

**ENGINEERING GEOLOGICAL CONTROLS ON FAILURE
MECHANISMS IN ROCK CUT-SLOPES IN THE TORLESSE
COMPOSITE TERRANE IN WELLINGTON, NZ**

A thesis

Submitted in partial fulfilment of the requirements for the degree of

Master of Science in Engineering Geology

at the

University of Canterbury

By

JESSICA FLORA BOYD

2019



UNIVERSITY OF CANTERBURY

ABSTRACT

The Torlesse Composite Terrane outcrops throughout both the North and South Islands of New Zealand. It is frequently encountered in cuttings along New Zealand's national road network thus it is important to understand the rock mass characteristics that control cut slope stability. As the Torlesse displays a high degree of variability in both lithology and structure, there is a need for geotechnical studies that can provide a qualitative assessment of the engineering geological conditions in the rock mass. This thesis investigates the range of rock mass conditions found in the Torlesse across the Wellington region. Seven sites were investigated in detail to provide an observational and qualitative assessment on the range of engineering geological conditions encountered. This included an evaluation of regional tectonic structures and their control on local rock mass defects and an analysis of the controlling factors that are likely to cause slope instability. Lithology and rock mass structure are identified as the dominant controls for slope stability. These attributes were integrated to develop a conceptual Torlesse rock mass classification (TRC). Eight rock mass types were identified, ranging from highly fragmented and brecciated fault crush through to massive sandstone-dominated rock masses.

Thickly-bedded sandstone has the best rock mass quality while mudstone-dominated units, being comparatively weaker generally display a higher frequency of defects, hence has a lower rock mass quality. Faulting and shearing are more commonly located within mudstone-dominated units. Proximity to major regional first order active faults is also a major influence on the rock mass. Rock masses adjacent to fault traces generally display increased levels of discontinuous and sub-systematic shearing, while shearing and faulting frequency decreases with distance away from the major fault traces.

Lithological proportions and tectonic structure are important tools for predicting rock mass condition. Defect properties, such as persistence and spacing, will determine the potential mode of failure and the likely volume of material involved. It is anticipated that the better rock mass types are likely to fail along persistent defect surfaces, irrespective of other rock mass characteristics. While poorer rock mass types are more likely to be controlled by a combination of rock mass conditions and structural defects. Jointing, which characteristically displays low persistence and close spacing, will only control small-scale failure, particularly in better rock mass types.

The quality and completeness of acquisition of the relevant rock mass characteristics through both surface (mapping and face logging) and subsurface (borehole and televiewer) investigations is evaluated using data from the Transmission Gully Project. Subsurface

information is only able to provide a 1-D profile of what can be a complex 3-D rock mass. Therefore, combining both surface and sub-surface investigations improves the accuracy of site-specific geological models for the purpose of detailed slope design.

The TRC developed in this study provides a simplified approach to classifying rock masses in heterogeneous, tectonised terranes. Although the approach is predominantly observational and qualitative in nature, it allows a first-order assessment of potential failure mechanisms in engineered rock cut slopes.

TABLE OF CONTENTS

Abstract	I
Table of Contents.....	III
List of Figures	VI
List of Tables.....	XIX
Acknowledgements	XXI
Chapter One Introduction	1
1.1 Context and Objectives.....	1
1.2 Background	1
1.3 Engineering in the Wellington Torlesse Composite Terrane.....	3
1.4 Desktop Study	4
1.5 Approach to Field Mapping	6
1.6 Rock Mass Analysis.....	8
1.6.1 General Methodology.....	8
1.6.2 Review of the Transmission Gully Structural Data.....	8
1.6.3 Classification Development	9
1.6.4 Rock Mass Development.....	9
1.7 Thesis Organization	9
Chapter Two Literature Review and Study Areas	11
2.1 Geological Setting.....	11
2.2 Rock Mass Structure	14
2.2.1 Fault and Shear Zone Characteristics	15
2.2.2 Rock Mass Defects	16
2.3 Active Faults	19
2.3.1 Ohariu Fault	21
2.3.2 Shepherd's Gully Fault.....	21
2.3.3 Wellington Fault	22
2.3.4 Moonshine Fault.....	23
2.4 Weathering versus Hydrology	24
2.5 Field Investigation Sites	24
2.6 Rock Mass Classifications	25
2.6.1 Read et al. (2000).....	26

2.6.2	<i>Irvine (2013)</i>	27
2.6.3	<i>Cammack et al. (2018)</i>	27
2.6.4	<i>Discussion and Synthesis</i>	28
2.7	<i>Summary</i>	30
Chapter Three Site Characterisation		31
3.1	<i>Terminology Adopted</i>	31
3.1.1	<i>Defect Type</i>	31
3.1.2	<i>Defect Infilling</i>	32
3.1.3	<i>Defect Shape</i>	33
3.1.4	<i>Defect Roughness</i>	34
3.1.5	<i>Defect Continuity and Termination</i>	34
3.1.6	<i>Folding</i>	34
3.2	<i>Rock Mass Site Characterisation</i>	36
3.2.1	<i>Transmission Gully North</i>	36
3.2.2	<i>Transmission Gully South</i>	43
3.2.3	<i>Kapiti Quarry</i>	48
3.2.4	<i>Horokiwi Quarry</i>	56
3.2.5	<i>Owhiro Bay Quarry</i>	63
3.2.6	<i>Wairaka Point</i>	67
3.2.7	<i>Makara Head</i>	75
Chapter Four Review of Transmission Gully Structural Domain Models.....		81
4.1	<i>Introduction</i>	81
4.1.1	<i>Design Site Investigation Data</i>	83
4.1.2	<i>Data Collection Methods</i>	83
4.1.3	<i>Transmission Gully Alignment Structural Domains</i>	84
4.2	<i>Comment on Design Structural Domains</i>	85
4.2.1	<i>Transmission gully North Study Zone</i>	86
4.2.2	<i>Transmission gully South Study Zone</i>	95
4.3	<i>Construction Mapping Data</i>	102
4.3.1	<i>Transmission gully North Study Zone</i>	102
4.3.2	<i>Transmission gully South Study Zone</i>	107
4.4	<i>Deviations from the Site Investigation Data</i>	112
Chapter Five Torlesse Rock Mass Classification		113
5.1	<i>Development</i>	113
5.2	<i>Overall Rock Mass Trends</i>	113
5.2.1	<i>Lithology</i>	113
5.2.2	<i>Rock Mass Structure</i>	118

5.2.3	<i>Poorly Correlated Rock Mass Trends</i>	131
5.3	Conceptual Classification System.....	133
5.3.1	<i>Rock Mass Classes</i>	133
5.3.2	<i>Nature of the Classification</i>	137
5.3.3	<i>Conceptual Development and Validation</i>	137
5.4	Plotting of the Study Site.....	140
5.4.1	<i>Transmission Gully North</i>	141
5.4.2	<i>Transmission Gully South</i>	142
5.4.3	<i>Kapiti Quarry</i>	144
5.4.4	<i>Horokiwi Quarry</i>	145
5.4.5	<i>Owhiro Bay Quarry</i>	147
5.4.6	<i>Wairaka Point</i>	148
5.4.7	<i>Makara Head</i>	150
5.5	Overall Rock Mass Types	151
5.5.1	<i>Type 1</i>	153
5.5.2	<i>Type 2</i>	154
5.5.3	<i>Type 3</i>	155
5.5.4	<i>Type 4</i>	157
5.5.5	<i>Type 5</i>	158
5.5.6	<i>Type 6</i>	159
5.5.7	<i>Type 7</i>	160
5.5.8	<i>Type 8</i>	161
5.6	Rock Mass Condition and Discussion	163
5.6.1	<i>Lithology</i>	163
5.6.2	<i>Defect Type and Persistence</i>	163
5.6.3	<i>Defect Condition</i>	165
5.6.4	<i>Defect Orientation</i>	166
5.6.5	<i>Suggested Approach for the TRC</i>	167
Chapter Six Comparisons With Other Classifications and Application to Cut-Slope Design		169
6.1	Torlesse Rock Mass Classification	169
6.1.1	<i>Comparison with Cammack et al. (2018)</i>	169
6.1.2	<i>Comparison with Suneson (1993)</i>	170
6.2	Controls on Rock Mass Condition.....	171
6.2.1	<i>Geological Controls</i>	171
6.2.2	<i>Weathering Effect</i>	178
6.2.3	<i>Groundwater</i>	178
6.2.4	<i>Discussion on Identified Controls</i>	178
6.3	Borehole versus Mapping Data Collection	179

6.4	Application to Slope Design	181
6.4.1	Potential Stability Mechanisms	181
6.4.2	Rock Mass versus Structurally-Controlled Failure	184
6.4.3	Ravelling and Rockfall Failures	186
6.5	Implications to Slope Design	187
6.5.1	Excavation	187
6.5.2	Slope Geometry	188
6.6	Constraints on the TRC for Future Projects	189
Chapter Seven Summary and Conclusions		191
7.1	Thesis Objectives	191
7.2	Rock Mass Site Observations	191
7.3	Transmission Gully Site Investigation and Construction Structural Data Review	193
7.4	TRC	193
7.5	Controlling Factors on Cut-Slope Design	196
7.6	Cut-Slope Design Implications	197
7.7	Future Work	198
7.8	Conclusion	199
References		201
Appendices		207
Appendix A: Transmission Gully North		207
A.1	Transmission Gully North Conceptual Structural Model	208
A.2	Transmission Gully North Outcrop Location Map	210
A.3	Transmission Gully North Raw Mapping Data	212
A.4	Transmission Gully North Graphs	224
A.5	Transmission Gully North Stereonet Analysis	231
A.6	Filtered Stereonet Analysis	234
A.7	Transmission Gully North Structural Domains	237
A.8	Transmission Gully North Engineering Geological Model	241
Appendix B: Transmission Gully South		243
B.1	Transmission Gully South Conceptual Structural Model	244
B.2	Transmission Gully South Outcrop Location Map	246
B.3	Transmission Gully South Raw Mapping Data	248
B.4	Transmission Gully South Graphs	255
B.5	Transmission Gully South Stereonet Analysis	261
B.6	Filtered Stereonet Analysis	265
B.7	Transmission Gully South Structural Domains	268

B.8	Transmission Gully South Engineering Geological Model	272
Appendix C: Kapiti Quarry		274
C.1	Kapiti Quarry Conceptual Structural Model	274
C.2	Kapiti Quarry Outcrop Location Map	276
C.3	Kapiti Quarry Raw Mapping Data	278
C.4	Kapiti Quarry Graphs	285
C.5	Kapiti Quarry Stereonet Analysis	291
C.6	Filtered Stereonet Analysis	295
C.7	Kapiti Quarry Structural Domains	298
C.8	Kapiti Quarry Engineering Geological Model	302
Appendix D: Horokiwi Quarry		304
D.1	Horokiwi Quarry Conceptual Structural Model	304
D.2	Horokiwi Quarry Outcrop Location Map	306
D.3	Horokiwi Quarry Raw Mapping Data	308
D.4	Horokiwi Quarry Graphs	314
D.5	Horokiwi Quarry Stereonet Analysis	321
D.6	Filtered Stereonet Analysis	324
D.7	Horokiwi Quarry Structural Domains	327
D.8	Horokiwi Quarry Engineering Geological Model	331
Appendix E: Owhiro Bay Quarry		333
E.1	Owhiro Bay Quarry Conceptual Structural Model	334
E.2	Owhiro Bay Quarry Outcrop Location Map	336
E.3	Owhiro Bay Quarry Raw Mapping Data	338
E.4	Owhiro Bay Quarry Graphs	343
E.5	Owhiro Bay Quarry Stereonet Analysis	349
E.6	Filtered Stereonet Analysis	352
E.7	Owhiro Bay Quarry Structural Domains	355
E.8	Owhiro Bay Quarry Engineering Geological Model	359
Appendix F: Wairaka Point		361
F.1	Wairaka Point Conceptual Structural Model	361
F.2	Wairaka Point Outcrop Location Map	363
F.3	Wairaka Point Raw Mapping Data	365
F.4	Wairaka Point Graphs	370
F.5	Wairaka Point Stereonet Analysis	377
F.6	Filtered Stereonet Analysis	381
F.7	Wairaka Point Structural Domains	384

F.8	Wairaka Point Engineering Geological Model	388
Appendix G: Makara Head.....		390
G.1	Makara Head Conceptual Structural Model.....	390
G.2	Makara Head Outcrop Location Map	392
G.3	Makara Head Raw Mapping Data	394
G.4	Makara Head Graphs	398
G.5	Makara Head Stereonet Analysis.....	406
G.6	Filtered Stereonet Analysis	410
G.7	Makara Head Structural Domains	413
G.8	Makara Head Engineering Geological Model	417
Appendix H: Transmission Gully Mapping		419
H.1	Domain K – Bedding	420
H.2	Domain K – Shearing.....	421
H.3	Domain H – Bedding.....	422
H.4	Domain H – Shearing	423
H.5	Domain U and No Domain – Bedding	424
H.6	Domain U and No Domain – Shearing	425
Appendix I: Rock Mass Trends		426
Appendix J: Statistical Calculations for the Torlesse Rock Mass Classification (TRC).....		441
J.1	Calculations	441
J.2	Individual Site Results.....	445

LIST OF FIGURES

Figure 1.1: Extent of the New Zealand's Torlesse Composite terrane (Read et al., 2000).	2
Figure 1.2: Schematic diagram of the key defect characteristics. Diagram is scale independent to mapping rock slopes or benches.....	6
Figure 2.1: Plate boundary features of the North Island and Northern South Island, New Zealand (Begg et al., 2008). Arrows and numbers indicate the rate and direction of the plate boundary convergence after (Begg et al., 2008).....	11
Figure 2.2: Scaled diagram illustrating the relationship between the Pacific and Australian plates in the Wellington area. The cloud of dark spots represents seismic activity between 1987 and 1993 from a zone within 20km of the top section line. This allows a relatively accurate estimation the location of the subduction interface (Begg and Johnston, 2000; Begg et al., 2008).	12
Figure 2.3: Faulting in the Wellington Region (Stevens, 1974).	13
Figure 2.4: Diagram of a cross-section through a fault zone showing the relationship between faulting and the fractured nature of the surrounding rock mass. Sourced from Stevens (1974) and is scale independent to higher magnitudes of faulting.	15
Figure 2.5: Map showing locations of study sites and active major 1 st order regional faulting. Detailed maps of each site are in Appendix A.1 through G.1. Information sourced from the GNS (2018)	20
Figure 2.6: GSI chart for heterogeneous rock masses (Marinos et al., 2005).	29
Figure 3.1: Drawing displaying the different scales and patterns associated with superimposed folding, interpretation taken from past literature (Suneson, 1992).....	35
Figure 3.2: Photographs of the groundwater flow escaping above the fault trace.	37
Figure 3.3: Photograph and sketch of a major cut in the Transmission Gully North study site. Photo taken 20th of March 2018 before shotcrete and other remedial measures were used to stabilise the darker fault crush material. The black dashed lines show bedding. The red are faults.	38
Figure 3.4: Flexure of bedding (black dashed lines), faulting (red) resulting in localising folding in the top of the cut. Shearing is presented by the red dashed line influencing folding such that bedding is thrust up producing fault propagation folding in the lower half of the cut. Light grey area indicates fault crush material.	39
Figure 3.5: Graph displaying the total percentage of defects shape in the Transmission Gully North study site.	40
Figure 3.6: Graph displaying the total percentage of the different major fraction infill types for defects recorded in the Transmission Gully north study site.	40

Figure 3.7: Graphs displaying the Transmission Gully North Shearing (Left) and Bedding (Right) waviness.	41
Figure 3.8: Graph displaying the defect roughness in the Transmission Gully North site.....	41
Figure 3.9: Graph displaying the total percentage of defect thickness, using the NZGS (2005) rock thickness terms, in the Transmission Gully North study site.	42
Figure 3.10: Contour diagram of bedding data for Transmission Gully North.....	43
Figure 3.11: Orientation arrangement of different generations of Folds associated with the Ohariu Fault. Figure 3.10 adapted from Twiss and Moores (1992)) subsidiary R, R', and P shear fracture arrangement model.	43
Figure 3.12: Photograph of a major cut in the Transmission Gully South study site looking south west. Photo taken 21 th of March 2018 before remedial measures were implemented. Bending of bedding (dashed black lines) in response to faulting (red lines) can be observed.	45
Figure 3.13: Graph displaying the total percentage of defect shape in Transmission Gully South.	46
Figure 3.14: Graphs displaying the Transmission Gully South Shearing (Left) and Bedding (Right) waviness.	47
Figure 3.15: Contour plot of the bedding data for Transmission Gully South. Interpretation of potential folding is indicated by the black and blue pi-girdle lines.	48
Figure 3.16: Shear zones (dashed red lines) within a thick sandstone bed. Contact between the extensively sheared mudstone rock mass and the thick sandstone bed (Grey line).	49
Figure 3.17: Photograph taken of mapping site 1. This area was mapped entirely as Lithofacies B.	50
Figure 3.18: Photograph and sketch of Kapiti Quarry displaying the water seepage (darker areas) on fault lines (red line) and axial surfaces of the synclines. The water also escapes on shear zones (dashed red lines) which are sub-parallel to bedding (dashed black lines) and coincide with the thicker sandstone units. Photo taken September 2018.....	51
Figure 3.19: Displaying Global scale failure controlled by continuous faulting leading to translational sliding. The black line shows the extent of the sliding failure. Photograph taken August 2018.....	52
Figure 3.20: Kapiti Quarry defect infill matrix grainsize fraction	53
Figure 3.21: Thickness of defects in Kapiti Quarry.	53
Figure 3.22: Kapiti Quarry dominant defect infill material.....	53
Figure 3.23: Fault crush material present on the lower bench on the south west corner of Kapiti Quarry. Hammer for scale, ~0.3 m.	54

Figure 3.24: Graphs displaying the Kapiti Quarry Shearing (Left) and Bedding (Right) waviness.	55
Figure 3.25: Contour plot of the bedding at Kapiti Quarry. Folding interpretations are overlaid showing the use of the π -girdle method.	55
Figure 3.26: Exposure of Fault disturbed rock mass in Horokiwi Quarry. Located near the Wellington Fault, in the south study area.	57
Figure 3.27: West study area in Horokiwi Quarry displaying the folding and continuity of the bedding in the “Margin Zone” area.	58
Figure 3.28: North study area in Horokiwi Quarry displaying “truncated” and continuous bedding in the “Margin Zone” area.	58
Figure 3.29: Displaying Margin Zone very widely spaced shearing forming conjugate (red arrow) to bedding.	59
Figure 3.30: Graphs displaying the defect waviness of Bedding (Right) and Shearing/Faulting (Left) at Horokiwi Quarry.	60
Figure 3.31: Thickness of the defects observed in Horokiwi Quarry.	61
Figure 3.32: Horokiwi Quarry defect roughness	61
Figure 3.33: A) Photograph of a Bedding shear and B) a Shear zone in "Margin fault" zone material. Geological hammer is provided for scale, ~0.3 m long.	62
Figure 3.34: Owhiro Bay Quarry photographs A) displaying thick mudstone bedding and B) rotated bedding due to faulting.	64
Figure 3.35: Shows a range of different rock mass conditions exposed in Owhiro Bay Quarry. Intersecting faulting and bedding defects form a number of failures in the upper benches.	64
Figure 3.36: Failure in the upper benches of Owhiro Bay Quarry. Appears to be bedding and fault controlled in a thick mudstone rich bed.	65
Figure 3.37: Graphs showing the waviness of Bedding (Right) and Shearing/Faulting (Left) in Owhiro Bay Quarry.	66
Figure 3.38: Owhiro Bay Quarry defect infill material.	66
Figure 3.39: Stereonet plot of bedding and shearing poles to planes of Owhiro Bay Quarry data. The red circle indicates the location of bedding clusters while the black circles are indicating shearing clusters.	67
Figure 3.40: Close up photograph of a large failure above mapped site 2 at Wairaka Point. Failure surface has been interpreted to occur on unfavourable oriented bedding and faulting (red line in Figure 3.42).	68

Figure 3.41: Photograph of mapped site 4 at Wairaka Point. Blue line indicates bedding upon which kinematic sliding has occurred.	69
Figure 3.42: Photograph and sketch displaying the location of a large failure above mapped site 2 at Wairaka Point. Failure surface has been interpreted to occur on unfavourable oriented bedding and faulting (Red line).	70
Figure 3.43: Folding observed at Wairaka Point. Left) observes tight to isoclinal inter-limb angles of first generation folding seen on shorelines while, Right) observes second generation folding which is more open. Geological Hammer and apple pencil are used for scale, approximately 0.3 m and 0.15 m respectively.	71
Figure 3.44: Photograph displaying the Bedding (Left) and shearing (Right) and Wairaka point. Geological hammer, ~0.3 m for scale.	72
Figure 3.45: Wairaka Point defect roughness.	72
Figure 3.46: Wairaka Point defect thickness.	73
Figure 3.47: Contour diagram of bedding and bedding shears for Wairaka Point.	73
Figure 3.48: Contour diagrams of Bedding and Bedding plane shear plots for structural Domains A) and B) at Wairaka Point. Use of the π -girdle method is shown to interpret folding.	74
Figure 3.49: Contour plot of A) all the “filtered” shearing data and B) all jointing data for Wairaka Point. Three shear sets can be identified in A).	75
Figure 3.50: Fault trace observed close to the study area.	76
Figure 3.51: Argillite bedding at Makara Head obscured by water and by cobbles and gravel material deposited onto the beach.	77
Figure 3.52: Defect infill material at Makara Head.	78
Figure 3.53: Graphs showing the defect waviness of shearing/faulting (Left) and Bedding (Right) at Makara Head.	78
Figure 3.54: Makara Head defect thickness.	79
Figure 3.55: Makara Head A) stereoplot of “filtered” shearing data, B) contour plot of the joints.	80
Figure 3.56: Stereoplot of bedding data collected from Makara Head. Shows the use of the π -girdle method to interpret folding.	80
Figure 4.1: Map showing the Transmission Gully alignment and the primary (1 st order) faults in the region. The Transmission Gully North and South study sites are highlighted. Data sources: LINZ and GNS.	82

Figure 4.2: Map showing the location of key cuts in the Transmission Gully North site. Imagery sourced from the Transmission Gully GIS Database (2019). See Figure 4.1 for the location of this site.....	85
Figure 4.3: Map showing the location of key cuts in the Transmission Gully South site. Imagery sourced from the Transmission Gully GIS Database (2019). See Figure 4.1 for location of this site.....	85
Figure 4.4: Domain K Stereonet displaying the televiewer shear and fault related shear data. Data sourced from PSM (2014).....	87
Figure 4.5: Stereonet displaying the bedding televiewer data in domain K. The red circle highlights a cluster of bedding data. The clusters, as indicated by the black circles have been overlaid from Figure 4.4 to aid in understanding the link between the shearing and bedding. Data is sourced from PSM (2014).....	87
Figure 4.6: Stereoplot of the bedding poles contour data for Domain K. The red, black and blue greater circles indicate potential fold orientations based on a π -girdle line of best fit. Data is sourced from PSM (2014).	88
Figure 4.7: Stereonet of design mapping shear and fault related shear data for Domain K. The red circles indicate the main clusters identified in Figure 4.4. Data is sourced from PSM (2014).	89
Figure 4.8: Stereonet of mapping bedding data for Domain K. The red circle indicates the main cluster of bedding data identified in Figure 4.5. Data is sourced from PSM (2014).	90
Figure 4.9: Domain H stereonet displaying televiewer shearing data. The black circle shows the location of the Data obtained from PSM (2014).	91
Figure 4.10: Domain H stereonet plot displaying the distribution of televiewer bedding data in Domain H. Data is obtained from PSM (2014).	91
Figure 4.11: Orientation arrangement of Folds associated with the Ohariu Fault. Figure 4.adapted from Twiss and Moore's (1993) subsidiary R, R', and P shear fracture arrangement model.	92
Figure 4.12: Contour diagram of the televiewer bedding data for Domain H. Data collected from PSM (2014).	93
Figure 4.13: Stereonet of the design mapping shear and fault related shear data. The red circle indicates the main cluster of shearing from the televiewer data in Figure 4.9. Data is obtained from PSM (2014).	94
Figure 4.14: Stereonet of the mapping bedding data. Data is obtained from PSM (2014).	94
Figure 4.15: Stereoplot of the Shearing televiewer data for Domain U. The black circles represent two clusters of shearing. Data is sourced from PSM (2014)	96

- Figure 4.16:** Stereoplot of bedding televiewer data for Domain U. Bedding has been grouped into two clusters represented by the black circles. Shearing clusters from Figure 4.15 are represented by the red circles. Data is sourced from PSM (2014). 97
- Figure 4.17:** Stereoplot of the design mapping shear and fault related shear data for Domain U. The red circles indicate the clusters of shearing from televiewer data. Data is sourced from PSM (2014). 98
- Figure 4.18:** Stereoplot of the design mapping bedding data for Domain U. The red circles represent the clusters of bedding from the televiewer data in Figure 4.10. Data sourced from PSM (2014). 99
- Figure 4.19:** Stereoplot of the televiewer shear and fault related data in the “No Domain” area within the Transmission Gully South study area. The black circles represent three clusters of shearing. Data is sourced from PSM (2014). 100
- Figure 4.20:** Stereoplot of the televiewer bedding data in the “No Domain” area within the Transmission Gully South study zone. Data is sourced from PSM (2014). 100
- Figure 4.21:** Stereoplot of the site investigation mapping shearing data in the No Domain area within the Transmission Gully South study zone. The red circles indicate the clusters of televiewer shearing from Figure 4.19. Data is sourced from PSM (2014). 101
- Figure 4.22:** Stereoplot of the site investigation mapping bedding data in the No Domain area within the Transmission Gully South study zone. Data is sourced from PSM (2014). 101
- Figure 4.23:** Relationship between persistence and defect width for (Top Left) Shearing and Faulting, (Top Right) Bedding and (Bottom) Jointing defects in the Transmission Gully North study area. Data obtained from PSM (2019). 103
- Figure 4.24:** Defect shape for the Transmission Gully north study area. Data obtained from PSM (2019). CU = Curved, IR = Irregular, PL = Planar, ST = Stepped, UN = Undulating. 103
- Figure 4.25:** Stereoplot of the shear and fault related shears from construction mapping data for Domain K. The red circles represent two clusters of shearing. Data is sourced from PSM (2019). 104
- Figure 4.26:** Stereoplot of bedding construction mapping data for Domain K. A single cluster represented by the black circles is shown. Data is obtained from PSM (2019). 105
- Figure 4.27:** Contour plot of the bedding poles from Figure 4.26 for domain K. The red black and blue greater circles indicated potential fold orientations based on a pi-girdle line of best fit. Data is sourced from PSM (2019). 105
- Figure 4.28:** Stereoplot displaying the construction mapping shear and fault related shear data for Domain H. Sourced from PSM (2019). 106
- Figure 4.29:** Stereoplot of bedding construction mapping data for Domain H. A single cluster represented by the black circle is shown. Data is obtained from PSM (2019). 107

Figure 4.30: Contour plot of the bedding poles from Figure 4.29 for domain H. The red black and blue greater circles indicated potential fold orientations based on a pi-girdle line of best fit. Data is sourced from PSM (2019).	107
Figure 4.31: Defect shape for the Transmission Gully south study area. Data obtained from PSM (2019). See Figure 4.24 for acronyms.	108
Figure 4.32: Stereoplot of bedding construction mapping data for Domain U. A single cluster represented by the black quadrilateral is shown. Data is obtained from PSM (2019).	109
Figure 4.33: Stereoplot of shears or fault related shears in the construction mapping data for the “No Domain” area. Two clusters represented by the black quadrilaterals are shown. Data is obtained from PSM (2019).	110
Figure 4.34: Stereoplot of bedding construction mapping data for the No Domain area. Two clusters represented by the black circles are shown. Data is obtained from PSM (2019).	110
Figure 4.35: Contour plot of the bedding poles from Figure 4.34 for the No Domain area. The red greater circle indicates potential fold orientations based on a pi-girdle line of best fit (black greater circle). Data is sourced from PSM (2019).	111
Figure 5.1: Relationship among lithology and discontinuity spacing relative to distance from major faults for Lithofacies B (Suneson, 1993, 1992).	116
Figure 5.2: Relationship among lithology and discontinuity spacing relative to distance from major faults for Lithofacies C (Red) and D (Green) (Suneson, 1993, 1992).	117
Figure 5.3: Distribution of bedding defect width observed from field sites (NZGS, 2005).	118
Figure 5.4: Overall percentage of all the defect types from all study areas. SR – Shear, SH – Shear zone, JN – Joint, FL – Fault, CZ – Crush Zone, BSH – Bedding Parallel Shear, and BG – Bedding.	119
Figure 5.5: Percentage of defect types recorded at each field area. Refer to Figure 5.4 for acronyms.	120
Figure 5.6: Average defect width (NZGS, 2005) of shearing features. See Figure 5.4 for acronyms.	121
Figure 5.7: Average percentage of rock fragments in defect infill across all study areas.	122
Figure 5.8: Major defect infill type across all sites. See Section 3.1.2 for infill type description.	122
Figure 5.9: Schematic diagram used to indicate defect continuity across engineered cut slopes in all study areas.	123
Figure 5.10: Schematic diagram used to indicate defect termination across engineered cut slopes in all study areas.	124

Figure 5.11: Continuity of defect types across all study sites. See Figure 5.9 for continuity explanation. See Figure 5.4 for acronyms.	124
Figure 5.12: Nature of the terminations for different defect types across all study area. See Figure 5.10 for termination type, See Figure 5.4 for acronyms.	125
Figure 5.13: Average defect type trace length across all study areas. For explanation on defect acronym see Figure 5.4.....	125
Figure 5.14: Relationship between continuity and persistence. For explanation on continuity terms see Figure 5.9 and 10.	126
Figure 5.15: A) Kapiti Quarry outcrop 3a, thin/moderately thin mudstone:sandstone: B) Owhiro Bay Quarry 2, thick to moderately thick mudstone:sandstone.	126
Figure 5.16: C) Horokiwi Quarry outcrop north, thin/thick mudstone:sandstone; D) Wairaka Point outcrop 1, thin/extremely thick mudstone;sandstone.	127
Figure 5.17: Average spacing of shearing defects across all study areas.....	127
Figure 5.18: Relationship between Wavelength and Inter-limb angle (PSM, 2010a).....	128
Figure 5.19: Bedding waviness across all study areas. Note that planar discontinuities are included.	129
Figure 5.20: Defect shape across all sites.	130
Figure 5.21: Average length (Persistence) of all the defects across all study sites.	132
Figure 5.22: Average defect width of shearing defects. See Figure 5.4 for acronyms.....	132
Figure 5.23: Torlesse rock mass classification.	138
Figure 5.24: Final Torlesse Rock mass Classification (TRC).....	139
Figure 5.25: Probability plot of the overall likelihood of defect classes and lithofacies combined.	139
Figure 5.26: Probability plot of the Transmission Gully North defect structural classes and lithofacies groups combined.....	141
Figure 5.27: Bird's eye perspective of the Transmission Gully North TRC (defined in Figure 5.24) plot and subsequent rock type clusters. Each cluster represents rock mass types 1, 2 and 3 explained in the previous paragraphs.....	142
Figure 5.28: Bird's eye perspective of the Transmission Gully South TRC (defined in Figure 5.24) plot and subsequent rock type clusters. Each cluster represents rock mass types 1 and 2 explained in the previous paragraphs.....	143
Figure 5.29: Probability plot of the Transmission Gully South defect structural classes and lithofacies groups combined.....	143

Figure 5.30: Probability plot of the Kapiti Quarry defect structural classes and lithofacies groups combined.	144
Figure 5.31: Bird's eye perspective of the Kapiti Quarry TRC (defined in Figure 5.24) plot and subsequent rock type clusters. Each cluster represents rock mass types 1 and 2 explained in the previous paragraphs.	145
Figure 5.32: Probability plot of the Horokiwi Quarry defect structural classes and lithofacies groups combined.	146
Figure 5.33: Bird's eye perspective of the Horokiwi Quarry TRC (defined in Figure 5.24) plot and subsequent rock type clusters. Each cluster represents rock mass types 1 and 2 explained in the previous paragraphs.	146
Figure 5.34: Bird's eye perspective of the Owhiro Bay Quarry TRC (defined in Figure 5.24) plot and subsequent rock type clusters. The cluster represents rock mass type 1 explained in the previous paragraphs.	147
Figure 5.35: Probability plot of the Owhiro Bay Quarry defect structural classes and lithofacies groups combined.	148
Figure 5.36: Bird's eye perspective of the Wairaka Point TRC (defined in Figure 5.24) plot and subsequent rock type clusters. The cluster (1) represents rock mass type explained in the previous paragraphs.	149
Figure 5.37: Probability plot of the Wairaka Point defect structural classes and lithofacies groups combined.	149
Figure 5.38: Bird's eye perspective of the Makara Head TRC (defined in Figure 5.24) plot and subsequent rock type clusters. The cluster (1) represents rock mass type explained in the previous paragraphs.	150
Figure 5.39: Probability plot of the Makara Head defect structural classes and lithofacies groups combined.	151
Figure 5.40: Bird's eye perspective of the combined TRC outcrop data (Figure 5.24). Overlay of rock mass types identified through individual site analysis.	152
Figure 5.41: Probability plot of the overall likelihood of defect classes and lithofacies combined. Copy of Figure 5.25.	152
Figure 5.42: Typical rock mass type 8 material. Containing gouge and brecciated material. A) Horokiwi Quarry South outcrop; B) Kapiti Quarry outcrop 1; C) Transmission Gully South outcrop 2a; D) Transmission Gully North Ohariu Fault trace and the related gouge and breccia material.	153
Figure 5.43: Typical outcrop of rock mass type 2 at Kapiti Quarry outcrop 3. Comprising of higher mudstone proportions and fragmented and brecciated mudstone and sandstone beds.	154

- Figure 5.44:** Fragmented and heavily sheared rock mass typical of Type 2. A) Kapiti Quarry outcrop 3; B) Kapiti Quarry outcrop 2. 155
- Figure 5.45:** Typical rock mass type 3. A) Horokiwi Quarry south outcrop displaying overprinted bedding; B) Discontinuous shearing and cross-cutting systematic shears in Transmission Gully North outcrop 2a; C) Continuous Crush zone in Transmission Gully North outcrop 1c. 156
- Figure 5.46:** Rock mass typical of type 4. A) Transmission Gully South outcrop 4, displaying continuous bedding which terminates again persistent (>20 m) faulting; B) Kapiti Quarry outcrop 1, bedding offset due to continuous shear zones and faulting to the left of the photograph. 157
- Figure 5.47:** Persistent (>20 m) bedding and shearing structures typical of rock mass type 5. A) Continuous bedding disrupted by folding in Horokiwi Quarry West outcrop; B) shearing forming conjugate to bedding in the Horokiwi Quarry North outcrop; C) bedding plane shearing in mudstone from Horokiwi Quarry West outcrop. 158
- Figure 5.48:** Thick to moderately thick interbedded sandstone-mudstone rock mass typical of Type 6. A) Continuous Bedding observed in Owhiro Bay Quarry outcrop 2; B) jointing and fragmented nature of the mudstone in Owhiro Bay Quarry outcrop 2; C) discontinuous jointing with persistence up to a metre in Owhiro Bay Quarry outcrop 1. 159
- Figure 5.49:** Typical defect infill of rock mass type 7 in A) Bedding plane shears; B) Shear zone; and C) shear at Makara Beach..... 160
- Figure 5.50:** Typical jointing that persists for >1 m. Presents a blocky characteristic for rock mass type 7. A) systematic jointing at Makara Head outcrop 3; B) Failure from intersecting persistent (~2 m) joints and shearing at Makara Head outcrop 2..... 161
- Figure 5.51:** Best possible rock mass quality typical of type 8. A) Persistent (>15 m) and continuous shearing and bedding which cross-cut in Wairaka Point outcrop 1; B) Persistent (>4 m) jointing intersecting with shears to form a wedge failure between Wairaka Point outcrop 2 and 3; C) Intersecting persistent (>4 m) systematic jointing forming local wedge and sliding failures at Wairaka Point outcrop 4..... 162
- Figure 5.52:** Flow chart of the suggested approach for the TRC..... 168
- Figure 6.1:** Representation of the interpreted failure scenarios with the typical pole plots and great circles likely to lead to such failures. Modified from Cook (2001) and González de Vallejo and Ferrer (2011). 182
- Figure 6.2:** Comparison between structurally controlled and rock mass condition failures adapted from González de Vallejo and Ferrer (2011). 186
- Figure 6.3:** Schematic displaying the nature of ravelling and rockfall mechanisms. Adapted from Hearn (2011). 187
- Figure 7.1:** Final rock mass classification. The green area represents the rock mass type adjacent to major 1st order regional faults. The grey area represents the rock mass type typical of fault crush or gouge material. The dashed lines are included to accommodate potential rock mass types that have yet to be or may be encountered. 195

LIST OF TABLES

Table 1.1: Irvine et al. (2018) fault order definitions.	4
Table 1.2: Structural Regimes from Cammack et al. (2018).....	7
Table 2.1: Summary of the different defect characteristics in greywacke rock masses from Read and Richards (2007).....	18
Table 2.2: Informal greywacke rock mass classification from Read et al. (2000).	27
Table 3.1: Defect type descriptions and terms, adapted from ISRM (1978) and PSM (2010a, 2010b).....	31
Table 3.2: Sequence of the infill terms.....	32
Table 3.3: Specific terms adopted for the recording of brecciated material among rock fragment percentages and defect coating descriptions (Jones, 2014; PSM, 2010a, b).....	33
Table 3.4: Specific terms adopted for Defect shape with related illustrations (PSM, 2010a).	33
Table 3.5: Specific codes adopted for Inter-limb angle (PSM, 2010a, b).....	33
Table 3.6: Specific codes adopted for defect roughness (PSM, 2010b).....	34
Table 3.7: Specific codes adopted for defect continuity and end termination nature (PSM, 2010a).....	34
Table 3.8: Scale of folding determined by Suneson (1993, 1992).	35
Table 3.9: Relationship between Suneson (1993, 1992) and Twiss and Moores (1992) folding terminology using wavelengths	36
Table 5.1: Summary bedding thicknesses and sandstone and mudstone ratios at each study site.	114
Table 5.2: Relative proportions of (Suneson, 1993, 1992) lithofacies at each study site.	115
Table 5.3: Definition of rock mass lithofacies	133
Table 5.4: Summary bedding thickness classification from PSM (2010)	134
Table 5.5: Dominant defect structures controlling slope stability. It is inferred that global scale structures will also control local failures as well, either by interacting with other similar or local structures.	136
Table 5.6: ISRM (1978) defect spacing classification.....	137

Table 5.7: Relative proportions of the adapted Suneson (1993) lithofacies groups and structural defect classes established in 5.3.1.....	140
Table 5.8: Sandstone and mudstone proportions displayed across all rock mass types	163
Table 5.9: Typical persistence of defect types across rock mass types	164
Table 5.10: Typical defect infill characteristics for each rock type.	166
Table 5.11: Typical orientation of continuous defects in relation to major regional faulting.....	167
Table 6.1: Comparison with Cammack et al. (2018) rock mass regimes and rock mass types derived in this study.	170
Table 6.2: Comparison between Suneson (1993) rock mass lithofacies and rock mass types derived through this study.	171
Table 6.3: Potential failure scenario irrespective of slope orientation	184

ACKNOWLEDGEMENTS

The time spent gathering and processing of both the primary and secondary data for this thesis could not have been done without the generous support of a number of people. So to take the time to formally thank them all is not only apt but deserving for their energy, time, resources and professionalism.

Firstly I would like to express my utmost gratitude to the Pells Sullivan Meynink (PSM) who provided me with an internship over the 2018 summer, giving me invaluable access to both their structural database, and to a number of sites in Transmission Gully alignment. A special acknowledgement is warranted to both Mark Eggers and Ralph Cammack for their generosity in sharing their professional guidance and considerable knowledge in this geologically complex field.

To my thesis supervisor, Clark Fenton (University of Canterbury) the personal guidance and challenging discussions have been both stimulating and reassuring thus shaping this thesis through to its final draft. A special thank you is also warranted to David Bell a co-supervisor (University of Canterbury) for his willingness to take the time to help, support and give advice during the study.

A number of sites were visited to collect the extensive amount of data in the process of forming this thesis. It is therefore important to acknowledge both the companies and their personnel that enabled my access to the sites (beyond that of PSM): The CPB and the geotechnical team on the Transmission Gully Project, Lawrence Snook (Kapiti Quarry Winestone Aggregates) and Ross Barker (Horokiwi Quarry).

I would also like to extend my gratitude to Adam Irvine and Tim Rutherford for facilitating access to the relevant Transmission Gully structural data. Your generosity of both your time and professional opinion was always valued. Support in the field by Mei Ai Khoo (Research student) and Matt Cockcroft (University of Canterbury, Geology Department) for his technical drone flying skills to help generate detailed map work.

To all my friends, colleagues and family thank you for all of your patience and understanding. Your endless encouragement, support and good humour have been powerful driving factors in completing this thesis.

CHAPTER ONE INTRODUCTION

1.1 Context and Objectives

The aim of this project is to investigate the engineering geological conditions governing large scale rock slope cuttings in the Wellington Torlesse Composite Terrane. The purpose of this study is to characterise the range of rock mass conditions in the Torlesse that can be assessed and utilised in a classification scheme that will provide the basis for a framework that will aid in the design of large rock cut-slopes.

The primary objectives of this thesis are to:

- Characterise the range of engineering geological conditions encountered within the Torlesse Composite Terrane of Wellington, New Zealand.
- Review and compare the structural data established from a preliminary site investigation phase and the construction mapping programme.
- Develop an engineering geological model approach for the evaluation of rock mass condition.
- Comment on the application of the approach to future engineering projects within the Torlesse Composite Terrane, within the Wellington region for slope design.

The motivation for this study is to utilise the design geotechnical database and exposures available during construction of the Transmission Gully project in Wellington. This project transects a range of geological conditions in the Torlesse rock mass and as such presents a rare opportunity to advance the understanding on engineering geological controls on rock slope design in this important geological unit in New Zealand.

To achieve these objects seven study sites were selected which represent a wide range of engineering geological conditions exposed in the Wellington Torlesse Composite Terrane. These sites are Transmission Gully North and South, Horokiwi Quarry, Kapiti Quarry, Owhiro Bay Quarry, Wairaka Point and Makara Head. Data collected from detailed engineering geological mapping was assessed and used to develop a characterisation system to classify the structural make-up of the Torlesse rock mass in the Wellington region. It is intended that this information will provide a framework that can be applicable to future rock cut-slope design projects in the Torlesse Composite Terrane, both within the Wellington region and in other areas.

1.2 Background

The Torlesse Composite Terrane is a widespread geological unit encountered in rock cuttings along the national road network in New Zealand (Figure 1.1). It consists of a large group of rocks

that has been exposed to severe tectonic deformation over its complex structural history, resulting in a wide range of engineering geological conditions (Begg and Johnston, 2000; Kamp, 2000). Slope design in these cuttings is therefore an important task during geotechnical studies for new road developments.



Figure 1.1: Extent of the New Zealand's Torlesse Composite terrane (Read et al., 2000).

Past geotechnical studies of the Torlesse Composite Terrane have typically focused on rock mass description and classification to enable the assessment of rock mass strength parameters (Cook, 2001; Pender, 1996; Read et al., 1999; Read and Richards, 2007; Read et al., 2000; Read et al., 1998; Stewart, 2007). More recent work by Irvine (2013) undertook to describe key engineering geological features that may be important to the assessment of mechanised tunnelling conditions in the Torlesse, while Cammack et al. (2018) adapted the Read et al. (2000) rock mass classification to include weathered and faulted materials. Relevant past

geological work includes Suneson (1993), which separates the Torlesse stratigraphy into several sub-units using a lithofacies classification system.

While the focus of past work has mainly been on rock mass description and classification, experience from existing road cuttings suggest that, outside of weathered and highly faulted rock, other factors are likely to control potential slope instability mechanisms in rock cuttings. As such, this study seeks to investigate the nature of these engineering geological controls with the aim to refocus the geotechnical effort to the important factors likely to control slope design of rock cuttings in the Torlesse Composite Terrane.

1.3 Engineering in the Wellington Torlesse Composite Terrane

There have been numerous studies of engineered rock slopes around the Wellington region and surrounding regions. Of the constructions very little provide information regarding large scale cut-slopes in the Torlesse. Slope height - slope angle charts presented in Grant-Taylor (1964) provides a method of assessing stable slope angles in the Wellington region. This method is based on observations from a number of natural hillside and cliff slopes with results anticipating a final life expectancy of fifty years or more. The graph is drawn from observed slope angles and as such only appears to allow for rock strength in the lower altitude faces. Because of this and the relatively small scale of the highest natural vertical rock face (around 30 m), it would appear that this method is only suitable for small scale rock slopes. Additionally the method does not mention the effect of structure on cut-slope stability, such as continuous shears and faults instead they predict that jointing will govern stability in much of the weathered Torlesse material.

Recent work has been undertaken on the Transmission Gully Project located in the northwest of the Wellington region. The project spans 27 km from Porirua to Paekakeriki passing through Cannons Creek, Pauatahau and Battle hill forest. Current knowledge held by PSM through tender, detailed design and construction studies is important to this study. The scheme crosses through a range of Torlesse rock mass conditions including deeply weathered zones, fractured less weathered rock and highly tectonically disturbed material associated with regional fault systems (Cammack et al., 2018). A Torlesse rock mass classification system has been developed for the purpose of facilitating geotechnical design of cuts in this project (Section 2.6.2).

Past work conducted within the Wellington urban motorway's Terrace Tunnel considered the different rock conditions, in particular weathering, jointing and faulting (Riddolls and Perrin, 1975). The 460 m long tunnel passes through intensely weathered and fault disrupted Torlesse (Riddolls and Perrin, 1975). It is recorded that a majority of the tunnel is situated in mostly clayey breccia of the Terrace fault zone while the existing slopes adjacent to the north portal are mostly in weathered bedrock (Riddolls and Perrin, 1975). Site investigation mapping provided enough

information to describe the overall rock condition in terms of six subjective classes, later used during logging of the investigation drive (Riddolls and Perrin, 1975). During construction, mapping indicates that adversely oriented faults, shears and crush zones were encountered in slopes (Riddolls and Perrin, 1975). This lead to proclamations emphasizing the need for stability measures after excavation due to the required steep cuttings (Riddolls and Perrin, 1975).

1.4 Desktop Study

Prior to conducting field work, a desktop study was carried out to understand the influence of bedrock structure on slope design and to develop conceptual models that predicted the likely rock mass conditions at each study site. This information was used to create field sheets that record important information in the field (Appendix A to G).

Conceptual models were created using aerial imagery in conjunction with the literature review to identify potential faulting in the landscape. Data sources included use of the fault database provided by Begg and Johnston (2000) and Irvine et al. (2018). This information was divided into the three fault orders (Table 1.1) that were previously defined by Irvine et al. (2018). The division is dependent on the strike length of each fault and based on the assumption that the structures with greater lengths are more likely to have a larger control on crust stress/strain. Many past studies (AECOM and PSM, 2015; Cotton, 1949; Irvine, 2013; Irvine et al., 2018; Stevens, 1974; Twiss and Moores, 1992) show that these longer structures are likely to have wider zones of structural influence which largely reflects on observe rock mass conditions. This understanding has been employed at a basic level to help convey and explain rock mass conditions.

Table 1.1: Irvine et al. (2018) fault order definitions.

Order	Strike length
Frist	> 10,000 m
Second	10,000 m – 2,500 m
Third	< 2,500 m

The aim of constructing conceptual models was to allow all existing knowledge on the regional (approximately 1:200,000) to district scale (approximately 1:400) structures to be presented in an illustrative way. Application of the current philosophy surrounding the major structures that incorporated various geometric models of all structural faults and folds was included. Due to the spatial extent of field areas, only individual district scale models were generated.

Knowledge from the conceptual models and literature review provided valuable insight into necessary information to be collected at outcrops and sites. Field sheets were created to provide a checklist and ensure consistency of information gathered. The basis of these sheets was provided from the NZGS (2005) field guide. This included weathering, strength, fabric, spacing,

bedding thickness and defect width. Defect infilling terms also used the NZGS (2005). These consisted of strength, weathering, and grain size of soil or rock fragments. Other information was derived from internal documents from Pells Sullivan Meynink (PSM, 2010a, b), after ISRM (1978). This information included defect characteristics such as: shape, type, waviness, Inter-limb angle, wavelength, termination, roughness, continuity, and saturation. Assessing the varying defect types was the main focus for this study.

Definitions of key defect characteristics are listed below (Figure 1.2):

Shape – refers to the surface shape of defects recorded over the surface trace length visible in an exposure or single bench.

Defect width – the perpendicular distance between adjacent defect walls.

Inter-limb angle (ILA) – is one of two measurements that are used to describe waviness. Recorded as the angle between two limbs, it is left blank where the shape is irregular, stepped or inaccessible.

Wavelength – is the second of two measurements for describing waviness. It is the recorded distance, in metres, between two identical peaks in a wave.

Persistence – is a measure of the defect trace length visible in an exposure or over a single bench. Recorded in metres.

Continuity – is measured over the visible surface trace from one termination (end) to the other, or over a single bench.

Termination – the way in which a defect ends (terminates) in a rock.

Spacing – is recorded as the perpendicular distance (metres) between adjacent discontinuities of the same type or set.

Infilling – material that separates adjacent defect walls.

Roughness – refers to the inherent surface roughness of a defect plane.

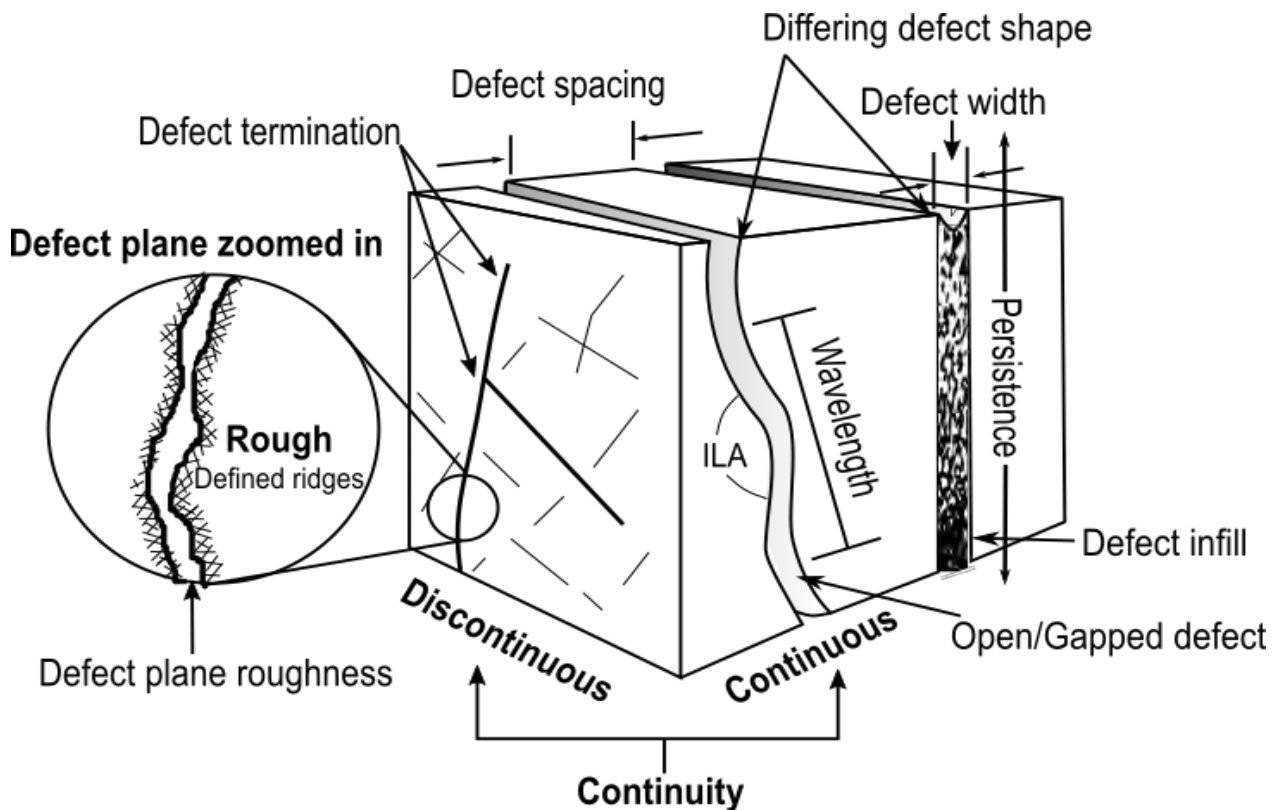


Figure 1.2: Schematic diagram of the key defect characteristics. Diagram is scale independent to mapping rock slopes or benches.

1.5 Approach to Field Mapping

Field areas were initially assessed to estimate the likely time it may take to observe and record outcrops. Mapping was not conducted in areas where access was problematic. In order to efficiently map all study areas, the methods that analyse small scale structures, such as scanline techniques or line mapping techniques used by Cook (2001), were not included. Furthermore, as the focus of this study is mostly on the more continuous and persistent structures, the use of small-scale methods was deemed nonessential.

Accessibility was examined at each outcrop as it appeared to dictate what outcrops could be observed. As most study areas were located in active quarries or construction sites, access was limited based on where operational business was being conducted. Each of these areas also had their own health and safety protocols that had to be followed. Therefore, the outcrops examined had to have relatively easy and safe access.

Each outcrop was first examined at a distance. All defect types were identified and labelled on a map. Once identified, defect character was recorded. Recording also included dip and magnetic dip direction. Due to the relative time constraints, defects typically than a metre in size were not recorded. Furthermore, where outcrops frequently exhibited similar defect types, such as bedding, then the number recorded was reduced and spaced throughout the outcrop to avoid repetitions. Generally, only one jointing plane from each outcrop was surveyed as they were

typically short and discontinuous and so was not suited with the focus of this study. Overall, outcrop descriptions were recorded using the NZGS (2005) field guide. Outcrops were also assessed for different lithological proportions and characterised using the (Suneson, 1993) sedimentary lithofacies classification system, which is as follows:

Lithofacies B (Arenaceous) – Amalgamated, thickly bedded (metres to tens of metres) to massive, fine to medium grained sandstone with minor thinly interbedded mudstone. Mudstone makes up less than 25% of the unit, and it is often sheared.

Lithofacies C (Arenaceous - Pelitic) – Interbedded sandstone and mudstone sequences, with bands generally 50mm to 5m thick. Individual sandstone beds are typically continuous at the outcrop scale. Mudstone content varies from ~ 25 to 50%. Mudstone beds are often sheared and frequently anastomosing.

Lithofacies D (Pelitic – Arenaceous) - Interbedded sandstone and mudstone sequences, with bands generally 50mm to 100mm thick. Poorly stratified to unstratified and pervasively sheared. Stratal continuity at the outcrop scale is an important characteristic. Mudstone to sandstone proportion is around 2:1.

Further description using Cammack et al. (2018) structural regimes was also use, which is described below. Combining both descriptions systems and defect structural data enabled an adequate description of the rock.

Table 1.2: Structural Regimes from Cammack et al. (2018)

Regime	Title	Occurrence
Regime A	Fractured Rock	Adjacent Margin Zone
Regime B	Margin Zone	Fault Margin Zone
Regime C	Fault Disturbed Zone	Close to Fault trace
Regime D	Fault Crush Zone	Adjacent Fault trace
Regime E	Mudstone Influenced	Varies by lithology
Regime F	Weathered Zone	Typically shallow

Regime A - Relatively less tectonically disturbed rock mass. Bedding and shearing structures are typically persistent (>50 m), continuous and planar. Isolated discrete sets are uncommon. Joints obtain a degree of randomness and may form relatively well defined sets with persistence still limited to a 10 to 20 m scale.

Regime B – Slightly more disturbed rock mass. Comprising of bedding and shearing that is less persistent (10 – 30 m). Bedding and may be truncated against other defects or disrupted by folding. Isolated discrete shearing is more frequent than in Regime A. Joints tend to form random patterns and are well defined with less visible at the >20 m scale.

Regime C – Characterised by a high degree of faulting associated with proximity of the rock mass in relation to major fault traces. Consists of pockets of regime B. Bedding can be persistent by is mainly truncated or overprinted. Shearing may form defined sets but is distinctly isolated and randomly oriented. Joints are generally random in orientation, short and discontinuous.

Regime D – Comprises mostly of brecciated or overprinted rock mass. Potential shearing tends to be oriented sub-parallel to major fault traces. Defined defect sets are rare.

Regime E – Increased proportions of mudstone tends to result in a higher degree of disturbance. Cross cutting, distinct and persistent defects are uncommon. Bedding is less distinct with bedding parallel shear planes typically forming wider shear zones.

Regime F – Encapsulates Highly weathered and Completely weathered material. Higher clay content tends to be included in infill material.

1.6 Rock Mass Analysis

The following section presents the rock mass analysis undertaken in this study.

1.6.1 General Methodology

All field information was transferred to spreadsheets that were divided into groups defined by their defect type - shearing/faulting, bedding or jointing. The computer program *DIPS v. 7.010* from Rocscience Inc. was used to produce stereographic projections of the poles to planes of each defect type. Clusters, fold axis, axial planes and π girdles were recognised on corresponding plots. Comparisons were made between different defect orientations at individual outcrops within each study site. Areas of similar bedding or structural set orientations were then grouped together and later combined with information collected from literature and field observations to produce structural domains. This was undertaken to assist in identifying common trends or patterns of defect orientations which were then compared with the conceptual models. This information was used in combination with field observations to generate 3D engineering geological models of individual sites. These models provide a detailed summary of the rock mass condition, and overall controls of the rock mass structure at each study area.

1.6.2 Review of the Transmission Gully Structural Data

Both the dominantly borehole based and construction mapping structural databases from the Transmission Gully project were assessed using the *DIPS v. 7.010* software. The data was split into previously defined structural domains established by the Geotechnical Investigation Team. Only the domains which encompass the selected study area extents were examined as other sites were not located within the project boundaries. Similar methods used in 1.6.1 were

undertaken and used to compare the mapping data against the borehole dominated design models.

1.6.3 Classification Development

All field information was plotted to find common rock mass trends or patterns across the Wellington Torlesse. Where no trends were observed, the information was cut. The Transmission Gully data, established trends and past literature were collectively analysed to determine which characteristics had a greater effect on the rock mass condition and, by association, slope stability. Groups which incorporate these characteristics were developed to produce a number of classes and lithofacies which, when compiled together, form the conceptual Torlesse rock mass classification (TRC). The classification was assessed against all study sites to validate the model and make modifications where new trends occurred.

1.6.4 Rock Mass Class Development

Each site was analysed and entered into the conceptual TRC. Individual plotting of each site on the diagram highlighted specific areas relating to certain rock mass types. These rock mass types were described using a number of different engineering geological characters. This was compared to the Transmission Gully project data for which rock cut slope implications can be assessed.

1.7 Thesis Organisation

Chapter 2 introduces the geological setting for the Wellington region and details of the field area localities. This is followed by a discussion on the current rock mass classifications specific to the Torlesse Composite Terrane.

Chapter 3 is split into two parts. The first is a detailed description and illustration of all the structures and features observed in this study. The second provides the site-specific results, which include the conceptual models, rock mass conditions, defect condition and stereonet projections.

Chapter 4 reviews the dominantly borehole structural data collected in the early stage of cut slope design on the Transmission Gully project and compares it with the construction mapping database. This chapter examines the structural domain models for the purpose of interpreting distribution patterns of shearing and bedding structures. Any variations and possible reasons for any departures from the revised structural domain models are discussed.

Chapter 5 begins with a discussion into the common physical properties of the defects that are typical across all the study sites. This is followed by an introduction into the development of the Torlesse rock mass classification diagram. This chapter concludes with a discussion on key rock mass characteristics that heavily influence the rock mass condition.

Chapter 6 provides a discussion into the Torlesse rock mass controls and potential slope instability mechanisms for rock cuttings. Further discussion addresses the implications and application of this research towards rock cut-slope design.

Chapter 7 summarizes and concludes the results of this study with suggestions for further research.

CHAPTER TWO LITERATURE REVIEW AND STUDY AREAS

2.1 Geological Setting

The Wellington region is located in a tectonically active area near the southern end of the Hikurangi subduction zone (Suneson, 1993). Known as the active transpressional boundary the rate of convergence is about 40 mm/yr (Figure 2.1), with the Pacific Plate being gently subducted at an azimuth of about 260° under the Australian Plate (Begg et al., 2008; Semmens, 2010; Van Dissen and Berryman, 1996). The gently northwest-dipping subduction interface lies at a depth of about 25-30 km beneath the city (Figure 2.2) (Begg et al., 2008).

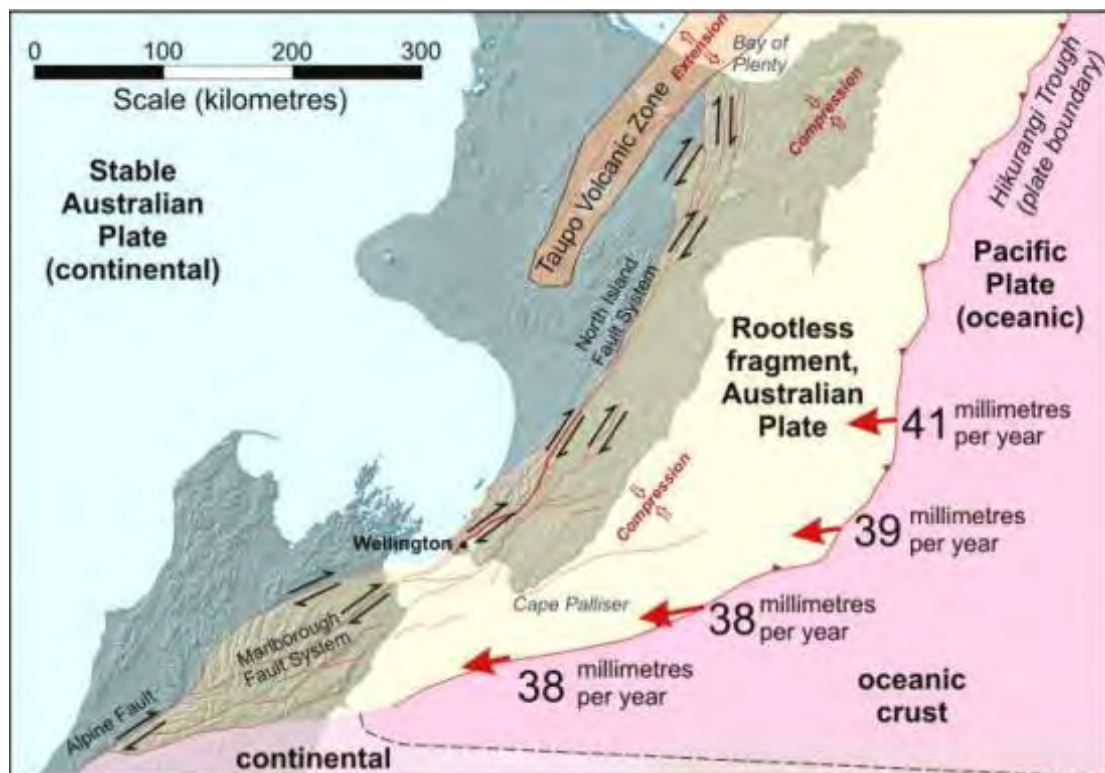


Figure 2.1: Plate boundary features of the North Island and Northern South Island, New Zealand (Begg et al., 2008). Arrows and numbers indicate the rate and direction of the plate boundary convergence after (Begg et al., 2008).

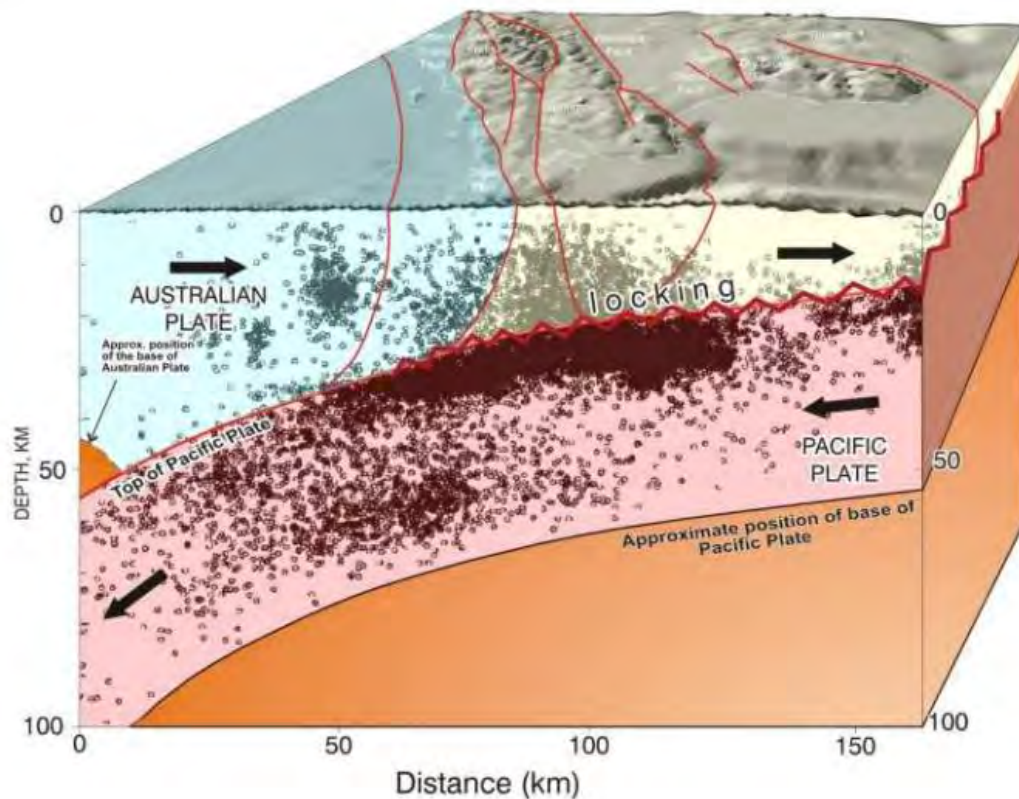


Figure 2.2: Scaled diagram illustrating the relationship between the Pacific and Australian plates in the Wellington area. The cloud of dark spots represents seismic activity between 1987 and 1993 from a zone within 20km of the top section line. This allows a relatively accurate estimation the location of the subduction interface (Begg and Johnston, 2000; Begg et al., 2008).

Development of this boundary began with a violent period of wrenching and tearing of the already metamorphosed Torlesse bedrock associated with the Kaikoura Orogeny (25 Ma to present) (Stevens, 1974). This resulted in northeast to southwest and north to south striking dextral-strike-slip faults and additional steeply dipping reverse fault alignments that correlate with a splinter pattern (Figure 2.3) (Eyles, 1982; Langridge et al., 2005b; Van Dissen et al., 1992).

Strain build-up from plate convergence is mostly stored and released on the “first order” northeast to southwest striking faults (Van Dissen et al., 1992). These faults are the dominant, persistent structures of the region that control the regional stress fields and orientation of the “second order” structures (Stevens, 1974)

The major active faults (“first order”) in this region separate blocks of Torlesse bedrock tilting them northwest (Stevens, 1974). These 1st order faults include; The West Wairarapa fault, the Wellington fault, the Ohariu fault and the Shepherds Gully-Pukerua fault (Figure 2.3) (Semmens, 2010; Stevens, 1974). Movement along these faults accommodates for some 60-90% of motion parallel to the plate boundary (Semmens, 2010).

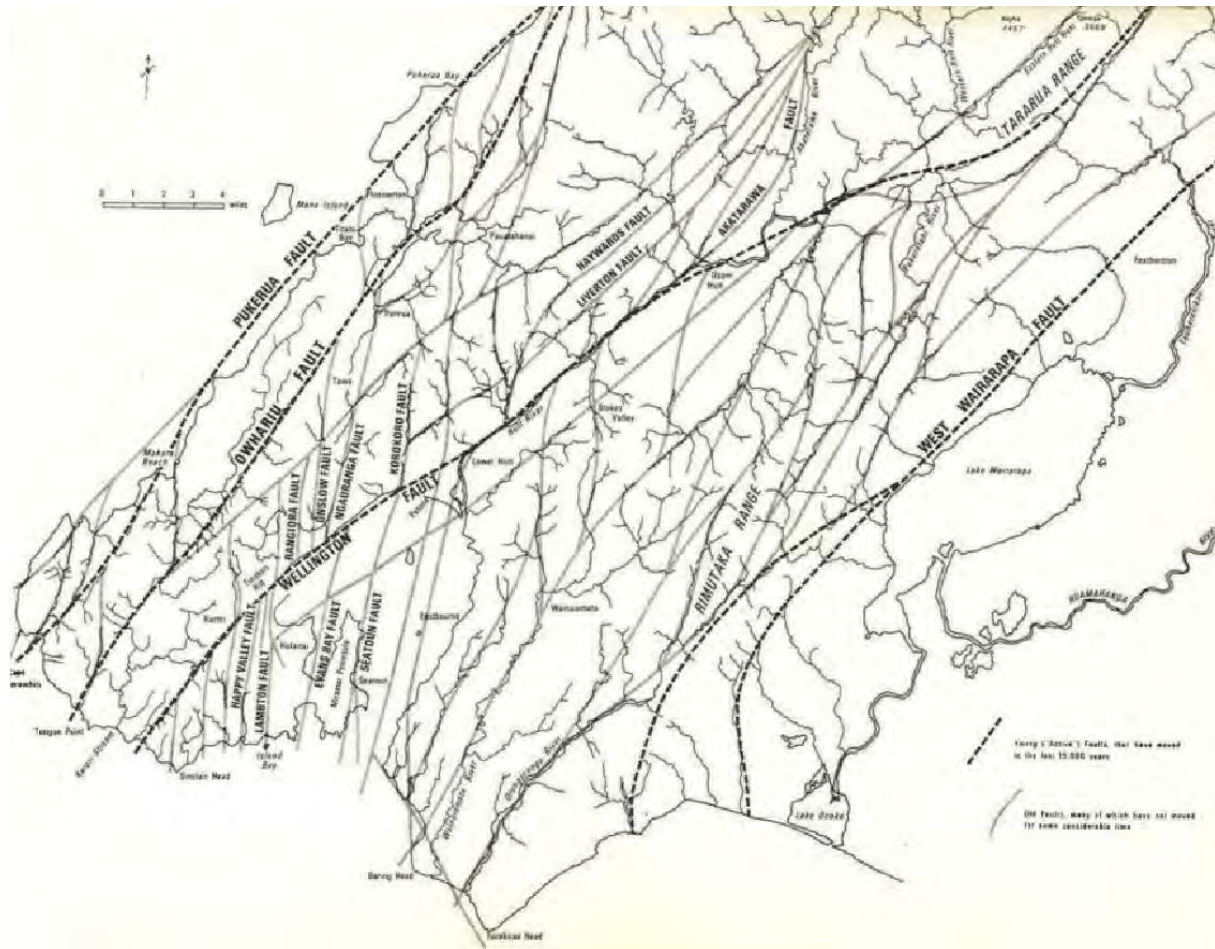


Figure 2.3: Faulting in the Wellington Region (Stevens, 1974).

Multiple smaller, 1st order faults are related to the splintering pattern along the major faults. Perceived as “second order” faults they are associated with the initial straining and tearing apart of the major active transpressional boundary (Stevens, 1974). These form in close proximity and parallel to major faults and accommodate a small portion of the predominantly margin-parallel motion (Langridge et al., 2005b; Stevens, 1974). Movement is observed as strike-slip and reverse, with examples including: The Moonshine, Akatarawa, Evans Bay, Whitemans Valley, and Otaki Forks faults (Figure 2.3) (Langridge et al., 2005a). Sites for this study are within close proximity to the Wellington Fault, the Ohariu fault, the Moonshine Fault and the Shepherds Gully-Pukerua Fault.

At local scales fault bending will control local stress fields and subsequently the local rock mass, which is reflected in the topography (Eyles, 1982).

Wellington’s underlying basement rock comprises mostly of quartzo – feldspathic sedimentary rock ranging in age from Late Permian to Early Cretaceous (Begg and Johnston, 2000). Known as the Torlesse Composite Terrane (also supergroup, complex) (Suneson, 1992) the rock is divided into three sub-terrane which are separated with the study areas in this thesis being

located within the Rakaia sub-terrane (Late Triassic) (Begg and Johnston, 2000; Suneson, 1993). Additional sub-terrane include the Pahau (Late Jurassic) and Esk Head (Orr et al., 1991).

The Torlesse rocks in the Wellington region are dominantly composed of strong to extremely strong quartzo-feldspathic sandstone (greywacke)-mudstone (argillite) sequences (Orr, 1984). These sequences are generally lightly metamorphosed to prehnite-pumpellyite grade and highly indurated (AECOM and PSM, 2015). There are minor amounts of conglomerate, volcanic and limestone material within the sub-terrane strata (Suneson, 1992).

Compositionally the sandstone contains detrital quartz with both plagioclase and potassium feldspars and lesser amounts of lithic fragments. Begg and Johnston (2000) discuss the quartz-feldspar-lithic fragment ratio (Q:F:L) to be approximately 40:43:17 within the Rakaia sub-terrane. The quartz present is mostly microcrystalline and the feldspar is dominantly plagioclase with a subordinate fraction of potassium feldspar at approximately a 19:1 ratio (Orr, 1984). Proportions of the alternating sandstone and mudstone lithofacies vary significantly throughout the region (Irvine, 2013; Suneson, 1992).

All material has been deposited in a submarine basin off the coast of Gondwana, near an active subduction zone, around 200 to 235 Ma (AECOM and PSM, 2015; Stevens, 1974). The type of material deposited at this time varied due to changing conditions along the coast. As a result deeper waters were able to obtain mud beds completely covered by coarse gravels and sands brought down by rivers and storms that form bedded sequences (Stevens, 1974).

At the same time the region endured a long period of compression, commonly recognized as the Rangitata Orogeny (Stevens, 1974). Constant shaking was a product of this period which sequentially generated turbidity currents that resulted in the deposition of coarser rocks in areas of usually fine-grained material (Suneson, 1993). This resulted in graded beds providing a means of recognizing the original top and bottom layers (Stevens, 1974).

Compression continued for several more million years subsequently burying, scraping and partially dragging beds down into the subduction system (Stevens, 1974). This formed an accretionary wedge environment with varying levels of induration within the accumulated sediments (AECOM and PSM, 2015). Later the sediments are folded, tilted, faulted and slightly metamorphosed (Orr et al., 1991).

2.2 Rock Mass Structure

The majority of the bedding in the Wellington Torlesse supergroup is observed as dipping greater than sixty degrees to sub-vertical with relatively high persistence (AECOM and PSM, 2015; Irvine et al., 2018). Conversely, joints are closely spaced, short and discrete (AECOM and PSM, 2015; Irvine et al., 2018; Pender, 1980; Stevens, 1974; Stewart, 2007; Suneson, 1993,

1992) the rock is also heavily fractured and faulted with common occurrences of overturned beds and tight, upturned folds (Begg and Johnston, 2000; Read and Richards, 2007; Suneson, 1993).

2.2.1 Fault and Shear Zone Characteristics

In the Torlesse the rock mass is heavily anisotropic (Irvine, 2013; Read and Richards, 2007). The argillite beds are generally more susceptible to deformation than the greywacke, as a result pervasive shearing is often displayed with a large number of shears running sub-parallel to bedding (Irvine et al., 2018; Suneson, 1992). Millimetre scale shear lengths are typically within the individual argillite beds, while the more persistent (tens of metres) shears are within the massive greywacke beds (Suneson, 1992). Despite the highly deformed nature of the rock mass, the intact rock strength between discrete structures is often moderately strong to strong (AECOM and PSM, 2015).

Ongoing movement of the major 1st order structures has formed zones of extremely fractured rock in the order of 10's to 100's of metres wide on each side of the fault (AECOM and PSM, 2015). Additional zones of fractured rock are generated with the degree of fracturing being higher closer to the fault and diminishing as distance from the fault increases (Figure 2.4) (Stevens, 1974). Close spacing of these faults regionally, has meant very few rocks escaped some degree of shattering (Stevens, 1974).

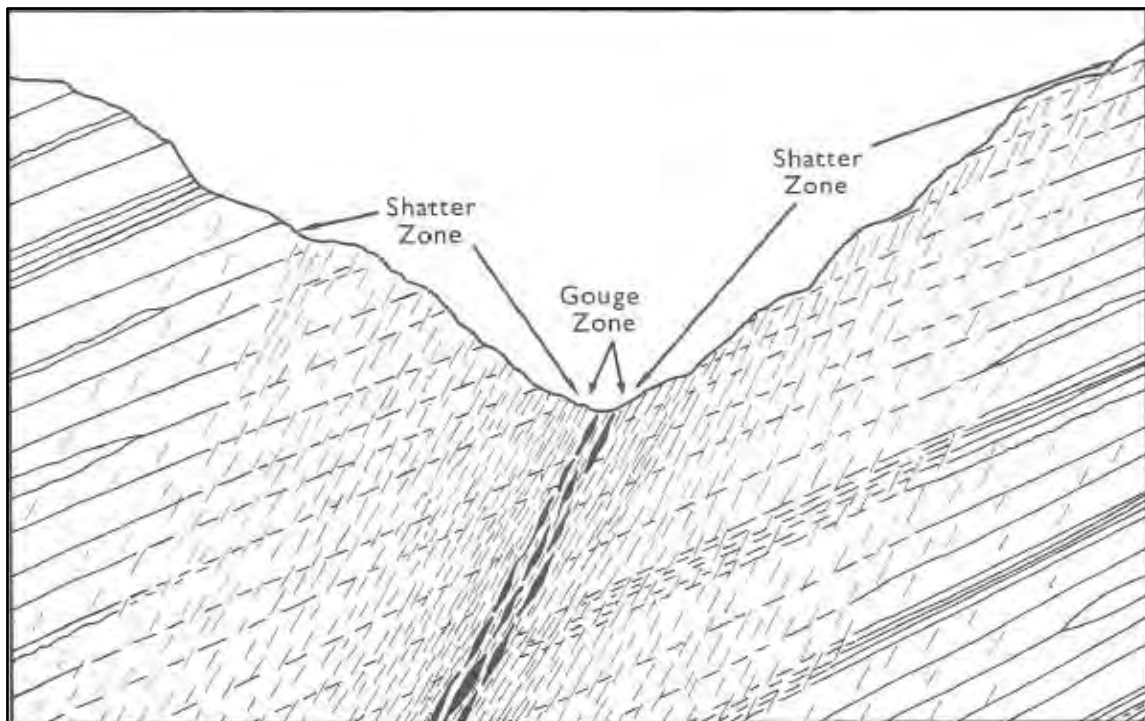


Figure 2.4: Diagram of a cross-section through a fault zone showing the relationship between faulting and the fractured nature of the surrounding rock mass. Sourced from Stevens (1974) and is scale independent to higher magnitudes of faulting.

Crush zones within the Torlesse, which are associated with faulting, are common and often contain gouge, or a brecciated zone several metres wide (AECOM and PSM, 2015; Stevens, 1974). This material has been well documented in literature. Numerous works for example have been carried out on a number of major active faults located within the Torlesse such as the Ohariu Fault and the Wellington Fault (AECOM and PSM, 2015; Cammack et al., 2018; Litchfield et al., 2009; Stevens, 1974; Van Dissen et al., 1992). All authors noted marked gouge zones around five metres wide, with brecciated zones approximately 400 m wide (Stevens, 1974). Along some of the smaller faults the gouge zone is only 50-75 mm wide with the brecciated zone 5-6 m wide (Stevens, 1974). Typically the fault crush material is very weak with most rock mass structure often overprinted or indistinct (AECOM and PSM, 2015). Structural regimes in Cammack et al. (2018) uses this information to help predict and guide interpretation of the likely rock mass characteristics around faults along the Transmission Gully alignment. The study has proven to be useful for predicting structure at cutting scale, specifically bedding and faulting/shearing. The results also allowed for an 'intelligent' interpretation of the borehole dominated structural database in heavily fractured rock (Cammack et al., 2018). This method of analysis can be directly applied to this study, however, being exercised on a much larger scale.

Suneson (1993) recognized up to four types of megascopic folds in the Rakaia sub-terrane. The majority of these folds were upright or overturned, with the less common inverted folds restricted to the south west of the Wellington regional coast and Titahi Bay (Begg and Johnston, 2000). The hinge zones are generally visible on the 1:1500 scale vertical aerial photographs used in the Suneson (1993) study. Most of the folds orientate sub parallel to bedding and are persistent for a few hundred metres to kilometres (Suneson, 1993). Limbs are generally moderate to tightly closed, of flexural-slip concentric style and east verging with a shallow plunge ((Begg and Johnston, 2000). Some smaller mesoscopic folds, visible at the outcrop scale have wavelengths ranging from centimetres to a few metres. They display widely varying plunges, from shallow SSW-dipping through vertical to shallow NNE dips (Begg and Johnston, 2000; Suneson, 1993). A few occurrences of box folds and local moderately tight to isoclinal folding is also mentioned (Begg and Johnston, 2000; Suneson, 1993).

2.2.2 Rock Mass Defects

The complex tectonic history and current seismically active environment in the Wellington region has resulted in an intensely disturbed rock mass with a high degree of variability in defect characteristics that can change significantly over short distances. Despite the highly fractured nature of the rock mass, relatively distinct structural patterns are visible. Understanding the geological structural patterns is important to this study for investigating the likely structural controls on potential slope instability mechanisms in rock cuttings. (AECOM and PSM, 2015) have examined the different defect types in Transmission Gully alignment and groups them into

two main structural categories (Cammack et al., 2018), systematic and sub-systematic defects. Systematic defects are comprised of more persistent structures typically bedding partings, faults, shears, shear zones, crush seams and some joints. These defects generally occur in well-defined sets unlike those of the sub-systematic defects which do not form sets or form poorly defined sets. Sub-systematic defects are usually more random in orientation and are often discontinuous, closely spaced (<20 - 200 mm) joints which tend to truncate each other (AECOM and PSM, 2015; Cammack et al., 2018). The focus of this study is on systematic defects as they are considered to be the governing control of large scale stability in the Torlesse (AECOM and PSM, 2015; Cammack et al., 2018).

Read and Richards (2007) summarizes the different defect characteristics for greywacke rock masses in New Zealand as seen in Table 2.1. Jointing is the most common defect identified (AECOM and PSM, 2015; Read and Richards, 2007) with up to six different joint sets at any one outcrop (Cook, 2001; Irvine, 2013). In highly tectonically disturbed areas joints tend to be more randomly oriented with a lack in persistence, and tend towards stronger defect sets in less tectonically disturbed areas (AECOM and PSM, 2015). Given the relatively close spacing of the major fault structures in this region jointing is not expected to typically form persistent defects or continuity at a large scale. Cammack et al. (2018) states that because of this joints will likely only influence local scale slope stability mechanisms. Therefore, for the purpose of this thesis joint sets are typically only assessed where considered critical and form well-defined sets. Faulting and shearing structures, such as shear and crush zones are thought to be of greater significance. These structures tend to be persistent, more widely spaced features which can occur in well-defined sets. If present in slope cuttings and sub-parallel to the slope orientation these features have the potential to cause large scale slope instability (AECOM and PSM, 2015; Cammack et al., 2018).

Table 2.1: Summary of the different defect characteristics in greywacke rock masses from Read and Richards (2007).

Table 3. Descriptions of defects in New Zealand greywacke rock masses.

	Bedding ¹	Vein ¹	Joint	Sheared zone	Crushed zone ²
Physical description	Defect where parting is parallel with rock texture	Defect with secondary mineralisation	Defect with little or no displacement	Roughly parallel sided zone with closely spaced joints	Roughly parallel sided zone with angular fragments including clay and/or gouge
Proportion	0–8%	0–10%	80–100%	0–2%	0–2%
Spacing	10 mm–5 m	Where present: 10 mm–2 m	20–600 mm	Where present: 1–20 m	Where present: 1–20 m
Persistence	<2 m–>10 m	<1 m–<10 m	<1 m–10 m	10–>100 m	10–>100 m
Width	n/a	n/a	n/a	<1 m	<2 m
Filling	Clean or silt/clay infill where relaxed	Secondary mineralisation (e.g. calcite or zeolite)	Clean or silt/clay infill where relaxed	n/a	n/a

¹ Not considered a defect where bedding is textural only (has no parting) or vein is annealed.

² Fault is a generic term for crushed zones with development of gouge from significant tectonic displacement and may be >2 m wide.

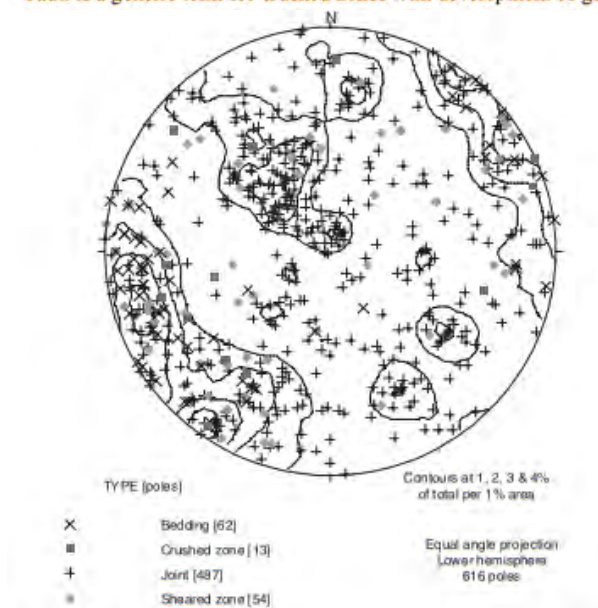


Figure 4. Stereographic plot of greywacke defects from Waitaki.

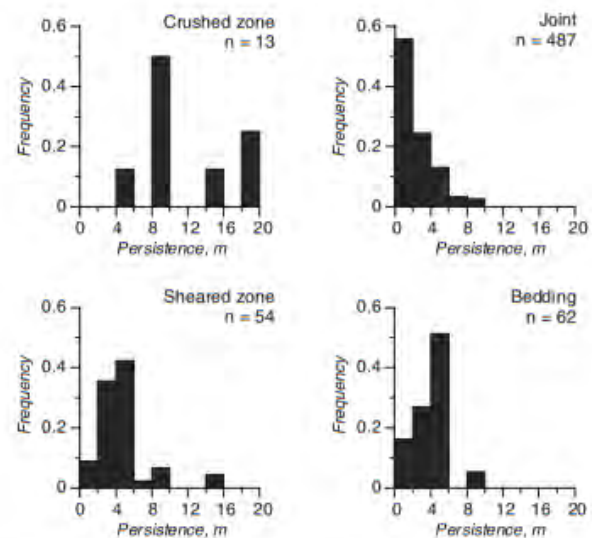


Figure 5. Frequency distributions for persistence of greywacke defects in Waitaki exposures.

It is highlighted in past studies that defects in this Wellington Torlesse composite terrane are highly variable in defect shape, roughness and infill characteristics (AECOM and PSM, 2015; Cammack et al., 2018; Irvine, 2013; Read and Richards, 2007). Defect infill material generally comprises of brecciated rock and soils containing silts and sands, with limited clays tending to occur in less weathered and tectonically disturbed areas. Clay infill is more dominant in the more weathered and faulted areas (Cammack et al., 2018). This variation has a significant influence on the rock mass shear strength as documented by Irvine (2013) who states that the defect condition will inevitably control any potential failure within the rock mass. Irvine (2013) also discusses the need for assessment of the relative age and maturity of shear zones in order to better predict rock mass conditions in rock masses. This is important to consider when differentiating conditions of sheared zones related to older, inactive fault zones from younger,

active faulting Irvine (2013). Characteristics presenting in the Torlesse rock mass suggest that older sheared zones are often healed or overprinted (AECOM and PSM, 2015; Irvine, 2013).

2.3 Active Faults

The active regional fault pattern is thought to by many (Begg and Johnston, 2000; Eyles, 1982; Grapes et al., 2011; Langridge et al., 2011) to control the shape of the entire Wellington landscape. More work by Irvine et al. (2018) recognized that the geometric relationships between these active regional faults are useful in predicting cutting scale structural patterns in the Torlesse rock mass in the Wellington region. This suggests that understanding the regional to district scale faulting pattern is useful for predicting cutting scale structure and therefore rock cut-slope design. As such, major 1st order regional faulting structures critical to this study are described in the sections that follow. Their location relative to each study site is presented in Figure 2.5 and in Section 1 of Appendix A to G.

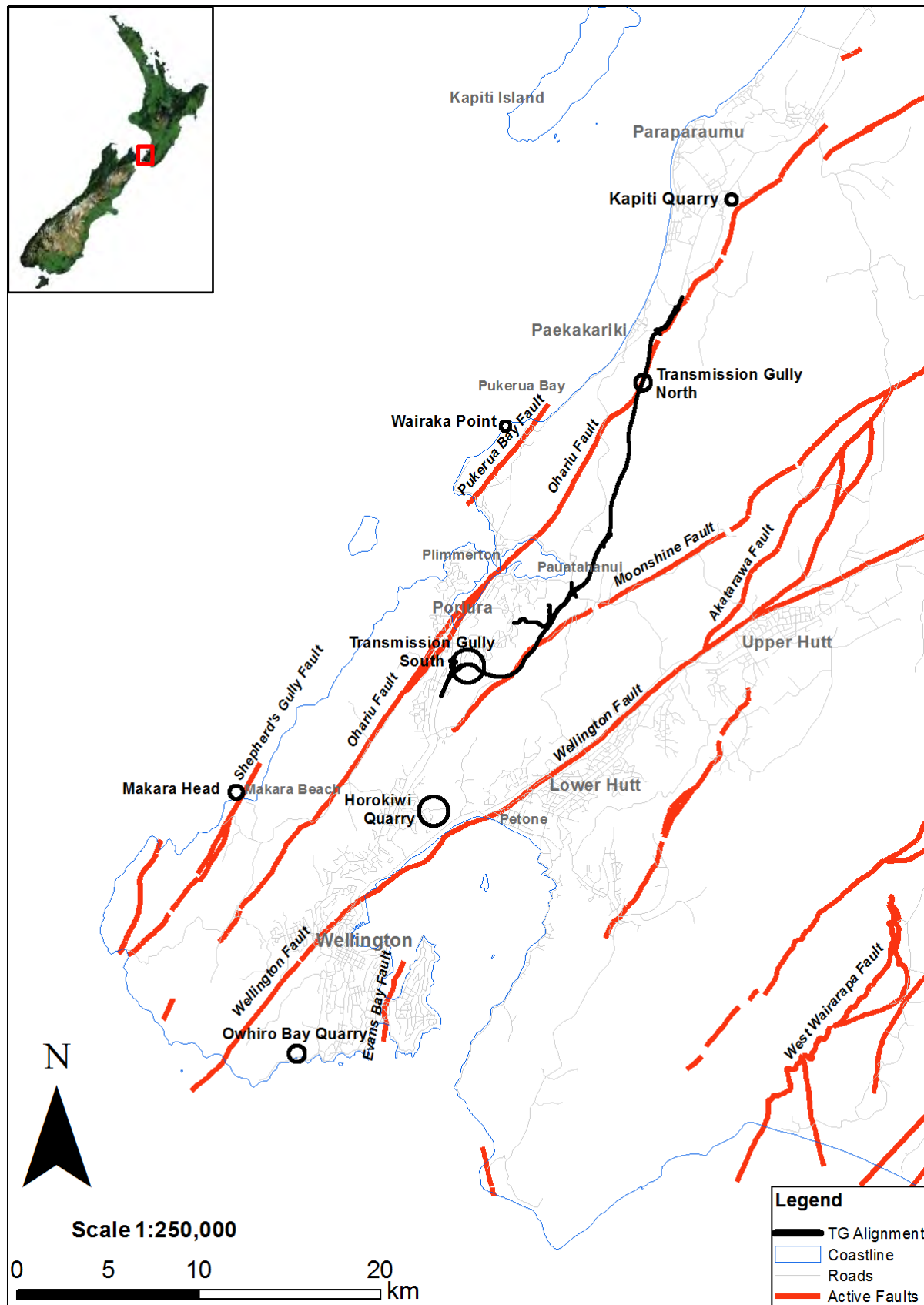


Figure 2.5: Map showing locations of study sites and active major 1st order regional faulting. Detailed maps of each site are in Appendix A.1 through G.1. Information sourced from the GNS (2018)

2.3.1 Ohariu Fault

The Ohariu Fault is one of the major active dextral strike-slip faults within the Wellington region. It has a large influence on the rock mass condition in a number of the selected study areas with some residing directly on top of or adjacent to the fault trace. A total of three study sites are affected by this fault: Kapiti Quarry, and Transmission Gully North and South. The Ohariu Fault is of particular interest in this study as the Transmission Gully alignment has a well-defined cut in the Northern section. This provides a great example of the influence major structures can have on rock mass condition.

The total on-land length of the fault is approximately 70 km trending NE/SW, with an average strike of 030-050°. The fault extends north eastwards from Tongue Point (near Waiariki Stream) on Wellington's southern coast through to Waikanae (Heron et al., 1998; Semmens, 2010). Just north of Waikanae the Northern Ohariu Fault appears to form the continuation of the Ohariu Fault in the Kapiti districts (Heron et al., 1998; Langridge et al., 2005b). The Ohariu Fault follows the Ohariu Valley running directly through the urban area of Porirua and transecting a number of major lifelines (Semmens, 2010). Offshore the fault can be followed for around 20 km as a series of discontinuous traces that lead from Tongue Point across the continental shelf to central Cook Strait. The fault trace is assumed to be a continuous feature with the exception of a 7 km section between Makara and Waiariki Stream, where the fault trace bifurcates (Semmens, 2010; Williams, 1975).

Slip rates on the Ohariu Fault are cited in Litchfield et al. (2009) and reported between 1-2 mm/year. This value was calculated from nine sites while vertical slip rates of > 0.006 mm/year were calculated from two sites in Heron et al. (1998). Horizontal displacements have been determined from the most recent event offsets at seven onland sites, a range between 3-5 m with a mean of 3.7 m (Heron et al., 1998).

Radiocarbon dates sourced from a number of different studies (Heron et al., 1998; Litchfield et al., 2006; Litchfield et al., 2009; Van Dissen et al., 1992) tend to correspond providing a recurrence interval of approximately 2200 years. This analysis took into account mean slip rates, single-event displacements, inter-event times between trenches and their uncertainties. The results obtained from Litchfield et al. (2006) also displayed a minimum and maximum 68% and 95% confidence interval limits of 1300 and 3800 years, and 800 and 7000 years, respectively (Litchfield et al., 2009).

2.3.2 Shepherd's Gully – Pukerua Bay Fault

Less information is available regarding the Shepherd's Gully – Pukerua Bay Fault. The Shepherds Gully segment of the fault zone is located to the south on the western edge of the Wellington Peninsula (Litchfield et al., 2013). The trace can be followed in a north easterly

direction towards Porirua, where it is assumed by Van Dissen and Berryman (1996) to join up with the Pukerua fault. The linear continuity of the trends of both faults are the basis for this assumption, with further support provided from results of seismic profiling (Thorpe, 1976) which identify a fault trace between Mana Island and the Mainland. Onshore fault traces are poorly preserved in the landscape, suggesting a low overall rate of movement (Semmens, 2010; Van Dissen and Berryman, 1996). These onland traces are also the only geomorphic expressions that are used to infer sense of movement, dip, and dip direction (Litchfield et al., 2013).

Slip rates are estimated from a combination of fluvial terrace offset data from the Pukerua Fault and slip rate budgets detailed in Robinson et al. (2011). Litchfield et al. (2013) records that the slip rate on the Pukerua-Shepherd's Gully Fault is between 0.3 and 0.6 mm/yr. This estimate is based on results recorded from one single-event displacement measured on the Shepherd's Gully segment of the fault. Slip rates yielded a tentative, poorly constrained, recurrence interval of 2500-5000 years with no direct data available regarding the timing of surface rupture on either of these faults (Langridge et al., 2005b). With the relatively poor preservation of onshore fault scarps it also suggests that the fault has not ruptured prior to the most recent primary fault rupture event on the nearby Ohariu Fault (Semmens, 2010). This implies that the last rupture event is greater than 1050-1000 years BP (Litchfield et al., 2004). A surface rupture centered on the Shepherd's Gully-Pukerua Fault system is anticipated to generate a moment magnitude (M_w) of 7.3-7.9 (Semmens, 2010). A total of two sites examined in this study are influenced by this fault, Wairaka Point and Makara Head.

2.3.3 Wellington Fault

The Wellington fault is one of the longest laterally persistent onshore faults in New Zealand (Semmens, 2010). It is one of the primary active faults of the North Island, with a dominantly dextral movement (Langridge et al., 2005a). Trending northeast – southwest the fault terminates approximately twenty kilometres in the Cook Strait to the south and runs some 420 km north, more or less continuously (Langridge et al., 2005a). From the southernmost known location, the fault runs through Wellington city, the Hutt Valley and the Tararua Range to the Manawatu River. Beyond the Manawatu River the fault continues towards the Bay of Plenty coastline as the Mohaka Fault where it is truncated by the active faults of the Taupo Rift (Begg et al., 2008). (Langridge et al., 2005b) describes the Wellington fault in the southern North Island in three parts: The Wellington Hutt Valley segment, The Tararua segment and the Pahiatua section. All study sites concerned with this fault are located in the Wellington-Hutt valley segment which spans from the southernmost part of the fault through to Kaitokie (Langridge et al., 2005b). This is 75 km long and includes two study sites, Owhiro Bay and Horokiwi Quarries. Location of these study sites relative to the Wellington fault display differences in proximity, presenting potential for variations in the rock mass condition.

Palaeoseismological studies conducted by Langridge et al. (2011), Langridge et al. (2005b), Little et al. (2010) and Van Dissen et al. (1992) all include trenching at a number of sites along the fault trace. The investigation's identified vital fault characteristics such as slip rate used for evaluating conditional fault rupture (Semmens, 2010). The fault along the Wellington-Hutt Valley segment has a high lateral rate of Quaternary slip rate of around 6-7.6mm/yr with varying rates of throw (Langridge et al., 2005b; Semmens, 2010; Van Dissen et al., 1992). A prior event is recorded approximately 670-830 cal. Yr BP (Langridge et al., 2005b; Van Dissen et al., 1992). A single surface rupture event has been observed at a few sites, such as near Te Marua and Long Gully, to have displacements in the range of 3.8-4.6 m (Langridge et al., 2005b; Van Dissen and Berryman, 1996). More recent works, in particular (Little et al., 2010) infers a best fit average moment magnitude (M_w) of 7.5 (7.3 to 7.6 1σ) with a late Holocene slip rate of $\geq 4.5 \pm 0.4$ mm/yr. Mean recurrence intervals are approximately 610-1100 years for this fault segment (Semmens, 2010). The estimated probability of a rupture in the next 100 years has been assessed by Rhoades et al. (2009) and found to be around 10-15%. Few exposures of the Wellington Fault also indicate that the fault plane is steeply dipping to vertical.

A surface rupturing earthquake centered on the Wellington Fault is calculated by Little et al. (2010) to have a mean single-event slip of 5.0 ± 0.24 m (95% confidence) on the Wellington-Hutt Valley segment. This is recognized by Van Dissen and Berryman (1996) to have moment magnitude of 7.5, which is considered to be New Zealand's greatest seismic risk, due to the obvious focus on the Wellington urban region (Langridge et al., 2005b; Rhoades et al., 2010).

2.3.4 Moonshine Fault

The Moonshine fault trace is one of the many active dextral strike-slip faults located at the southern end of the North Island. The fault trace extends from the headwaters of Duck Creek southward along Korokoro Stream passing through Cannons Creek (Begg and Johnston, 2000). The trend of the fault is about northeast with the sense of movement and dip direction being inferred from a combination of geomorphic expression and the Ohariu Fault along strike to the south (Litchfield et al., 2013). Past studies by Grant-Taylor et al. (1970) describe upthrow on the western side and down wraps at Bulls Run and Judgeford forming small basins. No strike-slip features have been recorded within the map area, however, according to Begg and Johnston (2000) the Akatarawa Stream is apparently dextrally offset at Cloustonville to the north. This would explain offsets in upper Duck Creek, Cannons Creek and Takapu Stream (Begg and Johnston, 2000).

Geomorphic expression of the fault is difficult to identify as most of the fault features are rounded and eroded, however, a few fault traces are exposed on the southeast side of lower Takapu Road (Litchfield et al., 2013). Vertical displacement is estimated to be 180 m at Judgeford and 240 m near Round Knob (Litchfield et al., 2013). Towards the south the topography is complex

making it difficult to estimate displacement. However, slip rates by Litchfield et al. (2013) estimated that fault movement is roughly 0.1-0.3 mm/yr. Recurrence interval stated in Cousins (2013) indicates that a 7.1 magnitude rupture on the Moonshine fault may occur approximately every 13,000 years.

2.4 Weathering versus Hydrogeological Factors

The effect of groundwater and weathering are a few of the important geological features that control the rock mass condition across the region (AECOM and PSM, 2015; Tating et al., 2013). As stated in AECOM and PSM (2015) the impact of weathering on the rock mass condition is to reduce the intact strength and degrade the structural fabric subsequently allowing for transportation by hydrogeological means. Irvine (2013) identified that the level of faulting and fracturing proximal to major faulting had direct effect on increasing the surface volume available for weathering. The degree of weathering is therefore often deeper closer to major faults (AECOM and PSM, 2015; Irvine, 2013). Further noted in AECOM and PSM (2015) are that these faults are often associated with compartmentalization of groundwater regimes and so frequent removal of the weaker weathered material tends to result in river and streams which follow the fault trace (Fetter, 2001; Stevens, 1974). Over time, continual down cutting of these rivers has led to the development of valleys (Eyles, 1982).

While these processes are important to understand the overall aim of this study is to focus more on the controls which govern the potential rock cut-slope failure mechanisms rather than assessing rock mass strength properties. Therefore weathering and hydrogeological processes in this study are not discussed in further detail.

2.5 Field Investigation Sites

Seven field areas around the Wellington region were selected to develop a widespread assessment of the Torlesse terrane. Locations of the study sites are shown in Figure 2.5. The aim was to incorporate a number of the large cuts of exposed greywacke and argillite rock in the region. The primary sites included two in Transmission Gully (one each in the north and the south areas of the alignment which comprise large cuts in this rock mass) accompanied by pit walls in three quarries, Owhiro Bay Quarry, Kapiti Quarry and Horokiwi Quarry. Two additional sites were investigated in natural coastal exposures, Wairaka Point and Makara Head. These sites were chosen for their large scale, displaying a range of rock mass conditions. Each of these sites obtains genetically similar material however, the rock mass and lithological structures vary throughout all the areas. The sites are located across the Wellington region solely in the Rakaia terrane.

Transmission Gully was chosen as the principal site of the study due to the proximity and complexity of good, fresh, exposures to major structures. Engineering geological mapping on the

largest working faces in the north and south provided a visual representation of the changes in rock mass conditions over varying distances. This included mapping across a combined total of 11 North and South bound benches, in parts presenting a valuable three dimensional insight, as most cuts are paired directly opposite each other. A total of 406 significant structures were recorded along with a number of rock mass descriptions.

Horokiwi and Kapiti quarries also provided a three dimensional insight due to their pit slope geometry. With Horokiwi quarry being a large and active quarry, health and safety was a major factor when collecting data. For this reason access was limited and so was not able to be as intensely investigated as other sites. A total of 89 significant structures were recorded. Kapiti Quarry is also active, however, it is not as large or as busy as Horokiwi and therefore access was not as limiting. A total of 140 significant structures were recorded at this site.

Owhiro Bay quarry was chosen as a study site primarily because of its accessibility and good exposure over a large scale. As the quarry has been inactive for a number of decades this provides valuable insight into how the rock mass behaves over time. A number of failures are logged on engineering geological maps and models including detail that is visible from 1:8500 scales. The bottom two benches have been mapped with a total of 70 significant structures having been logged.

Wairaka Point and Makara Head study sites enable a look into a number of naturally forming Torlesse rock slopes. Both of these areas lie on the coast and vary significantly from the other sites due to the lack of human influence. Access is good, however, exposures are relatively small compared to the other sites, specifically Makara Head. For this reason Makara Head has a low priority. Wairaka Point has a significant exposure and provides a further insight into how the rock mass behaves kinematically. A total of 102 significant structures at Wairaka Point and 67 at Makara Head have been recorded along with engineering geological mapping. Information gathered from these sites along with Owhiro Bay Quarry was used to compare rock mass conditions, character and performance with the larger database of results collected from Transmission Gully, Kapiti Quarry and Horokiwi Quarry.

2.6 Rock Mass Classifications

The advantage of using a classification is they provide simple estimates of rock mass parameters, although they are also limited by the intended applicability to a particular type of structure or rock mass (Sarkar et al., 2012; Stewart, 2007).

Past geotechnical studies on the Torlesse Composite Terrane have typically focused on rock mass description and classification to enable the assessment of rock mass strength parameters (Cook, 2001; Pender, 1996; Read and Richards, 2007; Read et al., 1998; Stewart, 2007). Study sites for all the works have been primarily centered outside of the Wellington region aside from

Cook (2001) who assessed the Torlesse rock mass in Belmont Quarry located in the Hutt Valley, Lower North Island.

2.6.1 Read et al. (2000)

Read et al. (2000) used the Belmont Quarry exposures when constructing a five class classification system, which is presented in Table 2.2. The classification system uses the application of the Hoek-Brown failure criterion to predict the rock mass strength of the New Zealand Greywacke. Results describe classes based on unweathered (fresh) or fresh-stained states of the Torlesse rock mass (Read et al., 2000).

(Read et al., 2000) identified that the use of a single numerical value does not represent the complexity of the Torlesse rock mass. For this reason a descriptive table such as the GSI was applied in order to support critical linkages between the strength and deformation properties that are assessed through laboratory triaxial testing and those assigned in the field. These linkages enable information to be computed into the Generalized Hoek-Brown Failure Criterion (Read et al., 2000). In applying this system Read et al. (2000) discovered that the rock mass strength estimates were unrealistically high for better quality rock, and low for lower quality rock Read et al. (2000). The suggestion was then to refine a rock mass classification, more specific than the GSI that recognizes the effect of the degree of tectonic activity specifically with defect spacing (Irvine, 2013).

Table 2.2: Informal greywacke rock mass classification from Read et al. (2000).

Rock material		Rock mass defects		Comments
CLASS	Lithology	Strength		
I	Homogeneous or faintly bedded medium-grained sandstone	Extremely strong to very strong	Joint spacing >150 mm, typically 200 – 300 mm, surfaces rough to smooth.	Little indication of major tectonic deformation in rock mass
	Fine-grained sandstone with some widely spaced interbeds of mudstone		Sheared, crushed or shattered zones generally absent	
II	Fine or very fine-grained sandstone with mudstone laminae	Very strong to strong	Joint spacing 60 – 200 mm, surfaces rough to slickensided.	Rock mass may contain minor very widely spaced zones of sheared and crushed rock
	Interbedded sandstone and mudstone		Minor narrow (<300 mm wide) sheared, crushed or shattered zones	
	Mudstone/sandstone with coarse podding			
III	Mudstone with extensive recrystallisation	Strong to moderately strong	Joint spacing <100 mm, surfaces smooth to slickensided.	Characterised by closely spaced defects (may be shattered) or recrystallised rock mass
	Interbedded sandstone and mudstone, often with podding and some veining		Narrow (<300 mm wide) sheared, crushed, or shattered zones	
IV	Interbedded sandstone and mudstone, with extensive podding	Strong to moderately strong	Joint spacing <60 mm, surfaces smooth to clay-lined.	Characterised by very closely spaced fractures with sheared zones ie. shattered and sheared rock mass with some crushed zones associated with fault zones
	Mudstone or very fine sandstone with extensive veining		Sheared with crushed zones (typically <500 mm wide), and may contain thin (<25 mm) gouge zones	
V	Mudstone or fine sandstone (rock material generally sheared and crushed)	Strong to moderately strong (or not applicable)	Joint spacing <20 mm, surfaces slickensided to clay-lined. Generally sheared or crushed zones which contain gouge zones	Characterised by very or extremely closely spaced fractures with crushed zones and gouges ie. crushed rock mass associated with major faulting

Classification based on rock mass in the *unweathered* (fresh) or *fresh-stained* state.

Podding refers to the disruption of bedding into irregular lenses or pods (not a common feature at Aviemore).

Recrystallisation refers to recementation of the rock mass and is often accompanied by veining.

2.6.2 Irvine (2013)

Irvine (2013) separates the Torlesse into eight different rock mass types for the purpose of assessing tunneling conditions. Development of the characterization identified that lithostructure and geological structure distributions are the main controls on major rock mass types. Proximity to major fault structures was discussed as a common link between these two main controls inferring that it was possible to predict rock mass conditions with some knowledge of the large scale structural setting. Currently the system is focused toward tunneling and does not examine cut slope design nor does it address the relative age of structural defects (Irvine, 2013). This information could be used to better predict variability in the Torlesse rock mass.

2.6.3 Cammack et al. (2018)

Recently Cammack et al. (2018) developed a site specific design methodology that considers the complexity of the structural variability of the Torlesse rock mass. The study describes six different structural regimes for rock cuttings on the Transmission Gully Highway project. The characterization is adapted from the Read et al. (2000) rock mass classification and addresses the importance of the geological history and geotechnical character on large scale performance

of cut slopes in the project area. Background for the design methodology is based on defect shear strengths for different failure mechanisms, with the assessment focusing on the scale for potential failures (Cammack et al., 2018). The study only considers a small part of the Wellington region and excludes the influence of age on structural defects. Cammack et al. (2018) also mentions that the structural regimes provides a means of grouping rock mass units according to their distribution in association with large fault systems, something that is also observed by Irvine (2013) and later discussed in Cammack et al. (2018).

2.6.4 Discussion and Synthesis

Most of the Torlesse lithotypes in the Wellington region can be described using the classification by Suneson (1993). The classification divides the Torlesse into several sub-units centered around the lithofacies classification established by Mutti and Ricci Lucchi (1978). Facies B (arenaceous) and C (arenaceous – pelitic) are the most common turbidite lithofacies in the Wellington Torlesse, with Facies D (pelitic) appearing less frequently, and Facies F (chaotic) and G (hemipelagic) observed rarely (Suneson, 1993).

Suneson's classification recognizes that the Torlesse bedrock originates from a non - or poorly channelized base-of-slope slope-apron system (Suneson, 1993). The importance of this is that originally the Torlesse rock is a sedimentary rock despite its low-grade metamorphism. However, it is a geological classification and so is limited in its geotechnical purpose as it does not address kinematic behavior or capture key engineering geological elements.

The use of widely known characterizations for rock mass properties is not included within this study. Bieniawski (1989) Rock Mass Rating (RMR) system, Barton et al. (1974) Q-system and Hoek and Marinos (2000) Geological Strength Index (GSI) are three examples of these external classifications systems all of which are primarily designed for tunneling applications (González de Vallejo and Ferrer, 2011). The degree of structural variability observed in the Torlesse rock mass means that these systems are practically unsuitable for providing a good representation of the rock mass condition, specifically the RMR and Q systems. Despite these limitations, the GSI can be useful as recent adaptations attempt to accommodate some of the more variable rock masses (Hoek and Marinos, 2000).

Both the RMR and Q systems are empirically derived rock classifications which require the evaluation of six parameters relating to the geometrical and mechanical properties of the rock mass (Barton et al., 1980). While these systems are typically great for the use of good quality rock masses they lack consideration for those of poor quality. To overcome these difficulties Hoek and Brown (1997) addressed these limitations by focusing on the strength of jointed rock masses (Read et al., 2000). This method is known as the Geological Strength Index (GSI). This system is split into six structural/fabric types and five types of defect surface conditions.

Together they are used to give a quantitative value ranged 0 to 100, where 100 is equivalent to intact rock mass (Cook, 2001; Marinos et al., 2005; Stewart, 2007). Hoek and Marinos (2000) has also extended the *GSI* to accommodate some of the more variable rock masses. Figure 2.6 shows the latest version of the Geological Strength Index for heterogeneous rock masses.

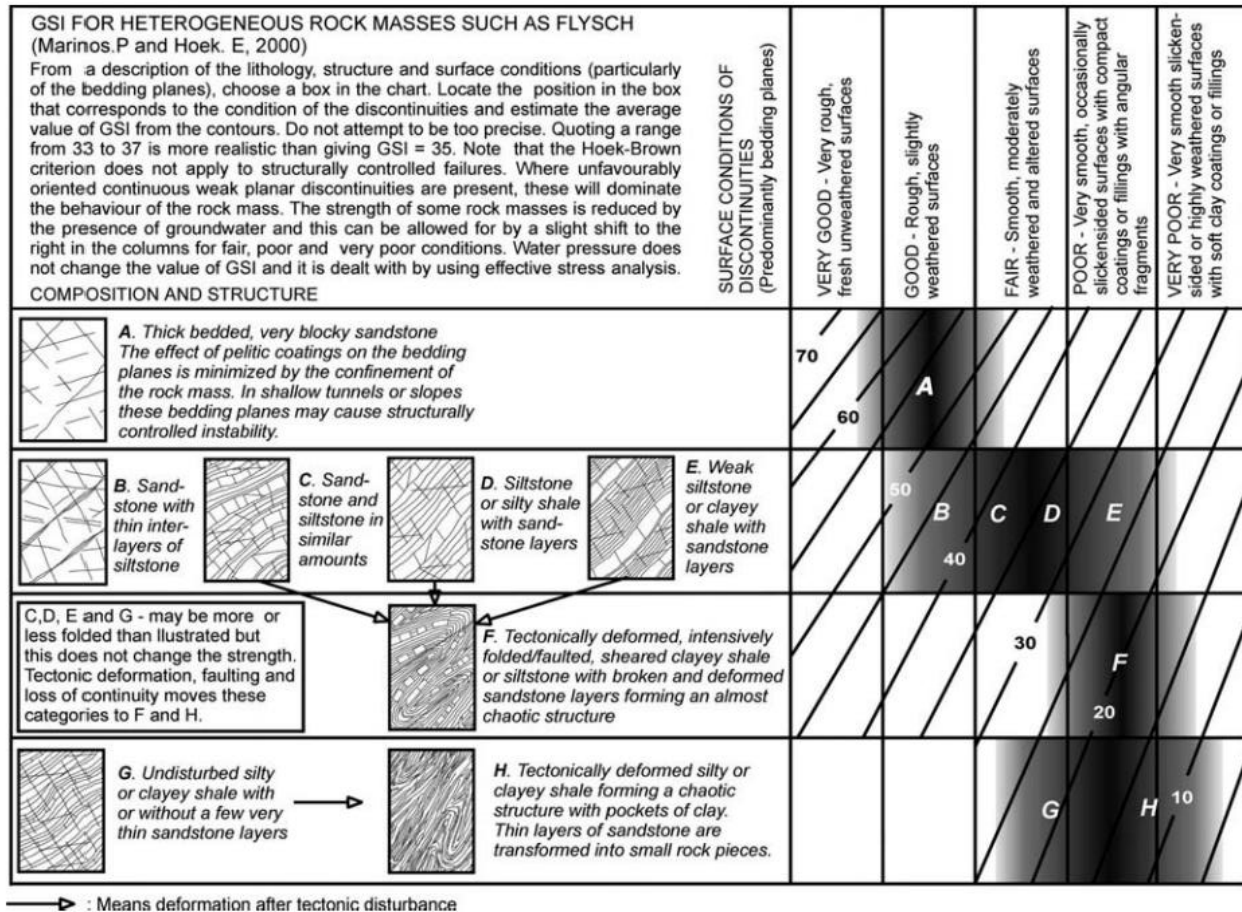


Figure 2.6: *GSI* chart for heterogeneous rock masses (Marinos et al., 2005).

While *GSI* has evolved to include weaker and sheared, poorer quality rock masses it is not intended to be used as replacement for the RMR or Q-system (Marinos et al., 2005; Palmstrom and Broch, 2006). As a result there is a need for a rock mass classification system that is more focused on the main attributes considered to control behavior of individual rock mass types.

Presently the *GSI* assumes the rock mass is undisturbed and that in-situ or induced stresses and groundwater pressures are not considered. For this reason (Marinos et al., 2005) suggests that this system not be used in tectonically disturbed rock masses in which the structural fabric has been destroyed. This also applies to weathered or blast damaged faces which are likely to receive some degree of disturbance upon the rock mass exposure (Cook, 2001; Marinos et al., 2005; Stewart, 2007). The *GSI* is also based on the assumption that a rock mass behaves isotropically (Marinos et al., 2005). Therefore, it is clear that this system not be applied to those rock masses in which there is a clearly defined dominant structural orientation. However,

Marinos et al. (2005) states that if the anisotropy does not control stability of rock masses then the *GSI* may be applied with caution.

2.7 Summary

This chapter presented an introduction to the geological context of the Torlesse Composite Terrane in the Wellington region. A description of the geologic and tectonic evolution was discussed and then related to the present day structural characteristics of the rock mass. Further description on the vast range of engineering geological conditions likely to be encountered at individual field investigation sites was included. Several rock mass classification methods were later summarized for the purpose of discussing how each classification utilizes different rock mass properties to predict specific rock mass characteristics. All of this information provides critical insight into the philosophy of the approach used within this thesis.

CHAPTER THREE SITE CHARACTERISATION

This chapter is subdivided into two parts: the first part deals with defining the terminology adopted for this study. The second part assesses the observed trends of these features through desktop study information, field mapping and stereonet analysis. This combined with the conceptual models, and portrayed rock mass character and conditions are used to derive the main characteristics at each site. Understanding what controls each rock mass is crucial for highlighting key relationships and information that will inevitably feed into a classification system.

3.1 Terminology Adopted

In this study overall outcrop descriptions were recorded using the NZGS (2005) field guide. However, a lack of descriptive defect terminology in the NZGS required other information derived from internal documents from such as PSM (2010a, 2010b), after ISRM (1978) to be applied. Therefore a discussion defining the adopted terminology is required.

The adopted methods used enabled the assessment of various defect parameters such as type, infilling, shape, continuity and the defect end termination nature. While roughness is recorded in the NZGS (2005) a different approach adopted from PSM (2010b) was used in order for more efficient field mapping. It is important to note

3.1.1 Defect Type

The general term for a defect refers to the plane of separation or weakness in a rock mass (Cook, 2001; González de Vallejo and Ferrer, 2011; ISRM, 1978). In the field these features can obtain a number of varying geological characteristics (Defect width, Persistence etc.), hence the need to establish the range of defect types observed across all the rock mass types (Table 3.1).

Table 3.1: Defect type descriptions and terms, adapted from ISRM (1978) and PSM (2010a, 2010b).

Code	Description
FL	Fault – a fracture along which displacement is observed, generally refers to large scale shears
SR	Shear- A fracture along which movement has taken place but may not be recognisable.
SH	Shear zone – Zone along a shear surfaces which concentrates strain resulting in a greater degree of deformation than the surrounding rock.
CZ	Crush zone – zone of roughly parallel, planar boundaries containing disoriented usually angular rock fragments of variable sizes in a soil matrix.
JN	Joint – A natural break of geological origin in a rock mass along which there has been no visible displacement.
BG	Bedding parting or fabric – Where a change in lithology upon which beds break up the homogeneity of the rock mass.
BSH	Bedding plane shear – A shear along a bedding plane

In the Wellington region there is ample evidence of many of these structures forming from brittle and or ductile deformation mechanisms. Despite the presence of ductile deformation, brittle deformation is the mode that is mainly observed. This is primarily due to the fault dominated structural environment of the Wellington region.

Previously stated in Chapter 2 is that defects can be grouped based on whether they are systematic or sub-systematic. The systematic defects are more persistent structures that occur in well-defined sets. It are these structures that are seen by many (AECOM and PSM, 2015; Cammack et al., 2018; Grant-Taylor, 1964; Hoek, 2007; Riddolls and Perrin, 1975) to be the main control largely governing global stability in the Torlesse. The term global is used to describe large scale exposures or engineering rock slopes. Both groups of defects are anticipated to control local scale mechanisms. The nature and behaviour of the systematic defects are assumed to be influenced by the district to regional scale geological structure.

3.1.2 Defect Infilling

As stated in Section 1.4 defect infilling consists of the material that separates adjacent defect walls. The infill may be soil, brecciated material, other minerals, and or a combination of all three. Typical infill descriptions record a wide range of physical characteristics which are mostly based on terminology derived from the NZGS (2005). These include grainsize, angularity, plasticity, strength of the material and weathering. Other internal documents from (Jones, 2014; PSM, 2010a, b) describe infill coating and rock fragment percentages along with their associated brecciated term (Table 3.3). A small comment on the precipitated mineralisation is also included. The infill description sequence is given below in Table 3.2 the whole sequence is written in lower case and separated by commas except where brackets and semicolons are indicated.

Table 3.2: Sequence of the infill terms.

Infill support	
(Brecciated type	
(Percentage of rock fragments %)	
Angularity of rock fragments	} Describes Clasts < 2 mm
Weathering of rock fragments	
Strength of rock fragments	
Coating;	
Colour	
Grainsize of the soil	} Describes Soil > 2 mm
Strength of soil	
Plasticity)	
Comment on precipitated mineralisation	

Table 3.3: Specific terms adopted for the recording of brecciated material among rock fragment percentages and defect coating descriptions (Jones, 2014; PSM, 2010a, b)

Infill support	Brecciated type	Percentage of rock fragments (>2mm)	Coating	
			Term	Description
Clast	Rock	99-100 %	Clean	No visible coating or staining
	Crackle	75-98%	Stain	Rock mass discoloured but no coating
Matrix	Mosaic	50-75%		
	Chaotic	30-49%	Veneer	Staining thinly coated
	Soil	< 30%	Coating	A visible coating > 1 mm thick.

3.1.3 Defect Shape

The shape of a defect refers to its surface waviness recorded over the trace length visible in an exposure or single bench. Shape can be described using common descriptive terms (Table 3.4) as well as by collecting measurements of inter-limb angles (ILA°) (Table 3.5) and wavelengths (λ) (PSM, 2010a). In this study a combination of all three has been collected. Where the overall defect shape is determined to be stepped, irregular or inaccessible, wavelength and ILA was left blank. If the shape is planar then the wavelength is the sole value left blank.

Table 3.4: Specific terms adopted for Defect shape with related illustrations (PSM, 2010a).






Term	Illustration
Planar	
Stepped	
Curved	
Wavy	
Irregular	

Table 3.5: Specific codes adopted for Inter-limb angle (PSM, 2010a, b).

Inter-limb angle (°)	Code
180 – 120	Gentle
120 – 70	Open
70 – 30	Close
30 – 0	Tight
0	Isoclinal

3.1.4 Defect Roughness

Five categories are used to describe the roughness of a defect surface as described in Table 3.6. Generally roughness can be characterised by the waviness of the defect walls. This is different from defect shape which looks at the waviness across the entire defect trace length.

Table 3.6: Specific codes adopted for defect roughness (PSM, 2010b).

Code	Description	
Ro1	Polished/ Slickensided	Very smooth, reflects light
Ro2	Smooth	Roughness not detected with finger
Ro3	Defined ridges	Sandpaper feel (fine to medium sandpaper)
Ro4	Small steps	Sandpaper feel (medium to coarse sandpaper)
Ro5	Very rough	Very well defined ridges and/or steps

3.1.5 Defect Continuity and Termination

The continuity and way in which a defect ends is adopted from PSM (2010a). Defect continuity is measured over the visible surface trace from one termination (end) to the other in natural slopes, or over a single bench in engineered slopes. Continuity is distinguished in three ways whereas the nature of the termination was distinguished in five, (Table 3.7).

Table 3.7: Specific codes adopted for defect continuity and end termination nature (PSM, 2010a).

Continuity		Terminations	
0	No ends visible	R	Terminates in Rock
1	1 end visible	D	Terminates against another defect
2	Both ends visible	S	Splits/Divaricated into multiple defects
		C	Continuous
		O	Obscured by debris, vegetation etc.

3.1.6 Folding

The Wellington region displays a variety of fold styles ranging in wavelengths from centimetres to hundreds of metres. In this study mesoscopic folds are defined as those recognisable at the outcrop scale and having wavelengths from centimetres to a few metres. Megascopic folds are generally visible from vertical aerial photographs (1:1500 scale) and have wavelengths that range from metres to 10's of metres. Map scale folds are larger and have wavelengths ranging from 100's of metres to kilometres (Suneson, 1992) (Table 3.8). Due to the limited range of exposed outcrops and scale of the map scale folds these folds are often difficult to identify in the field. The larger map scale folds also tends to be more open and can be identified where dip direction measurements change over some distance whereas, isoclinal and tight folding can only

be detected within outcrops. All other fold terminology follows commonly accepted terms (Twiss and Moores, 1992).

Table 3.8: Scale of folding determined by Suneson (1993, 1992).

Suneson (1993, 1992)Term	Scale	
	Visibility	Wavelengths
Mesoscopic	Outcrop	Centimetres to a few metres
Megascopic	Outcrop and aerial photographs (1:1500)	Metres to 10's of metres
Map scale	Aerial photographs and regional mapping	100's of metres to kilometres

The complexity of the structure in the Wellington region shows that the geometry of the rock mass is the result of more than one deformation event. These folds are referred to in literature as superposed folding (Suneson, 1992; Twiss and Moores, 1992), where **first generation** folding is refolded by the **second generation** and by all subsequent generations. The basic patterns of the orientations of fold hinges and axial surfaces of these generations generally result in superposition (Figure 3.1). Given that there are three different scales of folding identified from literature (Suneson, 1993, 1992) is likely that there may be three inherent generations of folding seen at each site. Map scale folding is the likely equivalent of **third generation** folding, megascopic folding is likely second generation, and mesoscopic folding is most likely first generation folds. This understanding implies that all generations developed at the same time everywhere, however, it is important to remember that this is not necessarily the case. Therefore at each study site the generation terms will be used to describe scale rather than chronological phases. This is also due to the high possibility that in areas where there is a high degree of shearing and faulting it is likely that folding may be overprinted. Where it is applicable to a specific study area a comparison will be made that comments on the relative age of the different scales of folding.

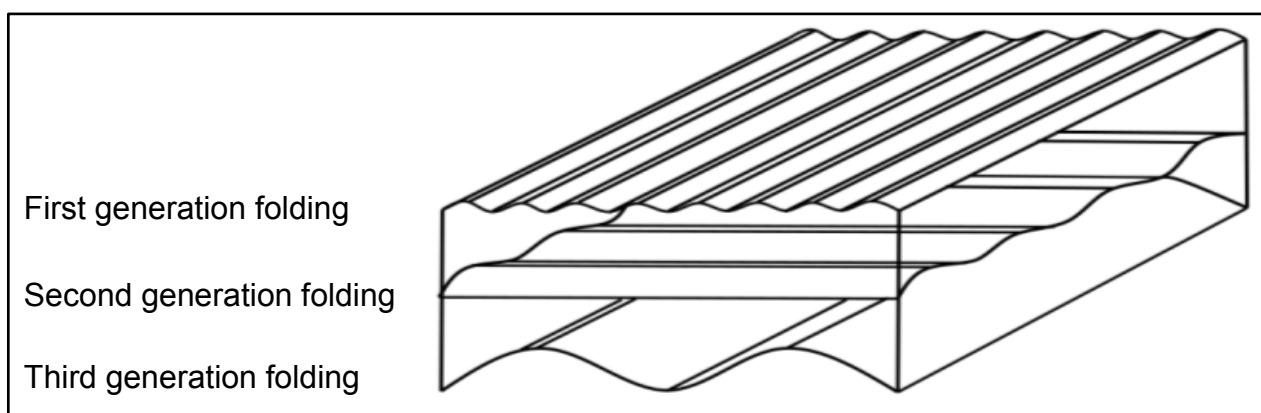


Figure 3.1: Drawing displaying the different scales and patterns associated with superimposed folding, interpretation taken from past literature (Suneson, 1992).

Table 3.9: Relationship between Suneson (1993, 1992) and Twiss and Moores (1992) folding terminology using wavelengths

Suneson (1992,1993) definition	Twiss and Moores (1992) Fold generations	Wavelength scale
Mesosopic	First	Centimetres to a few metres
Megascopic	Second	Metres to tens of metres
Map scale	Third	Hundreds of metres to kilometres

3.2 Rock Mass Site Characterisation

The following section shows observed trends through desktop study information and field mapping. Conceptual models and stereonet analysis are paired with the observed rock mass character to gather an understanding of the rock mass characteristics at each individual site. Full results are reproduced in Appendices A to G and are used to support findings.

3.2.1 Transmission Gully North

The following section describes the Transmission Gully North site characteristics.

Conceptual Model

The conceptual model can be seen in Appendix A.1 it states that the rock mass structure is heavily controlled by the active northeast striking Ohariu Fault and the Ohariu Splinter Fault, which transects this site. Strain is accommodated by a releasing bend where the Ohariu Fault steps over into the Horokiri valley, placing a part of this area into an extensional setting. The releasing bend is expected to transfer stress onto third order east-west oriented structures where it is anticipated to contribute to a high degree of dip slip movement. It is expected that the close proximity of the Ohariu Fault would cause a large volume of the Torlesse rock to be heavily sheared and fractured. Using this knowledge bedding and shearing is anticipated to strike sub-parallel to parallel to the NE/SW trending structures.

Rock Mass

Engineering geological mapping in the Transmission Gully North site identified Suneson (1993) Lithofacies Group B as the most dominant, along with the less common Lithofacies Group C. Other characterisation includes Cammack et al. (2018) “Fault Disturbed” Regime C, through to “Fault Crush” Regime D.

The presence of major faulting (Ohariu Fault) through the site has a large influence on the rock mass condition, particularly with shearing. The most influencing effect is that the closely spaced defects are not restricted to any particular bed. Further influences include a well-developed fault damage zone (high to very high degree of rock fracturing and a presence of a wide clay rich gouge zone) adjacent to the main Ohariu Fault trace. This clay rich zone appears to act as an

impermeable zone for which water cannot cross resulting in large volumes of groundwater escaping through the highly disturbed torlesse material above (Figure 3.2). Cross-cutting relationships are therefore apparent and roughly occur every metre or two, with spacing increasing as distance from the Ohariu Fault also increases.

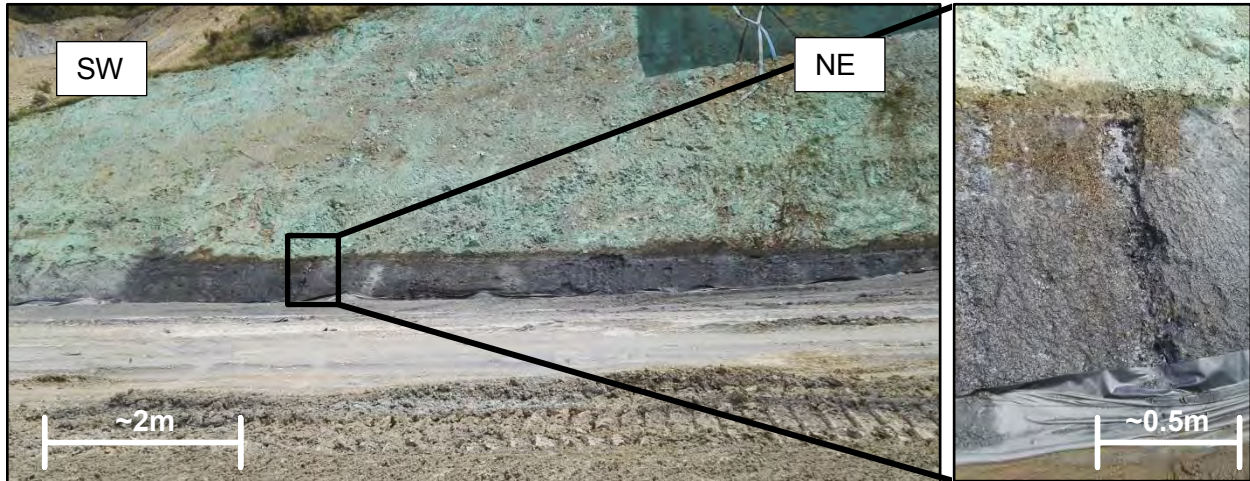


Figure 3.2: Photographs of the groundwater flow escaping above the fault trace.

Both brittle and ductile deformation is evident. Brittle behaviour is typified fractures or faults, while ductile behaviour appears as folding (Figure 3.3). Large faulting is exposed in this section continuing for ≥ 25 m. These structures are likely to be splays, trending roughly east-west. Bedding is mostly moderately thick too thick in sandstone and thin to moderately thin in mudstone. The sandstone was assessed as moderately strong as it could be fractured with a blow of a hammer whereas, the mudstone was assessed as weak. The rock mass is moderately weathered with highly weathered material exposure in the top 5 m of the north bound cuts (C5c.01 NB, See Figure 4.2). This is evident by the change in colour, from light grey to light brown, and a significant drop in strength from a fresh rock face. Jointing is closely to very closely spaced with very low persistence that tends to generate a very disturbed looking characteristic. The condition of the rock mass is therefore assessed as poor, with the sandstone member in vaguely better condition.



Figure 3.3: Photograph and sketch of a major cut in the Transmission Gully North study site. Photo taken 20th of March 2018 before shotcrete and other remedial measures were used to stabilise the darker fault crush material. The black dashed lines show bedding. The red are faults.

A range of different styles of folding has been identified. Figure 3.4 displays two different modes of folding in second generation folds; flexural and fault-propagation. Folding is observed to be symmetrical with wavelength scales roughly between 5-7 m. Shape of bedding overall is mostly wavy (Figure 3.5) with bedding dip appearing to flatten out towards the north. This is likely in response to the major fault first order faulting, as identified by the changing of structural domains in Appendix A.7. A total of five structural domains are identified in this site, A to E. All of these domains are bounded by mapped faults. First generation fold hinge lines are not exposed in this site. It is likely that the topographic high, described as the Wainui Saddle, is the result of convergence of the Ohariu Fault and the Splinter Fault, much like what is displayed in Figure 3.4 but over a larger scale. Third generation folds are likely to be overprinted due to the close proximity of the Ohariu Fault.

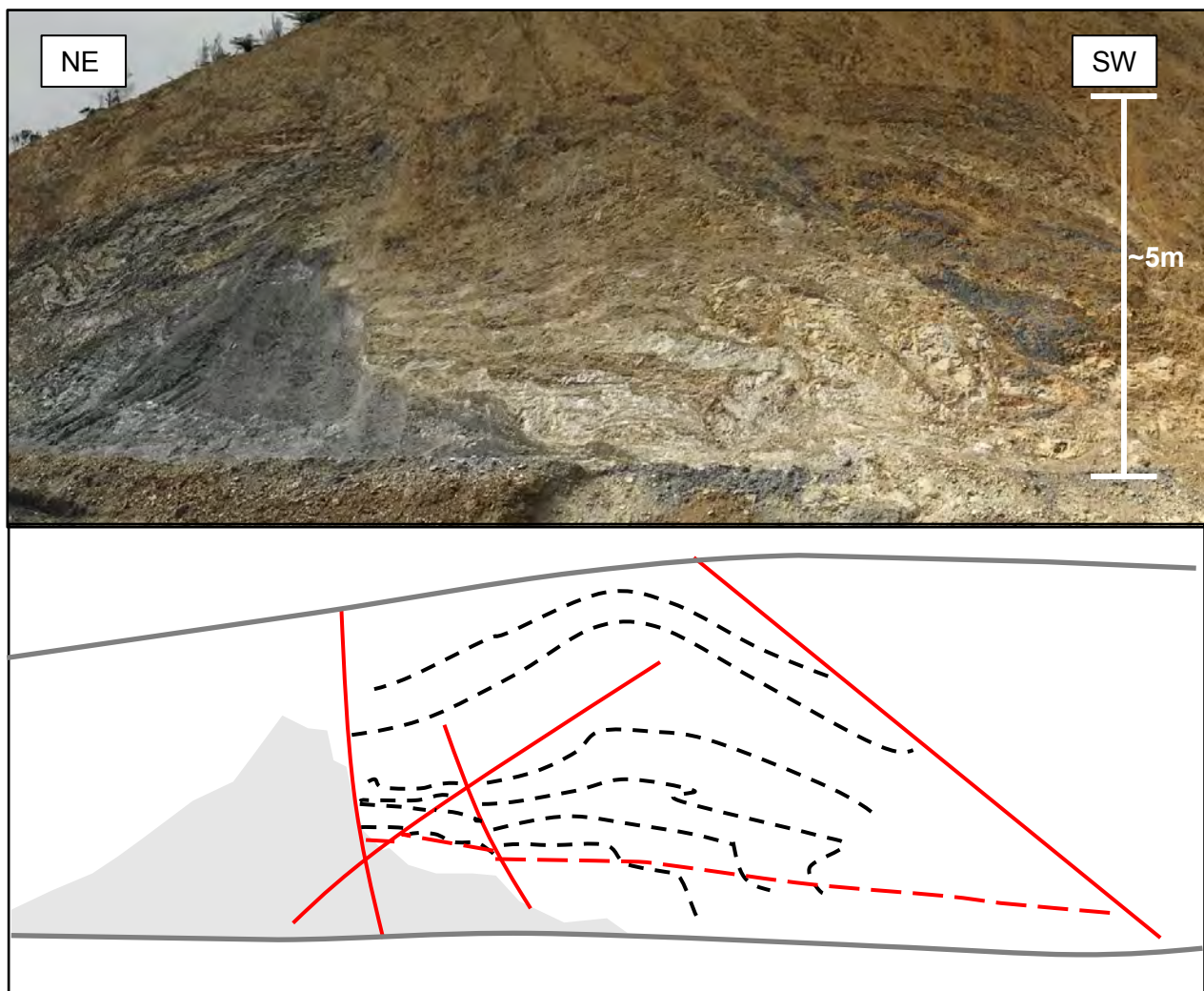


Figure 3.4: Flexure of bedding (black dashed lines), faulting (red) resulting in localising folding in the top of the cut. Shearing is presented by the red dashed line influencing folding such that bedding is thrust up producing fault propagation folding in the lower half of the cut. Light grey area indicates fault crush material.

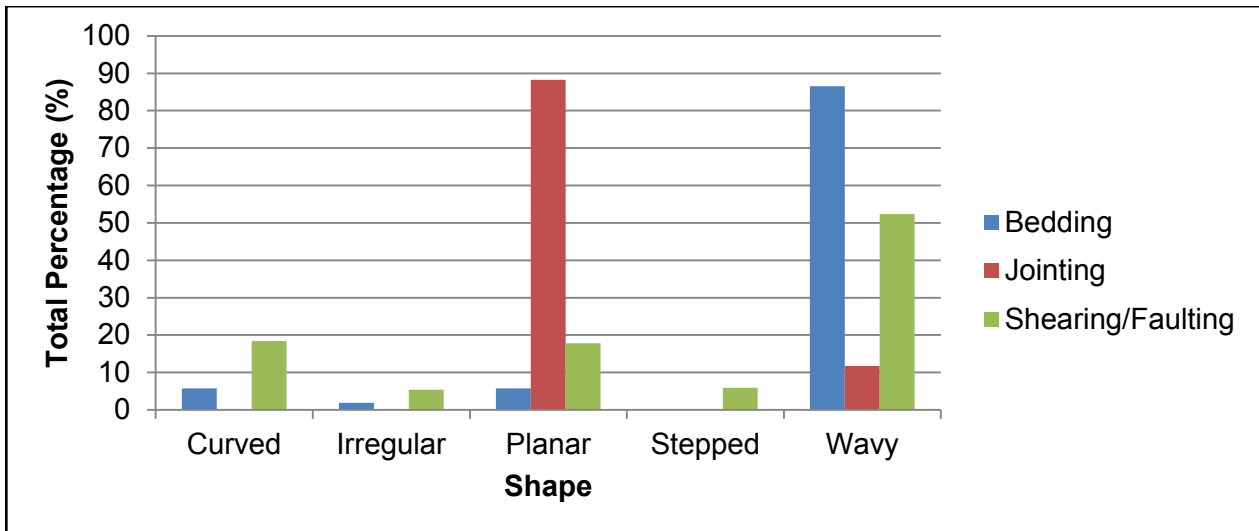


Figure 3.5: Graph displaying the total percentage of defects shape in the Transmission Gully North study site.

Discontinuity Condition

Defect infilling is dominated by rock fragments (Figure 3.6) within mostly wavy defects. Bedding appears to be the least planar of all the defects with inter-limb angles decreasing as wavelengths trend towards higher values. Alternatively, shearing trends towards more linear defect shapes at higher wavelengths (Figure 3.7). This is evident in faulting structures where over individual benches these features appear to be the more planar features (Figure 3.5). However, over multiple benches (Figure 3.3) faulting can be seen to take on more of a curve, bending more as the trace tends towards the topographic surface passing through increasingly weathered material.

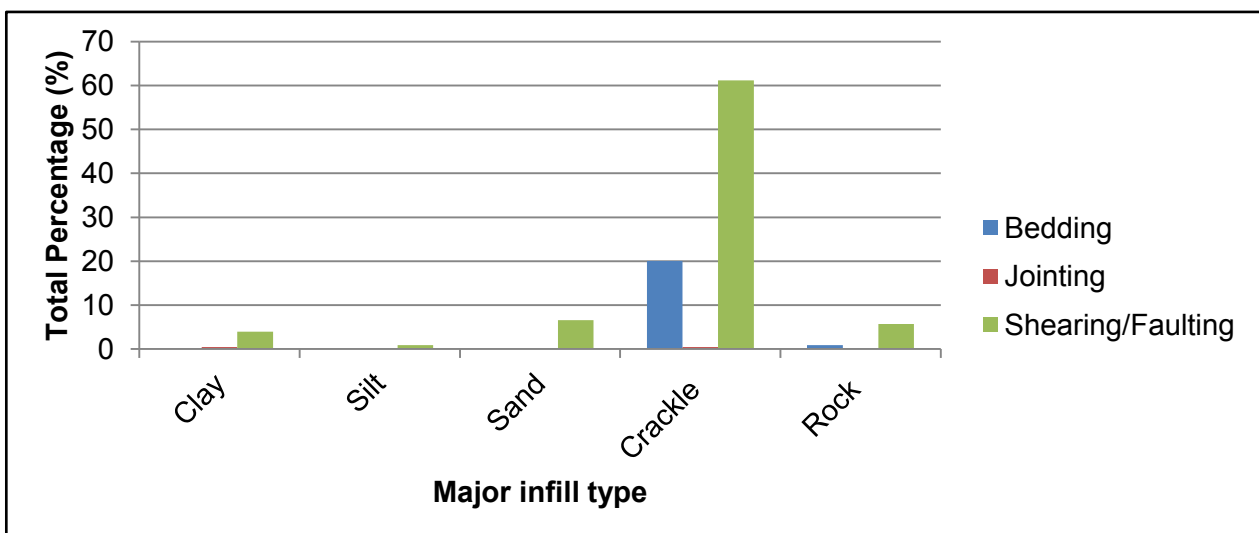


Figure 3.6: Graph displaying the total percentage of the different major fraction infill types for defects recorded in the Transmission Gully north study site.

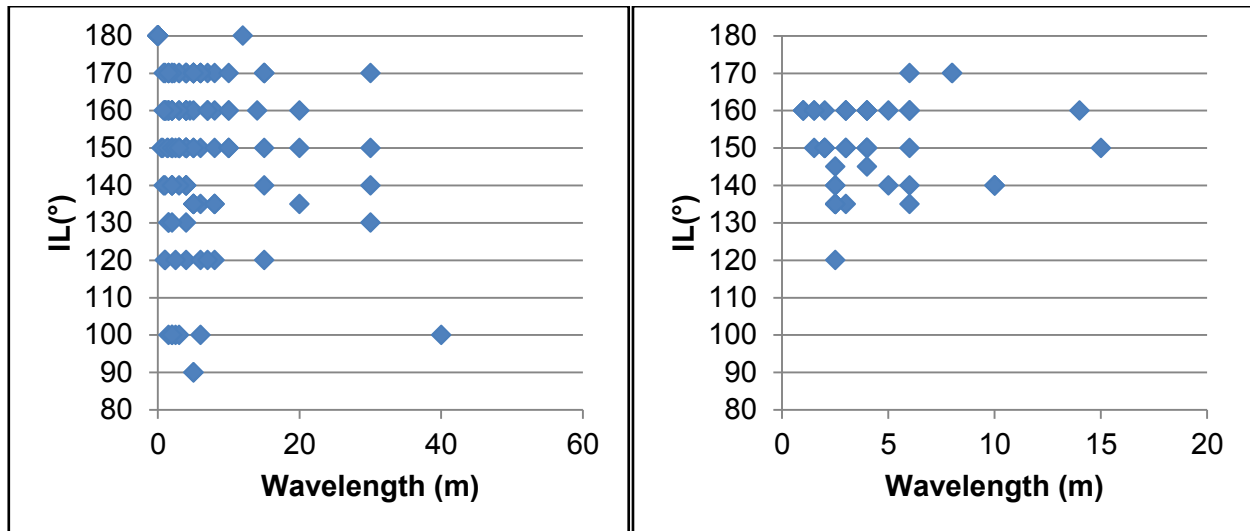


Figure 3.7: Graphs displaying the Transmission Gully North Shearing (Left) and Bedding (Right) waviness.

The average roughness of defects is Ro3 with an average width between 60 mm and 200 mm (NZGS (2005) - Wide) (Figures 3.8 and 3.9 respectively). Defect infill material in these structures is mainly comprised of weathered moderately strong or weak rock fragments surrounded by mostly sand sized grains. Rarely is the infill observed as clean or stained due to a lack of groundwater flow in the upper benches.

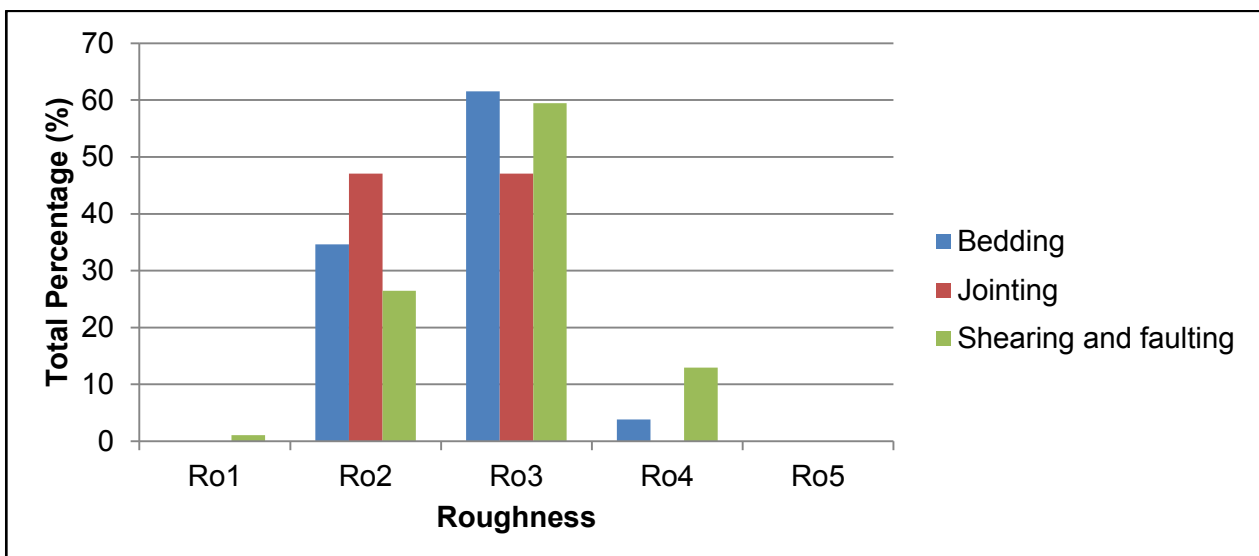


Figure 3.8: Graph displaying the defect roughness in the Transmission Gully North site.

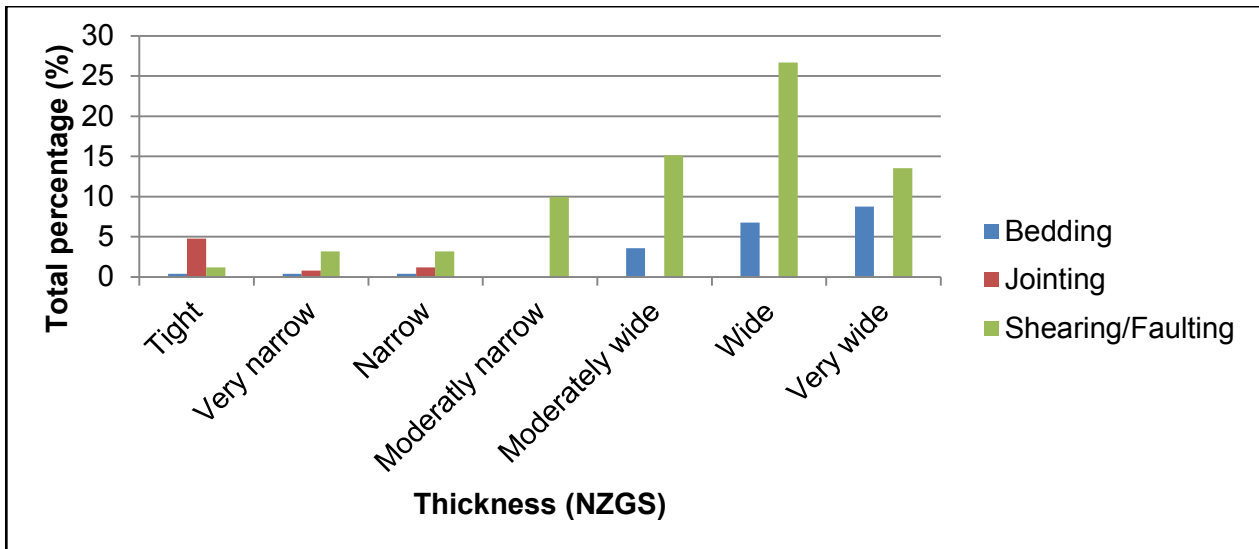


Figure 3.9: Graph displaying the total percentage of defect thickness, using the NZGS (2005) rock thickness terms, in the Transmission Gully North study site.

Stereonet Analysis

Stereoplots representing bedding and shearing orientations are collected in Appendix A.6. Distribution of the bedding and bedding plane shear poles appear to cluster mostly in the northern half of the stereonet, between 250° to 70° , striking roughly parallel with the west-east trending third order regional structures. Westward rotation of bedding across the site towards the north is observed and is seen in the contour diagram in Figure 3.10. This suggests that folding is present which corresponds with mapping observations. π -girdle best fit lines drawn on stereoplots (Figure 3.10) indicate that there are three potential fold orientations, two more than what was identified from field observations. The three folds are labelled F1, F2 and F3 and appear to conform to an echelon pattern (Figure 3.11). F1 when compared against the local topography and field data likely indicate third generation folding consisting of a wavelength that is likely to be around a kilometre wide. Despite this no visible hinge line is observed and so no formal inference can be made on the presence of third generation folding.

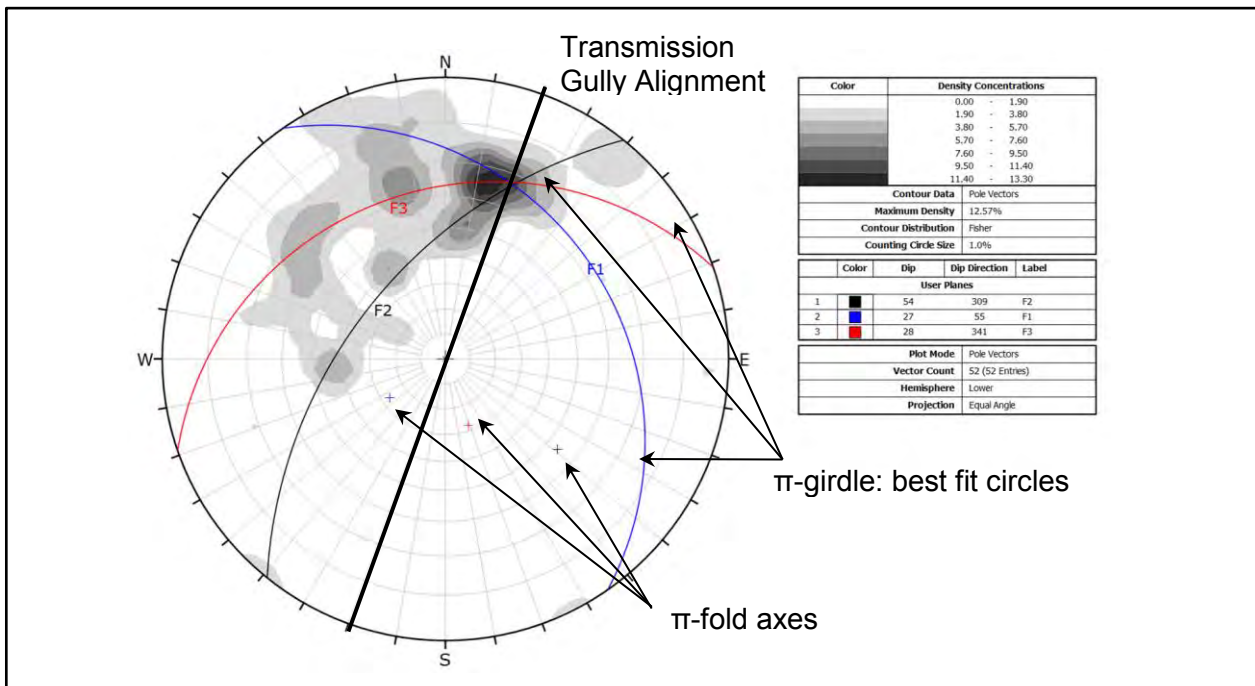


Figure 3.10: Contour diagram of bedding data for Transmission Gully North.

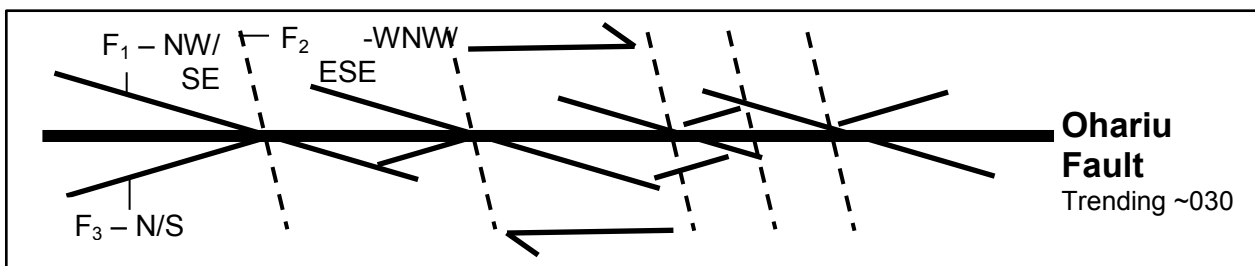


Figure 3.11: Orientation arrangement of different generations of Folds associated with the Ohariu Fault. Figure 3.10 adapted from Twiss and Moores (1992)) subsidiary R, R', and P shear fracture arrangement model.

Shearing stereoplots present an issue in regard to 'noise'. This required 'filtering' of the data so that only those defects that displayed lengths equal to or greater than the bench heights were visible. The result was that two vaguely defined conjugate defect sets that appear to be consistent across the hanging and footwall of the Ohariu Fault trace. Generally these conjugate sets tend to strike northwest-southeast and northeast-southwest, subparallel with the Ohariu Fault trace and roughly perpendicular.

3.2.2 Transmission Gully South

The following section describes the Transmission Gully South site characteristics.

Conceptual Model

The conceptual model for this site is located in Appendix B.1. Interpretations state that the rock mass structure is influenced by the Ohariu and Moonshine Fault converging towards the southwest. High angle cross faulting link these major faults and are likely accommodating and

transferring the regional tectonic stresses. A restraining bend on first order structures which is located within the site indicates that the immediate area is in convergence. Elastic strain is also accommodated by the cross faults due to the convergence of the major first order faults. This resulted in multiple fault bounded blocks, which appear to rotate anticlockwise as a means of accommodating this strain.

The distance from the controlling major faults is much more significant than what is observed in the northern study area. Despite the increased distance the close proximity of first order structures still appears to dissect the site. This means that shearing of any kind is un-avoidable. Using this knowledge bedding and shearing is anticipated to trend sub-parallel to parallel with the major northeast trending structures. Rotation of these features anticlockwise is likely in response to intra block rotation.

Rock Mass

Suneson (1993) Lithofacies Group B is the most dominant along with the less common Lithofacies Group C. Material is dominantly "Fault Disturbed" Regime C, with small occurrences of "Fault Crush" (Cammack et al., 2018).

Mapping has identified a number of large continuous fault structures (~30 m) striking northwest-southeast (Figure 3.12). A small volume of fault crush is observed directly adjacent to these structures which increases in width as depth also increases. These structures are likely to be third order faults due to their orientation. The increased distance from major faulting, relative to the Transmission Gully North area, seems to have a good effect on the rock mass condition. Defect spacing appears to have an increased to moderately widely to widely spaced with terminations mostly occurring against mudstone-sandstone contacts. The more persistent defects are mostly observed within the sandstone unit. Despite the relatively increased condition of the rock mass it is still highly fractured with smaller scale shearing observed to terminate against the more continuous, planar features. Cross-cutting of shears was also observed, occurring roughly every 2 m in sandstone units.

Bedding is mostly steeply to very steeply inclined with thick to very thickly bedded sandstone, and thinly bedded mudstone units. The sandstone member is assessed as slightly stronger than the mudstone, moderately strong in sandstone versus weak in mudstone. Bedding and bedding plane shears are occasionally observed to terminate against shears and faults. Jointing is closely spaced and obtains a low persistence (~0.15 m). This results in a moderately fractured to fractured rock mass that is also considered to be moderately weathered with highly weathered material exposed in the top few metres of the cut. There is no presence of groundwater. The condition of the rock mass is therefore assessed as mostly poor, with the sandstone member in vaguely better condition than the mudstone.

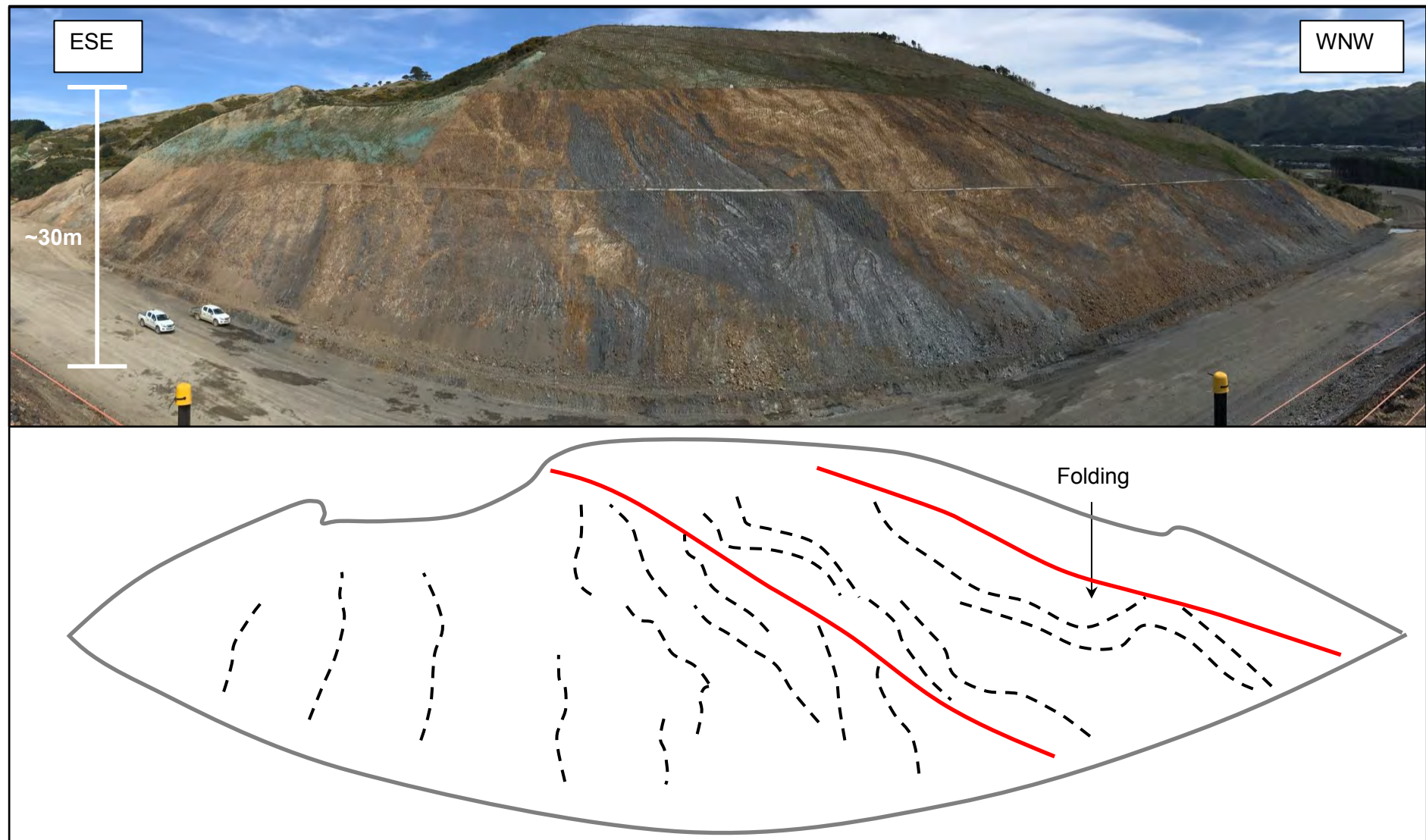


Figure 3.12: Photograph of a major cut in the Transmission Gully South study site looking south west. Photo taken 21th of March 2018 before remedial measures were implemented. Bending of bedding (dashed black lines) in response to faulting (red lines) can be observed.

Mapping only identified second generation folding due to a lack of visible hinge lines. Geometries of these folds are interpreted to be asymmetrical as bedding thicknesses vary over the wavelength distance. It is possible that these may be parasitic, Z folds given their orientation and shape. First generation folding is likely to be overprinted.

A total of five structural domains are identified in this site, A to E. All of these domains are bounded by mapped faults.

Discontinuity Condition

Defect infill is mostly comprised of crackle and rock type material within generally wide fracture or shearing surfaces. The strength of this material is typically weak to moderately strong and surrounded by soft sand or a clay matrix. Defect shape appears to behave similarly to TG North despite an increased proportion of planar shears or faults (Figure 3.13). Bedding is typically still observed to be gently undulating while faults and shears appear to increase waviness with increasing wavelengths (Figure 3.14). Average surface roughness is still Ro3 with no trend evident between roughness and defect type. Defects are dry and are clean or rarely stained. Faults and shears comprising clay material tend to exhibit slight plastic behaviours were occasionally moist. This clay material was commonly found as fault gouge adjacent to fault traces and as lens in shear zones.

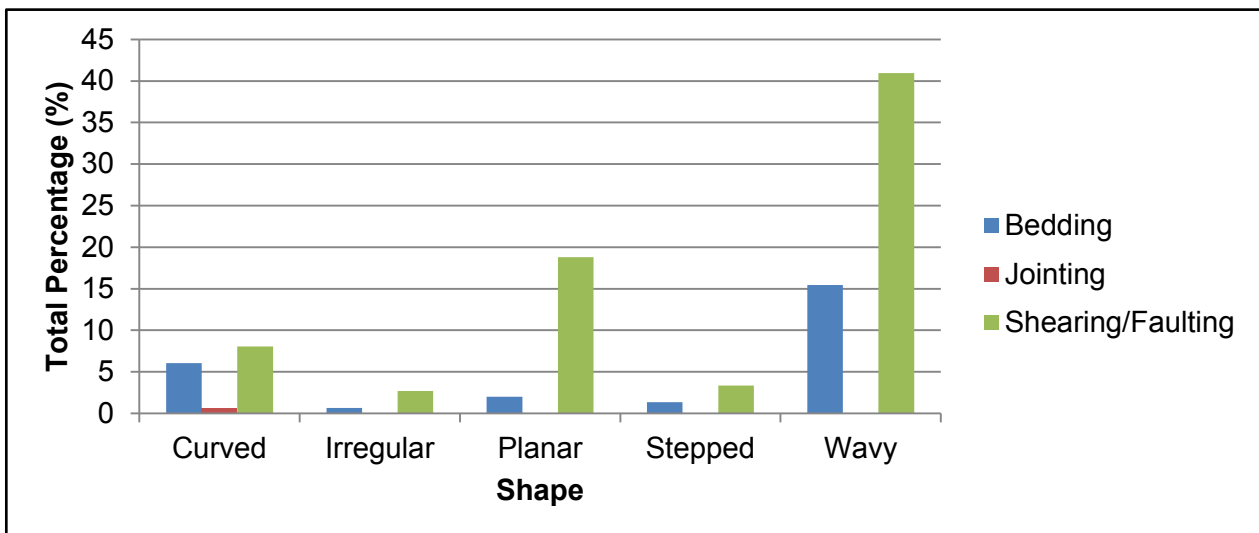


Figure 3.13: Graph displaying the total percentage of defect shape in Transmission Gully South.

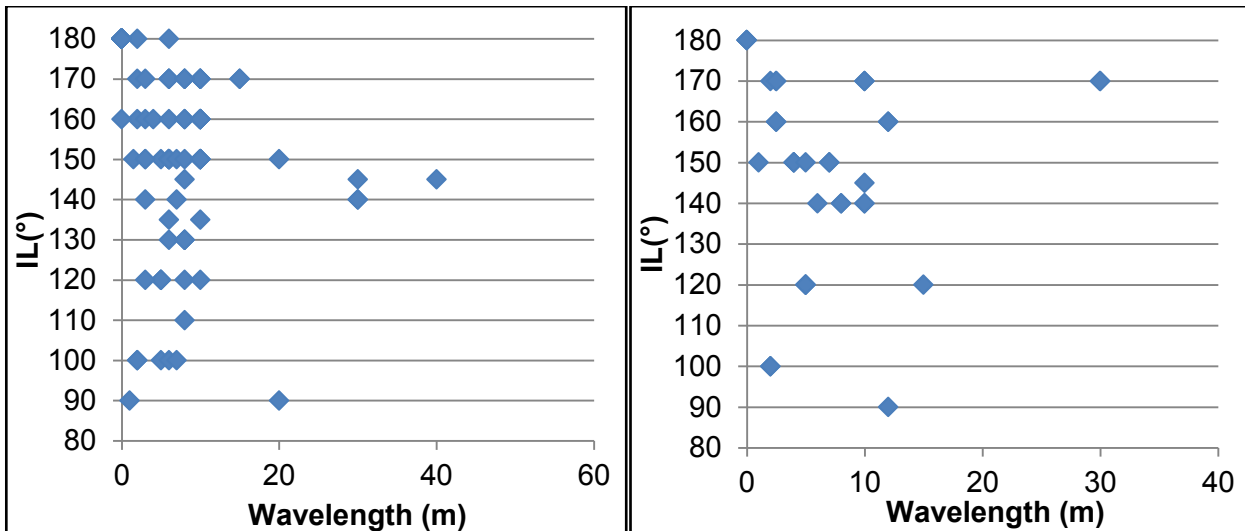


Figure 3.14: Graphs displaying the Transmission Gully South Shearing (Left) and Bedding (Right) waviness.

Stereonet Analysis

Stereoplots and contour diagrams for this site can be seen in Appendix B.6. These stereoplots display bedding poles that tend to form in two separate well defined clusters that are interpreted to rotate anticlockwise towards the east due to faulting. The two clusters examined appear to strike either north and south, or east and west. Overlap of shearing clusters indicates that shearing is antithetic with bedding, which is consistent throughout this site. Orientation of bedding and shearing tends to strike parallel to sub-parallel with the high angle cross faulting. Where bedding data does not follow this trend it seems to strikes sub-parallel to parallel with the third order faults that dissect (and mapped) in the area (Appendix B.7.2).

Shearing plots display similar scatter issues as seen in the Transmission Gully North site. Moderate scatter of these plots noted an issue in regard to 'noise' which resulted in 'filtering' the data in order to define distributions of shearing poles. The result was the two vaguely defined shearing clusters that appear to be antithetic with bedding.

Bedding and bedding plane shears distributed across this site appear to infer folding oriented roughly north-south and west-east (Figure 3.15). Since bedding is interpreted to rotate anticlockwise towards the west it is likely that the two folds identified are a part of same generation of folding. However, F1 and F2 display different fold geometries as indicated by the distribution of bedding poles on the π -girdle best-fit lines. F1 appears to have one long cluster whereas F2 is split into two separate bedding clusters, indicating that F1 is an open concentric fold and F2 is a gentle chevron fold. The geometry and orientation of the F1 seems to match the style of folding displayed in Figure 3.14, suggesting that these are possibly second generation folds. When F2 is compared to mapping data, specifically bedding orientations, F2 is more likely to be first generation. This interpretation corresponds with the trend that larger folds tend to be

more open whereas smaller fold tent to be more close and tight. However, a lack of visible first generation hinge lines means that no definitive orientation can be made.

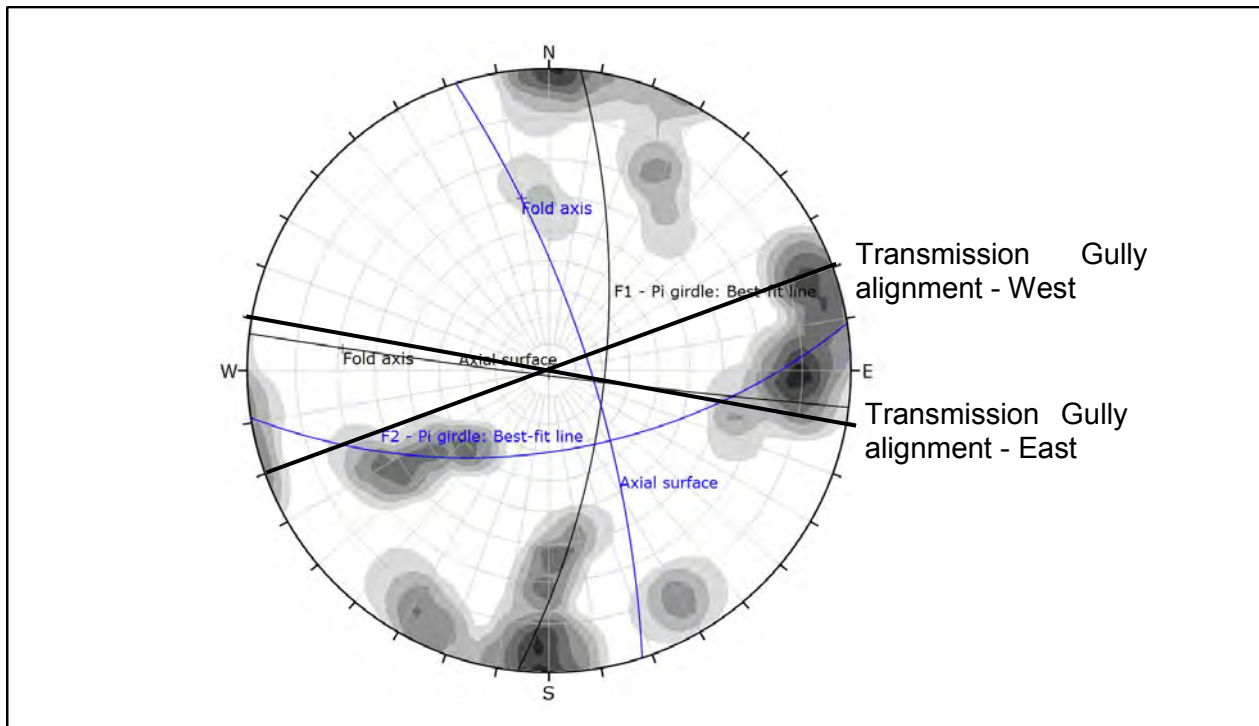


Figure 3.15: Contour plot of the bedding data for Transmission Gully South. Interpretation of potential folding is indicated by the black and blue pi-girdle lines.

3.2.3 Kapiti Quarry

The following section describes the Kapiti Quarry site characteristics.

Conceptual Model

The conceptual model displayed in Appendix C.1 shows that the major controls on rock mass structure in Kapiti Quarry is the Ohariu Fault. Interpretation of the Ohariu Fault geometry locates a releasing bend just south of this site, which is associated with normal faulting trending northwest-southeast. It is these NW-SE oriented second order structures that are likely accommodating the strain produced by the releasing bend. It is anticipated that this places Kapiti Quarry in an extensional setting. Bedding and shearing are therefore predicted to trend sub-parallel to the northwest-southeast oriented structures.

Rock Mass

Engineering geological mapping in the Kapiti Quarry site identified three (Suneson, 1993) Lithofacies Groups, labelled B, C and D. The most dominant is C, followed by B and then D. Of Cammack et al. (2018) characterisation, “Mudstone Influenced” Regime E is evident in association with “Fault Crush”, D, through to “Fault Disturbed”, C, zones.

Kapiti quarry displays a wide range of slightly weathered to unweathered Torlesse rock mass conditions. The rock mass condition at this site is assessed as poor to very poor. Mapping

identifies at least three faults transecting the site with associated fault crush material, including breccia and gouge, located adjacent to the fault traces. The rock mass is interpreted to be heavily sheared despite the increased distance from major fault traces, particularly when compared to what is observed in the Transmission Gully areas. It is suspected that the increase in mudstone content and the decrease in bedding spacing (noted from field mapping) is the most likely explanation for this. Mudstone is generally weaker than sandstone resulting in a fracture density increase. This leads to similar effects to what is observed in the Transmission Gully North area. Defects are generally not confined to a single bed with most terminations only against, or join up, with other larger defects or bedding (Figure 3.16). Therefore, bedding plane shearing is less distinct and more likely to consist of wider shear zones.

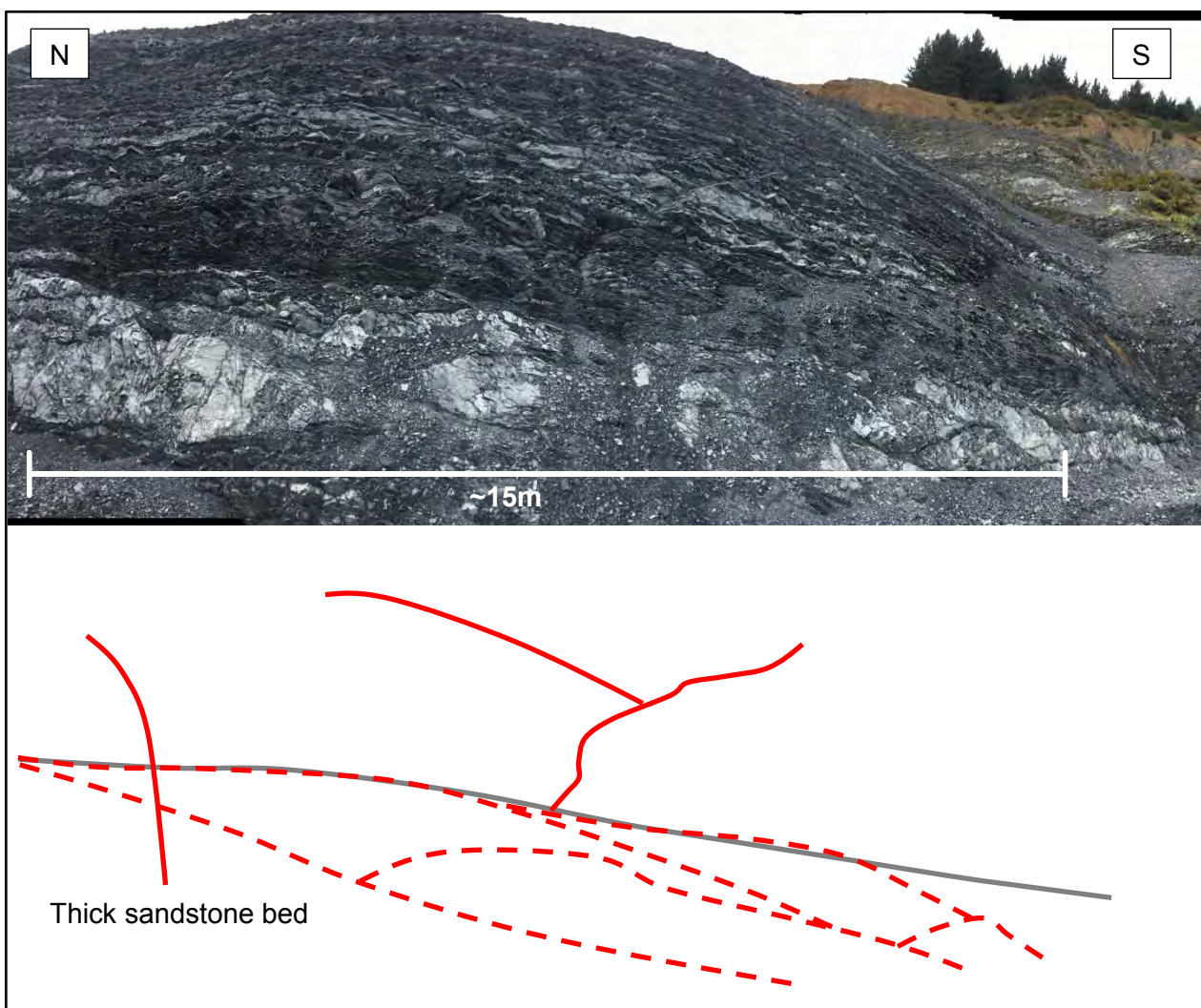


Figure 3.16: Shear zones (dashed red lines) within a thick sandstone bed. Contact between the extensively sheared mudstone rock mass and the thick sandstone bed (Grey line).

Persistence is generally low with those defects that are continuous tend to terminating against the rarer, stronger and thicker sandstone beds. Cross-cutting relationships are not well defined and less common with most occurrences only observed in Lithofacies B, with around a ~1.25 m

spacing (Figure 3.17). Shear zones are evident and appear to be continuous. These features tend to form sub-parallel with bedding and so are typically moderately inclined (Figure 3.16 and 17). Furthermore, thicknesses of alternating sandstone-mudstone beds are thinner in comparison to the TG sites, very thin to moderately thin bedding, with occasional thick sandstone beds (Figure 3.16). Sandstone intact rock mass strength is Strong to Very strong while mudstone is moderately strong to Strong. Jointing is typically discontinuous and very closely to closely spaced with clear surfaces only visible in the thick sandstone layers.

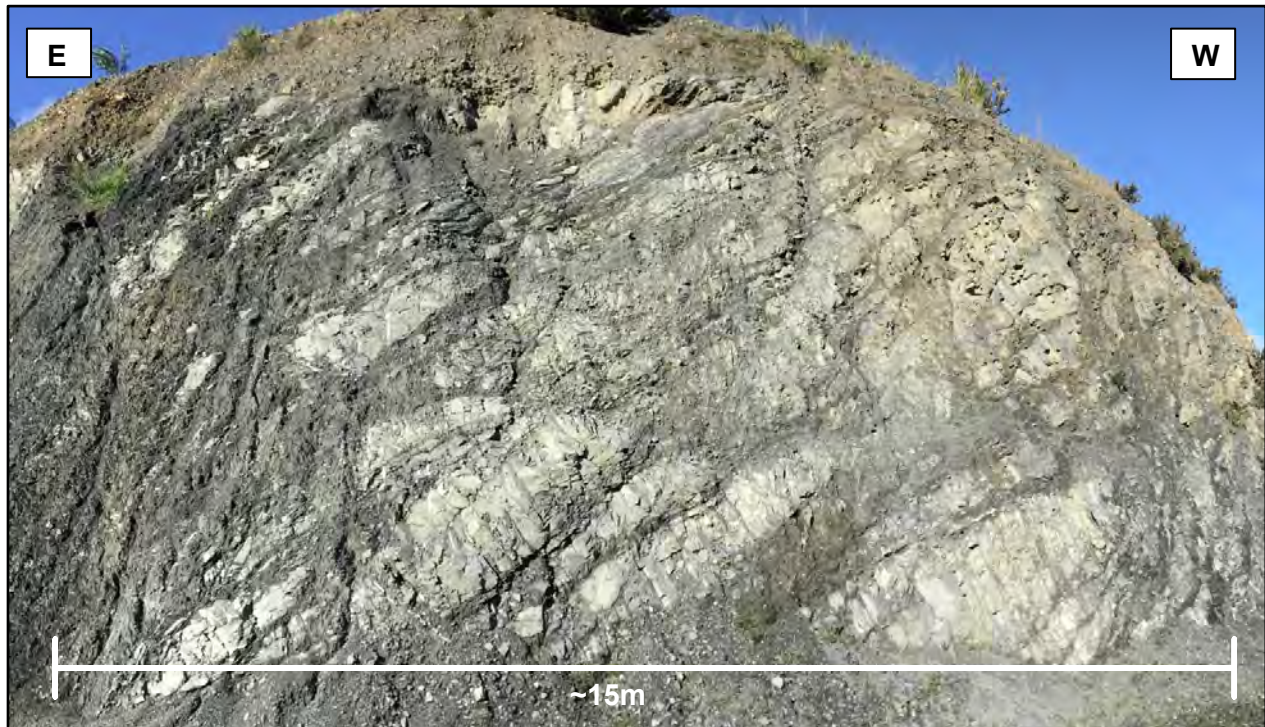


Figure 3.17: Photograph taken of mapping site 1. This area was mapped entirely as Lithofacies B.

Figure 3.18 indicates that there is a synclinal folding in Kapiti Quarry. Upon first inspection this was assumed to be a fault, however, bedding and shearing features remain fairly consistent across the assumed axial surface and appeared to only be offset by a 0.2 m wide sheared zone. Based on the scale of the synclinal wavelength it indicates that this is likely a first generation fold. Second generation folds appear to be the gently undulating nature of the bedding despite the vague visibility. Third generation folds are not visible and assumed to be overprinted.

Important to note is that there is water seepage that appears to form adjacent to fault traces and on the intersection of the observed syncline and shear zones. This can be observed in Figure 3.18 as indicated by the darker areas of the cut slopes with vegetation and orange brown iron staining. Water also seeps out on the contact between the mudstone and thicker sandstone units as well as through clay rich shear zones, which tend to form parallel to bedding and across thick fragmented mudstone bands.

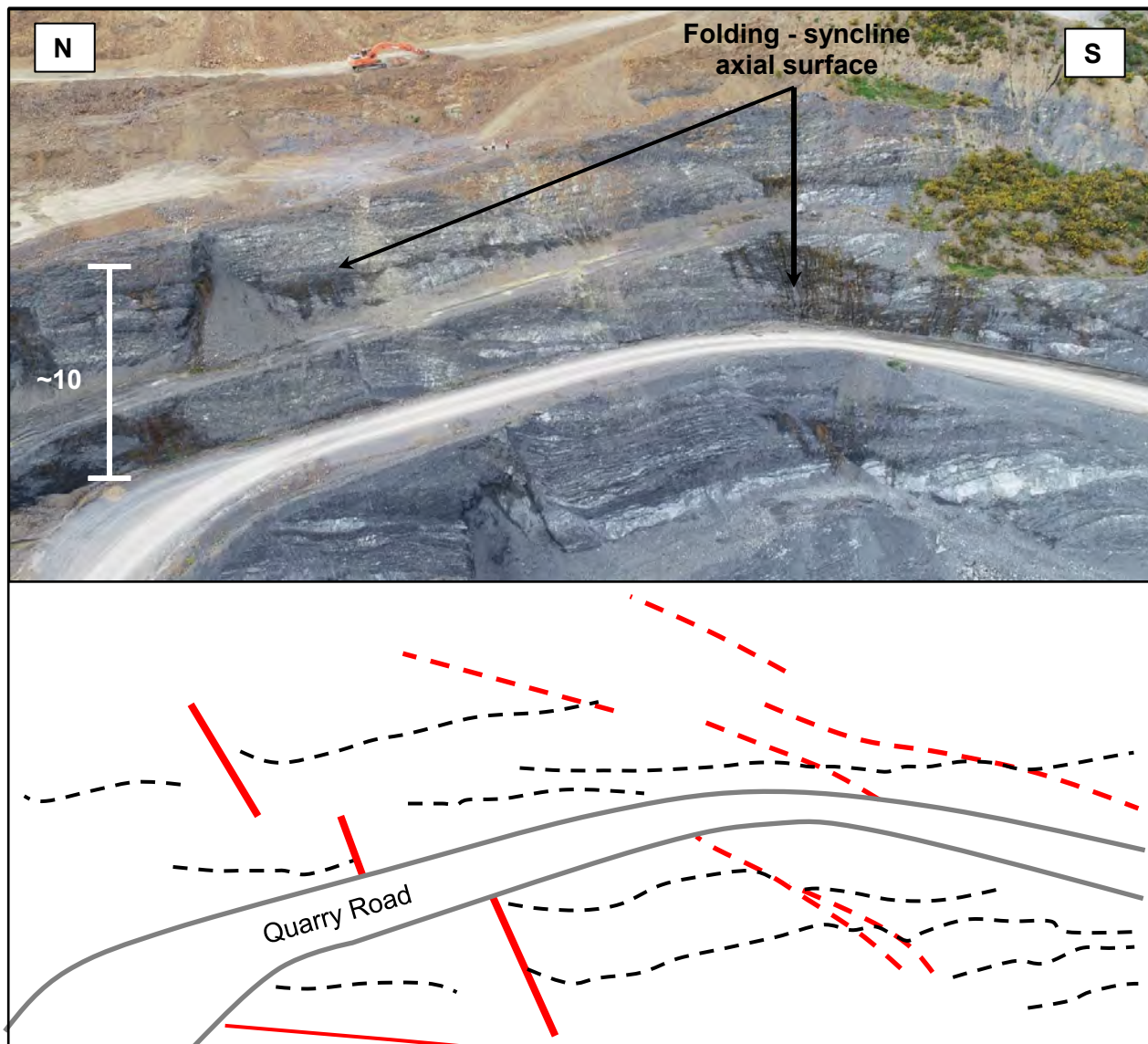


Figure 3.18: Photograph and sketch of Kapiti Quarry displaying the water seepage (darker areas) on fault lines (red line) and axial surfaces of the synclines. The water also escapes on shear zones (dashed red lines) which are sub-parallel to bedding (dashed black lines) and coincide with the thicker sandstone units. Photo taken September 2018.

Global scale failures are observed within this site on the north-western benches (Figure 3.19). A large translational slide is noted with continuous faulting being the main controlling feature. Local scale wedge failures are also present at this site and tend to fail on bedding and shearing intersections.

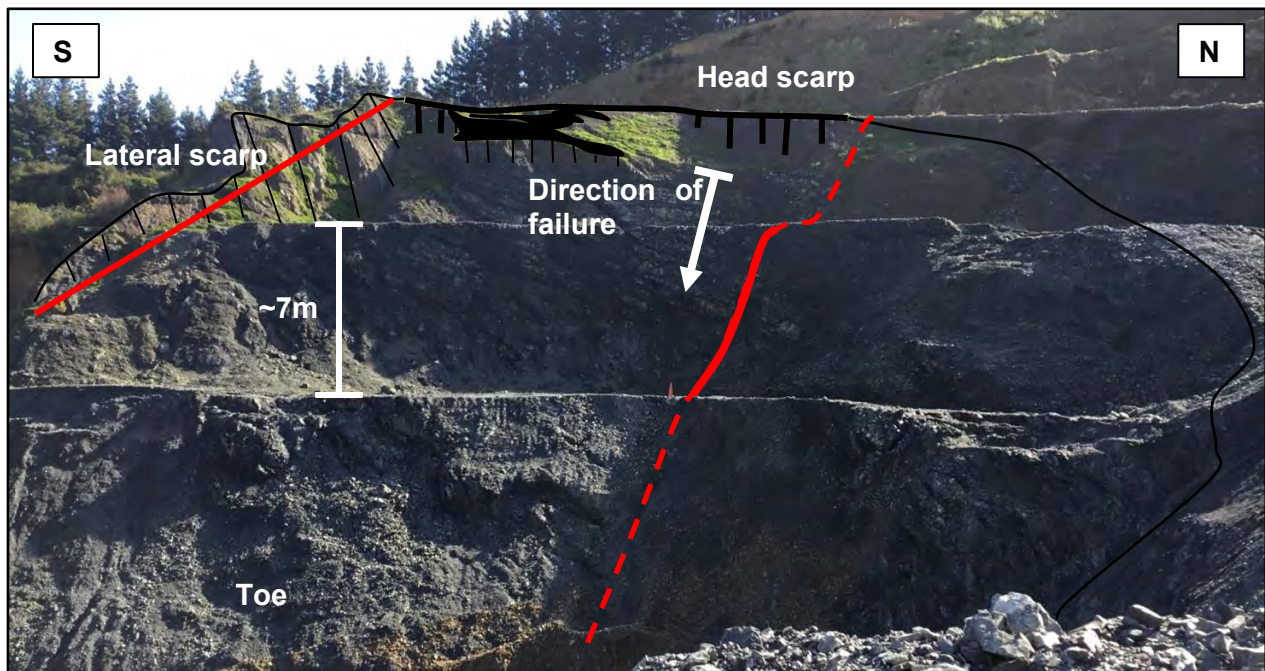


Figure 3.19: Displaying Global scale failure controlled by continuous faulting leading to translational sliding. The black line shows the extent of the sliding failure. Photograph taken August 2018.

Appendix C.7 displays the structural domains for this site. Three different domains, A to C, are defined with boundaries created by faulting.

Discontinuity Condition

Defect infill material in Kapiti Quarry is different from the previous sites. There is higher proportion of mudstone in the rock mass suggesting that there is an increase in the amount of clay and silt in defect infill material (Figure 3.20). Associated with this clay and silt rich material is an increase in plasticity and a decrease in clast strength. A number of defects are recorded to be damp with few displaying minor seepage. This has meant that some defect surfaces are stained. The groundwater flow through the area has also meant that defect infill is mostly completely too highly weathered and weak. Interestingly, Figure 3.21 shows the defect thickness is dominantly moderately wide, which is observed to be smaller than what is seen in the Transmission Gully areas. Despite these differences, defect infill still appears to be dominated by crackle comprising of mostly moderately strong, angular rock fragments (Figure 3.22). An increase in plastic clay gouge material was recorded, specifically in the southern faults in the mapped area (Figure 3.23). Thin seams of clay associated with silty Sands are particularly evident in moderately wide sheared and crush zones.

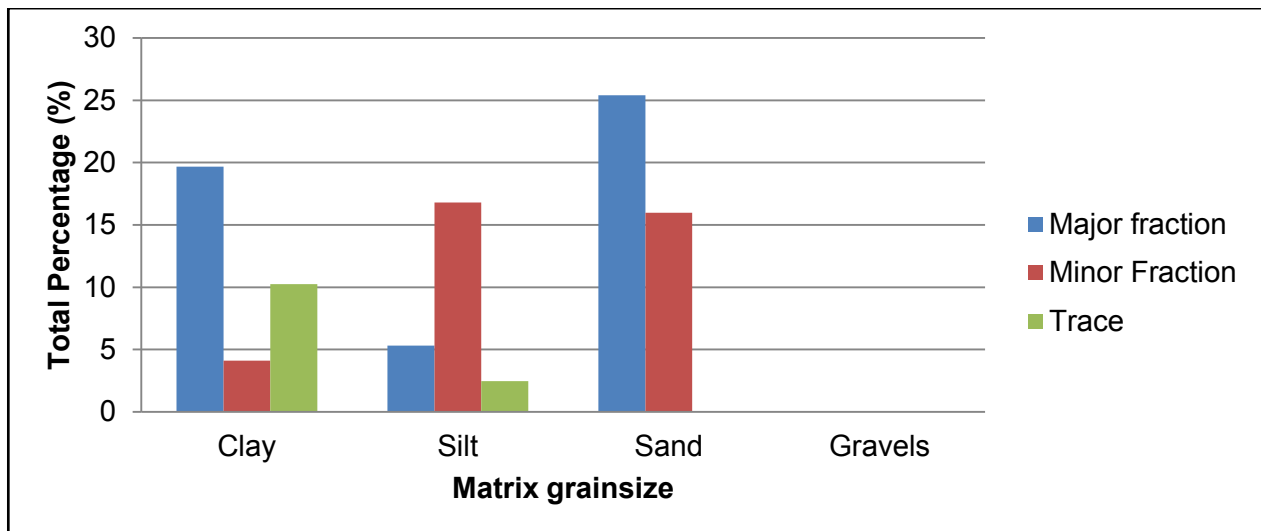


Figure 3.20: Kapiti Quarry defect infill matrix grainsize fraction

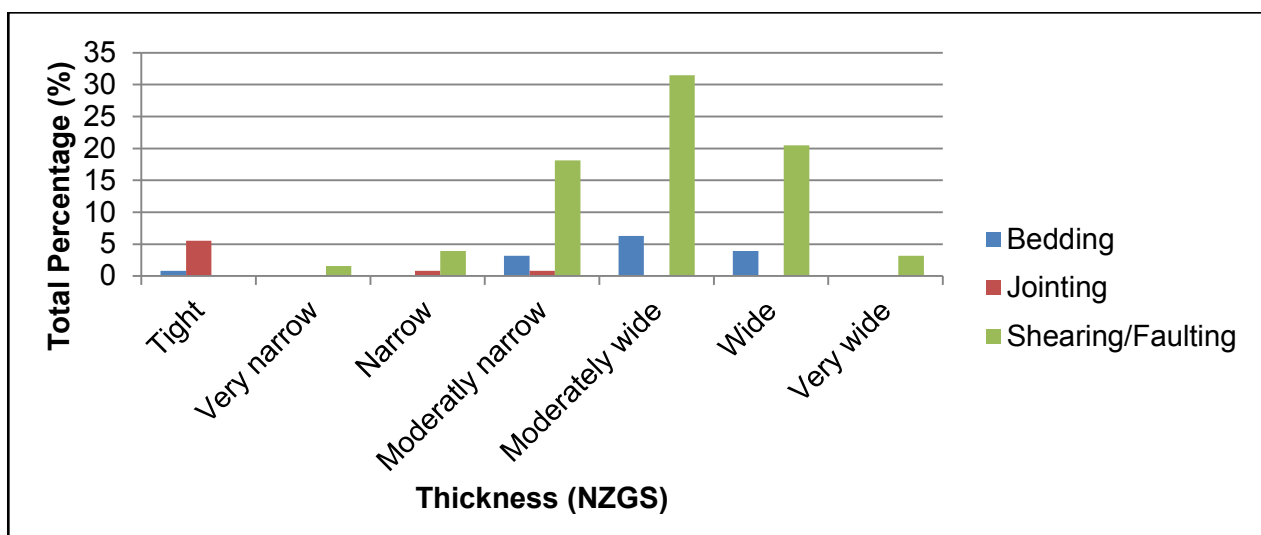


Figure 3.21: Thickness of defects in Kapiti Quarry.

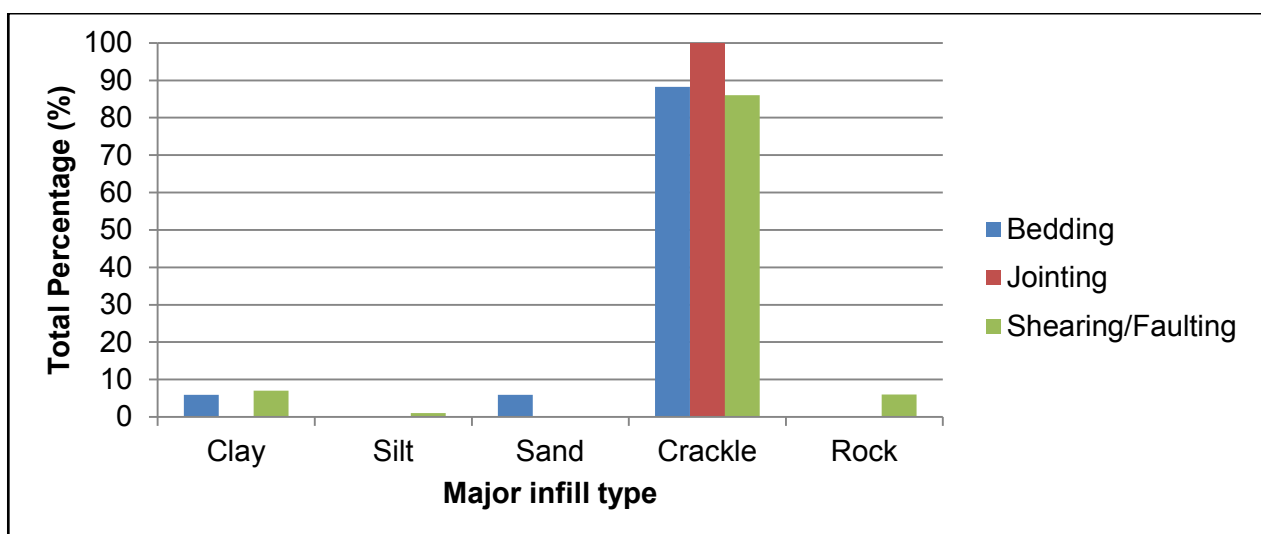


Figure 3.22: Kapiti Quarry dominant defect infill material.



Figure 3.23: Fault crush material present on the lower bench on the south west corner of Kapiti Quarry. Hammer for scale, ~0.3 m.

Defect shape also differs from previously assessed sites. Bedding and shearing still remain dominantly wavy but appear to increase in waviness over shorter wavelengths, indicating that the more continuous structures are more tightly curved (Figures 24). Roughness remains indifferent and jointing remains linear.

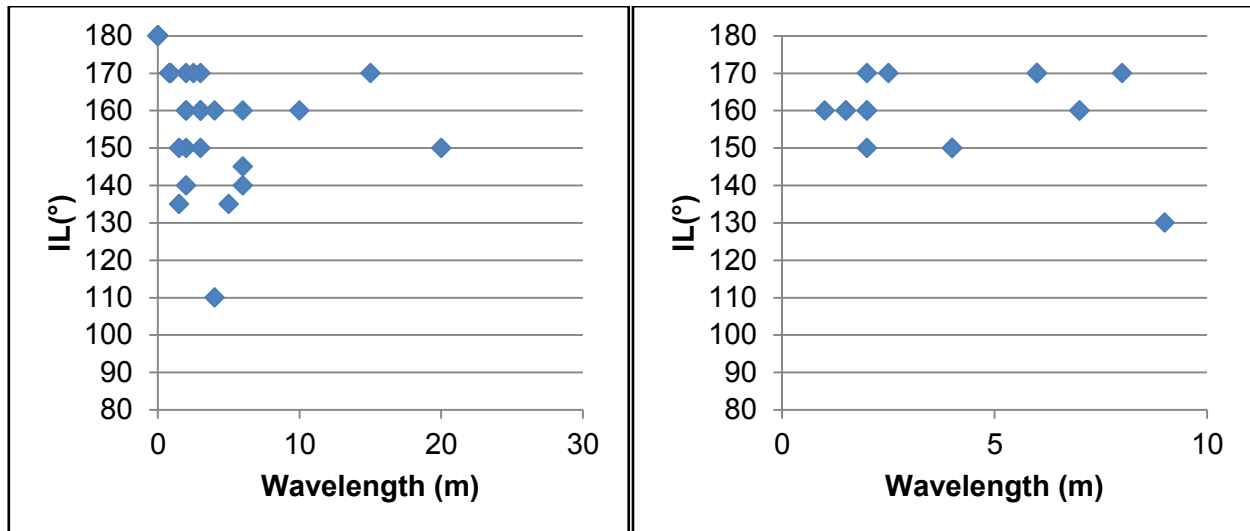


Figure 3.24: Graphs displaying the Kapiti Quarry Shearing (Left) and Bedding (Right) waviness.

Stereonet Analysis

A contour plot of the bedding data can be seen in Figure 3.25. It displays that bedding data can be inferred using the π -girdle method, to produce three potential folds labelled, F1, F2 and F3. Similar to the Transmission Gully North site these folds appear to produce an en echelon pattern (Figure 3.11). Based on the orientation of folds collected from mapping data (Section 3.2.1) F1 is likely to correspond to second generation folding. Due to a lack of hinge lines it is difficult to interpret third and first generation folding.

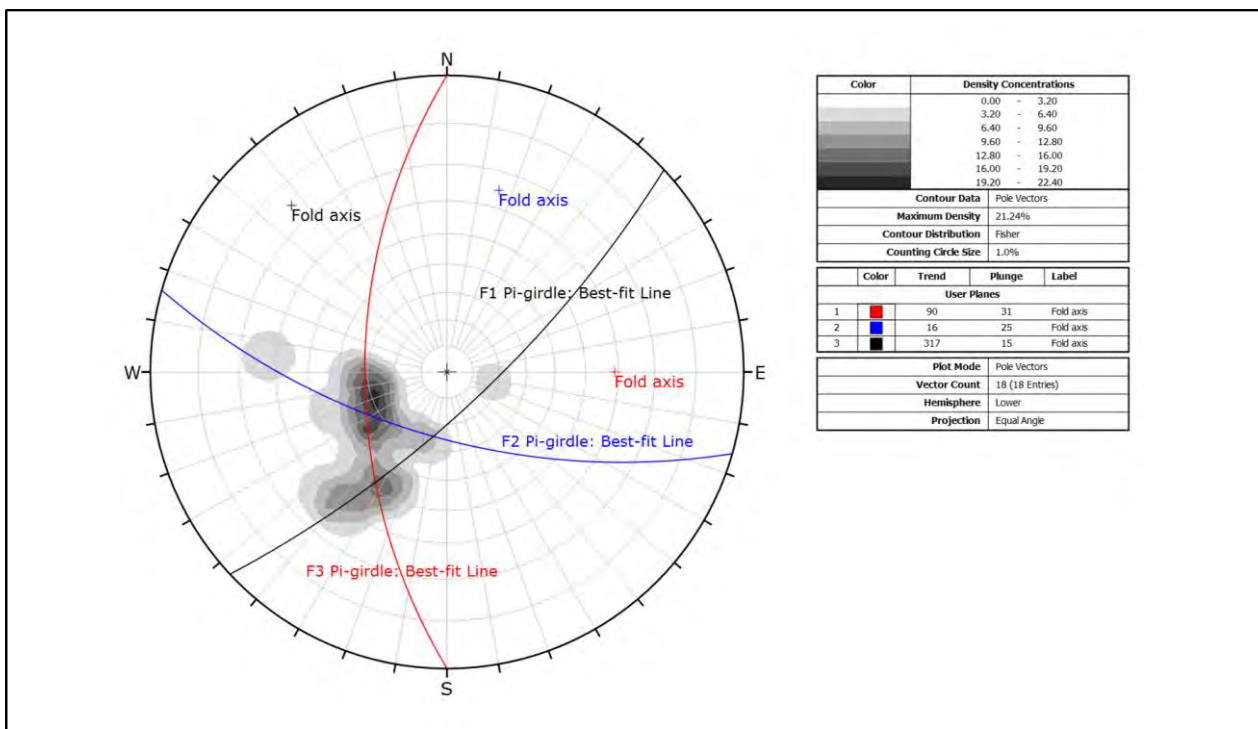


Figure 3.25: Contour plot of the bedding at Kapiti Quarry. Folding interpretations are overlaid showing the use of the π -girdle method.

Faulting in the quarry is clearly recognised. Two of these faults are interpreted to be orientated northwest to southeast, while the third appears to be oriented roughly west to east. Based on the orientation of these structures and the regional lineament analysis it is inferred that these faults are likely to be of the third order. Due to a lack of reference surfaces across the fault traces the fault movement is unable to be interpreted from observation in the field. It is assumed due to the direction of strike that the northwest-southeast oriented structures may obtain normal movement as indicated from the regional structural model.

Bedding and bedding shear poles can be confined to a cluster oriented between 095 and 010 with a dip between 20° and 65°. Overall bedding is dipping northeast and trending subparallel to the northwest-southeast oriented second order structures.

Shearing produced a large amount of “noise” in the stereoplots (Appendix C.6). This is primarily due to the large volume of random, discrete shearing displayed at this site. Therefore, this site required “filtering” for the more continuous and persistent shears in order to be able to identify patterns. A single well-defined cluster is identifiable dominantly consisting of shear zones that are antithetic with bedding. Another vaguely defined cluster is very steeply dipping to sub-vertical and appears to be trending subparallel to the northwest-southeast oriented second order structures. It is interpreted that this vaguely defined cluster forms conjugate to bedding and the antithetic shears.

3.2.4 Horokiwi Quarry

The following section describes the Horokiwi Quarry site characteristics.

Conceptual Model

Conceptual models seen in Appendix D.1 interpret that the rock mass structure for Horokiwi quarry is primarily controlled by the Moonshine and Wellington Faults. These faults place the study area in convergence with regional tectonic stresses and elastic strain being accommodated and transferred onto the linking unnamed high-angle cross faults. This resulted in multiple fault bounded blocks which are understood to rotate as a means of accommodating the strain. The close proximity of the quarry to the Wellington Fault means that a large volume of the Torlesse rock is heavily sheared and fractured within this site. This understanding provides that basis for bedding and shearing orientations. Bedding and shearing is anticipated to trend sub-parallel to parallel to the northeast-southwest trending structures. Folding and or shearing cross-cutting bedding is anticipated to produce some variation in bedding orientation.

Rock Mass

Engineering geological mapping at Horokiwi Quarry identified Suneson (1993) Lithofacies Group B as the most dominant along with the less common Lithofacies Group C. Also identified is Cammack et al. (2018) “Fault Disturbed” Regime, C, and “Margin Zone”, B.

The “Fault Disturbed” rock mass zone has a high degree of faulting and folding to the point that the original rock mass is overprinted (Figure 3.26). Persistent faulting and shearing in this zone is present but is commonly discontinuous and terminates against other structures. Mudstone beds range in thickness from 10 mm to 0.3 m and individual sandstone beds from 0.3 m to around 2m thick. Jointing is very closely spaced and discontinuous. The rock mass condition in this zone is typically poor. In the “Margin Zone” area the rock mass condition is increased. This zone displays truncated ‘fault blocks’ (Figure 3.27) that show bedding continuing over 10’s of metres before being disrupted by other defects or folding (Figure 3.28). These ‘fault blocks’ tend to be relatively close together resulting in a significant variation in bedding and shearing orientations over short distances. Individual sandstone beds in this material range from around 5 m to 0.3 m thick while mudstone beds are around a metre to 0.4 m thick. Jointing in this zone is typically random, closely spaced and starting to develop systematic sets (see Figure 3.28).



Figure 3.26: Exposure of Fault disturbed rock mass in Horokiwi Quarry. Located near the Wellington Fault, in the south study area.

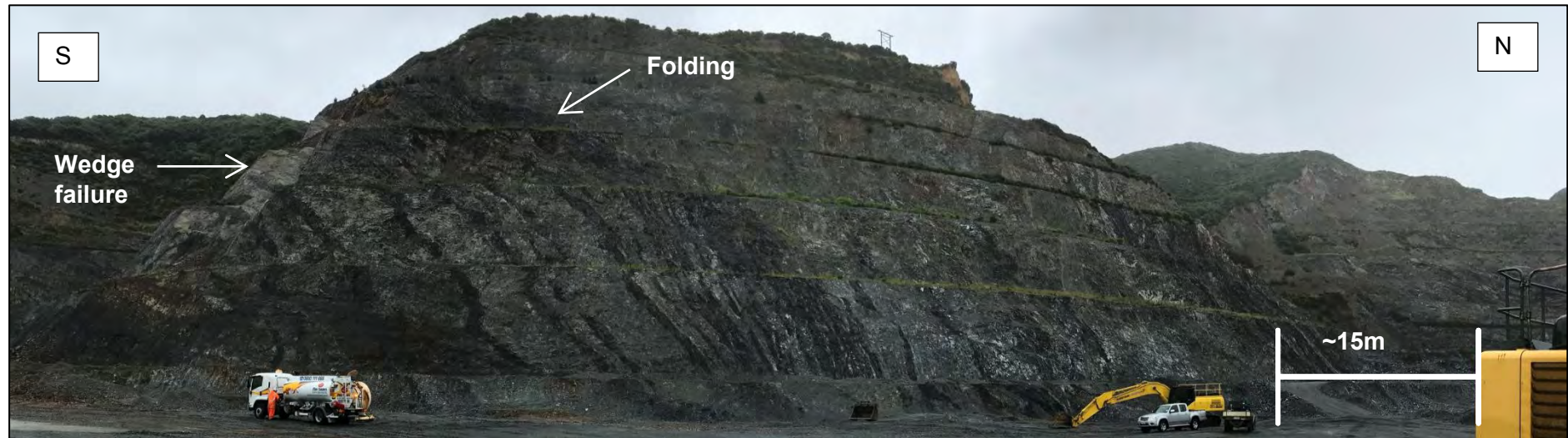


Figure 3.27: West study area in Horokiwi Quarry displaying the folding and continuity of the bedding in the “Margin Zone” area.



Figure 3.28: North study area in Horokiwi Quarry displaying “truncated” and continuous bedding in the “Margin Zone” area.

Overall continuous cross-cutting shears are approximately 10 m apart with spacing decreasing as distance to major faulting also decreases. Shearing commonly appears to form conjugate to bedding (Figure 3.29) and obtain relatively more persistence than seen in previous sites. Continuous defects tend to be very widely spaced with spacing decreasing in areas where there is higher mudstone content (Lithofacies C). Bedding is generally sub-vertical to steeply inclined with variation in dip angles due to faulting. The condition of the rock mass is moderately weathered to slightly weathered with groundwater flow only visible escaping through faults mapped in the northwest and south areas of the site. Data was collected in the rain so most defect infills obtain a slight saturation, however, it does not indicate groundwater flow. Shears, crush zones and shear zones are less common than in other locations. Rock mass strength is generally strong in sandstone to moderately strong in mudstone. Faulting is clearly visible and is continuous across the entire site.



Figure 3.29: Displaying Margin Zone very widely spaced shearing forming conjugate (red arrow) to bedding.

Gentle concentric third and second generation folding is visible in the margin zone whereas, only open second generation folding is observed in the fault disturbed zone. Furthermore, a global

wedge failure is recorded on the southern corner of the western mapping site (Figure 3.27). This failure is assessed to have been controlled by intersecting persistent shears.

A total of seven structural domains are identified in this site, A to G. These domains are all bounded by mapped faults. The high number of structural domains is primarily due to the large increase in outcrop exposure and the detail nature. It is anticipated that some areas could be grouped together such as E and F as they display similar structure and bedding orientation despite a minor degree of rotation clockwise. The distance from the mapped area in the south to the north is around 600 m. This is the longest and largest continual exposure used in this study.

Discontinuity Condition

Defect shape differs between the “Fault Disturbed” and the “Margin Zone” rock mass. Bedding and shearing in the “Fault Disturbed” zone is influenced by major faulting and so is generally more closed. Whereas, the “Margin Zone” is further away from major faulting and so is generally more planar. Figure 3.30 displays the waviness of the bedding and shearing data. In comparison to other sites the discontinuities in Horokiwi are evidently more planar, specifically in the margin zone material. Shearing and bedding thicknesses also appear to have decreased, similar to what is observed in Kapiti Quarry (Figure 3.31).

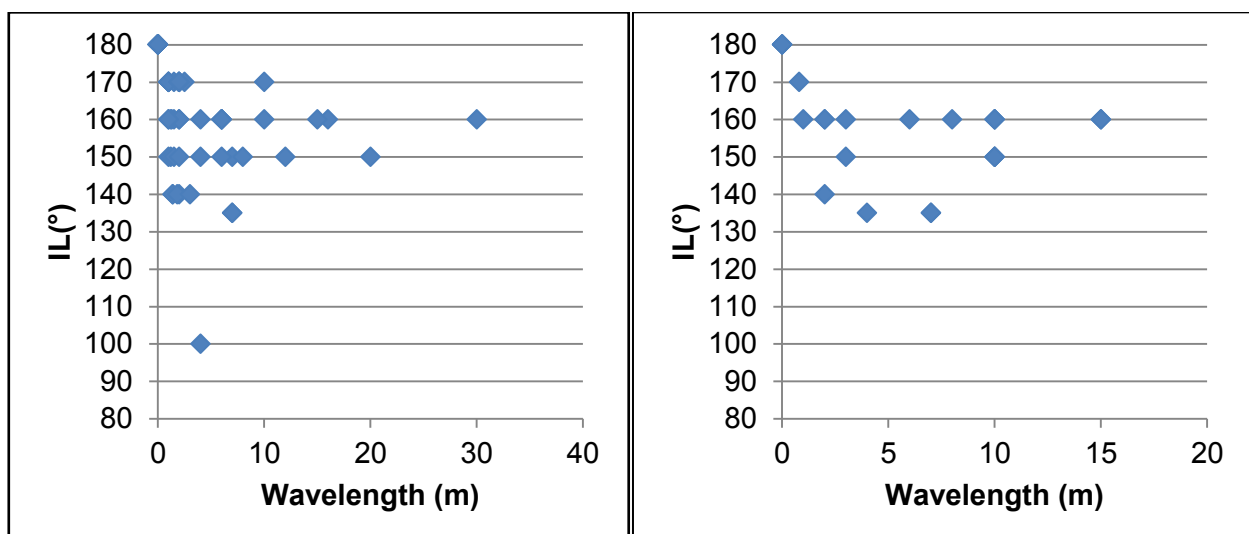


Figure 3.30: Graphs displaying the defect waviness of Bedding (Right) and Shearing/Faulting (Left) at Horokiwi Quarry.

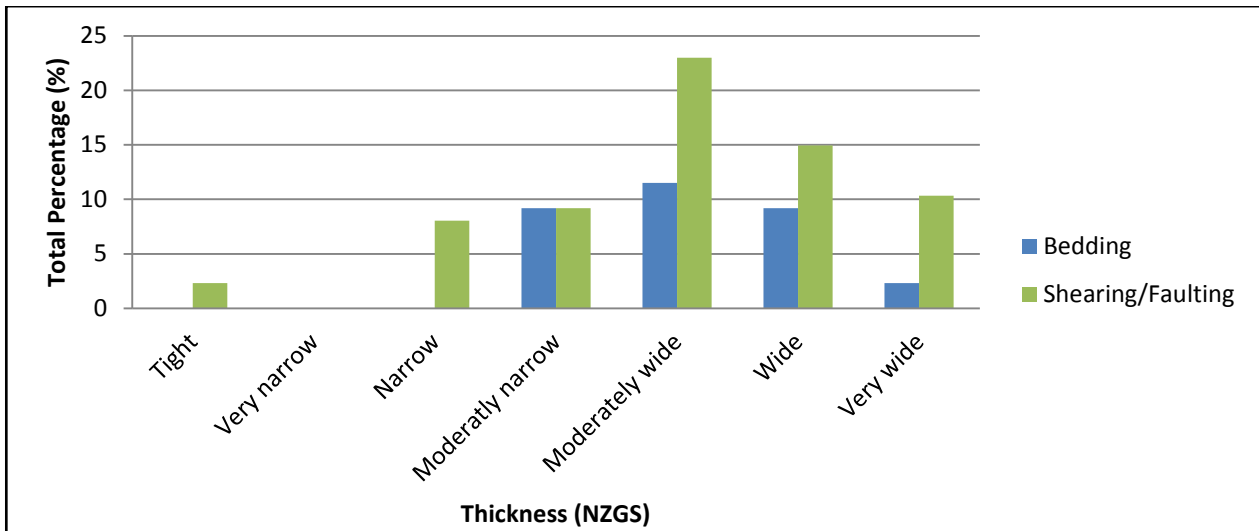


Figure 3.31: Thickness of the defects observed in Horokiwi Quarry.

The average Roughness is still Ro3 (Figure 3.31) and dominantly moderately wide, however, there is an increase in defects less than 20 mm thick (moderately narrow) (Figure 3.30). Jointing is generally random, clean or stained, and discontinuous despite being randomly defined. Defect infill material is mostly comprised of brecciated or gouge infill material, with a clayey or sandy matrix. The increase in fines in comparison to the Transmission Gully areas along with the wet conditions upon which this data was collected means that there is a slight plasticity is associated with this material, although not as much as what is observed in Kapiti Quarry. Rock fragments are mostly angular, moderately strong and highly weathered to moderately weathered. Occasional iron staining on shears is observed across the site (Figure 3.32), but is mostly overlooked due to a thin coating of clay or silt.

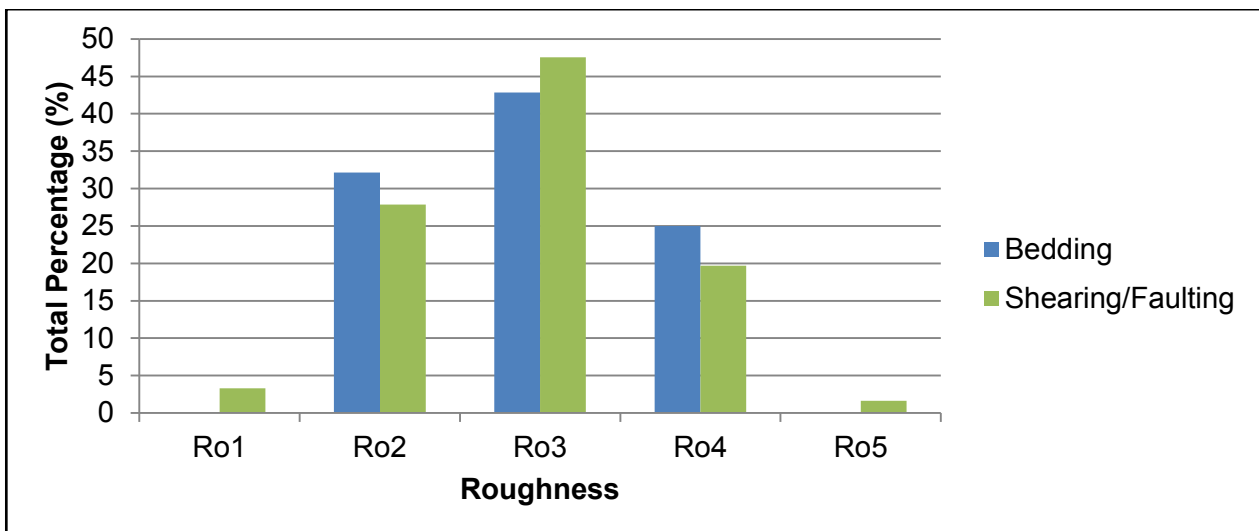


Figure 3.32: Horokiwi Quarry defect roughness



Figure 3.33: A) Photograph of a Bedding shear and B) a Shear zone in "Margin fault" zone material. Geological hammer is provided for scale, ~0.3 m long.

Stereonet Analysis

Bedding and shearing patterns are observed to vary significantly within this study area. This is primarily due to the close proximity of large faulting, folding and to a small amount the large spread between each of the mapped exposures. Therefore, no obvious overall pattern is observed. Despite this the structural domain model presented in Appendix D.7 displays two clusters of shearing typically forming conjugate or perpendicular to bedding. This is consistent throughout the site and is interpreted to rotate in response to faulting. Overall the bedding average is typically striking north-south.

3.2.5 Owhiro Bay Quarry

The following section describes the Owhiro Bay Quarry site characteristics.

Conceptual Model

Owhiro Bay Quarry is located approximately 4 km to the southeast of the active Wellington Fault (Appendix E.1). Multiple unnamed north-south trending faults extend from the south coast towards the Wellington Fault where they appear to terminate. Described by Begg and Johnston (2000) to be splays this places the area in convergence. Given the distance from the active faults the condition of the rock mass is anticipated to be relatively less disturbed. Using this knowledge bedding and shearing is likely to be more persistent and continuous and trending with orientation sub parallel to parallel with the Happy Valley Fault (2nd order structures).

Rock Mass

Engineering geological maps indicate that Suneson (1993) Lithofacies B, C and D are present. Lithofacies Group B is the most dominant, followed closely by Group C with rare occurrences of D. Cammack et al. (2018) “Margin Zone” is visible on the upper benches of the Quarry, however, the site is mostly dominated by “Fractured Rock”.

Rock mass condition in Owhiro Bay Quarry is assessed as relatively good when compared to other sites. This can be explained primarily by the increased distance from major regional faulting which results in less tectonically disturbed areas. Bedding appears to be thicker than most other sites, with mudstone beds forming approximately 2-3 m in places (Figures 34.a and 34.b) while sandstone beds are dominantly 2 to 10 metres thick. Bedding is also steeply inclined to sub-vertical with wide to very wide spacing. Bedding persistence can continue for fifty metres and more or until it terminates against faulting (Figure 3.34.b). Shearing is also persistent. Shearing relationships are very similar to what was observed in Horokiwi Quarry. The only difference is that cross-cutting relationships are wider spaced, 15 to 30 m, and fewer discrete sub-systematic shears are common. Jointing is still discontinuous despite being more defined with moderately wide spacing in sandstone and close to very close spacing in mudstone. Intact rock mass strength is assessed as strong to very strong with the mudstone lithology vaguely weaker. Folding is not observed.

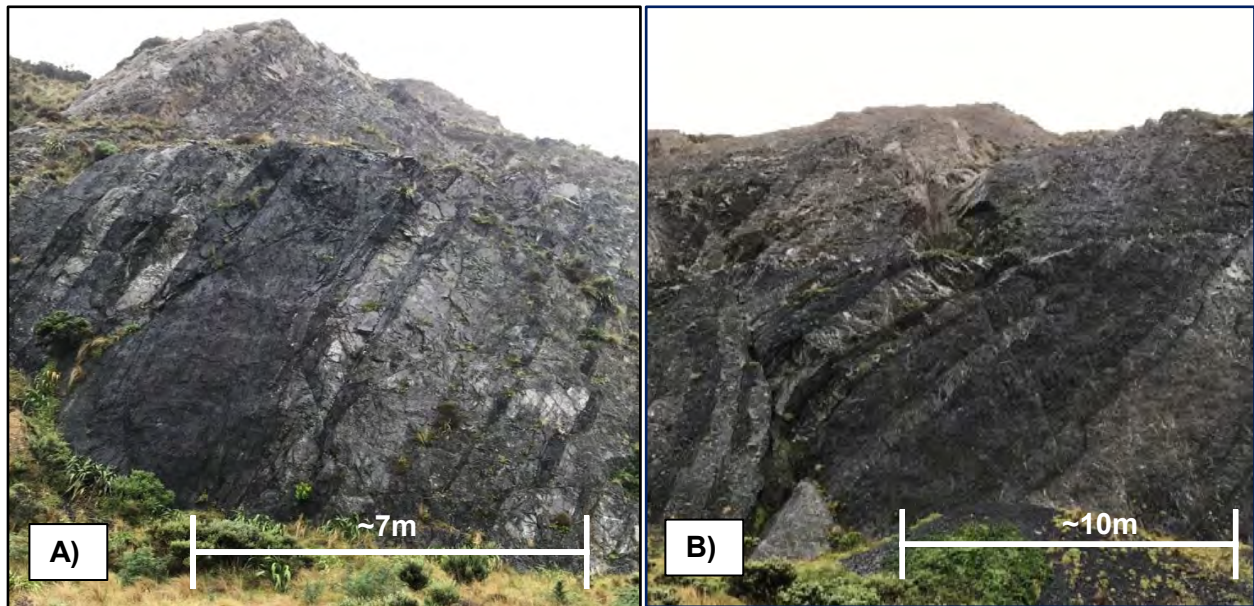


Figure 3.34: Owhiro Bay Quarry photographs A) displaying thick mudstone bedding and B) rotated bedding due to faulting.

Water seepage is recorded occurring mostly out of very wide shears at a rate of approximately 2 Lmin^{-1} . Most defects note a degree of saturation. This is primarily due to the wet conditions at the time data was collected. Vegetation and staining commonly indicate these areas.

Figure 3.35 and 3.36 displays a number of local and global failures occurring on the upper benches of the quarry. Important to note is that there appears to be a set of wedge failures evenly spaced out ($\sim 8 \text{ m}$) on the third bench up from the bottom (Figure 3.35). These failures all appear to fail locally on the intersection of bedding and continuous shears. Global failures appear to be commonly controlled by continuous faulting and bedding.



Figure 3.35: Shows a range of different rock mass conditions exposed in Owhiro Bay Quarry. Intersecting faulting and bedding defects form a number of failures in the upper benches.



Figure 3.36: Failure in the upper benches of Owhiro Bay Quarry. Appears to be bedding and fault controlled in a thick mudstone rich bed.

A total of three structural domains are identified in this site, A to C. All of these domains are bounded by mapped faults. Bedding orientations appear to change across the domains. Lithology appears to be fairly consistent throughout all the domains.

Discontinuity Condition

Discontinuity condition in Owhiro Bay Quarry does not differ greatly from the “Margin Zone” in Horokiwi Quarry. The main difference observed is that discontinuities appear to be more linear (Figure 3.37) with significantly less infill material, less than 0.06 mm in size (silt). Water saturation, and in some cases water flow, is the likely cause for a lack of finer material. The infill material that is displayed is mostly Crackle (Figure 3.38) that is highly weathered and moderately strong to strong. Rock fragments are generally angular and surrounded by mostly silty Sand material. Slight plasticity is associated with the finer material due to the wet weather conditions encountered when collecting structural data. The average roughness is still Ro3 and the thickness is mostly wide to very wide.

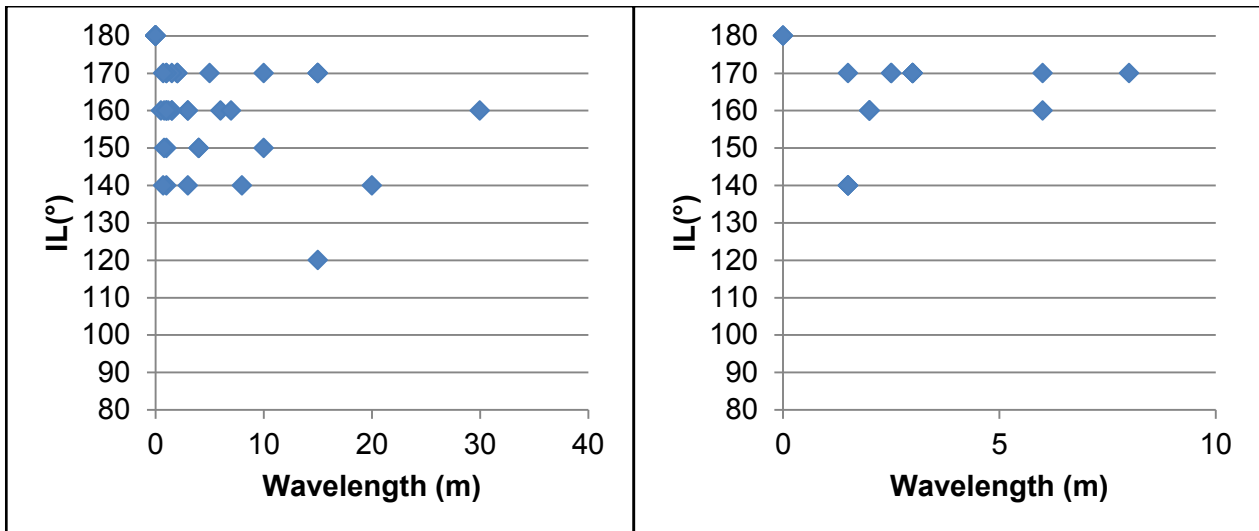


Figure 3.37: Graphs showing the waviness of Bedding (Right) and Shearing/Faulting (Left) in Owhiro Bay Quarry.

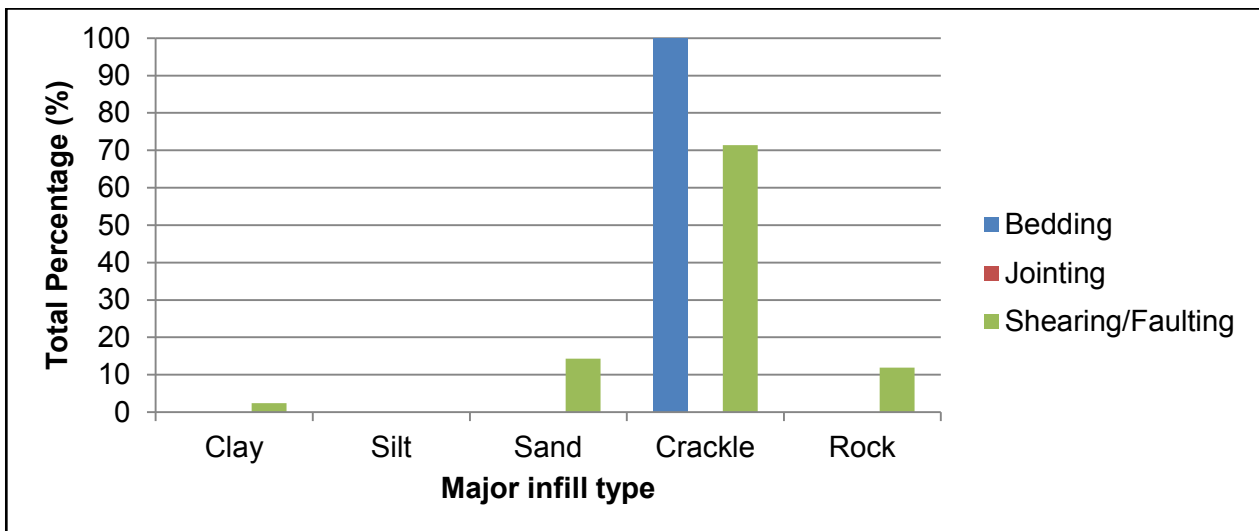


Figure 3.38: Owhiro Bay Quarry defect infill material.

Stereonet Analysis

Figure 3.39 displays a contour diagram of the poles to planes of the bedding and shearing data in Owhiro Bay Quarry. Bedding is observed to rotate clockwise from west to east throughout the site while predominantly oriented northwest-southeast. An absence of observed folding was noted therefore no further investigation was conducted. This would indicate a westward dipping homoclinal sequence for the entire site. This is supported by Grapes et al. (2011) and Suneson (1993) who also identified this feature.

The stereonet also indicates that Shearing tends to be dominantly oriented in two directions; northeast-southwest and northwest-southeast. This corresponds with observations noted in the conceptual model (Appendix E.1).

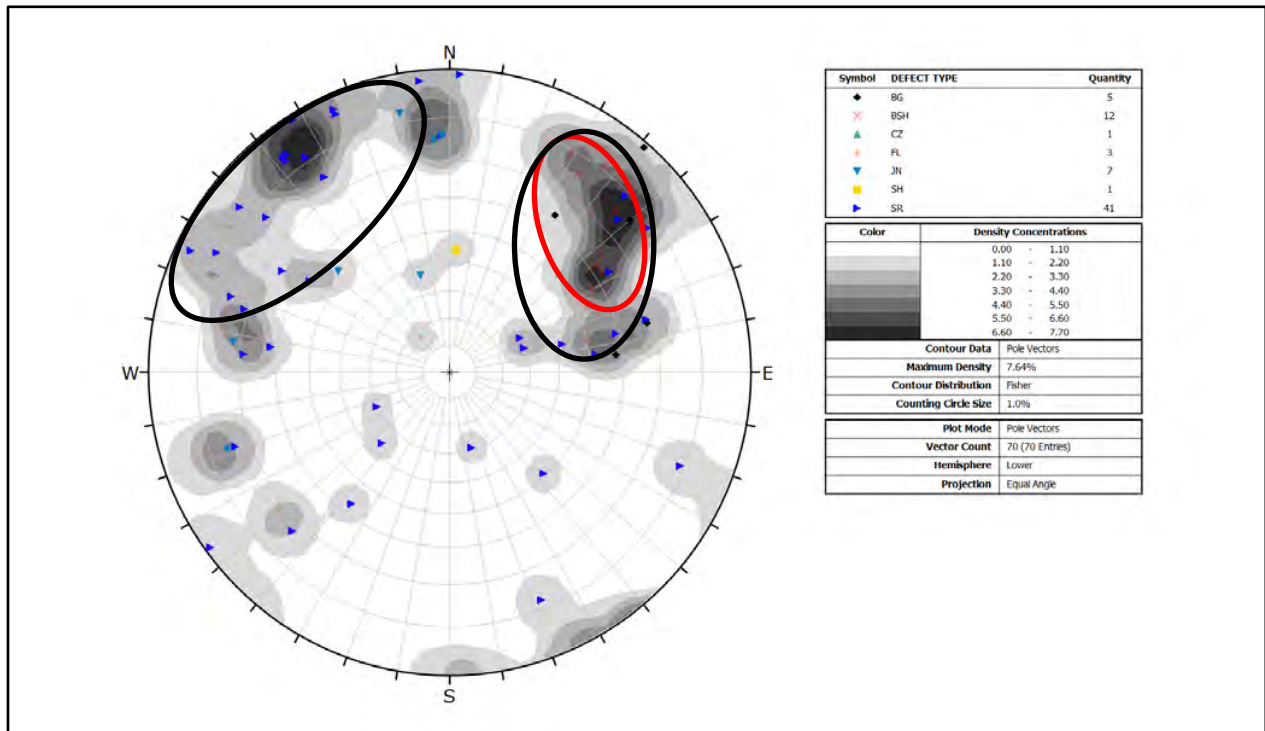


Figure 3.39: Stereonet plot of bedding and shearing poles to planes of Owhiro Bay Quarry data. The red circle indicates the location of bedding clusters while the black circles are indicating shearing clusters.

3.2.6 Wairaka Point

The following section describes the Wairaka Point site characteristics.

Conceptual Model

Conceptual models produced for this site are displayed in Appendix F.1. These models show that the major control on rock mass structure is primarily the Pukerua Fault and folding associated with the radial shear model explained by Twiss and Moores (1992). Interpretation of the inherent geometry of dextral strike-slip faults suggests that this area is placed in convergence. Superimposed folding is recorded in past literature with third generation folding anticipated to be oriented roughly 45 degrees or less to the Pukerua Fault. Second generation folding is predicted to orientate roughly perpendicular to the Pukerua Fault. Shearing is predicted to be well developed and trending sub-parallel to the Pukerua Fault. Bedding is anticipated to be oriented sub-parallel to the northwest-southeast trending structures.

Rock Mass

Engineering geological mapping was only able to identify (Suneson, 1993) Lithofacies Group B and Regime A, “Fractured Rock” zone, from Cammack et al. (2018).

Wairaka Point is different from other sites in that it is a naturally occurring rock slope that is approximately 50 m tall. Furthermore the exposures display a slightly weathered, strong to very strong rock mass that appears to be in fairly good condition. Shearing and bedding patterns

seem to form similarly to Horokiwi Quarry despite a lower persistence. Continuous defects are widely spaced with cross-cutting shears occurring approximately every 10-20 m. Generally discrete shearing terminates against bedding or the more continuous shearing features. Bedding is also continuous and tends to persist for ≥ 20 m (Figure 3.40), until it terminates due to faulting. Sandstone beds are generally 7-10 m thick and around 0.2-0.3 m where rare alternating mudstone and sandstone beds are visible. Mudstone beds do not tend to form thickness' greater than 0.3 m with occurrences of ≤ 4 mm typically exposed. This results in low mudstone proportions. Bedding is still steeply inclined. Jointing is well defined and persists for up to 4 m with moderately wide to wide spacing's (Figure 3.41).

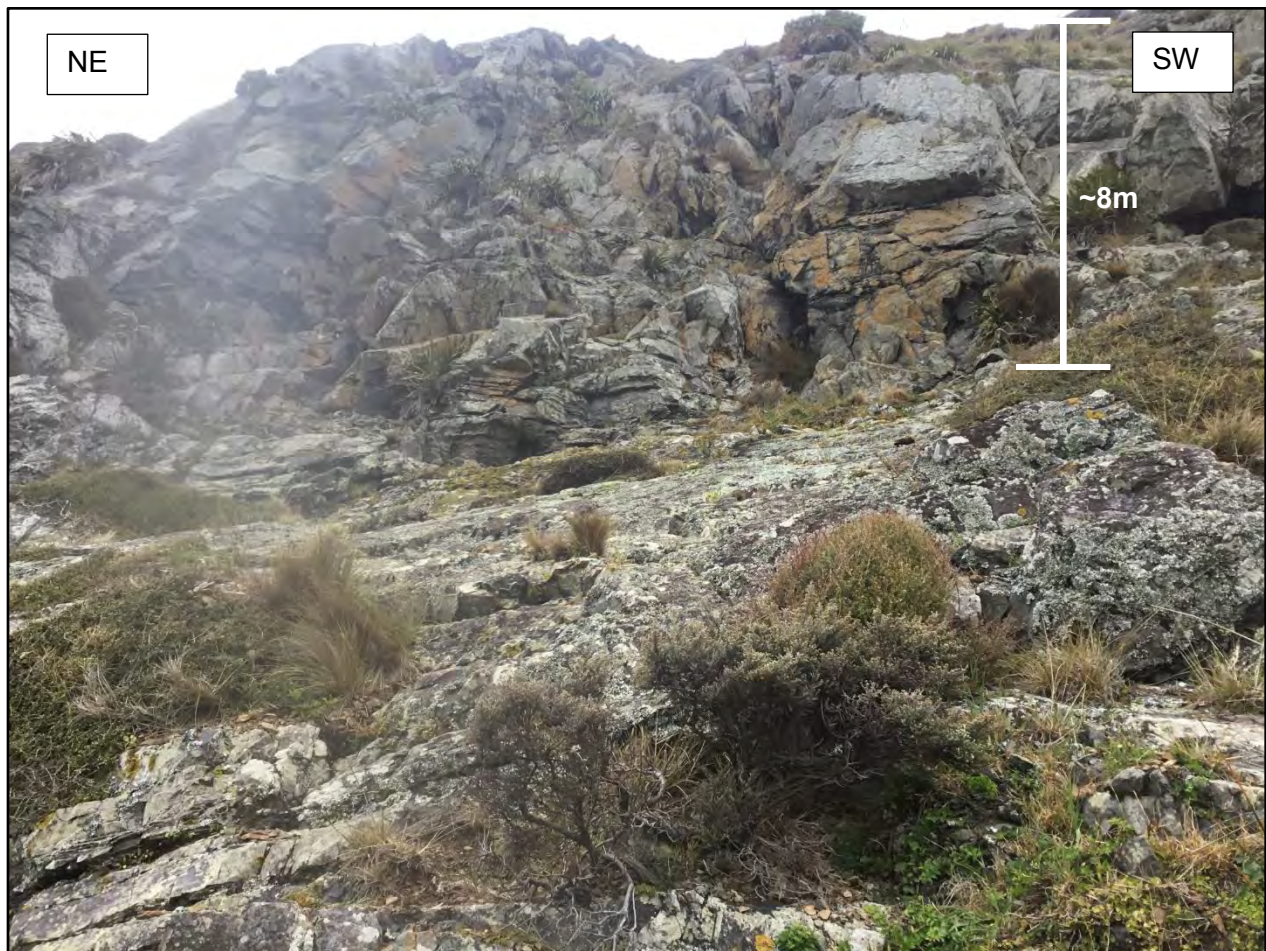


Figure 3.40: Close up photograph of a large failure above mapped site 2 at Wairaka Point. Failure surface has been interpreted to occur on unfavourable oriented bedding and faulting (red line in Figure 3.42).

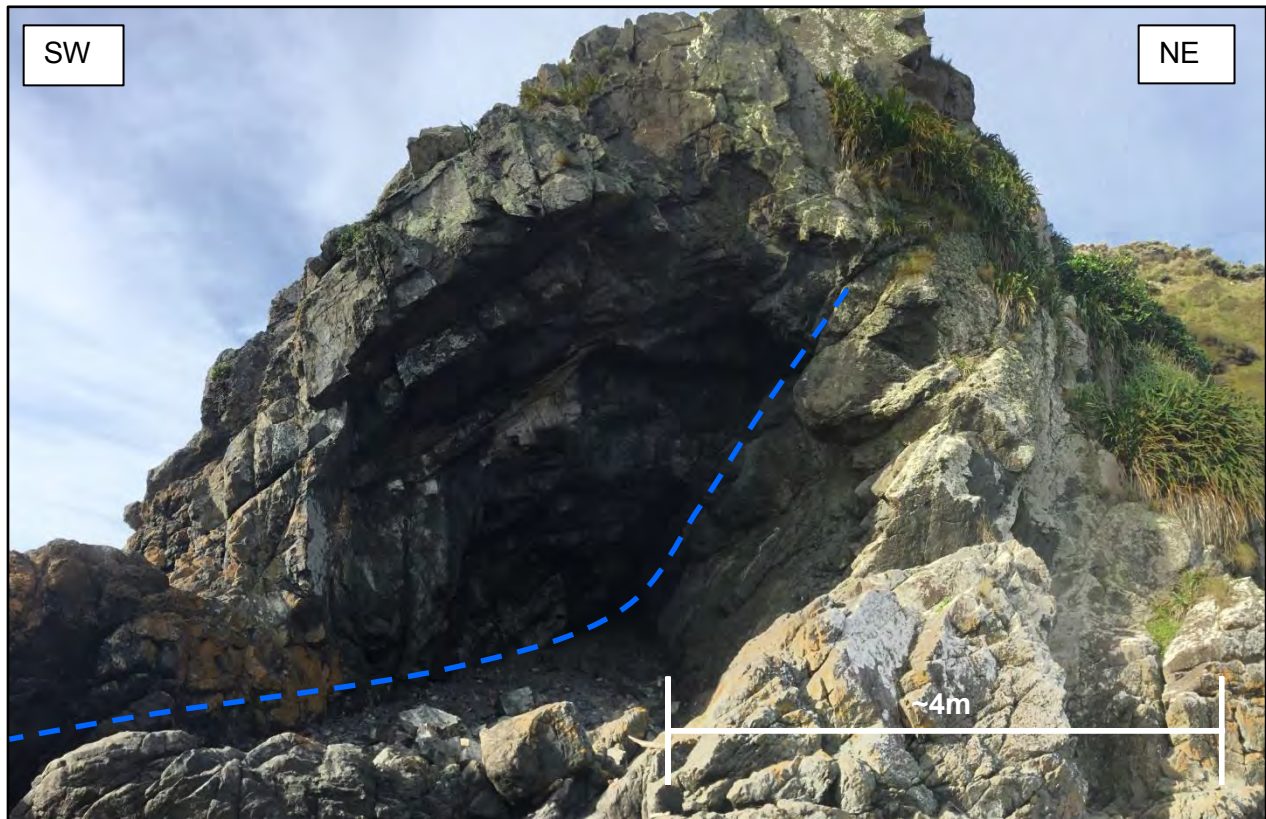


Figure 3.41: Photograph of mapped site 4 at Wairaka Point. Blue line indicates bedding upon which kinematic sliding has occurred.

Since Wairaka Point is a naturally occurring rock slope it therefore, generates a range of slope failures. Figure 3.42 displays a global scale failure above the second mapped study site. It is interpreted that this particular failure has occurred due to unfavourable oriented bedding intersecting with a fault that trends northwest-southeast. Multiple local scale failures have also been assessed throughout the site and are commonly occurring on persistent joint sets or bedding intersections. Jointing only ever appears to dislodge blocks less than a metre cubed, suggesting that these will only produce local scale failures rather than global ones. On the other hand continuous bedding has caused sliding in multiple locations (Figure 3.41).

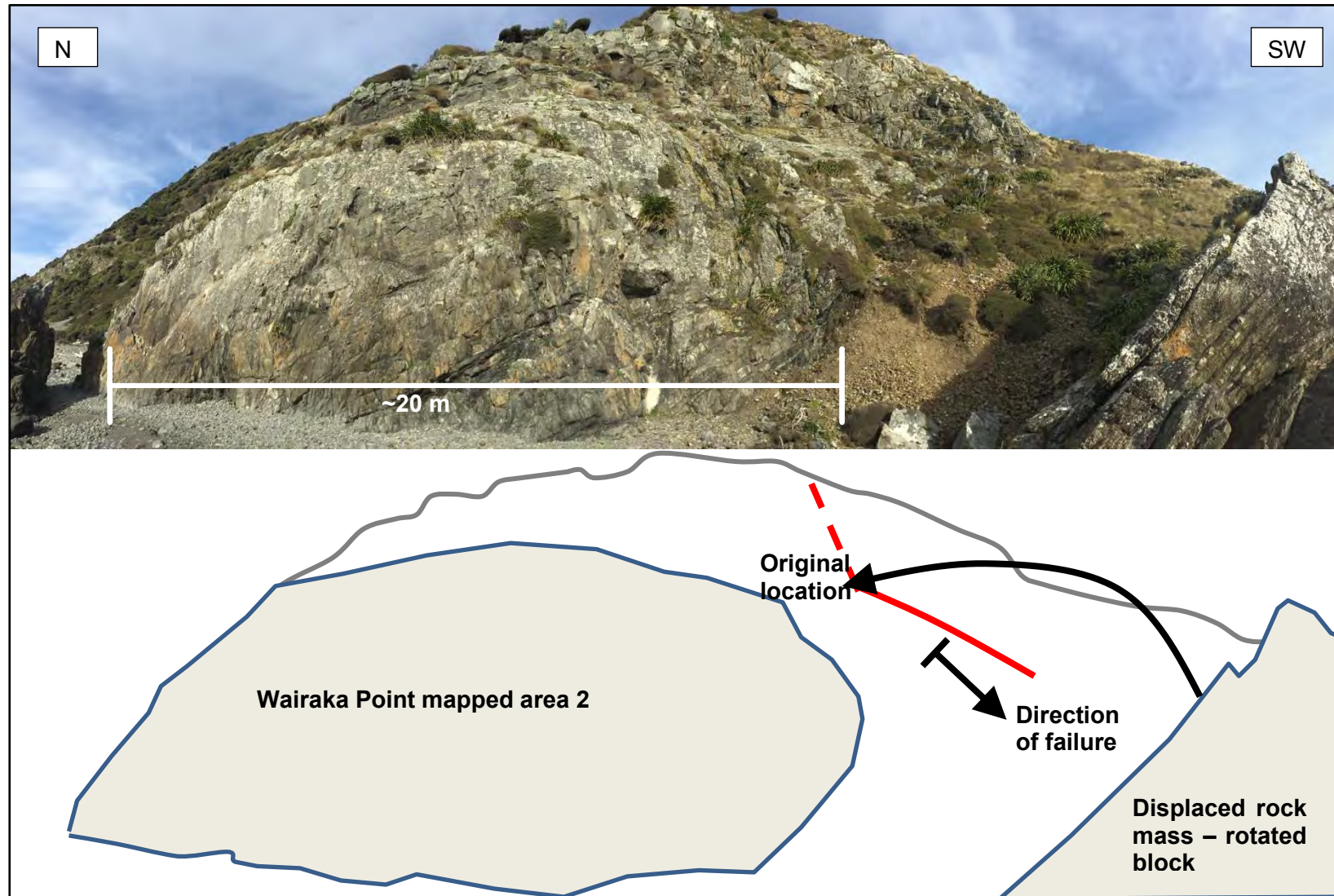


Figure 3.42: Photograph and sketch displaying the location of a large failure above mapped site 2 at Wairaka Point. Failure surface has been interpreted to occur on unfavourable oriented bedding and faulting (Red line).

This site also displays a wide scale of folding. Figure 3.43 shows first and second generation folding at this site. Hinge lines of third generation folds are not observed. First generation folding tends to trend roughly northeast-southwest, while second generation folding tends to be oriented northwest-southeast. The second generation folding is indirectly associated with the previously mentioned global failure. The moderately inclined and northwest moderately plunging fold axis is unfavourable oriented. This results in an increased susceptibility for slope failure. This fold is interpreted to be an open anticlinal box fold. Tighter folding appears to occur in higher mudstone content areas and is typically of the first generation. Folding is only observed where the alternating sandstone to mudstone sequences is exposed.



Figure 3.43: Folding observed at Wairaka Point. Left) observes tight to isoclinal inter-limb angles of first generation folding seen on shorelines while, Right) observes second generation folding which is more open. Geological Hammer and apple pencil are used for scale, approximately 0.3 m and 0.15 m respectively.

A total of two structural domains are mapped at this site, A and B. They are split by a fault seen between mapping site 3 and 2 and in Figure 3.42 (Appendix F.7).

Discontinuity Condition

Approximately 70% of defects are gapped and or clean (Figure 3.44). This is likely in response to weathering and erosion associated with coastal location of the site. Where there is infill material recorded it is mostly crackle or complete surrounded by a sand matrix. Rock fragments are mostly moderately weathered and strong to very strong.



Figure 3.44: Photograph displaying the Bedding (Left) and shearing (Right) and Wairaka point. Geological hammer, ~0.3 m for scale.

Defect shape does not seem to differ from Horokiwi Quarry. However, defect roughness and thickness appears to vary. Roughness averages Ro4 (Figure 3.45) and defect thickness is moderately narrow (Figure 3.46). This also differs from any of the other sites and could be a reflection of the coastal environment in which this area is located.

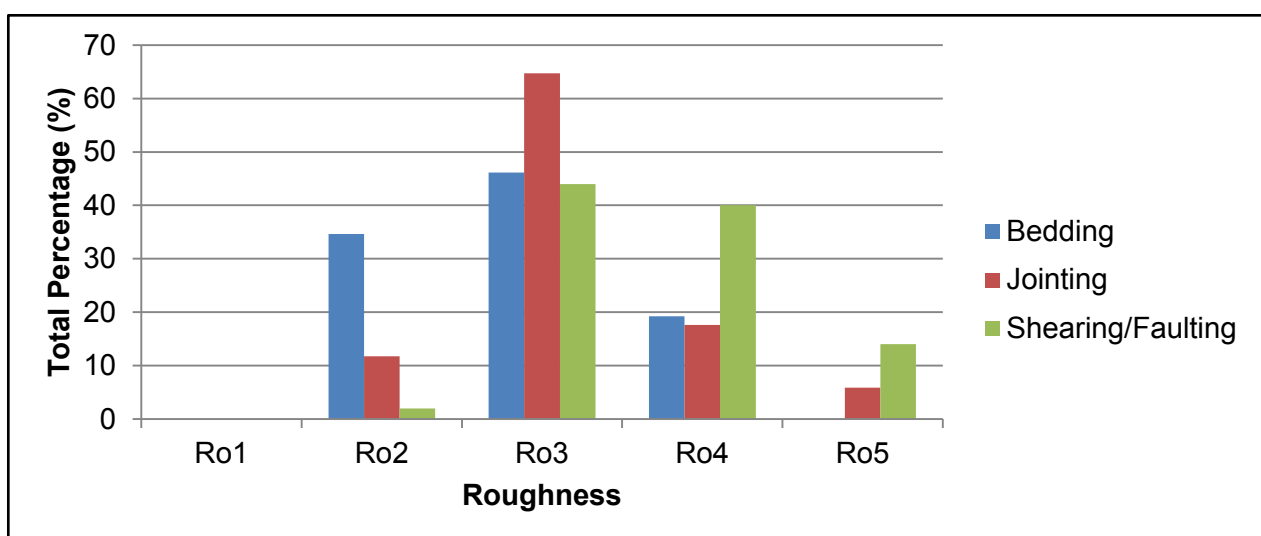


Figure 3.45: Wairaka Point defect roughness.

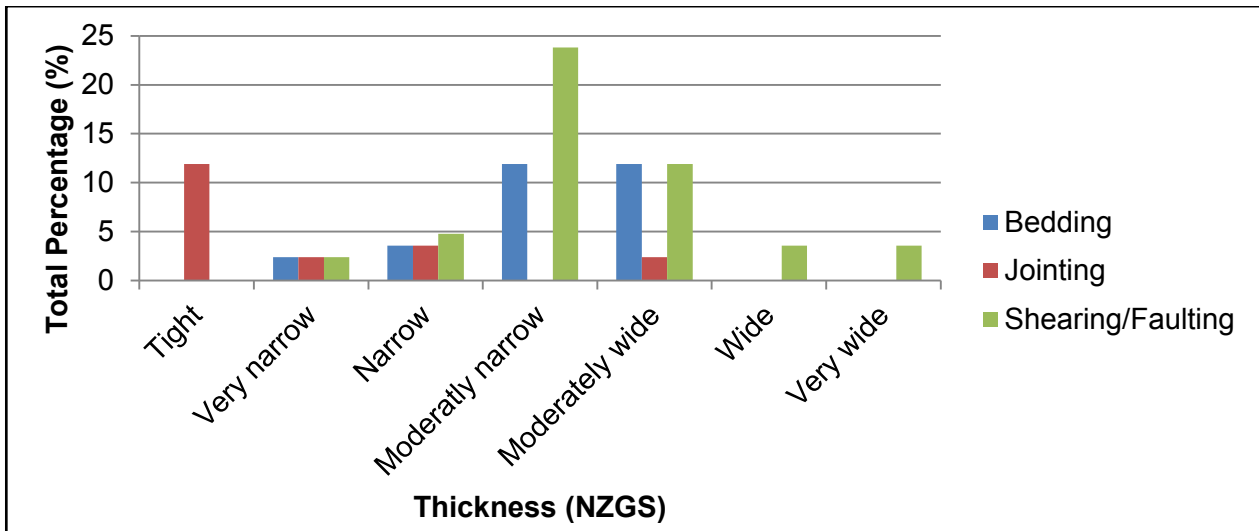


Figure 3.46: Wairaka Point defect thickness.

Stereonet Analysis

The overall pattern of bedding structures at Wairaka Point is clearly visible in the structural domain model and contour plots presented in Appendix F.6 and F.7 respectively. Contour plots showing the distribution of bedding and bedding shear poles to planes appear to form two clusters located about 50:290 and 35:010 (Figure 3.47). These clusters appear to be rotated by about 90° degrees from the north, in domain A, to the west in domain B (Figure 3.47). This rotation in bedding poles across the domains is likely in response to folding and northwest-southeast oriented faulting. Shearing plots also display a degree of rotation in a similar direction across all the mapped sites.

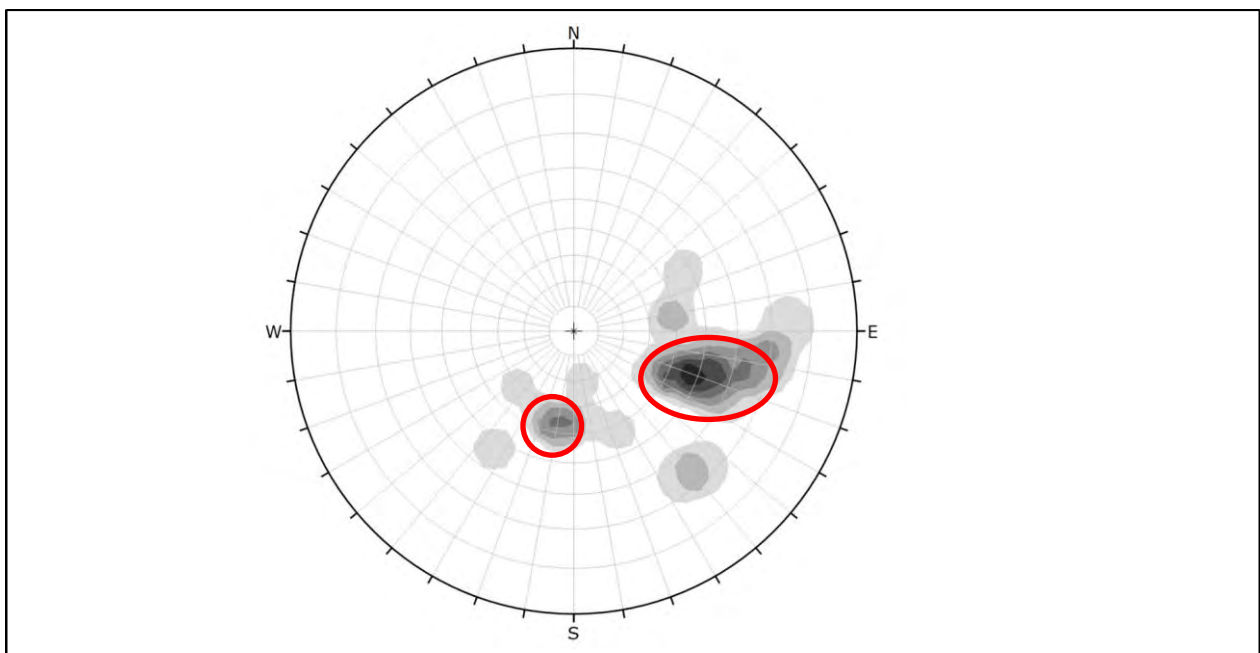


Figure 3.47: Contour diagram of bedding and bedding shears for Wairaka Point.

Further discussion on the overall pattern of bedding distribution is shown in Figure 3.48 as standard π -girdle diagrams. Three π -girdle best-fit lines labelled, F1, F2 and F3 (Figures 3.48.a and 3.48.b) are shown in both domains. F1 and F3 display significant rotation across the domains, obtaining a similar magnitude to what is observed by the bedding clusters in response to faulting. Based on the orientation and location of the folding identified from mapping exercises, it is interpreted that F3 is associated with third generation folding and F1 is associated with second generation folding. As rotation of the F2 π -girdle best-fit line is not as significant when compared to the observations for F1 and F3, it is therefore interpreted that F2 is most likely first generation folding. To further support this interpretation, the lack of rotation over the structural domains of the F2 feature implies there is less influence from faulting in relation to the F1 and F3 folds. A greater influence would indicate a larger degree of rotation. Therefore, development of F2 folding is likely to have occurred in the later stages of tectonic movement implying that F2 is relatively younger in comparison to F1 and F3. Despite that there is no first generation hinge line exposed at this site past literature suggests that there is first generation folding trending roughly north-south (Suneson, 1993) providing additional reasoning.

Overall, third generation folding is interpreted to be tight to isoclinal, moderately plunging and trending northwest-southeast to west-east. Second generation folding is likely open, gently to moderately plunging and oriented roughly northwest-southeast to southwest-northeast. Large scale first generation folding is interpreted to be gentle, moderately plunging and oriented roughly north-south. All folding is observed to be symmetrical.

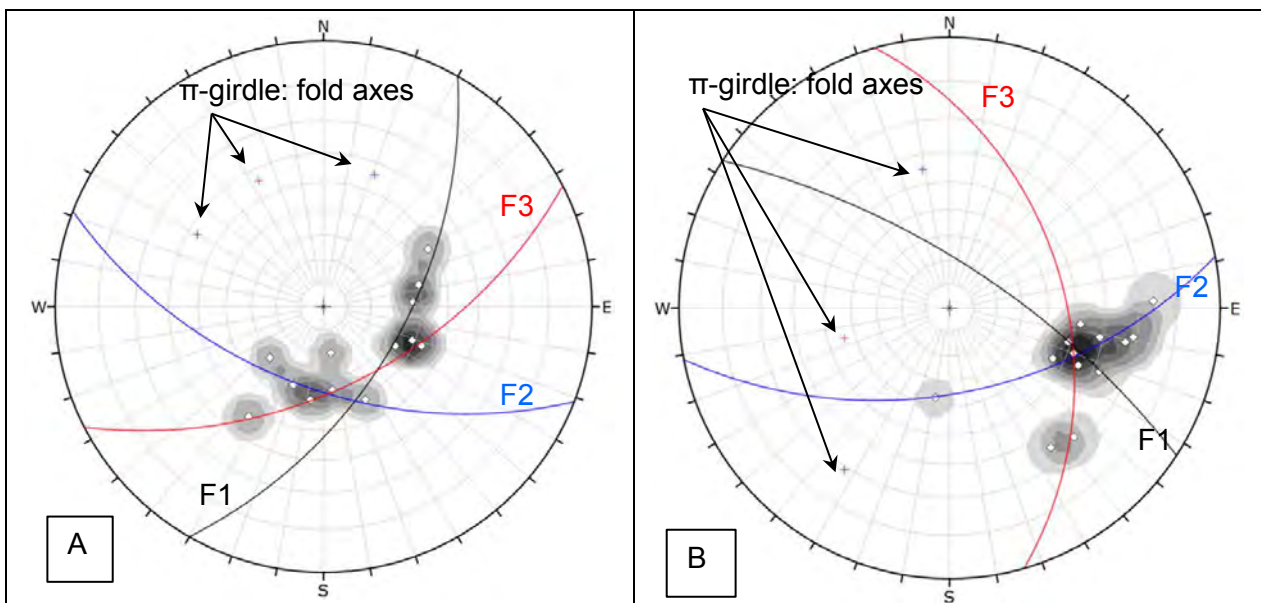


Figure 3.48: Contour diagrams of Bedding and Bedding plane shear plots for structural Domains A) and B) at Wairaka Point. Use of the π -girdle method is shown to interpret folding.

To further discuss patterns of shearing distributions, the shearing data is required to be “filtered” to show only the more continual structural features. This is primarily due to the relatively small and discontinuous rock outcrop extents at this site that limit the possibility of identifying continual shearing relationships. The result of the filtering process produced two fairly well-defined sub-vertical to very steeply dipping conjugate sets that are roughly orientated north-northwest-south-southeast and northwest-southeast. An additional vaguely defined cluster can be interpreted trending roughly west-east while also appearing to be horizontally to steeply dipping. A distinction can be made between the orientations of shearing and jointing sets. This is clearly visible in Figure 3.49.

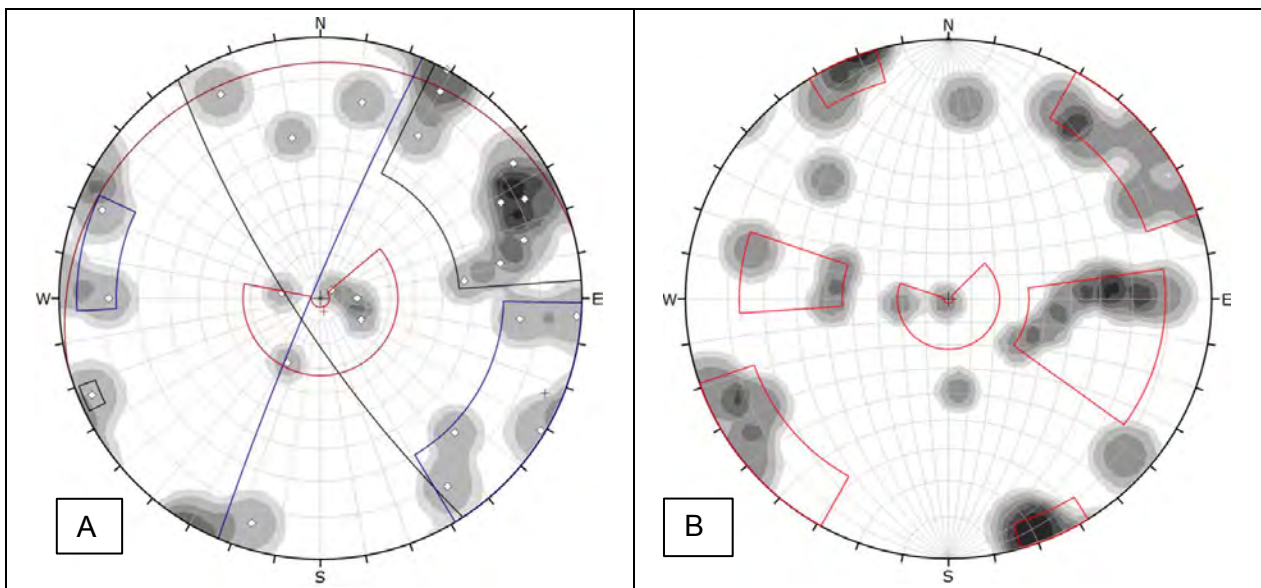


Figure 3.49: Contour plot of A) all the “filtered” shearing data and B) all jointing data for Wairaka Point. Three shear sets can be identified in A).

3.2.7 Makara Head

The following section describes the Makara Head site characteristics.

Conceptual Model

Stated in the conceptual models shown in Appendix G.1, is that rock mass structure is heavily controlled by the Shepherd’s Gully Fault trace and folding associated with the radial shear arrangement model (Twiss and Moores, 1992). To the south of this site the Shepherd’s Gully Fault merges from two fault traces. This zone is interpreted as a restraining bend resulting from a strike-slip duplex. Given the inherent geometry of strike-slip faults it is interpreted that this area is placed under convergence. Bedding and shearing orientations are therefore predicated to trend sub-parallel to parallel with the Shepherd’s Gully Fault.

Rock Mass

Engineering geological mapping indicated that (Suneson, 1993) Lithofacies Group B was the most dominant along with the “Fault Disturbed” and “Margin Zone” regimes of (Cammack et al., 2018).

Makara Head is similar to Wairaka Point in that it is a natural coastal exposure. This being said Makara Head is observed to be in relatively poorer condition, with exposures smaller and fewer. This is likely due to the close proximity of faulting (Figure 3.50) resulting in an increase in fracturing and deterioration of the landscape. The lack in exposed rock, specifically over large areas presented a problem in identifying continuous structures, specifically for shearing/faulting. Persistent shearing was only noticeable in three mapping areas, outcrop 4, 4b and 3 (Appendix G.2). The other areas showed large volumes of vegetation and scree that obscured any daylighting features. Shearing that was observed to be persistent generally terminated against other defects. Few cross-cutting shears were visible and spaced around 10 m apart. Bedding was typically persistent, for around 30 m, however, was often obscured by large dislodged boulders on the beach. Bedding was steeply to very steeply inclined with thickly bedded sandstone and moderately thick to moderately thin mudstone (Figure 3.51). Jointing was closely spaced, narrow, persistent (~4 m in places) and vaguely defined.



Figure 3.50: Fault trace observed close to the study area.

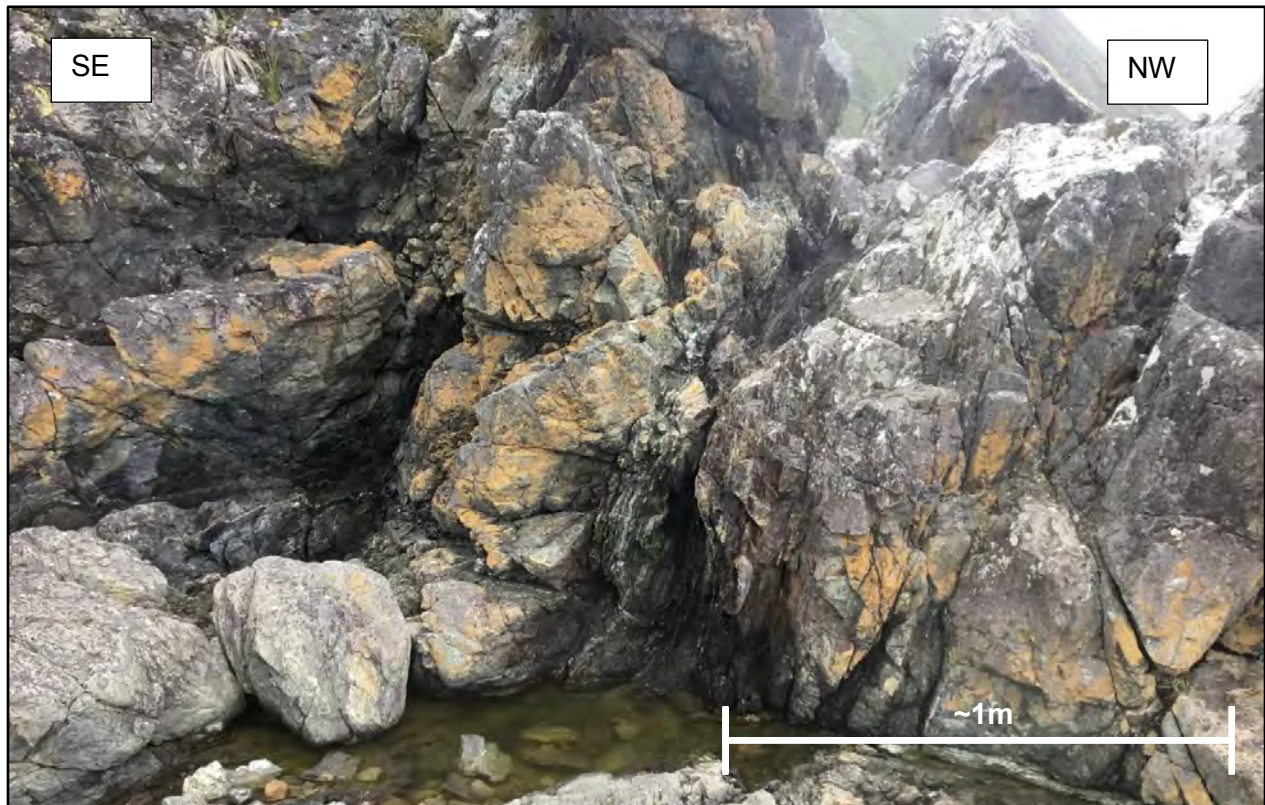


Figure 3.51: Argillite bedding at Makara Head obscured by water and by cobbles and gravel material deposited onto the beach.

The lack of exposed rock outcrops limited any detection of folding. Therefore, no hinge lines are observed.

Slope failure mechanisms are typically dominated by local scale wedge failures and global scale sliding failures. Wedge failures generally form on the intersection of joint sets or jointing and shearing. These tend to produce blocks of sandstone around a metre cubed, that is dislodged and tumble onto the beach. Sliding failures appear to have been caused adversely oriented and continuous shears.

A total of two structural domains are identified in this site, A and B (Appendix G.7).

Discontinuity Condition

Similar to Wairaka Point a number of the defects, approximately 24%, were gapped or clean. The defect infill material was also highly weathered, moderately strong and consisted of crackle or rock material (Figure 3.52). Defects that do record finer material indicate mostly sand sized grains. Some defects displayed a dampness this is likely due to close proximity of the site to the ocean.

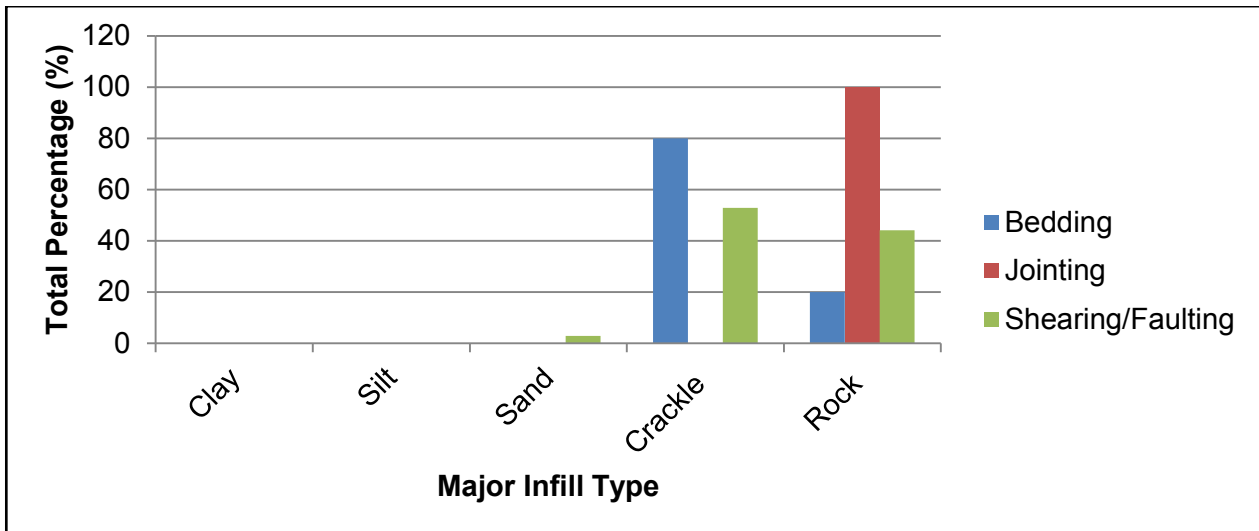


Figure 3.52: Defect infill material at Makara Head.

Shearing and Faulting shape appears to be wavier in comparison to most other sites (Figure 3.53). This is likely the result of smaller rock slope outcrops extents which unfortunately limit the ability to record the more continuous and persistent structures. Bedding appears to be more planar, with Inter-limb angles decreasing as wavelengths increase. The average defect roughness is Ro3. Defect thickness in bedding and shearing is dominantly moderately wide, while jointing is mostly tight to narrow (Figure 3.54).

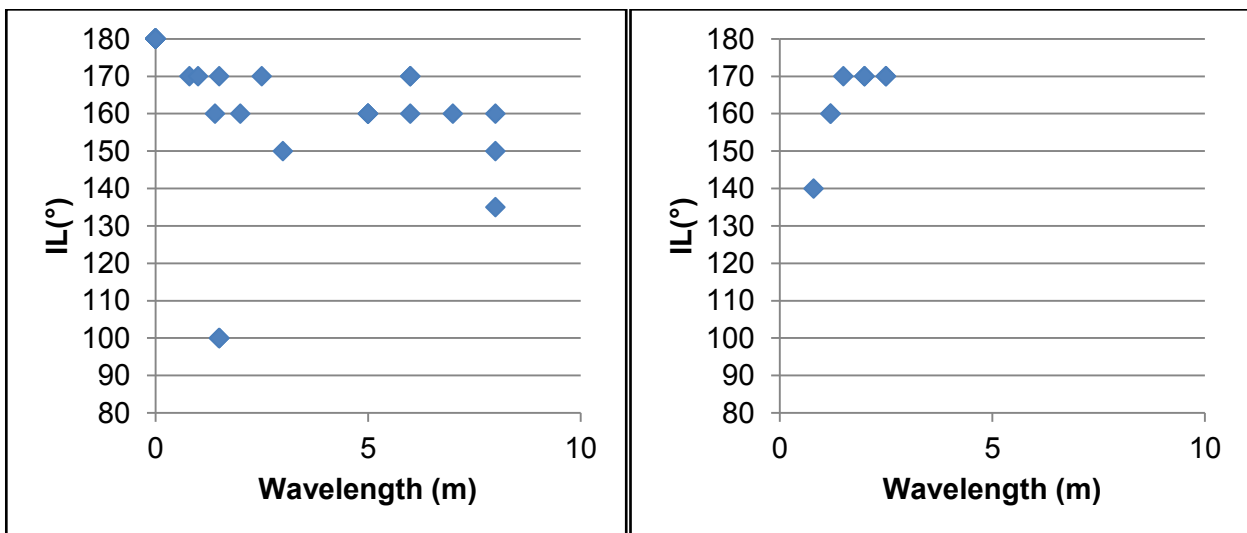


Figure 3.53: Graphs showing the defect waviness of shearing/faulting (Left) and Bedding (Right) at Makara Head.

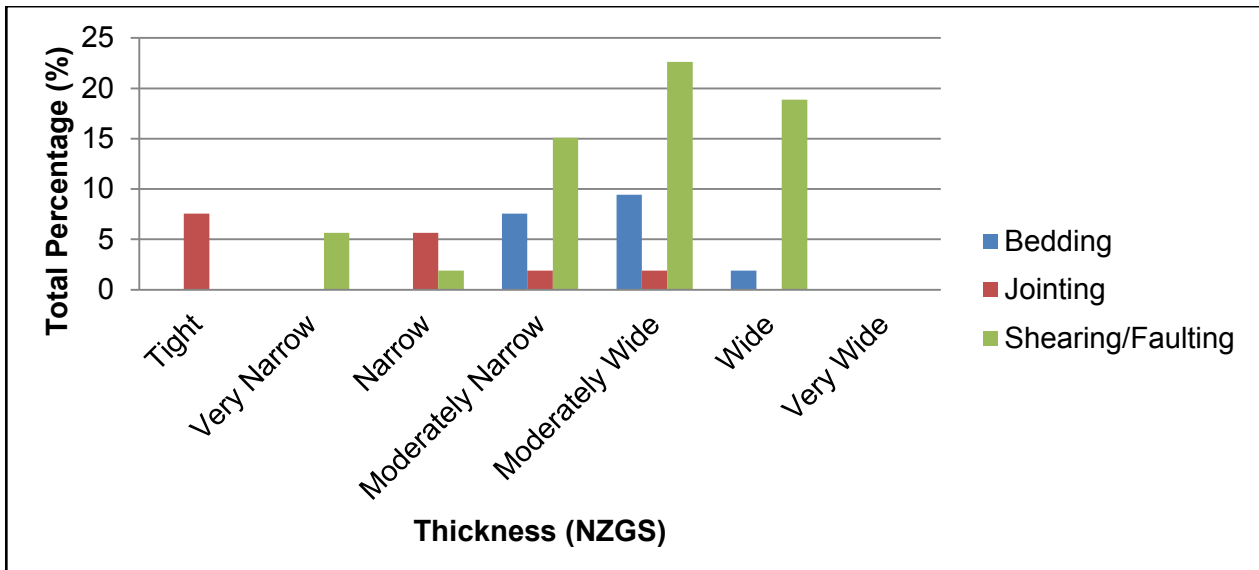


Figure 3.54: Makara Head defect thickness.

Stereonet Analysis

Bedding and shearing patterns are difficult to assess due to the limited exposure of rock outcrop. While the outcrop is mostly continuous around Makara Head most of the exposures are no more than 6 m high. This prevents identification of the more continual features (≥ 10 m) and rather increases occurrences of shorter less prevalent features included in the “filtered” data. The results indicate two vaguely defined conjugate forming shear sets that appear to rotate. Shear set one is trending northeast-southwest in the North to southeast-northwest in the South. Shear set two is not as well defined and is mostly trending in a singular direction, however, is mostly northwest-southeast to northeast-southwest. A number of isolated randomly oriented shears typically very steeply dipping is also displayed in the stereonet (Figure 3.55.a). Similar to Wairaka Point a distinction can be made between shearing and jointing sets (Figures 3.55.a and 3.55.b).

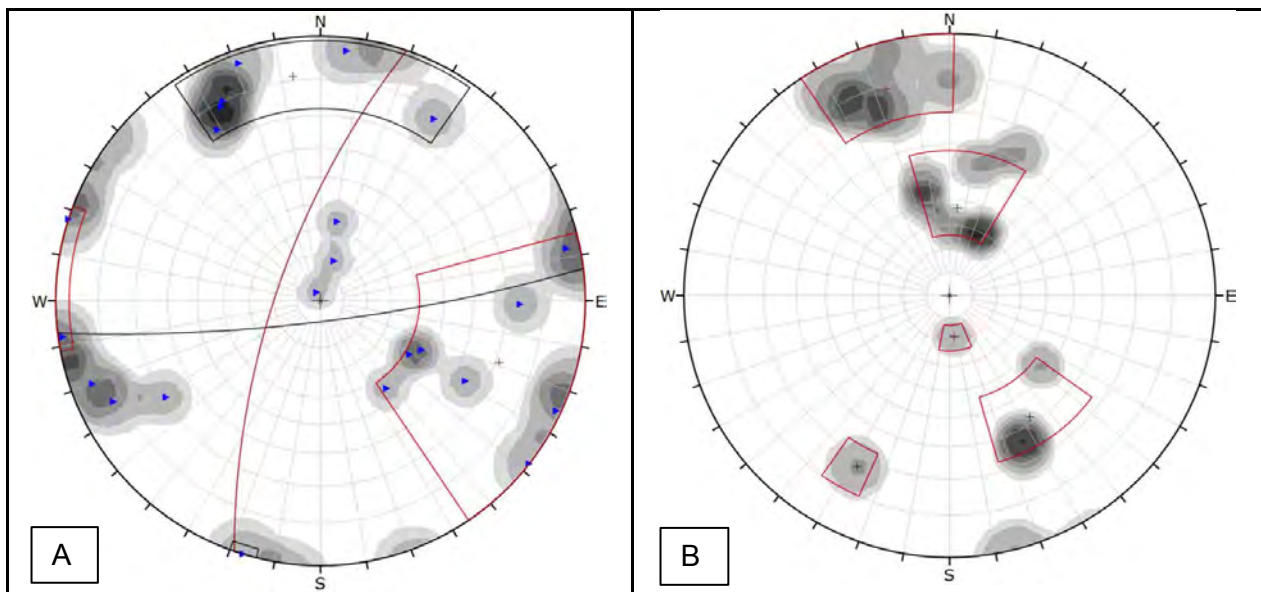


Figure 3.55: Makara Head A) stereoplot of "filtered" shearing data, B) contour plot of the joints.

Bedding also appears to rotate clockwise, likely in response to folding trending west-east. This is supported by Figure 3.56 which shows the use of the π -girdle method to interpret an upright, steeply plunging axial fold surface that is oriented west-east. Despite this no hinge line was visible. As mentioned in 3.1.6 this would suggest that there is no folding present. However, given that rock outcrop extents are relatively small and past papers such as Suneson (1992) also identified third generation folding trending west-east, it is perceived that folding is existent. No further analysis for folding is undertaken due to a lack of first and second generation folding.

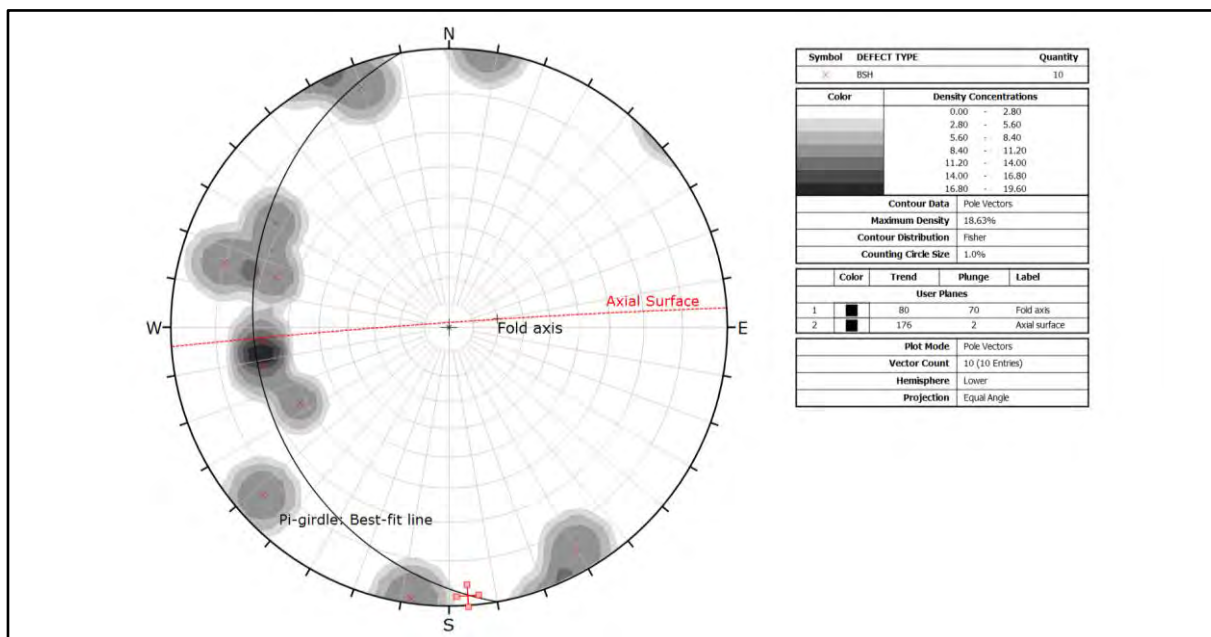


Figure 3.56: Stereoplot of bedding data collected from Makara Head. Shows the use of the π -girdle method to interpret folding.

CHAPTER FOUR REVIEW OF TRANSMISSION GULLY STRUCTURAL DOMAIN MODELS

4.1 Introduction

The design of rock cuts requires the collection of geotechnical data to identify conditions that may promote slope instability. This is often an iterative process, involving the collection of increasingly detailed data, initially from a far-field or regional scale to ultimately site-specific data. Investigations begin with initial field mapping programmes and evaluation of prior data and then progress through preliminary and final design stages, resulting in construction. During the latter stage, the observational method is implemented to update geological models developed in the previous stages, thereby leading to improved design and implementation of instability mitigation measures.

An important part of this process, particularly in regions of complex geology, is to define zones, in which similar lithological and structural characteristics are recognised. This process was used on the Transmission Gully project (Figure 4.1). Early identification of the complex sheared nature of the Torlesse composite terrane required additional geotechnical mapping and verification of the cut-slope design during the construction phase. The use of the observational method is a practical approach to designing in areas with unpredictable subsurface conditions.

The aim of this chapter is to explore and compare the structural zones established for the purpose of detailed design of the cut-slopes along the Transmission Gully alignment. Particular attention is given to comparison between the geotechnical data gathered from both preliminary and construction mapping phases in order to assess any variations and to identify the reasons for any departures from the established structural domain models.

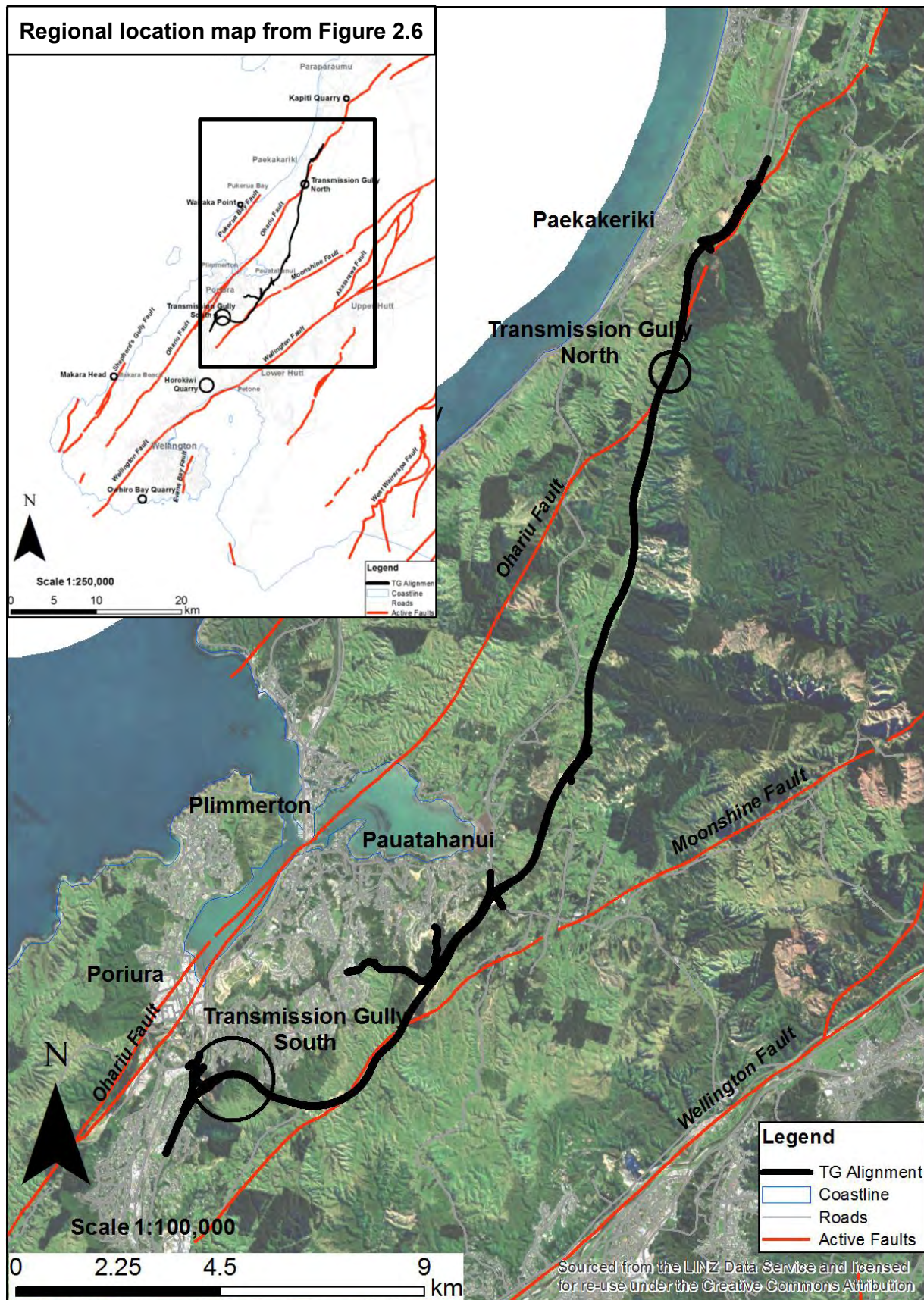


Figure 4.1: Map showing the Transmission Gully alignment and the primary (1st order) faults in the region. The Transmission Gully North and South study sites are highlighted. Data sources: LINZ and GNS.

4.2 Design Site Investigation Data

This section introduces the methods used in the early stages of cut-slope design for the Transmission Gully project. Information discussed here is useful in understanding the philosophy and methodology towards the final design of rock cut-slopes.

4.2.1 Data Collection Methods

Geological data collected in the early stages of cut slope design for the Transmission Gully project was mostly obtained by the use of borehole ATV (Acoustic Televiewer) and OTV (Optical Televiewer) surveys (AECOM and PSM, 2015). The use of ATV and OTV in borehole logging is common practice in capturing structural and geotechnical data. Televiewer surveys provide rapid and accurate high-resolution oriented images of borehole walls. Developed in the late 1960s (ATV) and 1987 (OTV) by the petroleum industry and as a stand-alone system (Weir, 2015) the two types of televiewer allow structural data to be captured from imagery by fitting sinusoids to discontinuity traces visible in the borehole wall. OTV uses lights and a camera to provide direct images of the drillhole wall and ATV uses the amplitude of a reflected acoustic signal. The combined application of ATV and OTV provides reliable structural data for sheared and fractured rock masses, such as the Torlesse, where the recovery of intact, oriented core may be difficult.

Additional site investigation methods included:

- Engineering geological mapping
- Test pits
- Hand auger holes
- Static cone penetration tests (CPT)
- Fault trenches
- Seismic refraction lines
- Piezometer instalments
- Laboratory testing

Field data were analysed to identify the critical drivers for potential global (large) slope instability. Structurally-controlled failure mechanisms, using persistent (mostly systematic) defects, were recognised as being the main source of instability along the project corridor. Thus, a rigorous assessment of the primary structural data sources was performed to identify the potential defect sets that may lead to instability. The design structural data set included 7639 measured defects, of which 6518 defects were solely detected from OTV and ATV surveys. Construction mapping recorded 1196 defects (as of February 2019). Design and construction mapping structural data are kept in separate databases for the duration of the Transmission Gully project.

The structural data gathered were classified into bedding and fabric related defects and shearing and fault-related defects. These structural data were plotted on aerial and terrestrial photographic panoramas and analysed using stereonet plots. Comparing the local changes in structural style with the regional (fault-bounded) structural domains allowed the identification of local structural domain zones. Although joints sets were also plotted on stereonets they were not used in the development of the structural domains.

4.2.2 Transmission Gully Alignment Structural Domains

Structural domain boundaries are dependent on the data at hand and are often developed based on intersections of major faults or changes in lithology (Mathis, 2016). Throughout the Transmission Gully alignment folds and minor regional faults and the associated structural patterns tend to cause a degree of variability within defined faulted 'blocks'. AECOM and PSM (2015) also mention that changes in bedrock lithology are subtle along the Transmission Gully route resulting in mostly structural lineaments and faults as the dominant selection for structural domain boundaries, others are selected based on changes in structural patterns between data points (AECOM and PSM, 2015). In areas where there was limited rock outcrop, or the ground is gently undulating, there was insufficient data to develop structural patterns so no domain was assigned. These areas had very few major cuttings so there was minimal impact on the cut slope design (AECOM and PSM, 2015).

A total of 22 domains, A through U, are defined along the length of the Transmission Gully alignment. No single domain spans less than 200 m of the alignment with whole cuts often occurring within one domain. In cases where whole cuts are split into more than one domain, these cuts tend to be larger in scale with more complex structural conditions. Such conditions can occur where proximity to regional faults or shearing may result in damage zones and associated faulting such as in the Wainui Saddle area (Figure 4.2). Smaller scale cuts typically remain entirely within soil or highly weathered rock zones enabling less internal variations resulting in a single structural domain, given that there are no adverse structural conditions or design conflicts identified. Domain A is an example of this. In this study the domain's that correspond with the selected study areas are those that will be examined and commented on. These domains include H, K and U. It is important to note that outcrop 1 (Appendix B.2) in the Transmission Gully South study area (Figure 4.3) does not have an assigned structural domain.

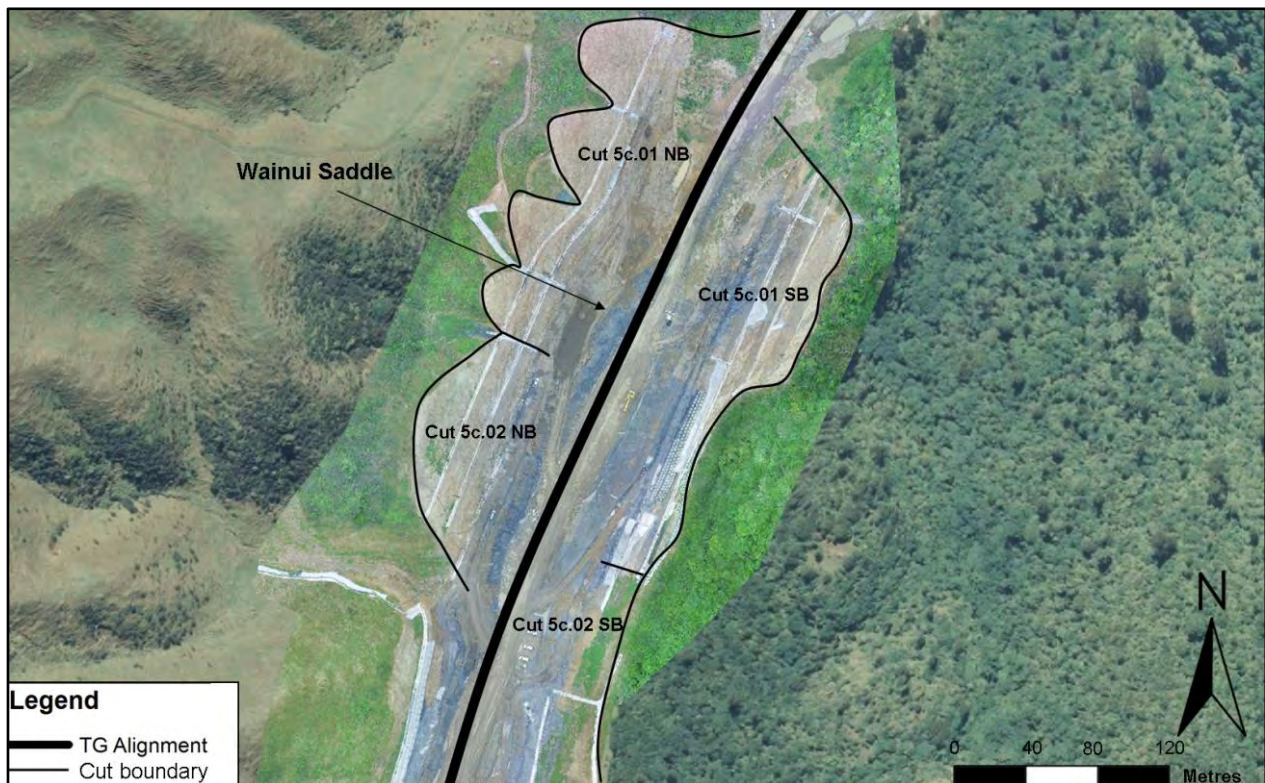


Figure 4.2: Map showing the location of key cuts in the Transmission Gully North site. Imagery sourced from the Transmission Gully GIS Database (2019). See Figure 4.1 for the location of this site.



Figure 4.3: Map showing the location of key cuts in the Transmission Gully South site. Imagery sourced from the Transmission Gully GIS Database (2019). See Figure 4.1 for location of this site.

4.3 Comment on Design Structural Domains

The following provides comment on the preliminary structural data provided from PSM (2014). Comments are based on observational information gathered from borehole logs and

interpretations from stereonet plots. In this section the stereoplots are separated into sub-surface (Borehole) and surface (Mapping) groups for the purpose of comparing 1D versus 2D views.

4.3.1 Transmission Gully North Study Zone

Drill core at the Transmission Gully North site indicates that the material present is mostly “Fault Disturbed” through to “Fault Crush Zone” Torlesse rock mass (Cammack et al., 2018).

The condition of the rock mass from the drill core is considered to be low quality. The “Fault Disturbed” rock mass has a high degree of faulting and folding with pockets of brecciated rock comprised of a mixture of “Fault Disturbed” and “Fault Crush” rock mass units. Typically, the rock mass is moderately weathered to unweathered with some areas indicating small amounts of highly weathered material. Intact rock mass strength is moderately strong to strong while defect infill material is generally comprised of weak to very weak brecciated or gouge infill. Joints are very closely to closely spaced and frequent bedding-parallel shears, shears and faults are moderately wide to widely spaced. Bedding is dipping steeply to very steeply. Logs also indicate groundwater very close to the surface, with seepage and saturated ground common in this area.

Low quality rock mass conditions at this site are intrinsically related to the proximity of the Ohariu Fault, which transects the study area (Appendix H.1 to H.4). The active Ohariu Splinter Fault also runs along the Transmission Gully alignment in the Horokiri Valley before meeting the main Ohariu Fault at the Wainui Saddle (located in the southern section of Domain K) (Figure 4.2). Rock fabric is therefore expected to have an increase in local shearing and faulting proximal to the major fault structure. This is also explained in Section 2.2. Given this interaction it is reasonable that the Ohariu Fault acts as a boundary between structural domains. A total of two structural domains, K and H, are examined in this section as they correspond with the Transmission Gully North study zone.

Domain K – East Side of Ohariu Fault

Bounded on the west by the Ohariu Fault, and by changes in structural patterns in the North, Domain K is markedly controlled by shearing and faulting (associated with the regional major structure). There are two cuts located within this domain, C5c.01 and C5c.02 South bound (Figure 4.2). The alignment is oriented around a bearing of 020° at this location.

On a stereoplot, shearing shows a large degree of scatter (Figure 4.4). However, there are two apparent clusters which are consistent across both the cuts. The general orientations of the clusters typically occur at around 46/142 and 48/320 (Dip/Dip-direction) with the later shear set appearing to dip sub-parallel with bedding (Shear set B). This interpretation is supported by Figure 4.5 which indicates that the overall bedding trend is towards the East. This correlation between bedding and shearing is a common characteristic throughout this domain.

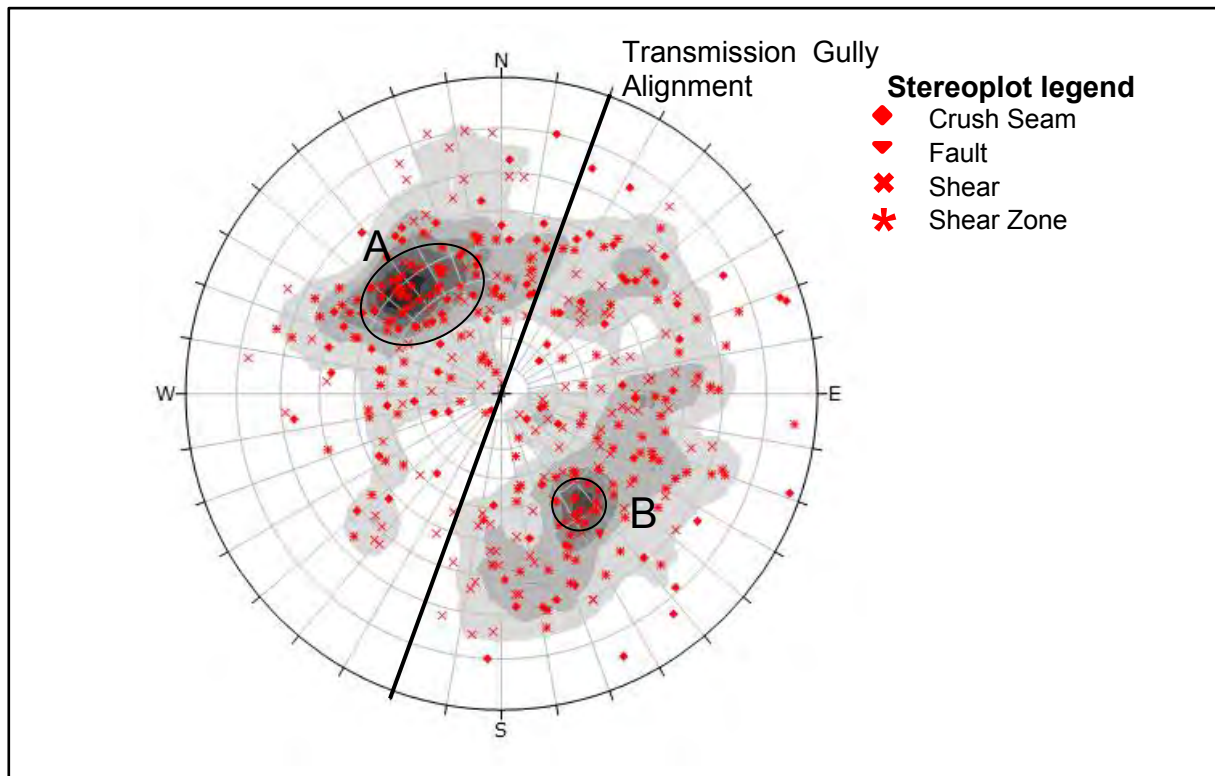


Figure 4.4: Domain K Stereonet displaying the televiewer shear and fault related shear data. Data sourced from PSM (2014).

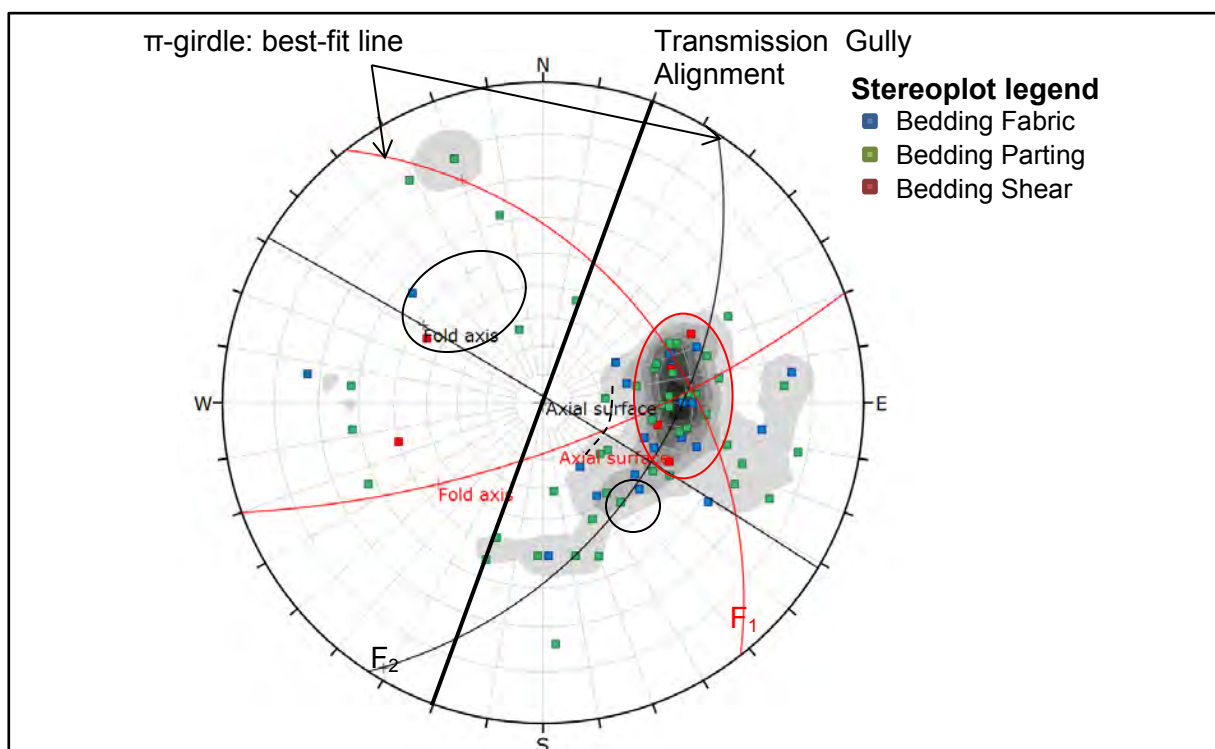


Figure 4.5: Stereonet displaying the bedding televiewer data in domain K. The red circle highlights a cluster of bedding data. The clusters, as indicated by the black circles have been overlaid from Figure 4.4 to aid in understanding the link between the shearing and bedding. Data is sourced from PSM (2014).

Further discussion on the overall pattern of the bedding poles is shown by the contour plots (Figure 4.6). Clearly, the data is mostly constrained in the eastern hemisphere of the stereonet inferring that the bedding is mostly dipping towards the west. Distribution of the bedding poles also shows a degree of rotation suggesting spread may account for a girdle distribution. Two π -girdle or best fit lines are presented here, labelled F_2 and F_1 . Examination of these π or best fit planes indicate that a high density of the poles lies between 050° - 200° for F_2 , and 050° - 120° for F_1 . The fold axis is the pole to the π circle which is trending roughly northwest and southwest, F_2 and F_1 respectively. Contour diagrams highlight the occurrence of asymmetrical folds within the F_1 fold and concentric folding in the F_2 fold. Computation of the F_1 fold orientation shows a degree of parallelism with the major first order fault structures implying that there is a direction of compression in the northwest-southeast direction. Given that deformation mechanisms (Ohariu Fault) are prevalent it is expected that folding will be produced, most likely forming an echelon arrangement as a result of the inherent geometry of strike-slip faults (Twiss and Moore, 1992). The F_2 fold axis is roughly west-northwest to east-northeast potentially indicating an anticline. The identified folds also appear to both be moderately plunging.

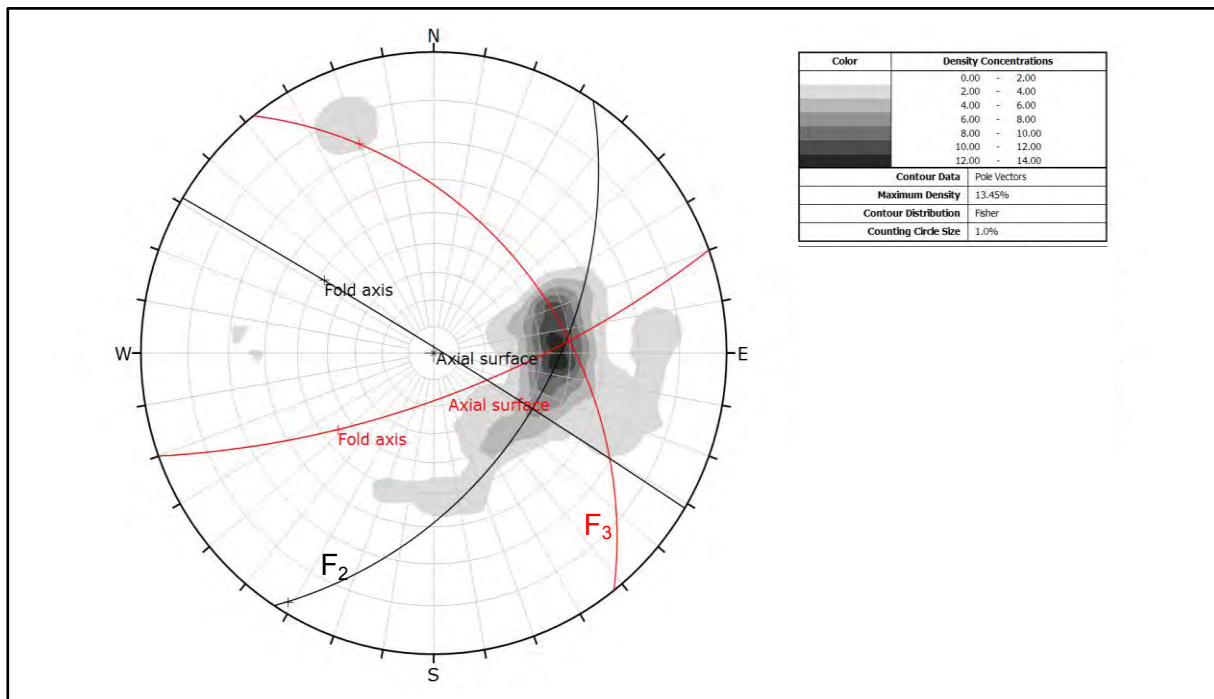


Figure 4.6: Stereoplot of the bedding poles contour data for Domain K. The red, black and blue greater circles indicate potential fold orientations based on a π -girdle line of best fit. Data is sourced from PSM (2014).

Bedding and shearing data collected from design mapping exercises are displayed in Figure 4.7 and Figure 4.8. There is significantly less data collected in the mapping design data compared to that sourced from the ATV and OTV surveys, in particular for the shearing data. While the data does show some correlation with shear set B the link is weak. For this reason, there can be no

unique interpretation made. However, this is not the same for the bedding data. While there is significantly less data there was sufficient to establish a pattern. The bedding pole plots and contour diagram (Figure 4.8) were used to draw best-fit pole girdle and highlights a northeast-southwest π -girdle trend. Examination of the bedding poles from Figure 4.8 indicates that a high density of the poles lie on the π -girdle best-fit line between 310° - 350° suggesting a potential fold dipping towards the southeast. On first glance the patterns identified from the design mapping data appear to produce no relationship to the televiewer data, however, a distinction between the orientations of the different folding can be identified. In the event that these folds do exist it is likely that the northwest trending fold from the televiewer data and the southeast trending fold from the mapping data form the same geological feature. The axial surface/planes of these two features are almost identical with the fold axes of the mapping data located on the axial surface of the televiewer logs. Relatively closely located design mapping bed data locations are then used to interpret all fold geometries. The result could infer a potential double plunging fold to the northwest and southeast generating a topographic high based on the changing dip orientations (Appendix H.1 and H.2).

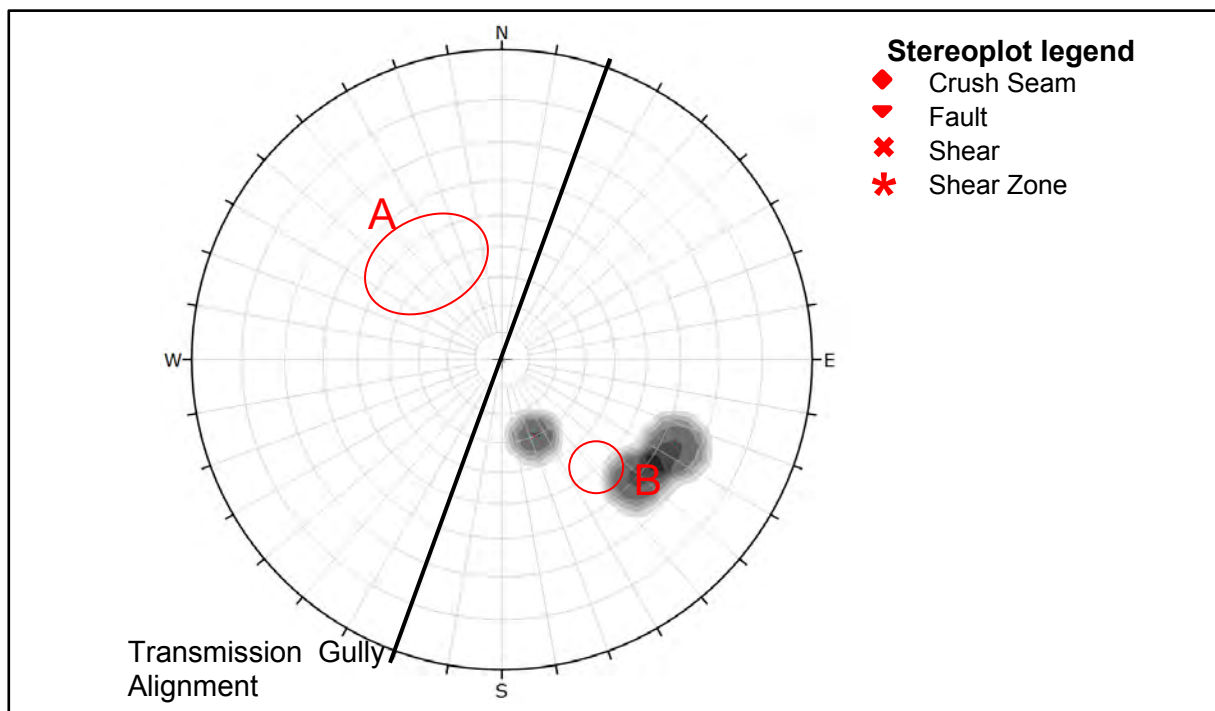


Figure 4.7: Stereonet of design mapping shear and fault related shear data for Domain K. The red circles indicate the main clusters identified in Figure 4.4. Data is sourced from PSM (2014).

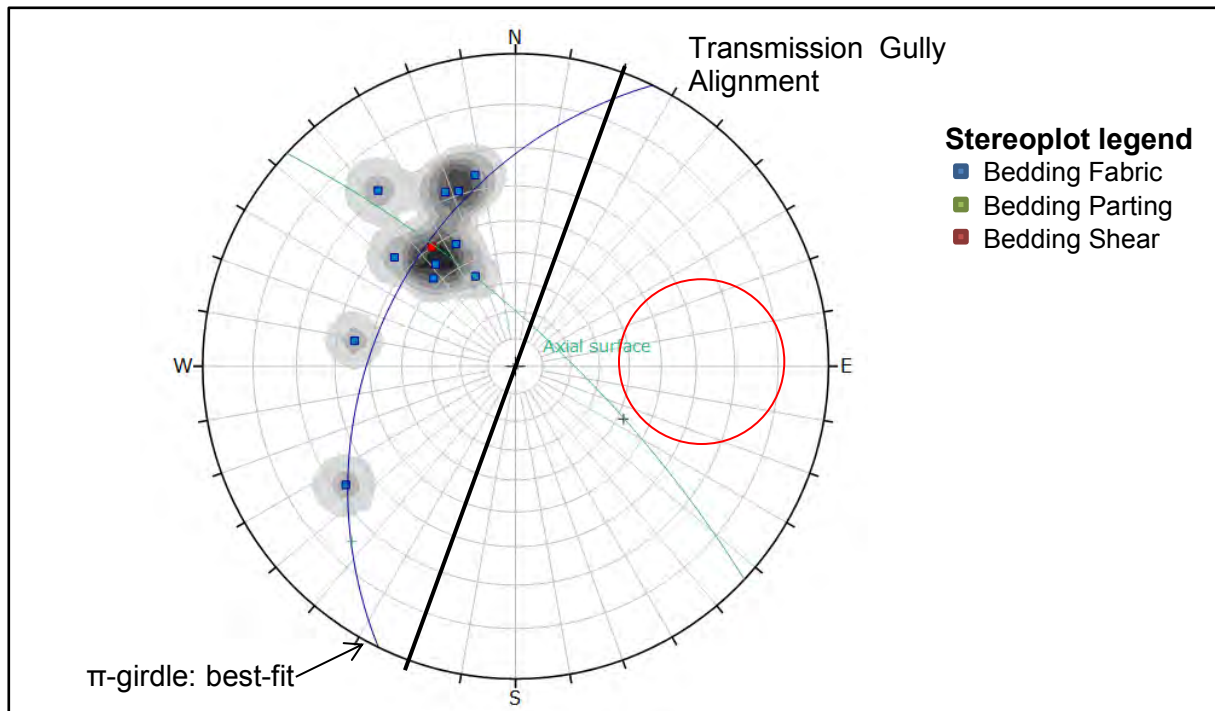


Figure 4.8: Stereonet of mapping bedding data for Domain K. The red circle indicates the main cluster of bedding data identified in Figure 4.5. Data is sourced from PSM (2014).

Domain H – West Side of the Saddle Cutting

Domain H is bounded by the Ohariu Fault to the east, a boundary which is shared with Domain K. Neighbouring Domain H to its north is Domain G, and Domain I lies to its south (Appendix H.3 and H.4). The domains are detailed by the changes in structural patterns. As in Domain K, the geological structure in this area is predominantly controlled by shearing and faulting associated with the regional major structures. There are three cuts located in this domain: C5c.01, C5c.02 and part of C5b.01 north bound (Figure 4.2). The alignment is oriented around a bearing of 020° at this location.

A stereographic plot of the shearing data taken from the televiwer dataset at Domain H is shown in Figure 4.9. The bulk of the poles to planes represent a cluster around 60/265 (Dip/ Dip-Direction) which is fairly consistent throughout the domain. Outside of this cluster the pattern of the poles is relatively scattered. Similarly, the bedding distribution displays some scatter as shown in a separate stereoplot (Figure 4.10). Since, the scatter of the bedding data is fairly large, there is no well-defined correlation between the bedding and shearing televiwer data. Despite this, a single dominant bedding set around 65/195 is shown in the figure below, and the main shear set at 60.265 is located proximal to the low-density bedding clusters dipping about 040 to 080 to the west. Therefore, while there is no well-defined correlation between bedding and shearing pole distributions an inference can still be made.

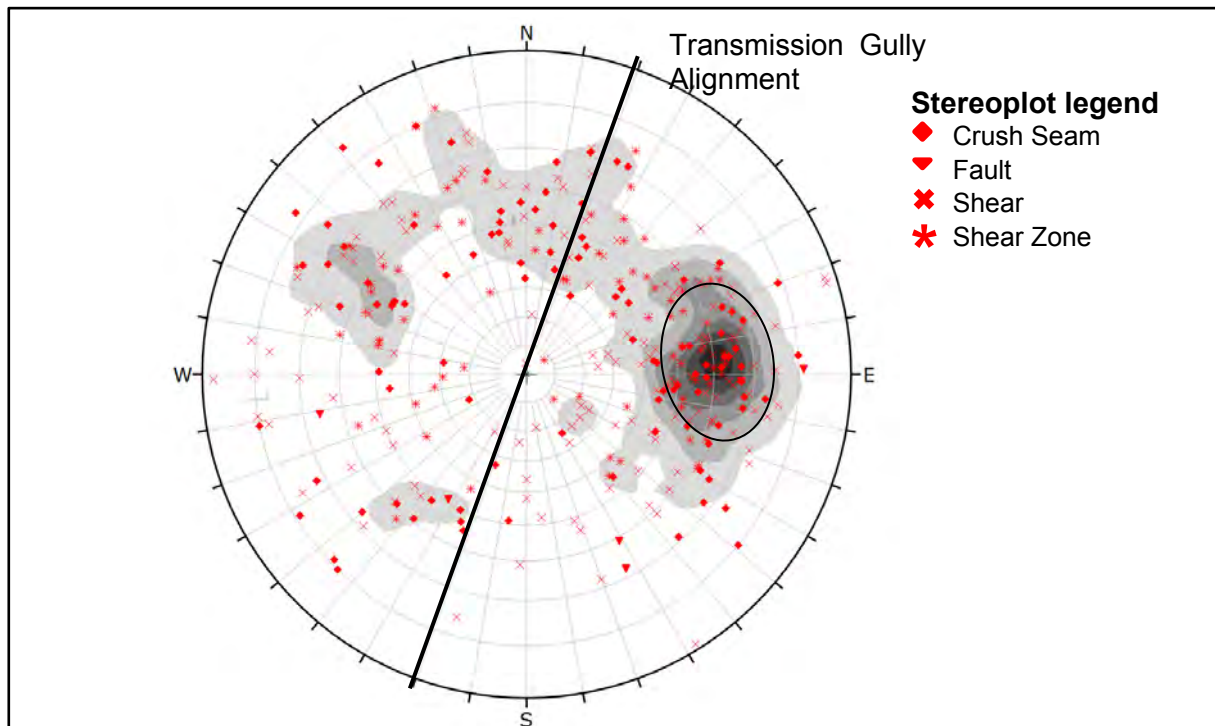


Figure 4.9: Domain H stereonet displaying televiewer shearing data. The black circle shows the location of the Data obtained from PSM (2014).

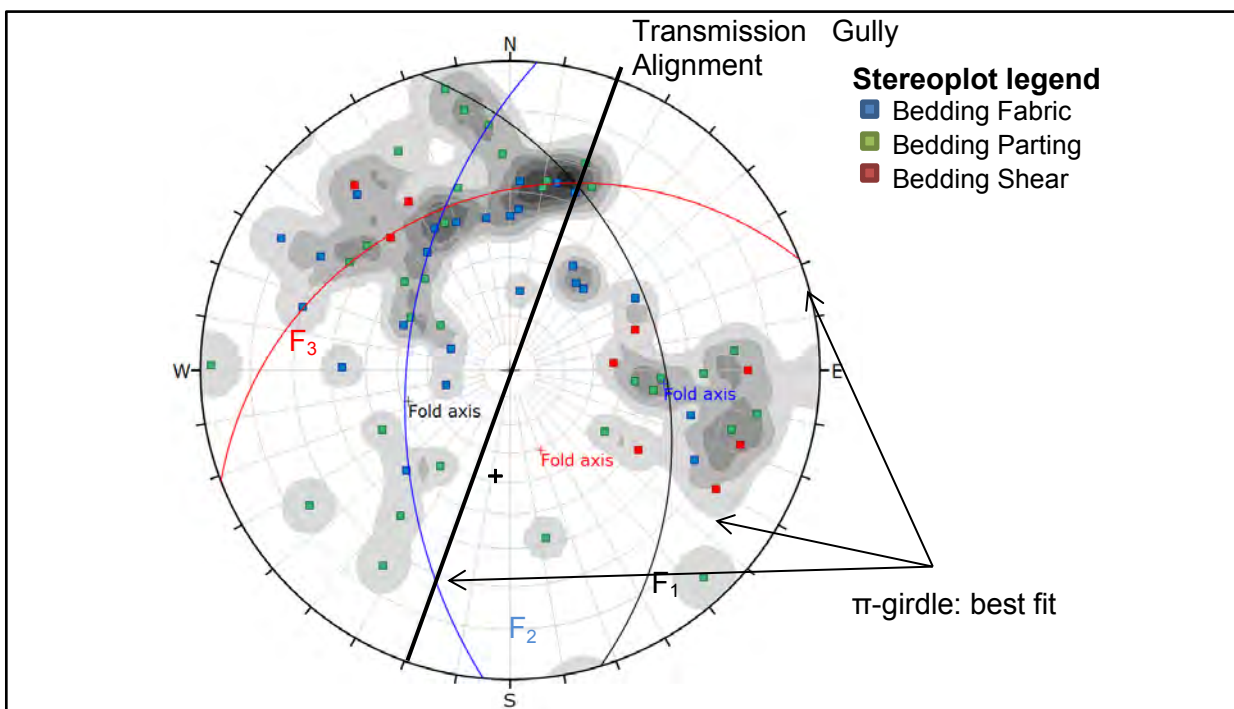


Figure 4.10: Domain H stereonet plot displaying the distribution of televiewer bedding data in Domain H. Data is obtained from PSM (2014).

Bedding and bedding plane shears distributed across the domain appear to infer folding trending northeast sub parallel to the alignment (Figure 4.10). Since, the data is widely spread within the overall distribution of the bedding stereoplots (Figure 4.10) there is no unique interpretation as the

bedding poles cannot be constrained to a large or small circle. However, a distinction is made between individual borehole bedding televiewer stereoplots, displaying the rotation of bedding about a potential synformal hinge oriented northeast-southwest (Appendix H.3 and H.4). Further investigation of the bedding stereoplot using a girdle distribution supports this interpretation. Three potential π -girdle best-fit lines are presented here (Figure 4.10), labelled F_1 , F_2 and F_3 . The axial surface of F_1 is oriented roughly southwest-northeast which is roughly parallel with the initial interpretation. F_2 while the π -girdle fold axis is oriented sub-parallel with F_1 the fold axial is trending west-east suggesting that these folds are not a part of the same geological structure. F_3 axis is trending southeast which is oriented roughly perpendicular to the Ohariu Fault. This F_1 , F_2 and F_3 pattern forms an en echelon arrangement which lines up with the typical model of strike slip faults (Figure 4.11).

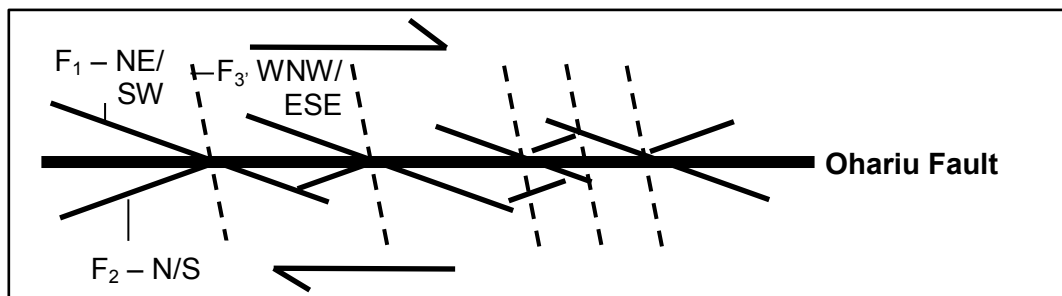


Figure 4.11: Orientation arrangement of Folds associated with the Ohariu Fault. Figure 4.adapted from Twiss and Moore's (1993) subsidiary R, R', and P shear fracture arrangement model.

Analysis of the contour diagram (Figure 4.12) highlights the fold geometries of stereonet projected folds, F_1 , F_2 and F_3 . Patterns in the stereonet of the degree of clustering correspond to the curvature of the folded surface. F_2 and F_3 present roughly identifiable planar limbs indicating concentric folding, whereas F_1 resembles mostly dual clusters of poles with one limb more pronounced than the other suggesting asymmetrical folding.

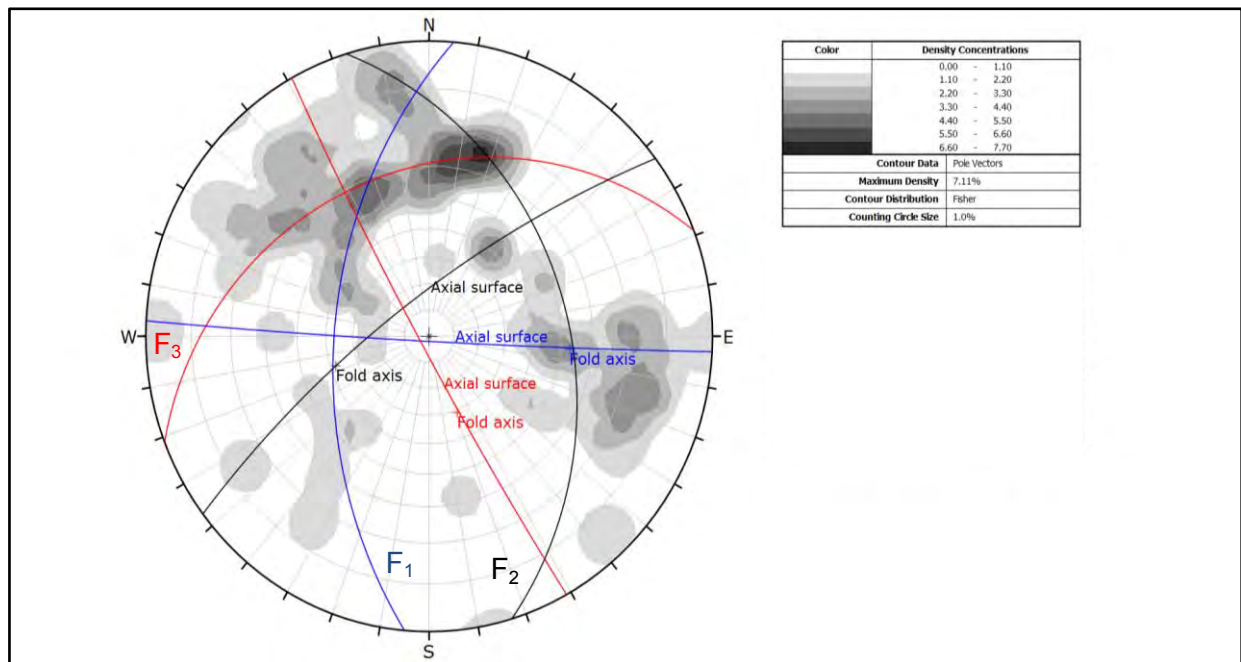


Figure 4.12: Contour diagram of the televiewer bedding data for Domain H. Data collected from PSM (2014)

Further bedding and shearing data collected from mapping carried out prior to this study for the purpose of the detailed design of the Transmission Gully project is presented in Figure 4.13 and Figure 4.14. As in Domain K there is significantly less data collected by mapping compared to the televiewer data. However, there is enough data available from the mapping dataset to make a number of important linkages for shearing and bedding orientations.

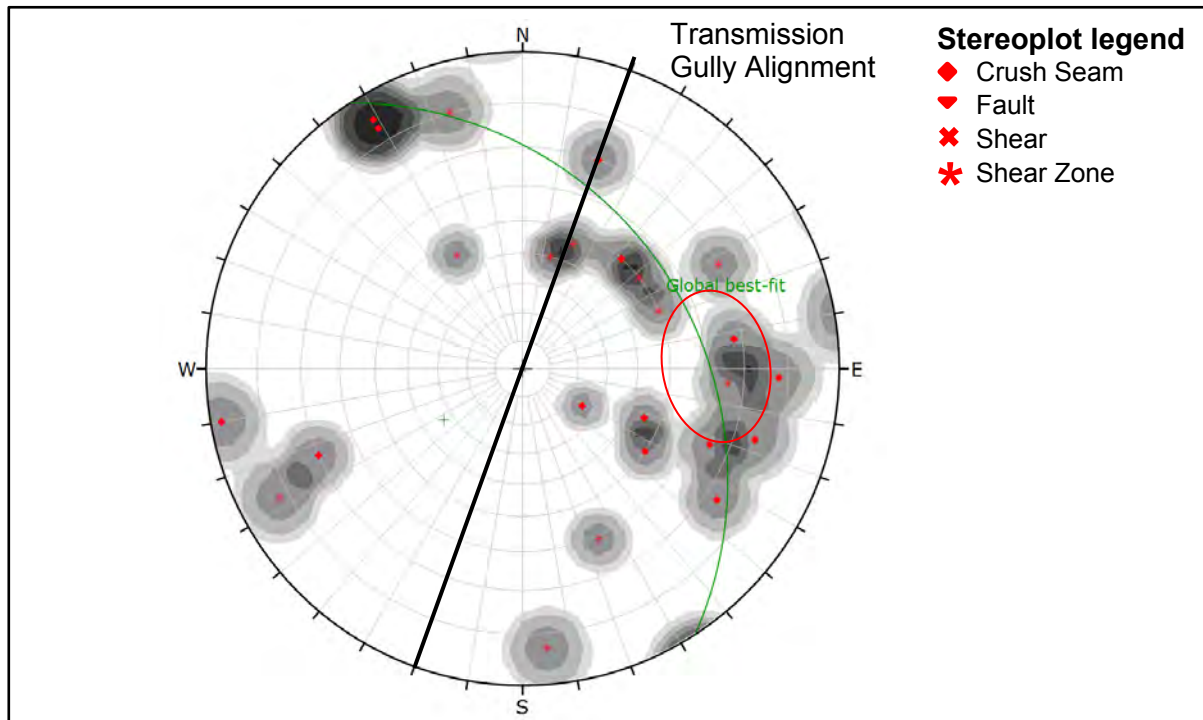


Figure 4.13: Stereonet of the design mapping shear and fault related shear data. The red circle indicates the main cluster of shearing from the televiewer data in Figure 4.9. Data is obtained from PSM (2014)

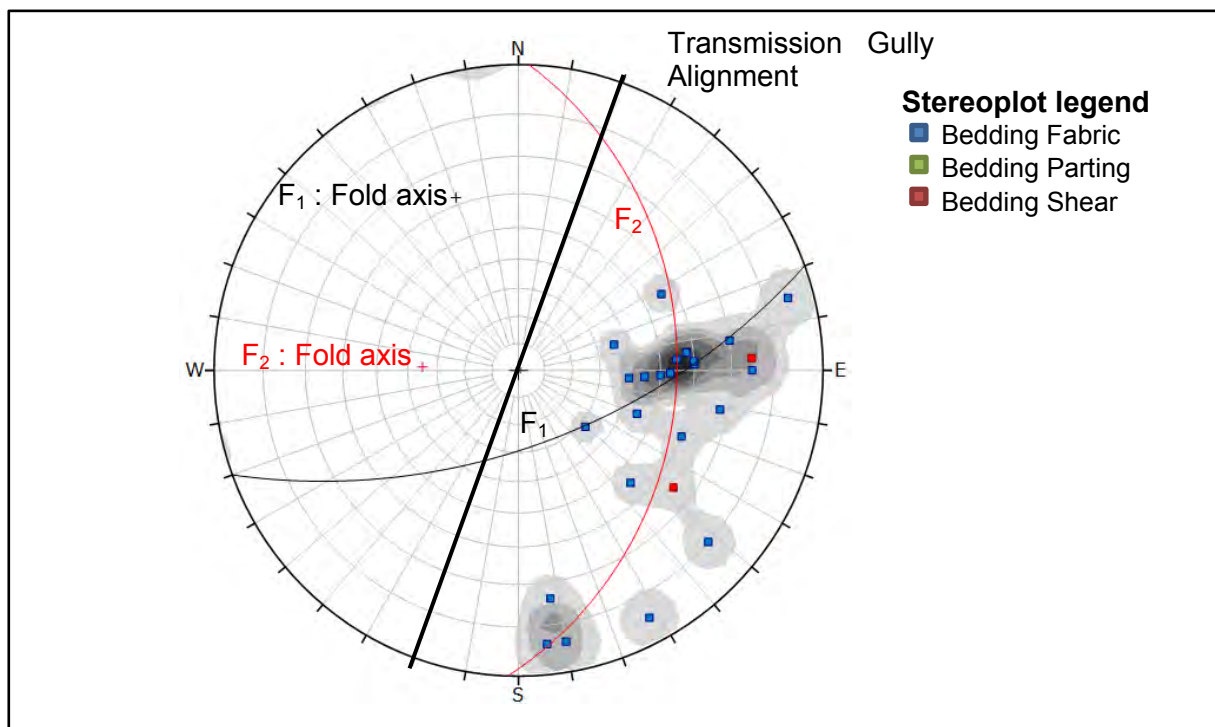


Figure 4.14: Stereonet of the mapping bedding data. Data is obtained from PSM (2014).

Distribution of the poles to the shearing planes from the mapping dataset displays a degree of scatter, making cluster interpretation difficult. Since the scatter is fairly wide the contours of the shearing feature poles were used to plot a best-fit line. The result is a broadly group of small

clusters centred close to the main shear set from Figure 4.13. Further examination of these stereoplots indicates potential shearing rotation, seeing that both televiewer and mapping stereoplots obtain two gaps in the dataset which are roughly the same size. These two gaps appear to have rotated clockwise from 270-230 and 200-150 in the televiewer data to 325-265 and 215-175 in the mapping data. This may be possible due to folding or given the increase in distance in the mapping locations from the boreholes, around fifty meters.

Distribution of the bedding data obtained from the mapping exercise appears to be typically orientated around 55/270 dipping to the east. This partially lines up with a small part of the distribution of bedding data collected from the televiewer. As with the televiewer data the mapped bedding poles distribution is fairly wide suggesting that the girdle method can be used. It is interpreted that two potential π -girdle/best-fit lines are observed with fold axes trending roughly north-northwest and west (Figure 4.14). The latter is almost identical to that of F_1 , while the former is trending in exactly the opposite direction to that of F_3 and is positioned close to the axial surface line. This suggests that the latter pairing maybe a part of the same geological feature indicating further that F_3 may be a double plunging fold.

4.3.2 Transmission Gully South Study Zone

Drill core at the Transmission Gully South site indicates that the material present is mostly “Margin Zone” through to “Fault Disturbed” Torlesse rock mass (Cammack et al., 2018).

The rock mass condition from drill core is understood to be in relatively better condition than the Transmission Gully North study zone. The Margin Zone material is associated with medium to high tectonic disturbance due to the increased distance away from major regional active fault lines. Shearing and faults are moderately widely spaced to widely spaced with silty-fine sandy infills, occasionally infill is comprised of brecciated rock or gouge material. Typically, the rock mass is moderately weathered to unweathered in mostly sandstone dominated material. Intact rock mass strength is moderately strong to strong while defect infill material ranges from moderately strong to very weak. Joints are generally very closely spaced to closely spaced clean, stained or sometimes with veneer infill. Logs indicate that mudstone proportions have slightly increased thicknesses relative to the north study site, with bedding that is typically disintegrated or sheared with an increasing frequency. Groundwater is relatively deeper with water levels in the East roughly between four and fifteen meters below the ground surface, and between twenty-four and fifteen in the West.

The nearest major fault traces are around five kilometres away, the Moonshine Fault is in the east and the Ohariu Fault in the west. A series of high angle cross faults link these structures and are thought to be actively accommodating the tectonic stresses in this area. It is expected that this faulting is the main influence controlling the rock mass structure in this study zone. Due

to the increased distance from major fault traces it is expected that rock fabric will have a decrease in local shearing and faulting. This is also explained in Section 2.2.

Unlike the North study zone the structural domains in this site is not split into north bound and south bound, instead the domains include both sides of the alignment (Appendix H.5 and H.6). Also, there is only one structural domain identified, Domain U, in the East of this site. However, there is borehole data available for this area so for the purpose of this study it will still be assessed and labelled as a made up “No Domain”.

Domain U – East of the Kenepuru Interchange

Domain U is bounded by a northeast trending fault to the west and by changes in bedding orientation in the east (Appendix H.5 and H.6). Faulting and shearing from high angle cross faults appear to be the main control on structure in this domain. There are two cuts located within the extents of this domain that obtain borehole data, C40.02 North and South bound (Figure 4.3). The alignment is oriented around a bearing of 100° at this location.

A stereoplot of televiewer shearing data in this domain is shown in Figure 4.15. This stereoplot displays two clearly defined clusters dipping roughly perpendicular to the alignment with some scattered data. These clusters typically dip parallel to bedding around 60/250 and 65/090 (Dip/Dip direction). This interpretation is supported by Figure 4.16 which indicates that bedding is trending parallel or sub-parallel to both shear sets.

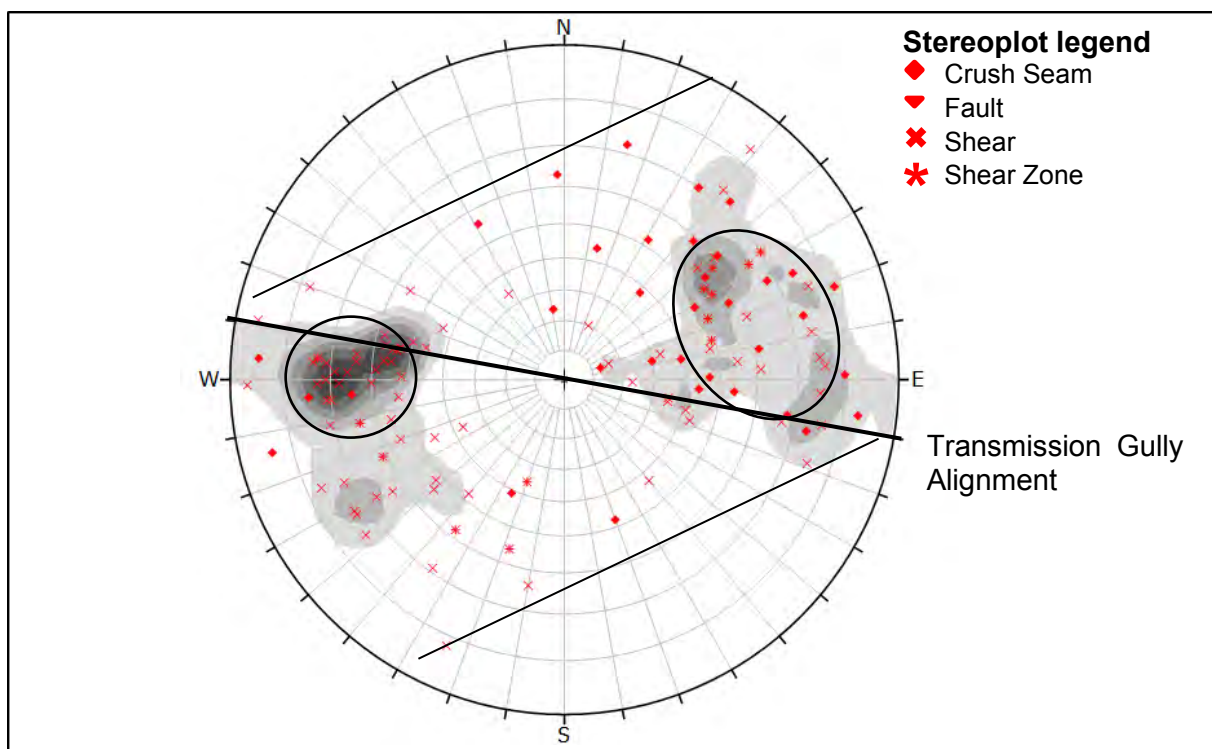


Figure 4.15: Stereoplot of the Shearing televiewer data for Domain U. The black circles represent two clusters of shearing. Data is sourced from PSM (2014)

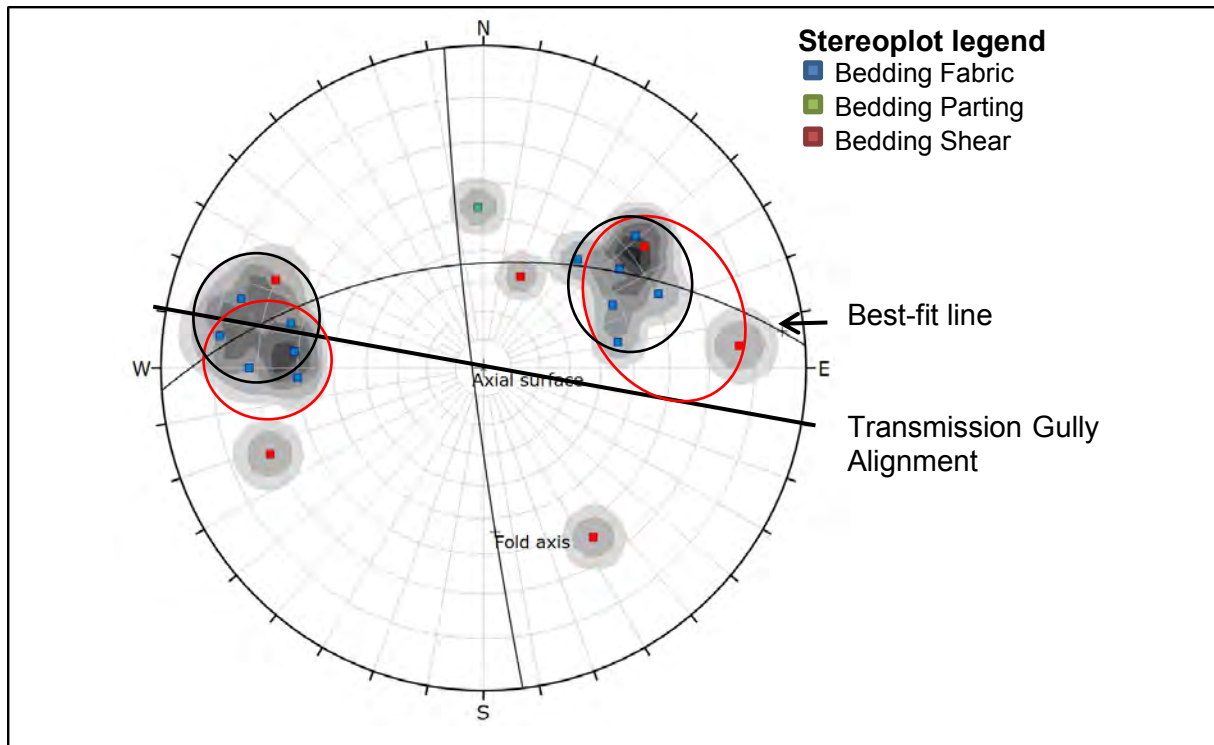


Figure 4.16: Stereoplot of bedding televiewer data for Domain U. Bedding has been grouped into two clusters represented by the black circles. Shearing clusters from Figure 4.15 are represented by the red circles. Data is sourced from PSM (2014).

Moderate scatter of the shearing poles may be interpreted as poles to planes of isolated discrete features. This is an important interpretation, one that is also made in the North study zone.

Further examination of the bedding distribution (Figure 4.16) suggests that folding with a hingeline oriented north-south is present. The two clusters described indicate two fold limbs that are 130° apart suggesting the geometry is a gentle, moderately plunging Chevron fold. Further comparison to the location of these boreholes indicates that this fold is likely to be an anticline that is sub-parallel to the nearest major fault traces.

There is a notable decrease in scatter compared to the North study site. This is likely due to a decrease in boreholes signifying less televiewer data in the South study zone, therefore reducing the amount of structural data available. Furthermore, another reason may be due to more complex structure in the north and therefore less variability is expected at this site. Another point worth acknowledging is the spatial distribution of the shearing scatter between borehole locations. There appears to be a confined area where shearing is limited too (Figure 4.15). Additionally, the shearing clusters appear to mimic that of the bedding. Shearing in the northern section of this domain presents poles that are mostly concentrated dipping towards the west likewise with bedding. The opposite orientation occurs in the south where bedding and shearing appear to mostly dip towards the east (Appendix H.5). This is likely a result of folding.

Bedding and shearing data collected from design mapping exercises conducted prior to construction are displayed in Figures 4.17 and 4.18. There is significantly less data collected from mapping compared to the data from ATV and OTV surveys. However, in this instance there is not enough data available in order to make any interpretation.

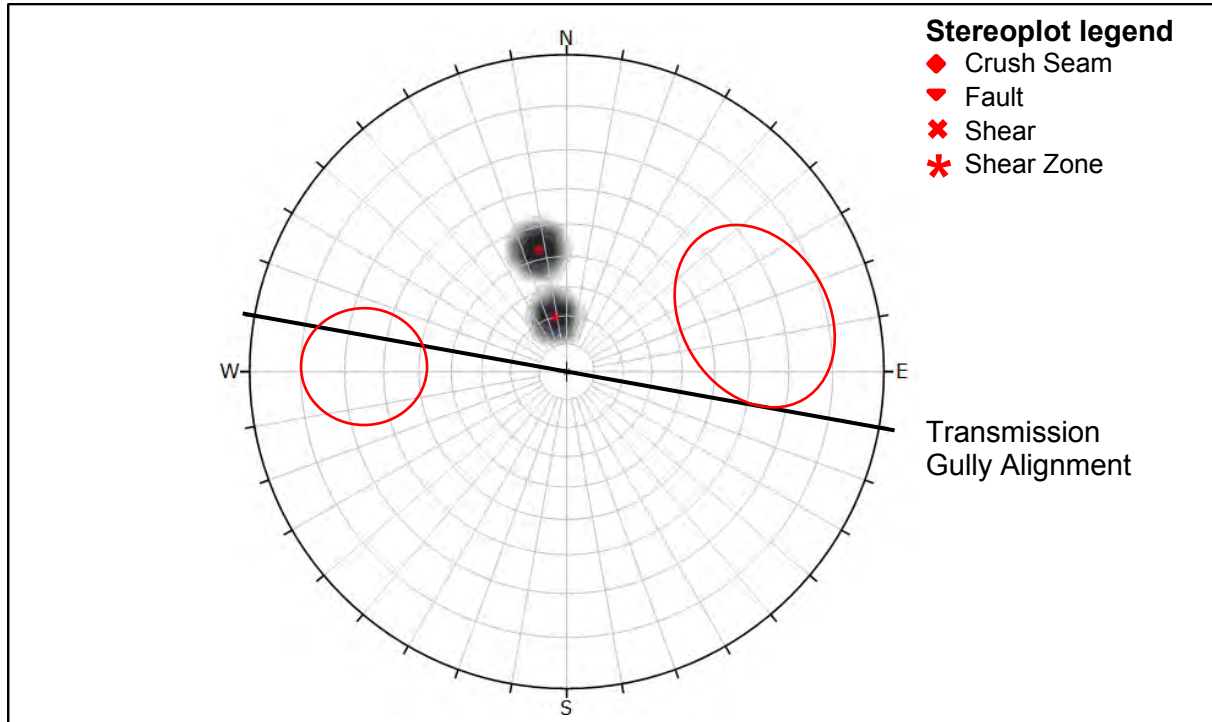


Figure 4.17: Stereoplot of the design mapping shear and fault related shear data for Domain U. The red circles indicate the clusters of shearing from televiewer data. Data is sourced from PSM (2014).

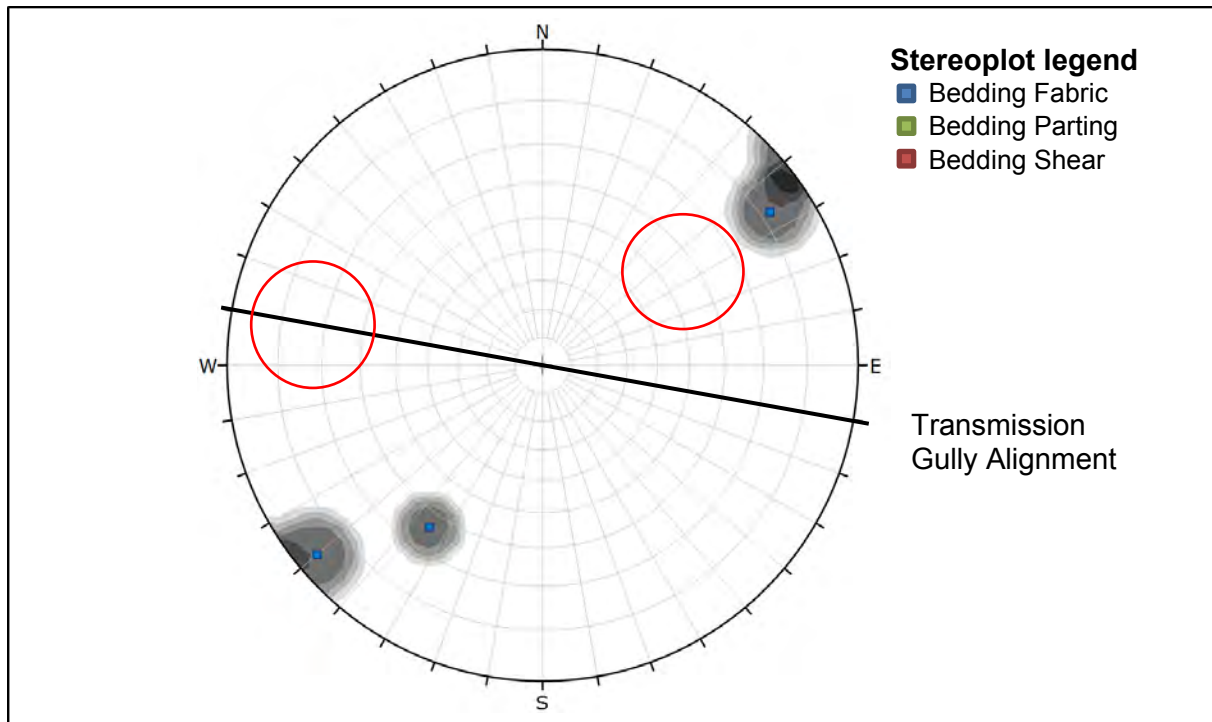


Figure 4.18: Stereoplot of the design mapping bedding data for Domain U. The red circles represent the clusters of bedding from the televiewer data in Figure 4.10. Data sourced from PSM (2014).

“No Domain” – Kenepuru Interchange

This area is not recognised as a structural domain and so is labelled as a “No Domain” area for the purpose of this study.

This area obtains only one faulted boundary in the east, which is shared with Domain U (Appendix H.5 and H.6). The Western boundary is not drawn on the map and its unknown how far along the Transmission Gully alignment it extends. The main influence controlling structure appears to be the faulting and shearing of the high angle cross faults. A number of cuts are located within this vast area however only two boreholes with televiewer data are present. These boreholes are located closest to largest cut in this area, C42.01 south bound (Figure 4.3). The alignment in this area trends approximately bearing 070°.

A stereographic plot of the televiewer shearing data in this area is presented in Figure 4.19. Similar to Domain U the stereoplot displays a moderate scatter of poles, likely representing discrete features however there are differences in the clustering. Unlike Domain U the bulk of the poles occur in three clusters that are vaguely defined, around 55/200, 70/035 and 45/065 (Dip: Dip-Direction). There is enough data to make some clear observations on the data spread however, the inferences are not backed by strong correlations leaving this area open to further interpretations. This could explain why this area had not been grouped into a domain and was left unlabelled. Bedding data collected from borehole data is displayed in Figure 4.20.

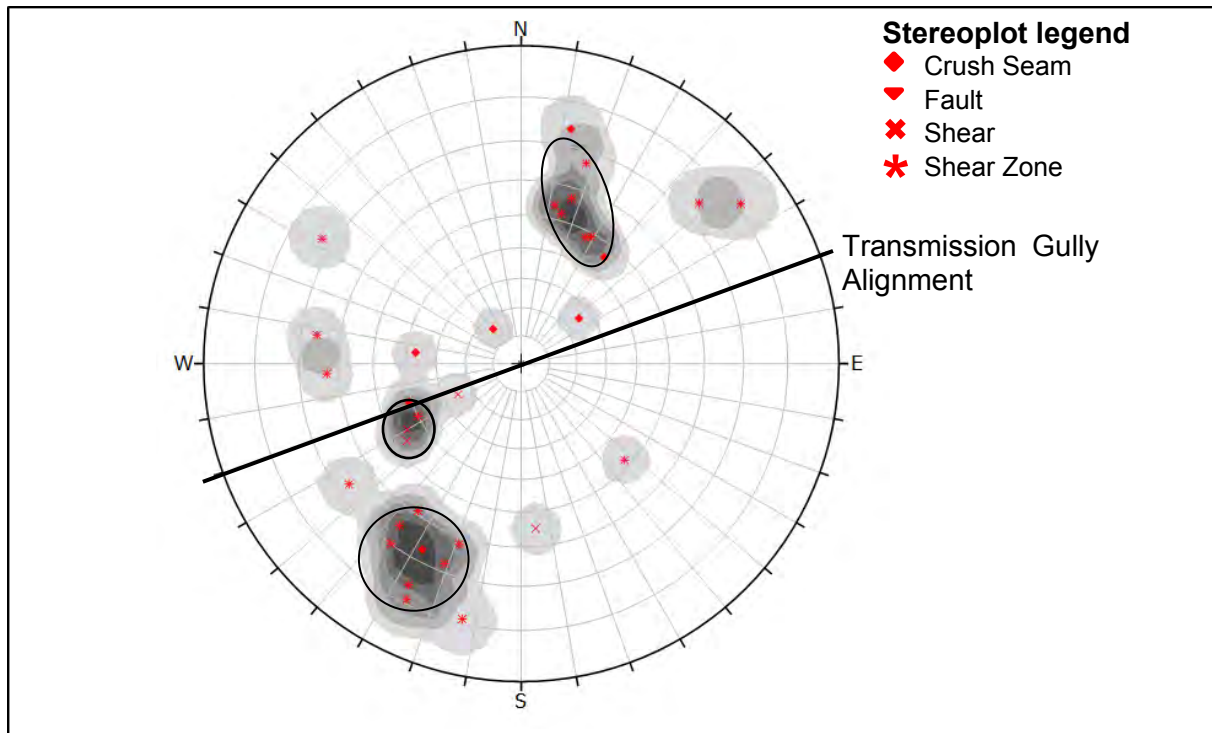


Figure 4.19: Stereoplot of the televiewer shear and fault related data in the “No Domain” area within the Transmission Gully South study area. The black circles represent three clusters of shearing. Data is sourced from PSM (2014)

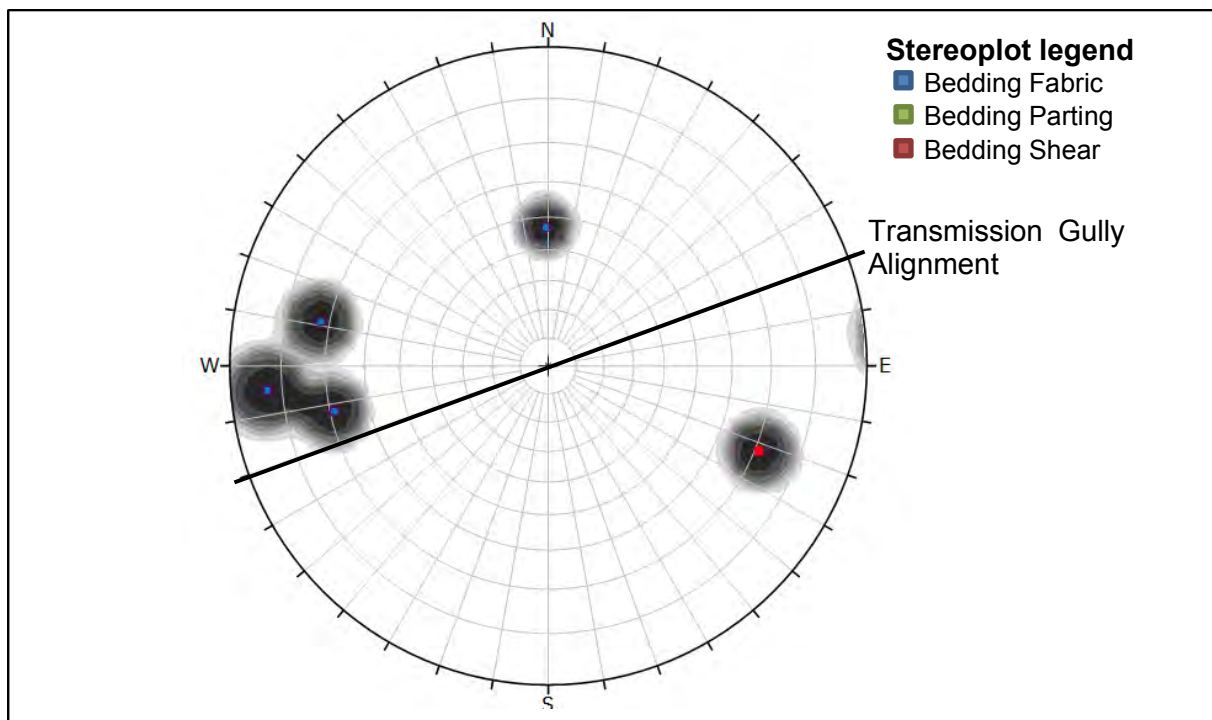


Figure 4.20: Stereoplot of the televiewer bedding data in the “No Domain” area within the Transmission Gully South study zone. Data is sourced from PSM (2014).

An attempt at further discussing the pattern of bedding and shearing orientations is provided by analysing the design mapping data for this area. Presented in Figure 4.21 and Figure 4.22, the

data is clearly fairly widely spread and insufficient to make any definite interpretation. This is the same with the bedding data collected from the borehole database (PSM, 2014).

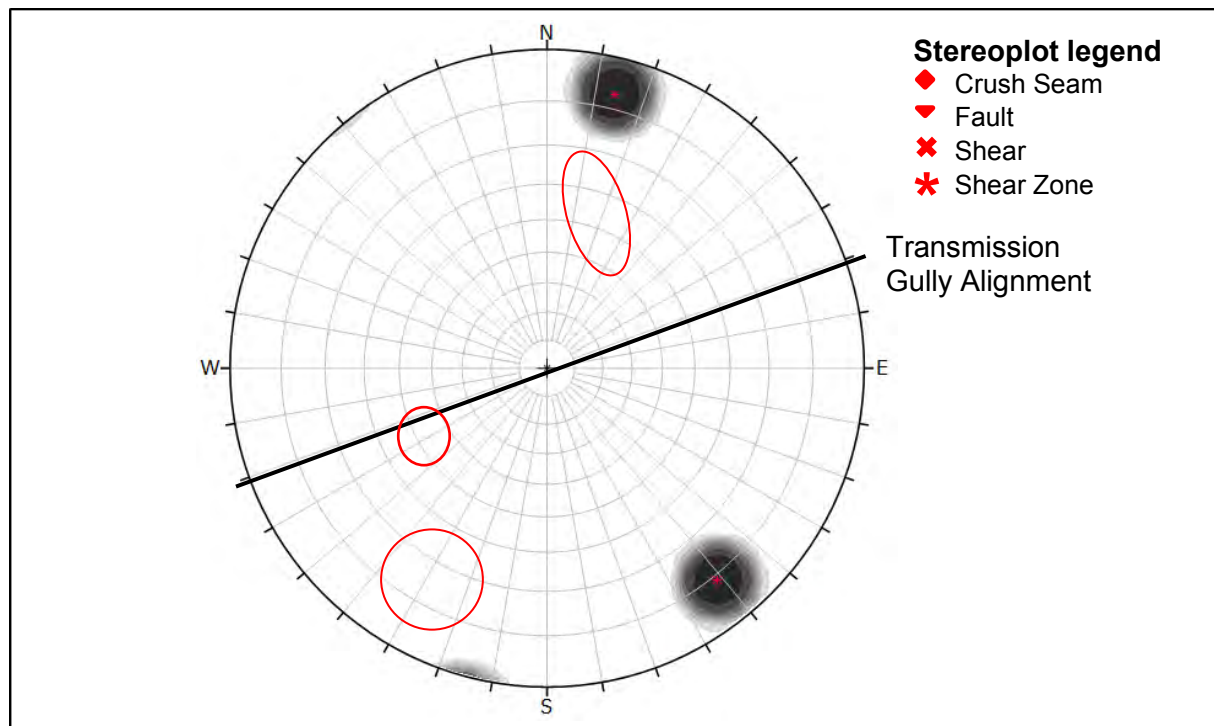


Figure 4.21: Stereoplot of the site investigation mapping shearing data in the “No Domain” area within the Transmission Gully South study zone. The red circles indicate the clusters of televiewer shearing from Figure 4.19. Data is sourced from PSM (2014).

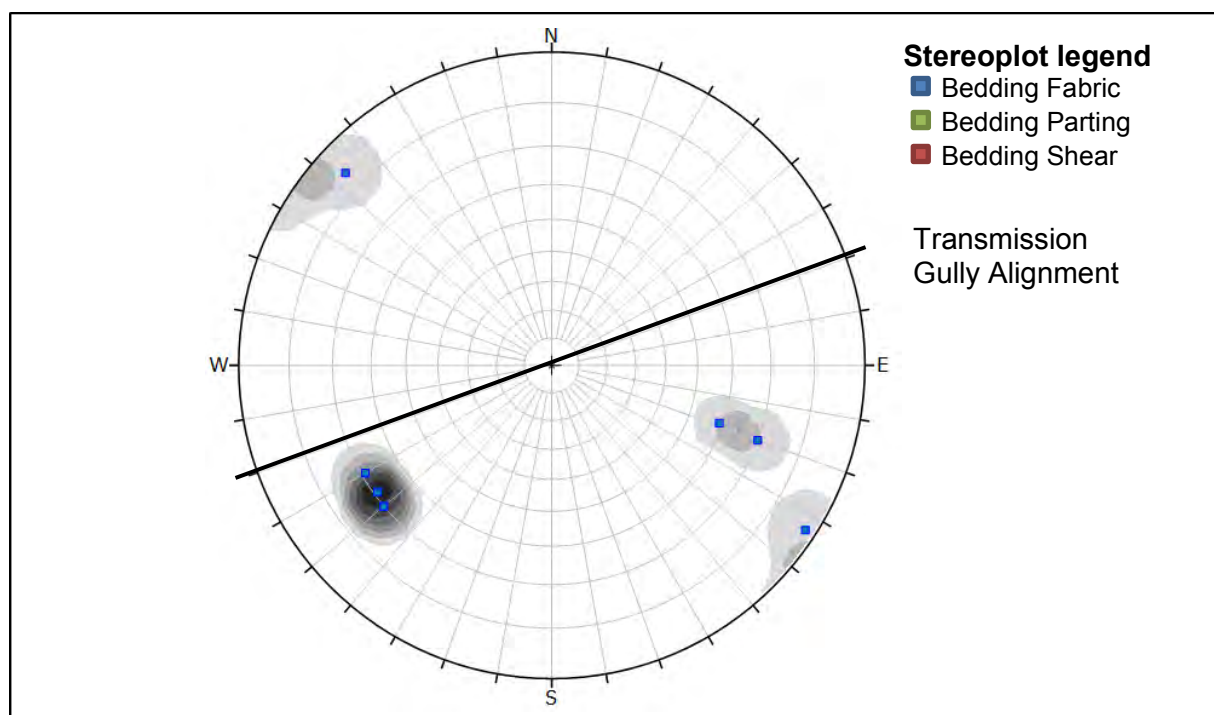


Figure 4.22: Stereoplot of the site investigation mapping bedding data in the “No Domain” area within the Transmission Gully South study zone. Data is sourced from PSM (2014).

4.4 Construction Mapping Data

Further structural data collected during construction on the Transmission Gully alignment reveals additional detail on defect shape and persistence. Furthermore, weathering and lithological extents are better established, which allows the geological model to be verified and or improved. Where the initial model differs from the observed conditions this may influence the detection and or distribution of structural domains and by association potential mechanisms and controls which govern rock slope stability. The following sections investigate and compare the construction mapping against the borehole and mapping design models from Section 4.3. Overall there appears to be little change across the domain extents, therefore, the focus is mostly on defect orientation and engineering geological condition.

4.4.1 Transmission Gully North

The overall condition of the rock mass from construction mapping does not appear to differ greatly from the site investigation analysis. Field mapping presents similar engineering geological conditions with additional information addressing defect persistence and shape. Both Domain H and K tend to be alike, with persistence dominating in bedding and shearing/faulting structures rather than jointing. The more continuous structures (Faults, shear and crush zones) tend to be the more persistent followed closely by bedding and then jointing, which comprises of relatively short structures (Figure 4.23). Jointing is dominantly the most planar which is then followed by shearing/faulting that tends to be gently undulating and lastly bedding (Figure 4.24).

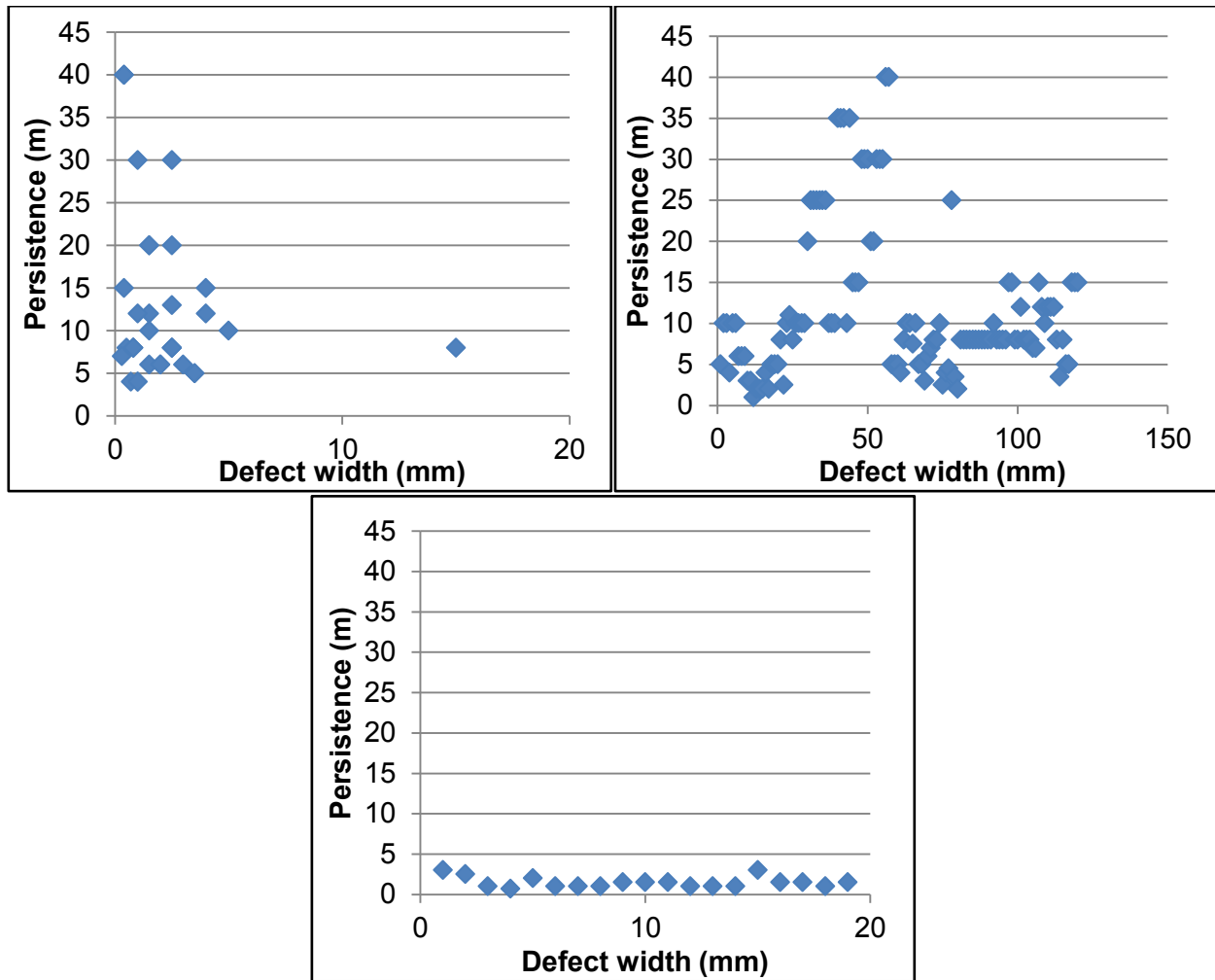


Figure 4.23: Relationship between persistence and defect width for (Top Left) Shearing and Faulting, (Top Right) Bedding and (Bottom) Jointing defects in the Transmission Gully North study area. Data obtained from PSM (2019).

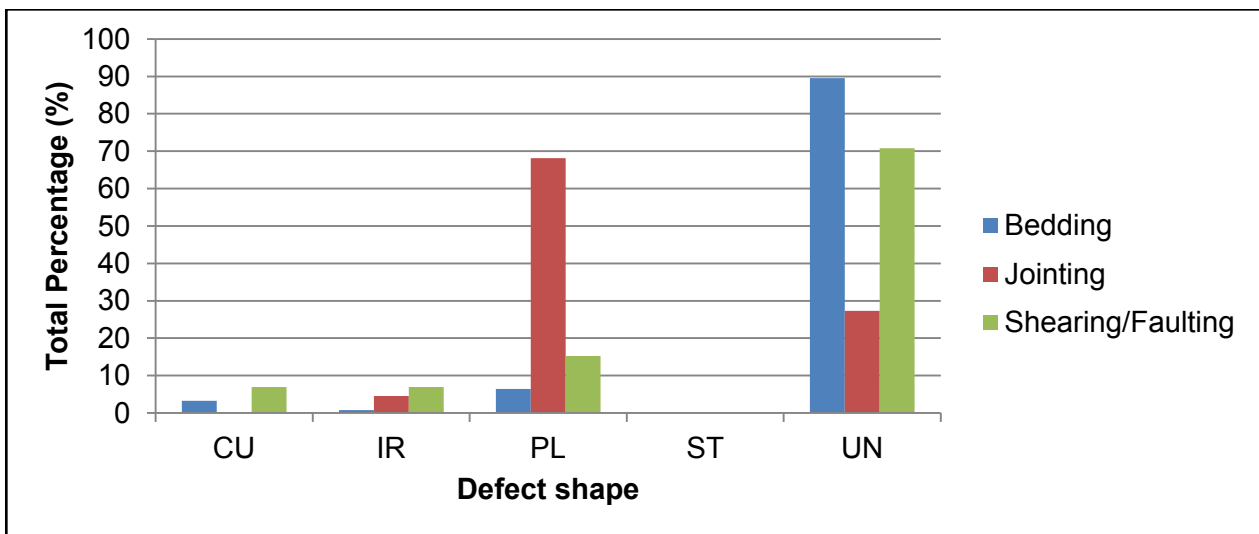


Figure 4.24: Defect shape for the Transmission Gully north study area. Data obtained from PSM (2019). CU = Curved, IR = Irregular, PL = Planar, ST = Stepped, UN = Undulating.

Domain K

Stereoplots of Domain K shearing shows a large degree of scatter (Figure 4.25). One defined cluster is displayed at around 60: 240 (Dip: Dip Direction) while another cluster which is not as clear, is oriented at approximately 60:010. This is not consistent with the site investigation televiewer data which indicated two clusters at approximately 46:142 and 48:318 (Dip: Dip direction). Bedding stereoplots (Figure 4.26) present a similar issue. It appears that the poles to bedding planes are around 60/145 roughly rotated 45° clockwise of the Ohariu Fault trace, which is rough trending 030 degrees. This is not what is observed in the Televiewer data, however, there still appears to be consistency in the cluster shape, suggesting that rotation due to faulting or folding may be the leading cause of this deviation. Supporting this is the location of the boreholes in relation to the cuttings, some of which are roughly positioned 600 metres apart. Further exploration of this rotation compares site investigation and construction mapping π -girdle best-fit lines, which identify a lack of π -girdle lines projecting through both clusters (Figure 4.27). Therefore, it is assumed that faulting is responsible for the large degree of rotation seen in the bedding data.

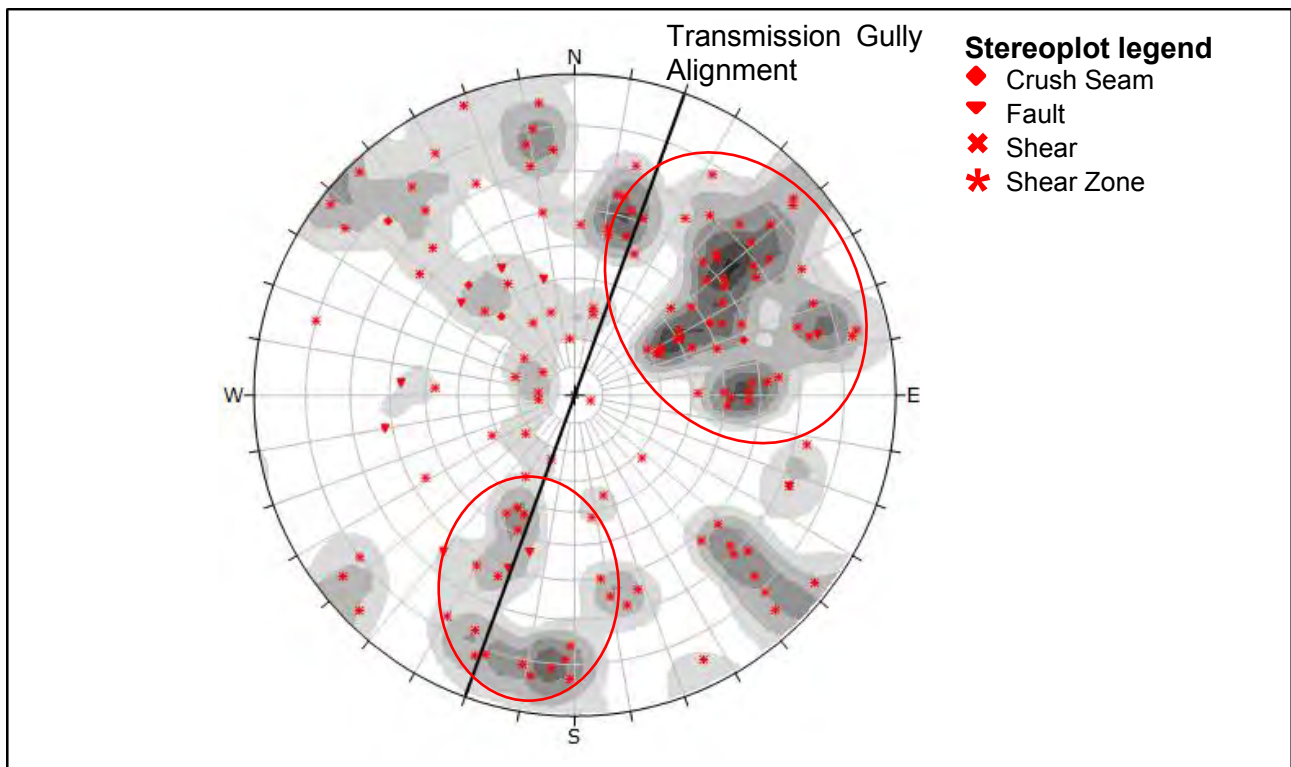


Figure 4.25: Stereoplot of the shear and fault related shears from construction mapping data for Domain K. The red circles represent two clusters of shearing. Data is sourced from PSM (2019).

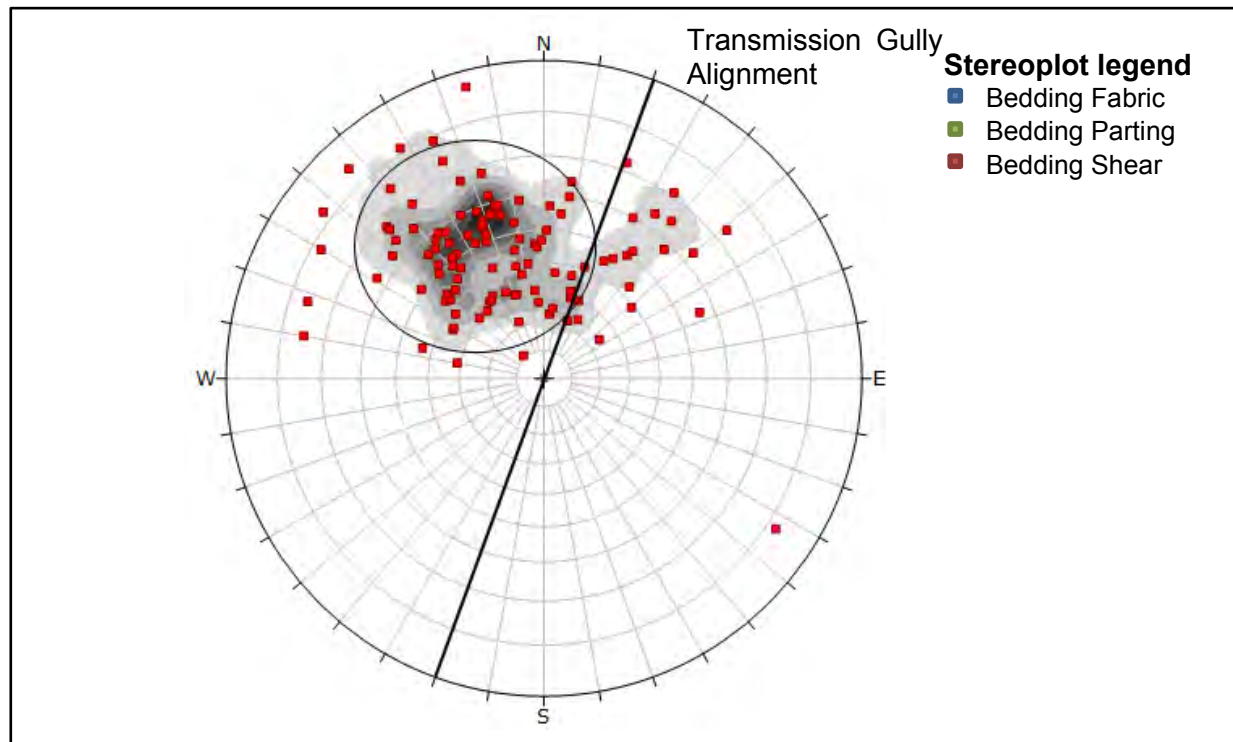


Figure 4.26: Stereoplot of bedding construction mapping data for Domain K. A single cluster represented by the black circles is shown. Data is obtained from PSM (2019).

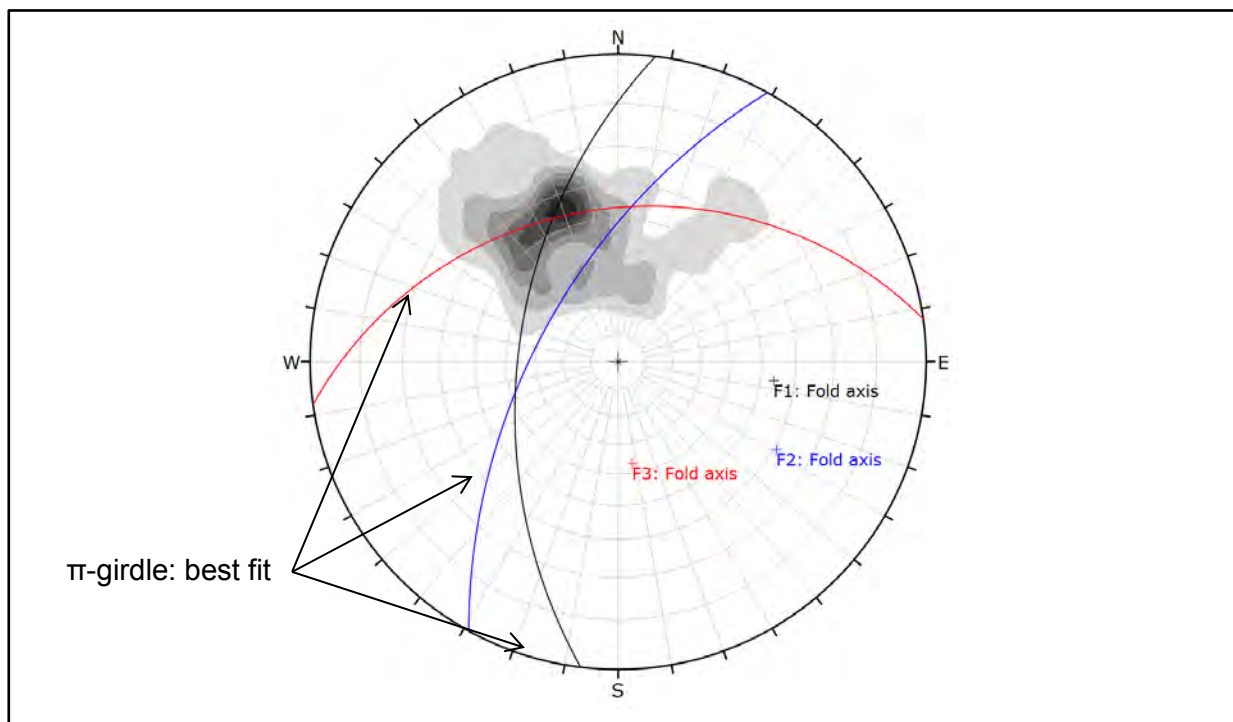


Figure 4.27: Contour plot of the bedding poles from Figure 4.26 for domain K. The red black and blue greater circles indicated potential fold orientations based on a pi-girdle line of best fit. Data is sourced from PSM (2019).

Domain H

Stereoplots of the shearing data for domain H is presented in Figure 4.28. The distributions of the bulk of the poles appear to be in several small loosely clustered set scattered at various orientations. However, a gap in the data is presented between 320° and 280°, these trends are poorly matched to the site investigation data presented in Section 4.2. It is unknown why this may be the case although, it is suspected that the proximity to major regional active faulting (Ohariu Fault which strikes at 030 degrees) is likely to have resulted in a large degree of rotation in shearing patterns.

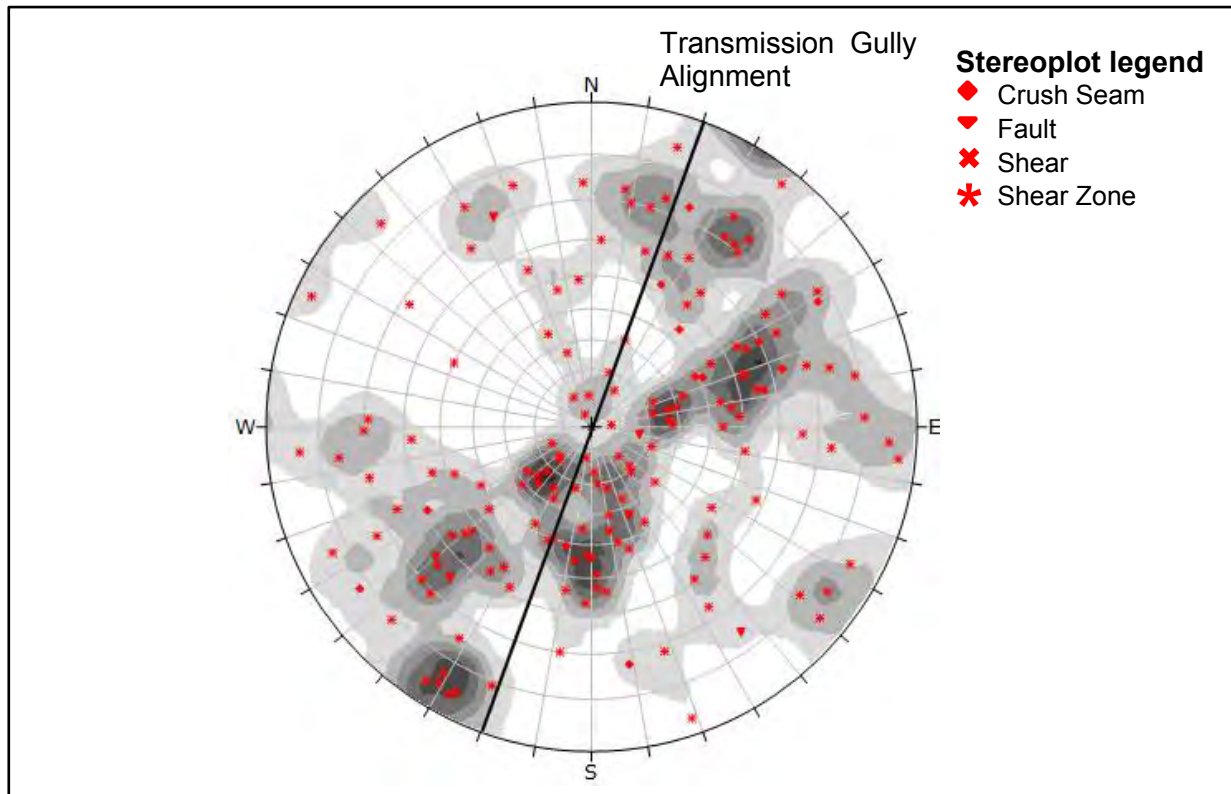


Figure 4.28: Stereoplot displaying the construction mapping shear and fault related shear data for Domain H. Sourced from PSM (2019).

Bedding stereoplots are presented in Figure 4.29 also appears to be poorly matched to the site investigation data. This plot displays a rather concentrated distribution of the bedding poles about 60/250 (Dip/Dip Direction), whereas, the site investigation data is noted to consist of wide scatter. Despite these differences both sets of data appear to infer folding trending roughly N-S and WSW and ENE (Figure 4.12 and Figure 4.30) suggesting that rotation about a potential syformal hinge (N-S) is the likely cause. This fits in with the en echelon fold arrangement model discussed in Section 4.3.1

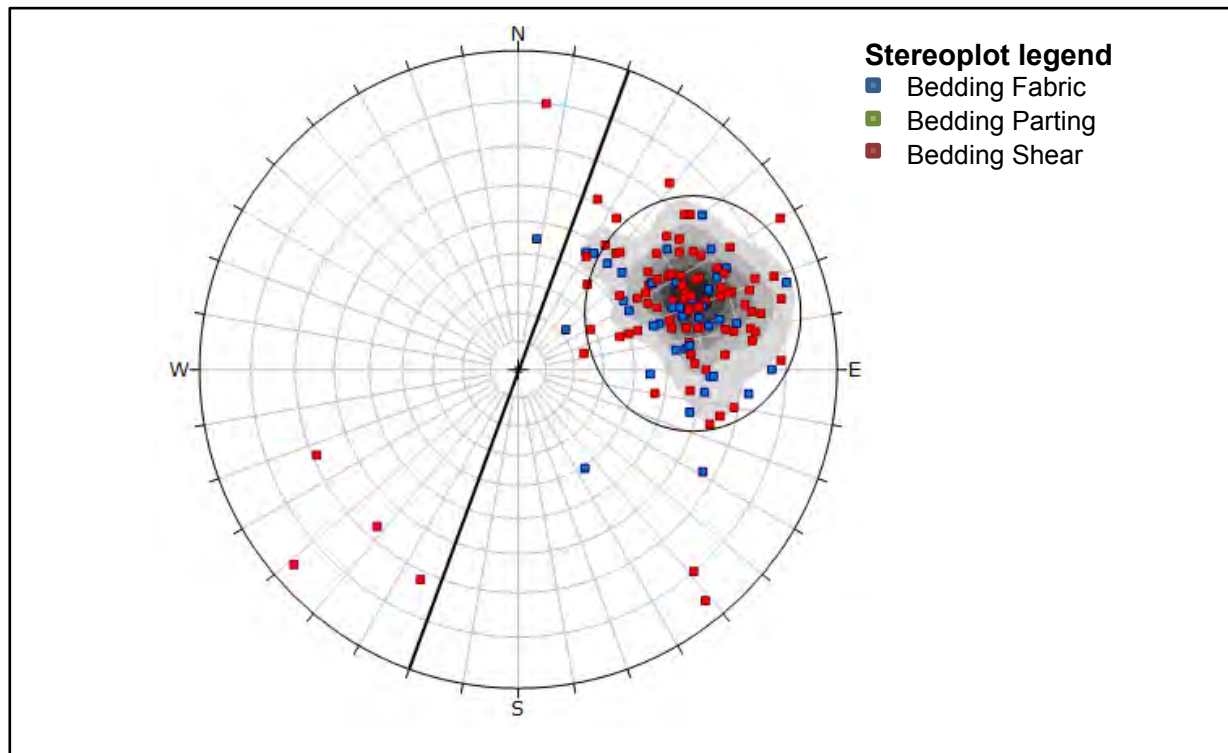


Figure 4.29: Stereoplot of bedding construction mapping data for Domain H. A single cluster represented by the black circle is shown. Data is obtained from PSM (2019).

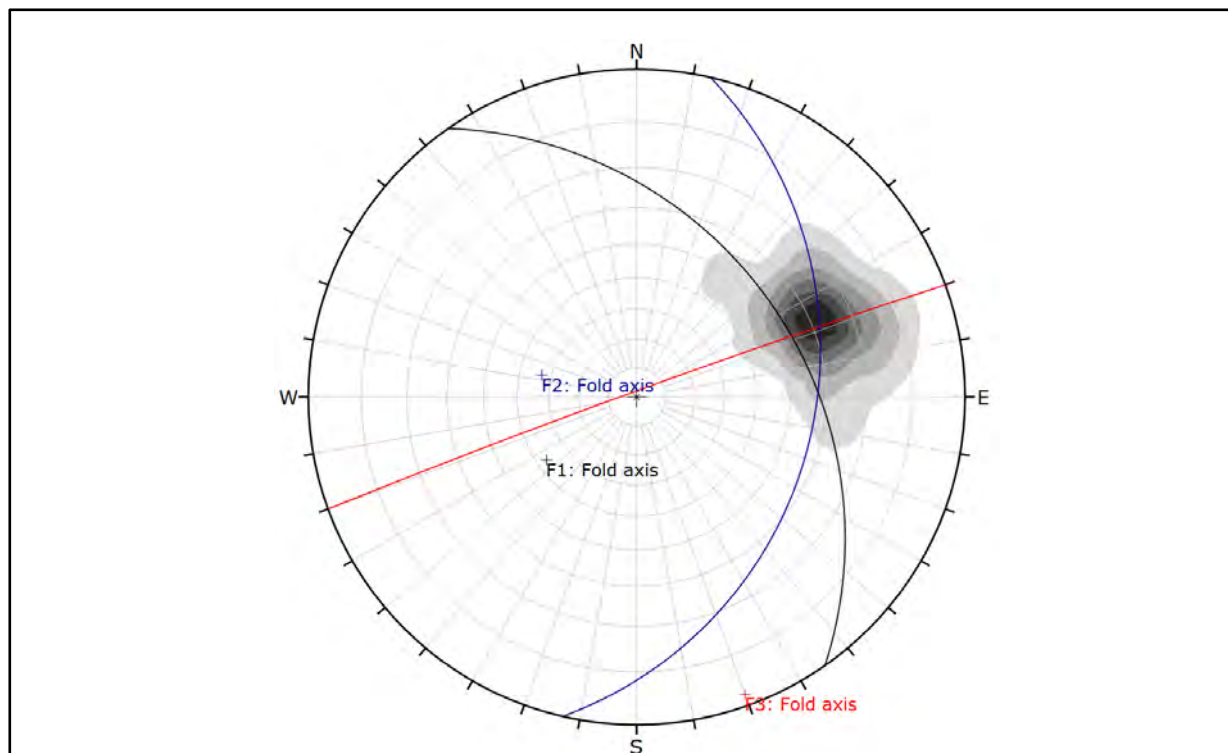


Figure 4.30: Contour plot of the bedding poles from Figure 4.29 for domain H. The red black and blue greater circles indicated potential fold orientations based on a pi-girdle line of best fit. Data is sourced from PSM (2019).

4.4.2 Transmission Gully South

Construction mapping data is limited in this area, such that there is not enough data collected for Domain U that can be used to make any shearing distribution evaluations. This may be due to the decrease of the cutting scale in comparison to the Transmission Gully North site, suggesting a reduced overall risk. Furthermore, interpretations indicated that this study area consists of relatively better rock mass condition than what is observed in the North. However, a distinction can still be made between the site investigation data and the construction mapping data of bedding structures in Domain U. The “No Domain” area also has a reduced dataset although, it is still sufficient enough to plot onto a stereonet.

Overall the rock mass condition does not appear to differ from the design geotechnical models. However, as indicated in Figure 4.31, defect shape shows that shearing and faulting defects are more planar instead of jointing. This differs from the North study area and may be due to a significant lack in the range of data recorded. Additionally, an absence of persistence data means that no further structural relationships can be identified.

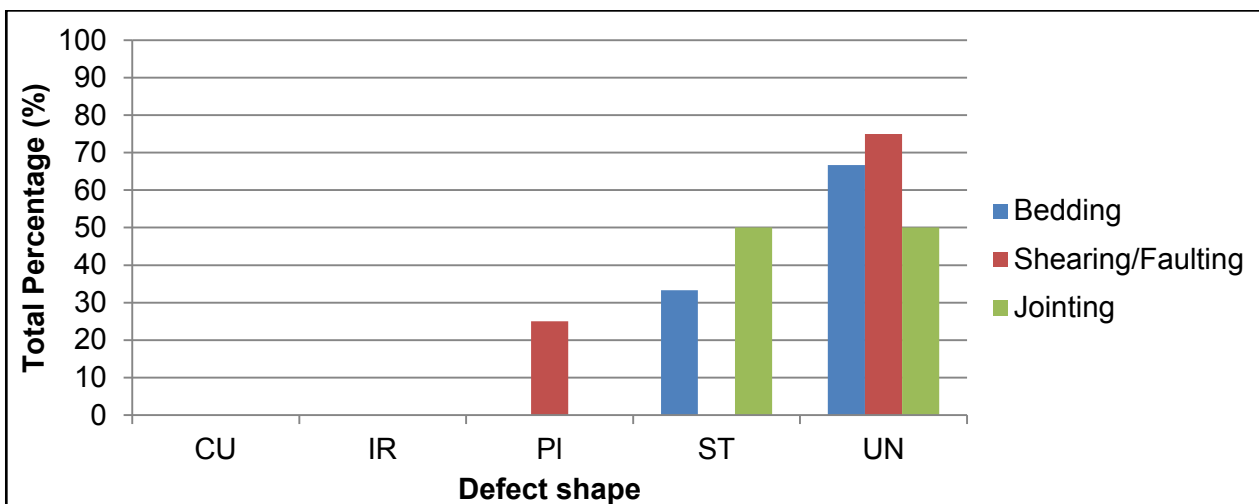


Figure 4.31: Defect shape for the Transmission Gully south study area. Data obtained from PSM (2019). See Figure 4.24 for acronyms.

Domain U

Bedding orientations displayed in Figure 4.32 show a correlation with the site investigation mapping data (Figure 4.16). Clustering identified in mapping stereoplots is located in roughly the same location about 85/240 (Dip/Dip Direction). From this, a single steeply dipping to sub-vertical limb can be derived. This is different from televiewer interpretations which suggest that folding is moderately plunging towards the south. As these interpretations are located in roughly the same area both folds may be a part of the same feature. However, there are no hinge lines exposed in this area suggesting that faulting which divides the site may have instead caused bedding to rotate.

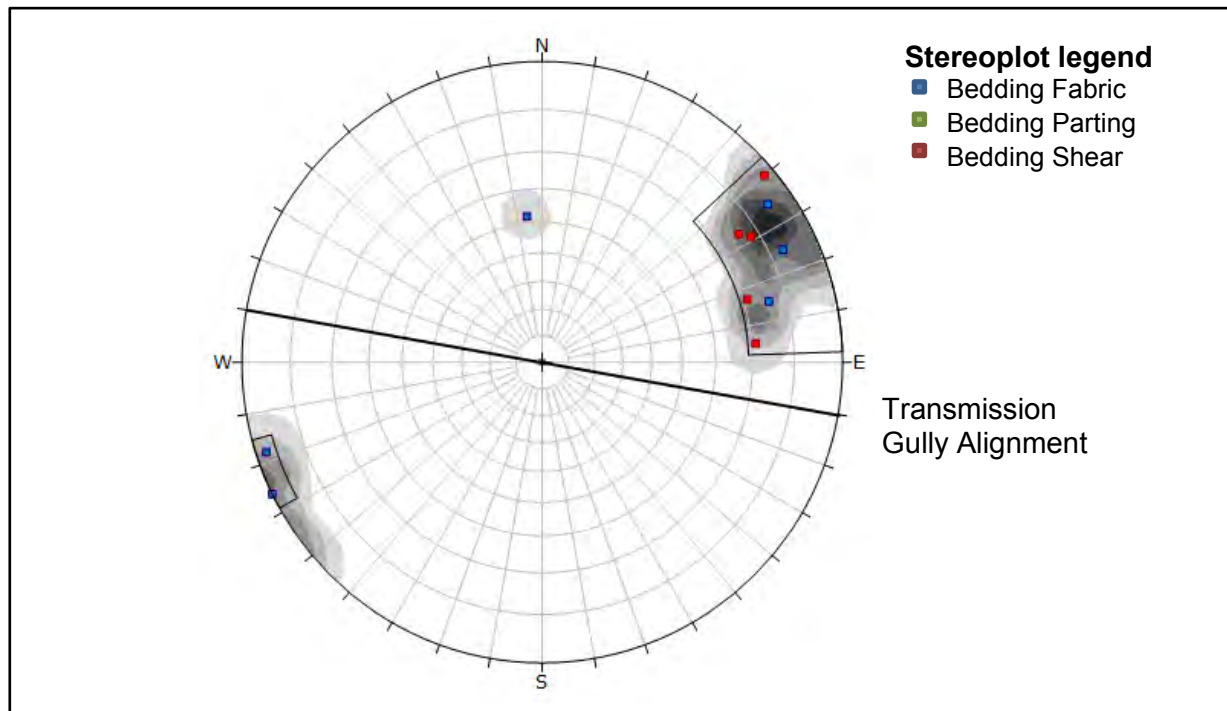


Figure 4.32: Stereoplot of bedding construction mapping data for Domain U. A single cluster represented by the black quadrilateral is shown. Data is obtained from PSM (2019).

“No Domain”

A stereographic plot of the shearing data in this area is presented in Figure 4.33. Clustering of the data about 65:215 and 75:090 appear to correlate with a single cluster identified in the televiewer data. The second cluster appears to dip sub-parallel to parallel with bedding, which also displays two clusters about 80/245 and 75/90 (Figure 4.34). Previous data was not significant enough to assess any clear interpretation about the orientation of the bedding. Therefore, construction mapping presented the only viable option in which a description could be identified. Contour plots utilise π -girdle methods and indicate a moderately plunging southward trending fold (Figure 4.35). A lack of visible hinge lines suggests that faulting in this area is more likely to influence any potential slope instability.

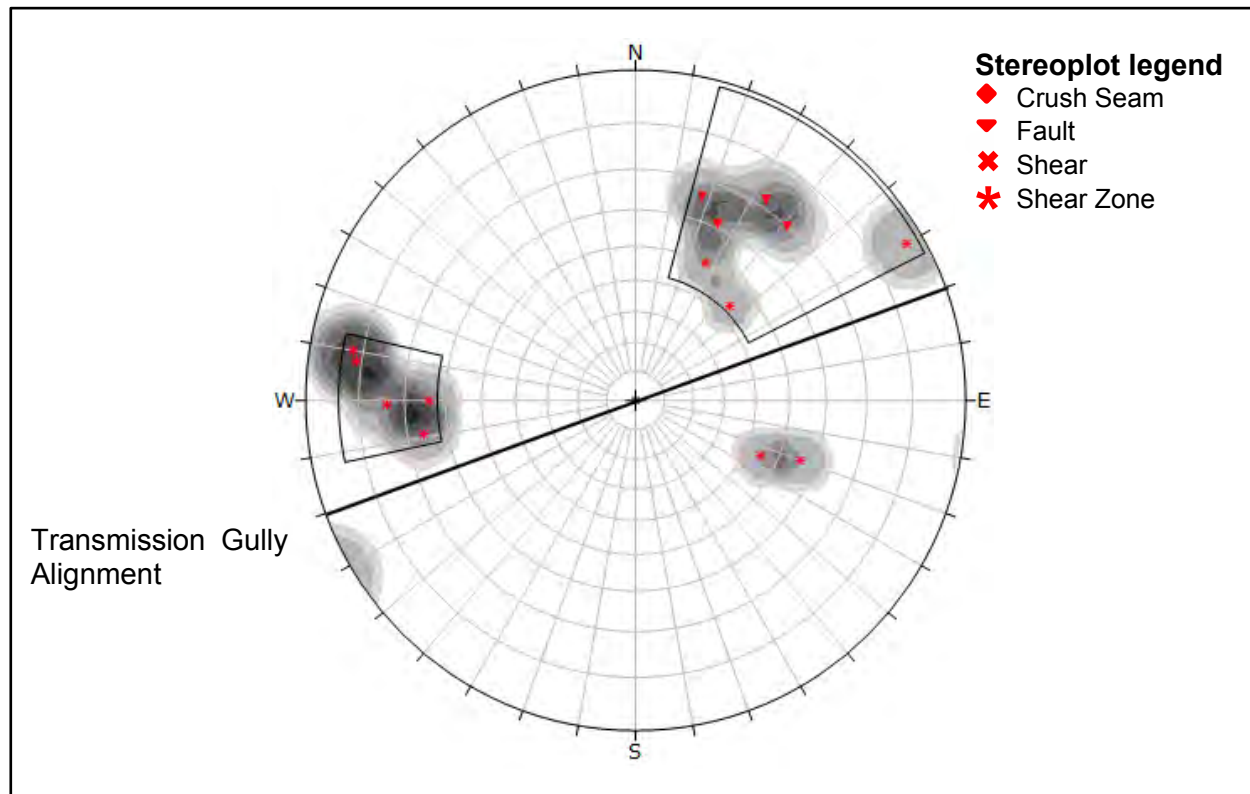


Figure 4.33: Stereoplot of shears or fault related shears in the construction mapping data for the “No Domain” area. Two clusters represented by the black quadrilaterals are shown. Data is obtained from PSM (2019).

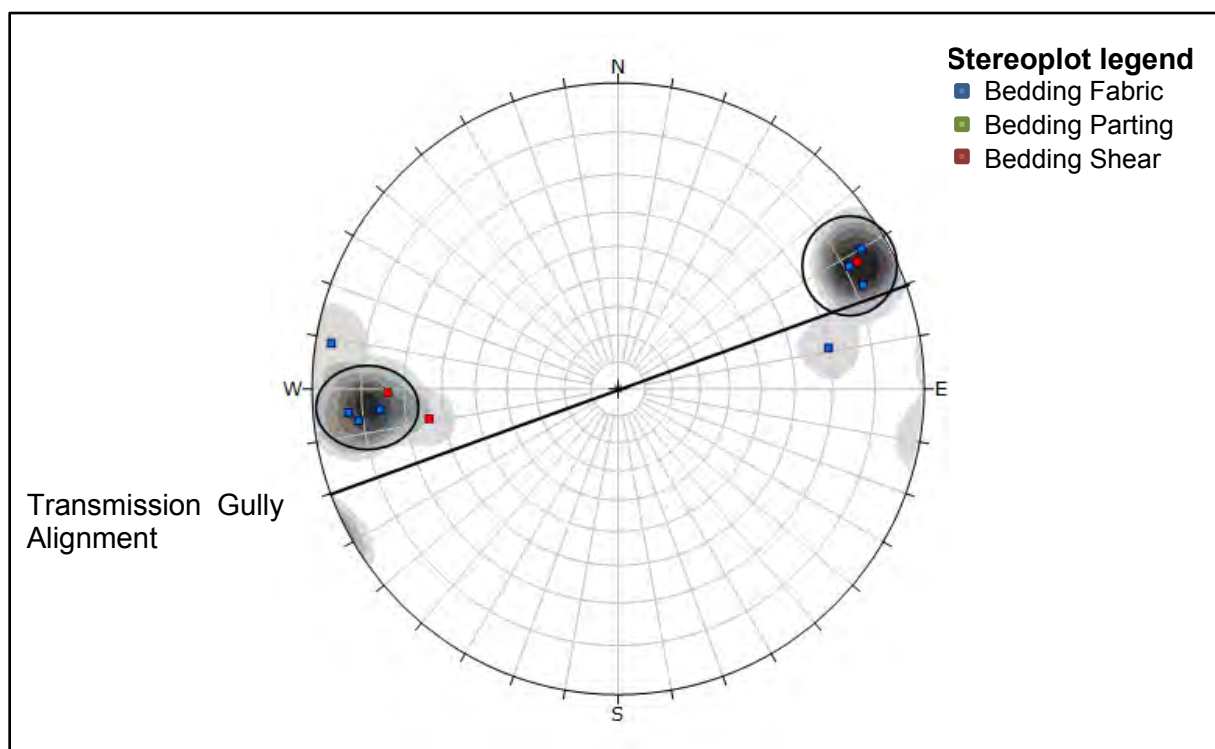


Figure 4.34: Stereoplot of bedding construction mapping data for the “No Domain” area. Two clusters represented by the black circles are shown. Data is obtained from PSM (2019).

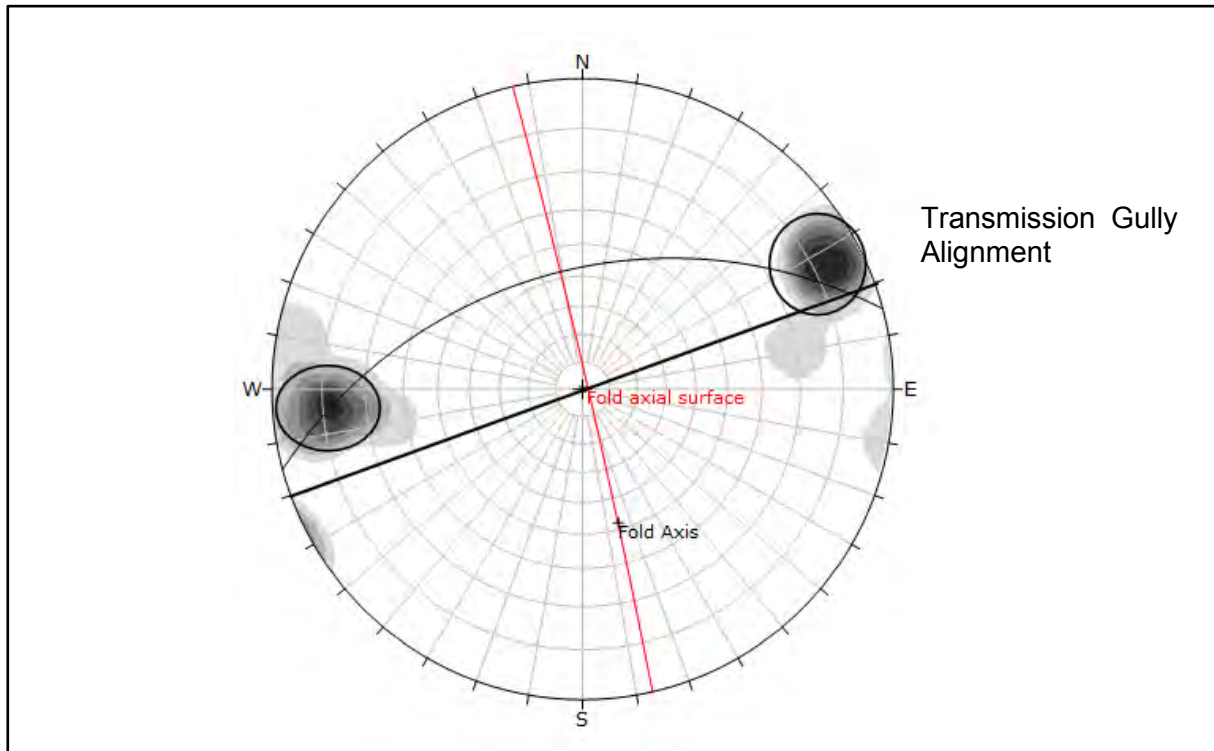


Figure 4.35: Contour plot of the bedding poles from Figure 4.34 for the “No Domain” area. The red greater circle indicates potential fold orientations based on a pi-girdle line of best fit (black greater circle). Data is sourced from PSM (2019).

4.5 Deviations from the Site Investigation Data

Observations made in Sections 4.3 to 4.4 clearly indicate that the overall rock mass condition was broadly similar in the early investigation data used for design to what is observed in the construction mapping records. However, construction mapping assessed defect orientations appear to noticeably deviate from the site investigation data. This may be a function of location bias, only a few boreholes were located at increased distances (~200 m see Appendix H.1 and H.2) away from the excavated cut slope face. This could lead to rotated due to faulting or folding mechanisms. However, a more likely interpretation is the impact on directional bias in the borehole dominated data. There is generally a lack of defect poles that are observed to dip vertically to very steeply. This is a result of angling the boreholes during drilling such that OTV and ATV surveys could be conducted. Therefore, any defects dipping parallel to the borehole inclination are under sampled. This is another reason why it is important to check and validate the initial design data during construction, such that bias like this is accounted for.

Furthermore, scatter presented in the design data may be interpreted as isolated discrete features. This could be the result of a degree of inaccuracy in the borehole imaging interpretation and measurements, however, it is more likely that this due to the highly deformed nature and complexity surrounding the structural history of the Torlesse rock mass. This point is worth noting as it provides a link between older generations of faulting and enables linkages to

be made to design of potential future cut-slopes. This is further discussed with a general sense towards the overall Wellington Torlesse in Chapter 6.

Where linkages were unable to be made, for example the bedding data in the “No Domain” area, there generally was a lack of sufficient data or defined clustering. Therefore, these areas did not show reason to deviate from the current structural domain extents.

CHAPTER FIVE TORLESSE ROCK MASS CLASSIFICATION

5.1 Development

Regional structural trends and characteristics of the Torlesse in the Wellington region are critical in identifying which parameters have a greater effect on rock mass condition. These patterns can be linked to geological controls with a specific focus on factors, in addition to weathered and heavily faulted rock that have the potential to predict slope instability mechanisms.

This chapter discusses these trends by finding common physical properties of defects that were identified by field mapping at each site. The principal driver in this iterative process was mainly provided for by geological field observations, which enabled further insight into the key controlling factors in cut-slope instability. Where clear relationships are observed they were then integrated into a classification framework that incorporated variability seen across all lithological and structural settings.

5.2 Overall Rock Mass Trends

The main controls of rock mass change were found to be lithology and rock mass structure. Lithology describes the mudstone to sandstone proportions and the dominant thickness of each identifiable bedding unit. Defect structure describes the occurrence of various structures, predominantly discontinuities, along with scale factors and infill conditions.

5.2.1 Lithology

Most of the Torlesse rock mass in the Wellington region can be described using lithofacies established by (Suneson, 1992). The lithofacies classification tends to cover a wide range of bedding thicknesses, particularly group C where occurrences of both very thickly bedded mudstone or sandstone can occur within mostly moderate to thinly bedded sequences. This is useful as it takes into account variation produced due to the depositional environment at the time the rock mass was deposited. However, mudstone has a lower intact rock mass strength and as such is prone to increased fracturing and subsequent accelerated weathering and erosion. As a result thicker mudstone beds may be hidden or obscured from surface exposures. This could mean that the naturally occurring rock slopes at Makara Beach and Wairaka Point may have higher mudstone proportions than what has been previously identified. Generally, the only occurrence of thin to very thin (> 200 mm) sandstone bedding was observed in the Kapiti Quarry area, where mudstone material was the most dominant of all the sites.

In bedded sequences bed thickness and sandstone to mudstone proportions are a major governing control on rock mass structure and condition (Crusoe Jr et al., 2016). However, these parameters are seen to be highly variable across all the study sites. Sandstone dominates with

six out of the seven study sites having sandstone proportions of 60% or higher (Table 5.1 and 5.2). Generally where sandstone content is greater bed thickness, and thus bedding plane spacing, within the sandstone members also increases. (Suneson, 1993) showed that as the ratio of mudstone to sandstone decreases the bedding spacing of Lithofacies B tends to also decrease (Figure 5.1) while groups C and D tend to increase (Figure 5.2) however, this trend is weak.

Table 5.1: Summary bedding thicknesses and sandstone and mudstone ratios at each study site.

Location	Dominant bedding thickness (NZGS, 2005)		Mud: Sand Ratio
	Mudstone	Sandstone	
Kapiti Quarry	Very thin to Moderately thin	Thin to Moderately thin	50:50
TG North	Thin to Moderately thin	Moderately thick to Thick	40:60
TG South	Thin to Moderately thin	Thick to Very thick	40:60
Owhiro Bay Quarry	Moderately thin to Moderately thick	Thick to Very thick	40:60
Horokiwi Quarry South and West	Very Thin to Moderately thick	Moderately thick to Very thick	30:70
Horokiwi Quarry North	Thin to Moderately thin	Moderately thick to Very thick	30:70
Makara Beach	Moderately thin to Moderately thick	Thick to Extremely thick (> 6 m)	20:80
Wairaka Point	Thin to Moderately thick	Moderately thick to Extremely thick (> 6 m)	20:80

Table 5.2: Relative proportions of (Suneson, 1993, 1992) lithofacies at each study site.

Study area	Width of outcrop	Relative proportion of lithofacies in percentage		
		B	C	D
TG North	460 m	80	20	
Outcrop 1	120 m	80	20	
Outcrop 2	30 m	80	20	
Outcrop 3	85 m	60	40	
Outcrop 4	90 m	70	30	
Outcrop 5	30 m	100		
Outcrop 6	25 m	100		
Outcrop 7	80 m	70	30	
TG South	450 m	70	27.5	2.5
Outcrop 1	80 m	60	30	10
Outcrop 2	140 m	80	20	
Outcrop 3	130 m	70	30	
Outcrop 4	100 m	70	30	
Kapiti Quarry	300 m	48	38	14
Outcrop 1	20 m	100		
Outcrop 2	180 m	15	65	20
Outcrop 3	100 m	30	50	20
Owhiro Bay Quarry	200 m	50	50	
Outcrop 1	100 m	60	40	
Outcrop 2	100 m	40	60	
Horokiwi Quarry	320 m	90	10	
Outcrop 1	20 m	80	20	
Outcrop 2	150 m	90	10	
Outcrop 3	150 m	100		
Wairaka Point	86 m	100		
Outcrop 1	40 m	100		
Outcrop 2	20 m	100		
Outcrop 3	20 m	100		
Outcrop 4	6 m	100		
Makara Head	100 m	100		
Outcrop 1	25 m	100		
Outcrop 2	15 m	100		
Outcrop 3	20 m	100		
Outcrop 4	40 m	100		

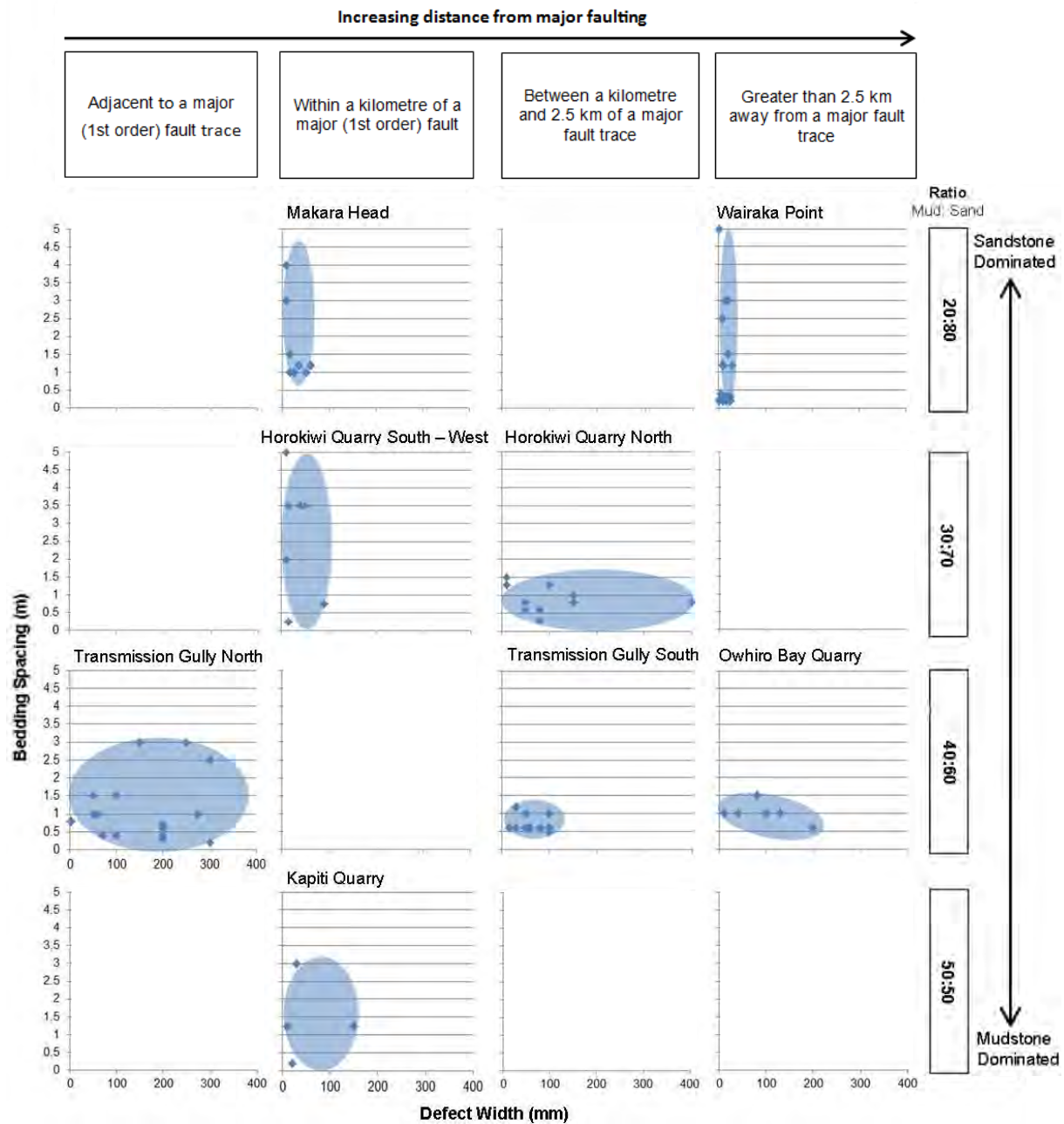


Figure 5.1: Relationship among lithology and discontinuity spacing relative to distance from major faults for Lithofacies B (Suneson, 1993, 1992).

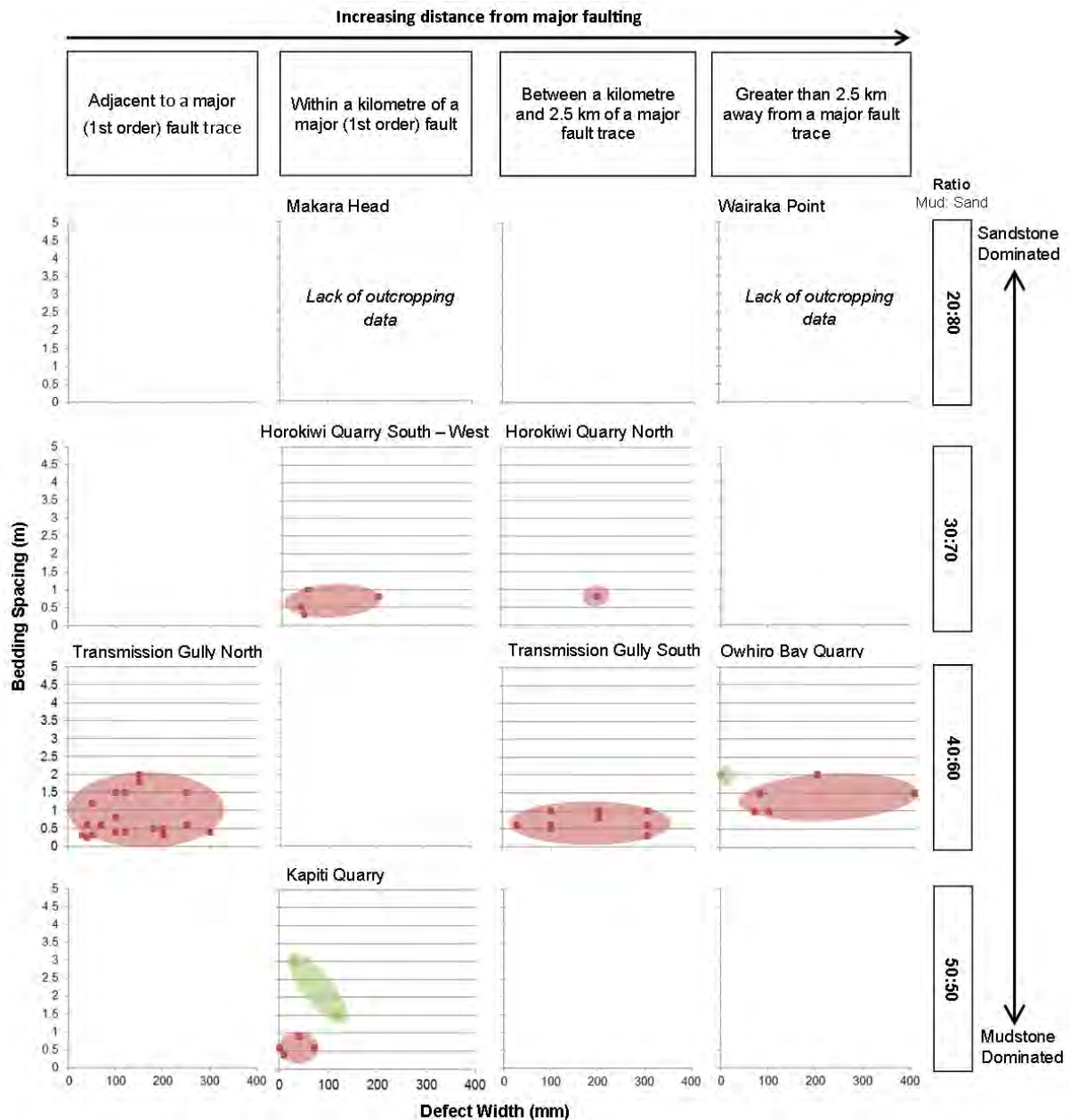


Figure 5.2: Relationship among lithology and discontinuity spacing relative to distance from major faults for Lithofacies C (Red) and D (Green) (Suneson, 1993, 1992).

Bedding defect width

Bedding defect width is strongly influenced by mudstone sandstone proportions. The defect width is generally greater in more mudstone dominated materials. However, this trend is also weak (Figure 5.1 and 5.2) as there is a general increase in defect width with proximity to major faults.

Over 75% of all bedding defect widths recorded in the field were moderately wide or greater (≥ 20 mm; Figure 5.3). Approximately three quarters of these defects were from areas where mudstone to sandstone proportions are less than 2:3 (Figure 5.1 and 5.2). However, due to heavily fractured nature of mudstone, distinct bedding fabric and shears may widen in areas

where the degree of tectonic disturbance is greater. Shear planes become wider shear zones (i.e. increasing damage zone width) with increasing strain that tends to follow bedding. Therefore, this trend may only hold true in certain mudstone to sandstone proportions.

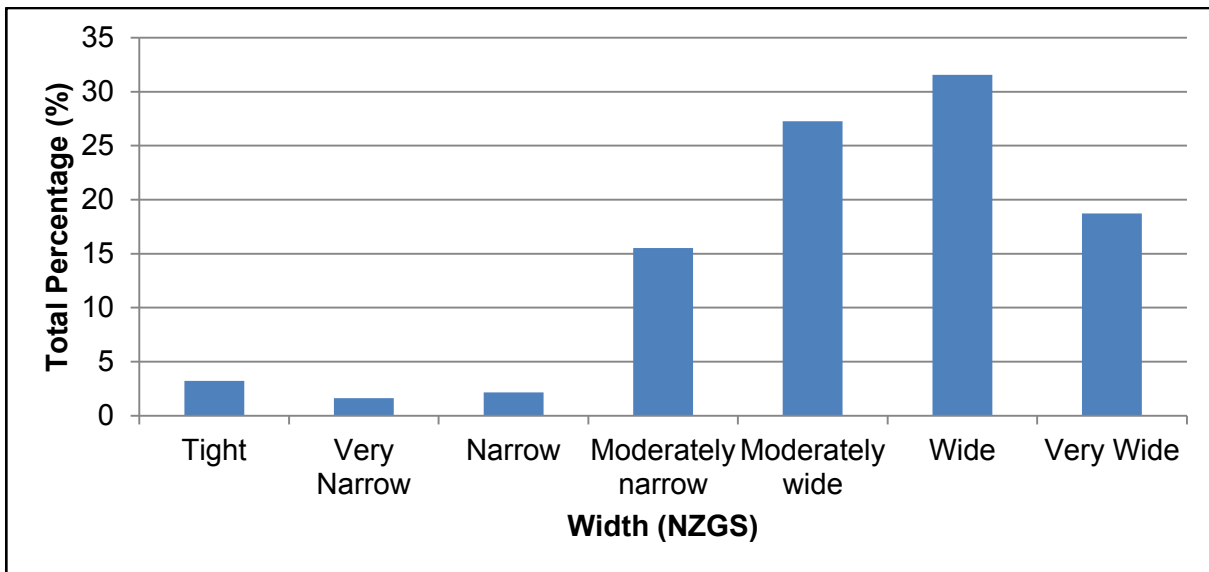


Figure 5.3: Distribution of bedding defect width observed from field sites (NZGS, 2005).

5.2.2 Rock mass structure

Rock mass structure is defined by defect type, infill, continuity, termination and waviness in the following sections:

1) Defect type

The dominant defect type recorded was a shear (SR). Shears make up about 55% of all defects recorded from field mapping (Figure 5.4). Figure 5.5 indicates the distribution of the different defect types at each of the field sites. As stated previously (Section 3.1.1) shears show a great deal of variability, and are formed by brittle deformation. Other shearing defects also created from brittle deformations include faults (FL), shear zones (SH) and crush zones (CZ), which typically form greater defect widths (Figure 5.6). These collectively make up roughly 11% of all recorded defects. Generally these larger structural defects are less common at increasing distances from major faulting. There are also more common in areas where there is a higher mudstone proportion (Figure 5.5).

The next most common group of defects includes bedding (BG) and bedding parallel shears (BSH). Totalling about 22%, these discontinuities are variable in defect width. Commonly bedding (BG) is sharp and distinct while bedding shears are generally wider as movement along the bedding surface has taken place leading to a more mature damage zone. Generally bedding is not easily identified in areas where there is a greater degree of deformation and the mudstone content is high. However, this overall trend is weak and dependent on the number of bedding

planes visible in a particular area (*i.e.*, bedding spacing). Increased bedding contacts are visible in areas where bedding thickness is lower. As discussed in Section 5.2.1, bedding thickness is ultimately dependent on the depositional environment. Furthermore, increasing tectonic strain in areas where mudstone contents are greater increases brecciation and disintegration of the rock mass. Thus, bedding parallel shears may become less distinct and instead form wider shear zones.

Jointing in this region tends to be closely spaced, randomly oriented and low to very low in persistence (ISRM, 1978). In previous studies (*e.g.* Read and Richards, 2007; Cook, 2001; and Irvine, 2013) have shown that joints which display these characteristics tend to have relatively high rock mass strengths. Additional investigations (*e.g.* AECOM and PSM, 2015; Grant-Taylor, 1964) also conclude that persistence is one of the main critical drivers related to large global failures. Hence, low persistent jointing will likely only influence local scale failure mechanisms. As previously stated, this study undertook an investigation with the aim of identifying the main geological controls governing slope instability. As a result jointing is only assessed where it is considered critical to cut-slope design. In the field only two sites identified jointing as a main control for slope instability. Both of these sites are natural rock slopes (Makara Head and Wairaka Point) where jointing is ≥ 2 m in persistence. Furthermore, these sites consist of relatively high sandstone proportions. Jointing in these areas appeared in strongly defined sets; mostly very narrow and little or no infill. Few occurrences of gapped and dilated infills were found, mostly in areas where failure mechanisms had occurred. Over all the sites, new or random joint fractures typically have tight to very narrow surfaces that are generally planar and rough.

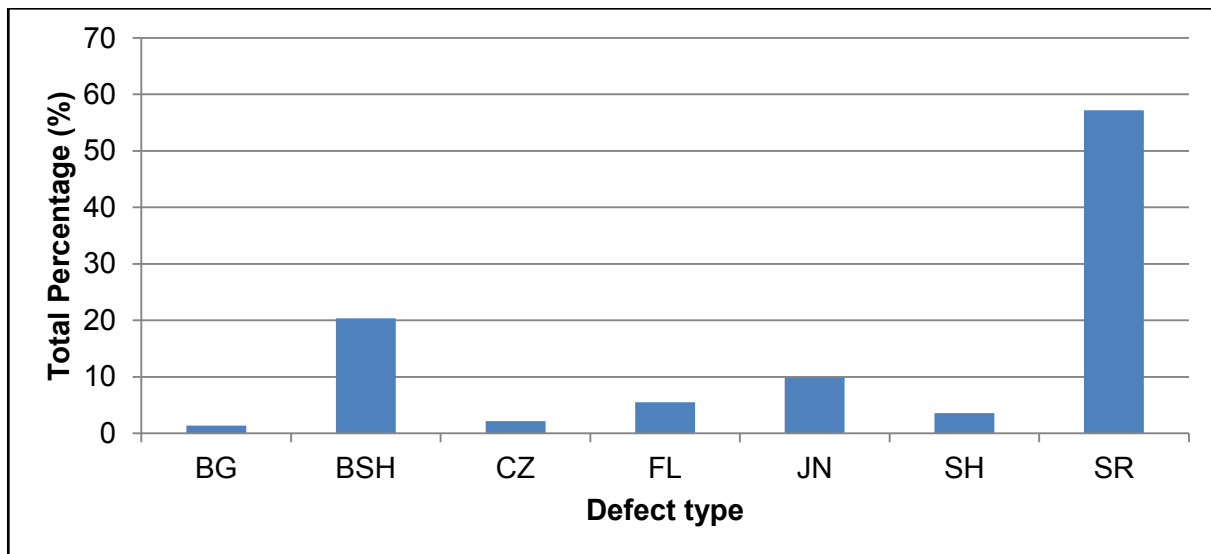


Figure 5.4: Overall percentage of all the defect types from all study areas. SR – Shear, SH – Shear zone, JN – Joint, FL – Fault, CZ – Crush Zone, BSH – Bedding Parallel Shear, and BG – Bedding

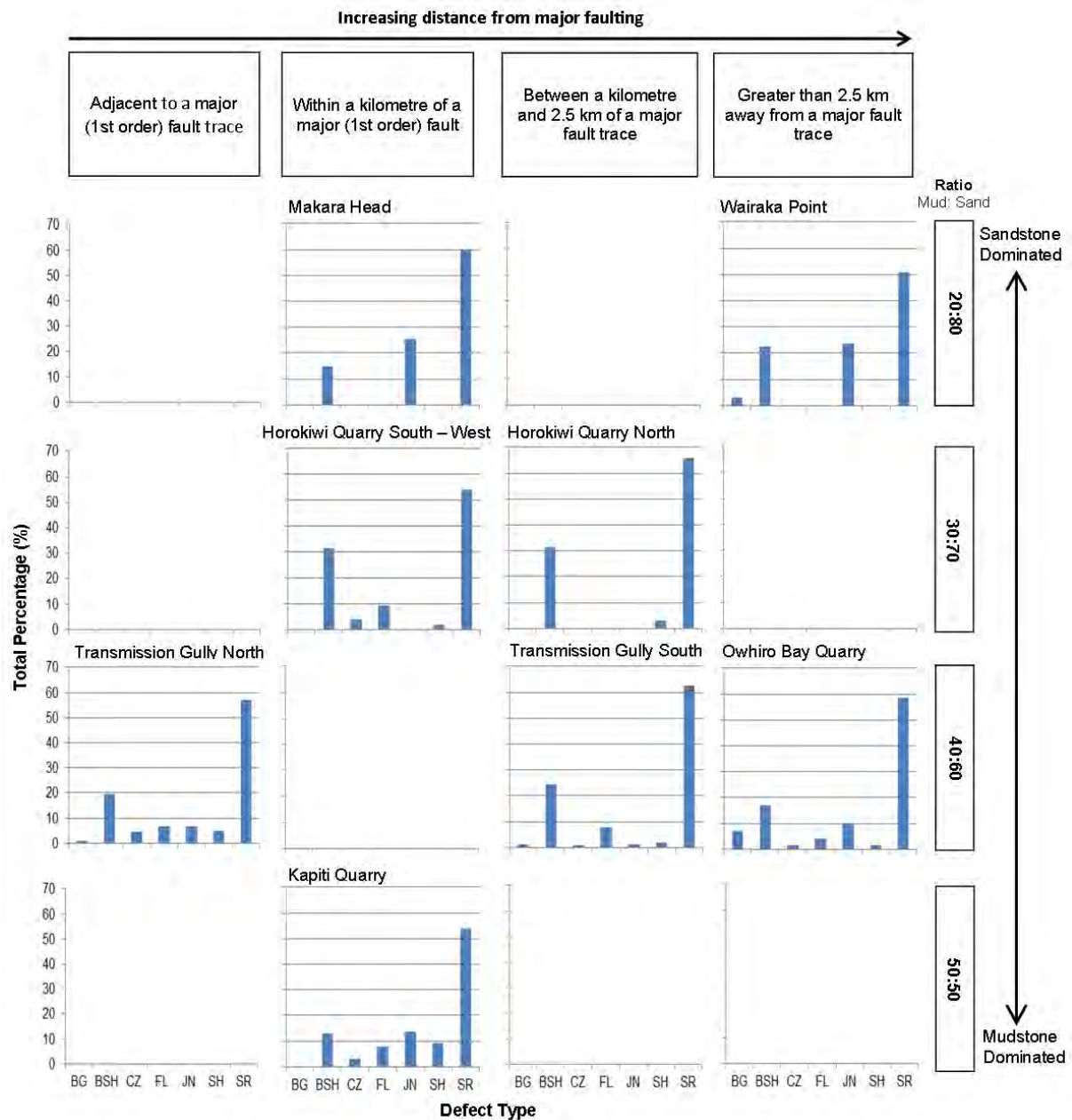


Figure 5.5: Percentage of defect types recorded at each field area. Refer to Figure 5.4 for acronyms.

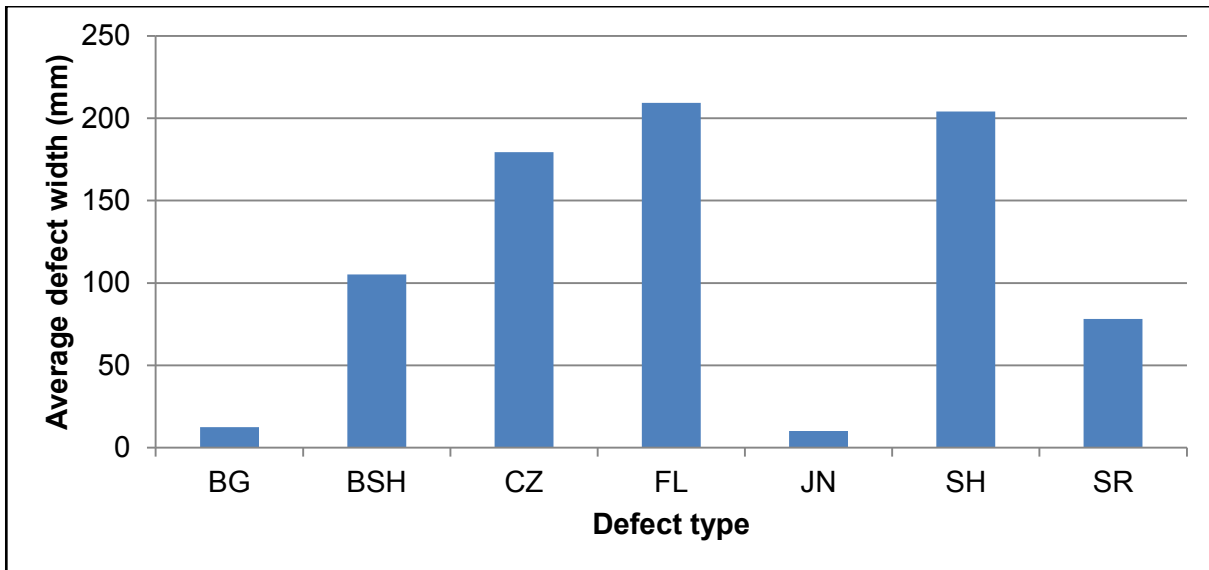


Figure 5.6: Average defect width (NZGS, 2005) of shearing features. See Figure 5.4 for acronyms.

2) Defect Infill

Discontinuities across all study sites consist of highly variable infill materials. (Appendix I Figures I.4 to I.6) The dominant infill material is crackle, which can be found in all defect types and characteristically shows brecciation (Figures 5.7 and 5.8). The clasts are often angular, moderately strong to weak and surrounded by a sand-sized matrix. Generally, as the distance from major faulting increases the volume of crackle and sand infilling material also increases. Finer materials (generally < 2 mm in width) tend to be more prominent where mudstone proportions and tectonic disturbance is greater. This trend is stronger for shears (SR).

Clay-rich infill materials are generally inactive and may have a slight plasticity as indicated from handling of the material in the field. More plastic materials are usually found in fault gouges or shear zones where moisture observed content is generally higher. Clays are commonly associated with sand in defect infill and are often as a coating or discontinuous lens on or adjacent to fracture surfaces. Typically, clean or stained surfaces are found where water is recorded or between narrow to tightly closed defect surfaces, such as joints. This would suggest that tightly formed defects prevent a lot of material from entering voids. Cook (2001) and Irvine (2013) state that these defects are not considered to be influenced by infilling.

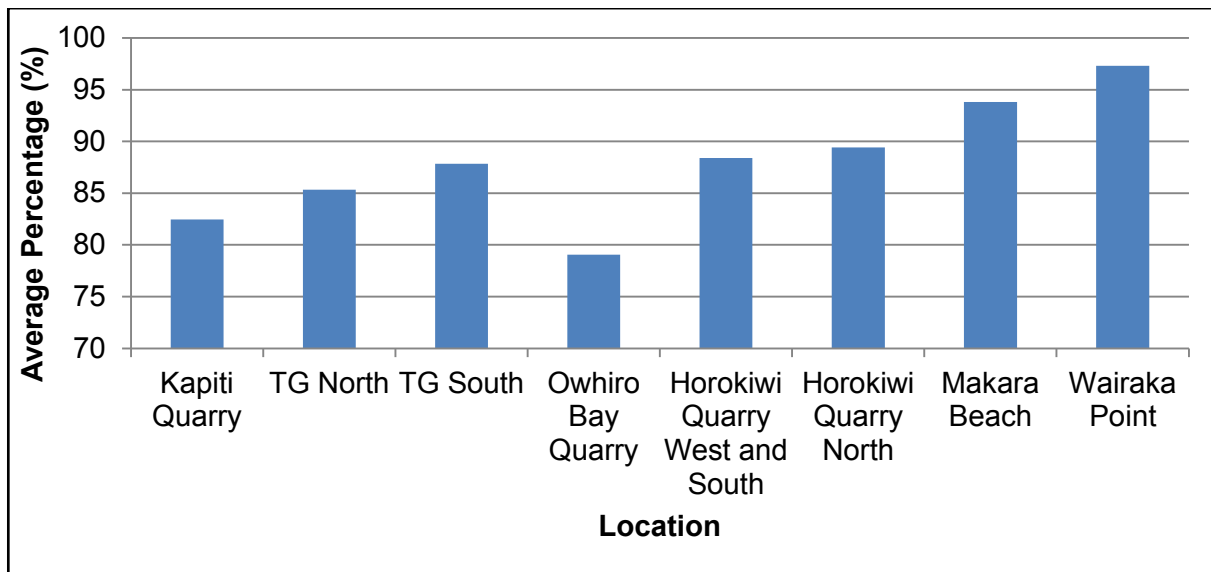


Figure 5.7: Average percentage of rock fragments in defect infill across all study areas.

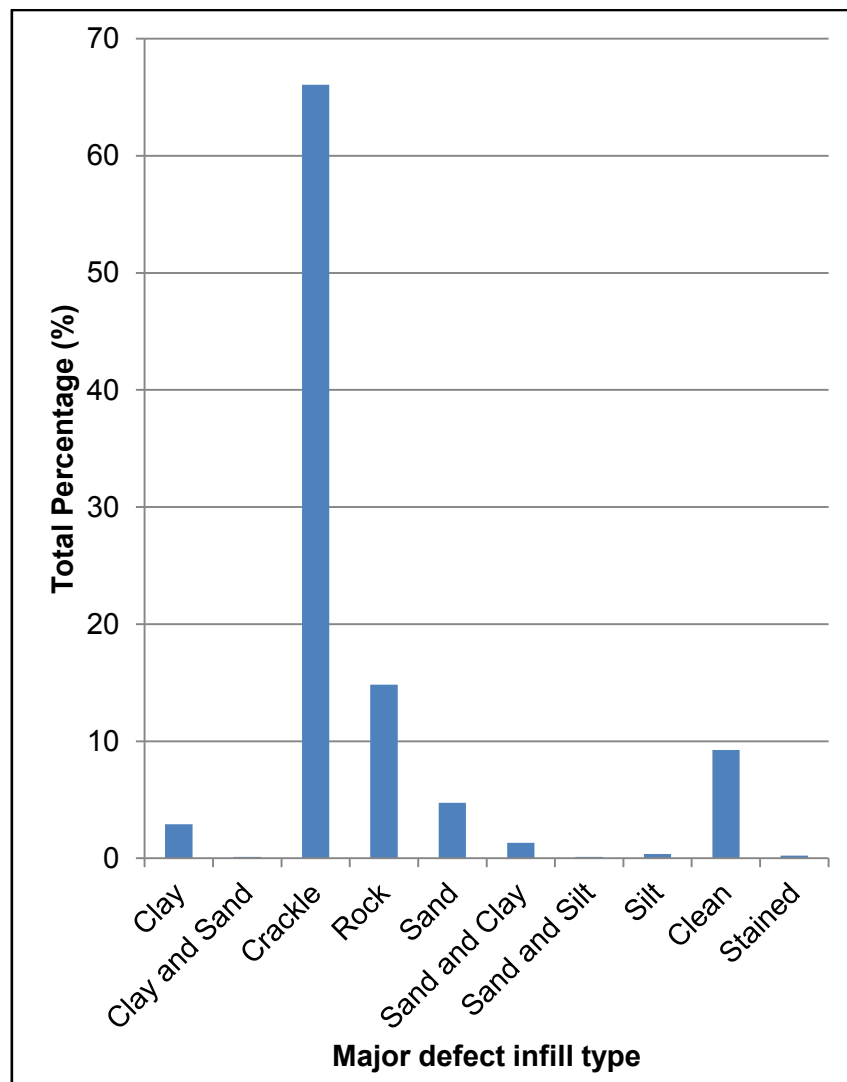


Figure 5.8: Major defect infill type across all sites. See Section 3.1.2 for infill type description.

Associated with most defect types are minor traces of mineralisation. The majority of defects observed in the field contain no traces of the mineralisation (about 63%) the remainder contain minor amounts, typically observed as randomly placed, white, hard, angular clasts or white sand-sized specks. Rarely is a defect fully filled with precipitated material (< 1%). Distribution of mineralised infilling increases in areas where there is less tectonic disturbance. However the trend is weak. Defects which display tight or dilated clean fracture surfaces do not appear to have any secondary mineralisation. Furthermore areas which display dominantly clast supported infilling also obtain less mineralisation.

a) Relationship with Shear Strength

Increasing mudstone content is likely to reduce the shear strength of defect planes. Associated with an increase in mudstone content is an increase of the finer grains in defect infill. Muds, particularly when there is a degree of moisture present, are commonly known to consist of significantly lower shear strengths than rock fragments or sand sized grains. Therefore where mudstone contents are higher the potential for slope instability is also higher.

b) Relationship with Bedding Thickness

As defect infill appears to be related to mudstone-sandstone ratios (Appendix I Figures I.4 to I.6) a distinction can be made between bedding thickness and the infilling rock fragments percentage. When dominant bedding thickness (Table 5.1) is compared to defect infill (Figure 5.7) it is seen that for lower mudstone-sandstone ratios with thin bedding the percentage of rock fragments in infilling increases.

3) Defect Continuity and Termination

Defect continuity was measured over the visible surface trace from one termination (end) to the other in natural slopes, or over a single bench in engineered slopes. Continuity was distinguished in three ways whereas the nature of the termination was distinguished in five, (Figure 5.9 and 5.10).

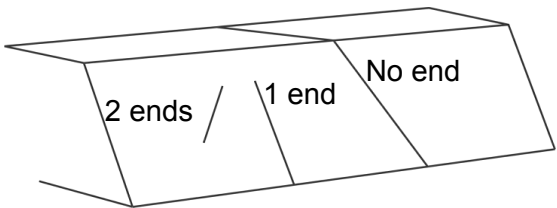
Continuity		
0	No ends visible	
1	1 end visible	
2	Both ends visible	

Figure 5.9: Schematic diagram used to indicate defect continuity across engineered cut slopes in all study areas.

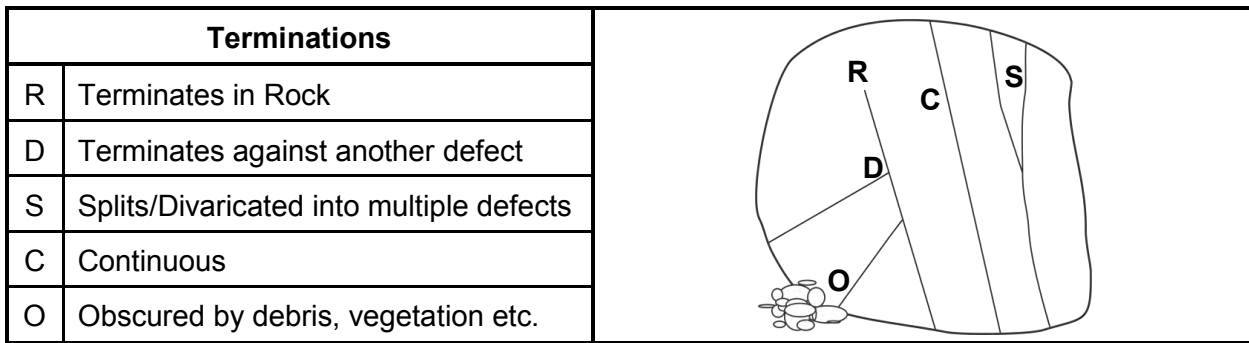


Figure 5.10: Schematic diagram used to indicate defect termination across engineered cut slopes in all study areas.

The more continuous structures tend to consist of the larger shearing (FL, SH and CZ) and bedding defects (Figure 5.11). The next continuous defect type is shears (SR), however, they mostly comprise of at least one visible termination (Figure 5.11). Jointing appears to be the least continuous of all the defects with over 65% of joints showing both terminations, which commonly occur against other joints or defects (Figure 5.12).

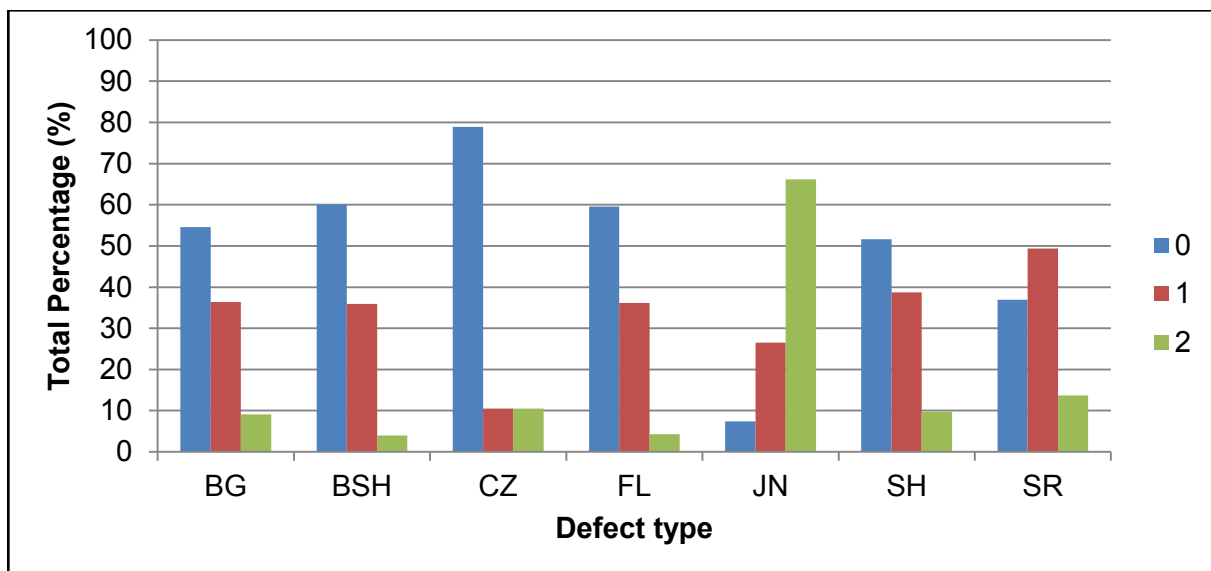


Figure 5.11: Continuity of defect types across all study sites. See Figure 5.9 for continuity explanation. See Figure 5.4 for acronyms.

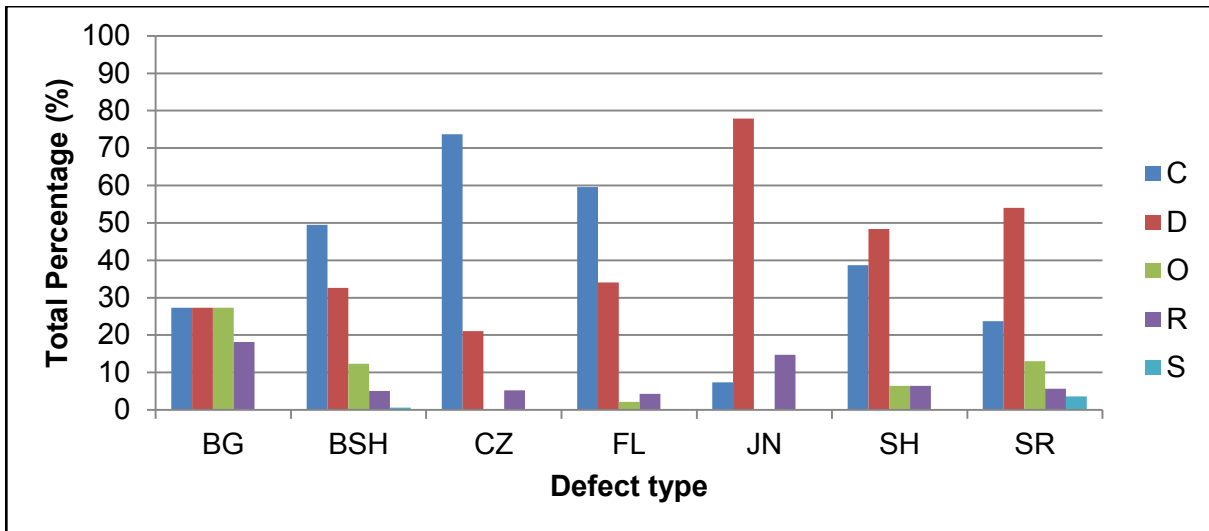


Figure 5.12: Nature of the terminations for different defect types across all study area. See Figure 5.10 for termination type, See Figure 5.4 for acronyms.

Generally, defect continuity is greater in areas further away from major fault traces and with higher sandstone proportions (Appendix I and Figure 5.7). This pattern correlates closely with the more continuous structures as previously indicated in this section. However, results from the two naturally forming rock slope sites (Makara Head and Wairaka Point) appear not to follow this trend. Defect continuity at these sites generally displays one defect end ($> 60\%$) which commonly terminates against another defect (about 50% of all defects).

a) Relationship with persistence

More “continuous” (FL, CZ, SH and BSH) defects (Figure 5.11) tend to correlate with a higher level of persistence (Figure 5.13). Evidence is presented in Figure 5.14, however the overall trend is weak. This is further explained in Section 5.2.7.

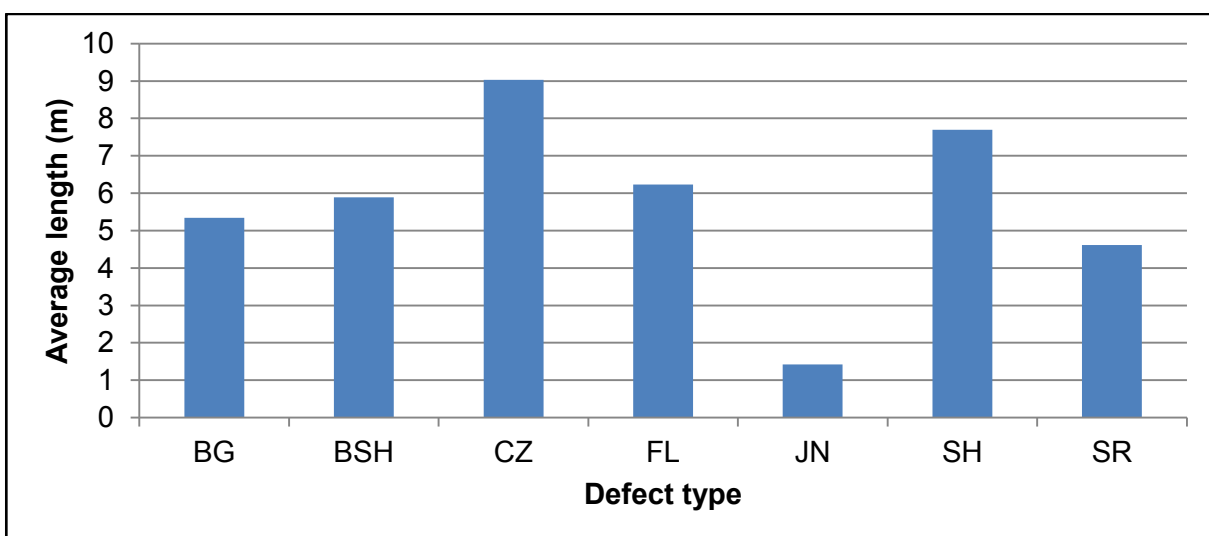


Figure 5.13: Average defect type trace length across all study areas. For explanation on defect acronym see Figure 5.4.

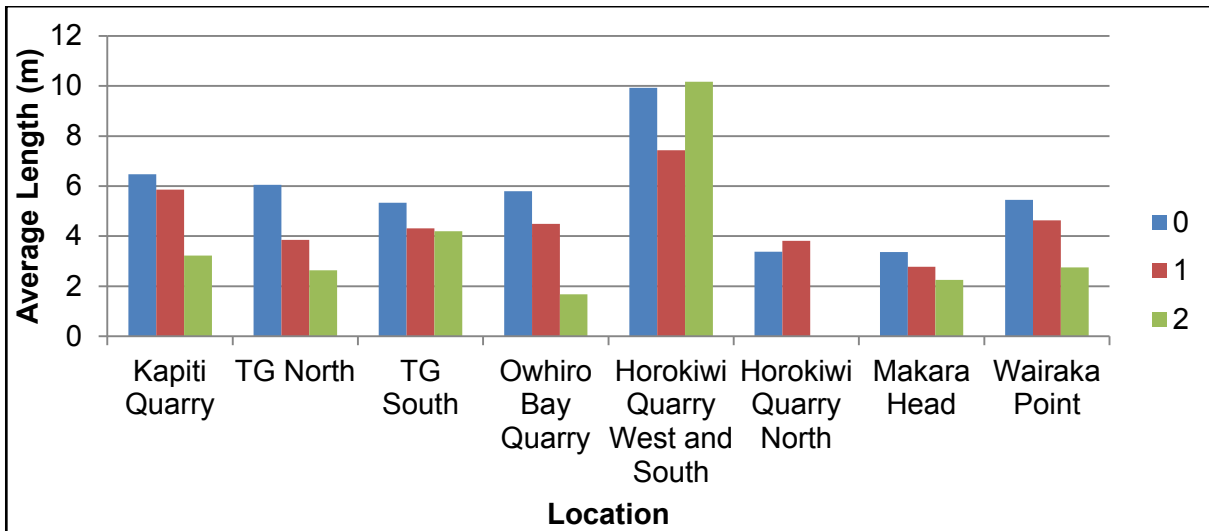


Figure 5.14: Relationship between continuity and persistence. For explanation on continuity terms see Figure 5.9 and 10.

4) Shearing Defect Spacing

Shearing defect types make up greater than two thirds of all recorded structural features (Section 5.2.2). Shearing is responsible for the disrupted appearance of many rock mass units (Sections 2.2). Therefore increased fracturing in a rock slope or bench generally decreases rock mass condition and increases the potential for slope instability. A range of different rock mass conditions are observed across different mudstone proportions study sites (Figure 5.15 and 5.16). It is generally observed that as mudstone proportions and the proximity to major faulting increases the degree of rock fracturing also increases (Figure 5.14). This is similar to bedding spacing trends, see Section 5.2.1 and Figure 5.17.

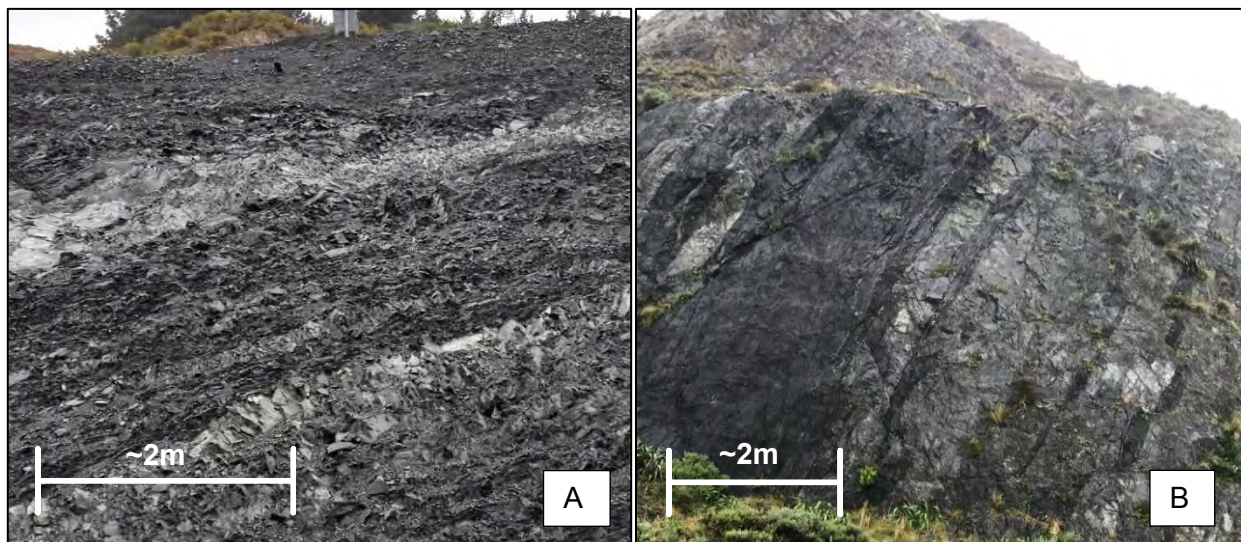


Figure 5.15: A) Kapiti Quarry outcrop 3a, thin/moderately thin mudstone:sandstone: B) Owhiro Bay Quarry 2, thick to moderately thick mudstone:sandstone.

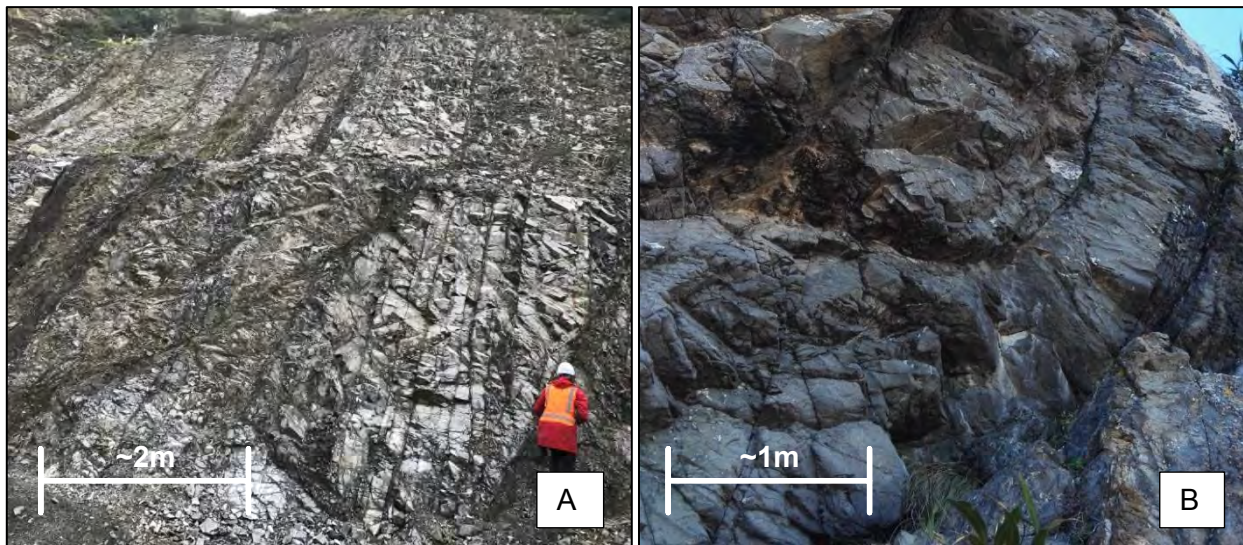


Figure 5.16: C) Horokiwi Quarry outcrop north, thin/thick mudstone:sandstone; D) Wairaka Point outcrop 1, thin/extremely thick mudstone;sandstone.

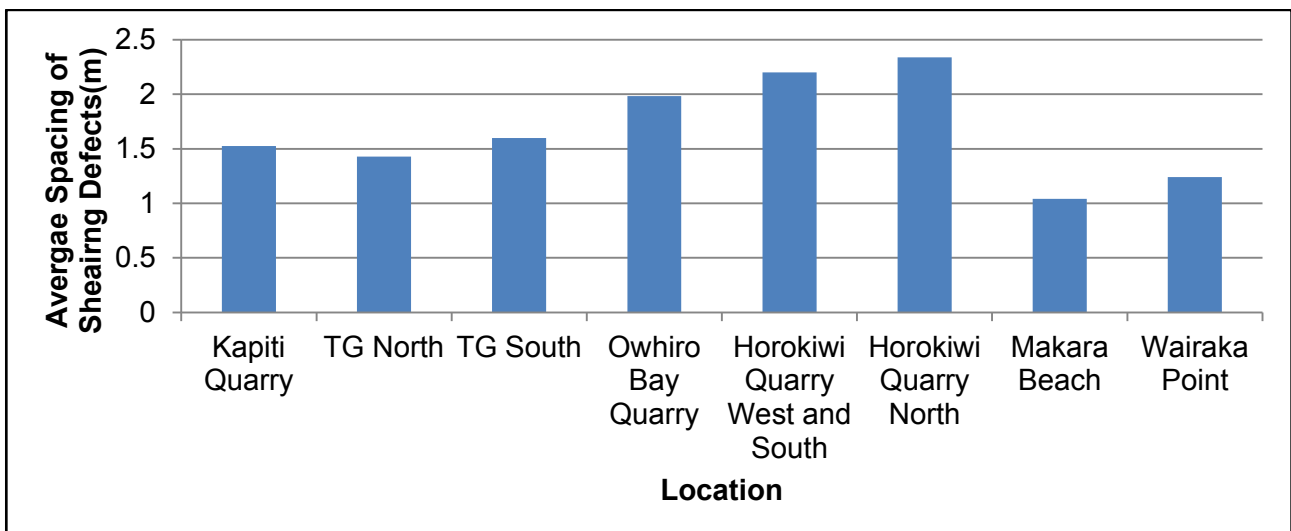


Figure 5.17: Average spacing of shearing defects across all study areas.

Spacing was determined by measuring the perpendicular distance between adjacent defects of the same type or set. This generally meant that spacing from larger, less frequent structures, such as faulting, shear zones and crush zones was more difficult to measure in areas of limited exposure.

It is important to note is that the two naturally forming rock slope sites (Makara Head and Wairaka Point) appear to have significantly lower defect spacing's than the other sites. This may be a result of the mostly discontinuous joint orientated shears (SR) (Section 3.1.1). This reduces the overall defect spacing. However, these shears are discontinuous and cannot be considered systematic.

a) Relationship Between Shearing Defect Type, Persistence and Spacing

More persistent shearing defects are generally more common in areas closer to major fault traces and where there is a higher mudstone proportion (Figure 5.5). This trend also correlates with a decrease in defect spacing. Therefore a differentiation can be made between defects which are categorically systematic or non-systematic (Section 2.2). It is apparent that systematic defects are progressively more closely spaced in areas where there is a higher degree of deformation and mudstone content. It is important to note that all sites present a degree of non-systematic shearing, therefore this trend is not only restricted to systematic defect sets. However, the pattern for non-systematic shearing is likely to be less distinctive due to the random orientation of sub-systematic defects.

5) Defect Waviness

Surface waviness was measured over the length of the visible trace of each discontinuity. Two measurements are used to describe the large scale shape of defect surfaces: Wavelength (λ) and inter-limb angle (ILA). Wavelength is used to record the distance between two adjacent identical peaks over the defect trace. The inter-limb angle is a record of the angle in degrees between the limbs of the defect trace. Figure 5.18 displays the relationship between inter-limb angle and wavelength. Estimates of these properties were collected from visual observations and recorded in data sheets displayed in Appendix I.12. Results of these characteristics are displayed in Figure 5.19. Generally where there is less tectonic disturbance and lower mudstone proportions bedding and shearing discontinuities tend to have smaller inter-limb angles as wavelengths get longer. Therefore defects appear to be more planar. This trend is weak and also limited by the scale of the outcrop exposed. By excluding any defects that were identified as planar this trend becomes clearer. Generally defects across the region show predominantly wavy profiles (Figure 5.20) with little control exerted by fault distance or lithology.

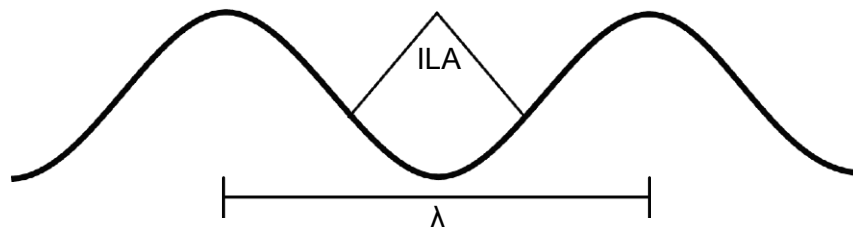


Figure 5.18: Relationship between Wavelength and Inter-limb angle (PSM, 2010a).

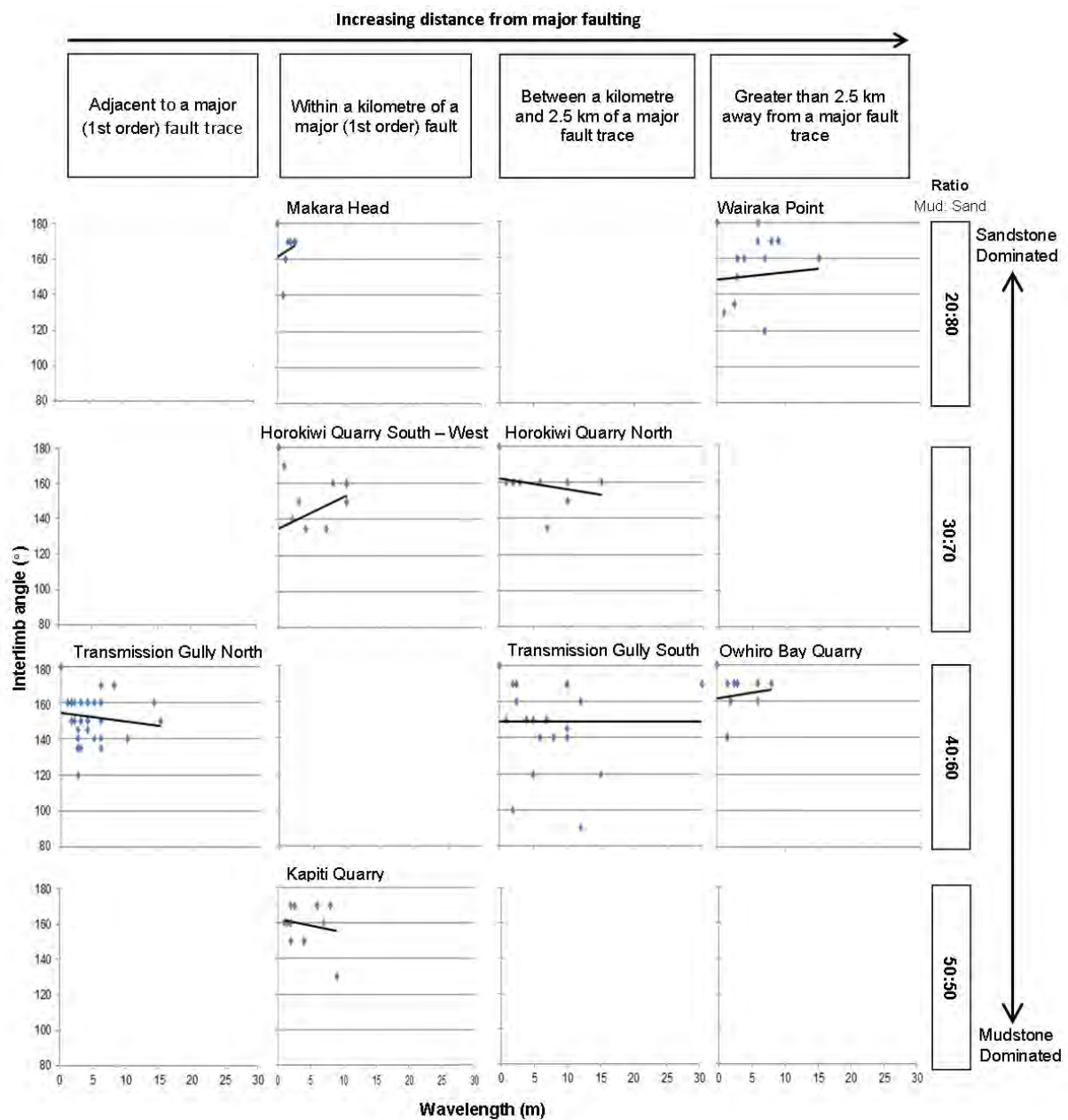


Figure 5.19: Bedding waviness across all study areas. Note that planar discontinuities are included.

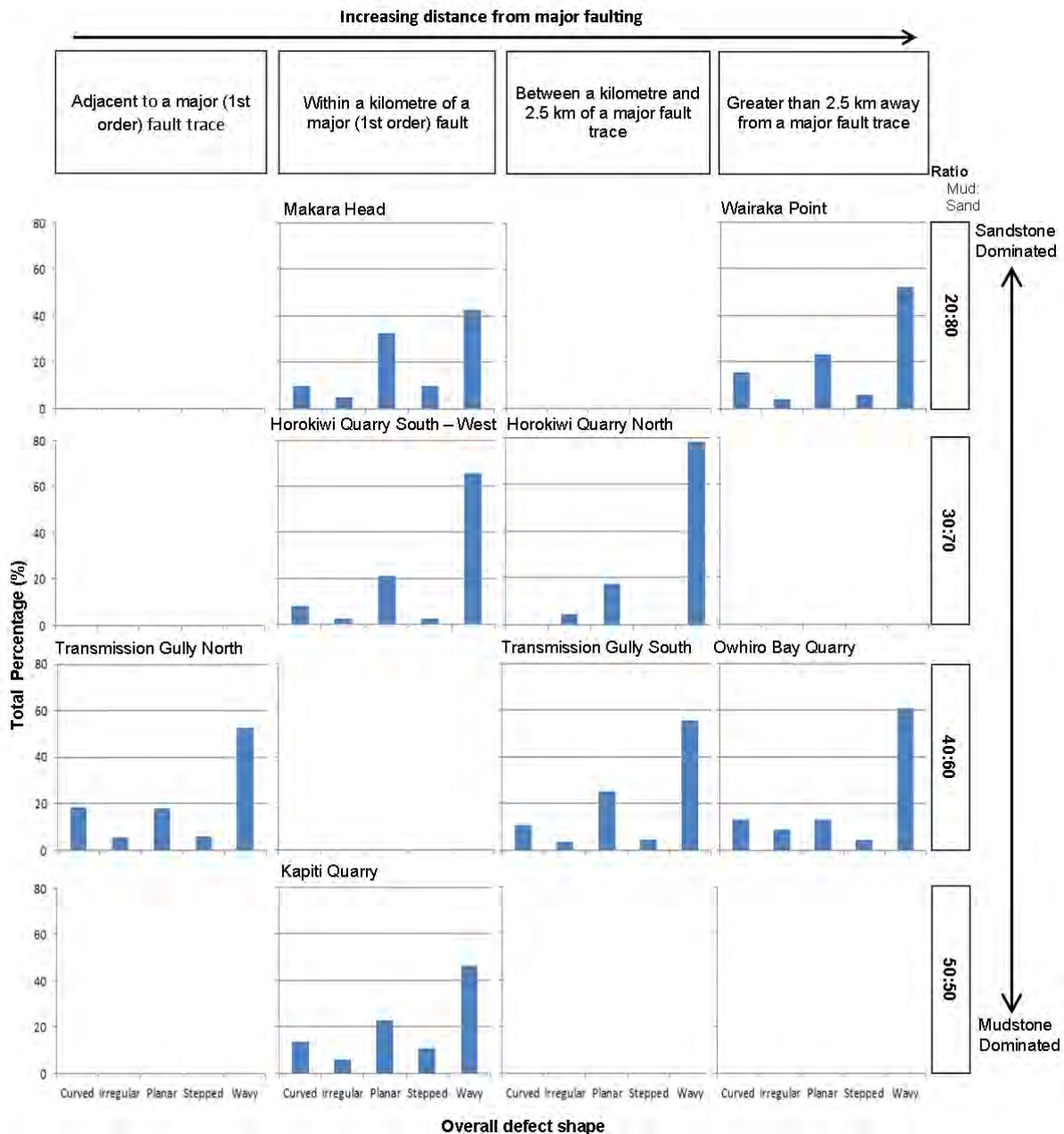


Figure 5.20: Defect shape across all sites.

a) Relationship with Shear Strengths

The shape of the defect plane can influence whether than failure can occur. Cook (2001) and Irvine (2013) along with many other authors (e.g. Reed and Richards, 2000) state that increasing the inter-limb angles on a defect plane can increase the shear strength. Therefore the wavier a defect is the less likely it is to cause a failure. More continuous and persistent defects generally occur where mudstone volumes and distances from major fault structures decrease (Section 5.2.2 part 3) this appears to correlate with the waviness trend identified. Therefore there is an anticipated increase in defect shear strength within discontinuities that obtain a degree of deformation.

5.2.3 Poorly Correlated Rock Mass Trends

Many rock mass variables did not show clear relationships in the field. In this study there is a focus on identifying the more persistent and continuous trends observed in large scale rock cut slopes which extend over multiple benches. In order to meet time requirements and assess large scale defect relationships the methods that analyse small scale structures, such as scanline or line mapping techniques used by Cook (2001), were not included. Other methods such as averaging the degree of fracture densities from multiple different outcrops, used by (Irvine, 2013), were also deemed unsuitable. In previous studies (AECOM and PSM, 2015; Cook, 2001; Irvine, 2013; Read and Richards, 2007; Read et al., 2000) have generally noted that low persistence, very closely to closely spaced, interlocked jointing tend to form higher rock mass strengths at smaller scales. Similar scales with tight, slightly rough to rough, and clean to stained joint surfaces are located throughout most of the sites investigated in this study. Jointing is still significant, however, it is only considered to contribute to local scale instability, either in combination with other short joints, or with larger more persistent structures (*i.e.* bedding or shearing defects).

Intact rock mass strength assessed using the (NZGS, 2005) field guide has similar issues. Due to the continuous nature of the majority of the study areas and the largely small range of weathering grades, there was a lack of rock mass strength trends. The focus of this study is to look at rock cut-slope stability controls and mechanisms outside of heavily faulted and weathered material therefore there was no need to assess a large range of weathering surfaces. Furthermore, this has already been addressed in classification systems established by Read et al. (2000), Cook (2001), Irvine (2013) and more recently Cammack et al. (2018).

There is no clear relationship between the recorded persistence at individual sites (Figure 5.21). Since persistence is a measure of the defect trace length visible in an exposure or over a single bench it is limited by the extent of the cut benches or rock slope exposed at each site. For example at Makara Head, where exposures are no greater than about six metres high and are frequently discontinuous, visible defect trace lengths appear to be significantly lower compared to exposures that are higher and wider, such as Owhiro Bay Quarry. Furthermore, in this study the rock slope benches examined are commonly much longer than they are high. If a defect is oriented sub-parallel to the width of an exposed bench or slope this would result in greater persistence than a perpendicularly orientated discontinuity. Likewise, an increase in the overall average within that area would be seen (*e.g.* Kapiti and Horokiwi Quarries). It is therefore important to compare the average defect persistence against the overall continuity and termination nature at each site (Figure 5.12).

In this study persistence is limited by the scale of rock exposures at each site. Therefore, persistence in areas where exposures are small can only be estimated, particularly for naturally

forming rock slopes. Fewer chances are available to record defect characteristics and parameters within these sites. Therefore only experienced and intelligent estimates based on probability theory and global observations can be given to predict the overall persistence. This must be considered in rock cut-slope design.

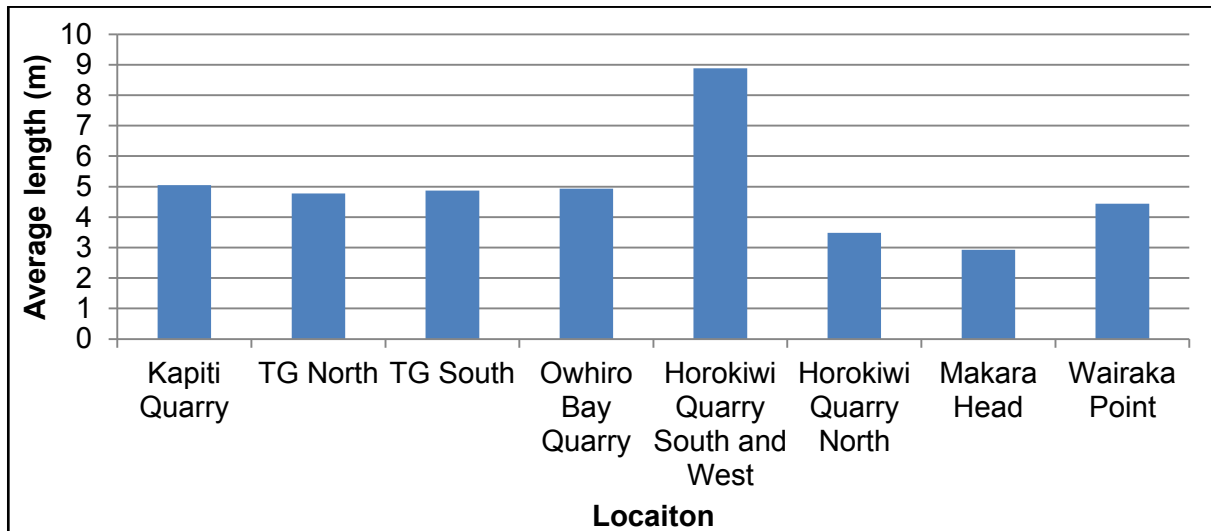


Figure 5.21: Average length (Persistence) of all the defects across all study sites.

The Torlesse rock mass is highly complex resulting from a number of tectonic events. Therefore not all rock mass characteristics will develop clear trends. As such, a large variation in defect width and roughness character was observed across all the study sites. Despite this it was observed that the larger more persistent structures (SH, FL, and CZ) displayed significantly larger defect widths (Figure 5.22) when compared to those of bedding and jointing (Figures 5.1 and 5.2). Faulting (FL) also appeared to be the more planar defect type.

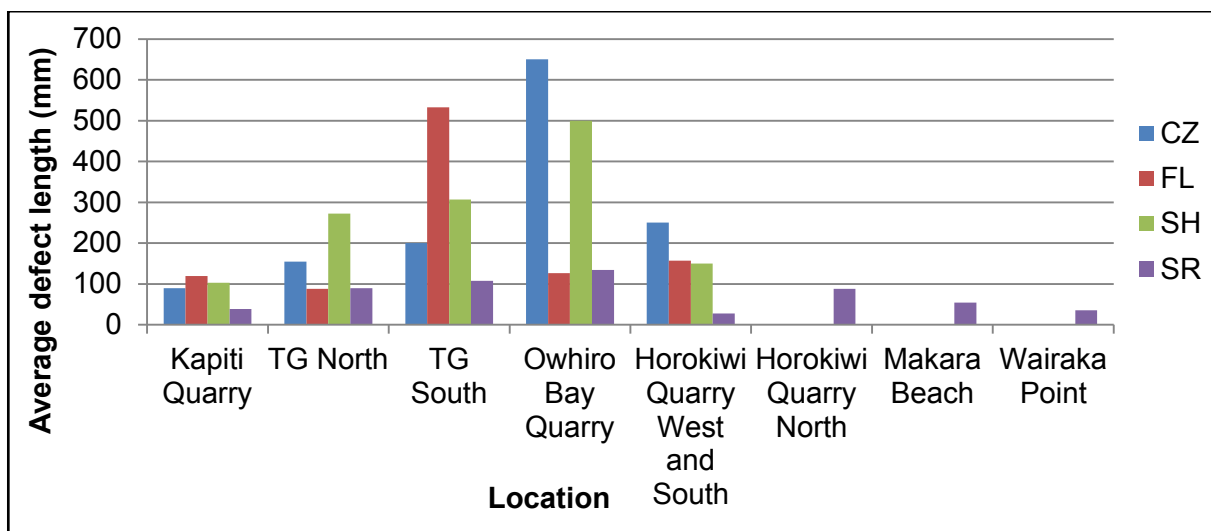


Figure 5.22: Average defect width of shearing defects. See Figure 5.4 for acronyms.

5.3 Conceptual Classification System

Defect structure and lithology as described in Sections 5.2.1 and 5.2.2 together make up the dominant controls influencing potential slope instability for the Torlesse. The relationships established in Section 5.2 are all related and used to form a conceptual rock mass classification for the Torlesse.

5.3.1 Rock Mass Classes

Observational trends and defect structure analysis identified two main principal controls for rock mass condition, lithology and defect structure.

Lithology

Lithology is used in an arbitrary way where it describes bedding thickness and mudstone to sandstone proportions. Areas of similar character have been grouped together and used to derive four rock mass classes that encapsulate/capture the variety of rock mass conditions observed.

In developing the principal lithological classes a similarity formed between the observed trends and the sedimentary lithofacies classification from Suneson (1993). Observational mapping consisted of describing the Torlesse rock mass in terms of Suneson (1993, 1992) sedimentary lithofacies classification. Each outcrop was grouped accordingly with results presented in Table 5.2. Some of the criteria used by (Suneson, 1992) to distinguish the different lithofacies are similar to the groups established in this study. Therefore there was a natural progression to describe the four rock mass groups as lithofacies which are represented in Table 5.3. The use of PSM's description of bedding thickness was also used (Table 5.4) as it can be related to NZGS (2005).

Table 5.3: Definition of rock mass lithofacies

Lithofacies	Dominant lithology	Dominant lithology bedding thickness	Sandstone: Mudstone Ratio
A	Sandstone (Arenaceous)	Massive to thick bedded sandstone	4:1 and fewer
B	Muddy sandstone (Arenaceous-Pelitic)	Medium bedded sandstone	4:1 to 1:1
C	Sandy mudstone (Pelitic-Arenaceous)	Medium to thinly bedded mudstone	1:1 to 1:2
D	Mudstone (Pelitic-Arenaceous)	Massive to thickly bedded mudstone	1:2 and greater

Table 5.4: Summary bedding thickness classification from PSM (2010)

Description	Bed thickness
Massive – No stratification	> 2 m
Very thickly bedded	>2 m
Thickly bedded	0.6 – 2 m
Medium bedded	0.2 – 0.6 m
Thinly bedded	60 mm – 0.2 m
Very thinly bedded	20 – 60 mm
Thickly laminated	6 – 20 mm
Thinly laminated	< 6 mm

Lithofacies A

Lithofacies A consists of massive to thickly bedded sandstone with occasional very thin to thin interbeds of mudstone. Sandstone beds range in thickness from 0.3 m to metres while the mudstone beds are generally between 40 mm and 150 mm thick. Mudstone to sandstone ratios are typically 1:4 or less. This is typical of Lithofacies B of Suneson (1992). Sandstone beds are rarely truncated and tend to have well-defined jointing. The larger natural rock slope exposures and generally correlates with better rock mass conditions.

Lithofacies B

This consists mostly of interbedded sandstone and mudstone. Sandstone tends to be medium bedded (around 0.4 m thick) while mudstone beds are generally thinly bedded (less than 0.2 m). However, both types can be very thickly bedded. This is similar to Lithofacies C and aspects from B from Suneson (1992). The major difference is that individual sandstone beds are thinner and mudstone to sandstone ratios are between 1:4 and 1:1.

Lithofacies C

In Lithofacies C individual sandstone beds tend to be thinner and mudstone contents tend to be higher. Mudstone to sandstone ratios generally range from 1:1 to 2:1. Mudstone beds vary from 60 mm to 0.6 m thick while sandstone beds are commonly 0.3 m thick. Thicker beds may be present but these are rare. This is similar to Lithofacies D from Suneson (1992). Lithofacies B and C commonly outcrop together and tend to grade into each other. Exposures of Lithofacies C rarely extend more than 50 m.

Lithofacies D

This massive mudstone lithofacies consists mostly of mudstone material while sandstone is typically rare or absent. Outcrops of this lithofacies are rare and often extensively sheared with

few visible very thin to thinly bedded sandstone interbeds. Outcrops examined in this study show bed thickness of no more than 2 m. Typically this lithofacies grades into Lithofacies C, and vice versa. Mudstone to sandstone ratios are greater than 2:1. This is similar to Lithofacies G of Suneson (1992).

Defect structure

Defect structure consists of the trends identified through field observations. It includes the defect characteristics that heavily influence potential mechanisms for failure in rock slopes. These are mostly observed to be the rock mass properties that represent rock mass condition, such as type and persistence. In developing a rock mass classification these factors were grouped into classes where similar conditions were observed. Each class considers the global and local stability influence of each component.

Large scale rock cuts design relies on subsurface information primarily drillhole data, in addition to limited surface mapping (Section 4.2). Throughout this study persistence has been highlighted as a key factor controlling to global slope failures. This rock mass property (Section 5.2.3) however is not able to be identified from borehole data due to the properties 2-D to 3-D characteristic. Thus, the previously described inputs for the defect structure classes must be adapted to include more information regarding features that presented relationships with persistence (Section 5.2.2). This includes defect infill characteristics and spacing. Defect structure classes are presented in Table 5.5. ISRM (1978) descriptions of spacing was applied as it provided more concise terminology and can be related to NZGS (2005) (Table 5.6).

Table 5.5: Dominant defect structures controlling slope stability. It is inferred that global scale structures will also control local failures as well, either by interacting with other similar or local structures.

Defect structure			
Class	Globally dominant structures (ISRM, 1978)	Local structures	Main Defect Infill
1	Persistent and continuous systematic shears and bedding (>50 m). Systematic shearing is extremely widely spaced. Faulting, shear zones, crush zones, cross-cutting and sub-systematic shears are rare but are persistent.	Persistent (≥ 4 m) well defined, Jointing, widely spaced.	Strong to moderately strong rock fragments (>95%). Sand matrix. Traces of Precipitation
2	Persistent and continuous systematic shears and bedding (>30 m). Systematic shears are very widely spaced to widely spaced. Persistent (>30 m) faults, shear zones, crush zones and cross-cutting shears are more frequent but still uncommon.	Discontinuous, moderately defined Jointing (~1 m), moderately spaced. Rare, sub systematic shears that are persistent (>30 m).	Moderately strong to weak rock fragments (>90%). silty Sand matrix. Few traces of precipitation.
3	Persistent and continuous (>20 m) bedding and Widely spaced systematic shears. Shearing that cross cuts may be spaced 10-30 m. Persistent faults, shear zones and crush zones start to become more frequent.	Discontinuous and random Jointing (~0.5m) closely spaced. Sub systematic shears are more common but are also discontinuous.	Weak rock fragments (>85%) Silty. Slight plasticity occurrences. Rare precipitation
4	Widely spaced to moderately spaced shearing structures that are continuous (>10 m) may form defined sets. Isolated shears are common. Most defects are discontinuous and tend to terminate other structures. Bedding may be persistent (>20 m) but these are often truncated or overprinted.	Jointing is closely spaced to very closely spaced discontinuous, random and sub-systematic. Discontinuous shearing and bedding and structures.	Weak to very weak rock fragments (>80%). silty Clay. Slight plasticity. No precipitation
5	Persistent defects are less common. Those that are continuous tend to be faults, sheared and crush zones. Cross-cutting Bedding may span the length of a bench (>10 m) but is commonly less distinct and tends to be overprinted, discontinuous and truncated.	Jointing is very closely spaced to extremely closely spaced. Sub-systematic and systematic shears are in approximately equal proportions.	Clay rich matrix, slight to moderate plasticity, Very weak rock fragments (<75%). No precipitation
6	Brecciated rock mass with potential shearing very closely spaced and limited persistence. Typical of sheared and crush zones		

Table 5.6: ISRM (1978) defect spacing classification

Description	Spacing
Extremely close spacing	< 20 mm
Very close spacing	20 – 60 mm
Close spacing	60 – 200 mm
Moderately spacing	200 – 600 mm
Wide spacing	600 – 2000 mm
Very wide spacing	2 – 6 m
Extremely wide spacing	> 6 m

Classifying both defect structure and lithology allows any outcrop to be assigned a representative engineering categorisation. Lithology is dependent on the depositional environment at the time of formation. Defect structure is also dependent on lithology, but is mostly controlled by the tectonic history of the region.

5.3.2 Nature of the Classification

One of the main objectives of this classification is to clearly and capture the complex variability in the Torlesse seen across all study areas. Trend analysis shows that there is a significant variation in bedding thickness and rock mass condition of the mudstone dominated lithofacies when compared to the sandstone dominated lithofacies (Section 5.2.1). As such, this classification attempts to capture this variability in lithological groups or facies. This is highly important for rock slopes as mudstone and sandstone proportions can change significantly over short distances.

5.3.3 Conceptual Development and Validation

Development of the conceptual Torlesse rock mass classification (Figure 5.23) was based on visual observations and trends identified in Section 5.2. In relating the key influences (*i.e.* defect structure and lithology) to rock mass condition, the best rock mass quality is defined by Lithofacies A which is not expected to comprise defect classes 5 or 6. Similarly, Lithofacies D and C, which define poorer rock masses, are not anticipated to contain defect classes 1 or 2. Therefore, the top right and bottom left hand corners are not included in the classification. Defect structural class 6 is suggestive of extremely poor rock mass condition, which typically describes fault crush material. This is highlighted in the rock mass classification as a “Fault crush zone”. Entire rock exposures that obtain this class are expected to be rare and only located adjacent to major regional faulting. Also captured are the rock masses that experience increased deformation close to major structures. This is termed the “Fault disturbed zone”. The classification graph also considers decreasing bed thickness.

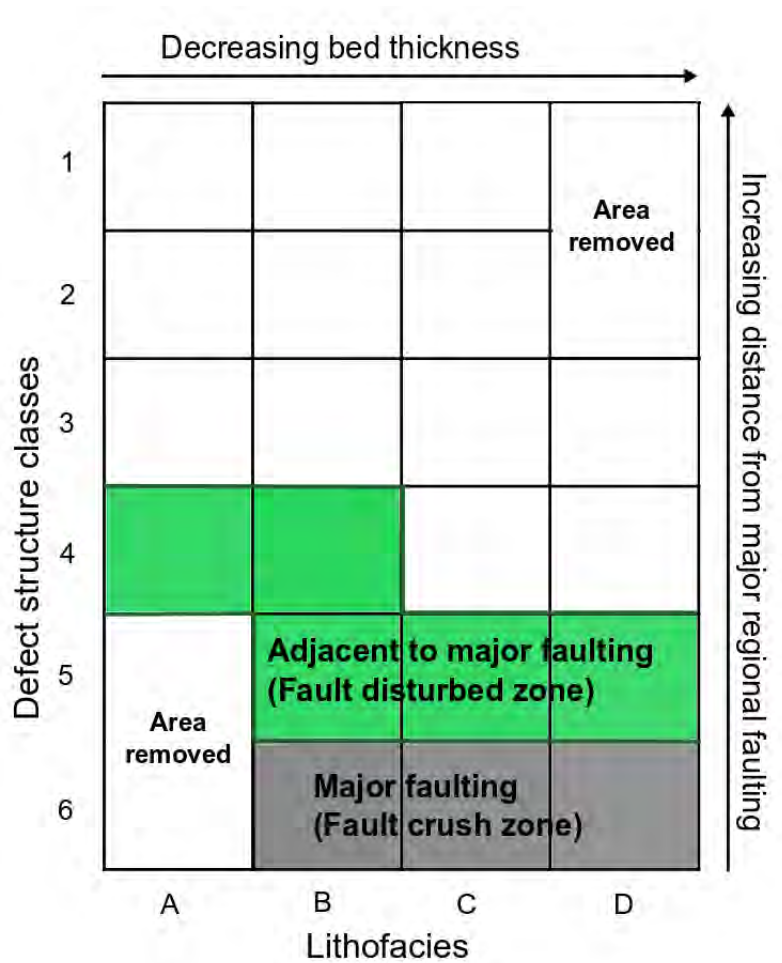


Figure 5.23: Torlesse rock mass classification.

The final classification (Figure 5.24) is validated by graphing individual site data (Figure 5.25). No outcrops appeared to obtain the rock masses of Lithofacies D with the favourable structural defect classes of 1 to 4. Despite the absence of these rock masses being encountered, the potential for defect classes 3 and 4 to exist still remains as indicated by previous studies (Begg and Johnston, 2000; Suneson, 1993). Additionally, the better quality rock masses of Lithofacies A with the unfavourable defect structural classes of 6 and 5 were not evident, but are also likely to be encountered. Therefore only defect classes 1 and 2 from the poorer rock masses were removed from the classification as they represent combinations that are not likely in the Wellington Torlesse rock mass. A margin of error has been included to accommodate the possibility of these rock masses that are still likely to be encountered, as represented by the dashed outlines in the lower section of the graph.

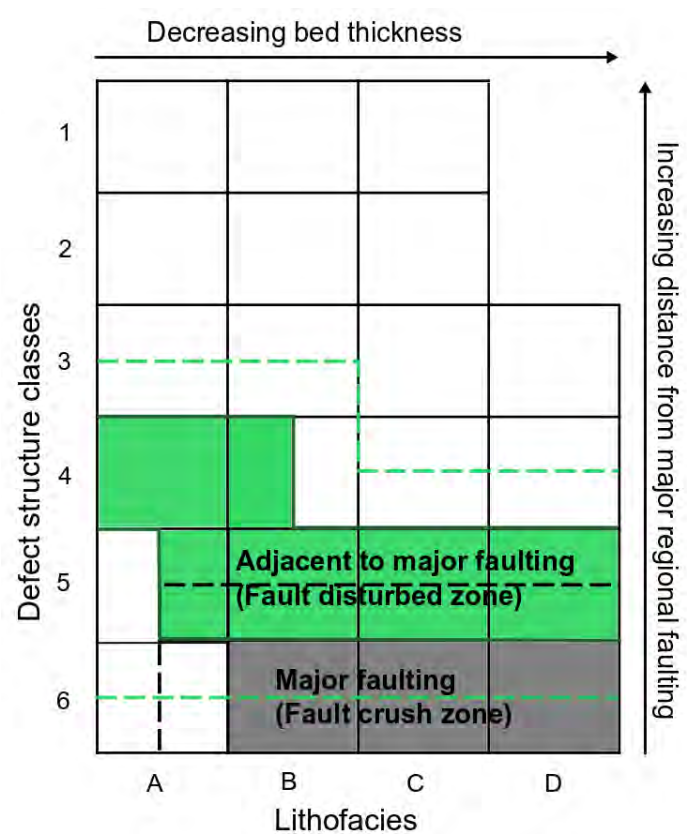


Figure 5.24: Final Torlesse Rock mass Classification (TRC).

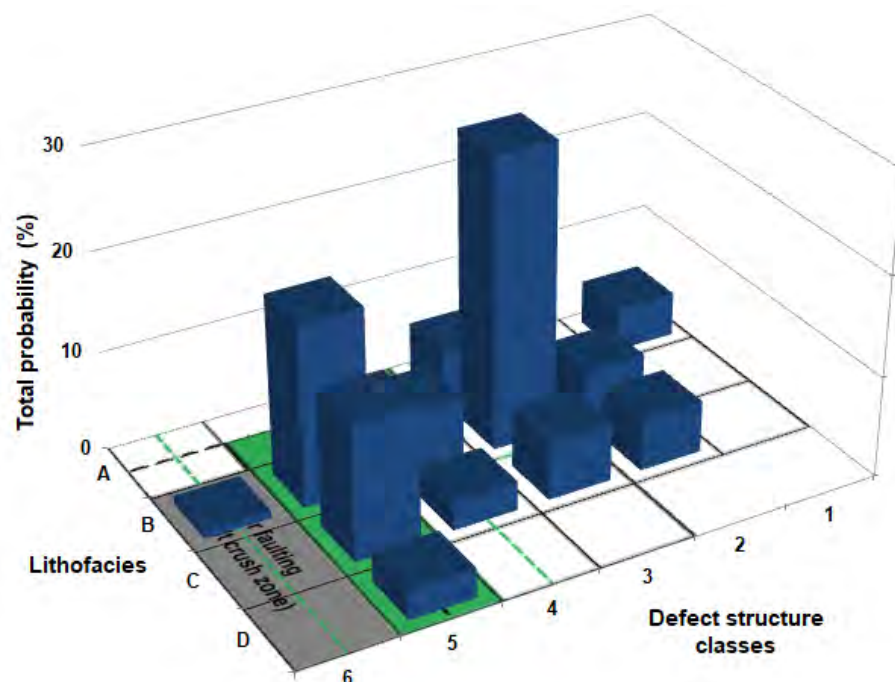


Figure 5.25: Probability plot of the overall likelihood of defect classes and lithofacies combined.

Given the complexity of the Torlesse tectonic history some of the areas display highly fractured appearances typical of defect structural classes 5 and 4, but do not appear to be situated within the presumed locations of these structural classes. Therefore, due to the highly variable nature

of the Torlesse rock mass the “Fault disturbed zone” interpretation should only be used as a guideline as this may not hold true for all locations.

5.4 Plotting Study Sites TRC

In using the lithofacies established in Section 5.3.1 the only difference observed between the results identified in Table 5.2 is that the two naturally forming rock exposures at Makara Head and Wairaka Point now obtain a Lithofacies Group of A. The other sites remain unchanged due to an excess of mudstone bedding thickness and proportions. Results of the defect structure classes and lithofacies Groups established in Section 5.3 can be seen in Table 5.7. All outcrops were grouped based on mapping and field observations.

Table 5.7: Relative proportions of the adapted Suneson (1993) lithofacies groups and structural defect classes established in 5.3.1.

Study area	Width of outcrop	Relative proportion of lithofacies in percentage				Relative proportions of defect classes in percentages					
		A	B	C	D	1	2	3	4	5	6
TG North	460 m	80	20						10	80	10
Outcrop 1	120 m	80	20							✓	
Outcrop 2	30 m	80	20							✓	
Outcrop 3	85 m	60	40						✓		
Outcrop 4	90 m	70	30							✓	
Outcrop 5	30 m	100	0							✓	✓
Outcrop 6	25 m	100	0							✓	
Outcrop 7	80 m	70	30							✓	
TG South	450 m	70	30					75	25		
Outcrop 1	80 m	60	40						✓		
Outcrop 2	140 m	80	20					✓			
Outcrop 3	130 m	70	30					✓			
Outcrop 4	100 m	70	30					✓			
Kapiti Quarry	300 m	50	40	10					33.3	66.7	
Outcrop 1	20 m	100	0						✓		
Outcrop 2	180 m	15	65	20						✓	
Outcrop 3	100 m	30	50	20						✓	
Owhiro Bay Quarry	200 m	50	50				100				
Outcrop 1											
Outcrop 2	100 m	60	40				✓				
	100 m	40	60				✓				
Horokiwi Quarry	320 m	90	10					66.7		33.3	
Outcrop 1	20 m	80	20							✓	
Outcrop 2	150 m	90	10					✓			
Outcrop 3	150 m	100						✓			
Wairaka Point	86 m	100				100					
Outcrop 1	40 m	100				✓					
Outcrop 2	20 m	100				✓					
Outcrop 3	20 m	100				✓					
Outcrop 4	6 m	100				✓					
Makara Head	100 m	100						100			
Outcrop 1	25 m	100						✓			
Outcrop 2	15 m	100						✓			
Outcrop 3	20 m	100						✓			
Outcrop 4	40 m	100						✓			

Statistical calculations of the data from individual sites were then undertaken to check and validate the conceptual Torlesse rock mass classification (Appendix J). This is displayed in the figures presented in the following sections.

5.4.1 Transmission Gully North

The Transmission Gully North study area (Figure 5.26) shows a dominant presence of rock masses located adjacent to major 1st order faults. This area is dominated by Lithofacies groups C and B which tend to outcrop together. Where outcrops consist only of Lithofacies C there tends to be a higher degree of shearing. Three defect structural classes (4, 5 and 6) are observed which combined with the lithofacies groups produce three main rock types displayed (Figure 5.27). Rock type 1 is generally indicative of the highly brecciated rock mass typical of fault crush material. This rock type is completely fragmented and represents the worst rock mass conditions observed. Rock type 2 represents discontinuous systematic and sub systematic fracturing with bedding that is rarely continuous. Jointing is very closely spaced and defect infill tends to obtain the highest proportion of finer materials (<2 mm). Rock type 3 displays more continuous structures in comparison to rock type 2. Shearing starts to form more defined sets and wavelengths tend to become longer. This rock type is generally observed in the higher benches or at increasing distances from the Ohariu Fault. Due to proximity of the major fault zone it is presumed that the regional stress is likely accommodated within the outcrop shearing. Jointing is therefore typically sub-systematic and randomly oriented. The features that tend to control global slope stability are the continuous shearing or faulting structures.

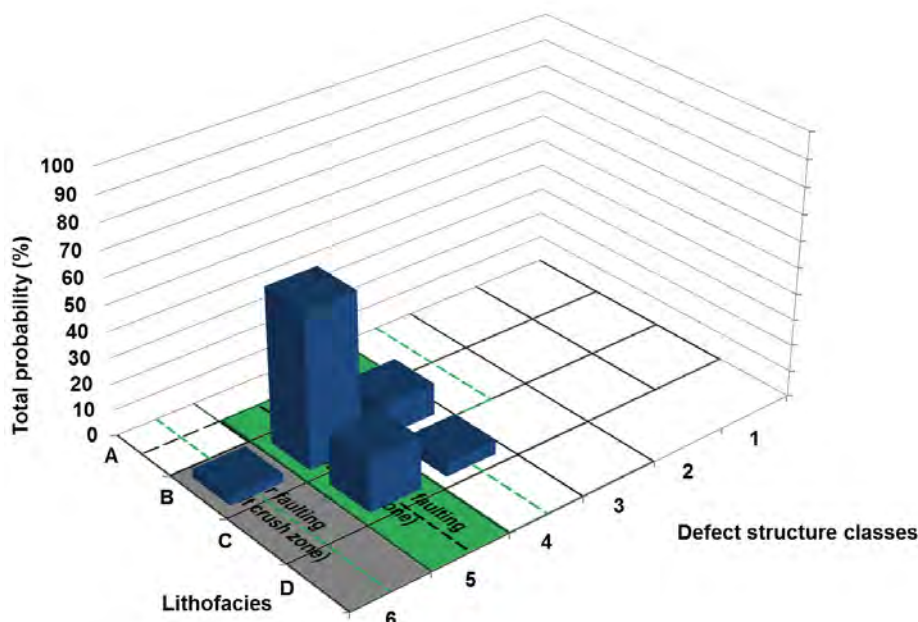


Figure 5.26: Probability plot of the Transmission Gully North defect structural classes and lithofacies groups combined.

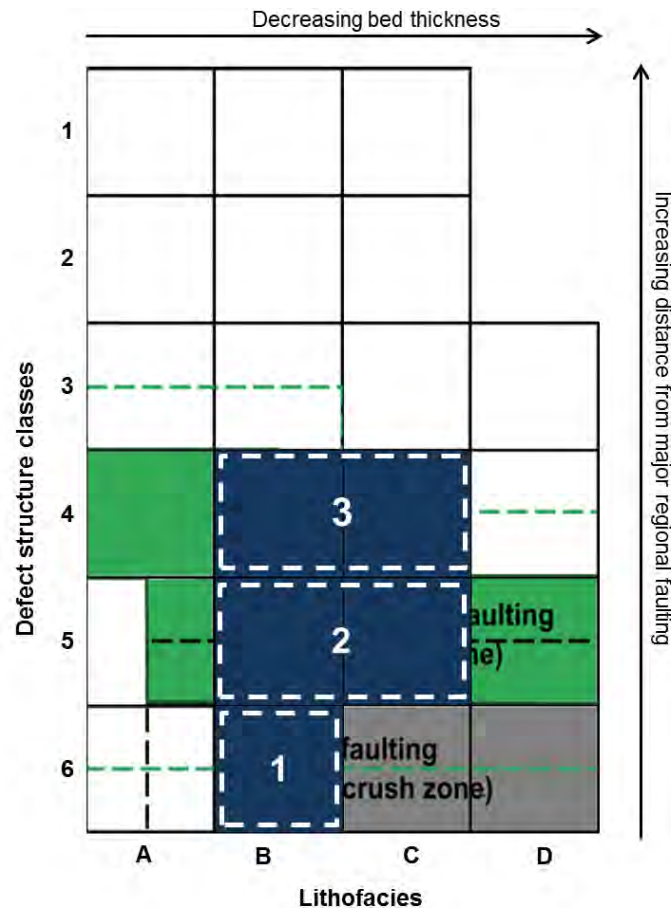


Figure 5.27: Bird's eye perspective of the Transmission Gully North TRC (defined in Figure 5.24) plot and subsequent rock type clusters. Each cluster represents rock mass types 1, 2 and 3 explained in the previous paragraphs.

5.4.2 Transmission Gully South

The Transmission Gully South study area is mostly controlled by the Ohariu and Moonshine faults which are located approximately 2.5 km to the West and East respectively. Two rock mass types are presented in Transmission Gully South TRC (Figure 5.28). Rock type 1 is represents the least amount of data for this site and similar characteristics to rock mass 3 at the Transmission Gully North (Figure 5.29). Rock type 2 represents the majority of the rock mass at this site. Structures appear to be more continuous with the larger defects such as faulting, crush zones and shear zone tend to persistent for >20 m, indicating a influence of major regional faulting on structures. Global instability is appears to be governed by the larger more persistent defect types and widely spaced systematic shear. Cross-cutting shears may be spaced 10-30 m apart. Jointing is starting to form a few systematic sets but is still closely spaced, planar and randomly oriented. Systematic shear sets are more common in areas that obtain higher proportions of Lithofacies group B indicating influences of mudstone to sandstone proportions. Lithofacies B still tend to dominate the site, however, the relative probability of Lithofacies C has increased from the Transmission Gully North study area.

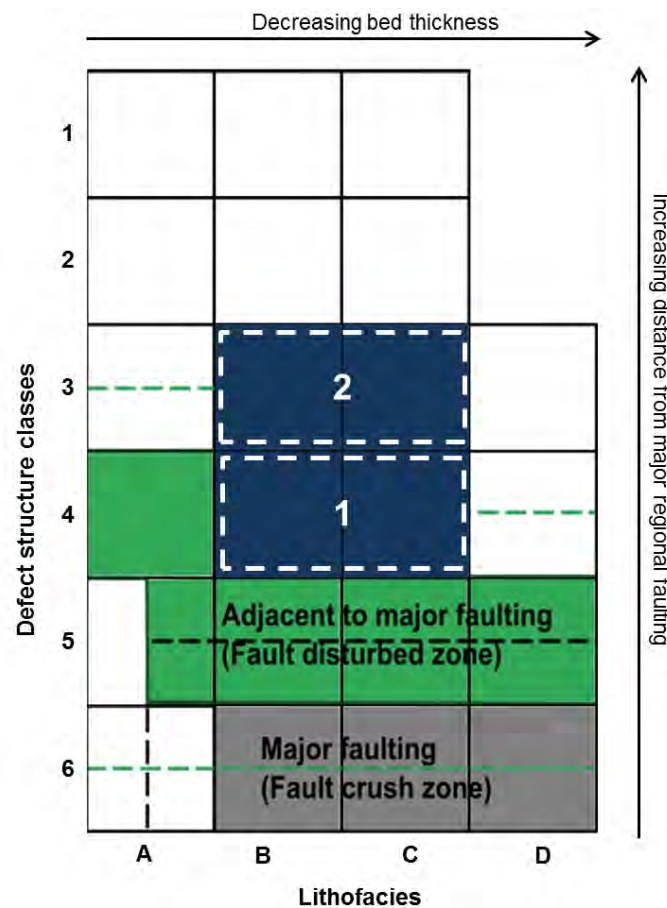


Figure 5.28: Bird's eye perspective of the Transmission Gully South TRC (defined in Figure 5.24) plot and subsequent rock type clusters. Each cluster represents rock mass types 1 and 2 explained in the previous paragraphs.

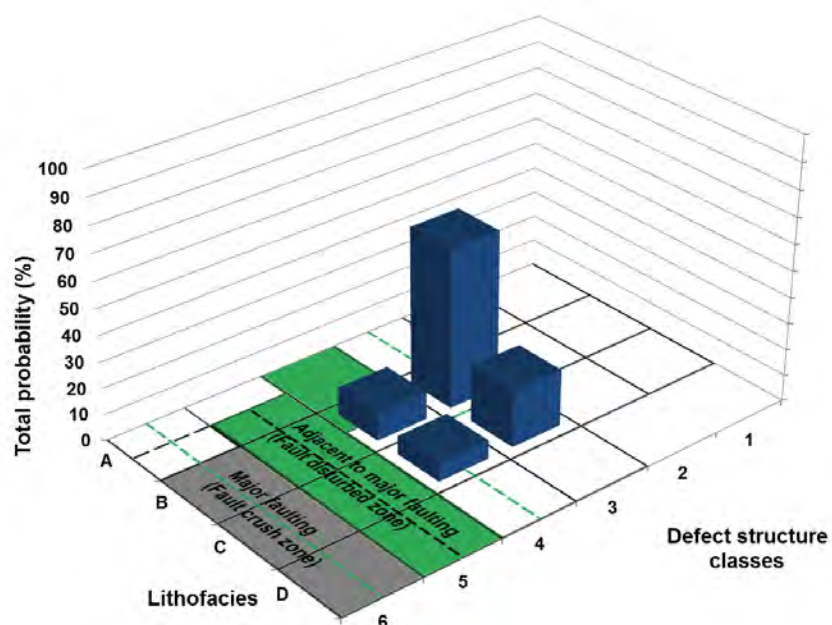


Figure 5.29: Probability plot of the Transmission Gully South defect structural classes and lithofacies groups combined

5.4.3 Kapiti Quarry

The Kapiti Quarry site represents the highest proportions of mudstone content across all the study areas (Figure 5.30). A wide range of lithofacies can be observed in the rock mass from B through to C. Typically the Lithofacies C and D are exposed together and tend to grade into each other. While Lithofacies D may be present it the least exposed of the three across all the sites (~18%; Figure 5.25). Lithofacies C tends to dominate while Lithofacies B appears to outcrop between beds of group C or as an individual group which is bounded on either side by faults. Two different rock mass types are presented here. Rock type 1 represents similar characteristics to rock mass 1 at the Transmission Gully South (Figure 5.31). Rock type 2 represents the highest mudstone rich rock type identified across all study sites. Located within a kilometre of the nearest major regional fault (Ohariu fault) the rock type is typically heavily sheared and fragmented within the mudstone units. Thick sandstone beds that display typically discontinuous, closely spaced jointing are infrequent and bedded between thick mudstone beds. Defects are typically discontinuous with bedding shears generally wide enough to form persistent (> 15 m) shear zones. It is these features (Shear zones) along with persistent (> 30 m) faults that tend to govern slope stability.

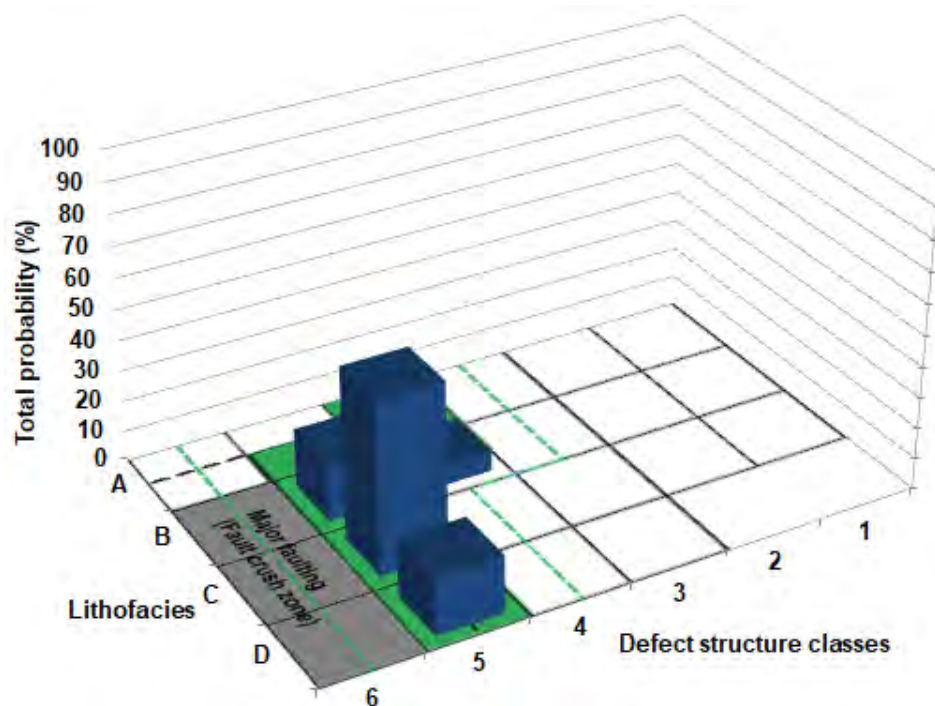


Figure 5.30: Probability plot of the Kapiti Quarry defect structural classes and lithofacies groups combined.

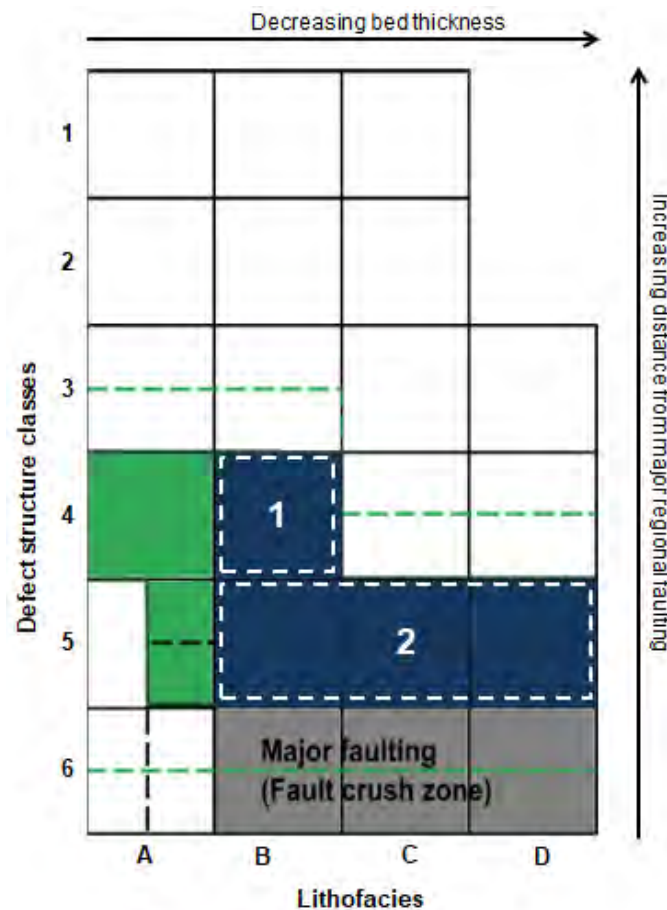


Figure 5.31: Bird's eye perspective of the Kapiti Quarry TRC (defined in Figure 5.24) plot and subsequent rock type clusters. Each cluster represents rock mass types 1 and 2 explained in the previous paragraphs.

5.4.4 Horokiwi Quarry

The rock mass displayed at the Horokiwi Quarry study site is mostly controlled by the Wellington Fault. Relative probabilities show that there is an increase in defect structure class 3 from 5 (Figure 5.32). This suggests that the distance from major faulting structures (Wellington Fault) is increasing. The dominant lithofacies group appears to be B with mostly intermittent occurrences of Lithofacies C. Two clusters are identified at this site (Figure 5.33). Rock type 1 presents a heavily overprinted rock mass which is characteristically similar to rock type 2 at the Transmission Gully North (Figure 5.27). This rock mass is dominantly heavily controlled by the close proximity of the Wellington fault and consists of mostly sub systematic shears and discontinuous bedding. Persistent structures such as faults will likely govern global slope stability. Rock type 2 comprises of characteristics that are similar to rock type 2 at the Transmission Gully South site. However, there appears to be a higher proportion of Lithofacies B. It presumed that the increase in Lithofacies B indicates a degree of lithological control on the rock mass type. As a result shearing appears to be more systematic with persistence around 20

m long. Rock type 2 is located in the north of the study area at an increased distance away from the Wellington Fault.

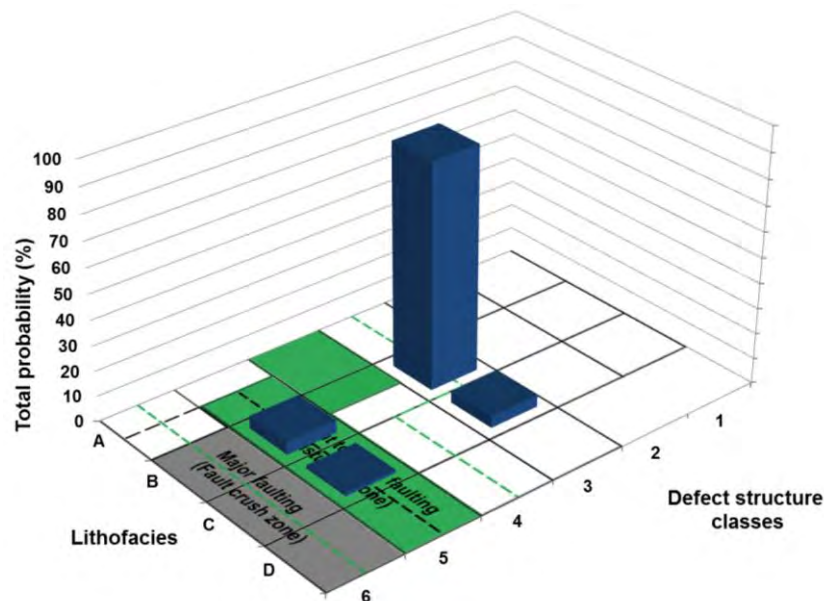


Figure 5.32: Probability plot of the Horokiwi Quarry defect structural classes and lithofacies groups combined.

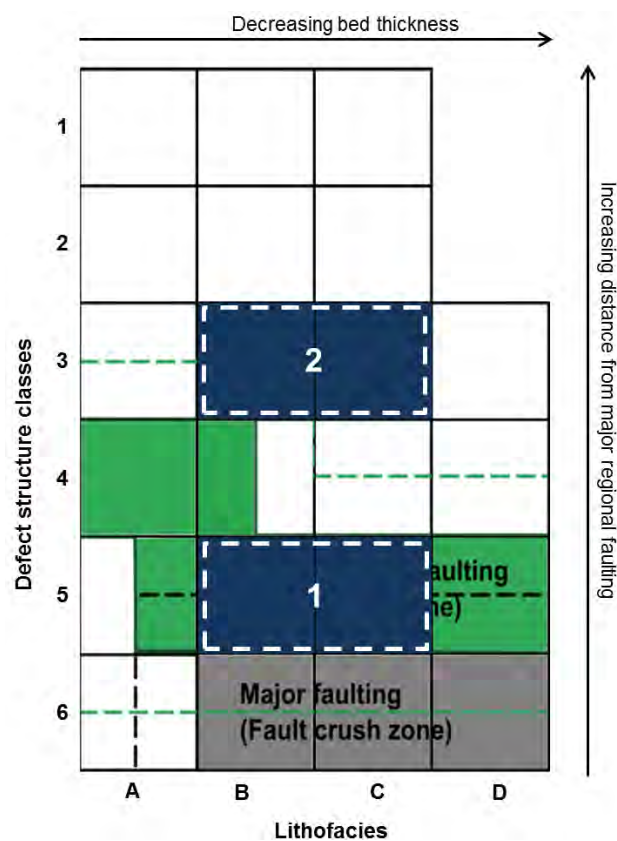


Figure 5.33: Bird's eye perspective of the Horokiwi Quarry TRC (defined in Figure 5.24) plot and subsequent rock type clusters. Each cluster represents rock mass types 1 and 2 explained in the previous paragraphs.

5.4.5 Owhiro Bay Quarry

The Owhiro Bay Quarry is located the furthest from major regional faults that consist of only Lithofacies C and B (Figure 5.34 and 5.35). This site obtains only one rock type which comprises of equal proportions of both lithofacies groups (Figure 5.35). The rock mass type at this site is dominated by persistent (>30 m) systematic shears that are mostly widely spaced with bedding that appears to be relatively planar. Most structures present at this are persistent (>40 m) including sub-systematic shears which are infrequent. This rock type represents the best rock mass conditions for Lithofacies C and D observed throughout the study. Jointing is still discontinuous but is starting to develop sets which may cause local instability, due to rock fall. It is anticipated that the persistent features will govern global stability.

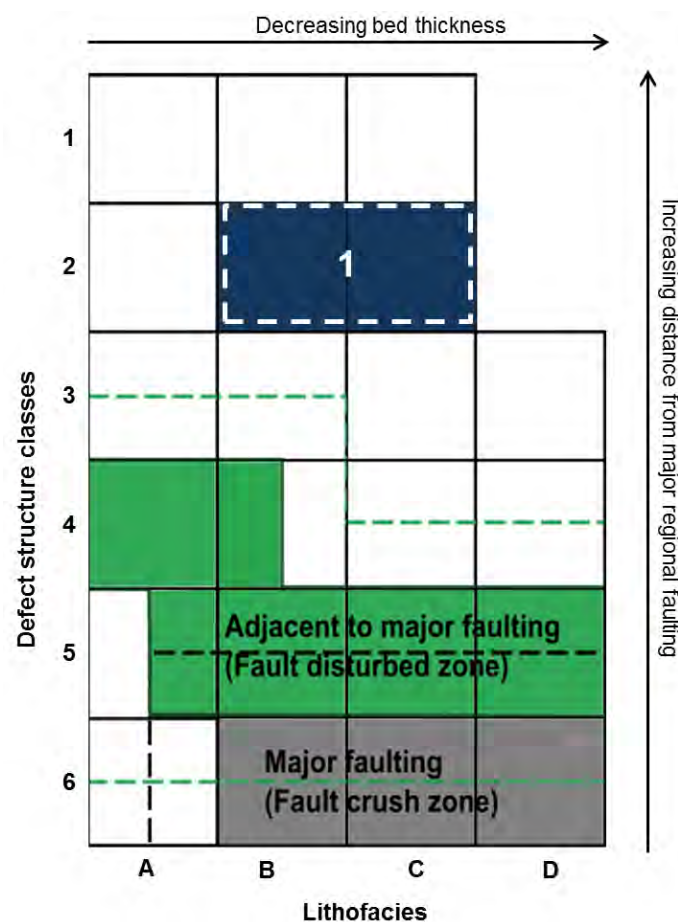


Figure 5.34: Bird's eye perspective of the Owhiro Bay Quarry TRC (defined in Figure 5.24) plot and subsequent rock type clusters. The cluster represents rock mass type 1 explained in the previous paragraphs.

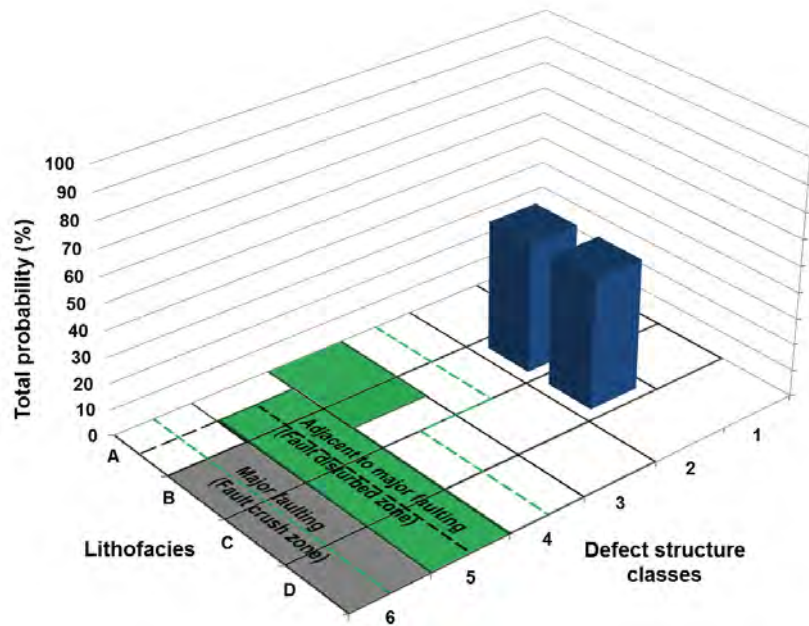


Figure 5.35: Probability plot of the Owhiro Bay Quarry defect structural classes and lithofacies groups combined.

5.4.6 Wairaka Point

The Wairaka Point site represents the best rock mass conditions in this study, despite its coastal location. Located at approximately 2.5 km away from the nearest active fault trace (Pukerua Bay Fault) this site is mostly controlled by folding and faulting generated from the radial shear arrangement model (Section 3.2.6 for further explanation). This site consists of only one rock type (Figure 5.36 and 5.37). This rock type represents persistent (>4 m) jointing that is widely spaced and well defined. Alternating mudstone to sandstone beds is infrequent extremely widely spaced, typical of Lithofacies group A. Bedding tends to be wavy due to folding. Shearing is continuous and appears to follow persistent joint sets. A lack of shear zones, crush zones and faulting is evident but are generally persistent where they are visible. Sub systematic shearing is rarely identified.

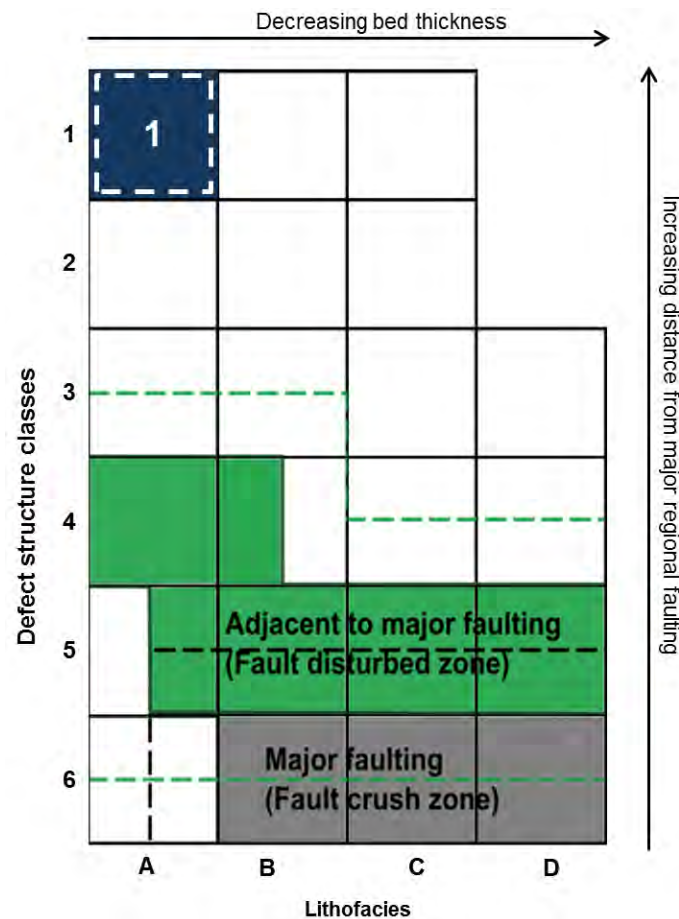


Figure 5.36: Bird's eye perspective of the Wairaka Point TRC (defined in Figure 5.24) plot and subsequent rock type clusters. The cluster (1) represents rock mass type explained in the previous paragraphs.

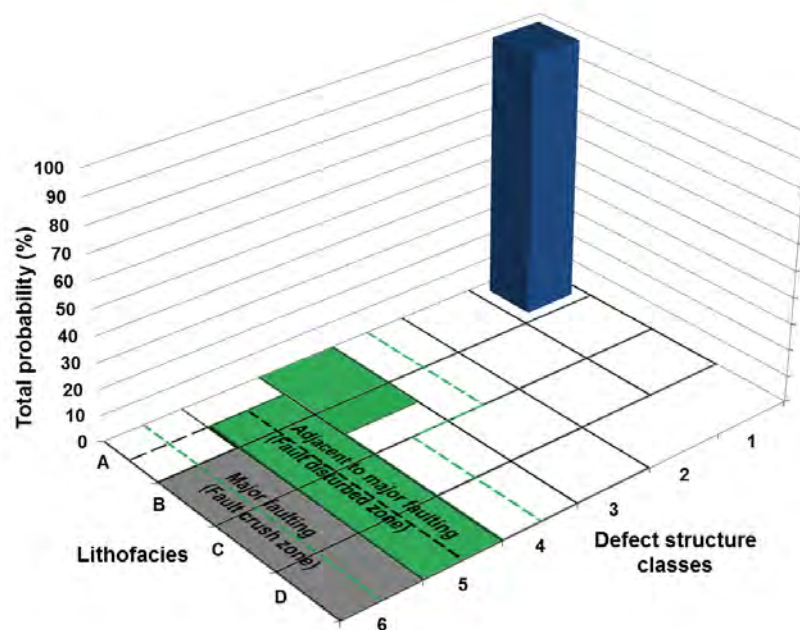


Figure 5.37: Probability plot of the Wairaka Point defect structural classes and lithofacies groups combined.

5.4.7 Makara Head

Makara Head is dominantly Lithofacies A and represents the rock type present at Wairaka Point but with a larger degree of shearing. Therefore there is only one rock type in the figure below (Figure 5.38 and 5.39). Typically the rock mass type obtains widely spaced defects with random and discontinuous closely spaced jointing. Sub-systematic shears and larger shearing features such as, crush zones, shear zones and faults are more frequent. This is due to the reduced distance from major regional faulting (Shepherd's Gully Fault). Bedding is infrequent but generally persistent for around twenty metres. It is predicated that the persistent and continuous structures will govern global stability. Jointing may local instability by dislodging random rock blocks.

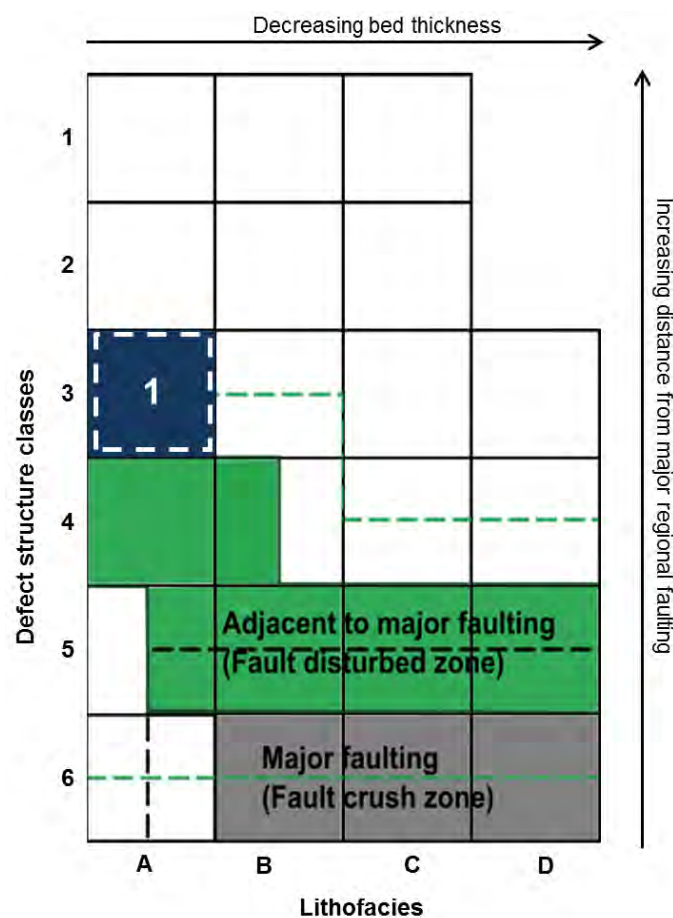


Figure 5.38: Bird's eye perspective of the Makara Head TRC (defined in Figure 5.24) plot and subsequent rock type clusters. The cluster (1) represents rock mass type explained in the previous paragraphs.

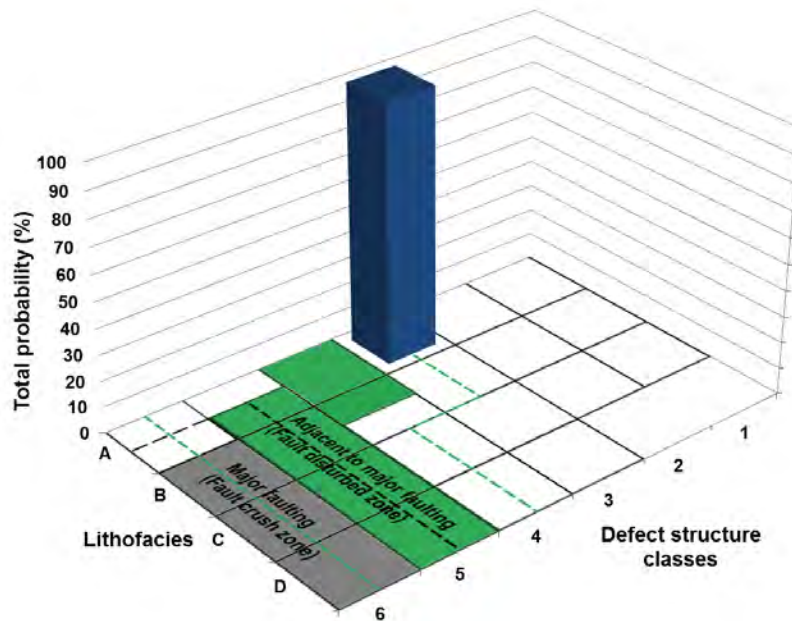


Figure 5.39: Probability plot of the Makara Head defect structural classes and lithofacies groups combined.

5.5 Overall Rock Mass Types

A wide range of rock mass conditions are likely to be encountered over short distances within the Torlesse in the Wellington region. By plotting each the Torlesse rock mass classification data of each site into a new diagram and then overlaying the clusters from each site a number of rock mass types can be identified. This enables a wide range of rock mass conditions to be characterised for the purpose of identifying groups of areas with similar trends. Important to note is that the rock mass types derived from this study are not to be relied upon for future projects. It is intended that future projects looking to implement the TRC will independently plot their own data in order to derive their own rock mass types, therefore the rock types will be more site specific. Results may show similar rock mass patterns however, other rock mass types may be identified. Overall eight rock mass types have been identified from the site analysis. The rock mass types are categorised such that the rock mass quality improves from Type 1 through to Type 8.

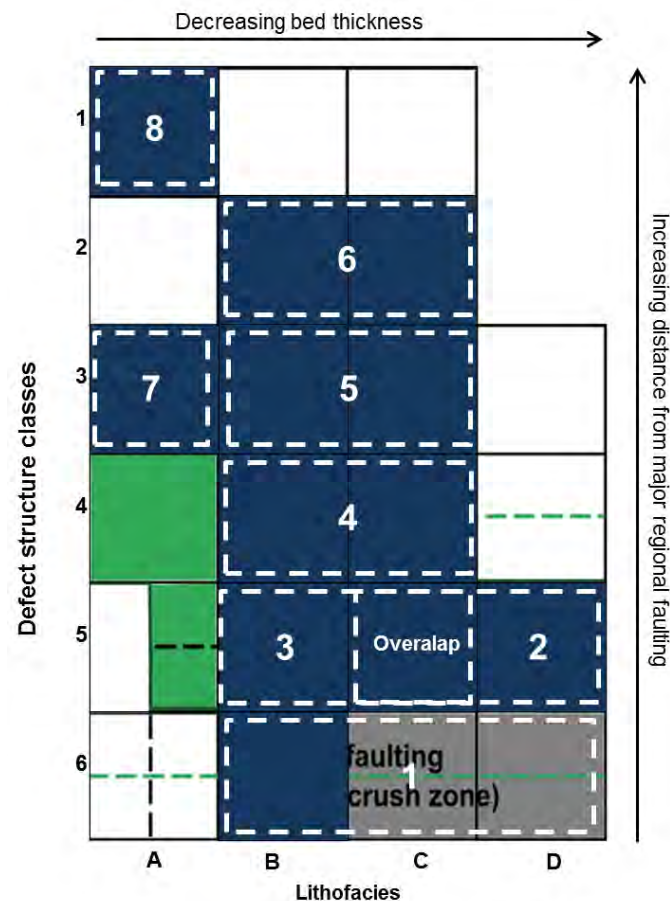


Figure 5.40: Bird's eye perspective of the combined TRC outcrop data (Figure 5.24). Overlay of rock mass types identified through individual site analysis.

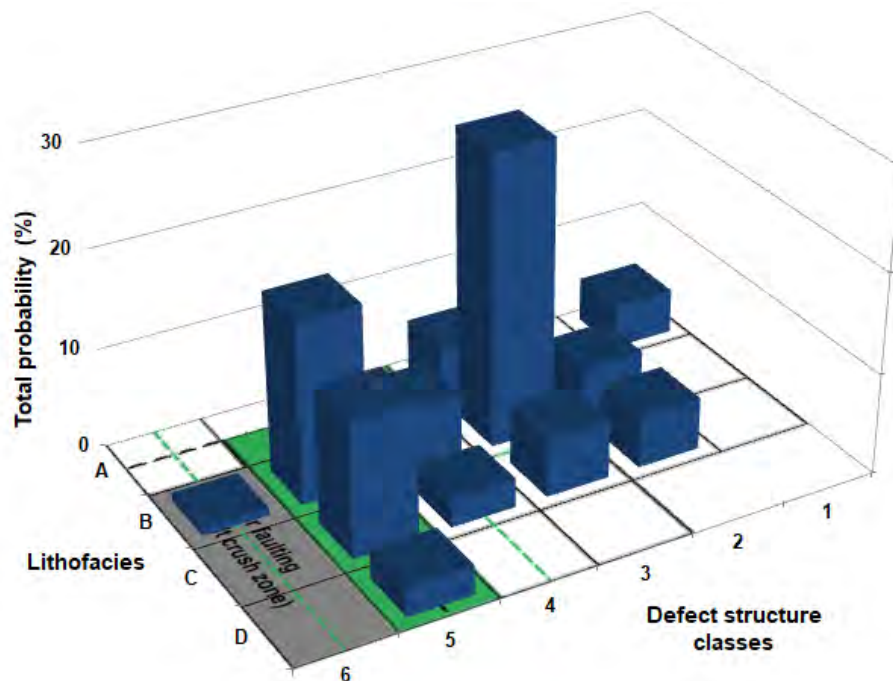


Figure 5.41: Probability plot of the overall likelihood of defect classes and lithofacies combined. Copy of Figure 5.25.

5.5.1 Type 1

Type 1 is the worst possible rock mass observed across all the study areas. The TRC defines this zone as “Fault Crush” material which contains of barely recognisable bedding. Shearing can be observed on varying scales as faults or localised shear zones that are very close to widely spaced. Geotechnically this rock type behaves like a soil (*i.e.* particles) comprised of dominantly weak to very weak rock fragments amongst a sandy silt matrix (Figure 5.42). Firm clay rich “gouge zones” are commonly associated with this rock mass and are observed to be approximately a few centimetres thick. Generally this rock type is located adjacent to fault traces. Where the magnitude of faulting is larger (Ohariu Fault) this rock mass tends to be wider.



Figure 5.42: Typical rock mass type 8 material. Containing gouge and brecciated material. A) Horokiwi Quarry South outcrop; B) Kapiti Quarry outcrop 1; C) Transmission Gully South outcrop 2a; D) Transmission Gully North Ohariu Fault trace and the related gouge and breccia material.

5.5.2 Type 2

The proportion of mudstone material tends to determine the character of this rock mass type (Figure 5.43). This rock mass typically consists of brecciated or fragmented thick mudstone bands which tend to grade into alternating medium to thinly bedded mudstone to thinly bedded sandstone sequences (Lithofacies C). Rare occurrences of individual thick sandstone beds may be present. Persistent cross-cutting shears are less common, those features that are persistent (>20 m) tend to be faults or shear zones (Figure 5.44.a). Most shears are discontinuous and either terminates in rock or joins up with other defects (Figure 5.44.b). Systematic and sub-systematic shearing are in approximately equal portions with most obtaining a higher degree of waviness compared to most other rock mass types. Bedding shears are less distinct and may form wider shear zones across the thick mudstone bands. Jointing is discontinuous and random typically very closely spaced to extremely closely spaced in the mudstone unit. Defect infilling material tends to comprise of the highest volume of clay material seen across all the rock types. The clay material is commonly slightly too moderately plastic and generally occurs as gouge material in fault or shear zones. Most infilling defects consist of around > 75% rock fragments. Infilling rock fragments are mostly very weak with a soft to very soft matrix. Generally, this rock type is observed in environments that obtain a higher degree of deformation.

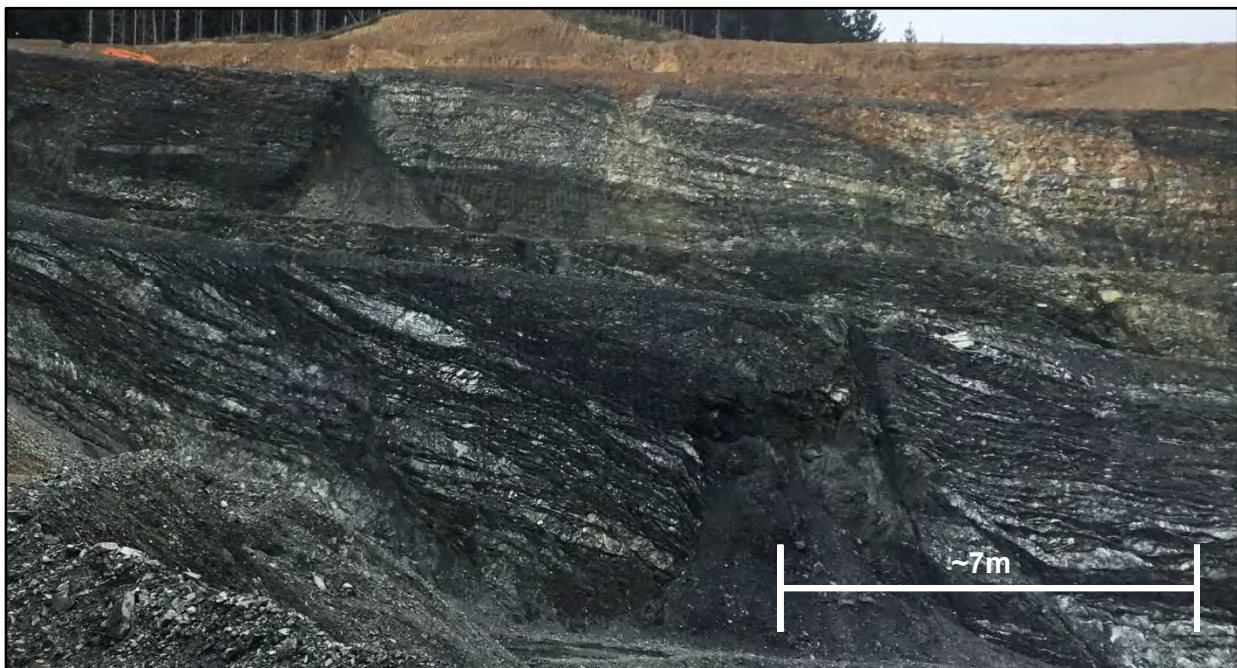


Figure 5.43: Typical outcrop of rock mass type 2 at Kapiti Quarry outcrop 3. Comprising of higher mudstone proportions and fragmented and brecciated mudstone and sandstone beds.



Figure 5.44: Fragmented and heavily sheared rock mass typical of Type 2. A) Kapiti Quarry outcrop 3; B) Kapiti Quarry outcrop 2.

5.5.3 Type 3

Type 3 is generally characterised by a high degree of deformation and is located close to major fault traces (Figure 5.45). It represents a more sandstone rich version of rock type 2. Sandstone and mudstone beds are generally medium to thinly bedded and commonly overprinted (Figure 5.45.a). Frequent occurrences of thick sandstone beds are rare. Bedding can be persistent but is commonly gently wavy and discontinuous. Generally, jointing is closely spaced, randomly orientated and discrete. Closely spaced systematic and sub-systematic shears are in approximately equal portions and tend to terminate against other defects (Figure 5.45.b). Few defects are persistent (> 10 m) with those that are tending to be shear zones, crush zones and faults (Figure 5.45.c). The continuous and persistent features are what are thought to govern global slope stability. Infilling is still dominated by rock clasts (<75 %) and obtains a slightly higher sand proportion in comparison to rock type 2, hence, the infilling material may obtain a slight plasticity. Defects are generally more planar than what is observed in rock type 2.



Figure 5.45: Typical rock mass type 3. A) Horokiwi Quarry south outcrop displaying overprinted bedding; B) Discontinuous shearing and cross-cutting systematic shears in Transmission Gully North outcrop 2a; C) Continuous Crush zone in Transmission Gully North outcrop 1c.

5.5.4 Type 4

This rock type generally obtains a higher degree of mudstone proportion in comparison to rock type 3 (Figure 5.46.a). Generally the rock mass is slightly less disturbed and tends to display relatively more continuous shearing features and bedding. However, bedding is commonly truncated by larger more persistent faults, crush and shear zones (Figure 5.46.a and 5.46.b). Systematic shearing appears to become more dominate with defined terminations that mostly occur against bedding and the larger structures which are likely to control the rock mass. Defect infill material is mostly a silty with weak rock fragments. Plasticity is not commonly observed. This rock type represents a high degree of deformation located close to low magnitude faults (larger 2nd order or smaller 1st order faulting).

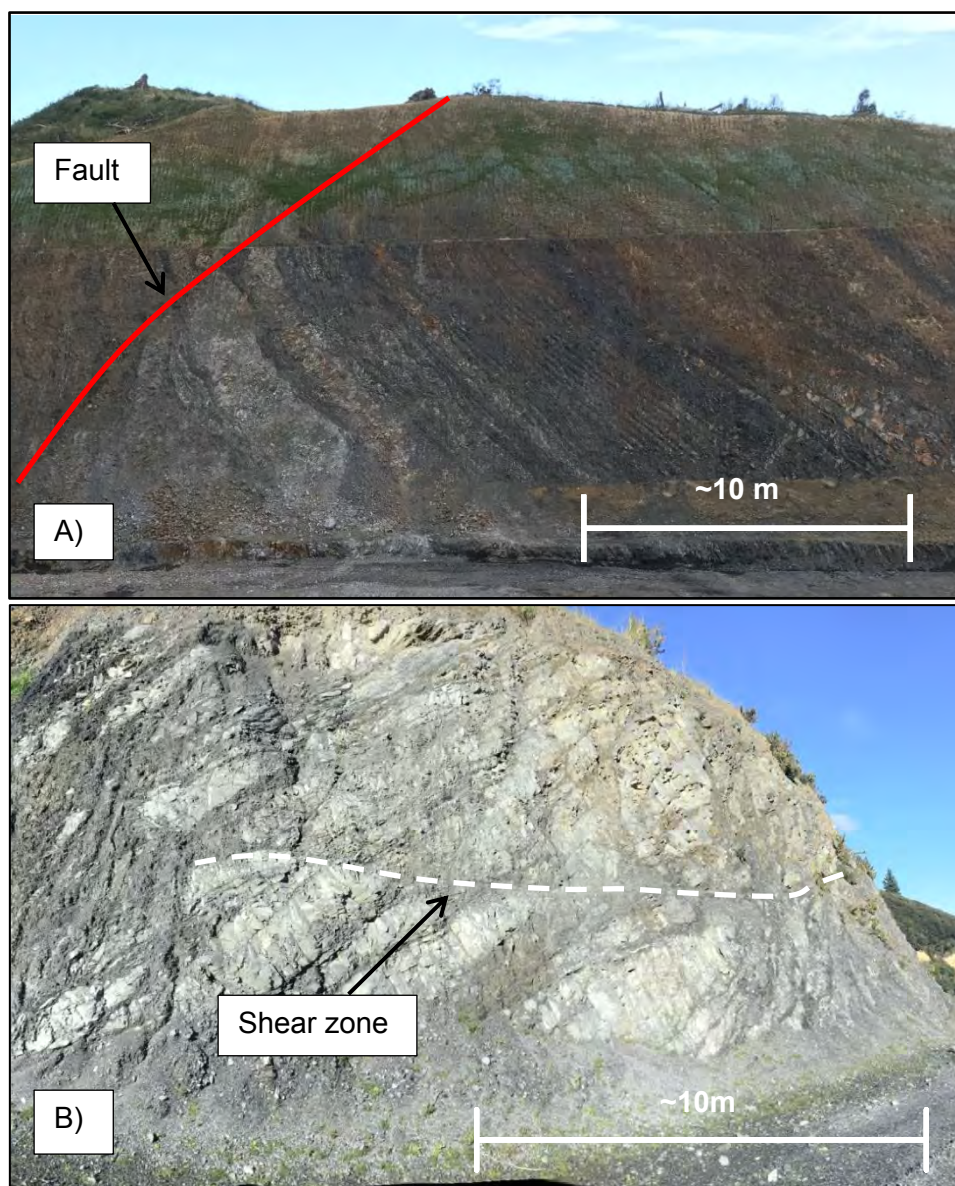


Figure 5.46: Rock mass typical of type 4. A) Transmission Gully South outcrop 4, displaying continuous bedding which terminates against persistent (>20 m) faulting; B) Kapiti Quarry outcrop 1, bedding offset due to continuous shear zones and faulting to the left of the photograph.

5.5.5 Type 5

Type 5 represents the most common rock type identified across all the study areas. It has the same bedding thickness to type 3, but is characterised by well-defined bedding that tends to persist for >20 m before truncating against other defects or folds (Figure 5.47.a). Jointing is still generally short, random and planar but is starting to develop systematic sets. Cross-cutting shears may be spaced 10-30 m while systematic shears tend to be widely spaced (Figure 5.47.b). Global stability is likely to be controlled by persistent (>20 m) shearing and bedding structures which commonly and tend to be wavy in shape. Some defects start to behave irregularly. Defect infill conditions are mostly comprised of > 85% rock fragments that are generally weak and surrounded by a silty matrix (Figure 5.47.c). Slight plasticity is observed where water flow can be observed. Few inclusions of white mineralisation are evident.



Figure 5.47: Persistent (>20 m) bedding and shearing structures typical of rock mass type 5. A) Continuous bedding disrupted by folding in Horokiwi Quarry West outcrop; B) shearing forming conjugate to bedding in the Horokiwi Quarry North outcrop; C) bedding plane shearing in mudstone from Horokiwi Quarry West outcrop.

5.5.6 Type 6

This rock type represents the best possible rock mass for Lithofacies B and C in this study. Persistent (>30 m) and continuous bedding (Figure 5.48.a) and systematic shears appear to largely control slope stability. Cross-cutting shears are less frequent and may be spaced >30 m. All defects are relatively planar. Faults, shear zones and crush zones are frequent but uncommon. Sub-systematic shears are rarely observed but are also persistent but tend to be discontinuous and wavy. Jointing is still discontinuous (Figure 5.48.b) but appears to persist for about a metre in the sandstone lithotype (Figure 5.48.c) and is moderately spaced, thereby controlling local scale instability mechanisms such as rock fall. Defect infill is comprised of mostly moderately strong to weak rock fragments. >90%, amongst a silty sand matrix. A few traces of precipitated material are evident in defect infills and tend to comprise of moderately strong, angular, elongated or tabulated gravel clasts. This rock mass type is typically located at increased distances away from major regional faulting.

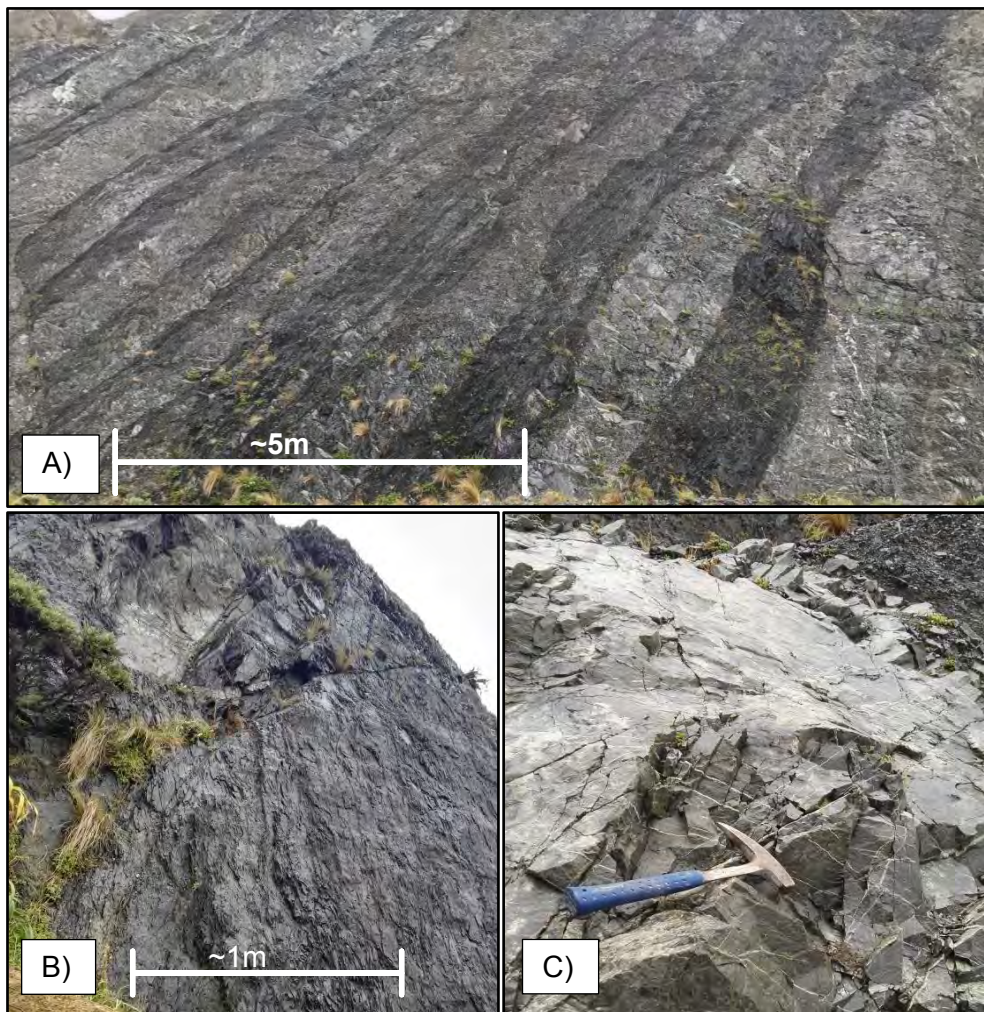


Figure 5.48: Thick to moderately thick interbedded sandstone-mudstone rock mass typical of Type 6. A) Continuous Bedding observed in Owhiro Bay Quarry outcrop 2; B) jointing and fragmented nature of the mudstone in Owhiro Bay Quarry outcrop 2; C) discontinuous jointing with persistence up to a metre in Owhiro Bay Quarry outcrop 1.

5.5.7 Type 7

The high proportion of sandstone material tends to influence the character of this rock mass type. Bedding is dominantly comprised of massive to very thick sandstone beds with occasional very thin to thin inter-beds of mudstone (Figure 5.49.a). This rock type represents the worst possible rock mass conditions of Lithofacies A observed through this study. Occurrences of this rock type tend to be located adjacent to major fault zones at an increased distance from types 1 and 2. It is typically characterised by jointing which is generally still short (>1 m; Figure 5.50.a 5.50.b), random and planar but is mostly developing systematic sets. Bedding and systematic shearing tends to persist (>20 m) and largely control global slope stability. Cross-cutting shears are spaced 10-30 m apart while shear zones, crush zones and faults are rarely observed. Rock mass structure is controlled by major regional fault structures (Shepherd's Gully Fault) and folding mechanisms, thereby defects are mostly wavy with small inter-limb angles and wavelengths. Infilling material is mostly comprised of weak to moderately strong rock fragments which dominate >90 % of defect infill (Figure 5.49.b and 5.49.c). A firm to soft silty sand matrix tends to surround the rock fragments.

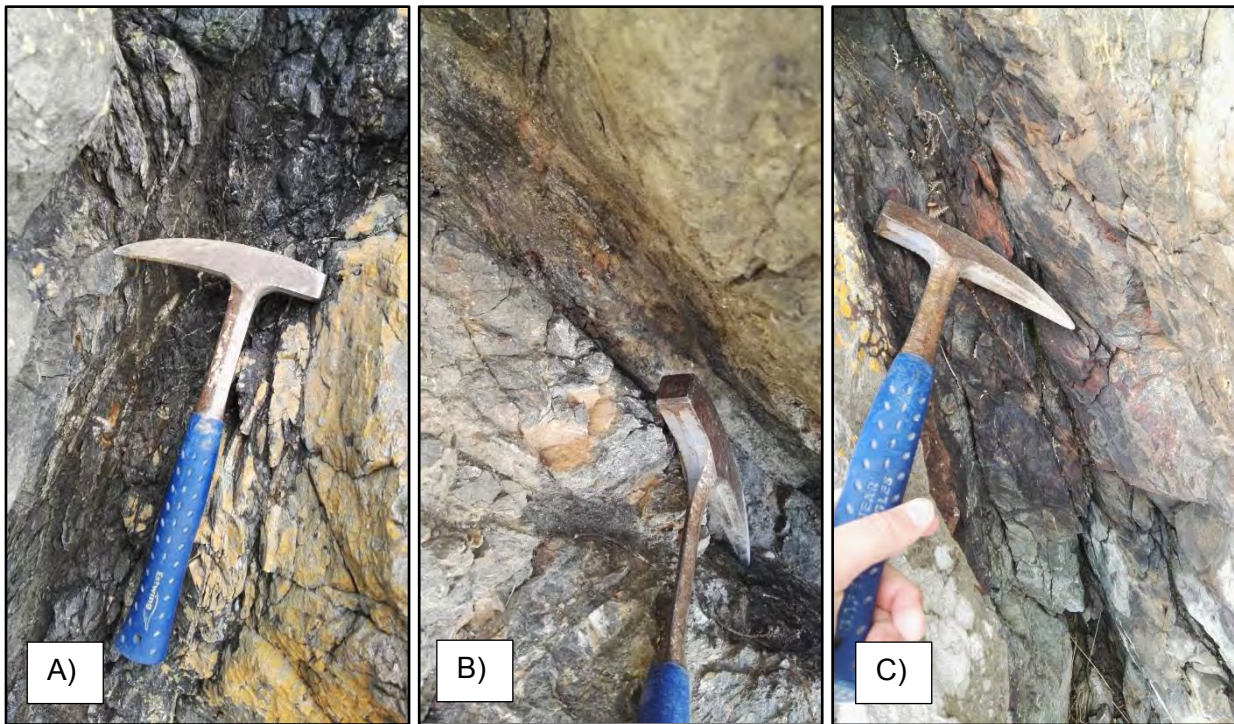


Figure 5.49: Typical defect infill of rock mass type 7 in A) Bedding plane shears; B) Shear zone; and C) shear at Makara Beach.

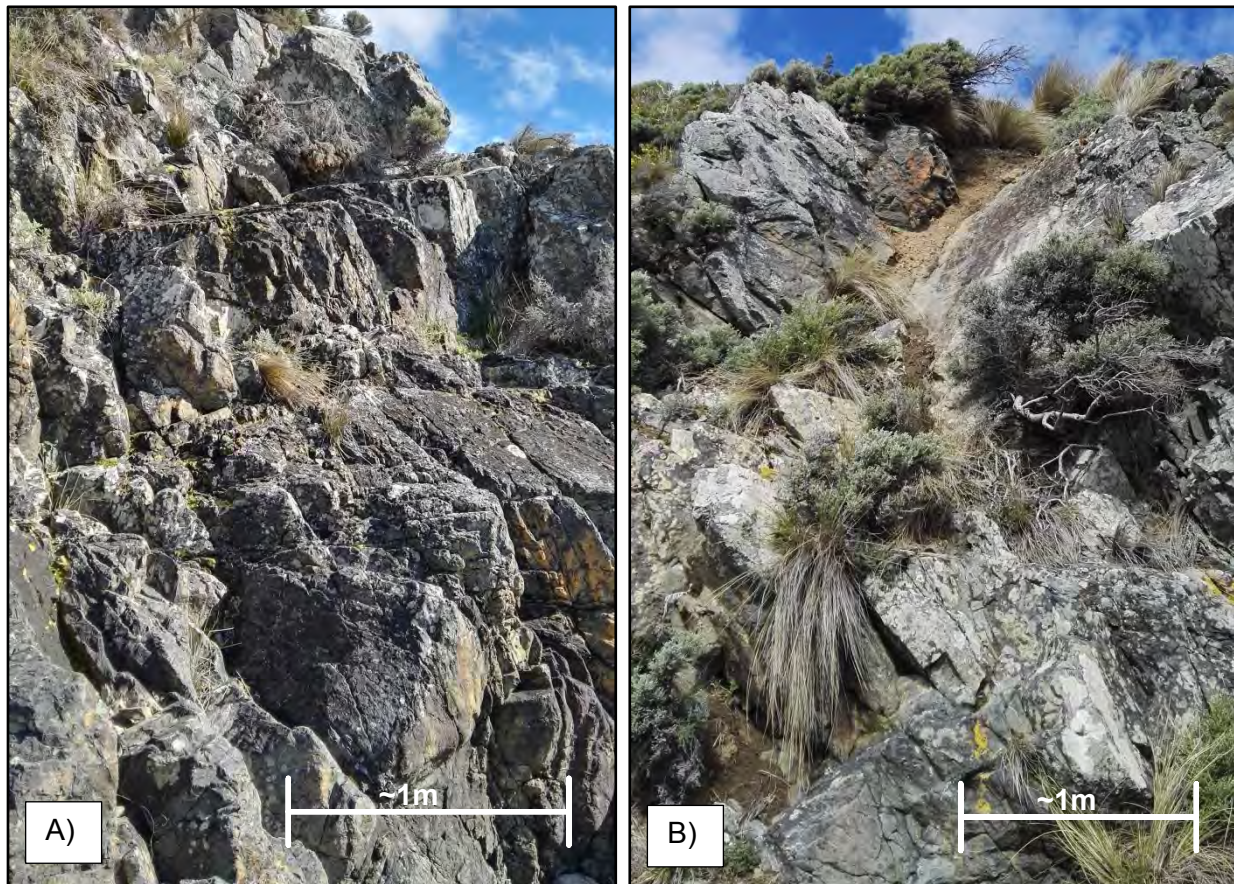


Figure 5.50: Typical jointing that persists for >1 m. Presents a blocky characteristic for rock mass type 7. A) systematic jointing at Makara Head outcrop 3; B) Failure from intersecting persistent (~2 m) joints and shearing at Makara Head outcrop 2.

5.5.8 Type 8

Type 8 is the best possible rock mass observed throughout this study. It contains the same bedding thickness as type 7 but occurrences of faulting and shearing has decreased. Controlling the rock mass character appears to be persistent (>4 m) jointing (Figure 5.51). However, continuous and persistent (>40 m) bedding and shears tend to govern global slope stability. Shears tend to follow similar orientations to Joints. Faulting, sheared and crush zones are rare. Defect infill is dominantly rock fragments (>95%), where matrix is observed it is mostly sand. Occurrences of this rock mass are located at increased distances from major regional faulting, in comparison to rock type 7. This increased distance means that rock mass structure is mostly controlled by folding mechanisms rather than faulting.

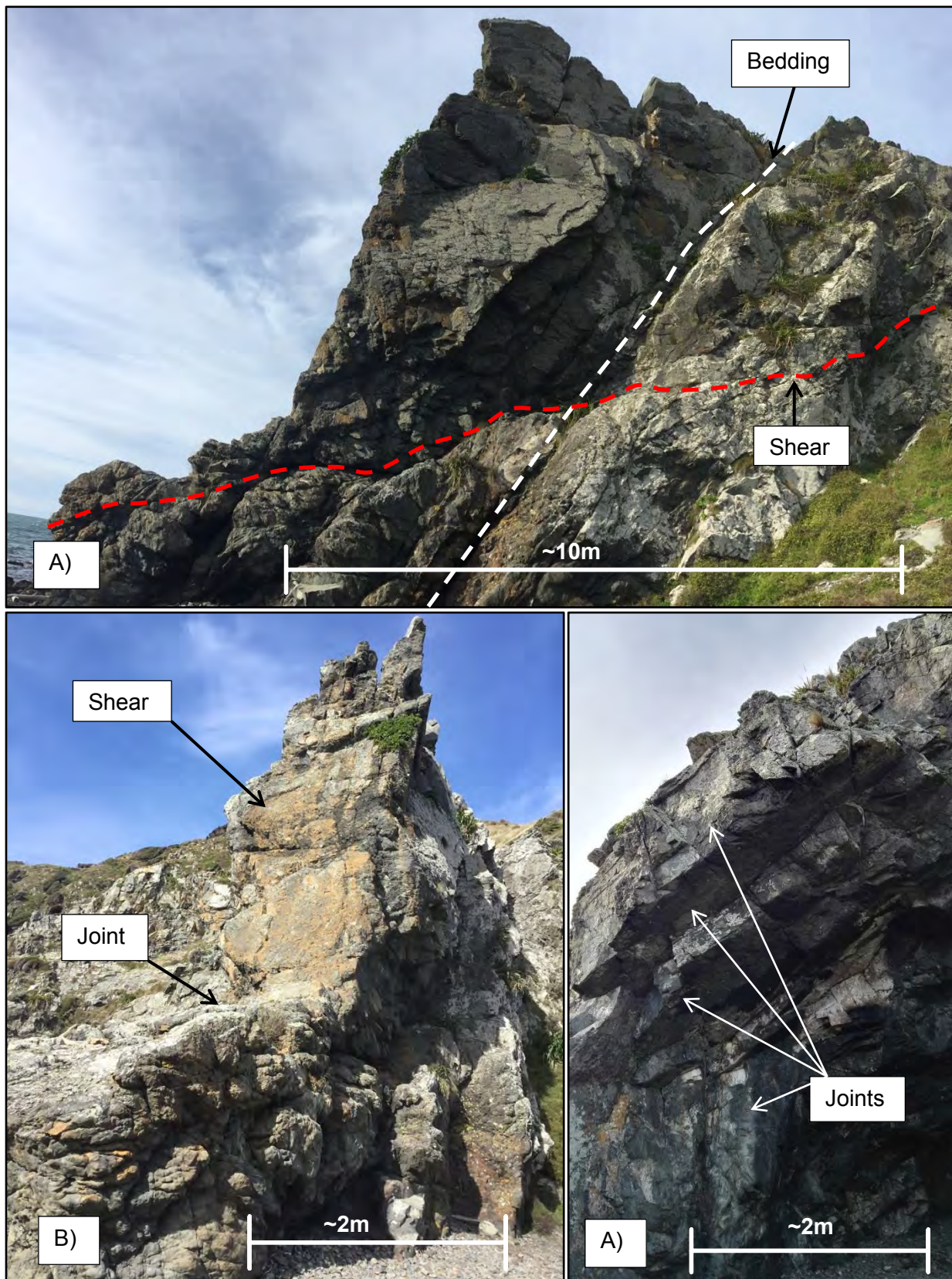


Figure 5.51: Best possible rock mass quality typical of type 8. A) Persistent (>15 m) and continuous shearing and bedding which cross-cut in Wairaka Point outcrop 1; B) Persistent (>4 m) jointing intersecting with shears to form a wedge failure between Wairaka Point outcrop 2 and 3; C) Intersecting persistent (>4 m) systematic jointing forming local wedge and sliding failures at Wairaka Point outcrop 4.

5.6 Rock Mass Condition and Discussion

The rock mass types identified through the use of the Torlesse Rock mass classification (TRC) in Section 5.3 to 5.4 show key trends as the rock mass quality improves from Type 1 to Type 8. The purpose of identifying these trends is to aid in the creation of a suggested approach in the use of the TRC. Only those that are assessed to have a large control on potential rock slope instability are further investigated.

5.6.1 Lithology

Across the various rock mass types major differences are observed in mudstone to sandstone proportions (Table 5.8). Due to large variations in bedding thicknesses across all outcrops a range of mudstone and sandstone proportions has been given for each rock mass type.

Table 5.8: Sandstone and mudstone proportions displayed across all rock mass types

Rock mass type	Sandstone		Mudstone	
	Range	Overall	Range	Overall
1	Variable			
2	40-60	40	40-60	60
3	60-70	60	30-40	40
4	60-70	60	30-40	40
5	60-70	70	30-40	30
6	60	60	40	40
7	80-100	80	0-20	20
8	80-100	80	0-20	20

Higher mudstone proportions are evident throughout rock mass type 2. This also appears to correlate with low relative probabilities from Figure 5.29. Therefore this rock mass type is less likely to be encountered than any of the other rock mass types. This also suggests that sandstone is the most dominant lithology in the Wellington Torlesse. This is important for assessing quantities of poorer mudstone rock masses which may require further remedial work.

5.6.2 Defect Type and Persistence

Defect persistence is the most important aspect relating to structural failures in a rock mass. Read and Richards (2007), Cook (2001) and Irvine (2013) among many others, all recognise that kinematic failures of a reasonable size will only occur if the plane of failure is persistent. Therefore it is important that typical rock mass type trends which derive defect persistence are described. In this study the presence of defects that persist over thirty metres (Type 6, 7 and 8) tend to indicate better systematic rock mass conditions. In more fragmented rock mass types (Types 1 and 2) persistence tends to be low and more sub-systematic (Table 5.9).

Table 5.9: Typical persistence of defect types across rock mass types

Rock mass type	Defect type and persistence
1	Typically over printed, however there is potential for localised shearing and faulting. Persistence is highly variable Jointing is extremely short
2	Bedding: May span the length of a bench (> 10 m) although is less distinct and tends to be overprinted Shearing/Faulting: Sub-systematic and systematic shears are discontinuous. Continuous features tend to be faults, sheared and crush zones (> 10 m) Jointing: very short, discontinuous, sub-systematic
3	Bedding: May span the length of a bench (> 10 m) however, it tends to be overprinted Shearing/Faulting: Sub-systematic and systematic shears are discontinuous. Continuous features tend to be faults, sheared and crush zones (> 10 m) Jointing: very short, discontinuous, sub-systematic
4	Bedding: Bedding may be persistent (>20 m) but these are often truncated or overprinted Shearing/Faulting: Continuous shears (> 10 m) may be systematic but are commonly sub-systematic. Persistent structures tend to be faults, shear zones and crush zones. Jointing: short, discontinuous, sub-systematic
5	Bedding: Typically continuous (> 20 m) Shearing/Faulting: Faults, shear zones and crush zones are less frequent but are persistent (> 20 m). Sub-systematic shears are less common and mostly discontinuous. Jointing: Short (< 0.5 m), discontinuous, sub-systematic starting to form systematic
6	Bedding: Persistent (> 30 m) and continuous Shearing/Faulting: Persistent (> 30 m) systematic shears. Faults, sheared and crush zones are infrequent but also persistent. Jointing: Still mostly discontinuous. Generally Sub-systematic but may form relatively well defined sets (~1 m).
7	Bedding: Typically continuous (> 20 m) Shearing/Faulting: Faults, shear zones and crush zones are less frequent but are persistent (> 20 m). Sub-systematic shears are less common and mostly discontinuous. Jointing: Short (< 0.5 m), discontinuous, sub-systematic
8	Bedding: Persistent (> 50 m) and continuous systematic shears. Shearing/Faulting: Rare faults, shear zones, crush zones and sub-systematic shears but are typically persistent (> 50 m). Mostly (> 20 m) persistent systematic shears. Jointing: > 4 m in persistence. Typically systematic few occurrences of sub-systematic

The majority of the jointing seen throughout the rock mass types (excluding rock type 7 and 8) tends to display dominantly non-persistent (< 2 m) and discrete jointing. It was found by Read and Richards (2007) that the effect of this low persistent jointing tends to create an interlocked rock mass, which results in higher shear strengths. Rock types 1 – 5 are expected to be interlocked, however, more so in rock mass types 1 - 3 as the observed persistence is lower. Read et al. (2000) states that when comparing regularly (systematic) jointing with irregular (sub-

systematic) jointing, provided that spacing is the same scale, the irregularly jointed rocks will interlock better and hence be stronger. Therefore, interlocking in the less persistent rock mass types (types 1-5) will dominantly control the rock mass strength. In the case of rock cut slopes, the more persistent structures will therefore determine the mode of failure.

Important to note is that persistence implies that the visible length of a defect over a rock slope or rock cut-slope is recorded. This only describes a 2-D representation of the recorded defect plane ultimately restricting the degree of persistence beneath the adjacent rock mass. Unfortunately there is no way of knowing how far into the rock mass defects may persist before they terminate and hence know the degree of which a rock mass may be involved in potential failures.

5.6.3 Defect Condition

Defect condition heavily influences the shear strength within any rock mass. Cook (2001) determined that surface roughness and infill type primarily control the initial shear strength within a rock mass. Patterns assessed in 5.2 identified that there was a lack of roughness trends therefore, this is unable to be discussed. However, trends that analysed defect infilling material suggested that as proximity to active regional fault traces and mudstone proportions increased, so do the volume of finer materials (< 2 mm). Appendix I Figure 5.I.4 displays this relationship strongly. Past studies (Cook, 2001; Irvine, 2013; Read et al., 2000) also state that defect widths of 3 mm or greater tend to have lower shear strengths. Furthermore, defect infills with weaker strengths tend to obtain low shear strength values (González de Vallejo and Ferrer, 2011). This applies to the majority of defects assessed in this study with the exception of Jointing (JN) and Bedding fabric (BG). It is therefore likely that defect infill will largely control the shear strength of a defect and thus have a greater influence on slope stability. Based on this understanding, it is expected that rock mass types 1, 2 and 3 will obtain lower shear strength values than any of the other rock types, while rock mass types 6, 7 and 8 will obtain higher shear strengths. Table 5.10 summarises the overall defect infill characteristics typical of the various rock mass types.

Table 5.10: Typical defect infill characteristics for each rock type.

Rock mass type	Infill type				
	Rock fragment percentage	Supporting matrix	Precipitation	Strength of soil	Strength of rock fragments
1	Variable, typically behaves like a soil, Fault crush				
2	< 75%	Clay, minor sand and silt	N/A	Soft to Very soft	Very weak
3	< 75%	silty Clay, traces of sand	N/A	Soft to Very soft	Weak to Very weak
4	< 80%	silty Clay, and sandy silt	N/A	Soft	Weak
5	< 85%	sandy Silt and Silts, traces of Clay	Rare	Soft to firm	Weak to Moderately strong
6	< 90%	silty Sand, traces of clay	Few traces	Firm	Moderately strong
7	< 85%	Sand traces of clay and silt	Rare	Firm	Moderately strong
8	< 95%	Sand	Traces	Stiff	Strong to Moderately strong

Where rock mass types are expected to obtain higher shear strengths precipitation and rock fragment percentages appear to be more prevalent. This would suggest that increasing volumes of precipitation and rock fragments in defect infilling material would indicate higher shear strengths. This is important for assessing kinematically derived failures in poorer quality rock masses.

5.6.4 Defect Orientation

The rock mass types are spread out across all of the study sites. They display differences in their orientation in relation to major regional faulting. Table 5.11 displays the typical orientation of the more continuous and persistent defects observed for each rock mass types. Typical orientations are assumed by comparing the conceptual and engineering geological models from individual study sites. While most sites comprise of more than rock mass type structural domains, location maps and individual outcrop data was consulted in order to differentiate between differing rock mass types. Generally most continuous faulting and shearing defects tend to present as systematic defects that form sets.

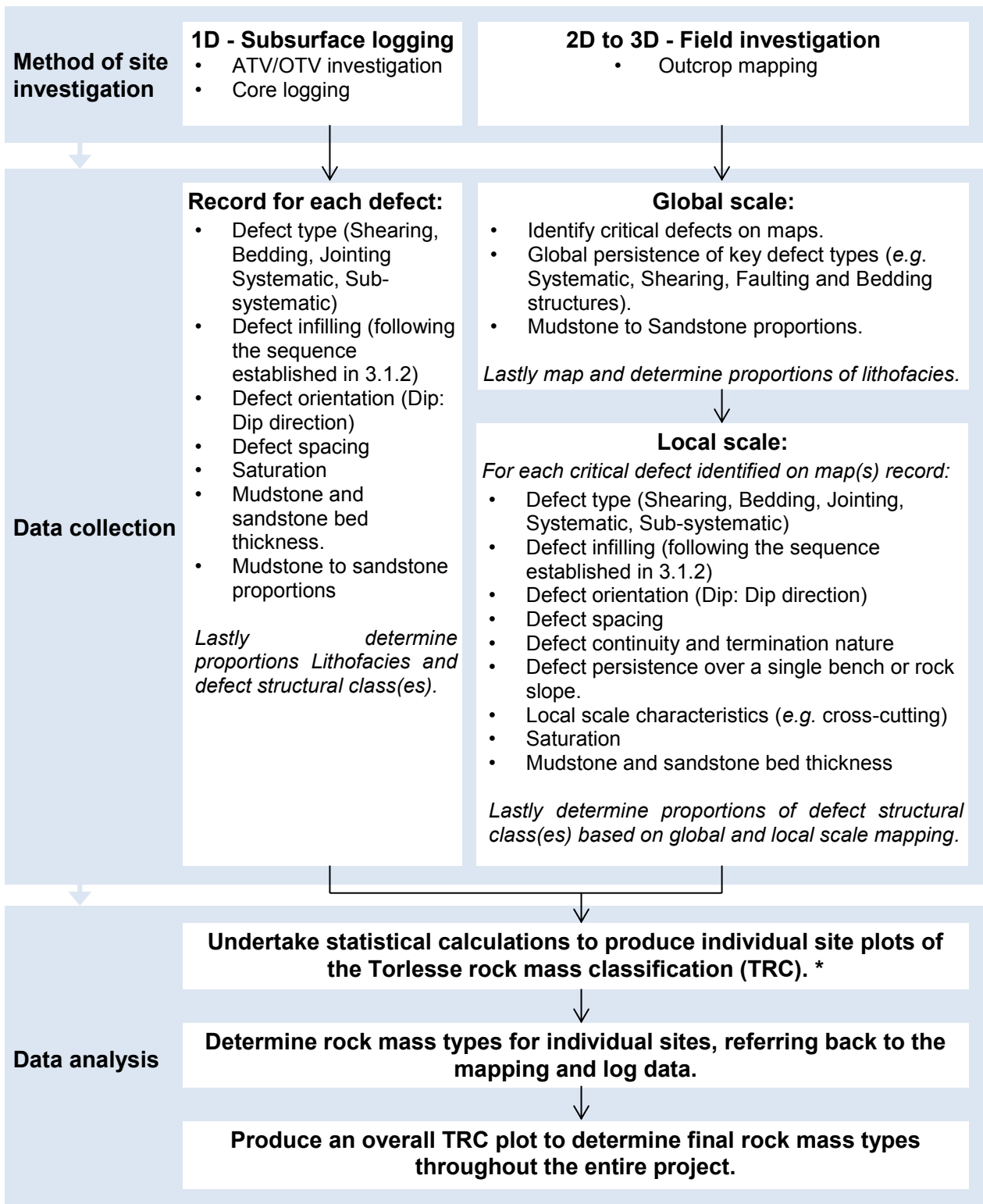
Table 5.11: Typical orientation of continuous defects in relation to major regional faulting.

Rock mass type	Typical orientation of defects in relation to regional faulting	
	Shearing and faulting orientations	Bedding orientations
1	Not applicable, continuous bedding and shearing is overprinted	
2	Requires filtering due the large occurrence of sub-systematic shears. Two systematic shear sets tend to strike roughly parallel with bedding and 1 st order structures.	Often overprinted and less distinct Striking sub-parallel with 3 rd order structures
3	Two systematic shear sets. Sub parallel with 1 st order and 2 nd order structures	Striking sub-parallel with 3 rd order structures
4	Two systematic shear sets. Sub-parallel and Antithetic with bedding.	Striking sub-parallel with high angle cross faulting typically 2 nd or 3 rd order.
5	Variable due to truncation. Tends to be perpendicular to bedding.	Variable, due to bedding truncation and rotation. the average strike is sub-parallel with 2 st order
6	Two systematic shear sets, sub-parallel with 1 st order and 2 nd order structures.	Striking sub-parallel with 2 nd order
7	Two systematic shear sets, sub-parallel with 1 st order and 2 nd order structures (Irvine et al., 2018).	Striking sub-parallel with R shears likely to be 2 nd order (Irvine et al., 2018)
8	Shearing appears to follow joint sets. The Sub-parallel with 1 st and 2 nd order structures. A third less well defined cluster appears to be sub-parallel with jointing and 3 rd order faulting.	Striking sub-parallel with 1 st order

As the rock mass condition improves (from 1 towards 8) the orientation of the bedding structures appear to become more parallel with the major regional 1st order faulting. Shearing and faulting orientations are generally sub-parallel with 1st and 2nd order regional faulting. However, in better rock mass types shearing and faulting defects start to be orientated along jointing surfaces, while in poorer rock mass types they tend to be oriented along bedding planes. This is likely the result of thinner beds and lower shear strength values identified in the mudstone unit (AECOM and PSM, 2015). It is therefore possible that the lithological proportions may control the orientation of defect structure and hence, the direction of failure.

5.6.5 Suggested Approach for the TRC

It is intended that future projects looking to implement the TRC will conduct a desktop study prior to site investigations, only then can this approach be used. As highlighted in 5.4, the TRC is designed such that future projects will plot their own data in order to derive their own rock mass types which are site specific. Observational data collected from subsurface or field investigations will provide the information required for this process as outlined in the flow chart below (Figure 5.52):



*See Appendix J for a step by step explanation of these calculations.

Figure 5.52: Flow chart of the suggested approach for the TRC.

CHAPTER SIX COMPARISONS WITH OTHER CLASSIFICATIONS AND APPLICATION TO CUT-SLOPE DESIGN

6.1 Torlesse Rock Mass Classification

The aim of the Torlesse Rock Mass Classification (TRC) is to provide an approach that incorporates the variability observed in the rock mass condition of Wellington Torlesse specific for cut slope design. To facilitate this evaluation, the approach takes into account that the design assessment of large cut slopes will encompass a range of preliminary mapping exercises and subsurface investigations at the inception of any new project. This information can then be incorporated into the TRC to identify specific rock mass types. Currently the classification produces gradational boundaries (Section 5.3.3). This is to accommodate for the range of geological controls on slope stability encountered within the Wellington Torlesse rock mass. The use of this scheme is not directly concerned with rock mass type, but rather defect structure classes and the lithofacies grouping. This scheme does not identify any rock mass strength parameters as no strength testing was conducted as part of this study. Therefore, specific site testing must be carried out to ultimately decide what rock mass type dominates a given area.

Each rock mass type is defined by a series of geological controls and defect conditions. This Chapter further discusses these conditions, which can then be used to interpret the potential mechanisms of slope failures imposed on different rock mass types. This allows for preliminary assessment of rock cut-slope behaviour that can lead to targeted site investigation planning.

6.1.1 Comparison with Cammack et al. (2018)

The TRC differs from other classifications, including the recently developed site-specific classification design methodology of Cammack et al. (2018). While both classifications partly achieve the same overall goal, the purpose of each classification is different. The Cammack et al. (2018) classification is extremely site-specific in nature and is only intended for application on the Transmission Gully alignment project. The main aim of the TRC scheme is that it is concerned with portraying a systematic approach that presents a way to allow future large-scale rock cut-slopes to identify their own rock mass types across the Wellington region. The significantly larger scale of this project means that there is a wider range of variation that is captured between all the study areas. This includes rock mass conditions and their associated controlling attributes.

Furthermore, the Cammack et al. (2018) classification addresses weathering and rock mass defect strength parameters, each of which are factors that have not been specifically addressed in the conceptual TRC. Despite this, there are similarities between the defect structure classes established in Section 5.3 and the rock mass attributes of persistence, continuity and systematic

versus sub-systematic proportions in the TRC. As the Cammack et al. (2018) classification also provides a connection between the fault proximity and the differing rock mass regimes, a correlation can be made between the two classifications (Table 6.1). It should be noted that the structural regimes of Cammack et al. (2018) do not specifically account for the effect of lithological variation. However, while Cammack et al. (2018) do consider a “mudstone influenced” regime, their approach does not address the opposite case which may be similar to but not limited to higher sandstone proportions.

Table 6.1: Comparison with Cammack et al. (2018) rock mass regimes and rock mass types derived in this study.

TRC	Cammack et al. (2018)
Type 1	Fault crush
Type 2	Mudstone influenced
Type 3	Fault disturbed
Type 4	Fault disturbed – Margin zone
Type 5	Margin zone
Type 6	Fractured zone
Type 7	Fault disturbed
Type 8	Fractured zone

6.1.2 Comparison with Suneson (1993)

The TRC differs from the Suneson (1993) sedimentary lithofacies classification for a number of reasons. While both classifications consist of describing the strata of the Wellington Torlesse, the end purpose is set up differently. The aim of Suneson (1993) was to identify the structural history of the Wellington area Torlesse. The main aim of the TRC was to generate a systematic approach for the purpose of large-scale rock cut-slopes. Therefore, the TRC mainly concentrates on the engineering characterisation of the Torlesse rock mass, whereas the Suneson (1993) classification is primarily geological. For this reason, mapping required for the TRC needed to include analysis of the outcrop-scale rock mass structure and its controlling attributes. None of these factors are assessed by Suneson (1993).

The lithofacies defined by Suneson (1993) can be compared to those characterised in Section 5.3. This classification can be correlated to bedding thickness attributes. However, slight modifications were made in order for it to correspond with this study. For example, Lithofacies B and C of Suneson (1993) do not have a defined mudstone-sandstone proportion and are solely characterised by qualitative attributes (Table 6.2). In this study lithofacies are also quantified by mudstone-sandstone proportions in addition to those descriptive attributes. There is also less

emphasis on the input of structural features, as this study assumes that rock mass structure is not restricted by the lithological strata.

Table 6.2: Comparison between Suneson (1993) rock mass lithofacies and rock mass types derived through this study.

TRC	Suneson (1993)
Type 1	-
Type 2	D
Type 3	C and B
Type 4	C and B
Type 5	C and B
Type 6	B
Type 7	C and B
Type 8	B

6.2 Controls on Rock Mass Condition

Development of cut-slopes requires effectively understanding what controls the rock mass at specific locations. There is a number of controlling rock mass factors specifically examined for the purpose of identifying those that are easily observed, quantified and recorded during standard site investigation and slope design processes. Ultimately these can be applied to the TRC rock mass types. This allows for a preliminary assessment of cut-slope design and comment on the potential implications during and after excavation over wide range of global and local scale cuts. The following section aims to address all the rock mass controlling factors which will provide for a more accurate preliminary assessment for the behaviour of future rock cut-slopes. This also provides further comment on rock slope conditions per type (TRC) that may implicate or constrain cut-slope design.

6.2.1 Geological Controls

The dominant Torlesse rock mass control governing the slope stability is rock mass condition, specifically rock structure. Analysis of these sites has indicated that structure has a significant impact on the rock mass condition in this region due to the effect of major fault proximity. Other controls on rock mass condition are weathering and Lithostructure but are considered to have a lower influence in controlling slope stability. Geological controls can aid in the prediction of rock mass conditions for cut slope design.

1. Defect Orientation

The orientation of defects is the primary geological factor controlling structural failure mechanism in a rock mass. For example, at Wairaka Point bedding is dipping unfavourably out of the rock mass and daylights on the slope. As a result, a global sliding event has previously occurred. Furthermore, two intersecting relatively persistent, joint sets in the sandstone unit dip at 55° and 86° out of the slope face. This creates potential for local wedge failures.

As the rock mass condition improves (from Type 1 to 8) the orientation of the bedding and shearing structures tend to become more aligned with the major regional faults. The improving rock mass tends to result in a decrease of sub-systematic defects, particularly shearing and faulting defects. Generally shearing and faulting structures are oriented sub-parallel to 1st and 2nd order regional faulting. However, in better rock mass types shearing and faulting defects start to be orientated along joint surfaces, while in poorer rock mass types they tend to be oriented along bedding planes. Furthermore, the orientation of bedding defects appears to become more parallel with the major regional 1st order faulting. It is therefore possible that the major defect sets in rock masses can be predicted from the regional fault model or lineament analysis. This could allow for the forecast of potential rock slope failures in proposed rock cut slope prior to construction of slope design.

2. Defect Condition

While defect orientation is the main geological factor influencing stability in any rock slope, other properties such as Waviness, spacing, defect width, shape, persistence, roughness and defect infill are also important. These factors will inevitably control the shear strength across any defect surface which is discussed in the following sections for the purpose of assessing their influence on rock mass shear strength and the friction angle. These factors are listed below:

a) Waviness

The majority of the rock types will consist of dominantly wavy or curved defects with inter-limb angles that trend towards higher wavelengths in stronger rock mass types (Types 5 to 8). This tends to result in an increase of planar defects with longer persistence. The effect of waviness in defect planes is that they may exert some control on the possible direction of failure (González de Vallejo and Ferrer, 2011). Furthermore, the shear strength of defect planes tends to vary along the direction of failure as any irregularities (larger inter-limb angles) makes movement along these defects more difficult (González de Vallejo and Ferrer, 2011). Thus the wavier a defect the higher the shear strength tends to be.

b) Spacing

Spacing of defects controls the block size of intact material in a rock mass. Rock mass Types 5 to 8 contain wide to extremely widely spaced defects, therefore are likely to produced larger rock

blocks. This influences the volume of localised small-scale rockfall or raveling events. Therefore, in rock mass Types 2 through 4, where defects are generally closely spaced, the volume of material that is likely to fail is anticipated to be smaller. It is important to note that while local scale failures may be smaller in Types 2 through 4 there is still the possibility of large global scale failures.

The closely spaced defects of rock mass Types 2 to 4 have been observed to yield interlocking conditions (Cook, 2001; Irvine, 2013; ISRM, 1978). As a result, this will effectively increase the rock mass strength, which may reduce the potential for local scale failures.

c) Defect Width

Defect width varies across all the sites, particularly within different defect types. The defect width is the perpendicular distance separating the adjacent rock walls of an open or filled discontinuity. Overall, Jointing generally has widths that are tight to moderately narrow. Bedding fabric tends to be narrow while bedding plane shears and fault related shearing structures tend to be wide to very wide. Steep or vertical defects that display tension are also thought to consist of wider defect widths (ISRM, 1978). In rock mass Type 2 the average defect width is about 100 mm while in rock mass Type 8 field area the average width is about 30 mm. This suggests that the orientation and proximity of each site to major regional active fault traces largely controls the defect width. Furthermore, increasing or dilating defects can cause a reduction in the shear strength of a rock mass (González de Vallejo and Ferrer, 2011), therefore increasing the potential for rock slope instability.

d) Shape

Overall defect shape, which is broadly referred to as waviness throughout this study plays a minor role in the shear strength of a rock mass. The more planar defects appear to be located in areas with higher degrees of faulting and folding. Jointing is often the most planar followed by shearing and then bedding as observed in the northern study site. However, the trend is weak. Past papers such as (Patton, 1966) identified that waviness only became significant under stress and strain conditions which result in shearing of asperities. For this reason shape is only concerned where it effects the defect orientation, for example where curving can cause slight adverse slope orientations. Therefore, it is important that defect shape is recorded as defect planes are rarely truly planar.

e) Persistence

Defect persistence determines the degree to which failure would extend in a rock mass. This defect property is arguably the most important aspect relating to structural failures in a rock mass Read and Richards (2007), Cook (2001) and Irvine (2013). The scale at which a defect can be traced in an exposure is therefore of major importance in the case of high rock slopes,

such as in Quarries or road cut-slopes. Typically, the close proximity of the rock mass to major faulting would suggest shorter more discontinuous defect lengths (Cammack et al., 2018). Different defect types, however, show variation in this trend as identified in 5.2.2. Generally the shear zones, crush zones and faults are the longer more persistent defects while the bedding plane shears and partings tend to be shorter and more discontinuous.

Where bedding thicknesses are greater, the persistence tends to be longer and rock masses are likely to be in better condition (Cook, 2001; Irvine, 2013). Thicker bedding tends to be in areas where there is relatively less deformation. It is therefore likely that where thinner bedded units are situated there is a greater degree of deformation, resulting in lower persistence levels.

f) Surface Roughness

The majority of the defects are dominantly Ro3 with the exclusion of Jointing (Ro2-Ro3). The slightly rough surfaces provide a degree of friction which diminishes with an increase in defect width and shear displacement (González de Vallejo and Ferrer, 2011). Cook (2001) identified that this defect width was approximately 3 mm wide suggesting that in any defects containing wider widths would be dependent on the infilling material for determining the defect shear strength. Given that the majority of the defects are greater than 3 mm it is therefore likely that infill material is going to control the overall initial shear strength rather than the roughness. Contradicting are joint defects, which are typically tight or narrow and are therefore the exception. The shear strength of joint is thus determined by the surface roughness conditions.

g) Infilling Material

The effect of infilling material within a defect can influence the shear strength of a rock mass. It is dependent on both the thickness and strength properties of the type of infilling material. Wyllie (2017) discuss the effect of inclusions of rock fragments in infilling when compared to material that is solely fine (clay, silt or sand). Generally, materials that have a combination of both types tend to consist of higher friction angles and shear strengths. As the majority of the infilling material in all study areas is rock fragments, with inclusions of clay, silt or sand it is assumed that shear strengths are likely to be relatively high.

Better quality rock masses (Types 5 to 8) tend to consist of stronger and higher proportions of rock fragments within the defect infilling. The effect of stronger infilling material tends to increase the shear strength of the defect whereas; weaker and smaller material tends to reduce shear strengths (Section 5.2.2). Therefore, where there is a higher percentage of rock fragments and a increase in the observed infill strength the potential for failure along these defects is less likely

3. Lithostructure

Despite fault proximity being the dominant control on rock mass structure and thus slope stability, lithostructure, specifically where mudstone occurs also has a significant effect.

Increases in sandstone content tend to result in better rock mass conditions. This is observed in rock mass Type 7, where the rock mass conditions are of better quality than rock mass Type 2, which is located at similar distances away from major 1st order active faults. Typically, sandstone rich rock masses contain relatively fewer occurrences of shearing, faulting and less discrete, non-systematic jointing as mudstone is generally weaker and thinner it is therefore more susceptible to deformation. Faulting, folding and shearing is therefore more concentrated in the mudstone lithology. The presence of these structural features is understood to influence the structural character of the rock mass. Increasing mudstone proportions are observed in Type 2 equating to poorer rock mass conditions. This is consistent across other sites examined in this study.

Overall mudstone bands are typically thinner, fragmented and display increased shearing when compared to the sandstone material. Increased proportions of mudstone appear to influence the structural character of rock masses, where mudstone content is higher in the north the degree of tectonic disturbance is relatively higher also. Being the weaker of the Torlesse lithologies, the mudstone appears to accommodate stresses within the rock mass resulting in higher strain. The effect of the high stresses causes deformation on the mudstone lithology. Where deformation concentrations are unable to be accommodated slip movement along bedding defects causes fracturing to the point of fragmentation and localised shearing parallel to the bedding contacts. This explains the heavy shearing of mudstone layers between thicker, stronger sandstone units. Furthermore, proximal major faults, which accommodate a majority of the crustal strain and stress, release a large amount of this energy into the nearby rock mass. As a result the mudstone units in the southern outcrop of Horokiwi Quarry are typically more sheared and faulted than in the North and observed to be in worse condition.

Where stress and strain is concentrated by mudstone and interbedded layers, the thicker bedded rock masses are likely to be in better condition. Thicker mudstone bedding is observed in rock mass Type 6 and as mentioned obtains relatively less deformation in relation to thinner bedded mudstone in rock mass Type 5. It is likely that where thinly bedded units are heavily deformed they have historically been favoured for accommodating the stress fields throughout the regions evolution (Irvine, 2013). Resulting in less stressed and better conditioned rock mass in the thicker member.

4. Anisotropy

Where there is a lack of mudstone interbedding, specifically in rock mass Types 6 and 8, there appears to be an increase in the observed intact strength. Typically, the presence of aligned defects in a jointed rock mass can lead to significant variations in the strength of the rock mass (Sainsbury and Sainsbury, 2017). The absence of thin interbedding allows a rock mass to behave more isotropically. This suggests that the rock mass Types 2 to 4 will tend to behave

more anisotropically due to the abundance of mudstone interbedding. This is further supported by the weaker observed rock mass intact strengths.

Major fault proximity has a significant effect on rock mass condition at different scales. When a movement occurs along a major fault line the rock in close proximity to the fault is shaken and jarred on both sides. Associated with this movement is a degree of disturbance varying with frequency and size of the rupture. Typically localised shearing and faulting is prevalent as a result. A shattered zone of rock being very close to the fault diminishes as the distance from each side increases. Beyond the shatter zone little rock is affected however the close spacing of the major faults in Wellington has meant that very few rocks have escaped some degree of shattering.

5. Fault Proximity

The effect of close proximity to a major fault is more evident within the poorer quality rock mass Types (1 to 4). Localised shearing and faulting observed in outcrop data and in past studies describes a severely shattered rock zone adjacent to the Ohariu Fault trace, typical of rock mass Type 1. Past studies indicate the extent of this zone is around 0.4 km (Stevens, 1974) near the Ohariu Fault trace, a distance able to encompass the majority of the Transmission Gully North study area. This has significant implications for cut-slope design as the stresses within the rock mass can be accommodated by movement along many of these defect planes. Increasing shearing and faulting towards major fault traces could reactivate older faults and shears from past tectonic deformation periods, resulting in potential slope instability.

The size of tectonic structure can also impact on different volumes of rock. Along some of the smaller Wellington Faults such as the Evans Bay Fault, the width of the directly affected rock is only about 5-6 m wide (Stevens, 1974). Major faults have moved substantially larger distances over a long time and are therefore marked by wider zones of severely shattered rock. Therefore identifying and understanding the regional structure will also aid as an indication of increasing structure proximity.

6. Fault Geometry

Variation in stresses and strains on the large major 1st order faults can alter the state or stress in the adjacent rock masses and therefore the condition. Near most of the study sites the primary rock mass controlling 1st order faults often contain releasing or restraining bends. These structural features are generally associated with the highest levels of crustal stress and strain along a fault, occurring in the principal directions of anisotropy (Chester and Fletcher, 1997). This suggests that the crustal stress associated with a bend in a fault will extend to much greater distances from the fault and therefore so will the degree of rock fracturing (Chester and

Fletcher, 1997). These models help explain the variation seen in field observations and signify the importance of understanding fault geometries near potential rock cut-slope projects.

The preferred orientation of shearing and faulting defects throughout the study was assessed to be mostly sub-parallel to bedding and major 1st order active faulting. Chester and Fletcher (1997) observed that weak bedding planes or weak interlayers can promote deformation by shearing in the direction of the principal stresses near fault bends. Chester and Fletcher (1997) go on to state that these principal stresses are mostly oriented parallel and perpendicular to sedimentary layering which will experience changes in stress state as it translates past fault bends. This suggests that in areas where a large degree of deformation is displayed in anisotropic materials close to fault bends (e.g., Transmission Gully North) major sets of shearing and faulting orientations can be inferred from the regional structural model. It is important to note, that while this is a useful tool for predicating orientations of major defect sets, the proximity of these sites to major active regional faults are almost certain to produce isolated, discrete and randomly oriented systematic shears and faults, which must also be considered in the design of rock cut slopes. Furthermore, intra-block rotation, as seen at the Transmission Gully site, is anticipated to result in localised changes in defect orientation.

7. Folding

Folding is associated within the regional tectonic environment and has numerous and varied effects on both natural and cut-slope stability. The majority of the study areas display folding features, in particular at Wairaka Point where folding is interpreted to be complex. Typically, folding forms an en echelon pattern above or beside the major regional fault structure. Where folding causes bedding to be unfavourably dipping out of a rock slope they are likely to facilitate slope instability. This is a typical failure at Wairaka Point.

Knowledge of the fold geometry and scale can also impact the significance of folding effects in rock slope stability. Typically folds may be associated with simple planar sliding on one limb and toppling mechanisms on the other limb, depending on their orientation with respect to a given slope face. However, asymmetrical folding indicates that one limb is longer, suggesting either sliding or toppling mechanisms maybe more probable. Furthermore folds with a smaller inter-limb angle generally have an increase in bedding dip, signifying the importance of understanding the fold shape and size when designing rock cut slopes.

Past papers describe that the tightness of a fold may not only influence the kinematics but may also indicate the degree of tectonic damage sustained by the rock mass. Weiss (1959) describes that open folds tend to show transverse, longitudinal, and conjugate discontinuities, whereas tight isoclinal folds may develop foliation and cleavage suggesting increased fault damage. Another point worth considering is the different generations of folding, where these features may

indicate plate tectonic stress relating to past deformation events instead of those in the present. While this is important to understand folding is ultimately an indirect effect of the regional tectonic environment, further signifying the importance of understanding the regional structure for cut-slope design.

6.2.2 Weathering Effects

Weathering impacts rock mass condition by reducing the intact strength and degrading the structural fabric. The Torlesse is variably weathered being fresh at the surface in some locations, to very deeply weathered in others. In the northern study zone the Torlesse appears to have a deeper weathering profile than the southern study zone. Drill core shows marginally better rock mass condition in the south compared to the north as described in Section 4.2. It is understood that this is related to the increased proximity of major fault structures in the north, with lesser amounts of fracturing reducing surface volume available for weathering. The level of faulting and shearing is still described as moderate to high with the rock mass still spaced moderately wide to wide. Implications of this suggest that the increase in rock condition in the south will initially mean that circular or combined failures may not be feasible.

6.2.3 Groundwater

Groundwater is a major geotechnical control on slope movement due to its capability to increase porewater pressures. It is observed at number of site particularly escaping from fractured rock above shear or fault zones which act as impermeable layers. It is noted by (Irvine, 2013) the presence of water generally indicate poorer rock mass types. While water may indicate poor rock mass conditions it usually a result of poor rock mass quality, where water is able to move easier due to higher permeability caused from an increase in fracturing. Furthermore water present in discontinuities reduces strength of the rock mass as a whole. The effect of water reduces normal stresses between the walls of discontinuities and will therefore reduce shear strengths providing an increased risk for all scenarios.

6.2.4 Discussion on Identified Controls

A common link between all of the controls is that they appear be heavily influenced by lithostructure or rock mass structure. Lithological bedding thicknesses and mudstone to sandstone proportions are dependent on the sedimentary environment at the time that the unit was deposited. Thus sedimentary facies must also be an overriding control on rock mass structure. In relating the rock mass structure to slope design it was identified that certain rock mass parameters such as defect orientation, infilling and scaler factors (for example persistence, defect width and spacing) tend to be more influential over rock mass stability than others. As previously discussed throughout this study, these factors appear to vary as distance from major

1st order regional faulting increases. This suggests that ultimately the rock mass structure is controlled by regional faulting.

6.3 Borehole versus Mapping Data Collection Methods

Subsurface information can, unfortunately only be collected from drillhole information. ATV and OTV is a very reliable and useful tool in providing adequate information regarding orientation data, however, it does not provide information regarding persistence. In slope instability defect persistence is widely assessed as the critical driver related to global failures. Forgoing input of this data implies a lower confidence level when recommending cut slope design. For this reason the TRC recommended to implement mapping during construction to highlight areas of instability when they arise. This approach is also successful in eliminating cuts where structure is not an issue and highlights areas where more structural analysis, through construction mapping may be required to validate the preliminary geological model.

The incredibly disturbed nature of the Torlesse rock mass means that the rock mass condition varies over small distances. This suggests that only using the mapping data, which is generally from small scale outcrops, is therefore not suitable for predicting patterns or structural behaviours over larger scales. In order to overcome this limitation a rigorous assessment based on identifying strong geological defect characteristics may be applied. It is anticipated that this assessment considers various defect scalar properties, such as spacing which is generally related to the persistence and termination of a defect, i.e. the more widely spaced the defects, the greater the persistence (Priest and Hudson, 1981). This understanding suggests that some kind of weighing process should be undertaken that assess the key characteristics of slope instability. For Transmission Gully this entailed a ranking system assigning defects either, first, second or third order based on assumed scales and whether or not they would form systematic or sub-systematic defects. Systematic structures are thought to have a higher importance than sub-systematic structure and so have a higher ranking. The first order is assumed to include bedding and faults while the second order is assumed to include systematic shearing. The third order is assumed to include joints and minor shears. It is this methodology combined with the rock mass and defect strength parameters that enable more robust domain models and preliminary cut slope designs (Cammack et al., 2018; Irvine et al., 2018). A classification system and structural regimes was a product of this investigation.

Even though all the above suggest that the borehole data presents a clear picture of what shearing and bedding is doing, most of the subsurface information fails to compare one or more of additional behaviours: the frequency of discrete, persistent cross-cutting defects, and the scale and distribution of folding.

Cross-cutting relationships for faults, shears and bedding have been recorded in various mapping in this study. At the cutting scale these features can be used to determine the relative age of each feature. Additionally if both features are unfavourably oriented with respect to rock cut slopes then potential wedge sliding may be feasible. Unfortunately this feature is not easily detectable in boreholes due to difficulties in differentiating scatter in stereoplots, therefore this relationship is mostly inferred from mapping and engineering judgement of the expected behaviour and characteristics of these features in the field. This can be problematic as these features can behave differently in different lithologies, sandstone versus mudstone. Typically we would expect these features to be more frequent in mudstone due to the weaker nature of the lithology, however, there is no definitive mention of the frequency of these features in either lithological unit. Furthermore, defect characteristics such as continuity, termination and shape, which are also unable to be identified from ATV/OTV methods, heavily influence how these features behave. Therefore careful consideration must be made when designing cut-slopes as presence of the more continuous cross-cutting features have the potential to prompt global slope instability.

Folding interpreted from borehole structural data (explained in Section 4.2) cannot accurately describe fold geometries as it is biased by the sampling method. Interpretations made in Section 4.3 frequently indicated the potential for folding based solely on a 1-D viewpoint represented by boreholes. While these interpretations may be possible, according to past literature on fold and thrust belts, it is also as just as likely that these areas could possess other fold styles due to a lack of spatial distribution of bedding data. This suggests that further checking in the field is required. However, given the limited exposures of good outcrop around the Wellington region and the close proximity of major fault structures this may not be possible. Other interpretations of folding that require further checking in the field is the en echelon arrangement. This is primarily due to the fact that the close proximity to major fault structures may have result in sheared out or overprinted fold axes. If this is the case then slope designs need to be adjusted in order to account for the change in rock mass structure, orientation and condition. Since there is generally a lack large of good rock exposures in the Wellington region, checking these interpretations may not be possible. Therefore these inferences will likely have to rely on engineering judgement.

In some cases it is assumed that access, particularly in steep terrain may prevent drilling or field techniques from being achieved. It is therefore important that location bias, particularly in unpredictable rock masses such as the Torlesse be understood, as it has the potential to change the position of the structural domain extents. This signifies the importance of validating the initial cut slope design through construction mapping during rock cut-slope projects, allowing for rock cut slope to be adapted when adverse conditions are exposed.

Further comments worth considering indicate that folding is used as a primary input for identifying structural domains as they can indicate a change in bedding orientations. Structural domain boundaries have the potential to move based on changes in lithology and or structure. Hence, the need to understand the folding scales and fold geometries when assessing kinematic failure and designing of rock cut-slopes.

6.4 Application to Slope Design

The aim of this section is to discuss the potential stability mechanisms on cut slope design. Implications for cut slope design across the range of rock types will then be derived from the TRC.

6.4.1 Potential Stability Mechanisms

To further discuss the potential mechanisms on slope instability, several possible failure scenarios are presented below (Figure 6.1):

Scenario 1: Isolated discrete features oriented sub-parallel to a cut-slope that are adverse and have potential for planar or wedge failure.

Scenario 2: Defined shears, bedding, faults or persistent joint structural defect sets oriented sub-parallel to a cut-slope that is adverse and has the potential for planar sliding.

Scenario 3: Defined defect sets (Bedding, persistent joints) dipping steeply into the cut slope with the potential to cause flexural toppling.

Scenario 4: Defined defect sets adversely oriented with the potential to combine to form wedge failure.

Scenario 5: Very closely spaced discrete and or defined discontinuities with poor quality rock mass that combine to form circular failures.

Scenario 6: Strong well-defined defect sets sub-parallel to cut-slope and poor rock mass conditions combine to form global scale cut-slope instability.

As there is a large degree of variability in defect orientation presented in all rock mass types. The potential exists for more than one scenario to be occur is a given rock mass type. Figure 6.1 illustrates scenarios and provides an example of the amount of dispersion in the area of the stereonet that may be required for kinematic assessment.

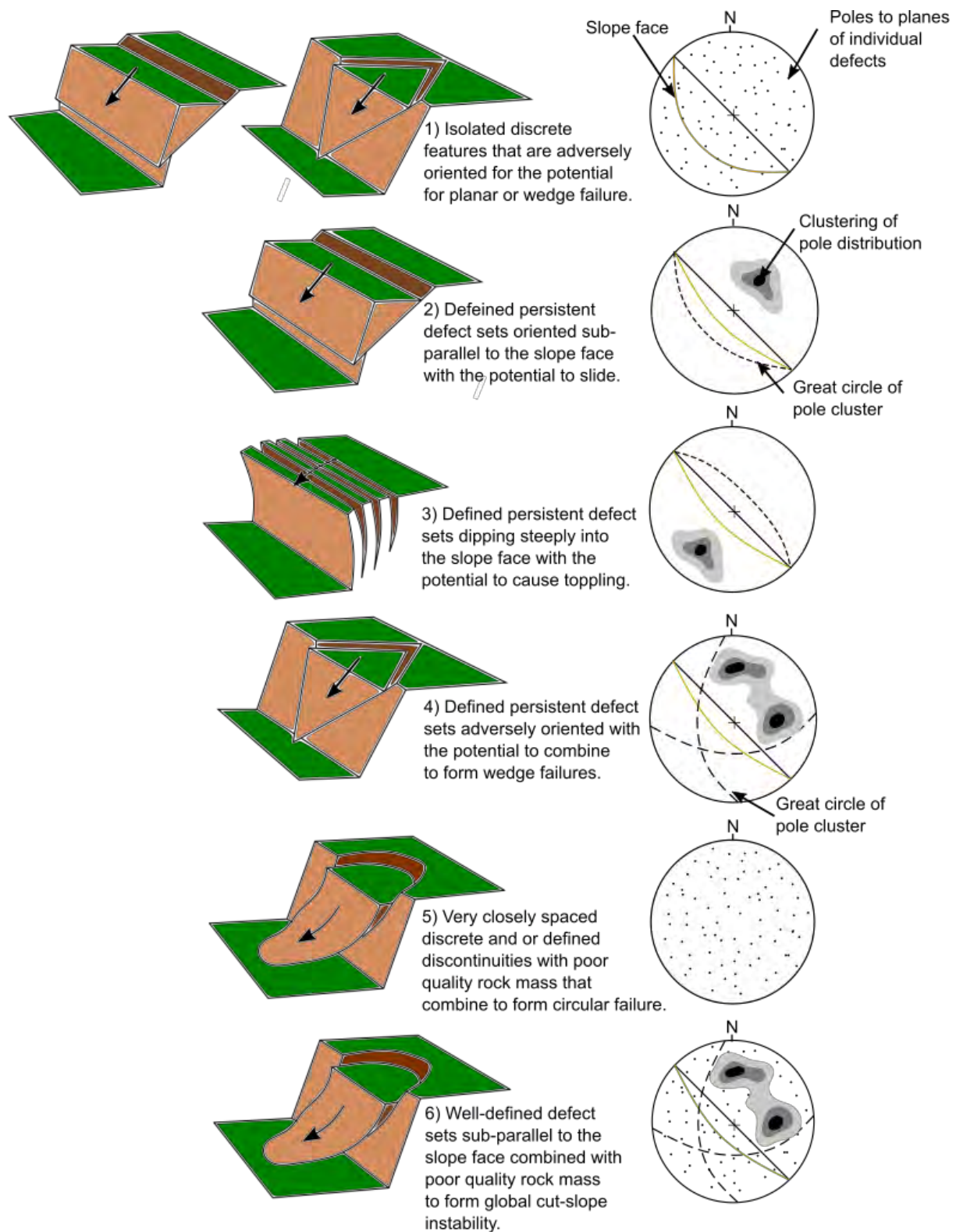


Figure 6.1: Representation of the interpreted failure scenarios with the typical pole plots and great circles likely to lead to such failures. Modified from Cook (2001) and González de Vallejo and Ferrer (2011).

Scenario 1

In Scenario 1, isolated discrete geological features suggest the potential for planar or wedge failures. Scatter examined in the stereoplots between all the study sites in Chapter 3, was the basis for this interpretation as poles to planes of the scattered data represented randomly oriented, isolated, discrete geological features. These features are expected to be non-systematic and at best only form weak defect sets that may represent older faults and shears from past tectonic deformation periods. Where these features are identified daylighting in unfavourable orientations to cut-slopes and or intersecting other geological or structural defects it is feasible that both planar sliding and wedge sliding may occur on a scale controlled by their persistence. Based on this the potential for this scenario to occur is probably too low to control design.

Scenario 2

In Scenario 2, the poles to planes of defined defect sets (shears, bedding, faults) indicate the potential for planar sliding. Where these defects are unfavourably orientated and daylight out of the slope sliding may be observed. These mechanisms are often dependent on the persistence and continuity within a rock slope or bench. Therefore the potential for this mechanism in the poorer rock mass Types (1-4) are less likely to due to their characteristically low or short persistence.

Scenario 3

Toppling mechanisms require long persistent, evenly spaced defect sets dipping steeply into the slope (González de Vallejo and Ferrer, 2011). In the Wellington Torlesse rock mass the only defects that are observed to form sets is bedding. As the rock mass is likely to be too disrupted by the complex deformation environment toppling mechanisms are not likely to cause slope instability. In past studies jointing has been known to display toppling failures however the persistence is typically much longer.

Scenario 4

Scenario 4 examines the potential for two defined defect sets intersecting to form a wedge failure. As with scenario 2 wedge failures are dependent the persistence and continuity of the defect failure surfaces within a rock slope or bench and so are unlikely to control design in the poor quality rock masses. Furthermore, these defects must be adversely oriented such that they daylight out of the slope.

Scenario 5

Scenario 5 reviews the condition of the rock mass for the purpose of assessing potential pure circular failures in the Torlesse. This scenario is defined by very closely spaced or fractured poor quality rock mass that is typically restricted to highly weathered or fault crush material. In both

cases the material obtains extremely low intact rock mass strengths which when combined with high groundwater pressures tend to facilitate failure.

Scenario 6

Scenario 6 assesses a combination mechanism of adverse structure and poor rock mass conditions with the potential to contribute to large-global scale cut-slope instability. This scenario is similar to scenario 5 in that it is also restricted to closely spaced or fractured poor quality rock masses. However, the way in which it fails involves well-defined defect sets that daylight and combine with “break through” or propagating defect planes through the highly fractured rock masses (Camones et al., 2013). Often this creates a stepped type failure surface. Again the need for high groundwater pressures is normally needed to drive failure. Combination failures are probably the most commonly occurring mechanism in the Torlesse, primarily due to the characteristically closely jointed nature.

Table 6.3 presents the interpreted failure scenarios for rock slope stability within each rock mass type; likely failure scenarios are irrespective of potential slope orientations.

Table 6.3: Potential failure scenario irrespective of slope orientation

TRC	Failure scenario irrespective of slope orientation
Type 1	1,5 and 6
Type 2	1,2,5 and 6
Type 3	1,2,4 and 6
Type 4	1,2,4 and 6
Type 5	1,2 and 4
Type 6	1,2,4
Type 7	1,2,4
Type 8	1,2,4

6.4.2 Rock Mass versus Structurally-Controlled Failure

Due to the range of rock mass and defect conditions encountered within the Torlesse, a number of rock mass failure mechanisms are likely to be encountered. Section 6.4.1 describes six potential failure scenarios that either fail along defect surfaces or through the rock mass. These scenarios can be applied to the TRC and for further analysis across the range of rock mass types that are derived from the TRC.

The importance of the TRC is that it essentially differentiates the various rock mass types between structurally controlled or rock mass failures. Better rock mass types (5-8) are likely to fail along defect surfaces, irrespective of the differences in rock mass condition. The poorest rock mass types (1-4) are more likely to be controlled by a combination of rock mass condition

and structural defects (Hearn, 2011). Given the dominance of rock mass structure in failure mechanism across all defect types, it is therefore more likely that the engineering geological properties that control overall defect condition are those that are more likely to control the rock slope stability mechanisms. To be noted is that the volume of material in a failure will vary as the size depends on the persistence and spacing of both bedding and shearing defects. As jointing tends to have shorter trace lengths and less spacing between sets it is likely that these structures will only control local failure in rock mass Types 5 to 7. Therefore, the more persistent defect types will have an important influence upon the scale of larger potential failures. These attributes will ultimately control structural failure mechanisms (Figure 6.1), with defect orientation determining the mode of failure. Therefore, the persistence, spacing and orientation of defects are the primary controls on the structural stability within a rock mass. It is anticipated that future engineering projects will comprise of individual site-specific design requirements that may necessitate varying slope angles and orientations, hence the absence of a thorough kinematic analysis.

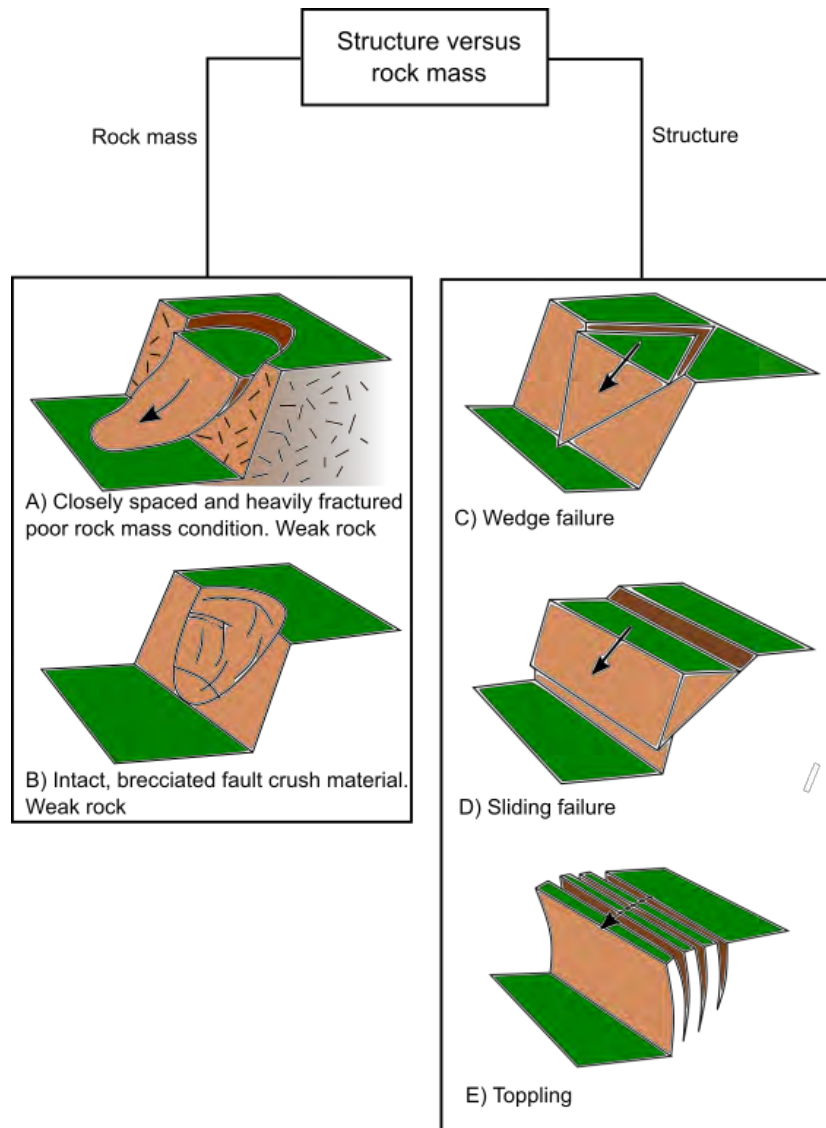


Figure 6.2: Comparison between structurally controlled and rock mass condition failures adapted from González de Vallejo and Ferrer (2011).

6.4.3 Ravelling and Rockfall Failures

Ravelling failure applies mostly to those rock mass types which consist of loosening of closely fractured, weak rock (Figure 6.2) (McMillian et al., 2000). This typically applies to failures within defect types 2 and 3, due to the presence of closely spaced, low persistence and discontinuous sub-systematic joints. Furthermore, relatively small rock blocks, delimited by the close spacing of the joints, are likely to detach from the rock mass and cause small-scale rockfalls (Figure 6.2). While these mechanisms are important to discuss, it is unlikely to cause global scale failure and so is excluded from the potential rock slope scenario list. As previously discussed by Cook (2001), Read and Richards (2007) and many other authors (e.g., Irvine (2013), Stewart (2007)), the interlocking nature of these joints generates a higher resistance to compression or shear loads. Therefore, supporting it is unlikely that this type of event will cause any global scale failures. It must be noted that ravelling will still have to be accounted for in the safety of a rock

slope. However, it is unsuitable to apply these small-scale failures in the overall design due their limited extent and therefore lower risk. Hence, only those mechanisms that may cause global failure are considered for the overall design.

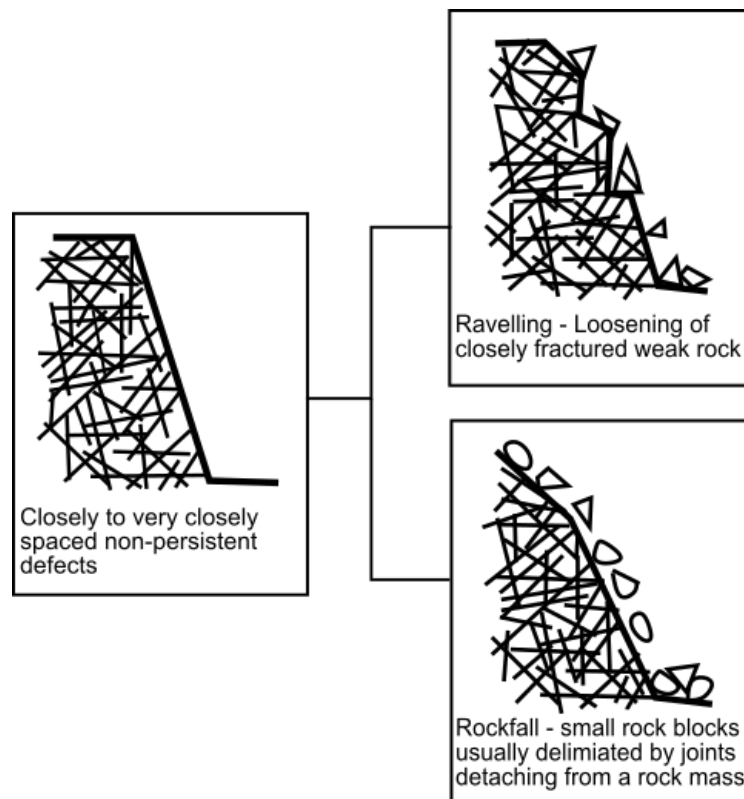


Figure 6.3: Schematic displaying the nature of ravelling and rockfall mechanisms. Adapted from Hearn (2011).

6.5 Implications to Slope Design

The aim of this section is to discuss and provide comments on cut slope design implementation, specifically for the rock types derived in the TRC. The intention is not to provide a thorough review or detailed assessment but to present philosophy towards the application of this approach.

6.5.1 Excavation

Slope excavation can be carried out by either mechanical means or by blasting. Ultimately the method of excavation will be selected based on the rippability of the materials.

Rippability versus Blasting

The high degree of fracturing observed in this study suggests that the Torlesse rock mass is rippable. Particularly, rock mass Types 2 to 4, as they present the smallest defect spacing and will likely have the highest productivity rates (Clark, 1996). Persistent and continuous defects of rock mass Types 5 and 7 will also make ripping easier however the increased spacing may require heavier machinery in order to keep production rates favourable (Clark, 1996). The widest

defect spacing present in this study is in rock mass Types 8 and 6. They also comprise of a smaller degree of fracturing which is generally associated with an increase in block sizes (Goodman and Shi, 1985). It is expected that this will cause an increase in the wear of ripper blades as well as decreasing the ease at which machinery can rip the rock mass. Therefore, a highly fractured rock mass will be easy to rip, whereas a massive rock mass may be very hard to rip (Clark, 1996).

Generally, the mudstone member is more fractured and sheared than the sandstone member. Higher proportions of mudstone are present in rock mass Types 2-4 which are expected to be less abrasive and easier to rip. This should result in higher productivity levels in those rock mass types that contain higher proportions of mudstone material.

Rock mass Types 8 and 6 are expected to present the most significant challenge to rock cut slope construction in the Wellington Torlesse. The wide defect spacing and lack of mudstone material suggests that ripping may not be a suitable excavation technique. Ripping would only be considered where there is a restriction on the use of explosives. Ripping is generally considered less hazardous however, blasting means less oversized material would need to be split before excavation. One of the main objects in rock blasting particularly in rock cut-slopes is to avoid excessive breakage (and further damage) of the rock mass. This could further stability problems therefore techniques such as pre-splitting and smooth blasting is essential to minimise structural damage to the rock mass. This should eliminate most dangers associated with blasting, however, blasting near urban areas may not even be permitted and so ripping may be the only choice. A further advantage of ripping machines is that they have more control over excavation dimensions therefore cut slopes will not be damaged when they could be damaged by blasting (Wyllie, 2017).

Rock mass Type 1 is anticipated to be encountered the least and is mostly comprised of extremely fractured material that is heavily favoured for scrapping. As the material is typically loose and already heavily fragmented ripping is not likely to be required. However, given that volumes of this rock mass type are low it may be more productive and cost effective to use the same machinery as the adjacent rock mass type. The decision between ripping and scraping should depend on the volume of the material expected to be in this rock mass type.

6.5.2 Slope Geometry

The common design requirement for rock cuts is to determine the maximum safe slope cut angle which corresponds with the planed height restrictions. This process is often dictated by economics as steeper cuts are usually less expensive to construct as smaller volumes of material are required to be excavated (Wyllie, 2017). However, the overall geometry of a cut slope is established by the orientation of defined defect sets. As discrete, isolated shearing is

often randomly oriented it is not suitable to design a rock cut slope around these features. It is generally more appropriate to allow for a few isolated features to outcrop and then implement stabilisation measures in order to prevent unwanted instability.

Most of the defined defect sets tend to dip steeply throughout the Wellington region. This is favourable for rock slope face angles however this is not necessarily the case everywhere. Some exposures, mainly at Wairaka Point, display bedding and shear sets that were moderately inclined. This is important, as the dip of the identified defect sets must be the same or larger to that of the rock cut- slope, particularly when the dips are in the same direction in order to prevent daylighting and subsequent potential instability.

Ditches act effectively as rock traps as they provide a barrier that captures minor rockfall or raveling failures, particularly from rock mass Types 1 through 4. Due to the close spacing of defects within these rock mass types, it is anticipated that loosened small-scale rock blocks are more likely to be detached than in the relatively stronger and wider spaced defects of rock mass types 5 to 8. It is still important to note that while ditches are important in the poorer rock mass types it is still recommended in rock mass types 5 to 8. The effect of the ditches significantly reduces the risk of rockfall impacting with potential users. Traditionally, ditches are built into each individual bench at the base of each rock slope face with the expectation that over time material will likely build up. If the accumulation of material is continued without clearing the effectiveness of the ditch will be reduced. As a result, regular clearance of accumulated material should be undertaken as part of post construction maintenance schedule. This signifies the importance of bench accessibility.

Furthermore, bench width is an important factor to be considered in the design rock mass slopes. All of the rock mass types obtain comprise of the potential for local scale failures, and given that they may occur will likely be captured by on the benches. This presents a similar impact to the implementation of ditches. Generally, bench widths are approximately 5 m although this is dependent on the height of the slope face (Wyllie, 2017). It is important to note that while the rule of thumb may be 5 metres, the width of the bench is ultimately decided in combination with the bench height as higher benches can cause more movement in locally displaced rock blocks. Generally, most bench heights are about 8 to 10 metres in the Wellington region.

6.6 Constraints on the TRC for Future Projects

Throughout all rock mass types it was identified that there was the potential for randomly oriented, isolated, discrete shearing. This presents a degree of unpredictability in the overall quantification of rock mass types, particularly in those rock mass types where there is a significant increase in sub-systematic defects (Types 2-5). While this discussion has attempted

to describe an approach that could be applied to future large cut-slope design projects, the unpredictable orientation of these structures in the Torlesse still remains a large known unknown. In order to account for these features, it is suggested that an observational approach be implemented during the construction of rock cut-slopes. Using this approach will allow for the design assumptions to be verified and local instability mechanisms to be managed. Furthermore, this approach will validate rock face conditions which will provide the potential for deviations from the initial design model in the event that adverse conditions require it.

The intended use of the TRC is that it is applied in future projects to aid in deriving their own individual site-specific rock mass types. Hence the rock mass types and the associated discussion provided in this chapter are not planned to be relied upon for future projects but are rather intended to provide an illustration of an approach that can be systematically used in other areas for slope design in the Torlesse or similar layered and tectonised materials.

When applying this classification to different investigation methods, certain rock mass parameters, such as defect persistence, continuity and fault proximity will exhibit more influence over other parameters when determining rock mass types. In relating this to future engineering projects and the rock cut-slope design methodology, specifically initial or preliminary design, linkages must be made. Most large-scale rock cut-slopes rely upon drillhole data in the preliminary rock cut design stages. It should be remembered that boreholes only provide a limited 1-D profile of what can be a complex, 3-D rock mass. Therefore, certain parameters such as persistence and continuity are unlikely to be obtained from these investigations. While this may appear to restrict the potential for successful classification, other defect structure parameters and infill characteristics (Section 5.2.2) are obtained and can be implemented in the TRC in order to account for these limitations. Using these other rock mass parameters (*e.g.*, defect infill, spacing, type and shape) along with lithostructure will provide the bases for the TRC during drillhole investigations. While boreholes do have their limitations, it often provides more valuable insight into furthering the understanding of the site specific geological model in the Wellington region. The current TRC presupposes good outcrop at a site, which is not strictly logical in the Wellington region due to the inherently fractured nature of the Torlesse rock mass. Therefore, it is expected that the TRC will not be the sole method used in site investigation methods for determining rock cut slope designs. It is intended that the TRC be used in combination with other preliminary site investigation methods such as site reconnaissance and laboratory testing where more information can be collected that can increase the accuracy of the site-specific geological model. This combined with safe engineering practices should result in achieving a lower risk for rock cut slope instability during and after construction.

CHAPTER SEVEN SUMMARY AND CONCLUSIONS

7.1 Thesis Objectives

The main objective of this study was to develop an engineering geological approach for the evaluation of the Wellington Torlesse rock mass condition that specifically addressed key factors which influence potential slope instability mechanisms in rock cuttings.

Previous work has mainly focused on 'traditional' rock mass description and classification approaches. However, experience from existing road cuttings suggests that, outside of weathered and highly faulted rock, there are other factors that are likely to control potential rock cut-slope instability mechanisms.

This investigation uses detailed engineering geological mapping, along with geotechnical databases obtained from prior site investigation and ongoing construction programs on the Transmission Gully project in Wellington, to characterise the Torlesse rock mass. The primary objective of this new approach was to focus more attention on regionally-controlled geological structure and defects when designing rock slopes in the Torlesse.

The objectives of this study (Chapter 1) are restated below:

- Characterise the range of engineering geological conditions encountered within the Torlesse Composite Terrane of Wellington, New Zealand.
- Review and compare the structural domain models established from a preliminary site investigation phase and the construction mapping programme.
- Develop an engineering geological model approach for the evaluation of rock mass condition.
- Comment on the application of the approach to future engineering projects within the Torlesse Composite Terrane, within the Wellington region for slope design.

Seven main study sites were investigated to gain an overall understanding of the range of engineering geological conditions exposed in the Wellington Torlesse. These were: Transmission Gully North and South; Horokiwi Quarry; Kapiti Quarry; Owhiro Bay Quarry; Wairaka Point; and Makara Head (Figure 2.5). A detailed engineering geological three-dimensional model for each site which, used in combination with structural mapping data, aided in the development of the engineering geological approach.

7.2 Rock Mass Site Observations

Each study site displayed different structural and lithological conditions. In Kapiti Quarry and Transmission Gully North, the rock mass condition is heavily influenced by major faulting (the

Ohariu Fault). While both sites display relatively similar rock mass properties, there is a greater proportion of mudstone to sandstone at Kapiti Quarry than at Transmission Gully North. An increase in shearing and faulting was observed at both sites, with defects tending to be discontinuous.

The Transmission Gully South site is located just outside this zone, in a relatively less disturbed rock mass. Although this zone is located at a greater distance from major regional active faults it contains similar mudstone to sandstone proportions as the Transmission Gully North site.

Decreased mudstone proportions are observed in Horokiwi Quarry. There are two distinct structural zones at this location. In the southern part of the quarry the rock mass is heavily disturbed by the Wellington fault. Intense shearing and faulting tend to overprint bedding producing poor rock mass conditions. Towards the northern part of the site, with increasing distance from the Wellington Fault the degree of tectonic disturbance decreases, resulting in a decrease in shearing but an increase defect persistence. Although there is a slight variation in lithology at Makara Head, the presence of the Shepherd's Gully Fault running through the site means that it displays similar rock mass characteristics to Horokiwi Quarry.

Although the structure at Owhiro Bay Quarry is influenced by the nearby Wellington Fault, it displays a relatively less disturbed rock mass. The distance between site and controlling fault is significantly greater than either Horokiwi or Makara. As a result, the rock mass shows a decrease in shearing and greater defect persistence. Wairaka Point is also assessed as part of this zone, however thicker sandstone beds, combined with a reduced mudstone content results in lower levels of shearing and greater joint persistence.

Thinly bedded mudstone sequences across all study sites were observed to be highly fractured, faulted and folded. These beds tended to concentrate increased levels of deformation in comparison to the thicker sandstone beds. The latter generally display less fracturing and higher levels of jointing. As the level of localised shearing and faulting increases in thicker interbedded sequences, the level of deformation also increases while there is a decrease in jointing.

Sandstone beds dominate the majority of the rock masses at all the study sites, with the notable exception of Kapiti Quarry. Mudstone is the weaker of the two lithotypes and is, therefore, mostly fragmented and deformed. As deformation is generally associated with poorer rock mass conditions, sites with a lower mudstone content tends to display better rock mass conditions.

The presence of finer defect infilling material (< 2 mm) was characteristic of rock masses with increased levels of mudstone and higher levels of deformation. Most infills were comprised of relatively high percentages of rock fragments (breccia), with the observed strengths tending to decrease as the rock mass condition decreased. Where less shearing and faulting was

observed, defect infilling consisted of cemented, precipitated material, indicating increased shear strength across the defects.

7.3 Transmission Gully Design and Construction Structural Data Review

Both the borehole-dominated design and construction mapping structural databases from the Transmission Gully project were examined. The defect information assessed included defect type, orientation, infilling material, defect thickness, spacing and persistence. Additional information on the rock mass condition was obtained from the original site investigation borehole logs in addition to supplied data on bedding thickness, spacing, colour, moisture, intact strength and weathering.

The problem of determining defect persistence, particularly from 1-D borehole and televiewer data was highlighted. Defect persistence is a significant factor governing slope instability and is found to vary significantly, sometimes over small distances. A number of other defect attributes (such as continuity, termination, shape, cross cutting relationships and folding properties) are also difficult to quantify from borehole and ATV/OTV data. This highlights the importance of making defect observations using other investigative techniques, primarily outcrop mapping, in order to support interpreted site investigation rock conditions.

Differences between the borehole data driven design model and the revised construction design model were mostly the result of directional bias. A number of defects are observed to dip vertically to very steeply (parallel) to the borehole inclination and so were under sampled. Further investigation looked at the result of potential location bias. Where changes in the rock mass condition over short distances may provide an inaccurate representation of the site-specific ground conditions. This is based on the assumption that sample locations are located at increased distances away from the proposed excavated cut-slope face.

7.4 TRC

Regional structural trends and characteristics of the Torlesse in the Wellington region were identified from observational field data. The main controls on rock mass were lithology and structure. Where clear relationships among these factors were observed, they were then integrated into a classification framework. The lithofacies and defect structural characteristics observed from individual outcrops at each study site were plotted against each other. Cluster analysis was used to identify a range of rock mass classifications.

Lithofacies are characterised by the mudstone to sandstone proportions and the dominant thickness of each identifiable bedding unit. Defect structure incorporates a description of the observed discontinuities, along with scale factors and infill conditions. In nearly all rock mass

types, thicker bedding was associated with better rock mass quality. Where bedding thickness decreased, the degree of fracturing generally increased. More prominently bedded sequences are related to decreases in the mudstone to sandstone proportions. Thus, lithofacies is a major control on rock mass condition.

Defect structure consists of defect properties which heavily influence potential mechanisms for rock slope failure. These include defect type, persistence, continuity, infilling and spacing. Both defect type and defect characteristics are closely related to the style of, and proximity, to regional structural features; in particular major 1st order, through-going faults. Poor quality rock mass types with very little defect persistence and closely-spaced defects are generally situated close to 1st order regional faults. As the proximity to faulting increases, so does the occurrence of sub-systematic defects and the degree of shearing or fracturing. An increase in shearing was also observed with an increase in the mudstone-sandstone ratio in thinly bedded rock masses.

A total of four categories (Lithofacies A through to D) describing different bedding sequences and mudstone to sandstone proportions are defined. Similarly, defect structure is described by six defect classes (Class 1 through 6). Plotting lithofacies against defect class provides the means to develop a conceptual model (Figure 7.1), termed the Wellington Torlesse rock mass classification (TRC). By plotting individual outcrops from each site, clusters of similar character can be identified across a range of lithologically and structurally heterogeneous region. Overall, eight different rock mass types were identified across all the study sites.

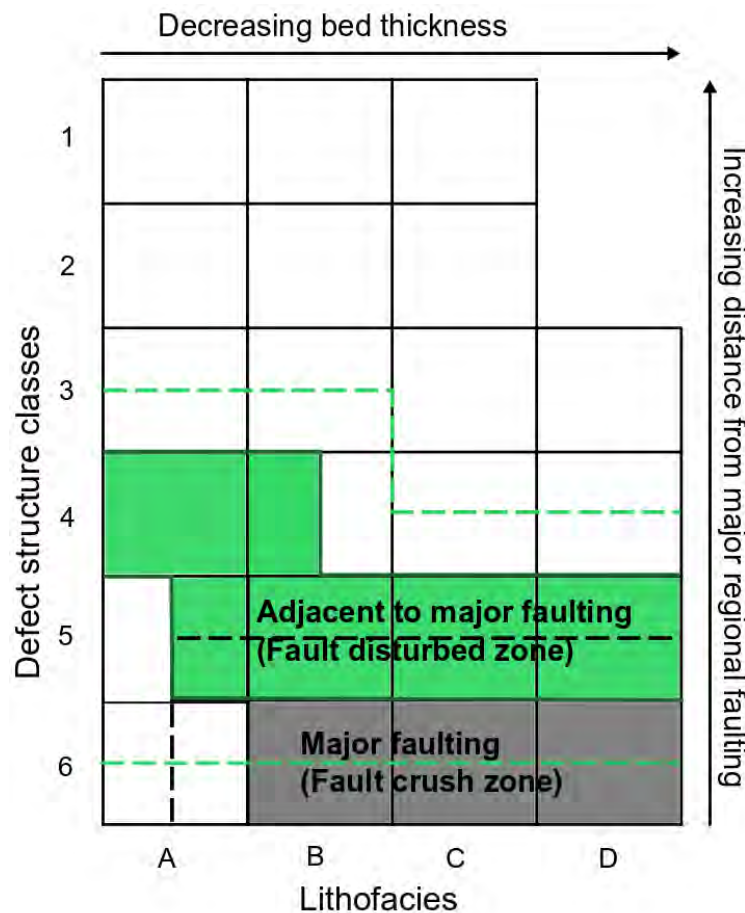


Figure 7.1: Final rock mass classification. The green area represents the rock mass type adjacent to major 1st order regional faults. The grey area represents the rock mass type typical of fault crush or gouge material. The dashed lines are included to accommodate potential rock mass types that have yet to be or may be encountered.

Rock mass Type 1 represents the poorest rock mass conditions. This generally defines fault crush material which is heavily fragmented with barely recognisable defects. Rock mass condition improves through rock mass Types 2 and 3, where shearing and bedding defects are easier to recognise and tend to form systematic and sub-systematic defects in approximately equal portions. Few defects are persistent (>10 m) and tend to be sheared zones, crush zones or faults. Jointing is generally closely to very closely spaced, randomly oriented and tends to produce a degree of interlocking. The main difference between Type 2 and 3 is that the former is comprised of higher mudstone proportions.

Decreasing levels of shearing and faulting, combined with increased bed spacing, define rock mass Types 4 and 5. Systematic shearing becomes more dominant, with defect terminations tending to be more developed. Persistent (>20 m) and continuous defects are more frequent with fewer faults, sheared and crush zones. The main difference between the two rock mass types is that Type 5 contains a greater proportion of the sandstone, as well as greater bedding thicknesses. Defect persistence increases in rock mass Type 6, with shearing and faulting

structures continuous over approximately 30 m or more. Faults, sheared zones, crush zones and sub-systematic defects are uncommon.

Rock mass Type 7 and 8 are the best possible rock mass types encountered across the Wellington region. This rock is generally characterised by high sandstone proportions and extremely wide beds. Relatively higher persistent jointing is observed in comparison to other rock mass types.

7.5 Controlling Factors on Cut-Slope Design

Development of cut-slopes requires effectively understanding what controls the rock mass conditions that have the potential for slope instability. The dominant controls for slope failure in the Wellington Torlesse were identified in this study to be lithology and rock mass structure. Lithology specifically applies to bedding thickness and mudstone to sandstone proportions while rock mass structure directly applies to defect orientation, infilling and other scalar factors (persistence, defect width and spacing). These identified controls are heavily influenced by other factors observed throughout this study. It was identified through data analysis that bedding thickness and mudstone to sandstone proportions are ultimately controlled by the depositional environment at the time that the material was deposited. Conversely, trends assessed in various defect properties identified that rock mass structure is heavily influenced by the proximity of a rock mass from major 1st order regional faulting. The overriding control on rock mass structure is, therefore, regional stress fields generated throughout the complex tectonic history of the Torlesse, which can be predicted from structural regional models.

Compared to other rock mass types, rock mass Types 8 and 6 are situated at the greatest distance away from 1st order regional faulting. Shearing in these rock mass types typically display systematic, widely spaced and continuous shearing that is also observed less frequently. Rock mass types that are located adjacent to 1st order fault traces tend to observe a larger degree of deformation with increased levels of shearing that are discontinuous and sub-systematic. These rock mass types generally consist of poorer defect conditions leading to increases in finer infilling material. Orientation of these defects are mostly sub parallel to bedding and with 1st order regional faulting, while the better rock mass types are generally oriented sub-parallel with 1st order and joint sets. Changes observed in fault geometry, such as releasing and restraining bends, also influence the degree of shearing and faulting within a rock mass, as is related with the highest levels of crustal stress and strain along a fault trace.

Increased bedding thicknesses and sandstone-mudstone proportions tend to indicate better rock mass conditions, as represented by rock mass Types 5 to 8. In these rock mass types, jointing appears to be more developed with fewer occurrences of sub-systematic, closely spaced jointing in comparison to the poorer rock mass Types (1 to 4). Conversely, dominant continuous

systematic shearing and faulting is less frequent but still evident. These rock mass types also tend to be comprised of increased mudstone proportions. Mudstone, being the weaker of the two lithotypes, appears to concentrate the majority of stresses within a rock mass, resulting in higher strains and fracturing in comparison to the sandstone unit. Therefore, rock mass types with decreased bedding thicknesses and increased mudstone proportions are typically characterised by short, discontinuous, sub-systematic jointing, along with higher fragmentation.

Other less significant rock mass controls observed through this study were defect properties such as shape, waviness and roughness. Defect shape and waviness only become significant where they affect defect orientation, while roughness is only concerned in defects where the width is less than approximately 3 mm wide. As these defect properties generally represent a transition between differing defect conditions, they cannot be assigned a major control on cut slope stability, despite their influence on rock slope stability.

7.6 Cut-Slope Design Implications

Due to the likelihood of local-scale failure mechanisms in all rock mass types, it is recommended that ditches and benches be implemented in future large-scale Torlesse rock cut slopes in the Wellington region. Benches and ditches will significantly reduce the risk of loss of life as it is expected these design features will capture any loose material before it reaches the bottom of the lowest bench. The width of the bench will be determined by the height of the bench as higher benches can cause more movement in locally displaced rock blocks.

Slope excavation across the Wellington region by mechanical means is expected to be reasonably favoured. Rock mass Types 1 to 4 are expected to produce the highest productivity rates due to a higher degree of fracturing resulting in relatively easy conditions for ripping. Rock mass Types 5 and 7 consist of persistent and continuous defects which will also make ripping easier to perform, however, heavier machinery may be required to keep production rates favourable. High proportions of mudstone will also make them easier to rip, resulting in increased productivity rates.

The wider spaced defects in rock mass Types 6 and 8 are expected to present the most significant challenge to rock cut slope construction. The wide defect spacing and lack of mudstone material may not be suitable for ripping techniques. Productivity of these rock mass types is anticipated to be lower and, in parts, the time and cost of machine maintenance may make blasting more cost-effective. If blasting is required, it should be conducted in a safe, controlled manner to avoid excessive breakage of the rock mass (which could result in further stability problems). While this should eliminate most dangers associated with blasting, blasting near urban areas may not be permitted; ripping may be the only choice. It is, therefore, important to consult local regulations if blasting is required.

Rock mass Type 1 is anticipated to be encountered the least. This rock mass type is mostly comprised of extremely fractured material that is heavily favoured for scrapping. However, it may be more cost effective to use the same machinery as the adjacent rock mass types. The decision between ripping and scraping should depend on the volume of the material expected to be in this rock mass type.

7.7 Future Work

The structural database recorded for this thesis is useful but by no means exhaustive. This study identified gaps where there was a lack in a range of rock mass conditions observed in outcrops and exposures. Therefore, further compilation of data from future rock slope engineering projects could possibly fill the data gaps and validate and/or refine the findings from this study. It is anticipated that, as the database becomes more comprehensive, it will provide valuable assistance into the design of rock cut-slopes in the Wellington Torlesse.

Compilation of data from other areas of Torlesse outcrop across New Zealand will be of significant benefit. This will allow testing of the method developed in this study. In addition, it will allow insight into the controls on the rock mass character in different tectonostratigraphic terranes. Regions such as the State Highway 1 corridor north and south of Kaikoura, where recent extensive rock slope engineering was required following the 2017 M7.8 earthquake, could provide a wealth of data, adding the additional factor of dynamic slope performance. The expanded database could provide a way of designing, assisting and planning for new geotechnical investigations by allowing for visualisation of the available data. For this to be feasible, the existing TRC must first be tested against other regions in order that rock mass implications and behaviours can be determined. If deviations are observed, this could be investigated and the controlling variables be considered in the next iteration of the TRC.

No laboratory rock mass strength testing was conducted for this study. Further development, therefore, recommends laboratory testing in order to provide shear and intact rock mass strengths for the different rock mass types. This can be compared with the results from previous investigations (e.g., Cook, 2001; Irvine, 2013), and construction projects, such as Transmission Gully, to better define the range of rock strength across each of the TRC Types. An issue exists around how best to conduct rock mass strength tests in rock mass Types 2 and 3, which are characteristically heavily fragmented, with closely to very closely spaced joints. The testing conducted by Cook (2001) may provide a means of accomplishing this. It is anticipated that sample sizes will be a major influence on the overall rock strength values.

Although not directly examined in this thesis, the incorporation of additional controls on rock mass strength, including weathering and hydrogeological factors, may provide further improvement and refinement of the TRC. In developing the TRC for these factors it is expected

that a wider range of rock mass types may be produced. Furthermore, input of external classifications, such as the GSI, may present an opportunity for the Torlesse rock mass to be assigned strength values. If this is deemed possible, it provides the potential for input into the Hoek-Brown criterion, which can then be related to other index classifications (e.g., RMR and the Q) for tunnelling and other underground engineering infrastructure projects.

7.8 Conclusion

This thesis assessed the variability of engineering geological conditions in the Torlesse Composite Terrane in the Wellington region. A total of seven study areas were chosen to represent a range of lithological and structural conditions. It was found through mapping and analysis of the defect properties, that lithology and rock mass structure were the dominant controls for slope instability. Further analysis, through the assessment of defect properties across each study site, identified that these factors were heavily influenced by other factors. Lithology and rock mass structure are ultimately dependent on the depositional environment at the time the rock was deposited and the district to regional scale geological structure, respectively.

These attributes were compiled together to form a conceptual Torlesse rock mass classification (TRC). Individual outcrops from the selected study sites were plotted on the TRC and used to derive rock mass types from clusters representative of a range of Torlesse rock mass conditions. Eight rock mass types were identified, ranging from fragmented and brecciated fault crush through to systematically controlled sandstone dominated rock masses.

The TRC enables various rock mass types to be differentiated between structurally controlled or rock mass failures. Instability in the better rock mass Types (5-8) are likely to fail along defect surfaces, irrespective of the differences in rock mass condition. While poorer rock mass Types (1-4) are more likely to be controlled by a combination of rock mass conditions and structural defects. Depending on the persistence and spacing of both bedding and shearing defects the volume of material in a failure will vary. Jointing tends to have shorter trace lengths and lower spacing so will only control small-local scale failures in rock mass Types 5 to 7. This information can then be used to assign potential stabilisation or support measures that are site and project specific.

Lithological proportions and proximity to major regional first order active regional faults enable rock mass predictions to be made prior to excavation and design of rock cut slopes. It is anticipated that the majority of rock mass Types (1 to 4) are rippable, but heavier machinery is may be required for better quality rock mass Types (5 and 7). Depending on local regulations, blasting may be more cost effective for rock mass Type 6 and 8. It is anticipated that large scale rock slopes are benched, along with the implementation of ditches so that local scale

mechanisms do not impact with nearby individuals. Where rock mass Type 1 outcrops occur amongst other rock mass types, it may be necessary that further stabilisation, either by shotcreting or other constructed retaining measures be implemented. It is anticipated that stabilisation measures will vary depending on individual site specific requirements, such as cost, design restrictions and regulations. Therefore, the TRC is not intended to provide future projects with site specific detailed design requirements but rather present a way of thinking towards the application of this approach.

In order to develop a robust TRC for future projects an integrated site investigation programme, involving both boreholes and detailed outcrop mapping will be required. Continuing mapping during construction will be required to identify isolated sub-systematic features, and hence update the TRC for each cut-slope. This will allow the preliminary geological design model to be validated and checked for any adverse stability conditions. The TRC allows for characterisation of site-specific Torlesse rock mass conditions in the Wellington region. It can be directly applied to assist in both preliminary design and construction development of cut-slope design, including the implementation of appropriate stabilisation measures.

REFERENCES

- AECOM and PSM. 2015. Transmission Gully PPP: Geotechnical Interpretive Report. Unpublished.
- Barnes, P. M., Nodder, S. D., Woelz, S. and Orpin, A. R. 2019. The structure and seismic potential of the Aotea and Evans Bay faults, Wellington, New Zealand. *New Zealand Journal of Geology and Geophysics*, 62, 46-71.
- Barton, N., Lien, R. and Lunde, J. 1974. Engineering classification of rock masses for the design of tunnel support. *Rock Mechanics Felsmechanik M canique des Roches*, 6, 189-236.
- Barton, N., Løset, F., Lien, R. and Lunde, J. 1980. Application Of Q-System In Design Decisions Concerning Dimensions And Appropriate Support For Underground Installations. *Conference on Sub-surface Space*. Rockstore, Stockholm.
- Begg, J. G. and Johnston, M. R. 2000. *Geology of the Wellington area.*, Lower Hutt, New Zealand, Institute of Geological & Nuclear Sciences Limited.
- Begg, J. G., Langridge, R. M., Van Dissen, R. J. and Little, T. 2008. Wellington Fault: Neotectonics and Earthquake Geology of the Wellington-Hutt Valley Segment. *GeoScience Feild Trip Guides*. GNS & Victoria University of Wellington.
- Bieniawski, Z. T. 1989. *Engineering rock mass classifications*, New York, John Wiley and Sons.
- Cammack, R., Eggers, M. J., Rouvray, B. and Rutherford, T. 2018. Torlesse rock mass classification system and structural regimes for rock engineering - Wellington, New Zealand. New Zealand: Pells Sullivan Meynink.
- Camones, L. A. M., Vargas, E. d. A., de Figueiredo, R. P. and Velloso, R. Q. 2013. Application of the discrete element method for modeling of rock crack propagation and coalescence in the step-path failure mechanism. *Engineering Geology*, 153, 80-94.
- Chester, J. S. and Fletcher, R. C. 1997. Stress distribution and failure in anisotropic rock near a bend on a weak fault. *Journal of Geophysical Research*, 102, 693-708.
- Clark, P. 1996. *Rock mass and rippability for a proposed open pit mine at Globe-Progress, near Reefton*. Master of Science, University of Canterbury.
- Cook, G. K. 2001. *Rock mass structure and intact rock strength of New Zealand greywackes*. . Master of Science, unpublished thesis, University of Canterbury, Christchurch, New Zealand.
- Cotton, C. A. 1949. A Review of Tectonic Relief in Australia. *The Journal of Geology*, 57, 280-296.
- Cousins, W. J. 2013. Wellington Without Water - Impacts of Large Earthquakes. *GNS Science Report*. Lower Hutt, New Zealand.
- CPB. 2019. Transmission Gully Project: GIS. Accessed online [21.02.2019].

- Crusoe Jr, G. E., Cai, Q.-x., Shu, J.-s., Han, L. and Barvor, Y. 2016. Effects of Weak Layer Angle and Thickness on the Stability of Rock Slopes. *International Journal of Mining and Geo-Engineering*, 50, 97-110.
- Eyles, R. J. 1982. Chapter 14 - Wellington. In: SOONS, J. M. & SELBY, M. K. (eds.) *Landforms of New Zealand*. Longman Paul.
- Fetter, C. W. 2001. *Applied hydrogeology*, Upper Saddle River, N. J, Pearson Education.
- GNS. 2018. New Zealand Active Fault Database. <https://data.gns.cri.nz/af/> [Accessed 15/01/2019].
- González de Vallejo, L. I. and Ferrer, M. 2011. *Geological engineering*, Leiden, The Netherlands, CRC Press/Balkema.
- Goodman, R. E. and Shi, G. 1985. *Block Theory and Its Application to Rock Engineering*, United States of America, Prentice-Hall INC.
- Grant-Taylor, T. L. 1964. Stable Angles in Wellington Greywacke. *NZ Engineering*.
- Grant-Taylor, T. L., Northey, R. D. and Adams, R. D. 1970. Microzoning for earthquake effects in the Pauatahanui area. Wellington, New Zealand: Department of Science and Industrial Research.
- Grapes, R., Campbell, H., Eagar, S. and Ruthven, J. 2011. A history of the geology of Wellington Peninsula, New Zealand: an analysis of nineteenth to early twentieth century observations and ideas. *Journal of the Royal Society of New Zealand*, 41, 167-204.
- Hearn, G. J. 2011. C4 Rock slope stabilization. *Geological Society, London, Engineering Geology Special Publications*, 24, 189-208.
- Heron, D., Van Dissen, R. and Sawa, M. 1998. Late Quaternary movement on the Ohariu Fault, Tongue Point to MacKays Crossing, North Island. *New Zealand Journal of Geology and Geophysics*, 41, 419-439.
- Hoek, E. 2007. *Practical Rock Engineering*, North Vancouver, British Columbia, Evert Hoek Consulting Engineering Inc.
- Hoek, E. and Brown, E. T. 1997. Practical estimates of rock mass strength. *International Journal of Rock Mechanics and Mining Sciences*, 34, 1165-1186.
- Hoek, E. and Marinos, P. 2000. GSI: A Geologically Friendly Tool for Rock Mass Strength Estimation. *Proc. GeoEng2000 Conference*. Melbourne.
- Irvine, A. G. 2013. *Engineering geological characterisation of the Torlesse Composite Terrane in Canterbury, New Zealand with reference to mechanised tunnelling*. Master of Science Thesis, University of Canterbury.
- Irvine, A. G., Eggers, M. J. and Cammack, R. 2018. Aspects of the regional tectonic and structural geological model of the Transmission Gully Project in Wellington, New Zealand for rock cutting slope design. *Proceedings of the 12th ANZ Young Geotechnical Professionals Conference*. Hobart, Australia: PSM.

- ISRM. 1978. Suggested Methods For The Quantitive Description of Discontinuities in Rock Masses. *International Society for Rock Mechanics*. , 15, 319-368.
- Jones, J. 2014. Transmission Gully -Phase 2 Site Investigation Works. In: BOSSELMANN, P. (ed.) *Rock Description Explanation Sheet - Transmission Gully*. Unpublished: Internal Document: Leighton HEB.
- Kamp, P. J. J. and Kamp, P. J. J. 2000. Thermochronology of the Torlesse accretionary complex, Wellington region, New Zealand. *Journal of geophysical research. B, Solid earth*, 105, 19253-19272.
- Langridge, R., Van Dissen, R., Rhoades, D., Villamor, P., Little, T., Litchfield, N., Clark, K. and Clark, D. 2011. Five Thousand Years of Surface Ruptures on the Wellington Fault, New Zealand: Implications for Recurrence and Fault Segmentation. *Bulletin of the Seismological Society of America*, 101, 2088-2107.
- Langridge, R. M., Berryman, K. R. and Van Dissen, R. J. 2005a. Defining the geometric segmentation and Holocene slip rate of the Wellington Fault, New Zealand: The Pahiatua section. *New Zealand Journal of Geology and Geophysics*, 48, 591-607.
- Langridge, R. M., Van Dissen, R. J., Cochran, U. A., Litchfield, N. J., Berryman, K. R., Begg, J. G., Villamor, P., Heron, D., Nicol, A. and Townsend, D. 2005b. Active Faulting and Paleoeearthquakes in the Wairarapa and Wellington regions *The 1855 Wairarapa Earthquake Symposium*. Lower Hutt, New Zealand: Geological & Nuclear Sciences.
- LINZ. NZ Topo50. Land Information New Zealand.
- Litchfield, N., Van Dissen, R., Heron, D. and Rhoades, D. 2006. Constraints on the timing if three most recent surface rupture events and recurrence interval for the Ohariu Fault: trenching results from MacKays Crossing, Wellington, New Zealand. *New Zealand Journal of Geology and Geophysics*, 49, 57-61.
- Litchfield, N., Van Dissen, R., Langridge, R., Heron, D. and Prentice, C. 2004. Timing of the most recent surface rupture event on the Ohariu Fault near Paraparaumu, New Zealand. *New Zealand Journal of Geology and Geophysics*, 47, 123-127.
- Litchfield, N., Van Dissen, R., Sutherland, R., Barnes, P. M., Cox, S. C., Norris, R., Nicol, A., Nodder, S. D., Lamarche, G., Barrell, D. J. A., Pettinga, J. R., Little, T., Pondard, N., Mountjoy, J. and Clark, K. 2013. A model of active faulting in New Zealand: fault zone parameter descriptions. *GNS Science Report 2012/19*.
- Litchfield, N. J., Van Dissen, R. J., Hemphill-Haley, M., Townsend, D. and Heron, D. 2009. Post c. 300 year rupture of the Ohariu Fault in the Ohariu Valley, New Zealand. *New Zealand Journal of Geology and Geophysics*, 53, 43-56.
- Little, T. A., Van Dissen, R., Rieser, U., Smith, E. G. C. and Langridge, R. M. 2010. Coseismic strike slip at a point during the last four earthquakes on the Wellington fault near Wellington, New Zealand. *Journal of Geophysical Research*, 115.
- Marinos, V., Marinos, P. and Hoek, E. 2005. The geological strength index: applications and limitations. *Bulletin of Engineering Geology and the Environment*, 64, 55-65.
- Mathis, J. I. Structural domain determination - practicality and pitfalls. Proceedings of the First Asia Pacific Slope Stability in Minning Conference, 2016 Perth, Australia. 203-213.

- McMillian, P., Harber, A. J. and Nettleton, I. M. 2000. Rock slope remedial and maintenance works. *Rock engineering guides to good practice*. Scotland: Transport Research Laboratory.
- Mutti, E. and Ricci Lucchi, F. 1978. Turbidites of the northern Apennines: introduction to facies analysis. *International Geology Review*, 20, 125-166.
- NZGS 2005. Field description of soil and rock. *Guidelines for the field classification and description of soil and rock for engineering purposes*. New Zealand Geotechnical Society.
- Orr, T. O. H. 1984. *The geology of the Torlesse Supergroup, Southern Tararua Range, North Island New Zealand*. Master of Science with Honours in Geology Thesis, Victoria University of Wellington.
- Orr, T. O. H., Korsch, R. J. and Foley, L. A. 1991. Structure of melange and associated units in the Torlesse accretionary wedge, Tararua Range, New Zealand. *New Zealand Journal of Geology and Geophysics*, 34, 61-72.
- Palmstrom, A. and Broch, E. 2006. Use and Misuse of Rock Mass Classification Systems with Particular Reference to the Q-system. *Tunnels and Underground Space Technology*, 21, 17.
- Patton, F. D. 1966. Multiple modes of shear failure in rock. *1st ISRM Congress*.
- Pender, M. J. 1980. Friction and Cohesion Parameters for Highly and Completely Weathered Wellington Greywacke. *Third Australia-New Zealand Conference on Geomechanics*.
- Pender, M. J. 1996. Aspects of the Geotechnical Behaviour of Some NZ Materials. *7th Australia NZ Conference on Geomechanics*.
- PSM. 2010a. PSM Guideline for Geotechnical Line Mapping.: Internal Document: Pells Sullivan Meynink.
- PSM. 2010b. PSM Guideline for Rock Description. Internal Document: Pells Sullivan Meynink.
- PSM. 2014. Transmission Gully Structural Database. Internal Document: Pells Sullivan Meynink.
- PSM. 2019. Transmission Gully Construction Mapping Database. Internal Document: Pells Sullivan Meynink.
- Read, S. A. L., Perrin, N. D. and Richards, L. R. 1999. Applicability of the Hoek-Brown Failure Criterion to New Zealand Greywacke Rocks. *9th ISRM Congress*. Paris, France: International Society for Rock Mechanics and Rock Engineering.
- Read, S. A. L. and Richards, L. 2007. Characteristics and classification of New Zealand greywackes. *1st Canada-US Rock Mechanics Symposium*.
- Read, S. A. L., Richards, L. and Perrin, N. D. 2000. Assessment of New Zealand Greywacke Rock Masses with the Hoek-Brown Failure Criterion.
- Read, S. A. L., Richards, L. R. and Perrin, N. D. 1998. Engineering parameters of closely-jointed rocks – Mapping and strength testing of greywacke from Aviemore and Belmont. *Institute of Geological & Nuclear Sciences Science Report 98/19*.

- Rhoades, D., Van Dissen, R., Langridge, R., Little, T., Ninis, D., Smith, E. G. C. and Robinson, R. 2009. It's Our Fault - Conditional probability of rupture of the Wellington-Hutt Valley segment of the Wellington Fault. *It's Our Fault*. GNS Science.
- Rhoades, D. A., Van Dissen, R. J., Langridge, R. M., Little, T., Ninis, D., Smith, E. G. C. and Robinson, R. 2010. It's Our Fault: Re-evaluation of Wellington Fault conditional probability of rupture. *New Zealand Society for Earthquake Engineering*. Wellington City: GNS Science.
- Riddolls, B. W. and Perrin, N. D. 1975. Wellington Urban Motorway - The Terrace Tunnel Engineering Geological Investigations. *NZ Engineering*, 30, 4.
- Robinson, R., Van Dissen, R. and Litchfield, N. 2011. Using synthetic seismicity to evaluate seismic hazard in the Wellington region, New Zealand. *Geophysical Journal International*, 187, 510-528.
- Priest, S. D. and Hudson, J. A. 1981. Estimation of discontinuity spacing and trace length using scanline surveys. *International Journal of Rock Mechanics and Mining Sciences & Geomechanics Abstracts*, 18, 183-197.
- Sainsbury, B. L. and Sainsbury, D. P. 2017. Practical Use of the Ubiquitous-Joint Constitutive Model for the Simulation of Anisotropic Rock Masses. *Rock Mechanics and Rock Engineering*, 50, 1507-1528.
- Sarkar, S., Kanungo, D. and Kumar, S. 2012. *Rock Mass Classification and Slope Stability Assessment of Road Cut Slopes in Garhwal Himalaya, India*.
- Semmens, S. 2010. *An engineering geological investigation of the seismic subsoil classes in the central Wellington commercial area*. Master of Science, University of Canterbury.
- Stevens, G. R. 1974. *Rugged Landscape*, A.H & A.W. Reed LTD.
- Stewart, S. 2007. *Rock Mass Strength and Deformability of Unweathered Closely Jointed New Zealand Greywacke*. Doctoral Thesis, University of Canterbury.
- Sunesson, N. H. 1992. Geology of Torlesse rocks around the Wellington coast between Paekakariki and Pencarrow Head. *Institute of Geological & Nuclear Sciences Science Report 92/8*, 52.
- Sunesson, N. H. 1993. The geology of the Torlesse Complex along the Wellington area coast, North Island, New Zealand. *New Zealand Journal of Geology and Geophysics*, 36, pages 369-384.
- Tating, F., Hack, R. and Jetten, V. 2013. Weathering effects on discontinuity properties in sandstone in tropical environment: case study at Kota Kinabalu, Sabah Malaysia. *Bulletin of Engineering Geology and the Environment*, 74.
- Thorpe, K. W. 1976. *A continuous seismic reflection survey of the entrance to Pukerua harbour*. B.Sci Honors Thesis, Victoria University of Wellington.
- Twiss, R. J. and Moores, E. M. 1992. *Structural geology*, New York, W.H. Freeman.
- Van Dissen, R. and Berryman, K. R. 1996. Surface rupture earthquakes over the last ~1000 years in the Wellington region, New Zealand, and implications for ground shaking hazard. *Journal of Geophysical Research*, 101, 5999-6019.

- Van Dissen, R. J., Berryman, K. R., Pettinga, J. R. and Hill, N. L. 1992. Paleoseismicity of the Wellington -Hutt Valley Segment of the Wellington Fault, North Island, New Zealand. *New Zealand Journal of Geology and Geophysics*, 35, 11.
- Weir, F. M. 2015. The future of structural data from boreholes. *International Journal of Geotechnical Engineering*, 9, 223-228.
- Weiss, L. E. 1959. Geometry of Superposed Folding. *Bulletin of the Geological Society of America*, 70, 91-106.
- Williams, D. N. 1975. Ohariu fault zone at Porirua, Wellington, New Zealand. *New Zealand Journal of Geology and Geophysics*, 18, 659-664.
- Woodcock, N. H. and Fischer, M. 1986. Strike-slip duplexes. *Journal of Structural Geology*, 8, 725-735.
- Wyllie, D. C. 2017. *Rock Slope Engineering: Civil Applicaitons*, Vancouver, Canada, Taylor & Francis Group.

APPENDICES

APPENDIX A: TRANSMISSION GULLY NORTH

The Transmission Gully North site lies in the north of the Transmission Gully alignment between Te-Puka Valley and the Wainui Saddle. The alignment is currently still under construction offering fresh rock exposures in an area that otherwise would not have any good outcrop coverage. The Ohariu Fault and its splinter fault converge within the area and the fault traces can be seen in the floor of the alignment. The intersection of the two faults form a very wide crush zone that spans the width of the alignment. It is therefore unsurprising that this area is heavily influenced by major faulting. A total of 7 outcrops were mapped (Appendix A.2).

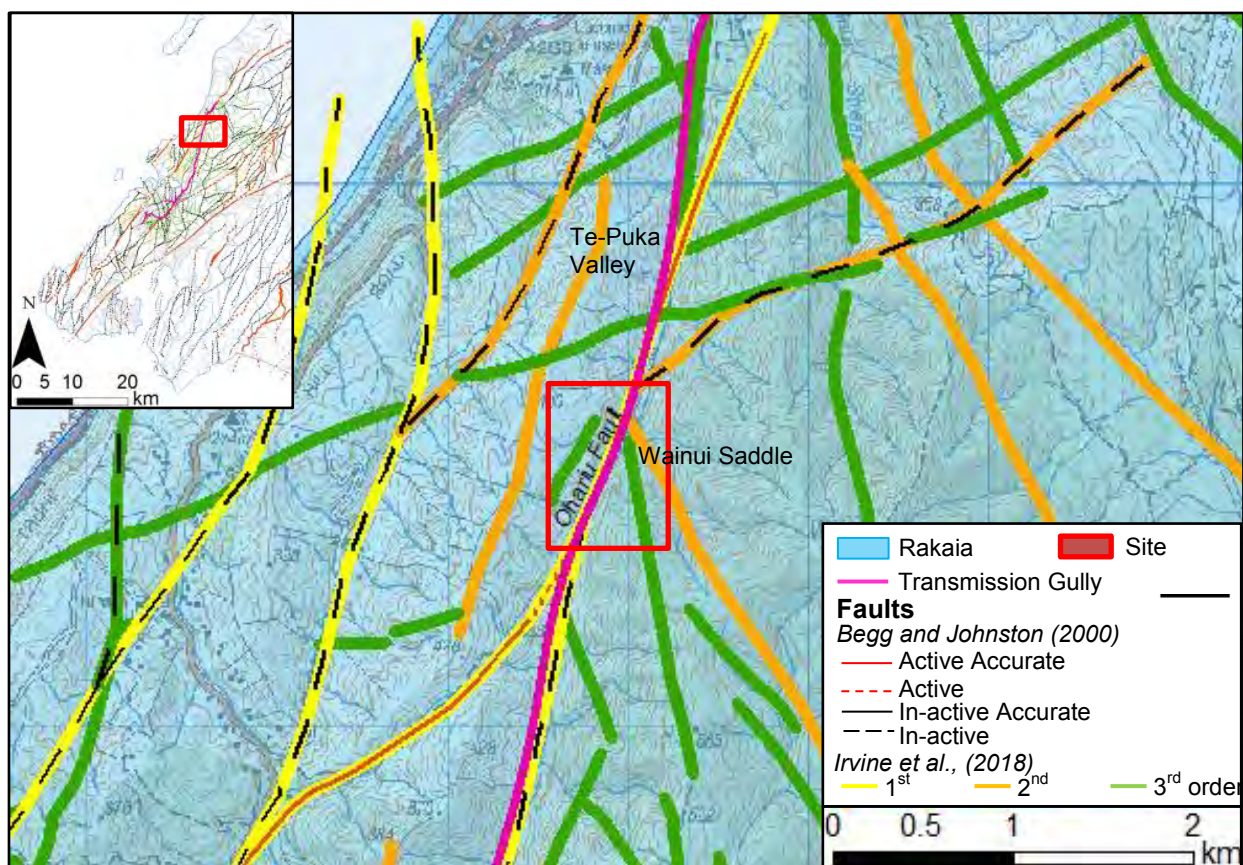


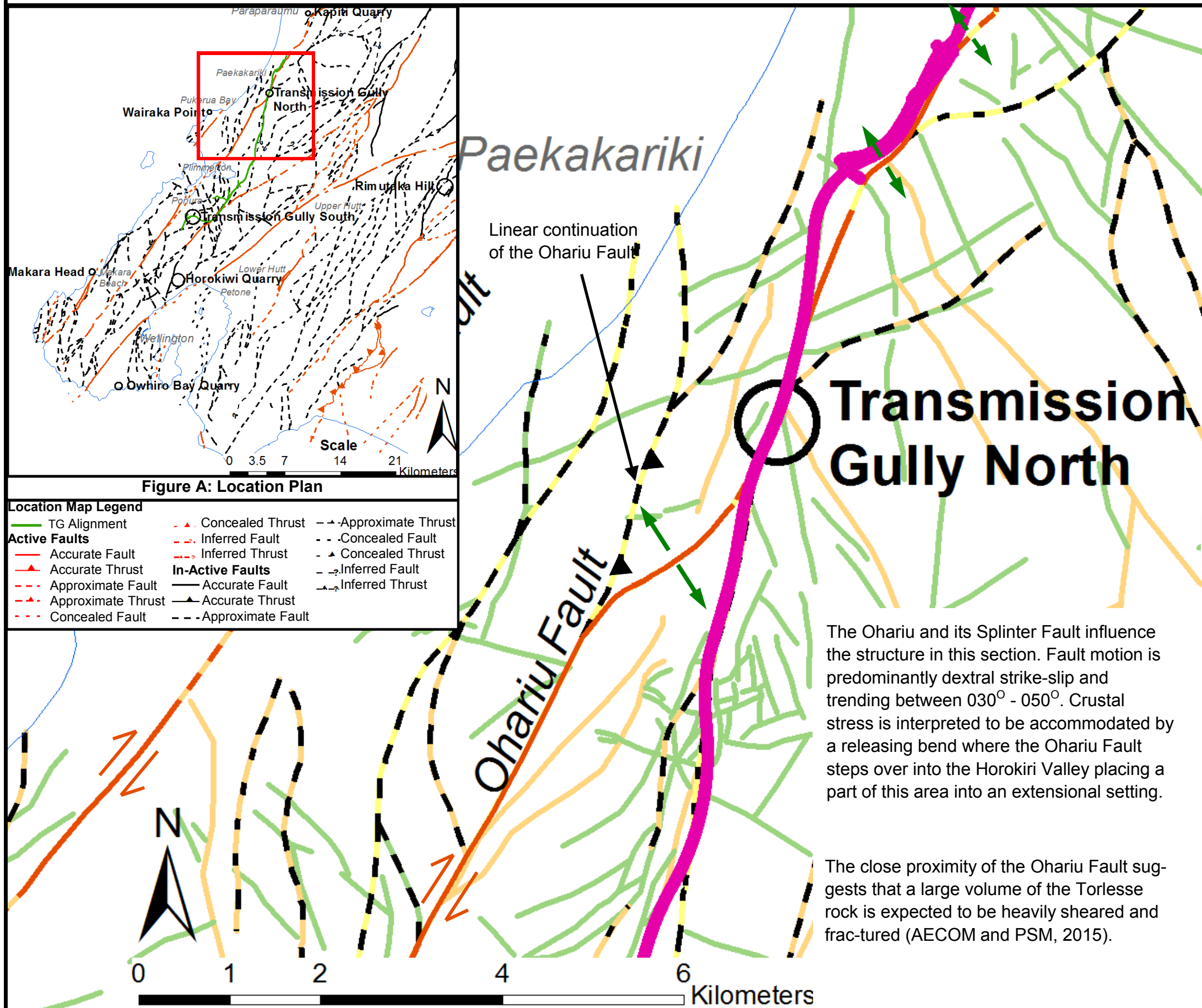
Figure A.1: Transmission Gully North site district scale map. Data sourced from GNS (2018) (Begg and Johnston, 2000) and Irvine et al. (2018). Refer to Section 1.4 for Irvine et al. (2018) order classification. Imagery from LINZ.

Results derived from conceptual models, raw mapping data, stereonet analysis and engineering geological models for the Transmission Gully North study site are displayed in the following sections.

A.1 Transmission Gully North Conceptual Structural Model

Preliminary structural assessment derived from GNS (2018) (Begg and Johnston, 2000) and Irvine et al. (2018) structural databases. Interpretations are based on information derived from past literature.

A.1 Conceptual Structural Model of Transmission Gully North



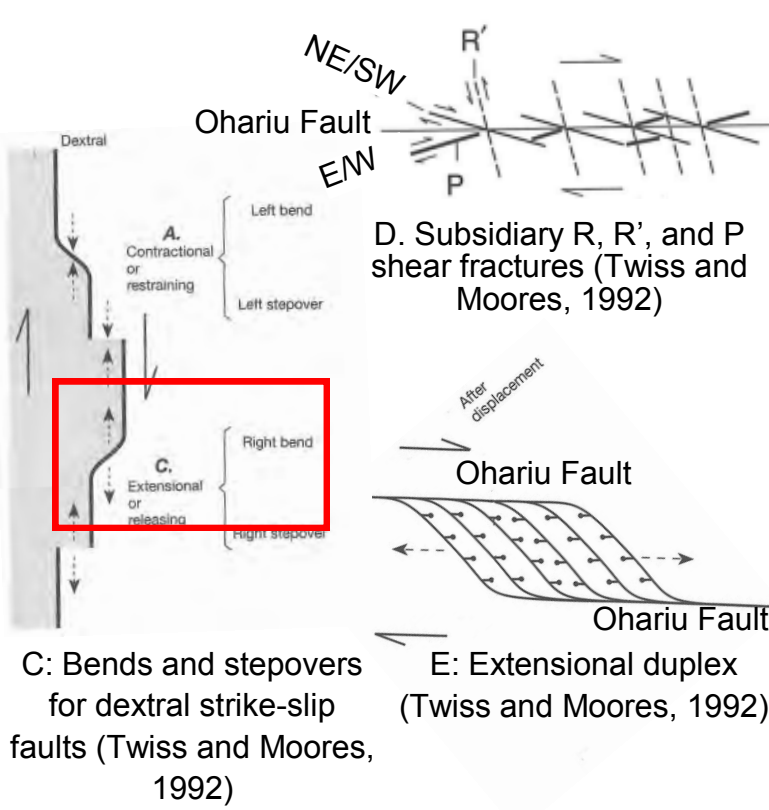
District Scale Legend:

- TG Alignment
- Restraining bend
- Coastline
- Active Faults
- Accurate Fault
- Accurate Thrust
- Approximate Fault
- Approximate Thrust
- Concealed Fault
- Concealed Thrust
- Inferred Fault
- Inferred Thrust
- In-Active Faults
- Accurate Fault
- Accurate Thrust
- Approximate Fault
- Approximate Thrust
- Concealed Fault
- Concealed Thrust
- Inferred Fault
- Inferred Thrust

Fault Analysis Overlay (Irvine et al., 2018)

- 3rd Order < 2,500 m
- 2nd Order 2,500 - 10,000 m
- 1st Order > 10,000 m

Conceptual Models:



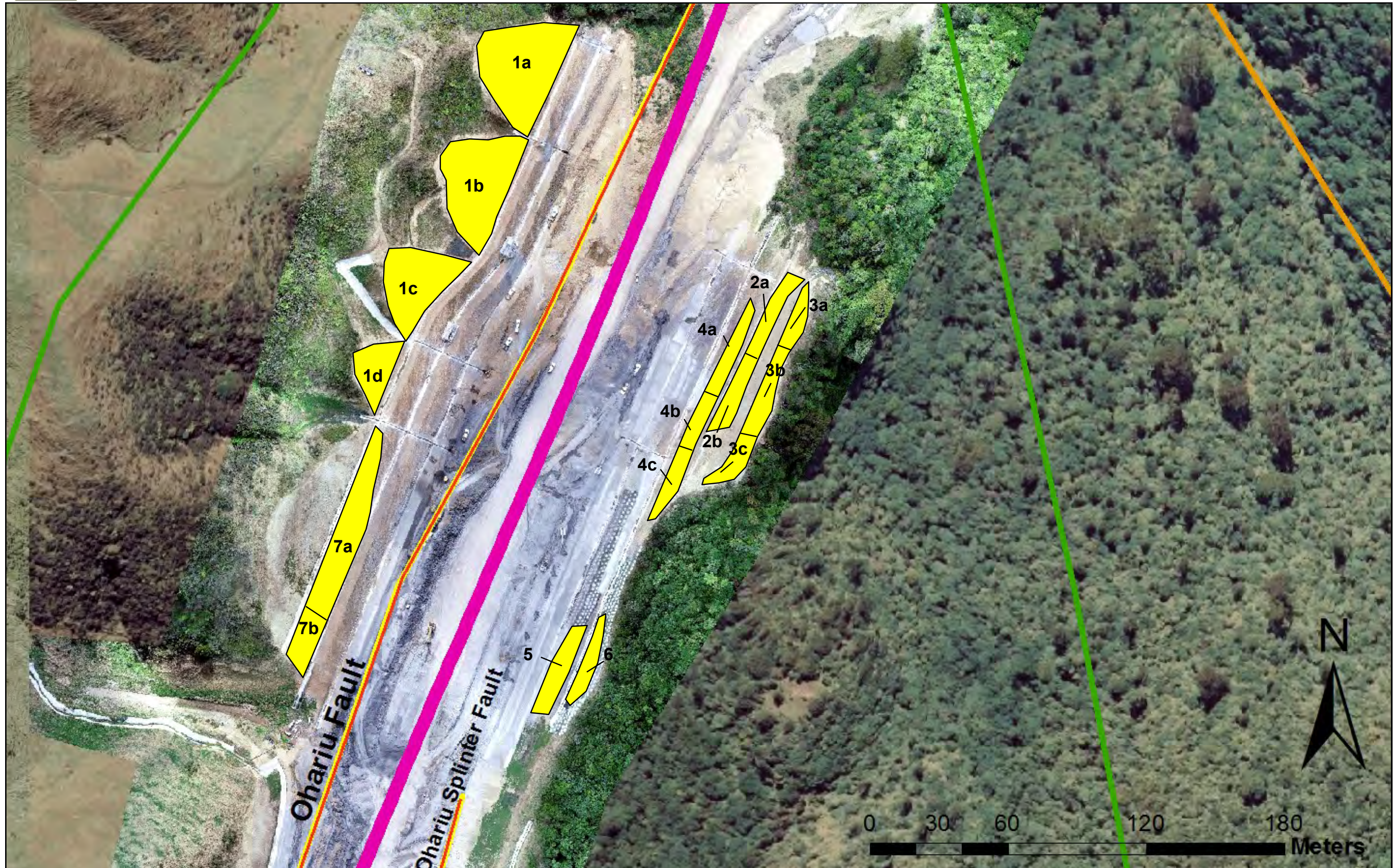
Bedding and Shearing Predictions:

Bedding and shearing is anticipated to strike sub-parallel to parallel to the NE/SW trending structures. The major structures will likely control the majority of bedding and shearing (Irvine et al., 2018).

A.2 Transmission Gully North Outcrop Location Map

Displays the location of the mapped outcrops within the Transmission Gully North study site.

A.2 Transmission Gully North



A.3 Transmission Gully North Raw Mapping Data

Structural data collected from the Transmission Gully North site. Where data is missing or blanked out information was either not able to be reached or was not relevant to the rock mass or defect condition (e.g. Planar defects did not contain a wavelength as outlined in Chapter 3).

A.3 Transmission Gully North - Raw Data

Transmission Gully North																								
ID	Defect Type	Dip	Dip Direction (Mag)	Dip Direction (True)	Structural Domain	Roughness	Thickness		% of rock fragments	Continuity	Persistence	Shape				Persistence - Trace Length (m)	Spacing (m)	Infill (Support (Breccia type (%Clasts), Angularity, weathering, strength, coating; colour, grainsize, strength, plasticity) precipitation)	Saturation	Latitude	Longitude	Comments	Cut ID	
							Width (mm)	Term				Inter-limb angle (degrees)	Term	Wavelength (m)	Term									
1	JN	58	325	302	B	Ro2	~0mm	Tight		2	D	~180°	Gentle		Planar	~0.6m	~0.2m		Dry	-41.009783	174.960962		C5c.01 SB B1	
2	SR	87	14	352	B	Ro3	~120mm	Wide	~75%	1	R	~100°	Open	~1.5m	Stepped	~2.5m		Clast supported (Mosaic (~75%), Angular, CW, Very weak, Coating; Light grey brown, silty Sand, Soft, NP) No visible precipitation	Dry	-41.009845	174.960996	Terminates in rock		
3	SR	39	356	334	B	Ro3	~100mm	Wide	~99%	1	D	~150°	Gentle	~5m	Wavy	~4m	~2m	Clast supported (Rock (~99%), Angular, MW, Weak, Coating; Dark brown grey, Sand, Very soft, NP) No precipitation	Dry	-41.009735	174.961059	Cross cuts SR4 and offsets it a little. Terminates against BSH		
4	SR	54	229	207	B	Ro3-4	~10mm	Moderately narrow	~99%	1	D	~150°	Open	~6m	Wavy	~8m		Clast supported (Rock (~99%), Angular, HW, Weak, Veneer; Light grey, Clay, Soft, LP) No precipitation	Dry	-41.009854	174.961082	Offset by SR3		
5	BSH	63	191	168	B	Ro3	~100mm	Wide	~99%	0	C	~170°	Gentle	~8m	Wavy	~8m	~1.5m	Clast supported (Rock (~99%), Angular, HW, Weak, Veneer; Light brown, Clay, Very soft, LP-NP) White sand sized specks of precipitation	Dry	-41.009809	174.960997	Continuous		
5	BSH	50	214	192	B	Ro4	~100mm	Wide	~99%	0	C	~170°	Gentle	~8m	Wavy	~8m	~1.5m	Clast supported (Rock (~99%), Angular, HW, Weak, Veneer; Light brown, Clay, Very soft, LP-NP) White sand sized specks of precipitation	Dry	-41.009755	174.961096	Continuous		
5	BSH	46	211	189	B	Ro3	~120mm	Wide	~90%	0	C	~170°	Gentle	~6m	Wavy	~8m	~1.5m	Clast supported (Crackle (~90%), Angular, HW, Weak, Coating; Light brown, silty Clay, Very soft, LP-NP) White sand sized specks of precipitation	Dry	-41.009755	174.961096	Continuous		
6	SR	51	251	228	B	Ro4	~200mm	Very wide	~75%	0	C	~170°	Gentle	~4m	Wavy	~1.5m		Clast supported (Mosaic (~75%), Angular, CW, Very weak, Coating; Light brown, silty Sand, Very soft, LP-NP) No precipitation	Dry	-41.009875	174.960942			
7	BSH	66	211	188	B	Ro3	~150mm	Wide	~95%	1	S	~150°	Gentle	~2m	Wavy	~7m	~2m	Clast supported (Crackle (~95%), Angular, HW, Weak, Veneer; Light brown grey, sandy Silt, Very soft, LP-NP) White elongated precipitation ~10mm thick	Dry	-41.009761	174.961024	Continuous, Same as BSH5		
8	BSH	71	208	185	B	Ro2	~300mm	Very wide	~95%	1	D	~160°	Gentle	~3m	Wavy	~4m	~2.5m	Clast supported (Crackle (~95%), Angular, HW, Weak, Coating; Light brown grey, silty Clay, Very soft, LP-NP) White elongated lenses of precipitation ~2mm thick	Dry	-41.009741	174.961114	Offset by SR10		
8	BSH	74	223	201	B	Ro3	~400 to 150mm	Wide to Very wide	~98%	1	D	~160°	Gentle	~1m	Wavy	~4m	~1m	Clast supported (Crackle (~98%), Angular, MW, Weak, Coating; Light brown grey, silty Clay, Very soft, LP-NP) White elongated lenses of precipitation ~2mm thick	Dry	-41.009682	174.961133	Offset by SR10		
9	SR	83	288	266	B	Ro3	~60 to 200mm	Moderately wide to Very wide	~70%	1	S	~150°	Gentle	~8m	Wavy	~8m		Matrix supported (Mosaic (~70%), Angular, CW, Very weak, Coating; Dark brown grey and light, silty Clay, Soft, LP-NP) No precipitation	Dry	-41.009703	174.961134	Terminates against SR10		
10	SR	41	128	106	B	Ro3	~300-400mm	Very wide	~90%	1	D				Stepped	~8m		Clast supported (Crackle (~90%), Angular, HW, Weak, Coating; Light brown grey, silty Sand, Soft, NP) No precipitation	Dry	-41.009758	174.960992	Terminates against BSH7		
11	SR	68	227	205	B	Ro3	~200mm	Very wide	~90%	0	C	~140°	Gentle	~4m	Wavy	~5m	~2m	Clast supported (Crackle (~90%), Angular, HW, Very weak to Weak, Coating; Light brown grey, silty Sand, Soft, NP) White sand sized specks of precipitation	Dry	-41.009655	174.961136	Terminates against SR10		
12	SR	50	123	101	B	Ro3	~150mm	Wide	~99%	1	D	~180°	Gentle		Planar	~2.5m		Clast supported (Rock (~99%), Angular, MW, Very weak to Weak, Coating) No precipitation	Dry	-41.009674	174.961122	Terminates against SR11 and BSH13		
13	FL	47	213	191	C&B	Ro3	~300mm	Very wide	~75%	0	C	~140°	Gentle	~15m	Curved	~7m	~10m	Clast supported (Mosaic (~75%), Angular, HW, Very weak to Weak, Coating; Light and dark brown , sandy Clay, Soft, LP) white tabulated gravel sized clasts of precipitation	Dry	-41.009622	174.961037			
14	SR	73	351	328	C&B	Ro3	~100mm	Wide	~75%	0	C	~140°	Gentle	~2m	Wavy	~8m	~10m	Clast supported (Mosaic (~75%), Angular, HW, Very weak to Weak, Coating; Light brown, silty Clay, Soft, LP) No precipitation	Dry	-41.009627	174.961247	Cross cuts BSH13		
15	SR	85	263	241	C	Ro2	~100mm	Wide	~90%	0	C	~150°	Gentle	~30m	Curved	~7m	~10m	Clast supported (Crackle (~90%), Angular, HW, Weak, Coating; Light brown, silty Clay, Soft, LP) No precipitation	Dry	-41.009558	174.961246	Offsets a number of SR's and follows bedding		
16	BSH	85	295	273	C	Ro2	~150mm	Wide	~90%	0	C	~160°	Gentle	~14m	Wavy	~6m	~3m	Clast supported (Crackle (~90%), Angular, HW-CW, Weak, Coating; Dark brown, Sand and Clay, Soft, LP) No precipitation	Dry	-41.009568	174.961208			
17	SR	45	330	307	C	Ro2	~10mm	Moderately narrow	~99%	1	D	~170°	Gentle	~7m	Curved	~2.5m	~1m	Clast supported (Rock (~99%), Angular, HW-CW, Moderately strong, Coating; Light brown, Silt , Soft, NP)	Dry	-41.009569	174.961191	Terminates against SBSH17		

18	SR	74	268	246	C	Ro2	~5mm	Narrow	~95%	1	D	~100°	Open		Curved	~4m	~1m	No precipitation Clast supported (Crackle (~95%), Angular, MW, Weak, Stained; Light brown, Clay, Soft, LP) White elongated ~3mm thick precipitation	Dry	-41.009489	174.961159	Terminates against SR20	
19	SR	59	205	182	C	Ro3	~100mm	Wide	~90%	1	D	~100°	Open	~2.5m	Wavy	~3m		Clast supported (Crackle (~90%), Angular, HW-CW, Moderately strong, Veneer; Light brown, clayey Silt, Very soft, LP) No precipitation	Dry	-41.009575	174.961139	Terminates against SR20	
20	SR	62	145	123	C	Ro3	~40 to 500mm	Moderately wide to Very wide	~85%	1	D	~180°	Gentle	~12m	Curved	~6m		Clast supported (Crackle (~85%), Angular, HW-CW, Weak, Veneer; Light brown, Clay and Silt, Very soft, MP and NP) No precipitation	Dry	-41.009635	174.961123	Terminates against BSH15	
21	SH	80	239	216	C	Ro3	~400mm thick narrows to 100mm	Wide to Very wide	~75%	0	C	~160°	Gentle	~7m	Wavy	~7m		Clast supported (Mosaic (~75%), Angular, HW, Weak, Veneer; Light brown, silty Sand and Clay, Very soft, NP-LP) No precipitation	Dry	-41.009538	174.96127	Offset by BSH16	
21	SH	80	239	216	C	Ro3	~400mm thick narrows to 100mm	Wide to Very wide	~75%	0	C	~160°	Gentle	~7m	Wavy	~7m		Clast supported (Mosaic (~75%), Angular, HW, Weak, Veneer; Light brown, silty Sand and Clay, Very soft, NP-LP) No precipitation	Dry	-41.009538	174.96127	Offset by BSH16	
22	BSH	70	178	156	C	Ro3	~200 to 300mm	Very wide	~80%	0	C	~160°	Gentle	~4m	Wavy	~6m	~3m	Clast supported (Crackle (~80%), Angular, HW-CW, Weak, Coating; Light brown, Sand and Clay, Soft, NP) No precipitation	Dry	-41.009475	174.961251	Offset a little by a SR	
23	SH	69	325	302	C	Ro3	~20mm	Moderately wide to Moderately narrow	~75%	0	C	~140°	Gentle	~4m	Wavy	~7m		Clast supported (Mosaic (~75%), Angular, HW, Weak, Clean; Light brown, silty Sand and Clay, Very soft, NP) No precipitation	Dry	-41.009469	174.961246	Offset by BSH22 and 16 also cross cuts SR29	
24	SH	68	217	194	C	Ro3	~300mm	Very wide	~75%	0	C	~140°	Gentle	~4m	Wavy	~7m		Clast supported (Mosaic (~75%), Angular, CW, Very weak, Stained; Light brown, silty Sand and Clay, Very soft, NP) No precipitation	Dry	-41.009421	174.961238	BSH22 causes the SR to bend eventually joins up with BSH22	
25	BSH	62	146	124	C	Ro3	~250mm	Very wide	~80%	0	C	~120°	Open	~2.5m	Wavy	~6m	~1.5m	Clast supported (Crackle (~80%), Angular, HW-CW, Weak, Coating; Light brown, Sand and Clay, Soft, NP) No precipitation	Dry	-41.009427	174.961232		
26	SR	76	341	318	C	Ro3	~200mm	Wide to Very wide	~80%	1	D	~160°	Gentle	~4.5m	Wavy	~6m		Clast supported (Crackle (~80%), Angular, HW-CW, Very weak, Stained; Light brown, silty Sand and Clay, Very soft, NP) No precipitation	Dry	-41.009385	174.96128	Cross cuts Bedding	
27	SR	84	253	230	C	Ro3	~200mm	Wide to Very wide	~80%	0	C	~160°	Gentle	~4m	Wavy	~6m		Clast supported (Crackle (~80%), Angular, HW-CW, Very weak, Stained; Light brown, silty Sand and Clay, Very soft, NP) No precipitation	Dry	-41.009414	174.961305	Offset slightly by BSH25	
28	SR	21	39	17	C	Ro3	~50mm	Moderately Wide	~80%	1	D		Gentle		Stepped	~15m		Clast supported (Crackle (~80%), Angular, HW, Very weak, Veneer; Light brown, silty Sand and Clay, Very soft, NP) No precipitation	Dry	-41.009296	174.961391	Transverses almost the entire face	
30	SR	88	191	169	C	Ro2	~50mm	Moderately Wide	~95%	0	C	~130°	Gentle	~30m	Curved	~7m		Clast supported (Crackle (~95%), Angular, HW-MW, Moderately strong, Stained; Light brown, Clay, Very soft, LP) No precipitation	Dry	-41.00955	174.961106	Cross cuts SR17,18 and 28	
31	JN	56	266	244	C	Ro3	~0-1mm	Tight	~95%	2	R	~180°	Gentle		Planar	~1.5m	~0.15m	Clast supported (Crackle (~95%), Angular, MW, Weak, Stained; Light brown, Clay, Very soft, LP) No precipitation	Dry	-41.009539	174.961186		
32	BSH	17	146	124	C	Ro3	~300 to 100mm	Wide to Very wide	~90%	1	D	~145°	Gentle	~4m	Wavy	~3m		Clast supported (Crackle (~90%), Angular, HW, Weak, Veneer; Light and dark brown, silty Clay, Very soft, NP) No precipitation	Dry	-41.009245	174.961378		
33	BSH	41	171	148	C	Ro3	~300 to 100mm	Wide to Very wide	~80%	0	C	~145°	Gentle	~2.5m	Wavy	~10m		Clast supported (Crackle (~80%), Angular, HW, Weak, Veneer; Light and dark brown, silty Sand and Clay, Very soft, LP) White tabulated randomly space gravel clasts of precipitation	Dry	-41.009459	174.961297	Offset slightly by faulting	
34	SR	28	23	0	C	Ro3	~3 to 150mm	Narrow to Wide	~80%	0	C	~180°	Gentle		Planar	~5m		Clast supported (Crackle (~80%), Angular, CW, Weak, Veneer; Light and dark brown, clayey Sand, Very soft, LP) No precipitation	Dry	-41.009234	174.961387	Cross cuts bedding causing offsets	
35	SR	78	209	187	C	Ro3	~150mm	Wide	~80%	0	C	~160°	Gentle	~4m	Wavy	~6m		Clast supported (Crackle (~80%), Angular, CW, Weak, Veneer; Light and dark brown, clayey Sand, Very soft, LP) No precipitation	Dry	-41.0093	174.961324	Cross cuts bedding	
1	SH	48	99	77	C	Ro3	~600mm	Very wide	~80%	0	C	~160°	Gentle	~2m	Curved	~7m		Clast supported (Crackle (~80%), Angular, HW, Weak, Coating; Light brown, silty Clay, Soft, MP) No precipitation	Dry	-41.0093	174.9612	Follows bedding	
2	BSH	44	102	80	C	Ro2	~70mm	Wide	~90%	0	C	~180°	Gentle		Planar	~6.5m	~0.6m	Clast supported (Crackle (~90%), Angular, HW, Weak, Veneer; Brown grey, silty Clay, Soft, MP) No precipitation	Dry	-41.0093	174.9613	Joins up with SH1 and terminates against FL4	
3	SH	48	160	138	C	Ro3	~250mm	Very wide	~95%	1	D	~90°	Open	~5m	Wavy	~3m		Clast supported (Crackle (~95%), Angular, HW, Weak, Coating; Light reddish brown, Sand and Clay, Soft, LP) small sand sized white flecks	Dry	-41.0092	174.9612	Terminates against SH1	
4	FL	42	219	197	C	Ro2	0mm	Tight		0	C	~150°	Gentle	~3m	Wavy	~7m			Dry	-41.0094	174.961	Displacement of ~25cm reverse fault	

C5c.01 SB B2

5	SH	78	318	296	C	Ro3	~100mm	Wide	~80%	0	C	~170°	Gentle	~15m	Wavy	~6m		Clast supported (Crackle (~80%),Angular, MW, Very weak, Stained; Light brownish grey, sandy Silt, Very soft, LP) No precipitation	Dry	-41.0094	174.9612	
6	SR	30	314	292	C	Ro4	~1mm	Very narrow	~99%	1	R	~100°	Open	~2m	Wavy	~1.5m		Clast supported (Rock (~99%),Angular, MW, Weak, Stained) No precipitation	Dry	-41.0094	174.9612	Cross cuts SR7 and terminates against SR2
7	SR	42	216	194	C	Ro2	~2mm	Very narrow to Narrow	~99%	1	D	~120°	Open	~4m	Curved	~1.5m		Clast supported (Rock (~99%),Angular, MW, Weak, Veneer; Grey, silty Sand, Very soft, NP) No precipitation	Dry	-41.0093	174.9612	Cross cuts SR6
8	SR	33	224	202	C	Ro2	~300mm	Very Wide	~95%	1	D	~120°	Open	~1m	Wavy	~3m		Clast supported (Crackle (~95%),Angular, HW, Weak, Veneer; Light brown, silty Clay, Very soft, LP) No precipitation	Dry	-41.0093	174.9612	Terminates against SH1
9	SR	86	298	276	C	Ro4	~200mm	Very Wide to Wide	~80%	0	C	~120°	Open	~15m	Curved	~3m		Clast supported (Crackle (~80%),Angular, HW, Weak, Veneer; Light orangey brown, sandy Silt, Soft, NP) small sand sized white flecks	Damp	-41.0094	174.9612	
10	SR	76	43	21	C	Ro3	~80mm	Wide	~80%	1	R	~180°	Gentle		Planar	~1.5m		Clast supported (Crackle (~80%),Angular, MW, Very weak, Clean; Light grey brown, silty Sand, Very soft, NP) No precipitation	Dry	-41.0094	174.9611	
11	JN	55	355	333	C	Ro2	~1mm	Narrow		2	D	~180°	Gentle	~0.8m	Planar	~1.5m	~0.05m		Dry	-41.0092	174.961	Cross cuts JN12
12	JN	40	224	202	C	Ro2	0mm	Tight		2	D	~180°	Gentle	~0.8m	Planar	~1m	~0.2m		Dry	-41.0093	174.9611	Cross cuts JN11
13	JN	35	306	284	C	Ro2	~1mm	Narrow		2	D	~180°	Gentle	~0.8m	Planar	~2m	~0.1m		Dry	-41.0094	174.9613	Terminates at BSH2
14	SR	86	251	229	C	Ro4	~100mm	Wide	~90%	0	C	~120°	Open	~1m	Wavy	~6m		Clast supported (Crackle (~90%),Angular, MW, Weak, Stained; Light grey brown, silty Sand, Soft, NP) No precipitation	Dry	-41.0094	174.9611	
15	SR	83	234	212	C	Ro2	~6mm	Moderately wide	~99%	1	D	~170°	Gentle	~3m	Wavy	~7m		Clast supported (Rock (~99%),Angular, MW, Moderately strong, Stained) No precipitation	Dry	-41.0093	174.9611	Terminates against SR15
16	SR	52	187	165	C	Ro3	~50mm	Moderately wide	~75%	1	D	~180°	Gentle		Planar	~2.5m	~1m		Dry	-41.0094	174.961	
17	SR	65	230	208	C	Ro2	~1mm	Narrow	~90%	1	D	~170°	Gentle	~15m	Curved	~3m		Matrix supported (Mosaic (~75%),Angular, HW, Weak, Veneer; Light grey brown, Sand and Silt, Soft, MP) No precipitation	Dry	-41.0094	174.961	Terminates at SR15
18	SR	80	304	282	C	Ro2	~300mm	Very wide	~80%	0	C	~180°	Gentle		Planar	~4m	~1.2m		Dry	-41.0094	174.9611	Terminates against SR21
19	SR	88	159	137	C	Ro2	~50mm	Moderately wide	~90%	0	C	~170°	Gentle	~8m	Wavy	~1.5m		Clast supported (Crackle (~90%),Angular, HW, Weak, Veneer; Light brown grey, sandy Silt, Soft, MP) No precipitation	Dry	-41.0094	174.9613	Terminates against SR21
20	FL	48	19	357	C	Ro2	~50mm	Moderately wide	~95%	1	D	~180°	Gentle		Planar	~1.5m		Clast supported (Crackle (~95%),Angular, MW, Weak, Veneer; Dark grey and brown, Sand, Very soft, NP) No precipitation	Dry	-41.0094	174.9611	Terminates in rock
21	SR	66	259	237	C	Ro3	~5mm	Narrow	~40%	0	C		Gentle		Stepped	~7m		Matrix supported (Chaotic (~40%),Angular, HW-CW, Very weak, Coating; Light grey, Sand with traces of gravels and silt, Soft, NP) small sand sized white flecks	Dry	-41.0094	174.9609	
22	FL	84	34	12	C	Ro2	~70mm	Wide	~80%	0	C	~150°	Gentle	~10m	Wavy	~7m		Clast supported (Crackle (~80%),Angular, HW-CW, Very weak, Coating; Light and dark brown grey, Clay, Soft, HP) No precipitation	Dry	-41.0095	174.9611	Approximately 40cm of offset, normal fault
23	FL	65	221	199	C	Ro3	~40mm	Moderately wide	~80%	1	R	~180°	Gentle		Planar	~2.5m		Clast supported (Crackle (~80%),Angular, MW, Weak, Stained; Light grey, Clay, Soft, HP) No precipitation	Dry	-41.0095	174.961	normal offset ~10cm. Offset by FL22
24	FL	60	345	323	C	Ro1	~20mm	Moderately wide	~80%	0	C	~120°	Open	~6m	Wavy	~3m		Clast supported (Crackle (~80%),Angular, MW, Weak, Stained; Light grey, Clay with traces of silt, Very soft, HP) small sand sized white flecks	Dry	-41.0095	174.961	~normal offset. Terminates at FL22
25	FL	75	246	224	C	Ro1	~70mm	Wide	~85%	1	D	~170°	Gentle	~30m	Wavy	~6.5m		Clast supported (Crackle (~85%),Angular, MW, Weak, Clean; Dark grey, sandy Silt, Soft, NP) No precipitation	Dry	-41.0094	174.9608	Joins up with FL30
26	FL	70	28	6	C	Ro2	~40mm	Moderately wide	~80%	0	C	~135°	Gentle	~2m	Wavy	~8m		Clast supported (Crackle (~80%),Angular, MW, Weak, Coating; Dark grey and brown, sandy Silt, Soft, NP) No precipitation	Dry	-41.0097	174.9611	Terminates against FL25
27	BSH	40	168	146	C	Ro2	~70mm	Wide	~85%	1	D		Gentle		Irregular	~1m		Clast supported (Crackle (~85%),Angular, HW, Weak, Veneer; Dark grey, sandy Silt, Soft, NP) No precipitation	Dry	-41.0096	174.9608	Terminates against FL26
28	SR	87	176	154	C	Ro2	0mm	Tight		2	D				Irregular	~2m			Dry	-41.0096	174.9609	Terminates against FL25 and another FL
29	SR	59	148	126	C	Ro3	~70mm	Wide	~80%	1	D				Irregular	~1.5m		Clast supported (Crackle (~80%),Angular, HW, Weak, Veneer; Dark grey, silty Clay, Very soft, LP-NP) No precipitation	Dry	-41.0093	174.9611	Terminates against another FL
30	FL	62	128	106	C	Ro2	~200mm	Very wide to Wide	~80%	1	D	~130°	Gentle	~4m	Wavy	~6m		Clast supported (Crackle (~80%),Angular, HW, Weak, Veneer; Light and dark brown grey, Clay, Soft, HP) No precipitation	Dry	-41.0096	174.961	Joins up with FL25
31	FL	61	229	207	C&B	Ro2	~200mm	Very wide to Wide	~80%	0	C	~180°	Gentle		Planar	~6m		Clast supported (Crackle (~80%),Angular, CW, Very weak, Coating; Dark grey and brown and light grey, Clay seems Sand, Very soft to Soft, HP and NP) small sand sized white flecks	Dry	-41.0096	174.961	
32	BG	41	170	148	B	Ro2				2	R	~180°	Gentle		Planar	~0.3m			Dry	-41.0093	174.9611	

1	BSH	59	129	107	B	Ro2	~200mm	Very wide	~95%	0	C	~150°	Gentle	~4m	Wavy	~5m	~0.6m	Clast supported (Crackle (~95%) Angular, HW, Moderately strong, Coating; Light brown grey and white, Clay and sand, Soft, NP) No precipitation	Dry	-41.010067	174.960653	Cross cuts SR2 and SR3	C5c01 SB B3
1	BSH	68	187	165	B	Ro2	~200mm	Very wide	~95%	0	C	~150°	Gentle	~4m	Wavy	~5m	~0.6m	Clast supported (Crackle (~95%) Angular, HW, Moderately strong to Weak, Coating; Light brown grey, Clay and sand, Soft, NP) No precipitation	Dry	-41.010109	174.960752	Cross cuts SR2, SR3, SR4 and SR5	
2	SR	83	288	266	B	Ro2	~50mm	Moderately wide	~85%	0	C	~170°	Gentle	~5m	Wavy	~4m		Clast supported (Crackle (~85%) Angular, HW to CW, Very weak, Coating; Light brown grey and black, Clay and sand, Soft, NP) No precipitation	Dry	-41.009999	174.960535	Cross cuts BSH1 and SR4	
3	SR	65	292	270	B	Ro3	~30mm	Moderately wide	~90%	0	C	~140°	Gentle	~2m	Wavy	~4.2m		Clast supported (Crackle (~90%) Angular, CW, Very weak, Coating; Light brown grey, Clay and sand, Soft, NP) No precipitation	Dry	-41.010064	174.960704	Cross cuts BSH1, SR4 and SR5	
4	SR	40	22	0	B	Ro4	~30mm	Moderately wide	~80%	0	C	~150°	Gentle	~15m	Wavy	~4m		Clast supported (Crackle (~80%) Angular, CW, Very weak, Coating; Light orangey brown grey, Clay and sand, Soft, NP) No precipitation	Damp	-41.010061	174.960635	Terminates against BSH1 and cross cuts SR3, SR5 and SR2	
5	SR	73	210	188	B	Ro2	~20mm	Moderately wide to Moderately narrow	~70%	0	C		Gentle		Stepped	~4.4m		Matrix supported (Mosaic (~70%) Angular, CW, Weak, Coating; Light grey, Clay with traces of sand, Stiff, LP) No precipitation	Damp	-41.010052	174.960661	Cross cuts SR3, SR4 and BSH1	
6	SR	44	92	70	B	Ro3	~100mm	Wide	~90%	2	D/R	~180°	Gentle		Planar	~2.2m		Clast supported (Crackle (~90%) Angular, HW, Weak, Coating; Light grey brown, Clay and sand, Soft, NP) No precipitation	Dry	-41.009924	174.960546	Terminates against SR4 and BSH8	
7	SR	43	60	38	B	Ro3	~100mm	Wide	~80%	1	D	~135°	Gentle		Curved	~2m	~1m	Clast supported (Crackle (~80%) Angular, CW, Weak, Coating; Light grey brown, Clay and sand, Soft, NP) No precipitation	Damp	-41.009936	174.960666	Cross cuts and terminates against BSH8	
8	BSH	63	186	164	B	Ro3	<200mm	Very wide	~80%	0	C	~140°	Gentle	~10m	Curved	~2m	~0.4m	Clast supported (Crackle (~80%) Angular, HW to CW, Weak, Coating; Light grey brown, Clay and sand, Soft, NP) No precipitation	Damp	-41.009936	174.960665		
8	BSH	66	153	131	B	Ro3	<200mm	Very wide	~80%	0	C	~140°	Gentle	~10m	Curved	~5m	~0.4m	Clast supported (Crackle (~80%) Angular, HW to CW, Weak, Coating; Light grey brown, Clay and sand, Soft, NP) No precipitation	Damp	-41.009891	174.960635	Cross cuts SR9	
8	BSH	89	173	151	B	Ro3	<200mm	Very wide	~80%	0	C	~140°	Gentle	~10m	Curved	~5m	~0.4m	Clast supported (Crackle (~80%) Angular, HW to CW, Weak, Coating; Light grey brown, Clay and sand, Soft, NP) No precipitation	Damp	-41.009907	174.960634	Cross cuts SR9 and SR7	
9	SR	56	31	9	B	Ro3	~100mm	Wide	~90%	1	D	~140°	Gentle		Curved	~3m	~1m	Clast supported (Crackle (~90%) Angular, HW, Weak to Moderately strong, Coating; Light orange brown, Sand, Soft, NP) No precipitation	Dry	-41.009914	174.960737	Cross cuts BSH8, BSH10 and BSH11 and terminates against BSH8	
9	SR	54	235	213	B	Ro3	~100mm	Wide	~90%	1	D	~140°	Gentle		Curved	~3m	~1m	Clast supported (Crackle (~90%) Angular, HW, Weak to Moderately strong, Coating; Light orange brown, Sand, Soft, NP) No precipitation	Dry	-41.009861	174.960606	Cross cuts BSH8, BSH10 and BSH11 and terminates against BSH8	
11	BSH	68	167	145	B	Ro2	~40mm	Moderately wide	~90%	0	C	~150°	Gentle	~1.5m	Wavy	~5m	~0.25m	Clast supported (Crackle (~90%) Angular, HW, Weak, Coating; Light brown grey, Clay and sand, Soft, NP) No precipitation	Dry	-41.009878	174.960645	Cross cuts BSH8 and SR9	
10	BSH	71	92	70	B	Ro2	~300mm	Very wide	~95%	0	C	~135°	Gentle	~2.5m	Wavy	~5m	~0.2m	Clast supported (Crackle (~95%) Angular, HW, Moderately strong to Weak, Coating; Light and dark brown grey, sandy Clay, Soft to Stiff, LP) No precipitation	Dry	-41.009873	174.960733	Cross cuts SR9, SR15 and CZ14	
12	JN	57	279	257	B	Ro3		Tight		2	R	~180°	Gentle		Planar	~0.6m	~0.2m		Dry	-41.009894	174.960611		
13	JN	43	268	246	B	Ro3		Tight		2	R	~180°	Gentle		Planar	~0.6m	~0.1m		Dry	-41.010018	174.960563		
14	CZ	77	206	184	B	Ro3	~30mm	Moderately wide	~80%	0	C	~160°	Gentle	~4m	Wavy	~5m	~1m	Clast supported (Crackle (~80%) Angular, MW, Moderately strong to Weak, Coating; Light and dark brown grey, sandy Clay, Soft to Stiff, LP) No precipitation	Dry	-41.009766	174.960714	Cross cuts BSH10, SR19 and SR15	
15	SR	78	269	247	B	Ro3	~200mm	Wide to Very wide	~80%	0	C	~160°	Gentle	~2m	Wavy	~4m		Clast supported (Crackle (~80%) Angular, HW to MW, Moderately strong to Weak, Coating; Light orange brown, Sand with traces of Clay, Soft, LP) No precipitation	Dry	-41.009785	174.960713	Cross cuts BSH10, SR19 and CZ14	
16	JN	66	289	267	B	Ro3		Tight		2	R	~180°	Gentle		Planar	~0.6m	~0.3m		Dry	-41.009883	174.960703		
16	JN	68	293	271	B	Ro3		Tight		2	R	~180°	Gentle		Planar	~0.6m	~0.3m		Dry	-41.009808	174.960725		
20	JN	56	279	257	B	Ro3		Tight		2	R	~180°	Gentle		Planar	~0.6m	~0.2m		Dry	-41.009748	174.960727		
17	CZ	89	302	280	B	Ro2	~120mm	Wide	~85%	0	C	~150°	Gentle	~4m	Wavy	~4m	~0.6m	Clast supported (Crackle (~85%) Angular, HW to CW, Weak, Coating; Light grey brown, Sand with traces of Clay, Soft, NP - LP) No precipitation	Dry	-41.009795	174.960743	Cross cuts SR30 and BSH21	
18	CZ	75	230	208	B	Ro2	~120mm	Wide	~85%	0	C	~150°	Gentle	~4m	Wavy	~5m	~0.6m	Clast supported (Crackle (~85%) Angular, HW to CW, Weak, Coating; Light grey brown, Sand with traces of Clay, Soft, NP - LP) No precipitation	Dry	-41.009745	174.960727	Cross cuts SR30 and BSH21	
19	CZ	77	205	183	B	Ro3	~30mm to ~200mm	Moderately wide to Very wide	~85%	0	C	~150°	Gentle	~4m	Wavy	~4.5m	~1m	Clast supported (Crackle (~85%) Angular, HW to CW, Weak, Coating; Light grey brown, Sand with traces of Clay, Soft, NP - LP) No precipitation	Dry	-41.009784	174.960816	Cross cuts CZ14 and SR15	
21	BSH	72	151	129	B	Ro2	~200mm	Moderately	~95%	1	D	~150°	Gentle	~4m	Wavy	~5.5m	~0.3m	Clast supported (Crackle (~95%) Angular, HW to CW,	Dry	-41.009763	174.960747	Terminates against CZ17	

21b	BSH	68	210	188	B	Ro2-3	~200mm	wide to Very wide	~95%	1	D	~150°	Gentle	~4m	Wavy	~2.5m	~0.3m	Weak to Very weak, Coating; Light grey brown, clayey Sand, Soft, NP - LP) No precipitation	Dry	-41.009749	174.960793	Terminates against CZ17	SB Central
22	SR	75	163	141	B	Ro2	~20mm	Moderately wide to Moderately narrow	~95%	1	D	~150°	Gentle	~4m	Wavy	~5m		Clast supported (Crackle (~95%) Angular, HW to CW, Weak to Very weak, Coating; Light grey brown, clayey Sand, Soft, NP) No precipitation	Dry	-41.009675	174.960802	Cross cuts SR23, SR28, SR29, SR24 and SR30. Terminates against FL25	
23	SR	89	223	201	B	Ro3	~20mm	Moderately wide to Moderately narrow	~75%	1	D	~160°	Gentle	~3m	Wavy	~4m		Clast supported (Mosaic (~75%) Angular, HW, Very weak, Coating; Light brown, Sand, Stiff, NP) No precipitation	Dry	-41.009732	174.96077	Terminates against FL26 and cross cuts SR30	
24	SR	49	342	320	B	Ro3	~70mm	Wide	~99%	1	D				Irregular	~4m		Clast supported (Rock (~99%) Angular, HW, Weak, Coating; Light brown grey, clayey Sand, Soft, NP) No precipitation	Dry	-41.009682	174.960834	Cross cuts SR28, SR29, FL26 and SR22. Terminates against FL25 and SR30	
25	FL	54	186	164	C&B	Ro3	~120mm	Wide	~95%	0	C	~160°	Gentle	~1m	Wavy	~4m		Clast supported (Crackle (~95%) Angular, HW, Weak, Coating; Light brown grey, clayey Sand, Soft, NP) No precipitation	Dry	-41.009616	174.960905	Cross cuts SR30 and offsets FL26	
26	FL	75	269	247	C&B	Ro4	~70mm	Wide	~90%	1	O	~180°	Gentle		Planar	~5.5m		Clast supported (Crackle (~90%) Angular, HW, Weak, Coating; Light grey brown, silty Sand, Soft, NP) No precipitation	Dry	-41.009615	174.960817	Offset by FL25 and cross cuts SR33, SR30, SR24, SR28, SR29 and SR22	
28	SR	82	251	229	B	Ro4	~10mm	Moderately narrow	~90%	0	C	~160°	Gentle	~1.2m	Wavy	~4m	~0.4m	Clast supported (Crackle (~90%) Angular, HW, Weak, Coating; Light grey brown, Sand with traces of Clay, Soft, NP) No precipitation	Dry	-41.009667	174.9609	Cross cuts SR24, SR22, FL26, SR29 and SR30	
29	SR	72	236	214	B	Ro4	~6mm	Moderately narrow to Narrow	~95%	0	C	~140°	Gentle	~0.8m	Wavy	~4m	~0.4m	Clast supported (Crackle (~95%) Angular, HW to CW, Very weak, Coating; Light grey brown, Sand with traces of Clay, Very soft, NP) No precipitation	Dry	-41.009679	174.960798	Cross cuts SR24, SR22, FL26, SR28 and SR30	
29	SR	77	266	244	B	Ro3	~50mm	Moderately wide	~95%	0	C	~150°	Gentle	~1.4m	Wavy	~2m		Clast supported (Crackle (~95%) Angular, HW, Very weak, Coating; Light brown grey, silty Sand, Soft, NP) No precipitation	Dry	-41.009624	174.960866	Cross cuts SR24, SR22, FL26, SR28 and SR30	
30	SR	16	72	50	C&B	Ro3	~70mm	Wide	~95%	2	D	~170°	Gentle	~4m	Wavy	~15m		Clast supported (Rock (~95%) Angular, HW, Weak, Coating; Light brown grey, clayey Sand, Soft, NP) No precipitation	Dry	-41.009544	174.96091	Terminates against FL32 and SR15. Cross cuts SR31, FL25, FL26, SR27, SR22, SR23, SR28, SR29, SR23, CZ18, CZ17 and BSH21	
31	FL	21	344	322	C	Ro3	~40mm	Moderately wide	~70%	1	D	~180°	Gentle		Planar	~5m		Matrix supported (Mosaic (~70%) Angular, HW to CW, Very weak, Coating; Light blue grey and white grey, clayey Sand and Clay, Stiff, LP) No precipitation	Dry	-41.009523	174.96087	Cross cuts FL32 and SR30. Terminates against FL25	
32	FL	46	170	148	C	Ro3	~60mm	Moderately wide to Wide	~75%	0	C	~180°	Gentle		Planar	~3m	~0.5m	Clast supported (Mosaic (~75%) Angular, HW, Weak, Coating; Light bluish white grey, clayey Sand, Stiff, NP) No precipitation	Dry	-41.009568	174.960813	Cross cuts FL31.	
33	SR	39	97	75	C	Ro4	~55mm	Moderately wide	~80%	2	D				Stepped	~4.5m		Clast supported (Crackle (~80%) Angular, HW, Weak, Coating; Light brown grey, silty Sand, Soft, NP) No precipitation	Dry	-41.009578	174.960817	Terminates against FL25 and FL32. Cross cuts FL26	
34	SR	87	6	344	C	Ro3	~180mm to ~220mm	Wide to Very wide	~80%	1	D	~180°	Gentle		Planar	~3m		Clast supported (Crackle (~80%) Angular, HW and CW, Very weak, Coating; Light white grey and Dark blue grey (Clay), silty Sand and Clay, Stiff and soft, MP) No precipitation	Damp	-41.00953	174.960842	Terminates against another FL	
35	SR	50	115	93	C	Ro3	~65mm	Wide	~80%	2	D	~150°	Gentle	~3m	Curved	~4m		Clast supported (Crackle (~80%) Angular, HW to CW, Weak, Coating; Light grey brown, Clay and sand, Soft, NP) No precipitation	Dry	-41.009509	174.960927	Terminates against SR34	
36	BSH	51	115	93	C	Ro3	~20mm to ~40mm	Moderately wide	~85%	2	D	~150°	Gentle	~2m	Wavy	~2.75 m	~0.3m	Clast supported (Crackle (~85%) Angular, HW, Weak, Coating; Light brown grey, silty Sand, Soft, NP) No precipitation	Dry	-41.009335	174.960997	Cross cuts SR37	
36	BSH	43	106	84	C	Ro3	~20mm to ~40mm	Moderately wide	~85%	2	D	~150°	Gentle	~2m	Wavy	~2.75 m	~0.3m	Clast supported (Crackle (~85%) Angular, HW, Weak, Coating; Light brown grey, silty Sand, Soft, NP) No precipitation	Dry	-41.009332	174.960904	Cross cuts SR37	
37	SR	38	90	68	C	Ro3	~10mm	Moderately narrow	~95%	2	D	~170°	Gentle	~1.5m	Wavy	~2.5m		Clast supported (Crackle (~95%) Angular, HW, Moderately strong to Weak, Coating; Light grey brown, Sand with traces of Clay, Very soft, NP) No precipitation	Dry	-41.009298	174.961054	Cross cuts BSH36	
38	SR	53	93	71	C	Ro3	~15mm	Moderately narrow	~95%	1	D	~180°	Gentle		Planar	~3.5m		Clast supported (Crackle (~95%) Angular, HW, Weak, Coating; Light blue grey, silty Sand, Soft, NP) No precipitation	Dry	-41.009406	174.960909		
38	SR	55	64	42	C	Ro3	~15mm	Moderately narrow	~95%	1	D	~180°	Gentle		Planar	~3.5		Clast supported (Crackle (~95%) Angular, HW, Weak, Coating; Light blue grey, silty Sand, Soft, NP) No precipitation	Dry	-41.00943	174.960978		
1	SR	61	164	142	B	Ro2	~80mm	Wide	~80%	0	C	~180°	Gentle		Planar	~4m		Clast supported (Crackle (~80%) Angular, CW, Weak, Coating; Light orange brown, sandy Clay, Soft, NP) White angular precipitation	Dry	-41.0104	174.9603	Continuous	
2	SR	52	347	325	B	Ro3	~1mm	Very narrow	~80%	1	O	~140°	Gentle	~3m	Curved	~6m		Clast supported (Crackle (~80%) Angular, CW, Weak, Coating; Light orange brown, sandy Clay, Soft, NP) No precipitation	Dry	-41.0104	174.9603	Cross cuts SR3 and BSH5.	

3	SR	31	97	75	B	Ro3	~20mm	Moderately narrow to Moderately wide	~80%	1	O	~140°	Gentle		Planar	~4m		Veneer; Light orange brown, sandy Clay, Soft , NP) White angular precipitation	Dry	-41.0104	174.9603	Terminates against SR1	
4	BSH	65	162	140	B	Ro3	~70mm	Wide	~80%	0	C	~150°	Gentle	~3m	Wavy	~2m	~0.4m	Clast supported (Crackle (~80%)Angular, CW, Weak, Veneer; Light orange brown, sandy Clay, Soft , NP) White angular precipitation	Dry	-41.0104	174.9603	Terminates against SR1 and cross cuts SR2	
5	BSH	56	177	155	B	Ro3	~70mm	Wide	~80%	0	C	~150°	Gentle	~3m	Wavy	~2m	~0.4m	Clast supported (Crackle (~80%)Angular, HW-CW, Very weak, Coating; Dark blue grey, sandy Clay, Stiff, NP) No precipitation	Dry	-41.0104	174.9602	Continuous	
6	JN	77	270	248	B	Ro3	~0mm	Tight		2	R	~135°	Gentle	~1m	Wavy	~0.6m	~0.05m	Clast supported (Crackle (~80%)Angular, HW-CW, Very weak, Coating; Dark blue grey, sandy Clay, Stiff, NP) No precipitation	Dry	-41.0105	174.9603		
7	SR	63	173	151	B	Ro3	~60mm	Moderately wide to Wide	~85%	0	O	~150°	Gentle	~4m	Wavy	~2m		Clast supported (Crackle (~85%)Angular, CW, Weak to Very weak, Coating; Light orange brown, Sand with traces of Clay, Soft, NP)	Dry	-41.0105	174.9602		
8	SR	54	170	148	A	Ro3	~40mm	Moderately wide	~80%	0	O	~180°	Gentle		Planar	~3m		Clast supported (Crackle (~80%)Angular, HW, Weak to Very weak, Coating; Light orange brown, Sand and Clay, Soft , NP and MP) No precipitation	Dry	-41.0106	174.9603	Cross cuts SR10	
9	SR	75	174	152	A	Ro3	~50mm	Moderately wide	~60%	0	O	~170°	Gentle	~10m	Wavy	~3m		Matrix supported (Mosaic (~60%)Angular, CW, Weak, Coating; Light orange brown, Sand and Clay, Soft, NP and MP) No precipitation	Dry	-41.0106	174.9603	Cross cuts SR10	
10	SR	67	147	125	A	Ro3	~100mm	Wide	~95%	1	R	~160°	Gentle	~10m	Wavy	~5m		Clast supported (Crackle (~95%)Angular, HW, Moderately strong to Weak, Coating; Light brown grey, Sand with traces of Clay, Soft, NP) No precipitation	Dry	-41.0106	174.9602	Cross cuts SR9 and SR8	
11	SR	84	325	303	A	Ro4	~40mm	Moderately wide	~80%	0	O	~170°	Gentle	~1.5m	Wavy	~8m		Clast supported (Crackle (~80%)Angular, MW-HW, Moderately strong to Weak, Coating; Orange brown grey, Sand with traces of Clay, Soft, NP) No precipitation	Dry	-41.0105	174.9602	Cross cuts SR12 and BSH13	
12	SR	76	179	157	A	Ro3	~100mm	Wide	~85%	0	C	~135°	Gentle	~6m	Wavy	~12m		Clast supported (Crackle (~85%)Angular, MW-HW, Moderately strong to Weak, Coating; Brown grey, Sand and Clay, Soft, NP and MP) No precipitation	Dry	-41.0106	174.9602	Cross cuts SR11	
13	BSH	51	143	121	A	Ro3	~200mm	Wide to Very wide	~80%	0	O	~150°	Gentle	~6m	Wavy	~15m	~0.7m	Clast supported (Crackle (~80%)Angular, HW-CW, Weak, Coating; Brown grey, silty Sand, Soft, NP) No precipitation	Dry	-41.0106	174.9601	Cross cuts SR11, SR15 and SR16	
13	BSH	28	138	116	A	Ro3	~200mm	Wide to Very wide	~80%	0	O	~135°	Gentle	~6m	Wavy	~15m	~0.7m	Clast supported (Crackle (~80%)Angular, HW-CW, Weak, Coating; Brown grey, silty Sand, Soft, NP) No precipitation	Dry	-41.0107	174.9601	Cross cuts SR11, SR15 and SR16	
14	CZ	47	150	128	A	Ro4	~300mm	Very wide	~80%	0	C	~135°	Gentle	~8m	Wavy	~14m	~0.5m	Clast supported (Crackle (~80%)Angular, HW-CW, Weak to Very weak, Veneer; Light grey brown, Sand and Clay, Soft, NP and MP) No precipitation	Dry	-41.0106	174.9601	Cross cuts SR16, SR15 and SR17	
14	CZ	46	141	119	A	Ro4	~300mm	Very wide	~80%	0	C	~135°	Gentle	~8m	Wavy	~14m	~0.5m	Clast supported (Crackle (~80%)Angular, HW-CW, Weak to Very weak, Veneer; Light grey brown, Sand and Clay, Soft, NP and MP) No precipitation	Dry	-41.0107	174.9603	Cross cuts SR16, SR15 and SR17	
15	SR	83	203	181	A	Ro3	~150mm	Wide	~80%	0	O	~160°	Gentle	~14m	Wavy	~10m		Clast supported (Crackle (~80%)Angular, HW-CW, Moderately strong, Veneer; Light brown grey, silty Clay, Soft, LP) No precipitation	Dry	-41.0106	174.9602	Cross cuts CZ14, SR12, BSH13 and SR16	
16	SR	49	356	334	A	Ro3	~20mm	Moderately narrow to Moderately wide	~90%	0	O	~170°	Gentle	~2m	Wavy	~12m	~1m	Clast supported (Crackle (~90%)Angular, HW, Moderately strong to Weak, Coating; Light grey brown, Sand with traces of Clay, Soft, NP) No precipitation	Dry	-41.0106	174.9602	Cross cuts SR15, SR12, BSH13 and CZ14	
17	SR	80	284	262	A	Ro2	~40mm	Moderately wide	~75%	0	C				Stepped	~8m		Clast supported (Mosaic (~75%)Angular, HW, Weak to Very weak, Coating; Light brown and grey, Sand, Soft, NP) No precipitation	Dry	-41.0107	174.9602	Cross cuts CZ14	
1	SR	71	325	303	B	Ro4	~100mm	Wide	~50%	1	O	~90°	Open	~5m	Wavy	~3.5m		Matrix supported (Chaotic (~50%) Angular, CW, Very weak, Coating; Light orange brown and light grey (Clay), Sand and Clay, Soft, LP) No precipitation	Dry	-41.0102	174.9602	Cross cuts SR4	
2	SR	58	155	133	B	Ro3	~80mm	Wide	~80%	1	D	~150°	Gentle	~2m	Wavy	~2m		Clast supported (Crackle (~80%) Angular, HW to CW, Weak, Coating; Dark grey (Clay) and light white grey (Sand), sandy Clay, Soft, LP) No precipitation	Dry	-41.0103	174.9601	Terminates against SR1	
3	SR	52	161	139	B	Ro3	~80mm	Wide	~80%	1	D	~150°	Gentle	~2m	Wavy	~2.5m	~0.8m	Clast supported (Crackle (~80%) Angular, HW to CW, Weak, Coating; Dark grey (Clay) and light white grey (Sand), sandy Clay, Soft, LP) No precipitation	Dry	-41.0104	174.9603	Cross cuts SR4	
4	SR	50	123	101	B	Ro3	~400mm	Very wide	~80%	1	D	~135°	Gentle	~5m	Wavy	~3m		Clast supported (Crackle (~80%) Angular, HW to CW, Weak, Coating; Dark grey (Clay) and light white grey (Sand), sandy Clay, Stiff, MP) No precipitation	Dry	-41.0104	174.9603	Cross cuts SR1 and SR3	
6	SR	52	155	133	B	Ro3	~80mm	Very wide	~80%	1	D	~135°	Gentle	~5m	Wavy	~1.5m	~0.8m	Clast supported (Crackle (~80%) Angular, HW to CW, Weak, Coating; Dark grey (Clay) and light white grey (Sand), sandy Clay, Stiff, MP) No precipitation	Dry	-41.0104	174.9603	Terminates against SR4	
8	SR	66	177	155	B	Ro3	~200mm	Very wide	~90%	1	D	~135°	Gentle	~5m	Curved	~2m		Clast supported (Crackle (~90%) Angular, HW, Weak,	Dry	-41.0105	174.9602	Terminates against SR15	

10	SR	53	113	91	B	Ro3	~200mm	Very wide	~70%	1	D	~180°	Gentle		Planar	~0.8m	Coating; Light white grey, sandy Clay, Soft, MP) No precipitation Matrix supported (Mosaic (~70%) Angular, CW, Very weak, Coating; Dark blue black and light white grey, sandy Clay, Soft and Stiff (Clay), LP) No precipitation Clast supported (Crackle (~95%) Angular, HW, Weak, Coating; Light blue black and light white grey, silty Clay, Soft, NP) No precipitation	Dry	-41.0105	174.9602	Terminates against SR4 and SR8	C5c01 NB Surt 1
9	SR	56	190	168	B	Ro3	~200mm	Very wide	~95%	1	D	~135°	Gentle		Curved	~1.5m	Clast supported (Crackle (~80%) Angular, HW, Weak and Moderately strong, Veneer; Light blue black and light white grey, sandy Clay, Soft,) No precipitation Clast supported (Crackle (~90%) Angular, HW, Weak and Moderately strong, Coating; Light orange brown , Sand and Clay, Soft, NP) No precipitation Clast supported (Rock (~99%) Angular, HW, Weak, Coating) No precipitation	Dry	-41.0105	174.9602	Terminates against SR11 and SR8	
5	SR	40	66	44	B	Ro3	~10mm	Moderately narrow	~80%	2	D	~170°	Gentle	~4m	Curved	~6m	~1m	Dry	-41.0105	174.9602	Terminates against SR15 and SR ~0.4m above SR4	
7	SR	56	114	92	B	Ro3	~100mm	Wide	~90%	1	D	~150°	Gentle	~4m	Curved	~6m		Dry	-41.0104	174.9603	Terminates against SR15	
16	SR	87	275	253	B	Ro3	~10mm	Moderately narrow	~99%	1	D	~180°	Gentle		Planar	~7m		Dry	-41.0105	174.9602	Cross cuts SR17 and SR15	
18	JN	51	271	249	B	Ro2	~0mm	Tight		2	D	~160°	Gentle	~0.5m	Wavy		~0.1m		-41.0105	174.9601	Cross cuts SR11	
21	SR	59	113	91	A	Ro3	~30mm	Moderately wide	~95%	1	D	~160°	Gentle	~1m	Wavy	~5m		Dry	-41.0106	174.9602	Cross cuts FL20 and SR17. Terminates against SR24	
21	SR	53	123	101	A	Ro3	~30mm	Moderately wide	~95%	1	D	~160°	Gentle	~1m	Wavy	~5m		Dry	-41.0105	174.9601	Cross cuts FL20 and SR17. Terminates against SR24	
20	FL	54	131	109	A&B	Ro3 -2	~150mm	Wide	~65%	0	C	~170°	Gentle	~2m	Wavy	~5m	~1.5m	Dry	-41.0105	174.9601	Cross cuts FL21	
27	SR	67	112	90	A	Ro3 -2	~15mm	Moderately narrow	~95%	1	D	~150°	Gentle	~0.5m	Wavy	~4m		Dry	-41.0106	174.9601	Terminates against BSH25 and cross cuts SR24	
24	SR	89	286	264	A	Ro3 -2	~80mm	Wide	~95%	0	C	~170°	Gentle	~1m	Wavy	~5m		Dry	-41.0106	174.9601	Cross cuts SR27	
20	FL	55	124	102	A	Ro2	~40mm	Moderately wide	~70%	0	C	~180°	Gentle		Planar	~5m	~1.5m	Dry	-41.0107	174.9601	Cross cuts SR21	
22	BSH	72	124	102	B	Ro3	~50mm	Moderately wide	~95%	1	R	~135°	Gentle	~2.5m	Wavy	~2.4m	~1m	Dry	-41.0103	174.9597		
22	BSH	62	140	118	B	Ro3	~60mm	Moderately wide to Wide	~95%	1	R	~135°	Gentle	~3m	Wavy	~2.5m	~1m	Dry	-41.0105	174.9599		
25	BSH	41	135	113	A	Ro3	~50mm	Moderately wide	~95%	0	C	~180°	Gentle		Planar	~6m	~1.5m	Damp	-41.0108	174.96	Cross cuts SR30	
28	SR	32	102	80	A	Ro4	~30mm	Moderately wide	~90%	1	D	~150°	Gentle	~0.7m	Wavy	~3.5m		Dry	-41.0108	174.96	Terminates against BSH25 and cross cuts SR29 and SR30	
26	BSH	37	113	91	A	Ro3	~100mm	Wide	~95%	0	C	~160°	Gentle	~3m	Wavy	~3m	~0.8m	Dry	-41.0108	174.96		
29	SR	87	285	263	A	Ro4	~10mm	Moderately narrow	~95%	1	D	~170°	Gentle	~2.3m	Wavy	~2m		Dry	-41.0107	174.96	Terminates against BSH25 and cross cuts SR28	
30	SR	59	154	132	A	Ro3	~15mm	Moderately narrow	~95%	0	S		Gentle		Irregular	~3m		Dry	-41.0108	174.9602	Terminates against BSH25 and cross cuts SR28	
15	SR	22	50	28	B	Ro3	~10mm	Moderately narrow	~85%	2	D		Gentle		Irregular	~6m		Dry	-41.0106	174.96	Terminates against SR19 and small FL between SR5 and SR15. Cross cuts SR16 and SR17	
15	SR	22	72	50	B	Ro3	~10mm	Moderately narrow	~85%	2	D		Gentle		Irregular	~6m		Dry	-41.0106	174.96	Terminates against SR19 and small FL between SR5 and SR15. Cross cuts SR16 and SR17	
1	SR	63	13	350	E	Ro3	1mm	Very narrow	~95%	0	C	~150°	Gentle	~2m	Wavy	~2.5m		Dry	-41.009529	174.959237	Cross cuts SR2	
2	SR	32	279	257	E	Ro2	100mm	Wide	~80%	0	C	~160°	Gentle		Planar	~12m	~2.5m	Damp	-41.009578	174.959263	Cross cuts SR1, all bedding shears and eventually transitions into SR15	
3	BSH	81	182	159	E	Ro3	120mm	Wide	~95%	0	C	~140°	Gentle	~5m	Wavy	~13m	~0.4m	Damp	-41.009569	174.959253	Cross cuts SR2 and SR11	

4	SR	46	273	251	E	Ro2	150mm	Wide	~95%	0	O	~140°	Gentle	~30m	Curved	~8m		Veneer; Dark brown grey, silty Sand, Soft, LP) No precipitation Clast supported (Crackle(95%) Angular, HW, Weak, Coating; Dark grey, silty Clay, Very soft, MP) No precipitation	Dry	-41.009522	174.959279	Cross cuts BSH5	
5	BSH	54	211	189	E	Ro3	50mm	Moderately wide	~90%	1	D	~160°	Gentle	~2m	Wavy	~1.5m	~1.2m	Clast supported (Crackle(90%) Angular, MW, Weak, Veneer; Dark brown grey, silty Clay trace of sand, Very soft, MP) No precipitation	Dry	-41.009528	174.959265	Terminates against SR4	
6	BSH	64	221	198	E	Ro3	250mm	Very wide	~95%	0	C	~135°	Gentle	~2.5m	Wavy	~8m	~0.6m	Clast supported (Crackle(95%) Angular, MW, Moderately strong, Coating; Dark brown grey, silty Clay, Very soft, MP) No precipitation	Dry	-41.009547	174.959276	Continuous, cross cuts SR2	
6	BSH	68	215	193	E	Ro3	250mm	Very wide	~95%	0	C	~135°	Gentle	~2.5m	Wavy	~8m	~0.6m	Clast supported (Crackle(95%) Angular, MW, Moderately strong, Coating; Dark brown grey, silty Clay, Very soft, MP) No precipitation	Dry	-41.00955	174.959267	Continuous, cross cuts SR2	
7	SR	26	279	256	E	Ro3	60mm	Moderately wide	~90%	1	D				Stepped	~5m		Clast supported (Crackle(90%) Angular, HW, Very weak, Coating; Dark brown grey, silty Clay, Very soft, MP) No precipitation	Dry	-41.009494	174.959205	Terminates against BSH3 and BSH6. Cross cuts BSH9	
8	SR	66	359	336	E	Ro2	3 mm	Narrow	~95%	2	D	~130°	Gentle	~1.5m	Curved	~2m		Clast supported (Crackle(95%) Angular, MW, Moderately strong, Veneer; Dark brown grey, sandy Clay, Very soft, LP) No precipitation	Dry	-41.009539	174.959253	Terminates against SR7 and SR4	
8	SR	66	340	317	E	Ro2	3 mm	Narrow	~95%	2	D	~130°	Gentle	~1.5m	Curved	~2m		Clast supported (Crackle(95%) Angular, MW, Moderately strong, Veneer; Dark brown grey, sandy Clay, Very soft, LP) No precipitation	Dry	-41.009527	174.959267	Terminates against SR7 and SR4	
9	BSH	68	229	206	E	Ro2	200 mm	Very wide	~80%	1	D	~140°	Gentle	~2.5m	Wavy	~4m	~0.4m	Clast supported (Crackle(80%) Angular, MW, Moderately strong, Coating; Dark grey brown, silty Clay trace of sand, Soft, MP) No precipitation	Dry	-41.009541	174.959289	Terminates against a SR just below transition into HW material	
9	BSH	59	214	192	E	Ro2	300 mm	Very wide	~80%	1	D	~140°	Gentle	~2.5m	Wavy	~4m	~0.4m	Clast supported (Crackle(80%) Angular, MW, Moderately strong, Coating; Dark grey brown, silty Clay trace of sand, Soft, MP) No precipitation	Dry	-41.009541	174.959279	Terminates against a SR just below transition into HW material	
10	BSH	75	196	174	E	Ro2	50 mm	Moderately wide	~95%	0	C	~140°	Gentle	~6m	Wavy	~6m	~0.3m	Clast supported (Crackle(95%) Angular, MW, Moderately strong, Coating; Dark grey brown, silty Clay trace of sand, Soft, MP) No precipitation	Dry	-41.009485	174.959109	Cross cuts SR2	
11	SR	72	194	172	E	Ro2	1 mm	Very narrow	~75%	1	D	~150°	Gentle	~3m	Wavy	~8m	~0.8m	Clast supported (Mosaic (75%) Angular, HW, Moderately strong, Coating; Dark grey, Clay, Soft, MP) No precipitation	Damp	-41.009427	174.959329	Cross cuts SR2 and terminates against BSH6	
12	SR	31	352	329	E	Ro2	200 mm	Very wide	~95%	0	C	~150°	Gentle	~3m	Stepped	~1m		Clast supported (Crackle(95%) Angular, MW, Moderately strong, Coating; Dark grey, silty Clay, Very soft, MP) No precipitation		-41.0095	174.9593	Cross cuts SR15	
13	JN	51	45	22	E	Ro3	5 mm	Narrow	~25%	2	D	~180°	Gentle		Planar	~0.5m	~0.2m	Matrix supported (Soil(25%) Angular, MW, Strong, Stained; Dark grey, sandy Clay, Soft, NP) No precipitation	Dry	-41.009479	174.959247		
14	JN	52	72	49	E	Ro2	0mm	Tight		2	D	~180°	Gentle		Planar	~5m	~0.15m		Dry	-41.0095	174.9592		
15	SR	34	34	12	E	Ro3	1 mm	Very narrow	~95%	1	R	~130°	Gentle	~2m	Wavy	~4m		Clast supported (Crackle(95%) Angular, MW, Moderately strong, Veneer; Dark grey, sandy Silt, Soft, NP) No precipitation	Dry	-41.009414	174.959327	Cross cuts BSH12	
1	SR	83	326	303	E	Ro2	0mm	Tight		1	D	~160°	Gentle	~4m	Curved	~2m	~1.5m		Dry	-41.009207	174.959384		
2	SR	33	316	293	E	Ro2	1mm	Very narrow	~95%	1	D	~180°	Gentle		Planar	~3.5m	~1.5m	Clast supported (Crackle (95%) Angular, MW, Moderately strong, Stained; Light brown, clay silty, Very soft, NP) No precipitation	Dry	-41.009261	174.959402	Cross cuts SR3	
4	SR	81	59	36	E	Ro3	50mm	Moderately wide	~95%	0	C	~140°	Gentle	~1m	Wavy	~4m		Clast supported (Crackle (95%) Angular, HW, Very weak, Veneer; Light brown, silty Clay, Very soft, NP) No precipitation	Dry	-41.009266	174.959433	Cross cuts SR2	
5	CZ	35	211	188	E	Ro3	100mm	Wide	~85%	0	C	~150°	Open	~5m	Wavy	~15m	~0.8m - ~1m	Clast supported (Crackle (85%) Angular, HW, Weak, Coating; Dark brown, sandy Clay, Soft to very soft, HP) No precipitation	Dry	-41.009241	174.959379	Offset by SH10	
6	CZ	52	210	188	E	Ro3	100mm	Wide	~85%	0	C	~170°	Open	~5m	Wavy	~15m	~0.8m - ~1m	Clast supported (Crackle (85%) Angular, HW, Weak, Coating; Dark brown, sandy Clay, Soft to very soft, HP) No precipitation	Dry	-41.009227	174.959384	Offset by SH10	
6	CZ	75	54	31	E	Ro3	100mm	Wide	~85%	0	C	~170°	Open	~5m	Wavy	~1.8m		Clast supported (Crackle (85%) Angular, HW, Weak, Coating; Dark brown, sandy Clay, Soft to very soft, HP) No precipitation	Dry	-41.009227	174.959441	Terminates against SH10	
7	BSH	65	216	193	E	Ro3	150mm	Wide	~95%	0	C	~160°	Gentle	~6m	Wavy	~2.5m	~1.8m	Clast supported (Crackle (95%) Angular, HW, Very weak, Coating; Dark reddish brown, silty Sand traces of clay, Soft to very soft, L-NP) No precipitation	Dry	-41.009175	174.959455	Offset by FL12 and terminates against SH10	
7	BSH	84	200	177	E	Ro3	150mm	Wide	~95%	0	C	~160°	Gentle	~6m	Wavy	~2.5m	~1.8m	Clast supported (Crackle (95%) Angular, HW, Very weak, Coating; Dark reddish brown, silty Sand traces of clay, Soft to very soft, L-NP) No precipitation	Dry	-41.00925	174.959584	Offset by FL12 and terminates against SH10	

C5c.01 NB Spur 2

7	BSH	62	220	197	E	Ro3	150mm	Wide	~95%	0	C	~160°	Gentle	~6m	Wavy	~2m	~1.8m	Clast supported (Crackle (95%) Angular, HW, Very weak, Coating; Dark reddish brown, silty Sand traces of clay, Soft to very soft, L-NP) No precipitation	Dry	-41.009164	174.959491	Offset by FL12 and terminates against SH10	C5c.01 NB Spur 3
8	SR	76	246	223	E	Ro3	80 mm	Moderately wide	~99%	1	D	~180°	Gentle		Planar	~3m		Clast supported (Rock (99%) Angular, MW, Moderately strong, Stained; Dark reddish brown, silty Sand traces of clay, Soft to very soft, L-NP) No precipitation	Dry	-41.009091	174.95968	Terminates against SH10	
9	JN	51	74	51	E	Ro2	1mm	Very narrow		1	D	~180°	Gentle		Planar	~0.6m	~0.2m		Dry	-41.009128	174.959593		
9	JN	51	78	56	E	Ro2	1mm	Very narrow		1	D	~180°	Gentle		Planar	~0.6m	~0.15m		Dry	-41.009135	174.959586		
10	SH	41	327	304	E	Ro3	100mm	Wide	~90%	0	C	~180°	Gentle		Planar	~20m		Clast supported (Crackle (90%) Angular, HW, Very weak, Veneer; Light brown, sandy Clay, Soft, LP) No precipitation	Dry	-40.907519	175.001092	Cross cuts Crush Zone and Bedding	
11	BG	63	238	216	E	Ro2	0mm	Tight		0	C	~160°	Gentle	~4m	Wavy	~1m			Dry	-41.009147	174.959553		
12	FL	68	356	333	E	Ro2	30mm	Moderately wide	~95%	1	R		Gentle		Stepped	~8m		Clast supported (Crackle (95%) Angular, HW, Very weak, Veneer; Light brown, sandy Clay, Soft, LP) No precipitation	Dry	-41.009128	174.959583	Terminates against CZ5 and cross cuts bedding	
13	SR	51	181	158	E	Ro3	Open			1	R	~180°	Gentle		Planar	~1m			Dry	-41.009112	174.959623		
1	SR	86	127	105	E	Ro3	~220mm	Very wide	~70%	0	C	~160°	Gentle	~1.5m	Wavy	~4m	~10m	Matrix supported (Mosaic (70%) Angular, CW, Weak to very weak, Coating; Light brown, clayey Sand, Soft, NP) No precipitation	Dry	-41.008917	174.959806	Cross cuts BSH2 and SR3	
2	BSH	66	228	206	E	Ro3	~200mm	Very wide	~85%	0	C	~150°	Gentle	~15m	Wavy	~10m	~0.5m	Clast supported (Crackle (85%) Angular, HW, Weak, Coating; Light grey brown, clayey Sand, Soft, NP) No precipitation	Dry	-41.008962	174.959828	Cross cuts SR3 and SR1	
3	SR	57	001	338	E	Ro3	15mm	Moderately narrow	~90%	0	C	~170°	Gentle	~5m	Stepped	~4m	~1.2m	Clast supported (Crackle (90%) Angular, HW, Weak, Coating; Light grey brown, clayey Sand, Soft, NP) No precipitation	Dry	-41.008868	174.959836	Cross cuts SR1 and BSH2	
4	BSH	64	265	242	E	Ro3	~180mm	Wide	~90%	0	C	~160°	Gentle	~1m	Wavy	~15m	~0.5m	Clast supported (Crackle (90%) Angular, HW, Moderately strong, Coating; Light grey brown, clayey Sand, Soft, NP) No precipitation	Dry	-41.008898	174.959817	Continuous	
4	BSH	79	187	165	E	Ro3	~200mm	Very wide	~90%	0	C	~160°	Gentle	~1m	Wavy	~15m	~0.5m	Clast supported (Crackle (90%) Angular, HW, Moderately strong, Coating; Light grey brown, clayey Sand, Soft, NP) No precipitation	Dry	-41.008784	174.959869	Cross cuts SR5	
5	SR	74	356	333	E	Ro3	50mm	Moderately wide	~75%	0	C	~140°	Gentle	~2m	Wavy	~3m	~1.5m	Clast supported (Mosaic (75%) Angular, CW, Moderately strong, Coating; Light grey brown and grey, clayey Sand, Stiff to firm, NP) No precipitation	Dry	-41.008731	174.95989	Terminates against SR parallel to SR11 (~1.5m above). Cross cuts SR10 and BSH4	
6	JN	43	079	057	E	-	0mm	Tight		2	D	~180°	Gentle		Planar	~0.8m	~0.2m		Dry	-41.008653	174.959931		
7	SR	73	090	068	E	Ro3	200-300mm	Very wide	~85%	0	C	~160°	Gentle	~5m	Wavy	~4m	~2m	Clast supported (Crackle (85%) Angular, CW, Very weak, Veneer; Light grey brown and grey, clayey Sand, Stiff to firm, NP) White sand sized specks of precipitation	Dry	-41.008639	174.959899	Terminates against SH10	
8	SR	30	336	314	E	Ro4	10mm	Moderately narrow	~95%	1	D	~170°	Gentle	~4m	Wavy	~5m	~1.5m	Clast supported (Crackle (95%) Angular, HW, Weak, Coating; Light grey brown, clayey Sand, Soft, NP) No precipitation	Dry	-41.008669	174.959846	Terminates against a SR in the centre of the cut. Cross cuts SH10 and BSH4	
9	SR	84	339	317	E	Ro4	1mm	Very narrow	~95%	0	C	~150°	Gentle	~1.3m	Irregular	~5m		Clast supported (Crackle (95%) Angular, HW, Weak, Coating; Light grey brown, clayey Sand, Soft, NP) No precipitation	Dry	-41.008705	174.959948		
10	SH	51	357	335	E	Ro3	~300mm	Very wide	~95%	1	R	~150°	Gentle	~2m	Wavy	~6m		Clast supported (Crackle (95%) Angular, HW, Weak, Coating; Light grey white, sandy Clay, Soft, NP) White sand sized specks of precipitation	Dry	-41.008535	174.959901	Terminates against a SR that is ~1.5m above and parallel to SR7. Cross cuts SR8 and SR5	
11	SR	83	239	217	E	Ro3	~30mm	Moderately wide	~90%	1	D	~160°	Gentle	~8m	Wavy	~3m	~1.5m	Clast supported (Crackle (90%) Angular, HW, Weak, Coating; Light grey white, sandy Clay, Stiff, NP) No precipitation	Dry	-41.008673	174.959923	Terminates against SR that splays off from SR9	
12	SR	82	222	199	E	Ro3	~150mm	Wide	~99%	0	C	~160°	Gentle	~1.5m	Wavy	~10m	~0.3m	Clast supported (Rock (99%) Angular, MW to HW, Moderately strong to strong, Coating; Light grey white, sandy Clay, Stiff, NP) No precipitation	Dry	-41.008642	174.959913	Continuous and cross cuts SR9 and SR7	
1	SR	28	108	086	E	Ro2	200mm	Very wide	~90%	0	C	~160°	Gentle	~20m	Curved	~6m		Clast supported (Crackle (~90%) Angular, HW, Weak, Coating; Light brown, clayey Sand, Soft, NP) No precipitation	Dry	-41.008443	174.959983	Cross cuts CZ2, SR3 and SR6	C5c.01 NB Spur 4
2	CZ	42	293	270	E	Ro3	300mm	Very wide	~70%	0	C	~170°	Gentle	~3m	Wavy	~6m		Matrix supported (Mosaic (~70%) Angular, CW, Very weak, Coating; Light orange brown, clayey Sand, Soft to Firm, NP) No precipitation	Dry	-41.008379	174.96003	Cuts through SR1	
3	SR	57	1	338	E	Ro3	20mm	Moderately narrow	~80%	0	D	~180°	Gentle		Planar	~4m		Clast supported (Crackle (~80%) Angular, CW, Weak, Coating; Light brown, clayey Sand, Soft, NP) No precipitation	Dry	-41.008379	174.96003	Terminates against CZ2	
4	BSH	48	203	181	E	Ro3	2mm	Very Narrow		0	D	~160°	Gentle	~1.5m	Wavy	~2.5m	~0.8m		Dry	-41.008401	174.959954	Terminates against CZ2	
5	BSH	44	192	170	E	Ro2	3mm	Narrow		0	D	~160°	Gentle	~1.5m	Wavy	~2m	~0.8m		Dry	-41.008444	174.960019	Terminates against CZ2	
6	CZ	54	339	316	E	Ro2	1mm	Very Narrow		1	D	~160°	Gentle	~3m	Wavy	~4m			Dry	-41.008436	174.960012	Terminates against CZ2 and cuts SR1 and SR3	
7	SR	37	259	237	E	Ro3	200mm	Very wide	~75%	0	D	~160°	Gentle	~2m	Wavy	~3m		Clast supported (Mosaic (~75%) Angular, CW, Very weak, Coating; Light brown, clayey Sand, Firm, NP) No precipitation	Dry	-41.008365	174.960023	Terminates against shear	

8	SR	32	233	211	E	Ro2	150mm	Wide	~80%	0	S	~120°	Open	~8m	Curved	~6m		Clast supported (Crackle (~80%) Angular, CW, Weak, Coating; Light brown, clayey Sand, Very soft, NP) No precipitation	Dry	-41.008308	174.960055	Cross cuts SR9 and SR11	C5c.02 NB B2
9	SR	89	119	97	E	Ro2	3mm	Narrow		1	D	~180°	Gentle		Planar	~4m			Dry	-41.008307	174.96022	Cross cuts SR8 and terminates against SR11	
10	SR	54	339	317	E	Ro3	10mm	Moderately narrow	~75%	0	D	~120°	Open	~2.5m	Wavy	~1.5m	~1.5m	Clast supported (Mosaic (~75%) Angular, CW, Very weak, Coating; Light brown, clayey Sand, Stiff to firm, NP) No precipitation	Dry	-41.008192	174.960095	Terminates against SR8	
11	SH	42	218	195	E	Ro3	600mm	Very wide	~90%	0	D	~120°	Open	~7m	Wavy	~2.5m	~1.5m	Clast supported (Crackle (~90%) Angular, CW, Weak, Coating; Light brown, clayey Sand, Soft, NP) No precipitation	Dry	-41.008202	174.960079	Cross cuts SR9 and SR8	
12	SR	85	67	44	E	Ro3	300mm	Very wide	~80%	1	D	~100°	Open	~3m	Wavy	~1m		Clast supported (Crackle (~80%) Angular, CW, Weak, Coating; Light brown, clayey Sand, Soft, NP) No precipitation	Dry	-41.008306	174.960053	Terminates against SR8	
31	SR	80	81	103	D	Ro3	40mm	Moderately wide	~95%	0	C	~160°	Gentle	~1.5m	Wavy	~6m		Clast supported (Crackle (~95%) Angular, HW, Weak, Coating; Light orange grey, silty Sand, Soft, NP) No precipitation	Dry	-41.0105	174.9589	Cross cuts SR27 and SR28	
30	SR	54	202	224	D	Ro4	80mm	Wide	~90%	0	C	~150°	Gentle	~20m	Curved	~6m		Clast supported (Crackle (~90%) Angular, HW, Weak, Coating; Light orange grey, silty Sand, Soft, NP) No precipitation	Dry	-41.0104	174.9589	Cross cuts SR26 and SR29	
29	SR	57	13	35	D	Ro3	80mm	Wide	~90%	0	C	~150°	Gentle	~2.5m	Wavy	~6.5m		Clast supported (Crackle (~90%) Angular, HW, Very weak, Coating; Light orange grey, silty Sand, Soft, NP) No precipitation	Dry	-41.0104	174.9589	Cross cuts SR30, SR26 and SR28	
28	SR	32	221	243	D	Ro3	60mm	Wide - Moderately wide	~80%	0	C	~160°	Gentle	~2m	Irregular	~7m		Clast supported (Crackle (~80%) Angular, CW-HW, Very weak, Coating; Light orange grey, silty Sand, Soft, NP) No precipitation	Dry	-41.0105	174.9589	Cross cuts SR29, SR27 and SR31	
27	SR	72	10	32	D	Ro3	40mm	Moderately wide	~95%	0	O	~180°	Gentle		Planar	~3.4m		Clast supported (Crackle (~95%) Angular, HW, Weak, Coating; Greyish brown, sandy Silt, Soft, NP) white angular tabulated gravel sized clasts	Dry	-41.0104	174.959	Cross cuts SR26, SR28 and SR31	
26	SR	17	240	262	D	Ro3	15mm	Moderately narrow	~95%	2	D	~170°	Gentle	~1m	Irregular	~3.5m		Clast supported (Crackle (~95%) Angular, HW, Weak, Coating; Greyish brown, sandy Silt, Soft, NP) white angular tabulated gravel sized clasts	Dry	-41.0104	174.9589	Terminates against SR31 and SR25. Cross cuts SR27, SR29 and SR30	
25	SR	86	40	62	E&D	Ro3	400mm	Very Wide	~80%	0	C	~170°	Gentle	~5m	Wavy	~6m		Clast supported (Crackle (~80%) Angular, HW, Very weak, Coating; Dark grey black, sandy Clay, soft, NP) No precipitation	Dry	-41.0104	174.959	Continuous	
25	SR	86	50	72	E	Ro3	400mm	Very Wide	~80%	0	C	~170°	Gentle	~5m	Wavy	~6m		Clast supported (Crackle (~80%) Angular, HW, Very weak, Coating; Dark grey black, sandy Clay, soft, NP) No precipitation	Dry	-41.0104	174.959	Continuous	
24	SR	78	358	20	E	Ro3	80mm	Wide	~85%	1	S	~150°	Gentle	~3m	Curved	~6.5m		Clast supported (Crackle (~85%) Angular, HW, Very weak, Stained; Light brown grey, silty Sand, Soft, NP) No precipitation	Dry	-41.0104	174.9588	Cross cuts SR21 and splits into 3 shears. Terminates against SR25	
23	SR	82	69	91	E	Ro3	50mm	Moderately wide	~95%	0	D	~150°	Gentle	~10m	Curved	~6.5m		Clast supported (Crackle (~95%) Angular, HW, Weak, Stained; Light brown grey, sandy Silt soft, NP) No precipitation	Dry	-41.0103	174.959	Offset by SH18. Cross cut buy BSH20	
22	SR	84	352	374	E	Ro4	100mm	Wide	~80%	1	D	~135°	Gentle	~20m	Curved	~3.5m		Clast supported (Crackle (~80%) Angular, CW, Very weak, Veneer; light brown grey, silty Sand, Soft, NP) No precipitation	Dry	-41.0101	174.9591	Terminates against SH18. Cross cuts SR19, SH8 and SR13	
21	SR	26	233	255	E	Ro3	200mm	Wide	~80%	2	D	~170°	Gentle	~6m	Curved	~2m		Clast supported (Crackle (~80%) Angular, CW, Very weak, Veneer; light brown grey, silty Sand, Soft, NP) No precipitation	Dry	-41.0104	174.959	Terminates against SR25 and SR24	
20	BSH	58	194	216	E	Ro2	40mm	Moderately wide	~95%	0	C	~160°	Gentle	~5m	Wavy	~5.4m	~0.6m	Clast supported (Crackle (~95%) Angular, MW, Weak, Veneer; Grey brown, silty Sand with traces of clay, Soft, NP) white gravel angular clasts	Dry	-41.0103	174.959	Cross cuts SH8, SH18 and SR23.	
19	SR	89	66	88	E	Ro3-4	70mm	Wide	~99%	1	D	~160°	Gentle	~7m	Wavy	~4m		Clast supported (Crackle (~99%) Angular, MW, Weak, Veneer; Grey brown, silty Clay, Soft, NP) No precipitation	Dry	-41.0102	174.9591	Cross cuts SR22, SH8 and SR13. Terminates against SH18	
18	SH	25	259	281	E	Ro3-4	300mm	Very Wide	~85%	1	D	~170°	Gentle	~15m	Wavy	~8m	~0.25m	Clast supported (Crackle (~85%) Angular, CW, Very weak, Veneer; light brown grey, silty Sand, Soft, NP) No precipitation	Dry	-41.0103	174.959	Terminates against SR24 and joins up with SH8. Cross cuts SR13, SR16, BSH20 and SR23	
17	SR	86	247	269	E	Ro3	150mm	Wide	~50%	2	D	~160°	Gentle	~10m	Curved	~2m		Matrix supported (Chaotic (~50%) Angular, CW, Very weak, Coating; Light grey brown, clayey Sand, very soft, NP) No precipitation	Damp	-41.0101	174.9591	Terminates against SH18 and SR16	
16	SR	61	206	228	E	Ro2	120mm	Wide	~90%	0	C	~180°	Gentle		Planar	~7m	~0.5m	Clast supported (Crackle (~90%) Angular, HW, Very weak, Coating; Light grey brown, clayey Sand, NP) No precipitation	Damp	-41.0102	174.9591	Cross cuts SH18, SR13 and SH8	
15	SR	44	168	190	E	Ro3	80mm	Wide	~99%	1	D	~160°	Gentle	~0.8m	Wavy	~0.8m		Clast supported (Rock (~99%) Angular, HW, Very weak, Stained; Light grey brown, clayey Sand, soft, NP) No precipitation	Dry	-41.0101	174.9591	Very little soil. Cross cuts SR9 and terminates against SR13	
14	SR	84	153	175	E	Ro2	100mm	Wide	~90%	1	D	~100°	Open	~2m	Wavy	~1.4m		Clast supported (Crackle (~80%) Angular, HW, Very weak, Coating; Light grey brown, clayey Sand, NP) no	Dry	-41.0101	174.9591	Cross cuts SR9 and terminates against SR10	

13	SR	53	314	336	E	Ro2	200mm	Wide	~80%	0	C	~100°	Open	~40m	Curved	~7.5m		visible precipitation Clast supported (Crackle (~80%) Angular, HW, Weak, Veneer; Light grey brown, sandy Clay, soft, NP) White sand to gravel sized, angular tabulated clasts	Dry	-41.0101	174.9591	Cross cuts SR19, SR22, SH8, SR16, SH18 and SR9
12	SR	76	43	65	E	Ro3	100mm	Wide	~80%	2	D	~180°	Gentle		Planar	~1.4m	~0.3m	Clast supported (Crackle (~80%) Angular, HW, Weak, Veneer; Light grey brown, sandy Clay, soft, LP) No precipitation	Damp	-41.0101	174.9591	Terminates against SH8 and the SR that offsets BSH11. Cross cuts BSH11
11	BSH	83	238	260	E	Ro2	100mm	Wide	~80%	1	C	~160°	Gentle	~3m	Wavy	~3m	~0.4m	Clast supported (Crackle (~80%) Angular, HW, Weak, Veneer; Light grey brown, sandy Clay, soft, LP) No precipitation	Damp	-41.01	174.9592	Cross cuts SR12. Terminates against SH8. Potentially offset however continuity is not visible
10	SR	60	204	226	E	Ro3	100mm	Wide	~80%	1	D	~170°	Gentle	~6m	Wavy	~6.5m	~0.5m	Clast supported (Crackle (~80%) Angular, HW, Weak, Veneer; Light grey brown, sandy Clay, soft, LP) No precipitation	Damp	-41.0101	174.9592	Cross cuts SH18 and terminates against SH8
10	SR	56	174	196	E	Ro2	100mm	Wide	~80%	0	C	~170°	Gentle	~6m	Wavy	~7m		Clast supported (Crackle (~80%) Angular, HW, Weak, Veneer; Light grey brown, sandy Clay, soft, LP) No precipitation	Damp	-41.0102	174.9591	Cross cuts SH8 and SR9
9	SR	52	271	293	E	Ro3	4mm	Narrow	~95%	2	D	~170°	Gentle	~2m	Curved	~5m		Clast supported (Crackle (~95%) Angular, HW-CW, Very weak, Veneer; light brown grey, silty Clay with traces of sand, Soft, NP)	Dry	-41.0101	174.9591	Cross cuts SR10, SR13, SR15 and SR14. Terminates between SR10 and SH8
8	SR	89	316	338	E	Ro2	300mm	Very Wide	~85%	0	C	~170°	Gentle	~5m	Wavy	~10m		Clast supported (Crackle (~85%) Angular, HW-CW, Very weak, Veneer; light brown grey, silty Clay with traces of sand, Soft, NP)	Dry	-41.01	174.9592	Cross cuts BSH20, SR19, SR22, SR13 and SR16
7	SR	60	4	26	E	Ro2	30mm	Moderately wide	~98%	2	D	~170°	Gentle	~0.8m	Wavy	~1m		Clast supported (Crackle (~98%) Angular, HW, Weak, Veneer; Light brown grey, soft, NP)	Dry	-41.0101	174.9592	Terminates between SR6 and SH8
6	SR	70	359	21	E	Ro2	60mm	Moderately wide - wide	~95%	1	S	~90°	Open		Irregular	~3m		Clast supported (Crackle (~95%) Angular, HW, Weak, Veneer; Light brown grey, sandy Silt, soft, NP) No precipitation	Dry	-41.01	174.9591	Splits and terminates against SH8 and cross cuts SH1
5	SR	69	132	154	E	Ro4	20mm	Moderately narrow	~95%	1	D	~180°	Gentle		Planar	~0.8m		Clast supported (Crackle (~95%) Angular, HW, Weak, Coating; Light brown grey, sandy Silt, Soft, NP) Sand sized white clasts	Dry	-41.0101	174.9592	Terminates against SH8
4	BSH	87	245	267	E	Ro4	100mm	Wide	~95%	1	D	~160°	Gentle	~4m	Wavy	~4m	~0.4m	Clast supported (Crackle (~95%) Angular, HW, Weak, Coating; Light brown, sandy Silt, Soft, NP) No precipitation	Dry	-41.01	174.9592	Terminates against SH1
3	SR	65	124	146	E	Ro3	100mm	Wide	~90%	0	O	~100°	Open	~6m	Curved	~2.5m		Clast supported (Crackle (~90%) Angular, HW-MW, Weak, Coating; Light grey, Clay with trace of sand, Soft, NP) No precipitation	Dry	-41.01	174.9592	Cross cuts BSH4
2	SR	41	354	16	E	Ro2	100mm	Wide	~90%	0	O	~180°	Gentle		Planar	~1.4m		Clast supported (Crackle (~90%) Angular, HW, Weak, Coating; Light brown orangey grey, Sand with traces of clay, Soft, NP) Sand sized white specks	Dry	-41.0099	174.9592	Continuous
1	SH	86	65	87	E	Ro4	200mm	Wide - Very wide	~80%	0	C	~170°	Gentle	~1.5m	Wavy	~4m		Clast supported (Crackle (~80%) Angular, HW, Weak to very weak, Veneer; Brown orangey grey, Sand with traces of clay, Soft, NP) Sand sized white specks	Dry	-41.0101	174.9591	Cross cuts BSH4 and SR6

A.4 Transmission Gully North Graphs

Defect and rock mass results from Transmission Gully North. Results are presented in graphs. Where percentages are used they display the respective occurrence of the dependent variable assessed.

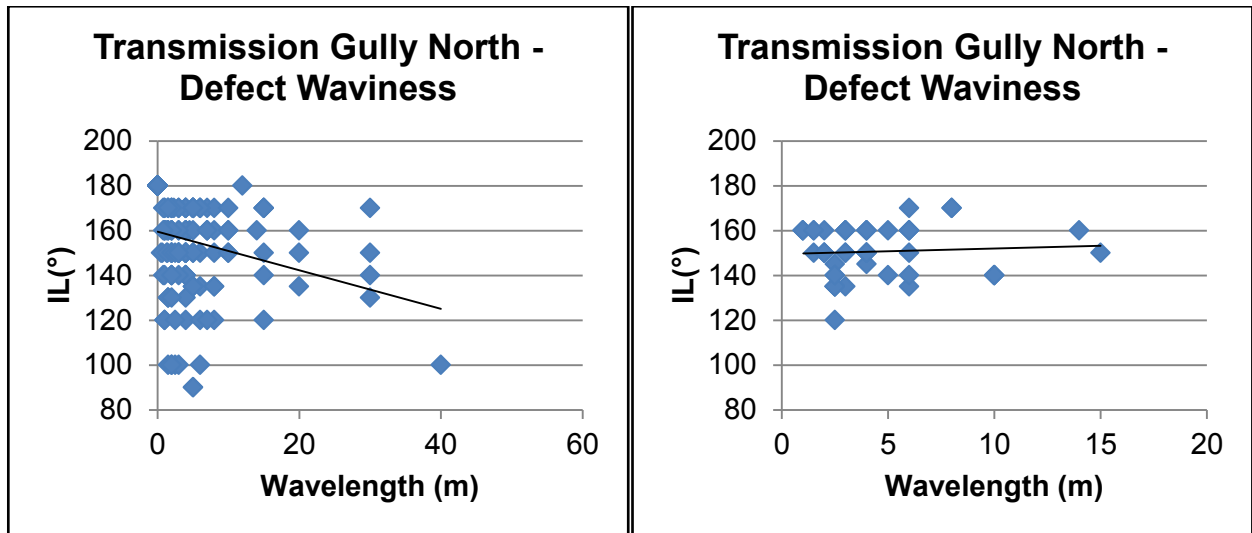
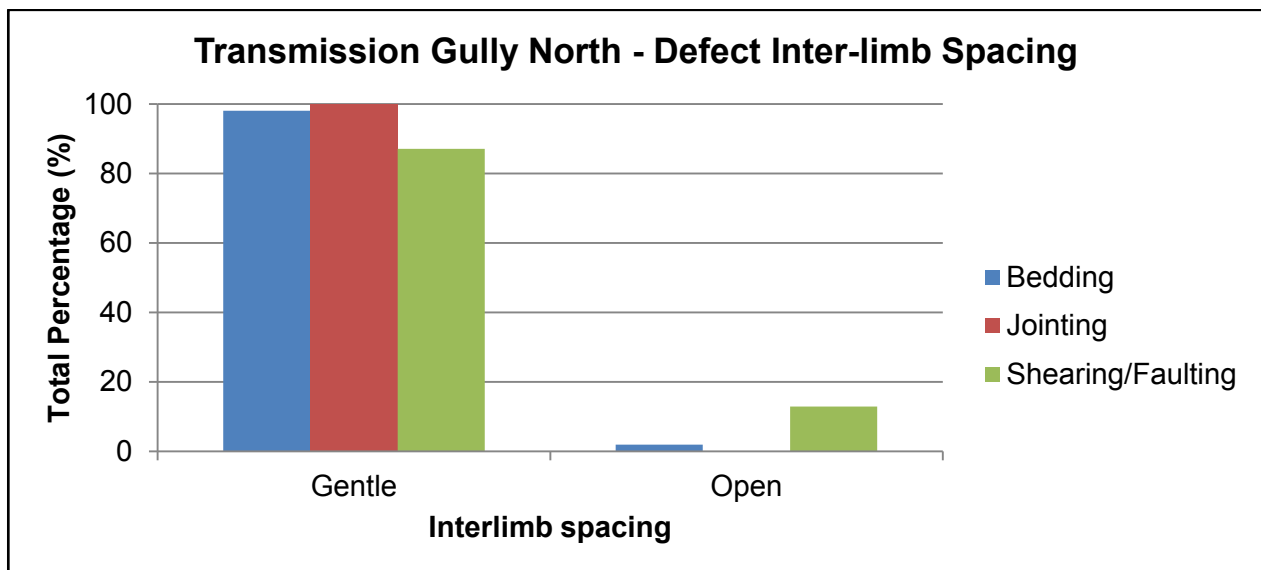
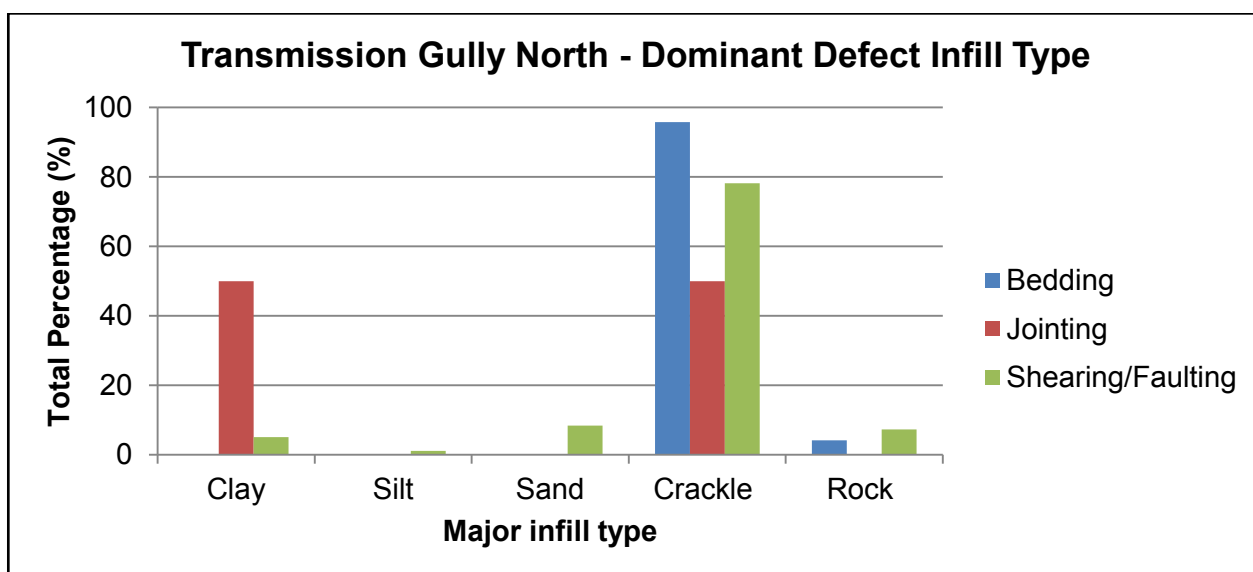
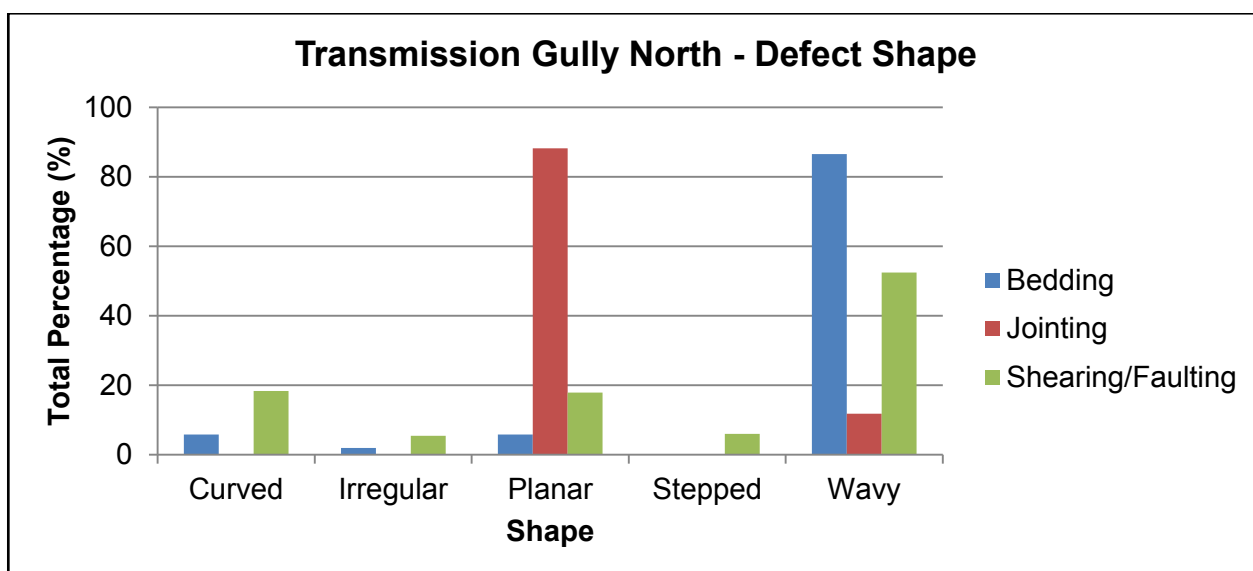
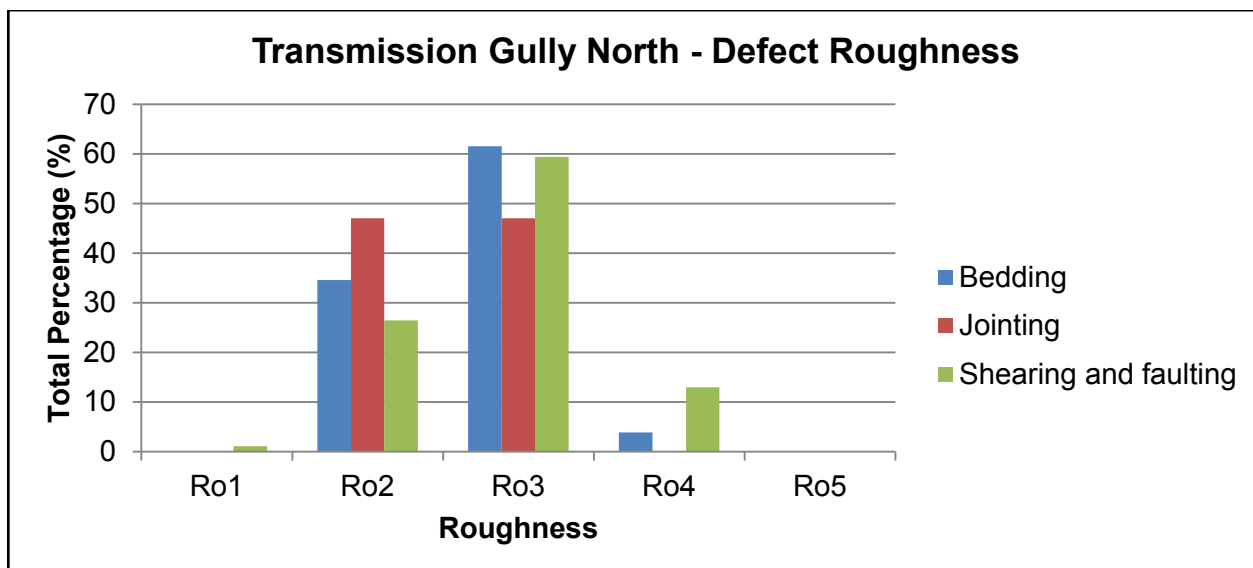
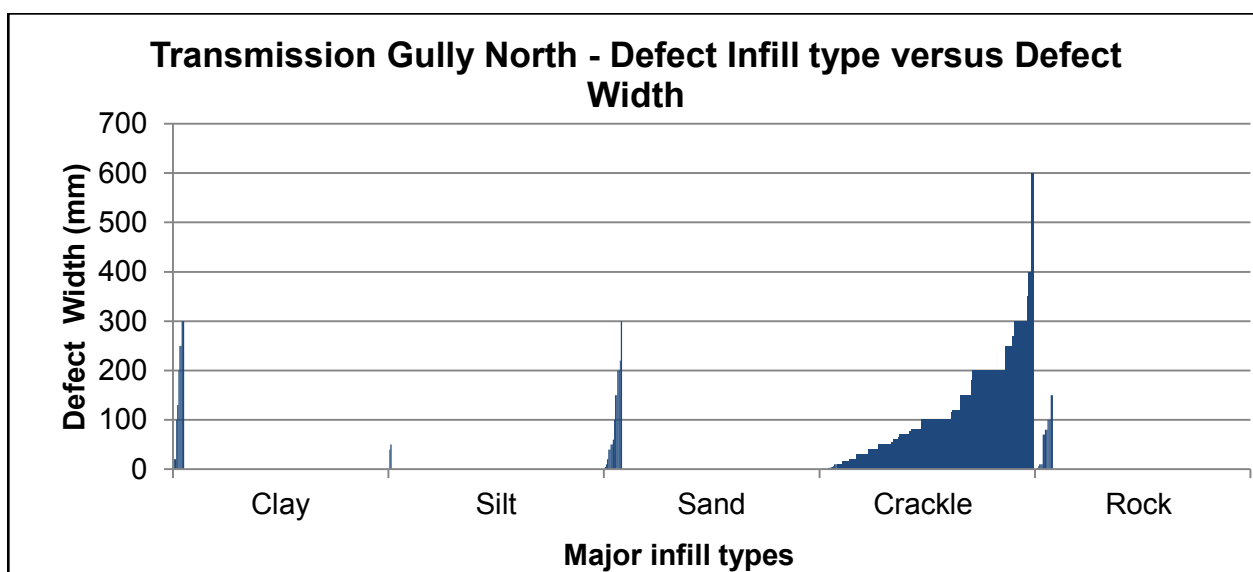
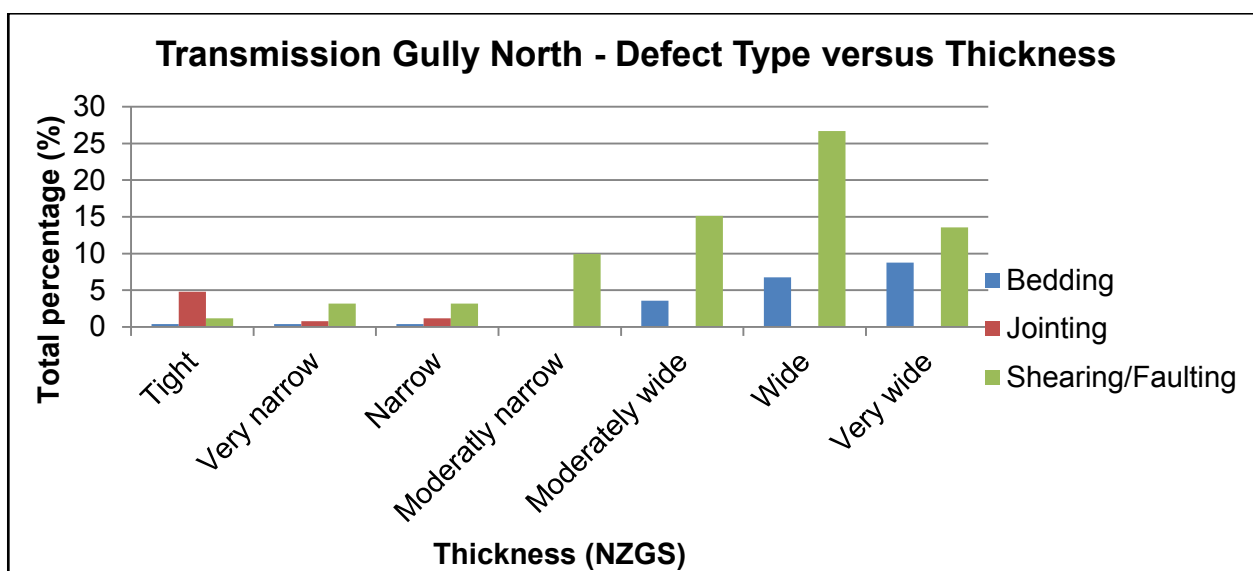
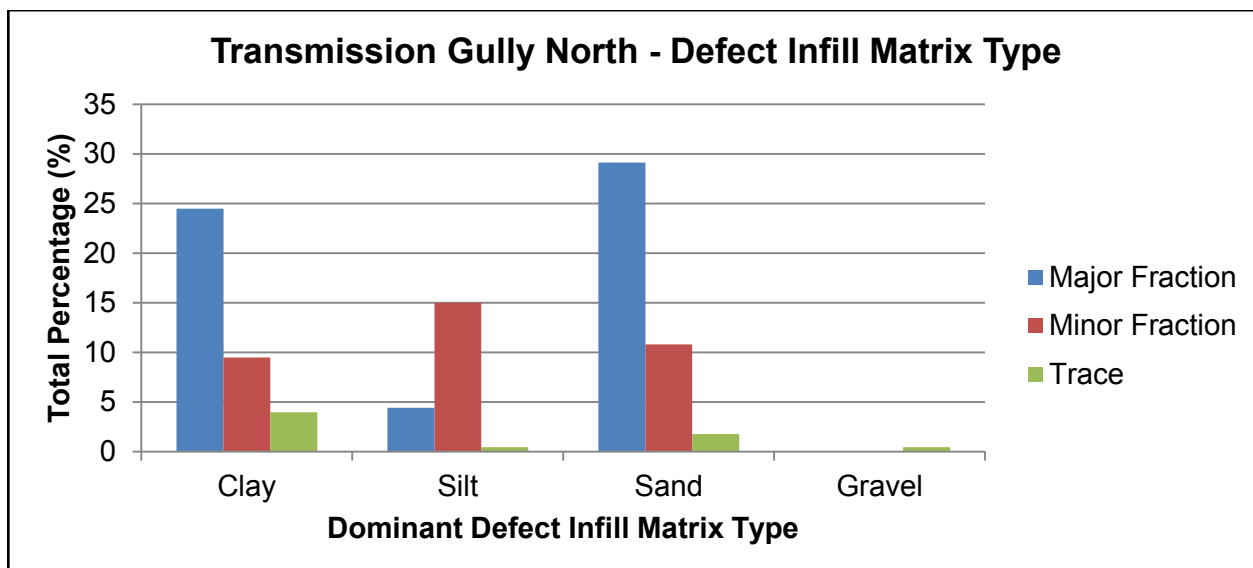
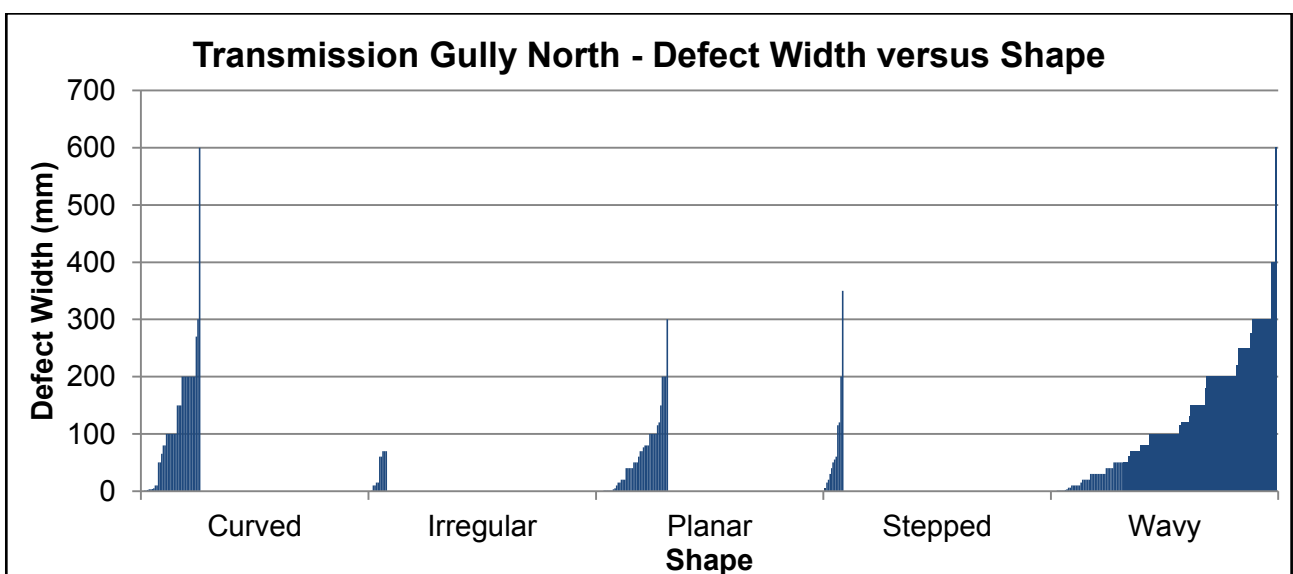
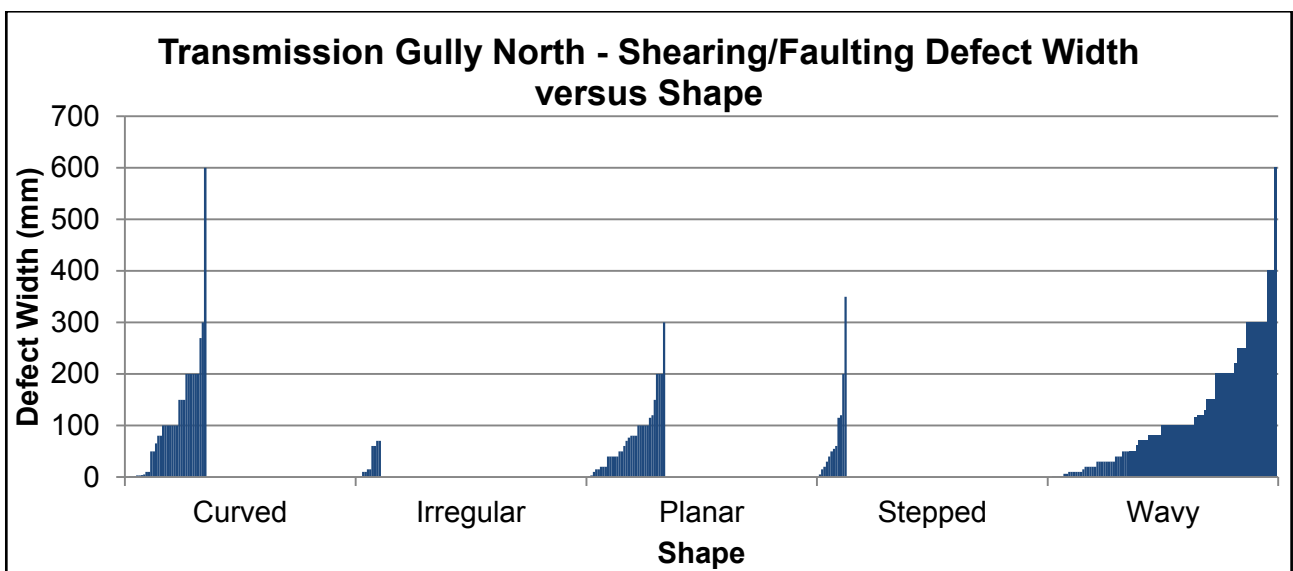
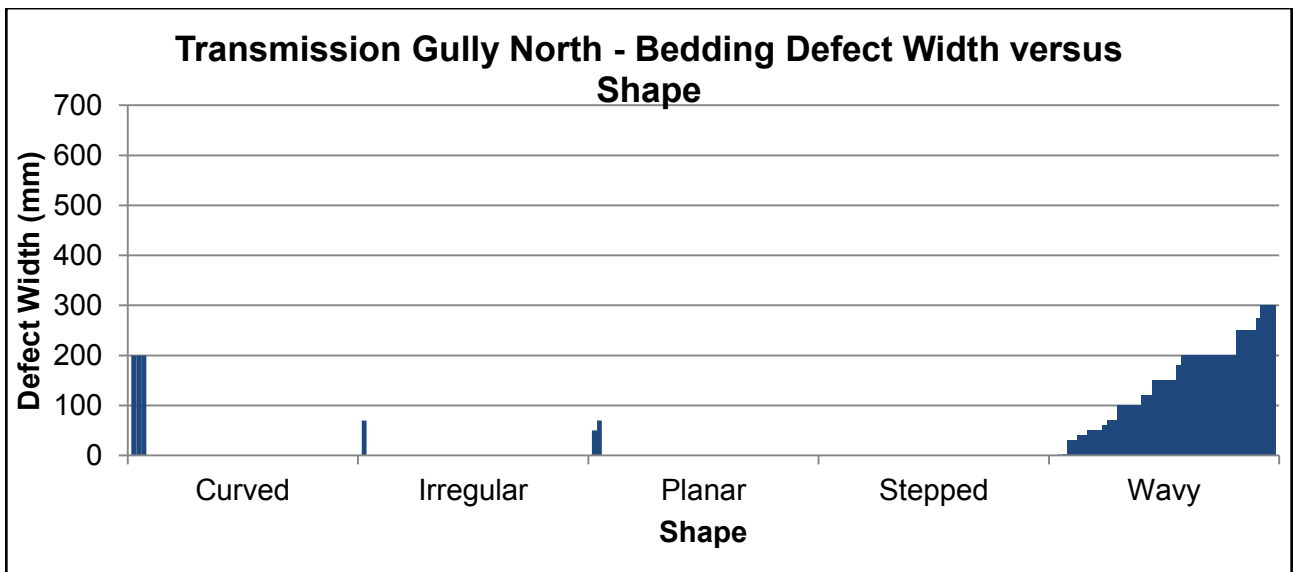


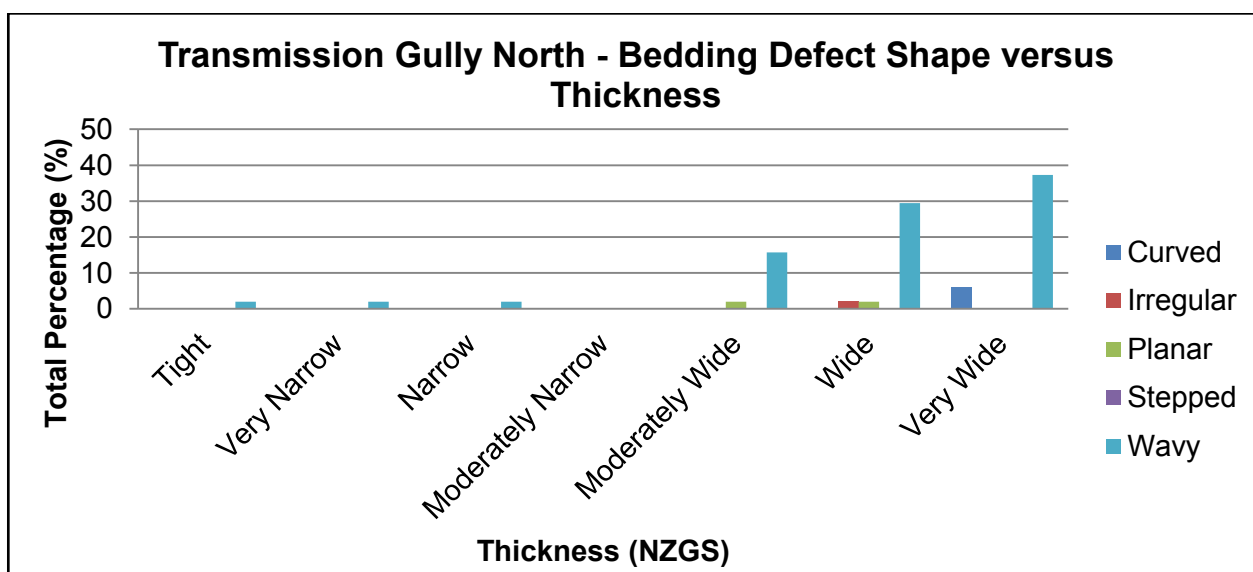
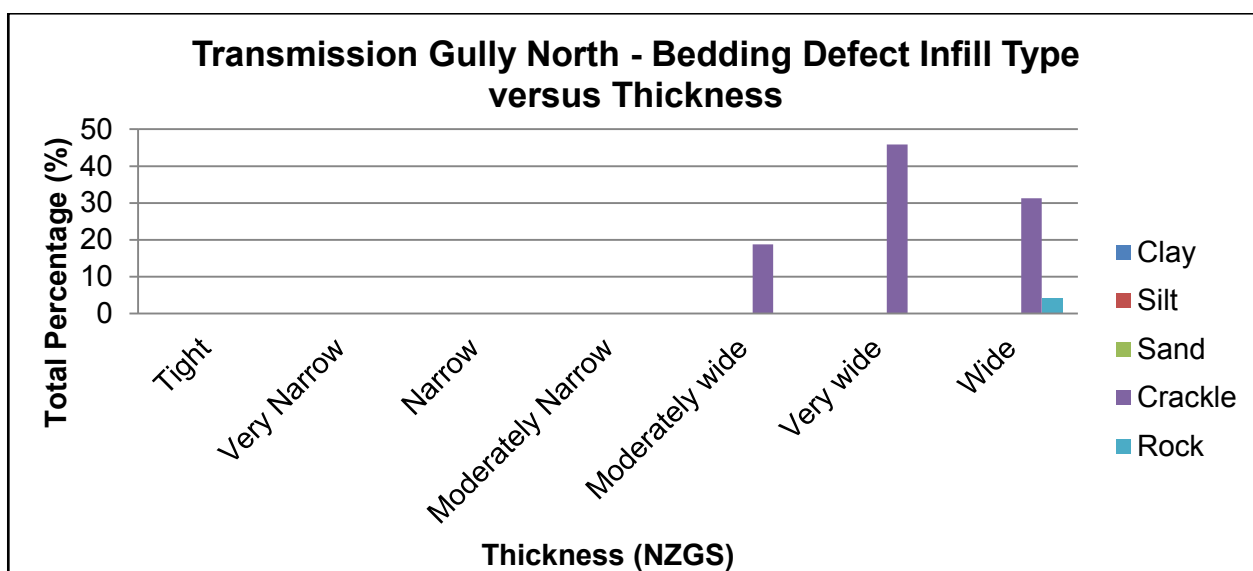
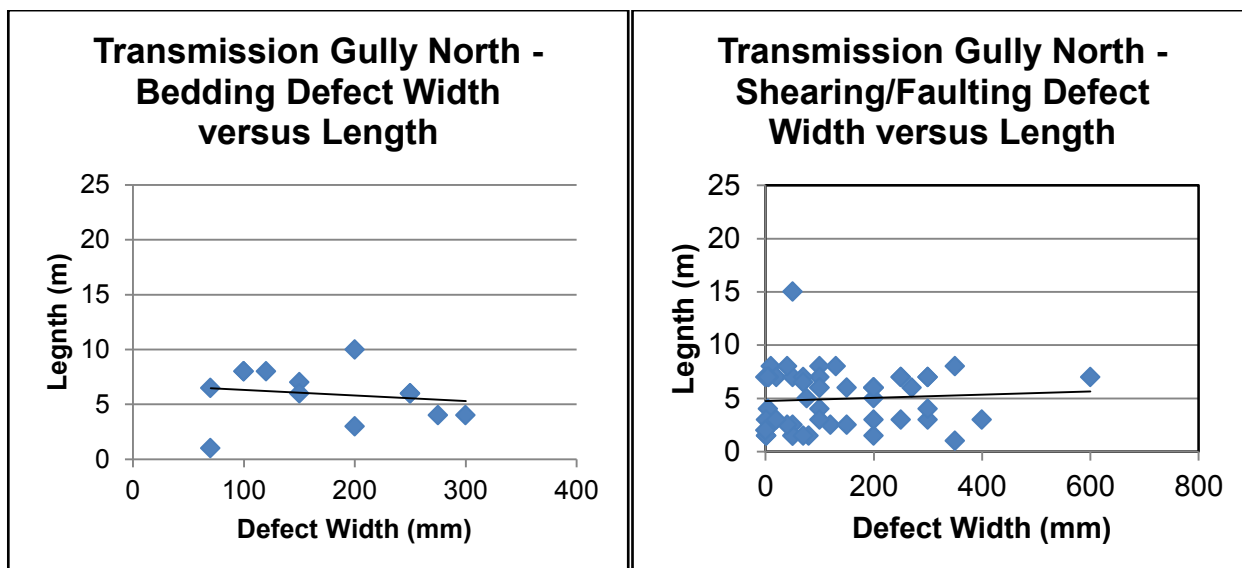
Figure A.4.1: Graphs displaying the Transmission Gully North Shearing (Left) and Bedding (Right) waviness.

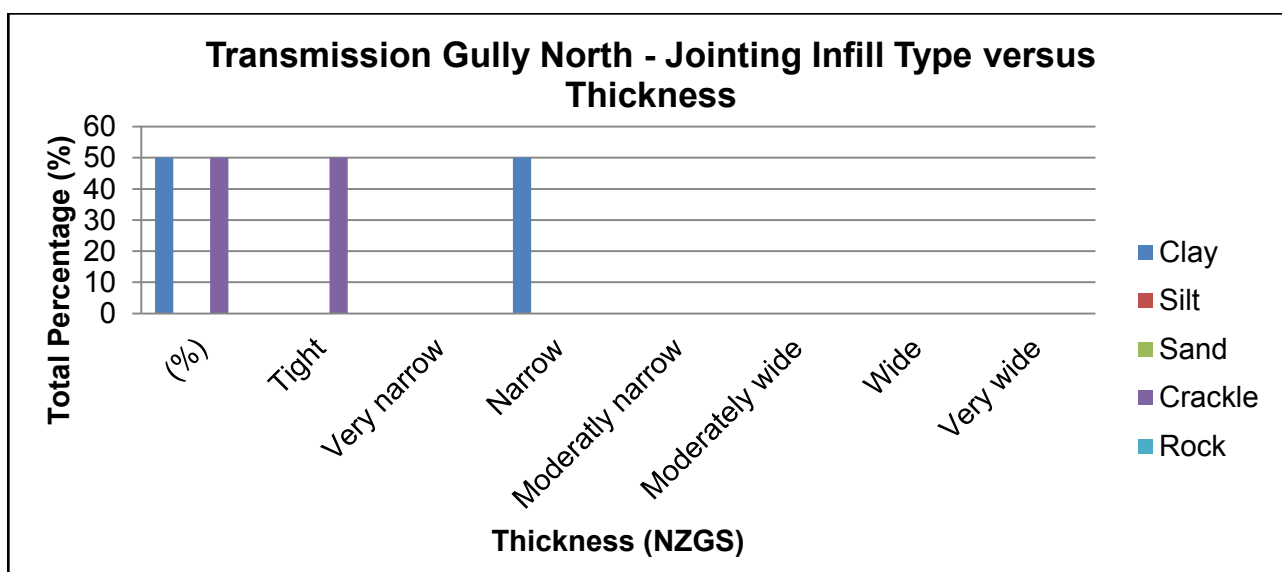
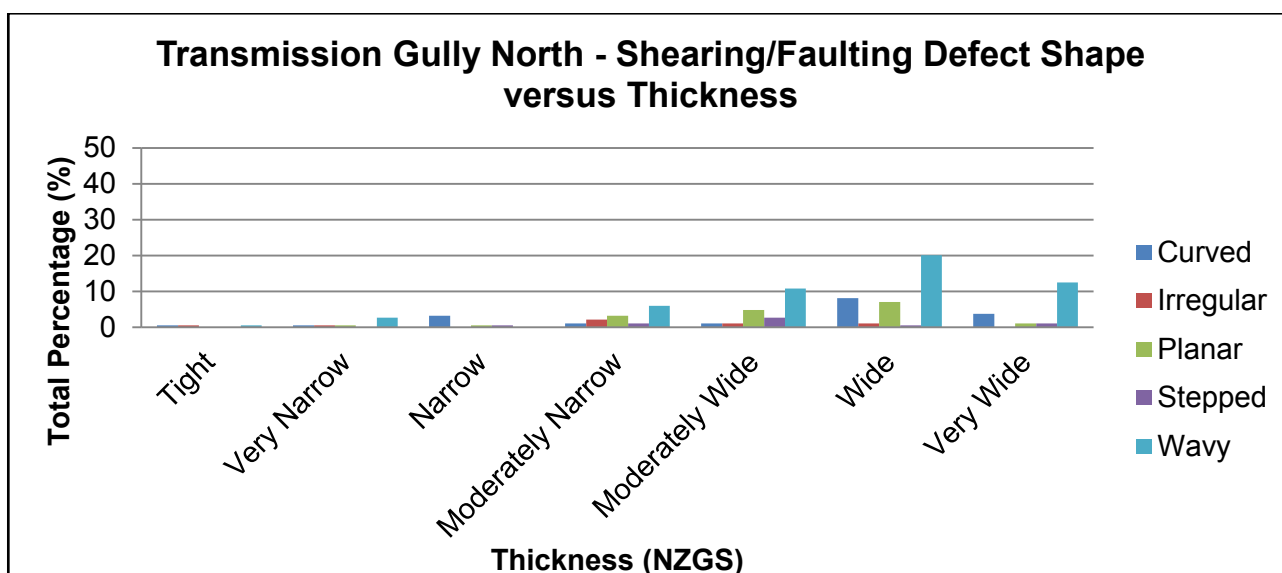
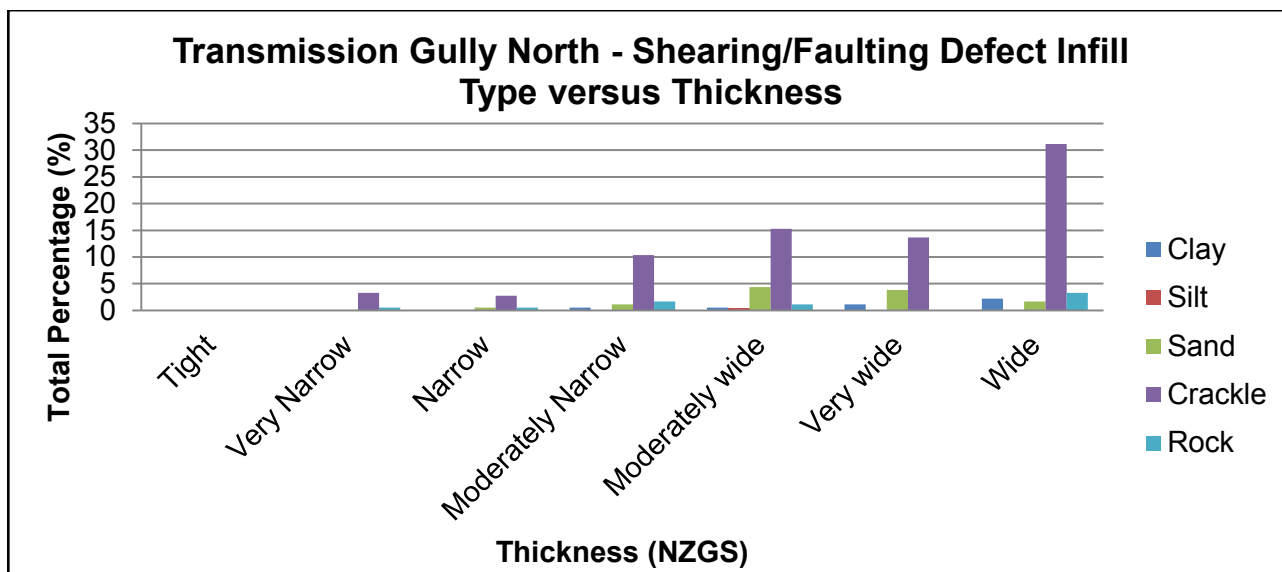


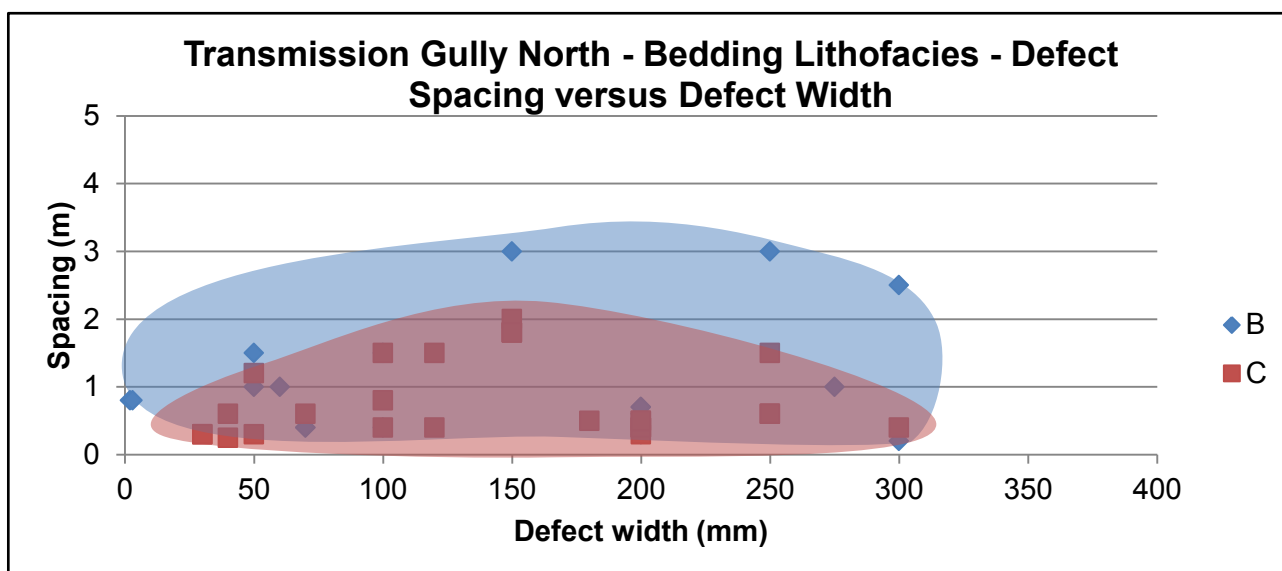
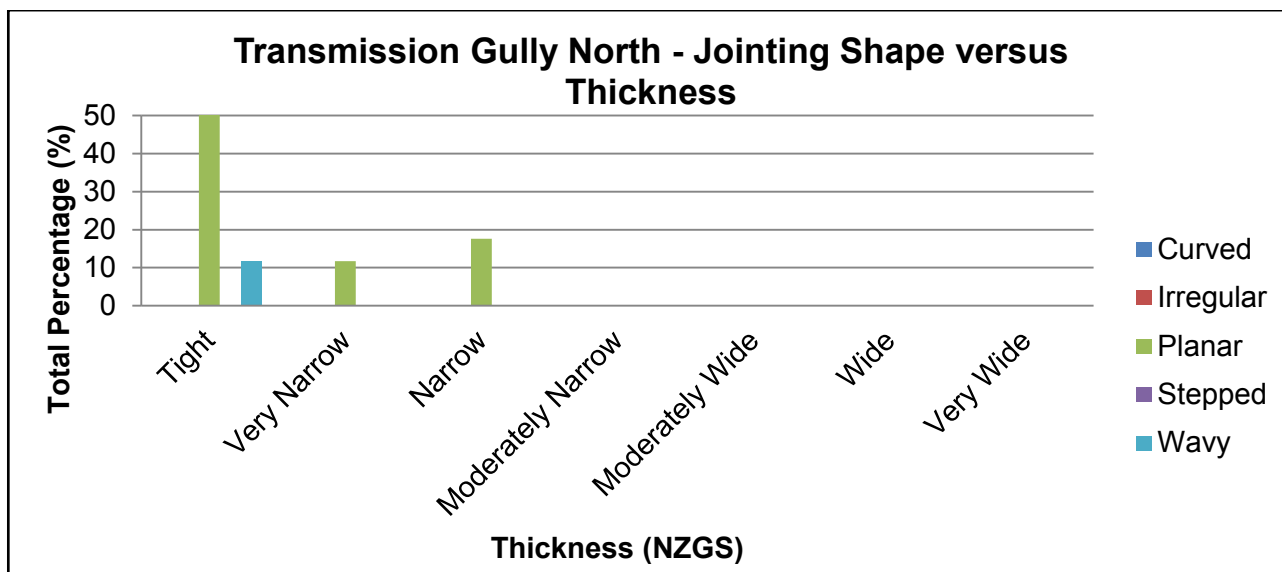








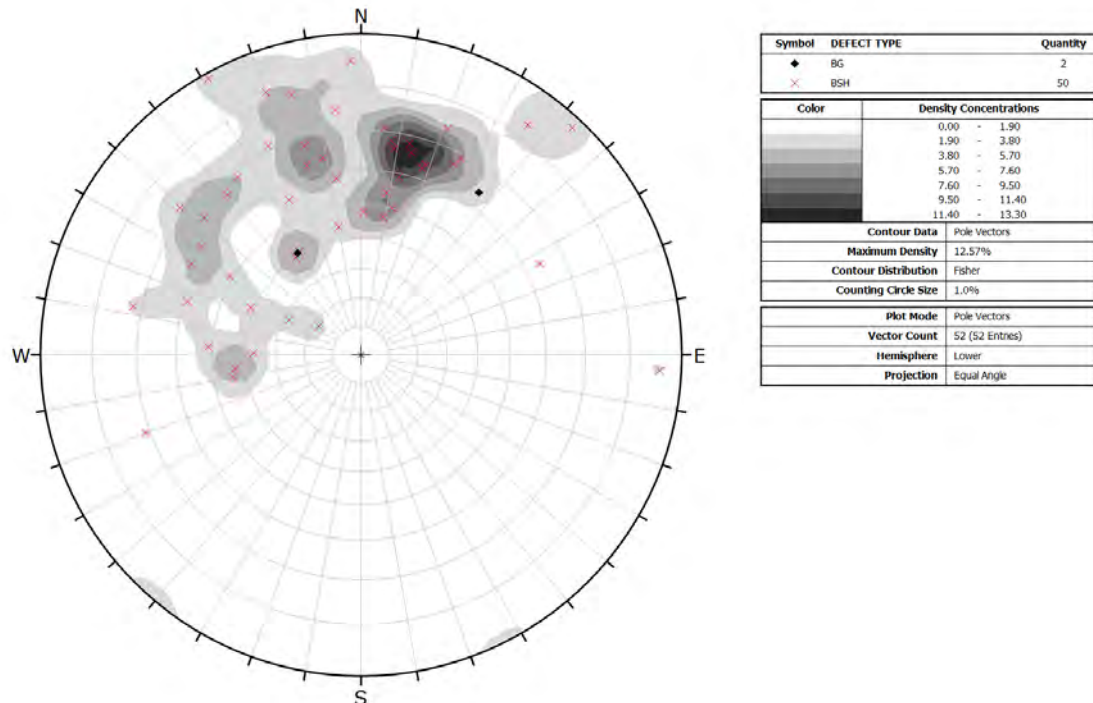




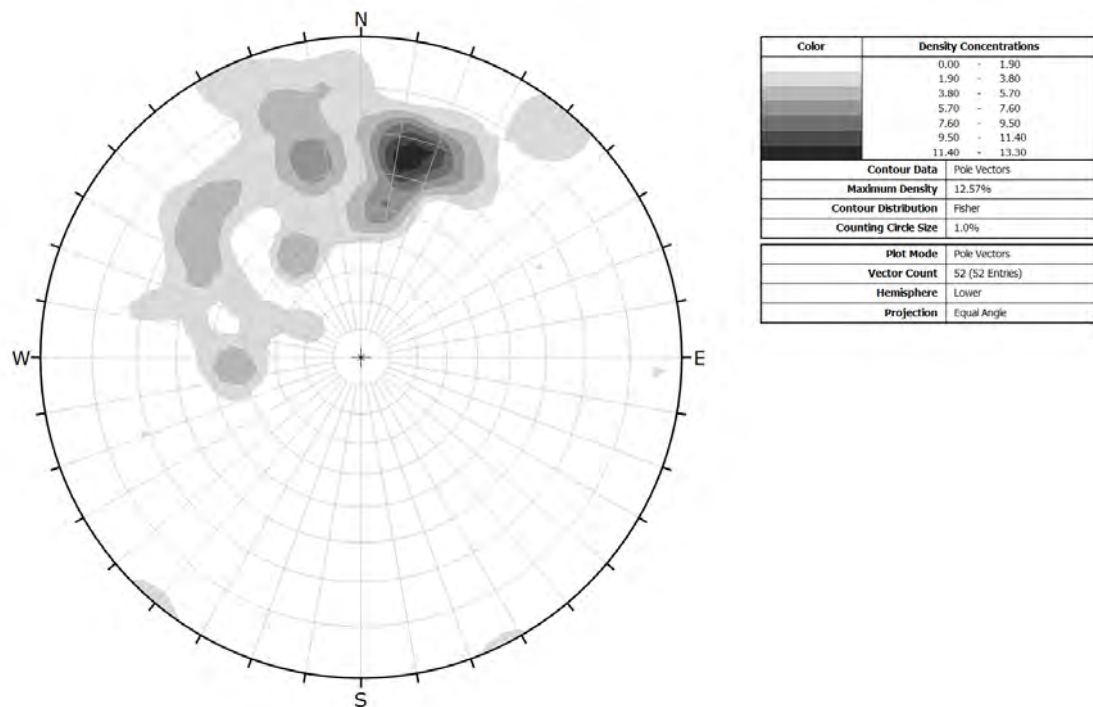
A.5 Transmission Gully North Stereonet Analysis

Stereonet Dip: Dip direction analysis of bedding, faults and shears respectively.

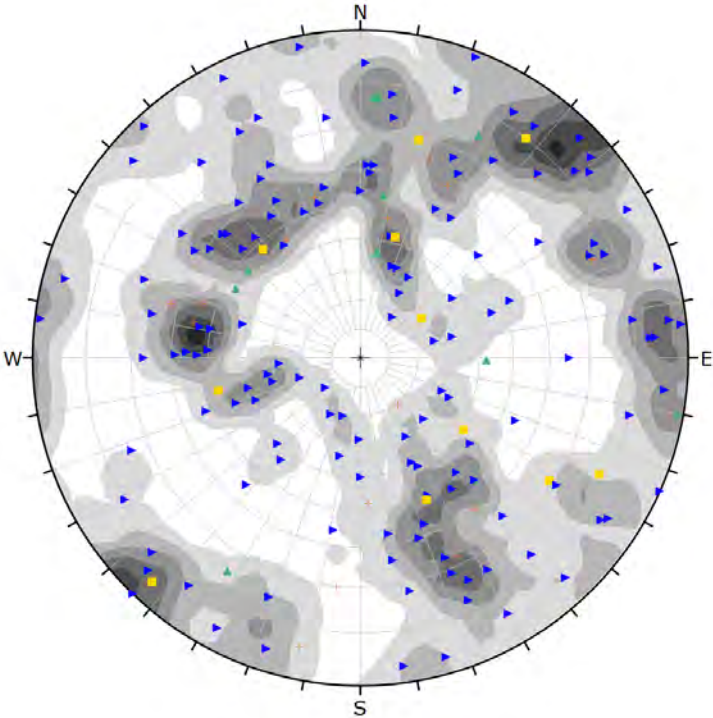
Bedding poles



Contour diagram of bedding clusters



Shearing poles



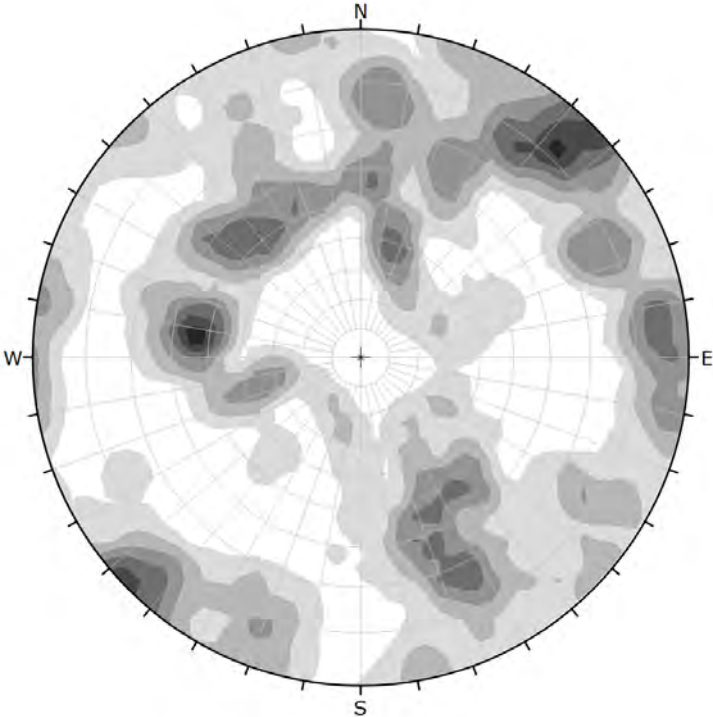
Symbol	DEFECT TYPE	Quantity
▲	CZ	11
+	FL	17
■	SH	12
▶	SR	145

Color	Density Concentrations
	0.00 - 0.60
	0.60 - 1.20
	1.20 - 1.80
	1.80 - 2.40
	2.40 - 3.00
	3.00 - 3.60
	3.60 - 4.20

Contour Data	Pole Vectors
Maximum Density	3.97%
Contour Distribution	Fisher
Counting Circle Size	1.0%

Plot Mode	Pole Vectors
Vector Count	185 (185 Entries)
Hemisphere	Lower
Projection	Equal Angle

Contour diagram of shearing and faulting clusters

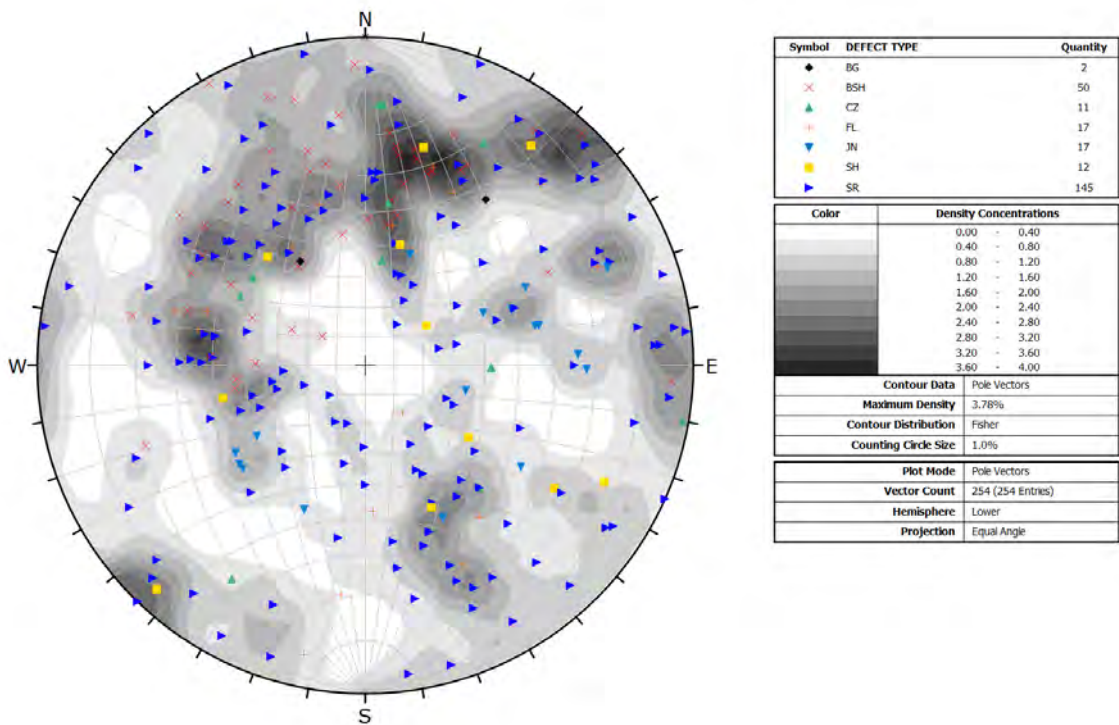


Color	Density Concentrations
	0.00 - 0.60
	0.60 - 1.20
	1.20 - 1.80
	1.80 - 2.40
	2.40 - 3.00
	3.00 - 3.60
	3.60 - 4.20

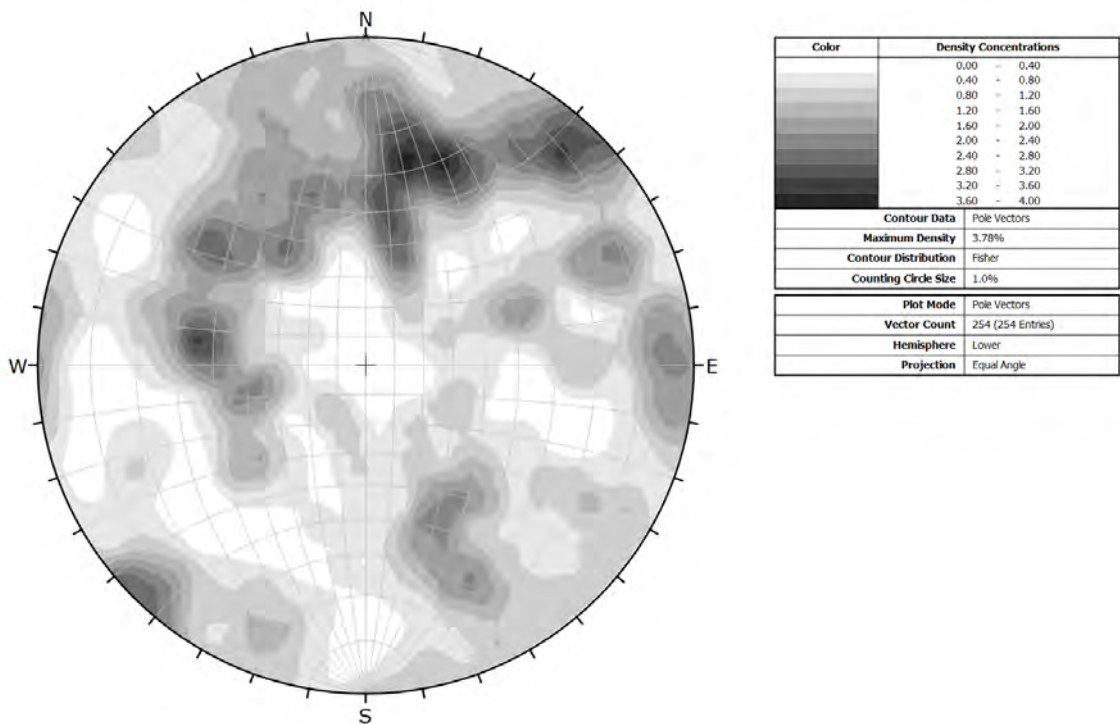
Contour Data	Pole Vectors
Maximum Density	3.97%
Contour Distribution	Fisher
Counting Circle Size	1.0%

Plot Mode	Pole Vectors
Vector Count	185 (185 Entries)
Hemisphere	Lower
Projection	Equal Angle

All defects poles



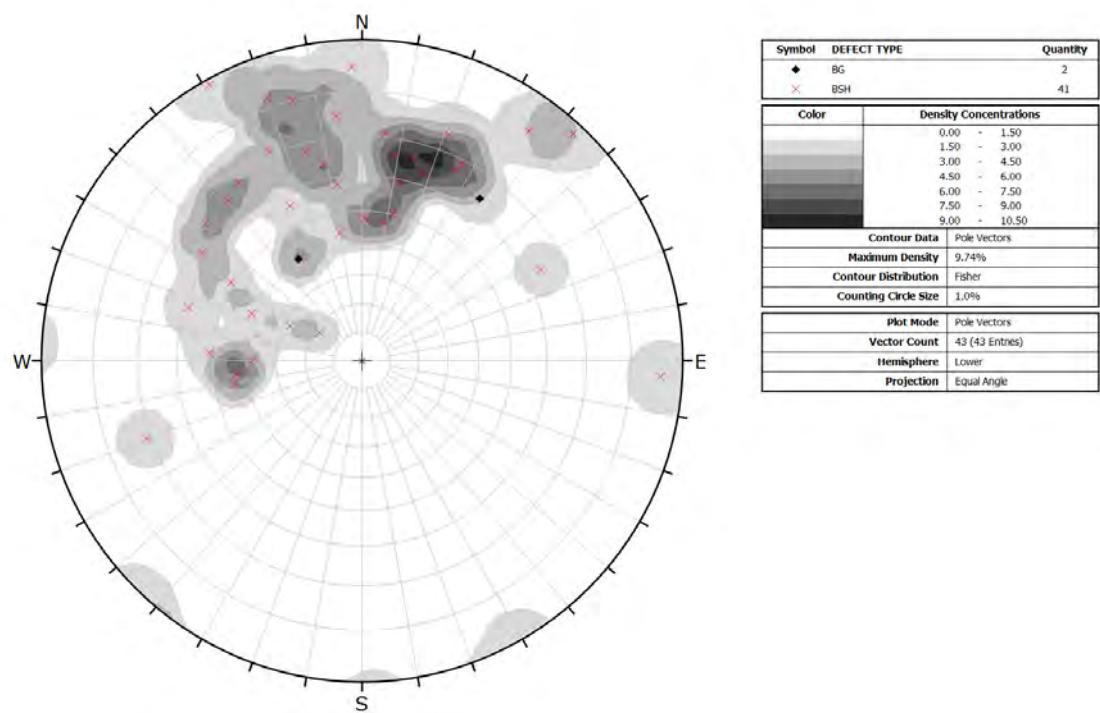
Contour diagram of all defects cluster



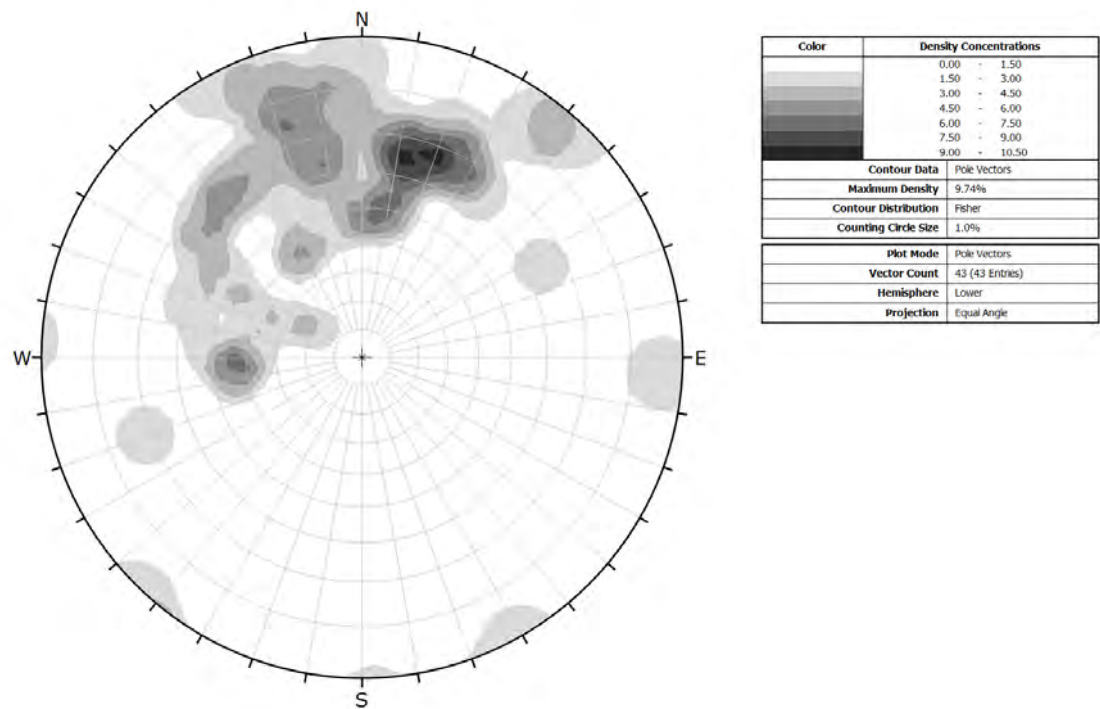
A.6 Filtered Stereonet Analysis

Stereonet from A.5 assessed for “noise”. The following only displays the poles of the continuous defects in Transmission Gully North.

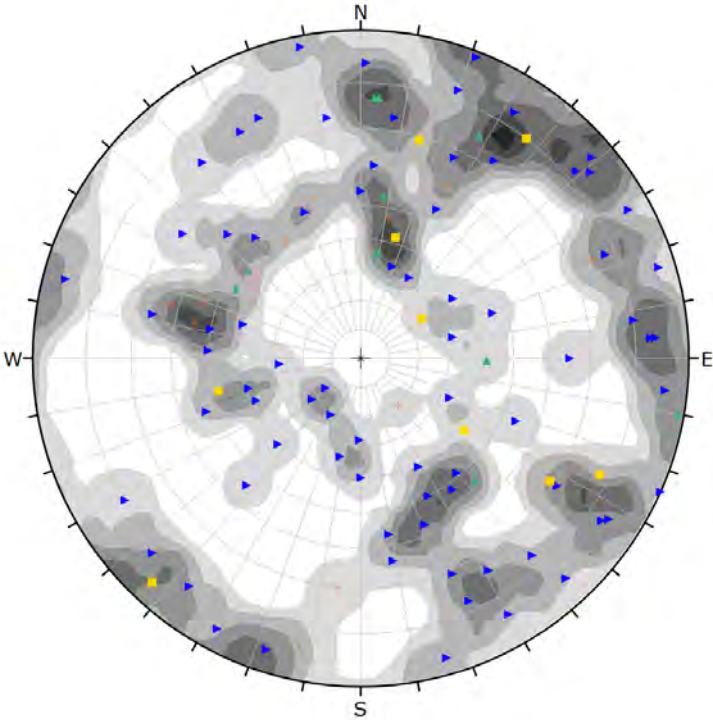
Bedding poles



Contour diagram of bedding clusters



Shearing poles



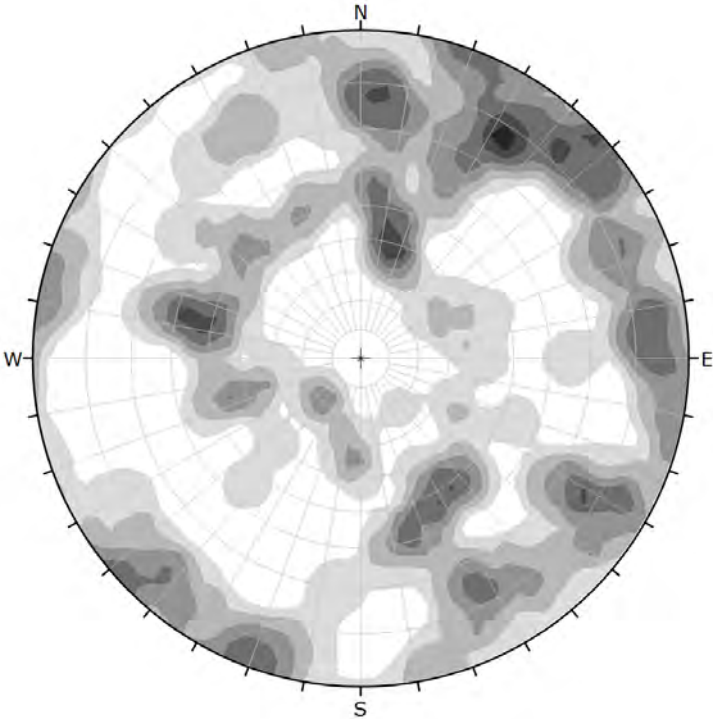
Symbol	DEFECT TYPE	Quantity
▲	CZ	10
+	FL	12
■	SH	10
▼	SR	78

Color	Density Concentrations
	0.00 - 0.60
	0.60 - 1.20
	1.20 - 1.80
	1.80 - 2.40
	2.40 - 3.00
	3.00 - 3.60
	3.60 - 4.20

Contour Data	Pole Vectors
Maximum Density	3.99%
Contour Distribution	Fisher
Counting Circle Size	1.0%

Plot Mode	Pole Vectors
Vector Count	110 (110 Entries)
Hemisphere	Lower
Projection	Equal Angle

Contour diagram of shearing and faulting clusters

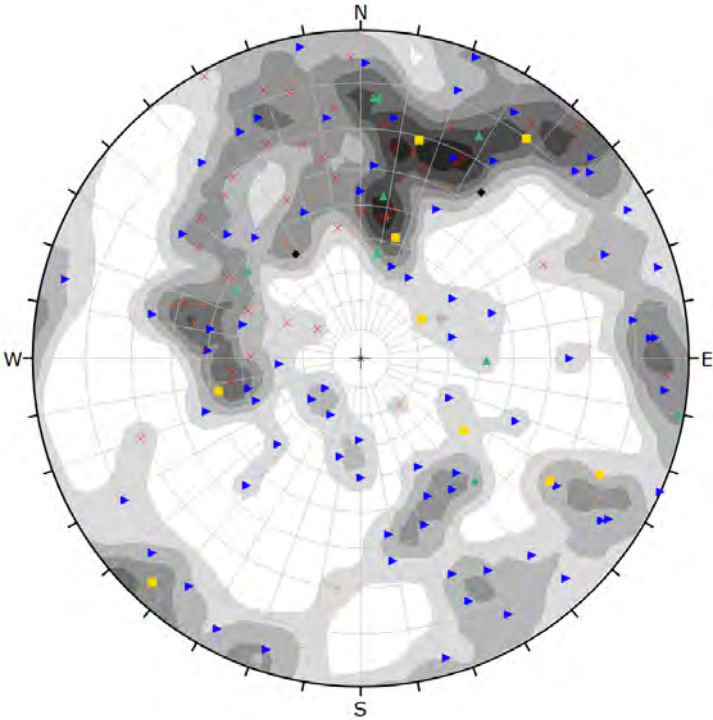


Color	Density Concentrations
	0.00 - 0.60
	0.60 - 1.20
	1.20 - 1.80
	1.80 - 2.40
	2.40 - 3.00
	3.00 - 3.60
	3.60 - 4.20

Contour Data	Pole Vectors
Maximum Density	3.99%
Contour Distribution	Fisher
Counting Circle Size	1.0%

Plot Mode	Pole Vectors
Vector Count	110 (110 Entries)
Hemisphere	Lower
Projection	Equal Angle

All defects poles



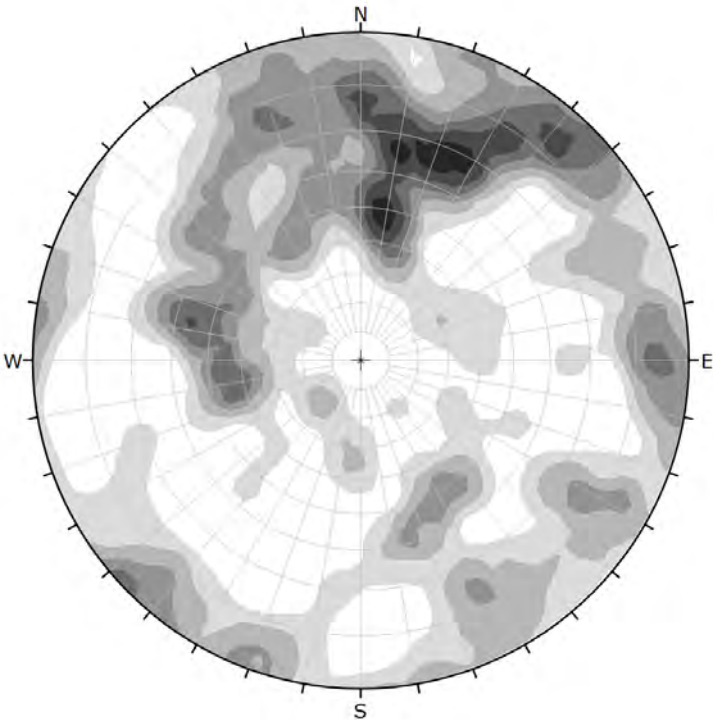
Symbol	DEFECT TYPE	Quantity
◆	BG	2
×	BSH	41
▲	CZ	10
+	FL	12
■	SH	10
▴	SR	78

Color	Density Concentrations
	0.00 - 0.60
	0.60 - 1.20
	1.20 - 1.80
	1.80 - 2.40
	2.40 - 3.00
	3.00 - 3.60
	3.60 - 4.20

Contour Data	Pole Vectors
Maximum Density	4.18%
Contour Distribution	Fisher
Counting Circle Size	1.0%

Plot Mode	Pole Vectors
Vector Count	153 (153 Entries)
Hemisphere	Lower
Projection	Equal Angle

Contour diagram of all defects cluster



Color	Density Concentrations
	0.00 - 0.60
	0.60 - 1.20
	1.20 - 1.80
	1.80 - 2.40
	2.40 - 3.00
	3.00 - 3.60
	3.60 - 4.20

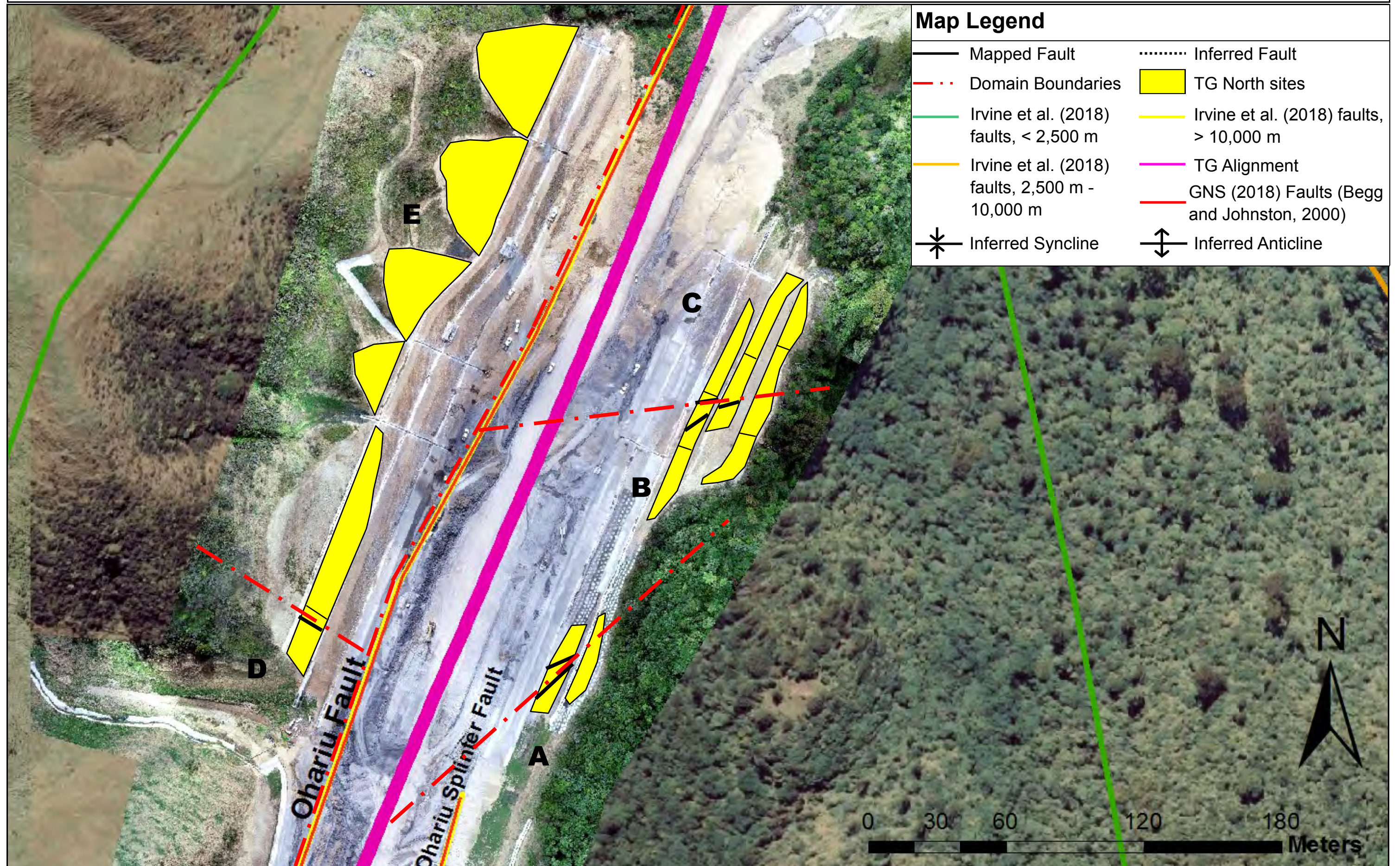
Contour Data	Pole Vectors
Maximum Density	4.18%
Contour Distribution	Fisher
Counting Circle Size	1.0%

Plot Mode	Pole Vectors
Vector Count	153 (153 Entries)
Hemisphere	Lower
Projection	Equal Angle

A.7 Transmission Gully North Structural Domains

Figures are based on mapping observations and stereonet analysis. The figures represent a very detailed interpretation of the changes in defect orientation across the Transmission Gully North site.

A.7.1 Transmission Gully North - Domains



Imagery sourced: LINZ aerial imagery, 2016 (Captured by AAM NZ Ltd (2017)) and from the Transmission Gully GIS Database (2019).

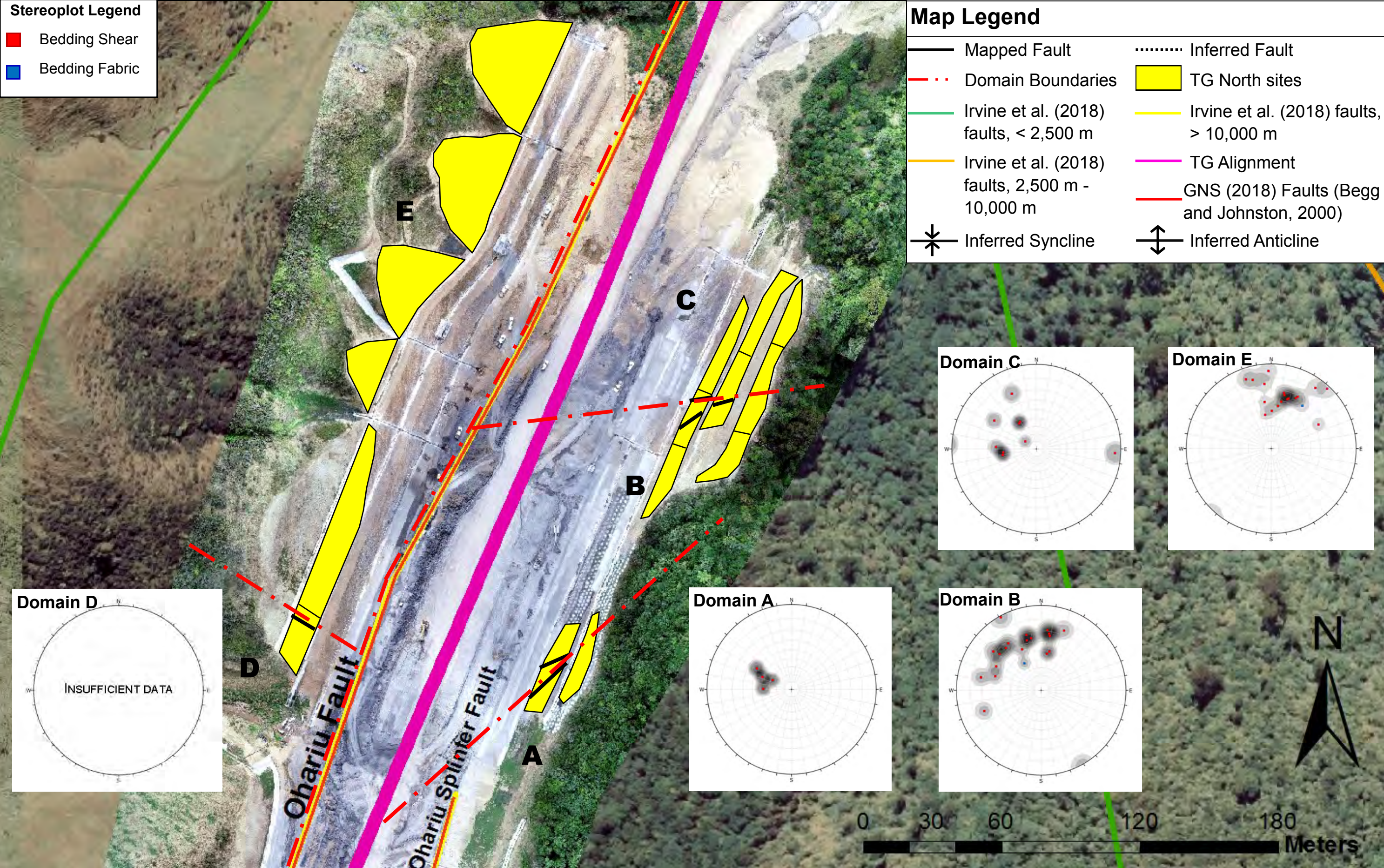
A.7.2 Transmission Gully North Domains - Bedding

Stereoplot Legend

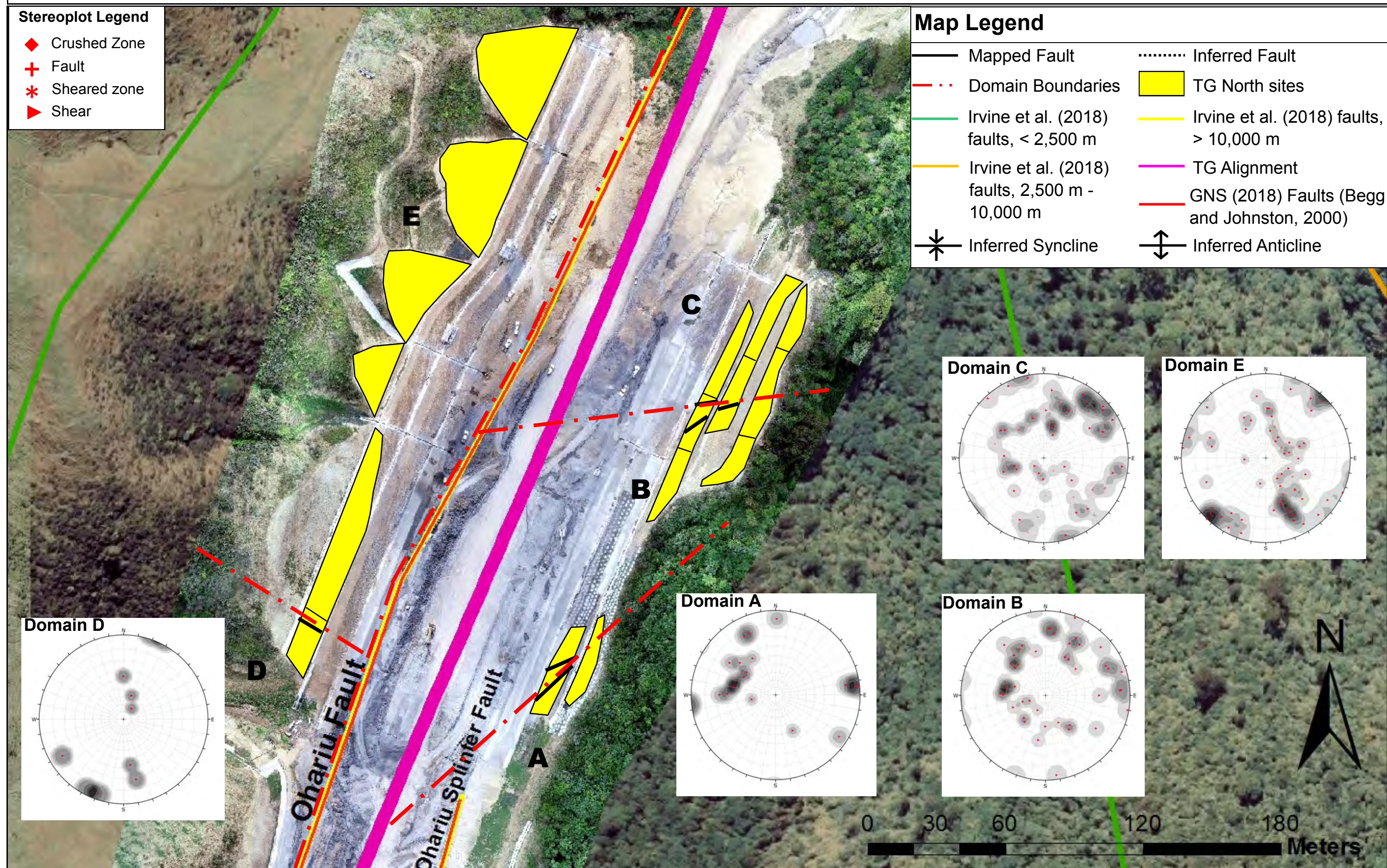
- Bedding Shear
- Bedding Fabric

Map Legend

- Mapped Fault
- Domain Boundaries
- Irvine et al. (2018) faults, < 2,500 m
- Irvine et al. (2018) faults, 2,500 m - 10,000 m
- Inferred Syncline
- Inferred Fault
- TG North sites
- Irvine et al. (2018) faults, > 10,000 m
- TG Alignment
- GNS (2018) Faults (Begg and Johnston, 2000)
- Inferred Anticline



A.7.3 Transmission Gully North Domains - Shearing



Imagery sourced: LINZ aerial imagery, 2016 (Captured by AAM NZ Ltd (2017)) and from the Transmission Gully GIS Database (2019).

A.8 Transmission Gully North Engineering Geological Model

Engineering geological model based on all available data. The model provides a summary of the rock mass and defect condition within the Transmission Gully North study site. Defect orientation and regional structural controls are also included.

A.8: Engineering Geological Model of Transmission Gully North

Key :
◆ BG ▲ CZ ▼ JN ▶ SR
✗ BSH + FL ■ SH

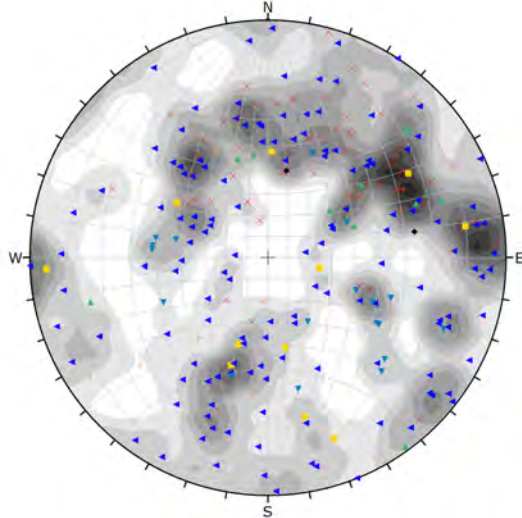


Figure 1: Stereonet of all the defect types and their orientation.

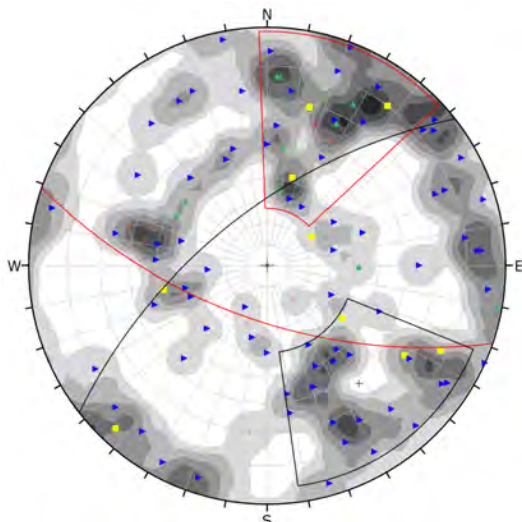


Figure 2: Stereonet of bench long shearing defects.

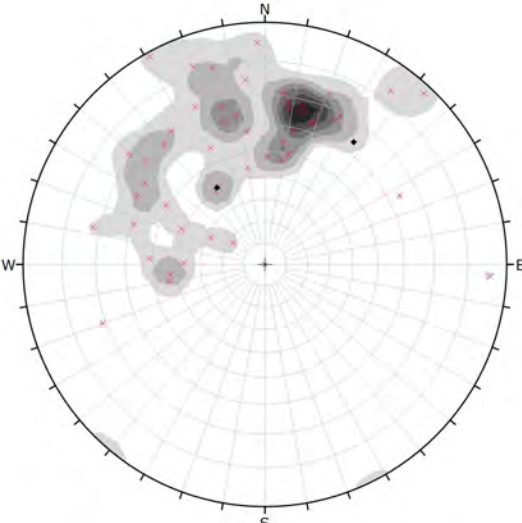
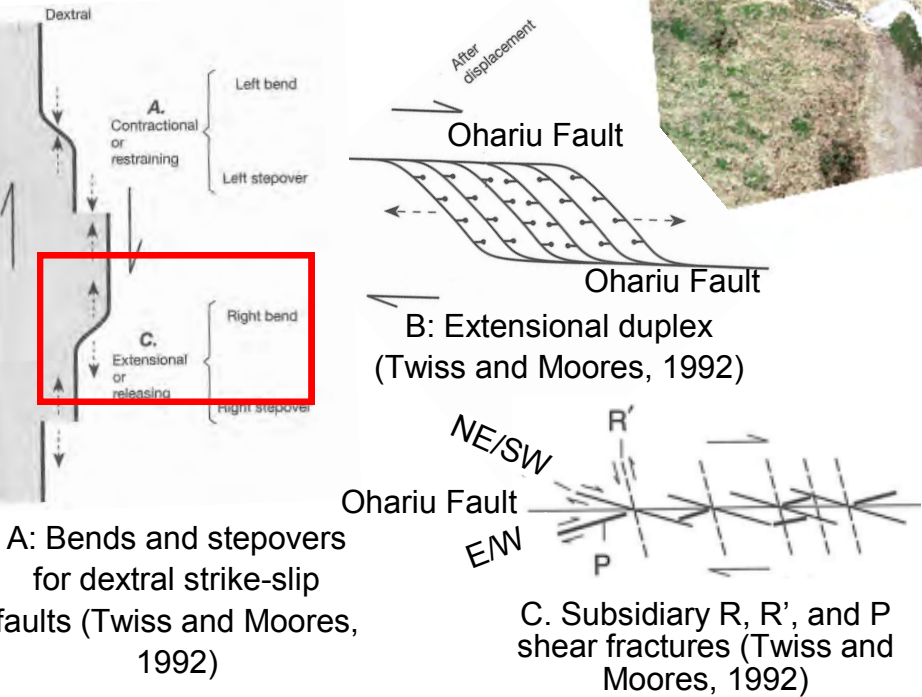


Figure 3: Stereonet of bedding.

Key:
— 1st Order >10,000m
— 2nd Order 2,500-10,000m
— 3rd Order <2,500m
— Mapped faults
..... Weathering profile

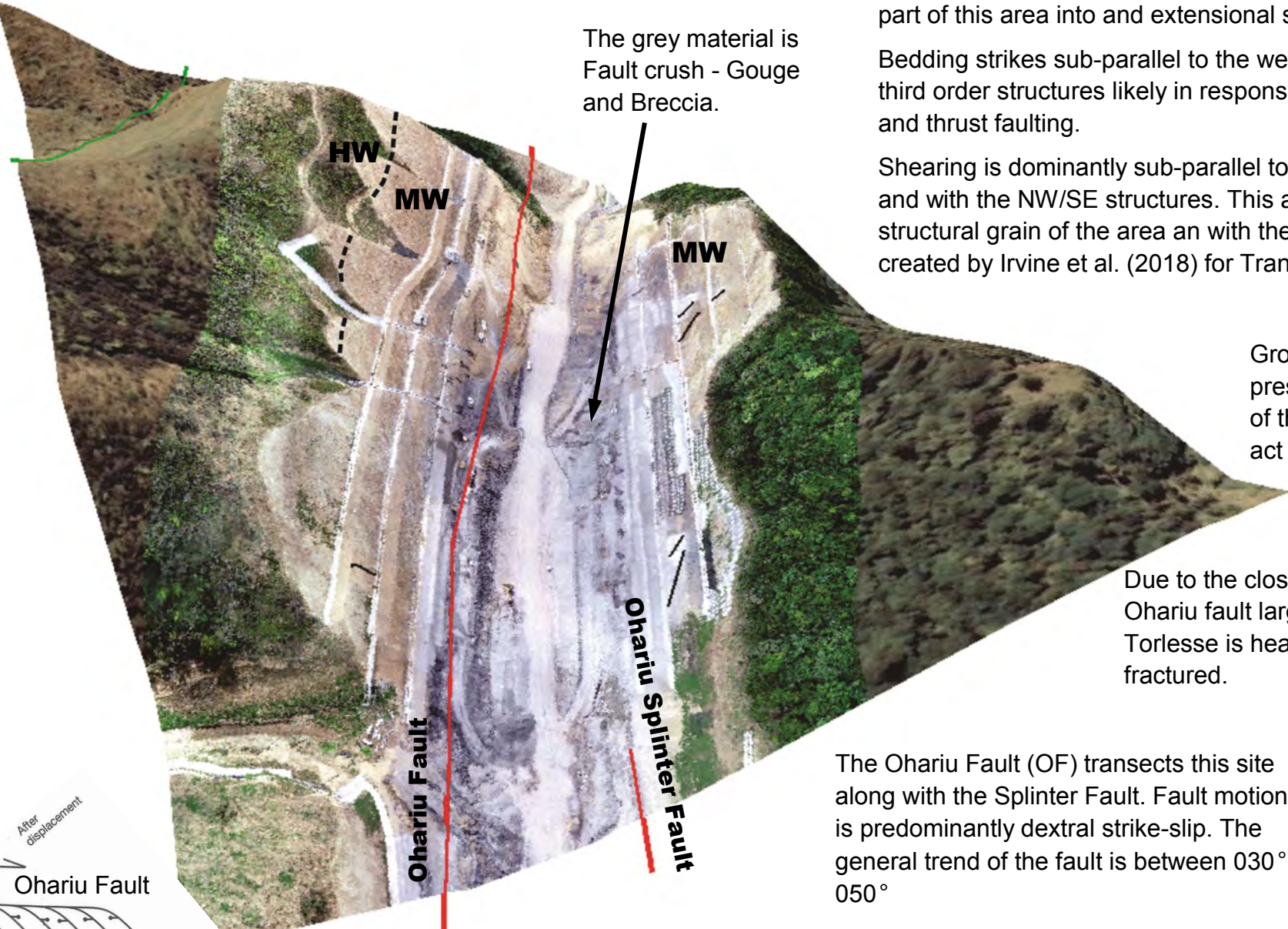
Individual sandstone beds are 2.5 m to 0.3 m thick and can be continuous. Mudstone beds are 3 mm to 0.3 m thick and heavily sheared. Traces of cross-cutting shears and faults are visible and persistent. Sheared zones are common.

Conceptual Models:



Weathering profile typically follows topography, faulting has minor influence

Bedding is dominantly sub-vertical to steeply inclined with variations occurring in response to faulting.



Rock mass structure at this site is controlled by the Ohariu and it's Splinter Fault. Crustal stress is interpreted to be accommodated by a releasing bend to just south and to the west of this site. This is where the Ohariu Fault steps over into the Horokiri Valley placing part of this area into an extensional setting.

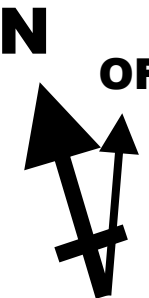
Bedding strikes sub-parallel to the west-east trending third order structures likely in response to their normal and thrust faulting.

Shearing is dominantly sub-parallel to the Ohariu Fault and with the NW/SE structures. This aligns with the structural grain of the area and with the regional model created by Irvine et al. (2018) for Transmission Gully.

Groundwater flow is present on both sides of the valley. Faults act as aquitards.

Due to the close proximity of the Ohariu fault large volumes of the Torlesse is heavily sheared and fractured.

The Ohariu Fault (OF) transects this site along with the Splinter Fault. Fault motion is predominantly dextral strike-slip. The general trend of the fault is between 030° - 050°



MUD : SAND 40: 60	Sandstone: Moderately to Highly weathered, light orange brown, SANDSTONE; Moderately Strong to Weak; 5 joint sets very closely spaced, narrow to tight joints [RAKAIA SUB-TERRANE Greywacke]	Mudstone: Moderately weathered, dark brown grey MUDSTONE; Weak [RAKAIA SUB-TERRANE Argillite]
Predominant Suneson lithofacies: B and C		
Scale 1:1,800 centimetres		
0 18.75 37.5 75 150 300 Meters		

APPENDIX B: TRANSMISSION GULLY SOUTH

The Transmission Gully South site lies in the south of the Transmission Gully alignment between Cannons Creek Bridge and Kenepuru Interchange (Figure B.1). This area is also located between the Moonshine and Ohariu Faults which converge in the southwest. High angle cross faulting link these major faults and are likely accommodating and transferring the tectonic stresses due to regional convergence. The close proximity of the major faults means that shearing of any kind is un-avoidable. The alignment is still under construction similarly offering fresh exposures in an area that would otherwise not have good exposure of the rock mass. A total of 4 outcrops were mapped (Appendix B.2).

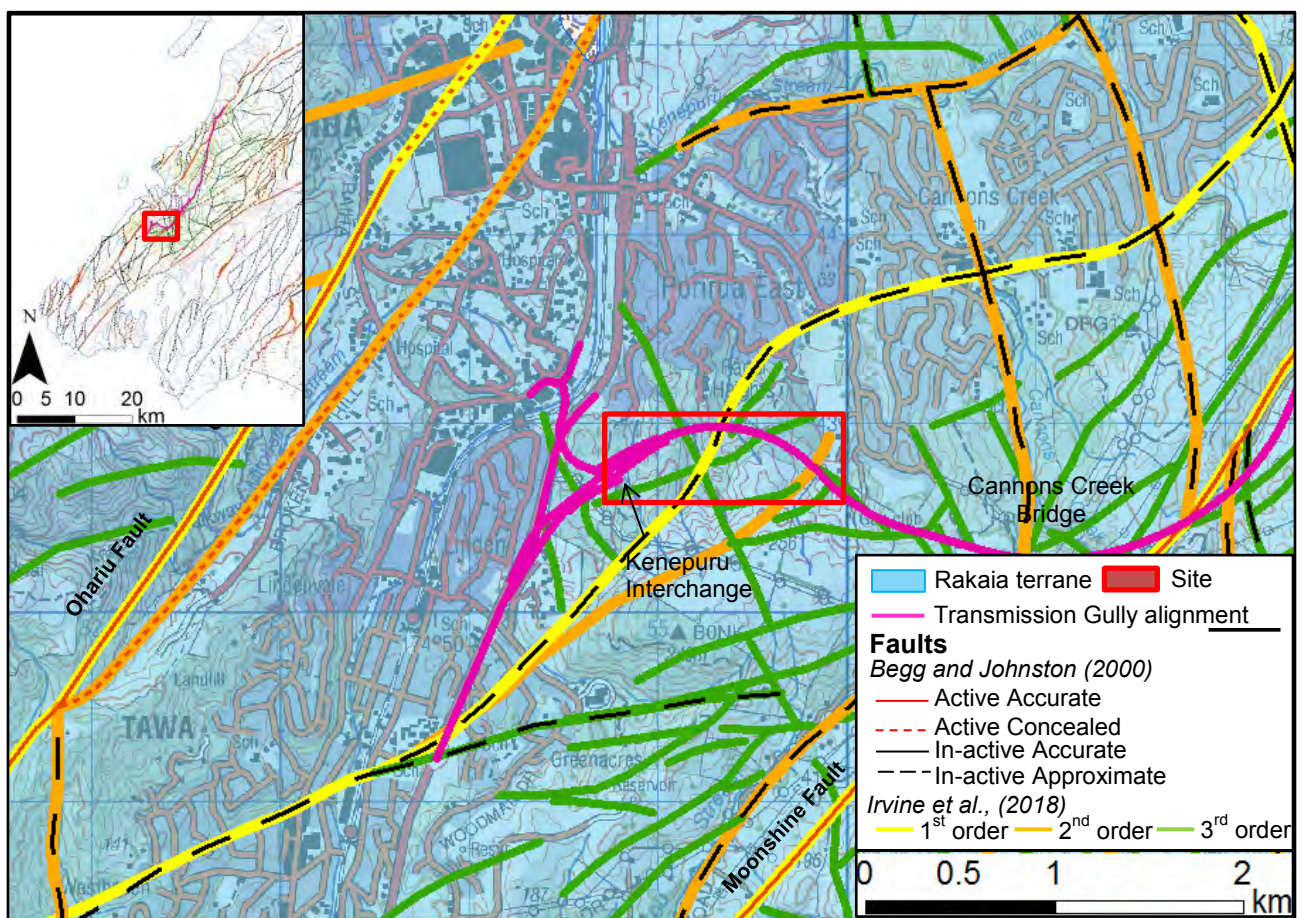


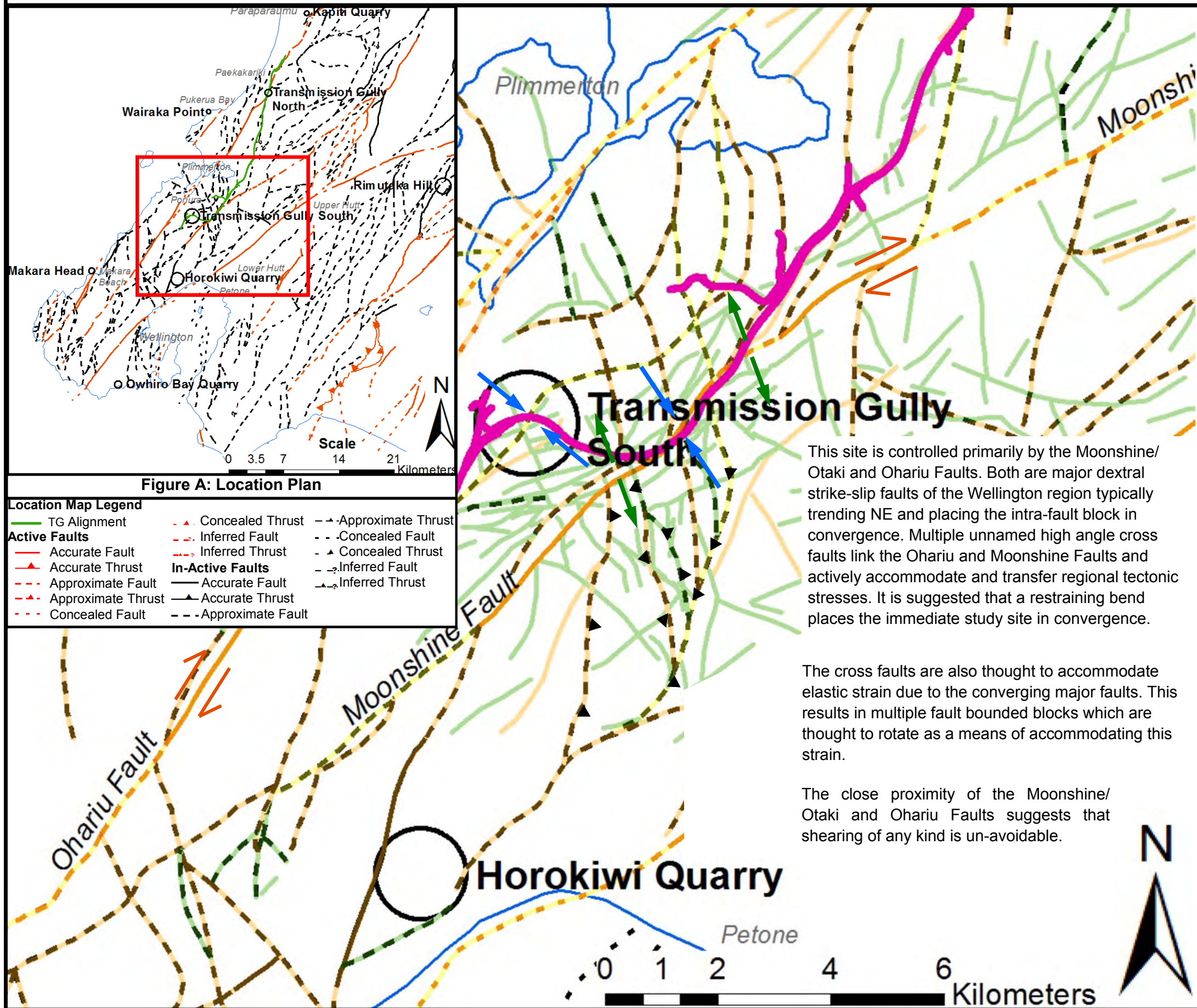
Figure B.1: Transmission Gully South site district scale map. Data sourced from GNS (2018) (Begg and Johnston, 2000) and Irvine et al. (2018). Refer to Section 1.4 for Irvine et al. (2018) order classification. Imagery from LINZ.

Results derived from conceptual models, raw mapping data, stereonet analysis and engineering geological models for the Transmission Gully South study site are displayed in the following sections.

B.1 Transmission Gully South Conceptual Structural Model

Preliminary structural assessment derived from GNS (2018) (Begg and Johnston, 2000) and Irvine et al. (2018) structural databases. Interpretations are based on information derived from past literature.

B.1 Conceptual Structural Model of Transmission Gully South



District Scale Legend:

- TG Alignment
- Restraining bend
- Coastline
- Strike Slip
- Releasing bend

Active Faults

- Accurate Fault
- Accurate Thrust
- Approximate Fault
- Approximate Thrust
- Concealed Fault
- Concealed Thrust
- Inferred Fault
- Inferred Thrust

In-Active Faults

- Accurate Fault
- Accurate Thrust
- Approximate Fault
- Approximate Thrust
- Concealed Fault
- Concealed Thrust
- Inferred Fault
- Inferred Thrust

Fault Analysis Overlay (Irvine et al., 2018)

- 3rd Order < 2,500 m
- 2nd Order 2,500 - 10,000 m
- 1st Order > 10,000 m

Conceptual Models:

A. Contractual or restraining

B. Left bend

C. Right bend

D. Contractional duplex (Twiss and Moores, 1992)

E. Development of dextral strike-slip duplexes (Woodcock and Fisher, 1986)

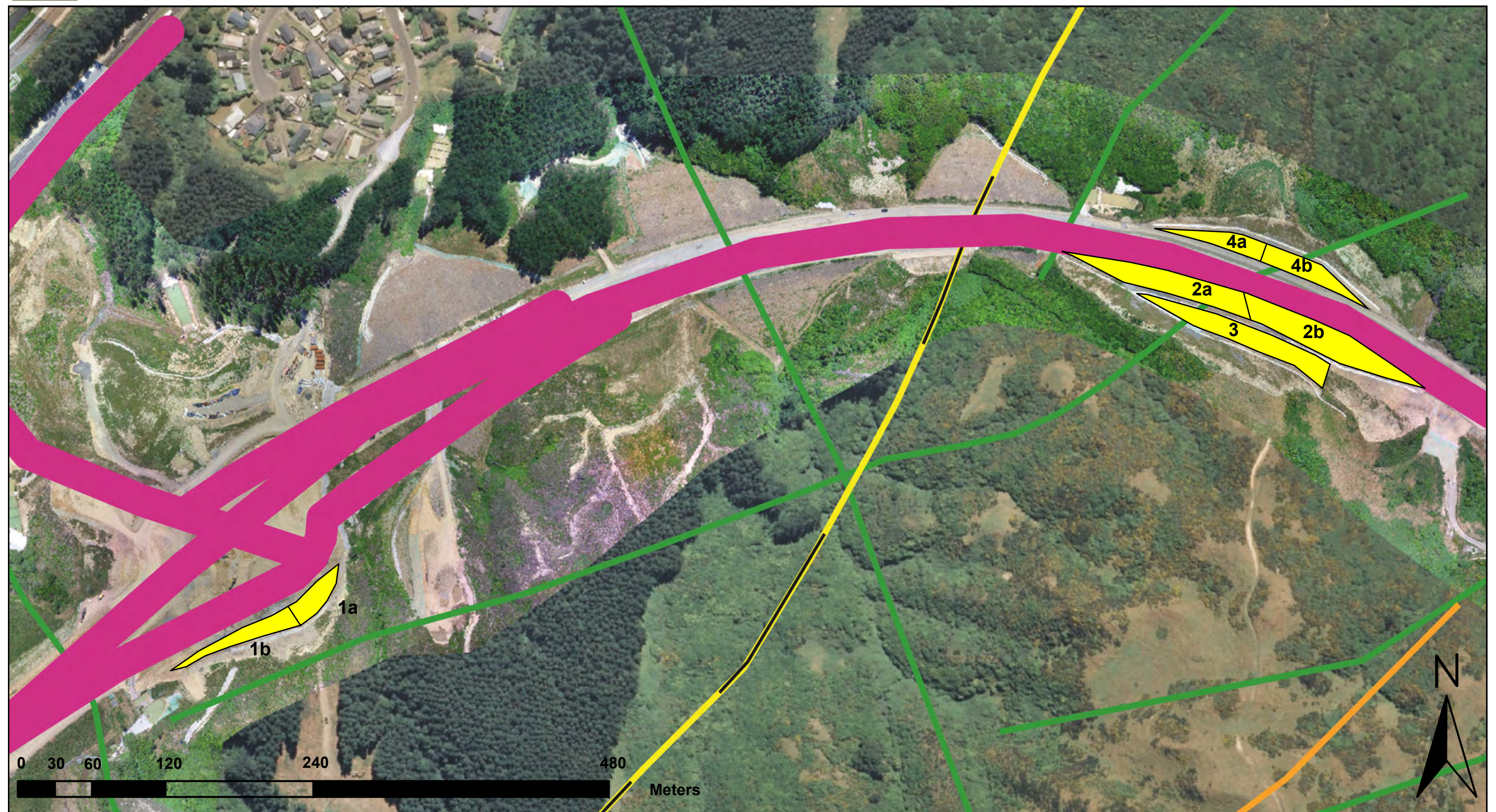
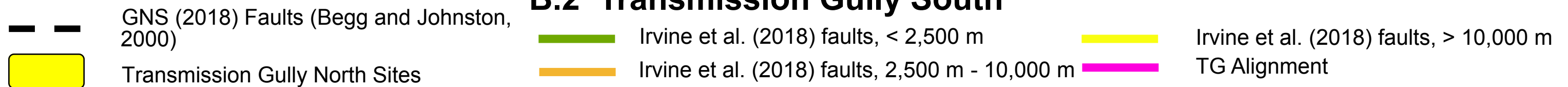
Bedding and Shearing Predictions:

Bedding is anticipated to trend sub-parallel to parallel with major fault structures however, intra block rotation suggests that the bedding may have rotated from NE to NW aligning sub-parallel with cross faulting (Irvine et al., 2018). Likewise, shearing is anticipated to trend sub-parallel to cross faulting (Irvine et al., 2018).

B.2 Transmission Gully South Outcrop Location Map

Displays the location of the mapped outcrops within the Transmission Gully South study site.

B.2 Transmission Gully South



Imagery sourced: LINZ aerial imagery, 2017 (NZ Aerial Mapping Ltd, 2017) and Transmission Gully GIS Database (2019)

B.3 Transmission Gully South Raw Mapping Data

Structural data collected from the Transmission Gully South site. Where data is missing or blanked out information was either not able to be reached or was not relevant to the rock mass or defect condition (e.g. Planar defects did not contain a wavelength as outlined in Chapter 3).

B.3.1 Transmission Gully South - Raw Data

Transmission Gully South																							
ID	Defect Type	Dip	Dip Direction (Mag)	Dip Direction (True)	Structural Domain	Roughness	Thickness		% of rock fragments	Continuity	Persistence	Shape			Persistence - Trace Length (m)	Spacing (m)	Infill (Support (Breccia type (%Clasts), Angularity, weathering, strength, coating; colour, grainsize, strength, plasticity)) precipitation	Saturation	Latitude	Longitude	Comments	Cut ID	
							Term	Width (mm)				Inter-limb angle (degrees)	Wavelength (m)	Term									
1	SR	79	22	360	F	Ro3	Moderately wide	50mm	~75%	0	C	~170°	Gentle		Curved	~3m		Clast supported (Crackle (~75%) Angular, CW, Weak to very weak, Coating; Orangey brown, Sand with traces of clay, Soft to stiff, NP) White sand sized specks	Dry	-41.1497	174.8534	Continuous	C40 NB B2
2	BSH	87	212	190	F	Ro3	Moderately wide	50mm	~75%	0	C	~170°	Gentle		Curved	~3m	~1m	Clast supported (Crackle (~75%) Angular, CW, Weak to very weak, Coating; Orangey brown, Sand with traces of clay, Soft to stiff, NP) White sand sized specks	Dry	-41.1497	174.8534	Continuous	
3	SR	81	184	162	F	Ro2	Moderately wide	40mm	~90%	1	D	~180°	Gentle		Planar	~5m		Clast supported (Crackle (~90%) Angular, HW, Weak to very weak, Coating; Orangey brown, sandy Clay, Firm, NP) White sand sized specks	Dry	-41.1497	174.8536	Cross cuts SR4	
4	SR	42	222	200	F	Ro3	Very narrow	0-1mm	~99%	0	C	~180°	Gentle		Planar	~4m	~1.5m	Clast supported (Rock (~99%) Angular, HW, Weak to Moderately Strong, Coating; Orangey brown, sandy Clay, Soft, NP) White sand sized specks	Dry	-41.1497	174.8536	Cross cuts SR3	
5	SR	76	178	156	F	Ro3	Moderately narrow	10mm	~99%	0	C	~170°	Gentle	~10m	Wavy	~6m	~1.5m	Clast supported (Rock (~99%) Angular, HW, Weak to Moderately Strong, Coating; Dark grey, Clay traces of sand, Stiff, NP) White sand sized specks	Dry	-41.1497	174.8537		
6	SR	72	258	236	F	Ro3	Wide	150mm	~60%	0	C	~150°	Gentle	~6m	Wavy	~5m		Matrix supported (Mosaic (~60%) Angular, CW, Very weak, Coating; Dark grey, clayey Sand and traces of gravels, Firm, NP) White sand sized specks	Dry	-41.1498	174.8538	Terminates against SR5	
7	SR	73	227	205	F	Ro3	Very wide	200mm	~50%	0	C	~170°	Gentle	~6m	Wavy	~6m		Matrix supported (Mosaic (~50%) Angular, CW, Very weak, Coating; Dark grey, silty Clay and traces of gravels, Stiff, LP to MP) White sand sized specks	Dry	-41.1497	174.8538	Continuous	
8	BSH	75	227	205	F	Ro3	Moderately wide	30mm	~80%	0	C	~120°	Open	~5m	Wavy	~6m	~0.6m	Clast supported (Crackle (~80%) Angular, CW, Weak, Coating; Dark grey, sandy Clay, Soft to stiff, NP) No precipitation visible	Dry	-41.1498	174.854	Terminates against SR9	
8	BSH	82	200	178	F	Ro3	Moderately wide	30mm	~80%	0	C	~120°	Open	~5m	Wavy	~6m	~0.6m	Clast supported (Crackle (~80%) Angular, CW, Weak, Coating; Dark grey, sandy Clay, Soft to stiff, NP) No precipitation visible	Dry	-41.1498	174.8539	Terminates against SR9	
9	FL	44	226	204	F	Ro3	Moderately wide	30mm	~99%	0	C	~180°	Gentle	~5m	Planar	~8m		Clast supported (Rock (~99%) Angular, HW, Moderately strong, Coating; Dark grey, sandy Clay, Soft to stiff, NP) No precipitation visible	Dry	-41.1498	174.8539	Cross cuts BSH10	
10	BSH	61	77	55	F	Ro2	Wide	100mm	~99%	0	C	~120°	Gentle	~5m	Wavy	~7m	~0.6m	Clast supported (Rock (~99%) Angular, HW, Moderately strong, Coating; Dark grey, sandy Clay, Soft to stiff, NP) No precipitation visible	Dry	-41.1498	174.8541	Cross cuts SR9	
10	BSH	49	83	61	F	Ro3	Wide	100mm	~85%	0	C	~120°	Gentle	~15m	Wavy	~7m	~0.6m	Clast supported (Crackle (~85%) Angular, HW, Weak, Coating; Dark grey, sandy Clay, Soft to stiff, NP) No precipitation visible	Dry	-41.1499	174.8542	Cross cuts SR9	
11	BSH	69	89	67	F	Ro2	Very wide	300mm	~80%	0	C	~170°	Gentle	~30m	Curved	~7m	~1m	Clast supported (Crackle (~80%) Angular, HW, Weak, Coating; Dark grey, silty Clay, Firm, HP) No precipitation visible	Dry	-41.1499	174.8542	Cross cuts SR12	
11	BSH	45	74	52	E&F	Ro2	Very wide	300mm	~80%	0	C	~170°	Gentle	~30m	Curved	~7m	~0.6m	Clast supported (Crackle (~80%) Angular, HW, Weak, Coating; Dark grey, sandy Clay, Firm, HP) No precipitation visible	Dry	-41.1499	174.8544	Cross cuts SR12	
12	SR	75	134	112	E	Ro2	Wide	30mm	~80%	0	C	~150°	Gentle	~10m	Wavy	~8m		Clast supported (Crackle (~80%) Angular, HW, Weak, Coating; Dark grey, sandy Clay, Firm, HP) No precipitation visible	Dry	-41.1499	174.8543	Cross cuts BSH11 and SR13	
13	SR	71	240	218	E	Ro3	Moderately wide	40mm	~90%	0	C	~170°	Gentle	~8m	Wavy	~7m		Clast supported (Crackle (~90%) Angular, HW, Weak to Moderately Strong, Coating; Dark grey brown, sandy Clay, Soft, NP) No precipitation visible	Dry	-41.1498	174.8543	Terminates against BSH11 and cross cuts BSH11	
14	SR	84	234	212	E	Ro2	Wide	80mm	~95%	0	S	~150°	Gentle	~10m	Wavy	~7m		Clast supported (Crackle (~95%) Angular, HW, Weak to Moderately Strong, Coating; Dark orangey brown, sandy Clay, Soft to stiff, NP) No precipitation visible	Dry	-41.1498	174.8545	Cross cuts BSH11 and SR15	
14B	SR	80	258	236	E	Ro2	Wide	80mm	~95%	0	S	~150°	Gentle	~10m	Wavy	~7m		Clast supported (Crackle (~95%) Angular, HW, Weak to Moderately Strong, Coating; Dark orangey brown, sandy Clay, Soft to stiff, NP) No precipitation visible	Dry	-41.1498	174.8545	Cross cuts BSH11 and SR15	
15	SR	47	171	149	E	Ro4	Narrow	4mm	~95%	1	D	~145°	Gentle	~40m	Irregular	~4m		Clast supported (Crackle (~95%) Angular, HW, Weak to moderately strong, Coating; Grey, sandy Clay, Soft to stiff, NP) No precipitation visible	Dry			Cross cuts SR14, BSH11 and SR17	
16	SR	21	238	216	E	Ro3	Wide	100mm	~80%	1	D	~145°	Gentle	~30m	Curved	~4m		Clast supported (Crackle (~80%) Angular, HW, Weak, Coating; Dark grey, silty Clay with traces of Sand, Firm, HP) No precipitation visible	Dry	-41.15	174.8545	Cross cuts BSH11 and terminates against SR19	
	JN	50	185	163	E	Ro2	Very wide	300mm	~80%	0	C	~170°	Gentle	~30m	Curved	~1m	~0.2m	Clast supported (Crackle (~80%) Angular, HW, Weak, Coating; Dark grey, silty Clay with traces of Sand, Firm, HP) No precipitation visible	Dry	-41.1499	174.8545		
18	BSH	67	80	58	E	Ro3	Very wide	300mm	~90%	0	C	~170°	Gentle	~10m	Wavy	~4m	~0.6m	Clast supported (Crackle (~90%) Angular, HW, Weak, Coating; Dark brown grey, sandy Clay, Soft to stiff, NP) No precipitation visible	Dry	-41.1499	174.8545	Offset by Horizontal Fault spanning ~50m	
18	BSH	56	74	52	E	Ro3	Very wide	300mm	~90%	0	C	~170°	Gentle	~10m	Wavy	~3m	~0.6m	Clast supported (Crackle (~90%) Angular, HW, Weak, Coating; Dark brown grey, sandy Clay, Soft to stiff, NP) No precipitation visible	Dry	-41.1498	174.8544	Offset by Horizontal Fault spanning ~50m	
19	SR	75	142	120	D&E	Ro3	Moderately wide	30mm	~95%	1	D	~180°	Gentle		Planar	~4m	~1.6m	Clast supported (Crackle (~95%) Angular, HW, Weak, Coating; Dark brown grey, sandy Clay, Soft to stiff, NP) No precipitation visible	Dry	-41.1499	174.8546	Terminates against BSH18	
21	SR	30	74	52	D	Ro3	Moderately wide	40mm	~95%	1	D	~170°	Gentle	~15m	Wavy	~5m		Clast supported (Crackle (~95%) Angular, HW, Weak to moderately strong, Coating; Dark grey brown, sandy Clay, Soft to stiff, NP) No precipitation visible	Dry			Terminates against BSH18 and cross cuts SR22	
22	SR	83	245	223	D	Ro3	Moderately wide	50mm	~95%	1	D	~140°	Gentle	~7m	Curved	~5m	~2m	Clast supported (Crackle (~95%) Angular, HW, Weak to moderately strong,	Dry	-41.1499	174.8547	Terminates against BSH18 and	

23	SR	85	140	118	D	Ro3	Moderately narrow	15mm	~50%	0	C	~160°	Gentle	~6m	Wavy	~5m		Coating; Dark brown, sandy Clay, Soft to stiff, NP) No precipitation visible Matrix supported (Mosaic (~50%) Angular, CW, Very Weak, Veneer; Dark brown, sandy Clay with traces of Gravels, Soft to stiff, NP) No precipitation visible	Dry	-41.15	174.8548	cross cuts SR21. Offsets SR24
24	BSH	63	195	173	D	Ro3	Wide	100mm	~95%	1	C	~140°	Gentle	~8m	Curved	~3m	~0.5m	Clast supported (Crackle (~95%) Angular, HW, Weak to moderately strong, Coating; Orangey brown, sandy Clay, Soft to stiff, NP) No precipitation visible	Dry	-41.1499	174.8547	offset by 22 and cross cuts SR23
24	BSH	54	204	182	D	Ro3	Wide	100mm	~95%	1	C	~140°	Gentle	~8m	Curved	~5m	~0.5m	Clast supported (Crackle (~95%) Angular, HW, Weak to moderately strong, Coating; Orangey brown, sandy Clay, Soft to stiff, NP) No precipitation visible	Dry	-41.1499	174.8547	Offset by 23 and cross cuts SR26
25	SR	86	177	155	D	Ro3	Moderately wide	50mm	~95%	0	C	~140°	Gentle	~30m	Curved	~4m		Clast supported (Crackle (~95%) Angular, HW, Weak to moderately strong, Coating; Dark brown, sandy Clay, Soft to stiff, NP) No precipitation visible	Dry	-41.1499	174.8547	Offset by 24
26	SR	82	13	351	D	Ro3	Moderately narrow	8mm	~99%	1	D	~180°	Gentle		Planar	~5m		Clast supported (Rock (~99%) Angular, HW, Strong, Coating; Dark orangey brown, Sand, Soft, NP) No precipitation visible	Dry	-41.1501	174.8549	Cross cuts BSH24, SR23 and offset by SR22. Terminates against SR22
	JN	58	197	219	D	Ro3	Moderately narrow to Moderately wide	20mm	gapped	0	C	~160°	Gentle	~8m	Wavy	~1m	~0.2m		Dry	-41.15	174.8547	
	FL	55	185	163	D															-41.1499	174.8538	
1	SR	44	237	215	D	Ro3	Wide	~70mm	~50%	0	O	~120°	Open	~5m	Wavy	~8m		Matrix supported (Mosaic (~50%) Angular, HW, Very weak, Coating; Orange brown and White, silty Sand, Stiff, NP) White, sand sized precipitation	Dry	-41.1505	174.8545	Splits
2	SR	61	121	99	D	Ro3	Moderately wide	~50mm	~75%	1	D	~120°	Open	~5m	Wavy	~8m		Clast supported (Crackle (~75%) Angular, MW, Very weak, Coating; Orange brown and White, silty Sand, Stiff, NP) White, sand sized precipitation	Dry	-41.1506	174.8547	Splits terminates against SR7
3	SR	75	22	0	F	Ro3	Moderately wide to Wide	~60mm	~90%	0	C	~150°	Gentle	~20m	Wavy	~7m		Clast supported (Crackle (~90%) Angular, MW, Weak, Coating; Orange brown, silty Sand, Stiff, NP) White, Strong, tabulated, sub angular gravel sized clasts	Dry	-41.1506	174.8546	Offset by CZ6 and SR2
4	SR	89	286	264	F	Ro4	Wide	~100mm	~80%	0	C	~150°	Gentle	~6m	Wavy	~6m		Clast supported (Crackle (~80%) Angular, HW, Weak, Coating; Orange brown and Dark grey (Clay), silty Sand and Clay, Soft, NP and HP (Clay)) White, Strong, tabulated, sub angular gravel sized clasts	Dry	-41.1505	174.8545	Cross cuts SR5
5	SR	79	272	250	F	Ro4	Wide	~100mm	~95%	1	D	~150°	Gentle		Irregular	~3m	~2m	Clast supported (Crackle (~95%) Angular, MW, Weak to Moderately strong, Coating; Orange brown, silty Sand, Soft, NP) White, Strong, tabulated, sub angular gravel sized clasts	Dry	-41.1505	174.8545	Cross cuts SR4 and terminates against CZ6
5B	SR	70	26	4	F	Ro3	Very wide to Wide	~200mm	~90%	1	D	~100°	Open		Irregular	~1.2m	~2m	Clast supported (Crackle (~90%) Angular, HW, Weak to Moderately strong, Coating; Orange brown and Dark grey (Clay), silty Sand and Clay, Stiff, NP an MP(Clays)) White, Strong, tabulated, sub angular gravel sized clasts	Dry	-41.1505	174.8545	Terminates against CZ6
6	CZ	33	230	208	F	Ro3	Very wide to Wide	~200mm	~90%	0	D	~120°	Open	~10m	Wavy	~10m		Clast supported (Crackle (~90%) Angular, HW, Weak to Strong, Coating; Orange brown and Dark grey (Clay), silty Sand and Clay, Stiff, NP an MP(Clays)) White, Strong, tabulated, sub angular gravel sized clasts	Dry	-41.1505	174.8543	Cross cuts bedding and offsets a number of SR's
6B	FL	69	30	8	F	Ro3	Wide	~80mm	~75%	0	C	~120°	Open	~3m	Wavy	~7m		Clast supported (Crackle (~75%) Angular, CW, Weak, Coating; Orange brown, silty Sand and Clay, Stiff, NP) White, Moderately strong, tabulated, sub angular gravel sized clasts	Dry	-41.1505	174.8544	Cross cuts CZ6
7	SR	72	310	288	F	Ro3	Wide	~120mm	~90%	1	D	~100°	Open	~6m	Wavy	~6m		Clast supported (Crackle (~90%) Angular, HW, Moderately strong, Coating; Orange brown, Clay, Soft, NP) White, Moderately strong, elongated, sub angular gravel sized clasts	Dry	-41.1505	174.8544	Terminate against FL6
8	SR	38	136	114	F	Ro3	Moderately wide	~30mm	~99%	2	D	~150°	Gentle	~6m	Curved	~8m	~5m	Clast supported (Rock (~99%) Angular, MW, Weak, Coating) No precipitation	Dry	-41.1504	174.8543	Terminates against Bedding and CZ6
9	BSH	89	45	23	F	Ro3	Moderately wide	~30mm	~95%	1	D	~150°	Gentle	~1m	Wavy	~6m		Clast supported (Crackle (~95%) Angular, HW, Very weak, Coating; Dark blue black, silty Clay, Soft, LP) No precipitation	Dry	-41.1504	174.8544	Offset by SR8 and some terminate against FL11
10	SR	82	254	232	F	Ro2-1	Wide	~120mm	~80%	1	D	~160°	Gentle	~10m	Wavy	~6m	~0.7m	Clast supported (Crackle (~80%) Angular, CW, Weak, Coating; Dark blue black, silty Clay with traces of sand, Soft, LP) White, sand sized precipitation	Damp	-41.1504	174.8543	Terminates against SR8
10B	SR	60	270	248	F	Ro3	Wide	~100mm	~95%	1	D	~100°	Open	~5m	Wavy	~5m	~0.7m	Clast supported (Crackle (~95%) Angular, HW, Moderately strong, Coating; Dark blue black, Silt with traces of sand, Soft, LP) White, Weak, tabulated, sub angular gravel sized clasts	Dry	-41.1505	174.8543	Terminates against SR8
11	FL	79	253	231	F	Ro2	Very wide	~300mm-1000mm	~80%	0	C	~180°	Gentle		Planar	~8m		Clast supported (Crackle (~80%) Angular, CW-HW, Weak to Very weak (White clasts), Coating; Dark blue black, silty Sand, Soft to Very soft, NP) White lenses of Strong, angular precipitation	Dry	-41.1504	174.8541	Continuous
11B	SR	45	263	241	F	Ro3	Moderately wide	~30mm	~90%	1	D	~90°	Open	~1m	Wavy	~2m		Clast supported (Crackle (~90%) Angular, HW, Weak, Coating; Dark blue black, silty Sand, Soft to Very soft, NP) White, sand sized precipitation	Dry	-41.1504	174.8541	Terminates against FL11
12	BSH	86	21	359	F	Ro2	Wide	~100mm	~90%	0	C	~90°	Open	~12m	Wavy	~7m	~1m	Clast supported (Crackle (~90%) Angular, HW, Moderately strong, Coating; Dark blue black, silty Sand, Soft to Very soft, NP) No precipitation	Dry	-41.1504	174.854	Offset by SR14
13	SR	88	32	10	F	Ro3	Wide	~130mm	~95%	0	C	~100°	Open	~6-8m	Wavy	~7m		Clast supported (Crackle (~95%) Angular, HW-MW, Weak to Moderately strong, Coating; Light brown grey, Silt with traces of clay and sand, Soft to Very soft, NP) No precipitation	Dry	-41.1504	174.8538	Cross cuts SR14 and multiple others
14	SR	22	119	97	F	Ro3	Moderately wide to Moderately narrow	~20mm	~99%	1	D	~160°	Gentle	~8m	Wavy	~13m	~2.5m	Clast supported (Rock (~99%) Angular, MW, Weak, Coating) No precipitation	Dry	-41.1504	174.8541	Terminates against FL11
15	SR	81	336	314	F	Ro3	Wide	~100mm	~95%	2	D	~110°	Open	~8m	Wavy	~5m		Clast supported (Crackle (~95%) Angular, MW, Moderately strong, Coating; Light brown grey, Silt with traces of clay and sand, Soft to Very soft, NP) White clasts that has been crushed to soil (Clay) precipitation	Dry	-41.1505	174.8538	Terminates against SR13 and SR14
15B	SR	73	31	9	F	Ro2	Wide	~100mm	~80%	0	C	~150°	Gentle	~8m	Wavy	~7m		Clast supported (Crackle (~80%) Angular, HW, Weak to Moderately strong, Coating; Light brown grey, Silt with traces of clay and sand, Soft to Very soft, NP) White, gravel sized, elongated sub angular to angular precipitation	Dry	-41.1503	174.8539	Cross cuts SR14

16	SR	54	232	210	F	Ro4	Very wide	~300mm	~90%	0	C	~130°	Gentle	~6m	Wavy	~7m	~3m	Clast supported (Crackle (~90%) Angular, HW-MW, Weak to Moderately strong, Coating; Light brown grey, Silt with traces of clay and sand, Soft to Very soft, NP) White, Strong, tabulated, sub angular gravel sized clasts	Dry	-41.1503	174.8537	Cross cuts SR14
16B	SR	79	255	233	F	Ro3	Very wide	~1000mm	~90%	0	C	~130°	Gentle	~8m	Wavy	~7m	~3m	Clast supported (Crackle (~90%) Angular, HW, Very weak to Weak, Coating; soil Light brown grey, Silt with traces of clay and sand, Soft to Very soft, NP) Lots of White, gravel sized, elongated sub angular to angular precipitation	Dry	-41.1503	174.8537	Cross cuts SR14
17B	SR	70	325	303	F	Ro3	Very wide	~300mm	~90%	0	C	~130°	Gentle		Stepped	~7m		Clast supported (Crackle (~90%) Angular, HW, Very weak, Coating; Light brown grey, Silt with traces of clay and sand, Soft to Very soft, NP) Lots of White, gravel sized, elongated sub angular to angular precipitation	Dry	-41.1502	174.8536	Cross cuts SR14
17	FL	85	259	236	F	Ro3	Very wide	~400mm-1000mm	~75%	0	C	~140°	Gentle	~30m	Wavy	~8m		Clast supported (Crackle (~75%) Angular, CW-HW, Very weak, Coating; Dark blue black, Silt with traces of clay and sand, Soft to Very soft, NP) Some randomly spaced specks of white precipitation	Dry	-41.1502	174.8535	
18	BSH	81	356	334	F	Ro3	Wide	~100mm	~90%	0	C	~150°	Gentle		Stepped	~7m	~0.8m to ~1.2m	Clast supported (Crackle (~90%) Angular, HW, Moderately strong, Coating; Light brown grey, Silt with traces of clay and sand, Soft to Very soft, NP) No precipitation	Dry	-41.1502	174.8534	Offset by SR19 and SR20
18B	SR	56	8	346	F	Ro4	Moderately narrow	~10mm	~90%	0	C	~150°	Gentle	~10m	Wavy	~2.5m		Clast supported (Crackle (~90%) Angular, HW, Weak, Coating; Light grey, Silt with traces of clay and sand, Soft to Very soft, NP) Some randomly spaced specks of white precipitation	Dry	-41.1502	174.8534	Offset by SR19 and SR20
19	SR	85	14	352	E&F	Ro4	Moderately narrow	~10mm	~95%	1	R	~150°	Gentle		Stepped	~5m		Clast supported (Crackle (~95%) Angular, HW, Weak, Coating; Light grey, Silt with traces of clay and sand, Soft to Very soft, NP) No precipitation	Dry	-41.1502	174.8533	Terminates against FL17
20	SR	85	99	77	E	Ro3	Wide	~80mm	~80%	1	R	~150°	Gentle	~1.5m	Wavy	~4m		Clast supported (Crackle (~80%) Angular, HW, Weak, Coating; Light grey brown, Silt with traces of clay and sand, Soft to Very soft, NP) No precipitation	Dry	-41.1502	174.8534	Terminates against FL17
21	BSH	73	289	267	E	Ro2	Very wide to Wide	~200mm	~90%	0	C	~150°	Gentle	~7m	Wavy	~6m	~0.8m	Clast supported (Crackle (~90%) Angular, HW, Weak, Coating; Light grey brown, Silt with traces of clay and sand, Soft to Very soft, NP) White lenses of Strong, angular precipitation	Dry	-41.1502	174.8533	Offset by SR19 and SR20
21	BSH	76	293	271	E	Ro2	Very wide to Wide	~200mm	~90%	0	C	~150°	Gentle	~7m	Wavy	~4.5m	~0.8m	Clast supported (Crackle (~90%) Angular, HW, Weak, Coating; Light grey brown, Silt with traces of clay and sand, Soft to Very soft, NP) some White lenses of Strong, angular precipitation	Dry	-41.1502	174.8533	Offset by SR19 and SR20
21B	SR	87	328	306	E	Ro2	Moderately wide	~50mm	~95%	1	D	~150°	Gentle	~7m	Wavy	~2.5m		Clast supported (Crackle (~95%) Angular, HW, Weak, Coating; Light grey brown, Silt with traces of clay and sand, Soft to Very soft, NP) Small amounts of white lenses of Strong, angular precipitation	Dry	-41.1502	174.8532	Terminates against SR20
21	BG	77	300	278	E															-41.1502	174.8533	
22	SR	54	31	9	E	Ro3	Moderately wide to Wide	~60mm	~75%	0	O	~100°	Open	~2m	Wavy	~3m		Clast supported (Crackle (~75%) Angular, HW, Weak, Coating; Orange brown, Sand, Stiff, NP) White, sand sized precipitation	Dry	-41.1507	174.8548	
23	SR	75	30	8	E	Ro3	Wide	~100mm	~75%	0	O	~120°	Open	~5m	Wavy	~2.5m		Clast supported (Crackle (~75%) Angular, HW, Weak, Coating; Orange brown, Sand, Stiff, NP) White, sand sized precipitation	Dry	-41.1506	174.8547	
1	BSH	38	68	46	E	Ro4	Very wide	~500mm	~85%	0	C	~150°	Gentle	~4m	Wavy	~2m	~2m	Clast Supported (Crackle (~85%), Angular, HW-CW, Very weak, Coating; Light and dark grey white, Sand and Clay, Very soft, NP) No precipitation	Dry	-41.1506	174.8552	Cross cuts SR2 and SR3
1	BSH	37	61	39	E	Ro4	Very wide	~500mm	~85%	0	C	~150°	Gentle	~4m	Wavy	~2.4m	~2m	Clast Supported (Crackle (~85%), Angular, HW-CW, Very weak, Coating; Light and dark grey white, Sand and Clay, Very soft, NP) No precipitation	Dry	-41.1506	174.8552	Cross cuts SR2 and SR3
1	BSH	58	18	356	E	Ro4	Very wide	~500mm	~85%	0	C	~150°	Gentle	~4m	Wavy	~3m	~2m	Clast Supported (Crackle (~85%), Angular, HW-CW, Very weak, Coating; Light and dark grey white, Sand and Clay, Very soft, NP) No precipitation	Dry	-41.1507	174.8552	Cross cuts SR6
2	SR	71	236	214	E	Ro2	Wide	~80mm	~95%	1	O	~180°	Gentle		Planar	~2m		Clast Supported (Crackle (~95%), Angular, HW, Weak, Veener; Light grey white, Sand and Clay, Very soft, NP) No precipitation	Dry	-41.1506	174.8553	Terminates in sandstone rock and cross cuts BSH1
3	SR	77	29	7	E	Ro3	Moderately wide	~40mm	~95%	1	S	~180°	Gentle	~2m	Wavy	~2.6m		Clast Supported (Crackle (~95%), Angular, HW, Weak, Coating; Light brown, Sand and Clay, Very soft, NP) No precipitation	Dry	-41.1506	174.8552	Terminates in sandstone rock
4	SR	33	123	101	D&E	Ro3	Wide to Moderately wide	~50-60mm	~95%	1	S	~180°	Gentle		Planar	~6m		Clast Supported (Crackle (~95%), Angular, HW, Very weak, Coating; Light grey white, Sand, Soft, NP) No precipitation	Dry	-41.1506	174.8551	Terminates against BSH1 and splits. Cross cuts SR6
5	SR	51	45	23	D	Ro3	Moderately wide	~50mm	~90%	0	C	~150°	Gentle	~5m	Wavy	~2m		Clast Supported (Crackle (~90%), Angular, HW, Weak to Very weak, Coating; Light brown grey, sandy Clay, Soft to Firm, NP) Elongated, white, sub angular gravel sized clasts of precipitation	Dry	-41.1505	174.8552	Offset by SR4 80cm.
6	SR	73	231	209	D	Ro3	Wide to Moderately wide	~50-60mm	~75%	0	S	~160°	Gentle	~10m	Wavy	~5m		Clast Supported (Crackle (~75%), Angular, HW-MW, Weak, Coating; Light grey white, Sand, Soft, NP) No precipitation	Dry	-41.1505	174.855	Cross cuts SR4, BSH1 and SR6 Splits into SR7
7	SR	74	276	254	D	Ro3	Wide to Moderately narrow	~20mm	~99%	1	D	~100°	Open	~2m	Wavy	~1.8m		Clast Supported (Rock (~99%), Angular, MW, Moderately strong, Veener; Dark brown, Sand and Clay, Soft, LP-NP) No precipitation	Dry	-41.1505	174.8549	Terminates against SR6
8	SR	71	51	29	D	Ro3	Wide	~100mm	~95%	0	C	~150°	Gentle	~3m	Wavy	~7m		Clast Supported (Crackle (~95%), Angular, HW, Moderately strong, Coating; Light brown grey, Sand, Soft, NP) No precipitation	Dry	-41.1505	174.855	Offset by SR6 by about 30cm. Cross cuts BSH10
9	SR	71	44	22	D	Ro3	Wide	~100mm	~99%	0	C	~150°	Gentle	~6m	Wavy	~2m	~1.4m	Clast Supported (Rock (~99%), Angular, MW, Moderately strong to Strong, brown grey, Clay, Soft, NP) No precipitation	Dry	-41.1504	174.8549	Offset by SR6 by about 30cm
10	BSH	68	24	2	D	Ro2	Very wide	~300mm	~70%	0	C	~160°	Gentle	~12m	Curved	~6m		Matrix Supported (Mosaic (~70%), Angular, CW, Very weak, Coating; Dark black blueish grey, clayey Sand, Soft, LP-NP) No precipitation	Dry	-41.1504	174.8548	Crush material, offset by a SR8 that is horizontal by ~30cm. Cross cuts SR41
10	BSH	81	57	35	D	Ro2	Very wide	~300mm	~70%	0	C	~160°	Gentle	~12m	Curved	~6m		Matrix Supported (Mosaic (~70%), Angular, CW, Very weak, Coating; Dark black blueish grey, clayey Sand, Soft, LP-NP) No precipitation	Dry	-41.1504	174.8548	Crush material, offset by a SR8 that is horizontal by ~30cm.
11	SR	74	46	24	D&E	Ro3	Wide	~150mm	~90%	0	C	~160°	Gentle	~8m	Wavy	~6m		Clast Supported (Crackle (~90%), Angular, HW, Moderately strong to Weak, Coating; Light brown grey, clayey Sand, Soft, NP) No precipitation	Dry	-41.1504	174.8548	
12	SR	32	95	73	E	Ro3	Moderately narrow	~10mm	~99%	0	C	~160°	Gentle		Planar	~6.5m		Clast Supported (Rock (~99%), Angular, HW-MW, Moderately strong to Weak, brown grey, clayey Sand, Soft, NP) No precipitation	Dry	-41.1504	174.8548	Cross cuts SR16 and SR15

C40 SB B2

13	SR	35	135	113	E	Ro3	Moderately narrow	~10mm	~99%	0	C	~160°	Gentle		Planar	~7m		Clast Supported (Rock (~99%),Angular, HW-MW, Moderately strong to Weak, brown grey, clayey Sand, Soft, NP) No precipitation	Dry	-41.1504	174.8548	Cross cuts SR15 and SR16 terminates against SR19
14	SR	27	92	70	E	Ro3	Moderately wide	~40mm	~95%	1	D	~160°	Gentle	~10m	Curved	~2.4m		Clast Supported (Crackle (~95%),Angular, HW, Weak, Coating; Light brown grey, clayey Sand, Soft, NP) No precipitation	Dry	-41.1504	174.8547	Terminates against SR15
15	SR	81	53	31	E	Ro3	Wide	~100mm	~99%	0	C	~160°	Gentle	~10m	Wavy	~7m		Clast Supported (Rock (~99%),Angular, HW, Moderately strong to Weak, Coating; Light brown grey, clayey Sand, Soft, NP) No precipitation	Dry	-41.1504	174.8546	Cross cuts SR13 and SR12
15	SR	75	64	42	E	Ro3	Wide	~100mm	~99%	0	C	~160°	Gentle	~10m	Wavy	~7m		Clast Supported (Rock (~99%),Angular, HW, Moderately strong to Weak, Coating; Light brown grey, clayey Sand, Soft, NP) No precipitation	Dry	-41.1504	174.8547	Cross cuts SR13 and SR12
16	SR	77	43	21	E	Ro3	Wide	~150mm	~95%	0	C	~180°	Gentle		Planar	~6m		Clast Supported (Crackle (~95%),Angular, HW, Weak, Coating; Light brown, Sand, Soft, NP) No precipitation	Dry	-41.1504	174.8546	Cross cuts SR13 and SR12
17	SR	74	124	102	E	Ro3	Moderately wide	~40mm	~80%	1	D	~135°	Gentle	~10m	Wavy	~4m		Clast Supported (Crackle (~80%),Angular, CW, Very weak to Weak, Coating; Light orange brown, Sand and Clay, Soft, NP) No precipitation	Dry	-41.1504	174.8545	Terminates against SR18
18	SR	84	57	35	E	Ro3	Very narrow to Tight	~0-1mm	~1%	1	D	~180°	Gentle		Planar	~3m		Matrix Supported (Soil (~1%),Angular, HW-MW, Moderately strong to Weak, Coating; Light orange brown, Clay, Soft, NP) Specks of Sand sized white precipitation	Dry	-41.1504	174.8545	Cross cuts SR14
19	SR	82	10	348	E	Ro3	Wide	~100mm	~90%	0	S	~145°	Gentle	~8m	Wavy	~8m	~2.5m	Clast Supported (Crackle (~90%),Angular, HW, Weak, Coating; Brown, sandy Clay, Soft, NP) No precipitation	Dry	-41.1502	174.8543	Splits
20	BSH	62	243	221	E	Ro3	Wide	~150mm	~80%	0	O	~145°	Gentle	~10m	Curved	~8m		Clast Supported (Crackle (~80%),Angular, HW, Weak, Coating; Light and dark blueish grey , sandy Clay, Soft, NP) No precipitation	Dry	-41.1503	174.8541	Continuous
21	FL	77	269	247	E	Ro3	Very wide	~3000m	~80%	0	C	~170°	Gentle	~15m	Wavy	~7m		Clast Supported (Crackle (~80%),Angular, MW-CW, Weak and Strong (Blocks), Coating; Light and dark blueish grey , sandy Clay, Soft to Firm, NP) Elongated, white, sub angular, gravel sized precipitation randomly spaced	Dry	-41.1501	174.854	Continuous
22	SR	79	259	237	E	Ro3	Wide	~100mm	~99%	1	D	~160°	Gentle	~3m	Wavy	~2m	~1.2m	Clast Supported (Rock (~99%),Angular, HW, Weak, Coating;, Clay, Soft,) No precipitation	Dry	-41.1502	174.8539	Terminates at a SR
23	SR	70	217	195	E&F	Ro4	Wide to Moderately wide	~60mm	~95%	0	C	-	Gentle		Stepped	~4m	~1.2m	Clast Supported (Crackle (~95%),Angular, HW, Weak, Veener; Bluish grey, silty Clay with traces of sand, Soft, LP-NP) No precipitation	Dry	-41.1502	174.8537	Continuous and cross cuts SR41, SR26 and SR43
24	SR	86	263	241	F	Ro3	Wide to Moderately wide	~60mm	~95%	2	D	~140°	Gentle	~3m	Wavy	~1m	~0.8m	Clast Supported (Crackle (~95%),Angular, HW-CW, Very weak, Coating; Bluish grey, Clay, Soft, LP) No precipitation	Dry	-41.1502	174.8538	Terminates between BSH27 and SR23
25	SR	78	22	0	F	Ro3	Moderately wide	~40mm	~95%	2	D	~160°	Gentle	~2m	Wavy	~2.6m	~0.8m	Clast Supported (Crackle (~95%),Angular, HW, Weak, Coating; Bluish grey, silty Clay with traces of sand, Soft, LP-NP) Specks of Sand sized white precipitation	Dry	-41.1502	174.8537	Terminates between SR41 and SR23, cross cuts SR26
26	BSH	70	233	211	F	Ro3	Wide	~100mm	~90%	2	D	~140°	Gentle	~6m	Wavy	~5m	~0.5m	Clast Supported (Crackle (~90%),Angular, CW, Weak, Coating; Brownish grey, Sand and Clay, Soft, NP) No precipitation	Dry	-41.1501	174.8536	Terminates against SR41 and SR27
27	SR	69	256	234	F	Ro3	Moderately wide	~40mm	~95%	1	D	~160°	Gentle	~10m	Wavy	~3.5m	~0.8m	Clast Supported (Crackle (~95%),Angular, CW, Weak, Coating; Brownish orange and white grey, Sand and Clay, Soft, NP) No precipitation	Dry	-41.1501	174.8537	Cross cuts SR41 and terminates against bedding
28	SR	17	99	77	F	Ro3	Moderately wide to Moderately narrow	~20mm	~85%	1	D	~170°	Gentle	~10m	Wavy	~4m	~2.2m	Clast Supported (Crackle (~85%),Angular, CW, Weak, Coating; Brownish orange, Sand and Clay, Soft, NP) No precipitation	Dry	-41.1501	174.8537	Terminates against SR31
29	SR	71	31	9	F	Ro3	Wide	~100mm	~95%	1	D	~135°	Gentle	~6m	Wavy	~4m		Clast Supported (Crackle (~95%),Angular, HW, Weak, Coating; Bluish grey, Clay, Soft, LP) No precipitation	Dry	-41.15	174.8534	Cross cuts SR40 and terminates against FL33
30	SH	52	279	257	F	Ro3	Very wide	~>400mm	~95%	0	C	~170°	Gentle	~6m	Wavy	~5m		Clast Supported (Crackle (~95%),Angular, HW, Weak, Coating; Bluish grey, Clay, Soft, LP) No precipitation	Dry	-41.1501	174.8534	Cross cuts SR40
31	SR	72	238	216	F	Ro3	Wide	~>70mm	~95%	1	S	~120°	Open	~8m	Curved	~6m		Clast Supported (Crackle (~95%),Angular, HW, Weak, Coating; Bluish grey, Clay, Soft, LP) Specks of Sand sized white precipitation	Dry	-41.15	174.8534	Terminates at SR41 and splits.
32	BSH	83	287	265	F	Ro2	Wide to Moderately wide	~60mm	~95%	1	D	~140°	Gentle	~10m	Wavy	~2m	~0.6m	Clast Supported (Crackle (~95%),Angular, HW-CW, Very weak, Coating; Dark bluish grey, Clay with traces of sand, Soft, NP) Specks of Sand sized white precipitation	Dry	-41.1501	174.8532	Terminates at FL33
32	BSH	83	298	276	F	Ro2	Wide to Moderately wide	~60mm	~95%	1	D	~140°	Gentle	~10m	Wavy	~1.8m	~0.6m	Clast Supported (Crackle (~95%),Angular, HW-CW, Very weak, Coating; Dark bluish grey, Clay with traces of sand, Soft, NP) Specks of Sand sized white precipitation	Dry	-41.15	174.8532	Terminates at FL33
33	FL	55	212	190	F	Ro1-2	Very wide	~200mm	~60%	0	C	~180°	Gentle		Planar	~7m		Matrix Supported (Mosaic (~60%),Angular, HW-CW, Very weak, Coating; Dark blue black , Clay with traces of sand, Very soft, MP to HP in the clay seam) Specks of Sand sized white precipitation some tabulated material	Damp	-41.15	174.8531	Unknown offset and cross cuts SR40
34	FL	87	286	264	F	Ro3	Very wide	~200mm	~60%	1	D	~150°	Gentle	~3m	Wavy	~1.6m		Matrix Supported (Mosaic (~60%),Angular, CW, Weak to Moderately strong (blocks) , Coating; Dark blue black , Clay with traces of sand, Very soft, MP to HP in the clay seam) Tabulated, white, sub angular, gravel sized precipitation	Damp	-41.15	174.8532	Fault joins up with FL34
35	SR	78	308	286	F	Ro2	Very wide	~300mm	~80%	0	C	~90°	Open	~20m	Curved	~4.5m		Clast Supported (Crackle (~80%),Angular, CW, Very weak, Coating; Dark blue black grey , Clay with traces of sand, Very soft, HP clay seam) Tabulated, white, sub angular, gravel sized precipitation	Dry	-41.1499	174.8528	Continuous
36	FL	61	254	232	F	Ro1	Very wide	~300mm	~50%	0	C	~180°	Gentle		Planar	~3.5m		Matrix Supported (Mosaic (~50%),Angular, CW, Very weak, Coating; orange white brown sand , Sand, Stiff to Very stiff (Clay), HP clay seam) Tabulated, white, sub angular, gravel sized precipitation	Damp	-41.1499	174.8527	Joins up with BSH35
37	SR	28	132	110	F	Ro3	Very wide	~300mm	~85%	1	D	~180°	Gentle		Planar	~1.5m		Clast Supported (Crackle (~85%),Angular, HW, Weak, Coating; Light orange brown, clay and sand, Soft to Very soft, NP) No precipitation	Damp	-41.1498	174.8528	Cross cuts bedding and terminates against SR35
38	BSH	65	311	289	F	Ro3	Moderately wide	~50mm	~60%	0	C	~100°	Open	~2m	Wavy	~4m	~0.6m	Matrix Supported (Mosaic (~60%),Angular, CW, Weak to Moderately strong (blocks) , Coating; Dark blue black , clay some sand, Very soft, MP to HP in the clay seam) Tabulated, white, sub angular, gravel sized precipitation	Damp	-41.1499	174.853	Cross cuts SR39
38	BSH	63	300	278	F	Ro3	Moderately wide	~50mm	~60%	0	C	~100°	Open	~2m	Wavy	~4m	~0.6m	Matrix Supported (Mosaic (~60%),Angular, CW, Weak to Moderately strong (blocks) , Coating; Dark blue black , clay some sand, Very soft, MP to HP in	Damp	-41.1499	174.853	Cross cuts SR39

39	SR	59	160	138	F	Ro3	Moderately wide to Moderately narrow	~20mm	~75%	1	D	~180°	Gentle		Planar	~4m		the clay seam) Tabulated, white, sub angular, gravel sized precipitation	Damp	-41.15	174.8527	Terminates against Bedding and cross cuts BSH38
40	SR	79	337	315	F	Ro3	Moderately wide to Moderately narrow	~20mm	~90%	1	D	~150°	Gentle	~10m	Wavy	~4m		Clast Supported (Crackle (~75%),Angular, HW-CW, Very weak to Weak, Coating; Light brown, silty Sand, Very soft, NP) No precipitation	Damp	-41.1501	174.8531	Terminates against SR31 and cross cuts SR29, SR30 and FL33
41	SR	74	167	145	F	Ro3	Moderately wide to Moderately narrow	~20mm	~90%	1	D	~160°	Gentle	~4m	Wavy	~10m		Clast Supported (Crackle (~90%),Angular, HW-CW, Weak, brown, Sand, Soft, NP) No precipitation	Dry	-41.1501	174.8533	Cross cuts BSH26, SR31, SR27, SR23 and SR43. Terminates against FL21
42	SH	74	351	329	F	Ro3	Moderately wide to Moderately narrow	~20mm	~90%	1	D	~160°	Gentle	~3m	Wavy	~5m	~1.4m	Clast Supported (Crackle (~90%),Angular, HW-CW, Weak, orangey brown, silty Sand, Soft, NP) No precipitation	Dry	-41.1503	174.8538	Terminates at FL21 and cross cuts BSH26
43	SR	77	359	337	E&F	Ro3	Moderately wide to Moderately narrow	~20mm	~90%	1	D		Gentle		Stepped	~4m	~1.4m	Clast Supported (Crackle (~90%),Angular, HW-CW, Weak, Coating; Light orangey brown, Sand, Soft, NP) No precipitation	Dry	-41.1503	174.8538	Terminates against a SR
1	BSH	67	20	358	C	Ro3	Moderately wide	~30mm	~30%	1	D	~180°	Gentle		Planar	~1.5m	~1.2m	Matrix supported (Chaotic (~30%)Angular, HW, Very Weak, Coating; Light orange black, Sand, Soft, HP) No precipitation	Damp	-41.1523	174.8449	Terminates against SR9 and cross cuts SR2
2	SR	47	127	105	C	Ro2	Wide	~100mm	~95%	0	O	~170°	Gentle	~2m	Wavy	~6m	~1.4m	Clast supported (Crackle (~95%)Angular, MW, Weak , Veneer; Light orange black, silty Clay, Soft, NP) No precipitation	Dry	-41.1523	174.8448	Terminates against BSH6 and cross cuts SR7 and SR1
3	SR	54	8	346	C	Ro3	Moderately narrow	~5mm	~99%	0	C				Irregular	~5m	~1.2m	Clast supported (Rock (~99%)Angular, MW, Moderately strong, Veneer)	Dry	-41.1523	174.8449	Cross cuts SR2 and SR9
4	BSH	82	349	327	C	Ro3	Wide	~100mm	~95%	1	D	~170°	Gentle	~2.5m	Wavy	~4m	~0.6m	Clast supported (Crackle (~95%)Angular, HW, Weak , Veneer; Light orange brown, sandy Silt, Soft, NP) No precipitation	Dry	-41.1523	174.8449	Cross cuts SR2 and SR9. Terminates against SR5
5	SR	46	94	72	C	Ro3	Wide	~100mm	~99%	1	D	~170°	Gentle	~6m	Curved	~2m		Clast supported (Rock (~99%)Angular, HW, Weak , Veneer; Light grey, Silt, Very soft, NP) No precipitation	Dry	-41.1523	174.8448	Terminates against SR2 and cross cuts BSH4
5	SR	54	97	75	C	Ro3	Wide	~100mm	~99%	1	D	~170°	Gentle	~6m	Curved	~2m		Clast supported (Rock (~99%)Angular, HW, Weak , Veneer; Light grey, Silt, Very soft, NP) No precipitation	Dry	-41.1523	174.8449	Terminates against SR2 and cross cuts BSH4
6	SR	88	277	255	C	Ro3	Wide	~100mm	~90%	1	D	~180°	Gentle		Planar	~4m	~2m	Clast supported (Crackle (~90%)Angular, HW, Weak , Coating; Dark orange brown, Sand, Soft, NP) No precipitation	Dry	-41.1523	174.8448	Cross cuts BSH4 and SR9. Terminates against SR5
6	SR	88	285	263	C	Ro3	Wide	~100mm	~90%	0	O	~180°	Gentle		Planar	~4m	~2m	Clast supported (Crackle (~90%)Angular, HW, Weak , Coating; Dark orange brown, Sand, Soft, NP) No precipitation	Dry	-41.1523	174.8449	Cross cuts SR9.
7	SR	69	124	102	C	Ro2	Very Narrow	~1mm		1	D	~180°	Gentle		Planar	~2.5m			Dry	-41.1523	174.8449	Terminates against BSH4 and cross cuts SR9 and SR2
8	SR	56	268	246	C	Ro3	Moderately wide	~50mm	~95%	1	D	~180°	Gentle		Planar	~2m		Clast supported (Crackle (~95%)Angular, MW, Moderately strong, Coating; Dark brown, Sand, Very soft, NP) No precipitation	Dry	-41.1523	174.8448	Cross cuts SR6 and terminates against SR6
9	SR	10	117	95	C	Ro3	Moderately wide to Moderately narrow	~20mm	~95%	1	D	~170°	Gentle	~10m	Wavy	~20m		Clast supported (Crackle (~95%)Angular, MW, Moderately strong, Stained; Light brown, sandy Silt, Soft, NP) No precipitation	Dry	-41.1523	174.8448	Cross cuts SR3, SR7, BSH4, SR6, SR15, SR10, BSH11 and terminates against SR13
9	SR	7	129	107	C	Ro3	Moderately wide to Moderately narrow	~20mm	~95%	1	D	~170°	Gentle	~10m	Wavy	~20m		Clast supported (Crackle (~95%)Angular, MW, Moderately strong, Stained; Light brown, sandy Silt, Soft, NP) No precipitation	Dry	-41.1524	174.8448	Cross cuts SR3, SR7, BSH4, SR6, SR15, SR10, BSH11 and terminates against SR13
10	SR	50	18	356	C	Ro4	Moderately wide	~50mm	~99%	1	D	~150°	Gentle	~6m	Curved	~4m		Clast supported (Rock (~99%)Angular, MW, Moderately strong, Veneer; Light grey, Sand, Soft, NP) No precipitation	Dry	-41.1524	174.8447	Terminates against BSH11 and cross cuts
11	BSH	84	48	26	C	Ro4	Very wide to Wide	~200mm	~95%	0	C	~170°	Gentle	~2m	Wavy	~4m	~0.8m	Clast supported (Crackle (~95%)Angular, HW, Weak , Veneer; Light brown, sandy Silt, Soft, LP) No precipitation	Dry	-41.152	174.8454	Cross cuts SR9.
12	SR	85	326	304	C	Ro3	Wide	~100mm	~99%	1	D	~180°	Gentle		Planar	~1m		Clast supported (Rock (~99%)Angular, MW, Moderately strong, Coating; Light orange brown, Sand, Very soft, NP) No precipitation	Dry	-41.1525	174.8446	Terminates against SR9
13	BSH	78	26	4	C	Ro2	Very wide	~300mm	~95%	1	D	~150°	Gentle	~5m	Curved	~1.4m	~0.3m	Clast supported (Crackle (~95%)Angular, MW, Moderately strong, Coating; Light orange grey, Sand, Soft, LP) No precipitation	Dry	-41.1525	174.8446	Terminates against FL14
14	FL	77	228	206	B&C	Ro3	Very wide	~300mm	~95%	0	C	~170°	Gentle	~8m	Wavy	~6m		Clast supported (Crackle (~95%)Angular, HW, Strong to Weak, Coating; Light brown, sandy Silt, Soft, LP) Small white elongated lenses of precipitation	Dry	-41.1525	174.8445	Continuous
14	FL	83	229	207	B&C	Ro3	Very wide	~300mm	~95%	0	C	~170°	Gentle	~8m	Wavy	~6m		Clast supported (Crackle (~95%)Angular, HW, Strong to Weak, Coating; Light brown, sandy Silt, Soft, LP) Small white elongated lenses of precipitation	Dry	-41.1525	174.8444	Continuous
15	SR	59	15	353	B	Ro3	Tight to Very narrow	<1mm		0	C	~180°	Gentle		Planar	~4m			Dry	-41.1524	174.8447	Cross cuts SR10 and SR9
16	BSH	57	8	346	B	Ro2	Moderately narrow	~15mm	~95%	0	C	~180°	Gentle		Planar	~6m	~0.6m	Clast supported (Crackle (~95%)Angular, MW, Weak , Veneer; Dark brown, Sand, Soft, NP) Small white elongated lenses of precipitation	Dry	-41.1525	174.8447	Cross cuts SR17 and SR18
17	SR	40	19	357	B	Ro2	Moderately wide to Moderately narrow	~20mm	~99%	1	R	~150°	Gentle	~10m	Curved	~5m		Clast supported (Rock (~99%)Angular, MW, Weak , Veneer; Light brown, Sand, Very soft, NP) No precipitation	Dry	-41.1524	174.8447	Cross cuts BSH16 and SR18
18	SR	87	303	281	B	Ro3	Moderately wide to Moderately narrow	~200mm	~99%	0	C	~130°	Gentle	~8m	Wavy	~6m		Clast supported (Rock (~99%)Angular, MW, Weak , Stained; Light brown, sandy Silt, Very soft, NP) No precipitation	Dry	-41.1524	174.8445	Cross cuts BSH16 and SR19
18	SR	87	284	262	B	Ro3	Moderately wide to Moderately narrow	~200mm	~99%	0	C	~130°	Gentle	~8m	Wavy	~6m		Clast supported (Rock (~99%)Angular, MW, Weak , Stained; Light brown, sandy Silt, Very soft, NP) No precipitation	Dry	-41.1525	174.8445	Cross cuts BSH16 and SR19
19	SR	18	272	250	B	Ro2	Tight to Very narrow	<1mm		2	D	~180°	Gentle		Planar	~5m	~1m		Dry	-41.1526	174.8444	Terminates against BSH16 and BSH22. Cross cuts SR18,

C42 SB B2

21	BSH	86	18	356	B	Ro3	Wide	~100mm	~95%	1	D		Gentle		Irregular	~2.6m	~0.6m	Clast supported (Crackle (~95%)Angular, MW, Moderately strong, Veneer; light orange grey, Silt, Soft, NP) No precipitation	Dry	-41.1526	174.8443	SR17, BSH21 and BSH16 Cross cuts SR19 and terminates against SR23
22	BSH	87	28	6	B	Ro3	Wide	~80mm	~95%	1	R		Gentle		Stepped	~1.2m	~0.6m	Clast supported (Crackle (~95%)Angular, MW, Weak , Veneer; light orange grey, silty Sand trace of Clay, Soft, NP) Small white elongated lenses of precipitation	Dry	-41.1526	174.8443	Cross cuts SR19 and terminates against SR23
23	SR	47	280	258	A	Ro3	Very wide	~800mm	~90%	1	D		Gentle		Stepped	~2.2m	~0.4m	Clast supported (Crackle (~90%)Angular, HW, Weak , Coating; Light blue black, sandy Silt, Very soft, NP) Small white elongated lenses of precipitation	Dry	-41.1526	174.8443	Continuous
24	SR	89	283	261	A	Ro3	Very wide	~800mm	~80%	0	C	~180°	Gentle		Planar	~3m	~0.4m	Clast supported (Crackle (~80%)Angular, HW, Very Weak, Coating; Dark blue black, sandy Silt, Soft, NP) Small white elongated lenses of precipitation	Dry	-41.1526	174.8444	Cross cuts SR25
24	SR	54	284	262	A	Ro3	Very wide	~800mm	~80%	0	C	~180°	Gentle		Planar	~3m	~0.4m	Clast supported (Crackle (~80%)Angular, HW, Very Weak, Coating; Dark blue black, sandy Silt, Soft, NP) Small white elongated lenses of precipitation	Dry	-41.1526	174.8444	Cross cuts SR25
25	SR	87	311	289	A	Ro3	Moderately wide	~25mm	~99%	2	D	~180°	Gentle		Planar	~3m		Clast supported (Rock (~99%)Angular, MW, Moderately strong, Coating; light grey white, Sand, Soft, NP) Elongated, tabulated, white precipitation	Dry	-41.1526	174.8443	Cross cuts SR24, SR26 and SR27. Terminates against SR23
29	SH	67	92	70	A	Ro3	Very wide	~500mm	~85%	0	C	~180°	Gentle		Planar	~4m		Clast supported (Crackle (~95%)Angular, MW, Moderately strong, Veneer; light orange grey, Silt, Soft, NP) No precipitation	Dry	-41.1526	174.8442	Continuous
30	BSH	82	269	247	A	Ro3	Moderately wide	~30mm	~90%	1	D	~180°	Gentle		Planar	~2m	~0.6m	Clast supported (Crackle (~90%)Angular, HW, Weak , Veneer; Dark blue grey, sandy Silt, soft, NP) Small white sand sized specks of precipitation	Dry	-41.1526	174.844	Terminates against SH29
31	FL	63	168	146	A	Ro3	Wide	~100mm	~95%	2	D	~180°	Gentle		Planar	~4m		Clast supported (Crackle (~95%)Angular, HW, Weak to Very weak, Stained; Light orange brown, sandy Silt, Soft, NP) Small white elongated lenses of precipitation	Dry	-41.1526	174.8441	Terminates against BSH32 and a SR
32	BSH	86	271	249	A	Ro3	Wide	~100mm	~90%	0	C	~160	Gentle	~2.5m	Wavy	~2m	~0.6m	Clast supported (Crackle (~90%)Angular, HW, Weak , Veneer; Dark blue grey, sandy Silt, Very soft, NP) Small white sand sized specks of precipitation	Dry	-41.1527	174.8441	Continuous
32	BSH	89	284	262	A	Ro3	Wide	~100mm	~90%	0	C	~160	Gentle	~2.5m	Wavy	~2m	~0.6m	Clast supported (Crackle (~90%)Angular, HW, Weak , Veneer; Dark blue grey, sandy Silt, Very soft, NP) Small white sand sized specks of precipitation	Dry	-41.1527	174.8439	Continuous
32	BG	85	276	254	A	Ro3	Wide	~100mm	~90%	0	C	~170°	Gentle	~2.5m	Wavy	~2m	~0.6m	Clast supported (Crackle (~90%)Angular, HW, Weak , Veneer; Dark blue grey, sandy Silt, Very soft, NP) Elongated, tabulated, white precipitation	Dry	-41.1527	174.8439	Continuous

B.4 Transmission Gully South Graphs

Defect and rock mass results from Transmission Gully South. Results are presented in graphs. Where percentages are used they display the respective occurrence of the dependent variable assessed.

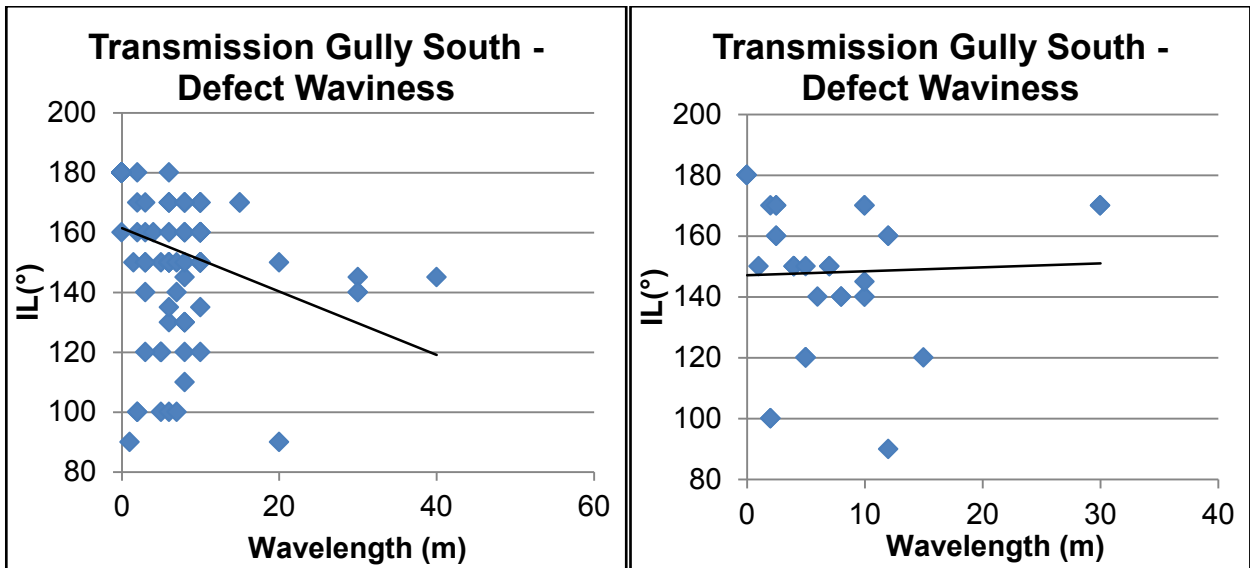
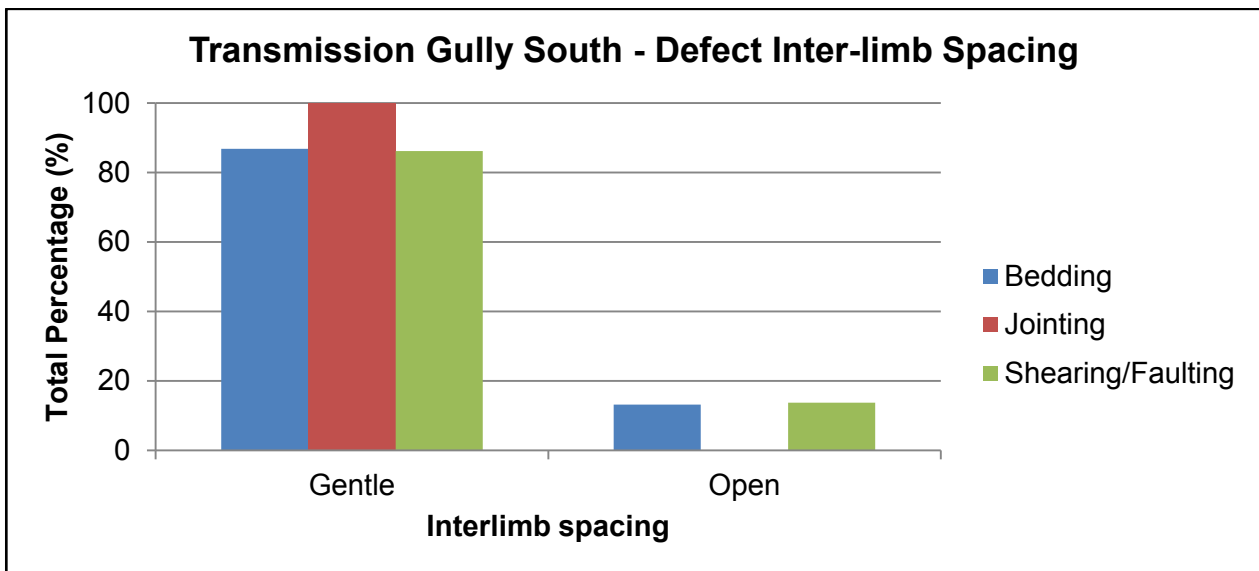
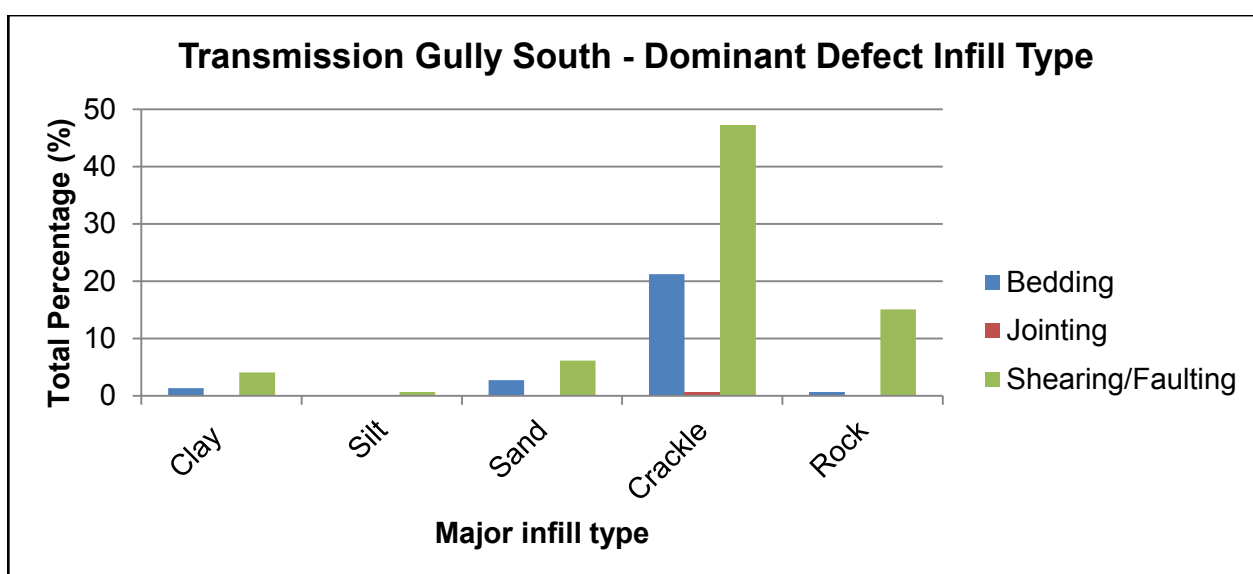
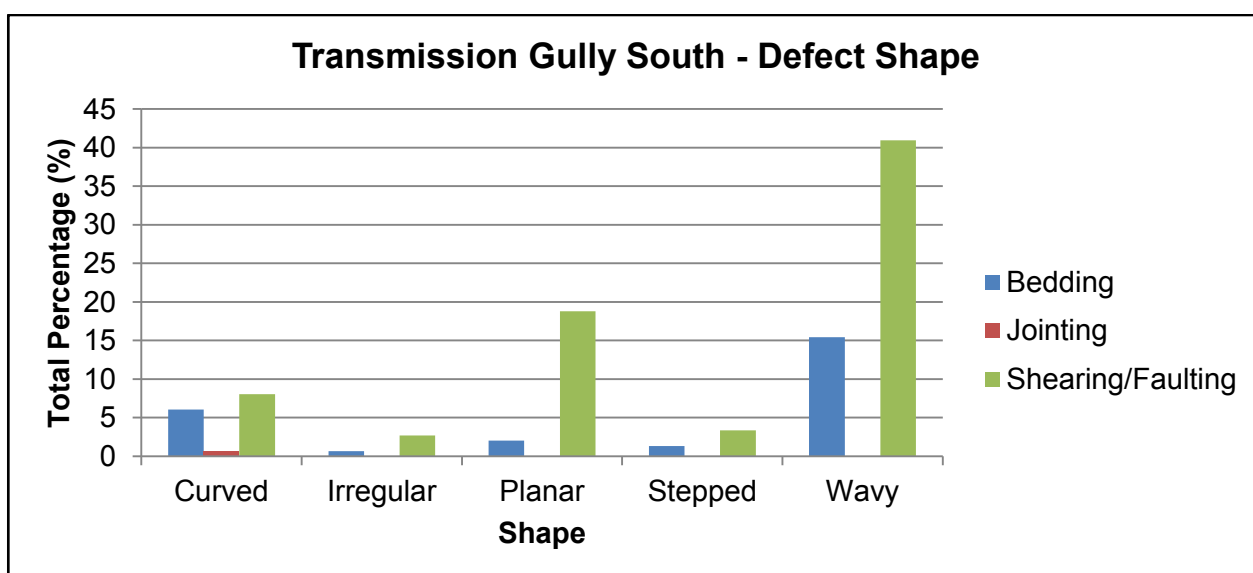
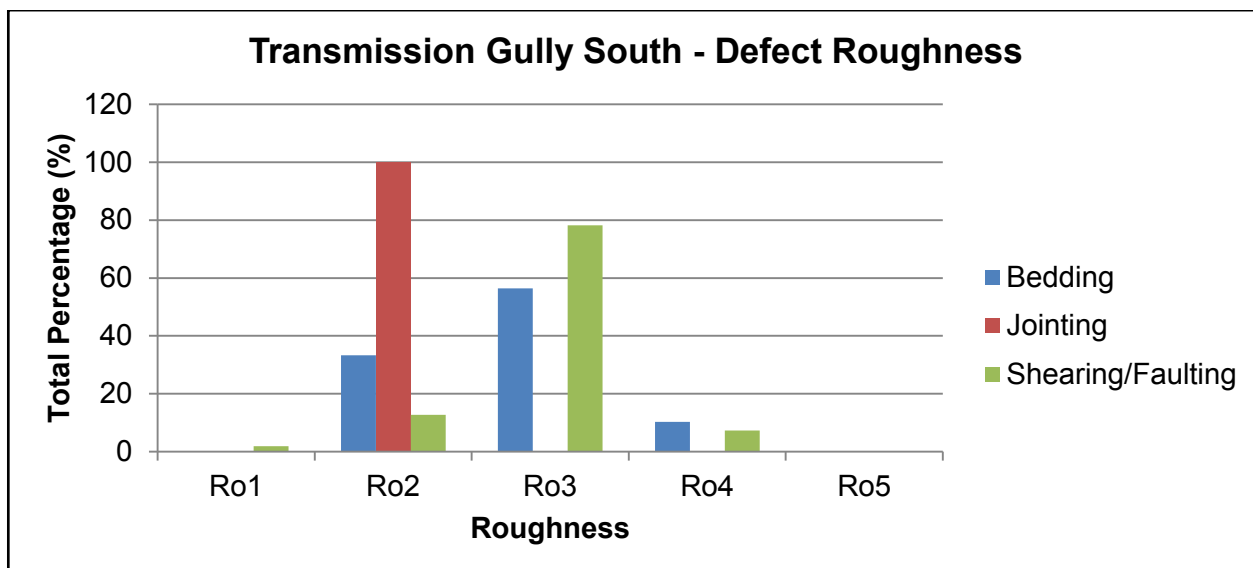
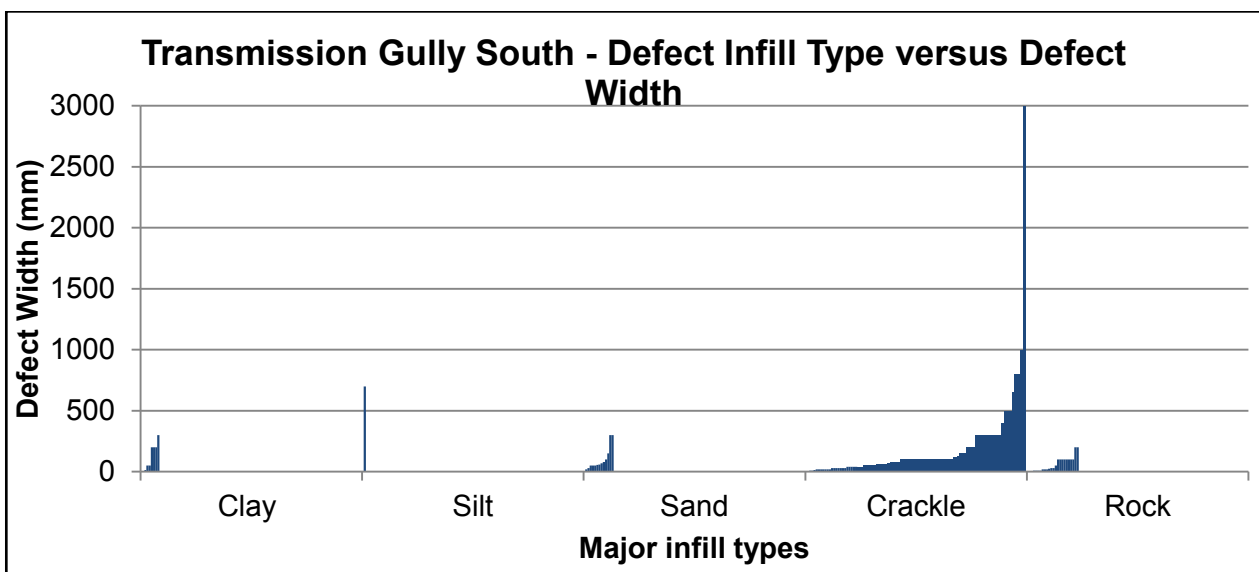
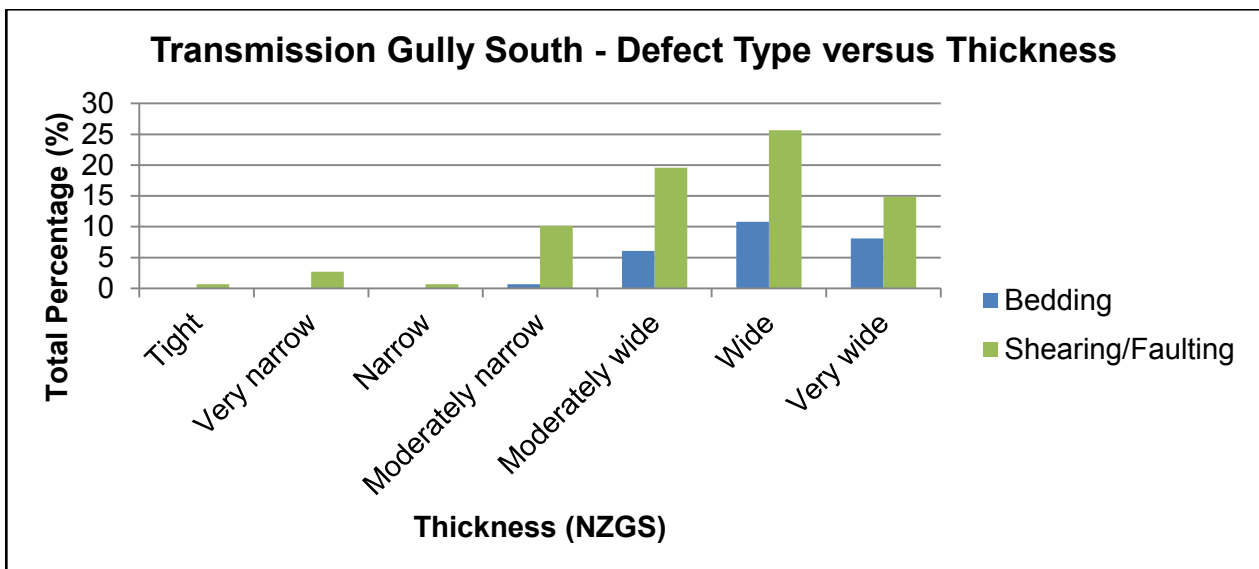
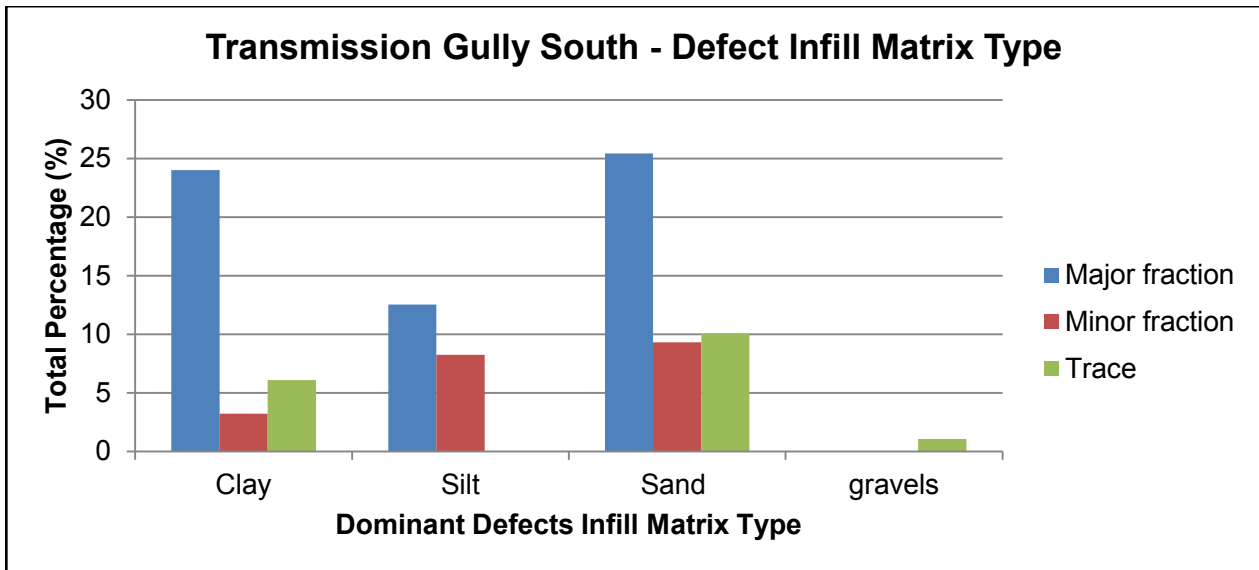
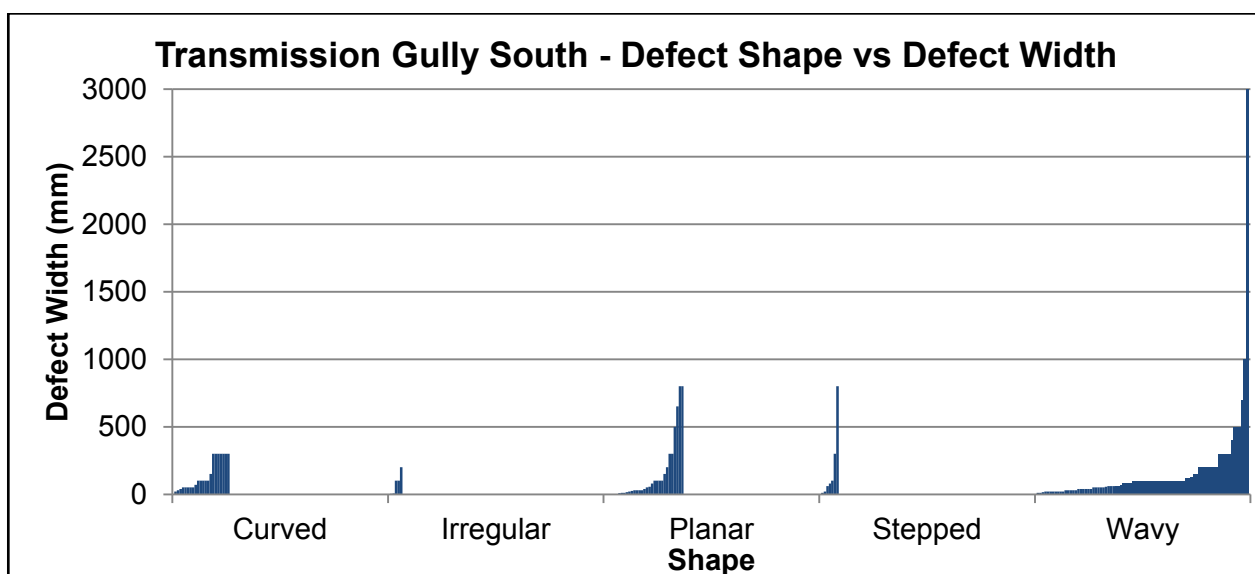
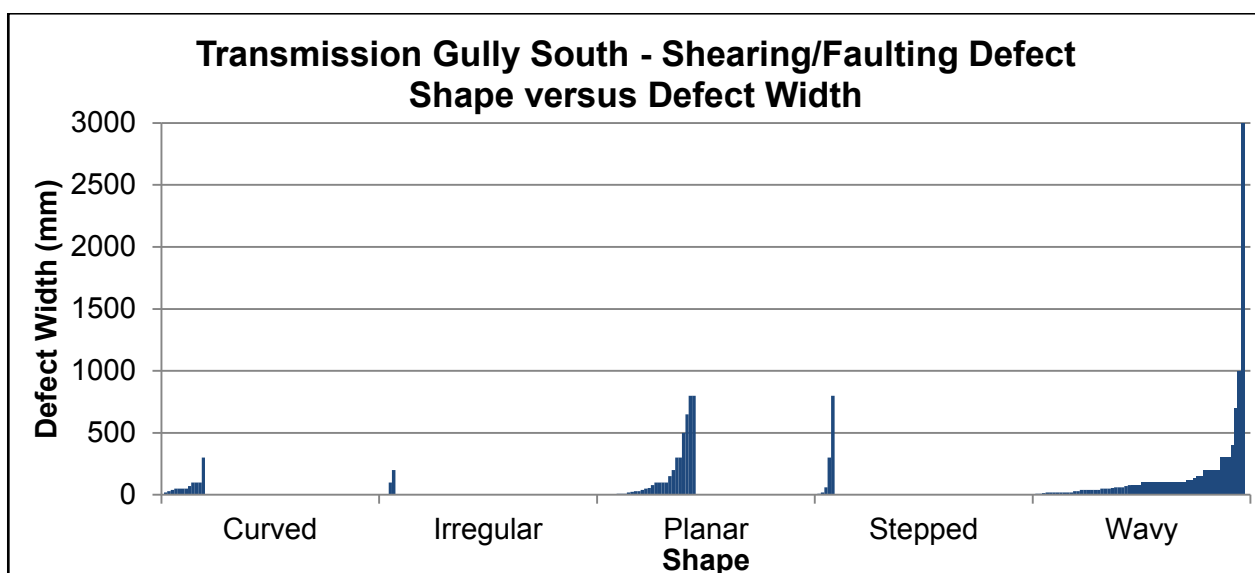
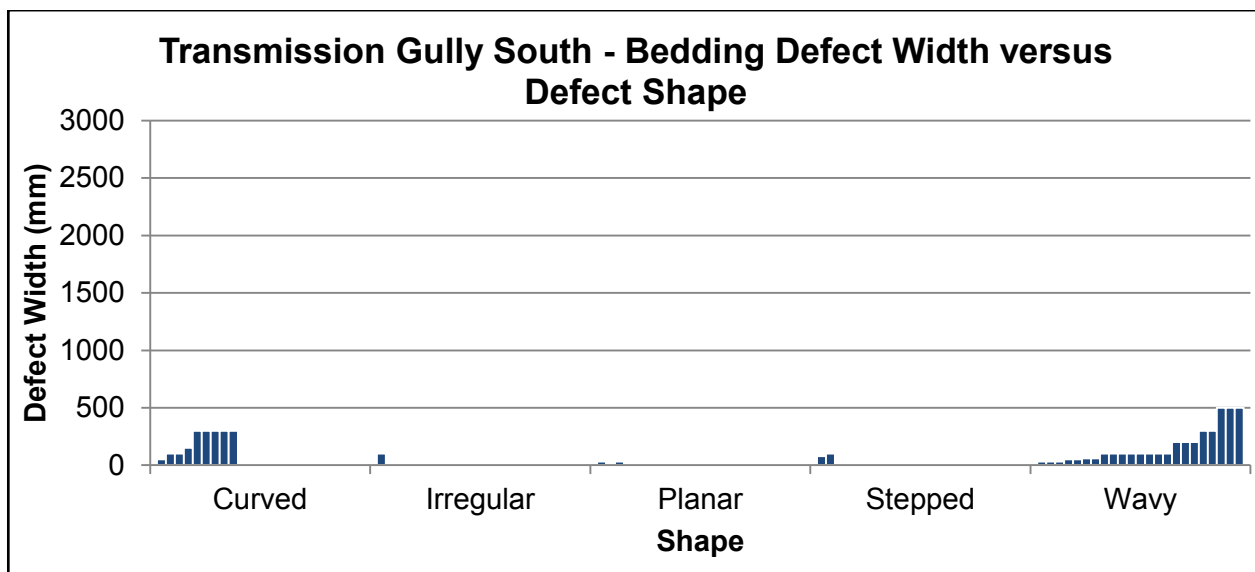


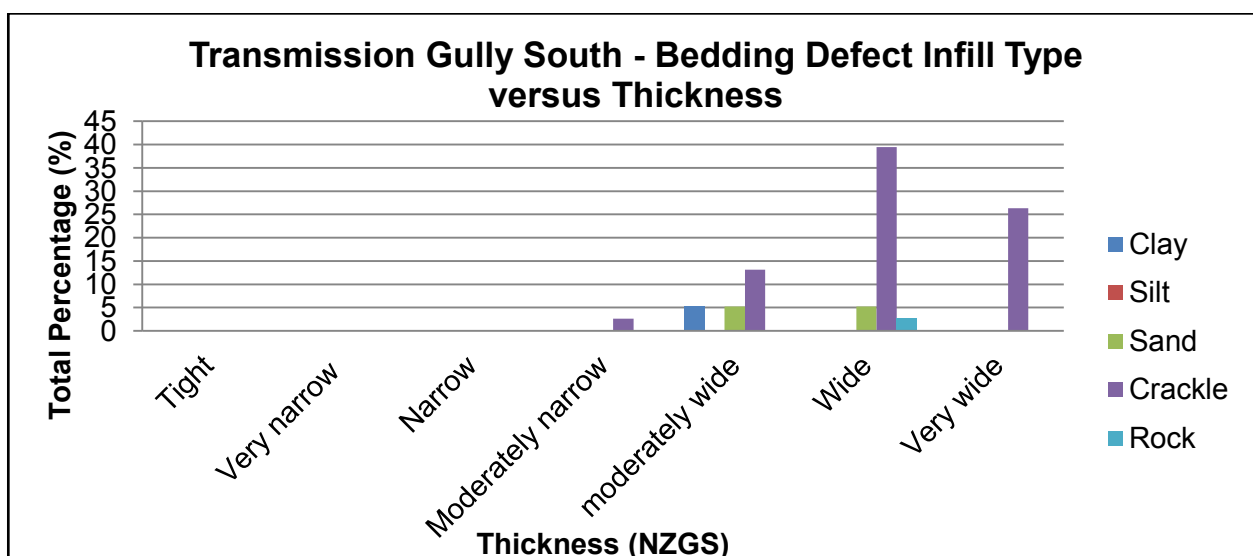
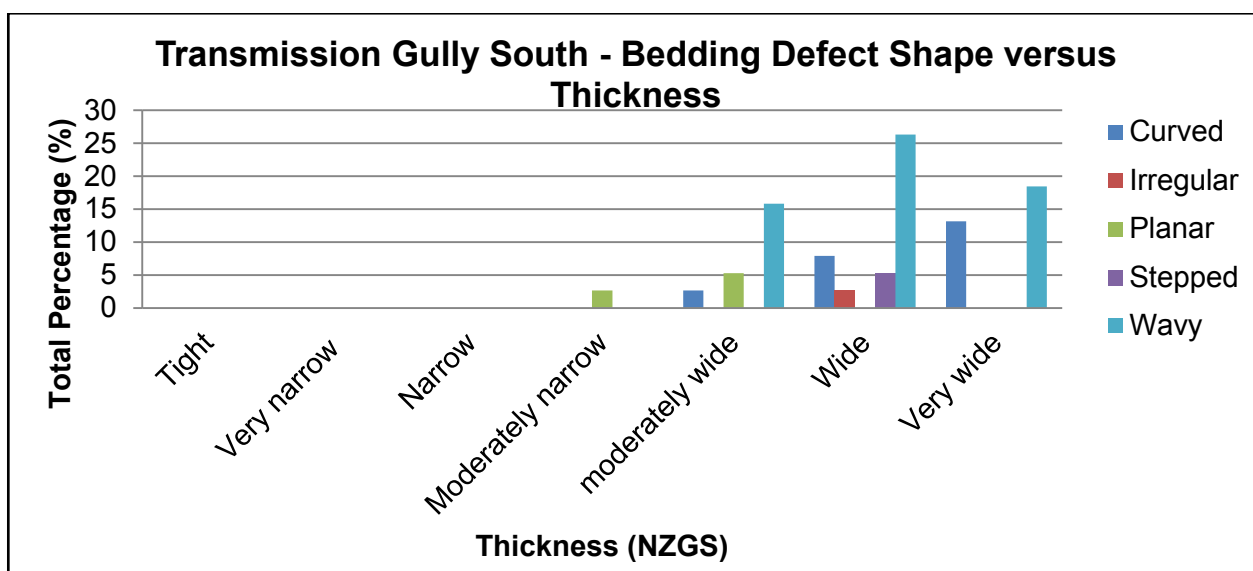
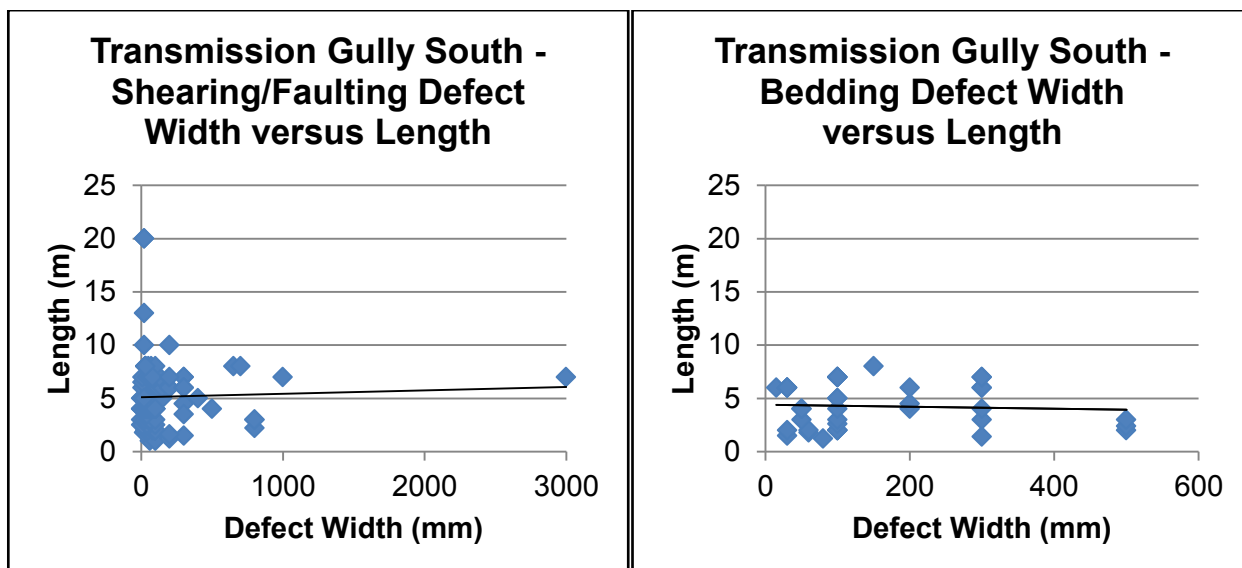
Figure B.4.1: Graphs displaying the Transmission Gully South Shearing (Left) and Bedding (Right) waviness.

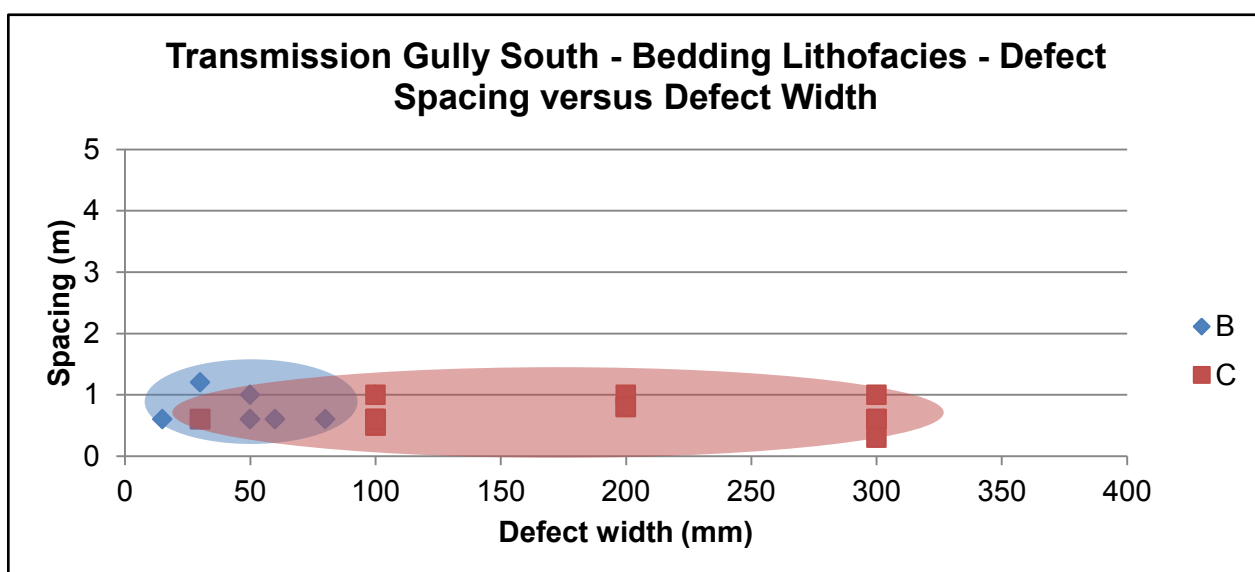
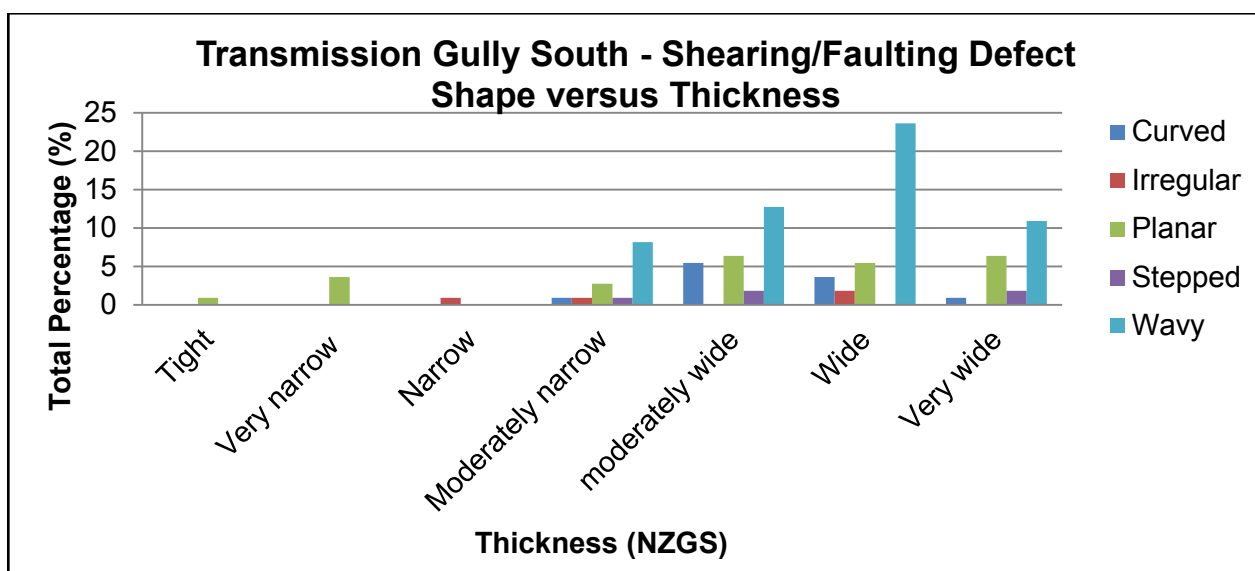
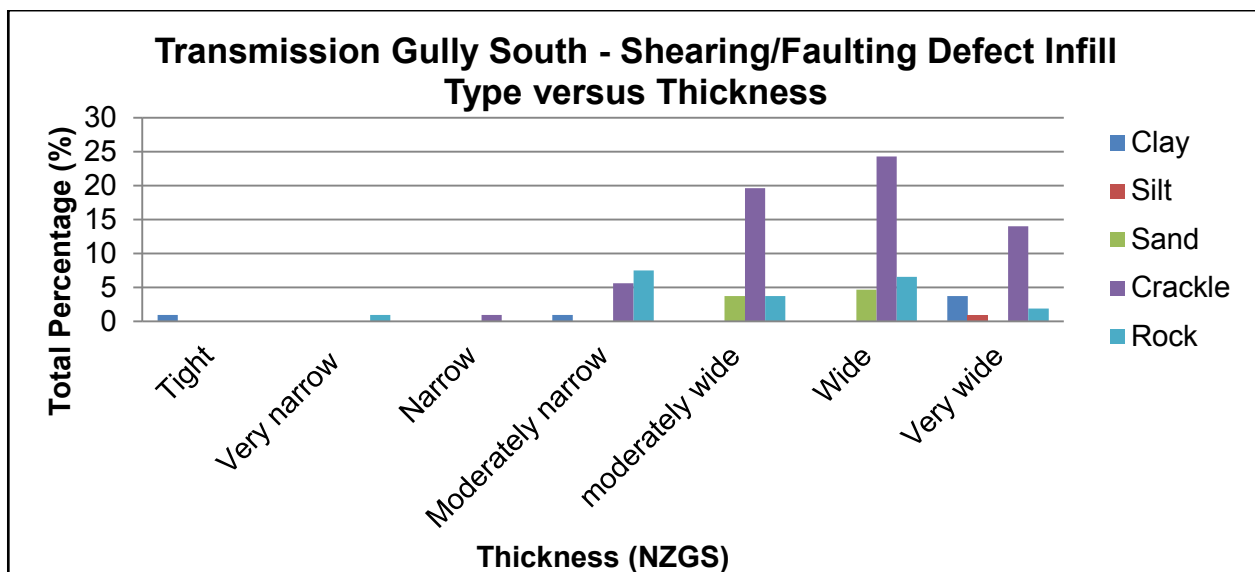








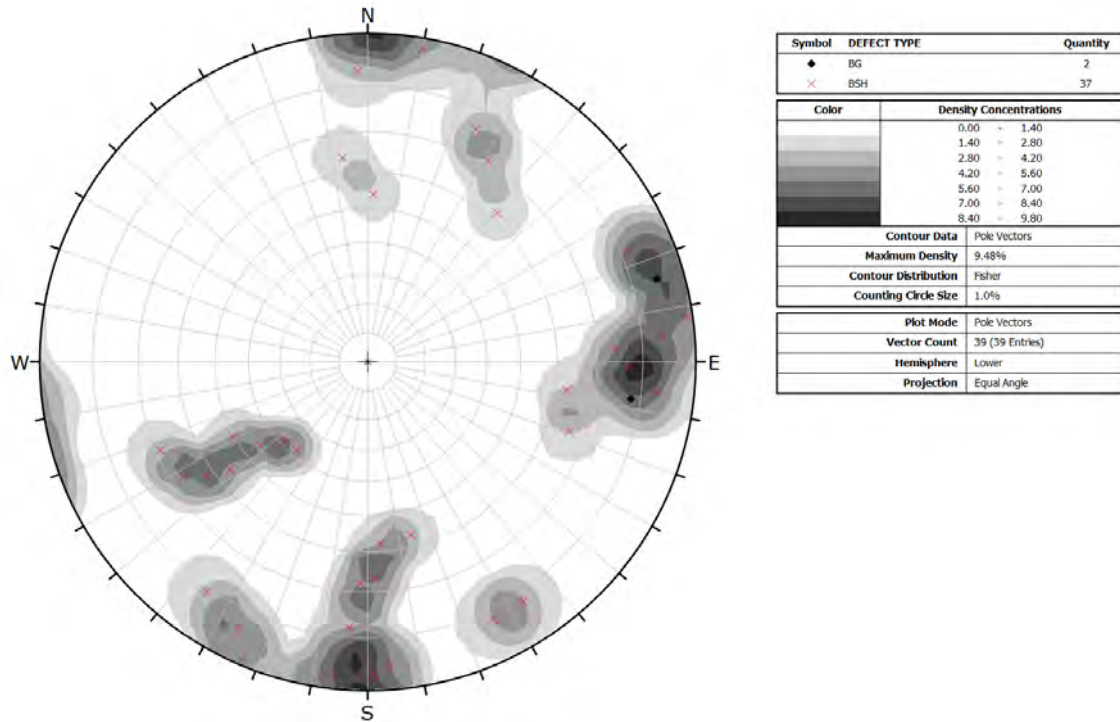




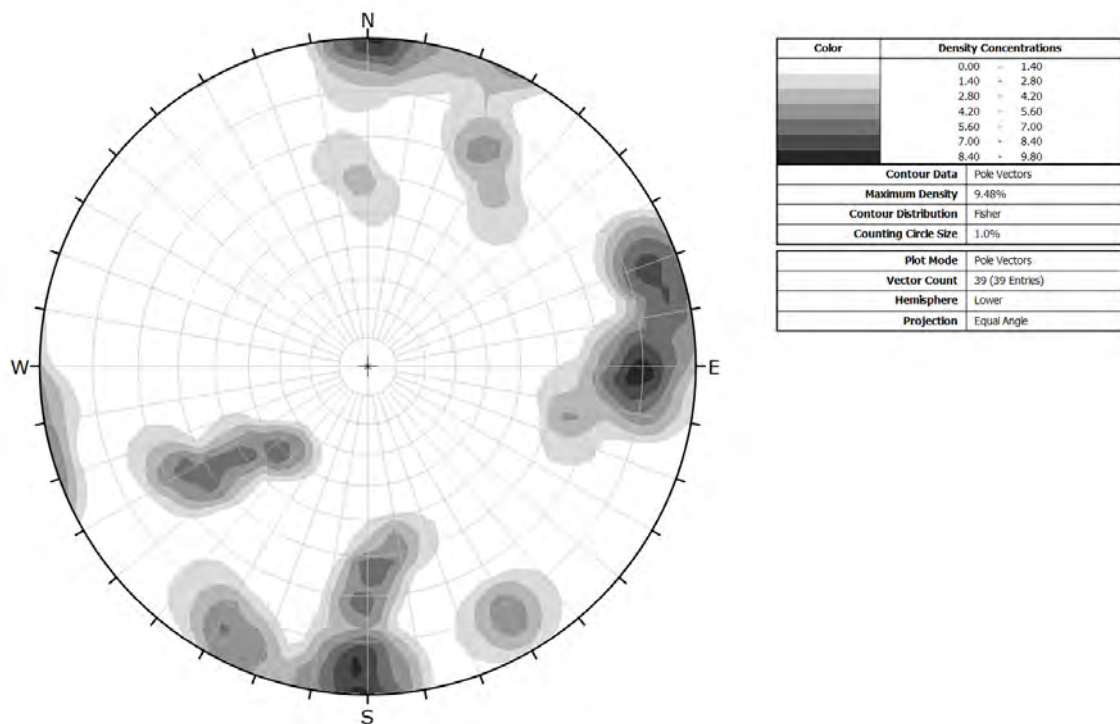
B.5 Transmission Gully South Stereonet Analysis

Stereonet Dip: Dip direction analysis of bedding, faults and shears respectively.

Bedding poles



Contour diagram of bedding clusters



Folding interpretation from Bedding

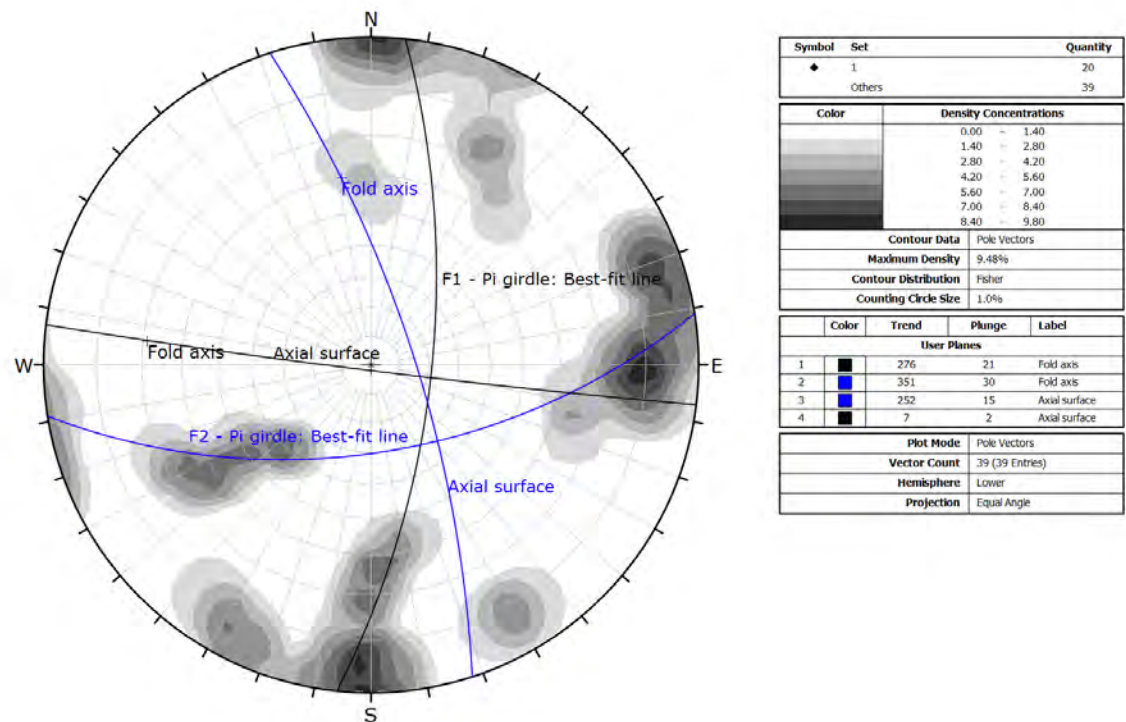
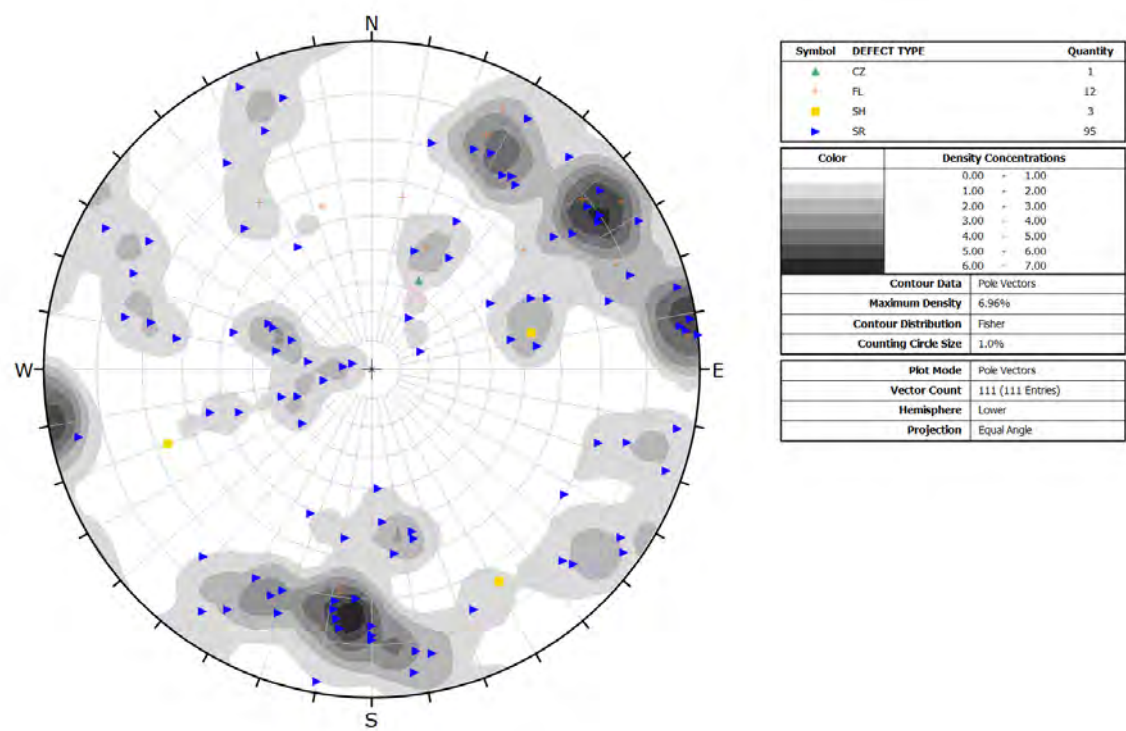
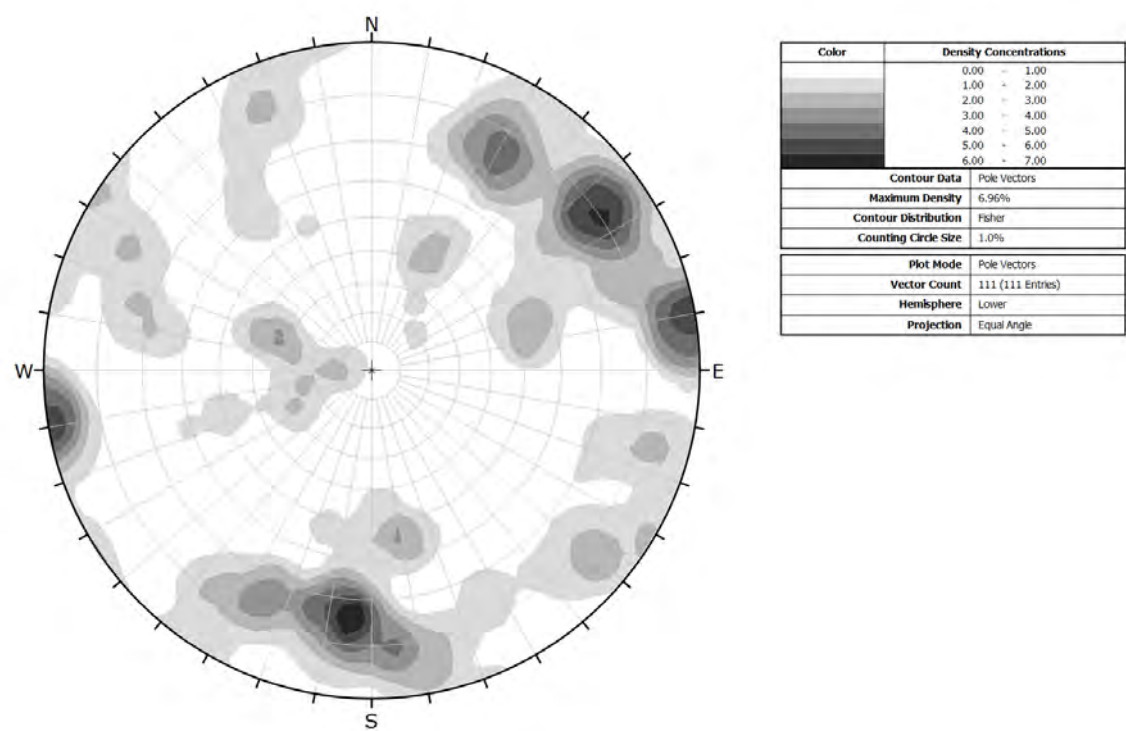


Figure B.5.2: Stereonet of the bedding data for Transmission Gully South. Interpretation of potential folding is indicated by the black and blue π -girdle lines.

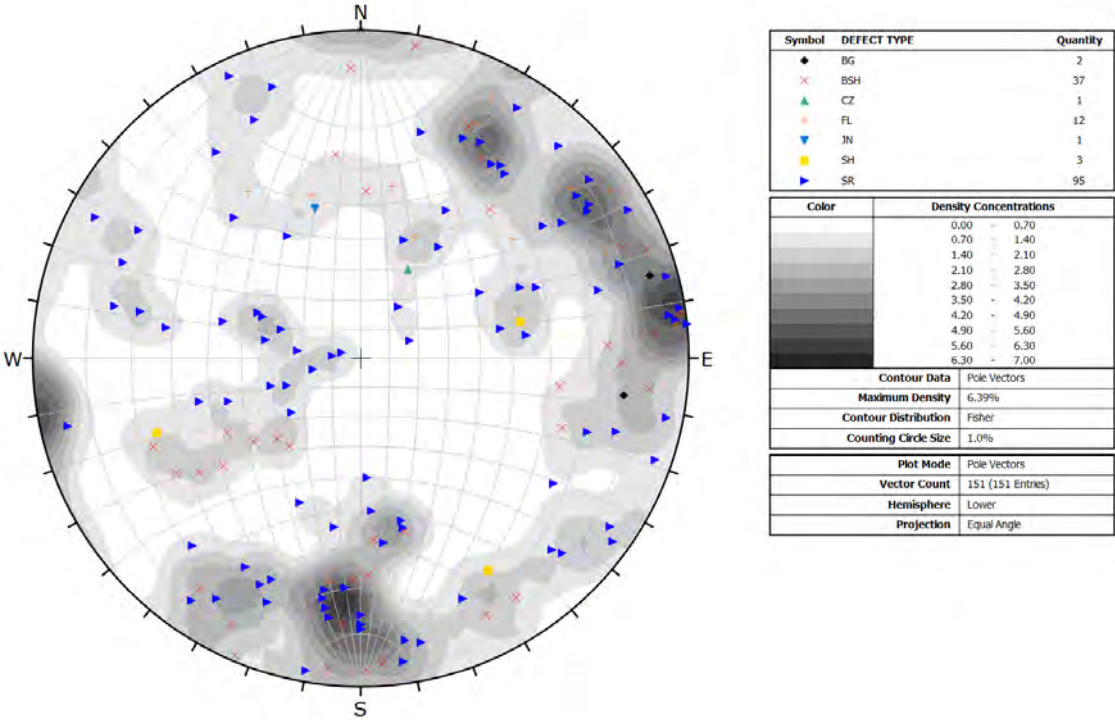
Shearing poles



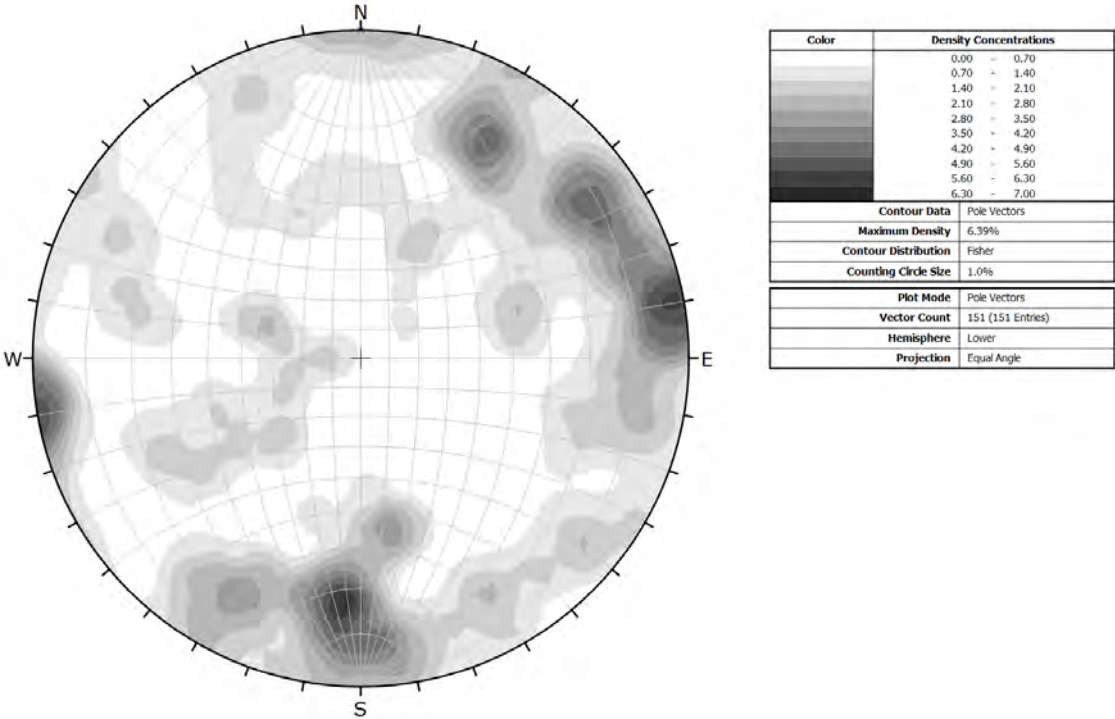
Contour diagram of shearing and faulting clusters



All defects poles



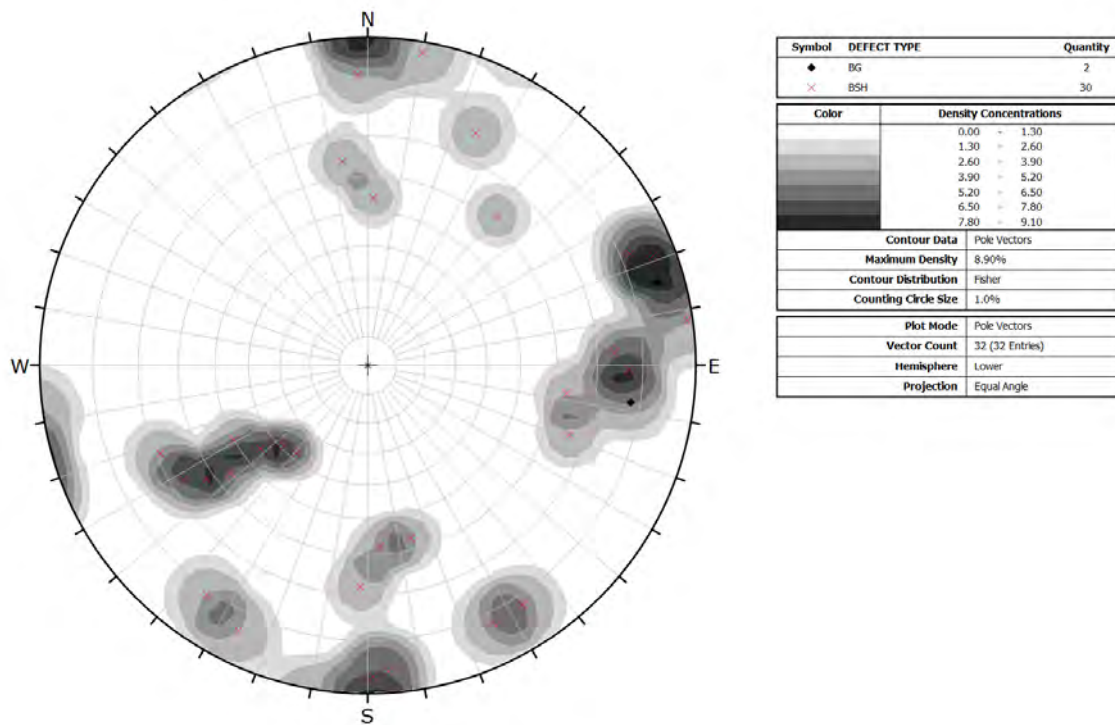
Contour diagram of all defects cluster



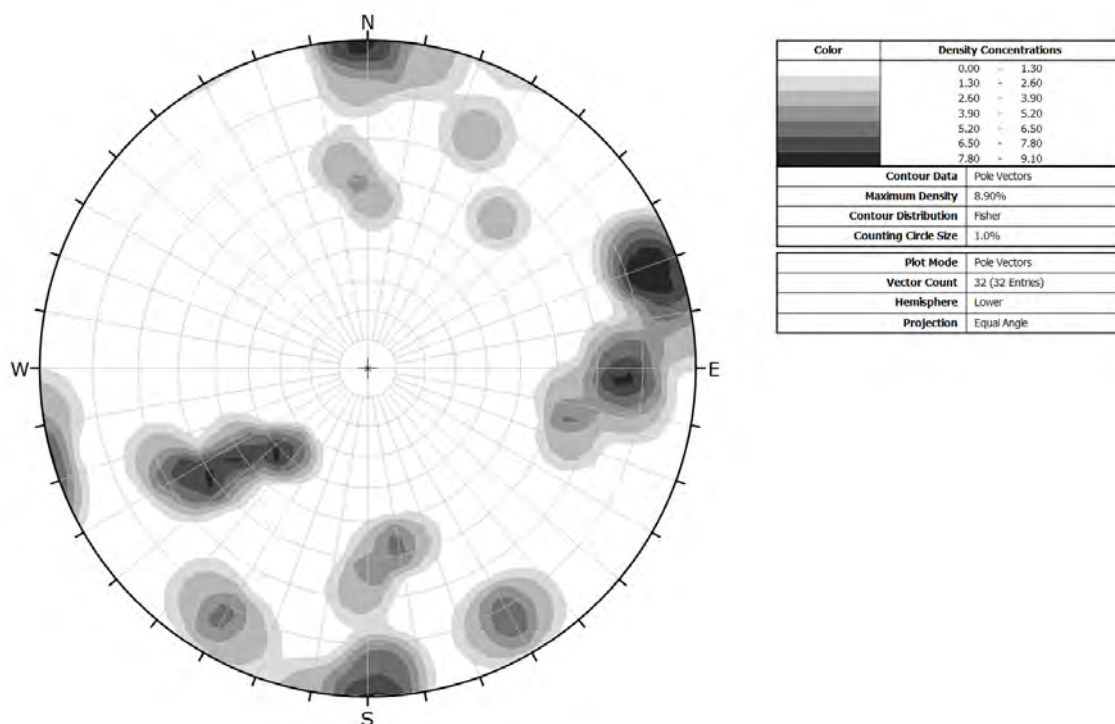
B.6 Filtered Stereonet Analysis

Stereonet from B.5 assessed for “noise”. The following only displays the poles of the continuous defects in Transmission Gully South.

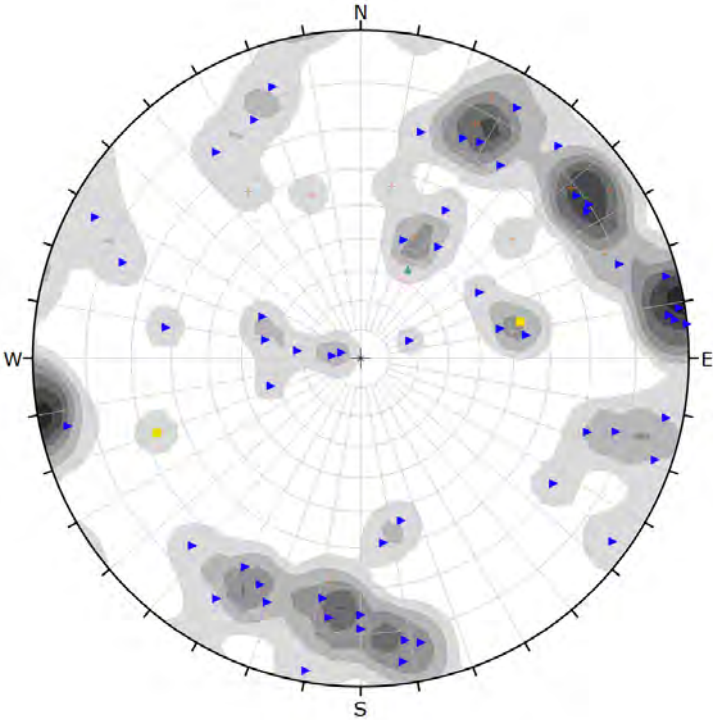
Bedding poles



Contour diagram of bedding clusters



Shearing poles



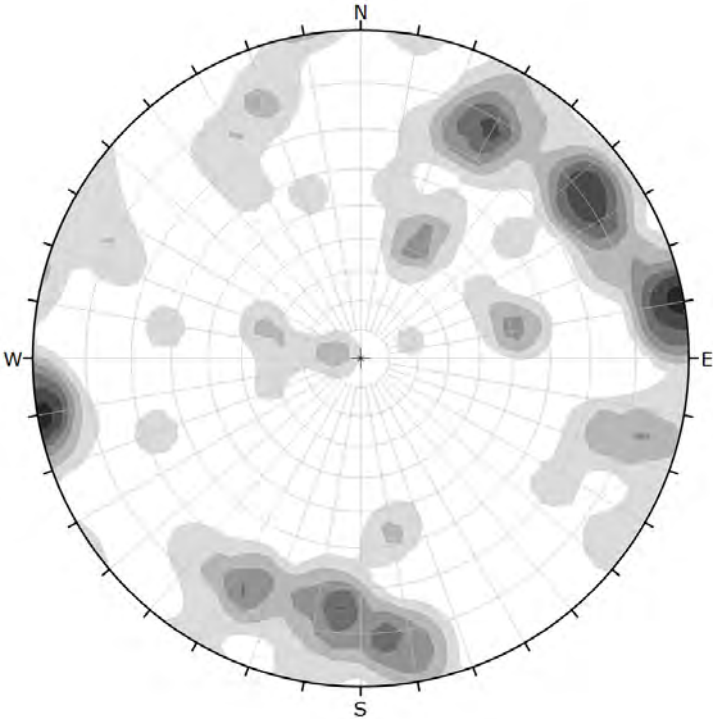
Symbol	DEFECT TYPE	Quantity
▲	CZ	1
+	FL	11
■	SH	2
▶	SR	56

Color	Density Concentrations
	0.00 - 1.20
	1.20 - 2.40
	2.40 - 3.60
	3.60 - 4.80
	4.80 - 6.00
	6.00 - 7.20
	7.20 - 8.40

Contour Data	Pole Vectors
Maximum Density	7.78%
Contour Distribution	Fisher
Counting Circle Size	1.0%

Plot Mode	Pole Vectors
Vector Count	70 (70 Entries)
Hemisphere	Lower
Projection	Equal Angle

Contour diagram of shearing and faulting clusters

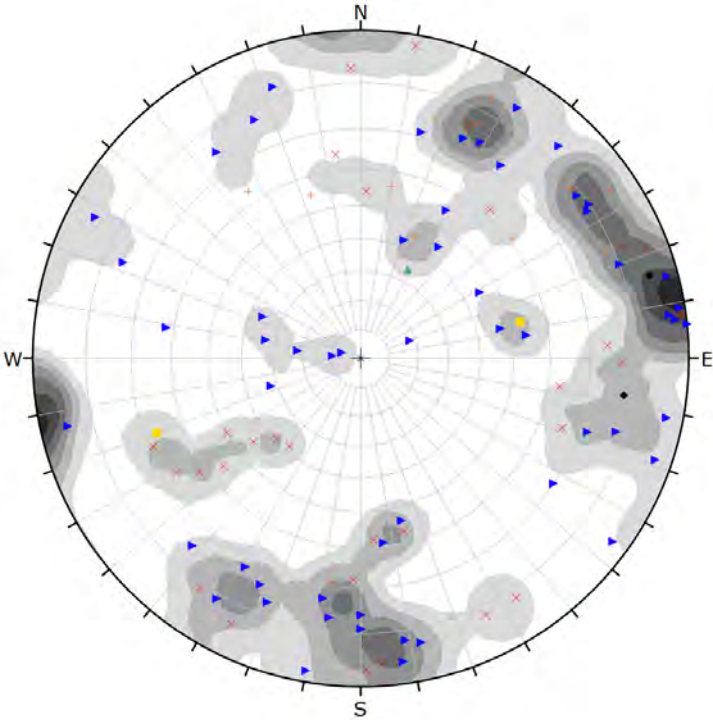


Color	Density Concentrations
	0.00 - 1.20
	1.20 - 2.40
	2.40 - 3.60
	3.60 - 4.80
	4.80 - 6.00
	6.00 - 7.20
	7.20 - 8.40

Contour Data	Pole Vectors
Maximum Density	7.78%
Contour Distribution	Fisher
Counting Circle Size	1.0%

Plot Mode	Pole Vectors
Vector Count	70 (70 Entries)
Hemisphere	Lower
Projection	Equal Angle

All defects poles



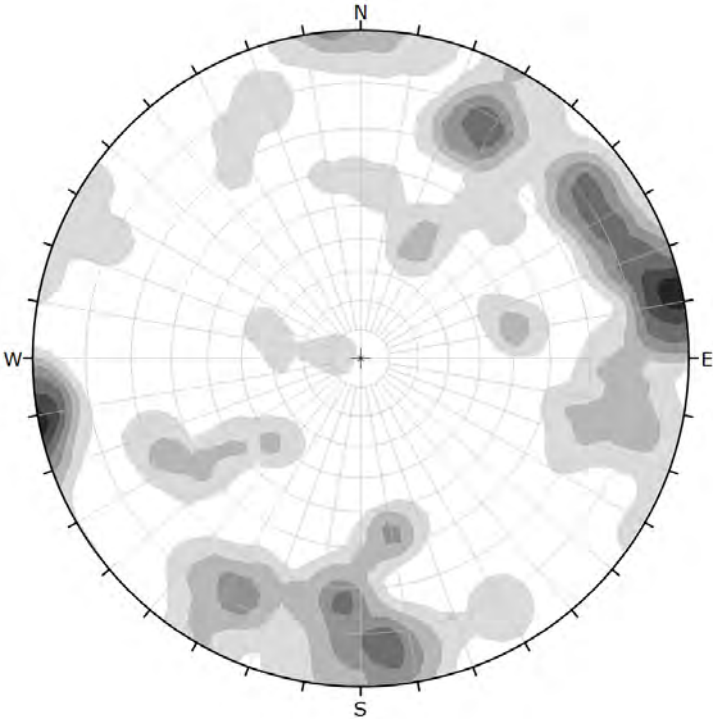
Symbol	DEFECT TYPE	Quantity
◆	BG	2
×	BSH	30
▲	CZ	1
+	FL	11
■	SH	2
▴	SR	56

Color	Density Concentrations
	0.00 - 1.10
	1.10 - 2.20
	2.20 - 3.30
	3.30 - 4.40
	4.40 - 5.50
	5.50 - 6.60
	6.60 - 7.70

Contour Data	Pole Vectors
Maximum Density	7.21%
Contour Distribution	Fisher
Counting Circle Size	1.0%

Plot Mode	Pole Vectors
Vector Count	102 (102 Entries)
Hemisphere	Lower
Projection	Equal Angle

Contour diagram of all defects cluster



Color	Density Concentrations
	0.00 - 1.10
	1.10 - 2.20
	2.20 - 3.30
	3.30 - 4.40
	4.40 - 5.50
	5.50 - 6.60
	6.60 - 7.70

Contour Data	Pole Vectors
Maximum Density	7.21%
Contour Distribution	Fisher
Counting Circle Size	1.0%

Plot Mode	Pole Vectors
Vector Count	102 (102 Entries)
Hemisphere	Lower
Projection	Equal Angle

B.7 Transmission Gully South Structural Domains

Figures are based on mapping observations and stereonet analysis. The figures represent a very detailed interpretation of the changes in defect orientation across the Transmission Gully South site.

B.7.1 Transmission Gully South - Domains

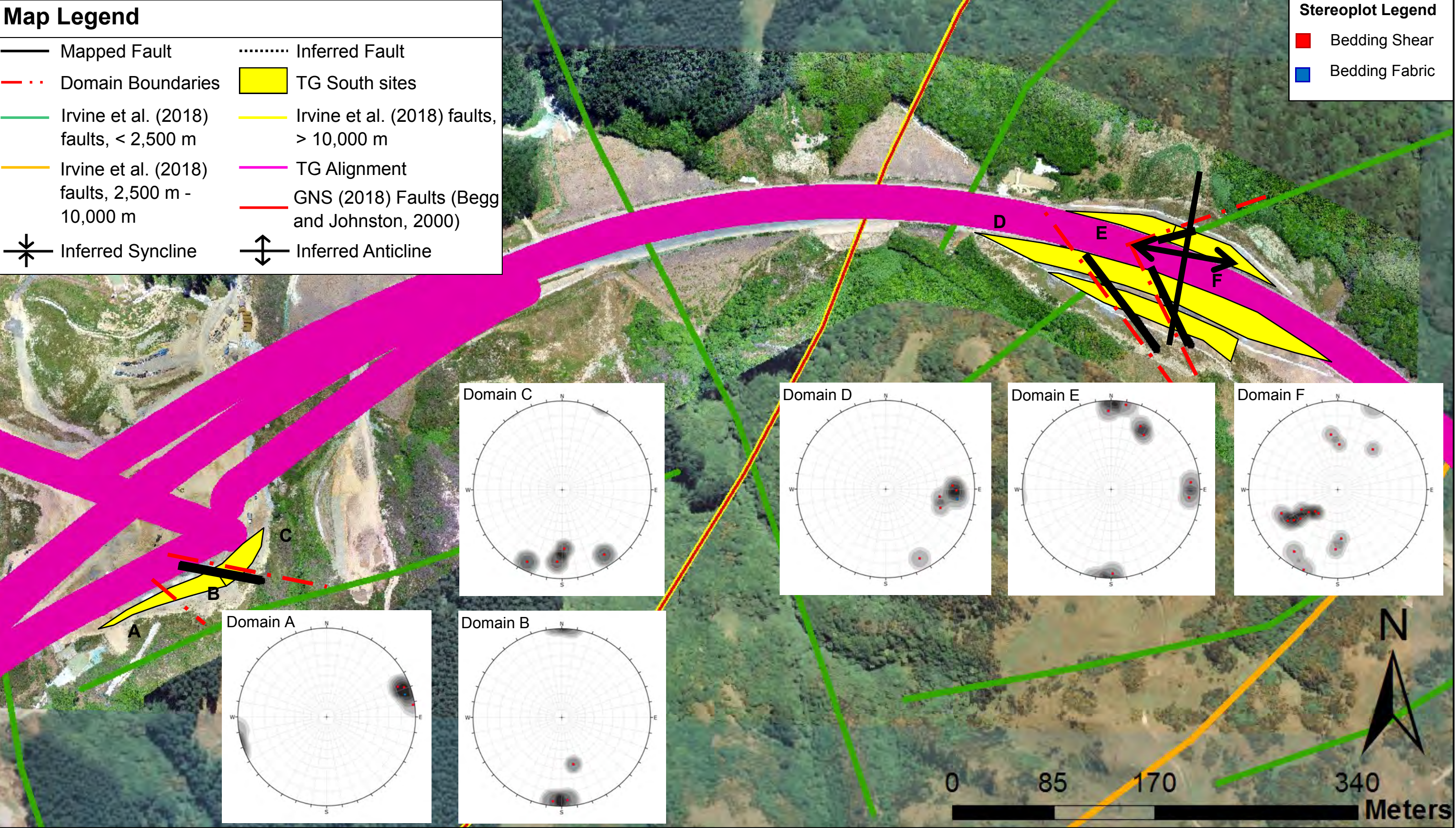
Map Legend

— Mapped Fault Inferred Fault
- . - Domain Boundaries	■ TG South sites
— Irvine et al. (2018) faults, < 2,500 m	— Irvine et al. (2018) faults, > 10,000 m
— Irvine et al. (2018) faults, 2,500 m - 10,000 m	— TG Alignment
✱ Inferred Syncline	— GNS (2018) Faults (Begg and Johnston, 2000)
⌈⌋ Inferred Anticline	



Imagery sourced: LINZ aerial imagery, 2017 (Captured by AAM NZ Ltd (2017)) and from the Transmission Gully GIS Database (2019)

B.7.2 Transmission Gully South Domains - Bedding



Imagery sourced: LINZ aerial imagery, 2017 (Captured by AAM NZ Ltd (2017)) and from the Transmission Gully GIS Database (2019)

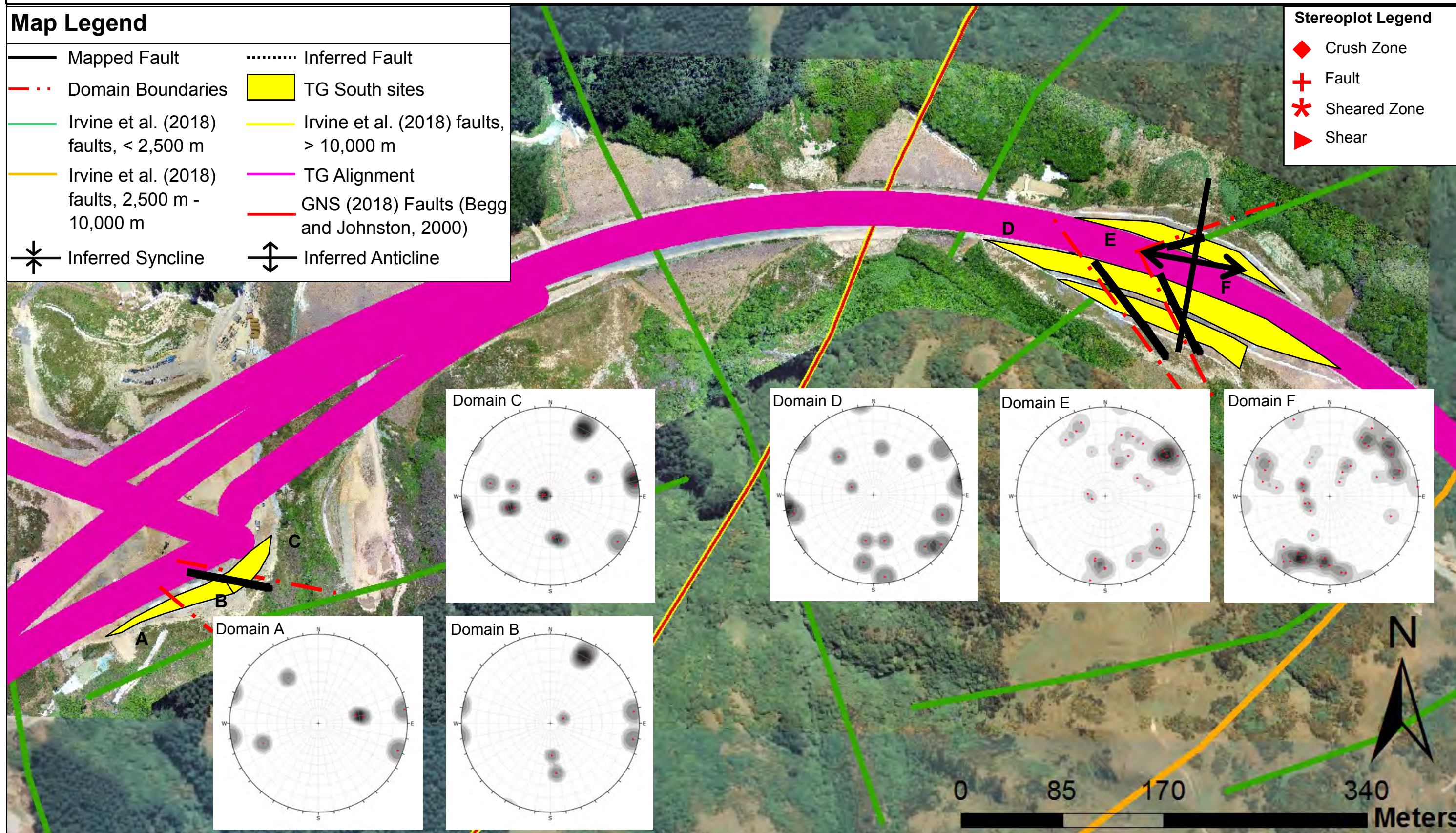
B.7.3 Transmission Gully South Domains - Shearing

Map Legend

- | | |
|---|---|
| — Mapped Fault | Inferred Fault |
| - . - Domain Boundaries | ■ TG South sites |
| — Irvine et al. (2018) faults, < 2,500 m | — Irvine et al. (2018) faults, > 10,000 m |
| — Irvine et al. (2018) faults, 2,500 m - 10,000 m | — TG Alignment |
| ✱ Inferred Syncline | — GNS (2018) Faults (Begg and Johnston, 2000) |
| | ⌈ Inferred Anticline |

Stereoplot Legend

- ◆ Crush Zone
- + Fault
- * Sheared Zone
- ▶ Shear



Imagery sourced: LINZ aerial imagery, 2017 (Captured by AAM NZ Ltd (2017)) and from the Transmission Gully GIS Database (2019)

B.8 Transmission Gully South Engineering Geological Model

Engineering geological model based on all available data. The model provides a summary of the rock mass and defect condition within the Transmission Gully South study site. Defect orientation and regional structural controls are also included.

B.8: Engineering Geological Model of Transmission Gully South

Key :
◆ BG ▲ CZ ▼ JN ▶ SR
✕ BSH + FL ■ SH

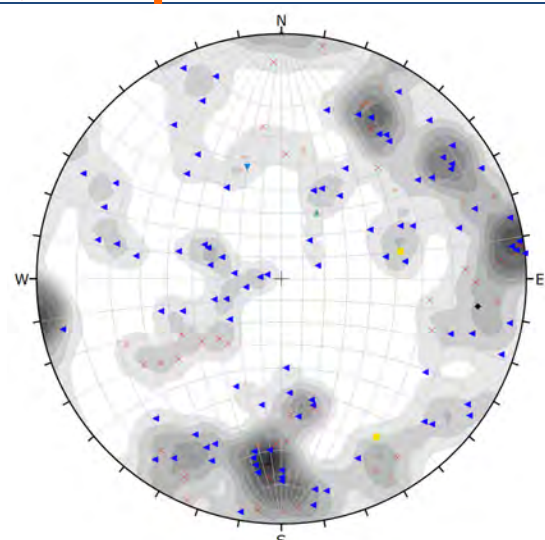


Figure 1: Stereonet of all the defect types and their orientation.

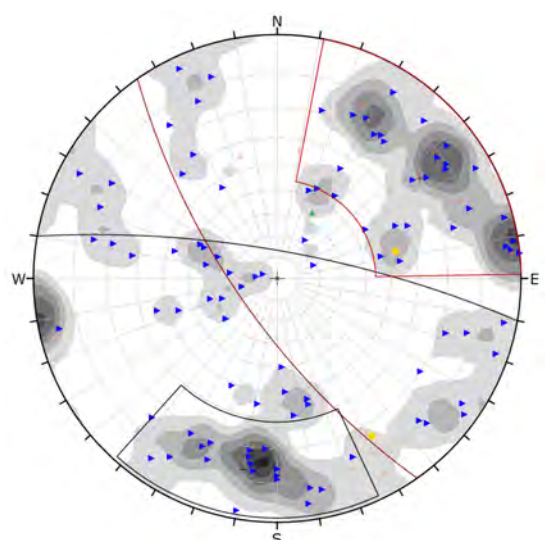


Figure 2: Stereonet of shearing.

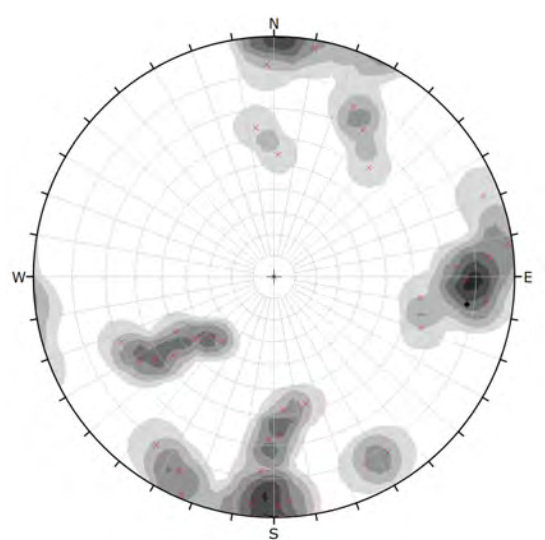


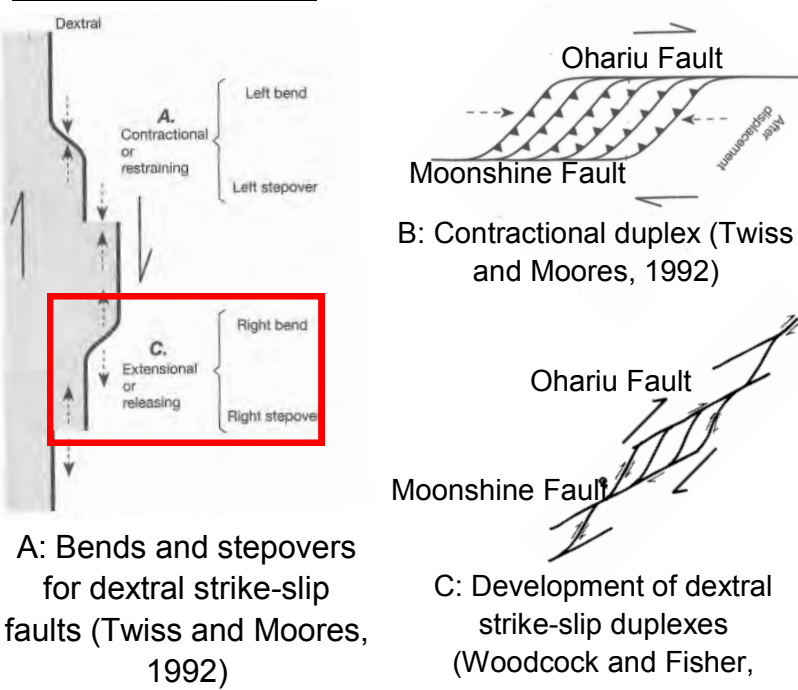
Figure 3: Stereonet of bedding.

Key:
— 1st Order >10,000m
— 2nd Order 2,500-10,000m
— 3rd Order <2,500m
— Mapped faults
..... Weathering profile

Individual sandstone beds are 2 m to 30 mm thick and continuous. Mudstone beds are 15 mm to 50 mm thick and heavily sheared. Traces of cross-cutting shears and faults are visible and persistent. Sheared zones are less common than other sites.

The Ohariu Fault (OF) and Moonshine/Otaki Faults (M/OF) are approximately 2 km to the northwest and the southeast respectively. Fault motion is predominantly dextral strike-slip. The general trend of the faults are between 030° - 050°

Conceptual Models:



Weathering profile typically follows topography, faulting has minor influence

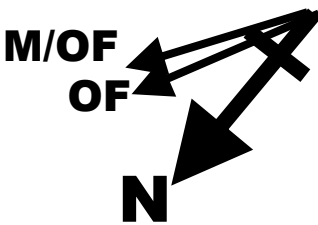
Rock mass structure at this site is controlled by the Ohariu and Moonshine/Otaki Faults converging to the southwest. High angle cross faulting link these major faults and are likely accommodating and transferring the regional tectonic stresses placing the area in convergence. Cross faulting is also thought to accommodate elastic strain due to the convergence. This results in multiple fault bounded blocks which rotate as a means of accommodating the built up of strain.

Bedding tends to strike sub-parallel to parallel with the high angle cross faulting . The cluster of data that does not follow this trend is heavily influenced by closely spaced faulting of the third order faults and so tend to strike sub-parallel to these structures. Shearing also trends parallel to sub-parallel to these structures. This aligns with the regional model created by Irvine et al. (2018) for Transmission Gully.

Bedding is dominantly sub vertical to steeply inclined with variations occurring in response to faulting.

Minor water seepage is present on both sides of the valley. Faults act as aquitards.

The close proximity of the Major faults means that shearing of any kind is un-avoidable.



MUD : SAND 40: 60	Sandstone: Moderately weathered, light orange brown and blueish grey, SANDSTONE; Moderately Strong to weak; 5 joint sets closely to very closely spaced, tight to narrow joints [RAKAIA SUB-TERRANE Greywacke]	Mudstone: Moderately weathered, dark brown and blueish grey, MUDSTONE; Weak [RAKAIA SUB-TERRANE Argillite]
Predominant Suneson lithofacies: B		
Scale 1:6,350 centimetres		
0 62.5 125 250 500 1000 Meters		

APPENDIX C: KAPITI QUARRY ANALYSIS

This site is located in Paraparaumu East at the base of the foothills (Figure C.1). The Ohariu Fault is located to the southeast approximately a kilometre away where the fault appears to bend to the right changing its strike to around 060°. This is interpreted as a releasing bend placing this site in an extensional setting, possessing a similar structural setting to the Transmission Gully North site. A total of 3 outcrops were mapped (Appendix C.2).

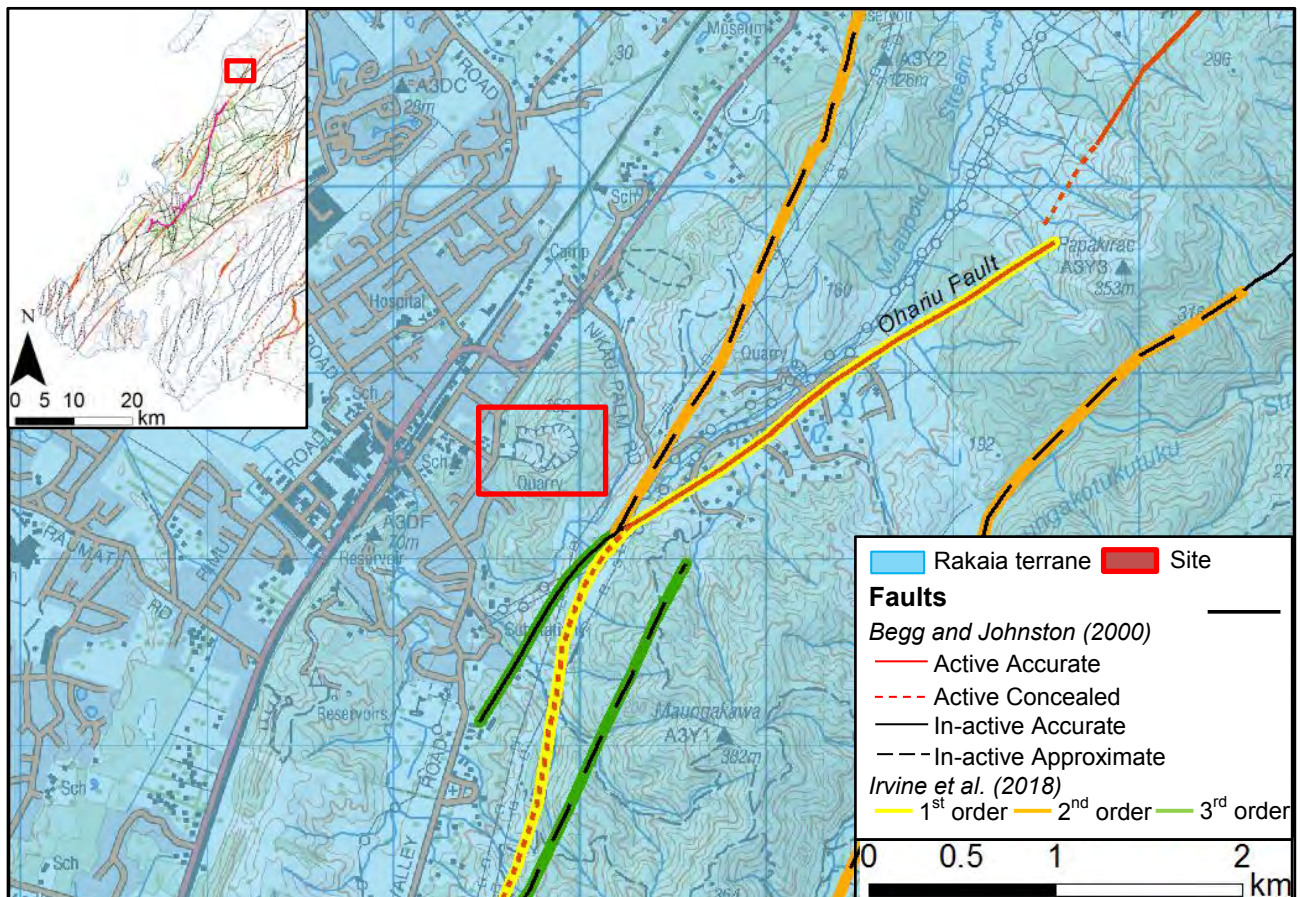


Figure 1: Kapiti Quarry site district scale map. Data sourced from GNS (2018) (Begg and Johnston, 2000) and Irvine et al. (2018). Refer to Section 1.4 for Irvine et al (2018) order classification. Imagery from LINZ.

Results derived from conceptual models, raw mapping data, stereonet analysis and engineering geological models for the Kapiti Quarry study site are displayed in the following sections.

C.1 Kapiti Quarry Conceptual Structural Model

Preliminary structural assessment derived from GNS (2010) (Begg and Johnston, 2000) and Irvine et al (2018) structural databases. Interpretations are based on information derived from past literature.

C.1 Conceptual Structural Model of Kapiti Quarry

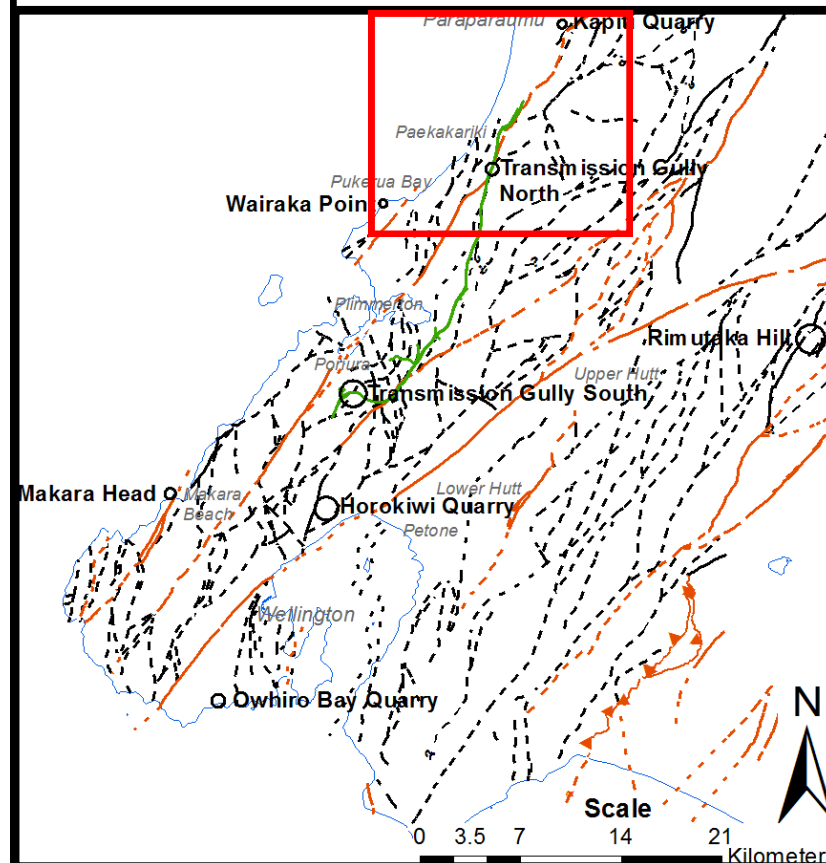


Figure A: Location Plan

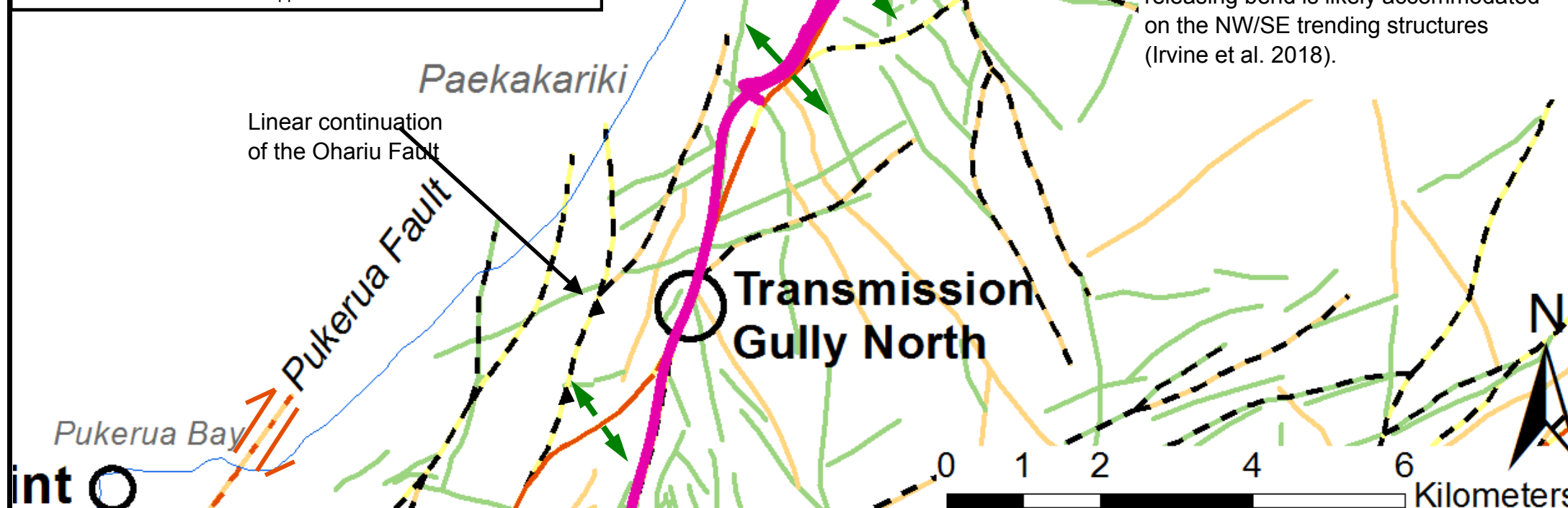
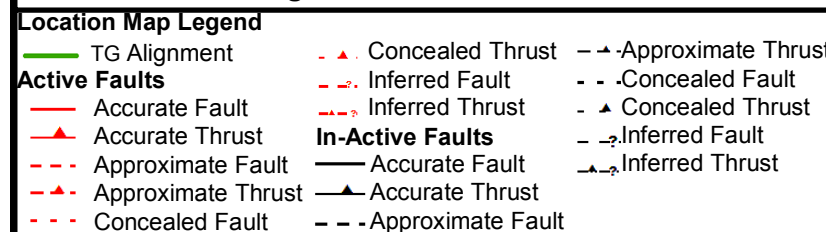
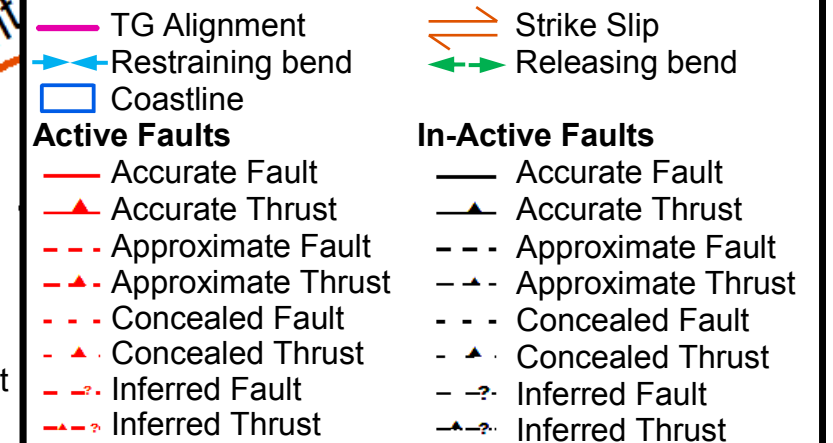
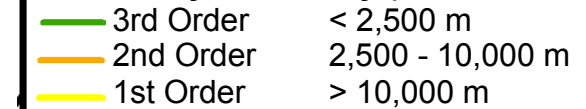


Figure B: District scale structures around Kapiti Quarry. Faults are sourced from GNS (2018) (Begg and Johnston, 2000) and from Irvine et al (2018).

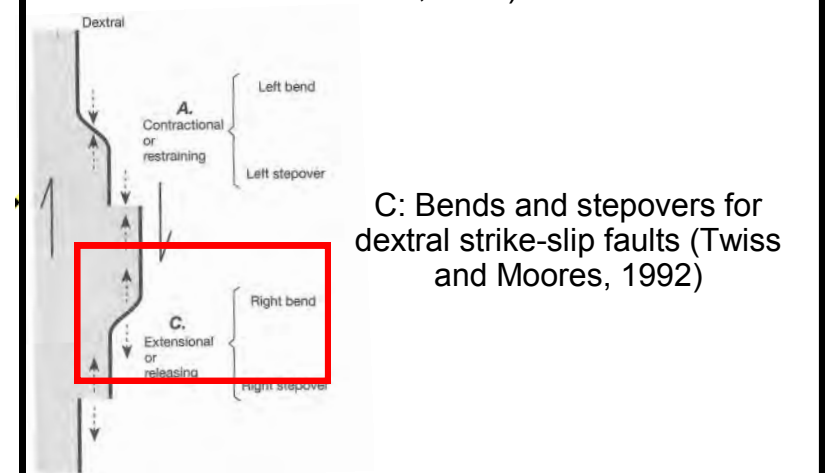
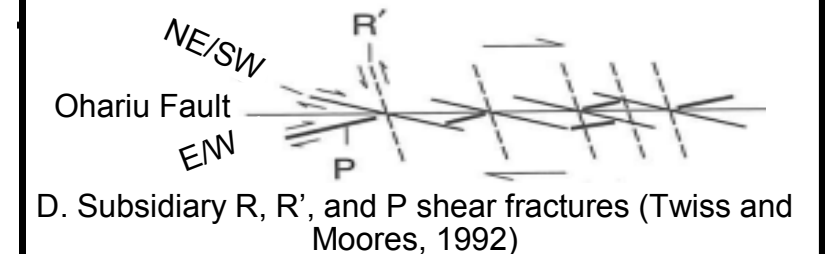
District Scale Legend:



Fault Analysis Overlay (Irvine et al., 2018)



Conceptual Models:



Bedding and Shearing Predictions:

Bedding is anticipated to strike sub-parallel to the NW/SE trending structures likely in response to the normal faulting of the 'second order' structures.

Shearing is predicted to occur sub-parallel to the Ohariu Fault and with the NW/SE structures. This aligns with the structural grain of the area (Irvine et al., 2018).

C.2 Kapiti Quarry Outcrop Location Map

Displays the location of the mapped outcrops within the Kapiti Quarry study site.

C.2 Kapiti Quarry

 Kapiti Quarry Sites



C.3 Kapiti Quarry Raw Mapping Data

Structural data collected from the Kapiti Quarry site. Where data is missing or blanked out information was either not able to be reached or was not relevant to the rock mass or defect condition (e.g. Planar defects did not contain a wavelength as outlined in Chapter 3).

C.3.1 Kapiti Quarry - Raw Data

Kapiti Quarry																							
ID	Defect Type	Dip	Dip Direction (Mag)	Dip Direction (True)	Structural Domain	Roughness	Thickness		% of rock fragments	Continuity	Persistence	Shape			Persistence - Trace Length (m)	Spacing (m)	Infill (Support (Breccia type (%Clasts), Angularity, weathering, strength, coating; colour, grainsize, strength, plasticity)) precipitation	Saturation	Latitude	Longitude	Comments	Cut ID	
							Term	Width (mm)				Inter-limb angle (degrees)	Wavelength (m)	Term									
1	BSH	26	53	31	B	Ro3	Tight	~0mm	-	1	D	~150°	Gentle	~4m	Wavy	~8m	~0.6m		Dry	-40.9161	175.0177	Offset by horizontal shear	Kapiti Quarry 1
2	BSH	36	113	91	B	Ro3	Wide	~70mm	~80%	1	D	~150°	Gentle	~4m	Wavy	~3m	~0.6m	Clast supported (Crackle (~80%), Angular, HW, Weak, Veneer, Dark grey with some brown, sandy Silt, Soft, MP) No precipitation	Damp	-40.91616	175.01766	Offset by FL3	
3	FL	89	189	167	A	Ro2	Wide	~150mm	~90%	1	D	~180°	Gentle		Planar	~3m		Clast supported (Crackle (~90%), Angular, HW, Weak, Veneer, Dark grey with some brown, sandy Silt, Soft, MP) White precipitation	Damp	-40.91616	175.01762	Terminates against FL4 and fault crush material	
4	FL	58	269	247	A	Ro4	Wide	~150mm	~90%	1	D	~180°	Gentle		Planar	~3m		Clast supported (Crackle (~90%), Angular, HW, Weak, Veneer, Dark grey with some brown, sandy silt, Soft, MP) No precipitation	Damp	-40.91608	175.01759	Failure plain for wedge failure	
5a	SR	60	55	33	A	Ro2	Moderately Narrow to Wide	~100-10mm	~75%	1	O				Stepped	~8m		Clast supported (Crackle (~75%), Angular, CW, Very weak, Coating, Dark grey and brown, sandy Clay with trace of silt, Very soft, MP) No precipitation	Damp	-40.91617	175.01757	SR4 terminates against it and offsets FL4-FL5b and is second wedge failure plain	
5b	FL	59	252	230	A	Ro2	Wide	~150mm	~25%	1	D	~170°	Gentle	~0.8m	Wavy	~6m		Matrix supported (Soil (~25%), Angular, CW-RS, Very weak, Coating, Dark grey and brown, sandy Clay with trace of silt, Very soft, HP) No precipitation	Minor Seepage	-40.9161	175.01748	SR4 terminates against it	
6	SR	77	304	282	A	Ro3	Moderately wide	~60mm	~10%	1	D	~170°	Gentle	~3m	Wavy	~2m	~1.5m	Matrix supported (Soil (~10%), Angular, CW, Very weak, Coating, Light grey and some brown, sandy Silt and Clay seams, Very soft, HP) Flecks of sand sized precipitation	Dry	-40.91614	175.0175	terminates against FL5b	
7	BSH	62	117	95	A	Ro3	Moderately wide	~10mm	~80%	1	D	~160°	Gentle	~7m	Wavy	~10m	~1.25m	Clast supported (Crackle (~80%), Angular, HW, Weak, Coating, Light grey, sandy Silt and Clay seams, Very soft, LP) No precipitation	Dry	-40.91615	175.01754	Terminates against FL5b and offset by CZ11	
7	BSH	34	82	60	A	Ro3	Moderately wide	~10mm	~80%	1	D	~160°	Gentle	~7m	Wavy	~10m	~1.25m	Clast supported (Crackle (~80%), Angular, HW, Weak, Coating, Light grey, sandy Silt and Clay seams, Very soft, LP) No precipitation	Dry	-40.91611	175.01751	Terminates against FL5b and offset by CZ11	
8	JN	61	288	266	A	Ro2	Tight	~0mm		2	D	~180°	Gentle		Planar	~0.4m	~0.4m		Dry	-40.9161	175.01753	Confined to sandstone beds	
8b	JN	72	331	309	A	Ro2	Tight	~0mm		2	D	~180°	Gentle		Planar	~0.4m	~0.4m		Dry	-40.91613	175.01754	Confined to sandstone beds	
9	SR	41	228	206	A	Ro2	Moderately wide	~5mm	~80%	1	D	~180°	Gentle		Planar	~2.5m		Clast supported (Rock (~100%), Angular, HW, Moderately strong, Coating, Light grey, sandy Silt and Clay seams, Very soft, LP) 100% precipitation, Fractured, angular and white	Dry	-40.91615	175.01754	offset by SR8 terminates in rock	
10	SR	81	331	309	A	Ro2	Moderately wide	~20mm	~99%	1	D	~160°	Gentle	~2m	Wavy	~1.5m	~1.25m	Clast supported (Rock (~99%), Angular, MW, Moderately strong, Stained, Light grey, sandy Silt and Clay seams, Very soft, LP) No precipitation	Dry	-40.91614	175.01745	Terminates against BSH7	
7	BSH	45	94	72	A	Ro2	Wide	~150mm	~95%	1	D	~160°	Gentle	~2m	Wavy	~12m	~1.25m	Clast supported (Crackle (~95%), Angular, HW, Weak, Coating, Light grey, sandy Silt with traces of clay, Very soft, NP) White tabulated precipitation	Damp	-40.91607	175.01744	Offset by SR11	
12	SR	61	40	18	A	Ro3	Moderately wide	~50mm	~80%	1	D	~160°	Gentle	~2m	Wavy	~10m	~1.25m	Clast supported (Crackle (~80%), Angular, HW, Very weak, Coating, Light blue grey, sandy Silt with traces of clay, Very soft, NP) White tabulated precipitation	Damp	-40.91614	175.01744	Offset by BSH7 and CZ11 and splits into two joins up with SR13	
13	SR	87	268	246	A	Ro3	Wide	~150mm	~95%	1	S				Irregular	~10m		Clast supported (Crackle (~95%), Angular, HW, Very weak, Coating, Light blue grey, sandy Silt with traces of clay, Very soft, HP) White tabulated precipitation	Dry	-40.91613	175.01749	Offset by BSH7 and CZ11 and SR12 terminates against it	
11	CZ	23	183	161	A	Ro4	Wide	~120mm	~80%	2	D	~180°	Gentle		Planar	~10m		Clast supported (Crackle (~80%), Angular, HW, Very weak, Coating, Light and dark grey with some orangey Brown, sandy Silt with Clay seams, Very soft, HP) No precipitation	Dry	-40.91613	175.01748	Offsets a number of BSH and causes terminations in a lot of SR's	
14	SR	90	13	351	A	Ro3	Very narrow	~2mm	~80%	0	C	~160°	Gentle	~3m	Wavy	~6m	~1m	Clast supported (Crackle (~80%), Angular, HW, Weak, Coating, Dark blue black, Sand, Very soft, NP) No precipitation	Dry	-40.91614	175.01742	Offset by BSH7 and CZ11 and terminates against it	
15	JN	85	326	304	A	Ro3	Tight	~0mm		2	D	~180°	Gentle		Planar	~0.6m	~0.6m		Dry	-40.91621	175.01754	Confined to sandstone beds	
16	JN	66	289	267	A	Ro3	Tight	~0mm		2	D	~180°	Gentle		Planar	~0.6m	~0.6m		Dry	-40.91614	175.01749	Terminates against sandstone between BSH7	
17	SR	85	1	339	A	Ro4	Moderately wide to Wide	~100-50mm	~80%	1	D				Stepped	~3m	~1.5m	Clast supported (Crackle (~80%), Angular, HW, Weak, Coating, Dark blue black, Sand with traces of clay, Soft, NP) White elongated precipitation	Damp	-40.91612	175.01741	Terminates against SR11	
7	BSH	52	56	34	A	Ro3	Moderately wide	~20mm	~90%	1	D	~160°	Gentle		Irregular	~3m	~0.2m	Clast supported (Crackle (~90%), Angular, HW, Weak, Coating, Dark blue black, sandy Clay with trace of silt, Soft, MP) White gravel sized clasts of tabulated precipitation	Damp	-40.91612	175.01743	Cross-cuts SR18	
18	SR	60	38	16	A	Ro3	Moderately Narrow	~10-5mm	~90%	1	D	~150°	Gentle	~2m	Wavy	~2m	~0.8-1m	Clast supported (Crackle (~90%), Angular, CW, Very weak, Coating, Dark blue black, sandy Clay, Soft, MP) No precipitation	Damp	-40.91608	175.01737	Cross-cuts bedding and terminates against bedding and SR11	

19	SR	78	49	27	A	Ro3	Moderately wide	~40mm	~80%	1	D	~180°	Gentle		Planar	~2.5m	~0.8-1m	Clast supported (Crackle (~80%), Angular, CW, Very weak, Coating , Dark blue black, sandy Clay, Very soft, MP) Flecks of sand sized precipitation	Damp	-40.91609	175.01741	Cross-cuts bedding and terminates at SR11
20	SR	65	37	15	A	Ro2	Wide	~80mm	~80%	1	D	~110°	Open	~4m	Irregular	~2.5m		Clast supported (Crackle (~80%), Angular, CW-HW, Very weak, Coating , Dark blue black, sandy Clay, Very soft, HP) Flecks of sand sized precipitation	Damp	-40.91611	175.01736	Cross-cuts bedding and terminates at JN21
21	JN	52	296	274	A	Ro2	Tight	~0mm		1	D	~180°	Gentle		Planar	~0.8m	~0.2m			-40.91613	175.0174	
1	BSH	31	82	60	B	Ro3	Moderately wide	~40mm	~95%	0	O	~130°	Gentle	~9m	Wavy	~9m	~0.9m	Clast supported (Crackle (~95%), Angular, MW, Weak, Veneer; Dark blue black, Sand with trace of clay, Soft to very soft, LP) No precipitation	Dry	-40.9162	175.018	Terminates against SH6
3	SR	35	218	196	B	Ro4	Very Wide	~200mm	~90%	0	O	~170°	Gentle	~15m	Curved	~6m	~1m	Clast supported (Crackle (~90%), Angular, CW, Very weak, Coating; Dark and light blue black grey, Sand with trace of clay, Soft to very soft, LP) No precipitation	Dry	-40.9163	175.018	Terminates against BSH1
3b	SR	20	233	211	B	Ro3	Moderately narrow	~10mm	~80%	2	D	~180°	Gentle		Planar	~2m	~1m	Clast supported (Crackle (~80%), Angular, CW, Very weak, Coating; Dark and light blue black grey, Sand with trace of clay, Soft to very soft, LP) No precipitation	Dry	-40.9163	175.018	Terminates against BSH and SR5
4	SR	48	153	131	B	Ro2	Wide	~100mm	~80%	1	D	~160°	Gentle	~3m	Wavy	~4m	~1.5m	Clast supported (Crackle (~80%), Angular, CW, Very weak, Coating; Dark and light blue black grey, sandy Clay, Very soft, HP) No precipitation	Damp	-40.9163	175.0181	Cross cuts BSH's and terminates against SH6
5	SR	79	216	194	B	Ro3	Moderately narrow	~10mm	~80%	1	D	~160°	Gentle	~6m	Curved	~3m		Clast supported (Crackle (~80%), Angular, CW, Very weak, Coating; Dark and light blue black grey, clayey Sand, Very soft, LP-NP) No precipitation	Damp	-40.9163	175.0181	Terminates against SR40 and SR39
6	SH	8	106	84	B	Ro2	Wide	~150mm	~80%	1	D	~180°	Gentle		Planar	~10m	~7m	Clast supported (Crackle (~80%), Angular, CW, Very weak, Coating; Dark and light blue black grey, sandy Clay, Very soft, HP) No precipitation	Damp	-40.9162	175.0181	Cross cuts bedding and terminates in rock
7	SR	42	71	49	B	Ro3	Moderately narrow	~8mm	~90%	1	D	~160°	Gentle		Curved	~5m		Clast supported (Crackle (~90%), Angular, HW, Weak, Coating; Dark and light blue black grey, Sand, Very soft, NP) No precipitation	Dry	-40.9162	175.0181	Terminates against SH6 is obscured by debris
8	SR	60	154	132	B	Ro3	Wide to Moderately wide	~60mm	~90%	1	D	~180°	Gentle		Planar	~4m	~1.5m	Clast supported (Crackle (~90%), Angular, HW, Weak, Coating; Light grey, Sand trace of silt, Very soft, NP) White tabulated angular precipitation	Dry	-40.9163	175.0181	Terminates against SH6 and cross cuts SR7
10	SR	79	259	237	B	Ro2	Wide to Moderately wide	~20-70mm	~60%	0	C	~160°	Gentle	~4m	Wavy	~7m		Matrix supported (Mosaic (~60%), Angular, CW, Very weak, Coating; Dark blue grey, sandy Clay, Very soft, MP) Random lenses of white sub angular precipitation	Damp	-40.9162	175.0182	Terminates against SH6 and cross cuts bedding
9	SR	55	234	212	B	Ro4	Wide to Very wide	~200-100mm	~80%	1	D	~170°	Gentle	~2m	Wavy	~4m	~0.1m	Clast supported (Crackle (~80%), Angular, HW, Weak, Coating; Light blue grey, sandy Clay, Very soft, NP) Sand sized flecks of white precipitation	Dry	-40.9162	175.0181	Terminates against SH6
11	BSH	33	69	47	B	Ro3	Moderately narrow to Moderately wide	~20mm	~95%	2	D	~170°	Gentle	~2m	Wavy	~4m		Clast supported (Crackle (~95%), Angular, MW, Moderately strong, Coating; Dark blue grey, Sand, Very soft, NP) Elongated angular white precipitation	Dry	-40.9161	175.0181	Terminates against SR10 and SH17 and offset by SR12
12	SR	83	9	347	B	Ro2	Moderately narrow	~8mm	~95%	2	D	~135°	Gentle	~1.5m	Wavy	~3m		Clast supported (Crackle (~95%), Angular, HW, Weak, Coating; Dark blue grey, Sand, Very soft, NP) Elongated angular white precipitation	Dry	-40.9161	175.0182	Off sets bedding and terminates against bedding
13	SR	17	179	157	B	Ro2	Moderately narrow	~8mm	~99%	2	D	~180°	Gentle		Planar	~3m		Clast supported (Rock (~99%), Angular, MW, Moderately strong, Coating; Light blue grey, Sand, Very soft, NP) Elongated angular white precipitation	Dry	-40.9162	175.0181	Terminates against SR12
14	SR	79	323	301	B	Ro5	Narrow	~5mm	~80%	1	D	~180°	Gentle		Stepped	~5m	~0.8m	Clast supported (Crackle (~80%), Angular, HW, Weak, Coating; Dark blue grey, Sand, Very soft, LP) No precipitation	Damp	-40.9161	175.0182	Terminates against SR16
15	JN	44	150	128	B	Ro2	Tight	~0mm		2	D	~180°	Gentle		Planar	~1.2m	~0.1m			-40.9161	175.0181	
16	SR	41	162	140	B	Ro3	Very narrow to narrow	~2mm	~95%	2	D	~180°	Gentle		Planar	~5m		Clast supported (Crackle (~95%), Angular, HW, Weak, Coating; Dark blue grey, Sand, Very soft, NP) Some white tabulated angular precipitation	Damp	-40.916	175.0182	Cross cuts SR12 and terminates against BSH11
17	SH	17	141	119	B	Ro3	Very wide	~200mm	~50%	1	D	~150°	Gentle	~3m	Wavy	~15m		Matrix supported (Mosaic (~50%), Angular, CW, Very weak, Coating; Dark blue grey and light, sandy Clay, Very soft, MP) Some white tabulated angular precipitation	Minor seepage	-40.9161	175.0181	Transitions into SH20 on the next map sheet
18	SR	17	263	241	B	Ro3	Wide to Very wide	~150-200mm	~80%	2	D	~180°	Gentle		Stepped	~6m	~0.6m	Clast supported (Crackle (~80%), Angular, CW, Very weak, Coating; Dark blue grey and light, sandy Clay, Very soft, MP) Some white tabulated angular precipitation	Minor seepage	-40.916	175.0181	Terminates against JN15
19	SR	88	346	324	C	Ro4	Wide to Very wide	~150-200mm	~90%	1	D	~180°	Gentle		Stepped	~4m		Clast supported (Crackle (~90%), Angular, CW, Very weak, Coating; Dark blue grey, (mostly washed out) sandy Clay, Very soft, NP) No precipitation	Minor seepage	-40.916	175.0182	Terminates against SH20/17
20	SH	31	114	92	B&C	Ro3	Very wide	~150mm	~20%	1	D	~135°	Gentle	~5m	Wavy	~20m		Matrix supported (Soil (~20%), Angular, CW, Very weak, Coating; Dark and light blue grey, sandy Clay, Very soft, MP) No precipitation	Damp	-40.9158	175.0182	Transitioned from SH17 and terminates against SR25
21	SR	10	12	350	C	Ro3	Moderately narrow	~10mm	~80%	2	D	~150°	Gentle	~1.5m	Wavy	~3m		Clast supported (Crackle (~80%), Angular, HW, Weak, Coating; Dark blue grey, Sand, Soft, NP) No precipitation	Damp	-40.9159	175.0182	Terminates in rock and against bedding/sandstone

22	SR	30	19	357	B	Ro3	Moderately wide to Wide	~60mm	~80%	1	R	~180°	Gentle		Planar	~6m		Clast supported (Crackle (~80%), Angular, CW, Very weak, Coating; Dark blue grey, Sand, Soft, NP) No precipitation	Damp	-40.9158	175.0183	Terminates against SH20
23	SR	37	140	118	C	Ro3	Moderately wide	~30mm	~80%	1	D	~160°	Gentle	~10m	Curved	~5m	~1.5m	Clast supported (Crackle (~80%), Angular, HW, Weak, Coating; Dark blue grey, Sand, Soft, NP) No precipitation	Dry	-40.9158	175.0183	Cross cuts SH20 and SR24
24	SR	17	256	234	C	Ro3	Moderately narrow to Moderately wide	~20mm	~80%	2	D	~180°	Gentle		Stepped	~8m		Clast supported (Crackle (~80%), Angular, HW, Weak, Coating; Dark blue grey, Sand, Soft, NP) No precipitation	Dry	-40.9156	175.0183	Cross cuts bedding and terminates against SH31
26	SR	41	137	115	C	Ro3	Moderately narrow to Moderately wide	~20mm	~90%	2	D	~150°	Gentle		Curved	~4m	~1.25m	Clast supported (Crackle (~90%), Angular, HW, Weak, Coating; Dark blue grey, Sand, Soft, NP) No precipitation	Dry	-40.9157	175.0185	Terminates against SR29 and in rock
27	SR	10	129	107	C	Ro3	Moderately narrow to Moderately wide	~20mm	~90%	2	D	~150°	Gentle		Curved	~4m		Clast supported (Crackle (~90%), Angular, HW, Weak, Coating; Dark blue grey, Sand, Soft, NP) No precipitation	Dry	-40.9156	175.0183	Terminates in rock and against SH32
28	JN	38	240	218	C	Ro3	Moderately narrow to Moderately wide	~20mm	~90%	2	D	~180°	Gentle		Stepped	~1m	~0.1m	Clast supported (Crackle (~90%), Angular, HW, Weak, Coating; Dark blue grey, Sand, Soft, NP) No precipitation	Dry	-40.9156	175.0182	Terminates against bedding and in rock
29	SR	15	349	327	C	Ro3	Moderately narrow to Moderately wide	~20mm	~90%	1	D	~180°	Gentle		Planar	~5m		Clast supported (Crackle (~90%), Angular, HW, Moderately strong, Coating; Dark blue black, Sand with trace of clay, Soft, LP for clay) Sand sized flecks of white precipitation	Dry	-40.9155	175.0182	Terminates against SR25 and SH32
31	SH	31	77	55	C	Ro2	Moderately wide	~50mm	~80%	1	D	~170°	Gentle	~2.5m	Wavy	~16m	~2m	Clast supported (Crackle (~80%), Angular, HW-CW, Weak, Coating; Dark blue grey, Clay with minor of sand, Very soft, HP) Random lenses of white sub angular precipitation	Dry	-40.9155	175.0183	Follows bedding
30	BSH	29	100	78	C	Ro2	Moderately narrow	~10mm	~95%	1	D	~170°	Gentle	~2.5m	Wavy	~16m	~0.4m	Clast supported (Crackle (~95%), Angular, MW, Weak, Coating; Dark blue grey, Sand with traces of clay, Very soft, HP) Random lenses of white sub angular precipitation	Dry	-40.9154	175.0183	Terminates against SH20
32	SH	48	211	189	C	Ro2	Moderately wide to Wide	~100-30mm	~80%	2	D	~170°	Gentle	~0.9m	Wavy	~3m	~2m	Clast supported (Crackle (~80%), Angular, HW-CW, Very weak, Coating; Dark blue grey and light brown, sandy Clay with traces of silt, Soft, HP) Random lenses of white sub angular precipitation	Dry	-40.9155	175.0183	Failure plain
34	CZ	43	147	125	C	Ro2	Wide to Moderately wide	~70cm then narrows to 30mm	~90%	0	C	~150°	Gentle	~20m	Curved	~8m		Clast supported (Crackle (~90%), Angular, HW-CW, Weak to moderately strong, Coating; Dark blue grey and light brown, Sand and Clay with minor silt, Soft to very soft, HP) No precipitation	Damp	-40.9155	175.0183	Terminates against SR29 and SH32
33	CZ	41	174	152	C	Ro3	Moderately narrow	~14mm	~80%	2	D	~180°	Gentle		Irregular	~2m		Clast supported (Crackle (~80%), Angular, HW, Weak to moderately strong, Coating; Dark blue grey and light brown, sandy Clay with traces of silt, Soft, LP) Sand sized flecks of white precipitation	Damp	-40.9155	175.0183	Cross cuts bedding and is the second failure plain
35	SR	89	230	208	C	Ro3	Moderately narrow	~15mm	~99%	2	D	~140°	Gentle	~6m	Curved	~2m		Clast supported (Rock (~99%), Angular, MW, Moderately strong, Coating; Light blue grey, sandy Clay, Soft, NP) Some elongated angular white precipitation	Dry	-40.9155	175.0183	Cross cuts bedding and terminates against SH31
36	SR	37	93	71	C	Ro3	Moderately wide	~30mm	~95%	2	D	~140°	Gentle	~2m	Curved to planar	~7m		Clast supported (Crackle (~95%), Angular, HW-MW, Moderately strong, Coating; Light blue grey, sandy Clay, Soft, NP) Some elongated angular white precipitation	Dry	-40.9155	175.0182	Terminates against SH31 and in rock
37	SH	42	72	50	C	Ro3	Wide	~150mm	~80%	0	C	~160°	Gentle	~3m	Wavy	~10m	~2m	Clast supported (Crackle (~80%), Angular, CW, Weak to very weak, Coating; Dark blue grey, sandy Clay, Soft, HP) Some Sand to Gravel sized angular clasts of white precipitation	Damp	-40.9153	175.0183	cross cuts bedding
38	SR	21	189	167	C	Ro3	Wide	~100mm	~80%	1	D	~145°	Gentle	~6m	Wavy	~12m		Clast supported (Crackle (~80%), Angular, CW-HW, Weak to very weak, Coating; Dark blue grey, sandy Clay, Soft, HP) Some Sand to Gravel sized angular clasts of white precipitation	Damp	-40.9153	175.0183	Splay off of BSH30
39	JN	40	253	231	C	Ro3	Narrow to Moderately narrow	~6mm	~85%	1	D	~180°	Gentle		Planar	~2m	~0.2m	Clast supported (Crackle (~85%), Angular, CW-HW, Weak to very weak, Coating; Dark blue grey and light brown, clayey Sand, Very soft, LP) Some Sand to Gravel sized angular clasts of white precipitation	Damp	-40.9154	175.0182	Terminates against SH37
39a	SR	44	135	113	C															-40.9154	175.0182	Random SR potential failure too far away to gather data
39b	SR	23	323	301	C															-40.9153	175.0182	Random SR potential failure too far away to gather data
40	SR	69	309	287	C	Ro2	Moderately wide	~25mm	~90%	1	D	~180°	Gentle		Planar	~2m		Clast supported (Crackle (~90%), Angular, MW, Moderately strong, Coating; Dark blue grey and light brown, clayey Sand, Very soft, LP) Some Sand to Gravel sized angular clasts of white precipitation	Damp	-40.9154	175.0181	Terminates against SR44

41	SR	28	298	276	C	Ro3	Moderately narrow	~15mm	~85%	2	D	~150°	Gentle	~6m	Curved	~3m		Clast supported (Crackle (~85%), Angular, HW, Weak, Coating; Dark blue grey, clayey Sand, Soft, NP) Some Sand to Gravel sized angular clasts of white precipitation	Dry	-40.9153	175.0181	Splays and terminates against SH37 and SR42
43	SR	77	136	114	C	Ro3	Moderately wide	~30mm	~80%	1	D	~170°	Gentle	~1.5m	Wavy	~3m		Clast supported (Crackle (~80%), Angular, HW, Weak, Coating; Dark blue grey, sandy Clay, Firm, NP) No precipitation	Dry	-40.9153	175.018	Offsets bedding
42	SR	65	95	73	C	Ro3	Moderately wide	~30mm	~80%	1	D	~180°	Gentle		Planar	~4m		Clast supported (Crackle (~80%), Angular, HW, Weak, Coating; Dark blue grey, sandy Clay, Firm, NP) No precipitation	Damp	-40.9152	175.0182	Terminates against FL43 and offsets bedding by approximately 10cm
44	SR	16	69	47	C	Ro3	Very narrow to narrow	~2mm	~95%	2	D	~180°	Gentle		Planar	~4m		Clast supported (Crackle (~95%), Angular, HW, Weak, Coating; Dark blue grey, Sand, Soft, NP) No precipitation	Dry	-40.9154	175.0181	Terminates against SR40 and SR39
45R	FL	80	271	249	C	Ro3	Wide	~150mm	~80%	0	C	~160°	Gentle	~1.2m	Irregular	~6m		Clast supported (Crackle (~80%), Angular, HW, Weak, Coating; Dark and light blue grey, clayey Sand and Clay, Soft and firm, NP and some HP) Some angular elongated white precipitation	Dry	-40.9152	175.0182	Terminates against FL45
45	FL	78	244	222	C	Ro3	Very wide	~800mm in parts narrows to 200mm	~80%	0	C	~160°	Gentle	~1.2m	Irregular	~6m		Clast supported (Crackle (~80%), Angular, CW, Weak, Coating; Dark and light blue grey, clayey Sand and Clay, Soft and firm, NP and some HP) Some angular elongated white precipitation	Dry	-40.9153	175.0181	Terminates against SR18
46	FL	54	124	102	D	Ro3	Narrow	~4mm	~95%	1	D	~160°	Gentle	~4m	Wavy	~5m		Clast supported (Crackle (~95%), Angular, HW, Weak, Coating; Dark Blue grey, Sand, Soft, NP) Some sand sized white flecks	Dry	-40.9153	175.0181	Terminates at FL45
47	BSH	28	107	85	D	Ro3	Moderately narrow	~10mm	~80%	1	D	~170°	Gentle	~6m	Wavy	~7m		Clast supported (Crackle (~80%), Angular, HW, Weak to very weak, Coating; Dark blue grey, sandy Clay, Very soft, NP) No precipitation	Dry	-40.9154	175.0181	Terminates against FL45
48	SR	85	152	130	D	Ro4	Moderately narrow to narrow	~15-4mm	~90%	1	D				Stepped	~3.5m		Clast supported (Crackle (~90%), Angular, HW, Weak, Coating; Light and dark blue grey, clayey Sand, Soft, NP) Some sand sized white flecks	Dry	-40.9152	175.0181	Terminates against SR47
49	SR	13	200	178	D	Ro4	Moderately narrow	~10mm	~90%	1	D				Stepped	~2.5m		Clast supported (Crackle (~90%), Angular, HW, Weak, Coating; Light and dark blue grey, clayey Sand, Soft, NP) Some sand sized white flecks	Dry	-40.9152	175.0181	Terminates against SR50
50	SR	77	159	137	D	Ro3	Moderately narrow	~15mm	~85%	2	D	~160°	Gentle		Wavy	~6m	~2.5m	Clast supported (Crackle (~85%), Angular, HW, Weak to very weak, Coating; Light and dark blue grey, Sand and Clay with minor silt, Soft and firm, LP) Some Sand to Gravel sized angular clasts of white precipitation	Dry	-40.9152	175.018	Terminates against BSH53 and SR47
51	SR	81	120	98	D	Ro3	Moderately narrow	~8mm	~90%	2	D	~150°	Gentle	~1.25 m	Curved	~2m		Clast supported (Crackle (~90%), Angular, HW, Weak, Coating; Dark blue grey, clayey Sand, Soft, NP) Some sand sized white flecks	Dry	-40.9152	175.0181	Terminates against SR50 and SR55
52	SR	37	101	79	D	Ro4	Moderately narrow	~15mm	~95%	2	D	-	Gentle		Stepped	~2m		Clast supported (Crackle (~95%), Angular, HW, Weak, Coating; Light blue grey, silty Sand, Very soft, NP) No precipitation	Dry	-40.9152	175.0181	Terminates against SR50 and SR55
53	SR	34	90	68	D	Ro3	Moderately wide to moderately narrow	~20mm	~90%	0	C	~170°	Gentle	~1.5m	Wavy	~5m		Clast supported (Crackle (~90%), Angular, HW, Weak, Coating; Light blue grey, Sand traces of clay, Soft, NP) Some sand sized white flecks	Damp	-40.9152	175.0181	Terminates against BSH1 also cross cuts SR2 and JN3b
54	SR	87	287	265	D	Ro4	Moderately narrow	~8-10mm	~95%	2	D	-	Gentle		Stepped	~2m		Clast supported (Crackle (~95%), Angular, HW, Weak, Coating; Light blue grey, Sand, Soft, NP) No precipitation	Dry	-40.9151	175.0181	Terminates against SR50 and cross cuts SR52
55	SR	31	345	323	D	Ro3	Moderately narrow	~15mm	~85%	1	D	~160°	Gentle		Wavy	~2.5m	~2.5m	Clast supported (Crackle (~85%), Angular, HW, Weak to very weak, Coating; Light and dark blue grey, Sand and Clay with minor silt, Soft and firm, LP) Some Sand to Gravel sized angular clasts of white precipitation	Dry	-40.9151	175.018	Terminates against BSH53
56	BSH	60	58	36	D	Ro2	Wide	~120mm	~50%	0	C	~160°	Gentle	~1.5m	Wavy	~10m	~1.5m	Matrix supported (Mosaic (~50%), Angular, CW, Very weak, Coating; Light blue grey, sandy Clay and Clay, Very soft, MP) No precipitation	Minor seepage	-40.9152	175.0181	
58	BSH	48	45	23	D	Ro2	Wide	~150mm	~35%	2	D	~160°	Gentle	~1m	Wavy	~7m		Matrix supported (Chaotic (~35%), Angular, CW, Very weak, Coating; Light and dark blue grey, Clay with minor of sand, Very soft, HP) Terminates against SR57 and CZ60	Minor seepage	-40.9151	175.018	Terminates against SR57 and CZ60
57	SR	51	134	112	D	Ro3	Moderately wide	~25mm	~60%	1	D	~160°	Gentle	~3m	Wavy	~4m		Matrix supported (Mosaic (~60%), Angular, CW, Very weak, Coating; Light grey, sandy Clay, Soft, NP) Some sand sized white flecks	Damp	-40.9152	175.0181	Terminates against SR58
59	BSH	59	68	46	D	Ro3	Moderately wide	~30mm	~80%	1	D	~160°	Gentle	~1.5m	Wavy	~1m	~3m	Clast supported (Crackle (~80%), Angular, HW, Weak, Coating; Light grey, sandy Clay and clayey Sand, Soft, NP) Some sand sized white flecks	Damp	-40.9149	175.018	Terminates against CZ60 and is cover by debris at the other end
60	CZ	85	220	198	D	Ro2	Wide	~175mm	~50%	0	C	~180°	Gentle		Planar	~2.5m		Matrix supported (Mosaic (~50%), Angular, CW, Very weak, Coating; Light and dark blue grey , Clay and Sand with traces of Clay, Very soft, NP) No precipitation	Minor seepage	-40.915	175.018	Too wet to roll a thread
61	SR	27	218	196	D	Ro3	Narrow	~5mm	~90%	1	O	~180°	Gentle		Planar	~3m		Clast supported (Crackle (~90%), Angular, HW, Weak, Coating; Light grey, Sand and Clay with minor silt, Firm, NP) No precipitation	Damp	-40.915	175.0179	Terminates against CZ60
62	SR	32	48	26	D	Ro3	Wide	~120mm	~80%	0	O	~160°	Gentle	~2m	Wavy	~1.5m		Clast supported (Crackle (~80%), Angular, HW-CW, Very weak, Coating; Light and dark blue grey, Sand and Clay, Soft to very	Minor seepage	-40.915	175.0179	Terminations obscured by debris

1	BSH	43	51	29	B	Ro3	Moderately wide	~30mm	~80%	0	C		Gentle		Stepped	~8m	~3m	soft, LP) No precipitation Clast supported (Crackle (~80%) Angular, HW, Weak to Very weak, Coating; Dark blue grey, silty Sand with traces of clay, Soft to Firm, NP) No precipitation	Dry to Damp	-40.9152	175.0179	Continuous
13	SH	25	157	135	C	Ro2	Moderately wide	~200mm	~90%	1	D	~140°	Gentle	~8m	Wavy	~8m	~0.5m	Clast supported (Crackle (~90%) Angular, HW, Weak, Coating; Dark and light blue grey, silty Sand and silty Clay, Soft, LP) White elongated and tabulated precipitation ~10mm thick	Dry	-40.9155	175.018	Cross cuts BSH1&2, transitions into SH13
3	SR	32	52	30	B	Ro3	Moderately wide	~40mm	~80%	0	O	~160°	Gentle	~6m	Wavy	~2m	~1.3m	Clast supported (Crackle (~80%) Angular, HW, Very weak, Coating; Dark and light blue grey, silty Sand with traces of clay, Soft, NP) Lenses of elongated tabulated white precipitation thick~8mm	Dry	-40.916	175.018	Terminates at SR4
2	BSH	18	304	282	B	Ro2	Moderately wide to Wide	~50-130mm	~80%	0	O	~170°	Gentle	~8m	Wavy	~8m		Clast supported (Crackle (~80%) Angular, HW-CW, Weak, Coating; Light blue grey, silty Sand and silty Clay, Soft to Firm, HP) White sand sized precipitation	Dry	-40.916	175.018	Cross cuts SH13 and SR5
4	SR	84	338	316	B	Ro3	Moderately wide	~25mm	~90%	0	O		Gentle		Stepped	~4m	~3m	Clast supported (Crackle (~90%) Angular, MW, Moderately strong, Coating; Dark blue grey, sandy Silt with traces of clay, Soft, NP) Lenses of elongated tabulated white precipitation thick~8mm	Dry to Damp	-40.9159	175.0179	Terminates at BSH2
6	SR	20	126	104	B	Ro3	Moderately wide	~50mm	~90%	1	D	~140°	Gentle	~10m	Curved	~4m		Clast supported (Crackle (~90%) Angular, MW, Moderately strong, Coating; Light blue grey, silty Sand, Soft, NP) Lenses of elongated tabulated white precipitation thick~15mm	Dry	-40.9161	175.0179	Terminates at SR4 and cross cuts bedding
8	BSH	43	69	47	B	Ro3	Moderately wide	~40mm	~80%	1	O	~170°	Gentle	~6m	Wavy	~8m		Clast supported (Crackle (~80%) Angular, HW-CW, Very weak, Coating; Dark blue grey, silty Sand and silty Clay, Firm, MP) Tabulated white precipitation thick ~3mm	Dry	-40.916	175.0179	Cross cuts SR10 &SR11 terminates against BSH12
9	SR	29	170	148	B	Ro3	Moderately wide	~50mm	~85%	1	D	~160°	Gentle	~5m	Wavy	~6m		Clast supported (Crackle (~85%) Angular, HW, Weak, Coating; Light blue grey, silty Sand and silty Clay, Firm, NP) White specks sand sized precipitation	Dry	-40.9161	175.0178	Terminates at BSH8 and BSH2
10	SR	89	351	329	B	Ro3	Moderately wide	~30mm	~90%	2	D	~170°	Gentle	~5m	Wavy	~5m		Clast supported (Crackle (~90%) Angular, MW, Moderately strong, Coating; Light and dark blue back, silty Sand and silty Clay, Firm, LP) White specks sand sized precipitation	Dry	-40.9161	175.0178	Cross cuts SR9 and BSH8
11	SR	72	288	266	B	Ro3	Moderately narrow to Moderately wide	~30-15mm	~80%	1	R	~150°	Gentle	~2m	Wavy	~5m		Clast supported (Crackle (~80%) Angular, HW-CW, Weak, Coating; Light and dark blue back, silty Sand and silty Clay, Firm, LP) White specks sand sized precipitation	Dry	-40.9158	175.018	Cross cuts SR9 and BSH8
12	BSH	28	33	11	B	Ro3	Moderately narrow to Moderately wide	~30-15mm	~80%	1	R	~150°	Gentle	~2m	Wavy	~5m		Clast supported (Crackle (~80%) Angular, HW-CW, Weak, Coating; Light and dark blue back, silty Sand and silty Clay, Firm, LP) White specks sand sized precipitation	Dry	-40.916	175.0178	Terminates against a FL3 on the top
14	JN	45	257	235	B		Tight	~0mm				~180°	Gentle		Planar	~0.8m	~0.25m			-40.9159	175.018	Terminates against bedding
16	SH	50	236	214	C	Ro2	Moderately wide to Wide	~50-130mm	~80%	0	O	~170°	Gentle	~8m	Wavy	~8m		Clast supported (Crackle (~80%) Angular, HW-CW, Weak, Coating; Light blue grey, silty Sand and silty Clay, Soft to Firm, HP) White specks sand sized precipitation	Dry	-40.9158	175.0181	
17	SR	34	277	255	C	Ro4	Moderately narrow	~10mm	~80%	2	D	~130°	Gentle	~2m	Wavy	~4.5m		Clast supported (Crackle (~80%) Angular, HW, Weak, Coating; Dark blue grey, silty Sand and silty Clay, Firm, LP) White specks sand sized precipitation	Dry	-40.9156	175.018	Terminates against SH21
18	SR	20	154	132	C	Ro4	Moderately narrow	~10mm	~80%	2	D	~160°	Gentle	~2m	Wavy	~3m		Clast supported (Crackle (~80%) Angular, HW, Weak, Coating; Dark blue grey, silty Sand and silty Clay, Firm, LP) White specks sand sized precipitation	Dry	-40.9157	175.0181	Terminates against SR17
19	SR	16	310	288	C	Ro3	Narrow to Moderately narrow	~6mm	~95%	1	D	~160°	Gentle	~5m	curved/wavy	~4m		Clast supported (Crackle (~95%) Angular, MW, Moderately strong to Strong, Coating; Dark and light blue grey, silty Sand and silty Clay, Very soft, NP) White lenses of tabulated and elongated precipitation ~5mm thick	Dry	-40.9155	175.018	Cross cuts bedding SH22, SH20, SR18 and SR23
20	SH	30	115	93	C	Ro2	Wide	~100-120mm	~80%	1	D	~150°	Gentle	~8m	Wavy	~8m	~1.6m	Clast supported (Crackle (~80%) Angular, CW-HW, Weak to Very weak, Coating; Dark and light blue grey, silty Sand and silty Clay, Soft to Firm, LP) White sand sized specks of precipitation	Dry	-40.9156	175.018	Terminates against FL30, cross cuts defects 23, 25, 26b, 26a and 27
21	SH	46	95	73	C	Ro3	Wide	~80mm	~90%	2	D	~150°	Gentle	~6m	Wavy	~3m		Clast supported (Crackle (~90%) Angular, HW, Weak, Coating; Dark and light blue grey, silty Sand, Soft, NP) No precipitation	Dry	-40.9156	175.018	Terminates against SH20 and SH22
21	SH	48	88	66	C	Ro3	Wide	~80mm	~90%	2	D	~150°	Gentle	~6m	Wavy	~3m		Clast supported (Crackle (~90%) Angular, HW, Weak, Coating; Dark and light blue grey, silty Sand, Soft, NP) No precipitation	Dry	-40.9156	175.018	Terminates against SH20 and SH22
22	SH	16	150	128	C	Ro2	Wide	~100-120mm	~80%	1	D	~150°	Gentle	~8m	Wavy	~8m	~1.6m	Clast supported (Crackle (~80%) Angular, CW-HW, Weak to Very weak, Coating; Dark and light blue grey, silty Sand and silty Clay, Soft to Firm, LP) White specks sand sized precipitation	Dry	-40.9156	175.018	Terminates against SH20
23	SR	52	144	122	C	Ro3	Moderately wide	~25mm	~99%	1	D	~160°	Gentle	~2m	Wavy	~2.5m		Clast supported (Rock (~99%) Angular, MW, Strong, Coating; Dark blue grey, silty Sand, Soft, NP) White lenses of precipitation thick~10-20mm	Dry	-40.9156	175.0181	Cross cuts SH20, SH22 and SR19
26a	SR	87	102	80	C	Ro3	Moderately narrow to Moderately wide	~20-15mm	~85%	2	D	~160°	Gentle	~2m	Wavy	~4m	~0.5m	Clast supported (Crackle (~85%) Angular, HW, Very weak, Coating; Dark blue grey, silty Sand, Soft, NP) White specks sand sized precipitation	Dry	-40.9156	175.018	Terminates against SR24
24	SR	30	101	79	C	Ro3	Moderately wide	~25mm	~99%	2	D	~170°	Gentle	~4m	Wavy	~1m		Clast supported (Rock (~99%) Angular, MW, Strong, Coating; Dark blue grey, silty Sand, Soft, NP) White lenses of precipitation	Dry	-40.9155	175.018	Terminates against SH20 &SR27

26b	SR	86	236	214	C	Ro3	Moderately narrow	~10mm	~90%	2	D	~160°	Gentle	~2m	Wavy	~1.5m	~0.5m	thick~10-20mm Clast supported (Crackle (~90%) Angular, HW, Very weak, Coating; Light blue grey, silty Sand, Soft, NP) White sand sized specks of precipitation	Dry	-40.9155	175.018	Terminates against SR24	
27	FL	74	147	125	C	Ro3	Moderately wide	~30mm	~85%	1	D	~160°	Gentle	~4m	Wavy	~4m		Clast supported (Crackle (~85%) Angular, HW, Moderately strong, Coating; Dark and light blue grey, silty Sand with traces of clay, Soft, NP) No precipitation	Damp and Dry	-40.9155	175.0179	Cross cuts SH20 and BSH28	
28	BSH	23	93	71	C	Ro3	Moderately narrow to Moderately wide	~20-15mm	~85%	2	D	~160°	Gentle	~2m	Wavy	~1m		Clast supported (Crackle (~85%) Angular, HW, Very weak, Coating; Dark blue grey, silty Sand, Soft, NP) White specks sand sized precipitation	Dry	-40.9156	175.018	Terminates against FL30	
30	FL	55	308	286	C	Ro5	Moderately wide to Wide	~60cm	~80%	0	C	~140°	Gentle	~8m	Wavy	~8m		Clast supported (Crackle (~80%) Angular, CW, Weak to Very weak, Coating; Dark and light blue grey, silty Sand with traces of clay, Soft, NP) Very few lenses of white elongated and thick ~15mm precipitation	Dry	-40.9154	175.0179	Continuous	
30	FL	82	249	227	C&D	Ro5	Moderately wide to Wide	~60cm	~80%	0	C	~140°	Gentle	~8m	Wavy	~8m		Clast supported (Crackle (~80%) Angular, CW, Weak to Very weak, Coating; Dark and light blue grey, silty Sand with traces of clay, Soft, NP) Very few lenses of white elongated and thick ~15mm precipitation	Dry	-40.9155	175.018	Continuous	
31	SR	22	269	247	D	Ro3	Moderately wide	~40mm	~80%	2	D	~180°	Gentle		Planar	~1.2m		Clast supported (Crackle (~80%) Angular, CW, Very weak, Coating; Dark blue grey, silty Sand with traces of clay, Firm, LP) No precipitation	Dry	-40.9153	175.0179	Terminates against FL30 and SR32b	
31	SR	11	295	273	D	Ro3	Moderately wide	~40mm	~80%	2	D	~180°	Gentle		Planar	~1.2m		Clast supported (Crackle (~80%) Angular, CW, Very weak, Coating; Dark blue grey, silty Sand with traces of clay, Firm, LP) No precipitation	Dry	-40.9154	175.0178	Terminates against FL30 and SR32b	
31	SR	11	296	274	D	Ro3	Moderately wide	~40mm	~80%	2	D	~180°	Gentle		Planar	~1.2m		Clast supported (Crackle (~80%) Angular, CW, Very weak, Coating; Dark blue grey, silty Sand with traces of clay, Firm, LP) No precipitation	Dry	-40.9154	175.0178	Terminates against FL30 and SR32b	
32a	SR	62	282	260	D	Ro3	Moderately wide	~30mm	~90%	2	D	~180°	Gentle		Planar	~1.5m	~1m	Clast supported (Crackle (~90%) Angular, HW, Weak, Coating; Dark blue grey, silty Sand with traces of clay, Soft, NP) No precipitation	Dry	-40.9154	175.018	Terminates against SR31 and FL30	
34	SR	30	150	128	D	Ro3	Moderately wide	~40mm	~80%	2	D	~140°	Gentle	~9m	Wavy	~8m		Clast supported (Crackle (~80%) Angular, HW, Very weak, Coating; Dark blue grey, silty Sand and Clay, Firm, MP (clay)) No precipitation	Damp	-40.9155	175.018	Terminates against SR32b	
35	SR	64	206	184	D	Ro4	Tight	~0mm		1	D		Gentle		Irregular	~6m				-40.9153	175.0179	Terminates against a SR	
37	FL	57	155	133	D	Ro2	Moderately wide	~30mm	~85%	1	D	~180°	Gentle		Planar	~4m		Clast supported (Crackle (~85%) Angular, MW, Moderately strong, Coating; Dark and light blue grey, silty Sand with traces of clay, Soft, NP) Sand sized specks and some lenses of elongated 15mm thick precipitation	Damp	-40.9154	175.0179	Terminates against SR35 and cross cuts SR36	
37	FL	57	156	134	D	Ro2	Moderately wide	~30mm	~85%	1	D	~180°	Gentle		Planar	~4m		Clast supported (Crackle (~85%) Angular, MW, Moderately strong, Coating; Dark and light blue grey, silty Sand with traces of clay, Soft, NP) Sand sized specks and some lenses of elongated 15mm thick precipitation	Damp	-40.9154	175.0179	Terminates against SR35 and cross cuts SR36	
36	SR	28	92	70	D	Ro3	Moderately wide	~25mm	~85%	1	D	~160°	Gentle	~7m	Curved	~7m		Clast supported (Crackle (~85%) Angular, MW, Moderately strong, Coating; Dark and light blue grey, silty Sand with traces of clay, Soft, NP) White sand sized specks precipitation	Damp	-40.9154	175.0178	Cross cuts FL37 offset ~4cm	
36	SR	26	97	75	D	Ro3	Moderately wide	~25mm	~85%	1	D	~160°	Gentle	~7m	Curved	~7m		Clast supported (Crackle (~85%) Angular, MW, Moderately strong, Coating; Dark and light blue grey, silty Sand with traces of clay, Soft, NP) White sand sized specks precipitation	Damp	-40.9153	175.0179	Cross cuts FL37 offset ~4cm	
38	SH	27	84	62	D	Ro2	Moderately wide to Wide	~60mm	~80%	1	D	~170°	Gentle	~6m	Wavy	~13m	~1m	Clast supported (Crackle (~80%) Angular, HW-CW, Weak, Coating; Dark and light blue grey, Clay, Firm, HP) White sand sized specks and some lenses of elongated 15mm thick precipitation	Damp	-40.9153	175.0179	Terminates against SR35	
39	SR	60	85	63	D	Ro2	Moderately wide	~30mm	~85%	1	D	~170°	Gentle	~4m	Wavy	~7m		Clast supported (Crackle (~85%) Angular, MW, Moderately strong, Coating; Dark and light blue grey, silty Sand with traces of clay, Soft, NP) White sand sized specks and some lenses of elongated 15mm thick precipitation	Damp	-40.9155	175.0179	Terminates against SR35	
-	JN	40	84	62						2	C	~180°	Gentle		Planar		~0.15m			-40.9155	175.018		
-	JN	42	174	152						2	C	~180°	Gentle		Planar		~0.07m						
-	JN	36	257	235						2	C	~180°	Gentle		Planar		~0.1m			-40.9155	175.018		
-	JN	45	180	158						2	C	~180°	Gentle		Planar		~0.15m			-40.9155	175.018		
-	JN	82	334	312						2	C	~180°	Gentle		Planar		~0.4m			-40.9155	175.018		
-	JN	56	160	138						2	C	~180°	Gentle		Planar		~0.1m			-40.9155	175.0179		
-	JN	73	57	35						2	C	~180°	Gentle		Planar		~0.15m			-40.9154	175.018		
-	JN	79	342	320						2	C	~180°	Gentle		Planar		~0.4m			-40.9155	175.018		
-	JN	82	292	270						2	C	~180°	Gentle		Planar		~0.4m			-40.9155	175.0179		
-	JN	23	221	199						2	C	~180°	Gentle		Planar		~0.2m			-40.9155	175.0182		

C.4 Kapiti Quarry Graphs

Defect and rock mass results from Kapiti Quarry. Results are presented in graphs. Where percentages are used they display the respective occurrence of the dependent variable assessed.

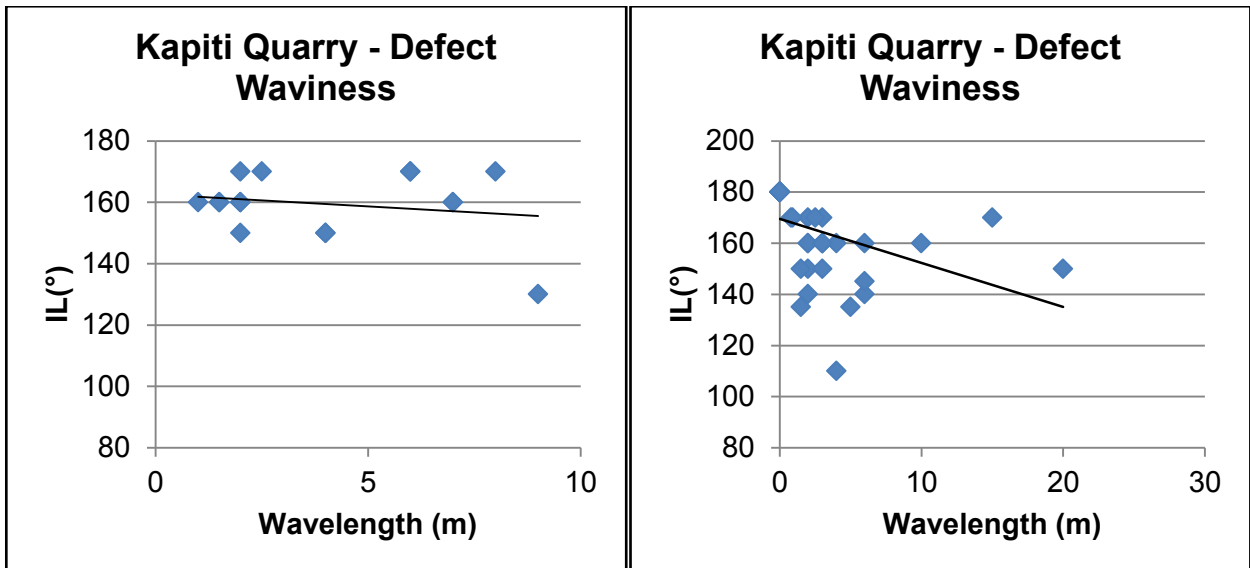
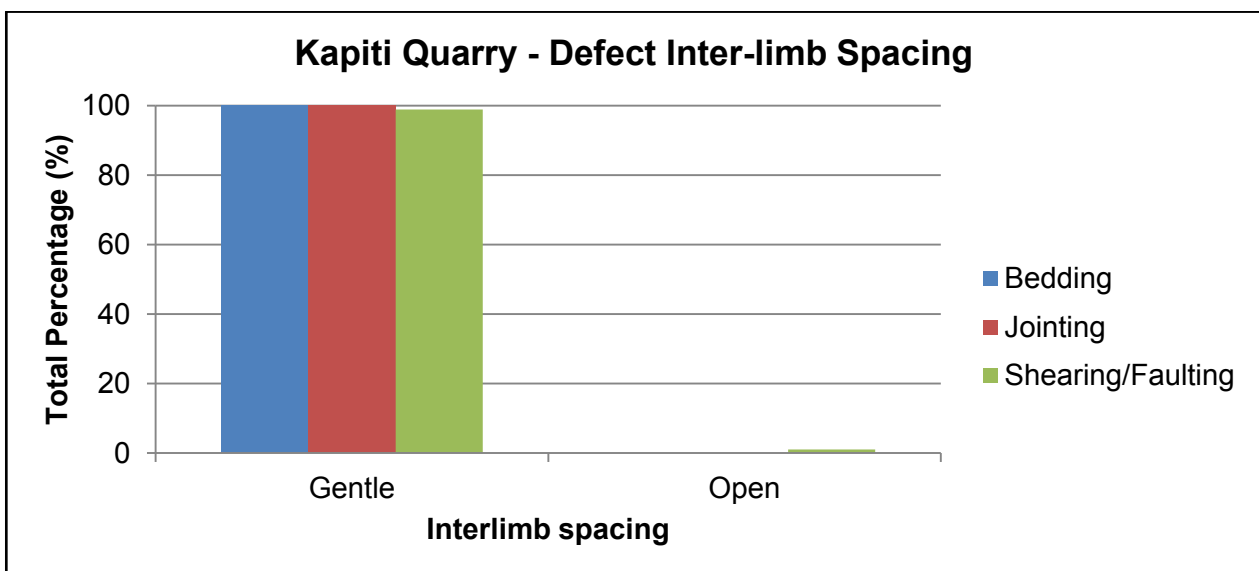
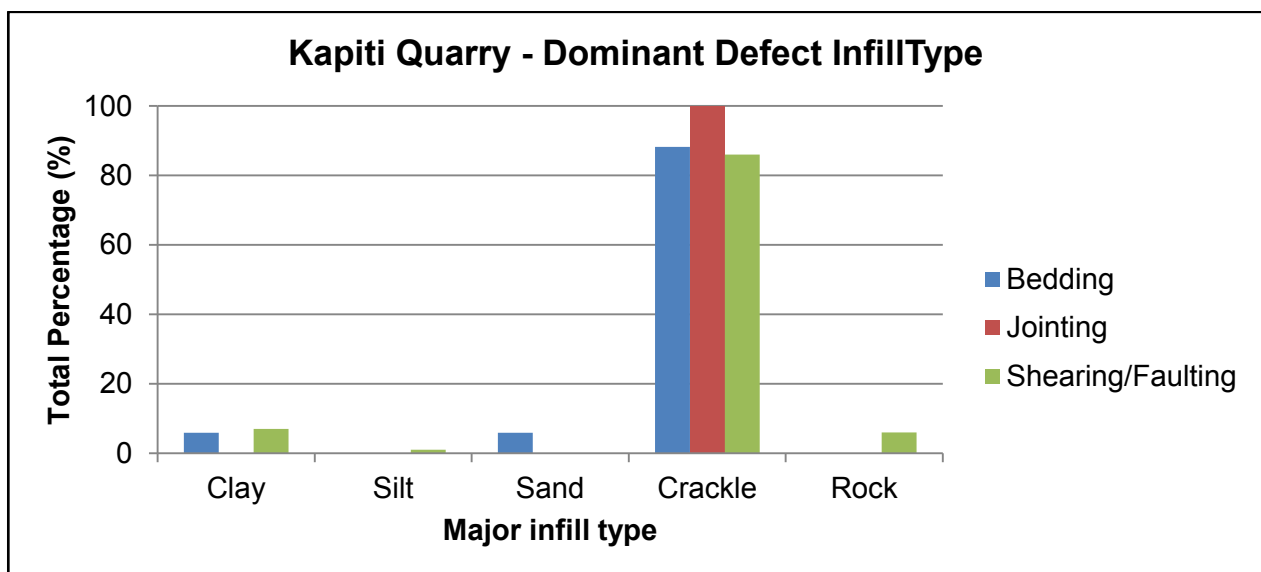
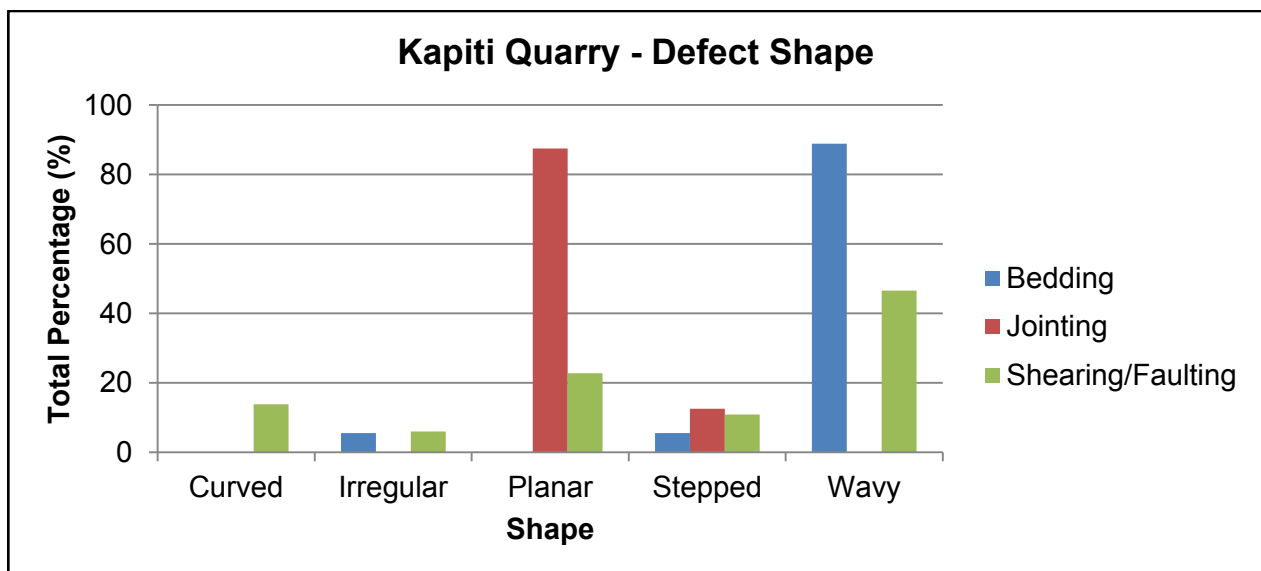
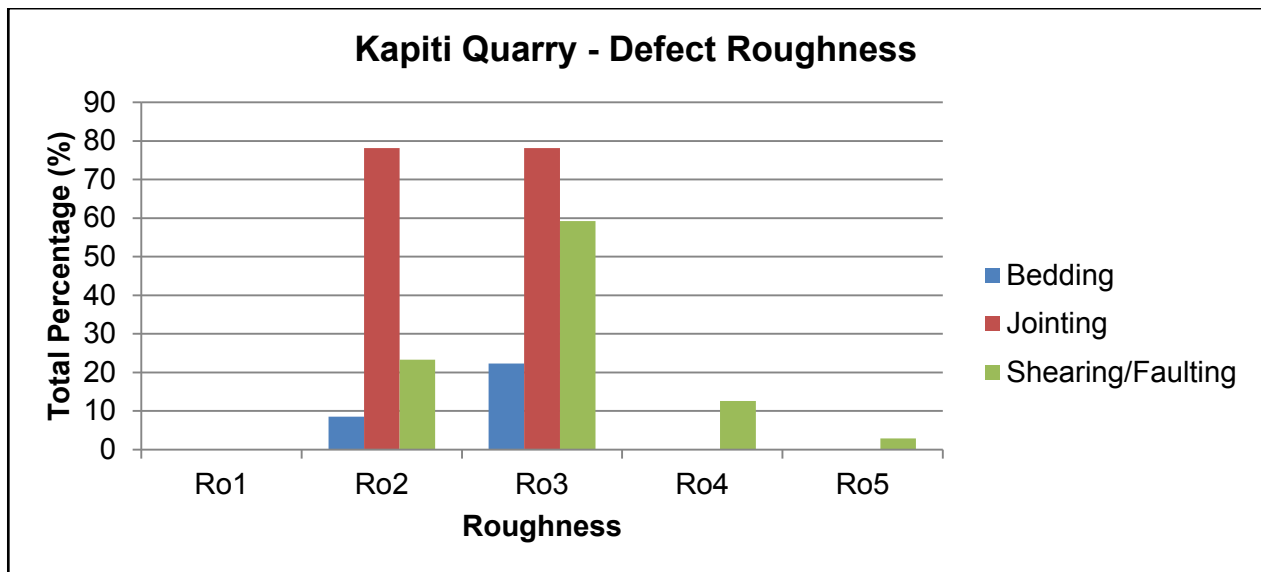
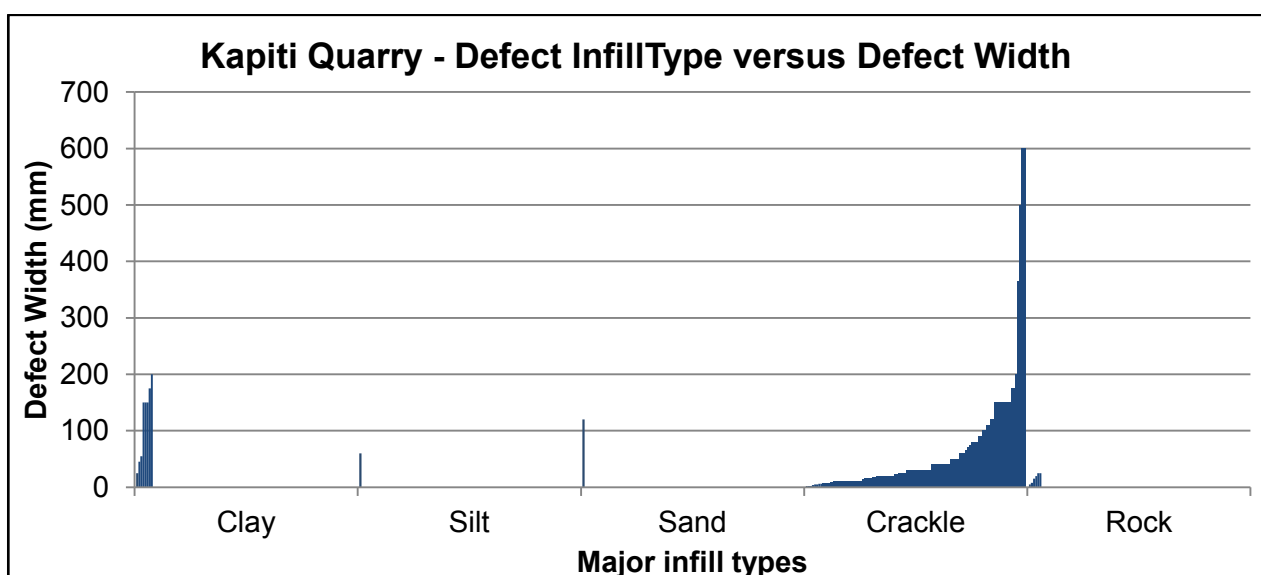
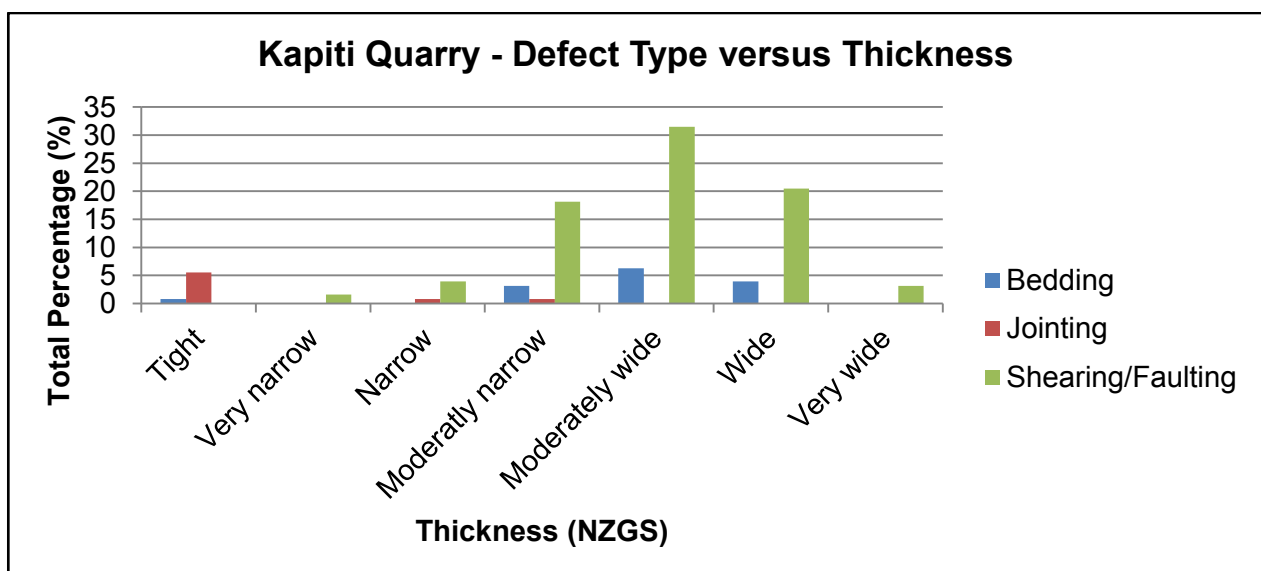
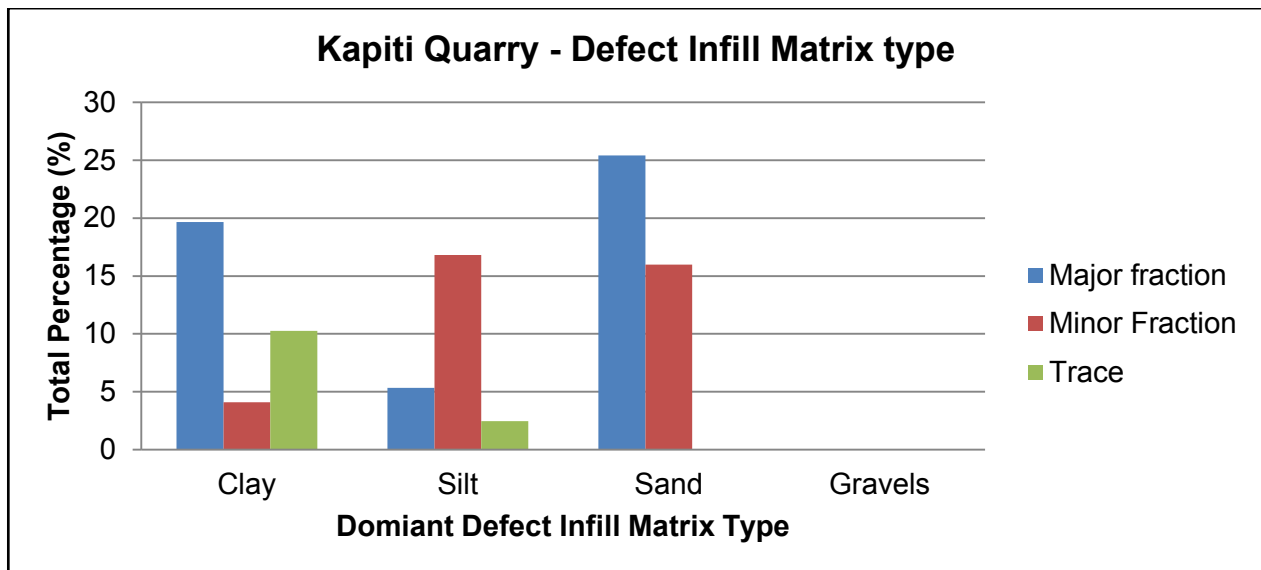
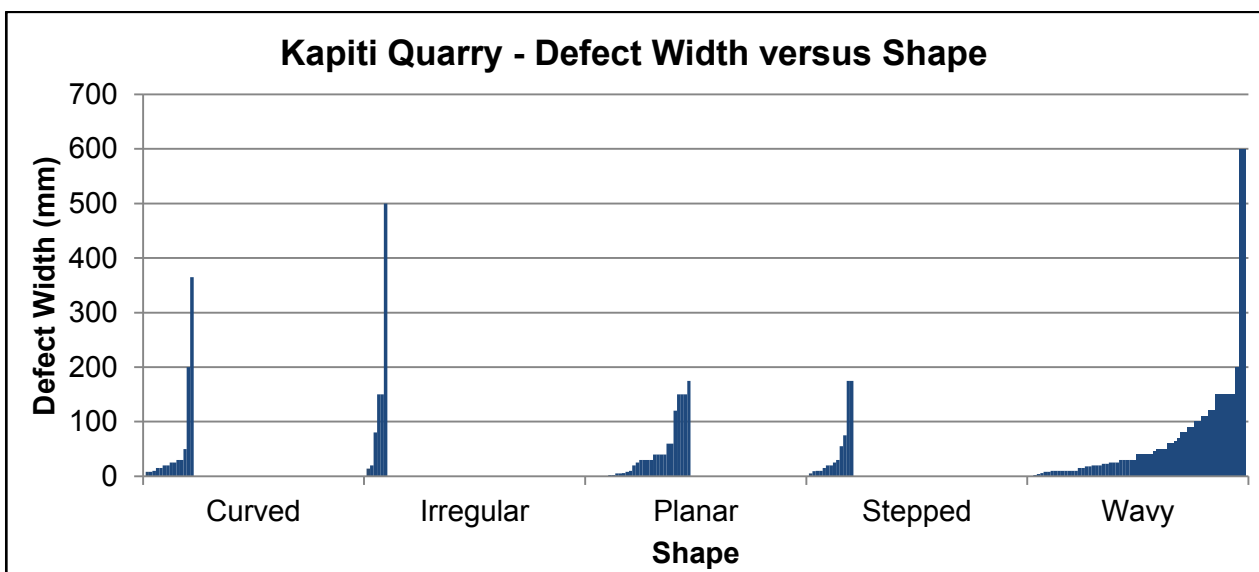
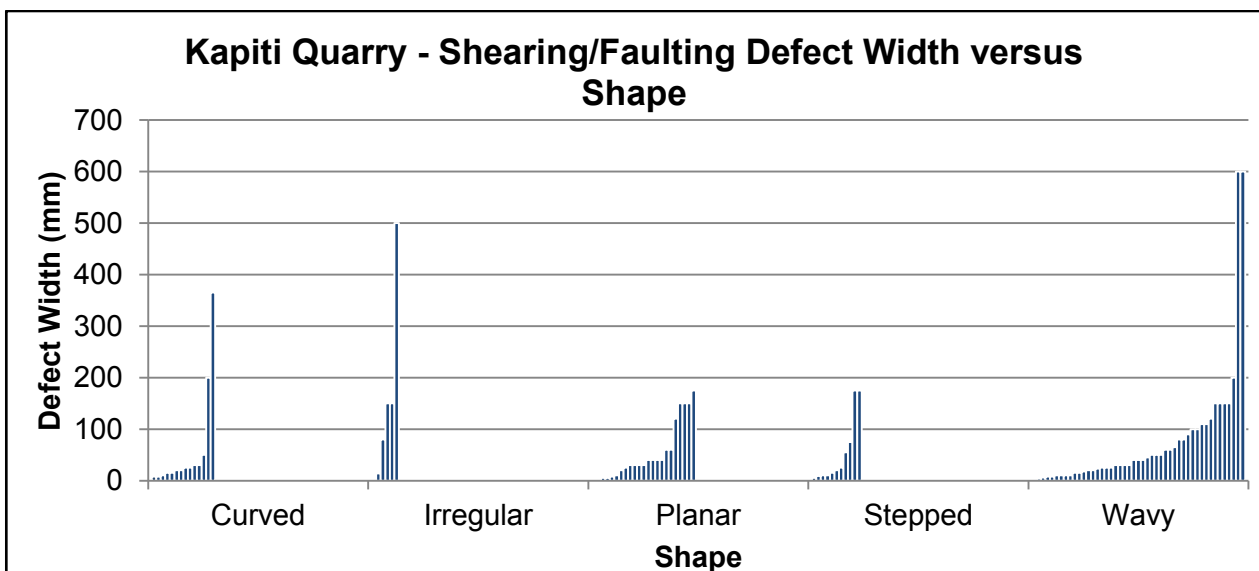
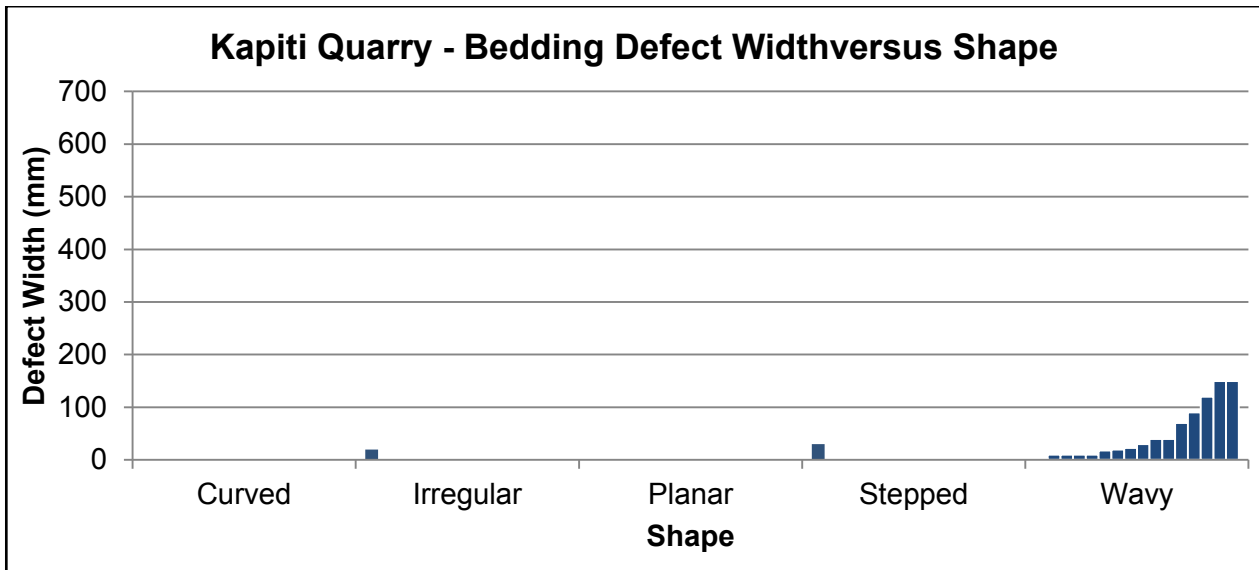


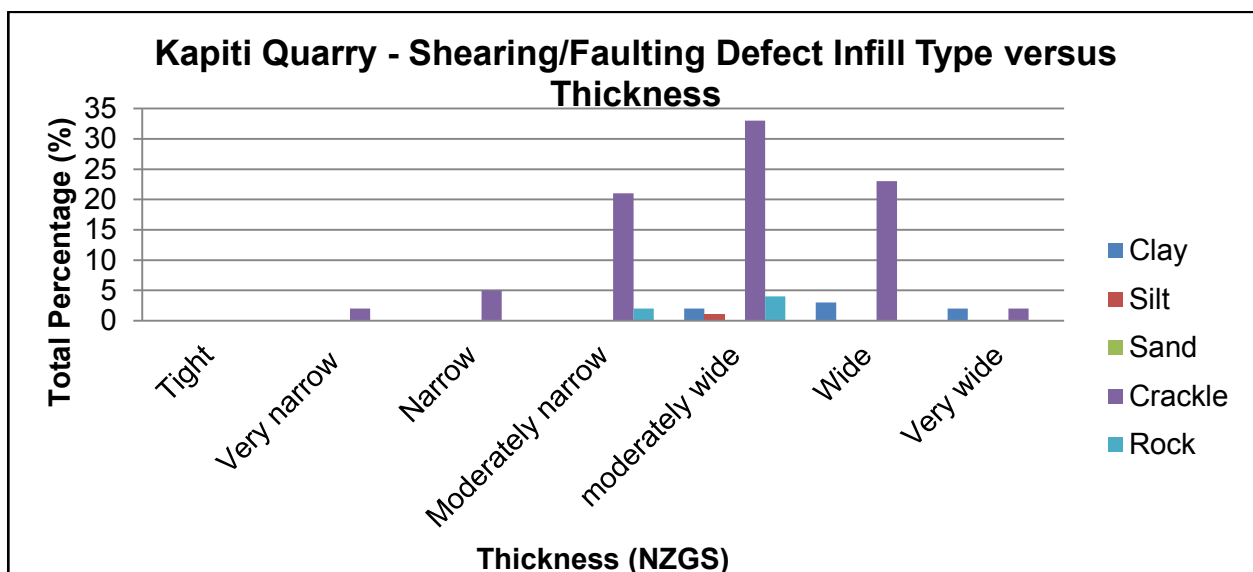
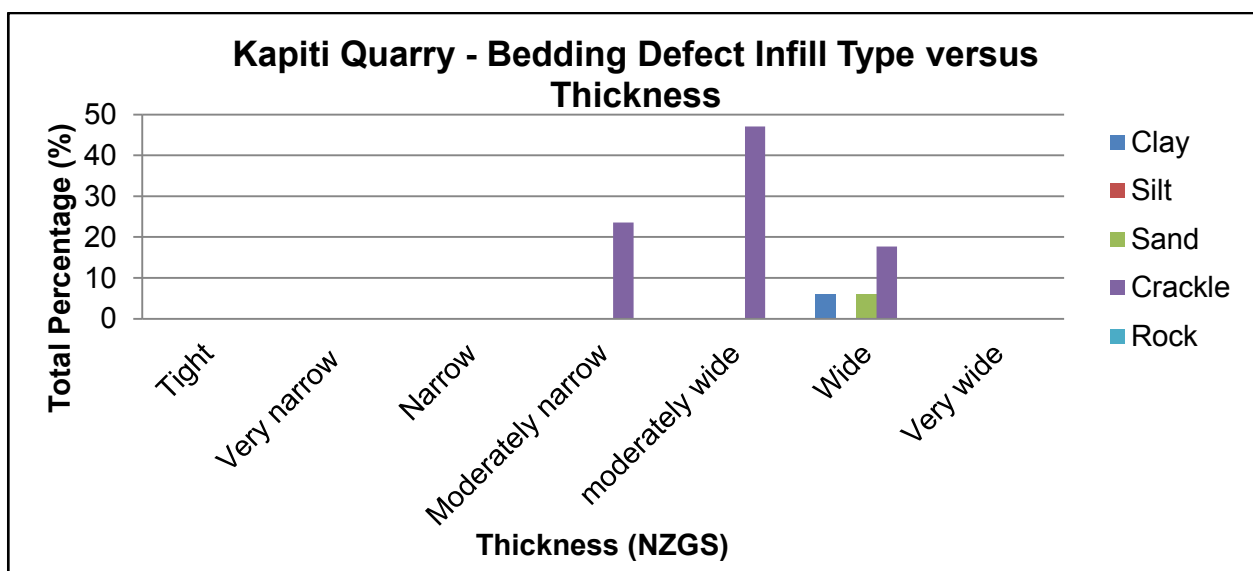
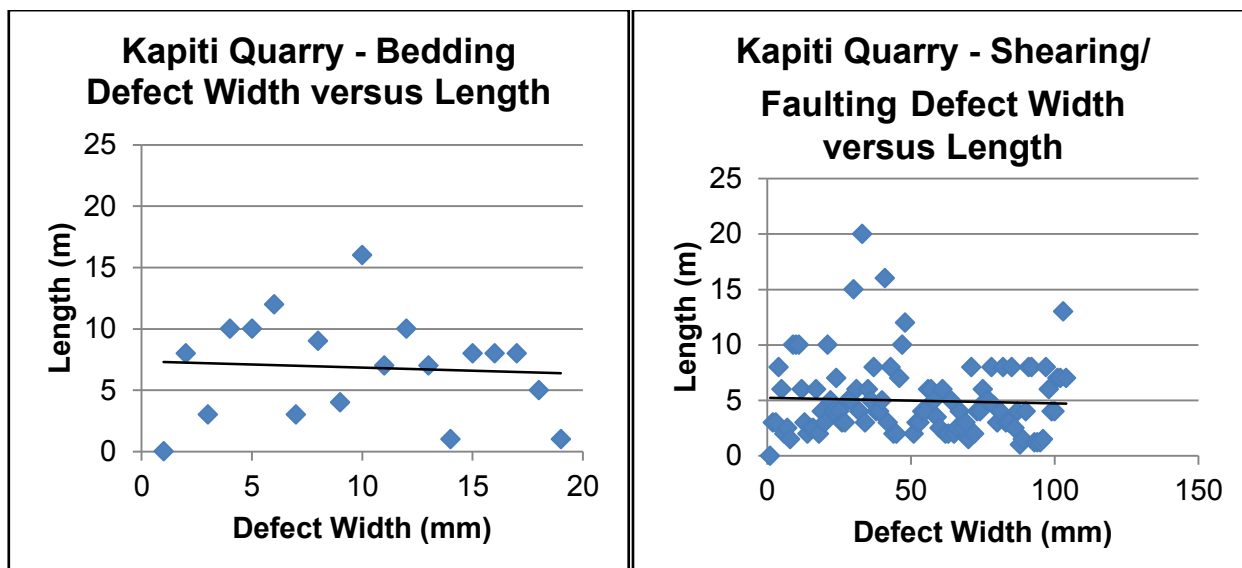
Figure C.4.1: Graphs displaying the waviness of shearing (Right) and bedding (Left) in Kapiti Quarry.

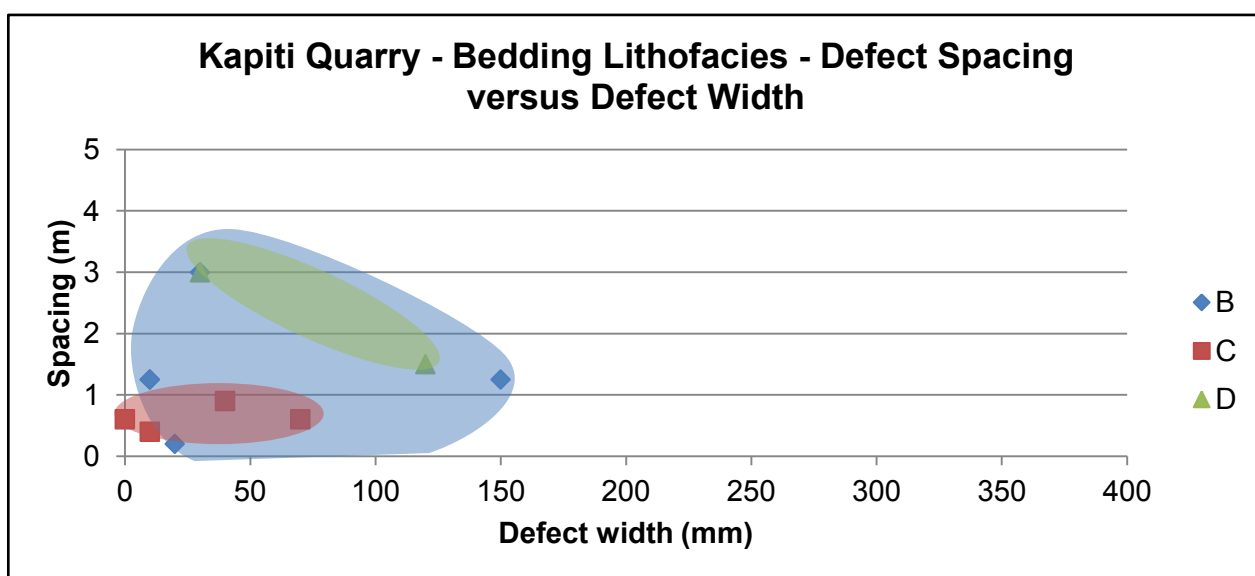
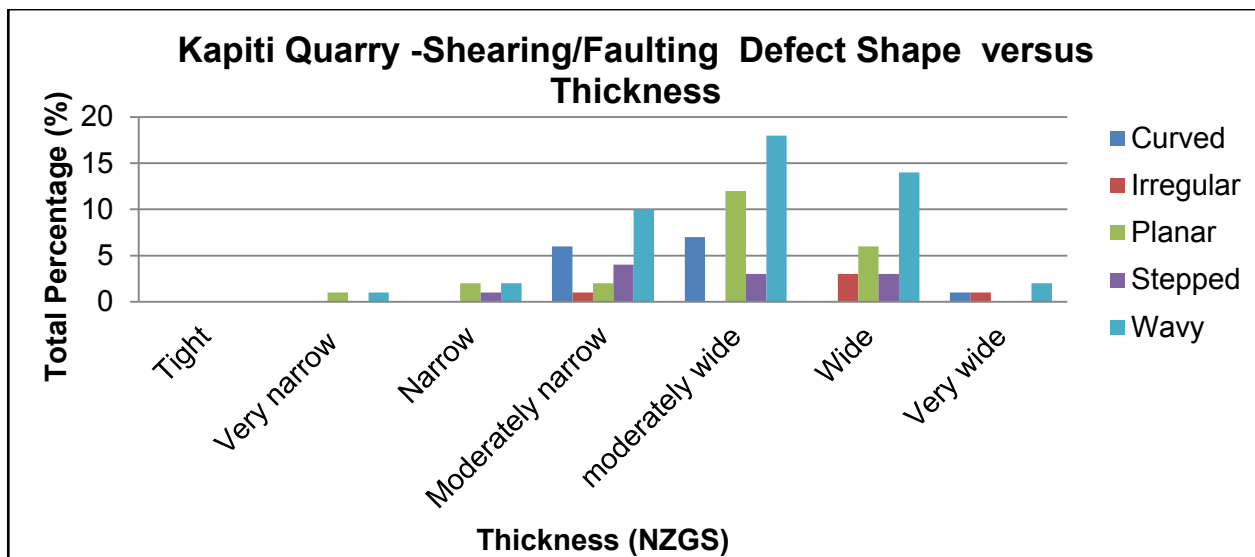
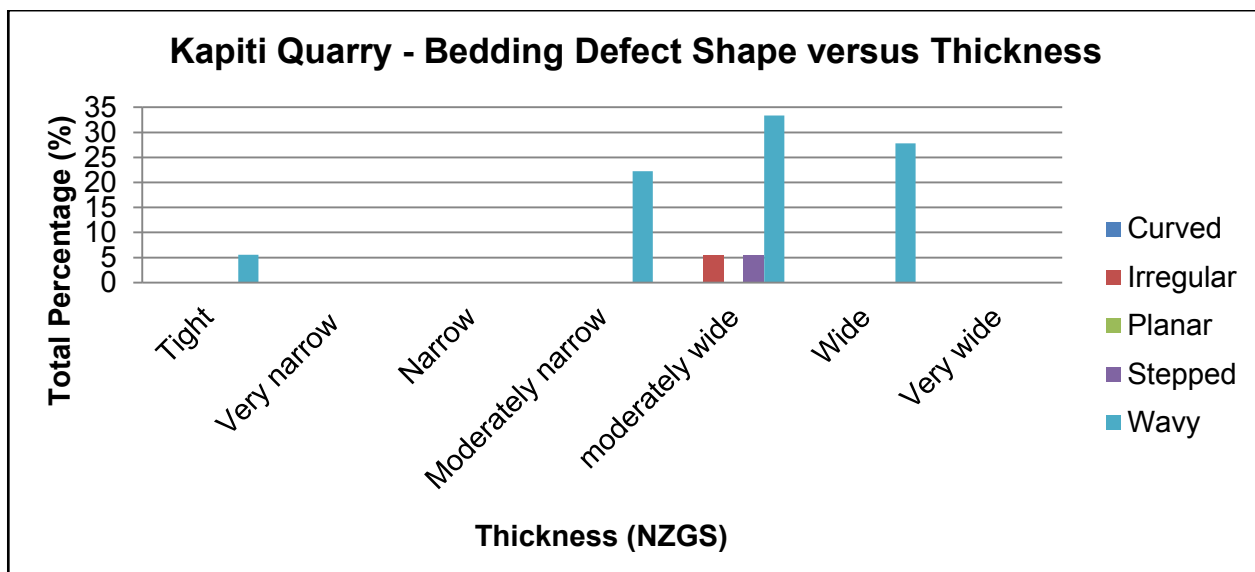








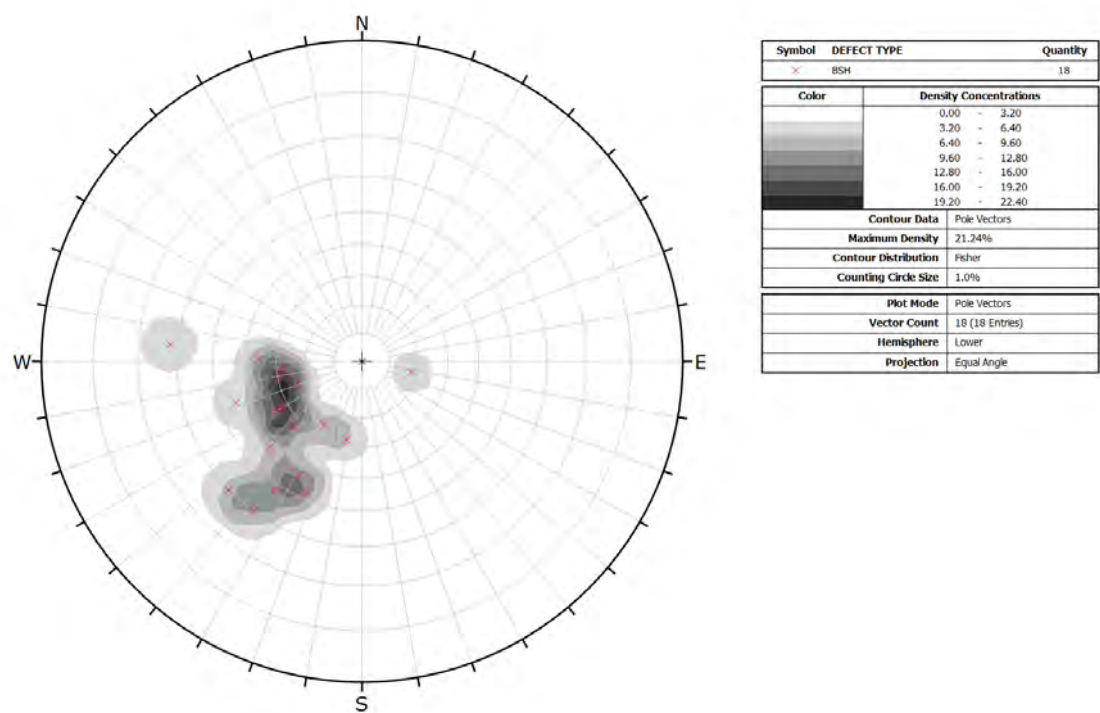




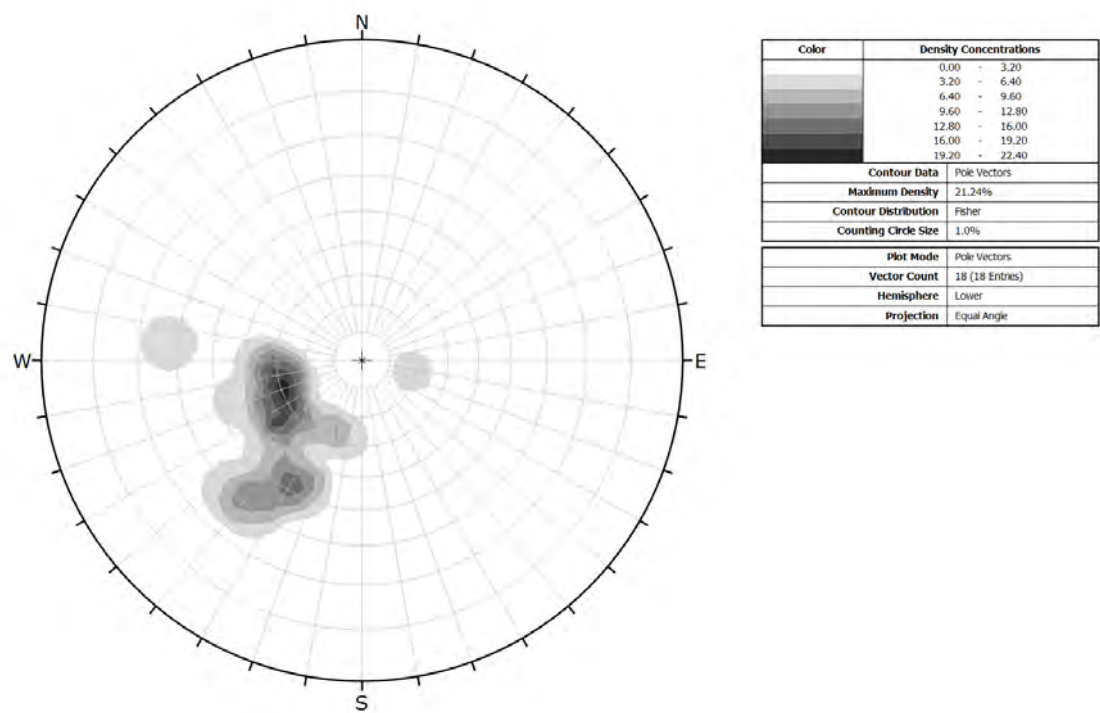
C.5 Kapiti Quarry Stereonet Analysis

Stereonet Dip: Dip direction analysis of bedding, faults and shears respectively.

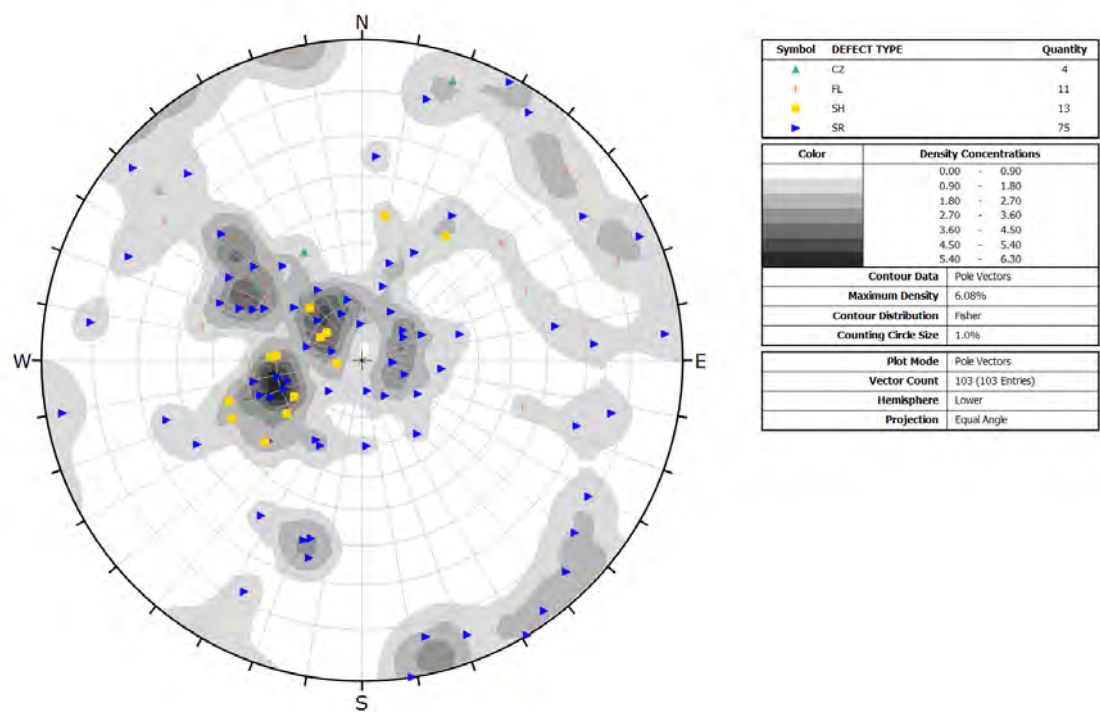
Bedding poles



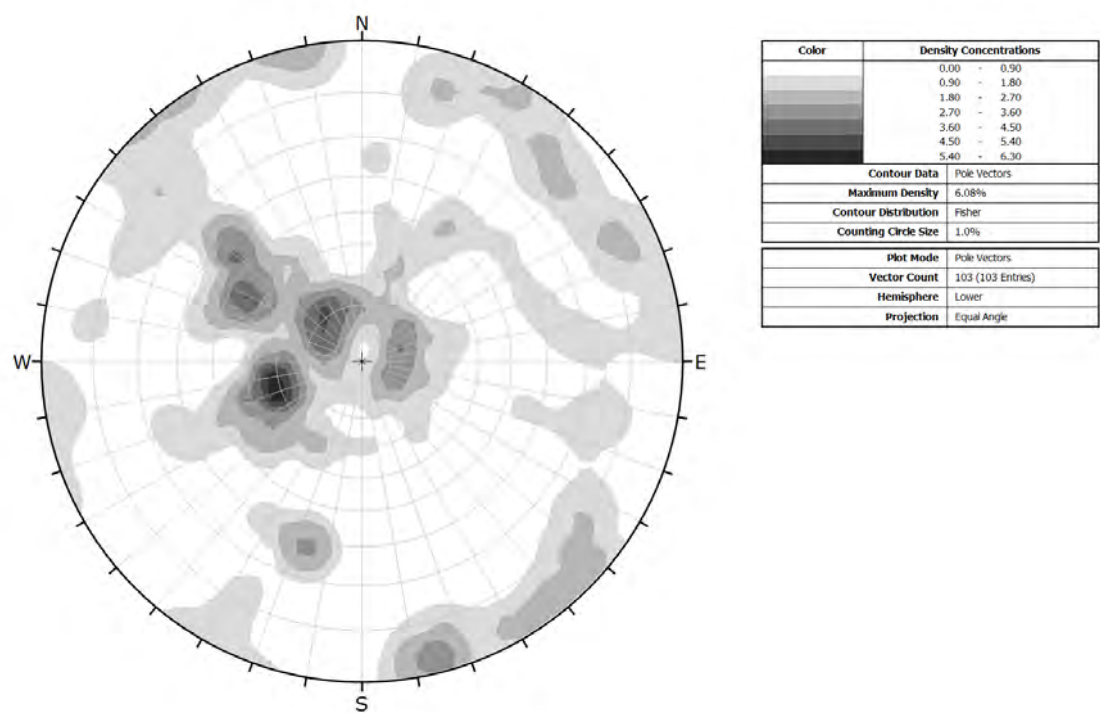
Contour diagram of bedding clusters



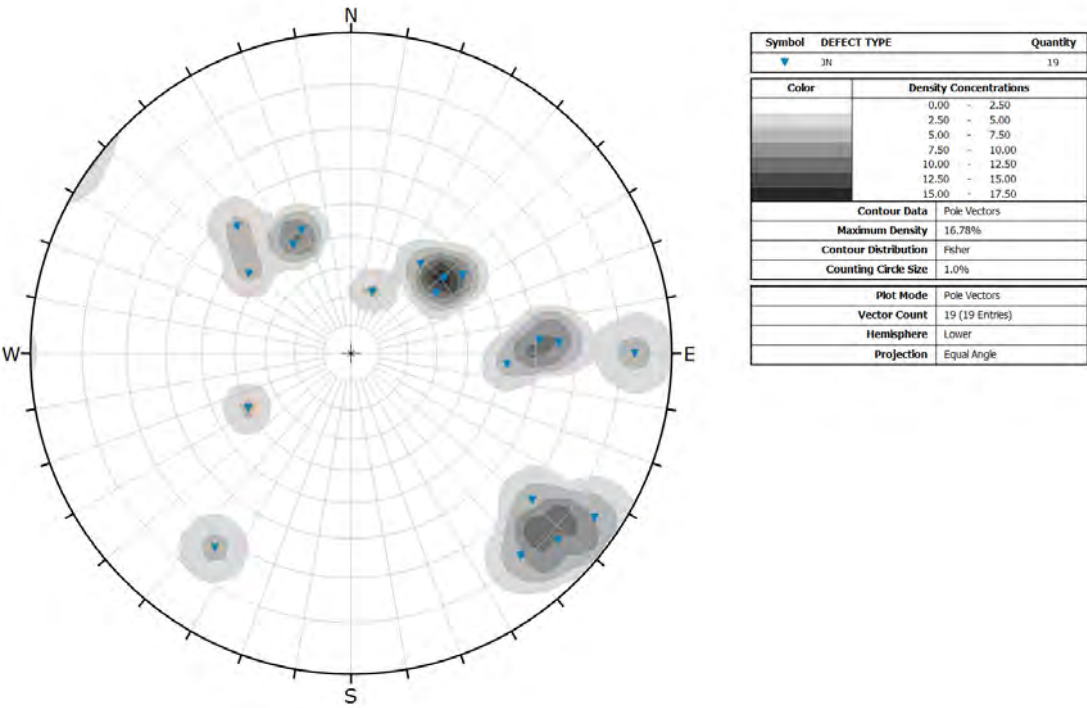
Shearing poles



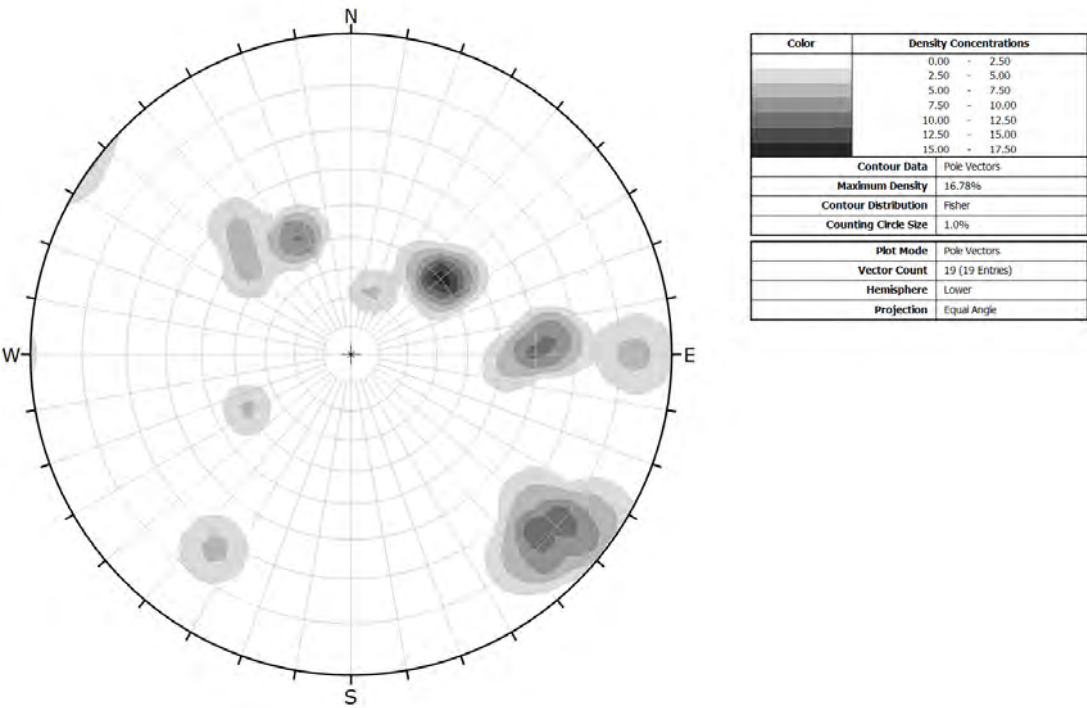
Contour diagram of shearing and faulting clusters



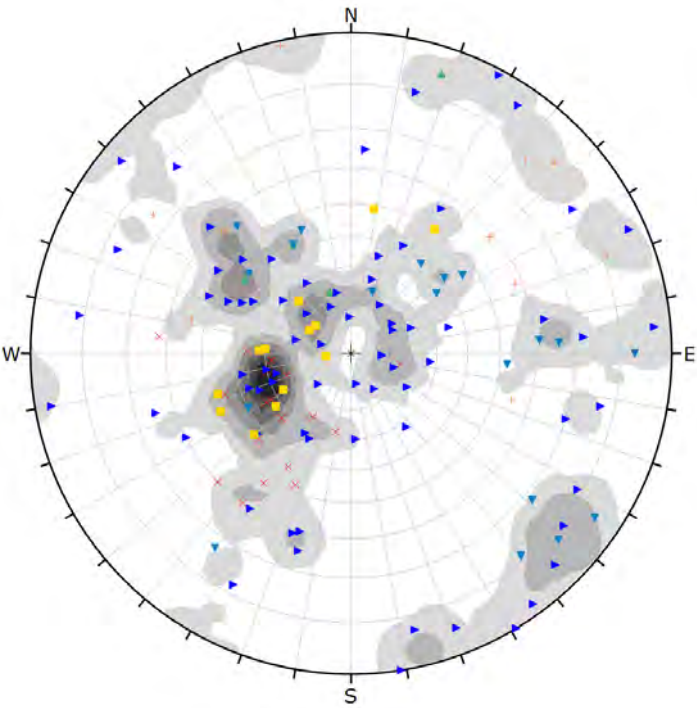
Jointing poles



Contour diagram of jointing clusters



All defects poles



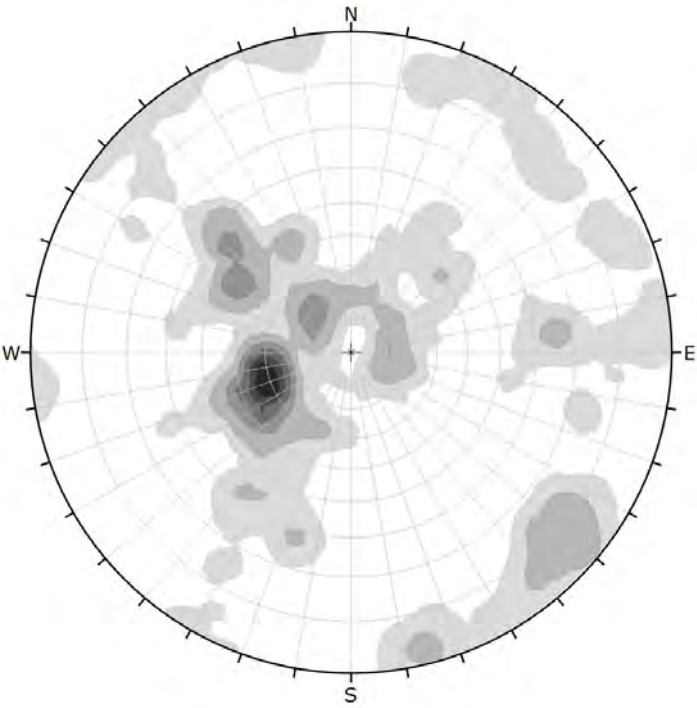
Symbol	DEFECT TYPE	Quantity
x	BSH	18
▲	CZ	4
+	FL	11
▼	JN	19
■	SH	13
▴	SR	75

Color	Density Concentrations
	0.00 - 1.00
	1.00 - 2.00
	2.00 - 3.00
	3.00 - 4.00
	4.00 - 5.00
	5.00 - 6.00
	6.00 - 7.00

Contour Data	Pole Vectors
Maximum Density	6.88%
Contour Distribution	Fisher
Counting Circle Size	1.0%

Plot Mode	Pole Vectors
Vector Count	140 (140 Entries)
Hemisphere	Lower
Projection	Equal Angle

Contour diagram of all defects cluster



Color	Density Concentrations
	0.00 - 1.00
	1.00 - 2.00
	2.00 - 3.00
	3.00 - 4.00
	4.00 - 5.00
	5.00 - 6.00
	6.00 - 7.00

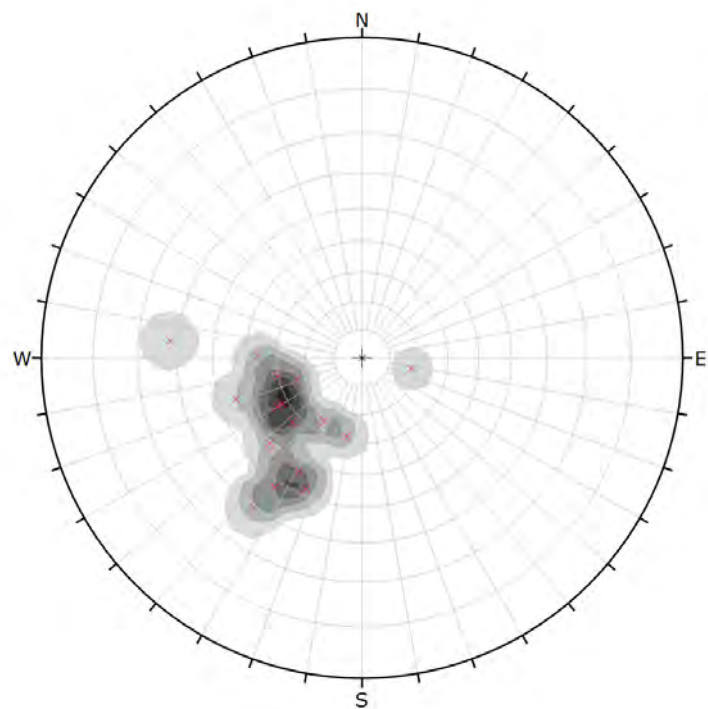
Contour Data	Pole Vectors
Maximum Density	6.88%
Contour Distribution	Fisher
Counting Circle Size	1.0%

Plot Mode	Pole Vectors
Vector Count	140 (140 Entries)
Hemisphere	Lower
Projection	Equal Angle

C.6 Filtered Stereonet Analysis

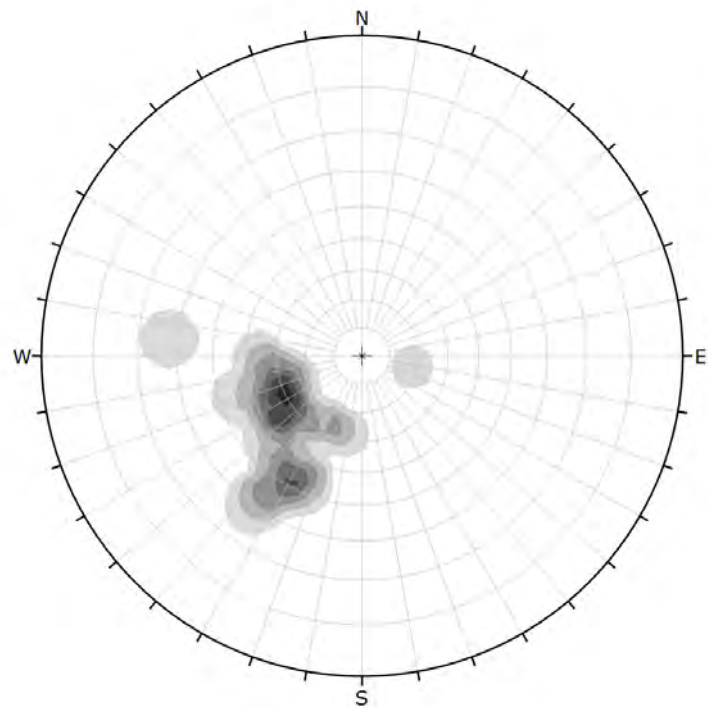
Stereonet from C.5 assessed for “noise”. The following only displays the poles of the continuous defects in Kapiti Quarry.

Bedding poles



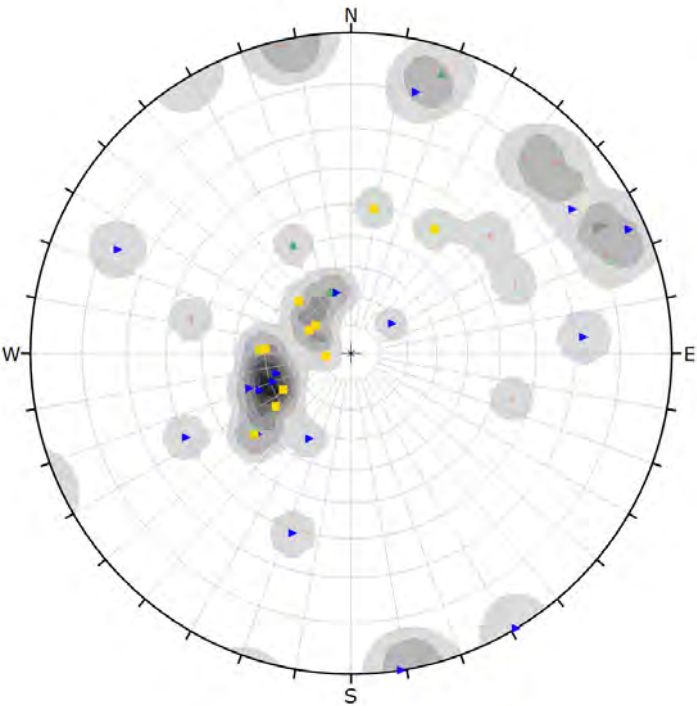
Symbol	DEFECT TYPE	Quantity
x	BSH	16
Color	Density Concentrations	
	0.00	- 3.20
	3.20	- 6.40
	6.40	- 9.60
	9.60	- 12.80
	12.80	- 16.00
	16.00	- 19.20
	19.20	- 22.40
Contour Data		Pole Vectors
Maximum Density		21.79%
Contour Distribution		Fisher
Counting Circle Size		1.0%
Plot Mode		Pole Vectors
Vector Count		16 (16 Entries)
Hemisphere		Lower
Projection		Equal Angle

Contour diagram of bedding clusters



Color	Density Concentrations	
	0.00	- 3.20
	3.20	- 6.40
	6.40	- 9.60
	9.60	- 12.80
	12.80	- 16.00
	16.00	- 19.20
	19.20	- 22.40
Contour Data		Pole Vectors
Maximum Density		21.79%
Contour Distribution		Fisher
Counting Circle Size		1.0%
Plot Mode		Pole Vectors
Vector Count		16 (16 Entries)
Hemisphere		Lower
Projection		Equal Angle

Shearing poles



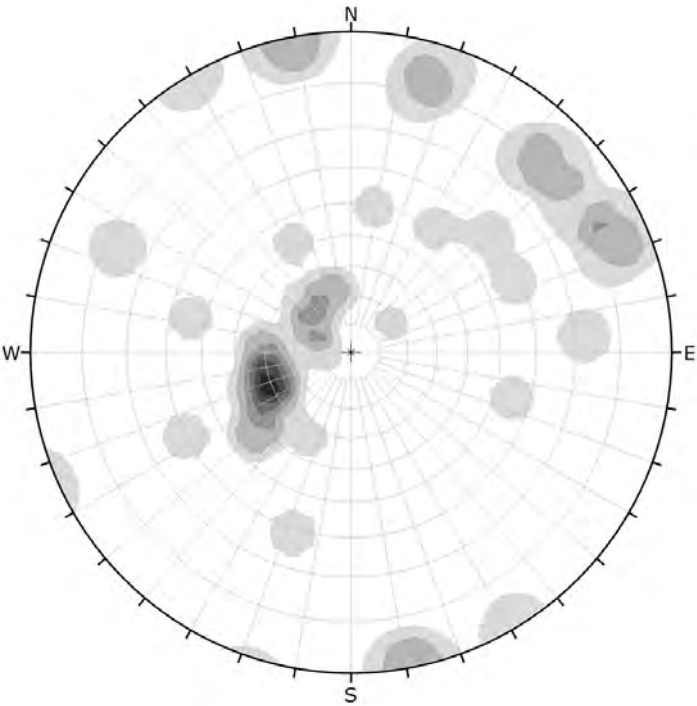
Symbol	DEFECT TYPE	Quantity
▲	CZ	3
▲	FL	8
▲	SH	11
▲	SR	17

Color	Density Concentrations
	0.00 - 1.90
	1.90 - 3.80
	3.80 - 5.70
	5.70 - 7.60
	7.60 - 9.50
	9.50 - 11.40
	11.40 - 13.30

Contour Data	Pole Vectors
Maximum Density	12.73%
Contour Distribution	Fisher
Counting Circle Size	1.0%

Plot Mode	Pole Vectors
Vector Count	39 (39 Entries)
Hemisphere	Lower
Projection	Equal Angle

Contour diagram of shearing and faulting clusters

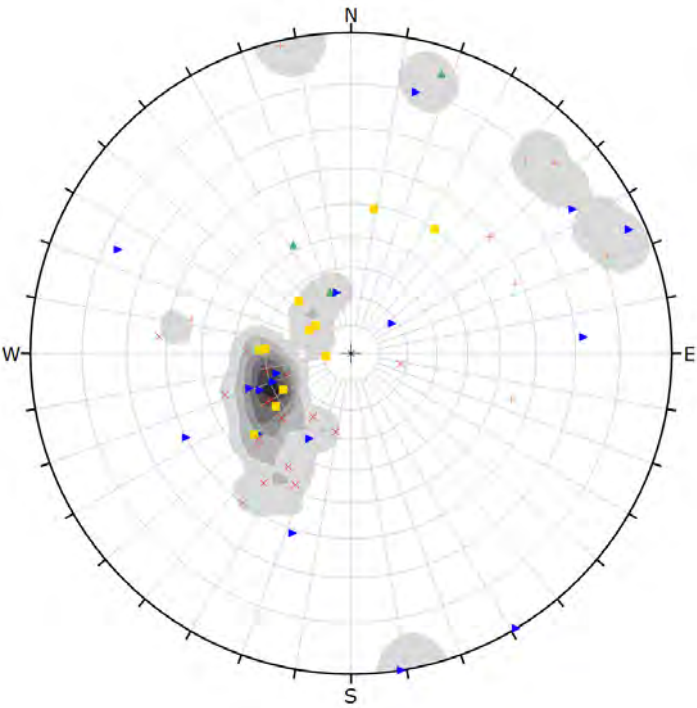


Color	Density Concentrations
	0.00 - 1.90
	1.90 - 3.80
	3.80 - 5.70
	5.70 - 7.60
	7.60 - 9.50
	9.50 - 11.40
	11.40 - 13.30

Contour Data	Pole Vectors
Maximum Density	12.73%
Contour Distribution	Fisher
Counting Circle Size	1.0%

Plot Mode	Pole Vectors
Vector Count	39 (39 Entries)
Hemisphere	Lower
Projection	Equal Angle

All defects poles



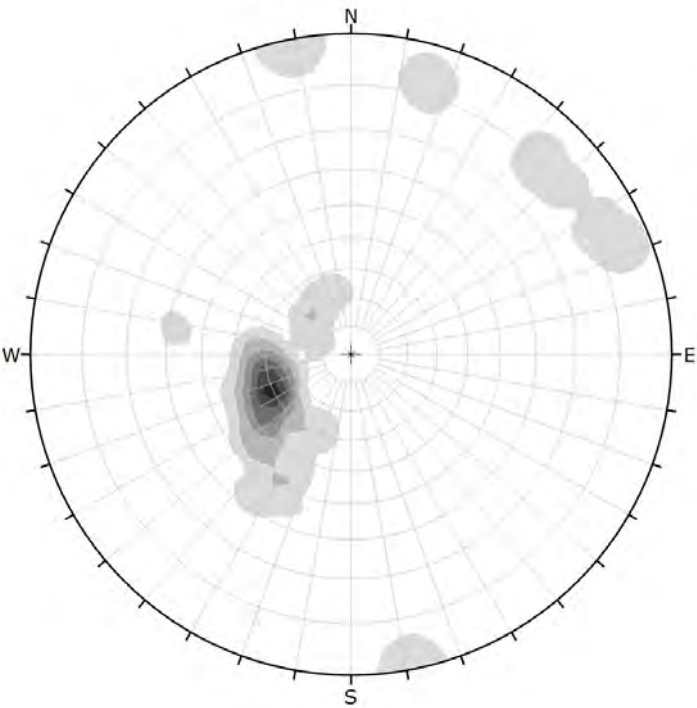
Symbol	DEFECT TYPE	Quantity
x	BSH	16
▲	CZ	3
+	FL	8
■	SH	11
▴	SR	17

Color	Density Concentrations
	0.00 - 2.30
	2.30 - 4.60
	4.60 - 6.90
	6.90 - 9.20
	9.20 - 11.50
	11.50 - 13.80
	13.80 - 16.10

Contour Data	Pole Vectors
Maximum Density	15.37%
Contour Distribution	Fisher
Counting Circle Size	1.0%

Plot Mode	Pole Vectors
Vector Count	55 (55 Entries)
Hemisphere	Lower
Projection	Equal Angle

Contour diagram of all defects cluster



Color	Density Concentrations
	0.00 - 2.30
	2.30 - 4.60
	4.60 - 6.90
	6.90 - 9.20
	9.20 - 11.50
	11.50 - 13.80
	13.80 - 16.10

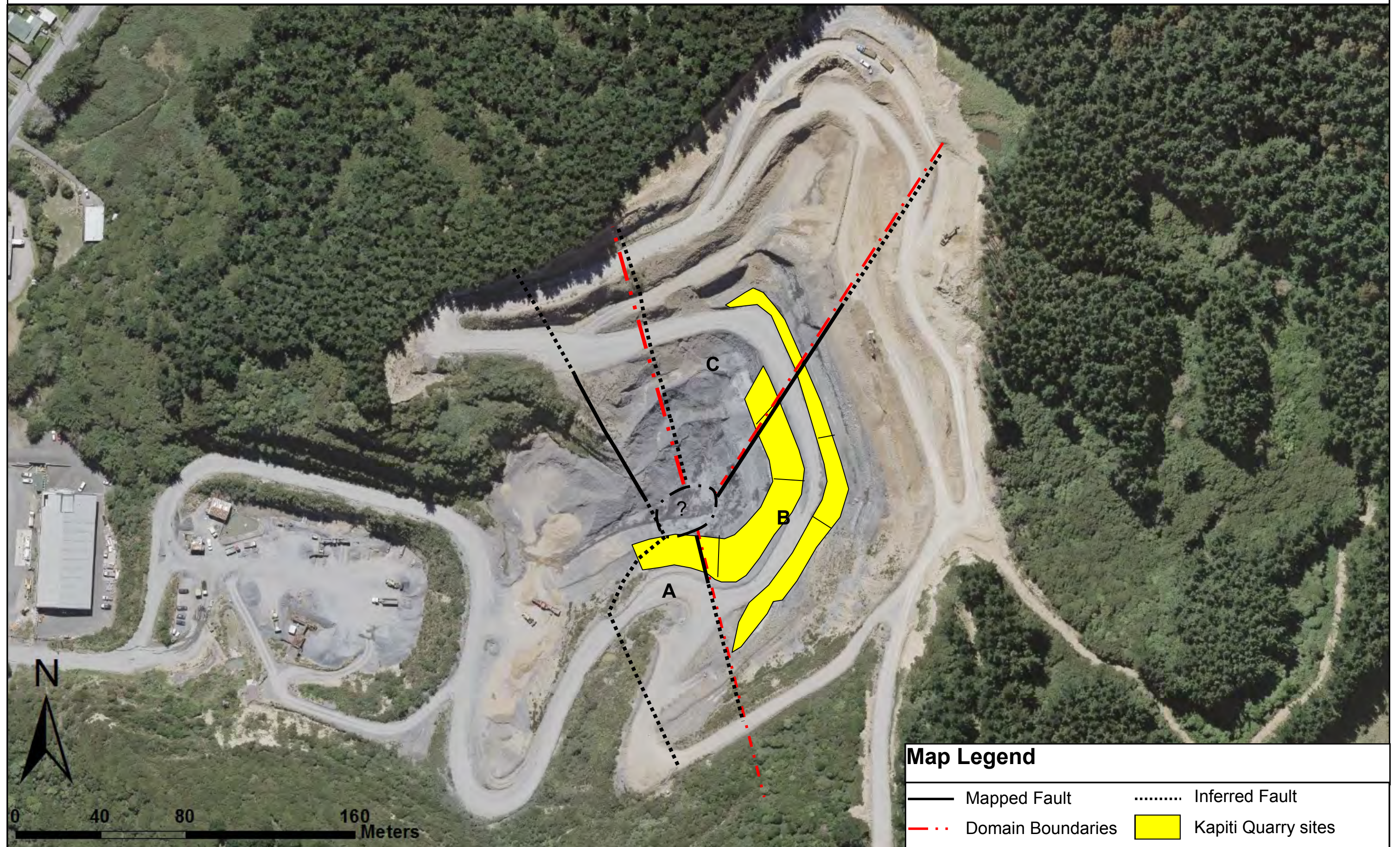
Contour Data	Pole Vectors
Maximum Density	15.37%
Contour Distribution	Fisher
Counting Circle Size	1.0%

Plot Mode	Pole Vectors
Vector Count	55 (55 Entries)
Hemisphere	Lower
Projection	Equal Angle

C.7 Kapiti Quarry Structural Domains

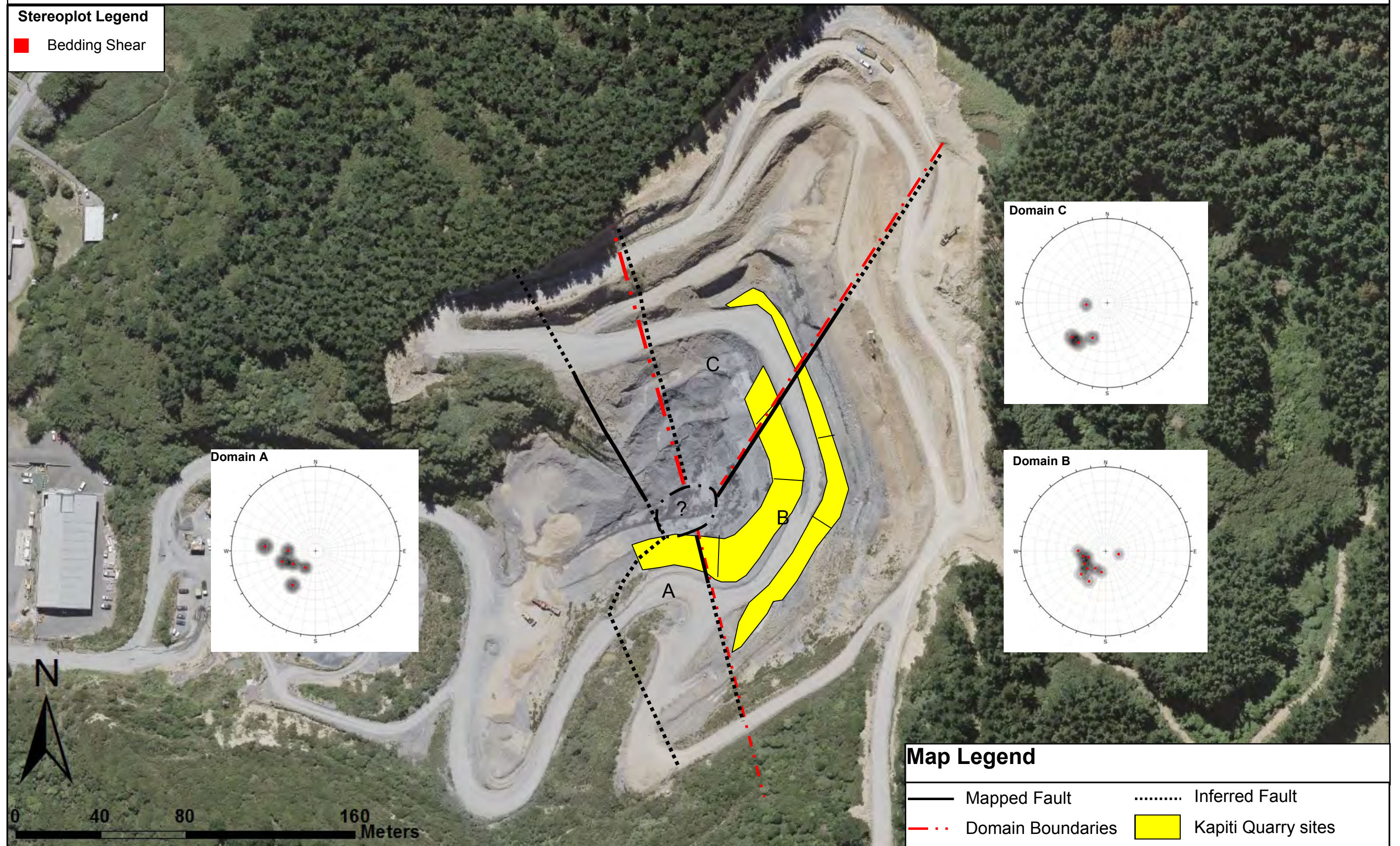
Figures are based on mapping observations and stereonet analysis. The figures represent a very detailed interpretation of the changes in defect orientation across the Kapiti Quarry site.

C.7.1 Kapiti Quarry Structural - Domains



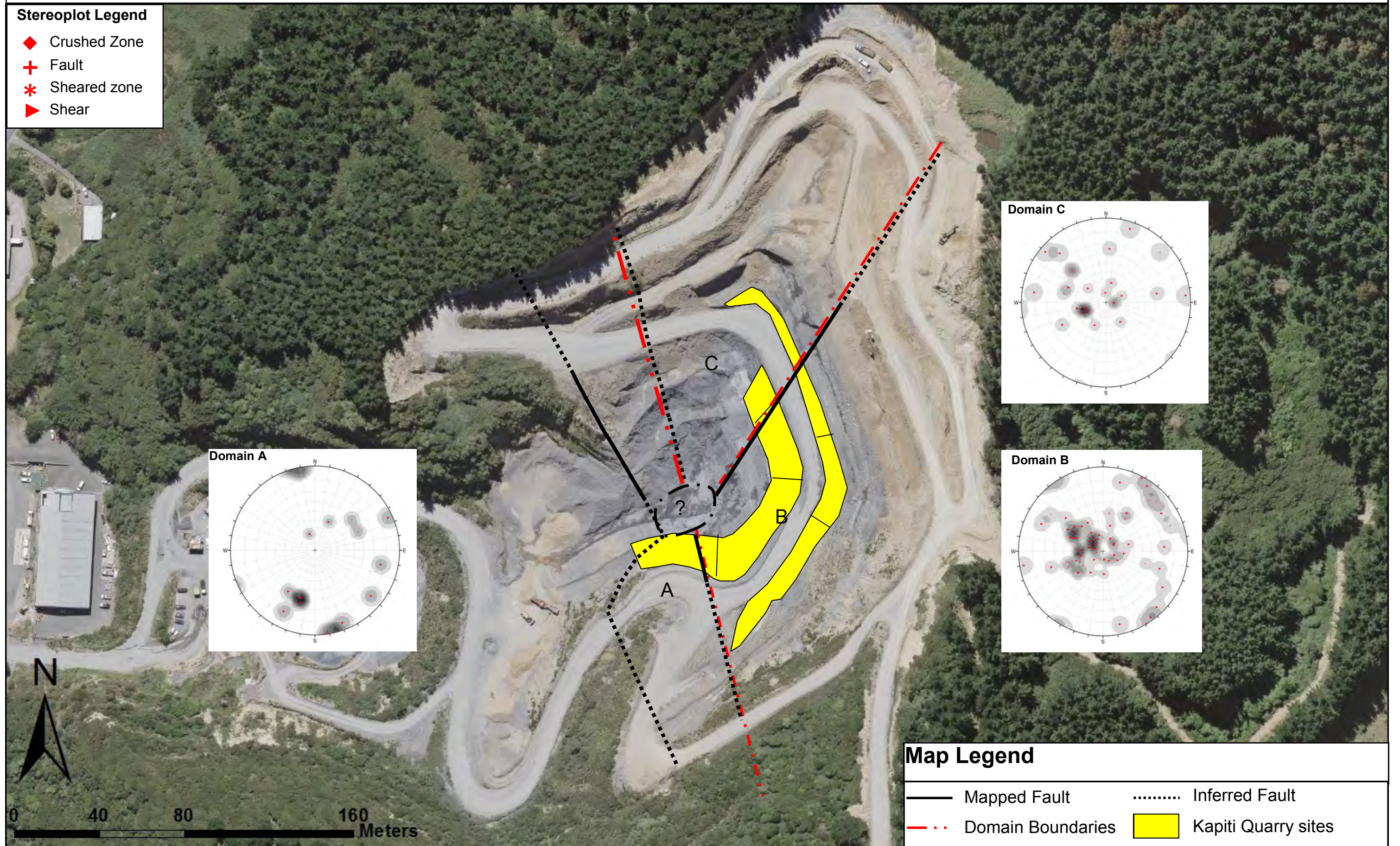
Imagery sourced: LINZ aerial imagery, 2017 (Captured by AAM NZ limited (2017))

C.7.2 Kapiti Quarry Structural Domains - Bedding



Imagery sourced: LINZ aerial imagery, 2017 (Captured by AAM NZ limited (2017))

C.7.3 Kapiti Quarry Structural Domains - Shearing



Imagery sourced: LINZ aerial imagery, 2017 (Captured by AAM NZ limited (2017))

C.8 Kapiti Quarry Engineering Geological Model

Engineering geological model based on all available data. The model provides a summary of the rock mass and defect condition within the Kapiti Quarry study site. Defect orientation and regional structural controls are also included.

C.8: Engineering Geological Model of Kapiti Quarry

Key :
 ◆ BG ▲ CZ ▼ JN ► SR
 ✕ BSH + FL ■ SH

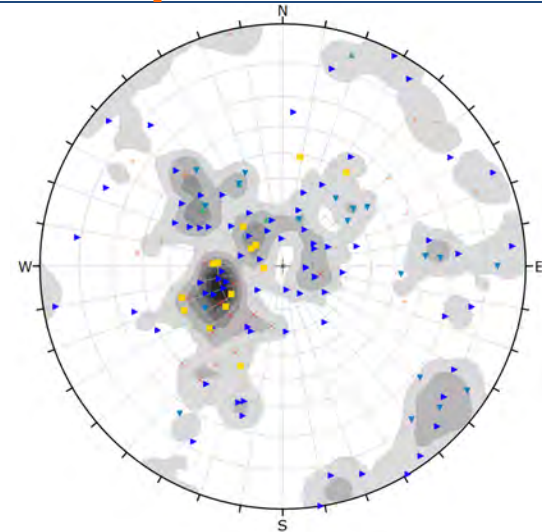


Figure 1: Stereonet of all the defect types and their orientation.

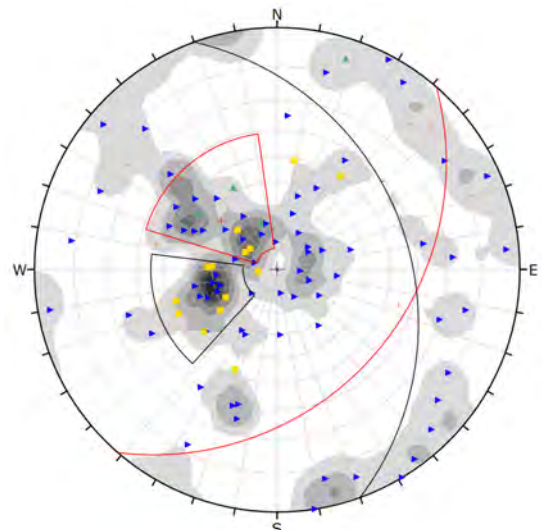


Figure 2: Stereonet of shearing.

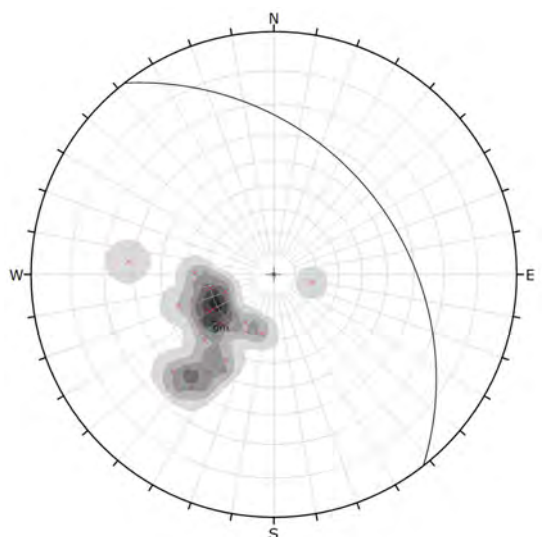


Figure 3: Stereonet of bedding.

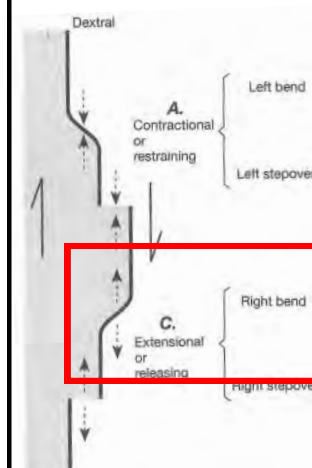
Rock mass structure in Kapiti Quarry is primarily controlled by the Ohariu Fault and normal faulting associated with a releasing bend (See map). Strain produced by the releasing bend is likely accommodated on the NW/SE trending structures (Irvine et al., 2018).

Bedding strikes sub-parallel to the NW/SE trending structures likely in response to the normal faulting.

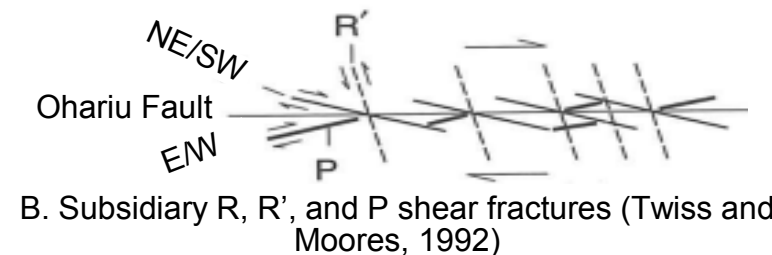
Shearing is dominantly sub-parallel to the Ohariu Fault and with the NW/SE structures. This aligns with the structural grain of the area and with the regional model created by Irvine et al. (2018) for Transmission Gully.

The weathering profile is influenced and follows the topography.

Conceptual models:



A: Bends and stepovers for dextral strike-slip faults (Twiss and Moores, 1992)



B. Subsidiary R, R', and P shear fractures (Twiss and Moores, 1992)

Individual sandstone beds are 50 mm to 2 m thick and continuous. Mudstone content is heavily sheared with discrete, persistent cross-cutting defects appearing to be less common. Sheared zones are much more common and wider than other locations.

Slide failure - translational.
 Fault and bedding controlled.

Interbedded sandstone and mudstone beds.

60:039 (Dip: Dip direction)
 Striking North West

Head scarp

Tension cracks

Lateral scarp

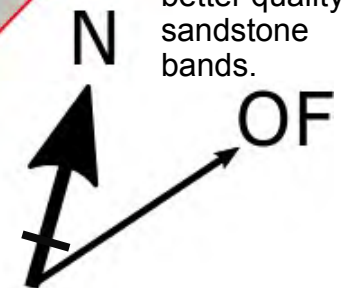
Fault - 81:268 (Dip: Dip direction) Striking North

Unsure where termination occurs, against the NW/SE structures or if it crosscuts.

The Ohariu Fault (OF) is located approximately a kilometre away, with fault motion predominantly dextral strike-slip. The general trend of the fault is between 030°-050° however just south of this location the fault bends to the right and strikes at around 060°. It is interpreted that this creates a releasing bend, placing this site in a extensional setting.

Minor water seepage occurring on the lowest point of the syncline

Heavily sheared thick mudstone beds overlying better quality sandstone bands.



Fault - 60:230 (Dip: Dip direction)
 Striking South East

MUD : SAND

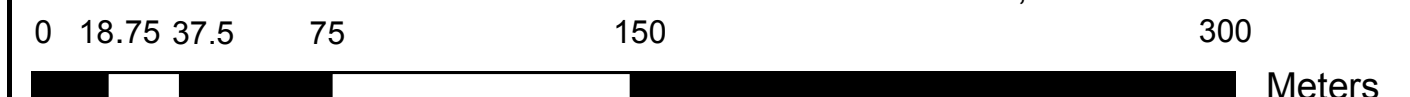
50: 50

Predominant Suneson lithofacies: C

Sandstone: Slightly weathered, light grey SANDSTONE; Strong; 5 joint sets very steeply inclined to moderately inclined closely spaced joints very narrow to tight [RAKAIA SUB-TERRANE Greywacke]

Mudstone: Slightly weathered, dark grey MUDSTONE; Moderately strong to weak [RAKAIA SUB-TERRANE Argillite]

Scale 1:1,875 centimetres



APPENDIX D: HOROKIWI QUARRY

This site is located off state highway 2 between Petone and Wellington (Figure D.1). The Wellington Fault is located less than 1.5 km away. North of this site the Moonshine Fault trace appears to be converging with the Wellington Fault. Cross faulting links these major structures and are likely accommodating and transferring the regional tectonic stresses. This is similar to the Transmission Gully South site however the faults associated with Horokiwi Quarry appear to be closer. The active quarry offers continuous large rock exposure over an extended distance. A total of 3 areas were mapped (Appendix D.2)

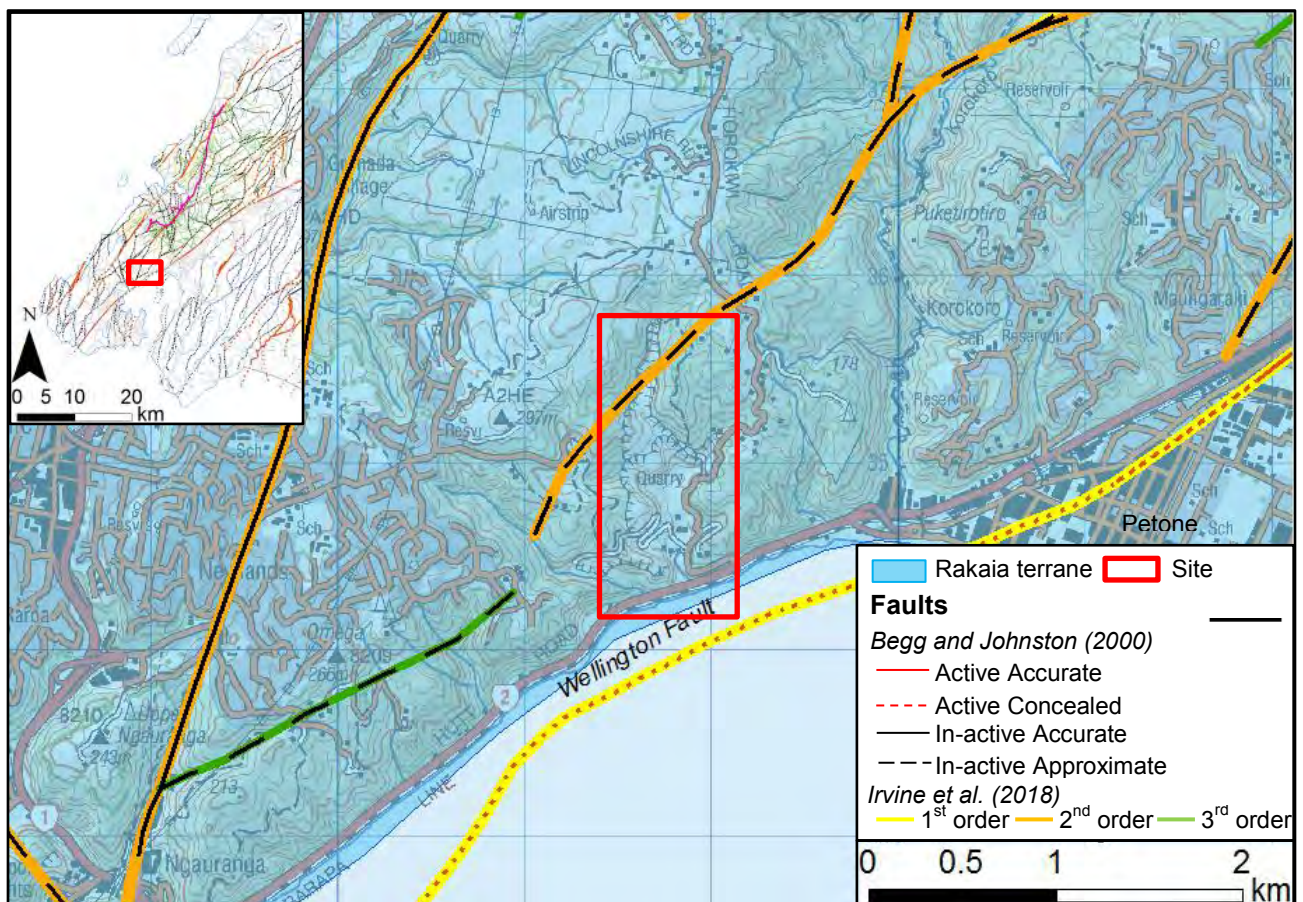


Figure D.1: Horokiwi Quarry site district scale map. Data sourced from GNS (2018) (Begg and Johnston, 2000) and Irvine et al. (2018). Refer to Section 1.4 for Irvine et al (2018) order classification Imagery from LINZ.

Results derived from conceptual models, raw mapping data, stereonet analysis and engineering geological models for the Horokiwi Quarry study site as displayed in the following sections.

D.1 Horokiwi Quarry Conceptual Structural Model

Preliminary structural assessment derived from GNS (2010) (Begg and Johnston, 2000) and Irvine et al. (2018) structural databases. Interpretations are based on information derived from past literature.

D.1 Conceptual Structural Model of Horokiwi Quarry

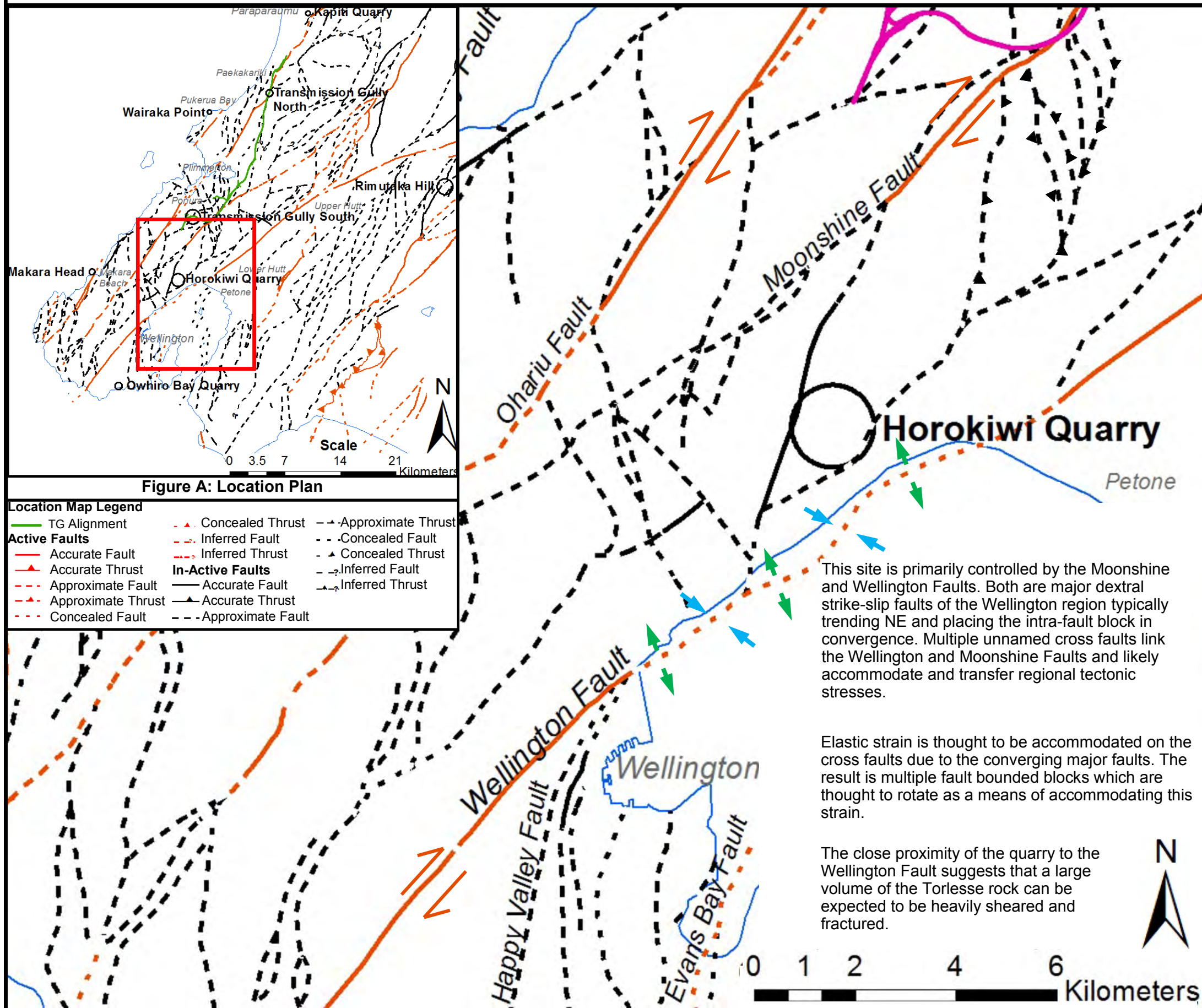
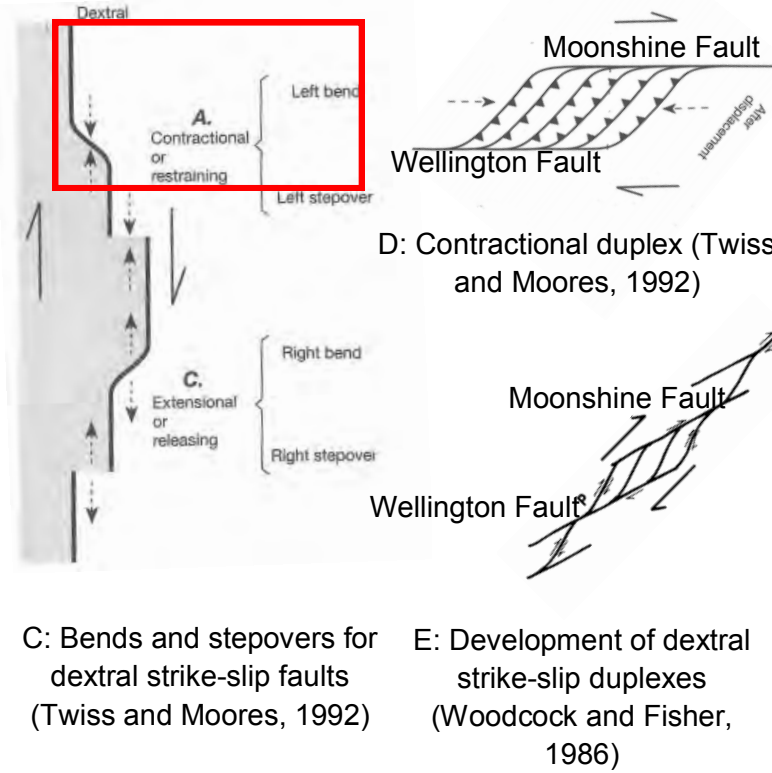


Figure B: District scale structures around Horokiwi Quarry. Faults are sourced from GNS (2010) (Begg and Johnston, 2000).

District Scale Legend:

- | | |
|-------------------------|--------------------|
| TG Alignment | Strike Slip |
| Restraining bend | Releasing bend |
| Active Faults | |
| Accurate Fault | Accurate Fault |
| Accurate Thrust | Accurate Thrust |
| Approximate Fault | Approximate Fault |
| Approximate Thrust | Approximate Thrust |
| Concealed Fault | Concealed Fault |
| Concealed Thrust | Concealed Thrust |
| Inferred Fault | Inferred Fault |
| Inferred Thrust | Inferred Thrust |
| In-Active Faults | |

Conceptual Models:



Bedding and Shearing Predictions:

Bedding and shearing is anticipated to strike sub-parallel to parallel to the NE/SW trending structures. Additionally, folding and/or shear cross-cutting of bedding is anticipated to produce some variation in bedding orientation (Irvine et al., 2018).

D.2 Horokiwi Quarry Outcrop Location Map

Displays the location of the mapped outcrops within the Horokiwi Quarry study site.

D.2 Horokiwi Quarry



D.3 Horokiwi Quarry Raw Mapping Data

Structural data collected from the Horokiwi Quarry site. Where data is missing or blanked out information was either not able to be reached or was not relevant to the rock mass or defect condition (e.g. Planar defects did not contain a wavelength as outlined in Chapter 3).

D.3.1 Horokiwi Quarry - Raw data

Horokiwi Quarry																							
ID	Defect Type	Dip	Dip Direction (Mag)	Dip Direction (True)	Structural Domain	Roughness	Thickness		% of rock fragments	Continuity	Persistence	Shape			Persistence - Trace Length (m)	Spacing (m)	Infill (Support (Rock (%Clasts), Angularity, weathering, strength, coating; colour, grainsize, strength, plasticity)) precipitation	Saturation	Latitude	Longitude	Comments	Cut ID	
							Term	Width (mm)				Inter-limb angle (degrees)	Wavelength (m)	Term									
1	SR	56	77	55	D	Ro3				1	R	~160°	Gentle		Wavy	~15m			-41.2249	174.8445	Failure plane 1 - wedge failure. Transects SR2	West Cut slope	
2	SR	60	190	168	D	Ro5				1	R	~160°	Gentle		Wavy	~15m			-41.2247	174.8445	Failure plane 2 - wedge failure. Transects SR1		
3	SR	25	349	327	C	Ro3	Moderately narrow to Moderately wide	~20mm	~95%	1	D	~160°	Gentle	~30m	Wavy	~15m	Clast supported (Crackle (~95%) Angular, HW, Weak, Coating; Light and dark blue grey, sandy Silt with traces of clay, Soft, NP) White sand sized specks of precipitation	Damp	-41.2244	174.8446	Cross cuts BSH5 and CZ7. Terminates against FL10		
4	SR	30	305	283	C	Ro3	Moderately narrow	~8mm	~95%	1	D	~170°	Gentle	~2.5m	Wavy	~7m	Clast supported (Crackle (~95%) Angular, HW, Weak, Coating; Light blue grey, silty Sand, Soft, NP) No precipitation	Damp	-41.2245	174.8446	Cross cuts BSH5. Terminates against BSH5		
5	BSH	74	84	62	C	Ro2	Moderately narrow	~10mm	~90%	0	C	~135°	Gentle	~4m	Wavy	~8m	~2m	Clast supported (Crackle (~90%) Angular, HW, Weak, Coating; Grey, sandy Clay, Soft, LP) No precipitation	Damp	-41.2245	174.8446		Cross cuts SR4, SR3 and FL10. Offset by FL10.
5	BSH	89	60	38	C	Ro2	Moderately narrow	~10mm	~90%	0	C	~135°	Gentle	~7m	Wavy	~8m	~5m	Clast supported (Crackle (~90%) Angular, HW, Weak, Coating; Grey, sandy Clay, Soft, LP) No precipitation	Damp	-41.2245	174.8446		Cross cuts SR4, SR3 and FL10. Offset by FL10
6	SR	86	3	341	C	Ro2	Moderately wide	~25mm	~80%	1	D	~150°	Gentle	~1m	Wavy	~3m		Damp	-41.2244	174.8446	Cross cuts CZ7. Terminates against SR3		
7	CZ	86	359	337	C&D	Ro4	Very Wide	~250mm	~85%	0	C	~140°	Gentle	~1.4	Wavy	~21m		Damp	-41.2245	174.8446	Cross cuts SR6, FL10, SR3, BSH9 and BSH4.		
7	CZ	86	14	352	C&D	Ro4	Very Wide	~250mm	~85%	0	C	~140°	Gentle	~1.4	Wavy	~21m		Damp	-41.2245	174.8446	Cross cuts SR6, FL10, SR3, BSH9 and BSH4.		
8	SR	45	121	99	D	Ro3	Moderately wide	~40mm	~80%	1	D	~140°	Gentle	~2m	Wavy	~5m	~1.5m	Clast supported (Crackle (~90%) Angular, HW, Weak, Coating; Dark blue black, silty Sand, Soft, NP) No precipitation visible	Damp	-41.2244	174.8448		Terminates against FL10 and cross cuts BSH9
9	BSH	58	317	295	D	Ro3	Moderately wide	~50mm	~90%	0	C	~150°	Gentle	~10m	Wavy	~20m	~3.5m	Clast supported (Crackle (~90%) Angular, HW, Weak, Coating; Light blue grey, sandy Clay, Very soft, LP) No precipitation	Damp	-41.2243	174.8446		Cross cuts CZ7 and SR8. Terminates against FL10
10	FL	48	293	271	C&D	Ro2	Very Wide	~250mm	~75%	0	C	~180°	Gentle		Planar	~15m		Damp	-41.2243	174.8447	Cross cuts CZ7 and BSH5.		
11	SR	85	301	279	D	Ro4	Moderately wide	~45mm	~90%	1	D	~150°	Gentle	~7m	Curved	~7m	~2m	Clast supported (Crackle (~90%) Angular, HW, Moderately strong to Weak, Coating; Light grey blue, silty Sand, Soft, NP) No precipitation	Damp	-41.2242	174.8447		Terminates against BSH12 and cross cuts BSH9 and SR13
9	BSH	87	341	319	D	Ro3	Moderately wide	~40mm	~80%	0	C	~150°	Gentle	~10m	Wavy	~20m	~3.5m	Clast supported (Crackle (~80%) Angular, CW, Weak, Coating; Blue grey, silty Sand with traces of Clay, Very soft, NP) White sand sized specks of precipitation	Damp	-41.2241	174.8447		Cross cuts SR11
12	BSH	68	76	54	D	Ro4	Moderately narrow	~15mm	~95%	0	C	~160°	Gentle	~8m	Wavy	~14m	~3.5m	Clast supported (Crackle (~95%) Angular, HW, Moderately strong, Coating; Blue grey, clayey Sand, Soft, NP) No precipitation	Damp	-41.2241	174.8447		Cross cuts SR13
13	SR	52	164	142	D	Ro4	Wide	~25mm	~80%	2	D	~180°	Gentle		Planar	~8m	~3m	Clast supported (Crackle (~80%) Angular, HW, Weak, Coating; Light and dark blue grey, silty Sand with traces of Clay, Soft, NP-LP) No visible precipitation	Damp	-41.2242	174.8446		Cross cuts BSH12, SR14, BSH5 and SR17. Terminates against BSH9 and SR16
14	SR	67	350	328	D	Ro3	Moderately wide	~30mm	~95%	0	C	~150°	Gentle	~8m	Wavy	~8m	~2m	Clast supported (Crackle (~95%) Angular, HW, Moderately strong, Coating; Light blue grey, silty Sand, Soft, NP) No precipitation	Damp	-41.2241	174.8446		Cross cuts BS15, SR13 and SR17
15	BSH	75	88	66	D	Ro2	Moderately wide	~40mm	~95%	0	C	~160°	Gentle	~10m	Wavy	~30m	~0.5m	Clast supported (Crackle (~95%) Angular, HW, Moderately strong, Coating; light blue grey, sandy Clay, Very soft, LP) No precipitation	Damp	-41.2241	174.8447	Cross cuts SR16, SR14 and SR13	
15	BSH	80	68	46	D	Ro2	Moderately wide	~40mm	~95%	0	C	~160°	Gentle	~10m	Wavy	~30m	~0.5m	Clast supported (Crackle (~95%) Angular, HW, Moderately strong, Coating; light blue grey, sandy Clay, Very soft, LP) No precipitation	Damp	-41.224	174.8448	Cross cuts SR16, SR14 and SR13	
16	SR	44	154	132	D	Ro4	Moderately narrow	~7mm	~99%	0	C	~150°	Gentle	~12m	Curved	~8m	~2m	Clast supported (Rock (~99%) Angular, MW, Moderately strong to Strong, Veneer) No precipitation	Damp	-41.2241	174.8446	Cross cuts SR23, BSH15, BSH20, SR17 and FL28	
17	SR	61	19	357	D	Ro3	Moderately wide	~25mm	~85%	1	D	~150°	Gentle	~1.2m	Wavy	~7m	~5m	Clast supported (Crackle (~85%) Angular, HW, Weak, Coating; Light blue grey, sandy Clay, Very soft, MP) No precipitation	Damp	-41.2241	174.8446	Cross cuts SR14, SR13 and SR23. Terminates against SR16	

18	SR	33	92	160	D	Ro3	Wide	~120mm	~95%	0	C	~160°	Gentle	~4m	Wavy	~8m	~2m	Clast supported (Crackle (~95%) Angular, MW, Weak, Coating; Light blue grey, sandy Clay, Soft, NP) No precipitation	Damp	-41.2241	174.8446	Cross cuts SR23, FL28 and BSH20	South Cut slope
19	SR	51	204	182	D	Ro3	Wide	~70mm	~80%	0	C	~170°	Gentle	~1.5m	Wavy	~4m	~2m	Clast supported (Crackle (~80%) Angular, HW, Moderately strong to Weak, Coating; Light blue grey (Sand) and Dark blue grey (Clay), silty Sand and Clay, Very soft to soft, MP to LP) No precipitation	Damp	-41.224	174.8447	Cross cuts SR23, FL28 and BSH20	
20	BSH	78	82	60	D	Ro4	Wide to Very wide	~200mm	~85%	0	C	~150°	Gentle	~3m	Wavy	~20m	~0.8m	Clast supported (Crackle (~85%) Angular, HW, Weak, Coating; Light and dark blue grey, silty Sand with traces of Clay, Soft , LP) White elongated precipitation	Damp	-41.224	174.8447	Cross cuts SR18, SR19, SR16 and BSH20	
21	SR	83	75	53	D	Ro3	Moderately wide	~40mm	~95%	1	D	~170°	Gentle	~1m	Wavy	~6m		Clast supported (Crackle (~95%) Angular, MW, Moderately strong, Coating; Dark blue black, silty Sand, Soft, NP) No precipitation	Damp	-41.224	174.8447	Terminates against FL28 and cross cuts SR23	
21	FL	81	113	91	D	Ro3	Wide	~150mm	~75%	1	D	~180°	Gentle		Planar	~6m		Clast supported (Mosaic (~75%) Angular, HW, Very weak, Coating; Light blue grey (Sand) and Dark blue grey (Clay), silty Sand and Clay, Very soft, MP and NP) No precipitation	Damp	-41.224	174.8447	Terminates against FL above splay off of FL28 and cross cuts SR23	
22	SR	45	165	143	D	Ro3	Moderately wide	~50mm	~50%	1	D	~160°	Open	~1.5m	Wavy	~7m		Matrix supported (Chaotic (~50%) Angular, CW, Very weak, Coating; Light blue grey, sandy Silt with traces of clay, Stiff, NP) White sand sized specks of precipitation	Damp	-41.2239	174.8448	Terminates against SR23 and Cross cuts SR24, FL28, SR27 and BSH25	
23	SR	30	342	320	D	Ro3	Narrow	~5mm	~90%	1	D	~170°	Gentle	~1m	Wavy	~20m	~3m	Clast supported (Crackle (~90%) Angular, HW, Weak, Coating; Light blue grey, clayey Sand, Very soft, NP) No precipitation	Damp	-41.2239	174.8447	Cross cuts SR21, FL21, BSH20, SR19, SR18, SR17, SR16, BSH15, SR14 and BSH12. Terminates against Shear set similar to SR11	
23	SR	30	341	319	D	Ro3	Narrow	~5mm	~90%	1	D	~170°	Gentle	~1m	Wavy	~20m	~3m	Clast supported (Crackle (~90%) Angular, HW, Weak, Coating; Light blue grey, clayey Sand, Very soft, NP) No precipitation	Damp	-41.2239	174.8447	Cross cuts SR21, FL21, BSH20, SR19, SR18, SR17, SR16, BSH15, SR14 and BSH12. Terminates against Shear set similar to SR11	
24	SR	56	74	52	D	Ro4	Moderately wide	~50mm	~95%	2	D	~150°	Gentle	~1.5m	Wavy	~2.5m		Clast supported (Crackle (~95%) Angular, MW, Moderately strong to strong, Coating; Light blue grey, silty Sand, Very soft, NP) White sand sized specks of precipitation	Damp	-41.2239	174.8447	Terminates against FL above splay off of FL28 and cross cuts SR23 and SR22	
25	BSH	62	68	46	D	Ro3	Moderately wide	~50mm	~95%	0	C	~170°	Gentle	~0.8	Wavy	~7m		Clast supported (Crackle (~95%) Angular, MW, Moderately strong to Strong, Coating; Dark blue black, clayey Sand, Soft, NP) White elongated precipitation	Damp	-41.2238	174.8446	Cross cuts SR23, FL28 and SR22	
26	SR	36	160	138	D	Ro3	Narrow	~5mm	~99%	1	D	~180°	Gentle		Planar	~1.5m		Clast supported (Rock (~99%) Angular, MW, Strong, Veneer; Light blue grey, Silt, Very soft, NP) No precipitation	Dry	-41.2239	174.8448	Terminates against FL28 and cross cuts SR27	
26	SR	34	159	137	D	Ro3	Narrow	~5mm	~99%	1	D	~180°	Gentle		Planar	~1.5m		Clast supported (Rock (~99%) Angular, MW, Strong, Veneer; Light blue grey, Silt, Very soft, NP) No precipitation	Dry	-41.2239	174.8448	Terminates against FL28 and cross cuts SR27	
27	SR	50	69	47	D	Ro4	Moderately wide	~40mm	~95%	1	D	~160°	Gentle	~6m	Wavy	~7m		Clast supported (Crackle (~95%) Angular, MW, Moderately strong, Coating; Light blue grey, sandy Silt, Soft, NP) No precipitation	Damp	-41.2238	174.8447	Terminates against SR set similar to SR23 and Cross cuts SR26	
28	FL	24	338	316	D	Ro3	Wide	~120mm	~80%	2	D	~170°	Gentle	~1m	Wavy	~20m	~3m	Clast supported (Crackle (~80%) Angular, HW to CW, Very weak, Coating; Light blue grey, silty Sand with traces of Clay, Very soft to soft, NP) White sand sized specks of precipitation	Damp	-41.2238	174.8447	Cross cuts SR22, BSH25, SR24, SR18 and SR21. Terminates against BSH20 and SR27	
29	SH	75	149	127	D	Ro4	Very Wide	~250mm	~50%	0	C	~160°	Gentle	~1.2m	Wavy	~7m		Matrix supported (Chaotic (~50%) Angular, CW, Very weak, Coating; Light blue grey (Sand) and Dark blue grey (Clay), silty Sand and Clay, Stiff and Soft, HP and NP) White sand sized specks of precipitation	Damp	-41.2237	174.8447	Cross cuts multiple shears not named here	
30	SR	79	157	135	D	Ro4	Moderately narrow	~15mm	~95%	0	C				Stepped	~8m		Clast supported (Crackle (~95%) Angular, HW, Weak, Coating; Light blue grey, silty Sand, Soft, NP) No precipitation	Damp	-41.2236	174.8448	Cross cuts bedding	
31	SR	63	102	80	D	Ro3	Narrow	~4mm	~99%	1	D	~180°	Gentle		Planar	~6m		Clast supported (Crackle (~99%) Angular, MW, Strong, Coating) No precipitation	Damp	-41.2236	174.8446	Terminates against SR set similar to SR23	
32	BSH	76	88	66	C	Ro3	Wide	~90mm	~95%	0	O		Gentle		Irregular	~12m	~0.75m	Clast supported (Crackle (~95%) Angular, MW, Moderately strong, Coating; Dark blue black, Sand, Soft, NP) No precipitation	Damp	-41.2237	174.8446	Follows bedding	
32	BSH	72	112	90	C	Ro3	Wide	~90mm	~95%	0	O		Gentle		Irregular	~12m	~0.75m	Clast supported (Crackle (~95%) Angular, MW, Moderately strong, Coating; Dark blue black, Sand, Soft, NP) No precipitation	Damp	-41.2237	174.8447	Follows bedding	
33	SR	63	340	318	C	Ro4	Narrow to Moderately narrow	~6mm	~95%	0	O	~160°	Gentle	~1.3m	Wavy	~1.5m		Clast supported (Crackle (~95%) Angular, HW, Weak, Coating; Light blue grey, Sand, Soft, NP) No precipitation	Damp	-41.225	174.8442	Cuts through bedding	
1	SR	63	53	31	B	Ro3	Moderately wide	~25mm	~99%	0	C	~140°	Gentle	~1.8m	Wavy	~8m	~0.6m	Clast supported (Crackle (~99%) Angular, MW, Moderately strong to Strong, Coating; Dark blue grey, Sand, Soft, NP) White elongated precipitation	Damp	-41.226	174.8447	Continuous	
2	SR	85	46	24	B	Ro3	Moderately wide	~20 to 50mm	~95%	1	R	~160°	Gentle	~2m	Wavy	~4m		Clast supported (Crackle (~95%) Angular, HW, Moderately strong to Strong, Coating; Dark blue grey, Clay, Very soft, MP) White elongated precipitation	Minor seepage	-41.226	174.8447	Terminates in rock	
3	SR	86	342	320	B	Ro2	Moderately	~20mm	~90%	1	D	~160°	Gentle	~16m	Curved	~6m	~0.2m	Clast supported (Crackle (~90%) Angular, MW, Moderately	Minor seepage	-41.226	174.8447	Terminates against SR4	

4	BSH	76	277	255	B	Ro3	narrow to Moderately wide										strong to Strong, Coating; Dark blue grey, silty Clay, Very soft, MP-LP) White elongated precipitation					
							Moderately narrow	~15mm	~90%	1	R	~140°	Gentle	~2m	Wavy	~8m	~0.25m	Clast supported (Crackle (~90%) Angular, MW, Moderately strong to Strong, Coating; Dark blue grey, silty Clay, Very soft, MP-LP) White elongated precipitation	Minor seepage	-41.226	174.8447	Terminates in rock
5	BSH	90	323	301	B	Ro4	Moderately wide	~55mm	~95%	1	R				Irregular	~5m	~1m	Clast supported (Crackle (~95%) Angular, HW, Moderately strong, Coating; Dark blue grey, silty Clay, Very soft, MP-LP) White tabulated, gravel sized precipitation	Minor seepage	-41.226	174.8447	Cross cuts FL7 and terminates against bedding
6	SR	88	343	321	B	Ro3	Narrow	~3mm	~99%	1	D	~170°	Gentle	~2m	Wavy	~6m		Clast supported (Crackle (~99%) Angular, MW, Moderately strong, Coating) White elongated precipitation	Damp	-41.226	174.8448	Cross cuts FL7 and terminates against BSH4
7	FL	48	276	254	B	Ro2	Moderately narrow	~15mm	~99%	1	D	~160°	Gentle	~6m	Wavy	~6m		Clast supported (Crackle (~99%) Angular, HW, Moderately strong, Coating; Dark blue grey, silty Clay, Soft, MP) No precipitation	Damp	-41.2261	174.8448	Terminates against BSH9 and cross cuts BSH5, SR6 and BSH8
8	BSH	83	65	43	B	Ro4	Moderately wide	~45mm	~99%	1	D	~70°	Close	~0.8m	Wavy	~6m	~0.3m	Clast supported (Crackle (~99%) Angular, MW, Moderately strong to Strong, Coating) Whit elongated precipitation	Minor seepage	-41.2261	174.8449	Terminates against FL7
9	BSH	75	291	269	B	Ro4	Moderately wide	~45mm	~99%	1	D	~70°	Close	~0.8m	Wavy	~6m	~0.3m	Clast supported (Crackle (~99%) Angular, MW, Moderately strong to Strong, Coating) Whit elongated precipitation	Minor seepage	-41.226	174.8449	Terminates against FL10
10	FL	68	310	288	A&B	Ro2	Very wide	~250mm	~80%	0	C	~180°	Gentle		Planar	~8m		Clast supported (Crackle (~80%) Angular, HW, Moderately strong, Coating; Light blue grey (Sand) and Dark blue grey (Clay), silty Sand and Clay, Very soft to Firm, MP and NP) White elongated precipitation	Significant seepage	-41.2261	174.8449	Continuous
11	BSH	80	42	20	A	Ro3	Moderately narrow	~10mm	~95%	0	C	~180°	Gentle		Planar	~8m		Clast supported (Crackle (~80%) Angular, HW, Moderately strong, Coating; Light blue grey (Sand) and Dark blue grey (Clay), silty Sand and Clay, Very soft to Firm, MP and NP) White elongated precipitation	Damp	-41.2262	174.845	Terminates against FL10
11	BSH	83	44	22	A	Ro3	Moderately narrow	~10mm	~95%	1	D	~180°	Gentle		Planar	~4m	~2m	Clast supported (Crackle (~95%) Angular, HW, Moderately strong, Coating; Light blue grey, silty Sand, Soft, NP) White sand sized speck of precipitation	Damp	-41.2262	174.845	Terminates against FL10
12	SR	86	138	116	A	Ro3	Moderately narrow	~10mm	~95%	0	C	~180°	Gentle		Planar	~4m	~2m	Clast supported (Crackle (~95%) Angular, HW, Moderately strong, Coating; Light blue grey, silty Sand, Soft, NP) White sand sized speck of precipitation	Damp	-41.2262	174.8451	Continuous
1	SR	59	321	298	E	Ro3	Wide	100mm	~90%	0	D	~160°	Gentle	~6m	Wavy	~4m	~1.5m	Clast Supported (Crackle (~90%), Angular, HW, Moderately strong clasts, Clean; Light brown, clayey Silt with traces of sand, Very soft, NP) No precipitation visible	Damp	-41.2214	174.8455	Cross cuts SR2
2	SR	46	200	177	E	Ro2	Tight	0mm		0	C	~180°	Gentle	~0m	Planar	~4m			Significant seepage ~10L/5mins	-41.2214	174.8458	Cross cuts BSH1 and SR3. Offset by SR3
2b	BSH	69	273	251	E	Ro3	Very wide	200mm	~85%	0	D	~160°	Gentle	~3m	Wavy	~4.5m	~0.8m	Clast Supported (Crackle (~85%), Angular, HW, Weak, Stained; Light grey, sandy Clay, Very soft, LP) white sand sized precipitation	Damp	-41.2213	174.8458	Cross cuts SR2 and SR3
3	SR	21	55	33	E	Ro3	Wide	100mm	~90%	1	D	~180°	Gentle	~0m	Planar	~3m		Clast Supported (Crackle (~90%), Angular, HW, Weak, Veneer; Light grey, sandy Clay, Very soft, LP) no visible precipitation	Damp	-41.2214	174.8459	Offsets SR2 and cross cuts BSH2
4	BSH	54	326	304	E&F	Ro3	Wide	80mm	~80%	1	D	~160°	Gentle	~6m	Wavy	~5m	~0.6m	Clast Supported (Crackle (~80%), Angular, HW, Weak, Veneer; Light grey brown, sandy Clay, Very soft, LP) white gravel sized angular clasts	Damp	-41.2214	174.8459	Cross cuts SR5. Terminates against SR9
5	SR	77	215	192	F	Ro3	Very wide	200mm	~90%	1	D	~150°	Gentle	~4m	Wavy	~3m		Clast Supported (Crackle (~90%), Angular, HW, Weak, Stained; Light grey, sandy Clay, Very soft, NP) white gravel sized angular clasts	Damp	-41.2215	174.8459	Cross cuts BSH4 and terminates against BSH4
6	SR	45	8	345	F	Ro3	Very wide	200mm	~90%	1	D	~150°	Gentle	~6m	Wavy	~3.5m		Clast Supported (Crackle (~90%), Angular, HW, Weak, Veneer; Light grey, silty Clay traces of sand, Very soft, LP) white elongated angular gravel clasts.	Damp	-41.2216	174.846	Cross cuts SR8, SR9 and SR10. Terminates against SR11
7	SR	71	217	194	F	Ro3	Moderately wide	40mm	~99%	0	C	~160°	Gentle	~6m	Wavy	~2.2m		Clast Supported (Rock (~99%), Angular, MW, Moderately strong to strong, Veneer; Light grey, silty Sand trace of clay, Very soft, NP) white gravel sized elongated angular clasts	Damp	-41.2216	174.846	Cross cuts SR8, BSH4 and SR9
8	SR	88	95	72	F	Ro3	Moderately wide	40mm	~85%	0	C	~140°	Gentle	~3m	Wavy	~2.6m		Clast Supported (Crackle (~85%), Angular, HW, Moderately strong to strong, Veneer; Light grey brown, silty Sand trace of clay, Very soft, LP) white gravel sized elongated angular clasts	Damp	-41.2215	174.8461	Cross cuts SR8, BSH4 and SR9
9	SR	59	84	62	F	Ro2	Moderately wide	60mm	~99%	0	C	~170°	Gentle	~2m	Wavy	~3.25m		Clast Supported (Rock (~99%), Angular, HW, Moderately strong to strong, Stained; Light grey brown, silty Sand trace of clay, Very soft, LP) white gravel sized elongated angular clasts	Dry	-41.2217	174.8459	Cross cuts SR8, BSH4 and SR7
10	SR	76	344	321	F	Ro2	Moderately wide	60mm	~99%	0	C	~170°	Gentle	~2m	Wavy	~6m		Clast Supported (Rock (~99%), Angular, HW, Moderately strong to strong, Coating; Light grey brown, silty Sand trace of clay, Very soft, LP) white gravel sized elongated angular clasts	Dry	-41.2215	174.8461	Cross cuts BSH4 and SR6
10	SR	77	349	326	F	Ro2	Moderately wide	60mm	~99%	0	C	~170°	Gentle	~2m	Wavy	~6m		Clast Supported (Rock (~99%), Angular, HW, Moderately strong to strong, Veneer; Light grey brown, silty Sand trace of clay, Very soft, LP) white gravel sized elongated angular clasts	Dry	-41.2215	174.8461	Cross cuts BSH4 and SR6

North Cut Slope

North Cut Slope

11	SR	81	245	223	F	Ro1	Moderately narrow	10mm	~99%	0	C	~160°	Gentle	~2m	Wavy	~3m		Clast Supported (Rock (~99%), Angular, HW, Weak to Very weak, Coating; Light grey brown, silty Sand trace of clay, Very soft, LP) All white precipitation	Dry	-41.2215	174.8463	Cross cuts BSH13 and SR12
11b	SR	79	225	203	F	Ro1	Very wide	300-200mm	~85%	0	C	~160°	Gentle		Wavy	~3m		Clast Supported (Crackle (~85%), Angular, HW, Moderately strong, Coating; Light grey, silty Clay trace of sand, Very Soft, MP) gravel and sand sized clasts white angular precipitation	Damp	-41.2215	174.8462	Cross cuts BSH13 and SR12
13	BSH	20	338	315	F	Ro2	Moderately narrow	10mm	~99%	0	C	~160°	Gentle	~2m	Wavy	~8m	~1.3m	Clast Supported (Rock (~99%), Angular, HW, Weak to Very weak, Coating; Light grey brown, silty Sand trace of clay, Very soft, LP) All white precipitation	Dry	-41.2216	174.8462	Cross cuts SR11, SR11b, SR17, SR15 and SR12
13	BSH	18	311	289	F	Ro2	Moderately narrow	10mm	~99%	0	C	~160°	Gentle	~2m	Wavy	~3m	~1.5m	Clast Supported (Rock (~99%), Angular, HW, Weak to Very weak, Veneer; Light grey brown, silty Sand trace of clay, Very soft, LP) All white precipitation	Dry	-41.2217	174.8462	Cross cuts SR17b, SR19 and SR18
12	SR	62	77	55	F	Ro4	Very wide	200mm	~85%	1	D	~100°	Open	~4m	Wavy	~2.4m	~1.5m	Clast Supported (Crackle (~85%), Angular, HW, Moderately strong, Coating; Light grey, silty Clay trace of sand, Very Soft, MP) white gravel sized elongated angular clasts	Damp	-41.2216	174.8463	Cross cuts SR11b, and BSH13. Terminates against SR11
17	SR	88	46	23	F	Ro2	Tight	0mm		1	D	~170°	Gentle	~10m	Wavy	~5.5m	~2m	Clast Supported (Rock (~99%), Angular, HW, Moderately strong, Coating; Light grey, silty Clay trace of sand, Very soft, MP) white gravel sized elongated angular clasts	Damp	-41.2216	174.8463	Cross cuts BSH14 and terminates against BSH13
17B	SR	80	242	220	F	Ro2	Wide	100mm	~90%	0	C	~150°	Gentle	~20m	Wavy	~4.5m	~2m	Clast Supported (Crackle (~90%), Angular, MW, Moderately strong, Coating; Light white grey, silty Clay trace of sand, Very soft, MP) gravel and sand sized clasts white angular precipitation	Damp	-41.2216	174.8463	Cross cuts BSH14, SR18 and BSH13
16	SR	59	294	272	F	Ro2	Wide	100mm	~90%	1	D	~150°	Gentle	~2m	Wavy	~5.5m		Clast Supported (Crackle (~90%), Angular, MW, Moderately strong, Coating; Light white grey, silty Clay trace of sand, Very soft, MP) gravel and sand sized clasts white angular precipitation	Damp	-41.2215	174.8463	Terminates against SR17b
14	BSH	19	5	342	F	Ro3	Wide	100mm	~80%	1	D	~150°	Gentle	~10m	Wavy	~3m	~1.3m	Clast Supported (Crackle (~80%), Angular, HW, Weak, Veneer; Dark brown, silty Sand trace of clay, Very soft, NP) gravel and sand sized clasts white angular precipitation	Damp	-41.2218	174.8463	Cross cuts SR17, SR17b, SR15, SR18 and SR19
18	SR	69	38	15	F	Ro3	Moderately wide	50mm	~99%	0	C	~160°	Gentle	~1m	Irregular	~6m	~1.7m	Clast Supported (Rock (~99%), Angular, MW, Moderately strong, Coating; Dark brown, silty Sand trace of clay, Very soft, NP) gravel and sand sized clasts white angular precipitation	Damp	-41.2217	174.8464	Cross cuts SR17b, SR17, SR15, BSH13 and BSH13
19	SH	83	57	35	F	Ro3	Moderately wide	50mm	~99%	0	R	~160°	Gentle	~1m	Irregular	~6m	~1.7m	Clast Supported (Rock (~99%), Angular, MW, Moderately strong, Coating; Dark brown, silty Sand trace of clay, Very soft, NP) gravel and sand sized clasts white angular precipitation	Damp	-41.2217	174.8465	Cross cuts BSH14 and BSH13
20	BSH	78	93	71	G	Ro2	Moderately wide	50mm	~99%	0	C	~180°	Gentle	~0m	Planar	~3m	~0.6m	Clast Supported (Rock (~99%), Angular, MW, Moderately strong, Veneer; Dark brown, silty Sand trace of clay, Very soft, NP) gravel and sand sized clasts white angular precipitation	Damp	-41.2217	174.8466	Failure plane 1 - Wedge failure. Transects SR20b
20b	SR	69	274	251	G	Ro2	Moderately wide	50mm	~99%	0	C	~180°	Gentle	~0m	Planar	~2.5m		Clast Supported (Rock (~99%), Angular, MW, Moderately strong, Veneer; Dark brown, silty Sand trace of clay, Very soft, NP) gravel and sand sized clasts white angular precipitation	Damp	-41.2217	174.8467	Failure plane 2 - Wedge failure. Transects BSH20
21	BSH	80	114	92	G	Ro3	Moderately wide	50mm	~99%	0	C	~160°	Gentle	~1m	Wavy	~2.8m	~0.8m	Clast Supported (Rock (~99%), Angular, MW, Moderately strong, Veneer; Dark brown, silty Sand trace of clay, Very soft, NP) gravel and sand sized clasts white angular precipitation	Damp	-41.2217	174.8467	Failure plane 1 - Wedge failure. Transects BSH22
22	BSH	82	93	71	G	Ro4	Wide	150mm	~80%	0	C	~160°	Gentle	~15m	Wavy	~2.8m	~1m	Clast Supported (Crackle (~80%), Angular, HW, Weak, Coating; Light and dark grey, silty Clay trace of sand, Very soft, LP) gravel and sand sized clasts white angular precipitation	Damp	-41.2218	174.8467	Continuous
23	SR	51	119	96	G	Ro4	Wide	150mm	~80%	0	C	~160°	Gentle	~15m	Wavy	~3m		Clast Supported (Crackle (~80%), Angular, HW, Weak, Coating; Light and dark grey, silty Clay trace of sand, Very soft, LP) gravel and sand sized clasts white angular precipitation	Damp	-41.2218	174.8468	Failure plane 2 - Wedge failure. Transects BSH21
24	BSH	86	277	254	G	Ro4	Wide	150mm	~80%	0	C	~160°	Gentle	~15m	Wavy	~3m	~0.8	Clast Supported (Crackle (~80%), Angular, HW, Weak, Coating; Light and dark grey, silty Clay trace of sand, Very soft, LP) gravel and sand sized clasts white angular precipitation	Damp	-41.2218	174.8469	Continuous
25	BSH	67	293	271	G	Ro2	Very wide	400mm	~80%	0	C	~160°	Gentle	~10m	Wavy	~2m	~0.8	Clast Supported (Crackle (~80%), Angular, HW, Weak, Coating; Light and dark grey, Clay with traces of silty Sand, Very soft, HP) gravel and sand sized clasts white angular precipitation	Damp	-41.2218	174.847	Continuous
26	SR	58	352	330	G	Ro2	Wide	80mm	~60%	0	C	~160°	Gentle	~10m	Wavy	~2.25m	~4m	Matrix Supported (Mosaic (~60%), Angular, HW, Very Weak, Coating; Light and dark grey, Clay with traces of silty Sand, Very soft, MP) gravel and sand sized clasts white angular precipitation	Damp	-41.2219	174.8471	Cross cuts SR28 and BSH25
27	SR	55	295	273	G	Ro2	Wide	80mm	~80%	0	C	~135°	Gentle	~7m	Wavy	~2m	~4m	Clast Supported (Crackle (~80%), Angular, HW, Very weak, Coating; Light and dark grey, silty Clay trace of Sand, Very soft, MP) gravel and sand sized clasts white angular precipitation	Damp	-41.2219	174.8471	Cross cuts SR28 and BSH25
28	SR	66	117	95	G	Ro2	Wide	80mm	~80%	0	C	~135°	Gentle	~7m	Wavy	~1m		Clast Supported (Crackle (~80%), Angular, HW, Very weak, Coating; Light and dark grey, silty Clay trace of Sand, Very soft, MP) gravel and sand sized clasts white angular precipitation	Damp	-41.2219	174.8471	Cross cuts SR27, BSH25 and SR26
25	BSH	78	276	253	G	Ro2	Wide	80mm	~80%	0	C	~135°	Gentle	~7m	Wavy	~2m	~0.3m	Clast Supported (Crackle (~80%), Angular, HW, Very weak, Coating; Light and dark grey, silty Clay trace of Sand, Very soft, MP) gravel and sand sized clasts white angular precipitation	Damp	-41.222	174.8472	Cross cuts SR28, SR26, SR28 and SR27

29	SR	43	327	305	G	Ro2	Moderately narrow	20mm	~90%	0	C	~180°	Gentle	~0m	Planar	~2m	~2m	Clast Supported (Crackle (~90%), Angular, MW, Strong to moderately strong, Coating; Light and dark brown, Clay with trace of silty Sand, Very soft, NP) all white precipitation	Damp	-41.2219	174.8472	Cross cuts BSH25	
----	----	----	-----	-----	---	-----	----------------------	------	------	---	---	-------	--------	-----	--------	-----	-----	---	------	----------	----------	------------------	--

D.4 Horokiwi Quarry Graphs

Defect and rock mass results from Horokiwi Quarry. Results are presented in graphs. Where percentages are used they display the respective occurrence of the dependent variable assessed.

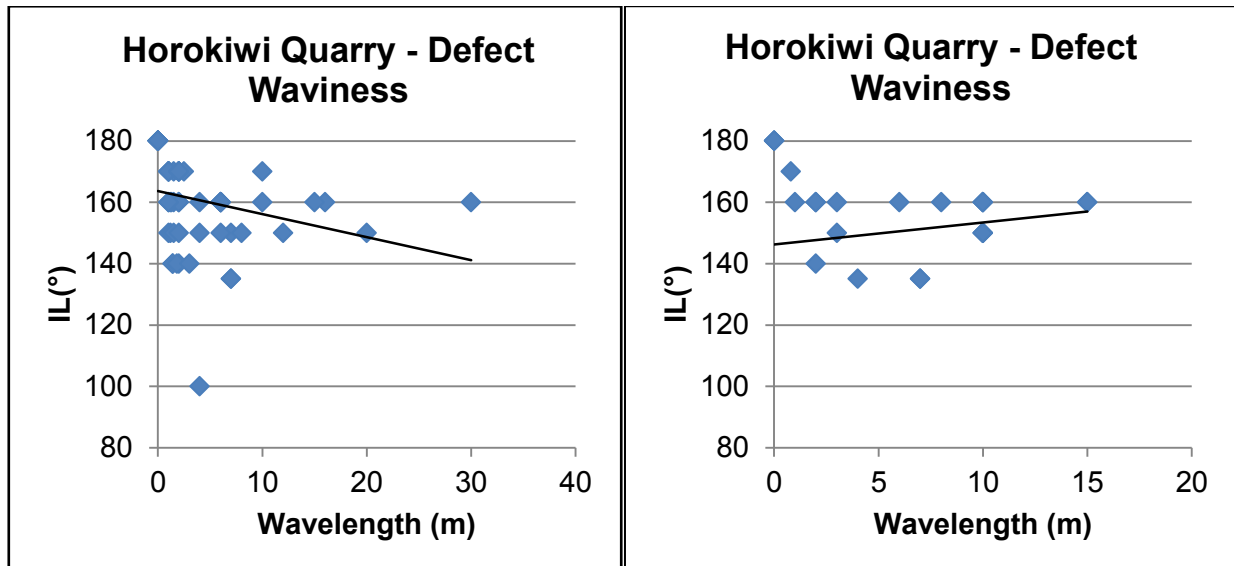
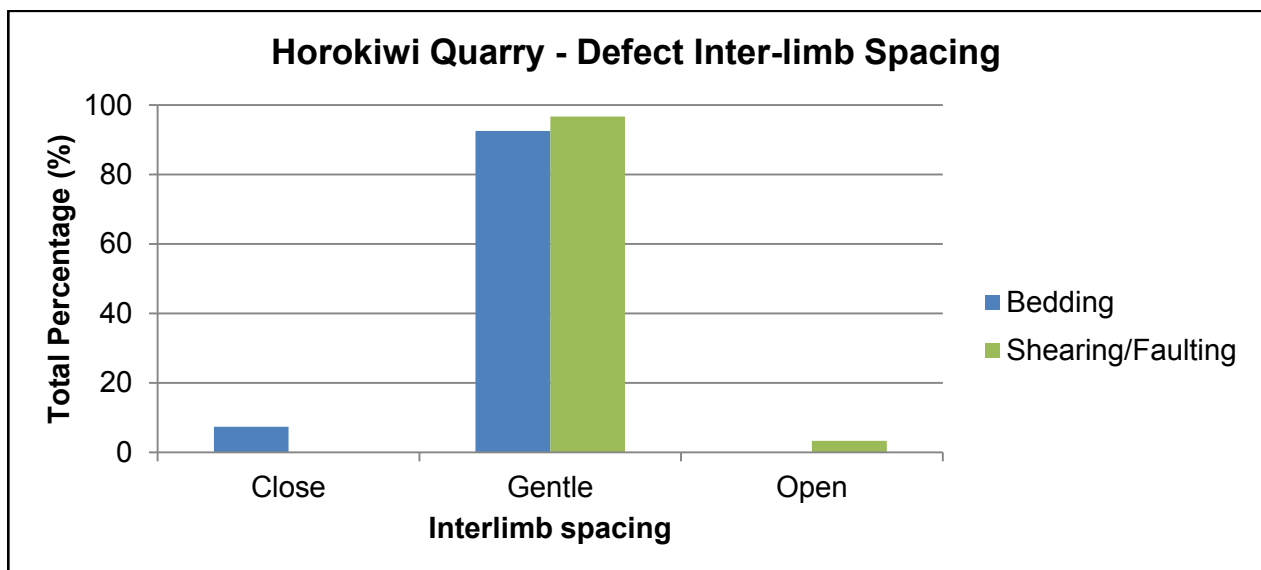
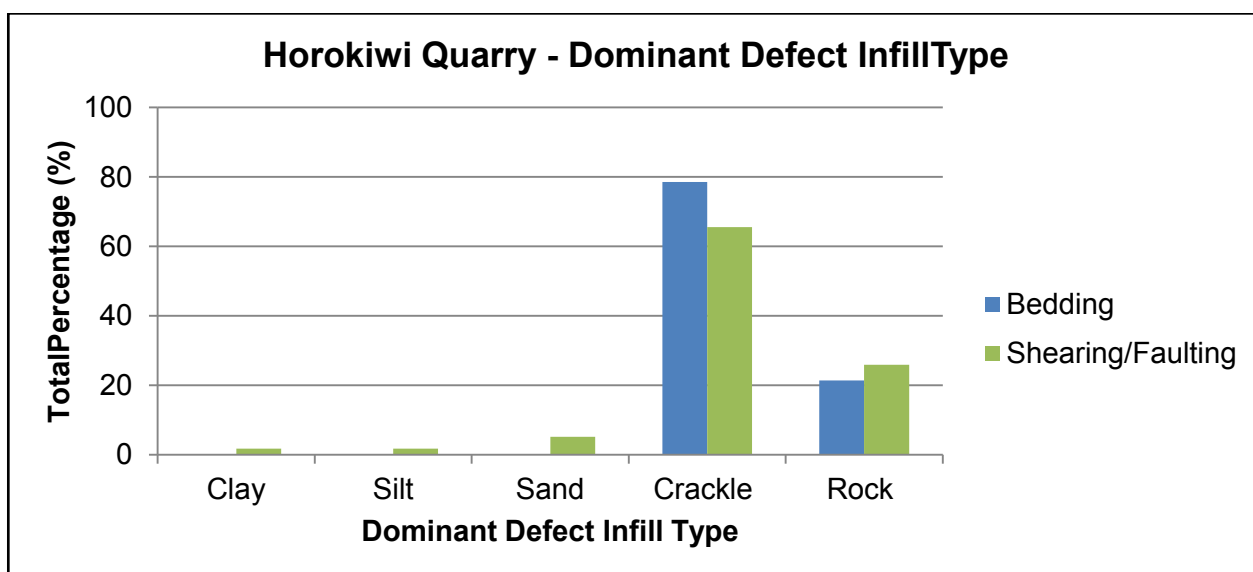
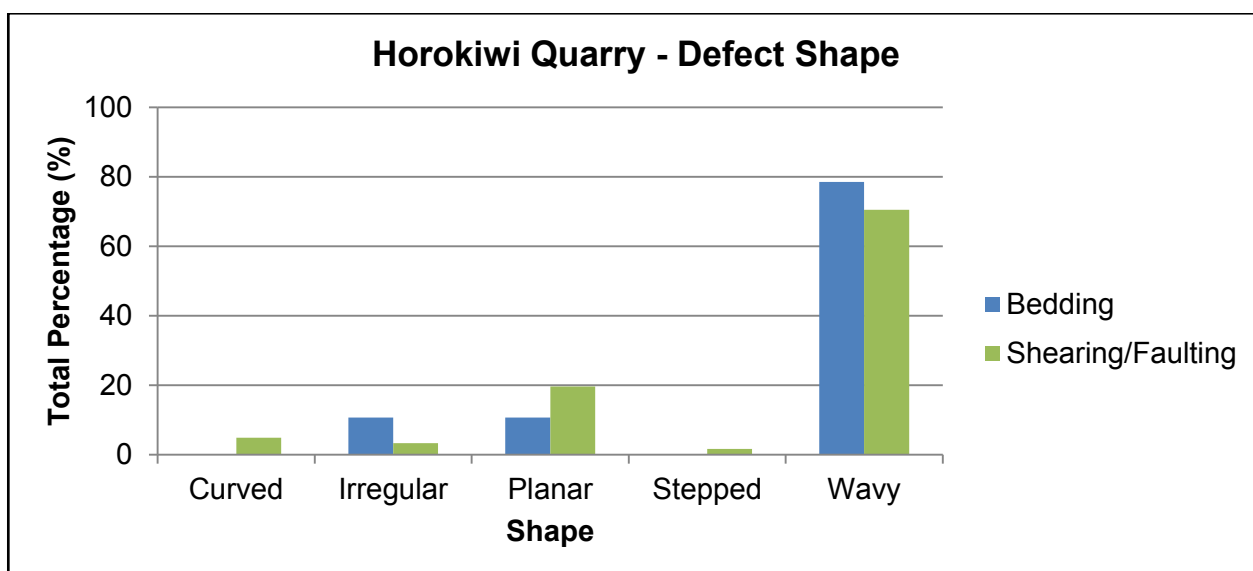
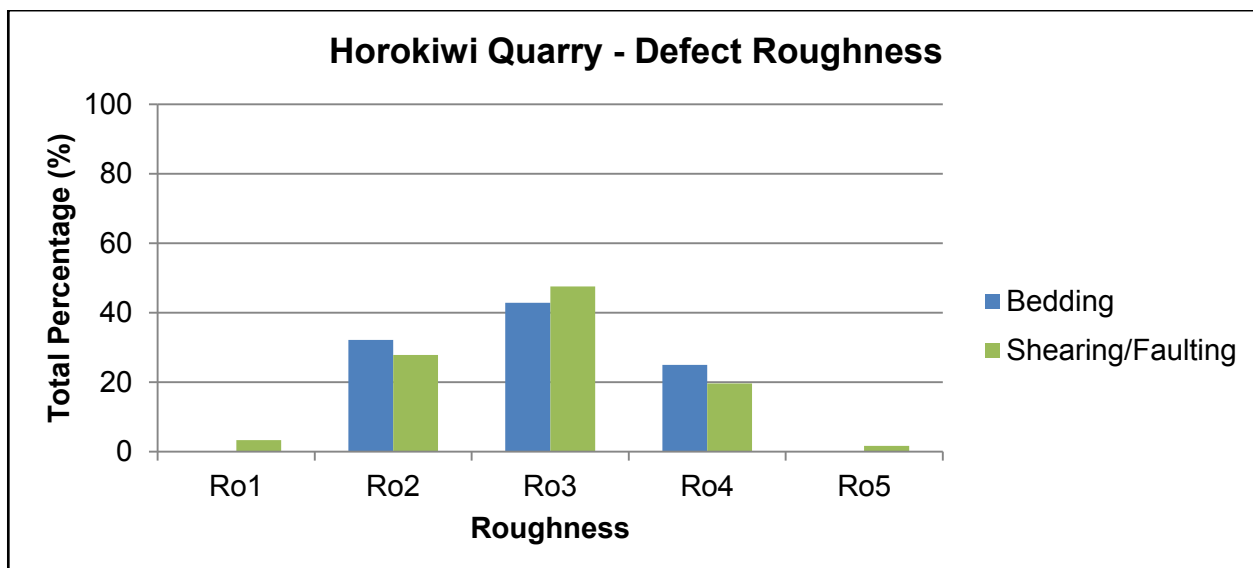
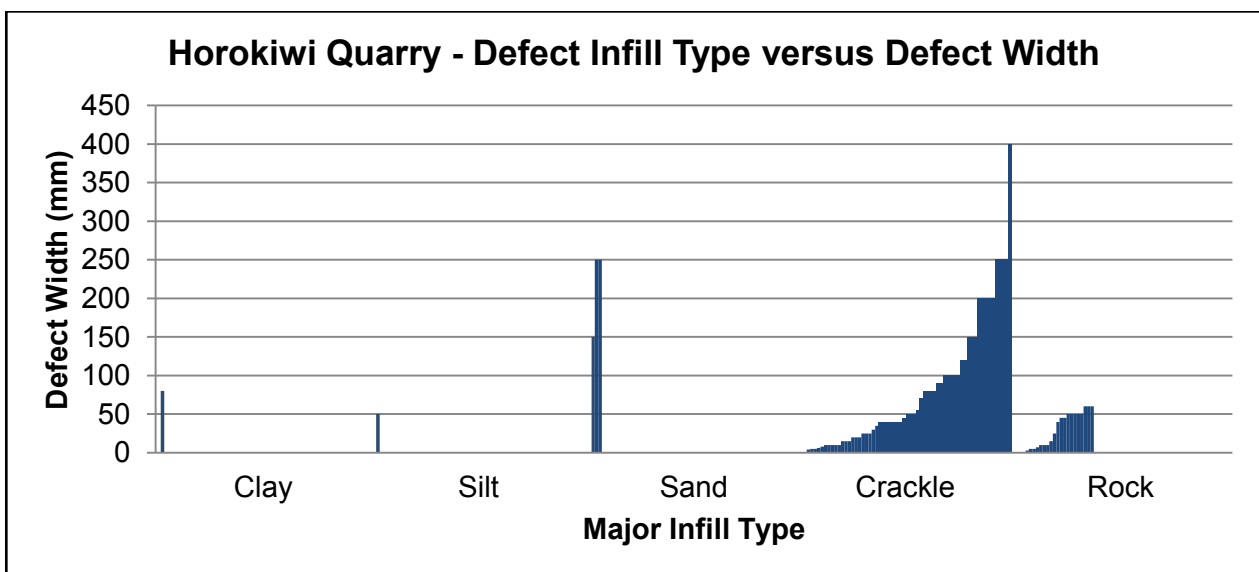
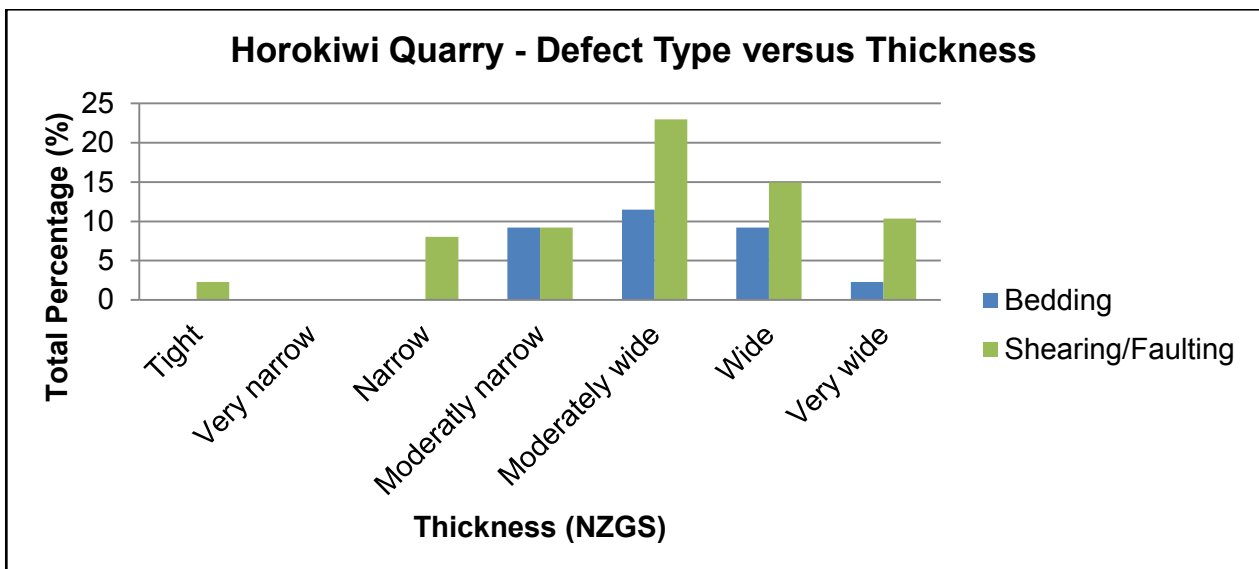
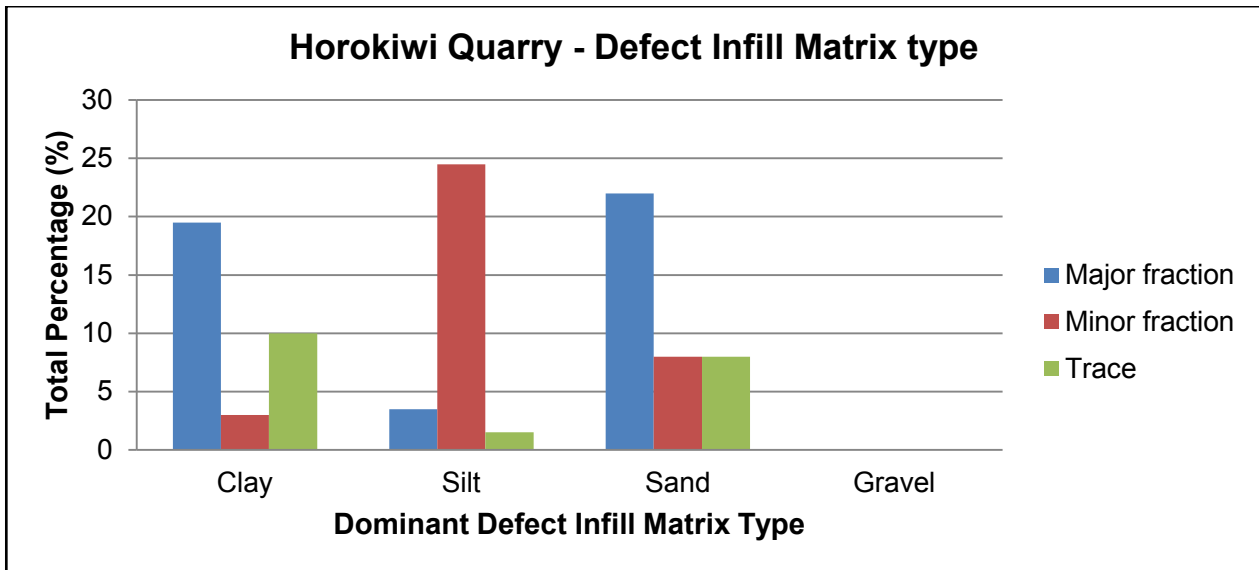
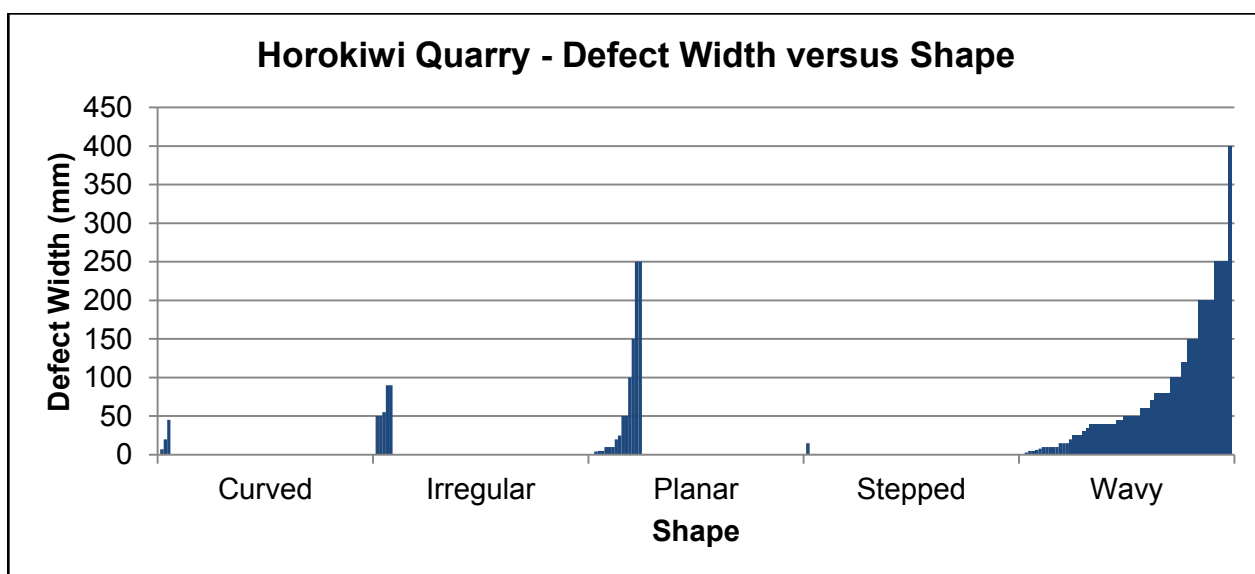
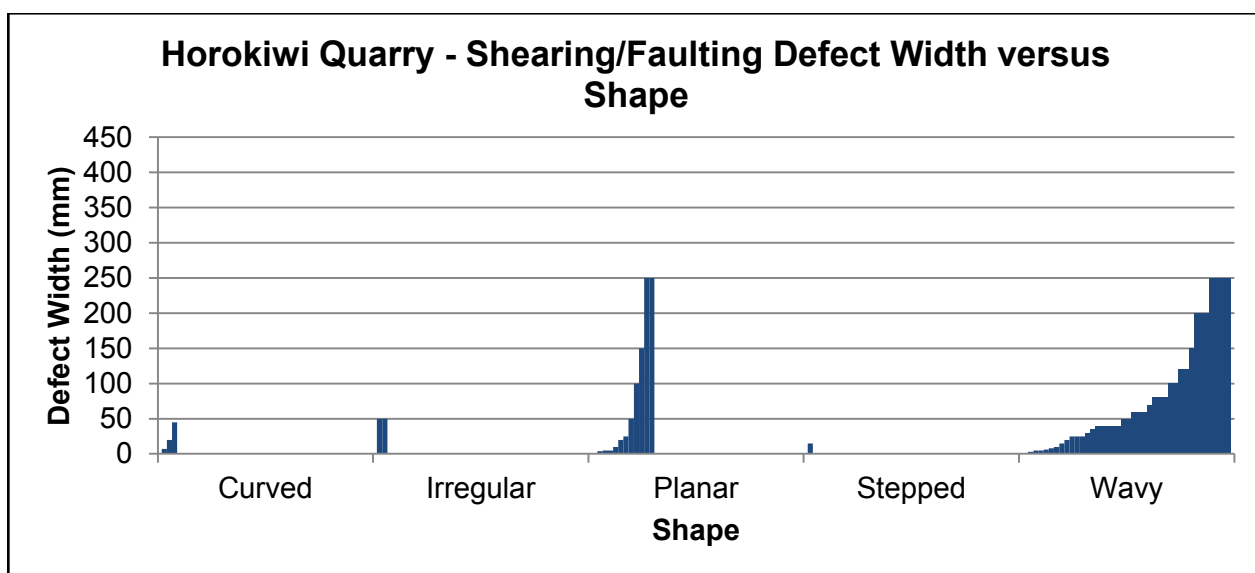
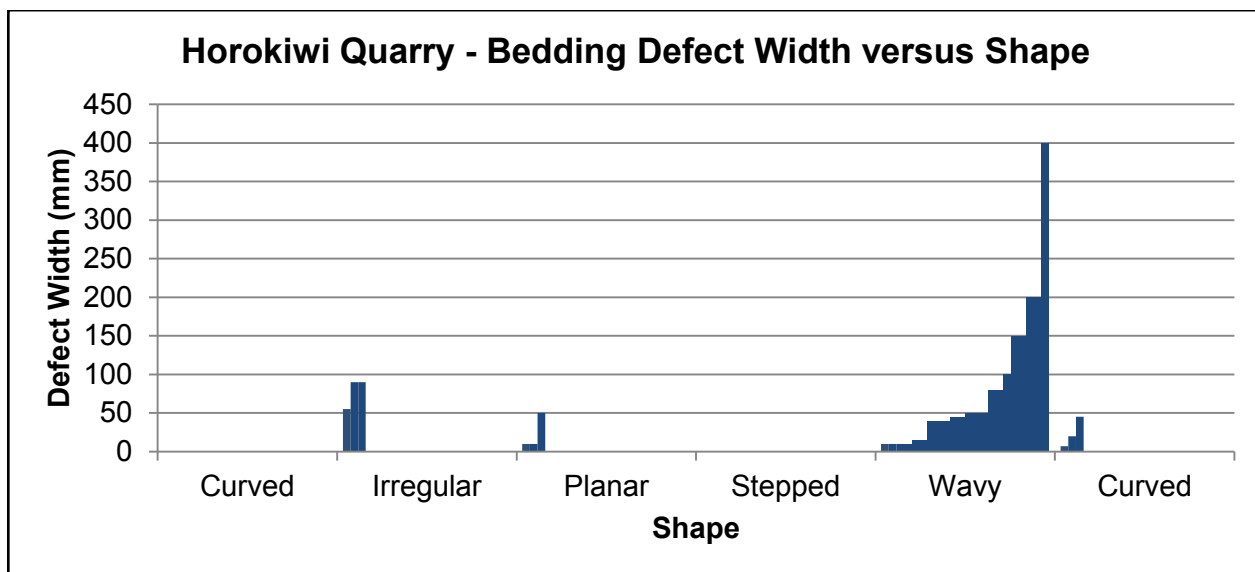


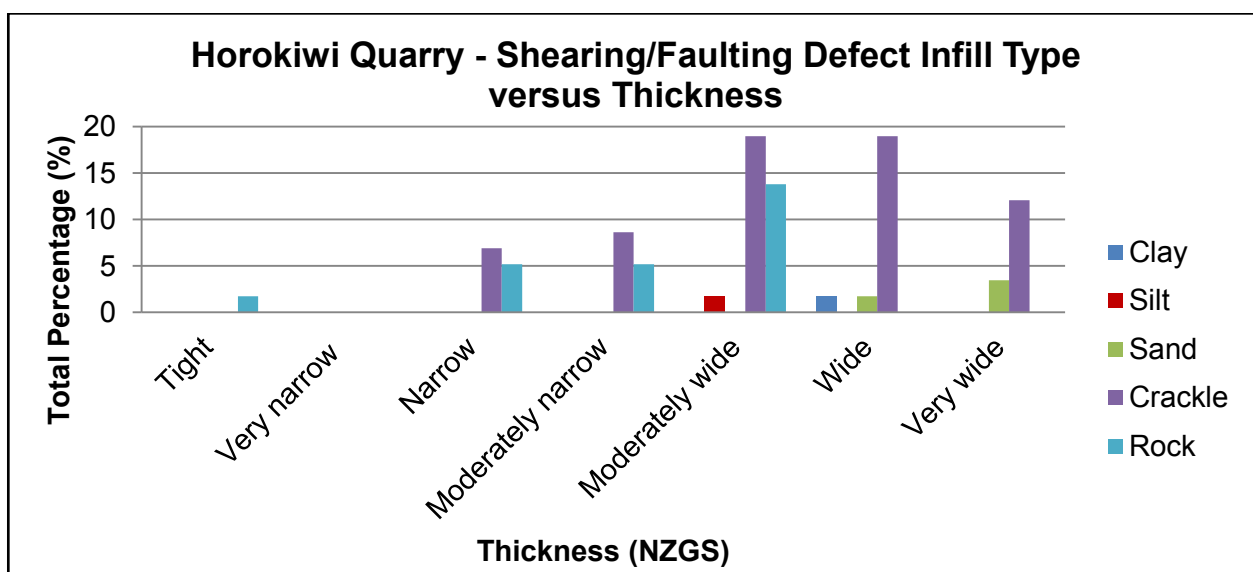
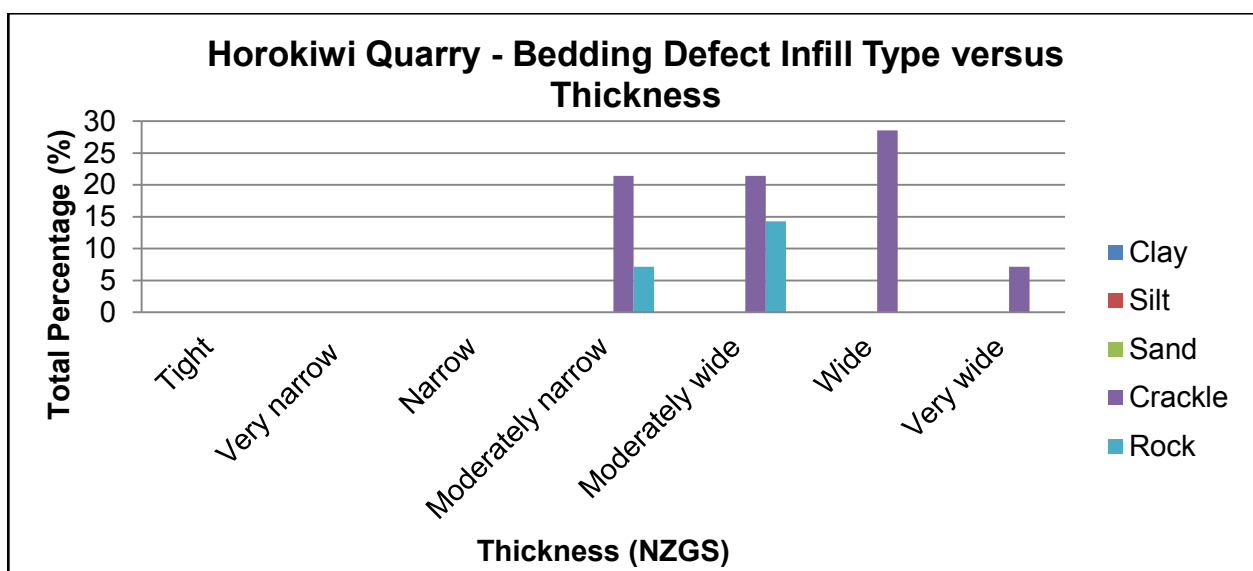
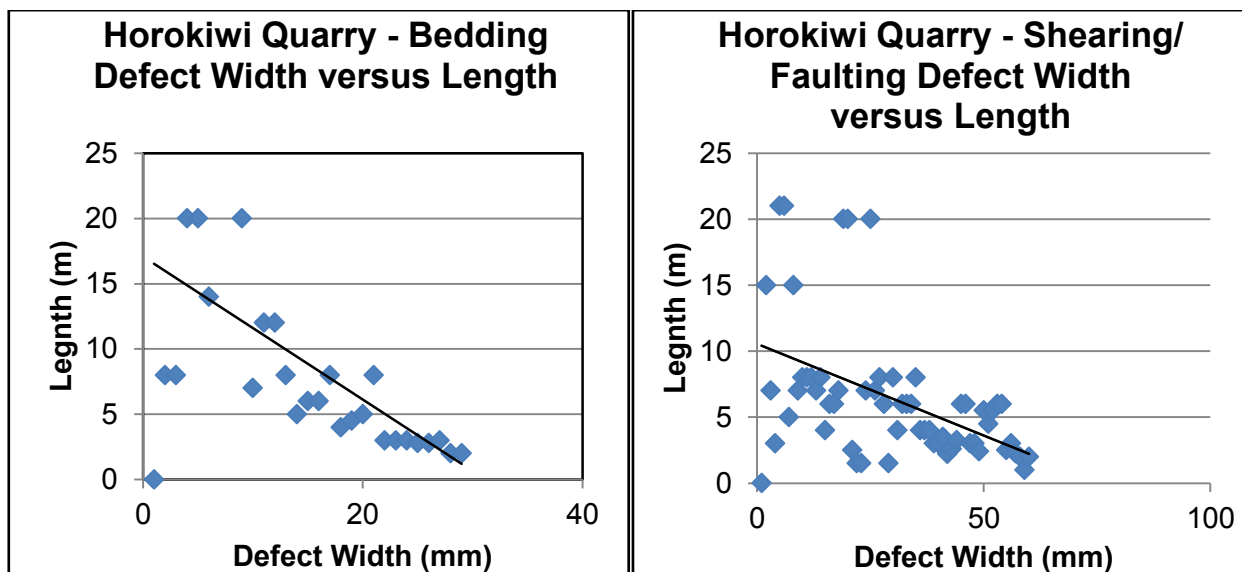
Figure D.4.1: Graphs displaying the defect waviness of Bedding (Right) and Shearing/Faulting (Left) at Horokiwi Quarry

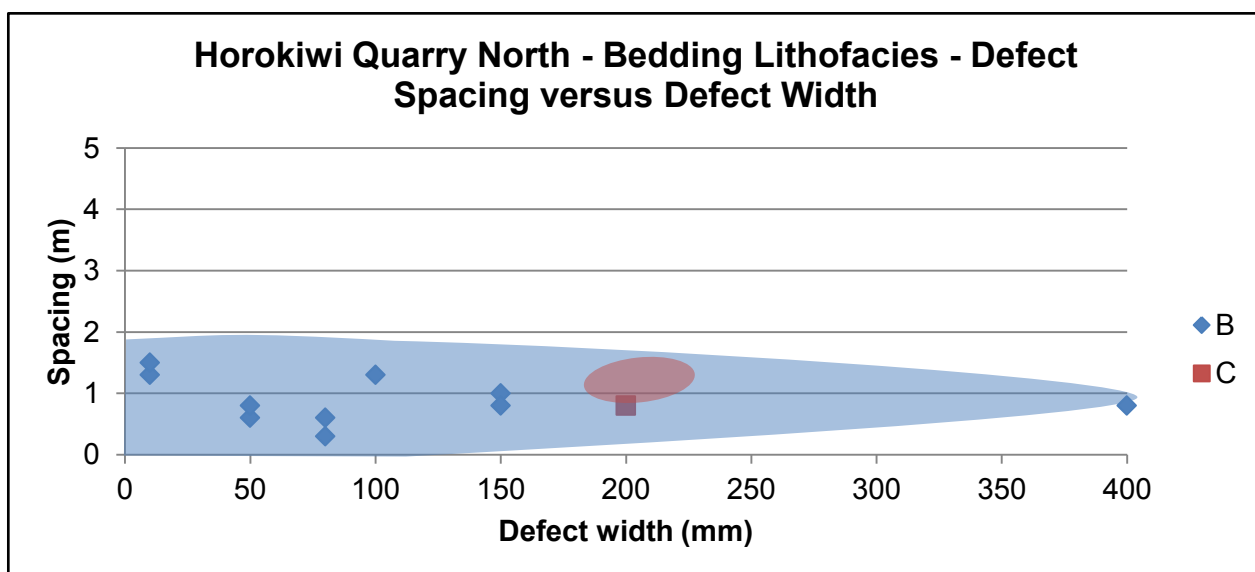
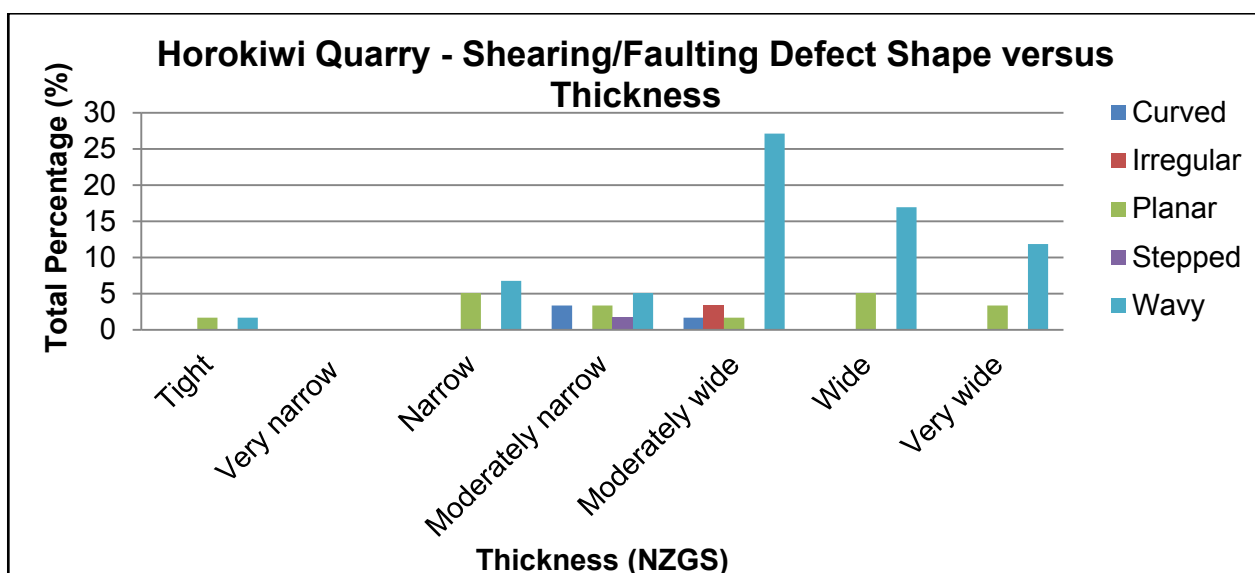
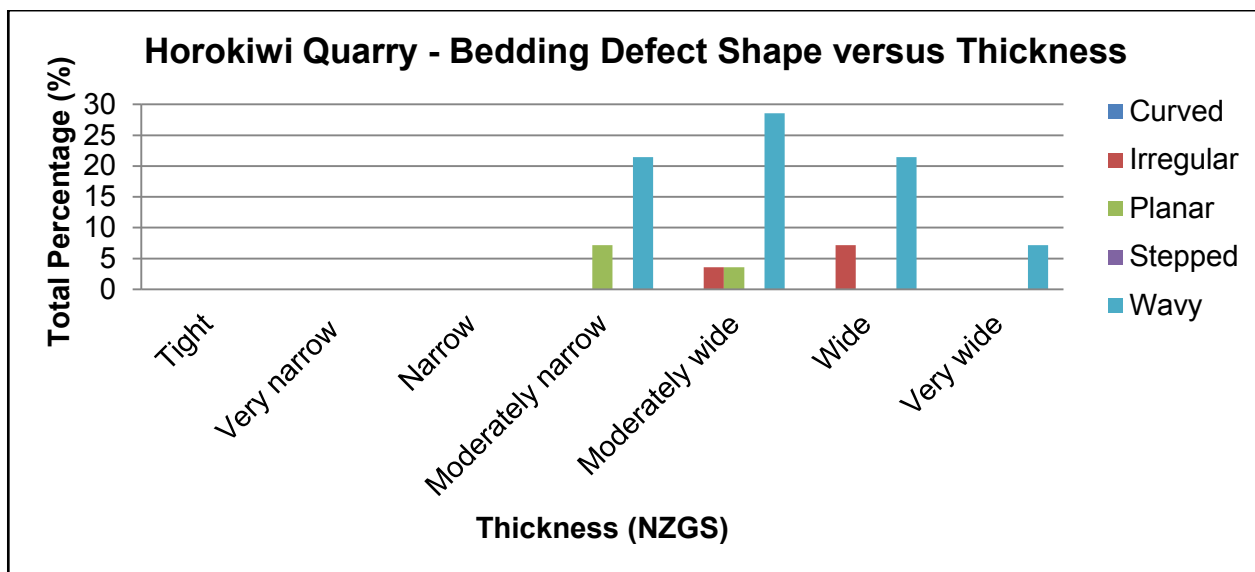


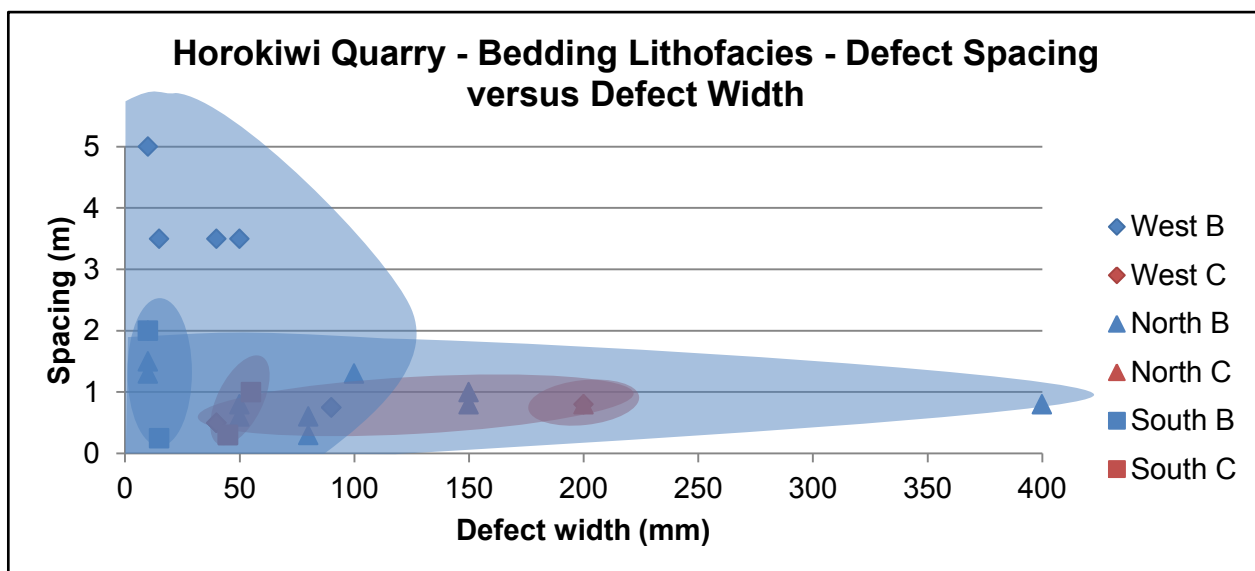
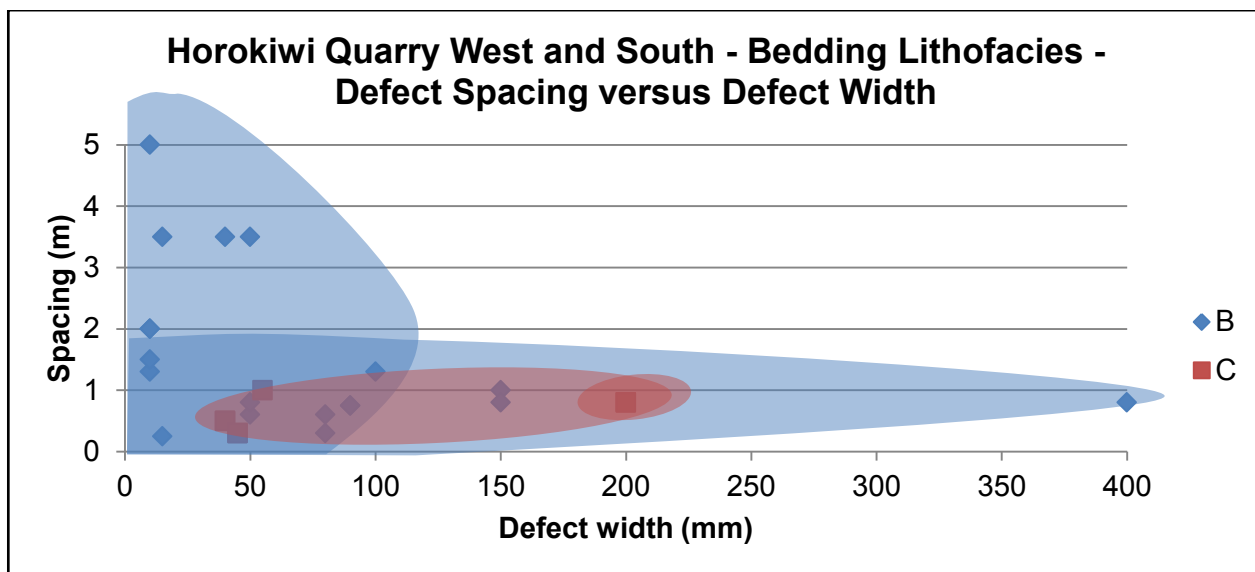








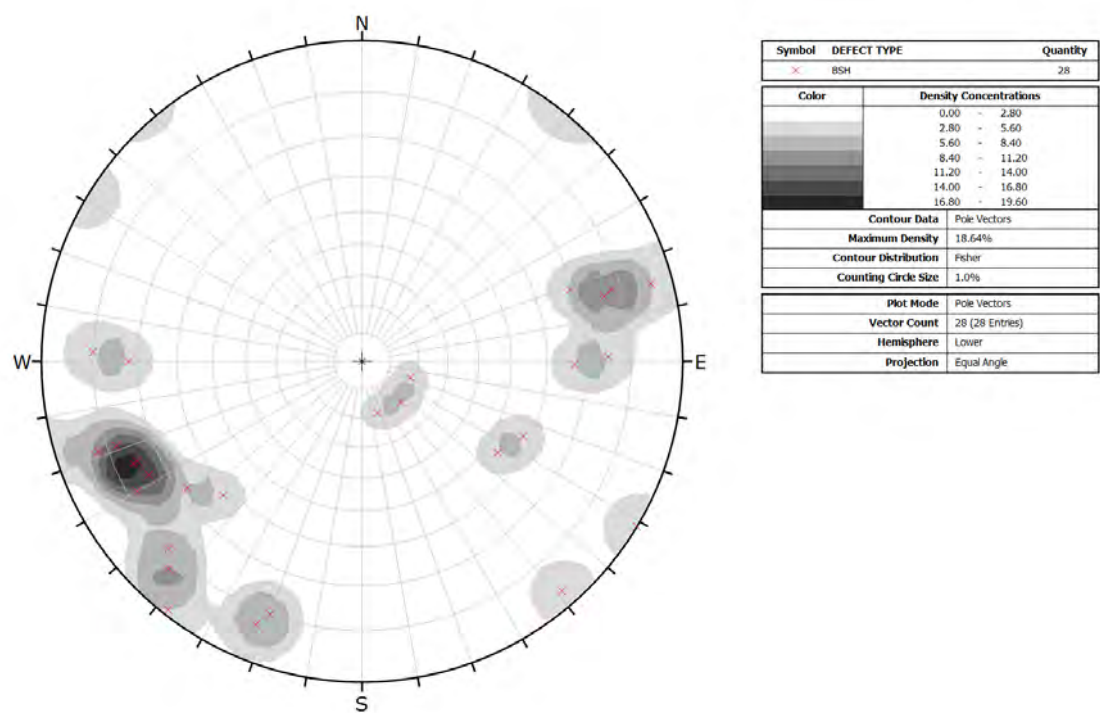




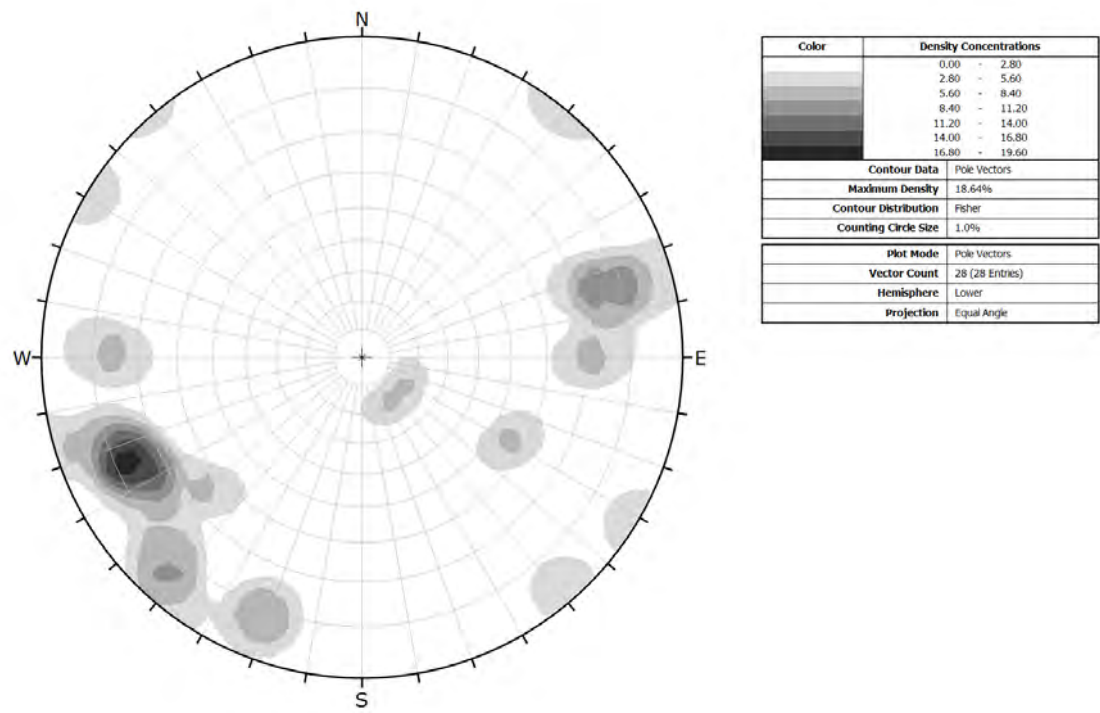
D.5 Horokiwi Quarry stereonet analysis

Stereonet Dip: Dip direction analysis of bedding, faults and shears respectively.

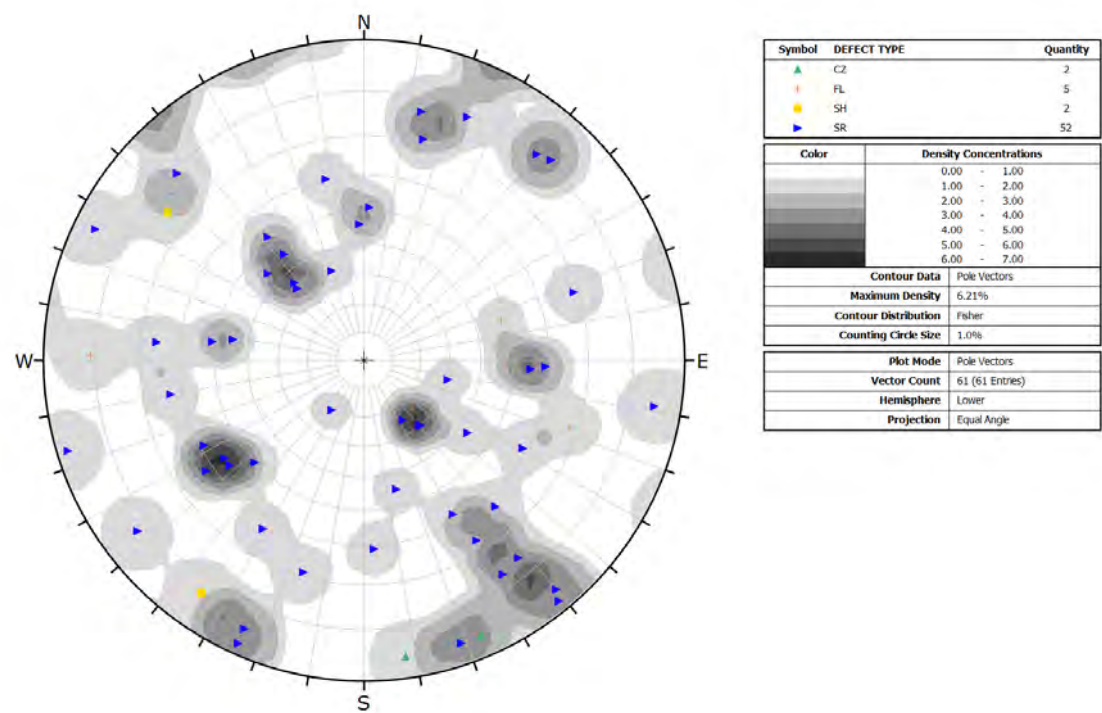
Bedding poles



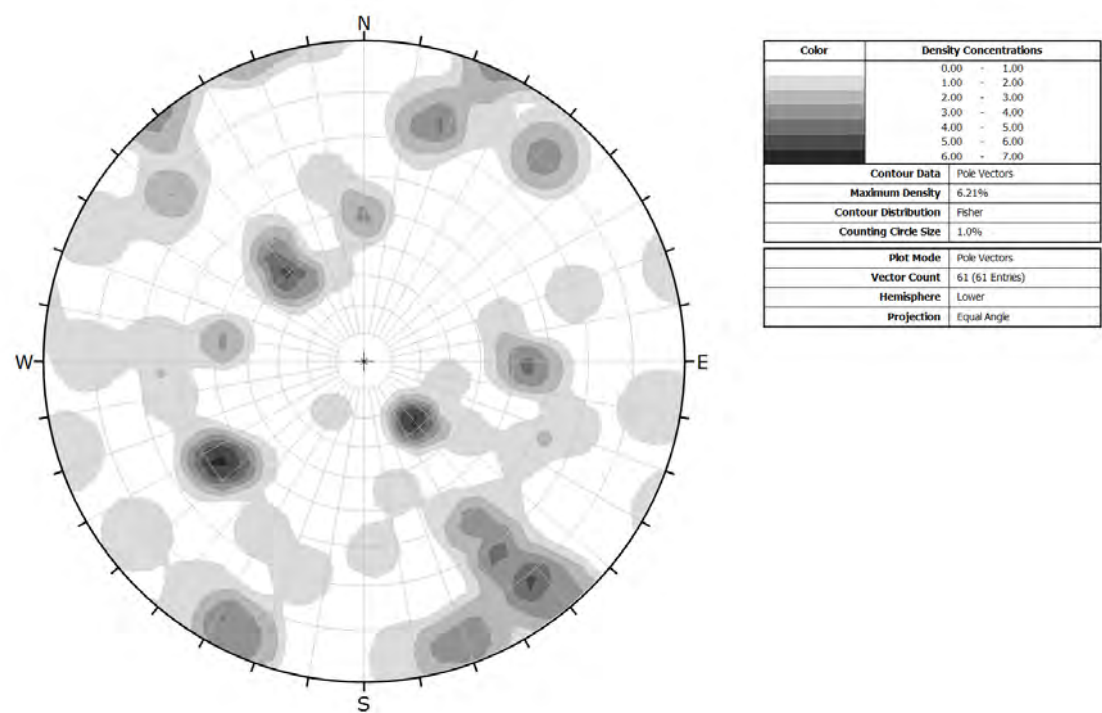
Contour diagram of bedding clusters



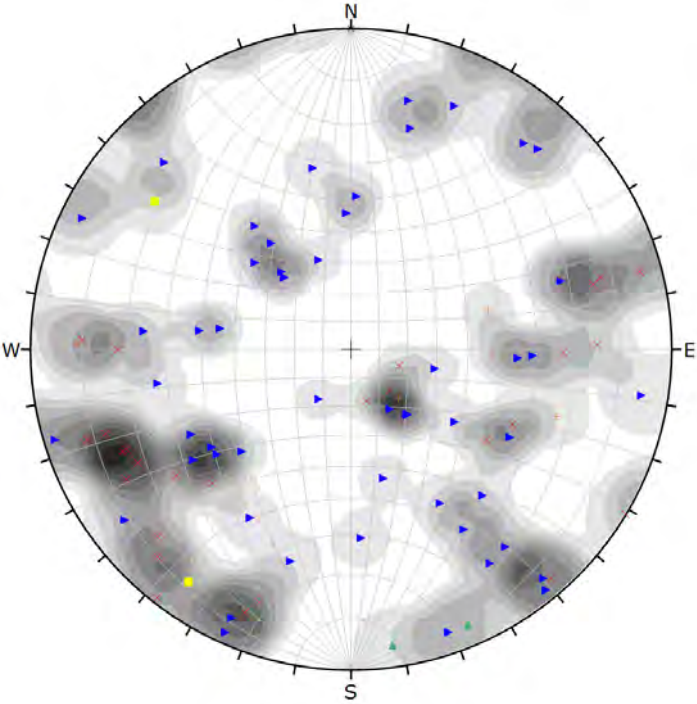
Shearing poles



Contour diagram of shearing and faulting clusters



All defects poles



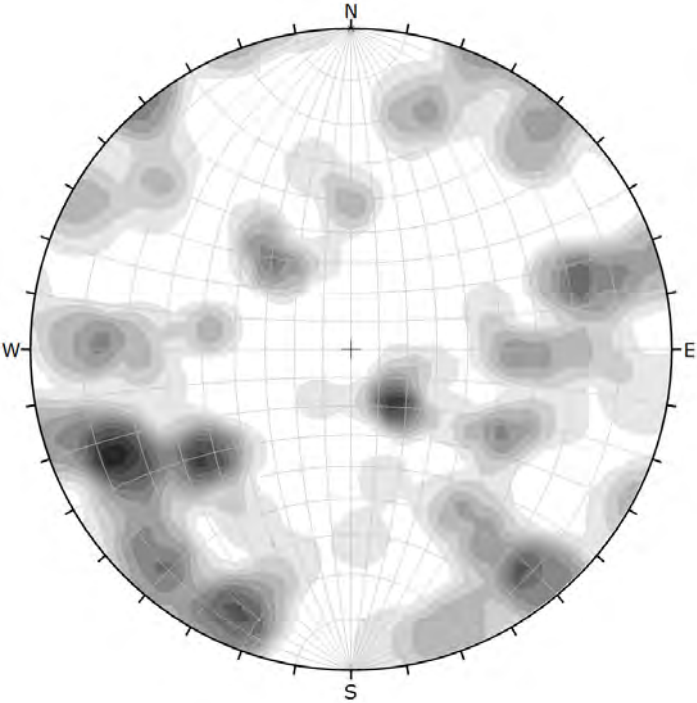
Symbol	DEFECT TYPE	Quantity
x	BSH	28
▲	CZ	2
■	FL	5
■	SH	2
▲	SR	52

Color	Density Concentrations
	0.00 - 0.60
	0.60 - 1.20
	1.20 - 1.80
	1.80 - 2.40
	2.40 - 3.00
	3.00 - 3.60
	3.60 - 4.20
	4.20 - 4.80
	4.80 - 5.40
	5.40 - 6.00

Contour Data	Pole Vectors
Maximum Density	5.88%
Contour Distribution	Fisher
Counting Circle Size	1.0%

Plot Mode	Pole Vectors
Vector Count	89 (89 Entries)
Hemisphere	Lower
Projection	Equal Angle

Contour diagram of all defects cluster



Color	Density Concentrations
	0.00 - 0.60
	0.60 - 1.20
	1.20 - 1.80
	1.80 - 2.40
	2.40 - 3.00
	3.00 - 3.60
	3.60 - 4.20
	4.20 - 4.80
	4.80 - 5.40
	5.40 - 6.00

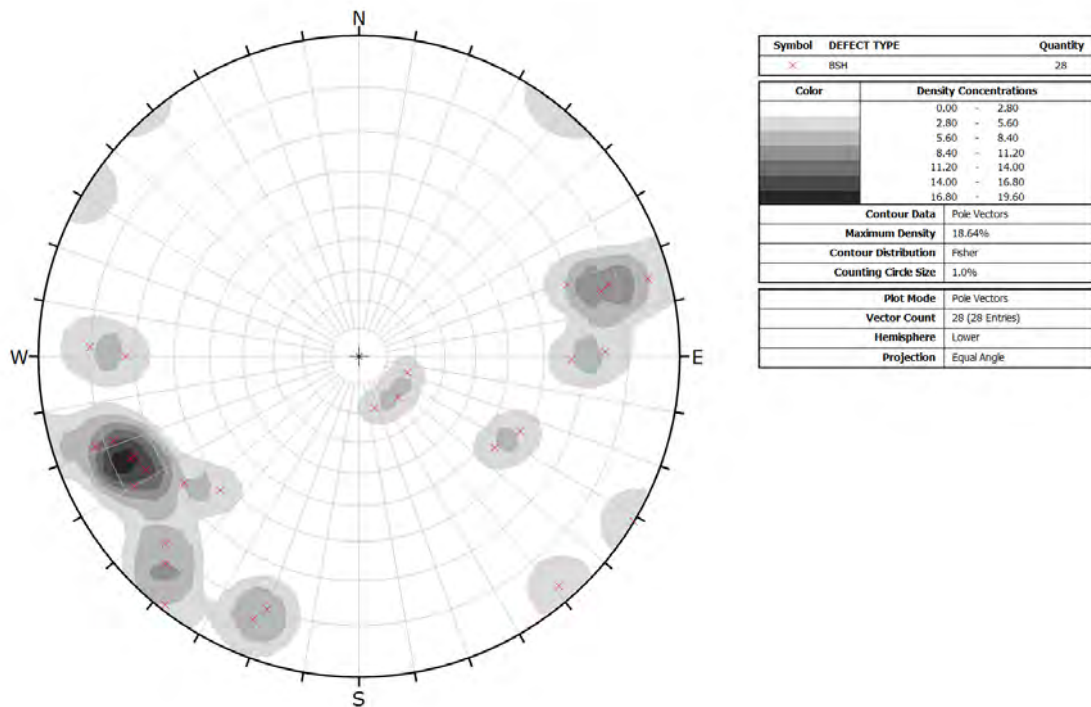
Contour Data	Pole Vectors
Maximum Density	5.88%
Contour Distribution	Fisher
Counting Circle Size	1.0%

Plot Mode	Pole Vectors
Vector Count	89 (89 Entries)
Hemisphere	Lower
Projection	Equal Angle

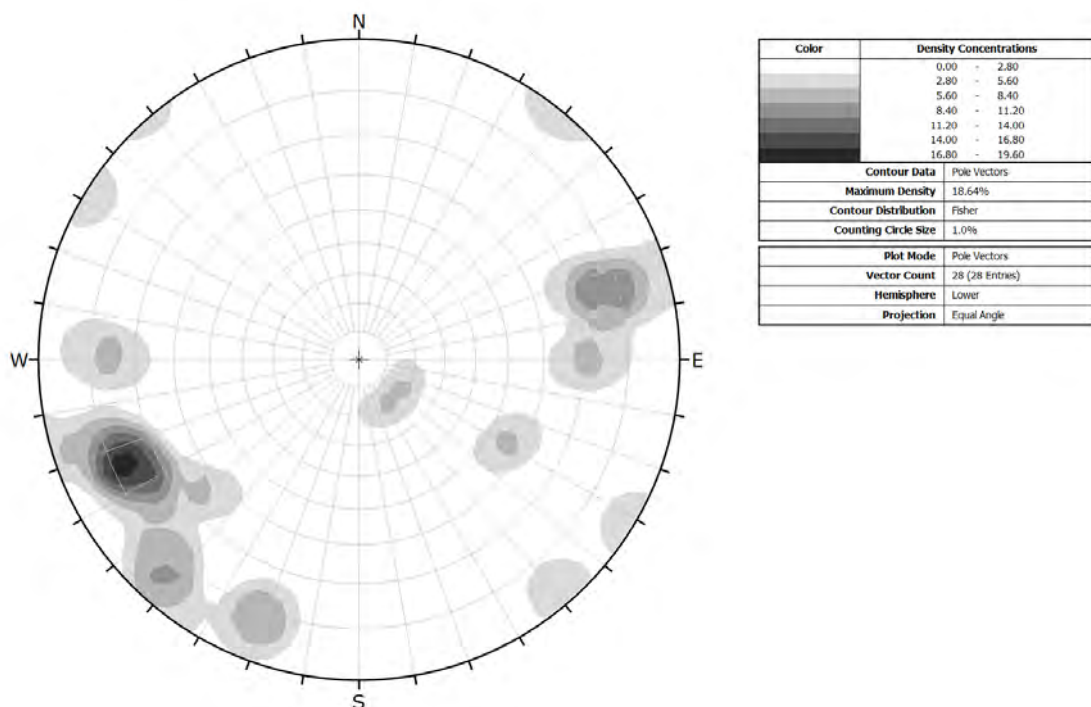
D.6 Filtered Stereonet Analysis

Stereonet from D.5 assessed for “noise”. The following only displays the poles of the continuous defects in Horokiwi Quarry.

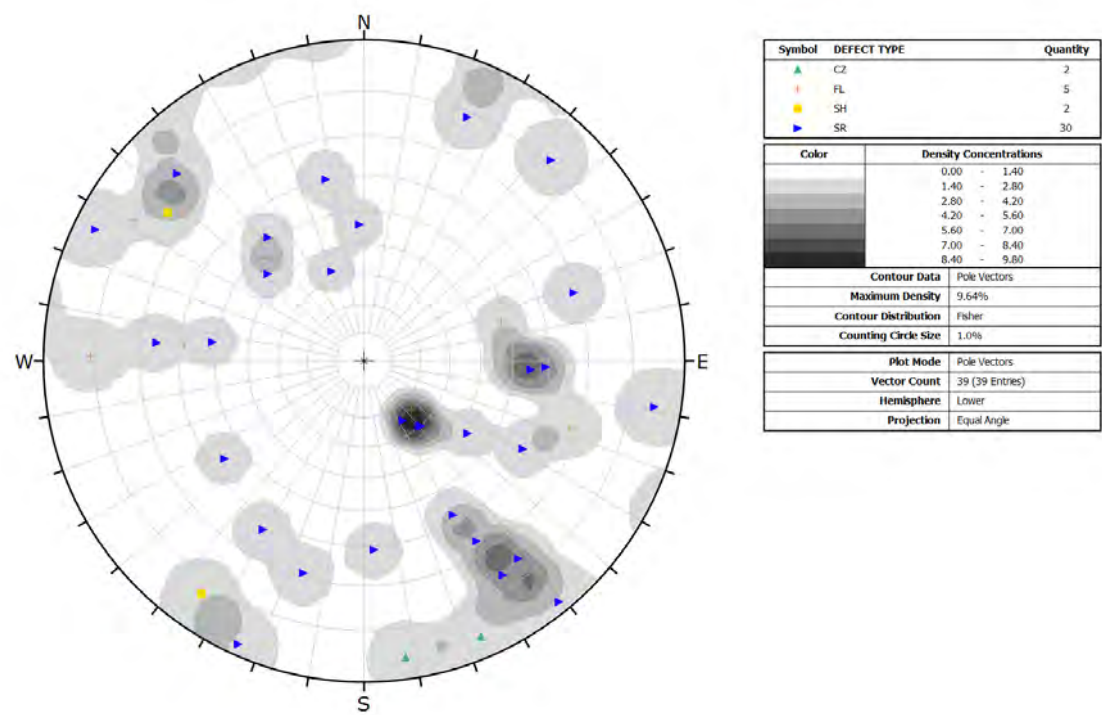
Bedding poles



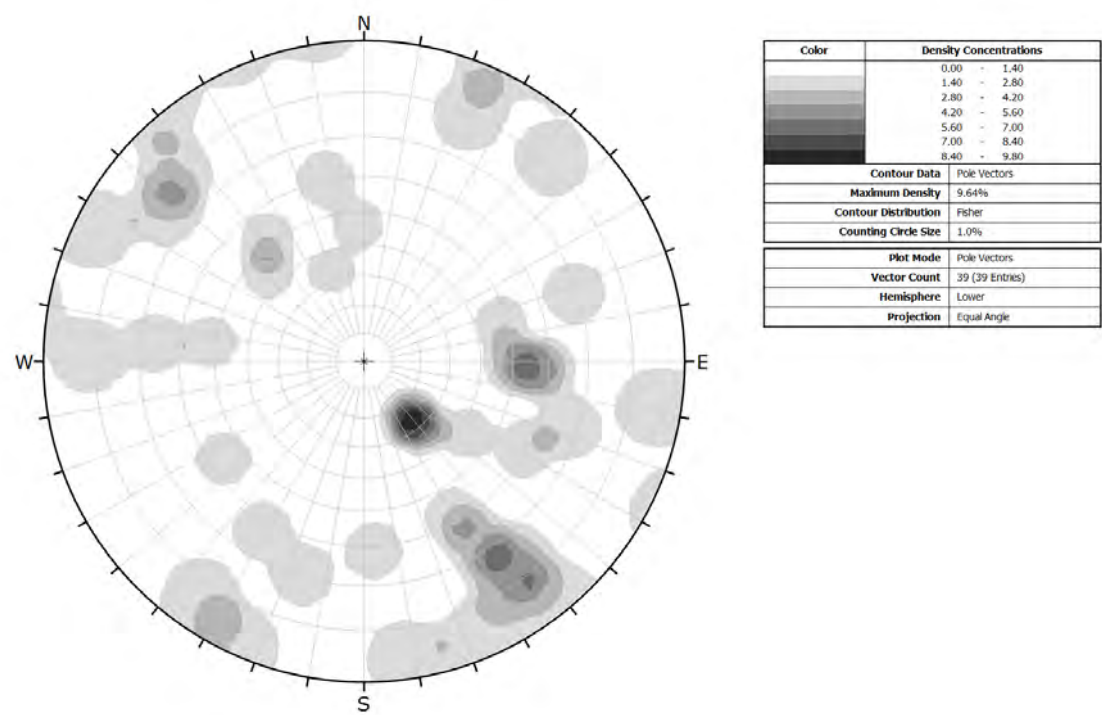
Contour diagram of bedding clusters



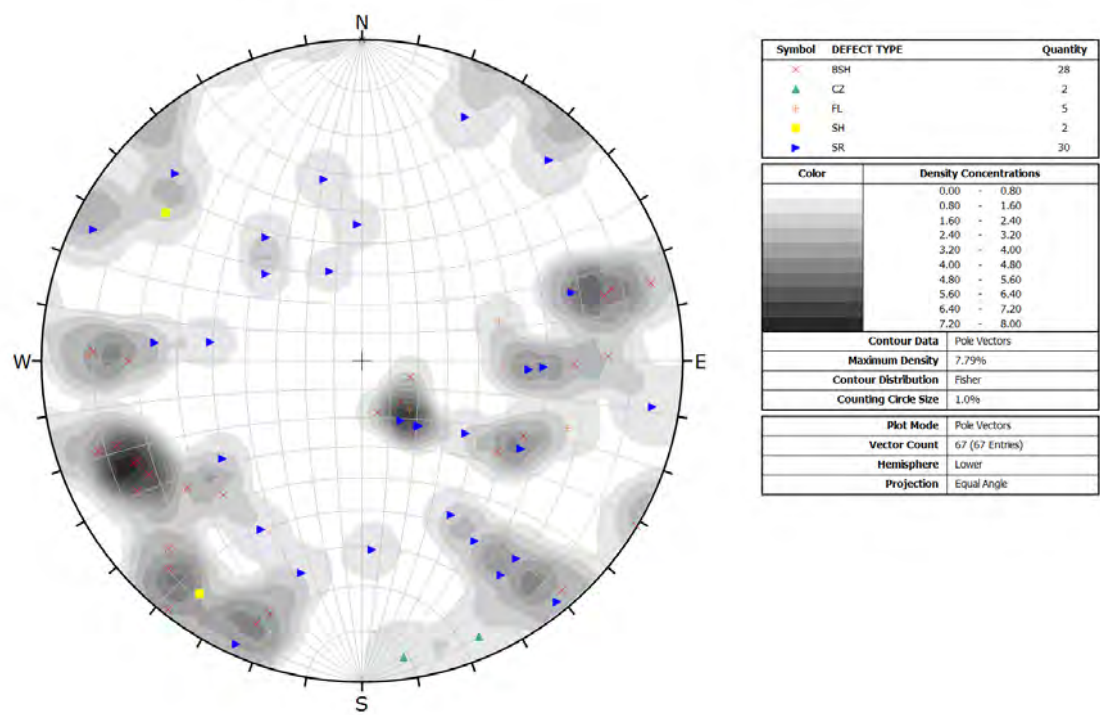
Shearing poles



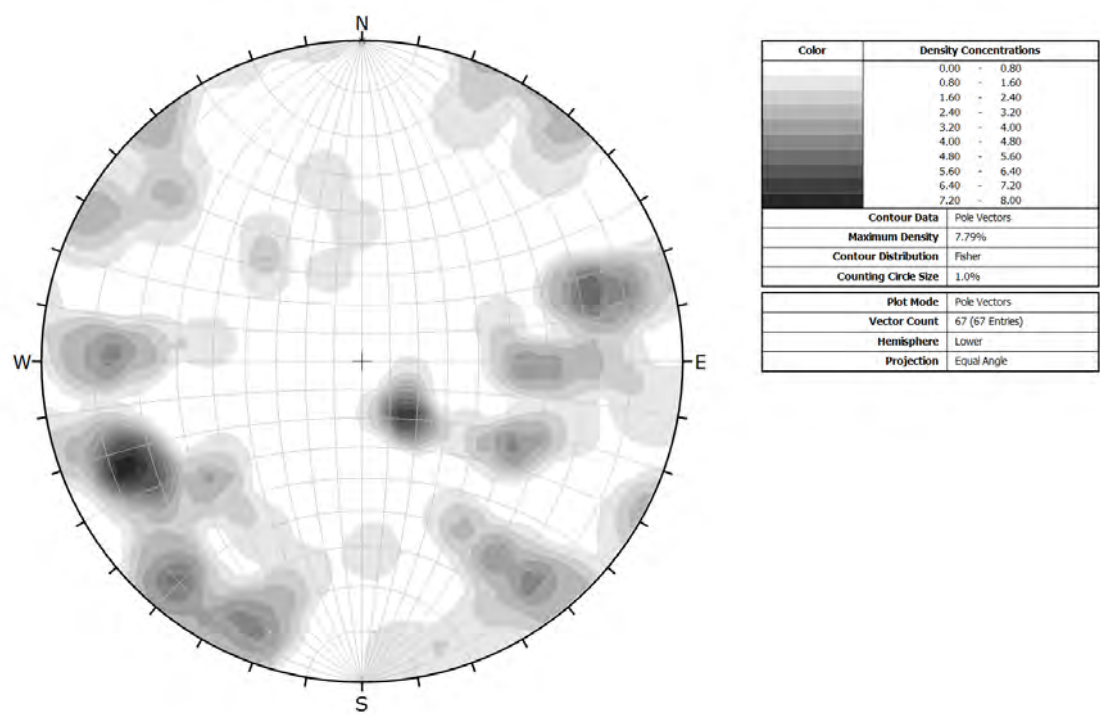
Contour diagram of shearing and faulting clusters



All defects poles



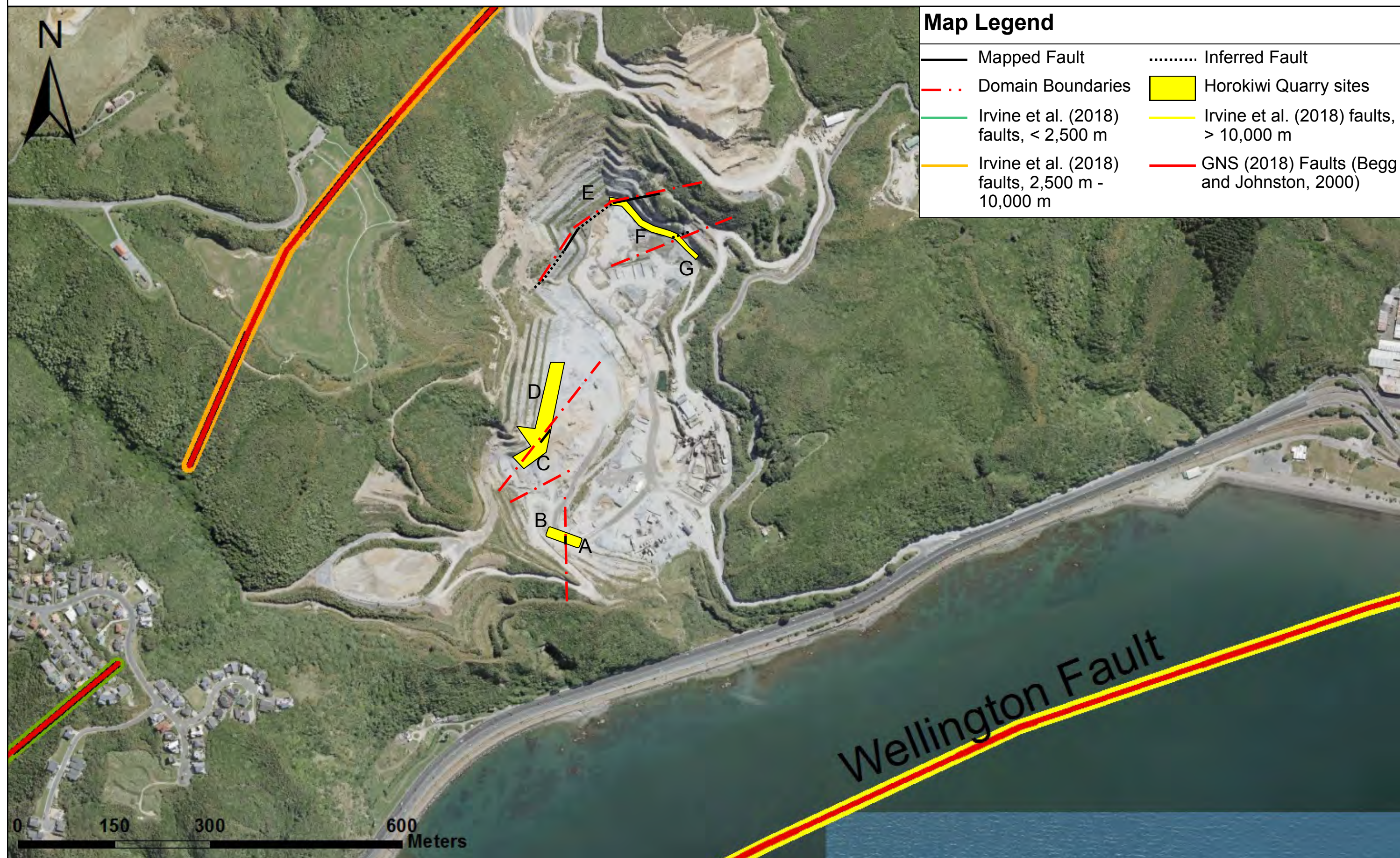
Contour diagram of all defects cluster



D.7 Horokiwi Quarry Structural Domains

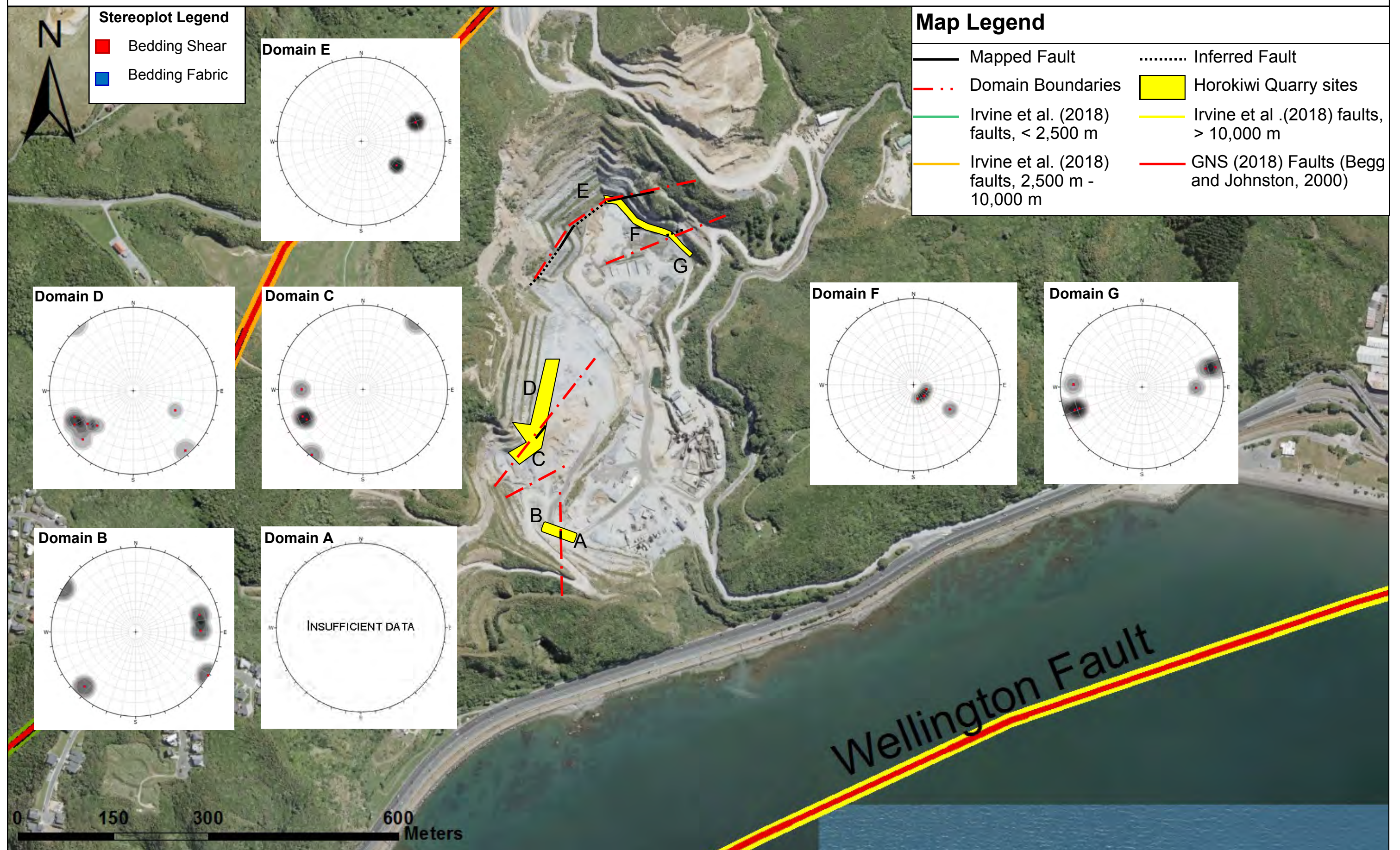
Figures are based on mapping observations and stereonet analysis. The figures represent a very detailed interpretation of the changes in defect orientation across the Horokiwi Quarry site.

D.7.1 Horokiwi Quarry - Domains



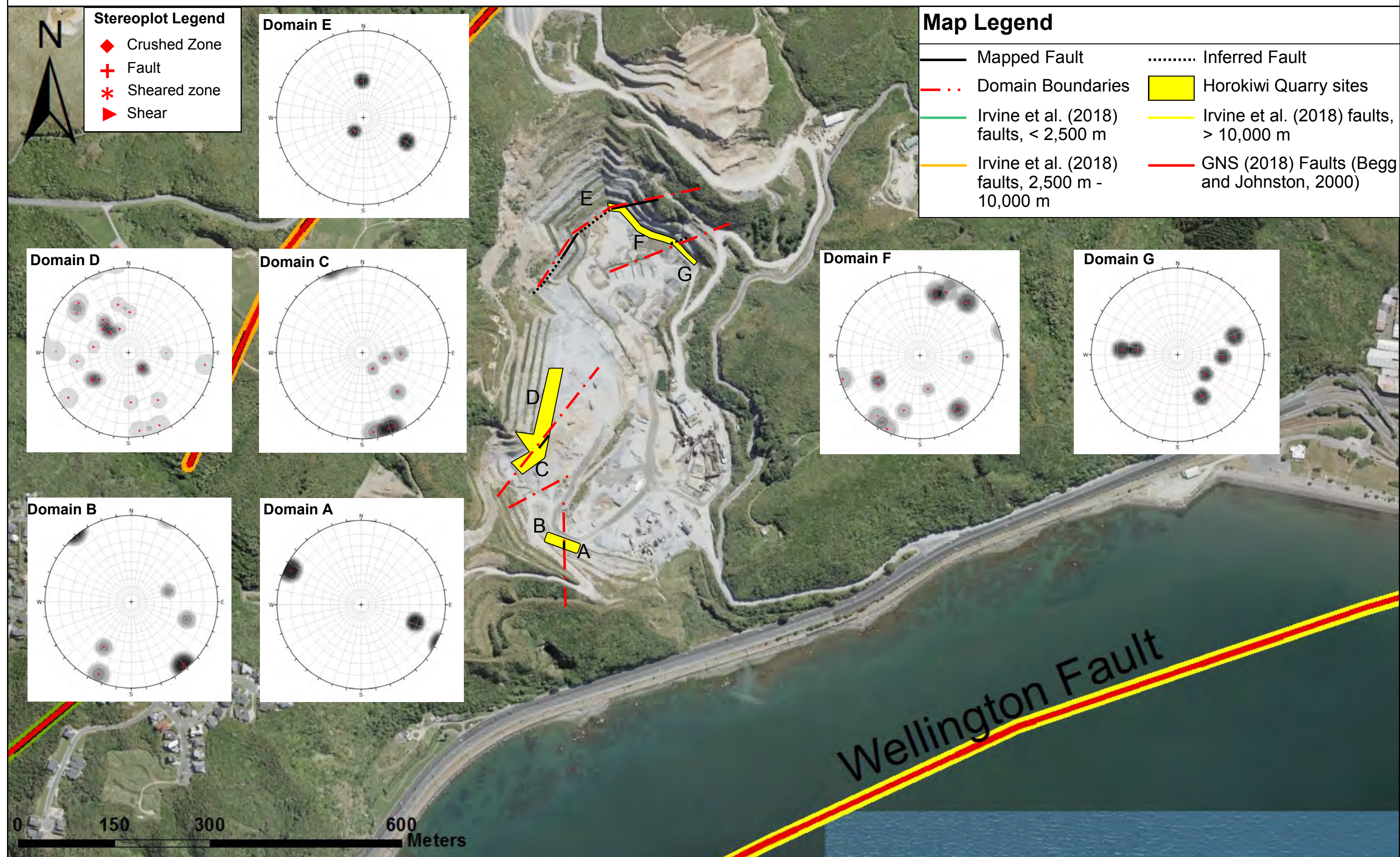
Imagery sourced: LINZ aerial imagery, 2016 (Captured by AAM NZ limited (2017))

D.7.2 Horokiwi Quarry Domains - Bedding



Imagery sourced: LINZ aerial imagery, 2016 (Captured by AAM NZ limited (2017))

D.7.3 Horokiwi Quarry Domains - Shearing



Imagery sourced: LINZ aerial imagery, 2016 (Captured by AAM NZ limited (2017))

D.8 Horokiwi Quarry Engineering Geological Model

Engineering geological model based on all available data. The model provides a summary of the rock mass and defect condition within the Horokiwi Quarry study site. Defect orientation and regional structural controls are also included.

D.8: Engineering Geological Model of Horokiwi Quarry

Key :
◆ BG ▲ CZ ▼ JN ► SR
✗ BSH + FL ■ SH

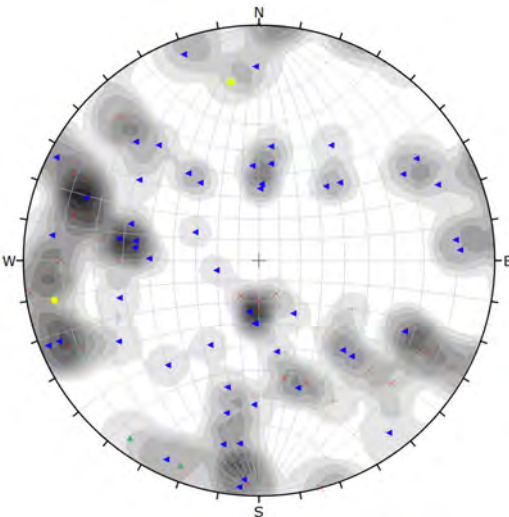


Figure 1: Stereonet of all the defect types and their orientation.

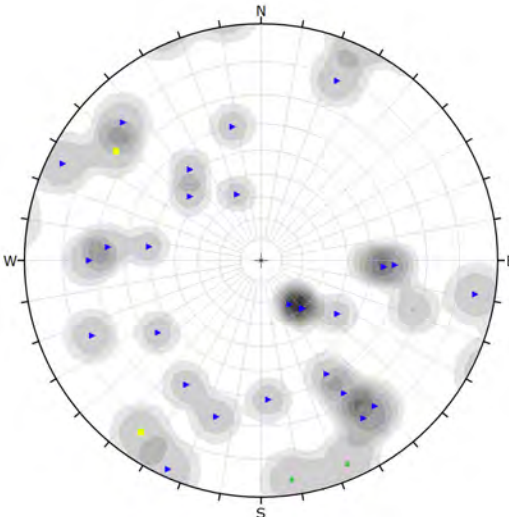


Figure 2: Stereonet of shearing in bench long defects

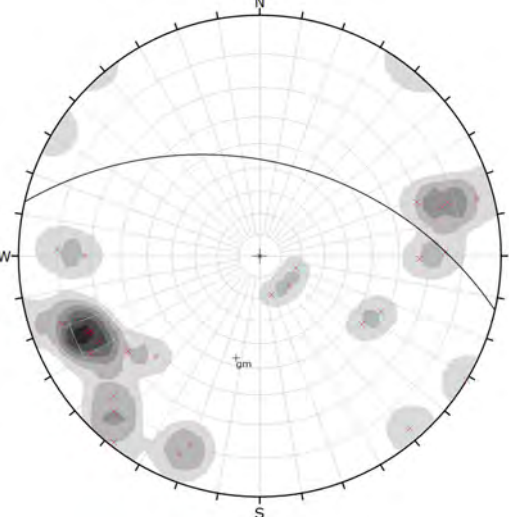


Figure 3: Stereonet of bedding.

Key:
— Mapped faults
..... Weathering profile

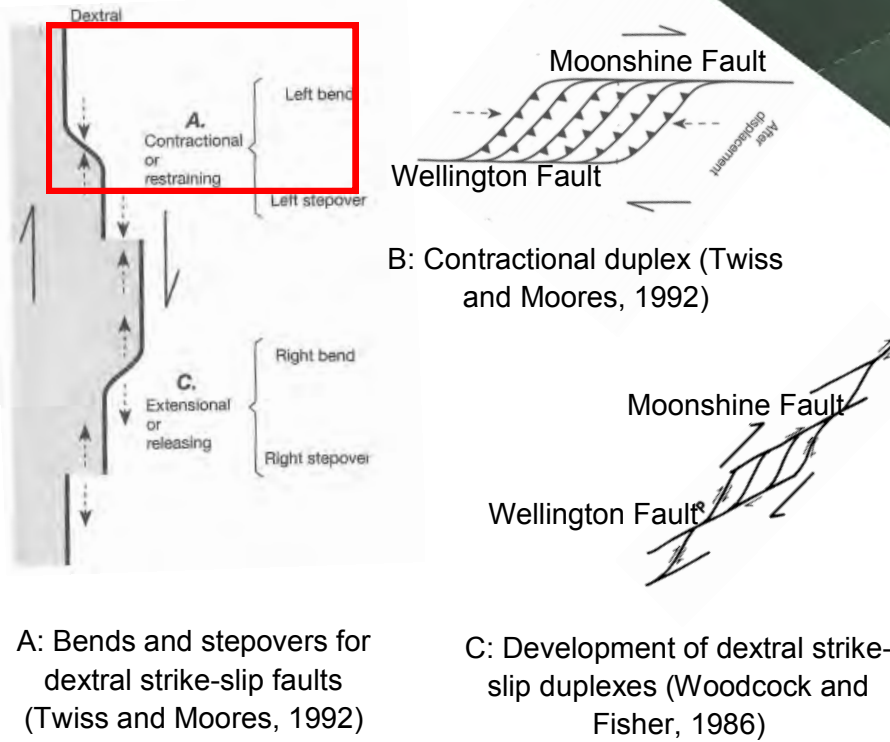
Rock mass structure in Horokiwi Quarry is primarily controlled by the Moonshine and Wellington Faults. Cross faulting links these major faults and are likely accommodating and transferring the regional tectonic stresses.

Elastic strain is thought to be accommodated on the cross faults due to the converging major faults. The result is multiple fault bounded blocks which are thought to rotate as a means of accommodating this strain.

The close proximity of the quarry to the Wellington Fault causes the original rock mass to be heavily sheared and faulted.

Fault disturbed rock due to close proximity of the Wellington Fault

Conceptual Models:



A: Bends and stepovers for dextral strike-slip faults (Twiss and Moores, 1992)

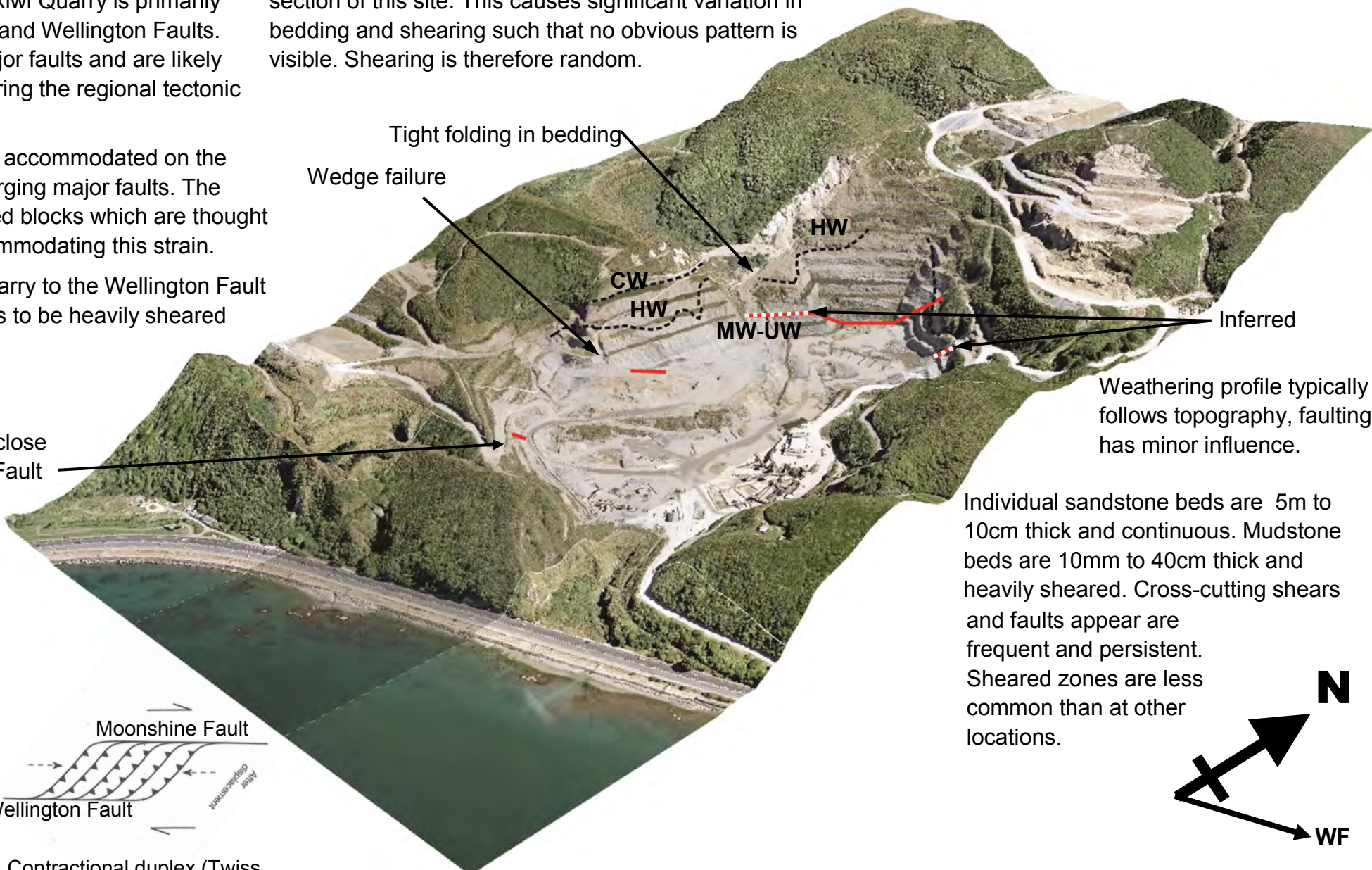
B: Contractual duplex (Twiss and Moores, 1992)

C: Development of dextral strike-slip duplexes (Woodcock and Fisher, 1986)

Bedding is dominantly sub-vertical to steeply inclined. There is variation in the bedding dip angle due to faulting however bedding is typically north-south striking.

Truncated fault blocks are well displayed in the Northern section of this site. This causes significant variation in bedding and shearing such that no obvious pattern is visible. Shearing is therefore random.

The Wellington Fault (WF) is located approximately less than 1.5 km away, with fault motion predominantly dextral strike-slip. The general trend of the fault is 045°.



Weathering profile typically follows topography, faulting has minor influence.

Individual sandstone beds are 5m to 10cm thick and continuous. Mudstone beds are 10mm to 40cm thick and heavily sheared. Cross-cutting shears and faults appear are frequent and persistent. Sheared zones are less common than at other locations.

<div><div><div>MUD : SAND</div><div>30: 60</div></div></div>	<div><div>Sandstone: Slightly weathered, light grey SANDSTONE; Strong; 5 joint sets very closely to closely spaced, very narrow to tight [RAKAIA SUB- TERRANE Greywacke]</div><div>Mudstone: Moderately weathered, dark grey MUDSTONE; Moderately Strong [RAKAIA SUB-TERRANE Argillite]</div></div>
<div><div><div>Predominant Suneson lithofacies:</div><div>B</div></div></div>	

Scale 1:6,700 centimetres

087.51753507001400

Meters

APPENDIX E: OWHIRO BAY QUARRY

This site is right at the entrance to the South Coast in Wellington (Figure E.1). Located about 4 km southeast from the nearest active fault trace (Wellington Fault) this quarry is influenced the least when compared to all the other sites. While the condition of the rock mass is anticipated to be relatively better it is likely that it will have some degree of shearing. Geological maps also show a series of north-south trending faults extending from the south coast towards and terminating against the Wellington Fault. These faults are described as potential splays and could be active due to Late Quaternary displacement (Begg & Johnston 2000). The nearest of these north-south trending faults is the Happy Valley Fault located around a kilometre to the east. Another fault running parallel to the Happy Valley Fault dissects this study site. This fault is most likely inactive due to a lack of geomorphic expression. A total of 2 areas were mapped (Appendix E.2).

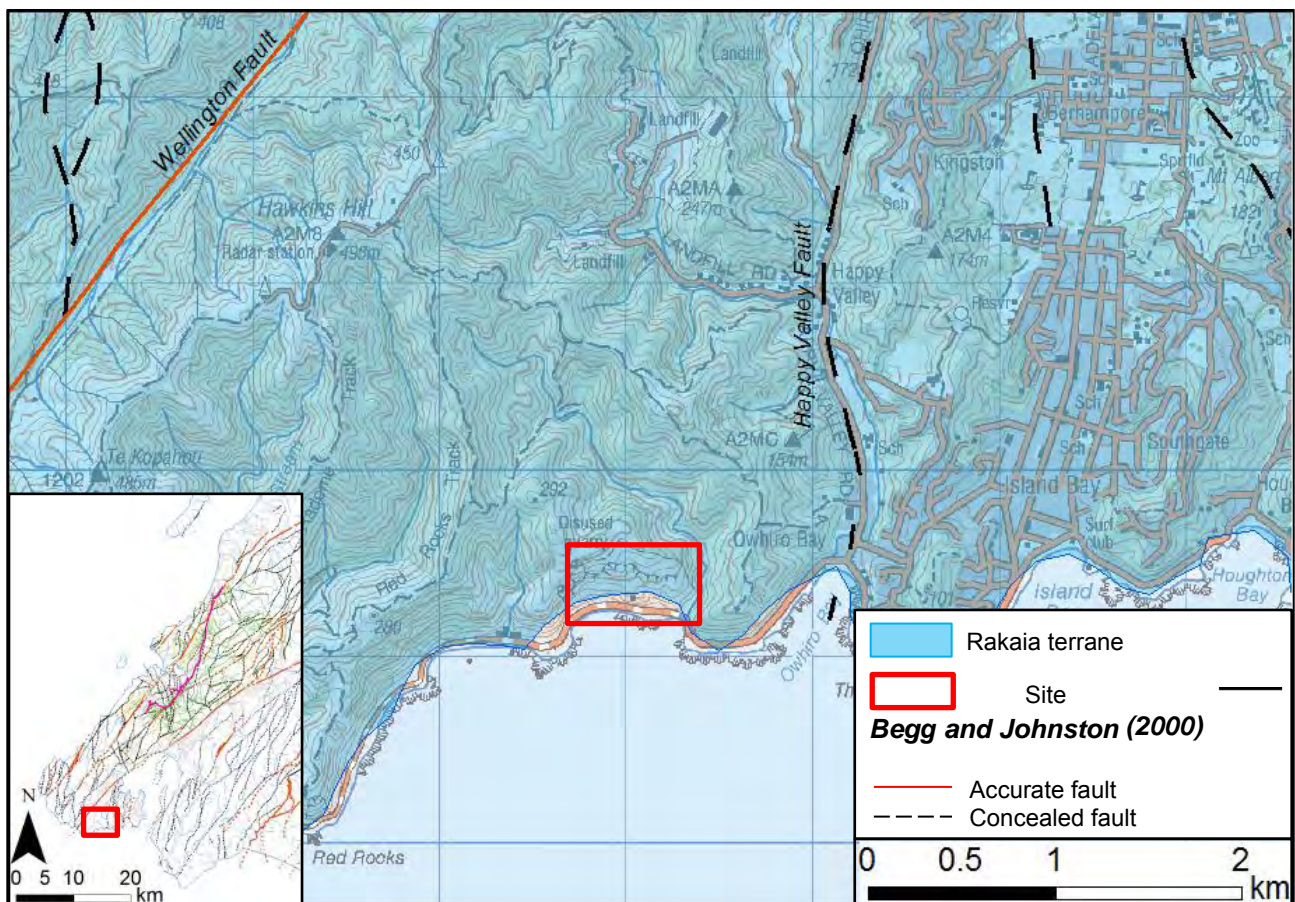


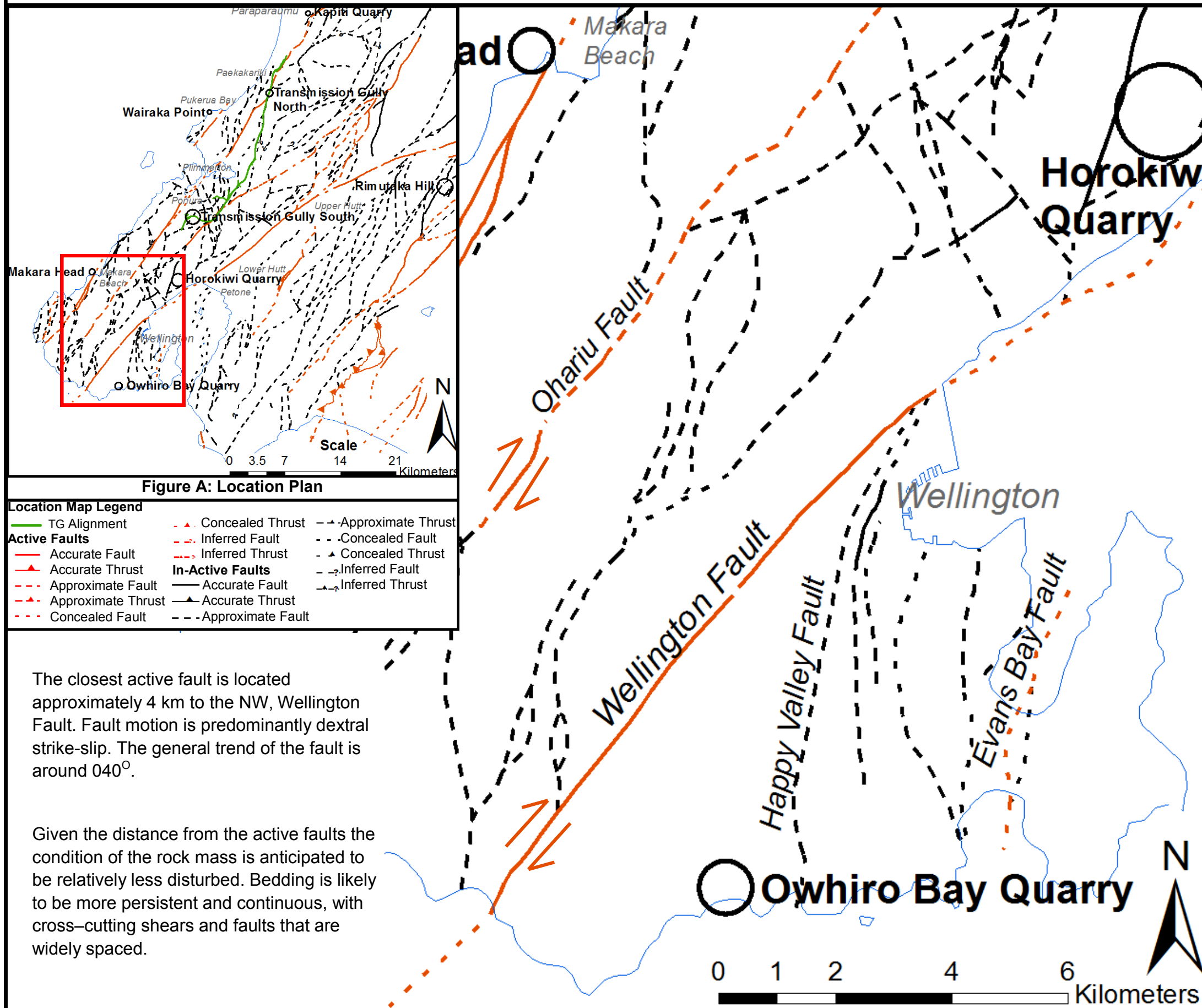
Figure E.1: Owhiro Bay Quarry site district scale map. Data sourced from GNS (2018) (Begg and Johnston, 2000). Refer to Section 1.4 for Irvine et al (2018) order classification Imagery from LINZ.

Results derived from conceptual models, raw mapping data, stereonet analysis and engineering geological models for the Owhiro Bay Quarry study site as displayed in the following sections.

E.1 Owhiro Bay Quarry Conceptual Structural Model

Preliminary structural assessment derived from GNS (2010) (Begg and Johnston, 2000) and Irvine et al. (2018) structural databases. Interpretations are based on information derived from past literature.

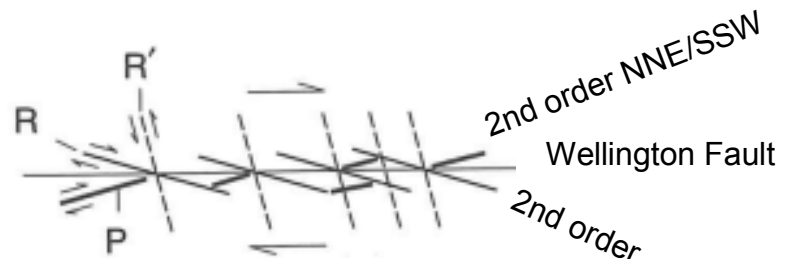
E.1 Conceptual Structural Model of Owhiro Bay Quarry



District Scale Legend:

- | | |
|---------------------------|---------------------------|
| ↗↘ Strike Slip | ↔↔ Releasing bend |
| ↖↗ Restraining bend | |
| Active Faults | |
| — Accurate Fault | — Accurate Fault |
| —▲ Accurate Thrust | —▲ Accurate Thrust |
| - - - Approximate Fault | - - - Approximate Fault |
| - - -▲ Approximate Thrust | - - -▲ Approximate Thrust |
| - - - Concealed Fault | - - - Concealed Fault |
| - - -▲ Concealed Thrust | - - -▲ Concealed Thrust |
| - - -? Inferred Fault | - - -? Inferred Fault |
| - - -▲? Inferred Thrust | - - -▲? Inferred Thrust |
| In-Active Faults | |
| — Accurate Fault | — Accurate Fault |
| —▲ Accurate Thrust | —▲ Accurate Thrust |
| - - - Approximate Fault | - - - Approximate Fault |
| - - -▲ Approximate Thrust | - - -▲ Approximate Thrust |
| - - - Concealed Fault | - - - Concealed Fault |
| - - -▲ Concealed Thrust | - - -▲ Concealed Thrust |
| - - -? Inferred Fault | - - -? Inferred Fault |
| - - -▲? Inferred Thrust | - - -▲? Inferred Thrust |

Conceptual Models:



C. Subsidiary R, R', and P shear fractures (Twiss and Moores, 1992)

Bedding and Shearing Predictions:

Bedding and shearing is anticipated to trend parallel to sub-parallel with the Happy Valley Fault (2nd order fault) (Irvine et al., 2018).

Figure A: Location Plan

- Location Map Legend**
- | | | |
|---------------------------|-------------------------|---------------------------|
| — TG Alignment | - - -▲ Concealed Thrust | - - -▲ Approximate Thrust |
| Active Faults | - - -? Inferred Fault | - - - Concealed Fault |
| — Accurate Fault | - - -▲ Inferred Thrust | - - -▲ Concealed Thrust |
| —▲ Accurate Thrust | In-Active Faults | - - -? Inferred Fault |
| - - - Approximate Fault | — Accurate Fault | - - -▲ Inferred Thrust |
| - - -▲ Approximate Thrust | —▲ Accurate Thrust | - - - Concealed Fault |
| - - - Concealed Fault | - - - Approximate Fault | |

The closest active fault is located approximately 4 km to the NW, Wellington Fault. Fault motion is predominantly dextral strike-slip. The general trend of the fault is around 040°.


Given the distance from the active faults the condition of the rock mass is anticipated to be relatively less disturbed. Bedding is likely to be more persistent and continuous, with cross-cutting shears and faults that are widely spaced.

Figure B: District scale structures around Owhiro Bay Quarry. Faults are sourced from GNS (2010) (Begg and Johnston, 2000)

E.2 Owhiro Bay Quarry Outcrop Location Map

Displays the location of the mapped outcrops within the Owhiro Bay Quarry study site.

E.2 Owhiro Bay Quarry

 Owhiro Bay Quarry Sites



E.3 Owhiro Bay Quarry Raw Mapping Data

Structural data collected from the Owhiro Bay Quarry site. Where data is missing or blanked out information was either not able to be reached or was not relevant to the rock mass or defect condition (e.g. Planar defects did not contain a wavelength as outlined in Chapter 3).

E.3.1 Owhiro Bay Quarry - Raw data

Owhiro Bay Quarry																						
ID	Defect Type	Dip	Dip Direction (Mag)	Dip Direction (True)	Structural Domain	Roughness	Thickness		% of rock fragments	Continuity	Persistence	Shape			Persistence - Trace Length (m)	Spacing (m)	Infill (Support (Breccia type (%Clasts), Angularity, weathering, strength, coating; colour, grainsize, strength, plasticity)) precipitation	Saturation	Latitude	Longitude	Comments	
							Term	Width (mm)				Inter-limb angle (degrees)	Wavelength (m)	Term								
1	BG	58	286	264	A	Ro2	Moderately Narrow	~10mm	~95%	1	R	~170°	Gentle	~2.5m	Wavy	~7m	~1m	Clast supported (Crackle (~95%) angular, HW, Weak, Veneer; Light brown grey, silty Sand, Very soft, LP) White angular clasts	Damp	-41.3459	174.7451	Cross cuts SR2b
2	SR	58	279	257	A	Ro3	Moderately Wide	~50mm	~95%	1	R	~170°	Gentle	~2m	Wavy	~1.6m	~2m	Clast supported (Crackle (~95%) angular, HW, Weak and strong (bigger blocks stronger), Coating; Light brown grey, silty Sand with clay seams, Very soft, LP-NP) No precipitation	Damp	-41.3459	174.7452	Cross cuts SR2b, 3 and 4b
2b	SR	29	6	344	A	Ro3	Very Narrow	~0-1mm	~99%	0	O	~150°	Gentle	~10m	Curved	~2.5m		Clast supported (Rock (~99%) angular, MW, Weak and strong (bigger blocks stronger), Coating; Light brown grey, silty Sand with clay seams, Very soft, LP-NP) No Precipitation	Damp	-41.3459	174.7452	Terminates against CZ4 and cross cuts SR1 and 2
3	SR	75	169	147	A	Ro3	Very Narrow	~0-1mm	~99%	1	R	~160°	Gentle	~6m	Wavy	~2.2m	~2.5m	Clast supported (Rock (~99%) angular, MW, Weak and strong (bigger blocks stronger), Coating; Light brown grey, silty Sand with clay seams, Very soft, LP-NP) No precipitation	Damp	-41.346	174.7452	Terminates against SR2b, cross cuts SR4b and SR2
4	CZ	52	250	228	A	Ro3	Very Wide	~1000mm narrows to 300mm	~80%	1	R	~170°	Gentle	~5m	Wavy	~8.8m		Clast supported (Crackle(~80%) angular, HW to CW, Moderately strong (bigger blocks) to very weak, Coating; Light brown blueish grey, silty Sand with clay seams, Very soft, MP) White angular clasts	Damp	-41.3459	174.7452	SR4b cross cuts
4b	SR	36	66	44	A	Ro3	Moderately Narrow	~10mm	~10%	1	D	~150°	Gentle	~1m	Wavy	~2.2m		Matrix supported (Soil (~10%) angular, MW, Moderately strong to strong, Coating; Light brown blueish grey, sandy Clay, Very soft, NP) White sand sized precipitation	Damp	-41.3459	174.7452	Cross cuts SR3, 2 and CZ4
5	SR	75	200	178	A	Ro2	Moderately Narrow	~10mm	~95%	0	R	~180°	Gentle		Planar	~2m	~2.5m	Clast supported (Crackle (~95%) angular, MW, Strong, Veneer; Light brown blueish grey, sandy Clay, Very soft, NP) White angular clasts	Damp	-41.3459	174.7453	Terminates against bedding
6	SR	81	168	146	A	Ro3	Wide	~100mm	~95%	1	D	~160°	Gentle	~3m	Wavy	~2.25m		Clast supported (Crackle (~95%) angular, MW, Strong (Greywacke) and weak (Argillite), Veneer; Light brown blueish grey, sandy Clay, Very soft, NP) White angular clasts	Damp	-41.3459	174.7453	Cross cuts bedding and CR5
7	BSH	79	231	209	A	Ro3	Wide	~150mm	~95%	0	O	~140°	Gentle	~1.5m	Wavy	~2.25m		Clast supported (Crackle (~95%) angular, HW, Weak (Argillite), Coating; Light brown blueish grey, silty Sand with traces of clay, Very soft, LP-NP) White angular clasts	Damp	-41.3459	174.7453	
7b	JN	75	198	176	A	Ro2	Tight	~0mm		2	D	~180°	Gentle		Planar	~0.6m	~0.3m			-41.3459	174.7453	
8	SH	44	205	183	A	Ro2	Very Wide	~500mm	~95%	0	O	~160°	Gentle		Curved	~2m	~3m	Clast supported (Crackle (~95%) angular, MW-HW, Strong to moderately strong, Veneer; Light brown blueish grey, silty Sand with traces of clay, Very soft, LP-NP) White angular clasts	Damp	-41.3459	174.7454	
9	SR	62	120	98	A	Ro2	Very Wide	~500mm	~95%	0	O	~150°	Gentle	~0.8m	Wavy	~1.2m		Clast supported (Crackle (~95%) angular, MW-HW, Strong, Veneer; Light brown blueish grey, silty Sand with traces of clay, Very soft, LP-NP) White angular clasts	Damp	-41.3459	174.7454	
10b	SR	79	314	292	A	Ro3	Wide	~200mm		1	R	~180°	Gentle		Planar	~1m		Clast supported (Crackle (~95%) angular, HW, Weak, Coating; Light brown blueish grey, silty Sand with traces of clay, Very soft, LP-NP) White angular clasts	Damp	-41.346	174.7455	
10	JN	36	185	163	A	Ro2	Tight	0mm		2	D	~180°	Gentle		Planar	~0.5m	~0.6m			-41.3459	174.7455	
11	JN	71	120	98	A	Ro3	Tight	0mm		2	D	~180°	Gentle		Planar	~0.5m	~0.5m			-41.346	174.7455	
12	BSH	75	248	226	A	Ro2	Wide	~100mm	~80%	0	C	~170°	Gentle	~8m	Wavy	~1.5m	~1m	Clast supported (Crackle (~80%) angular, HW, Weak, Coating; Light brown blueish grey, silty Sand with traces of clay, Very soft, LP-NP) White angular clasts	Damp	-41.346	174.7456	
12b	BSH	81	239	217	A	Ro2	Wide	~100mm	~80%	0	C	~160°	Gentle	~6m	Wavy	~1.6m	~1m	Clast supported (Crackle (~80%) angular, CW, Weak, Coating; Light brown blueish grey, silty Sand with traces of clay, Very stiff to Hard, LP-NP) White angular clasts	Damp	-41.346	174.7456	
13	SR	30	87	65	A	Ro2	Very Narrow	~1mm	~80%	0	O	~140°	Gentle	~0.6m to 1.5m	Irregular	~3.5m		Clast supported (Crackle (~80%) angular, HW-CW, Moderately strong to weak, Coating; Light brown blueish grey, Soft, LP) No precipitation visible	Damp	-41.346	174.7457	Terminates against BSH12b, offset by SR12b (~10cm)

14	JN	53	154	132	A		Tight	~0mm		2	D	~180°	Gentle		Planar	~0.8m	~0.4m	Clast supported (Crackle (~80%) angular, HW-CW, Strong (bigger Argillite blocks) and weak, Coating; Light brown blueish grey, silty Sand with traces of clay, Soft, LP) White angular seam like clasts		-41.3461	174.7457	
15	SR	63	260	238	A	Ro3	Wide	~80mm	~80%	0	O	~120°	Open	~15m	Wavy	~3.5m		Clast supported (Crackle (~90%) angular, HW, Moderately strong, Coating; Light brown blueish grey, silty Sand with traces of clay, Soft, LP) White angular randomly spaced gravel sized clasts	Damp	-41.3461	174.7457	
16	BSH	78	226	204	A	Ro3	Wide	~80mm	~90%	1	D	~140°	Gentle	~1.5m	Wavy	~3m	~1.5m	Clast supported (Crackle (~80%) angular, CW, Very weak, Coating; Light white blueish grey, Soft, NP) white angular precipitation	Damp	-41.3461	174.7458	Cross cuts SR19
18b	SR	48	339	317	A	Ro2	Moderately Narrow	~9mm	~80%	0	C	~160°	Gentle	~3m	Wavy	~5m		Matrix supported (Soil (~10%) angular, CW, Very weak, Coating; Light white blueish grey, silty Sand with traces of clay, Soft, NP) No precipitation	Damp	-41.3461	174.7458	Cross cuts BSH16, SR17, 17a, 19 and 19b
19b	SR	88	76	54	A	Ro2	Narrow	~5mm	~10%	2	D	~150°	Gentle	~4m	Wavy	~2m	~1m	Clast supported (Crackle (~90%) angular, HW, Moderately strong, Coating; Light brown blueish grey, silty Sand with traces of clay, Soft, LP) No precipitation	Damp	-41.3461	174.7459	Terminates between BSH16's and cross cuts SR18b
16	BSH	76	235	213	A	Ro3	Wide	~80mm	~90%	1	D	~140°	Gentle	~1.5m	Wavy	~3m	~1.5m	Clast supported (Crackle (~80%) angular, HW, Weak (Argillite) to moderately strong (Greywacke), Coating; Light white blueish grey, silty Sand with traces of clay, Soft, LP) white angular gravel clasts	Damp	-41.3461	174.7459	Cross cuts SR19, 18 and 18b. Terminates against SR17
17a	SR	77	256	234	A	Ro4	Wide	~150mm	~80%	0	R	~140°	Gentle	~8m	Wavy	~4m		Clast supported (Crackle (~80%) angular, HW, Moderately strong (Greywacke) and Weak (Argillite), Coating; Light blueish grey, silty Clay with trace of sand, Soft, MP) white angular seam like clasts	Damp	-41.3462	174.7458	Cross cuts 17b, a failure plane for image IMG_20180323_124756, rock topple. Also cross cuts SR19, BSH18, SR18b
17b	FL	83	93	71	A	Ro3	Wide	~200mm	~80%	0	C	~170°	Gentle	~10m	Wavy	~4m		Matrix supported (Soil (~10%) angular, CW, Very Weak, Coating; Light white blueish grey, silty Sand with trace of clay, Soft, NP) white sand size	Damp	-41.3462	174.7459	Cross cuts 17a, a failure plane for image IMG_20180323_124756, rock topple
19	SR	84	164	142	B	Ro2	Narrow	~5mm	~10%	0	D	~170°	Gentle	~15m	Wavy	~7m	~1m	Clast supported (Crackle (~80%) angular, HW, Weak (Argillite) and Moderately strong (Greywacke), Coating; Light blueish grey, silty Clay with trace of sand, Soft, MP) white sand size	Damp		174.7036	Cross cuts BSH16, SR17's, SR18b and SR18
19	SR	83	164	142	B	Ro2	Narrow	~5mm	~10%	0	D	~170°	Gentle	~15m	Wavy	~7m	~1m	Clast supported (Crackle (~80%) angular, HW, Weak (Argillite) and Moderately strong (Greywacke), Coating; Light blueish grey, silty Clay with trace of sand, Soft, MP) white sand size	Damp	-41.3462	174.7459	Cross cuts BSH16, SR17's, SR18b and SR18
19b	SR	83	165	143	B	Ro3	Wide	~200mm	~80%	1	D	~170°	Gentle	~15m	Wavy	~2m	~1m	Clast supported (Crackle (~95%) angular, MW, Weak, Coating; Light grey, silty Clay with trace of sand, Soft, MP) white angular clasts	Damp	-41.3462	174.7459	Terminates between BSH16's and cross cuts SR18b
20	SR	88	204	182	B	Ro2	Moderately Narrow	~10mm	~95%	0	O	~140°	Gentle	~0.7m	Wavy	~6m		Clast supported (Crackle (~95%) angular, MW, Moderately strong, Coating; Light grey, silty Clay with trace of sand, Soft, NP) no precipitation	Damp	-41.3462	174.746	Terminates against FL21 and cross cuts BSH18 and SR18
18	SR	52	285	263	B	Ro3	Very Narrow to Moderately Narrow	~1-10mm	~95%	1	O		Gentle		Stepped	~6m	~0.8m	Clast supported (Crackle (~90%) angular, HW, Moderately strong, Coating; Light grey, silty Clay with trace of sand, Stiff, NP) White elongated gravel angular seams	Minor seepage	-41.3462	174.746	Terminates against FL21 and cross cuts SR19 and 20
18	BSH	49	279	257	B	Ro3	Wide	~200mm	~90%	1	D	~170°	Gentle	~1.5m	Wavy	~7m	~0.6m	Clast supported (Crackle (~85%) angular, HW, Weak, Coating; Light grey, silty Clay with trace of sand, Stiff, MP) white sand sized	Damp	-41.3463	174.7461	Offset by FL21
21	FL	72	74	52	B	Ro2	Wide	~150mm	~85%	0	C	~180°	Gentle		Planar	~15m		Clast supported (Crackle (~85%) angular, HW, Weak, Coating; Light brown grey, silty Sand with trace of clay, Stiff, LP) white gravel to sand sized angular clasts	Damp	-41.3462	174.7462	Continuous, cross cuts SR17. One of the controlling mechanisms for wedge failures on the top benches
21b	SR	87	178	156	B	Ro4-3	Very Wide	~500mm	~85%	1	D	~160°	Gentle	~1.5m	Wavy	~7m		Clast supported (Crackle (~85%) angular, HW, Weak, Coating; Light brown grey, silty Sand with trace of clay, Stiff, LP) white gravel to sand sized angular clasts	Damp	-41.3463	174.7462	Cross cuts SR28
21b	SR	88	170	148	B	Ro4-3	Very Wide	~500mm	~85%	1	D	~160°	Gentle	~1.5m	Wavy	~7m		Clast supported (Crackle (~95%) angular, HW, Moderately strong, Coating; Light brown grey, silty Sand with trace of clay, Soft, NP) No visible precipitation	Damp	-41.3463	174.7462	Cross cuts SR28
22	BSH	61	256	234	B	Ro2	Wide	~70mm	~95%	0	O	~170°	Gentle	~6m	Wavy	~14m	~1m	Clast supported (Crackle (~90%) angular, HW, Weak, Veneer; Light brown grey, silty Sand with trace of clay, Soft, NP) white angular gravel sized clasts	Damp	-41.3464	174.7462	Offset by FL21 cross cuts SR24 and 23
23	SR	85	178	156	B	Ro3	Wide	~150mm	~90%	1	D	~160°	Gentle	~1.2m	Irregular	~8m		Clast supported (Crackle (~90%) angular, MW, Strong, Veneer; Light brown grey, silty Sand with trace of clay, Soft, NP) White elongated gravel angular seam like clasts	Damp	-41.3463	174.7463	Cross cuts BSH22 and SR18
24	SR	82	139	117	B	Ro2	Wide	~150mm	~90%	0	C	~170°	Gentle	~2m	Wavy	~7m		Clast supported (Crackle (~90%) angular, MW, Moderately strong, Coating; Light brown grey, silty Sand with trace of clay, Soft, NP) White elongated gravel angular seam like clasts	Damp	-41.3464	174.7463	Cross cuts SR27 and 28
24	SR	83	150	128	C	Ro2	Wide	~150mm	~90%	0	C	~170°	Gentle	~2m	Wavy	~7m		Clast supported (Crackle (~90%) angular, MW, Moderately strong, Coating; Light brown grey, silty Sand with trace of clay, Soft, NP) White elongated gravel angular seam like clasts	Damp	-41.3464	174.7463	Cross cuts SR27 and 28

24b	SR	57	145	123	C	Ro2	Wide	~200mm	~90%	0	D	~160°	Gentle	~0.8m	Wavy	~8m		Strong, Veneer; Light brown grey, silty Sand with trace of clay, Soft, NP) White elongated gravel angular seam like clasts Clast supported (Crackle (~90%) angular, MW, Strong, Coating; Light brown grey, sandy Silt with trace of clay, Very stiff, NP) White sand sized Clast supported (Crackle (~90%) angular, MW, Strong, Coating; Light brown grey, sandy Silt with trace of clay, Very stiff, NP) white angular elongated seams >1mm thick visible	Damp	-41.3464	174.7464	Terminates against SR18, cross cuts BSH22
22	BSH	64	254	232	C	Ro2	Wide	~130mm	~90%	0	C	~170°	Gentle	~2.5m	Wavy	~8m	~1m		Minor seepage	-41.3464	174.7463	Cross cuts SR26l, SR28, SR24 and SR27
25	FL	16	162	140	C	Ro2	Moderately Wide	~30mm	~99%	0	C	~180°	Gentle		Planar	~6m		Clast supported (Rock (~99%) angular, MW, Strong, Coating; Light brown grey, sandy Silt with trace of clay, Very stiff, NP) white angular clasts Clast supported (Rock (~99%) angular, MW, Very strong, Coating; Light brown grey, sandy Silt with trace of clay, Very soft, NP) white tabulated gravel clasts	Damp	-41.3464	174.7465	Terminates against BSH22 and cross cuts SR31
26l	SR	65	143	121	C	Ro2	Very Wide	~500mm	~99%	0	S	~140°	Gentle		Curved	~7m			Significant seepage ~10L/5mins	-41.3463	174.7465	Cross cuts BSH22, SR28 and 24b
26r	SR	77	152	130	C	Ro2	Very Wide	~500mm	~99%	0	S	~170°	Gentle		Curved	~8m			Significant seepage ~10L/5mins	-41.3464	174.7465	Cross cuts BSH22 and SR27
22	BSH	61	259	237	C	Ro3	Very Wide	~400mm	~90%	0	C	~170°	Gentle	~3m	Wavy	~8m	~1.5m	Clast supported (Crackle (~90%) angular, HW, Weak (Argillite) to moderately strong (Greywacke), Coating, Clay with silty Sand seams, Very soft, HP) white elongated angular seams	Minor seepage	-41.3463	174.7465	Cross cuts SR26's, SR27 and SR30
27	SR	88	196	174	C	Ro3	Narrow	~4mm	~90%	0	O	~180°	Gentle		Stepped	~8m		Clast supported (Crackle (~90%) angular, HW, Strong to moderately strong, Clean; Light brown grey, Coating, Clay with silty Sand seams, Very soft, NP) white elongated angular seams	Minor seepage	-41.3464	174.7465	Cross cuts BSH22, SR24's, 26's and SR28
22	BSH	56	262	240	C	Ro4	Wide	~200mm	~85%	0	C	~170°	Gentle	~3m	Wavy	~9m	~2m	Clast supported (Crackle (~85%) angular, HW, Moderately strong, Clean/ stained; Light brown grey, silty Clay and sand seams, Very stiff, MP) No precipitation	Minor seepage	-41.3464	174.7466	Continuous
22	BSH	54	266	244	C	Ro4	Wide	~200mm	~85%	0	C	~170°	Gentle	~3m	Wavy	~9m	~2m	Clast supported (Crackle (~85%) angular, HW, Moderately strong, Clean/ stained; Light brown grey, silty Clay and sand seams, MP) No precipitation	Minor seepage	-41.3464	174.7466	Continuous
28	SR	73	67	45	C	Ro2-3	Narrow	~5mm	~10%	2	D	~140°	Gentle	~20m	Curved	~7m		Matrix supported (Soil (~10%) angular, CW, Very Weak, Coating; Light white blueish grey, silty Sand with traces of clay, Soft, NP) white elongated gravel sized clasts	Damp	-41.3464	174.7465	Was too far away to be reached so assumed infill descriptions. Terminates against BSH22 and SR26r. Also cross cuts SR24, 27, 21b and 26l
29	JN	76	200	178	C		Tight	~0mm		2	D	~180°	Gentle		Planar	~1m	~0.15m			-41.3465	174.7465	
29	JN	82	191	169	C		Tight	~0mm		2	D	~180°	Gentle		Planar	~1m	~0.15m			-41.3464	174.7465	
30	SR	74	250	228	C	Ro2	Tight	~0mm		1	D	~180°	Gentle		Planar	~7m				-41.3465	174.7467	Terminates against BSH22
31	SR	71	129	107	C	Ro2	Very Wide	~800mm	~95%	0	C	~160°	Gentle	~7m	Wavy	~15m		Clast supported (Crackle (~95%) angular, MW, Weak, Coating; Light brown grey, sandy Silt with traces of clay, Very soft, MP) white elongated gravel seams	Damp	-41.3465	174.7467	Cross cuts FL25
32	SR	28	266	244	C	Ro2	Moderately Wide	~30mm	~95%	0	O	~180°	Gentle		Planar	~8m				-41.3466	174.7467	Terminates against SR31 and cross cuts BSH35, SR34 and SR33
34	SR	74	93	71	C	Ro3	Moderately Wide	~40mm	~95%	0	C	~160°	Gentle	~0.5m	Wavy	~6m		Clast supported (Crackle (~95%) angular, HW, Moderately Strong to strong, Stained; Light brown grey, sandy Silt with traces of clay, Stiff, MP) Angular clasts randomly spaced	Damp	-41.3466	174.7469	Cross cuts SR32
33	SR	79	247	225	C	Ro3	Very Wide	~300mm	~90%	0	O	~170°	Gentle	~1.5m	Wavy	~6m		Clast supported (Crackle (~90%) angular, HW, Moderately strong to weak, Coating; Light brown grey, Sand with traces of silt, Stiff, LP) white angular precipitation	Damp	-41.3466	174.7469	Cross cuts SR32 and 38
35	BG	75	252	230	C		Tight	~0mm		0	O	~180°	Gentle		Planar	~6m				-41.3466	174.747	Cross cuts SR32
38	SR	75	131	109	C	Ro2	Moderately Wide	~30mm	~80%	1	D	~170°	Gentle	~1m	Wavy	~5m		Clast supported (Crackle (~95%) angular, HW, Weak, Coating; Light brown grey, silty Sand, Very stiff, NP) white angular precipitation covering the lot	Damp	-41.3466	174.747	Cross cuts SR32 and 33
35	BSH	69	244	222	C	Ro3	Moderately Wide	~40mm	~90%	0	O	~160°	Gentle	~2m	Wavy	~5m	~1m	Clast supported (Crackle (~90%) angular, HW, Very weak, Coating; Light brown grey, clayey Sand, Very Stiff, LP) no precipitation	Damp	-41.3466	174.7471	Cross cuts SR32
36	BG	63	236	214	C		Tight	~0mm		0	O	~160°	Gentle	~2m	Wavy	~2.5m				-41.3467	174.7474	Failure plane for wedge failure. Presume joins up with SR37 despite inability to see the join.
37	SR	69	117	95	C					0	O	~150°	Gentle	~4m	Wavy	~2.5m				-41.3467	174.7472	Failure plane for wedge failure. Presume joins up with SR36 despite inability to see the join.
35	BG	67	278	256	C		Tight	~0mm		0	O	~160°	Gentle	~2m	Wavy	~5m				-41.3466	174.7472	
39	JN	76	93	71	C	Ro3	Tight	~0mm		1	D	~180°	Gentle		Planar	~0.8m	~0.1m			-41.3466	174.7471	
39	SR	78	0	338	C	Ro2	Moderately	~60mm	~80%	0	O	~160°	Gentle	~1m	Irregular	~5m		Clast supported (Crackle (~80%) angular, HW-CW,	Damp	-41.3466	174.7472	Cross cuts bedding

39b	SR	57	59	37	C		Wide										Very weak, Coating; Light brown grey, clayey Sand, Very stiff, LP) No precipitation				
							Tight	~0mm		1	D	~160°	Gentle	~1m	Irregular	~6m			-41.3466	174.7471	Cross cuts bedding and SR32
40	SR	87	137	115	C	Ro2	Moderately Narrow	~10mm	~80%	1	D	~160°	Gentle	~30m	Curved	~4m	Clast supported (Crackle (~80%) angular, HW, Very weak, Coating; Light brown grey, clayey Silt with traces of sand, Very stiff, LP) white elongated gravel sized seams	Damp	-41.3467	174.7475	Cross cuts SR43, SR41a, SR41b and BSH42.
42	BG	89	243	221	C		Tight	~0mm		0	C	~180°	Gentle		Planar	~4m			-41.3466	174.7475	Cross cuts SR41a, SR43 and SR40
41a	SR	42	278	256	C	Ro2	Moderately Wide	~30mm	~75%	0	O	~170°	Gentle	~1m	Wavy	~3m	Clast supported (Mosaic (~75%) angular, HW, Weak, Coating; Light brown grey, silty Sand with traces of sand, Soft, NP) no precipitation	Damp	-41.3466	174.7473	Cross cuts SR40 and terminates against BSH42
41b	SR	28	274	252	C		Narrow	~5mm	~75%	0	O	~140°	Gentle	~3m	Wavy	~2.5m	Clast supported (Mosaic (~75%) angular, HW, Moderately strong, Coating; Light brown grey, silty Sand with traces of sand, Soft, NP) no precipitation	Damp	-41.3467	174.7474	Terminates against SR40
43	SR	67	277	255	C	Ro3	Moderately Wide	~60mm	~80%	1	D	~170°	Gentle	~0.7m	Wavy	~3.5m	Clast supported (Crackle (~80%) angular, HW, Weak, Coating; Light brown grey, silty Sand with traces of sand, Soft, NP) white sand to gravel size angular clasts	Damp	-41.3467	174.7476	Cross cuts BSH42 and SR40. Offset by BSH42

E.4 Owhiro Bay Quarry Graphs

Defect and rock mass results from Owhiro Bay Quarry. Results are presented in graphs. Where percentages are used they display the respective occurrence of the dependent variable assessed.

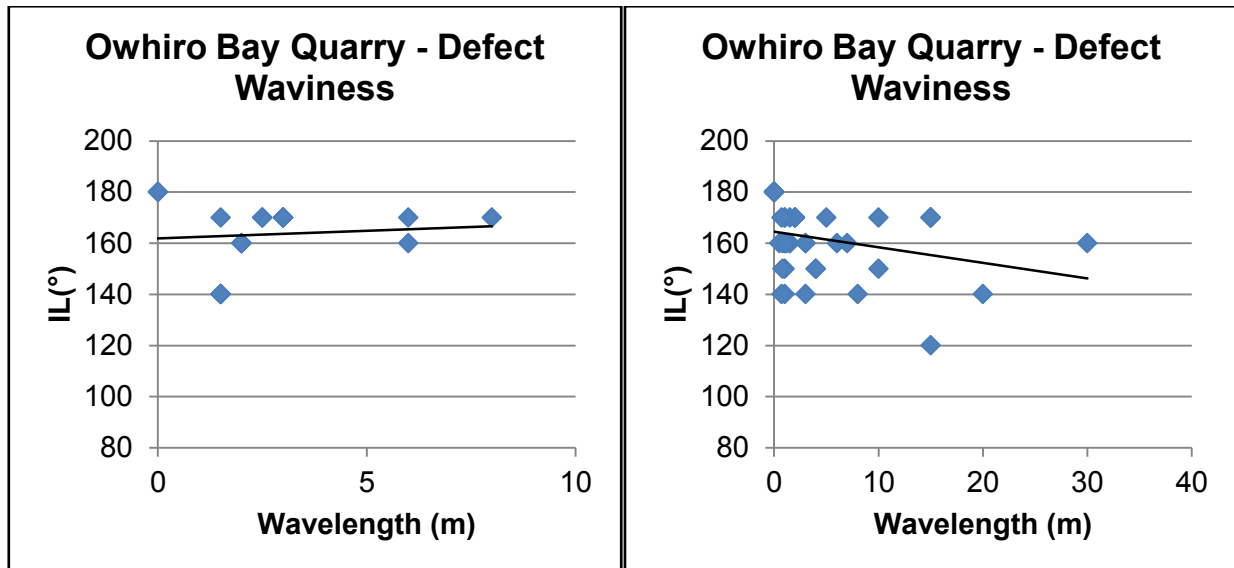
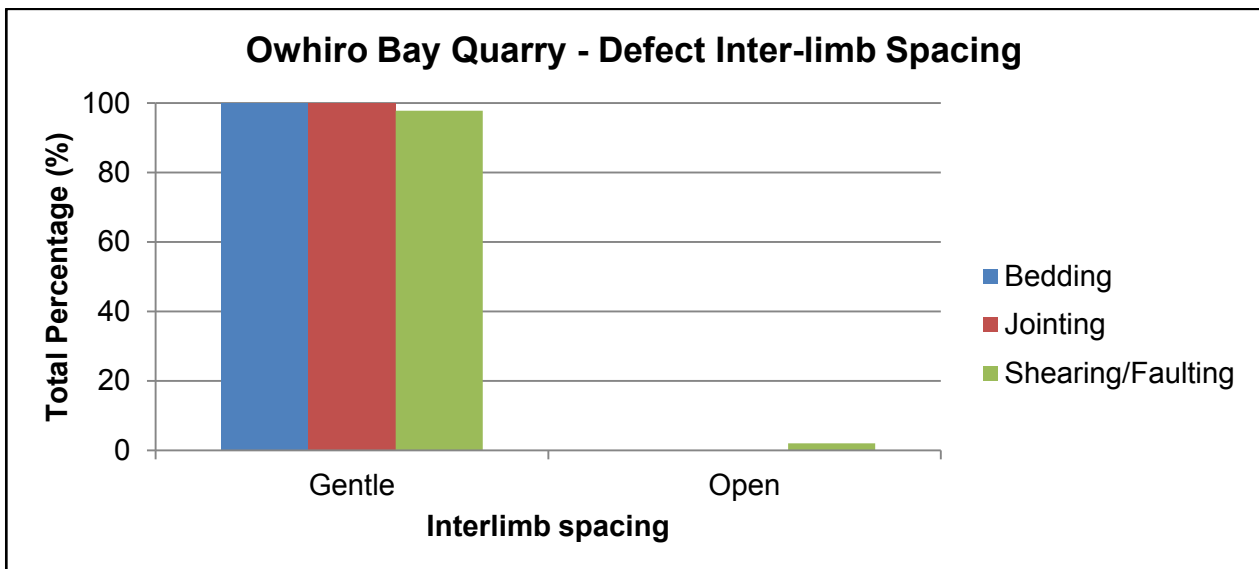
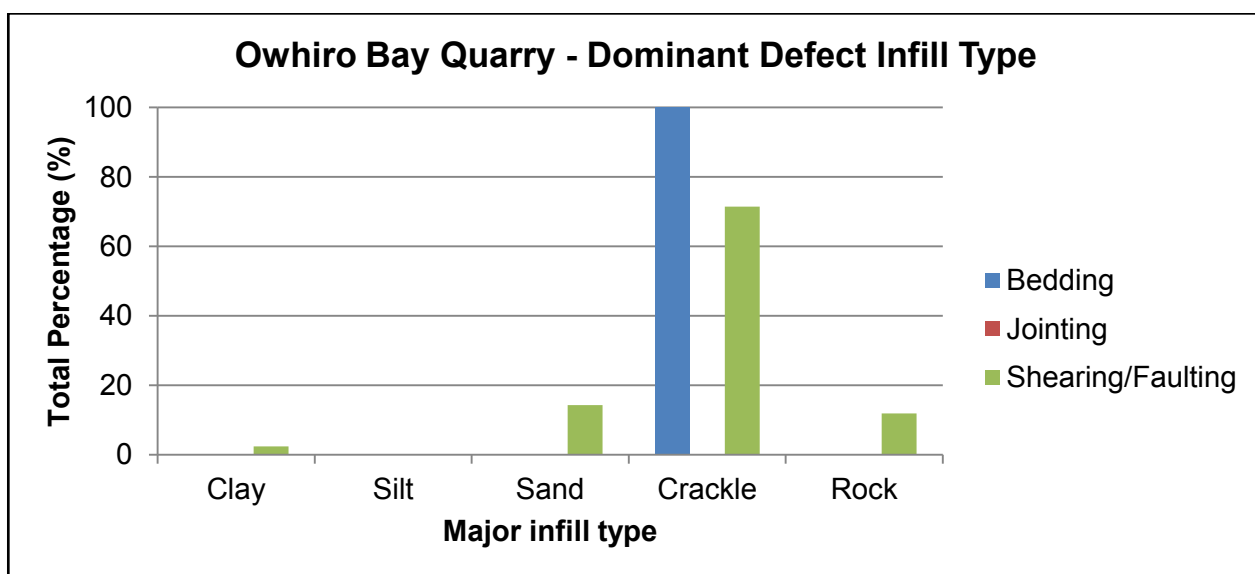
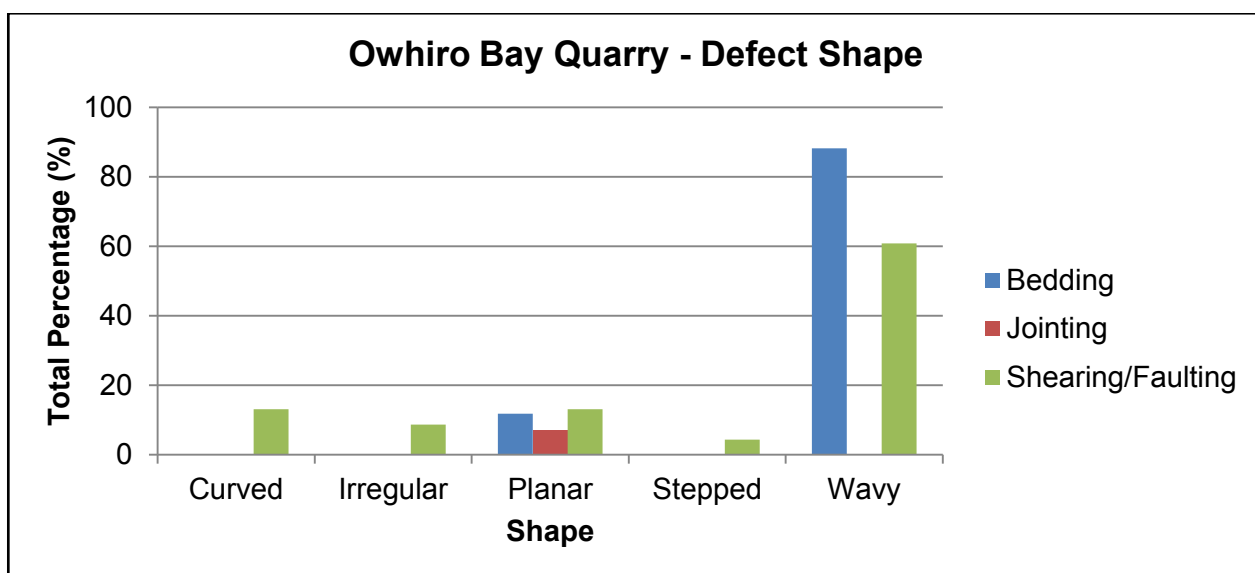
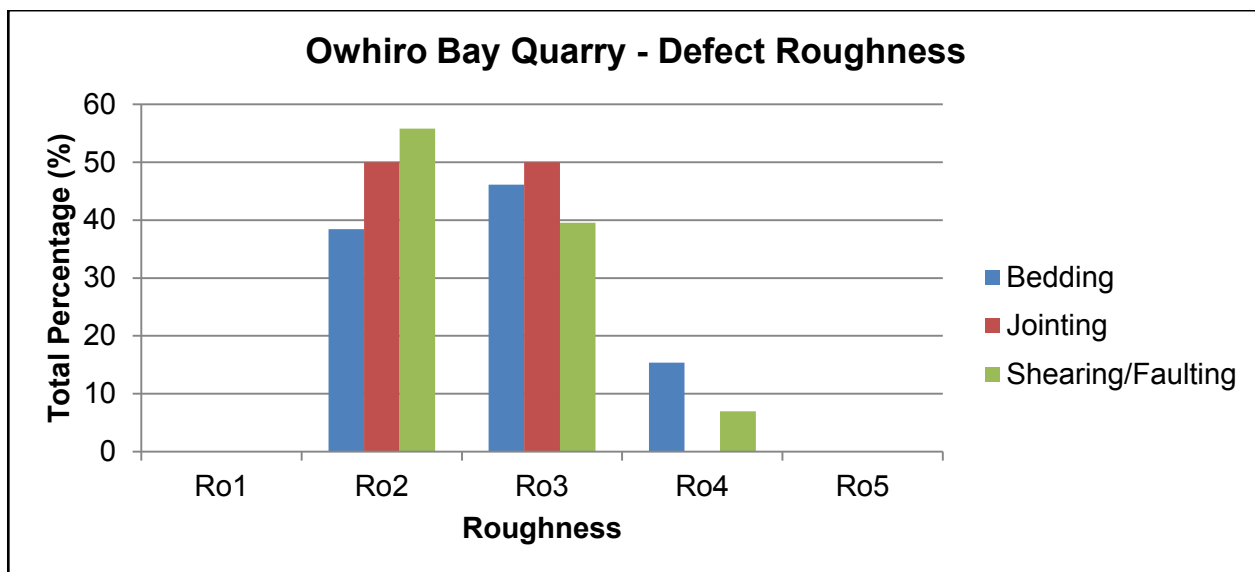
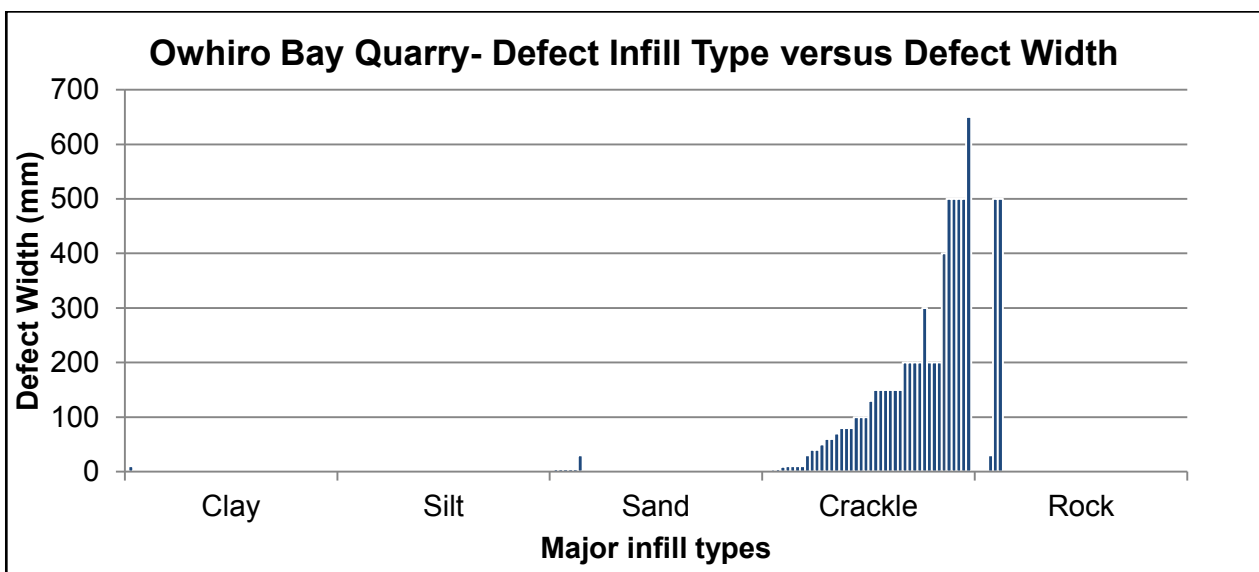
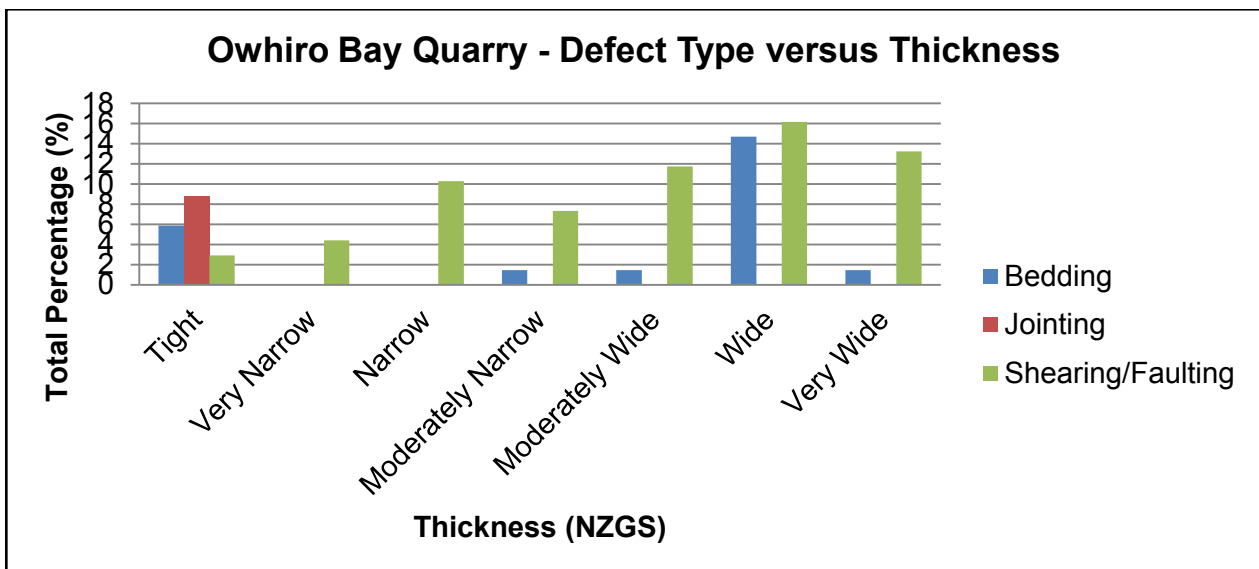
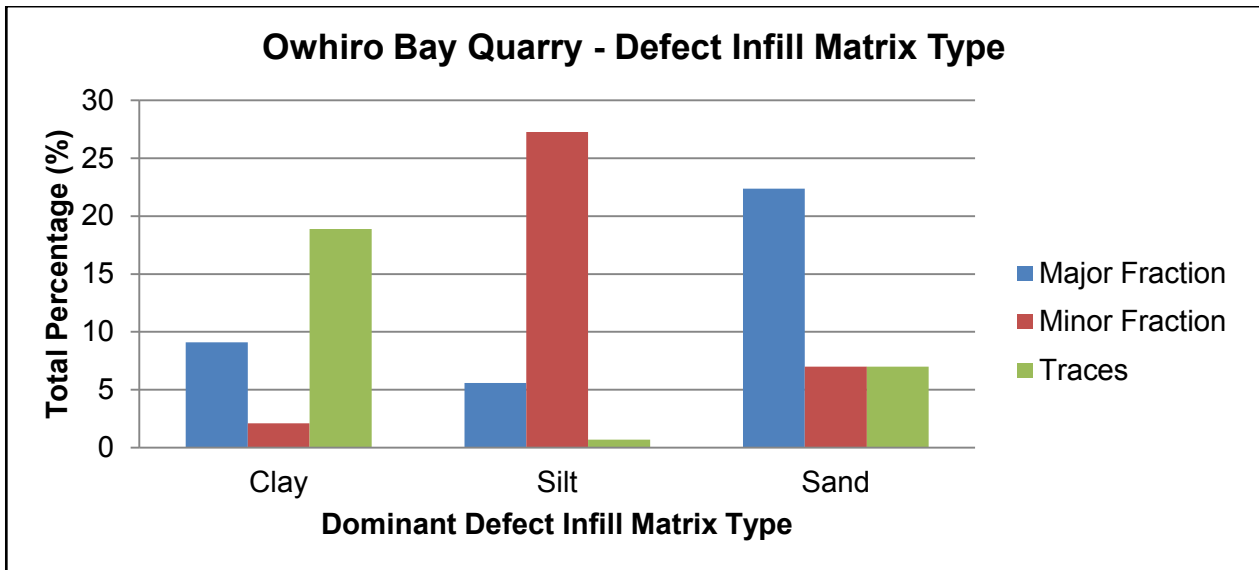
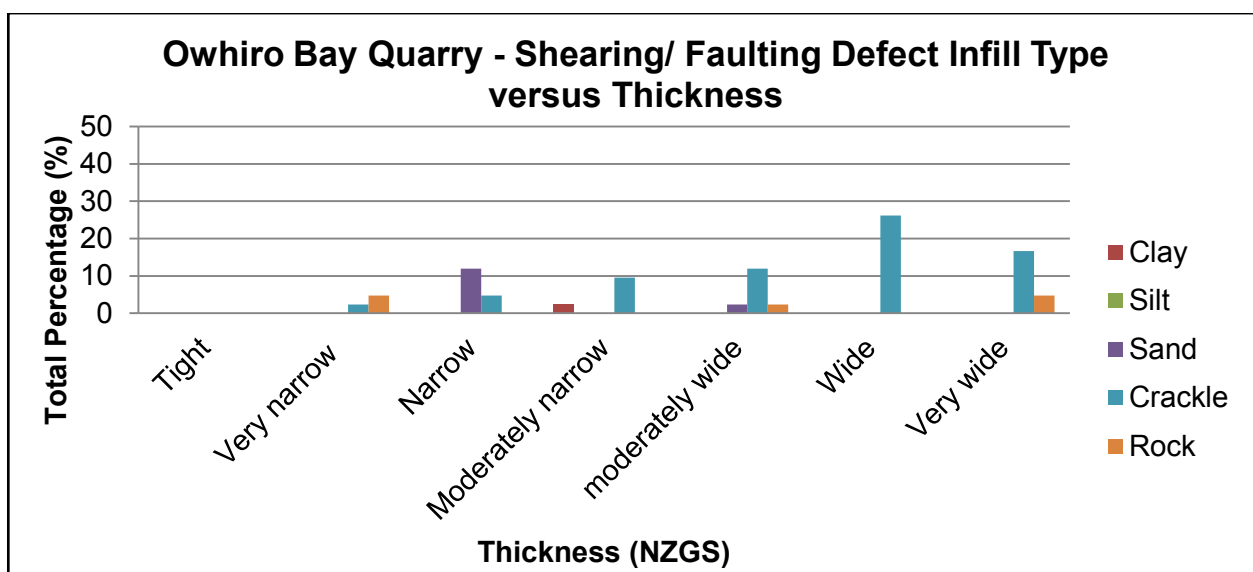
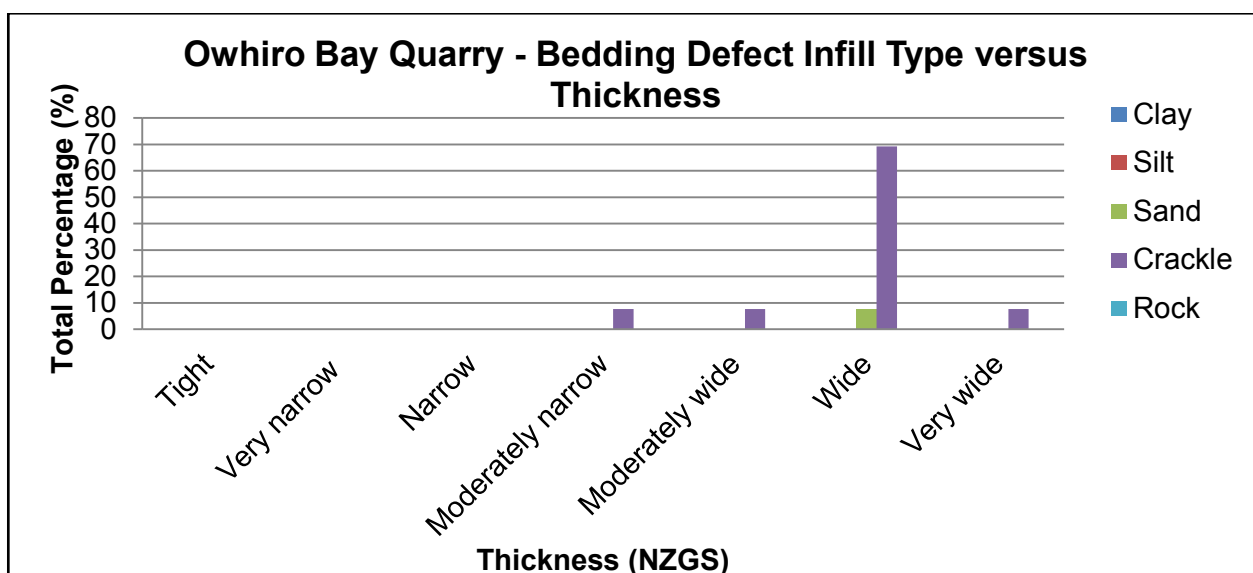
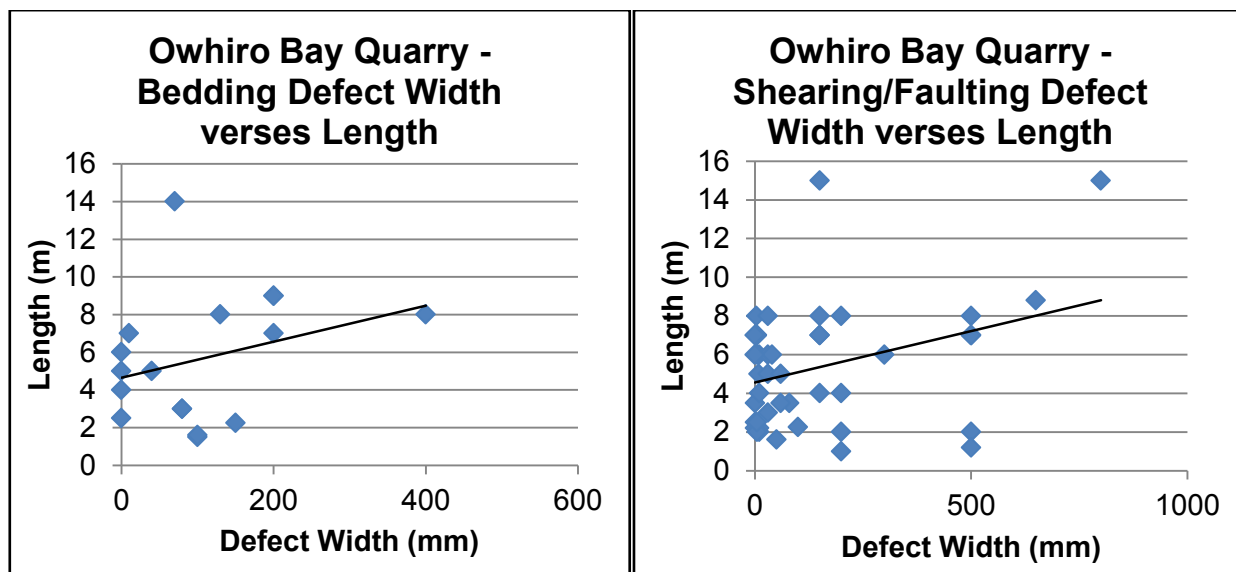


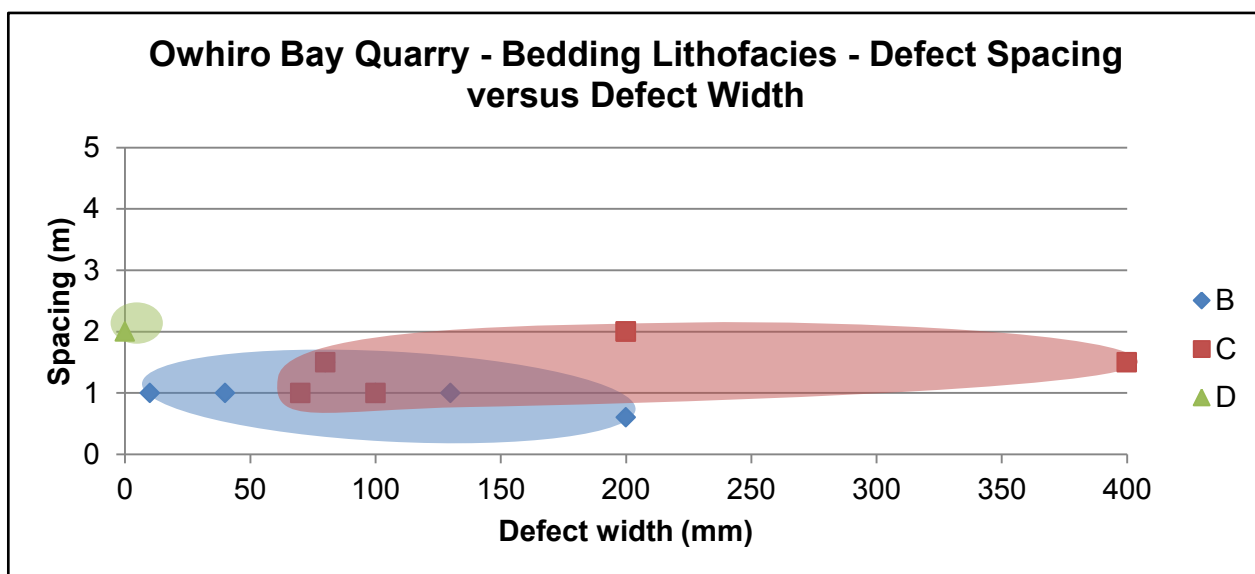
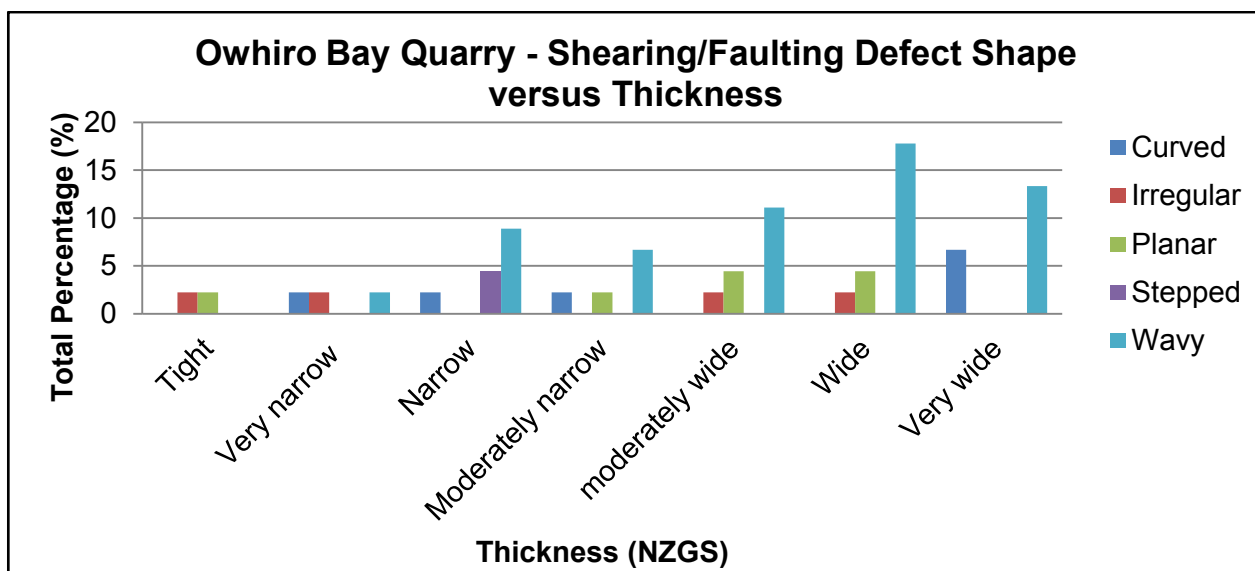
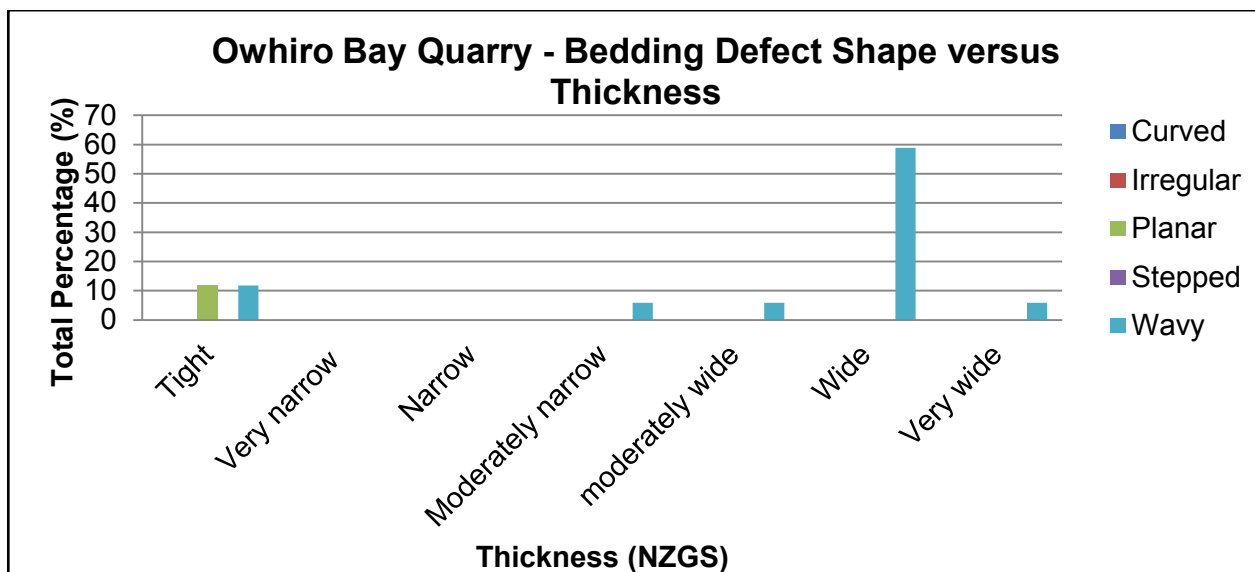
Figure E.4.1: Graphs showing the waviness of Bedding (Left) and Shearing/Faulting (Right) in Owhiro Bay Quarry







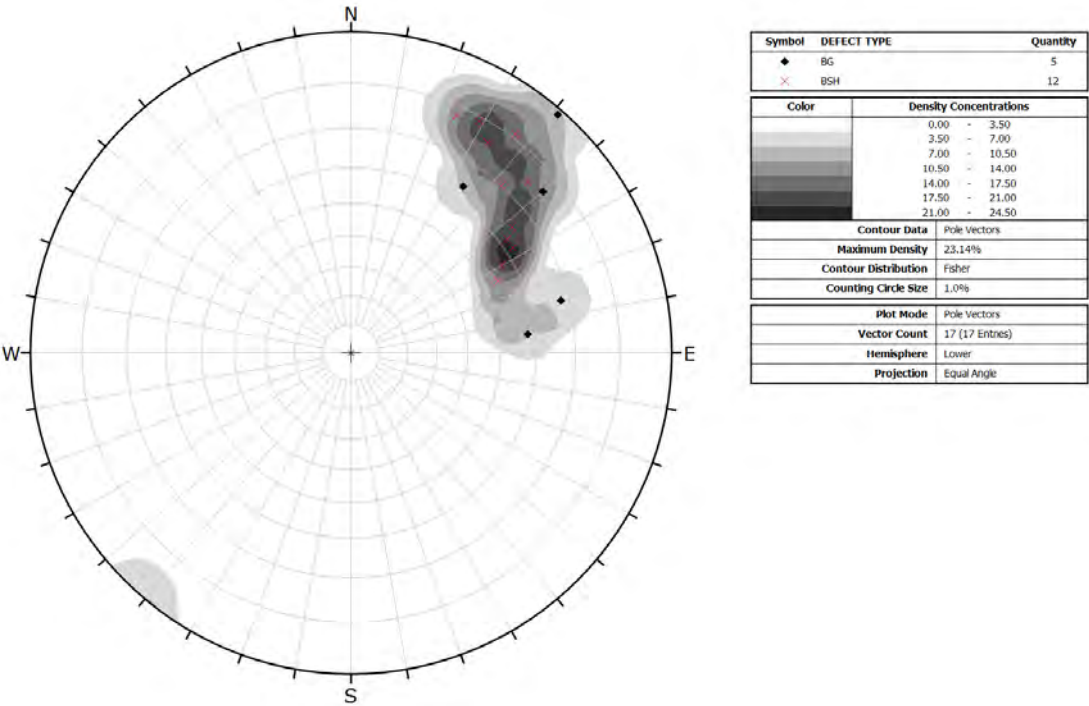




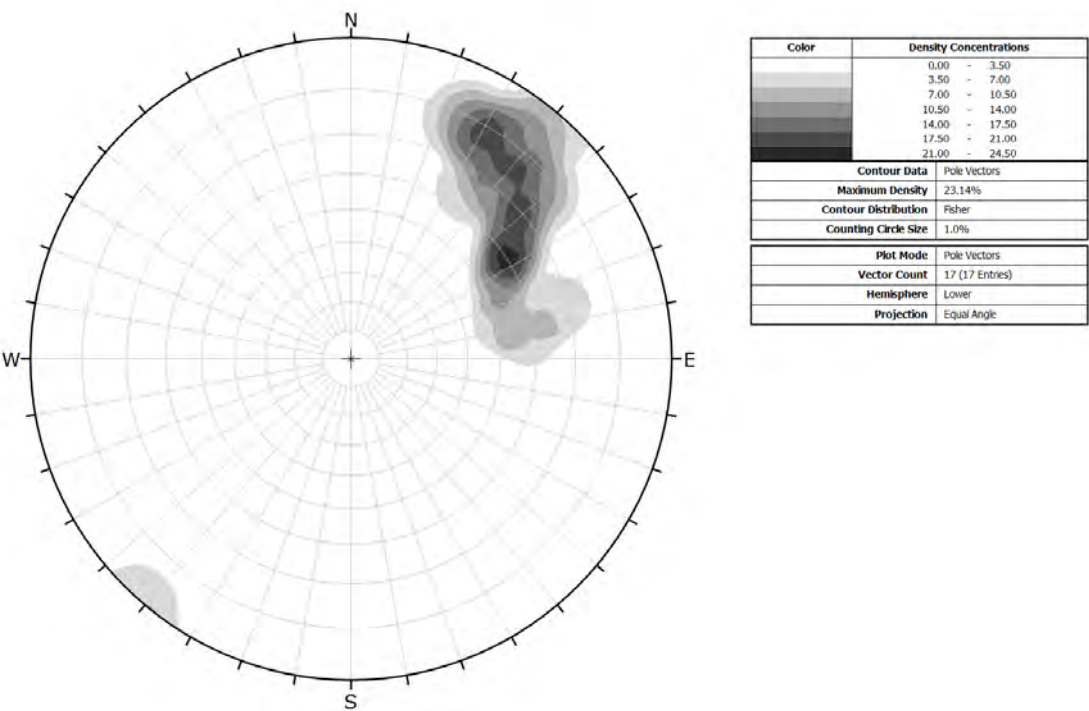
E.5 Owhiro Bay Quarry Stereonet Analysis

Stereonet Dip: Dip direction analysis of bedding, faults and shears respectively.

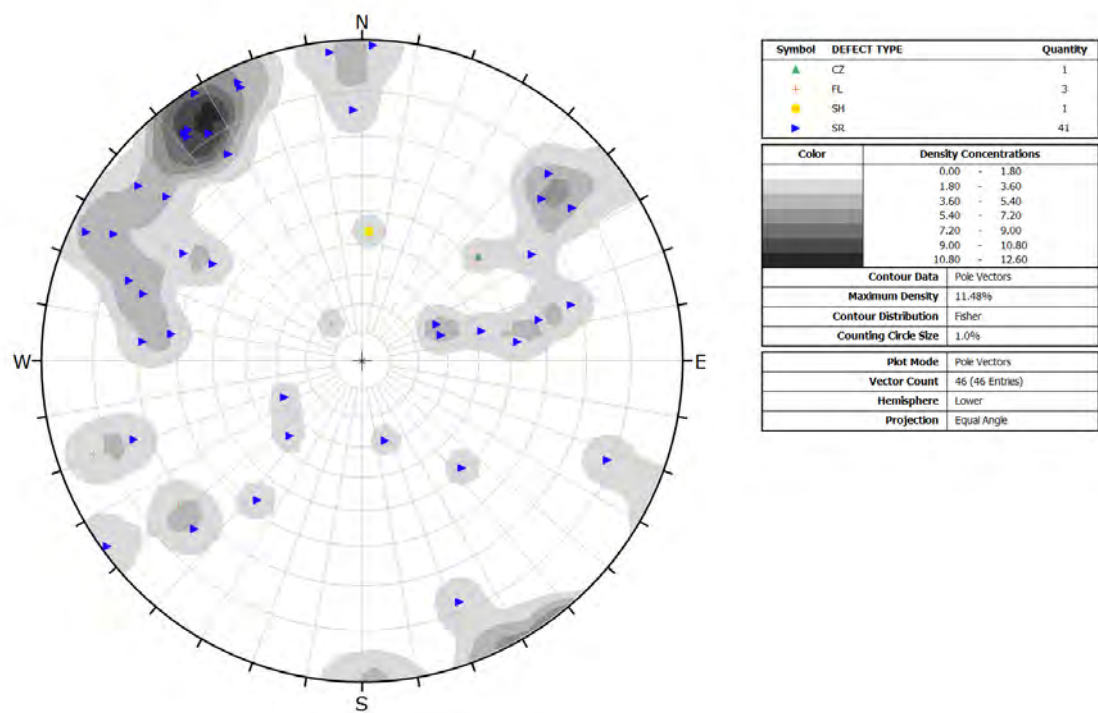
Bedding poles



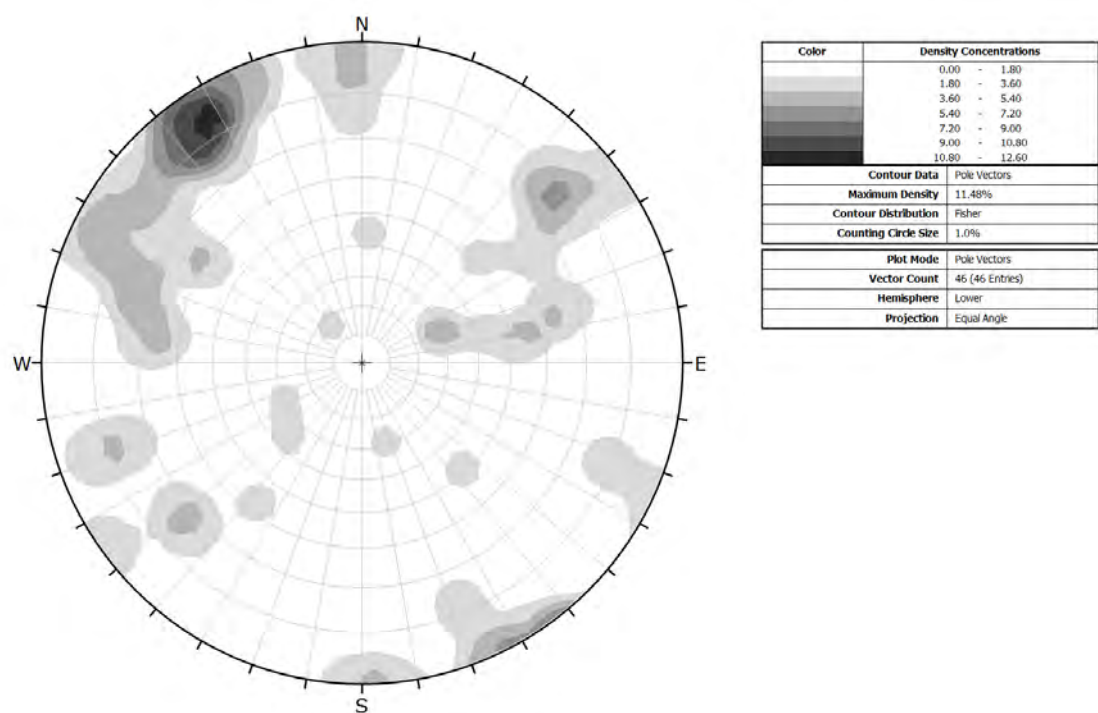
Contour diagram of bedding clusters



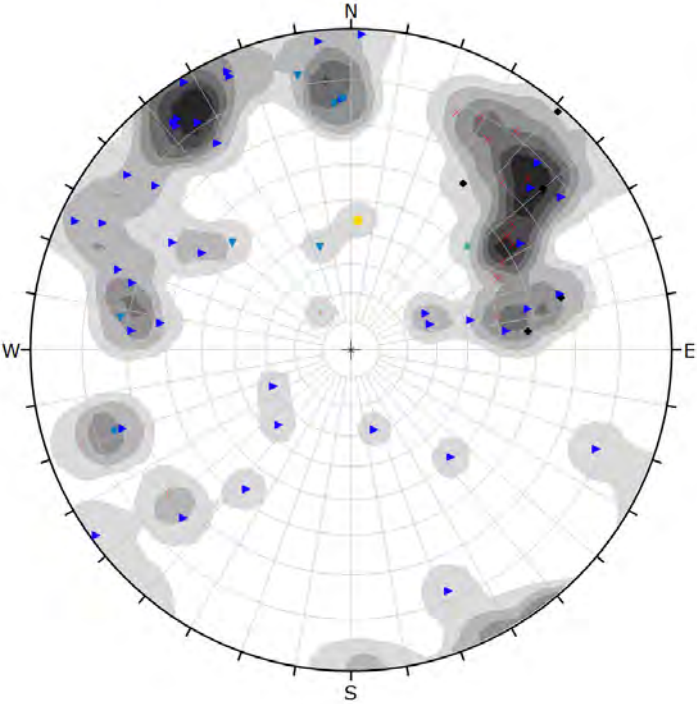
Shearing poles



Contour diagram of shearing and faulting clusters



All defects poles



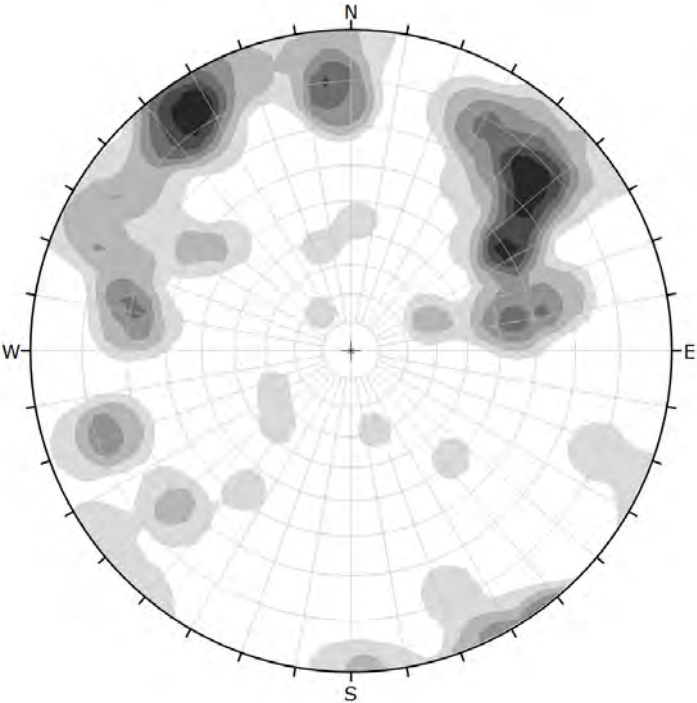
Symbol	DEFECT TYPE	Quantity
◆	BG	5
×	BSH	12
▲	CZ	1
★	FL	3
▼	JN	7
■	SH	1
▴	SR	41

Color	Density Concentrations
	0.00 - 1.10
	1.10 - 2.20
	2.20 - 3.30
	3.30 - 4.40
	4.40 - 5.50
	5.50 - 6.60
	6.60 - 7.70

Contour Data	Pole Vectors
Maximum Density	7.64%
Contour Distribution	Fisher
Counting Circle Size	1.0%

Plot Mode	Pole Vectors
Vector Count	70 (70 Entries)
Hemisphere	Lower
Projection	Equal Angle

Contour diagram of all defects cluster



Color	Density Concentrations
	0.00 - 1.10
	1.10 - 2.20
	2.20 - 3.30
	3.30 - 4.40
	4.40 - 5.50
	5.50 - 6.60
	6.60 - 7.70

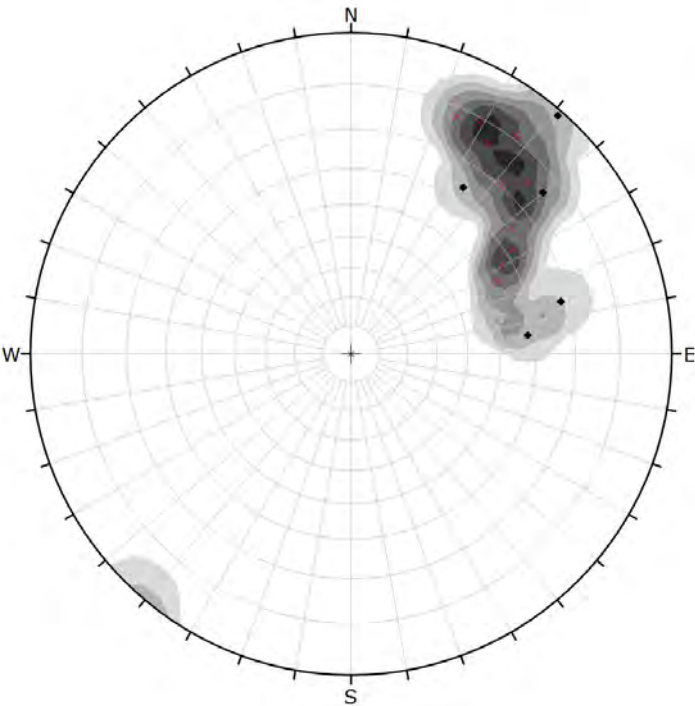
Contour Data	Pole Vectors
Maximum Density	7.64%
Contour Distribution	Fisher
Counting Circle Size	1.0%

Plot Mode	Pole Vectors
Vector Count	70 (70 Entries)
Hemisphere	Lower
Projection	Equal Angle

E.6 Filtered Stereonet Analysis

Stereonet from E.5 assessed for “noise”. The following only displays the poles of the continuous defects in Owhiro Bay Quarry.

Bedding poles



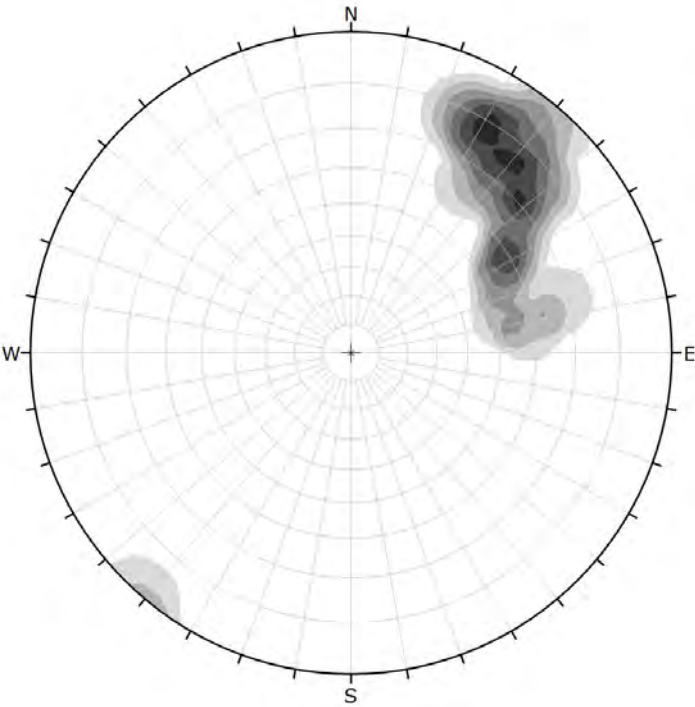
Symbol	DEFECT TYPE	Quantity
◆	BG	5
×	BSH	11

Color	Density Concentrations
	0.00 - 3.20
	3.20 - 6.40
	6.40 - 9.60
	9.60 - 12.80
	12.80 - 16.00
	16.00 - 19.20
	19.20 - 22.40

Contour Data	Pole Vectors
Maximum Density	21.13%
Contour Distribution	Fisher
Counting Circle Size	1.0%

Plot Mode	Pole Vectors
Vector Count	16 (16 Entries)
Hemisphere	Lower
Projection	Equal Angle

Contour diagram of bedding clusters

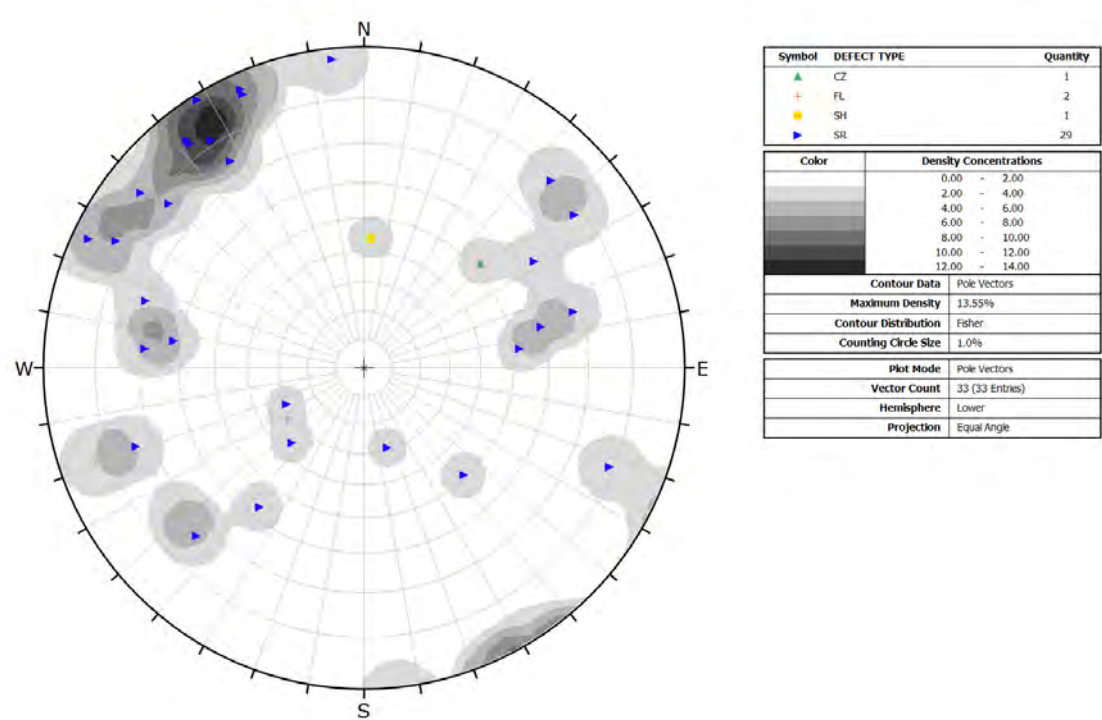


Color	Density Concentrations
	0.00 - 3.20
	3.20 - 6.40
	6.40 - 9.60
	9.60 - 12.80
	12.80 - 16.00
	16.00 - 19.20
	19.20 - 22.40

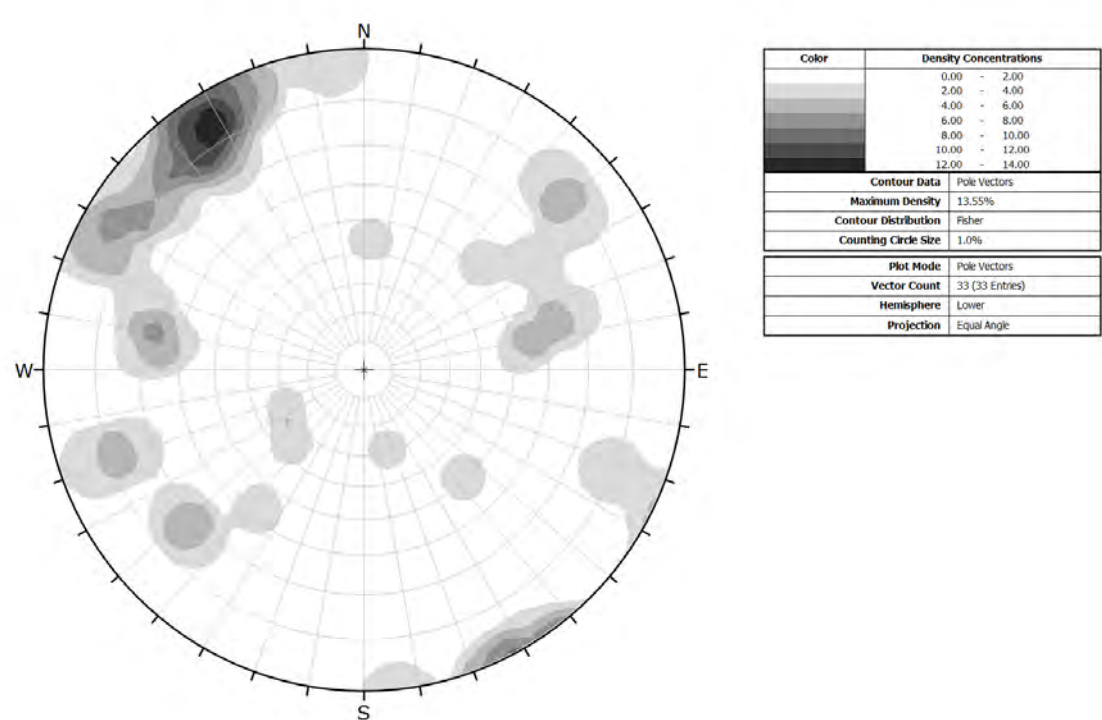
Contour Data	Pole Vectors
Maximum Density	21.13%
Contour Distribution	Fisher
Counting Circle Size	1.0%

Plot Mode	Pole Vectors
Vector Count	16 (16 Entries)
Hemisphere	Lower
Projection	Equal Angle

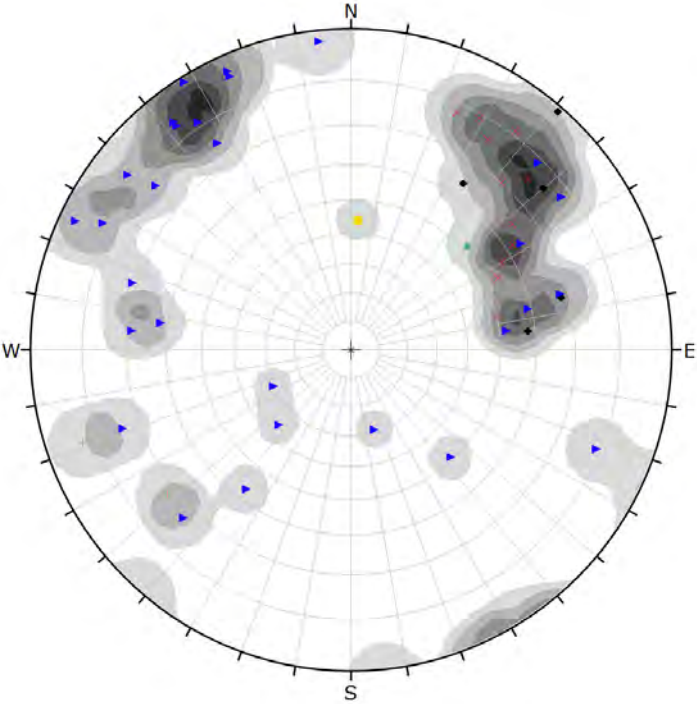
Shearing poles



Contour diagram of shearing and faulting clusters



All defects poles



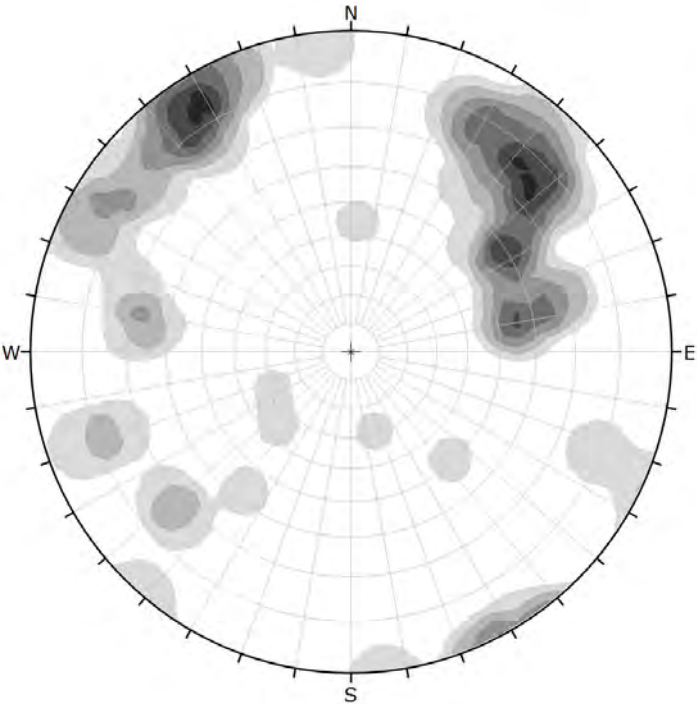
Symbol	DEFECT TYPE	Quantity
◆	BG	5
×	BSH	11
▲	CZ	1
■	FL	2
■	SH	1
▴	SR	29

Color	Density Concentrations
	0.00 - 1.40
	1.40 - 2.80
	2.80 - 4.20
	4.20 - 5.60
	5.60 - 7.00
	7.00 - 8.40
	8.40 - 9.80

Contour Data	Pole Vectors
Maximum Density	9.12%
Contour Distribution	Fisher
Counting Circle Size	1.0%

Plot Mode	Pole Vectors
Vector Count	49 (49 Entries)
Hemisphere	Lower
Projection	Equal Angle

Contour diagram of all defects cluster



Color	Density Concentrations
	0.00 - 1.40
	1.40 - 2.80
	2.80 - 4.20
	4.20 - 5.60
	5.60 - 7.00
	7.00 - 8.40
	8.40 - 9.80

Contour Data	Pole Vectors
Maximum Density	9.12%
Contour Distribution	Fisher
Counting Circle Size	1.0%

Plot Mode	Pole Vectors
Vector Count	49 (49 Entries)
Hemisphere	Lower
Projection	Equal Angle

E.7 Owhiro Bay Quarry Structural Domains

Figures are based on mapping observations and stereonet analysis. The figures represent a very detailed interpretation of the changes in defect orientation across the Owhiro Bay Quarry site.

E.7.1 Owhiro Bay Quarry - Domains



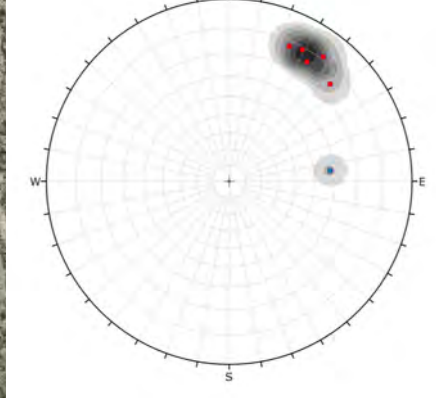
Imagery sourced: LINZ aerial imagery, 2017 (Captured by AAM NZ Limited (2017))

E.7.2 Owhiro Bay Quarry Domains - Bedding

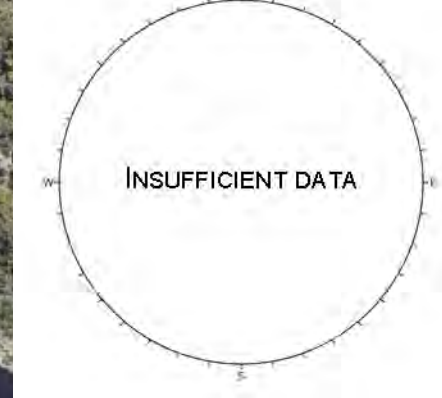
Stereoplot Legend

- Bedding Shear
- Bedding Fabric

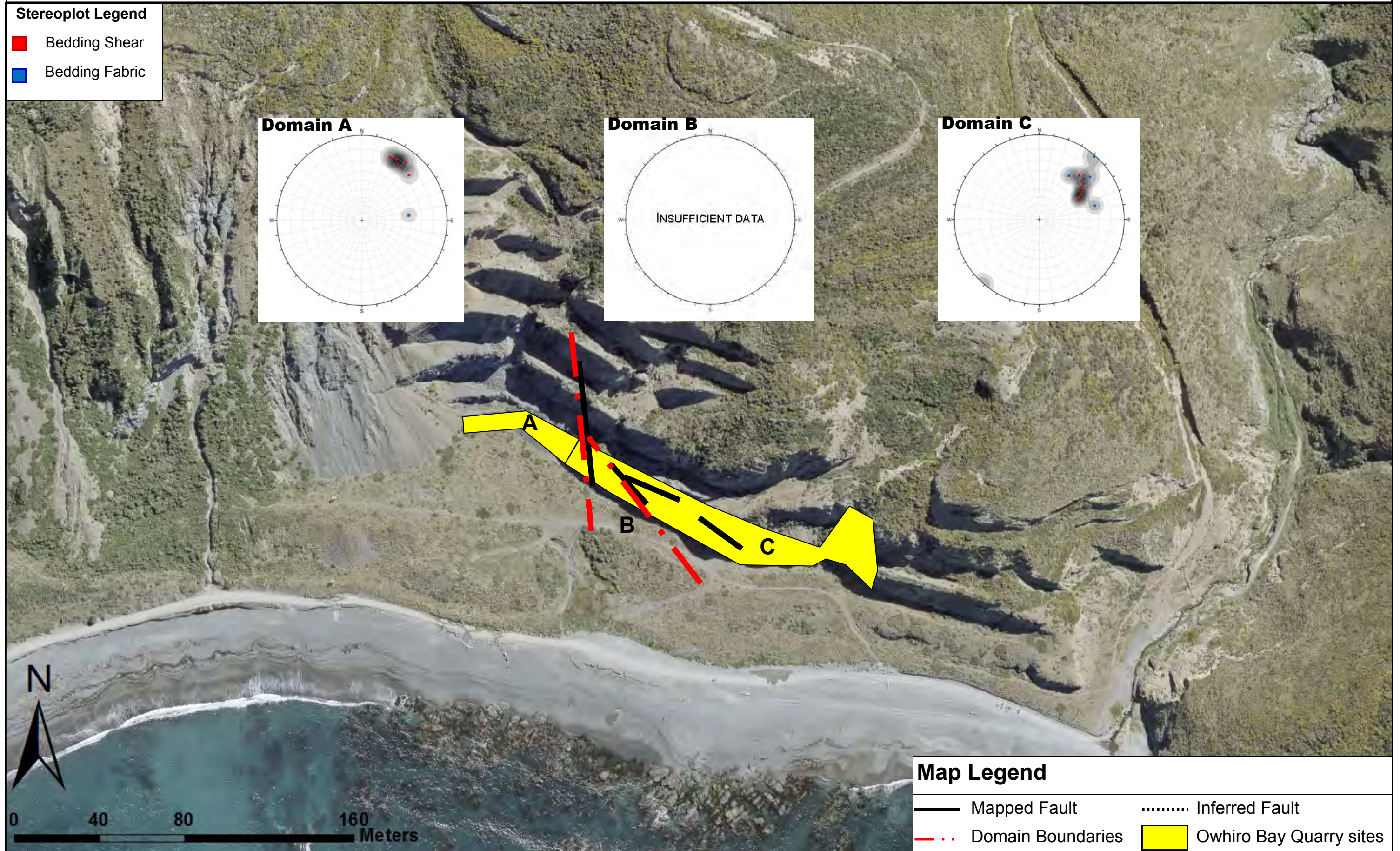
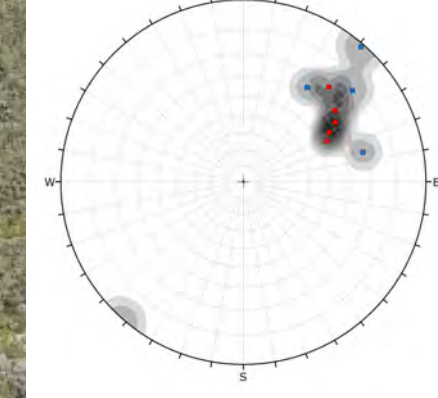
Domain A



Domain B



Domain C



Map Legend

- Mapped Fault
- - - Domain Boundaries
- Inferred Fault
- Owhiro Bay Quarry sites

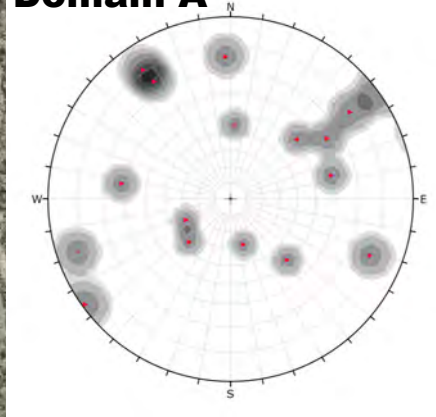
Imagery sourced: LINZ aerial imagery, 2017 (Captured by AAM NZ Limited (2017))

E.7.3 Owhiro Bay Quarry Domains - Shearing

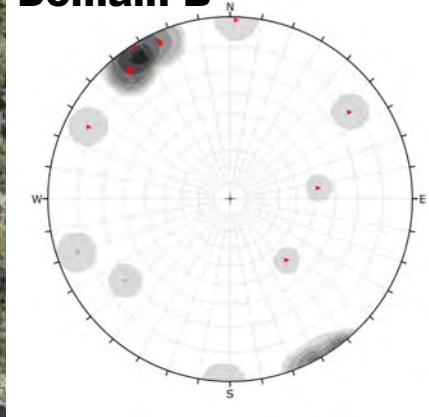
Stereoplot Legend

- ◆ Crushed Zone
- ✚ Fault
- * Sheared zone
- ▶ Shear

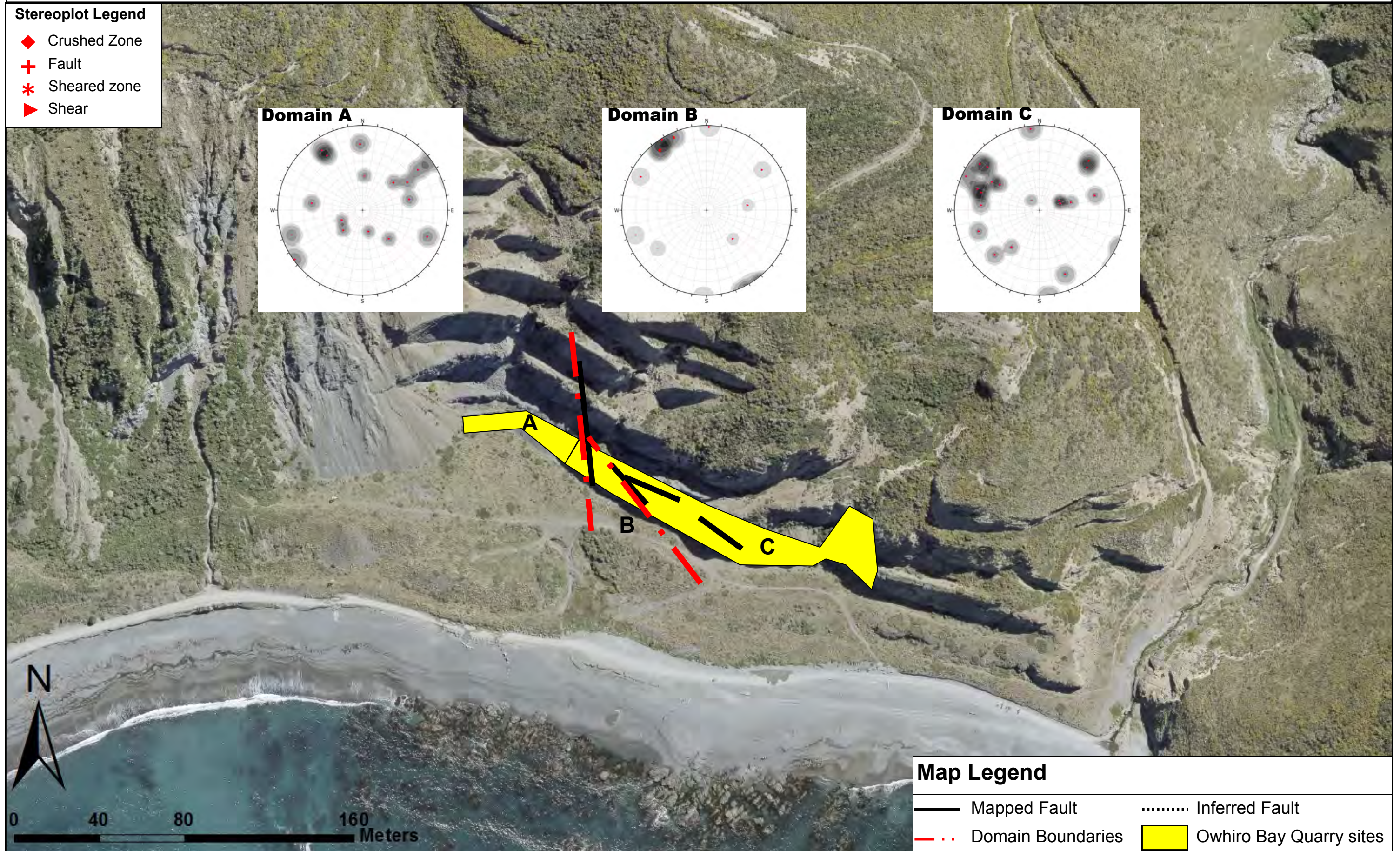
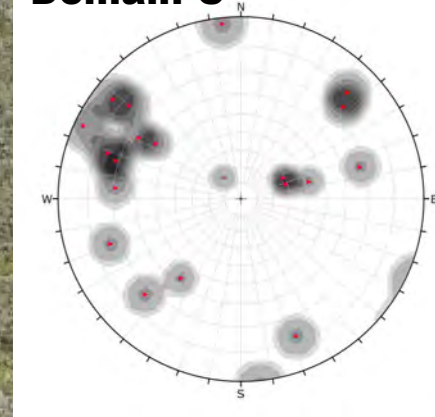
Domain A



Domain B



Domain C



Map Legend

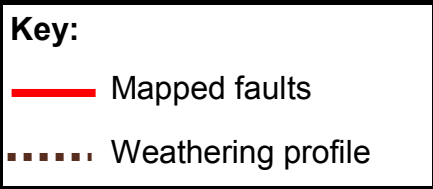
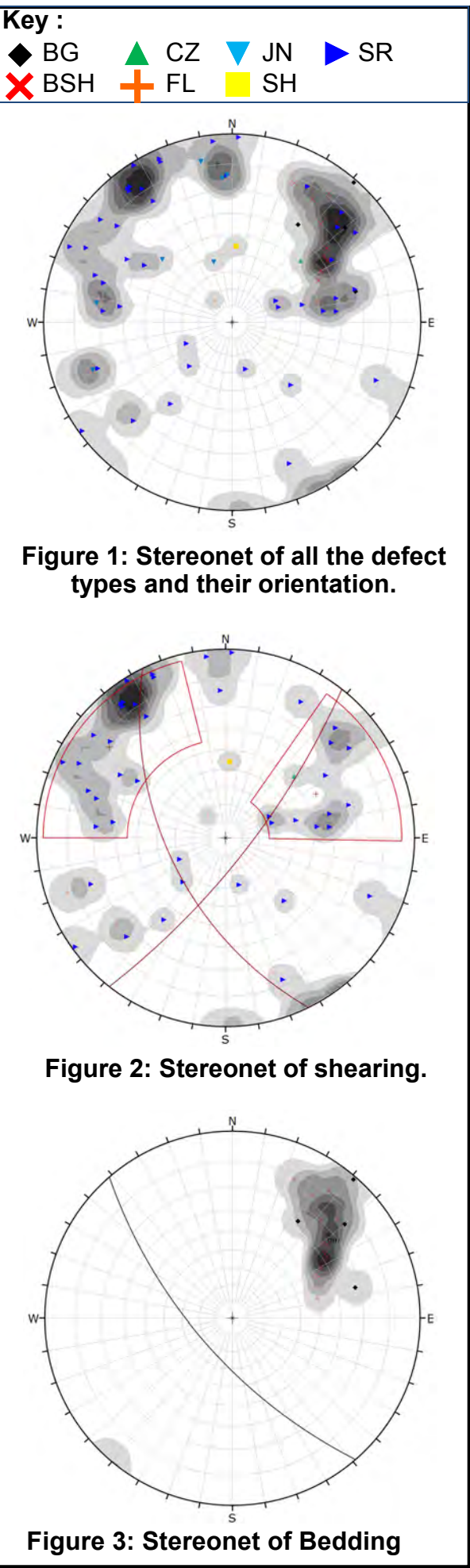
- Mapped Fault
- Inferred Fault
- - - Domain Boundaries
- Owhiro Bay Quarry sites

Imagery sourced: LINZ aerial imagery, 2017 (Captured by AAM NZ Limited (2017))

E.8 Owhiro Bay Quarry Engineering Geological Model

Engineering geological model based on all available data. The model provides a summary of the rock mass and defect condition within the Owhiro Bay Quarry study site. Defect orientation and regional structural controls are also included.

E.8: Engineering Geological Model of Owhiro Bay Quarry



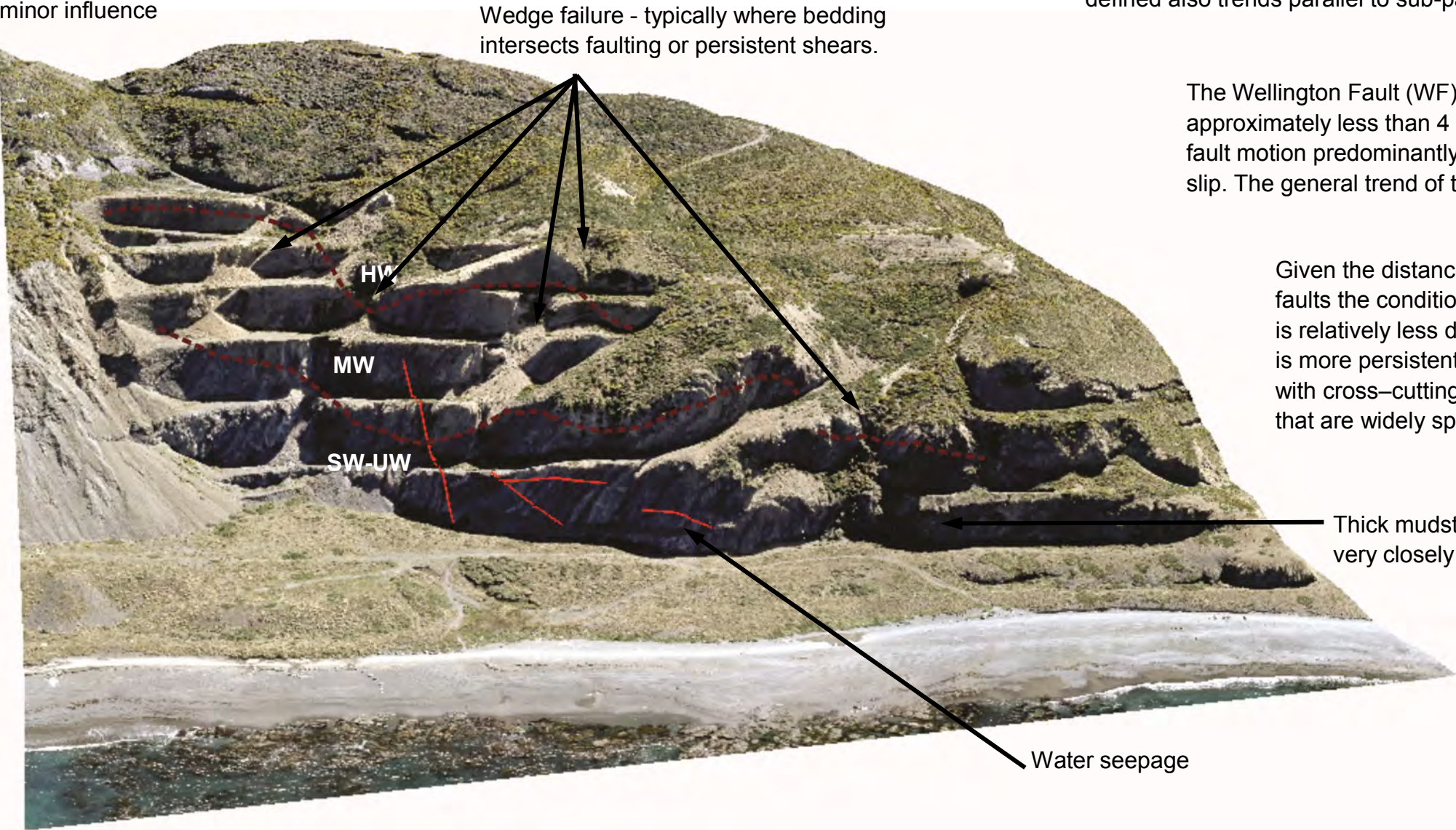
Weathering profile typically follows topography, faulting has minor influence

Bedding is dominantly sub vertical to steeply inclined with variations occurring in response to faulting.

Individual sandstone beds are 3 m to 0.6 m thick and continuous. Mudstone beds are 0.2 m to 2 m thick and heavily sheared. Cross-cutting shears and faults are apparent and persistent. Sheared zones are less common.

Rock mass structure at this site is controlled by the Wellington Fault, which is located some 4 km away.

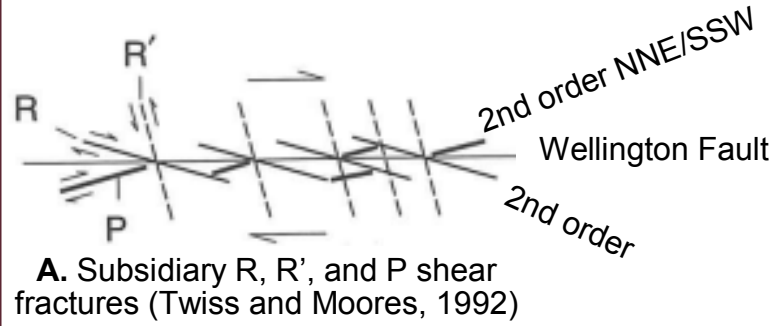
Bedding strikes sub-parallel to the 2nd order northwest-southeast trending structures. Shearing is dominantly sub-parallel with northeast-southwest trending structures (2nd order), a second conjugate set which is vaguely defined also trends parallel to sub-parallel with bedding.



The Wellington Fault (WF) is located approximately less than 4 km away, with fault motion predominantly dextral strike-slip. The general trend of the fault is 040°.

Given the distance from the active faults the condition of the rock mass is relatively less disturbed. Bedding is more persistent and continuous, with cross-cutting shears and faults that are widely spaced.

Conceptual Models:



<div><div><div>MUD : SAND</div><div>40: 60</div></div></div>	<div><div>Sandstone: Slightly weathered, light grey SANDSTONE; Strong; 5 joint sets, closely spaced , very narrow to tight joints [RAKAIA SUB-TERRANE Greywacke]</div><div>Mudstone: Slightly weathered, dark blueish grey MUDSTONE; Moderately Strong [RAKAIA SUB-TERRANE Argillite]</div></div>
<div><div><div>Predominant Suneson lithofacies:</div><div>B and C</div></div></div>	
<div><div>Scale 1:1,800 centimetres</div><div><div>018.7537.575150300</div><div><div></div><div></div><div></div><div></div><div></div></div><div>Meters</div></div></div>	

APPENDIX F: WAIRAKA POINT ANALYSIS

This site is located in Pukerua Bay 15 minutes' walk west from the beach carpark and is also directly west of the Transmission Gully North study area (Figure F.1). The dominant major structure of this area is the dextral strike slip Pukerua Bay Fault placing the area in convergence. Folding is evident within this area, with map scale folds possessing wavelengths ranging from 100 metres to kilometres generally plunging gently north-north east (Suneson 1993). A total of 4 outcrops were mapped (Appendix F.2).

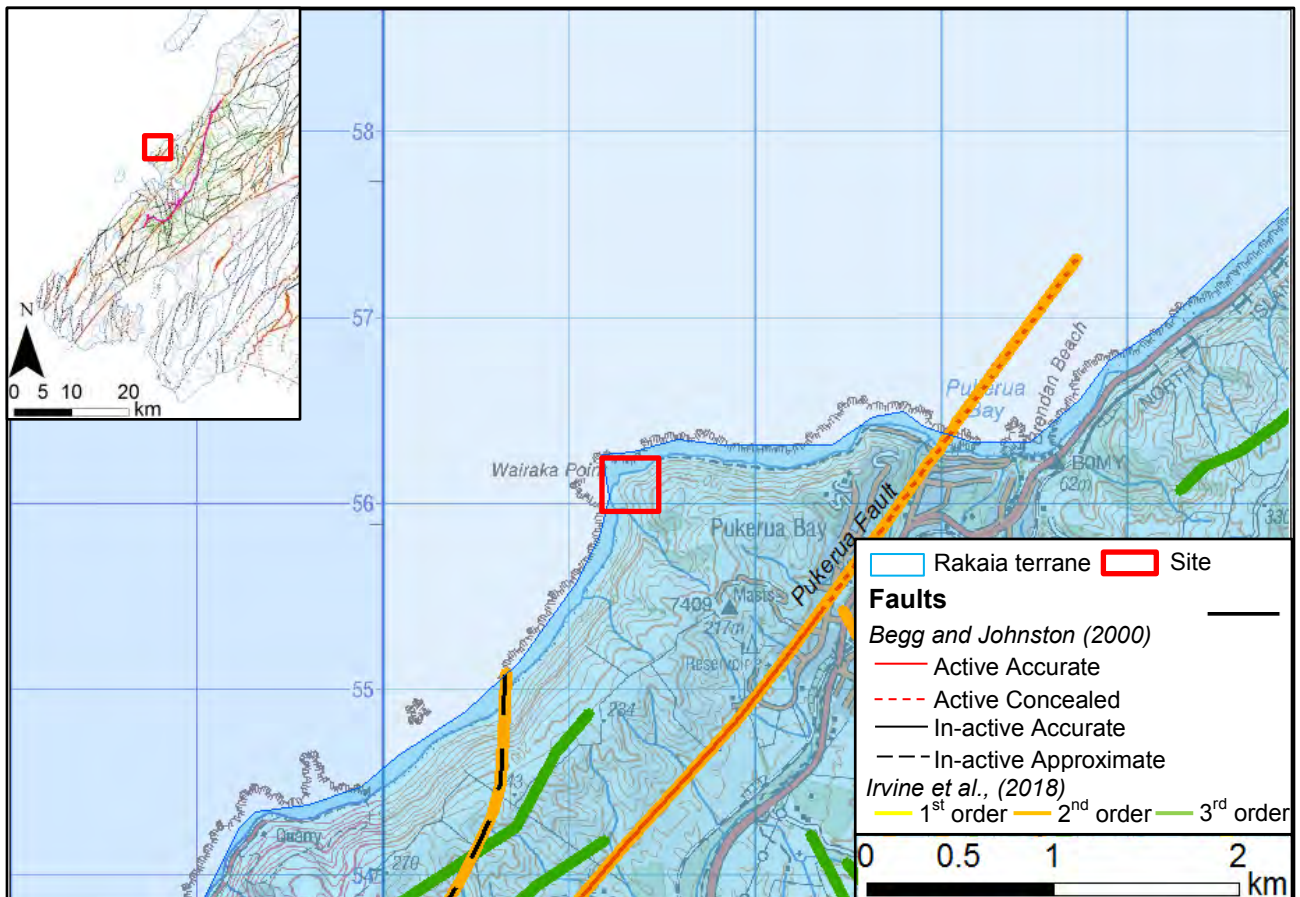


Figure F.1: Wairaka Point site district scale map. Data sourced from GNS (2018) (Begg and Johnston, 2000) and Irvine et al. (2018). Refer to Section 1.4 for Irvine et al (2018) order classification. Imagery from LINZ.

Results derived from conceptual models, raw mapping data, stereonet analysis and engineering geological models for the Wairaka Point study site as displayed in the following sections.

F.1 Wairaka Point Conceptual Structural Model

Preliminary structural assessment derived from GNS (2010) (Begg and Johnston, 2000) and Irvine et al (2018) structural databases. Interpretations are based on information derived from past literature.

F.1 Conceptual Structural Model of Wairaka Point

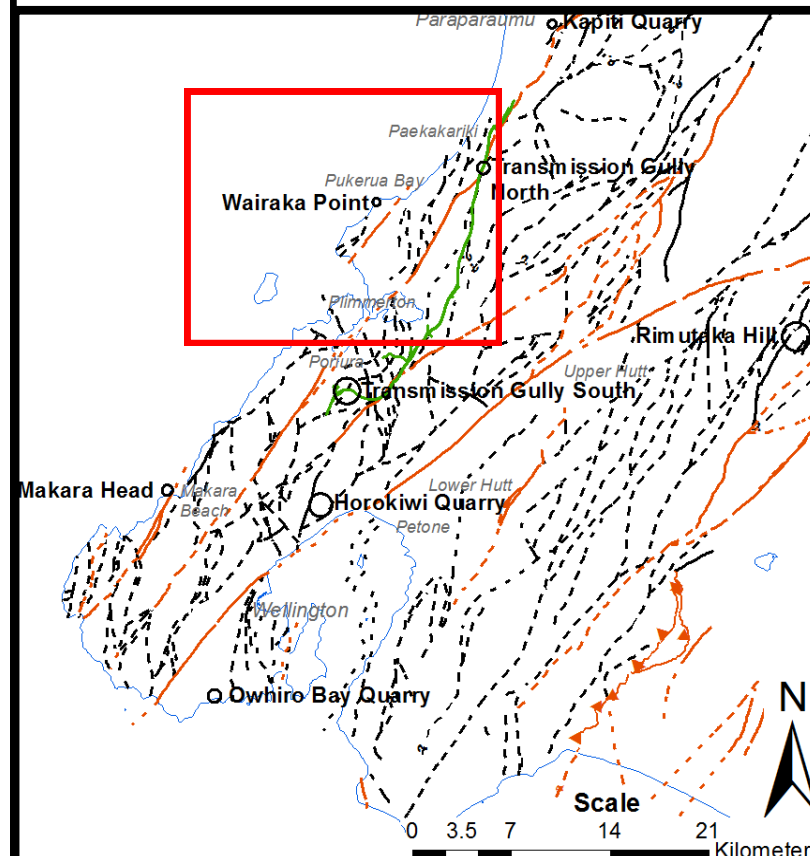
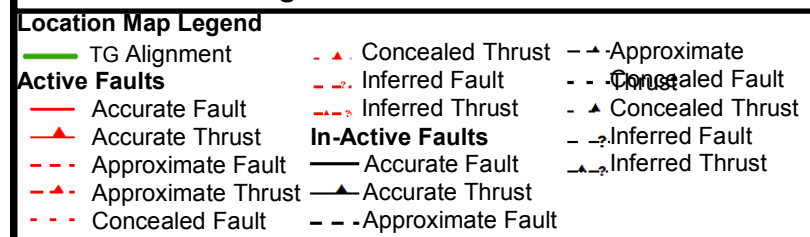


Figure A: Location Plan



Suneson (1992) describes numerous folds at different scales and orientation. It is interpreted that these folds are superimposed (see fold model produced below). These associated structures develop as a result of the inherent geometry of strike-slip faults explained by Twiss and Moores (1992).

Based on this understanding it is anticipated that there is a component of contraction oblique to the Pukerua Fault and roughly perpendicular to the trend of the first order folds. Also recorded is extension which is orientated obliquely to the Pukerua Fault and perpendicular to the SW/NE fault structures.

Rock mass structure is primarily controlled by the Pukerua Fault and folding associated with the radial shear model.

Fault motion on the Pukerua Fault is dextral strike-slip. The general trend of the fault is around 040°.

Wairaka Point

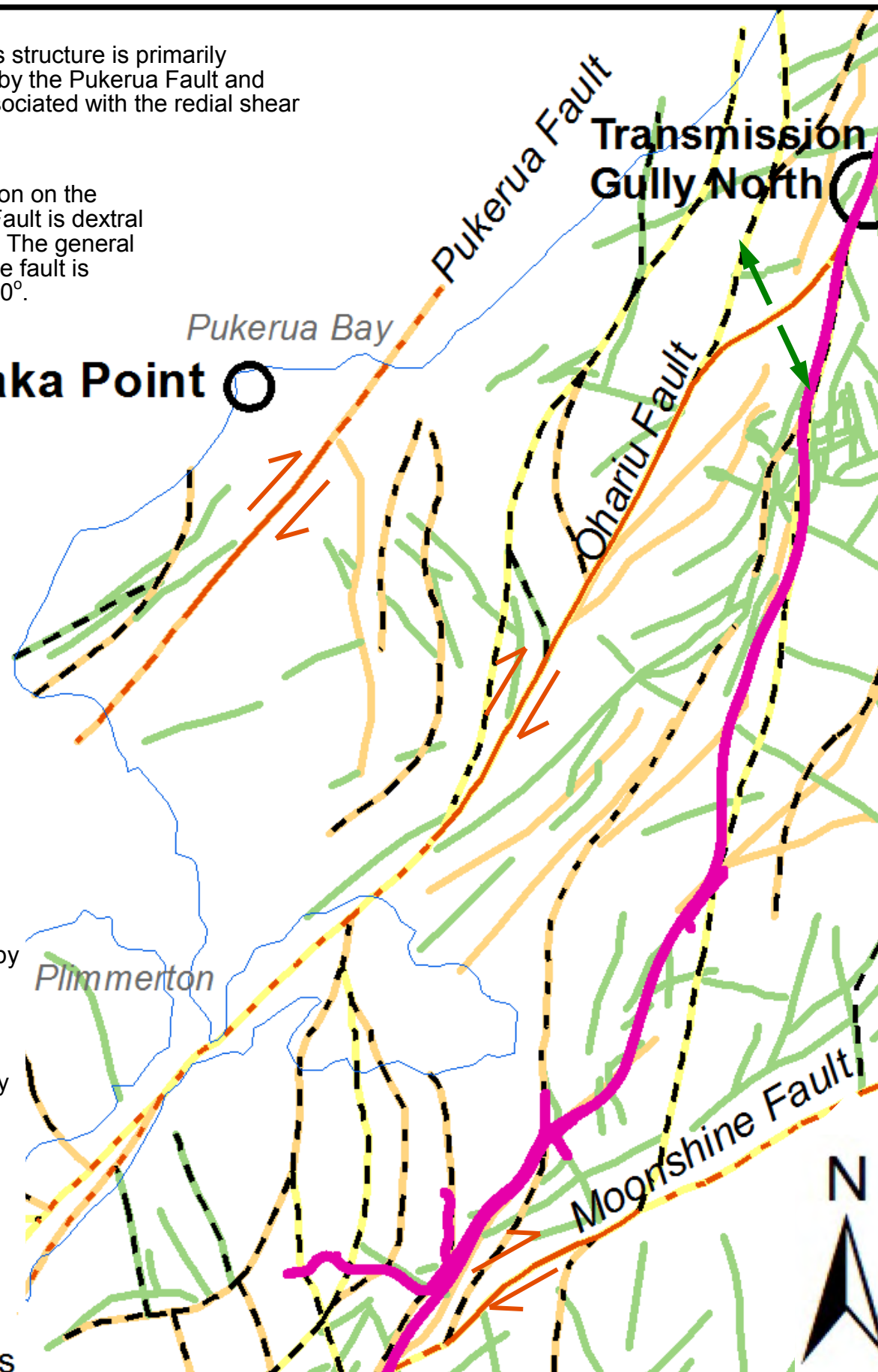
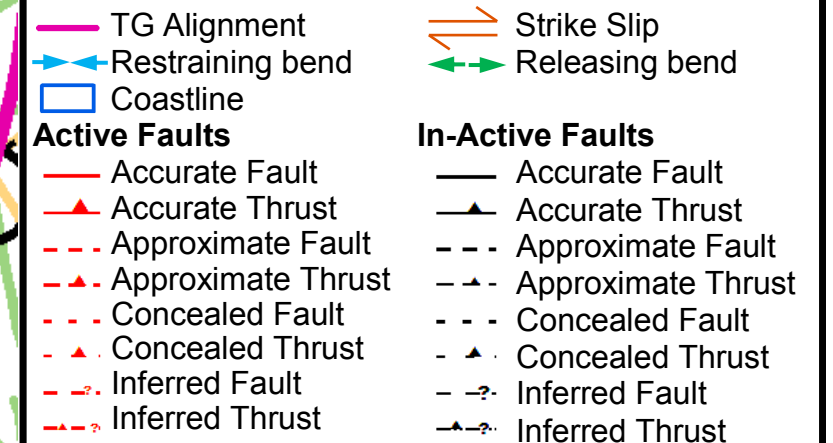
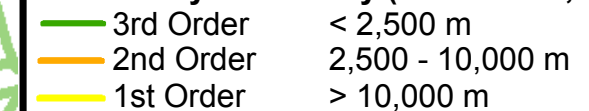


Figure B: District scale structures around Wairaka Point. Faults are sourced from GNS (2010) (Begg and Johnston, 2000) and from Irvine et al (2018).

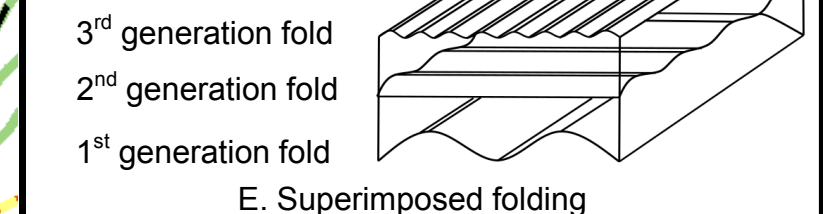
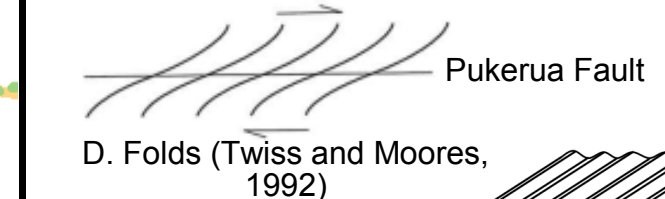
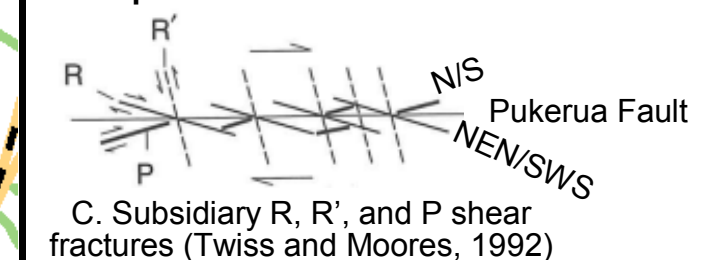
District Scale Legend:



Fault Analysis Overlay (Irvine et al., 2018)



Conceptual Models:



Bedding and Shearing Predictions:

Bedding is predicted to strike sub-parallel to the major fault structures (Suneson, 1992), with outcrop scale folds anticipated to orientate roughly perpendicular (2nd generation, a few metres to 10's of metres) and at roughly 45° or less (3rd generation, centimetre's to a few meters) to the Pukerua Fault. Shearing is anticipated to be well developed and trending sub-parallel to the Pukerua fault and bedding and NW/ SE structures.

F.2 Wairaka Point Outcrop Location Map

Displays the location of the mapped outcrops within the Wairaka Point study site.

F.2 Wairaka Point

 Wairaka Point Sites



F.3 Wairaka Point Raw Mapping Data

Structural data collected from the Wairaka Point study site. Where data is missing or blanked out information was either not able to be reached or was not relevant to the rock mass or defect condition (e.g. Planar defects did not contain a wavelength as outlined in Chapter 3).

F.3 Wairaka Point - Raw data

Wairaka Point																						
ID	Defect Type	Dip	Dip Direction (Mag)	Dip Direction (True)	Domain	Roughness	Thickness		% of rock fragments	Continuity	Persistence	Shape			Persistence - Trace Length (m)	Spacing (m)	Infill (Support (Breccia type (%Clasts), Angularity, weathering, strength, coating; colour, grainsize, strength, plasticity)) precipitation	Saturation	Latitude	Longitude	Comments	Cut ID
							Term	Width (mm)				Inter-limb angle (degrees)	Wavelength (m)	Term								
1	SR	43	93	70	B	Ro3	Moderately wide	~20mm	~95%	2	R	~160°	Gentle	~2m	Wavy	~1m	Clast supported (Crackle (~95%), Angular, MW, Strong, Veneer, Dark brown, Sand, Very soft, NP) No precipitation	Dry	-41.0307	174.871	Terminates in rock	#3
2	SR	89	117	95	B	Ro3	Moderately wide	~30mm	~95%	2	R&O	~180°	Gentle		Planar	~1m	Clast supported (Crackle (~95%), Angular, MW, Strong, Veneer, Dark brown, Sand, Very soft, NP) No precipitation	Dry	-41.0306	174.8711	Terminates between SR1 and SR3. Too high to get to safely	
3	SR	20	320	297	B					2	R&D	~160°	Gentle	~4.5m	Wavy	~5m		Dry	-41.0306	174.871	Terminates at SR5. Too high to reach	
4	SR	82	348	326	B	Ro5	Narrow to Moderately narrow	~5-10mm	~95%	2	R&D				Stepped	~2.2m	Clast supported (Crackle (~95%), Angular, MW, Strong, Veneer, Dark brown, Sand, Very soft, NP) No precipitation	Dry	-41.0307	174.871	Terminates against SR3	
5	SR	16	292	270	B	Ro4	Narrow	~5mm	~95%	0	C	~180°	Gentle		Planar	~10m	Clast supported (Crackle (~95%), Angular, MW, Strong, Stained, Dark brown, Sand, Very soft, NP) No precipitation	Dry	-41.0307	174.8709	Offset a little by BSH	
10	SR	85	305	283	B	Ro3	Moderately narrow	~10mm	~95%	1	R	~160°	Gentle	~6m	Wavy	~5m	Clast supported (Crackle (~95%), Angular, MW, Strong, Veneer, Dark brown, Sand, Very soft, NP) No precipitation	Dry	-41.0307	174.871	Terminates between SR5 and the SR running parallel to SR5	
6	BSH	65	346	323	B	Ro3	Narrow	~5mm	~99%	1	D	~130°	Gentle	~1m	Wavy	~2.4m	Clast supported (Rock (~99%), Angular, MW, Moderately strong, Stained, Dark brown, Sand, Very soft, NP) No precipitation	Dry	-41.0307	174.871	Terminates at SR running parallel to SR5 and SR7	
7	BSH	59	303	281	B	Ro3	Moderately narrow	~15mm	~95%	0	C	~135°	Gentle	~2.5m	Wavy	~14m	Clast supported (Crackle (~95%), Angular, MW, Moderately strong, Veneer, Dark brown, Sand, Very soft, NP) No precipitation	Dry	-41.0305	174.8708	Terminates against SR5	
8	JN	90	253	230	B	Ro3	Tight	~0mm		1	D	~180°	Gentle		Planar	~3m		Dry	-41.0307	174.8712	Cuts at SR running parallel to SR5	
9	SR	86	87	244	B	Ro3				1	D	~180°	Gentle		Planar	~3m		Dry	-41.0306	174.8709	Cuts at SR running parallel to SR5	
11	SR	78	276	253	B	Ro3				1	D	~180°	Gentle		Planar	~3m		Dry	-41.0307	174.8709	Terminates at BSH 6	
12	SR	84	257	234	B	Ro3				1	D	~180°	Gentle		Planar	~4m		Dry	-41.0307	174.8709	Terminates at JN13	
13	JN	21	106	84	B	Ro3	Narrow	~5mm	~95%	1	D	~180°	Gentle		Planar	~2m	Clast supported (Crackle (~95%), Angular, MW, Strong, Veneer, Dark brown, Sand, Very soft, NP) No precipitation	Dry	-41.0306	174.8709	Termination obscured by debris presumed terminates at JN11	
14	JN	39	16	354	B	Ro3	Very narrow	~2mm	~99%	1	D	~180°	Gentle		Planar	~2m	Clast supported (Rock (~99%), Angular, MW, Strong, Veneer, Dark brown, Sand, Very soft, NP) No precipitation	Dry	-41.0307	174.8709	Termination obscured by debris presumed terminates at JN11	
15	SR	76	264	242	B	Ro4			~99%	1	D				Stepped	~12m	Clast supported (Rock (~99%), Angular, -, Strong, Stained, Dark brown, Sand, Very soft, NP) No precipitation	Dry	-41.0306	174.8709	Cliff face	
1	JN	89	1	339	A	Ro3	Narrow	~3mm	~100%	1	D				Stepped	~2.8m	Clast Supported (Rock (~100%), Angular, MW, Strong, Stained) No precipitation	Dry	-41.0305	174.8716	Cuts across JN3	#2
2	SR	89	231	208	A	Ro3	Moderately narrow	~10mm	~100%	1	D	~170°	Gentle	~3m	Wavy	~6m	Clast Supported (Rock (~100%), Angular, MW, Strong, Veneer) No precipitation	Dry	-41.0305	174.8716	Failure plain with SR4. Terminates at SR1.	
4	SR	48	58	35	A	Ro4	Moderately wide	~20mm	~100%	1	R	~170°	Gentle	~1.4m	Wavy	~2m	Clast Supported (Rock (~100%), Angular, MW, Strong, Stained) Elongated white precipitation	Dry	-41.0305	174.8716	Failure plain with SR2. No obvious cutting characteristic	
3	JN	59	286	264	A	Ro3			~100%	0	C	~170°	Gentle	~2m	Wavy	~2m		Dry	-41.0305	174.8719	Terminates at SR2	
5	SR	71	56	33	A	Ro4	Moderately wide	~20mm	~100%	1	D	~160°	Gentle	~3m	Wavy	~4m	Clast Supported (Rock (~100%), Angular, MW, Strong, Veneer) No precipitation	Dry	-41.0307	174.872	Terminates at SR6	
6	SR	42	283	260	A	Ro4	Moderately narrow	~10mm	~100%	2	D	~150°	Gentle	~3m	Wavy	~2.5m	Clast Supported (Rock (~100%), Angular, MW, Strong, Stained) No precipitation	Dry	-41.0306	174.8715	Terminates at SR7 and JN3	
3	JN	79	82	60	A	Ro3	Tight	~0mm	~100%	0	C	~170°	Gentle	~2m	Wavy	~2m		Dry	-41.0306	174.8716	Terminates at SR13	
7	SR	31	49	26	A	Ro4	Moderately wide	~20mm	~100%	1	R	~160°	Gentle	~3m	Wavy	~7m	Clast Supported (Rock (~100%), Angular, MW, Strong, Coating) No precipitation	Dry	-41.0306	174.8715	Terminates at SR6	
8	SR	50	214	191	A	Ro5	Moderately narrow	~10mm	~90%	1	D	~180°	Gentle		Planar	~1m	Clast Supported (Crackle (~90%), Angular, MW, Strong, Veneer; Light grey, Sand, Soft, NP) No precipitation	Dry	-41.0305	174.8714	Terminates at BSH10	
9	SR	24	39	17	A	Ro3	Moderately narrow	~15mm	~100%	1	R	~160°	Gentle	10m	Wavy	~5m	Clast Supported (Rock (~100%), Angular, MW, Strong, Stained) No precipitation	Dry	-41.0306	174.8716	Terminates at BSH10	
10	BSH	34	16	354	A	Ro2	Moderately narrow	~15mm	~100%	1	D	~160°	Gentle	~15m	Wavy	~5m	Clast Supported (Rock (~100%), Angular, MW, Strong, Coating) No precipitation	Dry	-41.0307	174.8716	Terminates at SR14	
10	BSH	35	43	21	A	Ro2	Moderately narrow	~15mm	~100%	1	D	~160°	Gentle	~15m	Wavy	~5m	Clast Supported (Rock (~100%), Angular, MW, Strong, Coating) No precipitation	Dry	-41.0306	174.8715	Terminates at SR14	
11	SR	65	181	159	A	Ro3	Moderately wide	~25mm	~100%	2	D	~180°	Gentle		Planar	~1.5m	Clast Supported (Rock (~100%), Angular, MW, Strong, Veneer) No precipitation	Dry	-41.0307	174.8716	Terminates at BSH10	
12	BSH	31	68	46	A	Ro3	Moderately wide	~20mm	~100%	0	C	~160°	Gentle	~3m	Wavy	~1.5m	Clast Supported (Rock (~100%), Angular, MW, Strong, Coating) No precipitation	Dry	-41.0306	174.8714	Obscured by beach	
13	JN	87	91	69	A	Ro2	Moderately wide	~20mm	~100%	2	D	~180°	Gentle		Planar	~3m	Clast Supported (Rock (~100%), Angular, MW, Strong, Veneer) No precipitation	Dry	-41.0306	174.8715	Terminates against BSH10	

14	SR	69	281	258	A	Ro4	Moderately narrow	~10mm	~100%	0	C	~160°	Gentle	~10m	Wavy	~8m		Clast Supported (Rock (~100%), Angular, MW, Strong, Coating) No precipitation	Dry	-41.0307	174.8715	Cuts across bedding shears
15	SR	82	176	153	A	Ro4	Moderately wide	~20-40mm	~90%	0	C	~140°	Gentle	~15m	Wavy	~8m		Clast Supported (Crackle (~90%), Angular, MW, Strong, Veneer; Light grey, Sand, Soft, NP) No precipitation	Dry	-41.0307	174.8715	Cuts across bedding shears
16	SR	40	35	13	A	Ro4	Moderately narrow	~10mm	~95%	1	D	~150°	Gentle	~6m	Wavy	~3.5m		Clast Supported (Crackle (~95%), Angular, MW, Strong, Stained; Light blue black, Sand, Soft, NP) No precipitation	Dry	-41.0307	174.8715	Terminates against SR14. Cuts across SR15
17	BSH	39	30	8	A	Ro3	Moderately narrow	~8mm	~100%	1	D	~160°	Gentle	~3m	Wavy	~6m	~0.2m	Clast Supported (Rock (~100%), Angular, MW, Strong, Veneer) No precipitation	Dry	-41.0307	174.8715	Offset by SR18
17	BSH	52	56	34	A	Ro3	Moderately wide	~20mm	~100%	1	D	~160°	Gentle	~3m	Wavy	~6m	~0.3m	Clast Supported (Rock (~100%), Angular, MW, Strong, Coating) No precipitation	Dry	-41.0307	174.8716	Offset by SR18
18	SR	88	323	301	A	Ro3	Moderately wide to Wide	~20-100mm	~95%	1	D	~130°	Gentle	~3m	Wavy	~8m		Clast Supported (Crackle (~95%), Angular, MW, Strong, Veneer; Light blue black, Sand, Soft, NP) No precipitation	Dry	-41.0307	174.8715	
	BG	20	13	351	A					1	D	~160°	Open	~7m	Wavy	~15m	~0.3m		Dry	-41.0309	174.8714	Wait failure
	BG	40	279	257	A	Ro2	Very narrow	~1mm	~99%	1	D	~120°	Open	~7m	Curved	~8m	~0.2m	Clast Supported (Rock (~99%)), Angular, MW, Moderately strong, Clean) No precipitation	Dry	-41.0308	174.8715	Fold terminates against Fault
	BG	37	289	267	A	Ro2	Very narrow	~1mm	~99%	1	D	~120°	Open	~7m	Curved	~8m	~0.2m	Clast Supported (Rock (~99%)), Angular, MW, Moderately strong, Clean) No precipitation	Dry	-41.0308	174.8715	Fold terminates against Fault
	BSH	48	263	241	A	Ro2	Moderately wide	~10mm	~95%	1	D	~120°	Open	~7m	Curved	~6m	~0.2m	Clast Supported (Crackle (~95%), Angular, MW, Moderately strong, Clean; Dark blue black, Sand, Very soft, NP) No precipitation	Dry	-41.0309	174.8716	Fold terminates against Fault
	BSH	39	313	291	A	Ro2	Moderately wide	~25mm	~95%	1	D	~120°	Open	~7m	Curved	~7m	~0.2m	Clast Supported (Crackle (~95%), Angular, MW, Moderately strong, Clean; Dark blue black, Sand, Very soft, NP) No precipitation	Dry	-41.0309	174.8715	Fold terminates against Fault
	BSH	34	321	299	A	Ro2	Moderately wide	~25mm	~95%	1	D	~120°	Open	~7m	Curved	~8m	~0.2m	Clast Supported (Crackle (~95%), Angular, MW, Moderately strong, Clean; Dark blue black, Sand, Very soft, NP) No precipitation	Dry	-41.0309	174.8715	Fold terminates against Fault
	BSH	43	314	292	A	Ro2	Moderately wide	~15mm	~95%	1	D	~120°	Open	~7m	Curved	~8m	~0.2m	Clast Supported (Crackle (~95%), Angular, MW, Moderately strong, Clean; Dark blue black, Sand, Very soft, NP) No precipitation	Dry	-41.0309	174.8715	Fold terminates against Fault
	BSH	42	358	336	A	Ro3	Moderately wide	~10mm	~95%	1	D	~120°	Open	~7m	Curved	~8m	~0.3m	Clast Supported (Crackle (~95%), Angular, MW, Moderately strong, Clean; Dark blue black, Sand, Very soft, NP) No precipitation	Dry			Fold terminates against Fault
1	SR	58	285	262	B	Ro5	Very wide	<200mm	~99%	0	C	~170°	Gentle	~2m	Wavy	~14m		Clast supported (Rock (~99%), Angular, MW, Very strong, Stained)Elongated white precipitation gravel sized	Dry	-41.0308	174.8706	Cross cuts SR2
2	SR	6	255	232	B	Ro4	Wide	~150mm	~99%	1	D	~160°	Gentle	~6m	Wavy	~3m		Clast supported (Rock (~99%), Angular, MW, Very strong, Stained)No precipitation	Dry	-41.0307	174.8705	Cross cuts SR1
3	SR	25	338	315	B	Ro3	Moderately narrow	~10mm	~99%	1	D	~160°	Gentle	~4m	Curved	~2.5m		Clast supported (Rock (~99%), Angular, MW, Strong, Stained)Elongated angular white precipitation gravel 5mm thick sized	Dry	-41.0306	174.8709	Terminates at SR2
4	BSH	51	312	290	B	Ro4	Moderately narrow	~8mm	~95%	1	D	~180°	Gentle		Planar	~1m	~1.2m	Clast supported (Crackle (~95%), Angular, MW, Strong, Stained; Dark blue brown, Silty sand, Very soft, NP)Elongated angular white precipitation 5mm thick	Dry	-41.0306	174.871	Terminates at SR3
5	JN	1	57	35	B	Ro5	Narrow	~2-5mm	~99%	1	D	~150°	Gentle	~0.8m	Wavy	~2m	~1.4m	Clast supported (Rock (~99%), Angular, SW, Very strong, Stained)No precipitation	Dry	-41.0306	174.871	Terminates between BSH9 and SR3
6	SR	36	77	54	B	Ro3	Very Narrow	0-1mm	~99%	2	D	~180°	Gentle		Planar	~1m		Clast supported (Rock (~99%), Angular, SW, Very strong, Stained)No precipitation	Dry	-41.0308	174.8708	Terminates between BSH9 and SR3
7	SR	69	113	90	B	Ro4	Moderately narrow	~20mm	~95%	2	D	~150°	Gentle	~1.5m	Wavy	~3m	~0.8m	Clast supported (Crackle (~95%), Angular, MW, Strong, Stained; Dark brown, Sand, Very soft, NP)No precipitation	Dry	-41.0307	174.8708	Cross cuts SR12 and terminates at SR2
7	SR	10	249	227	B	Ro4	Moderately narrow	~20mm	~95%	2	D	~150°	Gentle	~1.5m	Wavy	~3m	~0.8m	Clast supported (Crackle (~95%), Angular, MW, Strong, Stained; Dark brown, Sand, Very soft, NP)No precipitation	Dry	-41.0307	174.8708	Cross cuts SR12 and terminates at SR2
8	SR	89	337	314	B	Ro4	Moderately narrow	~10mm	~95%	1	D				Irregular	~5.5m	~1.5m	Clast supported (Crackle (~95%), Angular, MW, Strong, Stained; Dark brown, Sand, Soft, NP)White sand sized flecks of precipitation	Dry	-41.0308	174.8708	Terminates at SR2
9	BSH	69	301	278	B	Ro3	Moderately wide	~25mm	~99%	0	C	~170°	Gentle	~9m	Wavy	~2.5m	~0.3m	Clast supported (Rock (~99%), Angular, MW, Strong, Stained)Elongated white precipitation gravel sized	Dry	-41.0307	174.8708	Terminates against SR2
9	BSH	61	315	292	B	Ro3	Moderately narrow	~15mm	~99%	0	C	~170°	Gentle	~9m	Wavy	~15m	~0.3m	Clast supported (Rock (~99%), Angular, MW, Strong, Stained)Elongated and tabulated white precipitation coarse gravel sized and larger	Dry	-41.0307	174.8709	Terminates against SR2
10	SR	65	307	285	B	Ro5	Moderately narrow	~10mm	~99%	1	R	~170°	Gentle	~30m	Wavy	~8m	~0.6m	Clast supported (Rock (~99%), Angular, SW, Very strong, Stained)No precipitation	Dry	-41.0307	174.8709	Terminates in rock
11a	JN	84	334	312	B	Ro4-3	Tight	~0mm	~99%	1	D	~180°	Gentle		Planar	~0.8m	~0.5m		Dry	-41.0307	174.8708	
11b	JN	77	291	269	B	Ro4-3	Tight	~0mm	~99%	1	D	~180°	Gentle		Planar	~0.8m	~0.5m		Dry	-41.0307	174.8708	Terminates against BSH22
9b	BSH	66	338	316	B	Ro3	Moderately wide	~30mm	~95%	2	D	~170°	Gentle	~9m	Wavy	~2.5m	~1.2m	Clast supported (Crackle (~95%), Angular, MW, Strong, Stained; Dark blue brown, Silty Sand, Very soft, NP)Elongated white precipitation gravel sized	Dry	-41.0307	174.8708	Terminates against SR2
12	SR	85	232	210	B	Ro3	Narrow	~5mm	~99%	1	R	~150°	Gentle	~3m	Wavy	~4m		Clast supported (Rock (~99%), Angular, MW, Strong,	Dry	-41.0306	174.8709	Terminates against SR1 and

#1

12b	SR	71	337	315	B	Ro3	Narrow	~5mm	~95%	1	R	~100°	Open	~3m	Curved	~4m		Clast supported (Crackle (~95%),Angular, MW, Strong, Stained; Dark brown, Sand, Soft, NP)No precipitation	Dry	-41.0307	174.8708	Transitions into SR12b Terminates in rock and transitions from SR12
13	SR	43	292	269	B	Ro3	Moderately wide	~8mm	~99%	2	D	~170°	Gentle	~1.5m	Wavy	~10m		Clast supported (Rock (~99%),Angular, MW, Strong, Stained)No precipitation	Dry	-41.0307	174.8709	Terminates against SR2 and cross cuts a BSH9
14	BSH	55	316	293	B	Ro4	Moderately narrow	~15mm	~99%	1	R	~170°	Gentle	~8m	Wavy	~3m	~0.2m	Clast supported (Rock (~99%),Angular, MW, Strong, Stained)Elongated white precipitation gravel sized	Dry	-41.0307	174.8708	Terminates in rock
14	BSH	45	318	296	B	Ro4	Moderately narrow	~10mm	~99%	1	R	~170°	Gentle	~8m	Wavy	~3m	~1.2m	Clast supported (Rock (~99%),Angular, MW, Strong, Stained)White sand sized flecks of precipitation	Dry	-41.0307	174.8708	Terminates in rock and cross cuts SR16
15	SR	30	63	40	B	Ro4	Moderately narrow	~20mm	~99%	1	D				Irregular	~1.2m		Clast supported (Rock (~99%),Angular, MW, Strong, Stained)White sand sized flecks of precipitation	Dry	-41.0306	174.8708	Cross cuts some BSH14
16	SR	46	136	114	B	Ro3	Very Narrow to Narrow	~1-3mm	~99%	1	D	~150°	Gentle	~1m	Wavy	~2.5m	~0.8m	Clast supported (Rock (~99%),Angular, MW, Strong, Stained)No precipitation	Dry	-41.0308	174.8709	Cross cuts BSH14 and some terminations against SR16
17	JN	67	291	269	B	Ro4	Tight	~0mm	~100%	1	D	~170°	Gentle	~1m	Wavy	~1m	~0.3m		Dry	-41.0307	174.8709	Failure plane for wedge failure. Presume joins up with SR36 despite inability to see the join.
18	BSH	51	299	277	B	Ro3	Moderately narrow	~8mm	~95%	1	O	~160°	Gentle	~4m	Wavy	~3m	~2.5m	Clast supported (Crackle (~95%),Angular, MW, Strong, Coating; Dark blue brown, Silty sand, Very soft, NP)Elongated white precipitation gravel sized	Dry	-41.0308	174.871	SR21 Cross cuts
19	JN	49	292	270	B	Ro3	Tight	~0mm		2	D	~170°	Gentle	~1.5m	Wavy	~2m	~0.4m		Dry	-41.0308	174.871	Terminates against SR20
20	SR	89	296	273	B	Ro3	Very wide	~300mm	~99%	1	D	~160°	Gentle	~3m	Wavy	~10m	~1m	Clast supported (Rock (~99%),Angular, MW, Strong, Stained)No precipitation	Dry	-41.0307	174.8709	SR13 cross cuts, dilated
26	BSH	67	303	280	B	Ro3	Narrow	~2mm	~95%	1	D	~170°	Gentle	~8m	Wavy	~4m	~5m	Clast supported (Crackle (~95%),Angular, MW, Strong, Coating; Dark blue brown, Silty sand, Very soft, NP)White sand sized flecks of precipitation	Dry	-41.0308	174.8709	Terminates against SR26
25	SR	75	214	192	B	Ro5				0	O	~160°	Gentle	~5m	Wavy	~2m			Dry	-41.0308	174.871	Failure plane
27	SR	36	11	348	B	Ro3	Moderately narrow	~10mm		1	D	~180°	Gentle		Planar	~2m			-41.0308	174.8709	Obscured by debris	
30	SR	31	6	344	B	Ro3	Moderately narrow	~10mm	~95%	0	O	~160°	Gentle	~9m	Curved	~1.5m	~2m	Clast supported (Crackle (~95%),Angular, MW, Strong, Coating; Dark brown, Sand, Very soft, NP)White sand sized flecks of precipitation	Dry	-41.0308	174.8709	Cross cuts SR33
33	SR	82	55	33	B	Ro4	Narrow to Moderately narrow	~5-15mm	~99%	0	O	~180°	Gentle		Planar	~1.5m		Clast supported (Rock (~99%),Angular, SW, Very strong, Veneer)No precipitation	Dry	-41.0308	174.8709	Cross cuts SR30 and terminates at SR29
28	SR	83	238	216	B	Ro3				1	O	~180°	Gentle		Planar	~2.5m				-41.0309	174.8709	Failure plane
29	SR	83	257	235	B	Ro4				1	O	~160°	Gentle	~3m	Wavy	~8m				-41.0309	174.8709	Failure plane
31	SR	64	192	169	B	Ro5	Moderately narrow	~10mm gapped then open		1	D	~150°	Gentle	~30m	Curved	~12m				-41.0309	174.8709	Terminates at SR29
32	BSH	37	31	9	B	Ro4	Narrow	~5mm		1	D	~150°	Gentle	~3m	Wavy	~2.5m	~0.4m			-41.0308	174.8709	Terminates against SR31
24	SR	81	266	243	B	Ro4				1	D	~160°	Gentle		Curved	~6m				-41.0308	174.8709	Failure plane
23	SR	72	233	211	B	Ro5				1	D				Stepped	~4m				-41.0308	174.8709	Failure plane
22	SR	84	39	16	B	Ro4	Very wide	>~200mm		1	D	~160°	Gentle	~2.5m	Wavy	~5m				-41.0308	174.8709	Terminates against SR18
21	SR	78	112	89	B	Ro4	Wide	~80mm		1	D	~150°	Gentle		Curved	~3m				-41.0308	174.8709	Terminates against SR18
10	SR	86	89	67	B	Ro4	Moderately wide	~50-30mm	~99%	0	O	~180°	Gentle		Planar	~2m		Clast supported (Rock (~99%)),Angular, MW, Strong, Clean; Dark blue grey, Sand, Soft, NP) No precipitation	Damp	-41.0314	174.8704	
9	JN	85	4	341	B	Ro3	Tight	~0mm		2	R	~180°	Gentle		Planar	~3m	~0.5-0.8		Dry	-41.0313	174.8705	
7a	BSH	49	308	286	B	Ro3	Moderately narrow to moderately wide	~20mm	~30%	1	R	~180°	Gentle	~6m	Planar	~2.5m	~3m	Matrix supported (Chaotic (~30%)),Angular, CW, Weak to Very Weak, Stained; Light blue grey, clayey Sand, Soft, LP) No precipitation	Damp	-41.0313	174.8703	
7b	JN	46	128	105	B	Ro2	Moderately narrow to moderately wide	~20mm	~90%	0	C	~150°	Gentle	~15m	Curved	~3m	~0.8m	Clast supported (Crackle (~90%)),Angular, MW, Strong, Veneer; Dark blue grey, sandy Clay, Very soft, NP) No precipitation	Damp	-41.0314	174.8703	Cross cuts JN5
6	SR	75	298	276	B	Ro3	Moderately narrow	~10mm	~95%	0	O	~170°	Gentle	~4m	Wavy	~4m		Clast supported (Crackle (~95%)),Angular, HW-MW, Moderately strong, Clean; Light grey, Sand, Very soft, NP) Minor elongated sub angular white precipitation	Minor seepage - likely due to coastline	-41.0314	174.8703	
5	JN	43	308	286	B	Ro3	Very narrow	0-2mm		2	R	~180°	Gentle		Planar	~4m	~0.5-0.6m		Dry	-41.0313	174.8703	Cross cuts SR7b and SR4
2b	SR	85	148	125	B	Ro3	Moderately narrow	~15mm	~99%	1	D	~170°	Gentle	~1.5m	Wavy	~2m		Clast supported (Rock (~99%)),Angular, HW-MW, Moderately strong, Stained)	Damp	-41.0313	174.8703	Terminates against BSH1 also cross cuts SR2 and JN3b
3b	JN	78	264	242	B	Ro3	Tight	~0mm		2	D	~180°	Gentle		Planar	~1m	~0.8m		Dry	-41.0313	174.8703	Terminates against SR2
2	SR	16	120	98	B	Ro3	Narrow	~5mm	~99%	1	R	~160°	Gentle	~8m	Curved	~3m		Clast supported (Rock (~99%)),Angular, HW-MW, Moderately strong, Stained; Light grey, Sand, Soft, NP) Minor amounts of small sub angular white precipitation	Dry	-41.0313	174.8704	Cross cuts SR2b
3	JN	74	126	104	B	Ro3	Tight	~0mm		2	R	~180°	Gentle		Planar	~1m	~0.8m		Dry	-41.0313	174.8703	
4	SR	84	134	111	B	Ro2	Moderately narrow to moderately wide	~20mm	~95%	0	C	~150°	Gentle	~15m	Curved	~4.5m		Clast supported (Crackle (~95%)),Angular, MW, Strong, Veneer; Dark blue grey, sandy Clay, Very soft, NP) No precipitation	Damp	-41.0313	174.8704	Cross cuts JN5
1	BSH	73	290	268	B	Ro3	Moderately narrow	~15mm	~99%	0	C	~170°	Gentle	~6m	Wavy	~2.5m	~0.2m	Clast supported (Rock (~99%)),Angular, MW, Moderately strong, Veneer)	Damp	-41.0313	174.8703	

	JN	77	243	221	B											~0.8m			-41.0313	174.8704		
	JN	66	157	135	B											~0.7m			-41.0312	174.8705		
	JN	48	110	88	B											~0.8m			-41.0313	174.8704		
	JN	35	325	303	B											~0.5m			-41.0313	174.8704		
	JN	79	232	209	B											~0.8m			-41.0313	174.8704		
	JN	83	171	149	B											~0.8m			-41.0313	174.8704		
	JN	73	207	184	B											~0.8m			-41.0313	174.8704		

F.4 Wairaka Point Graphs

Defect and rock mass results from Wairaka Point. Results are presented in graphs. Where percentages are used they display the respective occurrence of the dependent variable assessed.

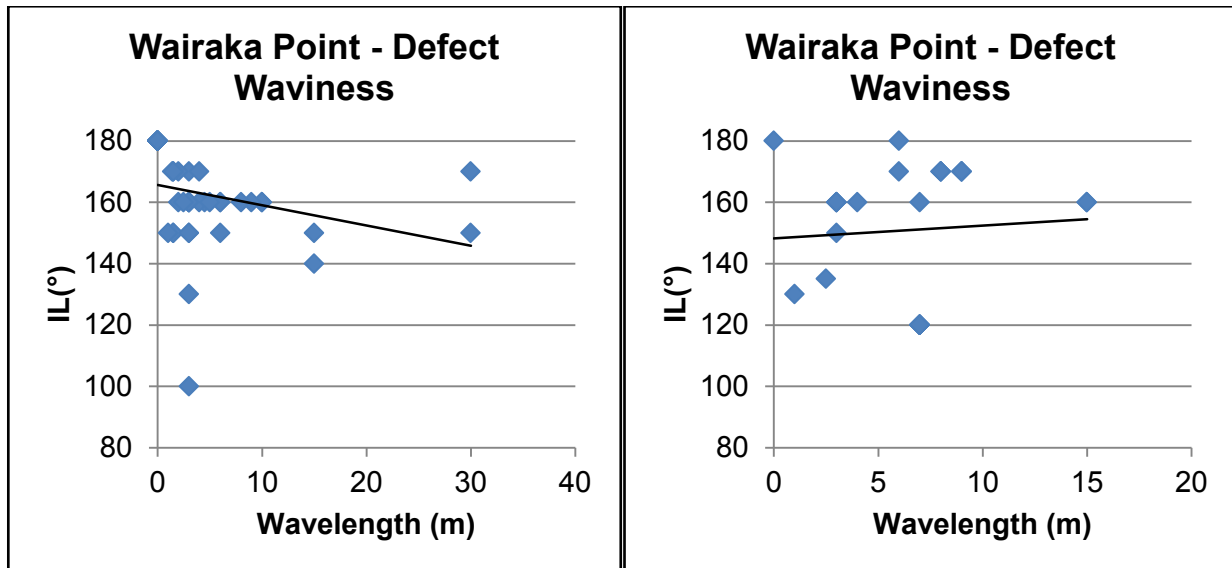
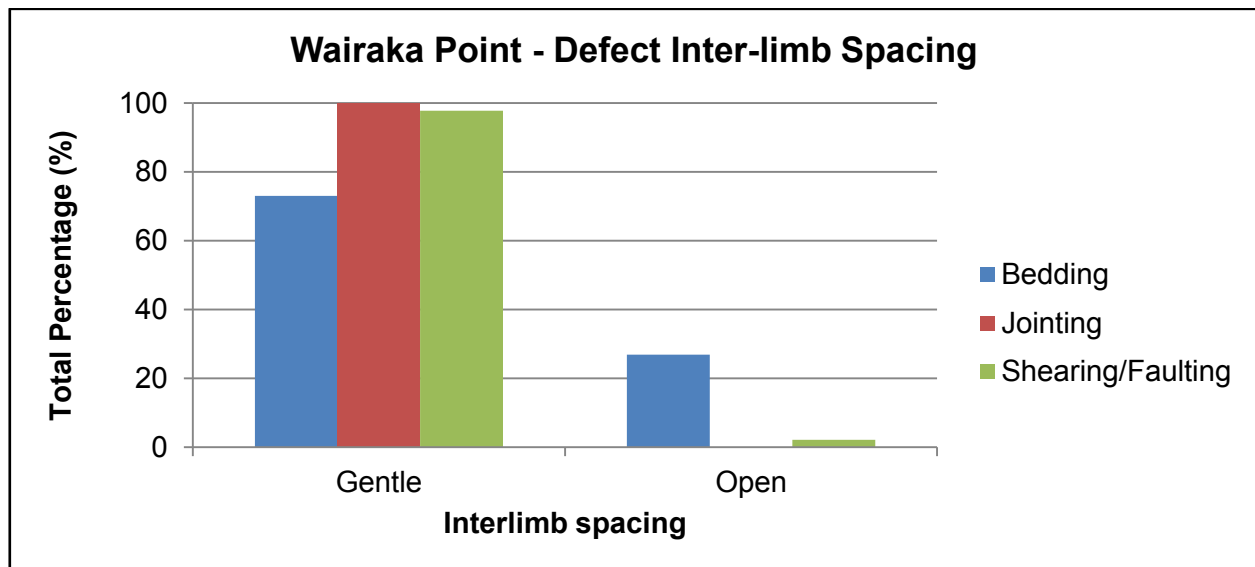
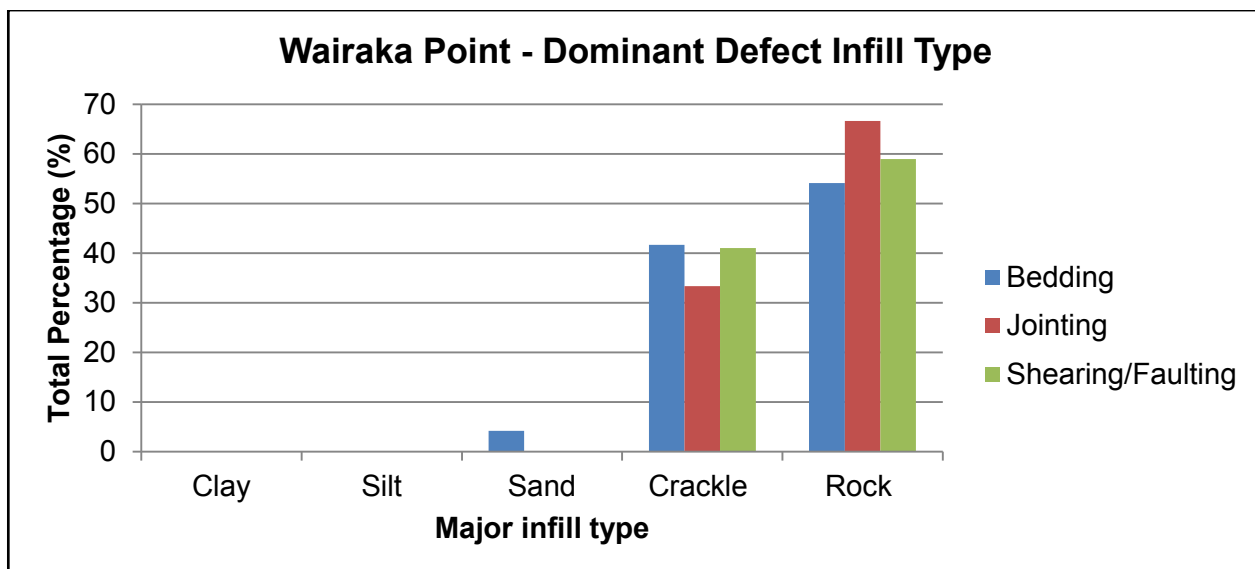
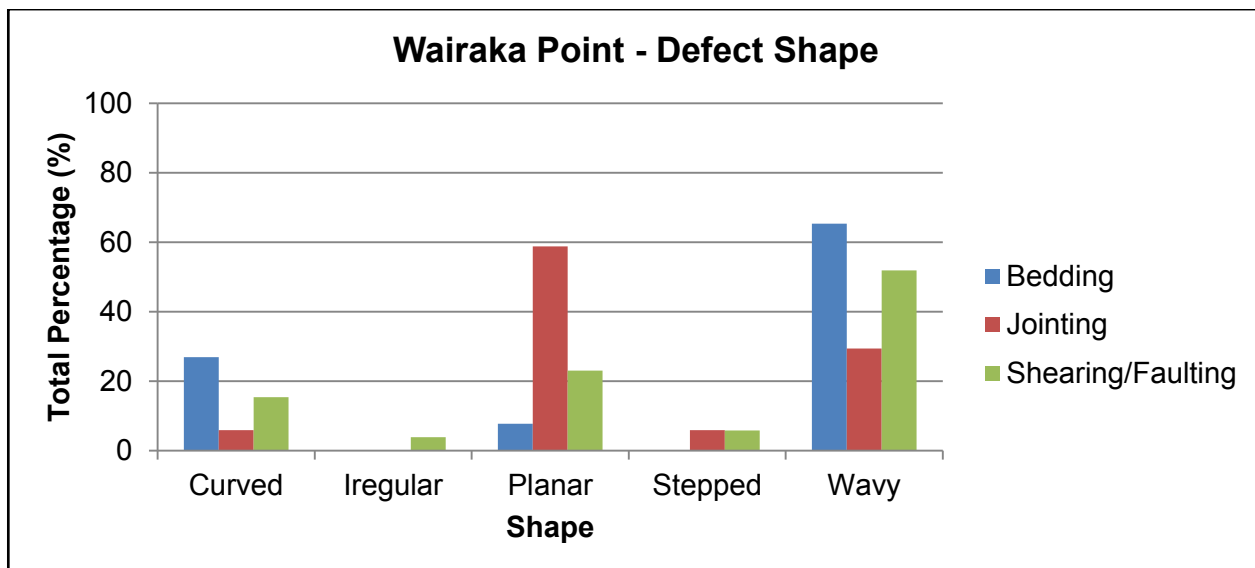
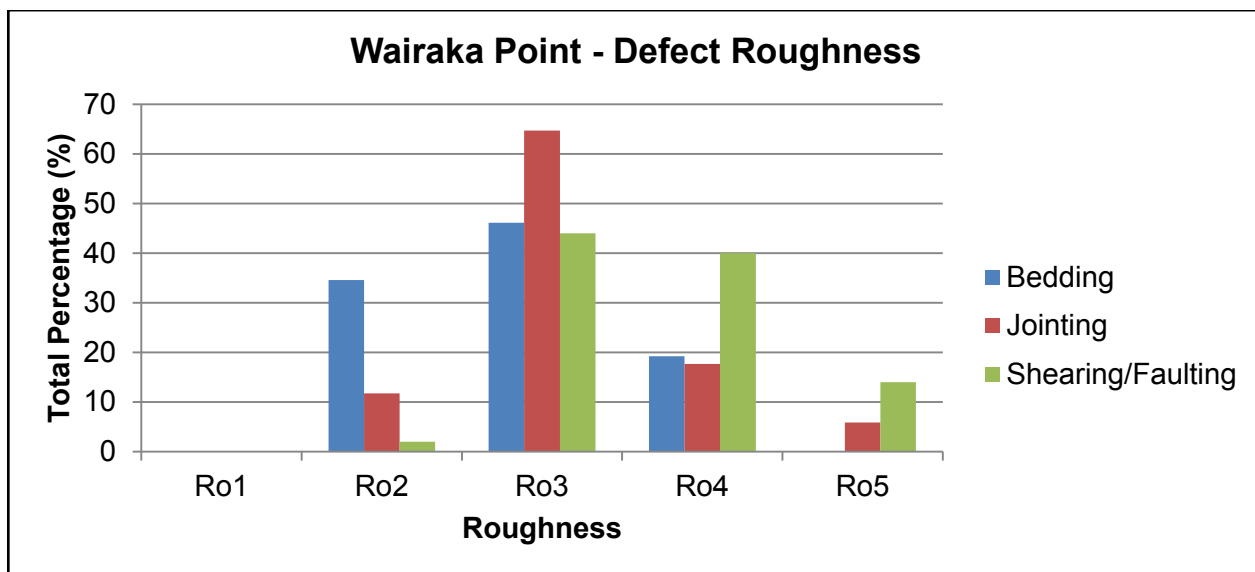
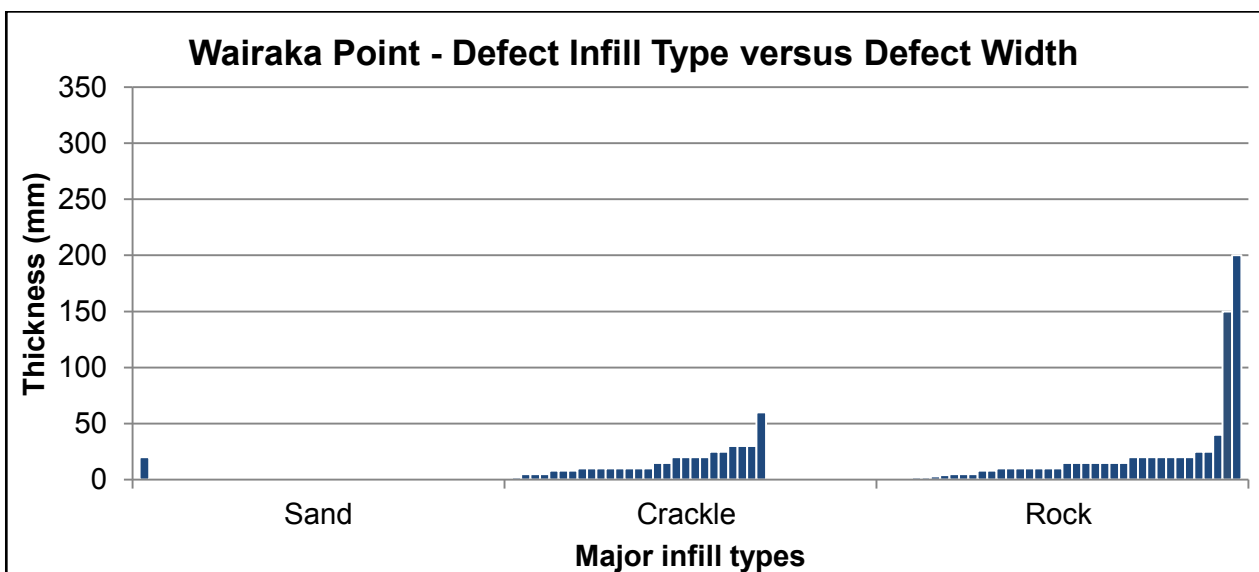
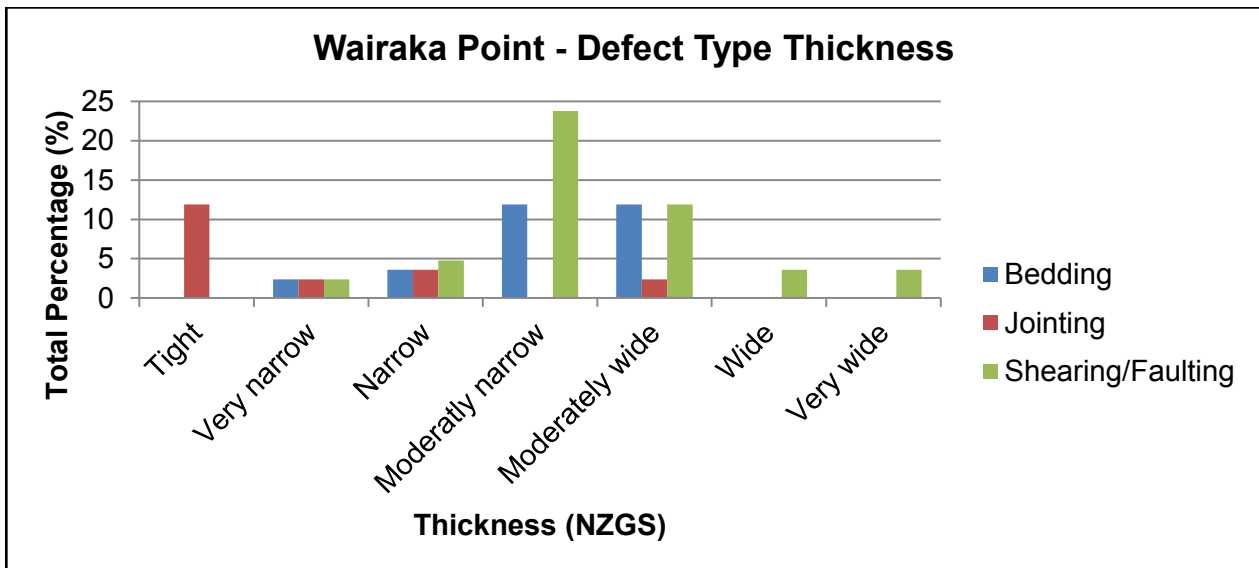
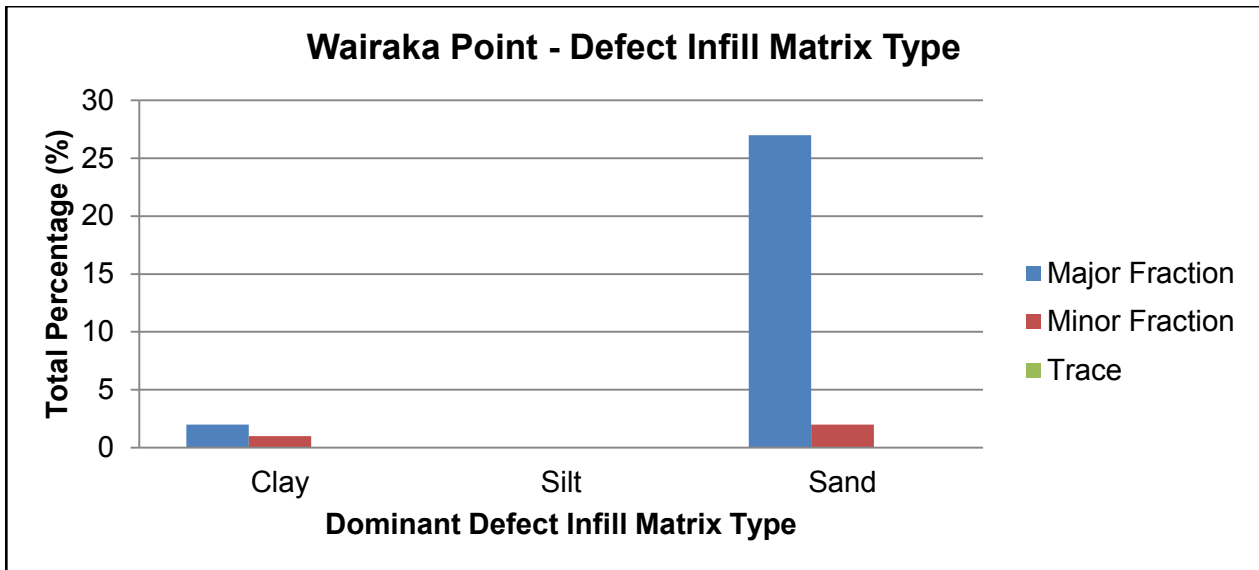
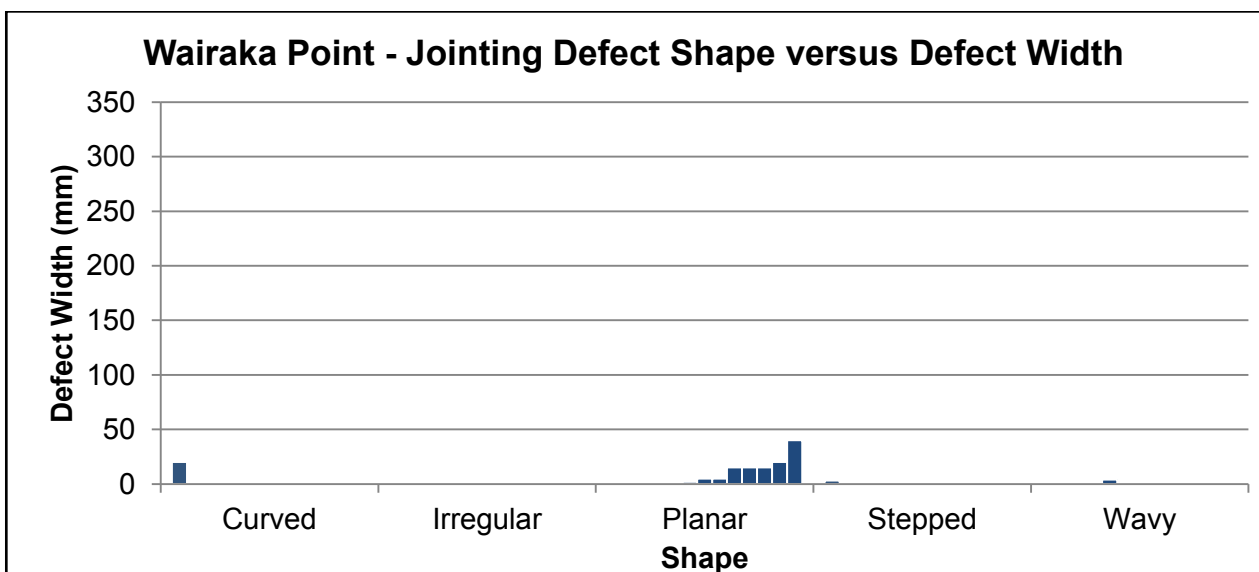
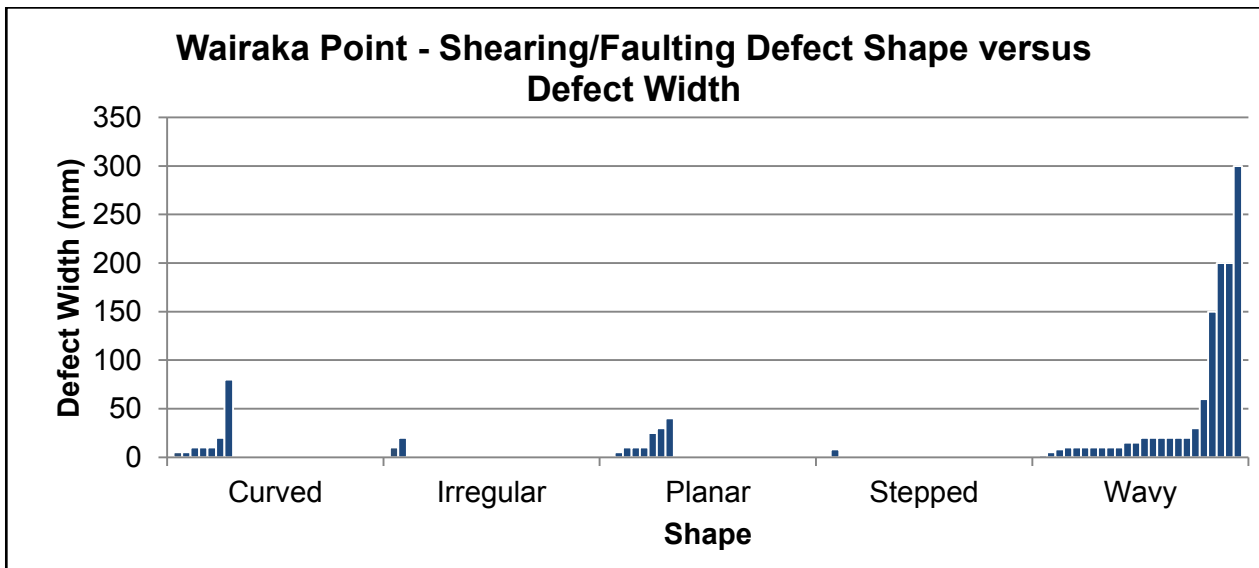
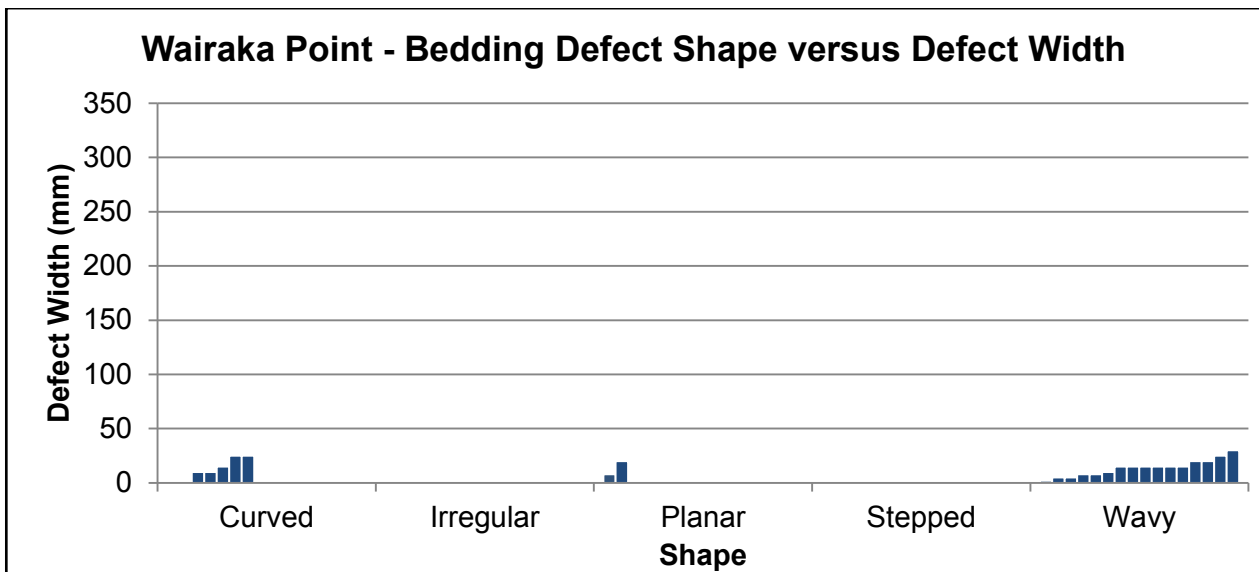


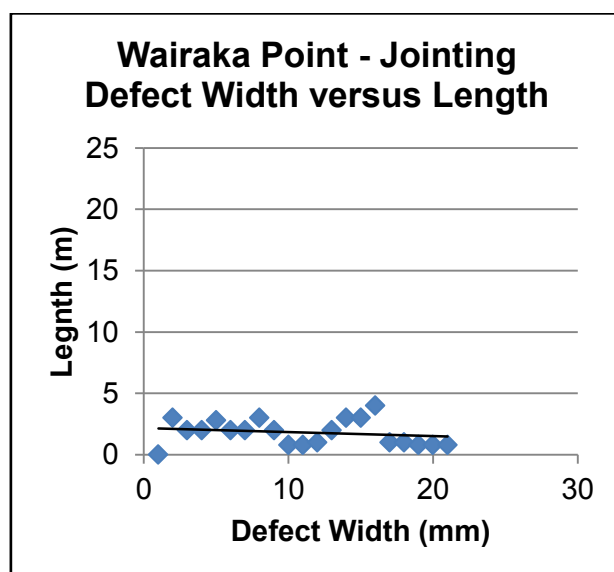
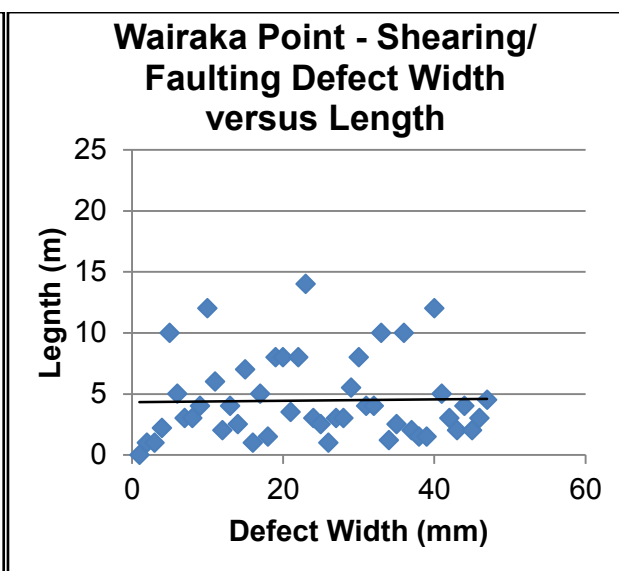
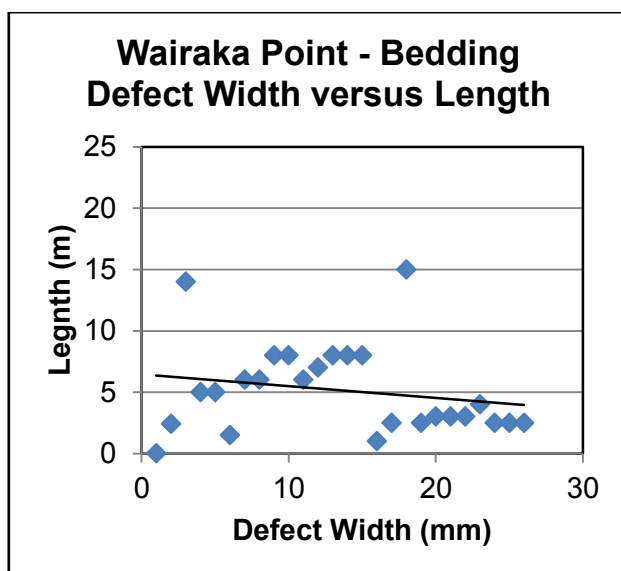
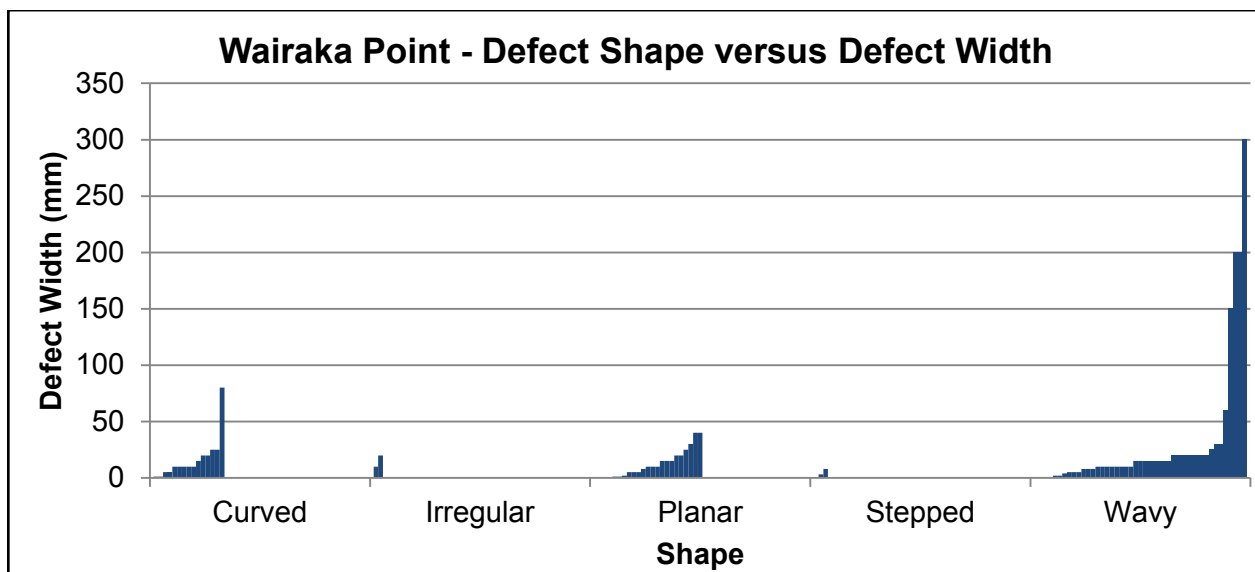
Figure F.4.1: Graphs displaying the Waviness of the Bedding (Right) and Shearing/Faulting (Left) at Wairaka Point

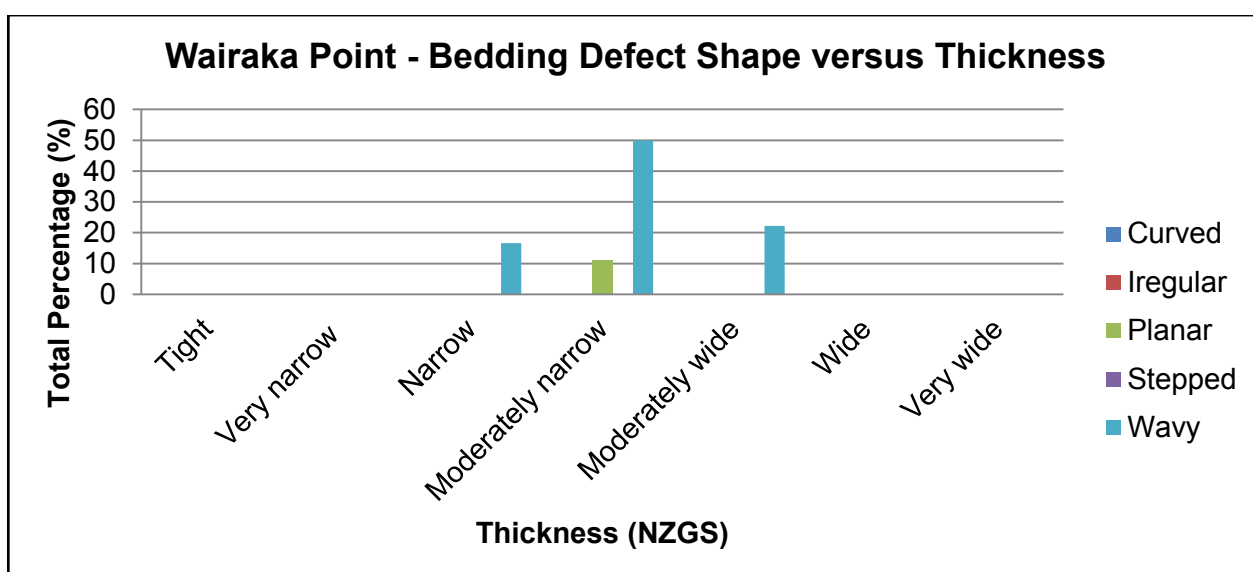
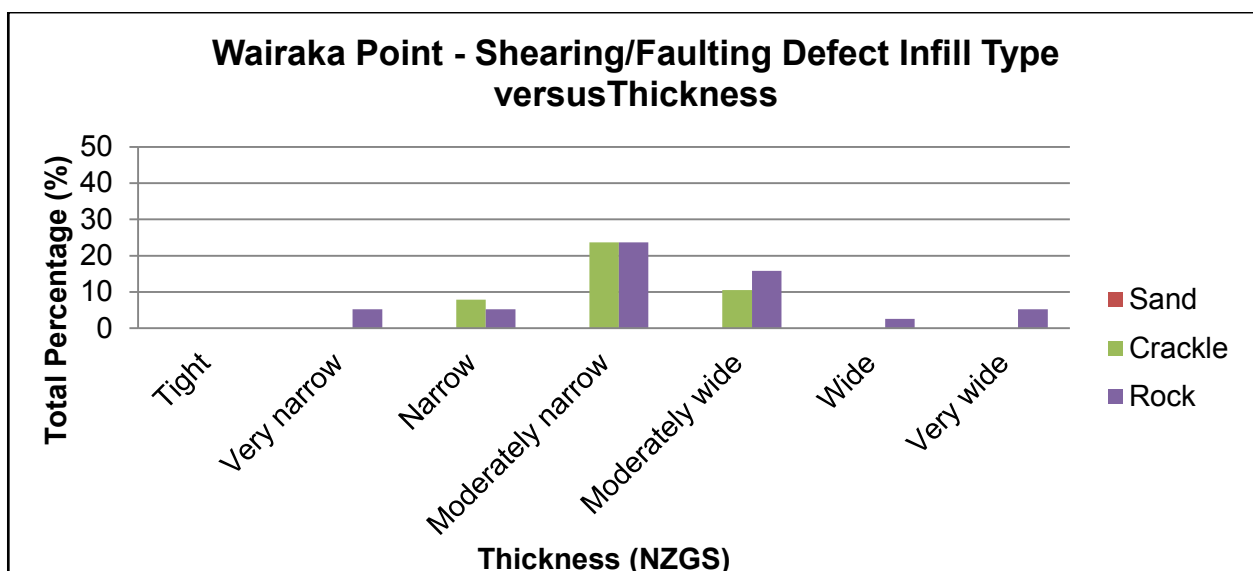
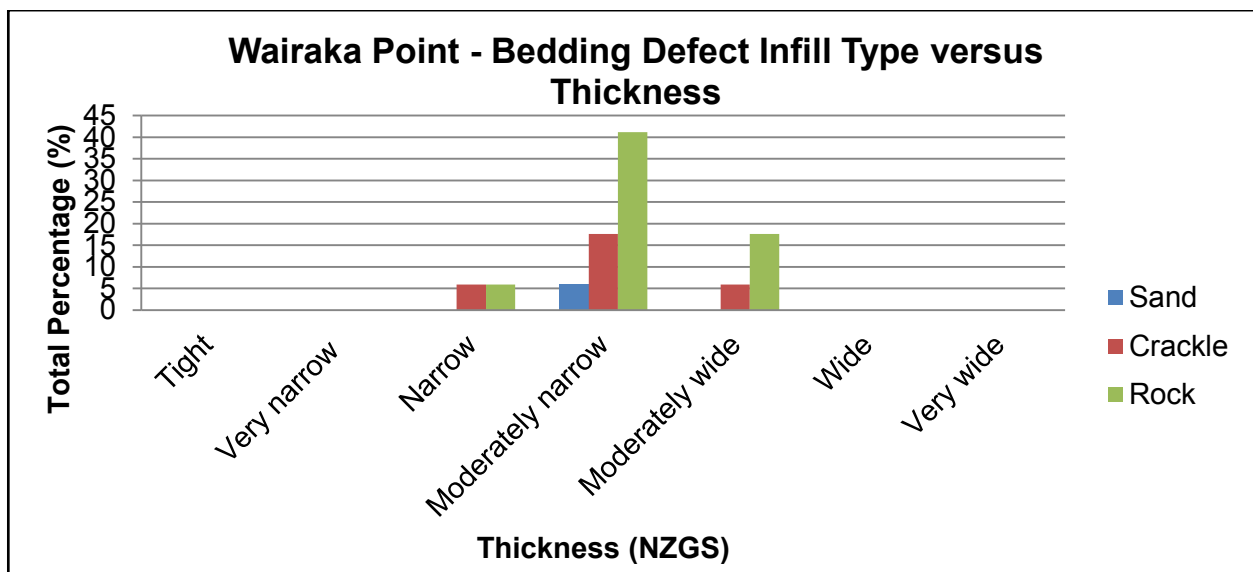


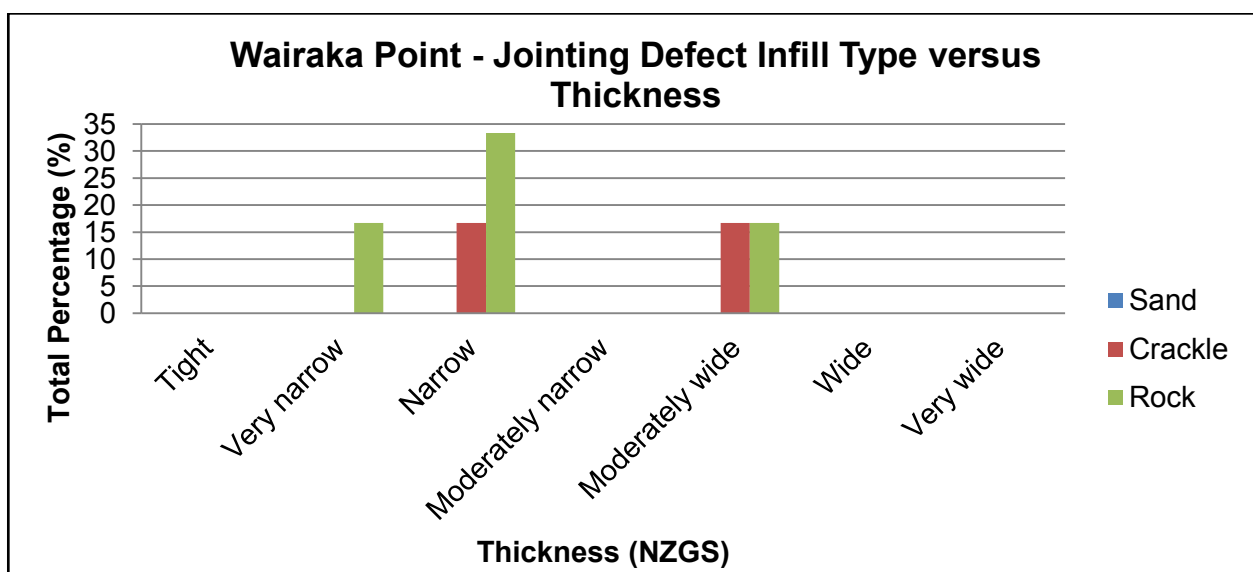
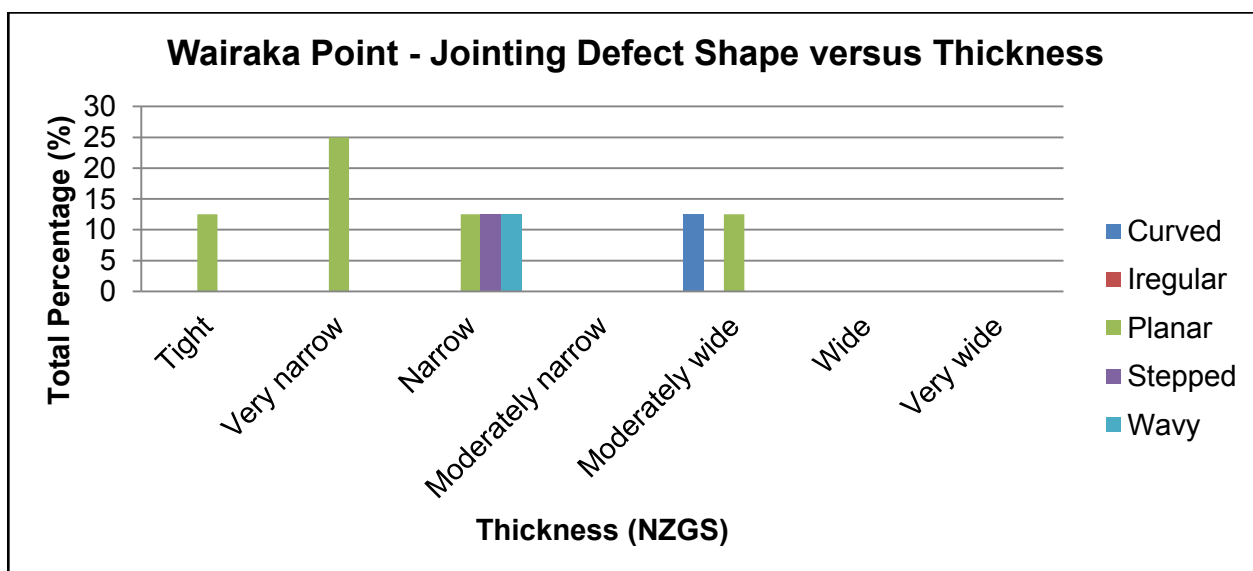
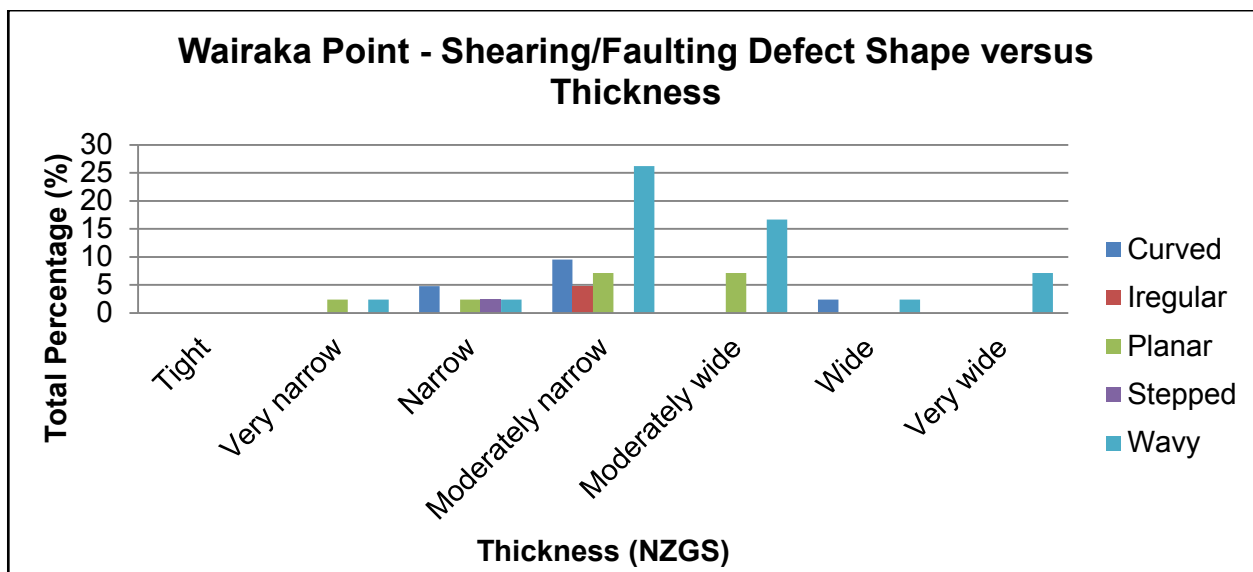








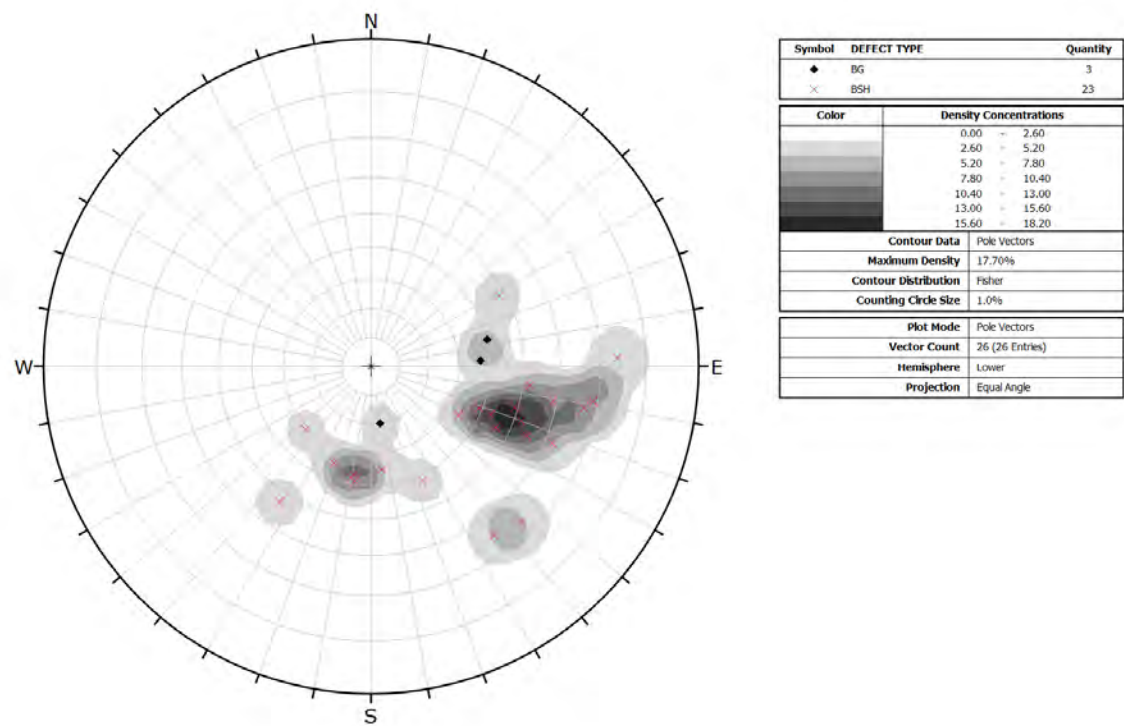




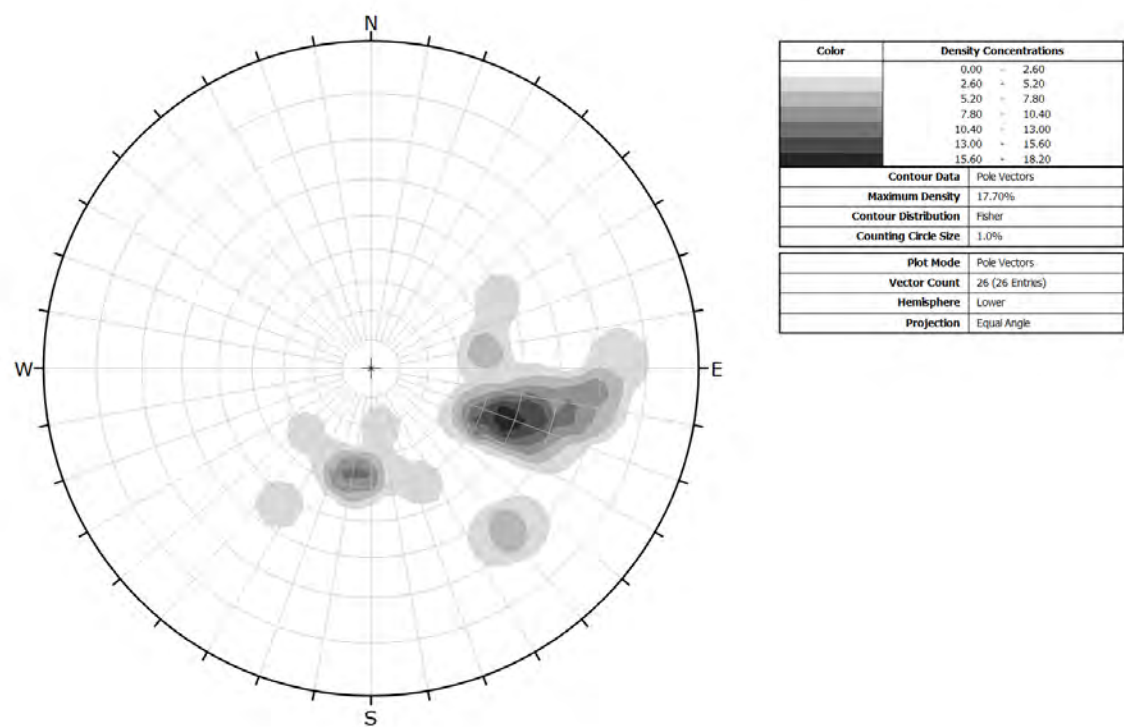
F.5 Wairaka Point Stereonet Analysis

Stereonet Dip: Dip direction analysis of bedding, faults and shears respectively.

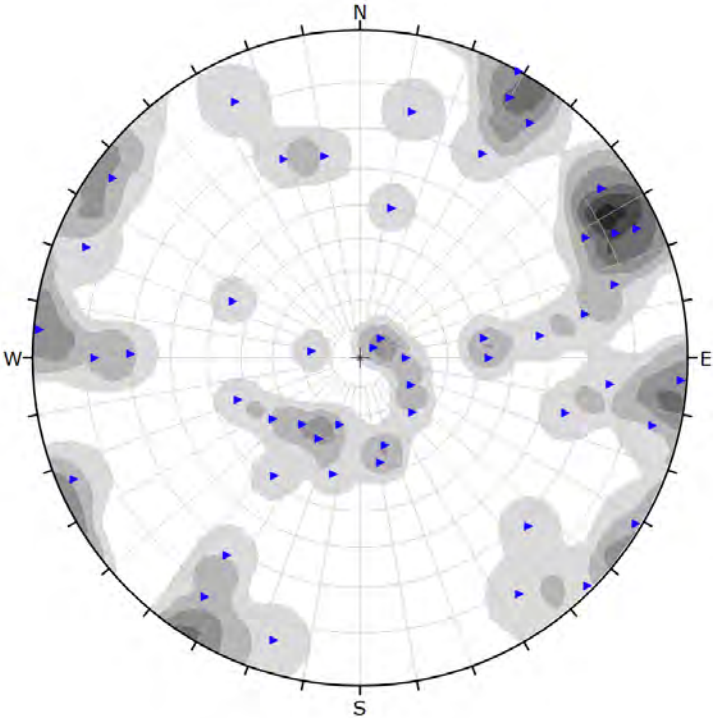
Bedding poles



Contour diagram of bedding clusters

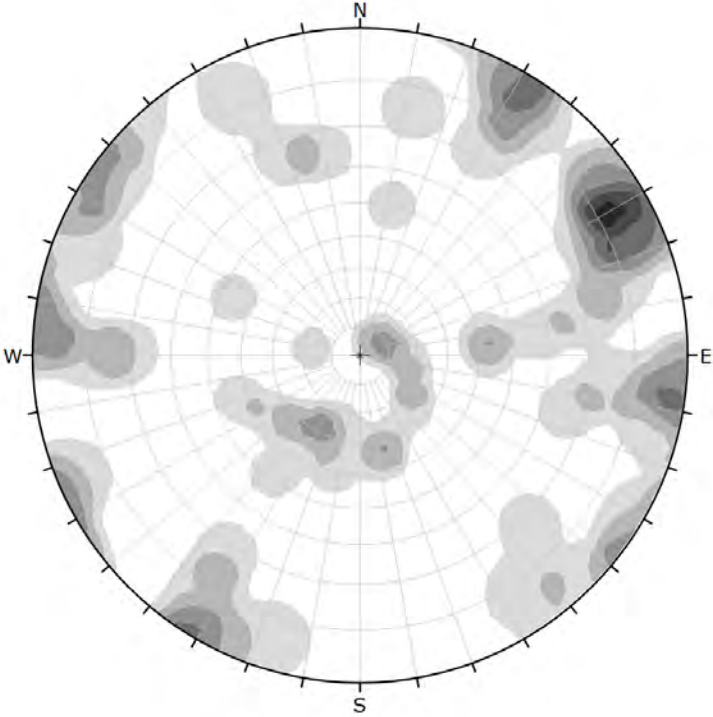


Shearing poles



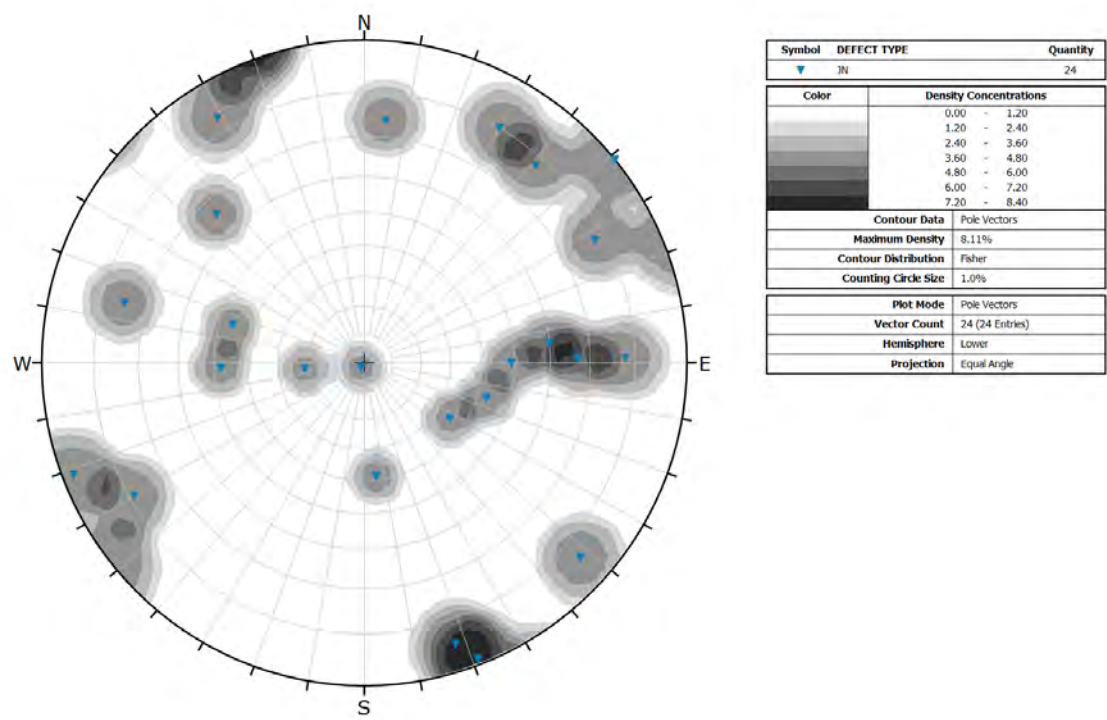
Symbol	DEFECT TYPE	Quantity
►	SR	52
Color	Density Concentrations	
	0.00	~ 1.20
	1.20	~ 2.40
	2.40	~ 3.60
	3.60	~ 4.80
	4.80	~ 6.00
	6.00	~ 7.20
	7.20	~ 8.40
Contour Data		Pole Vectors
Maximum Density		8.14%
Contour Distribution		Fisher
Counting Circle Size		1.0%
Plot Mode		Pole Vectors
Vector Count		52 (52 Entries)
Hemisphere		Lower
Projection		Equal Angle

Contour diagram of shearing and faulting clusters

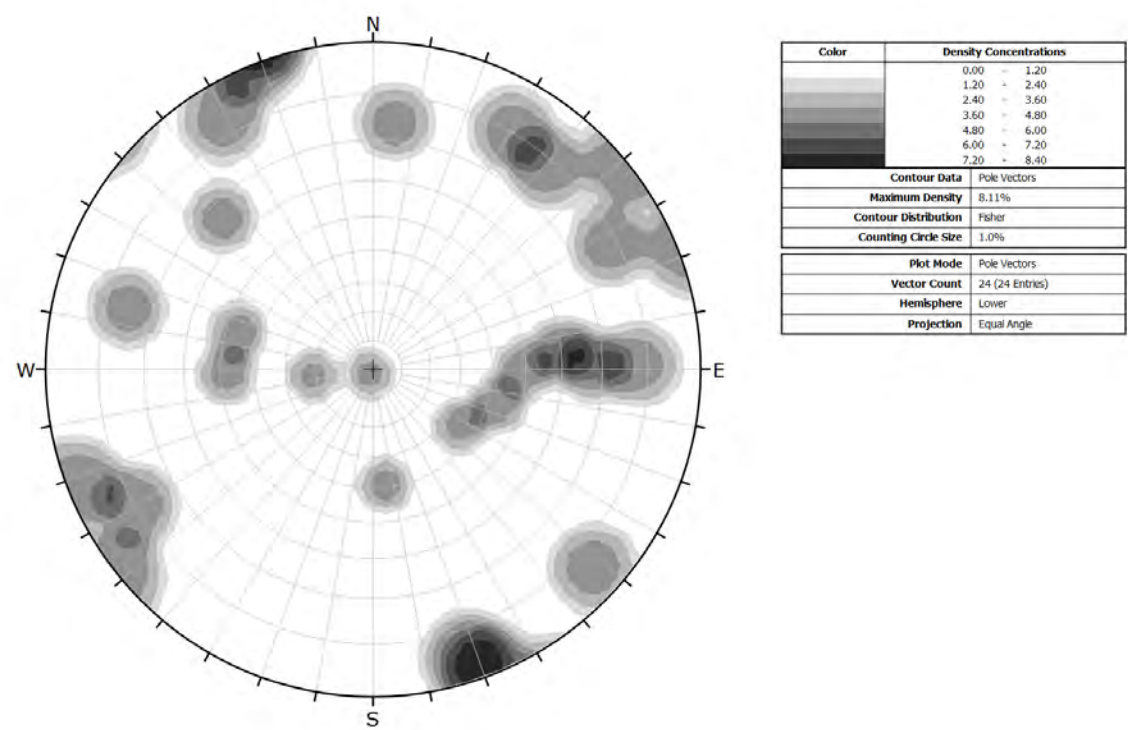


Color	Density Concentrations	
	0.00	~ 1.20
	1.20	~ 2.40
	2.40	~ 3.60
	3.60	~ 4.80
	4.80	~ 6.00
	6.00	~ 7.20
	7.20	~ 8.40
Contour Data		Pole Vectors
Maximum Density		8.14%
Contour Distribution		Fisher
Counting Circle Size		1.0%
Plot Mode		Pole Vectors
Vector Count		52 (52 Entries)
Hemisphere		Lower
Projection		Equal Angle

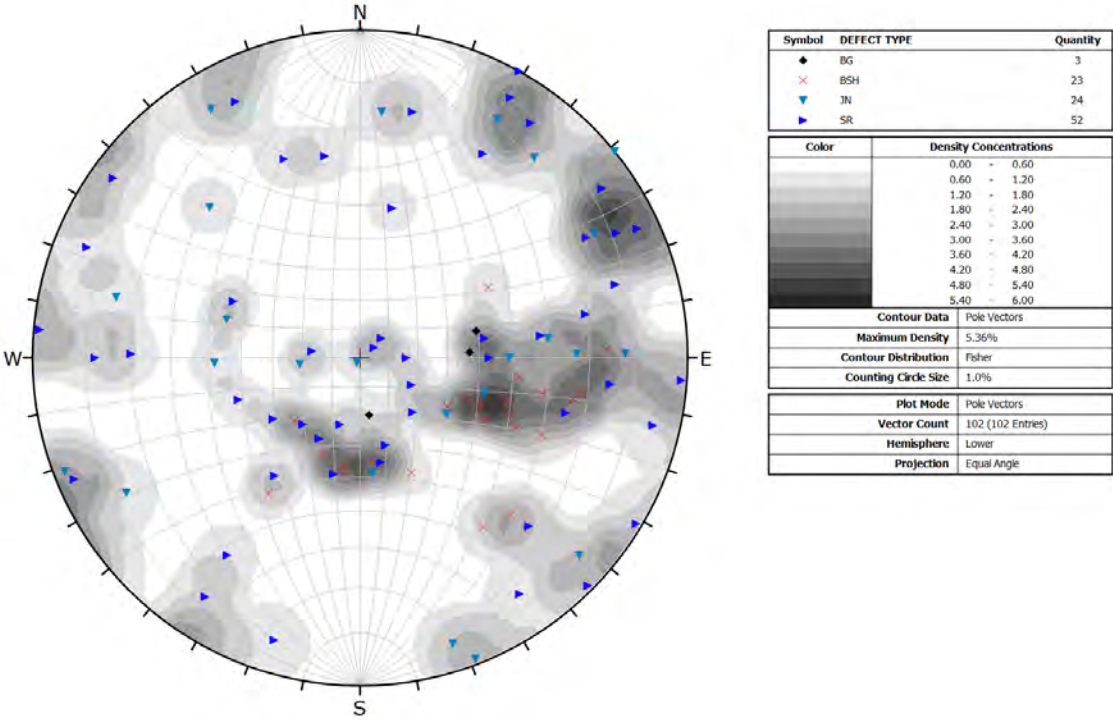
Jointing poles



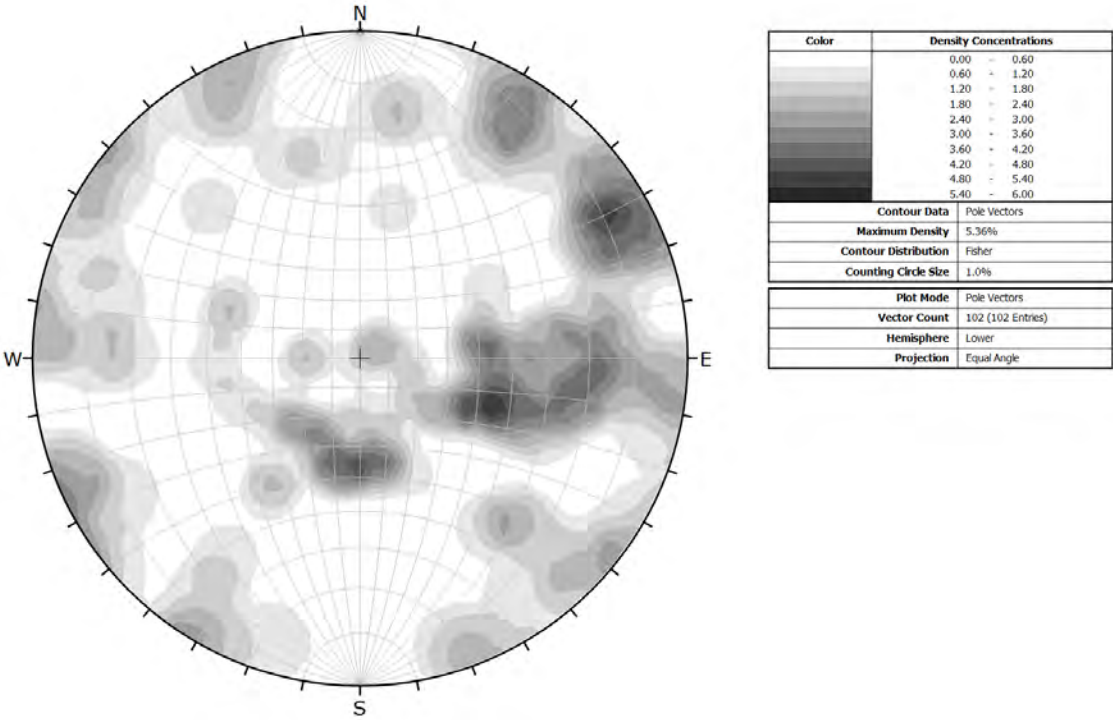
Contour diagram of jointing clusters



All defects poles



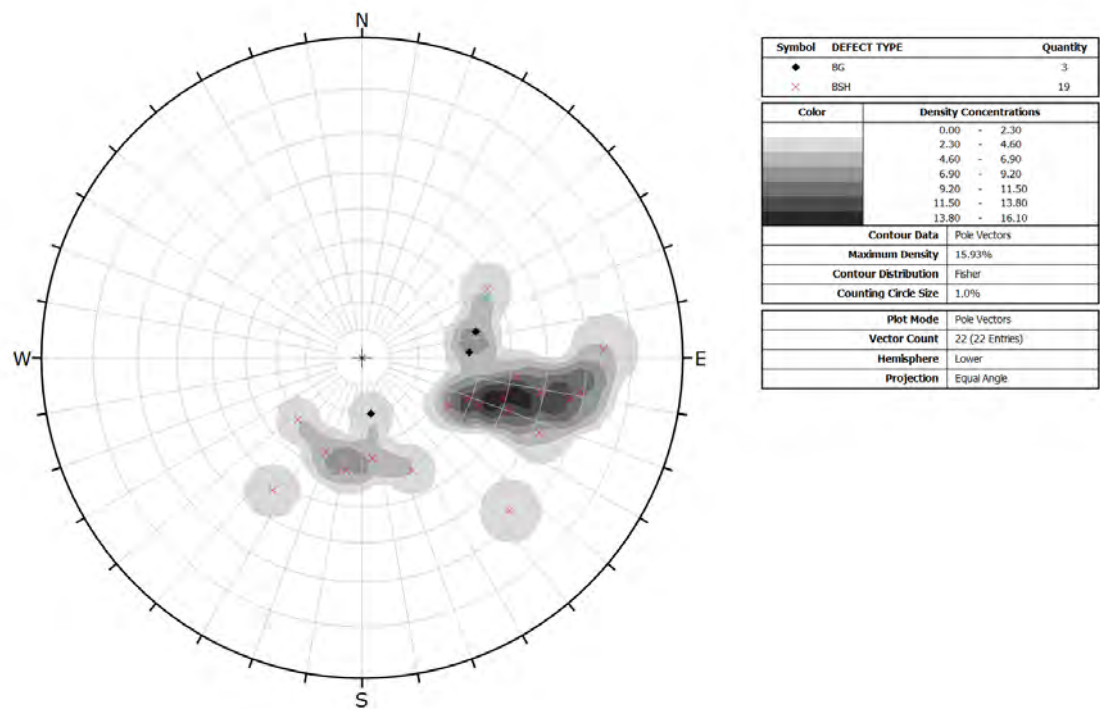
Contour diagram of all defects cluster



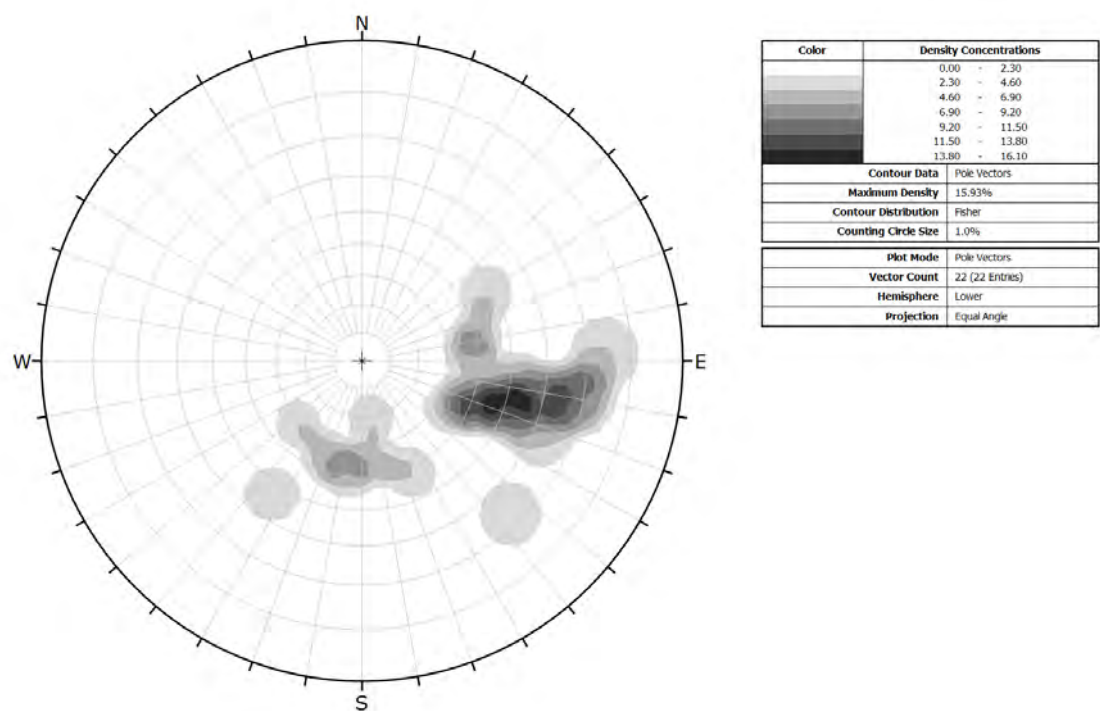
F.6 Filtered Stereonet Analysis

Stereonet from F.5 assessed for “noise”. The following only displays the poles of the continuous defects in Wairaka Point.

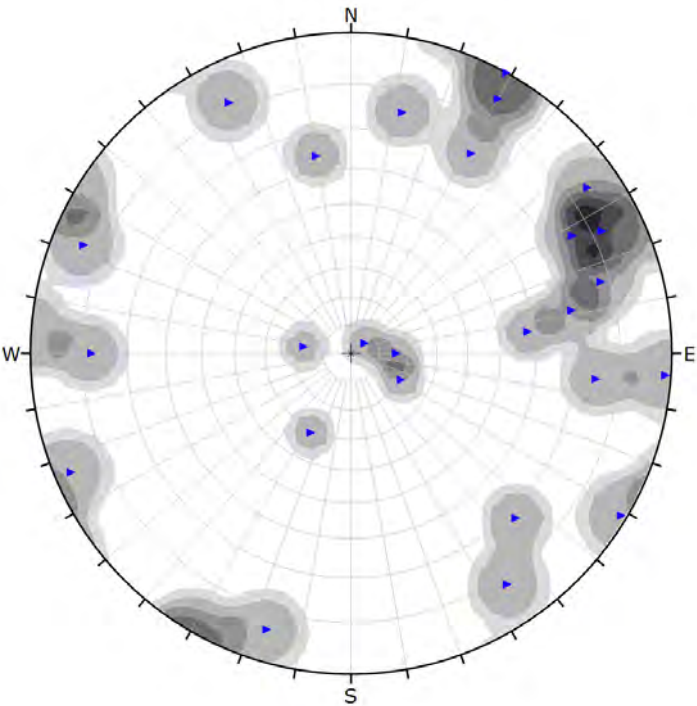
Bedding poles



Contour diagram of bedding clusters

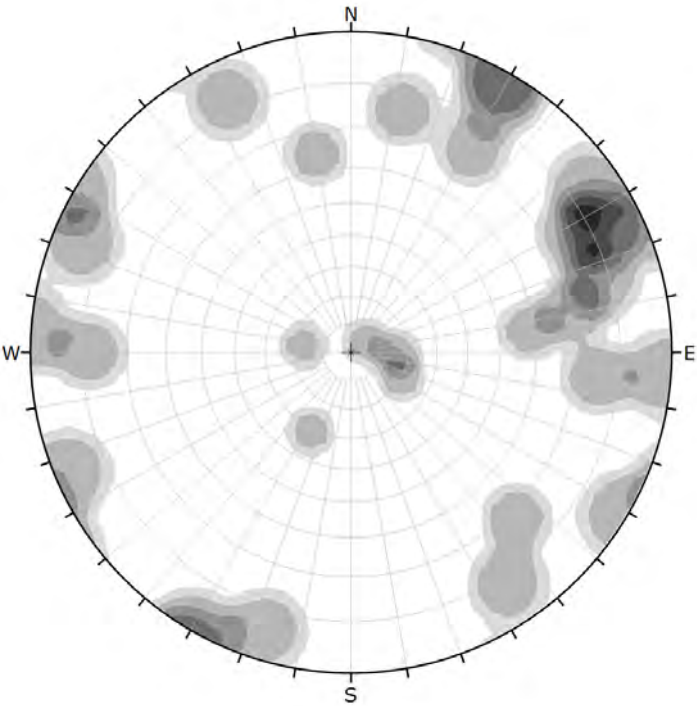


Shearing poles



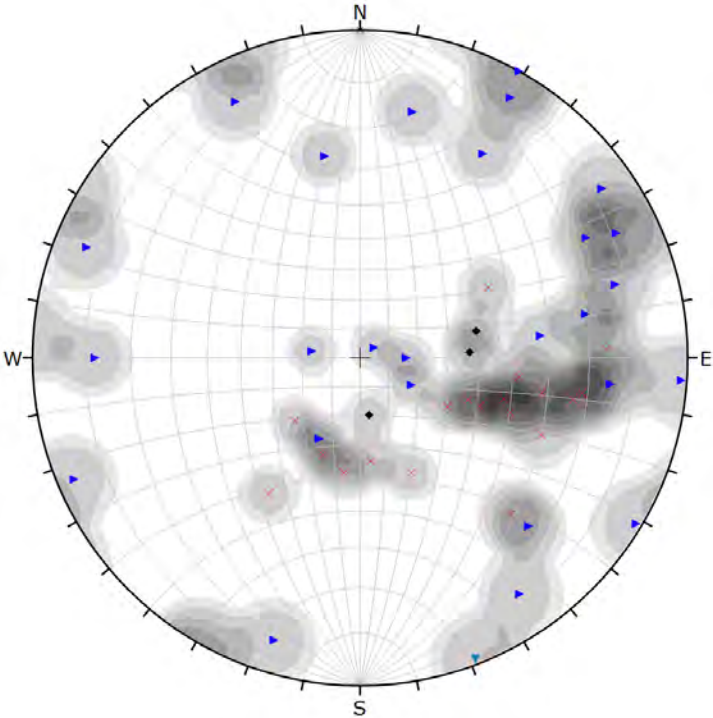
Symbol	DEFECT TYPE	Quantity
▶	SR	26
Color	Density Concentrations	
	0.00	1.50
	1.50	3.00
	3.00	4.50
	4.50	6.00
	6.00	7.50
	7.50	9.00
	9.00	10.50
Contour Data		Pole Vectors
Maximum Density		9.92%
Contour Distribution		Fisher
Counting Circle Size		1.0%
Plot Mode		Pole Vectors
Vector Count		26 (26 Entries)
Hemisphere		Lower
Projection		Equal Angle

Contour diagram of shearing and faulting clusters



Color	Density Concentrations	
	0.00	1.50
	1.50	3.00
	3.00	4.50
	4.50	6.00
	6.00	7.50
	7.50	9.00
	9.00	10.50
Contour Data		Pole Vectors
Maximum Density		9.92%
Contour Distribution		Fisher
Counting Circle Size		1.0%
Plot Mode		Pole Vectors
Vector Count		26 (26 Entries)
Hemisphere		Lower
Projection		Equal Angle

All defects poles



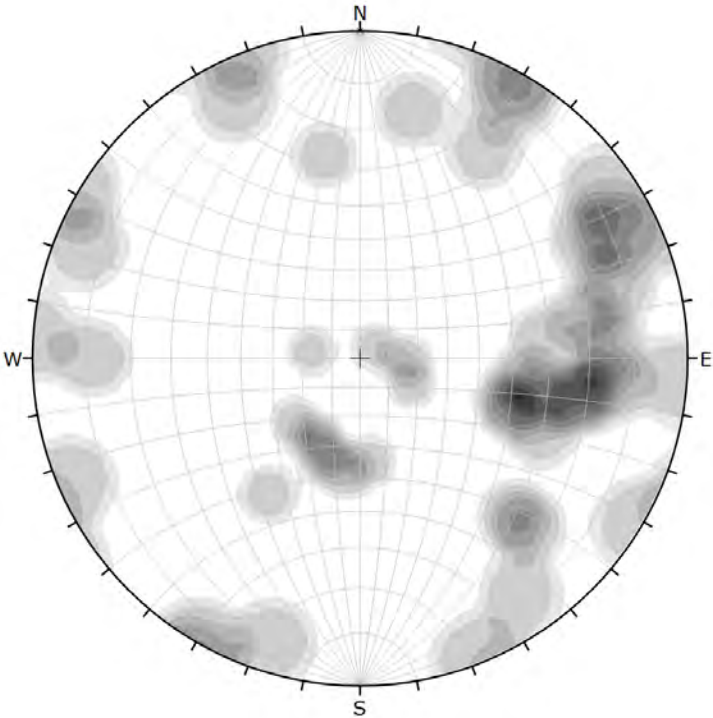
Symbol	DEFECT TYPE	Quantity
◆	BG	3
×	BSH	19
▼	JN	1
►	SR	26

Color	Density Concentrations
	0.00 - 0.80
	0.80 - 1.60
	1.60 - 2.40
	2.40 - 3.20
	3.20 - 4.00
	4.00 - 4.80
	4.80 - 5.60
	5.60 - 6.40
	6.40 - 7.20
	7.20 - 8.00

Contour Data	Pole Vectors
Maximum Density	7.15%
Contour Distribution	Fisher
Counting Circle Size	1.0%

Plot Mode	Pole Vectors
Vector Count	49 (49 Entries)
Hemisphere	Lower
Projection	Equal Angle

Contour diagram of all defects cluster



Color	Density Concentrations
	0.00 - 0.90
	0.90 - 1.80
	1.80 - 2.70
	2.70 - 3.60
	3.60 - 4.50
	4.50 - 5.40
	5.40 - 6.30
	6.30 - 7.20
	7.20 - 8.10
	8.10 - 9.00

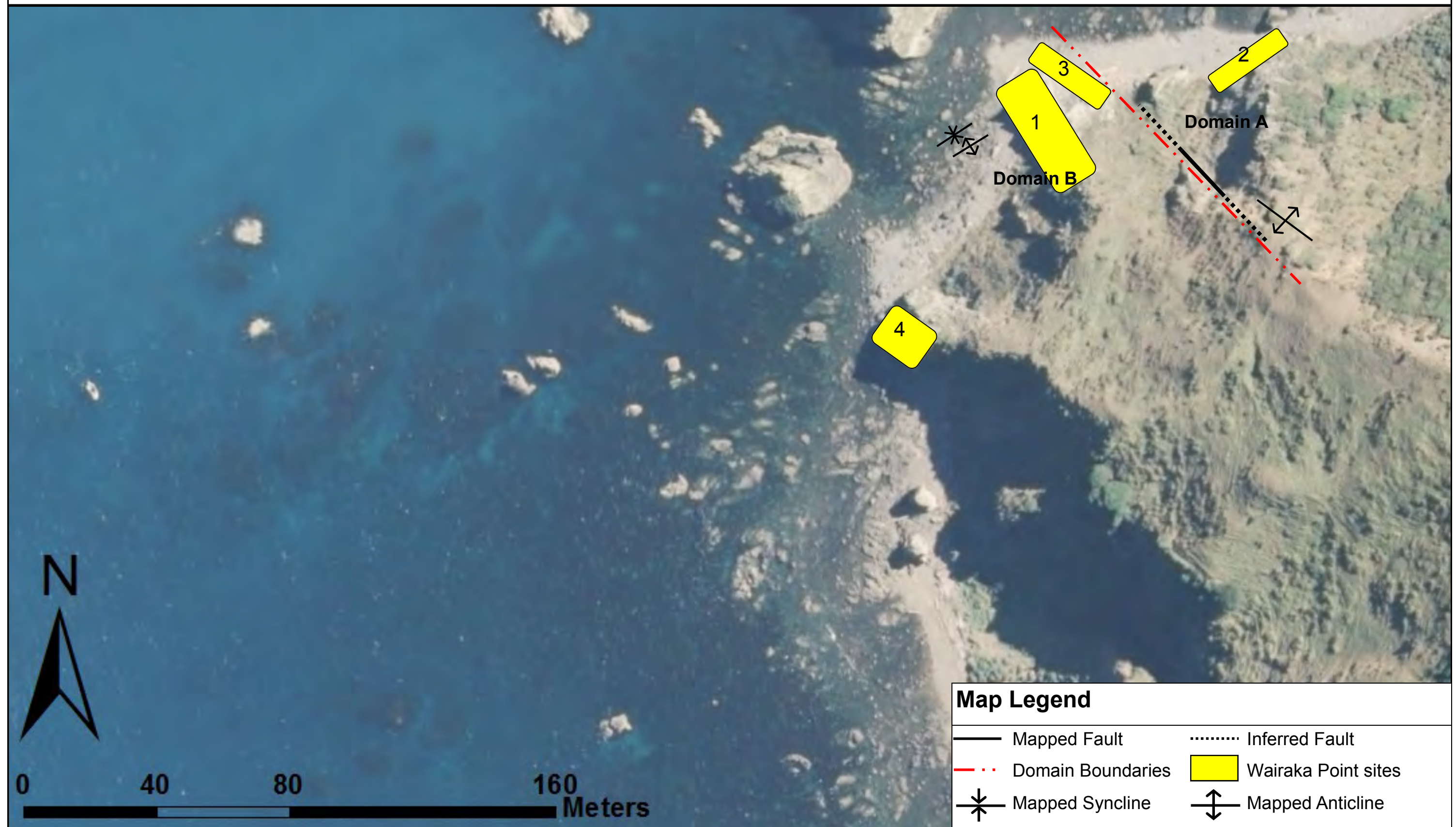
Contour Data	Pole Vectors
Maximum Density	8.39%
Contour Distribution	Fisher
Counting Circle Size	1.0%

Plot Mode	Pole Vectors
Vector Count	41 (41 Entries)
Hemisphere	Lower
Projection	Equal Angle

F.7 Wairaka Point Structural Domains

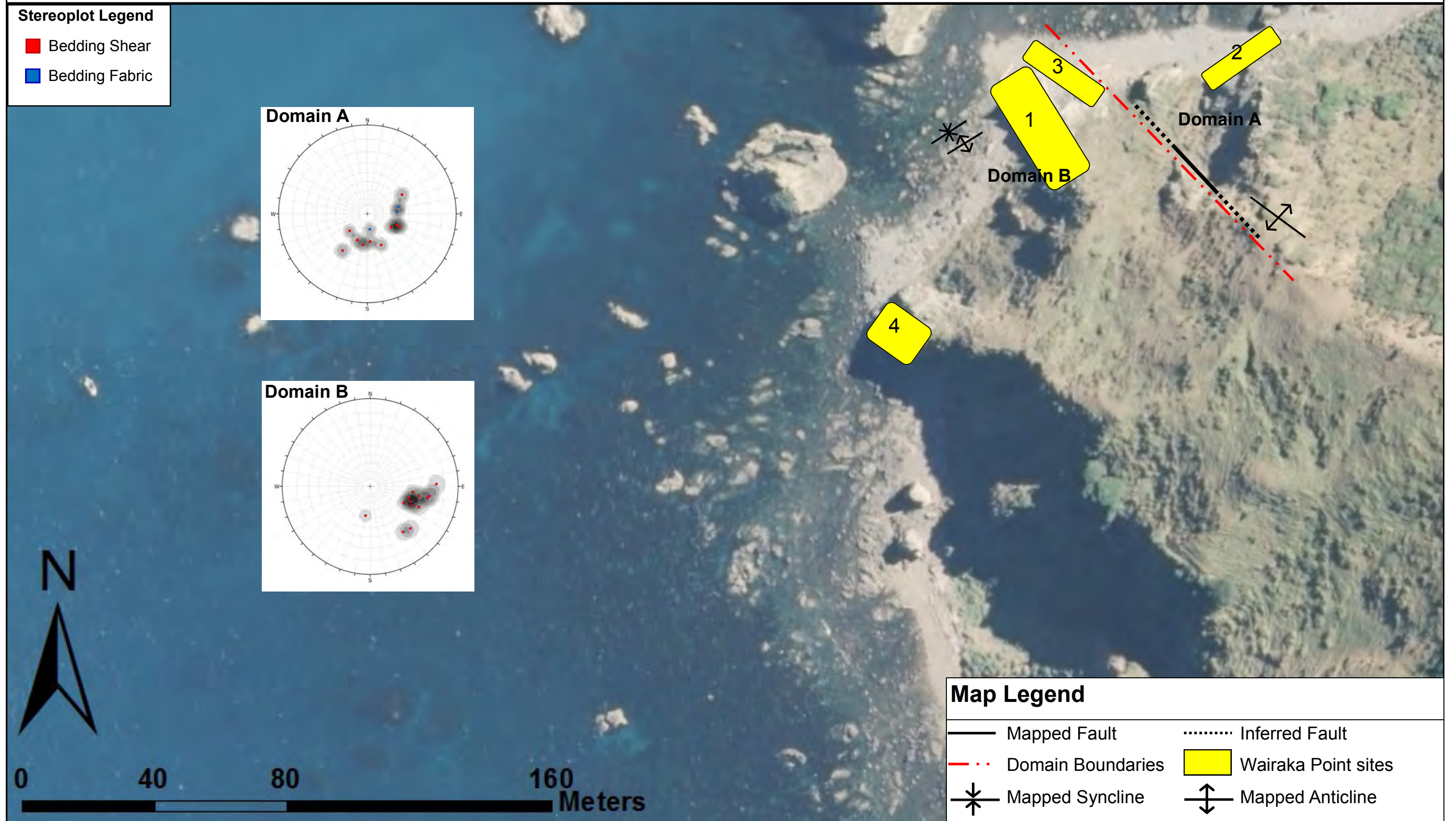
Figures are based on mapping observations and stereonet analysis. The figures represent a very detailed interpretation of the changes in defect orientation across the Wairaka Point site.

F.7.1 Wairaka Point Structural - Domains



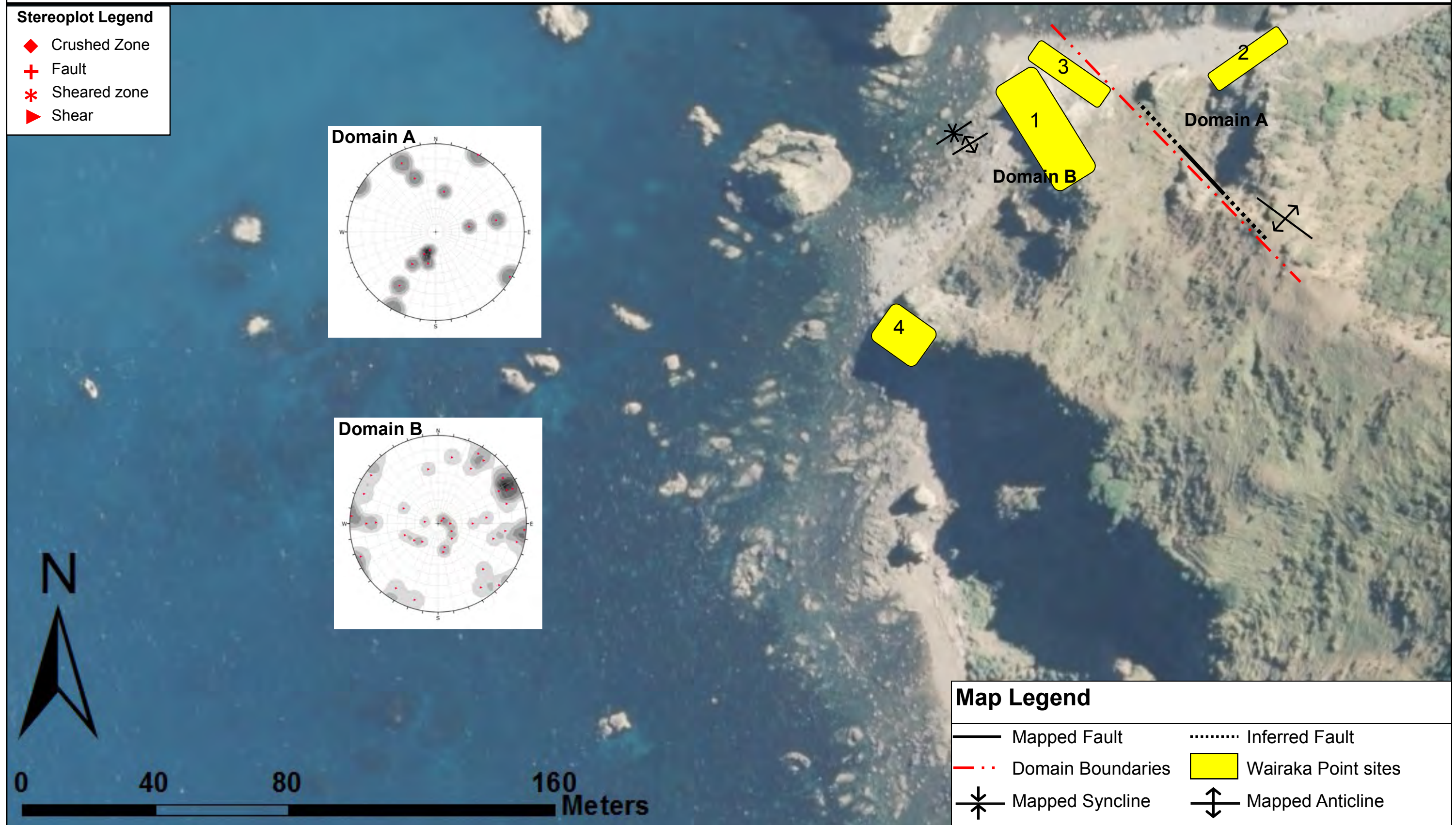
Imagery sourced: LINZ aerial imagery, 2016 (Captured by AAM NZ limited (2017))

F.7.2 Wairaka Point Structural Domains - Bedding



Imagery sourced: LINZ aerial imagery, 2016 (Captured by AAM NZ limited (2017))

F.7.3 Wairaka Point Structural Domains - Shearing



Imagery sourced: LINZ aerial imagery, 2016 (Captured by AAM NZ limited (2017))

F.8 Wairaka Point Engineering Geological Model

Engineering geological model based on all available data. The model provides a summary of the rock mass and defect condition within the Wairaka Point study site. Defect orientation and regional structural controls are also included.

F.8: Engineering Geological Model of Wairaka Point

Key :
 ◆ BG ▲ CZ ▼ JN ▶ SR
 ✕ BSH + FL ■ SH

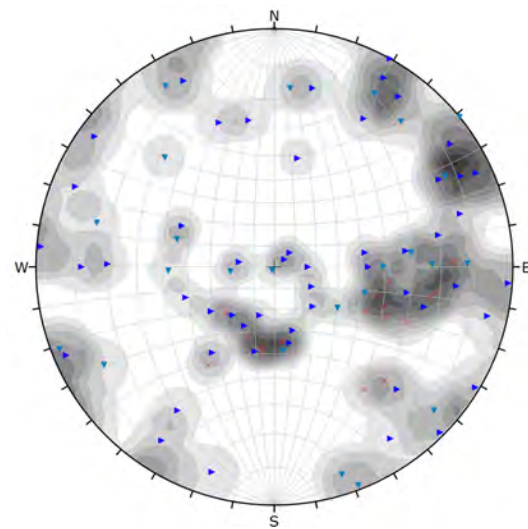


Figure 1: Stereonet of all the defect types and their orientation.

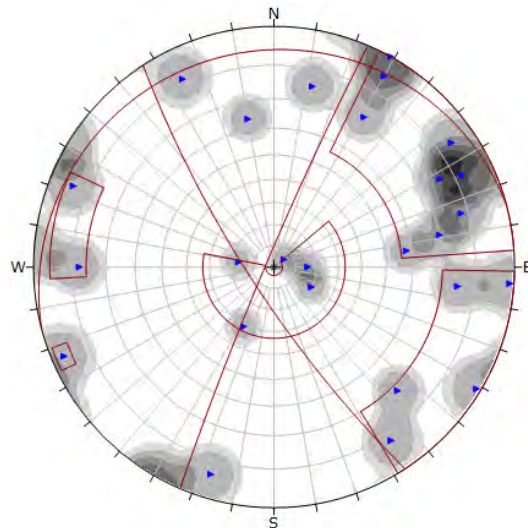


Figure 2: Stereonet of bench long shearing defects.

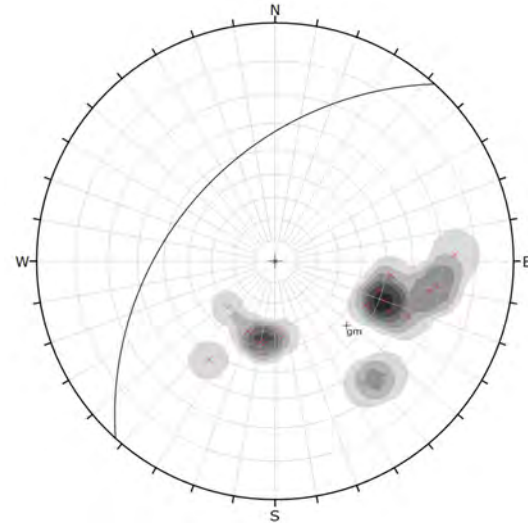


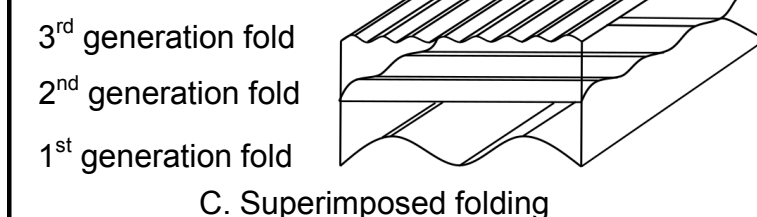
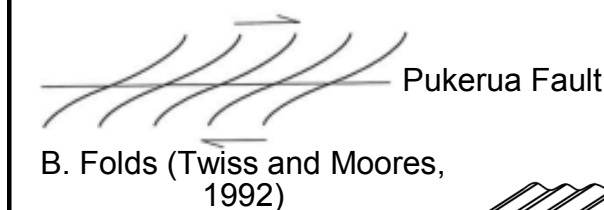
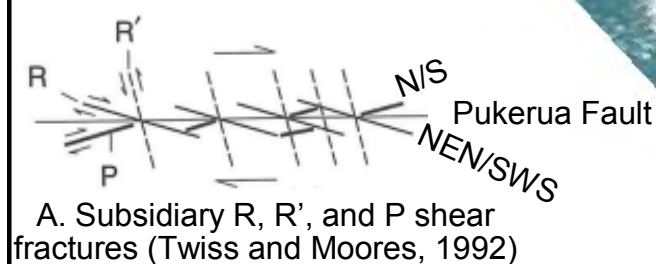
Figure 3: Stereonet of bedding.

Key:
 — Mapped faults
 - - - Failure
 — Mapped areas
 → Direction of failure

Individual sandstone beds are 6 m to 0.3 m thick and continuous. Mudstone beds are 2 mm to 4 mm thick and heavily sheared. Cross-cutting and conjugate shearing is present with rare faulting visible.

Bedding is dominantly moderately to very steeply inclined with variations occurring in response to faulting.

Conceptual Models:



Weathering profile typically follows topography however being located close to the coast has meant the weathering profile is not obvious.

Anticline trending NW

Failure is likely controlled by bedding and the mapped fault.

Rock mass structure at this site is controlled by the Pukerua Bay Fault (PF) and folding associated with the radial shear model.

Bedding typically strikes sub-parallel to parallel with the northeast-southwest trending structures while folds of the 2nd order are oriented perpendicular to bedding. 3rd order folding is oriented roughly parallel with the Pukerua Fault.

Shearing mostly forms in two fairly defined sets which dip sub-vertical to very steeply. They are roughly oriented NNW/SSE and NE-SW, which is sub-parallel with 1st order and 2nd order regional faults. A third less defined cluster appears to be mostly horizontally dipping.

The Pukerua Fault (PF) is located around 2.5 km away. Fault motion is predominantly dextral strike-slip. The general trend of the fault is between 040°.

Tight folding

Given the distance from the active faults the condition of the rock mass is relatively less disturbed. Bedding is more persistent and continuous, with cross-cutting shears and faults that are widely spaced.

MUD : SAND

20: 80

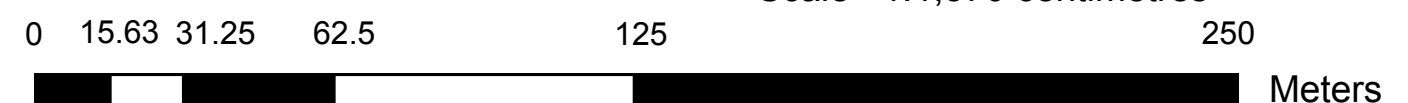
Predominant Suneson lithofacies:

B

Sandstone: Moderately to Slightly weathered, light brownish grey SANDSTONE; Strong to very strong; 5 joint sets moderately widely to widely spaced narrow to tight joints [RAKAIA SUB-TERRANE Greywacke]

Mudstone: Slightly weathered, dark blueish grey MUDSTONE; Strong to Moderately Strong [RAKAIA SUB-TERRANE Argillite]

Scale 1:1,570 centimetres



APPENDIX G: MAKARA HEAD ANALYSIS

This site is located on the north side of the peninsula at Makara Beach, 16 km north of Wellington (Figure G.1). The Shepherd's Gully Fault runs along the eastern edge of the peninsula likely controlling the topography and rock mass condition. Outcrop exposures are poor relative to the other sites. A total of 4 areas were mapped (Appendix G.2).

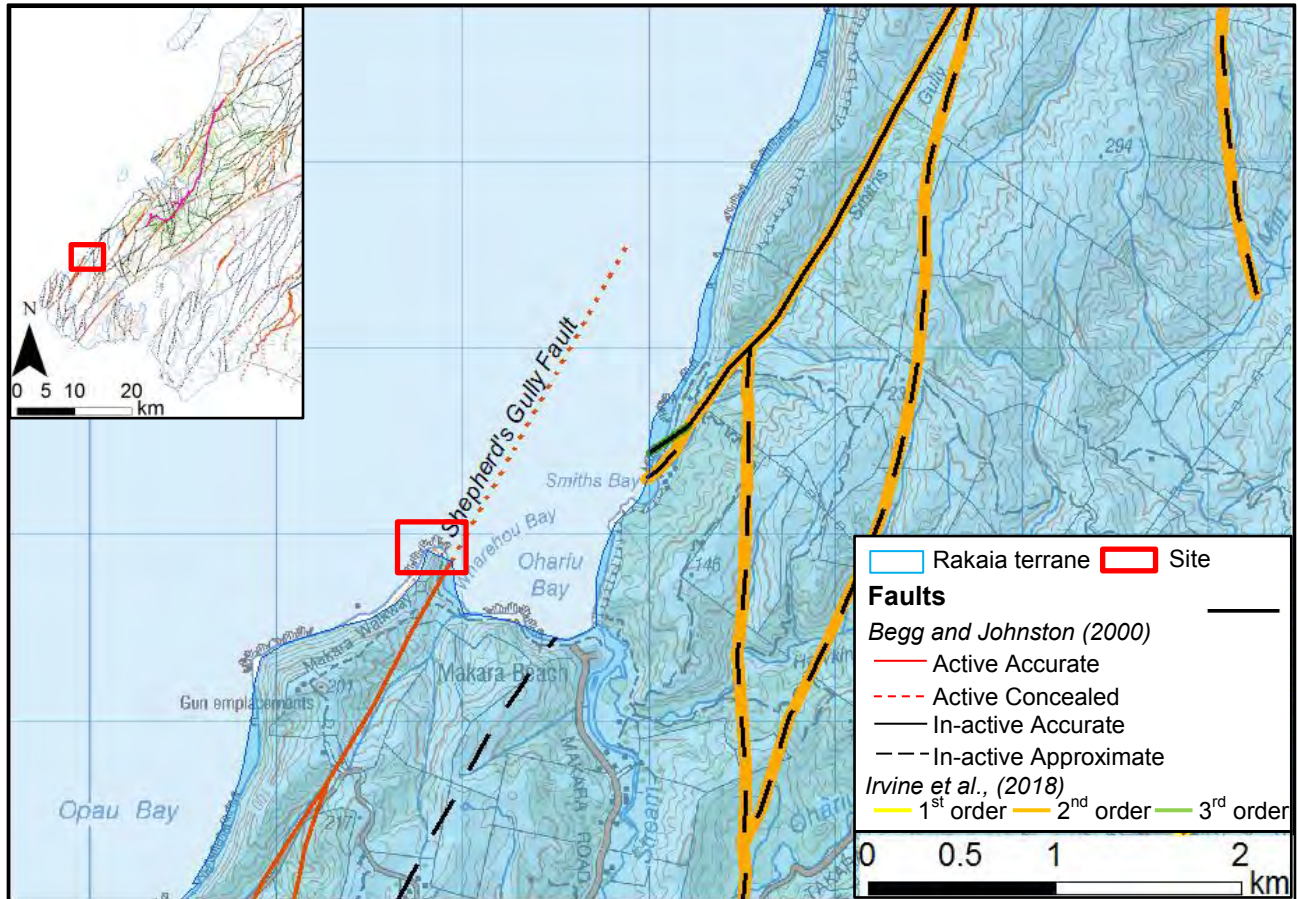


Figure G.1: Makara Head site district scale map. Data sourced from Begg and Johnston (2000) and Irvine et al. (2018). Refer to Section 1.4 for Irvine et al. (2018) order classification. Imagery from LINZ.

Results derived from conceptual models, raw mapping data, stereonet analysis and engineering geological models for the Makara Head study site as displayed in the following sections.

G.1 Makara Head Conceptual Structural Model

Preliminary structural assessment derived from GNS (2010) (Begg and Johnston, 2000) and Irvine et al (2018) structural databases. Interpretations are based on information derived from past literature.

G.1 Conceptual Structural Model of Makara Head

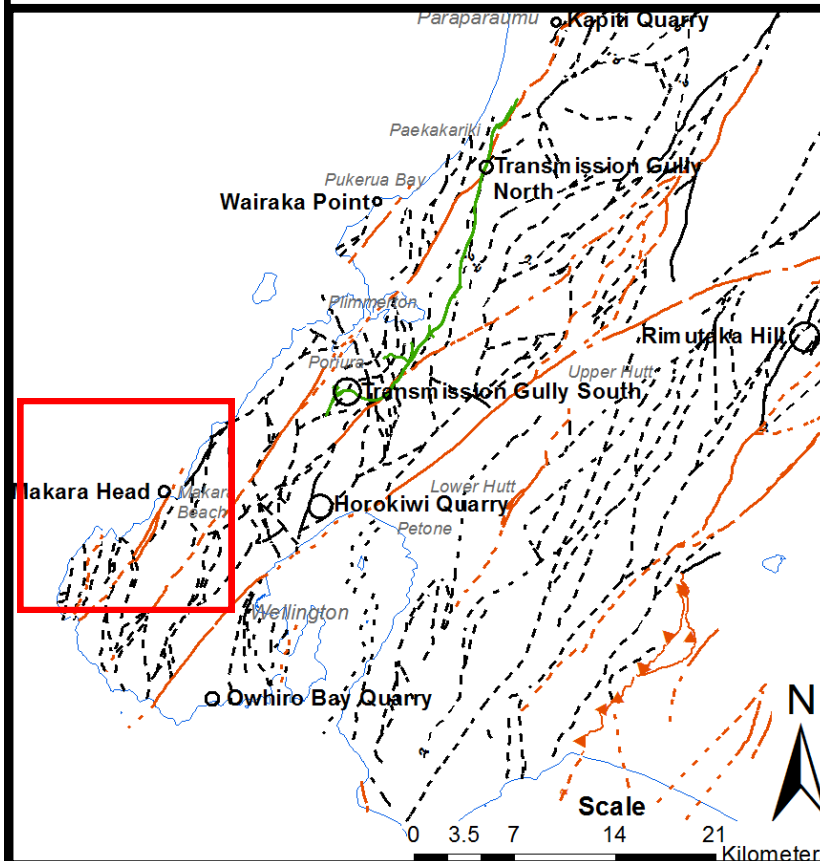
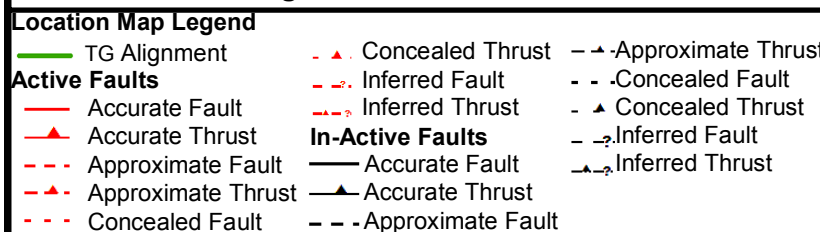


Figure A: Location Plan



Suneson (1992) notes that the area is mostly brecciated material which would infer that the condition of the rock is poor for cut-slope design. Further supporting this is the proximal distance of the Shepherds Gully Fault.

Suneson (1992) also mention's is associated folding at different scales and orientations.

Other studies such as Van Dissen and Berryman (1996) suggest that the Shepherds Gully and Pukerua Faults may be the same fault. If so, this site and Wairaka Point are a part of the same structural block.

Fault motion on the Shepherd's Gully Fault is dominantly dextral strike-slip faults. This fault is one of the major dextral strike-slip faults of the Wellington region. The general trend of the fault is around 030° and passes within 200 m of the study site.

Just south of the study site (~3 km) the fault merges from two fault traces. This split is interpreted as a restraining bend a structural feature resulting from strike-slip duplexes.

Rock mass structure is primarily controlled by the Shepherd's Gully Fault and folding associated with the Radial shear arrangement model. These structures develop as a result of the inherent geometry of strike-slip faults explained by Twiss and Moores (1992).

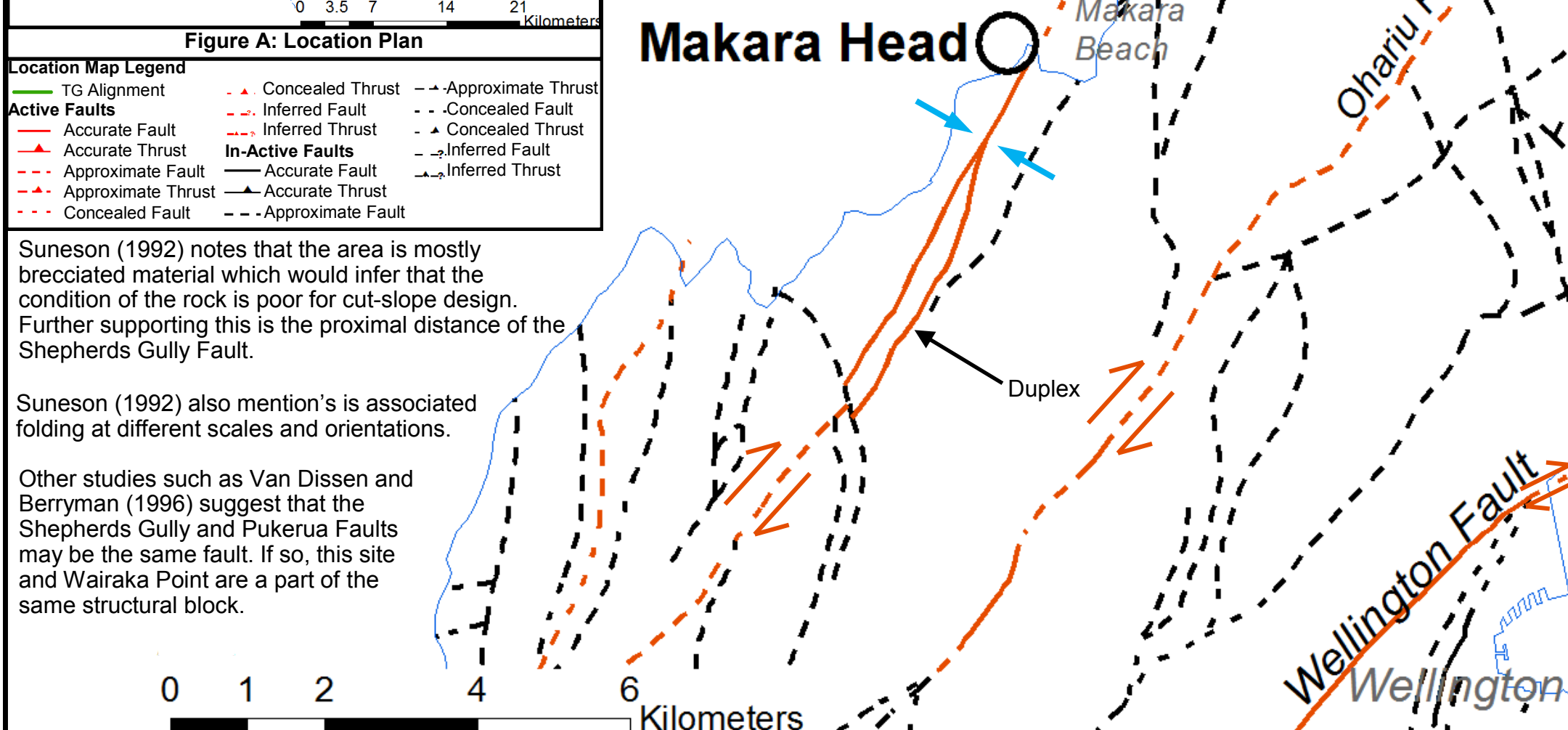
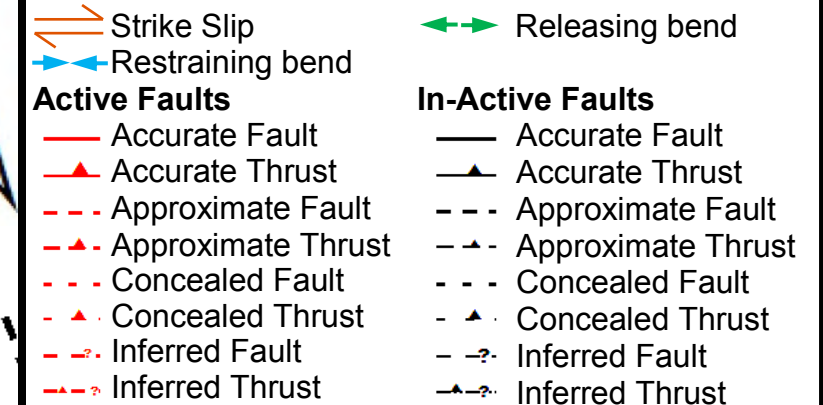
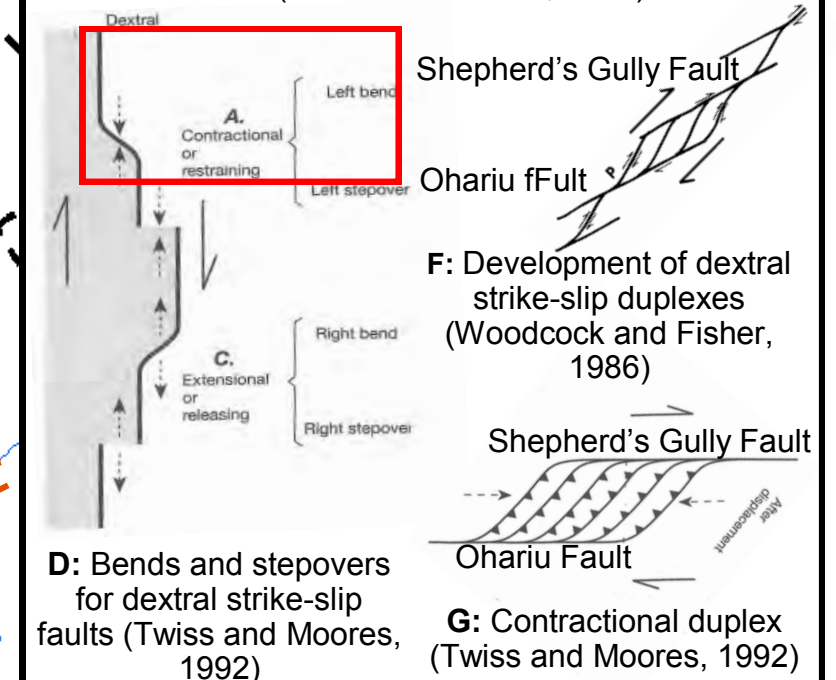
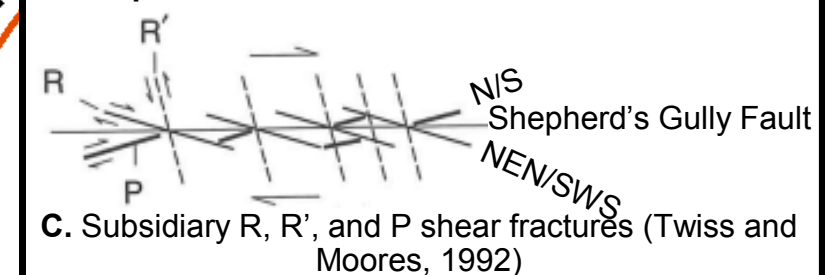


Figure B: District scale structures around Makara Head. Faults are sourced from GNS (2010)(Begg and Johnston, 2000).

District Scale Legend:



Conceptual Models:



Bedding and Shearing Predictions:

Bedding and shearing is anticipated to trend parallel to sub-parallel with the Shepherd's Gully Fault (Irvine et al., 2018, Suneson, 1992).

G.2 Makara Head Outcrop Location Map

Displays the location of the mapped outcrops within the Makara Head study site.

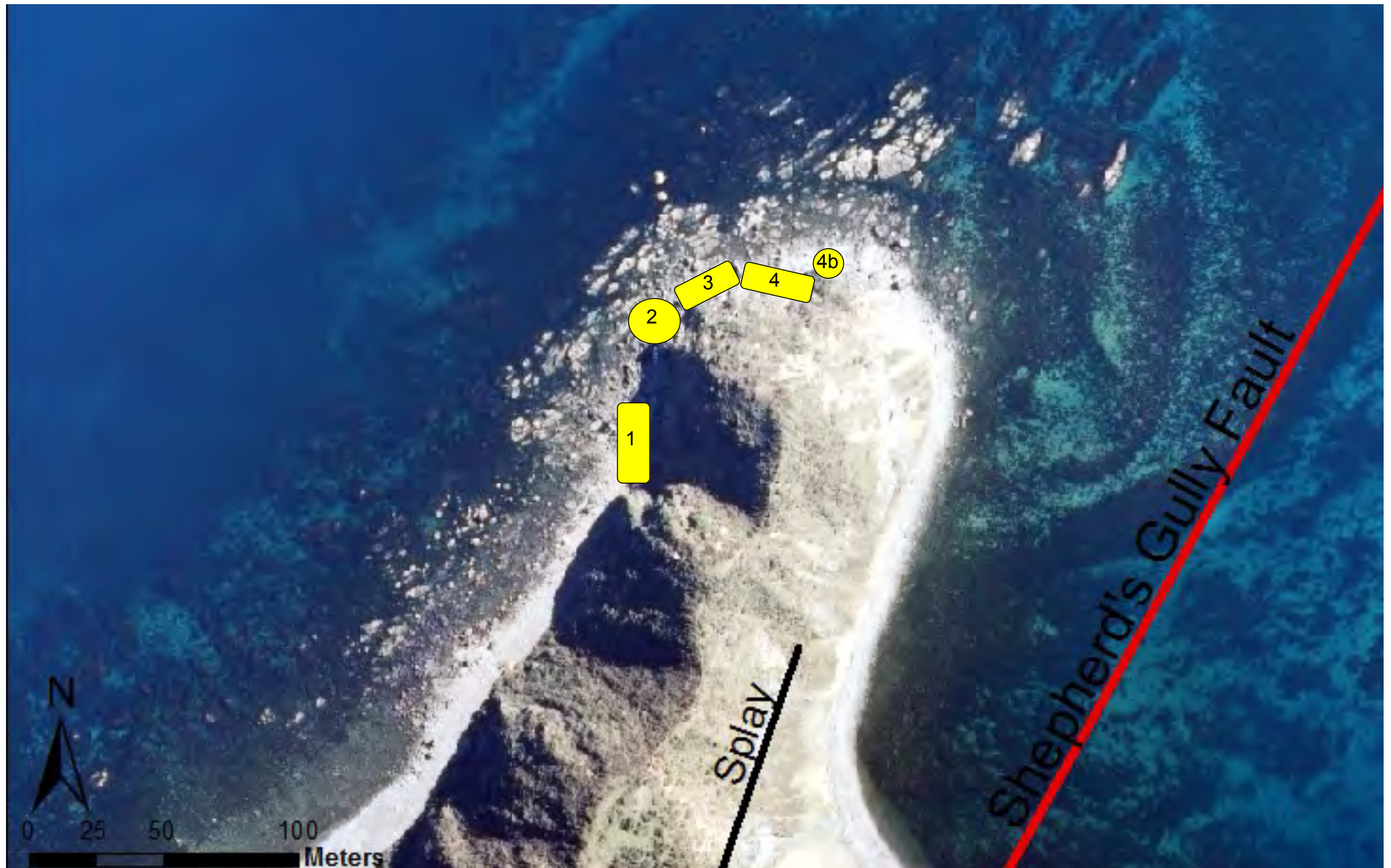
G.2 Makara Head



Makara Head Sites



GNS (2018) Faults (Begg and Johnston, 2000)



Imagery sourced: LINZ aerial imagery, 2016

G.3 Makara Head Raw Mapping Data

Structural data collected from the Makara Head study site. Where data is missing or blanked out information was either not able to be reached or was not relevant to the rock mass or defect condition (e.g. Planar defects did not contain a wavelength as outlined in Chapter 3).

G.3.1 Makara Head - Raw Data

Makara Head																					
ID	Defect Type	Dip	Dip Direction (Mag)	Dip Direction (True)	Structural Domain	Roughness	Thickness		% of rock fragments	Continuity	Persistence	Shape			Persistence - Trace Length (m)	Spacing (m)	Infill (Support (Breccia type (%Clasts), Angularity, weathering, strength, coating; colour, grainsize, strength, plasticity)) precipitation	Saturation	Latitude	Longitude	Comments
							Term	Width (mm)				Inter-limb angle (degrees)	Wavelength (m)	Term							
1	SR	87	208	185	A	Ro2	Wide	~80-100mm	~99%	0	O	~160°	Gentle	~2m	Wavy	~4m	Clast supported (Rock (~99%) Angular, HW, Weak to Moderately strong, Coating; Dark and light blue black, Sand, Soft, NP) White elongated lenses of precipitation	Dry	-41.2159	174.7035	Continuous
2	SR	89	229	207	A	Ro3	Wide	~150mm	~95%	1	D	~160°	Gentle	~6m	Wavy	~5m	Clast supported (Crackle (~95%) Angular, MW, Weak to Very weak, Coating; Light grey, silty Sand, Soft, NP) No precipitation	Dry	-41.216	174.7035	Terminates against SR3
6	SR	85	331	309	A	Ro2	Moderately wide	~55mm	~95%	1	D	~150°	Gentle	~8m	Wavy	~3m	Clast supported (Crackle (~95%) Angular, HW, Weak, Coating ; Light and dark grey, silty Sand, Soft, NP) White elongated precipitation	Dry	-41.216	174.7034	Terminates against a defect and cross cuts a SR that also terminates against SR1
8	SR	75	341	319	A	Ro2	Wide	~80mm	~95%	1	D	~180°	Gentle		Planar	~3m	Clast supported (Crackle (~95%) Angular, HW, Weak, Veneer ; Dark blue brown, silty Sand, Soft, NP) No precipitation	Dry	-41.2159	174.7033	Terminates against SR that cross cuts SR6 also
7	SR	83	267	244	A	Ro2	Wide	~150mm	~95%	1	D	~160°	Gentle	~8m	Wavy	~3m	Clast supported (Crackle (~95%) Angular, HW, Weak, Veneer ; Dark grey, silty Sand, Soft, NP) White elongated lenses of precipitation	Dry	-41.216	174.7034	Terminates against SR9
8b	SR	80	352	329	A	Ro2	Wide	~150mm	~90%	1	O	~135°	Gentle	~8m	Wavy	~3m	Clast supported (Crackle (~90%) Angular, HW, Weak, Coating ; Dark grey, silty Sand, Soft, NP) No precipitation	Dry	-41.2159	174.7033	Terminates at same SR as SR8
9	SR	68	80	58	A	Ro3	Wide	~150mm	~95%	0	O	~170°	Gentle	~6m	Curved	~2m	Clast supported (Crackle (~95%) Angular, HW, Weak to Moderately strong(greywacke clasts), Coating ; Dark grey, silty Sand, Soft, NP) No precipitation	Dry	-41.2159	174.7034	Terminates at SR2
3	SR	87	280	257	A	Ro4	Wide to Very wide	~150-200mm	~95%	0	C	~170°	Gentle	~6m	Wavy	~4m	Clast supported (Crackle (~95%) Angular, HW, Weak to Moderately strong(greywacke clasts), Coating ; Dark grey, silty Sand, Soft, NP) No precipitation	Dry	-41.2159	174.7034	Continuous
4	SR	89	39	17	A	Ro2	Very narrow to Moderately wide	~1-50mm	~95%	0	O	~180°	Gentle		Planar	~4m	Clast supported (Crackle (~95%) Angular, HW, Moderately strong, Veneer ; Grey, silty Sand, Soft, NP) No precipitation	Dry	-41.2158	174.7034	Continuous
5	SR	3	177	154	A	Ro3	Moderately wide	~25mm	~99%	0	O	~180°	Gentle		Planar	~1.5m	Clast supported (Rock (~99%) Angular, MW, Moderately strong, Veneer ; Grey, silty Sand, Soft, NP) No precipitation	Dry	-41.2159	174.7036	Continuous
10	JN	66	357	334	A	Ro3	Tight	~0mm		1	D	~180°	Gentle		Planar	~1.5m		Dry	-41.2157	174.7034	Failure plane
10	JN	62	355	332	A	Ro3	Tight	~0mm		1	D	~180°	Gentle		Planar	~1.5m		Dry	-41.2157	174.7034	Failure plane
11	JN	75	177	154	A	Ro3	Tight	~0mm		1	D	~180°	Gentle		Planar	~0.8m		Dry	-41.2157	174.7034	Failure plane
12	SR	81	86	64	A	Ro3	Wide to Very wide	~200 to 70mm	~90%	0	O	~160°	Gentle	~5m	Wavy	~4m	Clast supported (Crackle (~90%) Angular, MW, Moderately strong to Strong, Coating ; Light orange brown, silty Sand, Soft, NP) Some white tabulated precipitation	Dry	-41.2157	174.7034	Continuous
12b	JN	78	202	180	A	Ro3	Moderately wide	~30mm	~99%	1	D		Gentle		Stepped	~3m	Clast supported (Rock (~99%) Angular, MW, Strong, Veneer ; Light grey, Sand, Soft, NP) No precipitation	Dry	-41.2157	174.7035	Terminates against SR
13	SR	85	92	70	A	Ro4	Moderately narrow	~15mm	~99%	0	O		Gentle		Stepped	~4m	Clast supported (Rock (~99%) Angular, MW, Strong, Coating ; Light brown, Sand, Soft, NP) No precipitation	Dry	-41.2157	174.7035	Continuous
14	JN	28	202	180	B	Ro2	Narrow	~3mm		2	D	~180°	Gentle		Planar	~3m		Dry	-41.2156	174.7035	Gapped
14	JN	31	229	206	B	Ro2	Narrow	~3mm		2	D	~180°	Gentle		Planar	~3m		Dry	-41.2154	174.7034	Gapped - rock topple JN controlled, see map sheet. Terminates against JN's
15	JN	72	186	163	B	Ro2	Narrow	~5mm		2	D	~180°	Gentle		Planar	~3m		Dry	-41.2156	174.7035	Gapped - rock topple JN controlled, see map sheet. Terminates against JN's
16	SR	74	171	149	B	Ro4	Moderately narrow	~8mm	~99%	1	O	~110°	Open		Curved	~6m	Clast supported (Rock (~99%) Angular, MW, Moderately strong, Veneer ; Light brown grey, Sand, Soft, NP) No precipitation	Dry	-41.2156	174.7035	Termination obscured by debris
16	BSH	88	30	8	B	Ro4	Moderately narrow	~8mm	~99%	1	O	~110°	Open		Curved	~6m	Clast supported (Rock (~99%) Angular, MW, Moderately strong, Veneer ; Light brown grey, Sand, Soft, NP) Some lenses of white elongated precipitation	Dry	-41.2156	174.7035	Termination obscured by debris
17	BSH	66	128	105	B	Ro3	Moderately narrow to Moderately wide	~20 to 50mm	~90%	0	O	~170°	Gentle	~2.5m	Wavy	~3m	Clast supported (Crackle (~90%) Angular, HW, Weak, Coating ; Dark brown grey, silty Sand, Soft, NP) Some lenses of white elongated precipitation	Damp	-41.2156	174.7036	Continuous
17	BSH	83	70	47	B	Ro3	Moderately wide to Wide	~60mm	~90%	0	O	~170°	Gentle	~2.5m	Wavy	~3m	Clast supported (Crackle (~90%) Angular, HW, Weak, Coating ; Dark brown grey, silty Sand, Soft, NP) Some lenses of white elongated precipitation	Damp	-41.2156	174.7036	Continuous
16	BSH	68	108	85	B	Ro3	Moderately wide to Wide	~60mm	~90%	0	O	~170°	Gentle	~1.5m	Wavy	~4m	Clast supported (Crackle (~90%) Angular, HW, Weak to Very weak, Coating ; Dark brown grey, silty Sand, Firm, NP) Lenses of white elongated precipitation	Dry	-41.2156	174.7036	Continuous
18	SR	74	293	270	B	Ro3	Moderately narrow	~10mm	~90%	1	D	~170°	Gentle	~0.8m	Wavy	~2m	Clast supported (Crackle (~90%) Angular, HW, Weak to Very weak, Coating ; Dark brown grey, silty Sand, Soft, NP) No precipitation	Dry	-41.2155	174.7036	Terminates against SR31
19	JN	18	16	354	B	Ro3	Moderately narrow	~10mm		1	D	~180°	Gentle		Planar	~0.8m		Dry	-41.2155	174.7036	Gapped, cross cuts SR20
20	SR	55	250	228	B	Ro3	Moderately wide to	~20 to	~90%	1	D	~180°	Gentle		Planar	~3.5m	Clast supported (Crackle (~90%) Angular, HW, Weak to Very weak,	Dry	-41.2155	174.7036	Terminates against SR21 and

							Narrow	6mm									Coating ; Dark brown grey, silty Sand, Soft, NP) No precipitation Clast supported (Crackle (~90%) Angular, HW, Moderately strong, Veneer ; Light grey, Sand, Soft, NP) No precipitation					cross cuts JN19
21	SR	78	234	211	B	Ro3	Moderately narrow	~15-7mm	~90%	0	C	~160°	Gentle	~5m	Wavy	~6m		Dry	-41.2156	174.7037		
22	SR	53	250	227	B	Ro3				1	O	~180°	Gentle		Planar	~1.5m		Dry	-41.2156	174.7036		Terminates against SR21
23	SR	88	317	295	B	Ro3	Very narrow to Narrow	~2mm	~99%	1	D	~170°	Gentle	~1m	Wavy	~1.5m		Dry	-41.2155	174.7037		Terminates against BSH16
24	SR	89	130	108	B	Ro3				1	D	~180°	Gentle		Planar	~2m		Dry	-41.2156	174.7037		Terminates against BSH16
25	SR	17	221	198	B	Ro3	Moderately wide	~30mm	~99%	1	D	~180°	Gentle		Planar	~3m		Dry	-41.2156	174.7037		Terminates against JN's
27	SR	59	64	42	B	Ro3	Narrow to Moderately narrow	~6mm	~99%	1	D	~180°	Gentle		Stepped	~2m		Dry	-41.2156	174.7038		Terminates against SR25
28	SR	88	117	95	B	Ro3	Moderately wide	~30mm	~99%	1	D	~180°	Gentle		Stepped	~2m		Dry	-41.2155	174.7037		Terminates against SR25
29	SR	87	183	161	B	Ro3	Very narrow	~1mm	~99%	2	D	~160°	Gentle	~1.4m	Wavy	~2m		Dry	-41.2155	174.7037		Terminates against SR25
30	SR	34	214	191	B	Ro2	Moderately wide	~40mm	~95%	1	D	~180°	Gentle		Planar	~2m		Dry	-41.2156	174.7037		Terminates against BSH16
31	SR	24	224	202	B	Ro3	Moderately wide	~40mm	~99%	1	D	~180°	Gentle		Planar	~2m		Submerged in water	-41.2156	174.7035		Terminates against BSH17
31	SR	36	257	234	B	Ro3	Moderately wide	~40mm	~99%	1	D	~180°	Gentle		Planar	~2m		Submerged in water	-41.2155	174.7035		Terminates against BSH17
34	SR	68	309	286	B	Ro4				2	O	~180°	Gentle		Planar	~2m		Dry	-41.2156	174.7038		Failure plane 1
34	SR	85	71	49	B	Ro4				2	O	~180°	Gentle		Planar	~2m		Dry	-41.2156	174.7038		Failure plane 1
32	BSH	69	100	77	B	Ro3	Moderately wide	~50mm	~99%	0	O	~160°	Gentle	~1.2m	Wavy	~4m	~1m	Dry	-41.2156	174.7038		Failure plane 2 to the right
32	BSH	62	85	62	B	Ro3	Moderately narrow	~15mm	~95%	0	O	~160°	Gentle	~1.2m	Wavy	~2m	~1m	Dry	-41.2156	174.7037		
33	SR	75	104	82	B	Ro3	Moderately wide to Wide	~60mm	~50%	1	O	~180°	Gentle		Stepped	~2m	~1m	Dry	-41.2155	174.7038		Presume terminations against SR35
35	SR	87	183	161	B	Ro3	Moderately wide to Very wide	~300 to 30mm	~85%	1	O	~160°	Gentle	~5m	Curved	~6m		Dry	-41.2155	174.7039		soil fallen from above, Presume terminates against BSH37
36	JN	27	229	206	B	Ro3	Tight	~0mm		2	D	~180°	Gentle		Planar	~0.8m	~0.35m	Dry	-41.2156	174.7039		soil fallen from above but can see rock underneath, presume ~85% clasts
36	SR	74	259	236	B	Ro3	Moderately narrow to Moderately wide	~20 to 40mm	~75%	1	D	~160°	Gentle	~7m	Curved	~3m		Dry	-41.2155	174.7039		Terminates against CZ35
37	BSH	79	128	105	B	Ro2	Moderately narrow	~8mm	~80%	0	O	~180°	Gentle		Planar	~3m		Dry	-41.2156	174.7039		Continued from BSH32
39	SR	44	345	323	B	Ro5				0	O		Gentle		Irregular	~3m		Dry	-41.2155	174.704		Failure plane for sliding
40	SR	46	318	295	B	Ro5				0	O		Gentle		Irregular	~3m		Dry	-41.2155	174.704		Failure plane for sliding
42	SR	80	176	153	B	Ro3	Moderately wide	~30mm	~99%	0	O	~170°	Gentle	~1.5m	Wavy	~3m		Dry	-41.2155	174.7041		Failure plane for wedge failure, presume terminates against SR40
41	BSH	72	143	121	B	Ro3	Moderately wide	~25mm	~95%	0	O	~170°	Gentle	~2m	Wavy	~2.5m	~1m	Dry	-41.2155	174.7041		Presume terminates against SR40 also an extension of BSH37 and BSH32
41	BSH	84	182	159	B	Ro3	Moderately wide	~25mm	~95%	0	O	~170°	Gentle	~2m	Wavy	~2.5m	~1m	Dry	-41.2155	174.7041		Presume terminates against SR40 also an extension of BSH37 and BSH32
44	BSH	84	352	329	B	Ro3	Moderately narrow	~15mm	~95%	0	O	~140°	Gentle	~0.8m	Wavy	~2.5m	~1.5m	Dry	-41.2155	174.7042		Extension of BSH37 and BSH32
43	SR	78	175	152	B	Ro4	Narrow to Moderately wide	~4 to 20mm	~95%	1	D&S	~100°	Open	~1.5m	Wavy	~3m		Dry	-41.2155	174.704		Terminates against BSH41
43	SR	63	321	298	B	Ro4	Narrow to Moderately wide	~4 to 20mm	~95%	1	D&S	~100°	Open	~1.5m	Wavy	~3m		Dry	-41.2155	174.704		Terminates against BSH41
43	SR	42	323	301	B	Ro4	Narrow to Moderately wide	~4 to 20mm	~95%	1	D&S	~100°	Open	~1.5m	Wavy	~3m		Dry	-41.2155	174.704		Terminates against BSH41
45	SR	89	330	307	B	Ro4	Moderately wide	~40mm	~99%	0	O	~170°	Gentle	~2.5m	Wavy	~4m		Dry	-41.2154	174.704		Terminates against SR40 presume
46	SR	89	104	81	B	Ro5	Moderately wide	~40mm	~99%	0	O	~180°	Gentle		Planar	~5m		Dry	-41.2155	174.7042		Terminates against SR40 presume
47	SR	76	52	30	B	Ro3	Very narrow	~1mm	~99%	1	D	~150°	Gentle	~3m	Wavy	~3m		Dry	-41.2154	174.704		Terminates against SR45
	JN	40	187	164	B					2	D	~180°	Gentle		Planar		~0.2m		-41.2155	174.7041		

JN	47	330	308	B				2	D	~180°	Gentle		Planar		~0.25m			-41.2155	174.704	
JN	87	188	166	B				2	D	~180°	Gentle		Planar		~0.15m			-41.2155	174.7041	
JN	72	50	28	B				2	D	~180°	Gentle		Planar		~0.05m			-41.2155	174.7041	
JN	83	172	150	B				2	D	~180°	Gentle		Planar		~0.15m			-41.2155	174.7041	
JN	48	189	167	B				2	D	~180°	Gentle		Planar		~0.2m			-41.2155	174.704	
JN	62	228	205	B				2	D	~180°	Gentle		Planar		~0.08m			-41.2156	174.704	
JN	54	214	192	B				2	D	~180°	Gentle		Planar		~0.2m			-41.2156	174.7041	

G.4 Makara Head Graphs

Defect and rock mass results from Makara Head. Results are presented in graphs. Where percentages are used they display the respective occurrence of the dependent variable assessed.

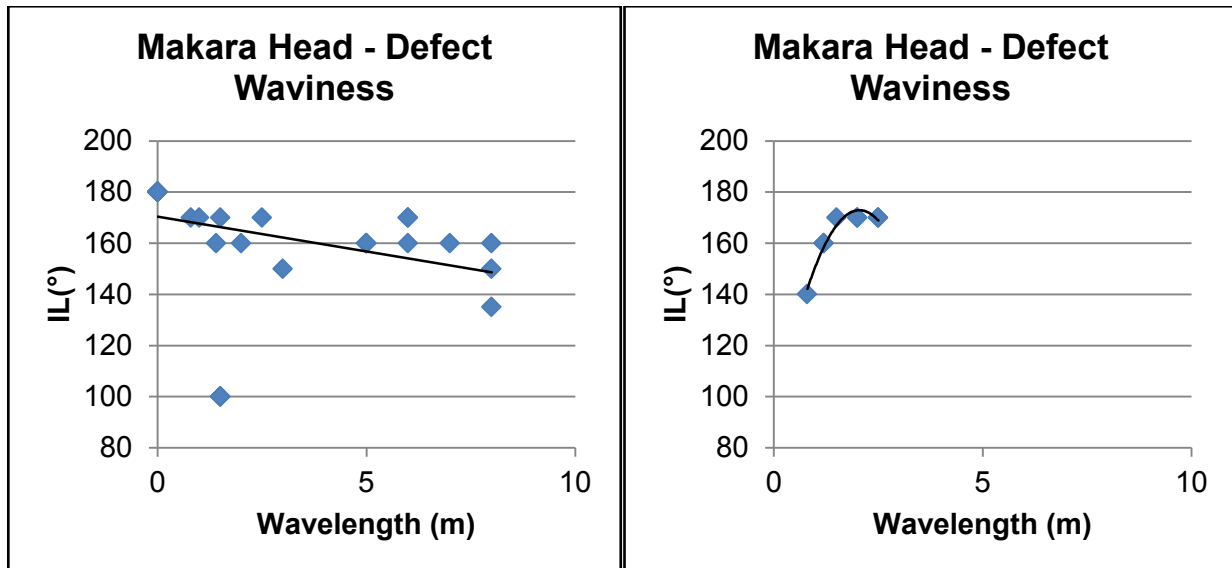
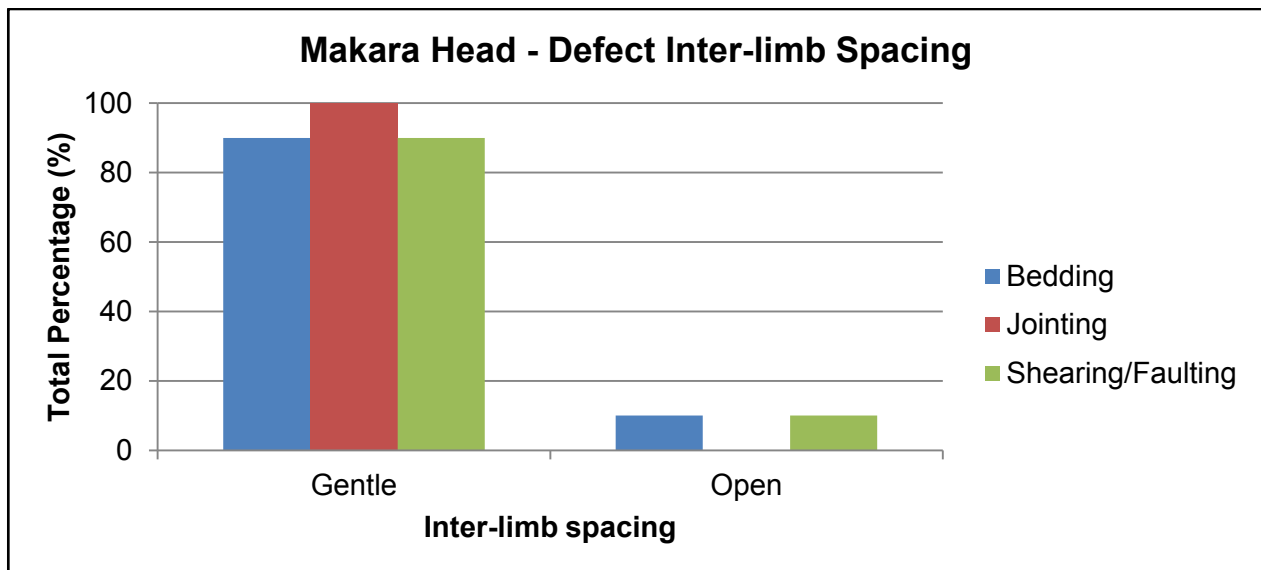
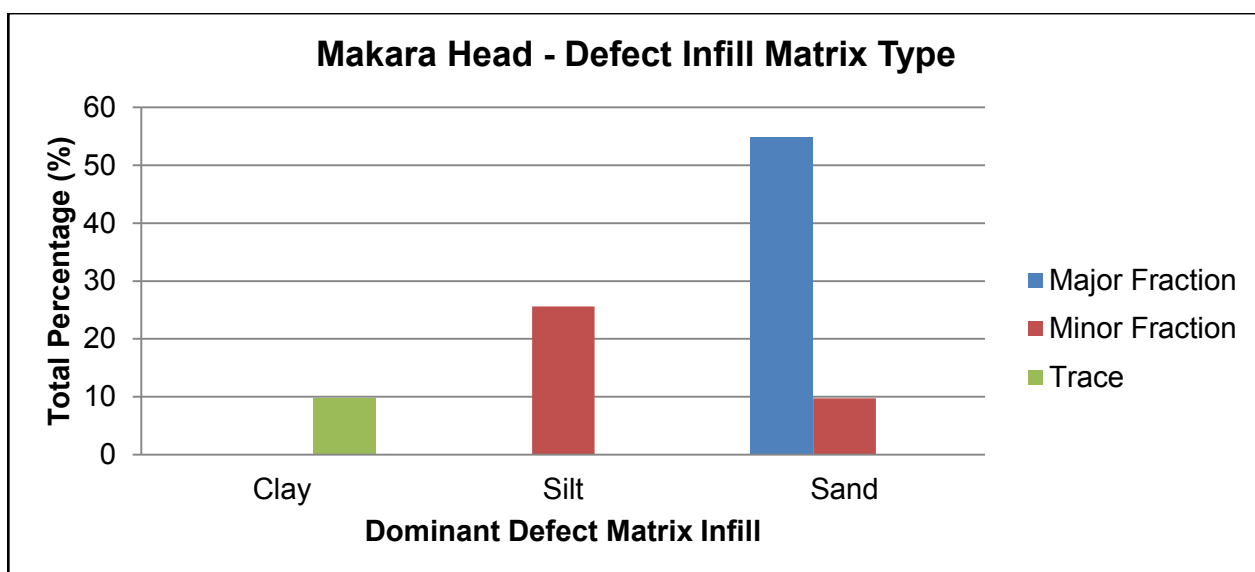
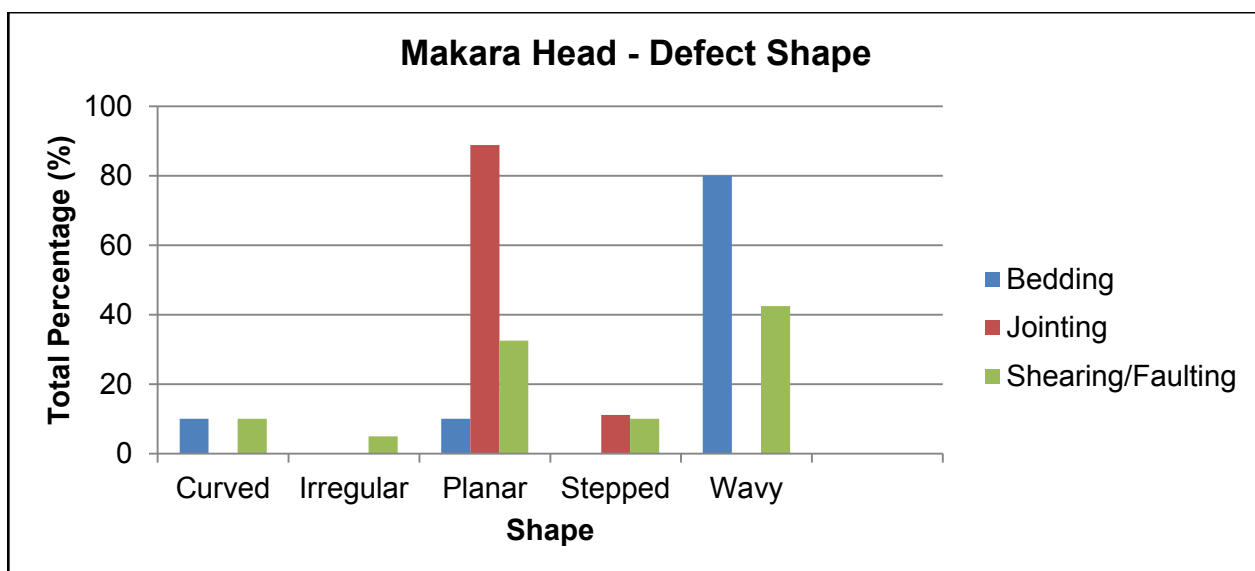
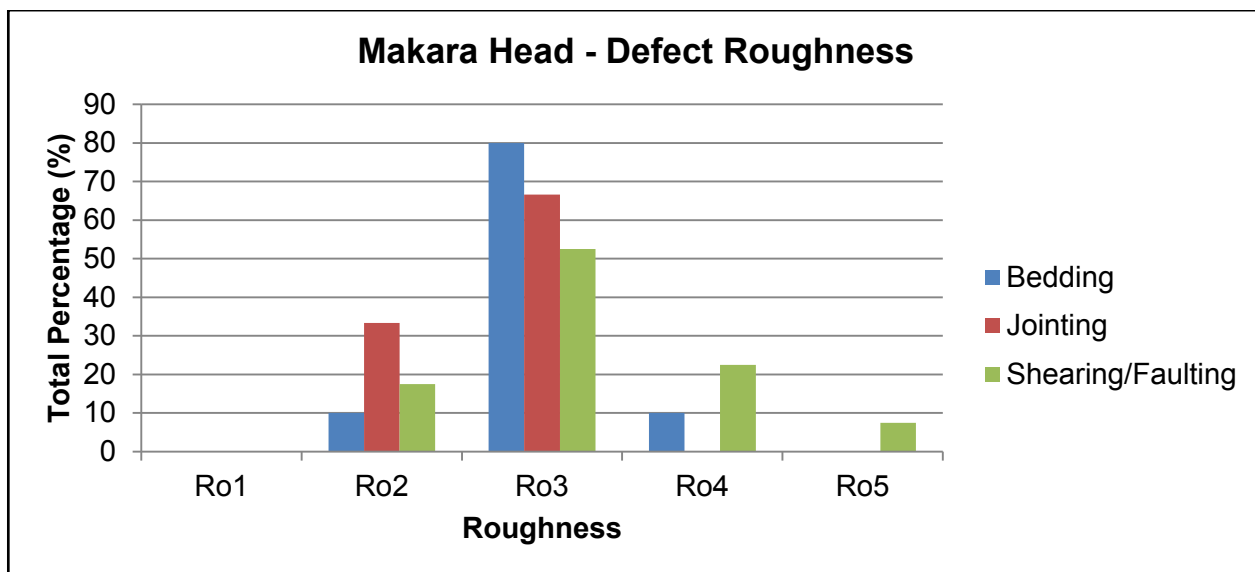
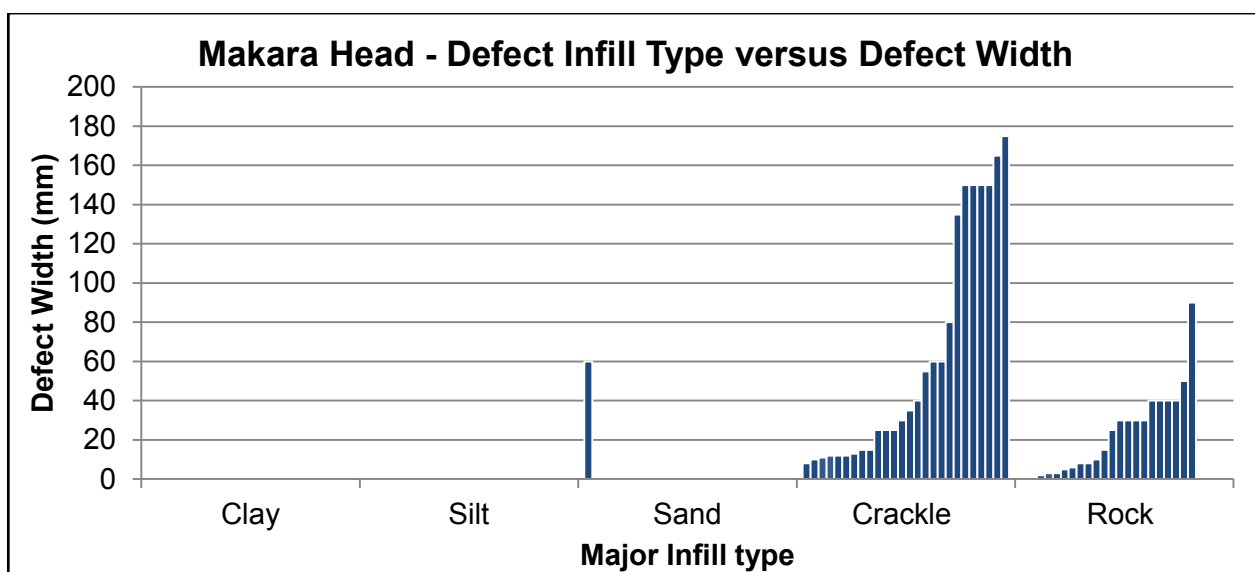
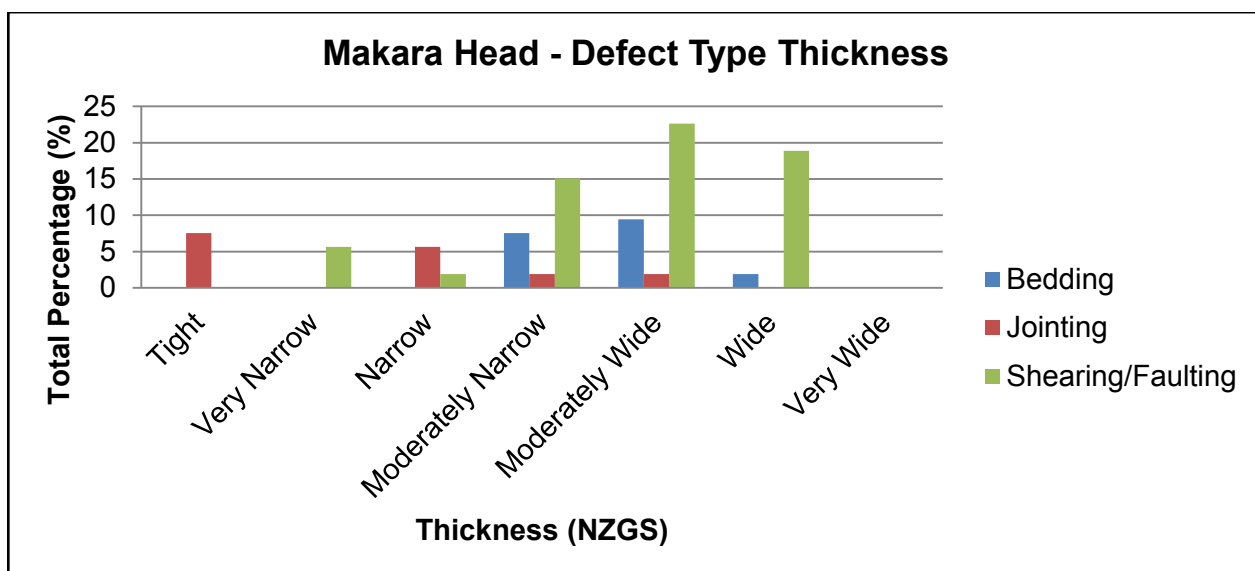
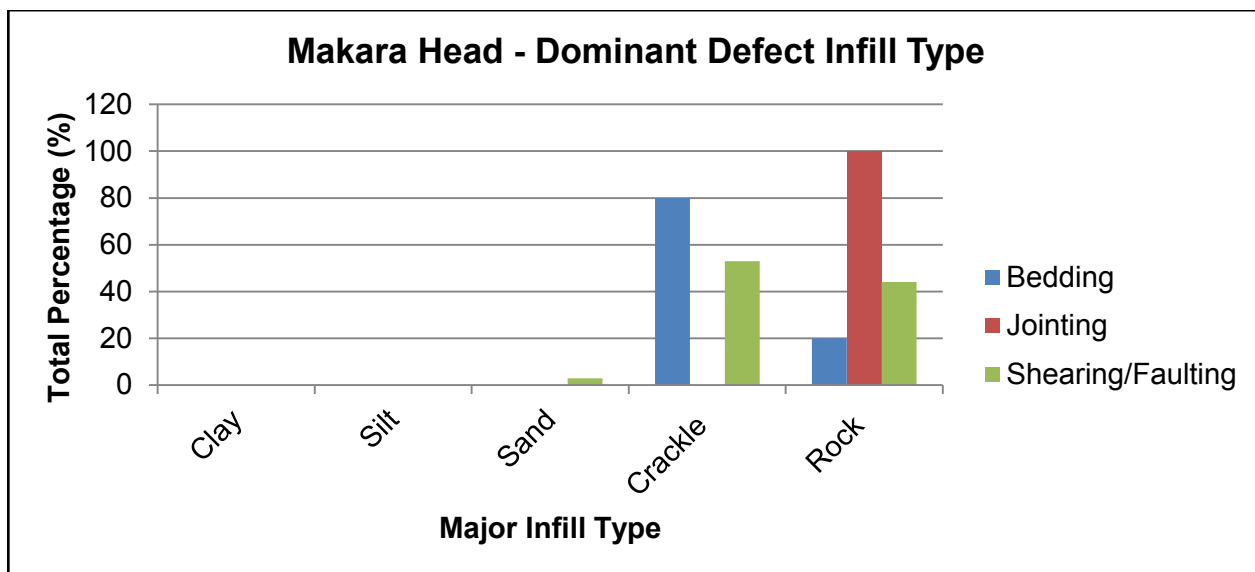
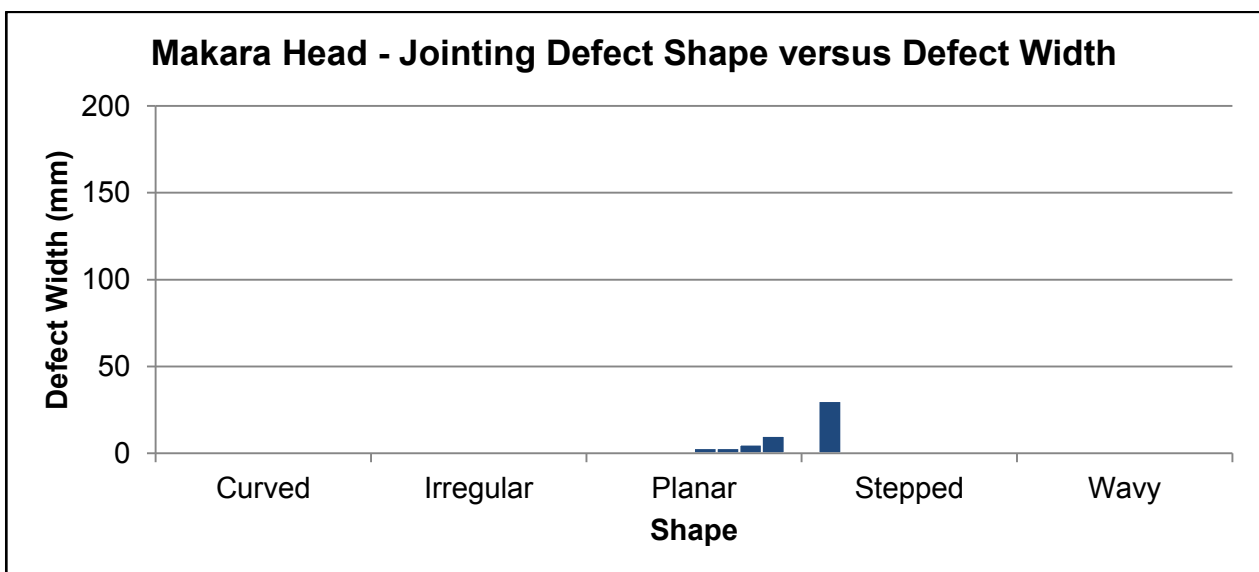
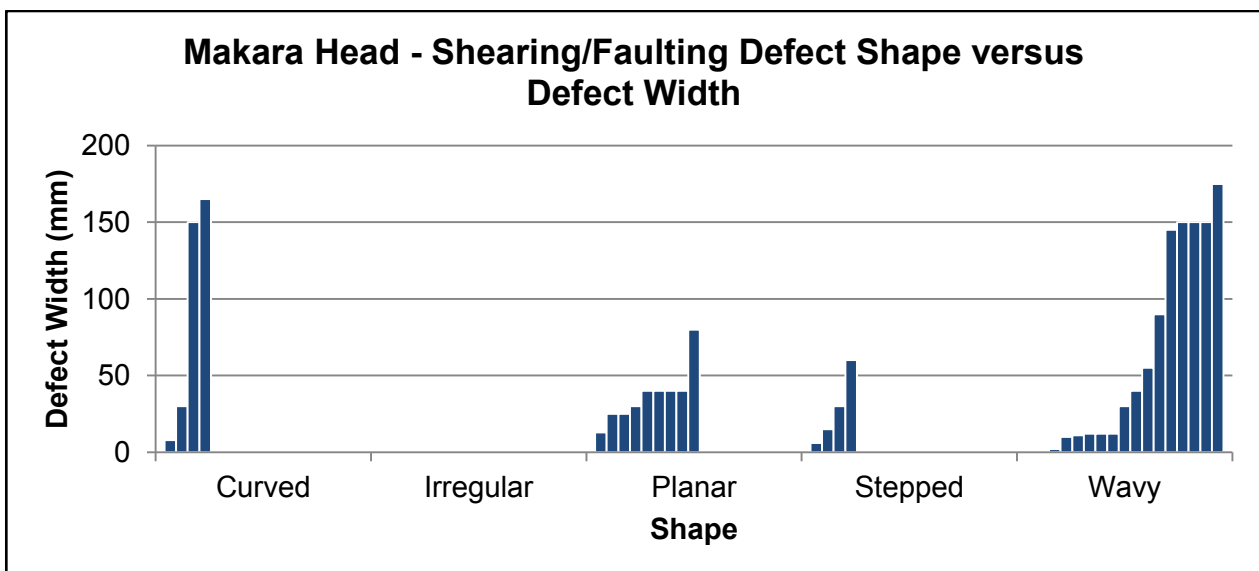
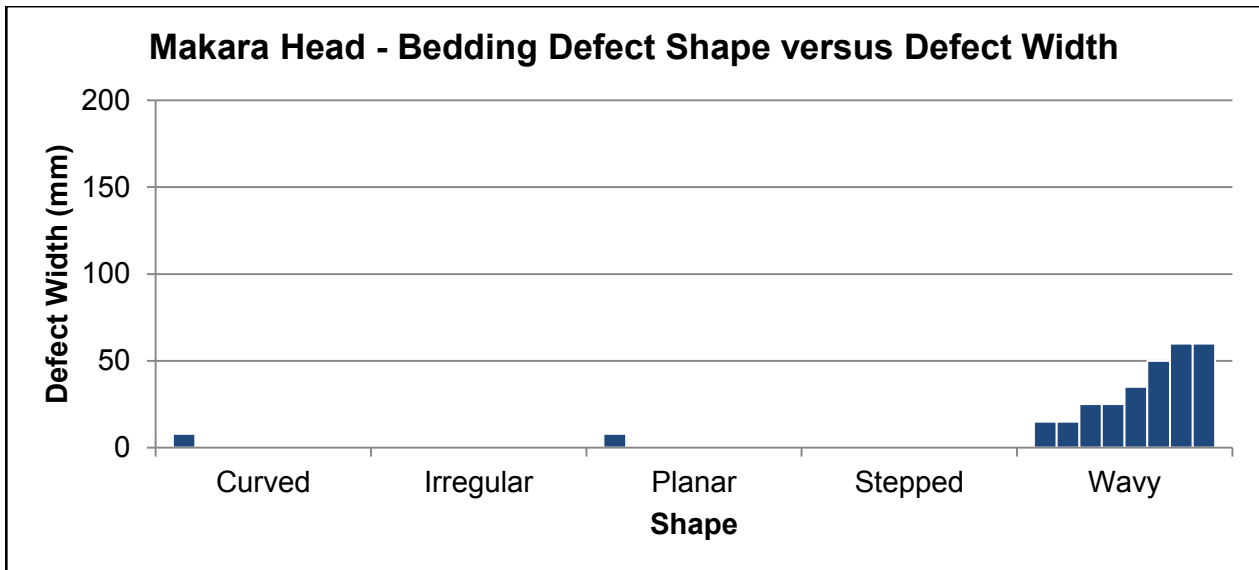


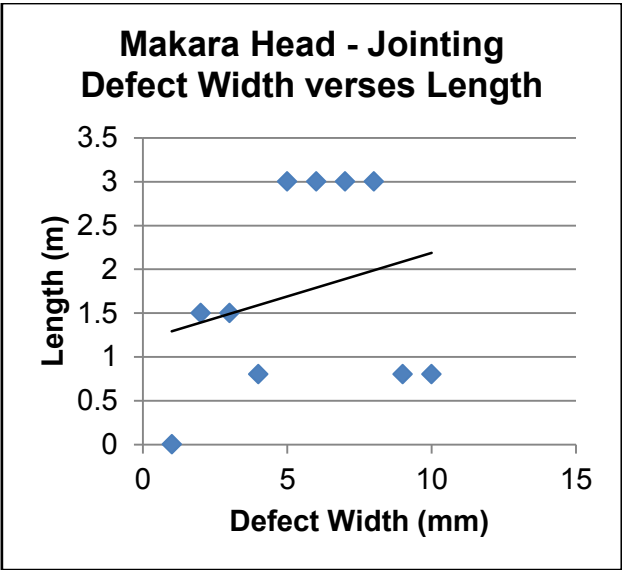
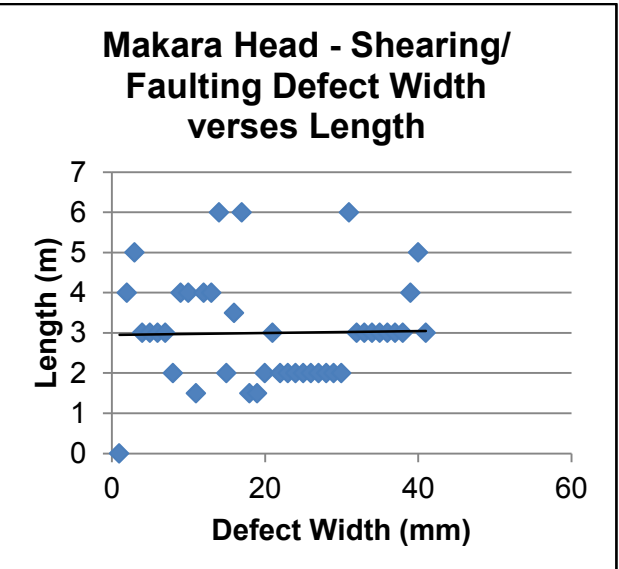
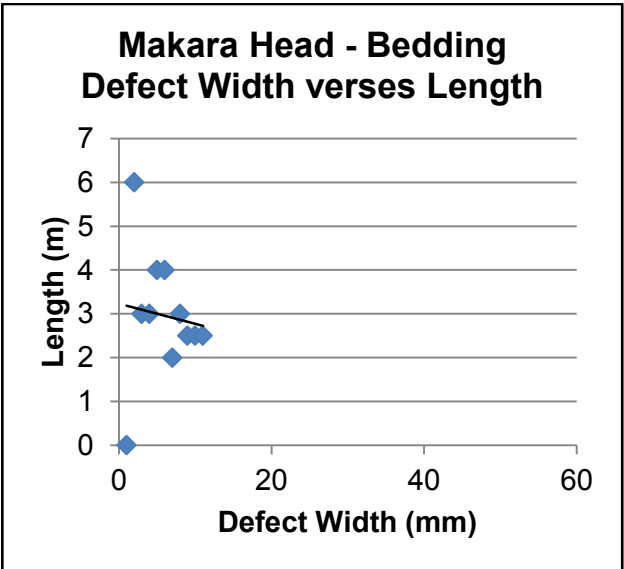
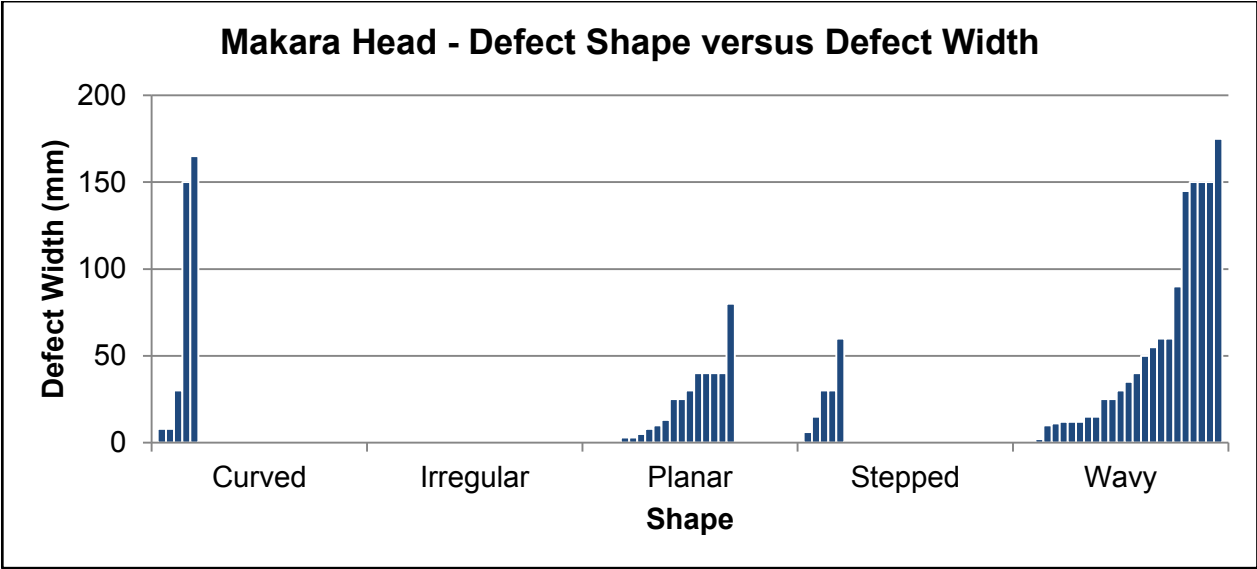
Figure G.4.1: Graphs showing the Makara Head Shearing (Left) and Bedding (Right) waviness.

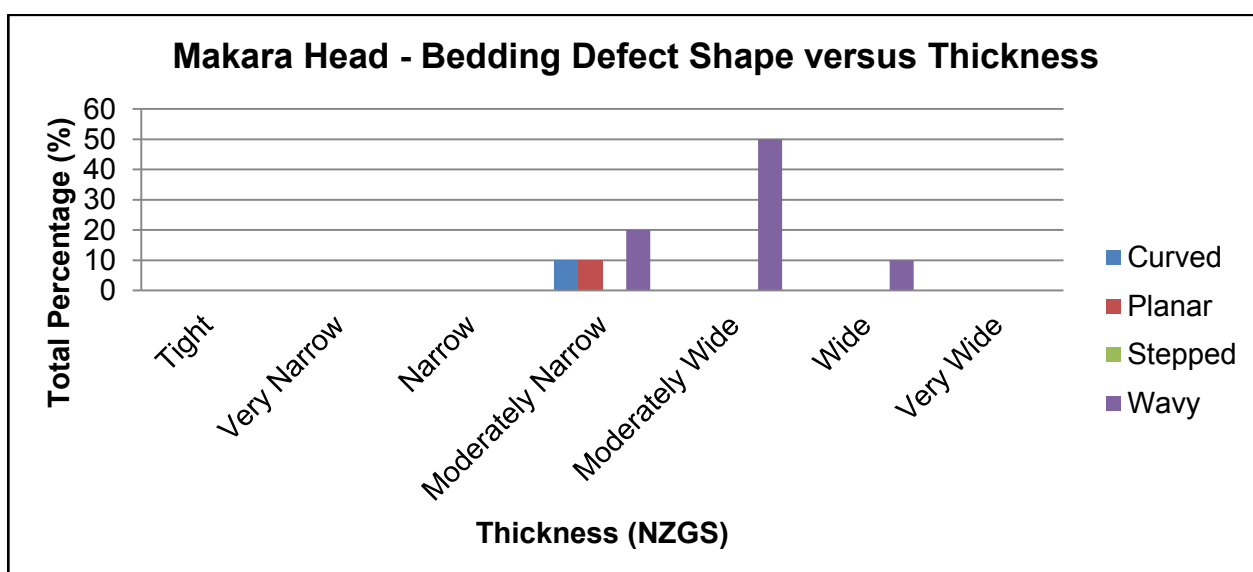
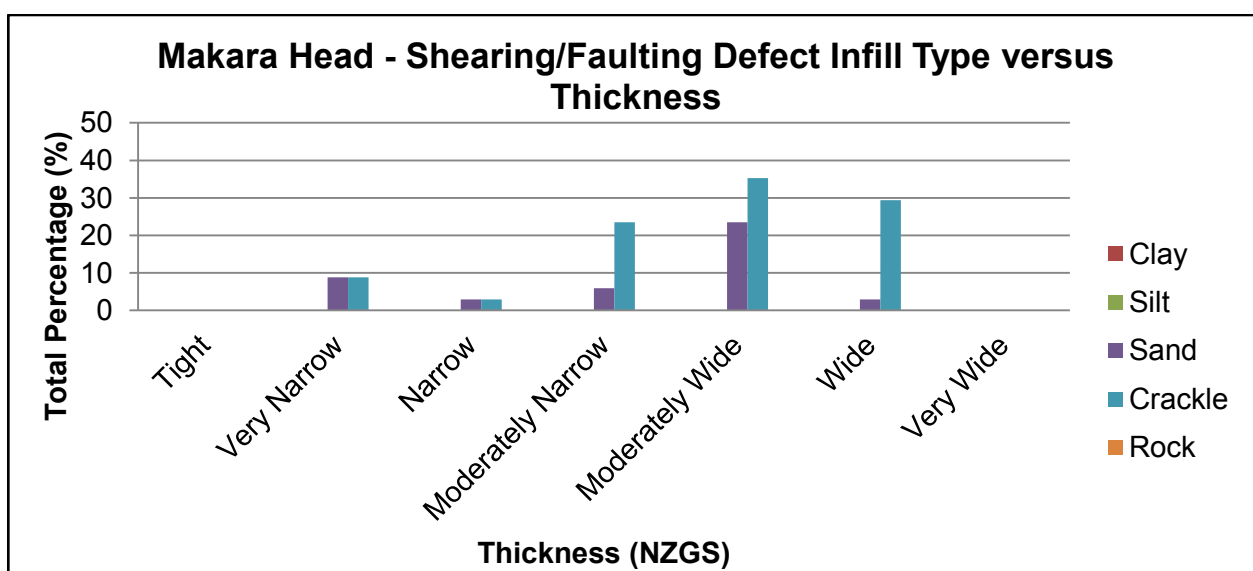
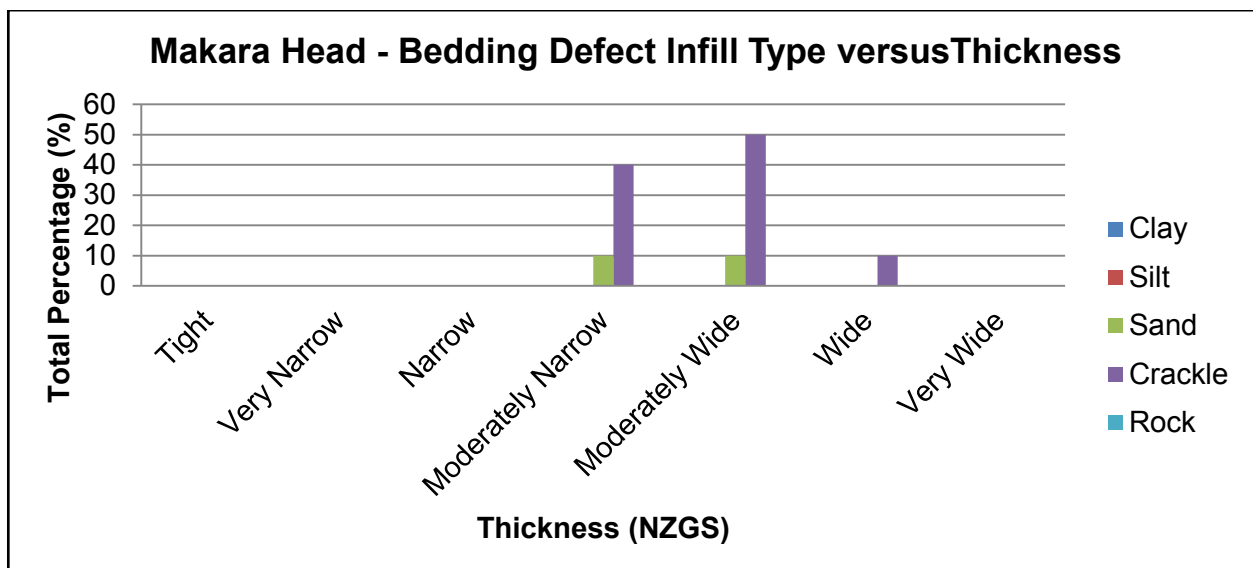


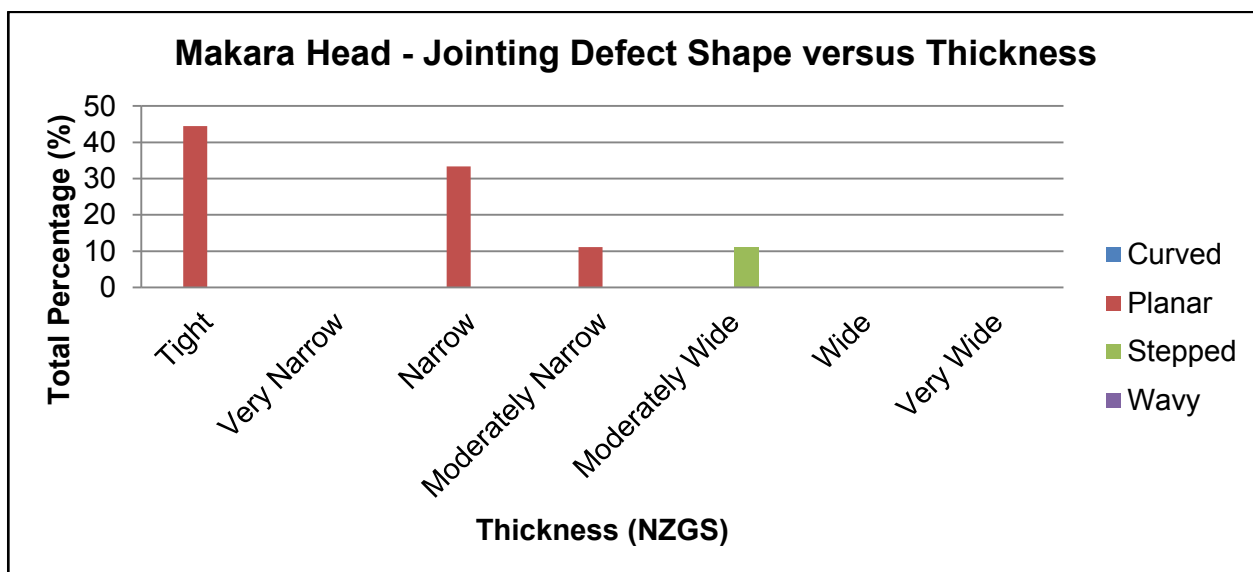
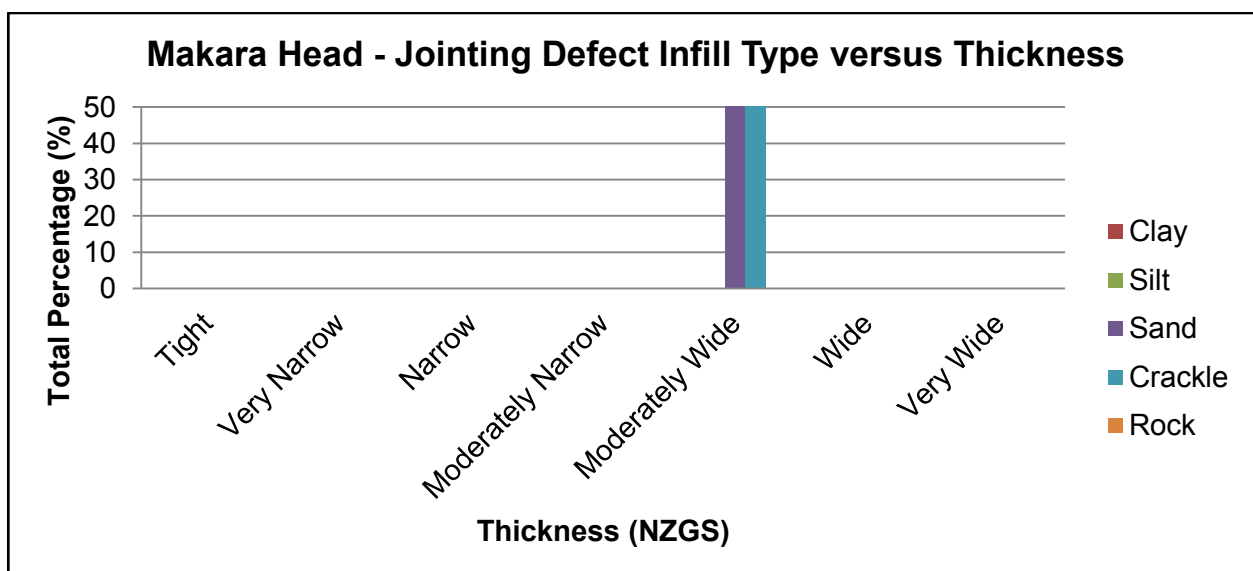
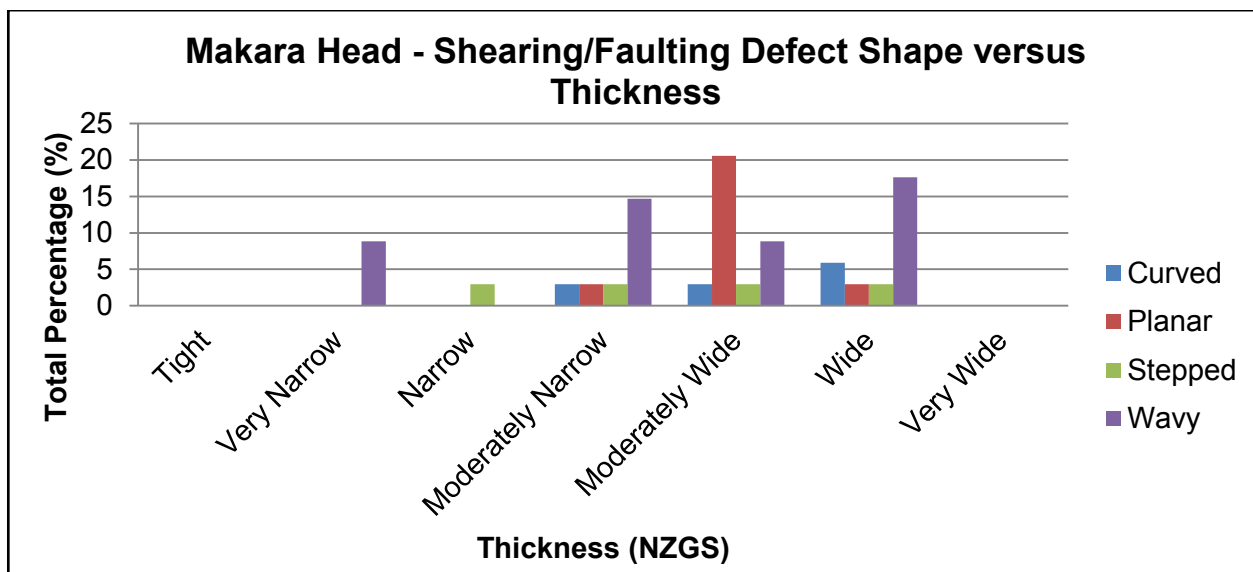


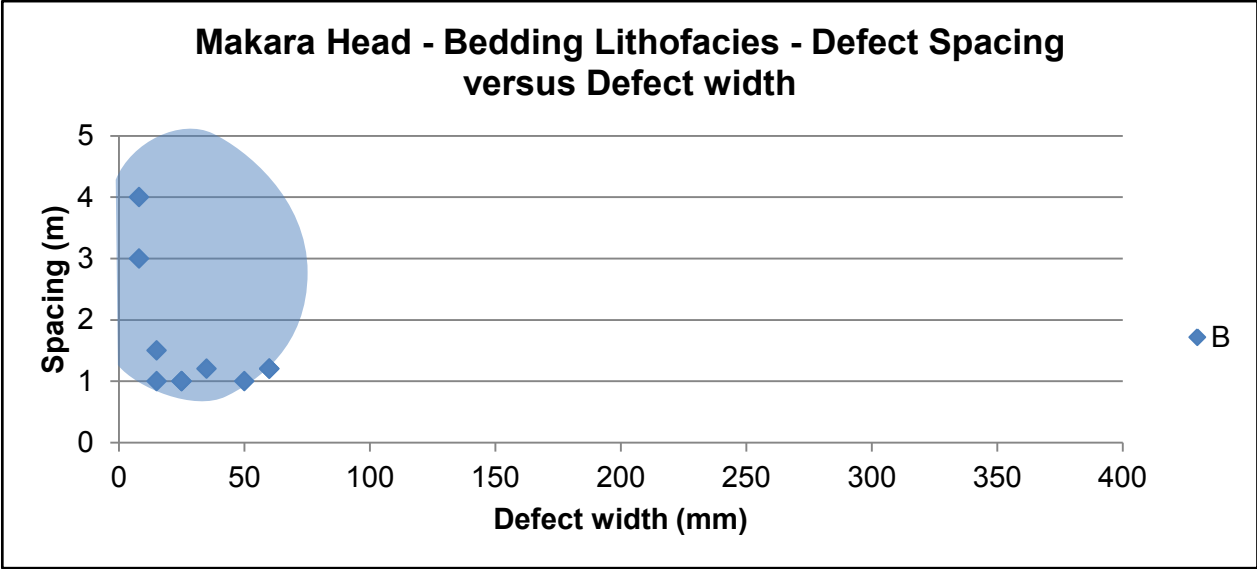








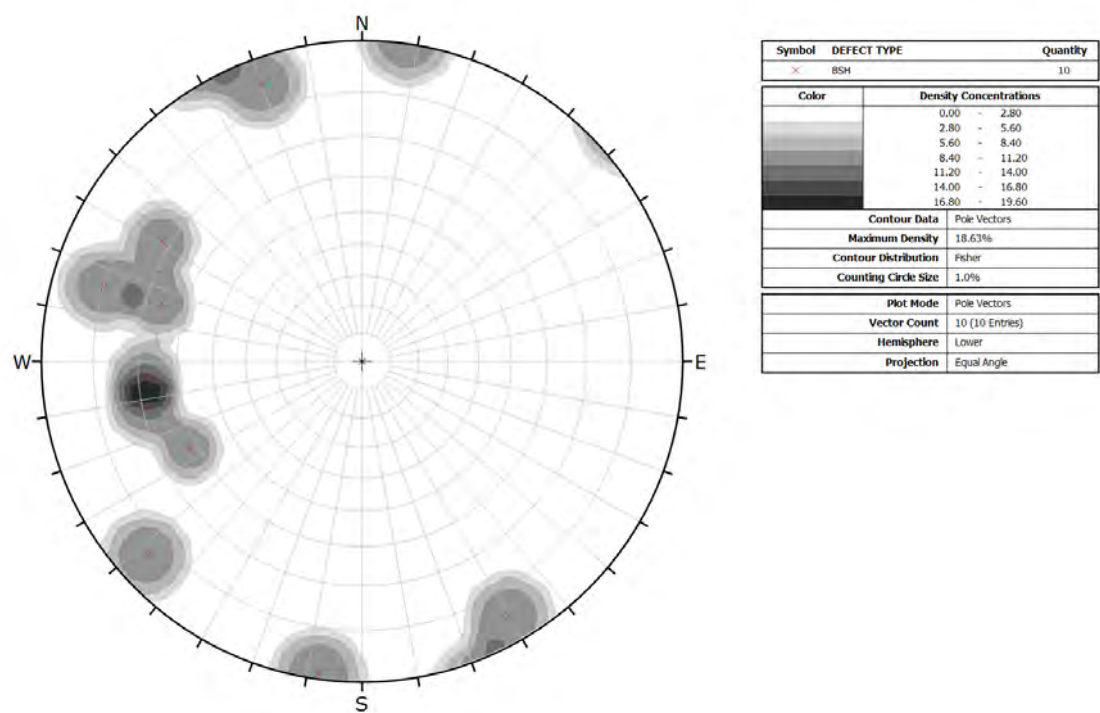




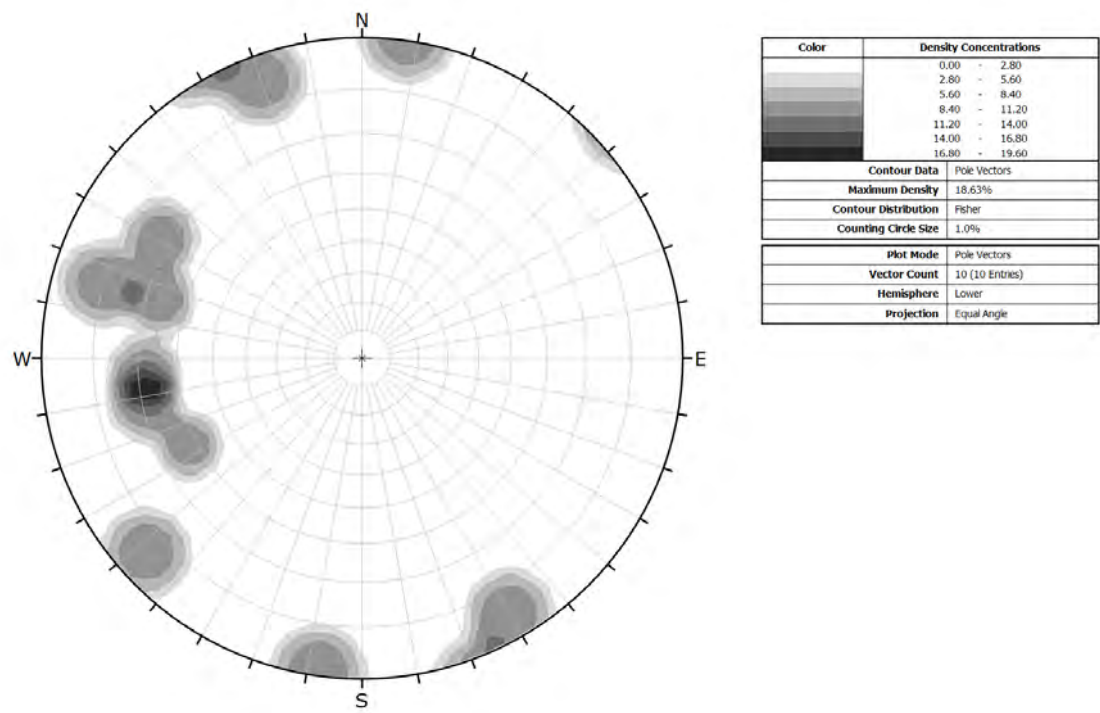
G.5 Makara Head Stereonet Analysis

Stereonet Dip: Dip direction analysis of bedding, faults and shears respectively.

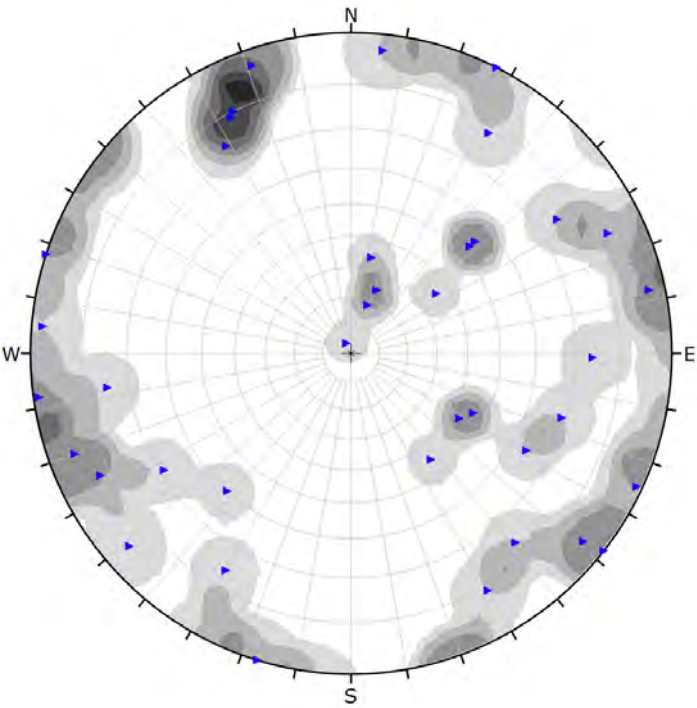
Bedding poles



Contour diagram of bedding clusters



Shearing poles



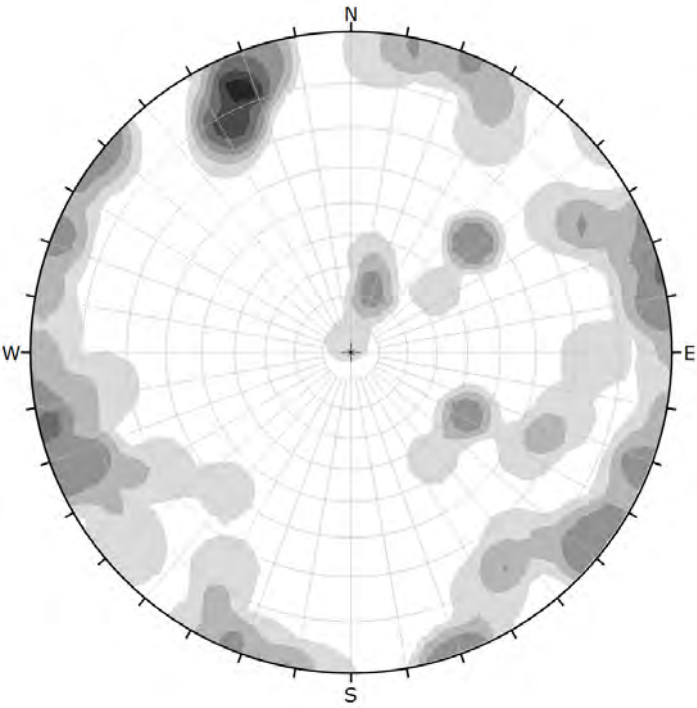
Symbol	DEFECT TYPE	Quantity
►	SR	40

Color	Density Concentrations
	0.00 - 1.30
	1.30 - 2.60
	2.60 - 3.90
	3.90 - 5.20
	5.20 - 6.50
	6.50 - 7.80
	7.80 - 9.10

Contour Data	Pole Vectors
Maximum Density	8.47%
Contour Distribution	Fisher
Counting Circle Size	1.0%

Plot Mode	Pole Vectors
Vector Count	40 (40 Entries)
Hemisphere	Lower
Projection	Equal Angle

Contour diagram of shearing and faulting clusters

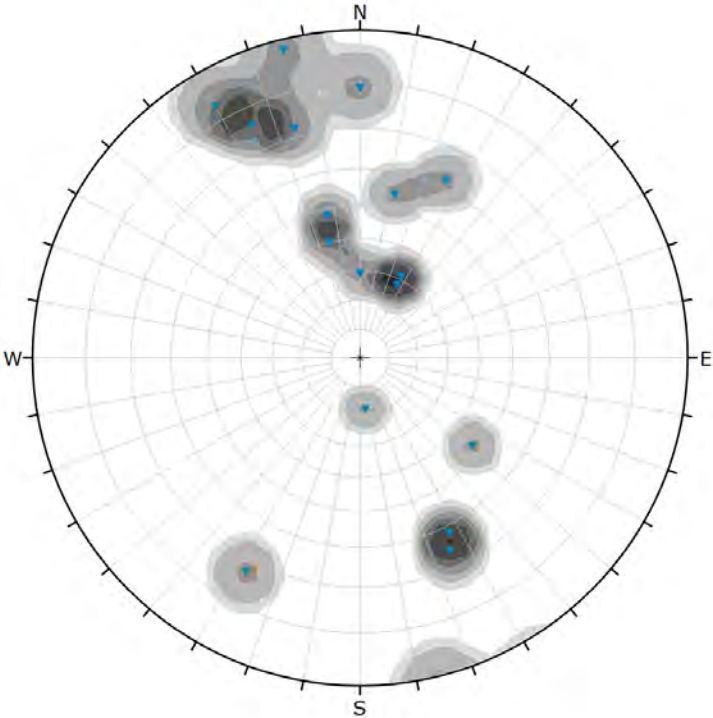


Color	Density Concentrations
	0.00 - 1.30
	1.30 - 2.60
	2.60 - 3.90
	3.90 - 5.20
	5.20 - 6.50
	6.50 - 7.80
	7.80 - 9.10

Contour Data	Pole Vectors
Maximum Density	8.47%
Contour Distribution	Fisher
Counting Circle Size	1.0%

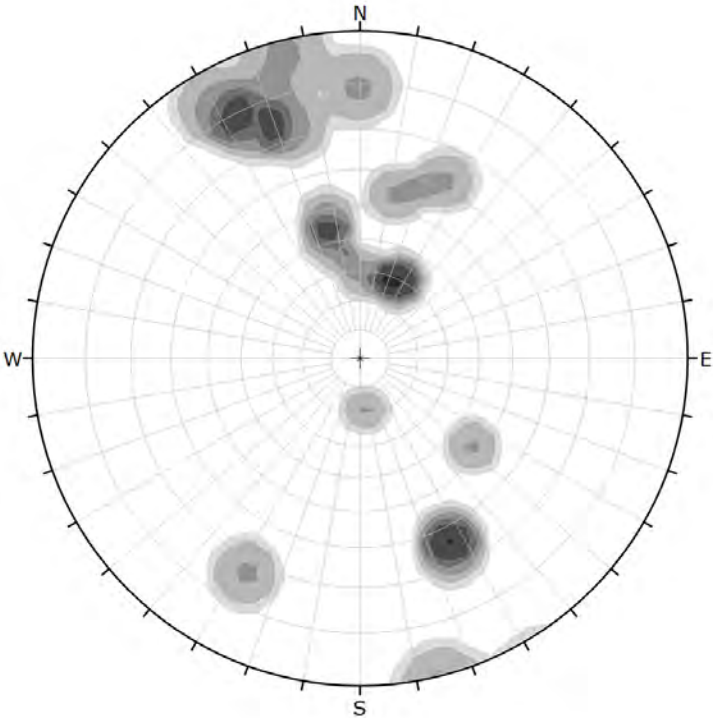
Plot Mode	Pole Vectors
Vector Count	40 (40 Entries)
Hemisphere	Lower
Projection	Equal Angle

Jointing poles



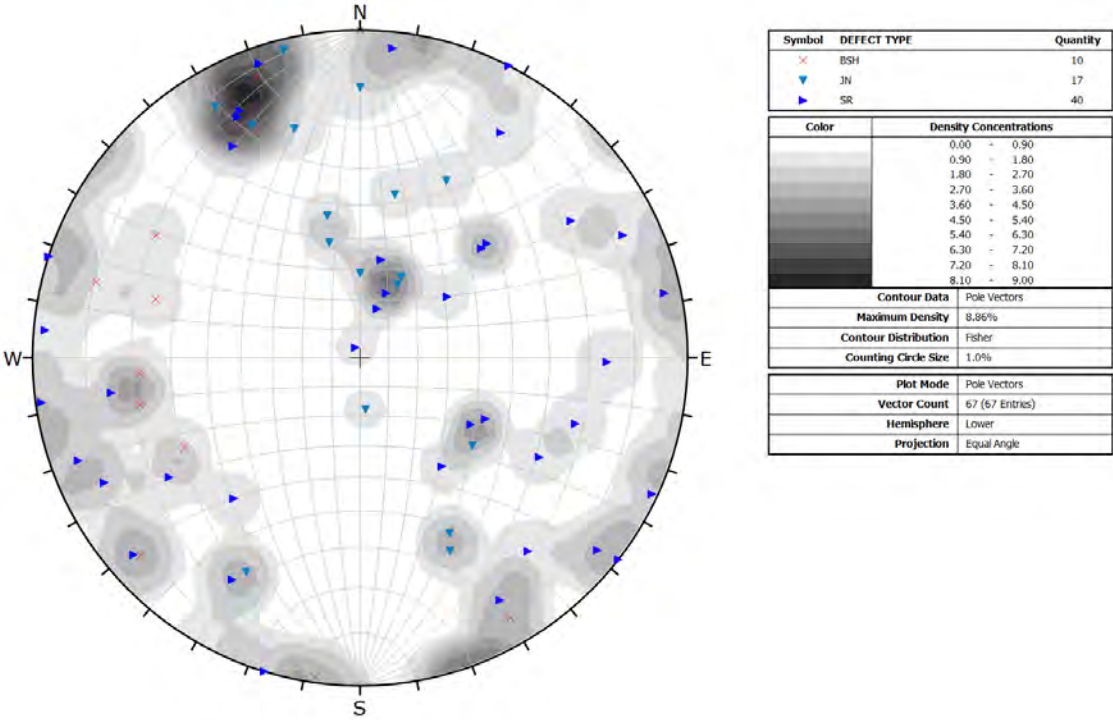
Symbol	DEFECT TYPE	Quantity
▼	IN	17
Color	Density Concentrations	
	0.00	~ 1.90
	1.90	~ 3.80
	3.80	~ 5.70
	5.70	~ 7.60
	7.60	~ 9.50
	9.50	~ 11.40
	11.40	~ 13.30
Contour Data		Pole Vectors
Maximum Density		12.31%
Contour Distribution		Fisher
Counting Circle Size		1.0%
Plot Mode		Pole Vectors
Vector Count		17 (17 Entries)
Hemisphere		Lower
Projection		Equal Angle

Contour diagram of jointing clusters

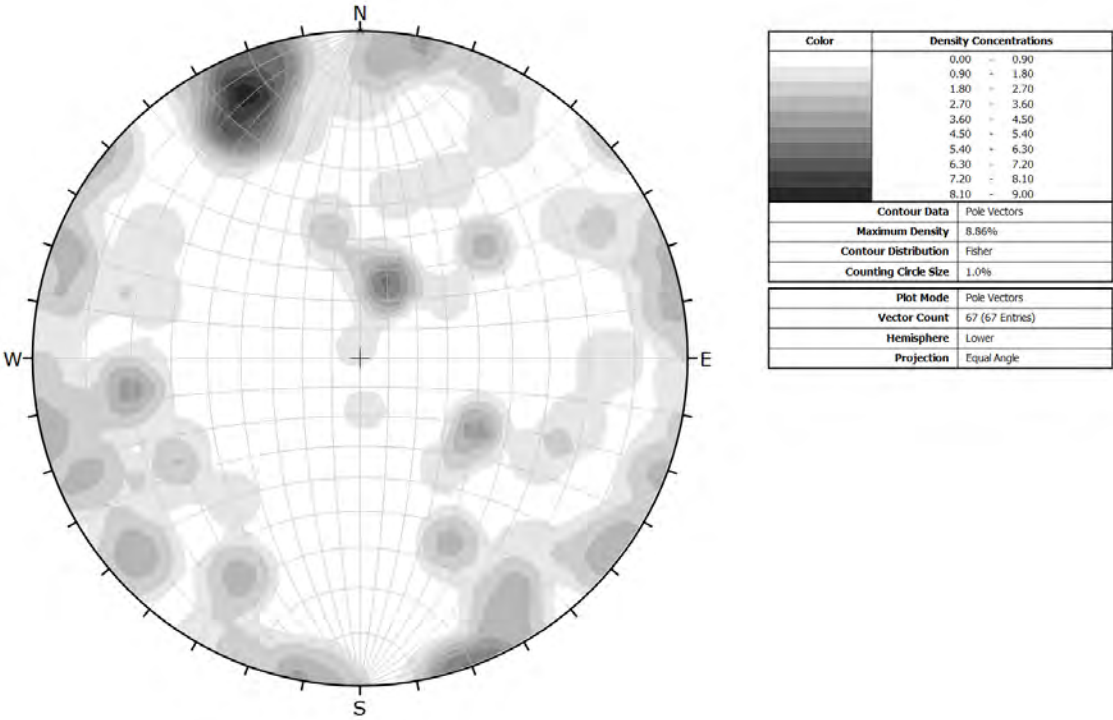


Color	Density Concentrations	
	0.00	~ 1.90
	1.90	~ 3.80
	3.80	~ 5.70
	5.70	~ 7.60
	7.60	~ 9.50
	9.50	~ 11.40
	11.40	~ 13.30
Contour Data		Pole Vectors
Maximum Density		12.31%
Contour Distribution		Fisher
Counting Circle Size		1.0%
Plot Mode		Pole Vectors
Vector Count		17 (17 Entries)
Hemisphere		Lower
Projection		Equal Angle

All defects poles



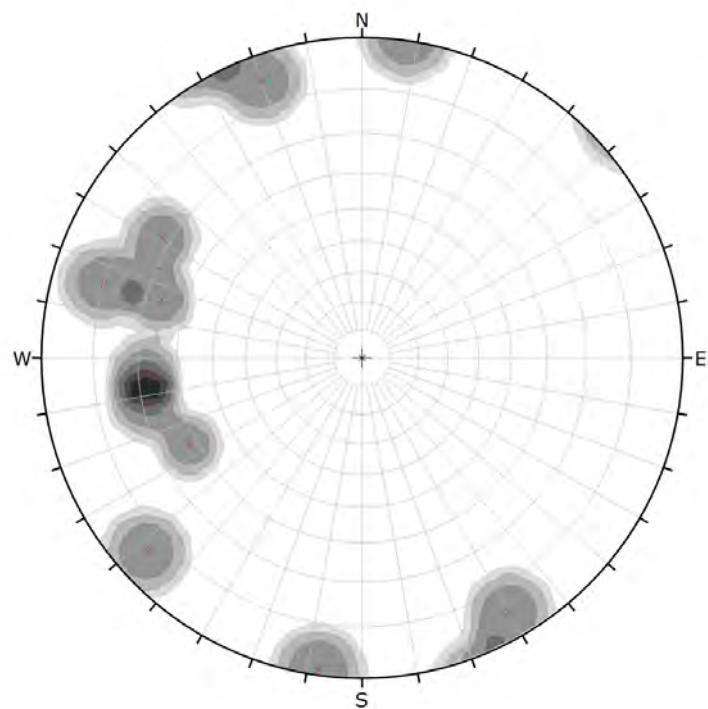
Contour diagram of all defects cluster



G.6 Filtered Stereonet Analysis

Stereonet from G.5 assessed for “noise”. The following only displays the poles of the continuous defects in Makara Head.

Bedding poles



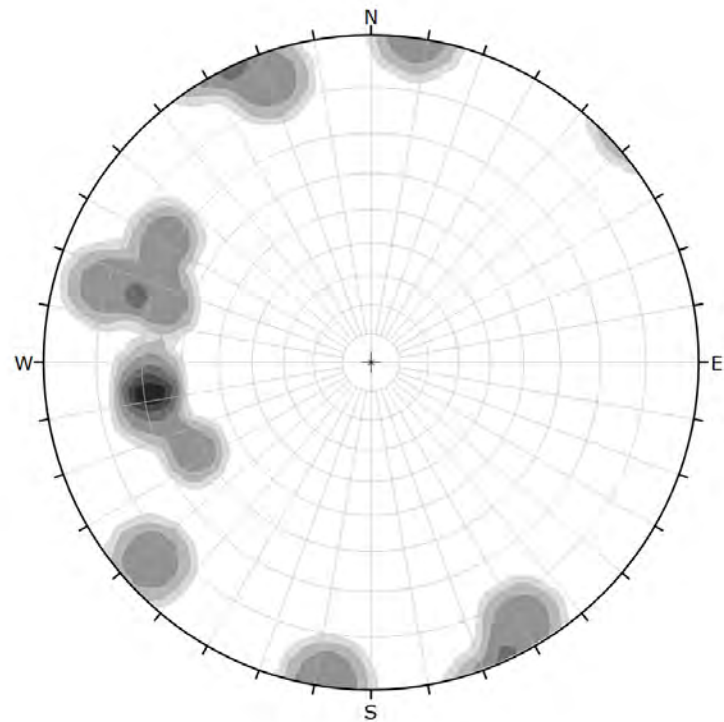
Symbol	DEFECT TYPE	Quantity
x	BSH	10

Color	Density Concentrations
	0.00 - 2.80
	2.80 - 5.60
	5.60 - 8.40
	8.40 - 11.20
	11.20 - 14.00
	14.00 - 16.80
	16.80 - 19.60

Contour Data	Pole Vectors
Maximum Density	18.63%
Contour Distribution	Fisher
Counting Circle Size	1.0%

Plot Mode	Pole Vectors
Vector Count	10 (10 Entries)
Hemisphere	Lower
Projection	Equal Angle

Contour diagram of bedding clusters

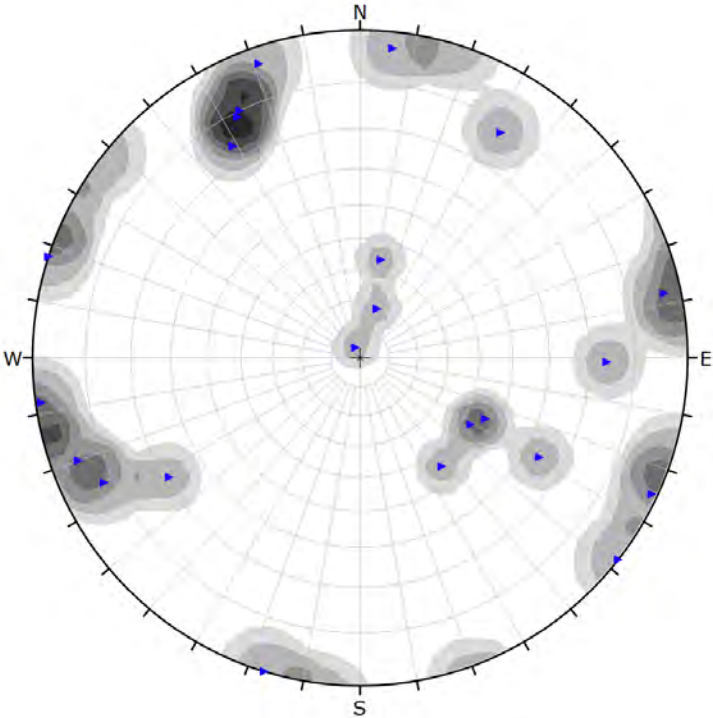


Color	Density Concentrations
	0.00 - 2.80
	2.80 - 5.60
	5.60 - 8.40
	8.40 - 11.20
	11.20 - 14.00
	14.00 - 16.80
	16.80 - 19.60

Contour Data	Pole Vectors
Maximum Density	18.63%
Contour Distribution	Fisher
Counting Circle Size	1.0%

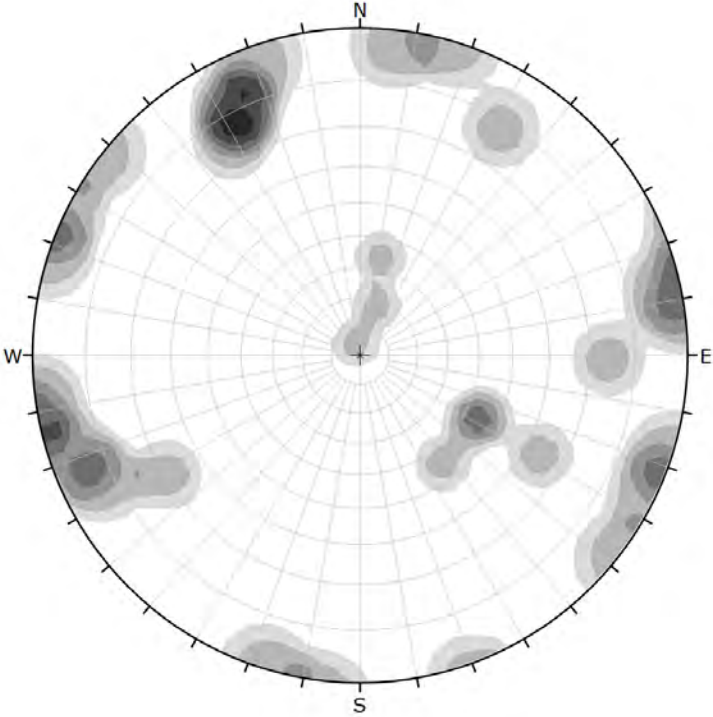
Plot Mode	Pole Vectors
Vector Count	10 (10 Entries)
Hemisphere	Lower
Projection	Equal Angle

Shearing poles



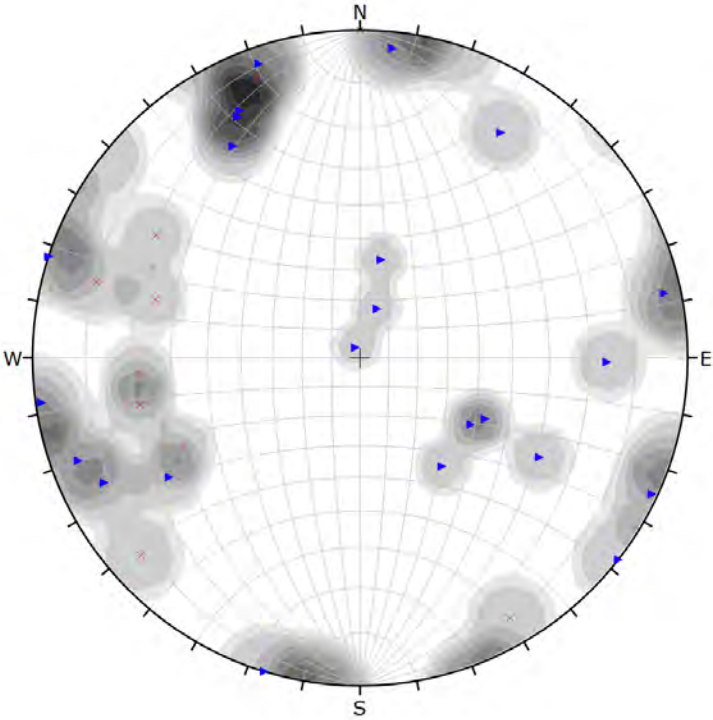
Symbol	DEFECT TYPE	Quantity
▶	SR	23
Color	Density Concentrations	
	0.00	~ 1.90
	1.90	~ 3.80
	3.80	~ 5.70
	5.70	~ 7.60
	7.60	~ 9.50
	9.50	~ 11.40
	11.40	~ 13.30
Contour Data		Pole Vectors
Maximum Density		12.38%
Contour Distribution		Fisher
Counting Circle Size		1.0%
Plot Mode		Pole Vectors
Vector Count		23 (23 Entries)
Hemisphere		Lower
Projection		Equal Angle

Contour diagram of shearing and faulting clusters



Color	Density Concentrations	
	0.00	~ 1.90
	1.90	~ 3.80
	3.80	~ 5.70
	5.70	~ 7.60
	7.60	~ 9.50
	9.50	~ 11.40
	11.40	~ 13.30
Contour Data		Pole Vectors
Maximum Density		12.38%
Contour Distribution		Fisher
Counting Circle Size		1.0%
Plot Mode		Pole Vectors
Vector Count		23 (23 Entries)
Hemisphere		Lower
Projection		Equal Angle

All defects poles



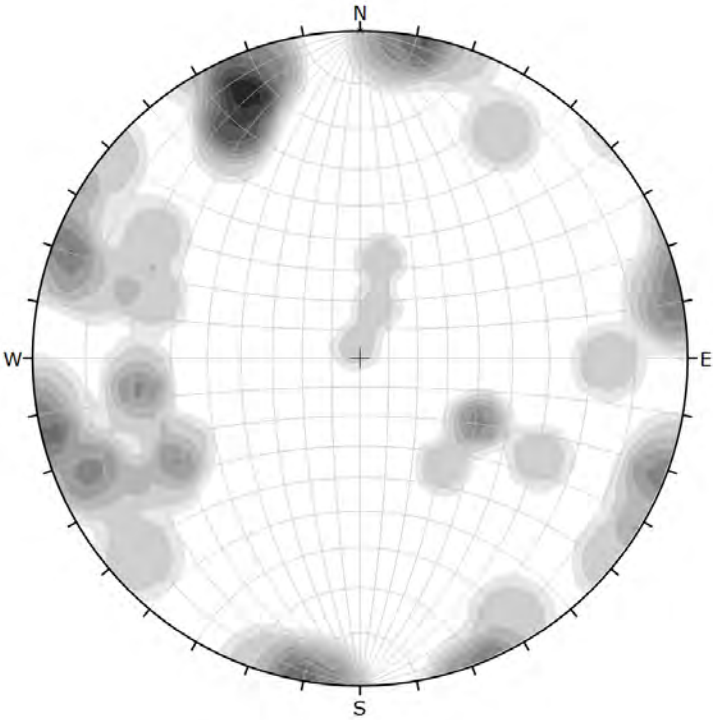
Symbol	DEFECT TYPE	Quantity
×	BSH	10
►	SR	23

Color	Density Concentrations
	0.00 ~ 1.10
	1.10 ~ 2.20
	2.20 ~ 3.30
	3.30 ~ 4.40
	4.40 ~ 5.50
	5.50 ~ 6.60
	6.60 ~ 7.70
	7.70 ~ 8.80
	8.80 ~ 9.90
	9.90 ~ 11.00

Contour Data	Pole Vectors
Maximum Density	10.85%
Contour Distribution	Fisher
Counting Circle Size	1.0%

Plot Mode	Pole Vectors
Vector Count	33 (33 Entries)
Hemisphere	Lower
Projection	Equal Angle

Contour diagram of all defects cluster



Color	Density Concentrations
	0.00 ~ 1.10
	1.10 ~ 2.20
	2.20 ~ 3.30
	3.30 ~ 4.40
	4.40 ~ 5.50
	5.50 ~ 6.60
	6.60 ~ 7.70
	7.70 ~ 8.80
	8.80 ~ 9.90
	9.90 ~ 11.00

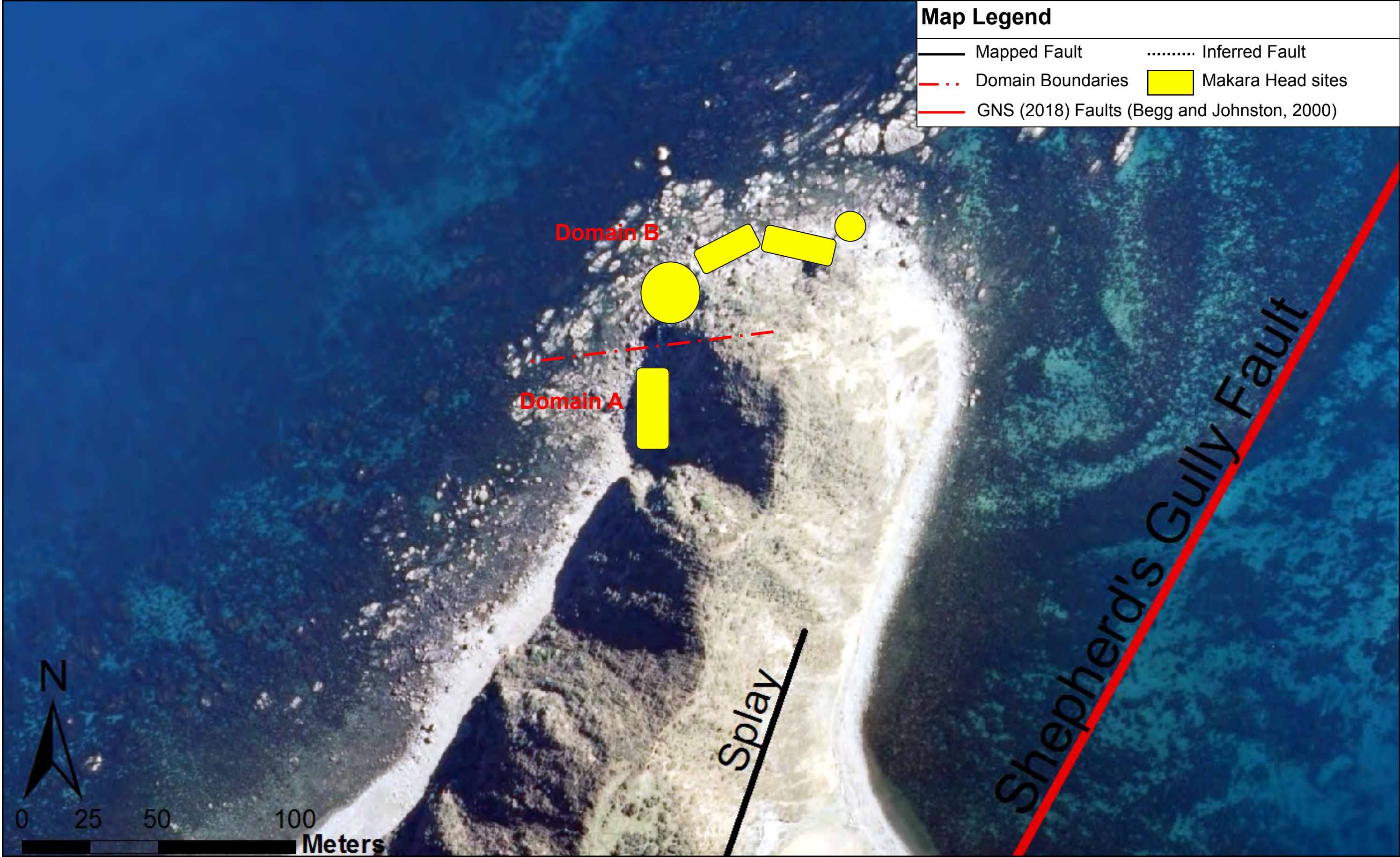
Contour Data	Pole Vectors
Maximum Density	10.85%
Contour Distribution	Fisher
Counting Circle Size	1.0%

Plot Mode	Pole Vectors
Vector Count	33 (33 Entries)
Hemisphere	Lower
Projection	Equal Angle

G.7 Makara Head Structural Domains

Figures are based on mapping observations and stereonet analysis. The figures represent a very detailed interpretation of the changes in defect orientation across the Makara Head site.

G.7.1 Makara Head - Domains



Imagery sourced: LINZ aerial imagery, 2017 (Captured by AAM NZ Ltd (2017))

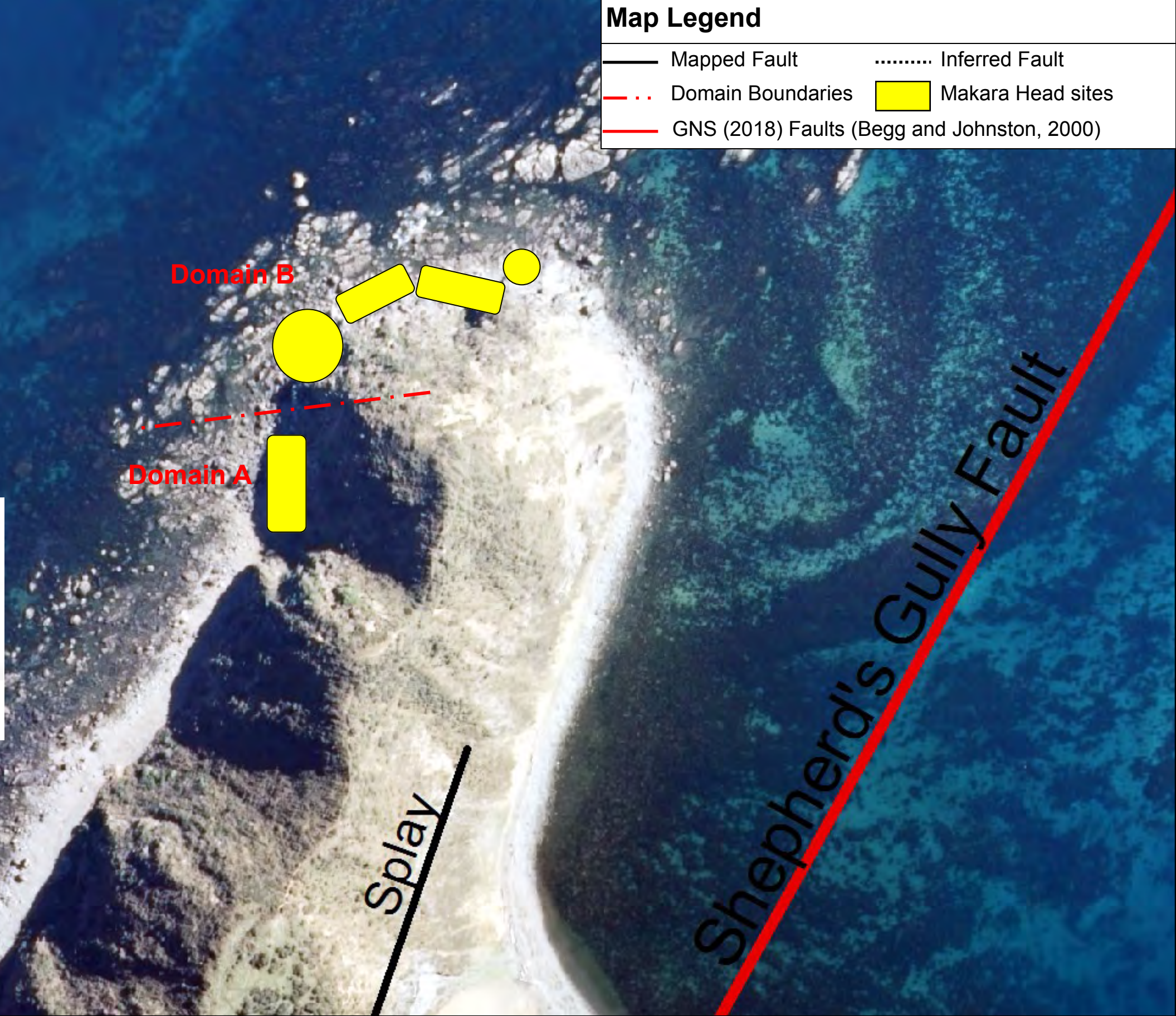
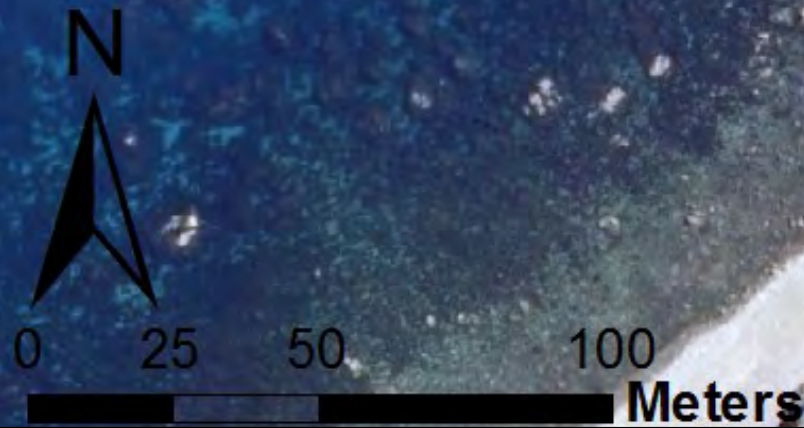
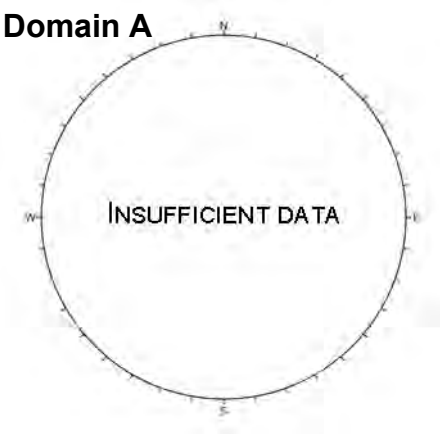
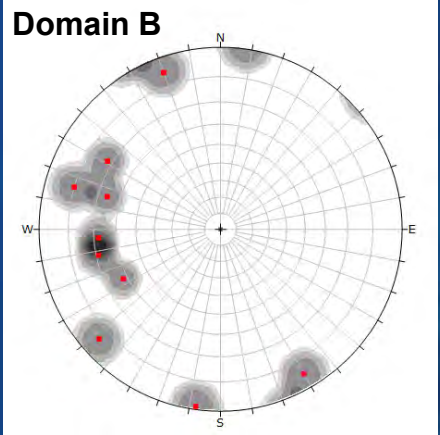
G.7.2 Makara Head Domains - Bedding

Stereoplot Legend

- Bedding Shear
- Bedding Fabric

Map Legend

- Mapped Fault
- Domain Boundaries
- GNS (2018) Faults (Begg and Johnston, 2000)
- Inferred Fault
- Makara Head sites



Imagery sourced: LINZ aerial imagery, 2017 (Captured by AAM NZ Ltd (2017))

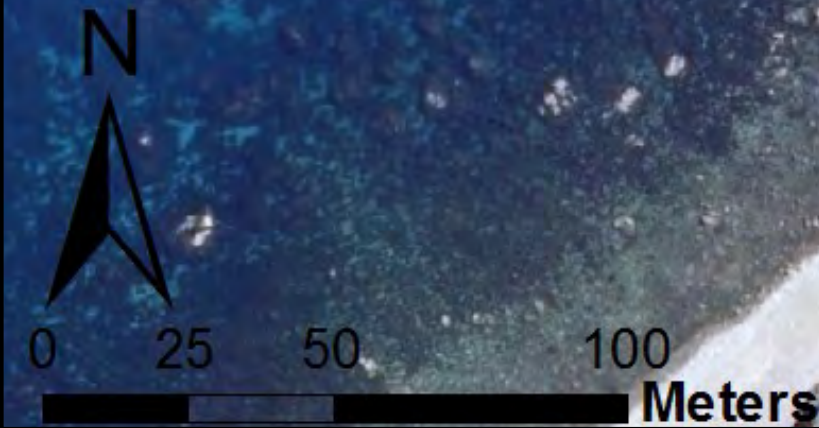
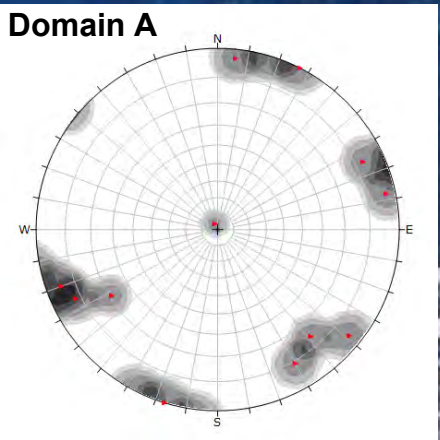
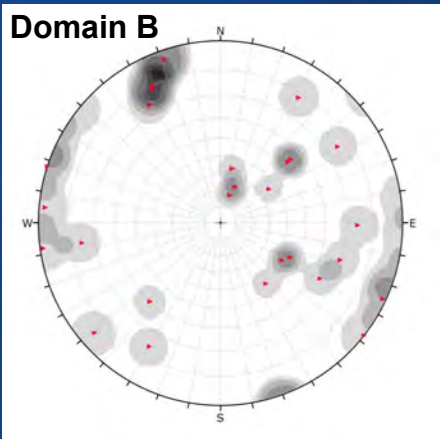
G.7.3 Makara Head Domains - Shearing

Stereoplot Legend

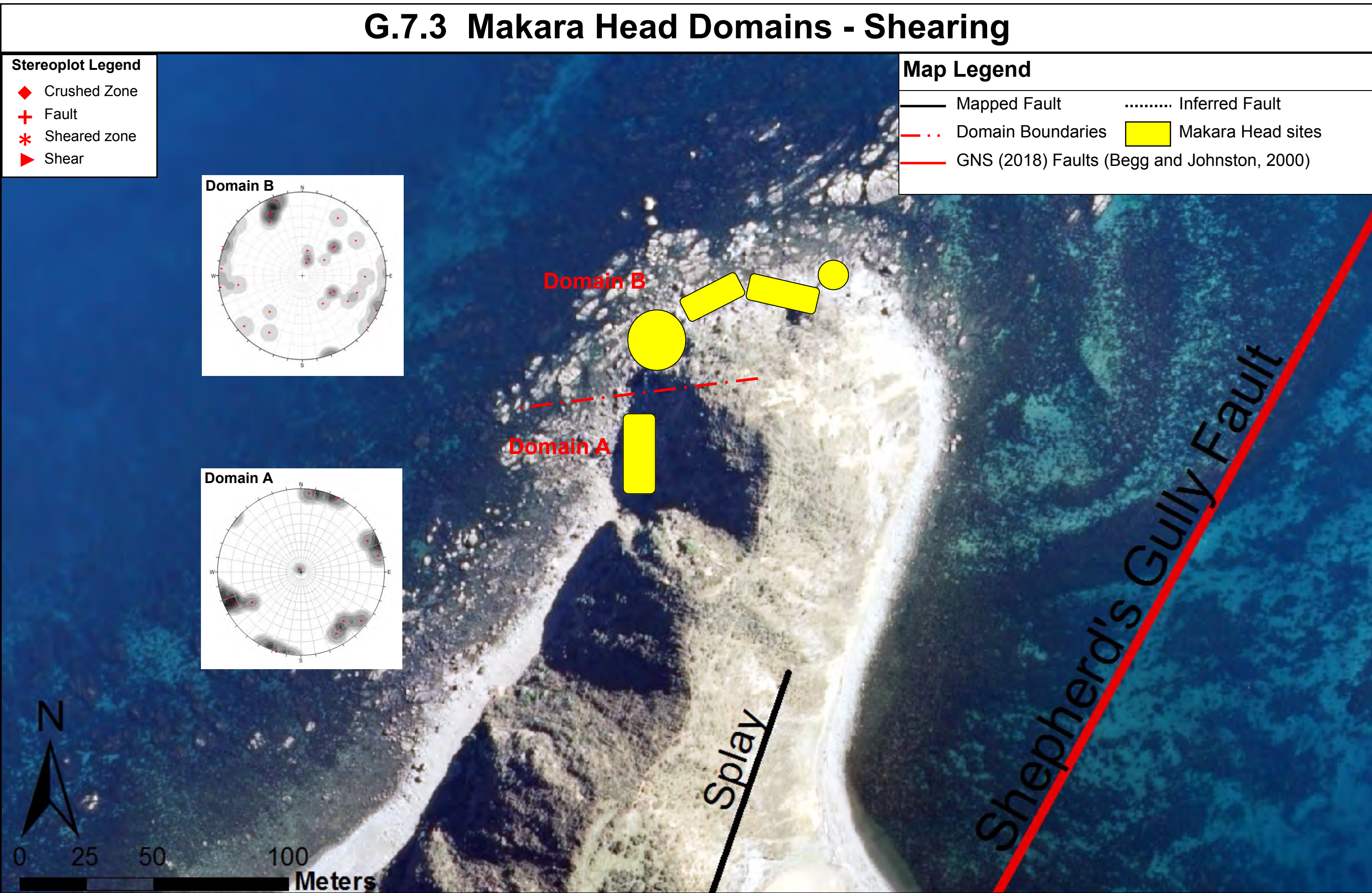
- ◆ Crushed Zone
- + Fault
- * Sheared zone
- ▶ Shear

Map Legend

- Mapped Fault
- Inferred Fault
- . - . Domain Boundaries
- Makara Head sites
- GNS (2018) Faults (Begg and Johnston, 2000)



Imagery sourced: LINZ aerial imagery, 2017 (Captured by AAM NZ Ltd (2017))



G.8 Makara Head Engineering Geological Model

Engineering geological model based on all available data. The model provides a summary of the rock mass and defect condition within the Makara Head study site. Defect orientation and regional structural controls are also included.

G.8: Engineering Geological Model of Makara Head

Key :
◆ BG ▲ CZ ▼ JN ► SR
✕ BSH + FL ■ SH

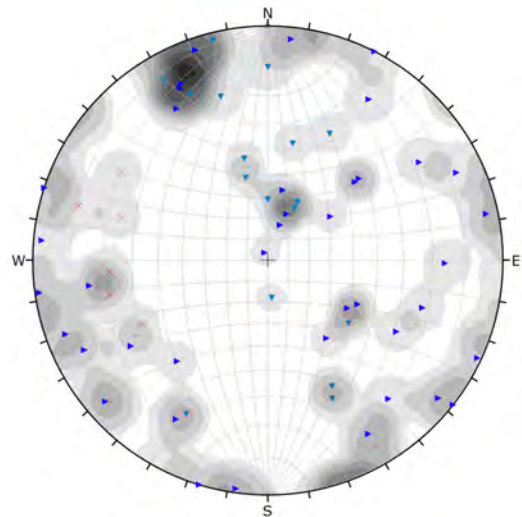


Figure 1: Stereonet of all the defect types and their orientation.

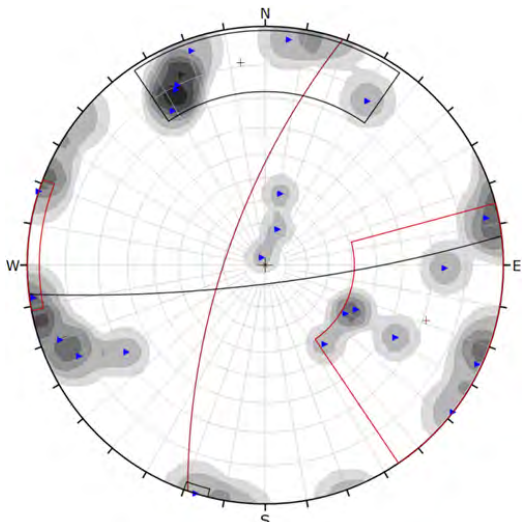


Figure 2: Stereonet of bench long shearing defects.

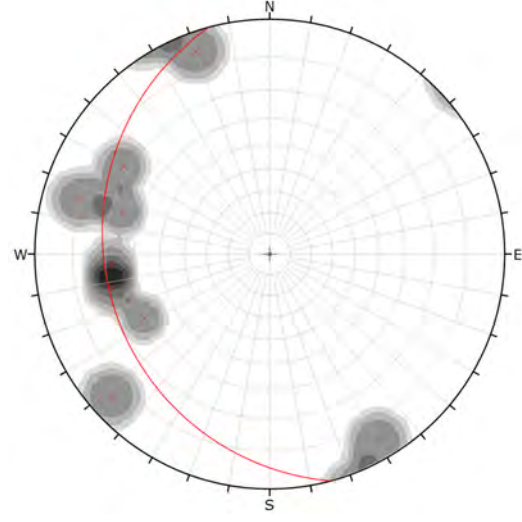
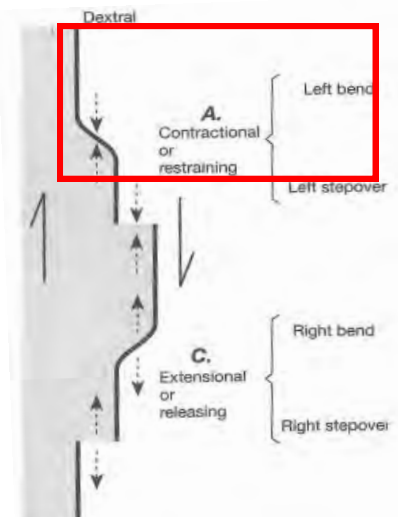


Figure 3: Stereonet of bedding.

Key:
— 1st Order >10,000m
— 2nd Order
— 3rd Order <2,500m
— Mapped areas

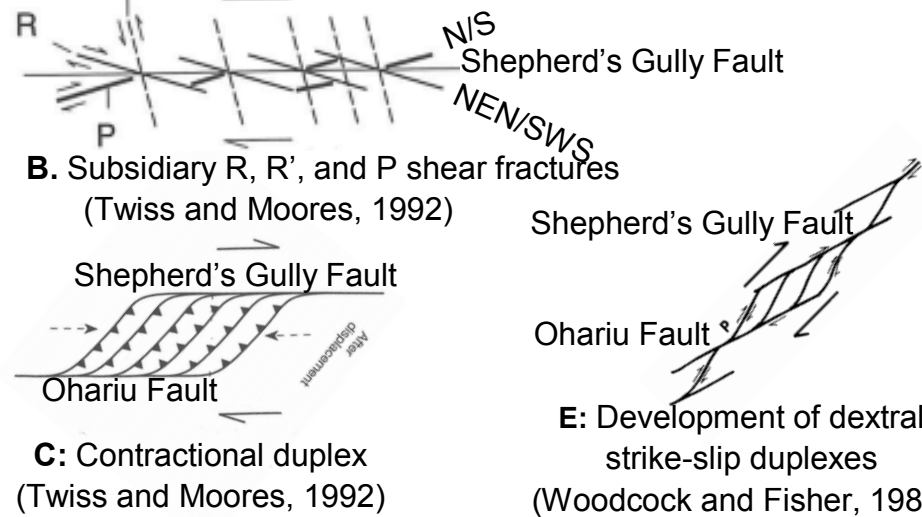
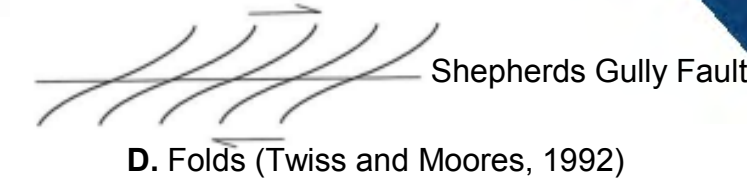
Individual sandstone beds are 1 m to 6 m thick and continuous. Mudstone beds are 8 mm to 60 mm thick and are heavily sheared. Cross-cutting shears tend to truncate each other, and faults are rarely seen.

Conceptual Models:



A: Bends and stepovers for dextral strike-slip

Shearing stereoplots appear to obtain a lot of scatter, which is anticipated when so close to major fault structures. However, there appears to be two vaguely defined sets of shears that trend sub-parallel with the likely 2nd order N/S fault structures and likely third order W/E trending structures.

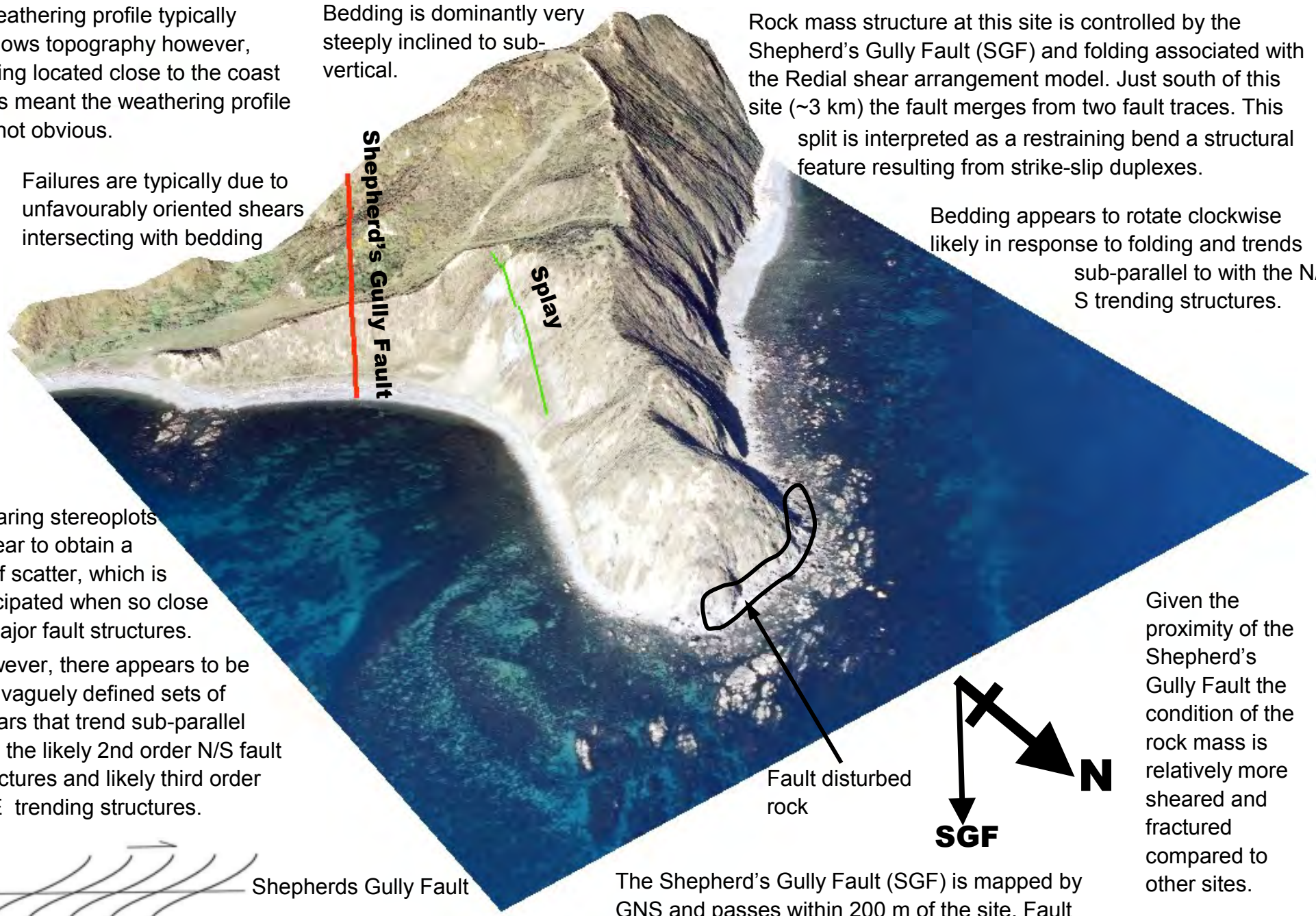


E: Development of dextral strike-slip duplexes (Woodcock and Fisher, 1986)

Weathering profile typically follows topography however, being located close to the coast has meant the weathering profile is not obvious.

Failures are typically due to unfavourably oriented shears intersecting with bedding

Bedding is dominantly very steeply inclined to sub-vertical.



Rock mass structure at this site is controlled by the Shepherd's Gully Fault (SGF) and folding associated with the Radial shear arrangement model. Just south of this site (~3 km) the fault merges from two fault traces. This split is interpreted as a restraining bend a structural feature resulting from strike-slip duplexes.

Bedding appears to rotate clockwise likely in response to folding and trends sub-parallel to with the N/S trending structures.

The Shepherd's Gully Fault (SGF) is mapped by GNS and passes within 200 m of the site. Fault motion is predominantly dextral strike-slip and the general trend is around 030°.

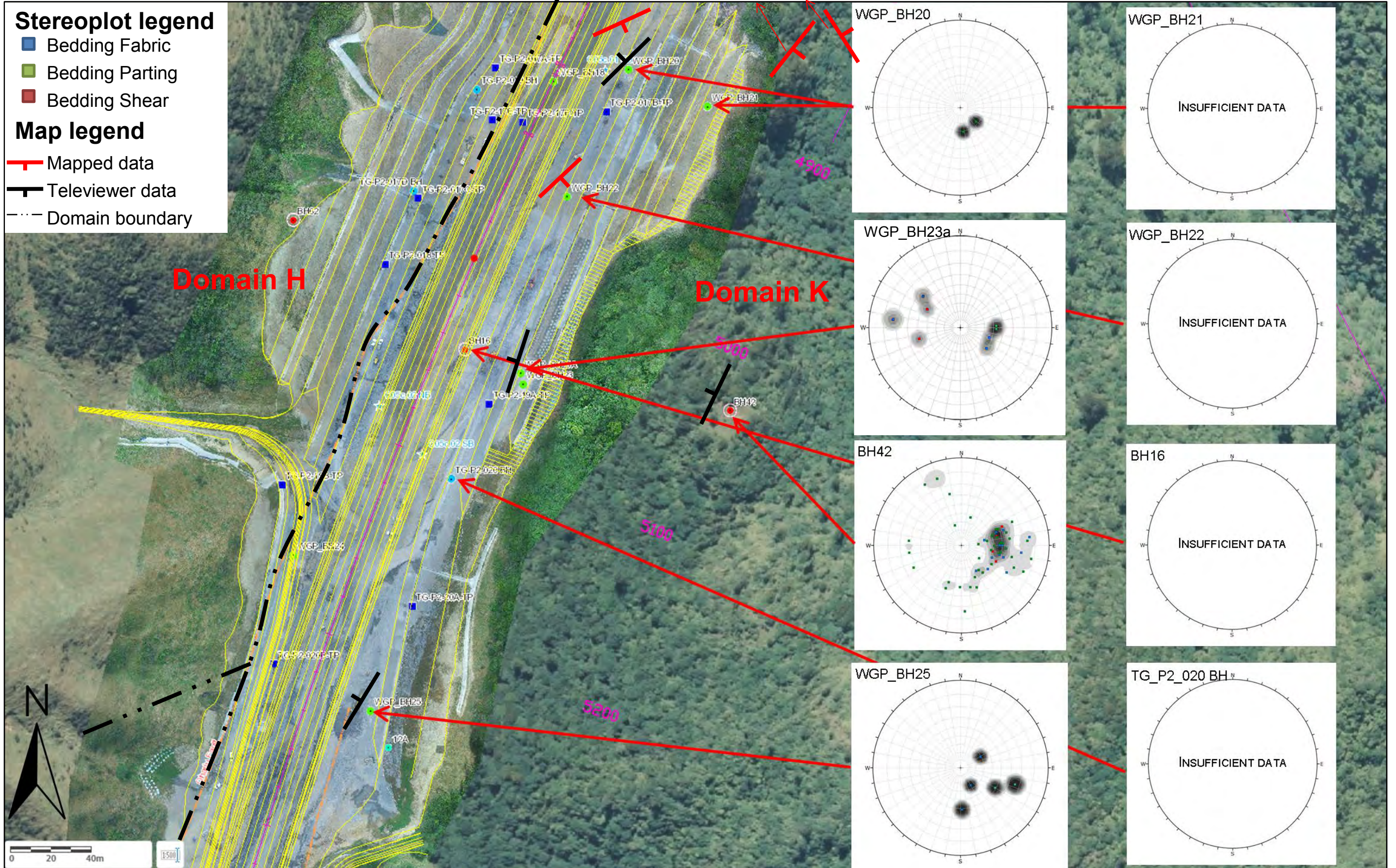
Given the proximity of the Shepherd's Gully Fault the condition of the rock mass is relatively more sheared and fractured compared to other sites.

MUD : SAND 20: 80	Sandstone: Moderately weathered, light grey SANDSTONE; Strong; 5 joint sets closely spaced, tight to narrow [RAKAIA SUB-TERRANE Greywacke]	Mudstone: Moderately weathered, dark grey MUDSTONE; moderately strong [RAKAIA SUB-TERRANE Argillite]
Predominant Suneson lithofacies: B		
Scale 1:2,920 centimetres		
0 29.375 58.75 117.5 235 470 Meters		

APPENDIX H: TRANSMISSION GULLY MAPPING

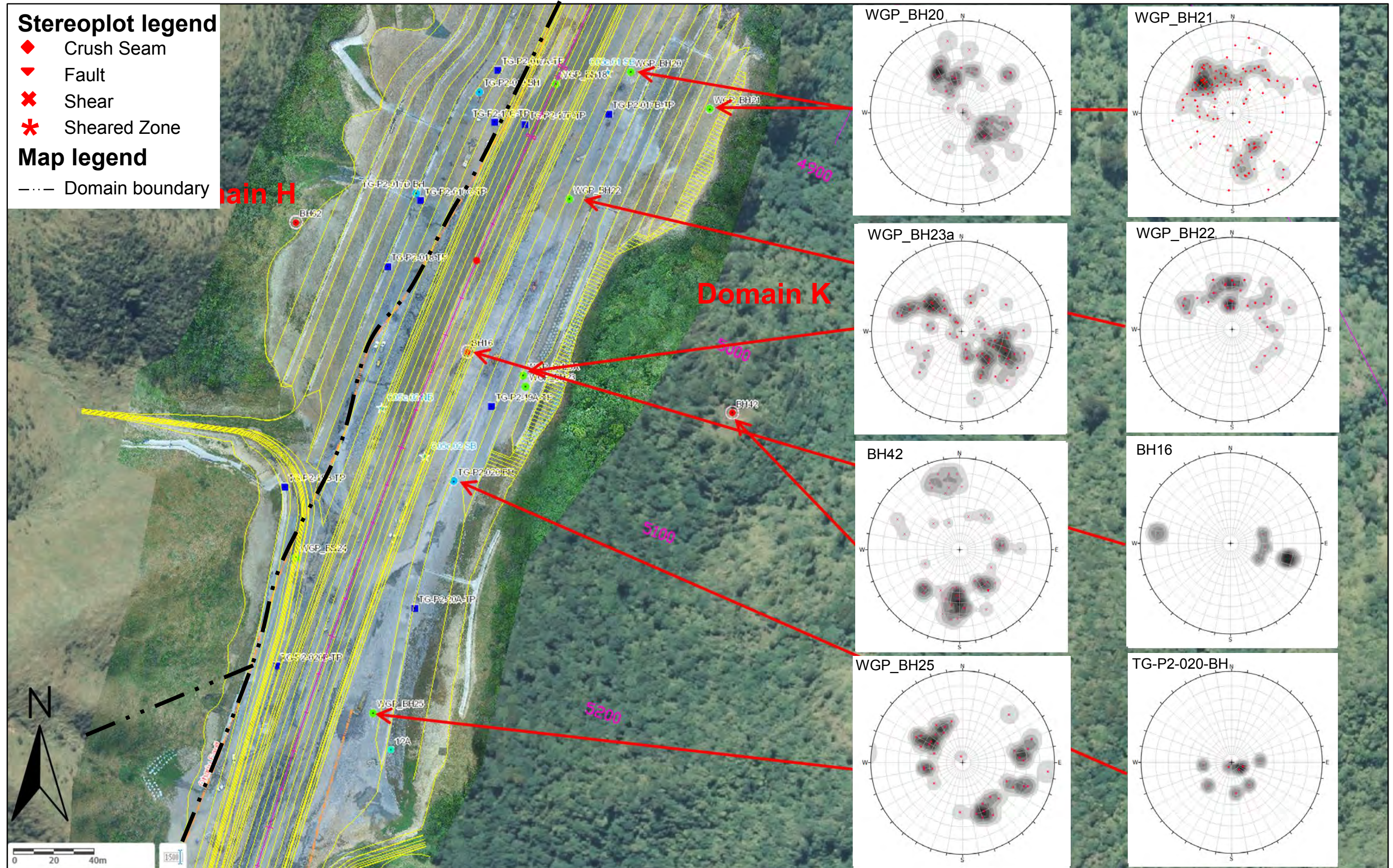
Borehole and construction mapping data from the Transmission Gully project is reproduced on aerial photographs supplied by the geotechnical team. Drillholes and mapping locations were able to be supplied allowing for geological models to be developed (PSM, 2014). Data is presented in stereoplots and overlaid in aerial extents shown in Figures H.1 through H.8.

H.1 Domain K – Bedding



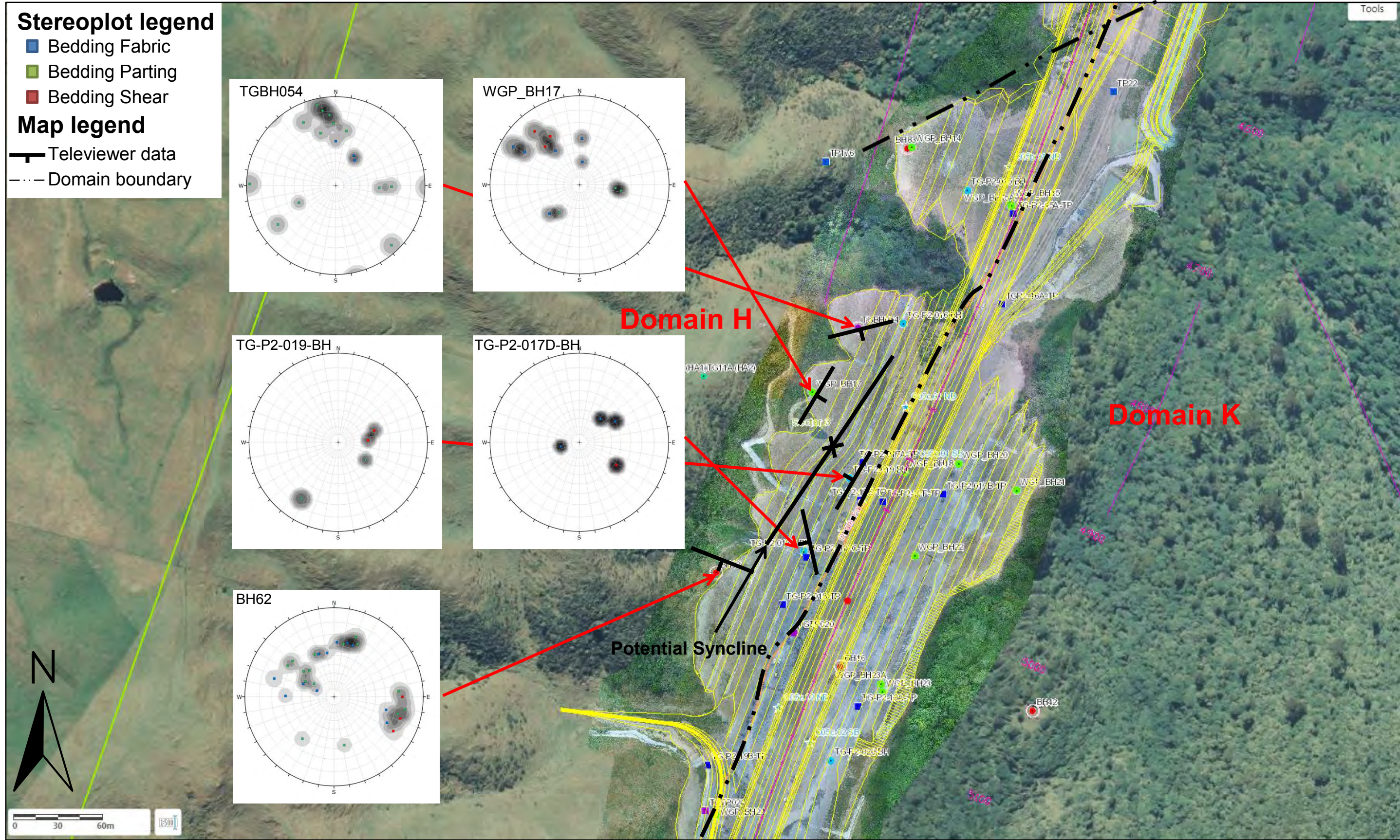
Data and imagery sourced from PSM (2014) and the Transmission Gully GIS Database (2019).

H.2 Domain K - Shearing



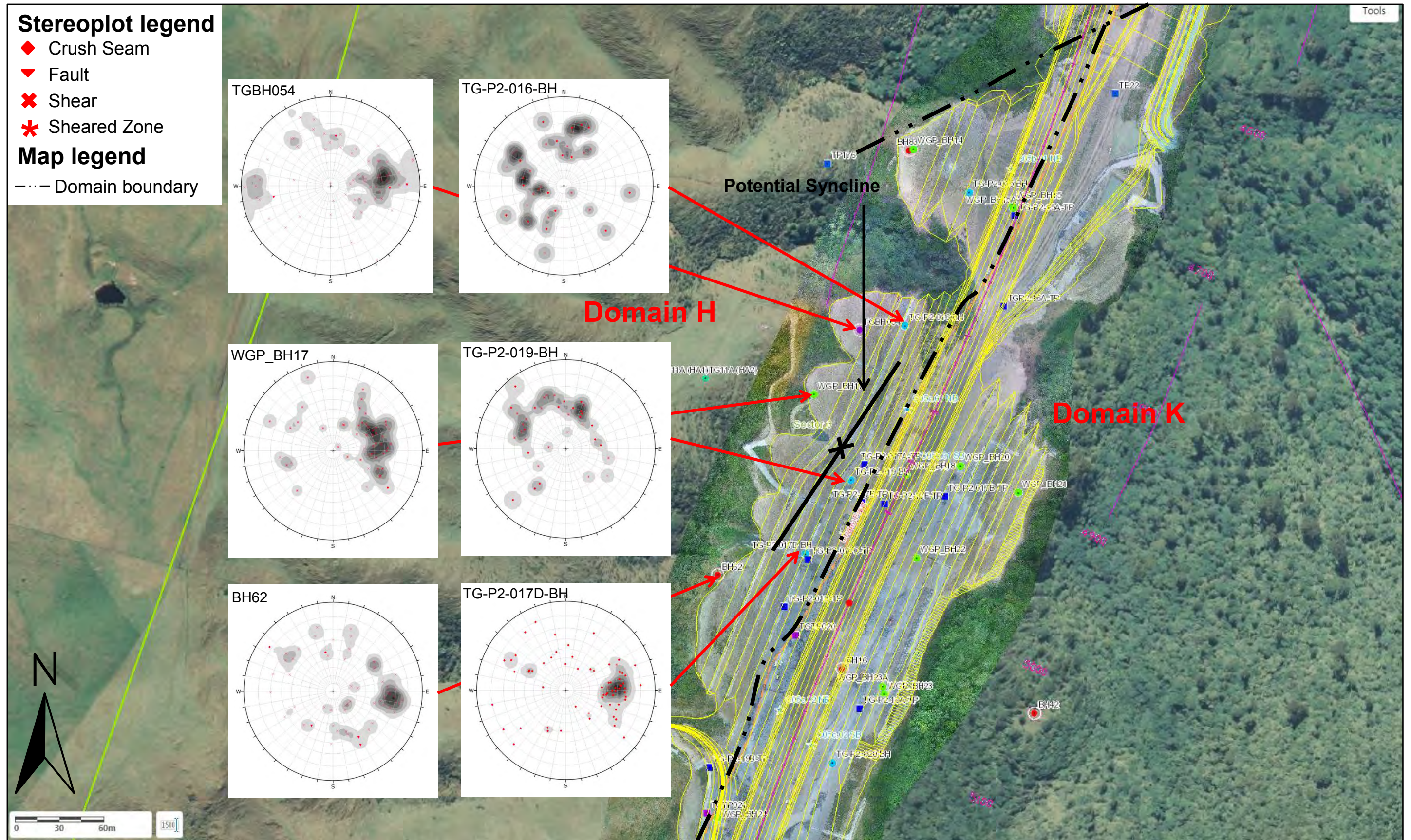
Data and imagery sourced from PSM (2014) and the Transmission Gully GIS Database (2019).

H.3 Domain H - Bedding



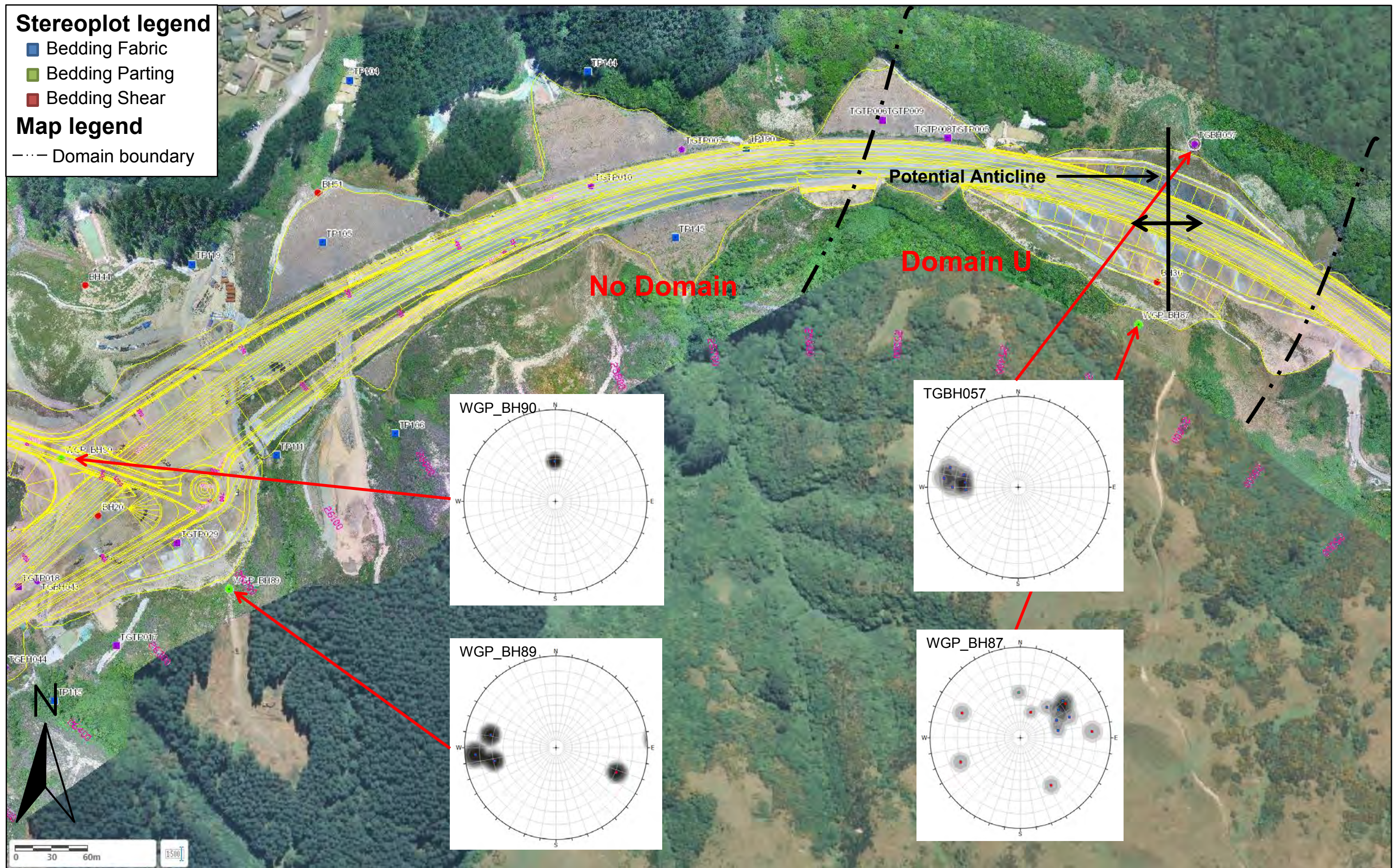
Data and imagery sourced from PSM (2014) and the Transmission Gully GIS Database (2019).

H.4 Domain H - Shearing



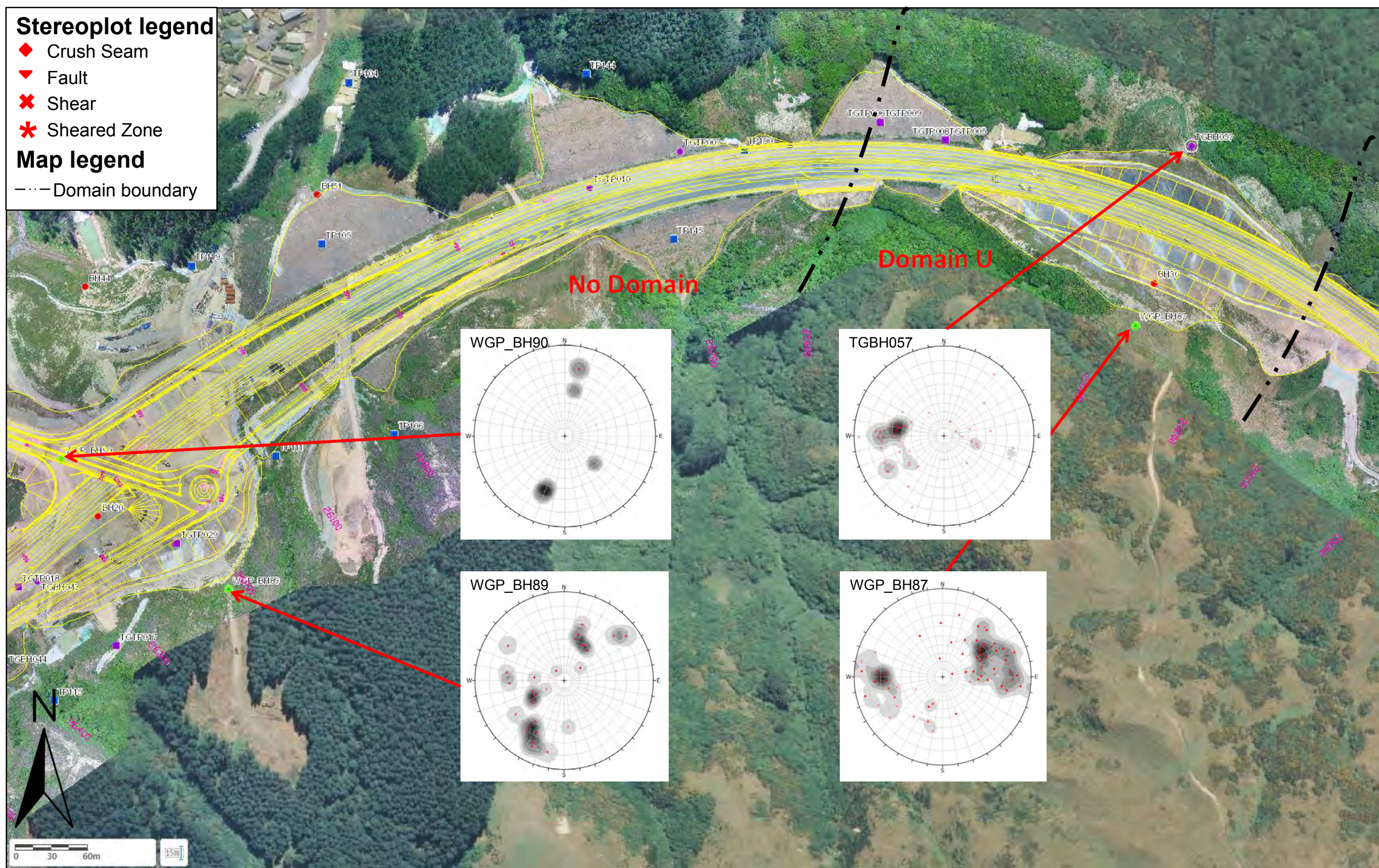
Data and imagery sourced from PSM (2014) and the Transmission Gully GIS Database (2019).

H.5 Domain U and No Domain - Bedding



Data and imagery sourced from PSM (2014) and the Transmission Gully GIS Database (2019).

H.6 Domain U and No Domain - Shearing



Data and imagery sourced from PSM (2014) and the Transmission Gully GIS Database (2019).

APPENDIX I: ROCK MASS TRENDS

Comparison against all the defect characteristics identified through individual site rock mass characterisation. Each site has been grouped based on relative lithological proportions and the distance from major 1st order faulting.

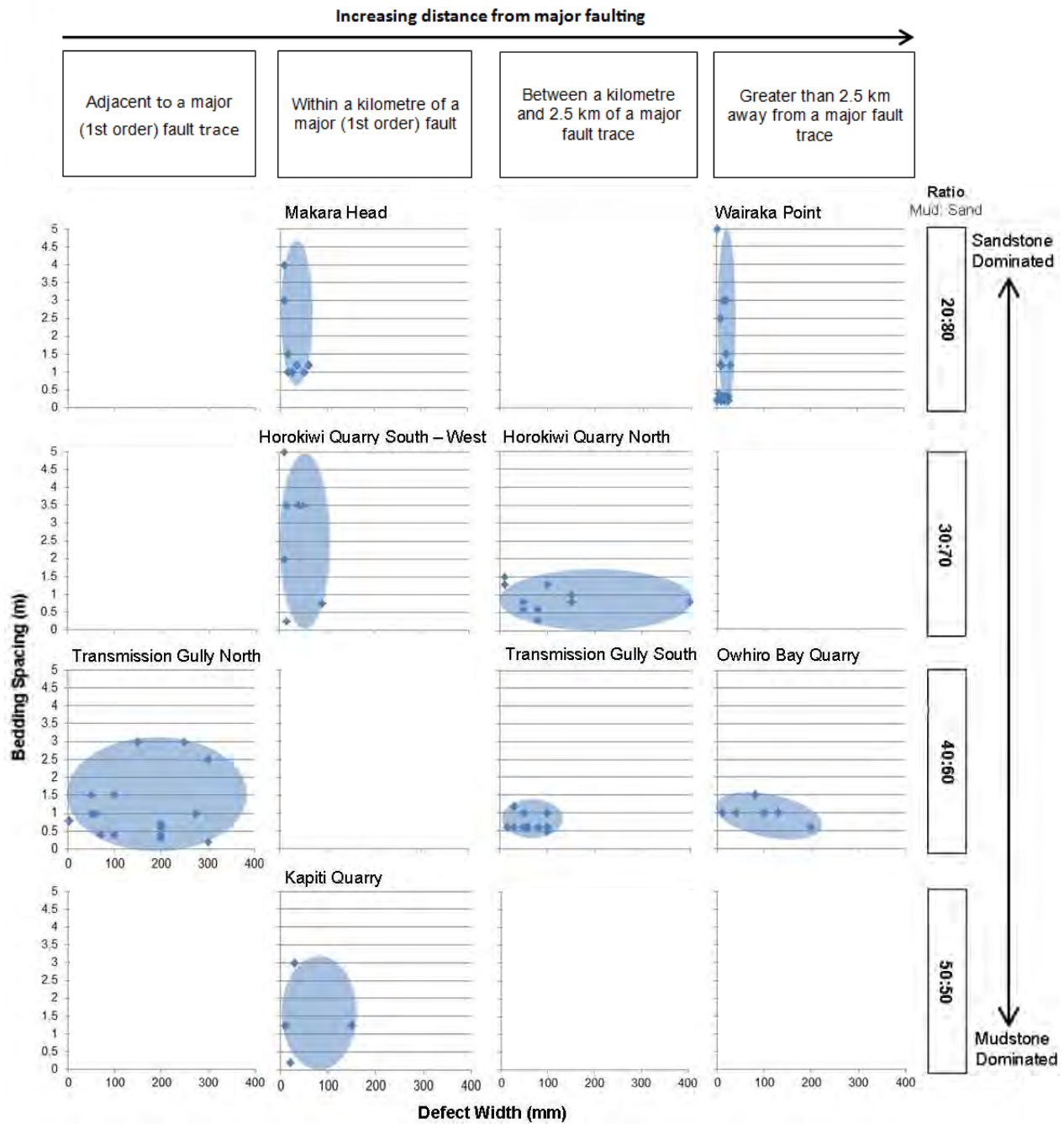


Figure I.1: Relationship among lithology and discontinuity spacing relative to distance from major faults for lithofacies B (Suneson, 1992).

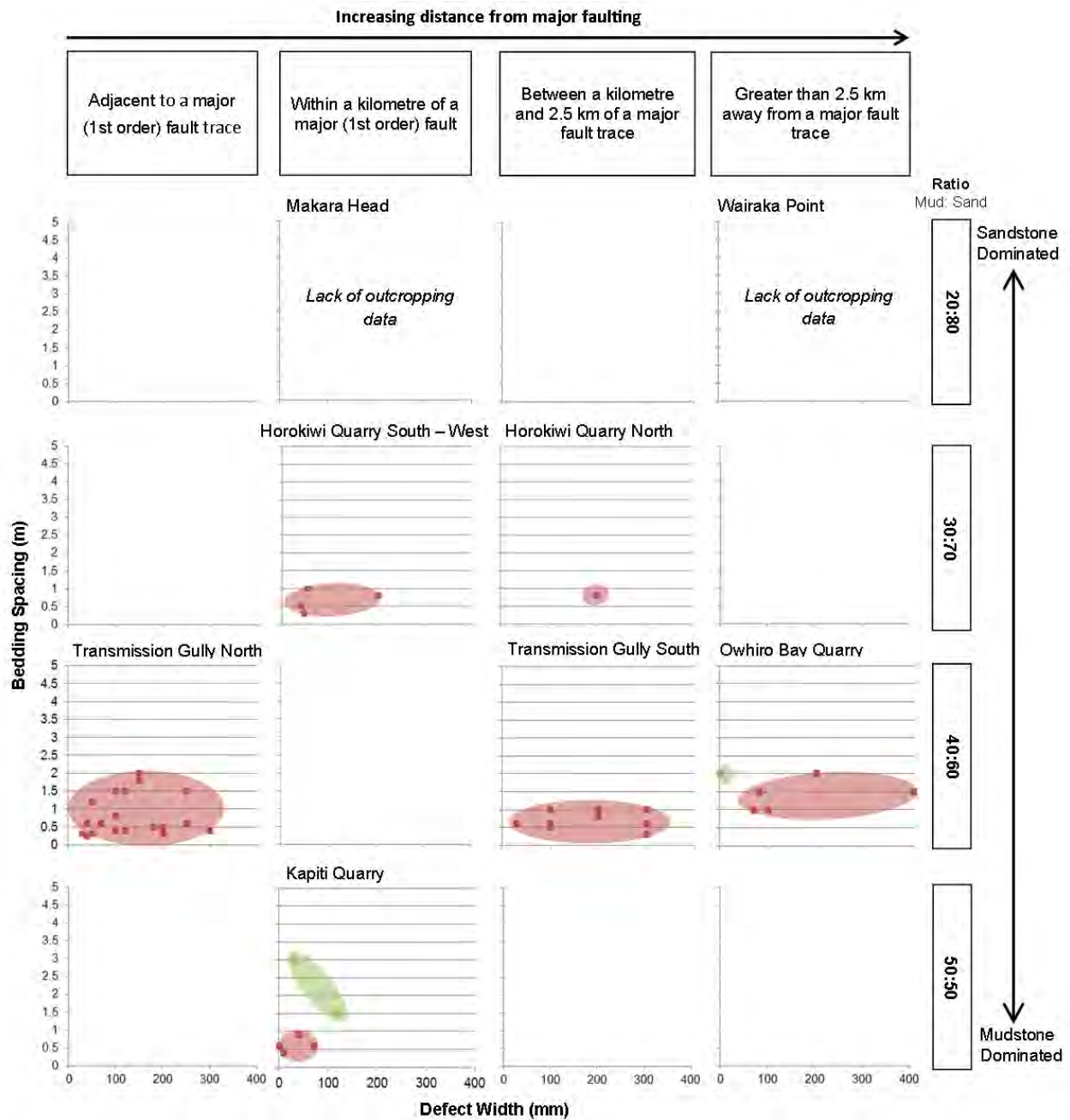


Figure I.2: Relationship among lithology and discontinuity spacing relative to distance from major faults for lithofacies C (Red) and D (Green) (Suneson, 1992).

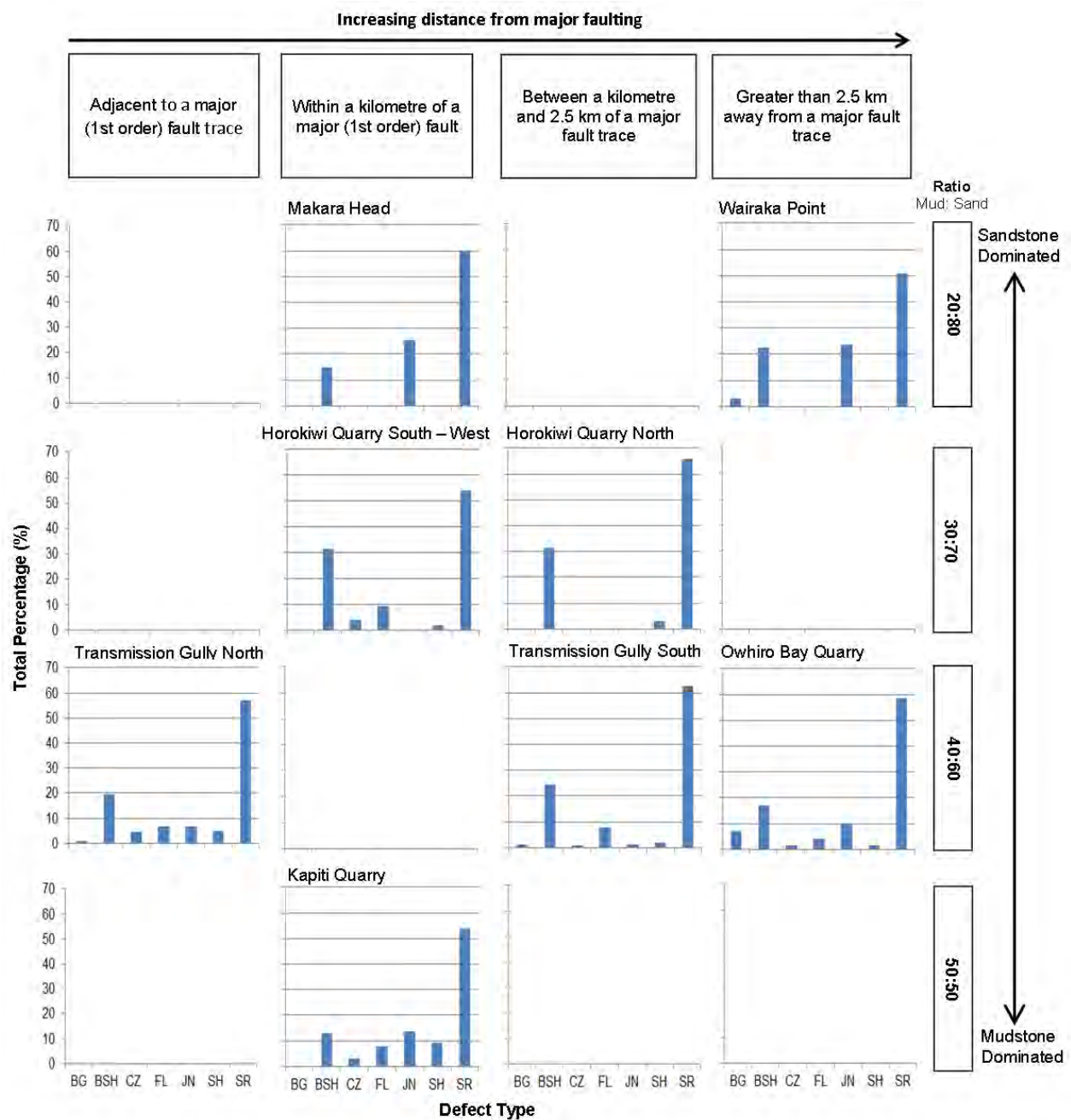


Figure I.3: Percentage of defect types recorded at each field area. SR – Shear, SH – Shear zone, JN – Joint, FL – Fault, CZ – Crush Zone, BSH – Bedding Parallel Shear, and BG – Bedding. Also shows the relationship between lithology and defect type relative to the distance from major faults.

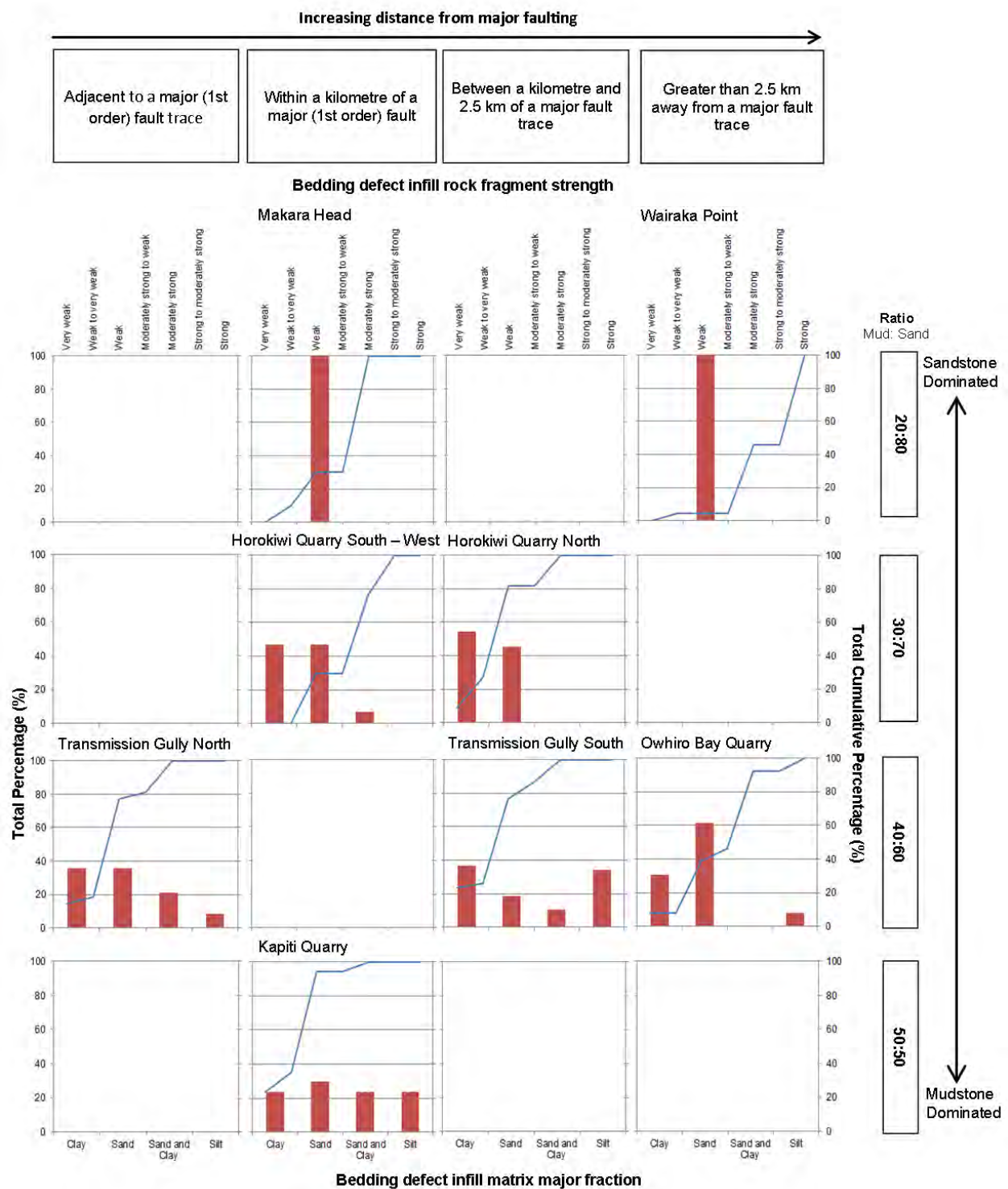


Figure I.4: Relationship between the bedding defect infill matrix grainsize and the infill rock fragment strength. Also displays further relationships between these defect properties among lithology and relative distances from major faults.

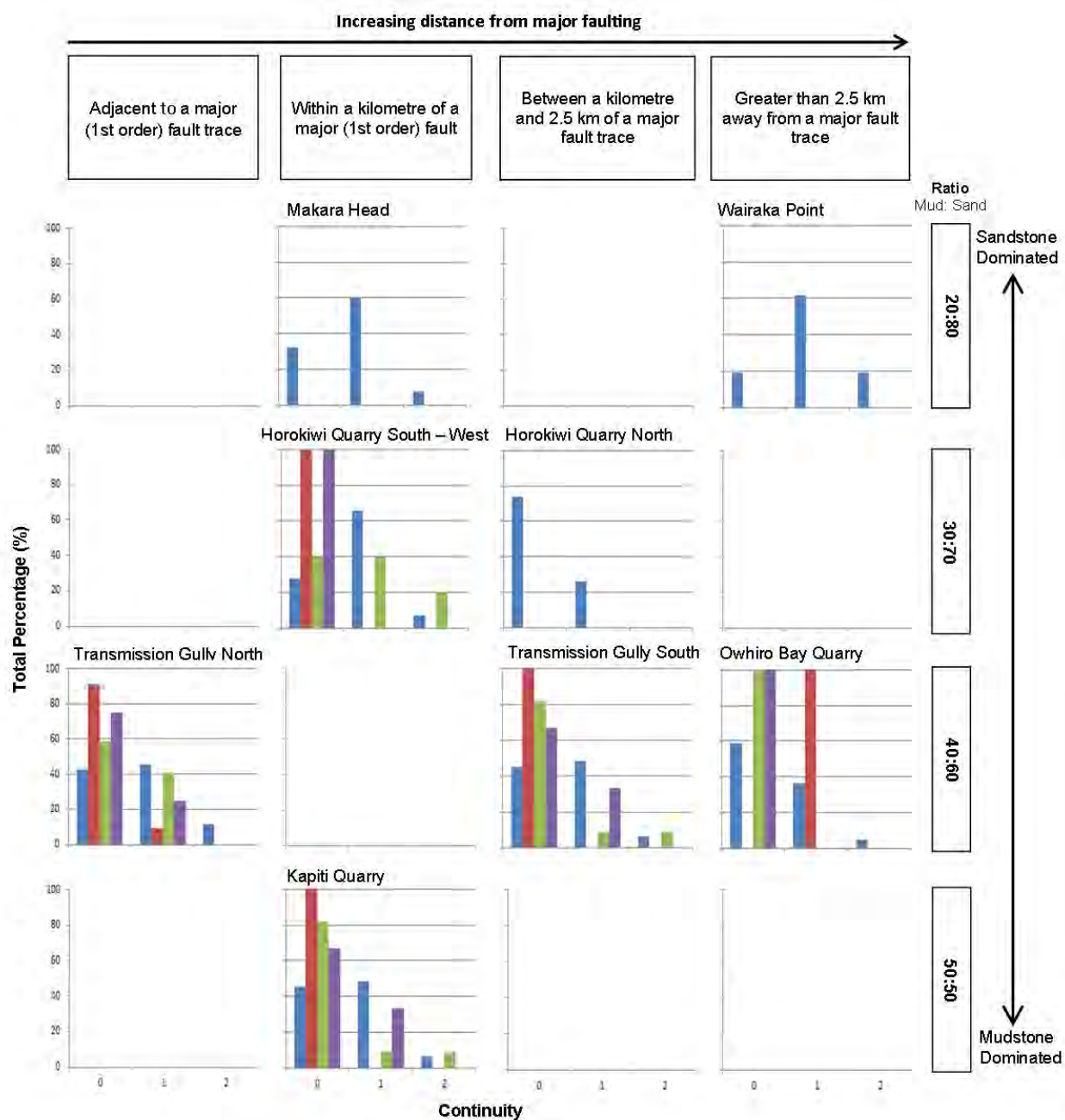
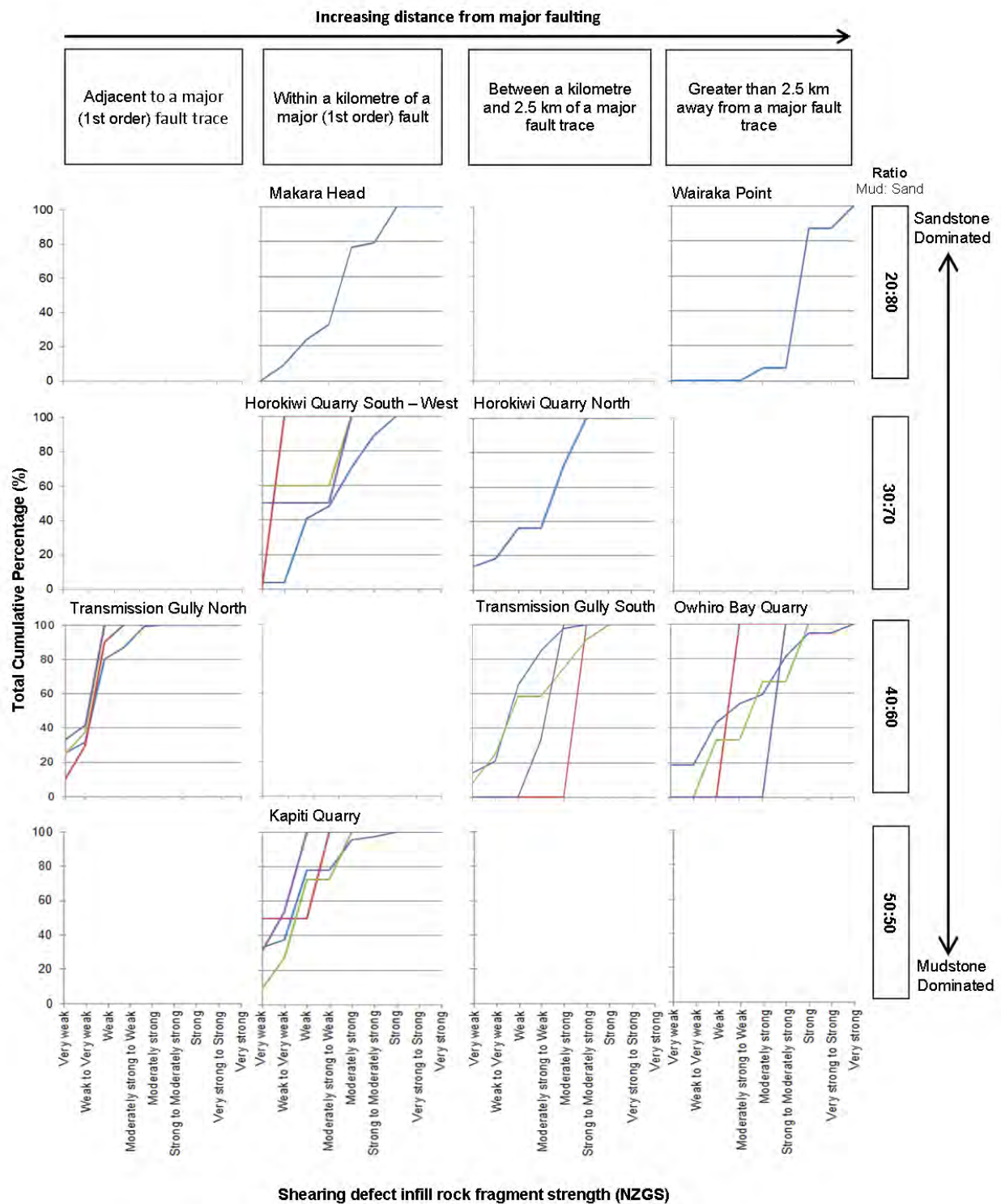


Figure I.7: Relationship among lithology and defect continuity relative to distance from major faults. Blue = SR, Red = FL Green = CZ, Purple = SH.



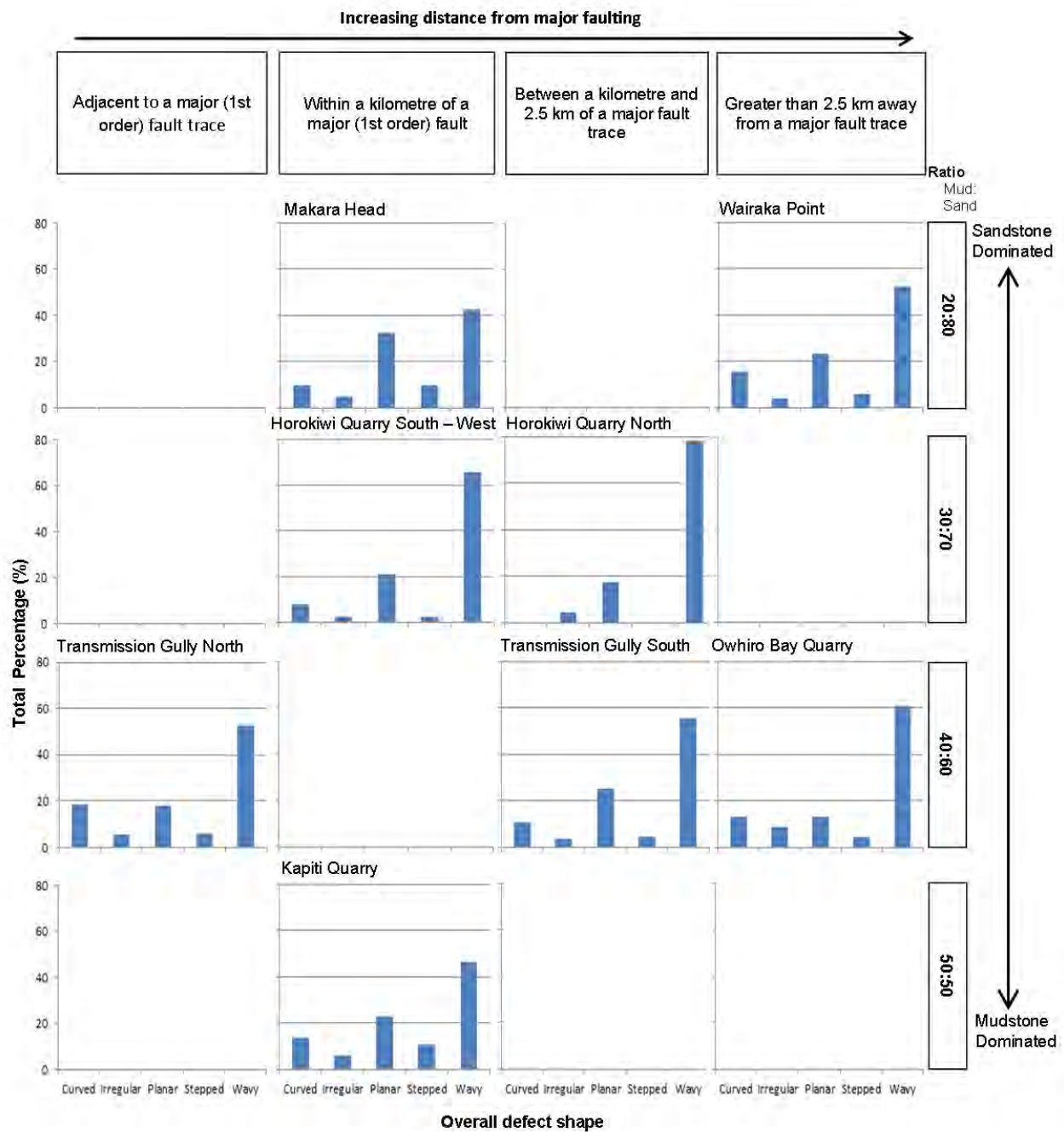


Figure I.9: Relationship between lithology and defect shape relative to distance from major faults.

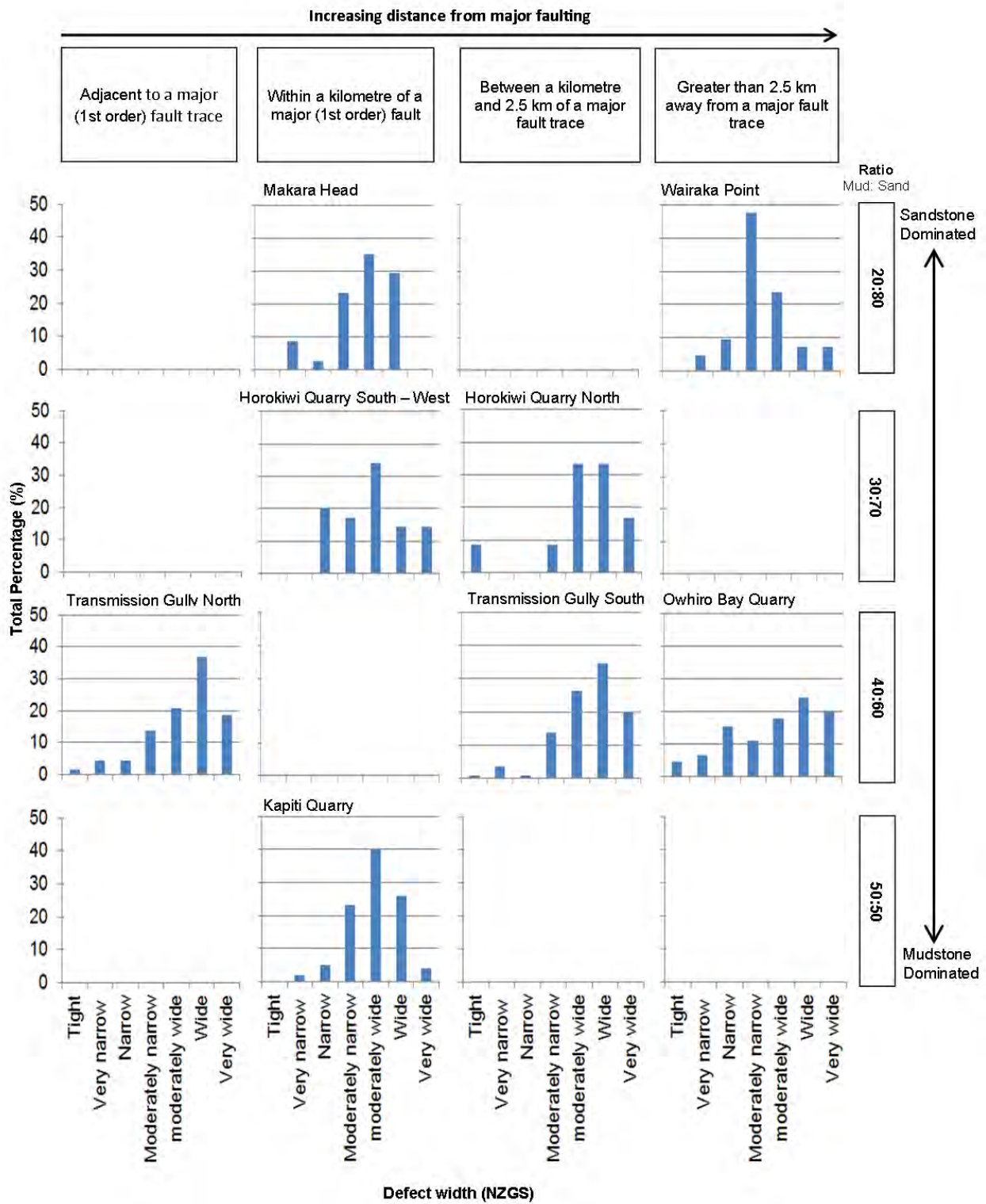


Figure I.10: Relationship between lithology and defect width relative to distance from major faults.

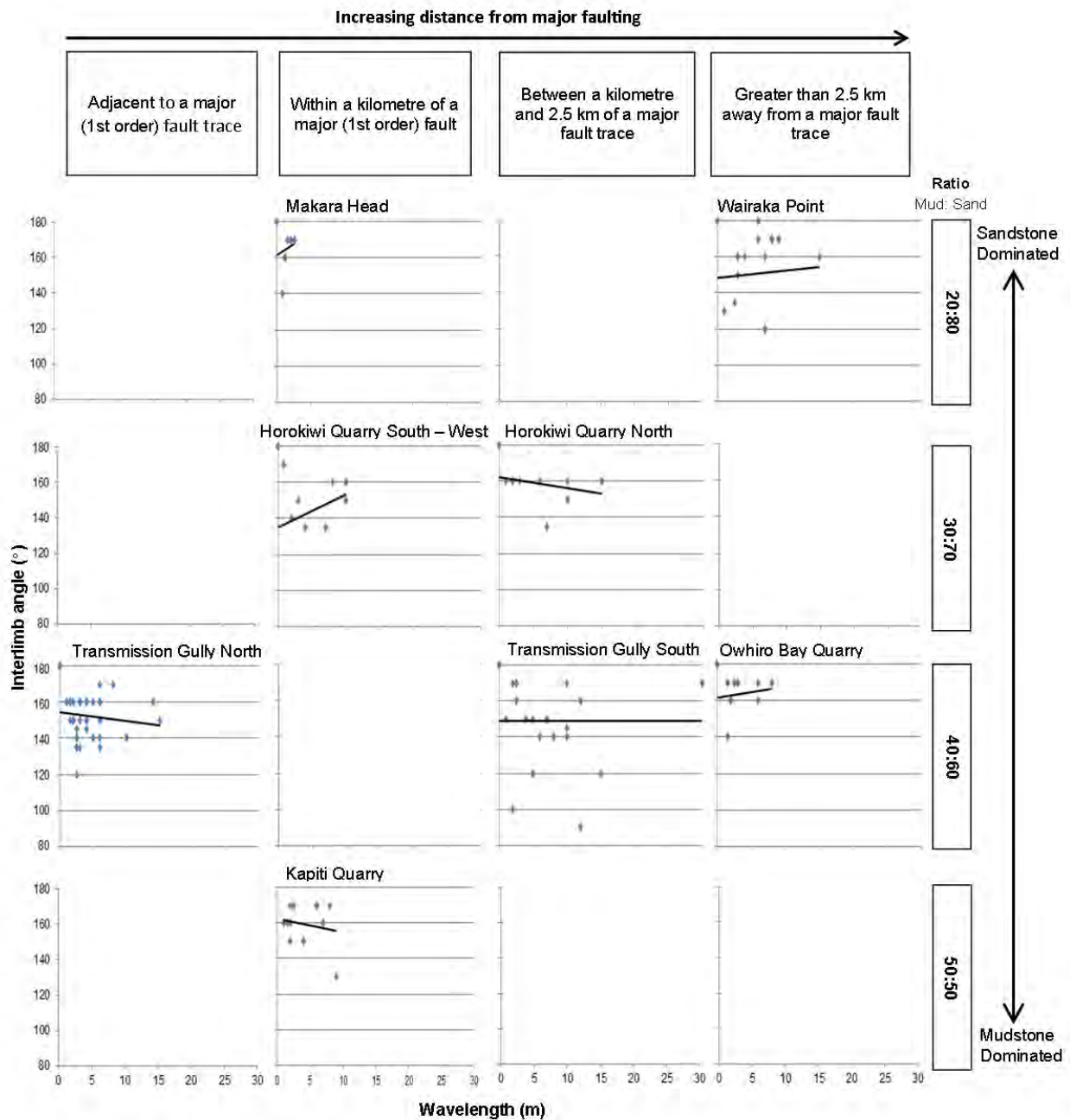


Figure I.11: Bedding waviness across all study areas. Note that planar discontinuities are included. Also shows the relationship between lithology and bedding waviness relative to the distance from major faults.

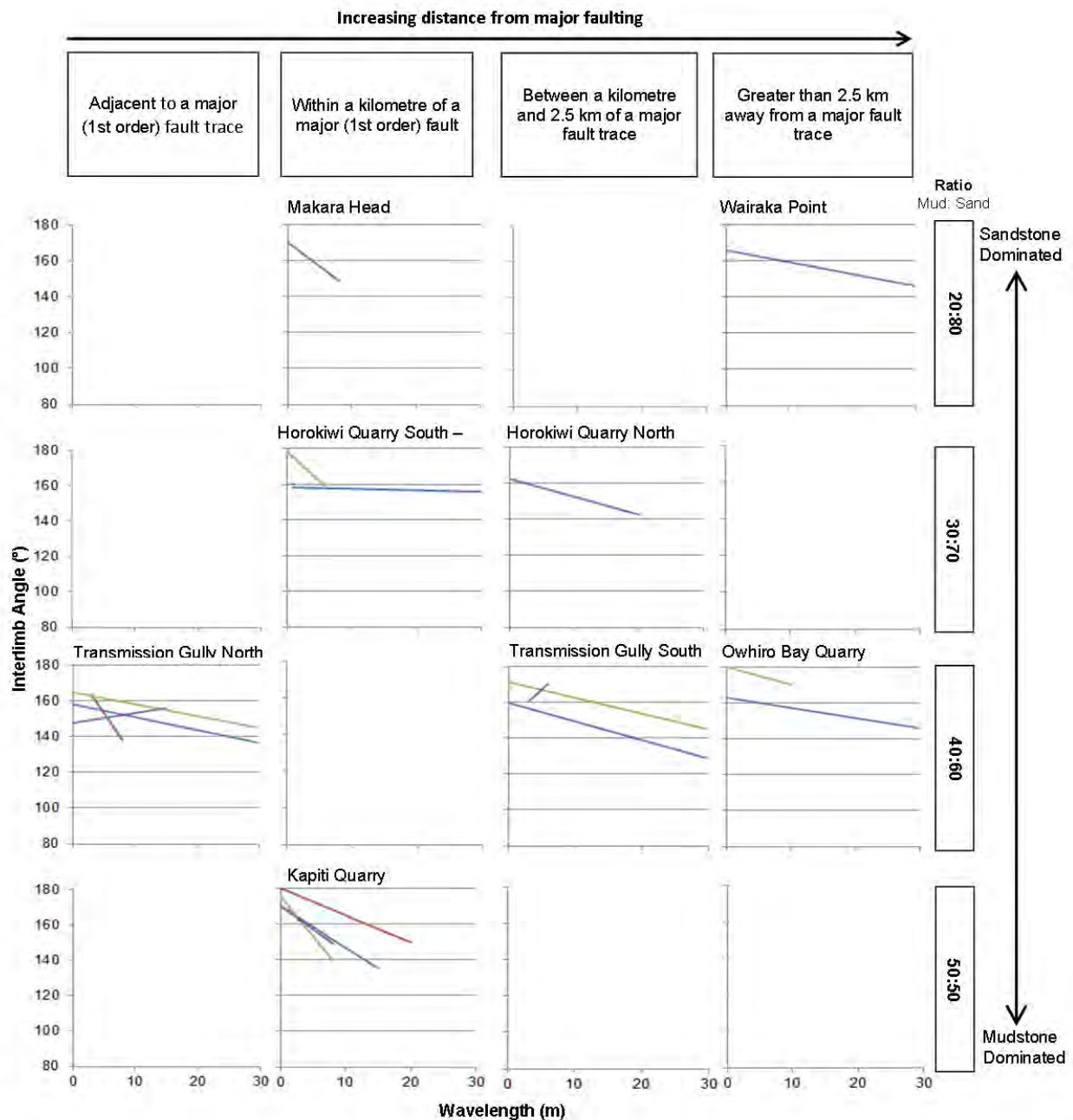


Figure I.12: Shearing waviness across all study areas. Note that planar discontinuities are included. Blue = SR, Purple = SH, Green = FL, Red = CZ. Also shows the relationship between lithology and shearing/faulting defect waviness relative to the distance from major faults.

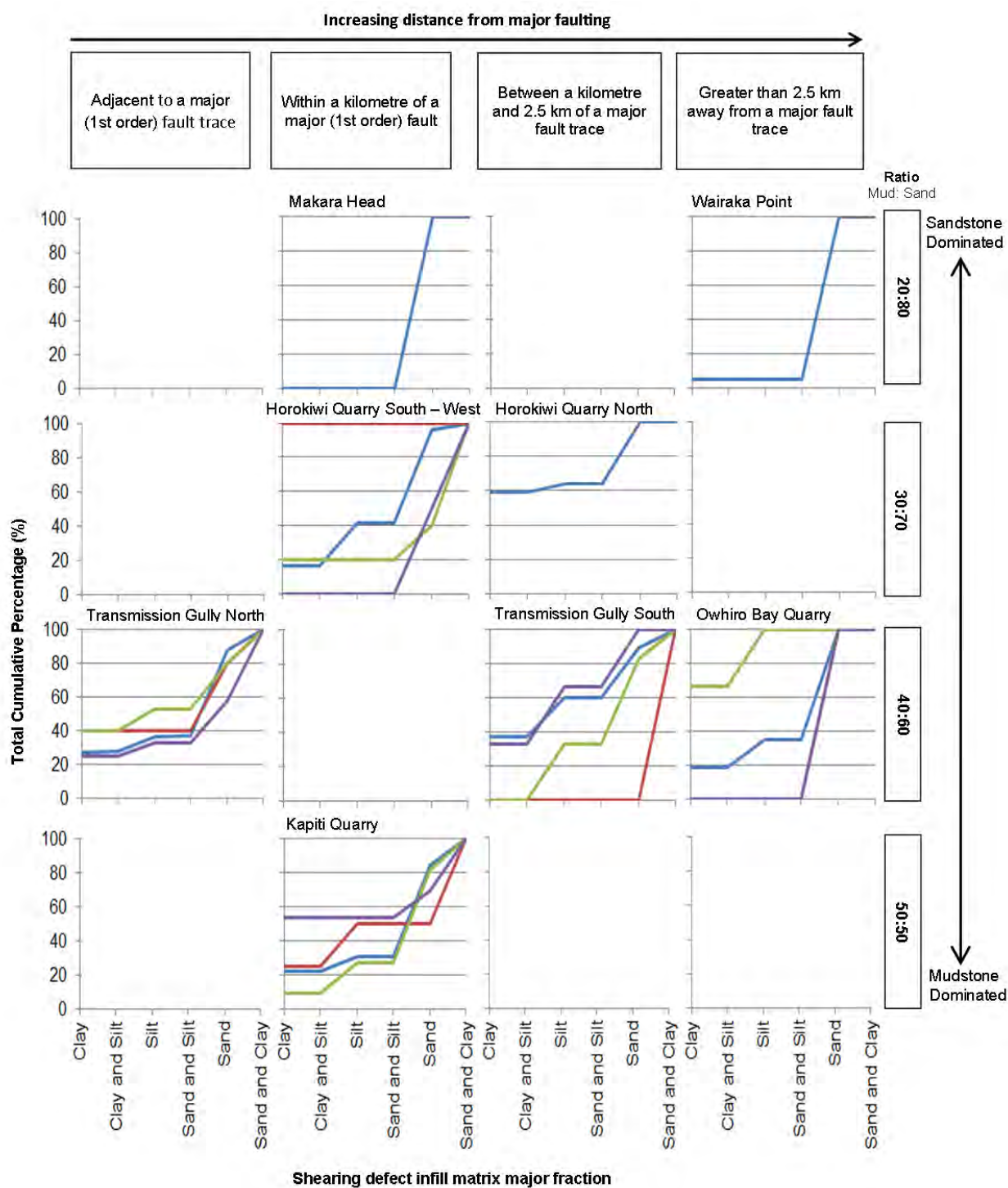


Figure I.13: Relationship between lithology and shearing defect infill grainsizes relative to distance from major faults. Also shows the relationship among other shearing and faulting structures. See Figure 12 for acronym explanation.

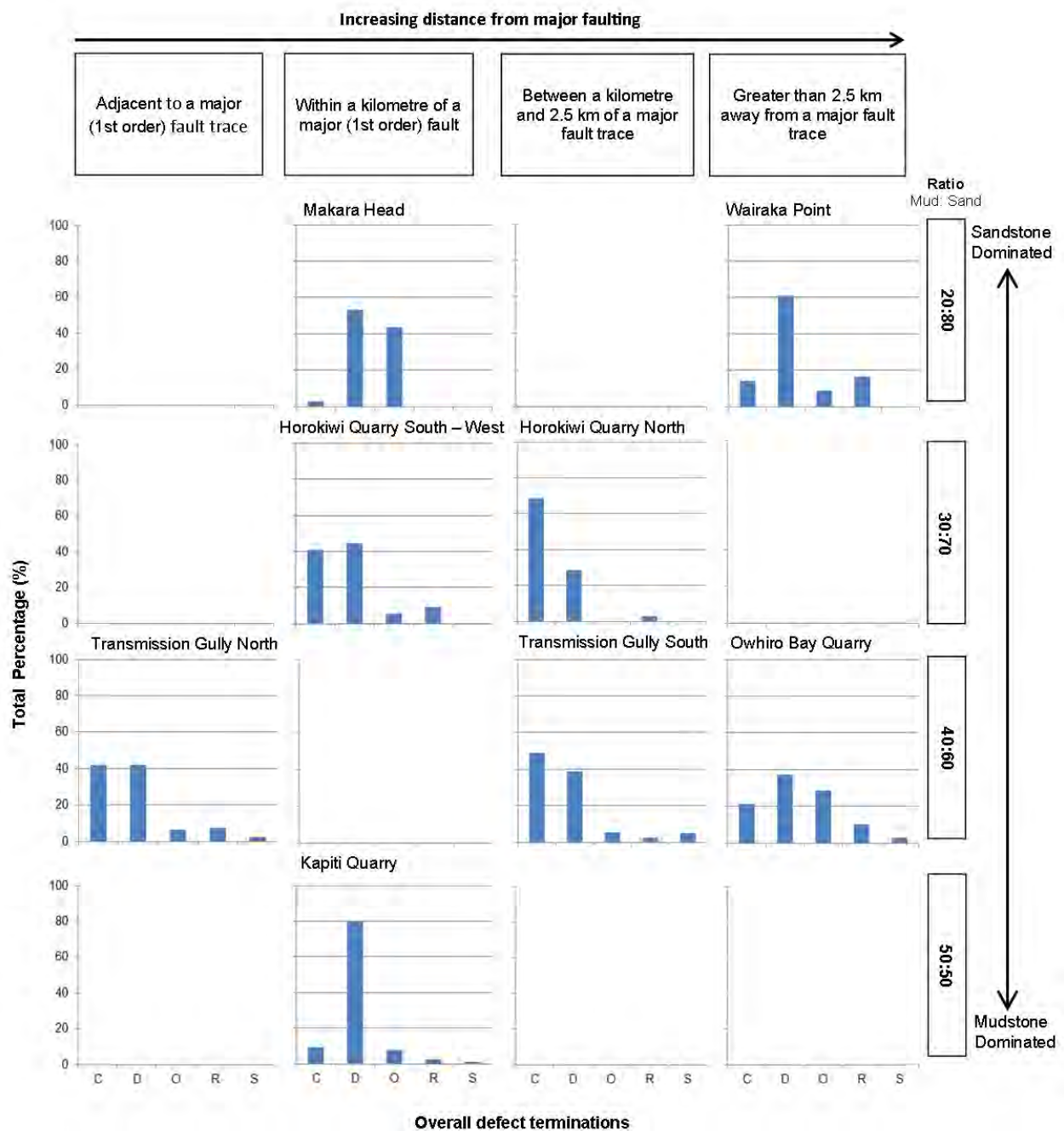


Figure I.14: Relationship among lithology and defect termination relative to distance from major faults.

APPENDIX J: STATISTICAL CALCULATIONS FOR THE TORLESSE ROCK MASS CLASSIFICATION (TRC)

In using the TRC it is suggested that further calculations be conducted. These calculations primarily determine the likelihood of lithofacies group, X, occurring simultaneously with defect structural class, Y, across a specific site or entire project. These results aid in the overall identification of potential rock mass types. These calculations can be followed in a step by step procedure outlined below.

J.1 Calculations

Step 1: Identify the probability (P) of each outcrop within a site.

The probability (P) of each outcrop is calculated by dividing the width of one outcrop (O_n) by the total width of the site (S_n), where the total width of the site is the sum of all the mapped outcrop widths within the site extents. This is shown in Equation one below:

$$P(O_n \text{ in } S_n) = \frac{\text{width of } O_n}{\text{width of } S_n} \quad \text{Equation 1}$$

Where, “O” represents the Outcrop and “S” represents the Site. “n” defines the number of the site or outcrop.

Step 2: Calculate the probability of each event “E” (i.e. Lithofacies group X, with Defect structural class, Y)

The probability of each event occurring within a site can be determined using Equation 2 and Equation 3. Where, the product of lithofacies (X) and defect structural class (Y) proportions are further multiplied by the result of Equation 1.

$$P(E \text{ in } O_n) = P(X \text{ and } Y) = P(X) \times P(Y) \quad \text{Equation 2}$$

$$P((E \text{ in } O_n) \text{ in } S) = P(E \text{ in } O_n) \times P(O_n \text{ in } S_n) \quad \text{Equation 3}$$

The sum of each outcrop (Equation 4) will determine the overall probability of each event occurring within a specific site, $P(E \text{ in } S_n)$.

$$P(E \text{ in } S_n) = P((E \text{ in } O_1) \text{ in } S) + P((E \text{ in } O_2) \text{ in } S) + P((E \text{ in } O_n) \text{ in } S_n) \quad \text{Equation 4}$$

The $P(E \text{ in } S_n)$ can then be multiplied by a 100 in order to find the total percentage of each event per site. This information is then used to produce graphs and identify rock mass types within each site.

Step 3: Determine the probability of each event occurring across all sites

For determining the probability of the certain rock mass types being identified across an entire project or site further calculations are required. This can be derived by multiplying each event probability per site (determined in step 2) by the probability of the specified site occurring within a project, Equation 5.

$$P(E) = P(S_n) \times P(E \text{ in } S_n) \quad \text{Equation 5}$$

The probability of the specified site occurring within a project can be calculated in a similar way to step 1, instead O_n is replaced with S_n , which is also substituted for the total project width, Equation 6.

$$P(S_n) = \frac{\text{width of } S_n}{\text{total width across all field sites}} \quad \text{Equation 6}$$

This information is then used to compare against individual site data in order to determine key rock mass types across the entire field area. A blank Torlesse rock mass classification is presented on the following page to aid in further work (Figure J.1). Results from this thesis are presented in Tables J.1 section J.2.

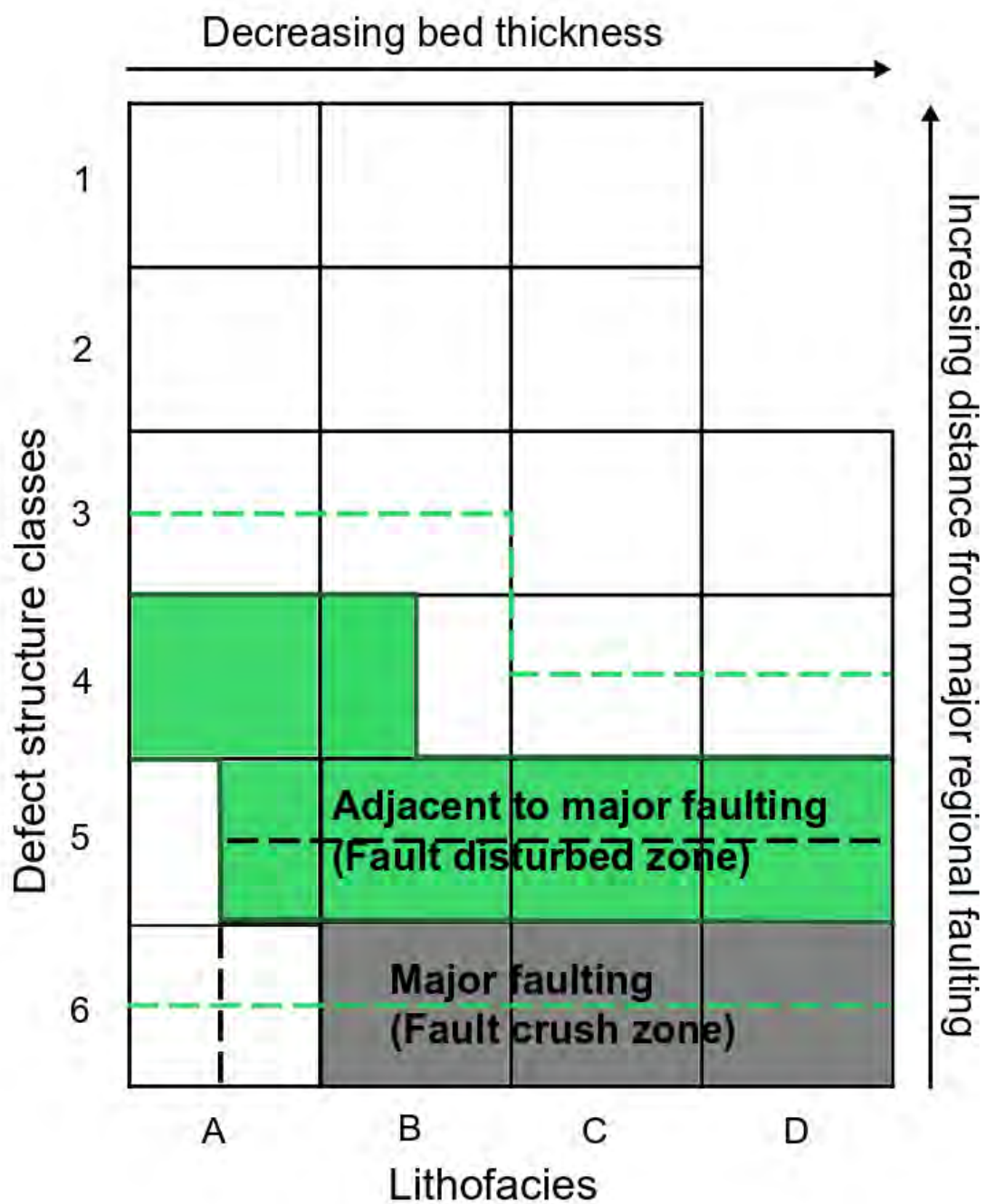


Figure J.1: Blank Torlesse rock mass classification

Table J.1: Site data and Calculations

Study area	Width study area	$P(Q_n \text{ in } S_n) \times 100$	$P(S_n) \times 100$	Relative proportion of lithofacies in percentage (%)				Relative proportions of defect classes in percentages (%)					
				A	B	C	D	1	2	3	4	5	6
TG North	460 m		24.01%		80	28					35.87	60.87	3.26
Outcrop 1	120 m	26.09%			80	20						100	
Outcrop 2	30 m	6.52%			80	20						100	
Outcrop 3	85 m	18.48%			60	40					100		
Outcrop 4	90 m	19.57%			70	30						100	
Outcrop 5	30 m	6.52%			100							50	50
Outcrop 6	25 m	5.43%			100							100	
Outcrop 7	80 m	17.39%			70	30						100	
TG South	450 m		23.49%		70	30				75	25		
Outcrop 1	80 m	17.78%			60	40					100		
Outcrop 2	140 m	31.11%			80	20				100			
Outcrop 3	130 m	28.89%			70	30				100			
Outcrop 4	100 m	22.22%			70	30				100			
Kapiti Quarry	300 m		15.66%		50	40	10			66.67		33.33	
Outcrop 1	20 m	6.67%			100					100			
Outcrop 2	180 m	60.00%			15	65	20					100	
Outcrop 3	100 m	33.33%			30	50	20					100	
Owhiro Bay Quarry	200 m		10.44%		50	50			100				
Outcrop 1	100 m	50.00%			60	40			100				
Outcrop 2	100 m	50.00%			40	60			100				
Horokiwi Quarry	320 m		16.70%		95	5				66.67		33.33	
Outcrop 1	20 m	6.25%			80	20						100	
Outcrop 2	150 m	46.88%			90	10				100			
Outcrop 3	150 m	46.88%			100					100			
Wairaka Point	86 m		4.49%	100				100					
Outcrop 1	40 m	46.51%		100				100					
Outcrop 2	20 m	23.26%		100				100					
Outcrop 3	20 m	23.26%		100				100					
Outcrop 4	6 m	6.98%		100				100					
Makara Head	100 m		5.22%	100						100			
Outcrop 1	25 m	25.00%		100						100			
Outcrop 2	15 m	15.00%		100						100			
Outcrop 3	20 m	20.00%		100						100			
Outcrop 4	40 m	40.00%		100						100			

J.2 Individual Site results

Transmission Gully North					
	A	B	C	D	Total
1	0	0	0	0	0
2	0	0	0	0	0
3	0	0	0	0	0
4	0	0.233	0.126	0	0.359
5	0	0.485	0.124	0	0.609
6	0	0.033	0	0	0.033
Total	0	0.75	0.25	0	1

Transmission Gully South					
	A	B	C	D	Total
1	0	0	0	0	0
2	0	0	0	0	0
3	0	0.607	0.216	0	0.822
4	0	0.107	0.071	0	0.178
5	0	0	0	0	0
6	0	0	0	0	0
Total	0	0.713	0.287	0	1

Owhiro Bay Quarry					
	A	B	C	D	Total
1	0	0	0	0	0
2	0	0.5	0.5	0	1
3	0	0	0	0	0
4	0	0	0	0	0
5	0	0	0	0	0
6	0	0	0	0	0
Total	0	0.5	0.5	0	1

Kapiti Quarry					
	A	B	C	D	Total
1	0	0	0	0	0
2	0	0	0	0	0
3	0	0	0	0	0
4	0	0.067	0	0	0.067
5	0	0.190	0.557	0.187	0.933
6	0	0	0	0	0
Total	0	0.257	0.557	0.187	1.000

Wairaka Point					
	A	B	C	D	Total
1	1	0	0	0	1
2	0	0	0	0	0
3	0	0	0	0	0
4	0	0	0	0	0
5	0	0	0	0	0
6	0	0	0	0	0
Total	1	0	0	0	1

Horokiwi Quarry					
	A	B	C	D	Total
1	0	0	0	0	0
2	0	0	0	0	0
3	0	0.891	0.047	0	0.938
4	0	0	0	0	0
5	0	0.05	0.013	0	0.063
6	0	0	0	0	0
Total	0	0.941	0.059	0	1

Makara Head					
	A	B	C	D	Total
1	0	0	0	0	0
2	0	0	0	0	0
3	1	0	0	0	1
4	0	0	0	0	0
5	0	0	0	0	0
6	0	0	0	0	0
Total	1	0	0	0	1

Overall					
	A	B	C	D	Total
1	0.045	0	0	0	0.045
2	0	0.052	0.052	0	0.104
3	0.052	0.302	0.058	0	0.412
4	0	0.054	0.029	0	0.084
5	0	0.181	0.137	0.029	0.347
6	0	0.008	0	0	0.008
Total	0.097	0.597	0.277	0.029	1